VACUUM

The International Journal and Abstracting Service

for

VACUUM SCIENCE AND TECHNOLOGY

1.
.0
960

VOLUME 10

(1960)

PERGAMON PRESS

NEW YORK OXFORD LONDON PARIS

VACUUM

The International Journal and Abstracting Service for Vacuum Science and Technology and their Applications in Research and Industry

BOARD OF EDITORS

Mr. A. S. D. BARRETT, Finsbury Pavement House, 120, Moorgate, London, E.C.2.

Mr. A. H. BECK, Engineering Laboratories, University of Cambridge, Trumpington Street, Cambridge.

Mr. B. B. DAYTON, Technical Director, Consolidated Vacuum Corp., 1775, Mt. Read Blvd., Rochester 3, N.Y., U.S.A.

Dr. J. M. DUNOYER, École Nationale Supérieure de Mécanique de Nantes, Université de Rennes, 3, rue Marechal-Joffre, Nantes, France.

Professor Dr. R. JAECKEL, Physikalisches Institut der Universität, Abt. Vakuum, Nussallee 6, Bonn, Germany.

Mr. W. G. MATHESON, Sylvania Electric Products, Inc., 60, Boston Street, Salem, Mass., U.S.A.

Mr. P. A. REDHEAD, National Research Council, Radio and Electrical Engineering Division, Ottawa, Canada.

Professor Dr. E. THOMAS, École Royale Militaire, Centre des Sciences Nucléaires, 30, Avenue de la Renaissance, Bruxelles 4, Belgium.

Mr. J. YARWOOD, Head of the Department of Mathematics and Physics, The Polytechnic, 309, Regent Street, London, W.1.

Secretary to the Board of Editors: G. E. SATTERTHWAITE

HONORARY INTERNATIONAL EDITORIAL ADVISORY BOARD

E. N. DA C. ANDRADE (London)
C. H. BACHMAN (Syracuse)
C. BALAKRISHNAN (Bombay)
J. BLEARS (Manchester)
R. N. BLOOMER (Aldermaston, Berks)
J. R. BOWMAN (Evanston)
H. L. J. BURGESS (London)
J. H. CARMICHAEL (New Hyde Park, N.Y.)
K. DIELS (Köln)
L. DUNOYER (Paris)
H. EBERT (Braunschweig)
F. D. EDWARDS (Crawley—*Joint Chairman*)
A. J. GALE (Burlington, Mass.)
C. L. GOULD (Brookhaven)
A. GUTHRIE (San Francisco)
W. HAENLEIN (Nürnberg)
C. HAYASHI (Tokyo)
K. C. D. HICKMAN (Rochester, N.Y.—*Joint Chairman*)
H. KLUMB (Mainz)
W. H. KOHL (Los Altos, Calif.)
J. H. LECK (Liverpool)
G. LEWIN (Princeton, N.J.)
A. LORENZ (Hainau-am-Main)
C. LOVINFOSSE (Bruxelles)
I. R. MAXWELL (Publisher)
C. R. MEISSNER (Atlanta, Georgia)
G. L. MUNDAY (Genève)
H. NAKAGAWA (Tokyo)
N. OCHERT (Israel)
G. W. OETJEN (Köln)
J. POLLARD (Baldock, Herts)
P. DELLA PORTA (Milano)
L. E. PREUSS (Detroit)
W. PUPP (Giessen)
L. RIDDIFORD (Birmingham)
N. W. ROBINSON (Salford)
D. J. SANTELER (Schenectady)
K. SCHAEFER (Frankfurt-am-Main)
R. F. STRICKLAND-CONSTABLE (London)
E. A. TRENDELENBURG (Balzers)
A. H. TURNBULL (Harwell)
H. VON UBISCH (Sweden)
A. VENEMA (Eindhoven)
M. W. WELCH (Chicago)
O. WINKLER (Liechtenstein)

Publishing Offices: Headington Hill Hall, Oxford (Oxford 64881)

Annual subscription (including postage) :

(A) For libraries, government establishments and research institutions £10 ($28.00)

(B) For individuals who write directly to the publisher and certify that the journal is for their personal use £5 5s. ($15.00)

Copyright © 1961 Pergamon Press Ltd.

PERGAMON PRESS LTD.

Headington Hill Hall,
Oxford

122 East 55th Street,
New York 22, N.Y.

CONTENTS OF VOLUME 10

Numbers 1/2

International Symposium on Residual Gases in Electron Tubes and Related High Vacuum Systems

page

Opening Speech by G. POLVANI 1

SESSION I

Residual Gases and Final Vacuum

W. DAHLKE and H.-J. SCHÜTZE : Residual Gas Pressure in Electron Tubes. Part I—Method of Measurements.. 3
H.-J. SCHÜTZE and H.-W. EHLBECK : Residual Gas Pressure in Electron Tubes. Part II—Experimental Results.. 5
A. KLOPFER, S. GARBE and W. SCHMIDT : Residual Gases in Vacuum Systems 7
S. P. WOLSKY and E. J. ZDANUK : The Investigation of Residual Gases in Vacuum Systems 13
J. C. FRANCKEN and J. VAN DER WAAL : Residual Gases in Picture Tubes 22
R. H. COLLINS and J. C. TURNBULL : Evolution and Absorption of Gases in Electron Tubes 27

SESSION II

Methods of Measuring Residual Gases during the Manufacture and Life of Tubes

W. TRETNER : An Electrostatic Mass Spectroscope 31
G. REICH and F. FLECKEN : Analysis of Partial Pressure by Means of Omegatron and Farvitron. Comparative View of the Ranges of Application 35
J. P. FREYTAG : Emploi d'une Diode d'Essais comme Moyen de Contrôle des Matériaux de Construction des Tubes Électroniques 40
R. J. WARNECKE, JR. : Emploi du Spectromètre de Masse dans la Technologie des Tubes Électroniques 49
F. A. BAKER and T. A. GIORGI : The Applicability of the Omegatron to Continuous Analysis of Residual Gases.. 58
G. CALVI : Double Pirani Bridge Leak Detector 64

SESSION III

Origin of Residual Gases. Studies on the Condition of Internal Surfaces of Tubes and their Gas Sorption and Desorption. Effects Caused by Surface Alterations due to Gas Sorption

A. NASINI, F. RICCA and G. SAINI : Clean Surfaces and Sorption of Gases 68
N. W. ROBINSON : The Action of Molybdenum, Tungsten, Tantalum and Nickel on Residual Gases in a Vacuum System 75
S. GARBE, A. KLOPFER and W. SCHMIDT : Some Reactions of Water in Electron Tubes 81
S. H. CROSS : System Design and the Choice of Materials for the " Nimrod " Vacuum System 86
K. HASHIMOTO, H. IWANAYAGI and H. FUKUSHIMA : Measurement of Gas Evolution and Absorption from Materials used in Vacuum Tubes 92

SESSION IV

Influence of Residual Gases in Tube Life

R. W. LAWSON : The Influence of Residual Gas on the Performance of the British Post Office Submarine Telephone Repeater Valve Type 6P12 100
N. W. W. SMITH : Noise Reduction in Microwave Tubes by Getter-Ion Pumping 106
J. R. TEW : A Pumping Schedule for a Power Travelling Wave Tube 110
T. H. BRIGGS and S. NADEAU : Effects of Continuous Gas Clean-up upon Cathodes Emission and Cathode Interface Impedance 112

ol.
10
960

AUTHOR INDEX Volume 10 (1960)

(B.R.) denotes a Book Review

Argano, E. pp. 194, 223
Armbruster, W. p. 405
Baker, F. A. p. 58
Bateman, S. K. p. 329
Batey, H. p. 263
Bierig, R. p. 382
Biolley, E. p. 151
Bloomer, R. N. p. 260
Briggs, T. H. p. 112
Bumm, H. p. 474
Calvi, G. p. 64
Charlton, M. G. pp. 189, 212
Collins, R. H. p. 27
Cotson, S. p. 266
Cross, S. H. p. 86
Dahlke, W. p. 3
Davis, F. N. p. 377
Ehlbeck, H.-W. p. 5
Elsworth, L. p. 266
Ermrich, W. p. 128
Flecken, F. p. 35
Florescu, N. A. pp. 250, 329
Francken, J. C. p. 22
Fransen, J. J. B. p. 199
Freytag, J. P. p. 40
Fukagawa, S. p. 178
Fukushima, H. p. 92
Garbe, S. pp. 7, 81
Giorgi, T. A. p. 58
Günther, K.-G. p. 293
Habraken, L. p. 412
Haefer, R. A. p. 118
Hannon, L. p. 435
Harper, M. E. p. 444
Harte, A. p. 133
Hashimoto, K. pp. 92, 156
Hawley, R. p. 310
Hetherington, J. S. p. 390 (B.R.)
Hejzlar, J. p. 231
Holland, L. p. 133
Horáček, V. p. 231
Iwanayagi, H. p. 92
Jenkins, R. O. p. 319
Jerič, S. pp. 234, 240
Kansky, E. pp. 234, 240
Kitagawa, K. p. 156
Klopfer, A. pp. 7, 81, 128, 363
Kobayashi, H. p. 153
Korn, O. p. 474
Langlais, J. B. p. 143
Lawson, R. W. p. 100
Levaux, J. p. 435
Malter, L. p. 121
Mandoli, H. p. 121
Mellor, J. D. p. 245
Misra, R. P. p. 188
Nadeau, S. p. 112
Nasini, A. p. 68
Newson, D. p. 189
Ogiermann, G. p. 454
Ohye, D. F. p. 245
Origlio, S. pp. 194, 227
Perdijk, H. J. R. pp. 199, 204
Podgurski, H. H. p. 377
Porta, P. della pp. 181, 194, 215, 223, 227
Pressel, O. p. 141
Reich, G. p. 35
Ricca, F. pp. 68, 215
Robinson, N. W. p. 75
Rubin, L. G. p. 382
Saini, G. p. 68
Schmidt, W. pp. 7, 81, 363
Schuchhardt, G. p. 373
Schütze, H.-J. pp. 3, 5
Schwerdtfeger, P. p. 330
Smith, N. W. W. p. 106
Smith, W. J. p. 444
Sourdillon, J. M. pp. 162, 166
Southam, F. H. p. 212
Takayama, H. p. 153
Tew, J. R. p. 110
Tougarinoff, B. p. 466
Tretner, W. p. 31
Trodden, W. G. p. 319
Turnbull, J. C. p. 27
Vucht, J. H. N. van p. 170
Waal, J. van der p. 22
Warnecke, R. J. p. 49
Whitchurch, P. J. p. 189
Wolsky, S. P. pp. 13, 382
Yarwood, J. p. 268 (B.R.)
Yazawa, K. M. p. 210
Zdanuk, E. J. pp. 13, 382

page

R. N. BLOOMER : On the General Principles of Chemical and Ionic Pumping 260
H. BATEY : Carbon Contamination of Glassware used for Vacuum Purposes 263
Letters to the Editor
S. COTSON : Note on Vacuum and Condensing Temperature Requirements for the Freeze-Drying of Tissue.. 266
L. ELSWORTH : Calibration Factors of Ionization Gauges for Hydrocarbon Gas Mixtures 266
Book Review
" Proceedings of the Fourth National Conference on Tube Techniques " (Reviewed by J. YARWOOD).. .. 268
Vacuum Notes 269
Classified Abstracts 270

Number 4

K.-G. GÜNTHER : Ein Partialdruckvakuummeter nach dem Prinzip des electrischen Massenfilters ; A Partial Pressure Vacuum Gauge working according to the Principle of the Electrical Mass Filter 293
R. HAWLEY : Vacuum as an Insulator 310
R. O. JENKINS and W. G. TRODDEN : Physical Processes in Small Titanium Ion Pumps 319
Letters to the Editor
S. K. BATEMAN : The Formation of Luminescent Films by Evaporation 329
N. A. FLORESCU : Improvement in Operation with McLeod Gauge.. 329
P. SCHWERDTFEGER : A Tetrode Ionization Gauge 330
International Organization for Vacuum Science and Technology : News Bulletin No. 7 333
Classified Abstracts 341

Number 5

A. KLOPFER and W. SCHMIDT : An Omegatron Mass Spectrometer and its Characteristics 363
G. SCHUCHHARDT : Ion Movements in an Omegatron 373
H. H. PODGURSKI and F. N. DAVIS : A Precision McLeod Gage for Volumetric Gas Measurement 377
E. J. ZDANUK, R. BIERIG, L. G. RUBIN and S. P. WOLSKY : An Omegatron Spectrometer, its Characteristics and Application 382
Book Review
" Transactions of the Vacuum Metallurgy Conference, 1959 " (Reviewed by J. S. HETHERINGTON) 390
International Organization for Vacuum Science and Technology : News Bulletin No. 8 391
Classified Abstracts 397

Number 6

One Day Symposium on Vacuum Metallurgy, Brussels, 13 June, 1960

Preface
W. ARMBRUSTER : Le Traitemente sous Vide des Métaux et de l'Acier en particulier 405
L. HABRAKEN : Techniques du Vide et Propriétés des Métaux ; Vacuum Techniques and Metal Properties .. 412
J. LEVAUX et L. HANNON : Coulée sous Vide de l'Acier ; Vacuum Casting of Steel 435
M. E. HARPER and W. J. SMITH : Design Considerations for Vacuum Metallurgical Equipment 444
G. OGIERMANN : Schmelzen im Elektronenstrahlofen ; Melting in the Electron Beam Furnace 454
B. TOUGARINOFF : Quelques Cas d'Application pratique du Vide dans la Métallurgie des Métaux non ferreux ; Some Practical Examples of the Use of Vacuum in Non-ferrous Metallurgy 466
H. BUMM et O. KORN : Application de la Technique du Vide à la Fabrication des Transistors 474

Index to Abstracts—Volume 9.. 482
Index to Abstracts—Volume 10 489

page

SESSION V

Methods Employed in the Evacuation of the Tubes

R. A. HAEFER : On the Use of Metal–Oil Diffusion Pumps when Operating with Discharge Tubes Sensitive to Hydrocarbons 118
L. MALTER and H. MANDOLI : Electron Tube Processing with Getter-Ion Pumps 121
A. KLOPFER and W. ERMRICH : Properties of a Small Titanium-Ion Pump 128
L. HOLLAND and A. HARTE : The Gas Sorption Characteristics of Penning Pumps and Titanium Films 133
O. PRESSEL : Method for Ageing of Electron Valves 141

SESSION VI

The Function of the Getters during the Manufacture and Life of the Tubes

J. B. LANGLAIS : Les Getters du Baryum dans les Tubes Électroniques de Reception 143
E. BIOLLEY : On the Use of Getters in TV Cathode-ray Tubes 151
H. TAKAYAMA and H. KOBAYASHI : Clean-up of Gases in TV Picture Tubes by Barium Getters 153
K. HASHIMOTO and K. KITAGAWA : Some Barium Getter Problems on the Vacuum Tubes 156
J. M. SOURDILLON : Use of Zirconium Sintered Getters 162
J. M. SOURDILLON : Test of Use of Titanium as Getter 166
J. H. V. VAN VUCHT : The Ceto Getter—its Chemical Structure and Hydrogen Gettering Properties 170
S. FUKAGAWA : Gettering Activity of Zr, Ti and Ba for Oxygen Gas under the Mercury Vapour 178

SESSION VII

Techniques for Measuring Getter Activity

P. DELLA PORTA : Apparatus and Techniques for Measurements of the Adsorption of Gases by Evaporated Getters 181
R. P. MISRA : Use of the A.S.T.M. Reference Planar Diode for Studying Getter Properties 188
M. G. CHARLTON, D. NEWSON and P. J. WHITCHURCH : An Automatic Apparatus for the Testing of Getter Adsorption 189

SESSION VIII

Getter Activity on Various Gases and Gas Mixtures. Parameters of Concern

P. DELLA PORTA, S. ORIGLIO and E. ARGANO : The Influence of Ionizing Electron Currents and Hot Filaments on the Gas Adsorption by Barium Films 194
J. J. B. FRANSEN and H. J. R. PERDIJK : The Absorption of Gases by Barium Getter Films Applied as a Tool .. 199
H. J. R. PERDIJK : Structure of Barium Getter Films 204
K. M. YAZAWA : Study of the Surface Structure of Barium Getter Deposited Film by an Electron Microscope .. 210
M. G. CHARLTON and F. H. SOUTHAM : The Adsorption of Methane by Barium Films in the Presence of a Thermionic Current 212
F. RICCA and P. DELLA PORTA : Carbon Monoxide Sorption by Barium Films 215
P. DELLA PORTA and E. ARGANO : Nitrogen Sorption by Barium Films 223
P. DELLA PORTA and S. ORIGLIO : Hydrogen Sorption by Barium Films 227
J. HEJZLAR and V. HORÁČEK : Selective Getters 231

SESSION IX

Various

S. JERIČ and E. KANSKY : A Method for Measuring of Caesium Vapour Pressure in Photoelectric Tubes 234
E. KANSKY and S. JERIČ : Some Results of the Measurement of Caesium Vapour Pressure in Photoelectric Tubes during their Manufacture and Life 240

Number 3

J. D. MELLOR and D. F. OHYE : An Ampoule Freeze-Dryer for Microbiological Research 245
N. A. FLORESCU : The Theoretical Development of the Vapour Vacuum Pump 250

Vol
10
196

VACUUM

The International Journal and Abstracting Service

for

VACUUM SCIENCE AND TECHNOLOGY

Vol.
10
1960

VOLUME 10

(1960)

CLASSIFIED SUBJECT INDEX

PERGAMON PRESS

OXFORD · LONDON · NEW YORK · PARIS

NUMERICAL LIST OF PAPERS PUBLISHED

	page	article
W. DAHLKE and H.-J. SCHÜTZE : Residual Gas Pressure in Electron Tubes. Part I—Method of Measurements	3	1
H.-J. SCHÜTZE and H.-W. EHLBECK : Residual Gas Pressure in Electron Tubes. Part II—Experimental Results	5	2
A. KLOPFER, S. GARBE and W. SCHMIDT : Residual Gases in Vacuum Systems	7	3
S. P. WOLSKY and E. J. ZDANUK : The Investigation of Residual Gases in Vacuum Systems	13	4
J. C. FRANCKEN and J. VAN DER WAAL : Residual Gases in Picture Tubes	22	5
R. H. COLLINS and J. C. TURNBULL : Evolution and Absorption of Gases in Electron Tubes	27	6
W. TRETNER : An Electrostatic Mass Spectroscope	31	7
G. REICH and F. FLECKEN : Analysis of Partial Pressure by Means of Omegatron and Farvitron. Comparative View of the Ranges of Application	35	8
J. P. FREYTAG : Emploi d'une Diode d'Essais comme Moyen de Contrôle des Matériaux de Construction des Tubes Electroniques	40	9
R. J. WARNECKE, Jr. : Emploi du Spectromètre de Masse dans la Technologie des Tubes Electroniques	49	10
F. A. BAKER and T. A. GIORGI : The Applicability of the Omegatron to Continuous Analysis of Residual Gases	58	11
G. CALVI : Double Pirani Bridge Leak Detector	64	12
A. NASINI, F. RICCA and G. SAINI : Clean Surfaces and Sorption of Gases	68	13
N. W. ROBINSON : The Action of Molybdenum, Tungsten, Tantalum and Nickel on Residual Gases in a Vacuum System	75	14
S. GARBE, A. KLOPFER and W. SCHMIDT : Some Reactions of Water in Electron Tubes	81	15
S. H. CROSS : System Design and the Choice of Materials for the " Nimrod " Vacuum System	86	16
K. HASHIMOTO, H. IWANAYAGI and H. FUKUSHIMA : Measurement of Gas Evolution and Absorption from Materials used in Vacuum Tubes	92	17
R. W. LAWSON : The Influence of Residual Gas on the Performance of the British Post Office Submarine Telephone Repeater Valve Type 6P12	100	18
N. W. W. SMITH : Noise Reduction in Microwave Tubes by Getter-Ion Pumping	106	19
J. R. TEW : A Pumping Schedule for a Power Travelling Wave Tube	110	20
T. H. BRIGGS and S. NADEAU : Effects of Continuous Gas Clean-up upon Emission and Cathode Interface Impedance	112	21
R. A. HAEFER : On the Use of Metal–Oil Diffusion Pumps when Operating with Discharge Tubes Sensitive to Hydrocarbons	118	22
L. MALTER and H. MANDOLI : Electron Tube Processing with Getter-Ion Pumps	121	23
A. KLOPFER and W. ERMRICH : Properties of a Small Titanium-Ion Pumps	128	24
L. HOLLAND and A. HARTE : The Gas Sorption Characteristics of Penning Pumps and Titanium Films	133	25
O. PRESSEL : Method for Ageing of Electron Valves	141	26
J. B. LANGLAIS : Les Getters du Baryum dans les Tubes Electroniques de Reception	143	27
E. BIOLLEY : On the Use of Getters in TV Cathode-ray Tubes	151	28
H. TAKAYAMA and H. KOBAYASHI : Clean-up of Gases in TV Picture Tubes by Barium Getters	153	29

Vol. 10 196

	page	article
K. HASHIMOTO and K. KITAGAWA : Some Barium Getter Problems on the Vacuum Tubes	156	30
J. M. SOURDILLON : Use of Zirconium Sintered Getters	162	31
J. M. SOURDILLON : Test of Use of Titanium as Getter	166	32
J. H. V. VAN VUCHT : The Ceto Getter—its Chemical Structure and Hydrogen Gettering Properties	170	33
S. FUKAGAWA : Gettering Activity of Zr, Ti and Ba for Oxygen Gas under the Mercury Vapour	178	34
P. DELLA PORTA : Apparatus and Techniques for Measurements of the Adsorption of Gases by Evaporated Getters	181	35
M. G. CHARLTON, D. NEWSON and P. J. WHITCHURCH : An Automatic Apparatus for the Testing of Getter Adsorption	189	36
P. DELLA PORTA, S. ORIGLIO and E. ARGANO : The Influence of Ionizing Electron Currents and Hot Filaments on the Gas Adsorption by Barium Films	194	37
J. J. B. FRANSEN and H. J. R. PERDIJK : The Absorption of Gases by Barium Getter Films Applied as a Tool	199	38
H. J. R. PERDIJK : Structure of Barium Getter Films	204	39
K. M. YAZAWA : Study of the Surface Structure of Barium Getter Deposited Film by an Electron Microscope	210	40
M. G. CHARLTON and F. H. SOUTHAM : The Adsorption of Methane by Barium Films in the Presence of a Thermionic Current	212	41
F. RICCA and P. DELLA PORTA : Carbon Monoxide Sorption by Barium Films	215	42
P. DELLA PORTA and E. ARGANO : Nitrogen Sorption by Barium Films	223	43
P. DELLA PORTA and S. ORIGLIO : Hydrogen Sorption by Barium Films	227	44
J. HEJZLAR and V. HORÁČEK : Selective Getters	231	45
S. JERIČ and E. KANSKY : A Method for Measuring of Caesium Vapour Pressure in Photoelectric Tubes	234	46
E. KANSKY and S. JERIČ : Some Results of the Measurement of Caesium Vapour Pressure in Photoelectric Tubes during their Manufacture and Life	240	47
J. D. MELLOR and D. F. OHYE : An Ampoule Freeze-Dryer for Microbiological Research	245	48
N. A. FLORESCU : The Theoretical Development of the Vapour Vacuum Pump	250	49
R. N. BLOOMER : On the General Principles of Chemical and Ionic Pumping	260	50
H. BATEY : Carbon Contamination of Glassware used for Vacuum Purposes	263	51
S. COTSON : Note on Vacuum and Condensing Temperature Requirements for the Freeze-Drying of Tissue	266	52
L. ELSWORTH : Calibration Factors of Ionization Gauges for Hydrocarbon Gas Mixtures	266	53
K.-G. GÜNTHER : Ein Partialdruckvakuummeter nach dem Prinzip des electrischen Massenfilters ; A Partial Pressure Vacuum Gauge working according to the Principle of the Electrical Mass Filter	293	54
R. HAWLEY : Vacuum as an Insulator	310	55
R. O. JENKINS and W. G. TRODDEN : Physical Processes in Small Titanium Ion Pumps	319	56
S. K. BATEMAN : The Formation of Luminescent Films by Evaporation	329	57
N. A. FLORESCU : Improvement in Operation with McLeod Gauge	329	58
P. SCHWERDTFEGER : A Tetrode Ionization Gauge	330	59
A. KLOPFER and W. Schmidt : An Omegatron Mass Spectometer and its Characteristics	363	60
G. SCHUCHHARDT : Ion Movements in an Omegatron	373	61
H. H. PODGURSKI and F. N. DAVIS : A Precision McLeod Gage for Volumetric Gas Measurement	377	62

ol.
10
960

	page	article
E. J. ZDANUK, R. BIERIG, L. G. RUBIN and S. P. WOLSKY : An Omegatron Spectrometer, its Characteristics and Application	382	63
W. ARMBRUSTER : Le Traitmente sous Vide des Métaux et de l'Acier en particulier	405	64
L. HABRAKEN : Techniques du Vide et Propriétés des Métaux ; Vacuum Techniques and Metal Properties	412	65
J. LEVAUX et L. HANNON : Coulée sous Vide de l'Acier ; Vacuum Casting of Steel	435	66
M. E. HARPER and W. J. SMITH : Design Considerations for Vacuum Metallurgical Equipment	444	67
G. OGIERMANN : Schmelzen im Elektronenstrahlofen ; Melting in the Electron Beam Furnace	454	68
B. TOUGARINOFF : Quelques Cas d'Application pratique du Vide dans la Métallurgie des Métaux non ferreux ; Some Practical Examples of the Use of Vacuum in Non-ferrous Metallurgy	466	69
H. BUMM et O. KORN : Application de la Technique du Vide à la Fabrication des Transistors	474	70

Classified Subject Index

Volume 10

The numbers refer to the numbers in the Numerical List of Papers Published

Absorption and Adsorption
6, 13, 14, 15, 17, 25, 26, 27, 29, 30, 31, 32, 33, 34, 35, 36, 37, 38, 41, 42, 44, 45, 50, 56

Alloys and Metals
17, 21, 31, 32, 33, 34, 39, 40, 41, 42, 43, 44, 45, 46, 47, 64, 65, 66, 68, 70

Analysis of Gases
4, 5, 6, 8, 10, 11, 54, 60, 63

Biological Technique
48, 52

Coaters and Coating
20, 38, 39, 40, 41, 42, 43, 44, 57

Drying
48

Electrical Engineering
55

Electron Tubes and Electronics
1, 2, 3, 4, 5, 6, 7, 9, 10, 11, 14, 15, 17, 19, 20, 21, 22, 23, 26, 27, 28, 29, 30, 31, 32, 37, 38, 45, 47, 51, 55, 61, 63, 70

Gases
53

Gauges
1, 2, 3, 4, 5, 7, 8, 9, 10, 11, 12, 35, 53, 54, 58, 59, 60, 61, 62, 63

Getters
27, 28, 29, 30, 31, 32, 33, 34, 35, 36, 37, 38, 39, 40, 41, 42, 43, 44, 54

Glass
15

Heating Equipment
67

Ionization of Gases
55

Kinetic Theory
49

Leaks
12

Metallurgy (Vacuum)
64, 65, 66, 67, 68, 69, 70

Outgassing
3, 4, 5, 6, 8, 10, 11, 13, 14, 15, 16, 17, 18, 21, 24, 25, 26

Particle Acceleration
16

Plastics
16

Pressure Measurement
1, 2, 3, 4, 5, 7, 8, 10, 11, 17, 35, 36, 46, 62

Pumping Systems
25, 26, 51, 56, 64, 65

Pumps
19, 22, 23, 25, 26, 27, 37, 49, 50, 56, 67

Radiation
57

Vacuum Systems
16, 22, 35, 67, 68

Valves
36

Vapour Pressure
46, 47

Vol.
10
196

SOCIETÀ ITALIANA DI FISICA
(Italian Society of Physics)
50, Via Saldini, MILAN, Italy

INTERNATIONAL SYMPOSIUM ON RESIDUAL GASES IN ELECTRON TUBES AND RELATED HIGH VACUUM SYSTEMS

TRANSACTIONS

Under the editorial supervision of
PAOLO DELLA PORTA

23rd, 24th and 25th September, 1959
Building of the Amministrazione Provinciale,
COMO, Italy

01.
10
960

Vol.
10
1960

SOCIETÀ ITALIANA DI FISICA
(Italian Society of Physics)
50, Via Saldini, MILAN, Italy

INTERNATIONAL SYMPOSIUM ON RESIDUAL GASES IN ELECTRON TUBES AND RELATED HIGH VACUUM SYSTEMS

Under the Patronage of the
International Organisation for Vacuum Science and Technology, Brussels, Belgium
and the auspices of the
Consiglio Nazionale delle Ricerche, Rome, Italy
and in the program of the
Ente Villa Monastero di Varenna, Como, Italy

ol.
10
960

Held on the
23rd, 24th and 25th September, 1959
in the building of the Amministrazione Provinciale,
80, Via Borgovico, COMO, Italy

Vol.
10
1960

Scientific and Organizing Committee

President

Prof. G. POLVANI,	Chairman : Società Italiana di Fisica, Milan.

Secretaries

Dr. Ing. P. DELLA PORTA,	Managing Director : S.A.E.S. Getters and Edwards Alto Vuoto S.p.A., Milan. Director : Getters Electronics Inc., Niagara Falls, N.Y. (U.S.A.).
Prof. E. GATTI,	Professor : Milan Polytechnic.

Members

Dr. Ing. E. CAMURATI,	Director : Philips S.p.A., Milan.
Prof. A. NASINI,	Professor : University of Turin.
Dr. Ing. U. QUINTAVALLE,	General Manager and Director : F.I.V.R.E., Milan.
Prof. B. RISPOLI,	Professor : Institute of Physics at the University of Rome.
Prof. R. SARTORI,	Director : National Electronic Institute " Galileo Ferraris ", Turin.
Dr. Ing. F. TEDESCHI,	Vice President : Associazione Elettrotecnica Italiana, Milan.
Dr. Ing. B. VALSECCHI,	General Manager and Director : Marconi Italiana S.p.A., Genoa.

ol.
10
960

Vol.
10
1960

VACUUM

Opening Speech*

G. POLVANI
President

THIS Symposium has a short story which I think is worth while telling.

I shall begin by saying that the idea belongs completely to Dr. Paolo della Porta, Managing Director of S.A.E.S. and Edwards Alto Vuoto, who, together with Prof. Nasini, approached me about two years ago and proposed that the Italian Society of Physics should sponsor a Symposium on residual gases in Electron Tubes or, more generally, in high vacuum tubes.

This proposal was presented by me to the Board of Directors of the Society. However, it was not favourably accepted. It was pointed out that, a Symposium of interest mainly to manufacturers, diverged too much from the Symposiums up to then sponsored, in which physicists had been mainly interested. Further, the argument of this proposed Symposium, that is to say technological physics, would have been too far removed from fundamental physics, which had up to then been the subject of our meetings.

As you may see, even our Board, which has a reputation of imagination in producing and developing new ideas, was in this case too conservative, which is a bad sign!

ol.
10
960

Subsequently, discussing the matter further with both Dr. della Porta and the Board, it happened that those reasons which seemed against the sponsoring by the Society of the proposal, changed, and became favourable.

The Board was then convinced that it would be opportune that some of its meetings should turn their attention to problems of non-fundamental physics, and to these meetings not only pure physicists should participate, but also technologists and those manufacturers who would benefit in their production by the most apt solution of their technological problems.

The Board agreed that the proposal put forward by Dr. della Porta offered the best opportunity to break with tradition. Therefore, we must be grateful to him, as indeed we are.

Of course, once things got moving, the Society made up for the lost time, and taking the initiative gave it all the help it could.

The members of the Organizing Committee have collaborated in the execution of the programme. In particular the two Secretaries of the Symposium, that is Prof. Gatti and Dr. della Porta, the latter a dynamic, wise and precious collaborator.

I wish to express the deepest thanks to everyone just mentioned on behalf of the whole Italian Society of Physics, the Board and myself.

Equally we wish to express our gratitude to the various Members of the Honorary Committee, in particular to the Prefect of Como for the importance he attached to the Symposium, equally to Consiglio Nazionale delle Ricerche and to its President, Prof. Giordani, and to the International Organization for Vacuum Science and Technology and to its President, Prof. E. Thomas, for having given it their patronage ; to the Amministrazione Provinciale di Como and to its President, Dr. Rossi, and to Amministrazione Comunale di Como and to the Lord Mayor, Comm. L. Gelpi, for their kind hospitality, to Ente Villa Monastero and to its President, Avv. Bosisio, for having included the Symposium in the activities of the Ente ; to the Ente Provinciale per il Turismo, Como, and to its President, Comm. Russo, for the help given with respect to accommodation.

I want to express my thanks to S.A.E.S. for the help given to the organization of the Symposium and to Pergamon Press Ltd. for the publication of the proceedings.

It is clear that sincere thanks must be given to participants to the Symposium, especially to those presenting papers on their research and study. Without them this Symposium could not take place. Many thanks again for having accepted the invitation of our Society to take part in this Symposium.

My talk could finish here, without touching on scientific or technical questions concerning our meeting. However, I would like to say something quite general on the subject.

*Translation from Italian.

Even though the production of vacuum in a container is a problem more than three centuries old, it is only during the last 70 years that this field has become particularly active.

Then studies were begun concerning the properties of various surfaces under vacuum, and in particular of the complex emission of molecules, atoms and electrons, which occur as a function of temperature, the life history of the surface, external conditions, etc.

In recent years the attainment of high vacuum has been greatly improved by coupling to the usual means offered by mechanical and diffusion pumps which we may term external means, the internal means of chemical processes, and in particular of getters —concerning which it is my pleasure to remind you that among the pioneers in this technique was the Italian Malignani.

The problems become more difficult when from ordinary electron tubes we require a longer, more reliable and extremely stable mode of operation ; three characteristics which appear more and more necessary and must be further emphasized to fulfil the requirements imposed by some applications. The number of these applications increases from day to day and is becoming an essential part of our modern way of life.

The problem of producing a vacuum is therefore associated to the more difficult one of maintaining it.

It is in fact difficult to obtain the highest vacuum, for instance in an ordinary radio tube, if we do not pay the necessary attention to those surfaces which confine the high vacuum, to see that they do not outgas or if so to provide the necessary means for the released gases to be adsorbed. This problem is of particular importance in miniature tubes, due to the high temperatures attained by all their component parts.

Hence, as is easily understood, the problem of construction of such tubes, or more generally of ultra high vacuum tubes possessing the required characteristics, gives rise to an extremely complex technology, both in so far as it must attain an initial high vacuum, and also because the construction materials employed must ensure that this vacuum does not deteriorate.

Problems similar to these, but in a far more general way, are presented by gas filled tubes.

Now that the very full programme of the Symposium is beginning, one can easily be surprised how fundamental problems relating to the subject of our Symposium will give rise to numerous questions, many of them from important physicists and technologists.

I think that this Symposium will, surely without a doubt, be of remarkable importance for the contribution that it will give to our knowledge, due to the arguments and discussions ; but I think also that the continuous development of science and technology will compel, with the progress of time, further meetings of a similar nature.

Therefore this meeting, which is the first of its kind, could be preceded by an adjective which belongs to it, that is to say the FIRST INTERNATIONAL SYMPOSIUM ON RESIDUAL GASES etc., etc., and could fix where and when the second Symposium should take place.

I also think, speaking on a different subject, more peculiar to Italy, that this Symposium could offer the beginning and the incentive to those who in our country deal with the problems of vacuum, to form an Italian Association, or an Italian group, call it as you like, of technologists and vacuum specialists.

With this wish and with the more general one that the work during these three days of proceedings in hospitable Como will be successful, I declare THE FIRST INTERNATIONAL SYMPOSIUM ON RESIDUAL GASES IN ELECTRON TUBES open.

Vol.
10
196

SESSION I

Residual Gases and Final Vacuum

Residual Gas Pressure in Electron Tubes

PART I : METHOD OF MEASUREMENTS

W. DAHLKE and H.-J. SCHÜTZE

Telefunken G.m.b.H., Ulm/Donau, Germany

IN ORDER TO determine the residual gas pressure in an electron tube its electrode system is circuited as ionisation gauge. The positive current

$$I_+ = I_{ion} + I_{st} \tag{1}$$

collected by the ion collector is measured. This current consists of the ion current I_{ion} and a stray current I_{st}. Using Barkhausen's equation, the gas pressure

$$P = \frac{1}{k_g}\frac{I_{ion}}{I_-} \tag{2}$$

is calculated from the ratio of the measured ion current I_{ion} and the electron current I_-. The gas ion constant k_g, being independent of p, is determined by calibration.

Allowing a maximum error of 10 per cent for pressure measurements a lower limit of measurable pressure

$$P_{min} = 10\frac{\Delta I_{ion}}{k_g I_-} \tag{3}$$

is obtained. ΔI_{ion} represents the absolute value of the error of I_{ion} measurement. Equation (3) indicates that a large product of $k_g I_-$ is favourable for low values of P_{min}. The dependence of k_g on the geometry, the circuit and the operating conditions of the tube under test is discussed in

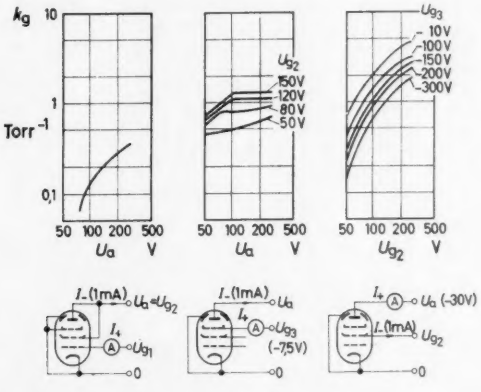

FIG. 1.

Fig. 1. For a pentode it is useful to operate the tube with the plate being ion collector.

The stray current

$$I_{st} = I_+^0 + k_x I_- \tag{4}$$

is represented by a linear function of the electron current I_-. The term I_+^0 can be measured directly. It is identical with the collector current I_+, the electron current being zero. I_+^0 is composed generally of a leakage current, a photoelectric current due to illumination by light and a thermionic emission of the ion collector. The term $k_x I_-$ in equation (4), which is produced by photoelectric emission of the collector due to soft X-rays, is determined by measuring the collector current I_+ at very low pressures. The photoelectric current is strongly dependent on the operating potentials. In a pentode, for instance, it may be suppressed rather perfectly using the plate as ion collector and supplying a suitable negative potential to the 3rd grid, as shown in Fig. 2.

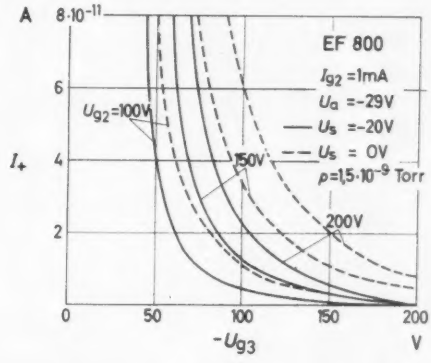

FIG. 2.

Finally, the gas pressure p and the pressure limit P_{min} are obtained by introducing into equations (2) and (3) the ion current

$$I_{ion} = I_+ - I_+^0 - k_x I_- \tag{5}$$

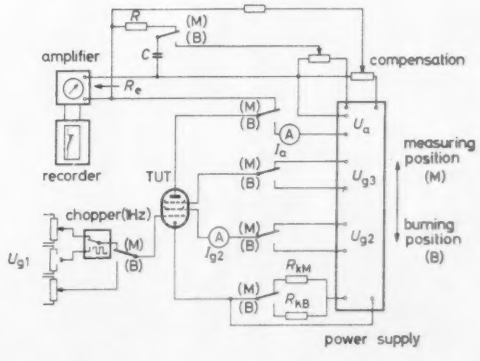

FIG. 3.

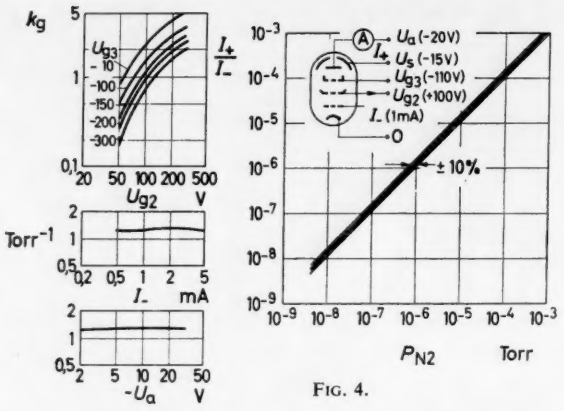

FIG. 4.

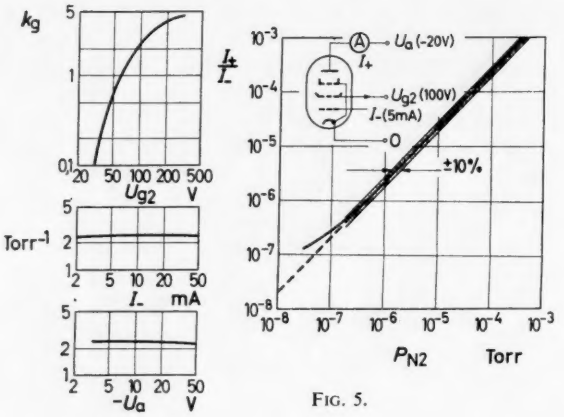

FIG. 5.

as function of measured quantities. A practical pressure measuring-set using the differential method following equation (5) is described in Fig. 3. Results are given for a broad-band pentode, a power pentode and a television

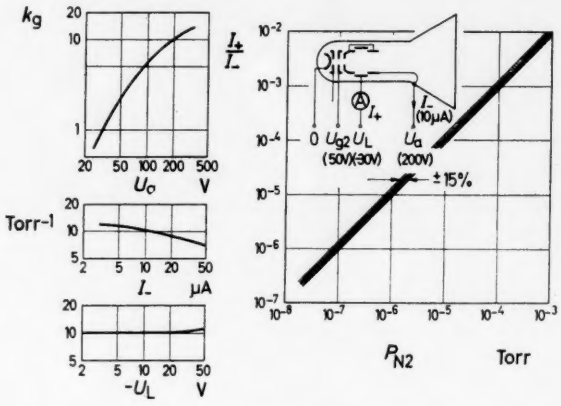

FIG. 6.

picture tube, as shown in Figs. 4, 5 and 6. The corresponding limits of pressure measurements are compiled in the following table :

Tube Type	EF 800	PL 36	AW 53–88
P_{min}/Torr	5.10^{-9}	2.10^{-7}	$<3.10^{-8}$

DISCUSSION

Question from Mr. J. C. Francken

When measuring the gas pressure in picture tubes, a higher value of k_g and a lower value of k_x has been found in the case where the focus lens is used as an ion collector than in the case where the final anode is used as such. How can this be explained ?

Cannot smaller external leakage be expected in the latter case when there is a long leakage path between anode and base ?

Answer. Comparing the two possibilities of using the plate and the focus lens as ion collector, the value of k_g was found to be about a factor of two higher if the lens electrode was used. This result is probably due to the longer ionisation path of the electrons. The low value of k_x can be explained by a screening effect, as the lens electrode is mounted in the shadow of the X-rays.

The leakage of the ion collector, the focus lens or the plate respectively, is effected by the external leakage path as well as by the internal leakage due to the conductivity of the glass mounts for TV-guns. The leakage current was found to be smaller if the lens electrode was used as an ion collector.

Residual Gas Pressure in Electron Tubes

PART II : EXPERIMENTAL RESULTS

H.-J. SCHÜTZE and H.-W. EHLBECK

Telefunken G.m.b.H., Ulm/Donau, Germany

Results of measurement of the residual gas pressure in electron tubes are presented. These results were obtained during the processing and the life-tests of sealed-off tubes. The pressure is determined by using the electrode system of the tube itself as ionisation gauge. For easy observation of the pressure variations the collector current was recorded by an automatic recorder having a sensitivity of 10^{-12} *amperes per scale.*

THE gas pressure during the getter process was studied in receiving pentodes like the EF 800, their lowest measurable gas pressure $P_{min} = 5.10^{-9}$ Torr being remarkably low. Flashing the getter after sealing-off the tube, the residual gas pressure even before flashing was found to be dependent on the type of the getter used, the maximum firing temperature of the getter and its temperature at sealing-off, as shown in Fig. 1. Pressures of 10^{-6} Torr were obtained by using getters with active additives like Th, Ti and Zr as shown in Fig. 1.

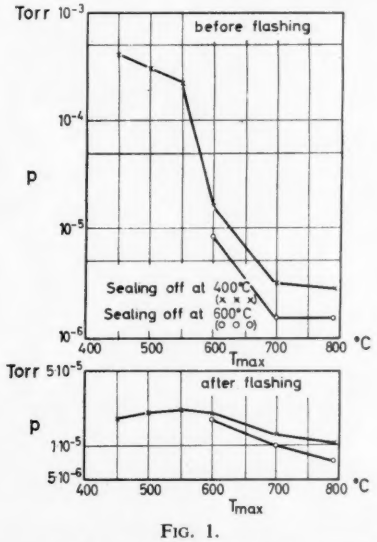

FIG. 1.

The gas pressure before flashing the getter was found to be strongly affected by the stay time of the tubes on the pump, especially if rotary pumps were used, as shown in Fig. 2. The stay time is the difference of time between the last processing step for the getter and sealing-off. In the case of using rotary pumps just a few minutes of stay time were sufficient to increase the pressure by about 2 orders of magnitude. After flashing the Ba-getters with or without active additives in the sealed-off tubes, gas pressures between 8.10^{-6} and 2.10^{-5} Torr were measured independent of the bulb temperature, as shown in Fig. 2.

Flashing the getter before sealing-off the residual gas pressure was affected remarkably by the stay time and by the

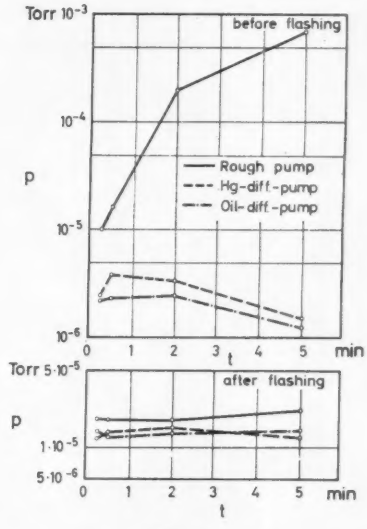

FIG. 2.

type of the pump too. Using oil diffusion pumps, low pressures of $p < 10^{-6}$ Torr were found, as shown in Fig. 3.

The gas pressure remained constant after flashing the getter until the electron current was switched on. Then the pressure was decreased due to electrical clean-up effects. The rate of clean-up was increased if the electron current and the potentials at the electron and ion collectors were raised, as shown in Fig. 4. The pressure in receiving tubes decreased about 2 orders of magnitude during the activation process, as shown in Fig. 5. Pressures between 5.10^{-9} and 10^{-8} Torr were found during life-test experiments, which are represented in Fig. 6. Under standby conditions a gradual increase of 1 to 2 orders of magnitude of the pressure was observed, corresponding to the applied heater voltages.

The residual gas pressure was especially affected by the

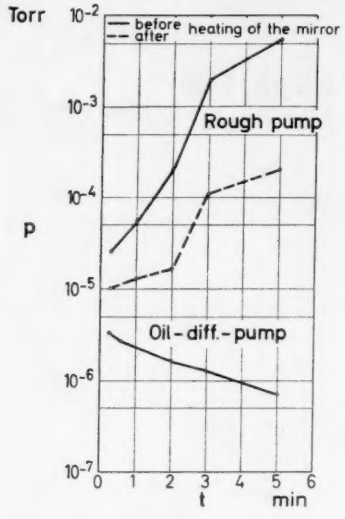

FIG. 3.

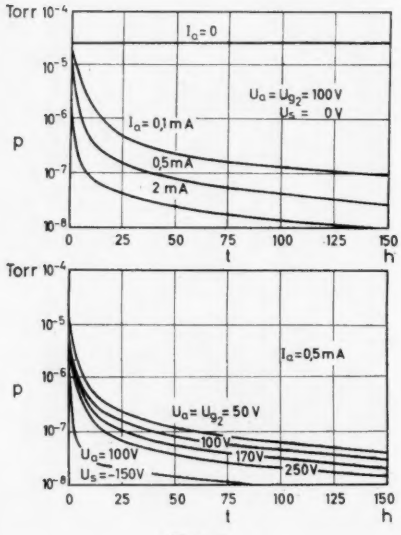

FIG. 4.

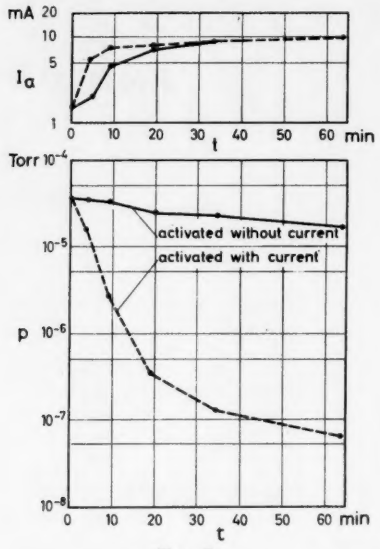

FIG. 5.

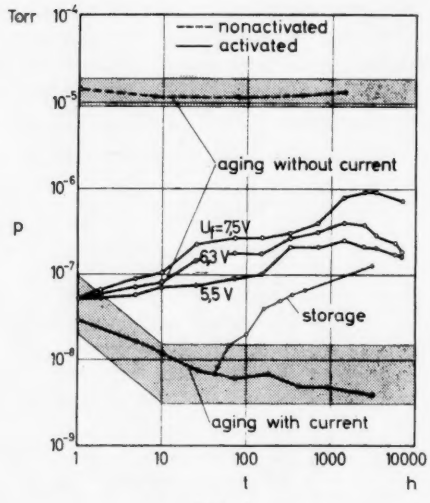

FIG. 6.

dissipated power at the plate of a power pentode or at the screen of a television picture tube. The pressure increased strongly while raising the power load of the electrodes. In the pentode PL 36 and the picture tube AW 53–88 under load, final gas pressures between 10^{-7} and 10^{-6} Torr were measured during life-test experiments.

DISCUSSION

Question from Mr. L. Holland

Have you any idea of the residual gas which is activated by the electron current, e.g. could this contain argon only exhausted by ion-pumping?

Answer. As far as I know there is no method available analysing the gas composition in sealed-off bulbs without using additional means. Therefore I can't give you exact data, but I believe that the amount of argon, present in receiving tubes, must be smaller than the amount of hydrocarbons (which are indicated by von Zanten, Klopfer and Garbe), because the residual gas pressure in sealed-off ionisation gauges, operated under standby conditions, was found also to be about 10^{-5} Torr immediately after flashing the getter, but then decreased within 100 hours about 1.5 orders of magnitude. This effect can hardly be explained by argon-pumping of the filament only.

Question from Mr. L. A. Petermann

You have shown some pressure-rise occurring in a sealed-off tube during shelf storage (up to 5,000 hr). How much of this rise could be due to helium leakage through the glass walls?

Answer. We have not calculated the pressure increase due to the penetration of helium through the glass walls, which in our case were made of soft glass.

Question from Dr. Rohde

What role has the getter during the activation and the life of the tube as regards clean-up?

Answer. The gases towards which the getter shows a considerable sorption capacity during the activation and life of the tube, are undoubtedly gettered even when the gases are not activated by an electric discharge.

The residual gas pressure in the receiving tube 10^{-5} Torr can, however, be reduced only by the activating effect produced by the electric discharge.

Residual Gases in Vacuum Systems

A. KLOPFER, S. GARBE and W. SCHMIDT

Allgemeine Deutsche Philips G.m.b.H., Zentrallaboratorium, Aachen, Germany

Investigations of the gas composition in sealed-off high and ultra-high vacuum systems with the aid of the omegatron have shown that the gas evolution of the materials and interactions between the gases and the surfaces determine the kind of gases which are present. Such interactions are : adsorption, chemical and exchange reactions. The results obtained on radio tubes, TV picture tubes and systems consisting of glass and metal only are given in this paper. It appears possible to classify the composition of residual gases on the basis of the conditions prevailing in the systems in question.

1. Introduction

In this paper a general survey will be given of the gases which are most frequently found in vacuum systems. Further, an effort will be made to explain the origin of these gases. In these respects unambiguous results can only be obtained if the systems under consideration meet the following conditions :

(a) The system may only contain materials which are commonly used in the manufacture of ultra-high vacuum systems and thermionic tubes.
(b) The vapour pressures of the materials used must be negligible at the prevailing temperatures.
(c) The permeation of gases through the walls from the surrounding atmosphere should not contribute to the amount of gas given off by the sealed-off system.
(d) In gettered systems the getter should not exhaust during the lifetime of the system.
(e) The preceding history of the system, i.e. all previous treatments such as degassing and pumping processes, must be fully known.

These conditions have not been chosen at random for the purpose of this paper, but they apply to every high and ultra-high vacuum system and to every thermionic tube.

From the conditions stated above it follows that the subjects of the considerations are :

full-glass systems ;
glass/metal systems ;
electronic tubes, from small radio tubes to TV picture tubes.

2. Evolution of gases in vacuum systems

When a system is disconnected from the vacuum pump after evacuation and degassing, the gases evolving from the materials are mainly responsible for the temporary pressure increase. The gas evolution rate of a given system depends on the pumping process and the applied method of degassing. In principle the following gases evolve from common materials : H_2, H_2O, N_2, CO, O_2 and CO_2, but their amount depends on the materials used as well as on the previous treatments and on impurities. To give some examples : heating of barium getters always leads to release of argon because these getters are prepared in an argon atmosphere ; metals which have been annealed in a forming-gas atmosphere ($H_2 + N_2$) will give off these gases when placed in a vacuum ; the glass walls release large amounts of H_2O and CO_2 during evacuation.

From what has been said so far it seems impossible that a prediction about the composition of the residual gases in a vacuum system can be made ; there are many possible combinations due to the large number of different materials and evolving gases. However, there are some of dominating effects, permitting the vacuum systems to be arranged in a few groups, each with its own predictable residual-gas composition. These dominant effects are the interactions between the surfaces and the gases. Interactions between various gases may be excluded, the mean free path in high vacuum being large with respect to the vessel diameter.

3. The surface-gas reactions

These reactions are dependent on the surface properties, on pressure, temperature, and catalytic influences. A thermodynamic equilibrium may be calculated in very simple cases, but reaction rates can only be studied by experiments.

(1) *Adsorption on cold surfaces*

During pumping and baking large amounts of H_2O and CO_2 are present. On degassing the system these gases react with the hot metal parts of the equipment, thus giving rise to metal oxides and carbides. While the system is cooled down, gases such as H_2, CO and N_2 leave the residual gas rapidly. As the cooling walls constitute a sorption pump for strongly adsorbable gases such as H_2O and CO_2, these gases can be pumped away only partly. Also in systems which are sealed-off before the walls being cooled down, the partial pressures of H_2O and CO_2 drop with decreasing temperature until an equilibrium between sorption and desorption is reached. The magnitude of this equilibrium

pressure depends on the coverage of the surfaces*. Due to exchange reactions between the gases in the adsorbed state mostly H_2O and CO_2 stick to the walls.

Therefore the partial pressure of water will, at low temperatures, not contribute very much to the total pressure in vacuum systems, except in the case of non-degassed and un-gettered ones. The diffusion of H_2O from deep-seated parts of glasses is negligible at room temperature. At higher temperatures, however, the evolution rate of H_2O may be considerable.

As the adsorption of water is accompanied by a considerable H_2 desorption and as oxygen is consumed by chemical reactions, therefore hydrogen, nitrogen and carbon monoxide will be mostly found in vacuum systems without getters.

(2) *Reactions between the gases and the getter*

If a getter is employed in a vacuum system the composition of the gas content is completely different from that found in a system without getter. The partial pressures of chemically active gases are determined by the equilibrium between the gas evolution rate and the gettering rate ; the latter can only be high (some l./sec $\times$ cm^2), if the surface coverage is very low. At increasing gas influx the gettering rate drops.

Measurements with the omegatron have shown that the ultimate partial pressures of CO, CO_2, O_2 and N_2 above an unsaturated getter are very low (see Table I). This indicates

TABLE I

Residual pressures above Ba-film (3.5 *mg*)

Film	Gas	Quantity of gas absorbed in Torr $\times$ 1	Residual pressure in omegatron (Torr)	Remarks
A	CO	1×10^{-3}	1.3×10^{-9}	Film unsaturated
	N_2	5×10^{-4}		
	CO_2	2×10^{-5}	1.6×10^{-9}	
	H_2	1×10^{-5}	2×10^{-10}	
B	CO	1×10^{-2}	5×10^{-9}	Film unsaturated
	CO	3×10^{-2}	4×10^{-9}	Film saturated at 20 °C; remainder removed
	CO	4.5×10^{-1}	1×10^{-8}	Film saturated at 300 °C; remainder removed

The gases listed were applied to film A at the same time; film B was saturated step by step with CO.

that the vapour pressures of reaction products or the equilibrium pressures between gas and solid phase must be very low for these gases. The measurement of such equilibrium pressures by means of a mass spectrometer is very complicated, because there is always a dynamic equilibrium between the gas evolution rate from the measuring system and the gettering rate.

Getter metals such as Ti, Zr and Ta show an equilibrium of solution with hydrogen, depending on temperature and pressure. If very low pressures have to be reached only a very small amount of hydrogen may have been taken up by the getter. Especially when the getter is subjected to large changes in the temperature, as it is the case during the operation of electronic tubes, the partial pressure of hydrogen will vary also.

When water reacts with barium and titanium, hydrogen is evolved. The partial pressure of hydrogen above the getter surface is governed by the water vapour pressure, the degree of saturation of the getter and the temperature. The amounts of hydrogen developed per second at a titanium surface to which water is supplied are given in Table II. The gas evolution at a clean titanium surface at room temperature was found to be unmeasurable.

TABLE II

Hydrogen evolution at a Ti film relative to the H_2O pressure and the temperature

Getter temperature	P_{H_2O} in Torr	Q_{H_2} in Torr $\times$ 1/sec
20 °C	1.2×10^{-7}	1×10^{-10}
200 °C	1.2×10^{-7}	2×10^{-8}
after 1 hour and at raised H_2O pressure:		
200 °C	2.5×10^{-7}	2.5×10^{-7}
20 °C	2.5×10^{-7}	1×10^{-8}

The lowest pressures obtainable with getter layers are still more influenced by reactions which form chemically inactive gases. At unsaturated barium and titanium getters reactions take place between water and the carbon impurities or the carbide-like constituents, giving rise to saturated hydrocarbons such as CH_4, C_2H_6, C_3H_8. As a rule the amounts occur in a ratio of 100 : 15 : 1. At higher temperatures even hydrocarbons with 1 to 5 carbon atoms may be found.

Cl, C and H_2 in the getter material are very unfavourable for the pressures after flashing the getter. The presence of Cl and H_2 leads to the formation of hydrochloric acid ; at the partial pressure of hydrogen prevailing during the getter evaporation, and at the flash temperatures, hydrocarbons are formed. The amount of hydrocarbons formed in this way during getter evaporation can be very much reduced by removal of H_2, i.e. by a thorough degassing of the getter. In the case of a non-degassed getter an amount of about 1×10^{-6} to 1×10^{-5} Torr $\times$ 1 of hydrocarbons was measured, which was formed by 1 mg of evaporated getter material, whereas this production of hydrocarbons could be reduced to about 2×10^{-8} to 1×10^{-7} Torr $\times$ 1/mg by thorough degassing of the getter.

Due to these reactions the residual gas in degassed systems consists almost entirely of hydrocarbons after the getter has been flashed. In the case of non-degassed systems the partial pressure of H_2O will at first predominate, but later only the hydrocarbons determine the pressure. In a system consisting of an omegatron, an ion gauge and a titanium getter, the water pressure had dropped to 2×10^{-8} Torr after two days, whereas the CH_4 pressure could only be kept within the measuring range of the omegatron with the aid

*See S. Garbe, A. Klopfer, and W. Schmidt, ' Reactions of Water in Electron Tubes ' (*International Symposium on Residual Gases in Electron Tubes, etc., Como, Sept.* 1959).

of a hot tungsten cathode. After three weeks the H_2O pressure was only 10^{-9} Torr. The system had not been degassed.

The low CH_4 production in a properly degassed system is shown by the residual-gas spectrum of a simple vacuum system with a barium layer (Fig. 1).

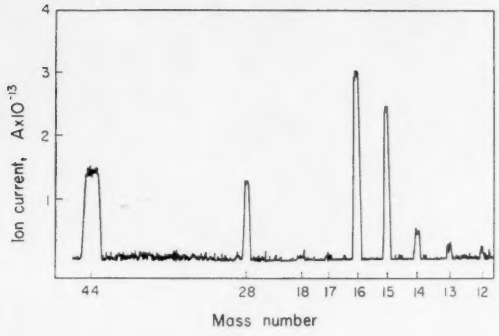

FIG. 1.

(3) *Reactions between gas and cathode*

The processes taking place at hot cathodes are very complicated due to temperature differences, for the temperatures decrease gradually from the operating value at the cathode surface to room temperature at the supports of the cathode. Measurements of the gases evolved by hot cathodes always show the result of the gases liberated by the various parts of the system and the reaction products at the hot surfaces. The gases released by the cathode have been measured many times and they have been mentioned at the beginning of this paper. Special mention should be made of the gas evolution from mica, which, depending on the degree of degassing, gives off mainly H_2O or CO, N_2 and H_2. The evaporation products of the solids such as Ba or W will not be discussed here.

In the following section some simple reactions taking place on the cathode will be considered. Oxygen and carbon dioxide react with the cathode material while forming metal oxides or metal oxides and carbon monoxide. The reaction rate depends on the surface properties, the materials used and the temperature. Similarly the reaction of water with the hot surfaces leads to the formation of oxides and also of hydrogen. The thermal dissociation of H_2O and CO_2 is negligible. However, in the case of hydrogen and hydrocarbons a purely thermal dissociation can be observed. As has been known for a long time, hydrogen dissociates into atomic hydrogen which is very reactive and is either strongly adsorbed on the surfaces or gives rise to other reaction products. Fig. 2 shows the methane decomposition at cathodes of equal surfaces ($\sim$8 mm^2) but of different temperatures. The volume of the reaction vessel was 1 l.

Gases which contain oxygen can react with the carbon impurities of the cathode. In the case of water and carbon the equilibrium is far towards the formation of CO, if the temperature is high enough and the pressure is low. Fig. 3 gives some information, gained by experiment, on the reaction rate of water with a tungsten cathode and a directly-heated oxide cathode. Similar reactions were observed for oxygen-containing gases and thoriated platinum–iridium

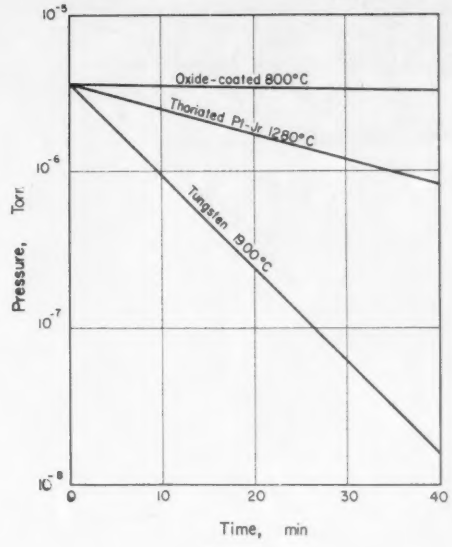

FIG. 2.

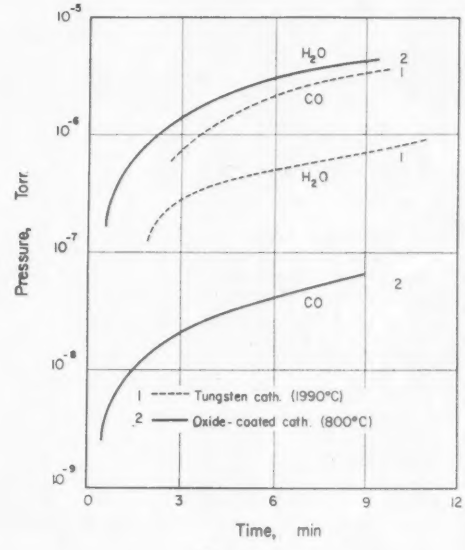

FIG. 3.

cathodes. In general the reaction rate decreases with the operating temperature of the cathode.

At the thoriated Pt–Ir cathode and at the oxide cathode a considerable amount of CO_2 was seen to be formed in addition to CO, when H_2O or O_2 was present. The ratio between the rates at which CO and CO_2 were produced, were strongly influenced by the amount of O_2 or H_2O present. At pressures of about 10^{-6} Torr the amount of CO was of the same order of magnitude as that of CO_2. There must be more than one mechanism for these reactions leading to the formation of carbon oxides. First there is the formation of CO or CO_2, then the carbon dioxide may react further with the hot metals while forming metal oxides and CO and finally there is the reaction

$$C + CO_2 \rightleftharpoons 2CO.$$

The free carbon originating from the dissociation of CH_4

at hot surfaces can reduce metal oxides, thus forming CO. The amount of CO formed and the rate of this reduction depend on the extent to which the metal surfaces are oxidised (see Fig. 4). After a while the CO-production diminishes

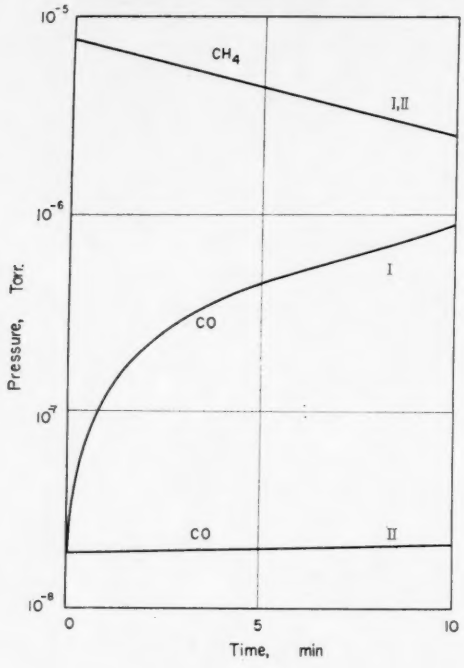

FIG. 4.

as a result of the decrease in the amount of oxygen available (compare curves II and III in Fig. 4). So far the experiments show that the evolution of gases from cathodes is not influenced only by the presence of gases, desorbed from the cathode, but that it is very strongly dependent on the atmosphere in which the cathodes are operating.

In addition to the reactions of the oxygen-containing gases with the carbon impurities, catalysed reactions take place also, giving rise to hydrocarbons. Further, the barium vapour released by the oxide cathode and deposited on the walls may be converted into carbide, and lead to the formation of hydrocarbons.

The observations given so far need some support from measuring results obtained on electronic tubes. Fig. 5 shows the pressure plotted against time, which was measured in an un-gettered type AW 43/80 picture tube with overheated cathode (9 V). In the main, hydrogen and nitrogen are given off by the hot parts of the cathode, while CH_4 is desorbed and also formed. After some time an equilibrium is reached between the pumping action of the cathode and the formation of CH_4. The pressure of the other gases which are given off, such as CO and CO_2, are much lower, viz. a factor of 10 to 100 lower. With normally heated cathodes (6.3 V) the gas formation is about a factor of 5 lower.

After flashing the getter, the residual gas consists almost

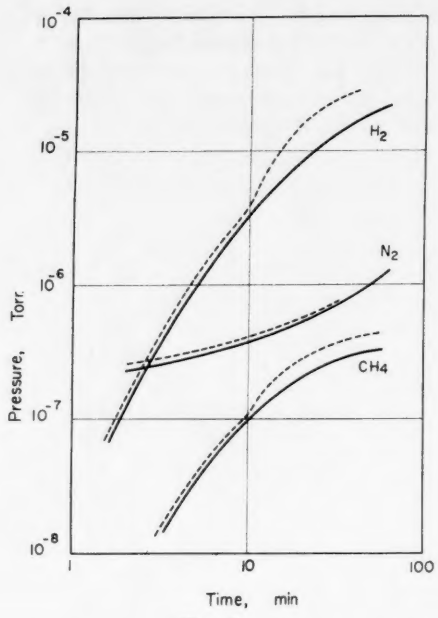

FIG. 5.

exclusively of CH_4 and some of the higher hydrocarbons (and of course also of argon from the barium getter), but the hydrocarbon pressure drops as soon as the cathode is turned on*. The reaction products, hydrogen and carbon, are taken up by the getter film or adsorbed on other surfaces.

(4) *Effects of ion-pumping*

When the gas composition in an electronic tube or in an ion gauge is examined, the purely electrical clean-up must also be considered. The change of pressure in the vacuum system is governed by the pumping speed of the ion pump, the release of gas during the electron bombardment of the electrodes (see Fig. 5) and by exchange reactions on the surfaces collecting the ions. Weakly adsorbed gas particles may be released by other gas molecules or atoms with higher heat of sorption. Ion bombardment will also cause a desorption of gas. So, after some time an equilibrium pressure is reached which depends on the amount of gas pumped away by the ion pump. In the case of small radio tubes, e.g. the type PCC 88, the argon pressure diminishes from about 10^{-5} Torr to some 10^{-7} Torr within the first hours of operation and it remains at that value during its whole life (the measurements were extended up to 10,000 hours). When partial pressures in a TV picture tube were measured during the first 250 operating hours, however, it was found that the argon pressure decreased slowly and continuously from some 10^{-7} Torr at the beginning to about 10^{-9} Torr. The initial pumping speed for argon in the case of the AW 43/80 picture tubes is only 1×10^{-4} l./sec. The electrical pumping speed in gettered electronic tubes is negligible in relation to the other pumping effects, as far as the partial pressures of the chemically active gases are concerned.

Electron bombardment of electrodes not only liberates

*See J. C. Francken and J. van der Waal, 'Residual Gases in Television Picture Tubes' (*International Symposium on Residual Gases in Electron Tubes, etc., Como, Sept. 1959*).

adsorbed gases, but also induces dissociation of chemical compounds on the surfaces. As an example the liberation of oxygen from dissociated metal oxides may be mentioned.

4. Conclusions and examples

Due to the reactions between the gases and the surfaces, the residual gases in vacuum systems are characteristic for the state of conditions of the systems. One such state is, for instance, determined by the temperature of the cathode and the presence of an active getter material. A statement on the prevailing residual gases not based on mass-spectrometric measurements is only unambiguous if the system meets the conditions mentioned at the beginning of this paper and if the reactions are completed for the major part or if an equilibrium has been reached. Table III shows the

TABLE III

Residual-gas schedule at various states in vacuum systems

Temperature of cathode	Without getter	With getter	With getter and ion pump
20 °C	H_2, N_2, CO, CH_4	CH_4, C_2H_6, C_3H_8 (A)	H_2, N_2, CH_4 (A)
900–1200 °C	H_2, N_2, CH_4, CO	H_2, CH_4, N_2 (A), CO	H_2, N_2, CH_4 (A) CO
1500–2000 °C	CO, N_2	CH_4, CO, N_2 (A)	CH_4, CO, N_2 (A)

composition of the main constituents of the residual gases at some typical states of condition of vacuum systems. Column 1 gives the cathode temperature, column 2 the main gases at the respective cathode temperatures, column 3 the gases in the event of a getter material such as barium or titanium being present, while column 4 states the gas composition if also an ion pump is present ; the gas appearing at the highest intensity is underlined. For the other gases the pressure decreases in the order at which they have been entered in the table, when this is read from left to right. The absolute value of the partial pressure cannot be given in the table as it is dependent on the degree of degassing. For un-gassed systems column 2 of Table III does not apply.

The results comprised in the " residual-gas schedule " were checked and confirmed by a large number of gas analyses with the omegatron. An example is the case of the gases in electron tubes with indirectly-heated oxide cathodes. After seal-off these tubes traverse the schedule from left to right. In the un-gettered state hydrogen is the main constituent after completion of the reactions on surfaces. When the cathode is heated and the tube is in full operation the hydrogen pressure rises steeply (Figs. 5 and 6). After the getter has been flashed the gas content changes completely : now hydrocarbons are the main gases ; but there is also argon if the getter material is barium. After the tube has been switched on, the gas composition and the partial pressures again change very rapidly. Methane is removed at a high rate and hydrogen becomes the main constituent, but the hydrogen pressure is much lower than in the un-gettered case (see Figs. 7 and 8). The curves denoted by

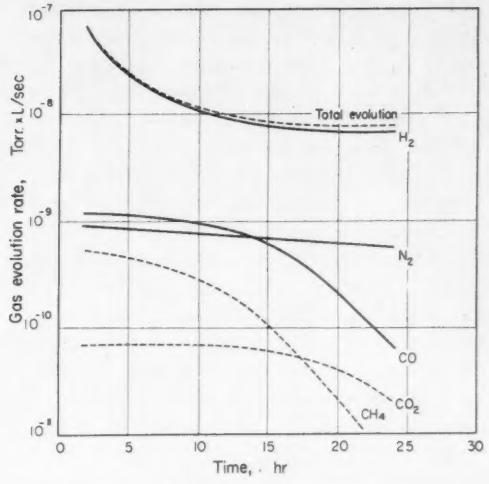

FIG. 6.

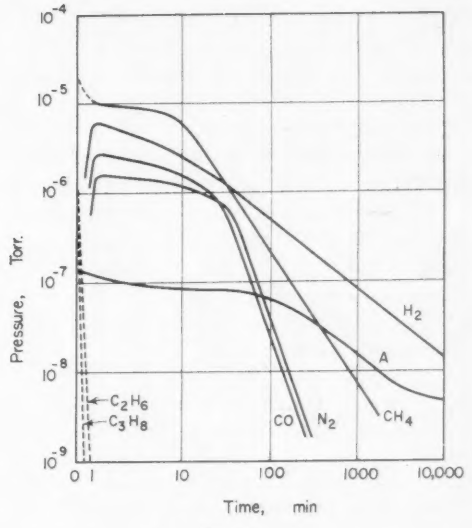

FIG. 7.

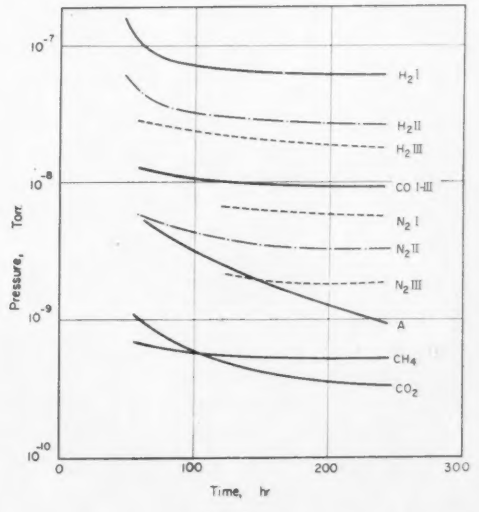

FIG. 8.

I in Fig. 8 are valid when the screen of a type AW 43/80 picture tube is bombarded, the curves denoted by II are valid when only the cathode is operated, while curves III apply to the tubes being out of operation. The residual pressures of the chemically active gases are very low in cold tubes after the getter has been flashed. In part the partial pressures measured with the omegatron are caused by gases evolved by the mass spectrometer itself. The omegatron, with its directly-heated oxide coated cathode (temperature about 700 °C), ranges between the first and the second line of Table III.

When gettered systems are stored after operation a temporary rise in the pressure of the hydrocarbons can be observed in most cases. The magnitude of the rise is determined by the prevailing water pressure and the time during which the tube had operated before it was put in the store (because during that time degassing took place).

When stored radio tubes were switched on a considerable pressure increase occurs. Fig. 9 shows the change in the pressure in a volume which is enlarged by that of the omegatron measuring system (total volume 0.7 l, tube volume 0.01 l). If only the tube is considered, an increase of the pressure of about 2×10^{-3} Torr will be found.

The residual-gas schedule given in this table is also valid for systems without cathode but with parts made of reactive metals which are kept at a high temperature (e.g. evaporating plants). When the surfaces of the hot metals are large with respect to the surface of a cathode in a conventional electronic tube, then the gases mentioned in the table move upwards. For instance, if all electrodes of an electronic tube are heated to 1000 °C, the pumping rate of the hot surfaces for hydrogen

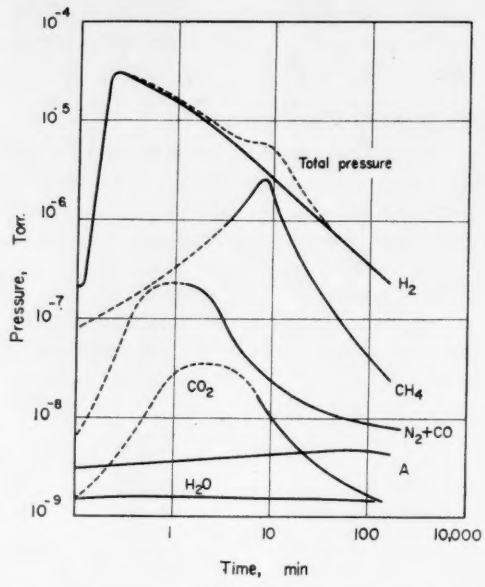

FIG. 9.

will exceed the production of this gas so that mainly gases such as CO and N_2 will be found, i.e. gases that are one line lower in the schedule.

If the conditions stated in the beginning of this paper are known, the residual-gas schedule permits the main residual gases in a system to be deduced from a number of data concerning treatment, temperature, etc. " Getter ion pumps " fully obey the residual-gas schedule.

Vol. 10 1960

DISCUSSION

Questions from Mr. R. P. Misra.—You mentioned about getting better vacuum when the getter is fired before tip-off.

1. How long before tip-off do you fire getter ?
2. How good is the vacuum when the getter is fired before tip-off compared to after tip-off ?

Answers.

1. Ba-getters are fired up to 800 °C for at least 15 min. in order to get the lowest possible CH_4-production.
2. The pressure can be reduced by a factor of 100.

The Investigation of Residual Gases in Vacuum Systems

S. P. WOLSKY and E. J. ZDANUK

Research Division, Raytheon Company, Waltham 54, Massachusetts, U.S.A.

(Received 26 October 1959)

Considerable information has been obtained concerning the origin of residual gases in evacuated systems. The experimental equipment involved in this research includes: (1) *an omegatron mass spectrometer,* (2) *a sensitive quartz microbalance,* (3) *an apparatus for determining the adsorptive properties of getter films, and* (4) *associated vacuum systems. Preliminary data concerning the residual gas content of miniature electron tubes is presented. The application of the omegatron to the study of gases generated during tube processing and lifetime is outlined briefly.*

1. Introduction

The residual gas content of evacuated systems is of considerable importance in certain fields of basic research as well as in the electronic industry. In electron tubes the overall behaviour and life is greatly dependent upon the residual gases in the sealed envelope. In studies of the chemical and electrical properties of clean surfaces, extremely low partial pressures of reactive species are required if reliable and meaningful results are to be obtained. Even an inert residual gas can produce detrimental effects through ionisation, subsequent bombardment of tube components and walls causing sputtering or desorption of other gaseous species. Due to the presence of hot filaments and potentials of varying magnitudes, the particular physical state, i.e. atomic, molecular or ionised, of the residuals and the exact nature of their interaction with tube elements can be quite complex. Consequently, basic information concerning the origin and nature of the ambient impurities in evacuated systems and of their interaction with materials commonly used in tubes is necessary for the better understanding of electron tube behaviour and for the design of reliable long-lived vacuum devices.

The original interest in this laboratory in the residual gas content of vacuum systems arose during our investigation of the adsorptive properties of atomically clean surfaces of semiconductor materials[1–3]. The rigorous experimental requirements involved in the preparation and study of clean surfaces and some anomalies in their behaviour necessitated a consideration of the changes in the composition of the gas in the system during an experiment[4]. The techniques evolved in this work are being applied to the investigation of the ambient in electron tubes and to problems in general vacuum technology. Simultaneously a study of the properties of getter material has been initiated. It is the purpose of this paper to present some preliminary results of our electron tube investigations and also to discuss pertinent information obtained from our surface studies. The experimental techniques will be described fully.

2. Experimental

The apparatus involved in this programme consists essentially of: (1) an omegatron type mass spectrometer, (2) a very sensitive quartz microbalance, (3) a modified Wagener[5] getter system, (4) associated equipment, including vacuum systems employing oil, mercury, ion and cryogenic pumping. The vacuum microbalance itself was not used extensively in the work reported here. Due to its widespread applicability to the study of gas–solid phenomena, its use is planned in many of our future experiments.

A. *The Omegatron*

The need for relatively simple and inexpensive equipment for gas analysis has led to the development of the omegatron spectrometer. The omegatron (Fig. 1), a device operating

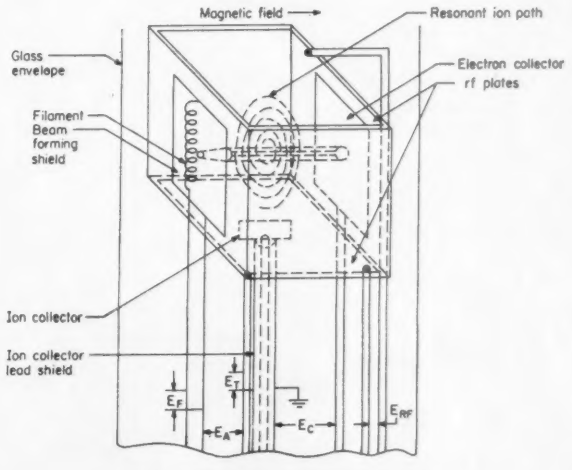

FIG. 1. Diagram of an omegatron.

on a cyclotron resonance principle, may be used to determine the composition of a gas in the pressure range of 10^{-5} to 10^{-10} Torr. In this range, knowledge of the partial pressure of a gas component is more valuable than that of the total

pressure as recorded with an ion gauge. Its reasonable resolution at high sensitivity, the ability to withstand bakeout and its small volume (100–200 cc) make it an extremely convenient and reliable analytical tool for the investigation of residual gases in electron tubes and vacuum systems.

The general characteristics, sensitivity and resolution of the omegatron have been discussed previously by us[6] and by other workers[7–9]. The double rf plate tube used in these studies had a sensitivity of 5×10^{-10} mm with sufficient resolution to separate completely masses 40 and 44. The sensitivity is defined as the pressure of gas yielding an ion current of 10^{-14} A.

As the capabilities of this type of device are becoming more widely known its use in vacuum investigations is increasing sharply. The ability to determine residual gas composition without itself causing any significant perturbation of the system ambient is an advantage which cannot be realised from the conventional mass spectrometer. The economy of having several omegatron tubes on different apparatus but with only one or two portable detection-recorder systems is also of interest to the research worker. The chief limitation of the omegatron is the inverse relationship of the sensitivity and resolution which restricts the effective mass range. In our laboratory we have achieved adequate resolution and sensitivity to mass 100, the highest we have investigated. It is felt that with a double plate or grid-like rf structure the mass range may be substantially increased. Certainly its applicability to the common gases present in the atmosphere has been well established.

Preliminary experiments indicate that the omegatron can provide a convenient means of studying the kinetic energy distribution of ions involved in dissociative ionisation processes. A brief discussion of this application has been presented elsewhere[4].

B. *The Vacuum Microbalance*

The gravimetric vacuum microbalance technique is one of the most powerful experimental tools available for the investigation of gas–solid interface phenomena. The apparatus consists essentially of a very sensitive quartz microbalance operating directly in vacuum and providing a continual record of the experimental process. A schematic representation of the balance is shown in Fig. 2. A detailed description of the design, fabrication and use of such balances has been presented elsewhere[3, 10, 11]. In general, weight changes of 0.15 μg could be detected with a reproducibility of ± 20 to 30 per cent.

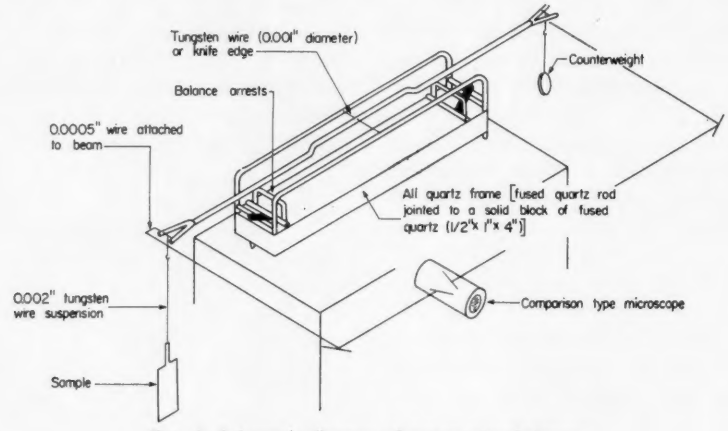
Tungsten wire (0.001" diameter) or knife edge
Counterweight
Balance arrests
0.0005" wire attached to beam
All quartz frame [fused quartz rod jointed to a solid block of fused quartz (1/2"x 1"x 4")]
0.002" tungsten wire suspension
Comparison type microscope
Sample

FIG. 2. Schematic diagram of quartz microbalance.

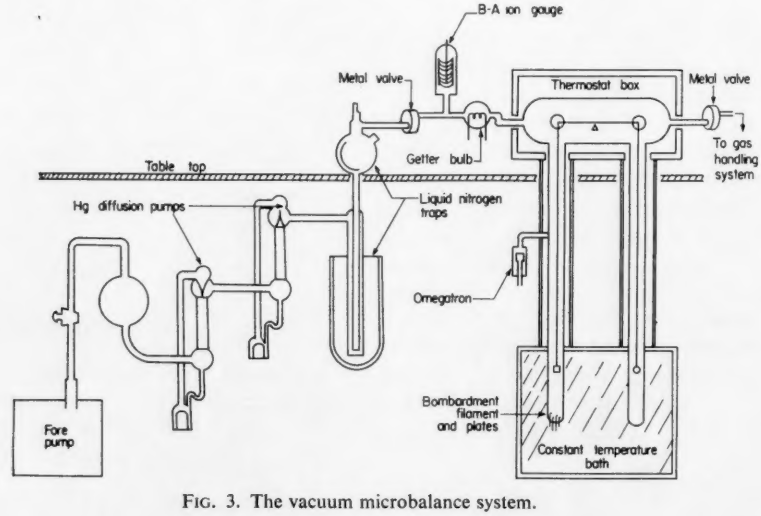

FIG. 3. The vacuum microbalance system.

The vacuum microbalance system is shown in Fig. 3. The all-quartz balance was enclosed in a Pyrex case which was connected through a double liquid nitrogen trap to two mercury diffusion pumps operating in series. After a bakeout of at least 12–24 hr, pressures of 10^{-10} mm are obtained. The bakeout temperature is limited to 200–250°C since the fused silver chloride used to cement the supporting wires to the beam exhibits plastic flow at about 300°C. Short periods of bakeout above this temperature do not appear to be harmful. Titanium and molybdenum getters in the form of small helical wires which could be joule heated are used in some instances to reduce further the partial pressure of reactive impurity gases.

With the sensitive microbalance, it is possible to work with single crystal samples of about 10 cm^2 total surface area. Large-area powdered samples may, of course, also be used. Experiments with single crystal slices allow the measurement of a property as a function of crystal orientation. The details of sample preparation and installation[1, 3, 11] have also been adequately described elsewhere. Of importance to the discussion of this paper is the fact that the sample is heated with a small external resistance heater which fits closely around the balance sample tube. Quartz is used in the sample region so that temperatures up to 1000°C were possible. The system is also designed to allow measurements of the effects of positive ion bombardment on the solid surface. The rates of sputtering of germanium and silicon as a function of ion energy at current densities of 1–10 $\mu a/cm^2$ have already been reported[11]. As will be discussed below, although only the sample has a directly applied potential, the quartz environment also is exposed to the bombardment.

That the vacuum microbalance is an extremely versatile apparatus is evidenced from its use in our laboratory to determine the gas content of samples[12], rates of sputtering[11], vapour pressures, surface areas and the adsorptive properties of materials over a wide range of pressures and temperatures[3]. Its application to the study of similar properties of getter, cathode and other tube materials is obvious. The combination of the microbalance and omegatron as in our present system, provides information concerning simultaneous changes both in the weight of the sample and the composition of its ambient.

C. *Getter Studies Apparatus*

The apparatus for determining the adsorption properties of metal films using the Wagener technique[5] is shown schematically in Fig. 4. The complete apparatus has been designed to withstand high temperature bakeout so that ultimate pressures of 10^{-10} mm can be attained. In addition to a mercury diffusion pump vacuum system similar to that employed with the microbalance, this system is designed to allow oil-diffusion, ion, and cryogenic pumping. The effect upon getter behaviour of the residual ambient characteristic of these pumping techniques may then be tested. It is, of course, desirable to obtain a clean metallic film free of contaminants introduced during the initial heating of the evaporation filament. In order to accomplish this, a filament shielding cap has been added to our system. This cap is moved with an external magnet until it completely covers the filament and is in contact with a small mica shield on the filament leads. The sample is subsequently degassed at a high temperature without deposition of material on the walls of the reaction flask. After completion of the degassing procedure the cap is withdrawn into the extension tube, which may be sealed. Magnetically operated shutters are used to isolate the reaction system during evaporation and to prevent the deposition of any metal film outside the reaction flask. The ion gauges are the usual Alpert type and may be operated at very low emission currents to minimise their effect upon the pressure-measurement. As an alternative procedure we

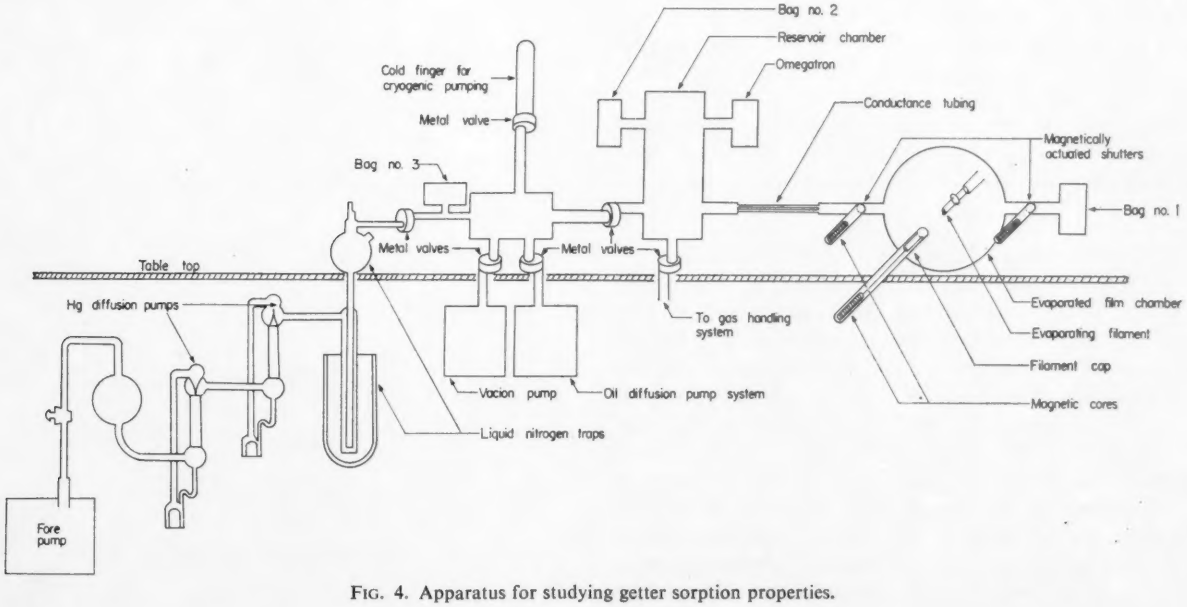

FIG. 4. Apparatus for studying getter sorption properties.

have been investigating the use of ion gauges with lanthanum boride filaments. The obvious advantage is the ability to obtain the desired emission currents at substantially lowered temperatures. The getter apparatus is at present being calibrated and no experimental data has yet been obtained.

D. *Gas Handling System*

The introduction of pure gases into an evacuated system without contamination from the preparation system requires special precautions. In our work the microbalance and getter systems are connected to a gas handling section (Fig. 5) through a metal high-vacuum valve and a series of glass breakoff tips or a ground-glass greaseless valve. In this sealed region, pumped by its own vacuum system (using mercury pumps), gas samples of known pressure are prepared. Stopcocks greased with Apiezon N are present in the system. All glass and metal parts are thoroughly outgassed prior to an experiment. Mass spectrographic grade gases are passed successively through a liquid nitrogen trap, a freshly flashed molybdenum getter bulb and a copper foil liquid nitrogen trap prior to admission to the sample area. The final purity of these gases has been determined with the omegatron and will be discussed below.

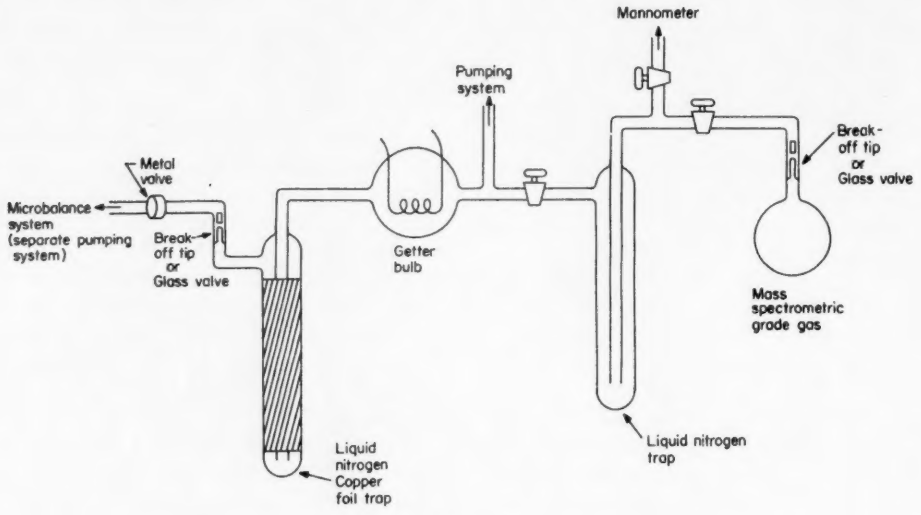

FIG. 5. Gas handling system.

E. *Other Experimental Techniques*

In order to investigate the residual ambient in sealed tubes the simple tube cracking device shown in Fig. 6 (a) is used. The electron tubes are scratched with a file before being placed in the system. After lifting magnet A, the first tube is slid into position by magnet B and broken by dropping A. After the experiment the broken tube is moved away and the second tube slid into position. The apparatus is so designed that the whole system except the small length of tubing containing the sample tubes could be baked out. The experimental set-up (Fig. 6 (b)) is used for studying gases evolved from the heating of flashless getter pellets used in the tube production. The extension arm is heated to outgas it completely and the pellets then slid into the heated region and the change in gas ambient recorded with the omegatron.

3. Results and Discussion

The observed mass spectra are not necessarily indicative of the exact species present in the sample region. The hot tungsten filaments of the ion gauge and omegatron could initiate reactions with the subsequent appearance of masses not due directly to the sample under study. In an attempt to reduce this effect lanthanum boride filaments are being

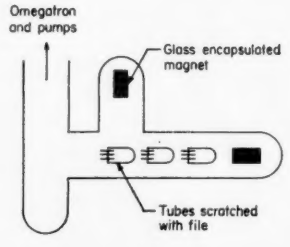

(a)
ELECTRON TUBE AMBIENT APPARATUS

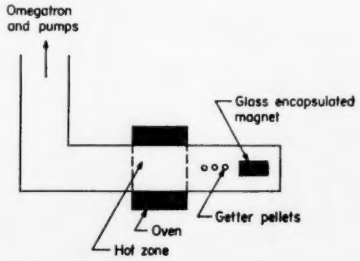

(b)
GETTER MATERIAL HEATING APPARATUS

FIG. 6.

Vol 10 196

studied as the emission source of the omegatron as well as for use in the ion gauges. It has been found that the desired emission current can be obtained from the boride filaments at about half the operating temperature of a tungsten filament.

A. *Origin of Residual Gases*

In the following discussion a number of different sources of ambient impurities in an evacuated system are considered.

1. *The Vacuum System*

The residual gas content of an evacuated system is, of course, influenced by the method employed to obtain the lowered pressure. It is desirable, therefore, to determine the effect of the more common vacuum techniques upon residual gas composition. Figs. 7, 8 and 9 show the ambient composition in : (a) an oil-diffusion pumped apparatus at a total pressure of $p = 6 \times 10^{-7}$ mm, (b) a mercury system at a pressure almost an order of magnitude greater, and (c) the same mercury system with a pressure of 1×10^{-9} mm after 40 to 50 hr of bakeout. The masses in the 44 range in Fig. 7

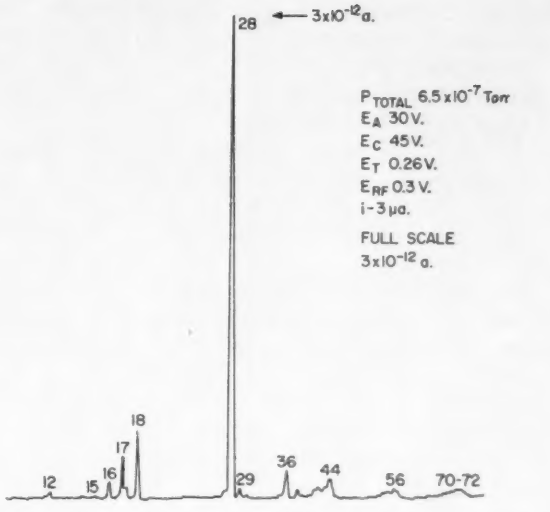

FIG. 7. Mass scan of residual gases of an oil-diffusion pump system.

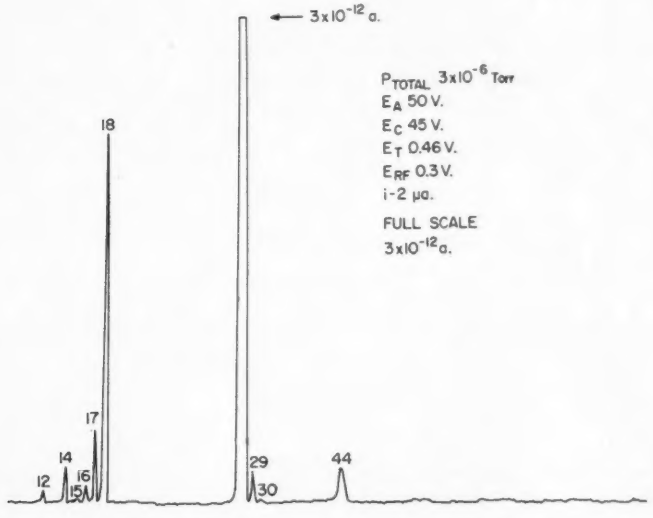

FIG. 8. Mass scan of residual gases of a mercury-diffusion pump system.

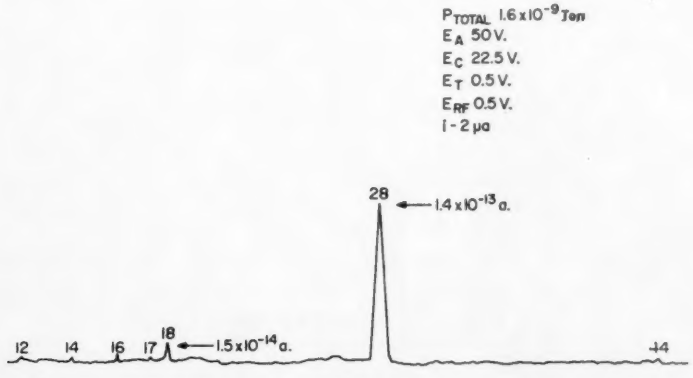

FIG. 9. Mass scan of residual gases of a mercury-diffusion pump system (extensively baked).

are characteristic of the long chain hydrocarbons due to the pump oil. These contaminants were absent in the mercury systems where the chief ambient constituents were CO and H_2O. After extended bakeout of the latter system, the only peak of significance was that at mass 28.

Although ion-pumping is used in our systems no detailed investigation has been made of the residual gas composition. Others[13, 14], however, have reported the ability to obtain systems free of hydrocarbon contamination by such a technique.

The results presented here do not rule out the possibility that a well-baked, carefully trapped (as with copper foil traps) and baffled oil-pumped system could produce a residual ambient free of hydrocarbon contaminants. It can be concluded, however, that special care must be taken at all times to prevent back diffusion of the oil vapours. The most desirable vacuum technique is one free of exposure to any oil even that of the mechanical forepump. Such systems employing cryogenic pumping have been described in the literature[13]. One could expect the residual gas content in such an apparatus to be free of hydrocarbons and to have extremely low partial pressures of reactive gases.

2. *Quartz Tubing*

The possible effect of gases desorbed from the quartz tubing used in the sample region of our vacuum microbalance has led us to examine the adsorption–desorption properties of quartz. This was accomplished by continually monitoring the ambient composition during a typical oxidation experiment which involved the positive ion bombardment (with argon) and heating of a sample. Since the sample had been thoroughly outgassed previously, its contribution to residual gas content in this experiment was limited to the desorption of argon adsorbed during the bombardment process.

Table I is a tabulation of the ambient composition at various stages of the experimental procedure. The analysis in column A was that following ~52 hours of bakeout. Column H records the results at the heating of an empty quartz tube used in many previous microbalance experiments. The empty system was not extensively baked, so that the initial pressure was only 3×10^{-8} mm. Both tubes were washed with de-ionised water and C.P. methylalcohol and dried in a flow of dry N_2 prior to being joined to the microbalance system by a direct glass to glass seal. All pressures were those in a dynamic system. No attempt was made to measure the total gas evolved.

A consideration of Table I leads to the following conclusions :

(1) Ion bombardment did not affect the composition of the residual ambient in the system. Any gases driven from the bombarded surfaces were either adsorbed elsewhere in the system or removed while pumping the argon used in the bombardment procedure.

(2) The major ambient constituents during the heating were masses 18 (H_2O) and 28 (CO/N_2). The only organic species observed was CH_4 (mass 16).

(3) The more copious evolution of gases during the first

Vol. 10 196

TABLE I

	A	B	C	D	E	F	G	H	
	Prior to experiment	After A^+ bombard. 11 min–700v	Sample heating Temp. 25–180 °CC	Sample heating Temp. 350–600 °C	After 1.5 hours at 615 °C	After pumping 15 hours at room temp.	Reheat—after 2 hours at 615 °C	Empty quartz tube initial pressure 3×10^{-8} mm after 30 min 600 °C	Ionic species
Mass no.	*Partial pressure in mm Hg*								
>44	—	—	—	1.6×10^{-9}(74)[a]	1.2×10^{-9}(85)[a]	—	T(85–86)[a]	—	GeO^+, Ge^+
44	T	T	2.2×10^{-9}	5.6×10^{-9}	3.1×10^{-9}	—	6.0×10^{-10}	2.0×10^{-8}	CO_2^+
40	—	2.5×10^{-8}	4.6×10^{-7}	1.2×10^{-6}	1.0×10^{-7}	T	1.8×10^{-8}	5.0×10^{-9}	A_{40}^+
28	3.6×10^{-9}	3.5×10^{-9}	2.9×10^{-8}	2.2×10^{-7}	1.7×10^{-7}	1.9×10^{-9}	1.6×10^{-8}	1.0×10^{-7}	CO^+, N_2^+
18	6.0×10^{-10}	6.0×10^{-10}	7.8×15^9	4.1×10^{-8}	2.2×10^{-8}	T	7.6×10^{-9}	4.0×10^{-7}	A_{36}^{++}, H_2O^+
17[b]	T	T	T	1.1×10^{-8}	5.4×10^{-9}	—	1.6×10^{-9}	3.5×10^{-8}	OH^+
16[c]	T	T	8.4×10^{-9}	1.1×10^{-8}	6.1×10^{-9}	—	8.0×10^{-10}	1.0×10^{-8}	CH_4^+, O^+, O_2^{++}
15[b]	T	T	T	6.7×10^{-9}	3.6×10^{-9}	—	T	N	CH_3^+
14[b]	T	T	T	7.8×10^{-9}	5.4×10^{-9}	—	6.0×10^{-10}	N	N^+, CH_2^+
12[b]	T	T	T	6.8×10^{-9}	3.6×10^{-9}	—	T	3.0×10^{-9}	C^+
2[c]	N	N	N	N	2.0×10^{-9}	N	6.0×10^{-10}	N	H_2^+
Total pressure	5.0×10^{-9}	3.0×10^{-8}	6.0×10^{-7}	1.4×10^{-6}	3.0×10^{-7}	2.1×10^{-9}	4.5×10^{-8}	6.0×10^{-7}	

[a] = Mass number.
[b] = Mass of ions which represent fragments of molecules.
[c] = Mass 16 due predominantly to CH_4.
T = Trace (partial pressure $< 5 \times 10^{-10}$ mm).
N = Not measured.

heating cycle indicates that their origin was one of adsorption and permeability at the surface during cleaning and glass-blowing procedures. The nature of the species observed were typical of those to be expected from the handling process. A disturbance of the quartz surface structure by the ion bombardment with the subsequent desorption of previously trapped dissolved gases could possibly contribute somewhat to the total gas evolved.

(4) The substantial release of argon at low temperatures and its continued presence even in the empty tube which had been cleaned and baked since last being used in a bombardment experiment indicates that a bombarding gas is apparently adsorbed with a wide range of binding energies.

(5) The net effect of changes in the concentration of the ambient constituents caused by heating quartz may be quite complex. The oxidising nature of the water vapour and the reducing action of the carbon monoxide could readily result in an irreproducibility in the behaviour of the system being evaluated.

(6) If adsorption from the atmosphere during handling is the prime source of contaminants, alternate pumping and flushing with a pure, dry inert gas could help to reduce appreciably the undesirable desorption during heating.

3. *Gas Atmosphere*

The need for pure gas atmosphere in many experimental processes is quite widespread. There is, however, always a serious danger of introducing contaminants into an originally high-grade gas during the transfer procedure. We have considered this problem in regard to the gas-handling section

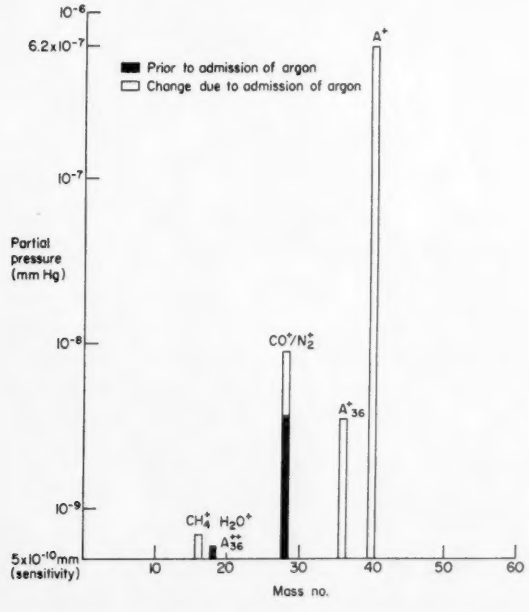

FIG. 10. Composition of argon from gas-handling section.

of the microbalance and getter systems. The experiment consisted of determining the residual gas composition in the microbalance system prior to and after the admission of a sample of argon gas at an arbitrarily chosen pressure of 6×10^{-7} mm. This dynamic pressure was held constant by adjusting the leak rate of the vacuum valves. The results of this study are shown graphically in Fig. 10. The initial pressure in the microbalance apparatus was 5×10^{-9} mm. It can be seen that the changes in ambient composition, represented by the open areas, are extremely small with mass 16, probably CH_4, being the only new impurity. The H_2O content was, if anything, somewhat lowered by the slow flushing process. (In the argon system, A_{36}^{++} also contributes to the total height of the 18 peak.) Most importantly it can be concluded that stopcocks can be used in a properly designed transfer system without introducing any of the higher hydrocarbons characteristic of stopcock greases.

In the above experiment the gas source was of mass spectrographic purity. It was also of interest to determine the impurity content of ordinary tank argon being used to provide an inert atmosphere in a crystal-growing operation. The tank was coupled directly to the apparatus with a copper tube. Rather surprisingly it was found that the tank gas in the controlled atmosphere had an impurity content of the same order of magnitude as that provided by a complex gas purification train using drying columns, deoxo units and traps.

4. *Getter Materials*

An obvious source of residual gas contaminants is the desorption produced during activation of the getter in the electron tube. The nature of the desorption products from the getter depend to a large extent upon the care in preparation and handling. Table II presents the results of an

TABLE II

Mass No.	Prior to Heating	Zr Getter $T = 120$–160 °C
>44	—	2.0×10^{-8}(85)[a]
44	3.5×10^{-8}	4.5×10^{8}
36	—	1.3×10^{-8}
28	2.1×10^{-7}	2.4×10^{-7}
19	—	1.2×10^{-8}
18	2.4×10^{-7}	2.7×10^{-7}
17	4.9×10^{-8}	5.2×10^{-8}
16[b]	6.2×10^{-9}	1.1×10^{-8}
15	—	7.5×10^{-9}
14	3.3×10^{-9}	1.4×10^{-8}
13	—	5.0×10^{-9}
12	4.4×10^{-9}	1.6×10^{-8}
P_{total}	6.0×10^{-7}	8.0×10^{-7}

[a] = Mass number.
[b] = Predominantly methane.
T = Trace (partial pressure $< 5 \times 10^{-10}$ mm).
N = Not measured.

investigation of the gases evolved on heating a zirconium hydride flashless getter. The pressures were those in a dynamic system so that the data can be used only to obtain an idea of the nature and relative magnitudes of the desorbed species. It should also be noted that special procedures such as dry boxes or inert atmospheres were not used in the storage of the sample pellets.

From Table II it is possible to arrive at several very general conclusions.

(1) The hydrocarbons observed probably resulted from oils introduced during the preparation of the getter materials. Special precautions should be taken to remove all oil and other hydrocarbons from the final getter.

(2) The failure of the CO or H_2O peaks to increase indicate either that these species are not readily adsorbed by the getter or that they are not easily desorbed at such low temperatures.

(3) The nature of mass 19 is not known, but it is of interest since it has been observed in the residual ambient of a sealed tube.

Heating of this material at 350–400 °C activated the getter, releasing, as expected, substantial quantities of hydrogen. Information concerning gaseous species present on activation was difficult to obtain since the getter was then actively and rapidly adsorbing from the ambient. The rate and capacity of a getter can be appreciably reduced by reaction with its own desorption products. The outgassing of the getter before activation, therefore, is extremely important. Unfortunately in the production of many tube types the pumping rate is restricted by the constrictions necessary for the eventual sealing-off ; and the overall time on the automatic processing machine is too short to allow complete removal of the large partial pressures of undesirable reactive species.

B. *Residual Gases in Electron Tubes*

The previous discussion was concerned with the origin of the residual gas content of evacuated systems. An analysis was also made of the composition of the gases present in subminiature electron tubes processed identically on an automatic indexing machine at a rate of about one every minute. A comparison was made between the ordinary tube with an activated getter, the same tube without a getter and a completely structureless tube. The gas pressures in the getterless and structureless tubes were estimated to be 10^{-3} to 10^{-5} mm. The composition of the residual gases in these tubes consisted of the usual inorganic species H_2O, CO/N_2 and CO_2. The most significant factor was the absence of any appreciable quantities of hydrocarbon. This indicates that the tubes were not exposed to the oil pumps of the machine long enough to allow diffusion of hydrocarbons into the envelope.

Tubes with getters showed two types of behaviour. In some instances the residual pressure in the tube was so low that no increase in any ambient constituents could be detected. For such tubes obviously a much lower background pressure than that used here is necessary. In other gettered tubes large total pressures were observed, an appreciable portion of which was attributable to an increase in hydrocarbon content of the system. Mass 19 was also observed in the gettered tubes. It is conceivable that this mass is fluoride present as a contamniant in the getter and in some manner occurring as the free fluoride ion in the mass spectrum. It does appear conclusive that the mass 19 is associated with our getter material. In this study it is obvious that the getter material influenced the nature of the residual gases in the tubes to a greater extent than the vacuum technique employed on the machine.

C. *Measurement of Residual Gases During Tube Processing and Operation*

The ideal system for the evaluation of production methods and the investigation of the effect of residual gases on electron tube behaviour involves the simultaneous observation of ambient composition and tube parameters in a sealed tube. If such measurements are to be significant the mass analysing device employed must be one which will not contribute appreciably to the gas content of the tube or interact with electrical or magnetic fields necessary for its proper operation. The omegatron spectrometer appears well suited for an application of this type. In our studies it is planned to include an omegatron as an integral part of one of the larger microwave tubes. The volume and surface area of the mass analyser will be a small fraction of that of the tube itself. Suitable placement of the omegatron will prevent any effect upon normal tube operation. The correlation of tube parameters and ambient composition should establish the relative importance of the different residual gases to tube behaviour.

The addition of an omegatron to a tube also allows the monitoring of residual gases throughout the manufacturing procedure. For small volume tubes a direct application of this type is not feasible. It is possible, however, to use the omegatron for automatic sampling of the residual gases at various stages of production, as, for example, before and after getter activation. The information so obtained is of value to the engineer in correlating production procedures with yield.

4. Conclusion

The detrimental effect of residual gases on electron tube behaviour has encouraged research on new pumping and gettering techniques. The availability of simple mass analysing devices serves to stimulate further the effort on this problem. It is improper to assume, however, that all electron tube problems are directly attributable to the residual gas content. The work in progress will lead to the development of tubes in which residual gas effects are negligible. It will be possible at that time to investigate other basic phenomena pertinent to electron tube behaviour.

Acknowledgement

The authors wish to thank Mrs. P. M. Rodriguez and Mr. R. Chase for their assistance in this work and to acknowledge the co-operation of Mr. F. Barry and others of our Industrial Tube Division. The omegatron tubes were made under the supervision of Mr. T. Driscoll of our Spencer Laboratory.

Vol.
10
196

References

[1] S. P. Wolsky and A. B. Fowler ; *Semiconductor Surface Physics* (University of Pennsylvania Press, Philadelphia, Pennsylvania, 1957), p. 139.

[2] S. P. Wolsky ; *J. Phys. Chem. Solids*, **8**, 771 (1957).

[3] S. P. Wolsky ; *Semiconductor Products*, **2**, 36 (1959).

[4] S. P. Wolsky and E. J. Zdanuk ; *Proceedings of* 1959 *Symposium on Vacuum Technology of the American Vacuum Society*, Philadelphia, Pennsylvania.

[5] S. Wagener ; *Brit. J. Appl. Phys.*, **1**, 225 (1950).

[6] E. J. Zdanuk, R. Bierig, L. G. Rubin, and S. P. Wolsky ; *Report on 19th Annual Conference on Physical Electronics* (M.I.T., Cambridge, Mass., 1959), p. 162. Also submitted for publication elsewhere.

[7] D. Alpert and R. S. Buritz ; *J. Appl. Phys.*, **25**, 202 (1954).

[8] P. A. Redhead ; *Trans. Roy. Soc. Can.*, **47**, 134 (1953).

[9] D. Charles and R. J. Warnecke ; *Le Vide*, **73**, 25 (1958).

[10] T. N. Rhodin ; *Advances in Catalysis* (Academic Press, New York, 1953), vol. v, pp. 40–114. See also E. A. Gulbransen in *Advances in Catalysis* (Academic Press, New York, 1953), vol. v, pp. 120–174.

[11] S. P. Wolsky ; *Phys. Rev.*, **108**, 1131 (1957).

[12] H. A. Papazian and S. P. Wolsky ; *J. Appl. Phys.*, **27**, 1561 (1956).

[13] E. V. Kornelsen ; *Proceedings of the 19th Annual Conference on Physical Electronics* (M.I.T., Cambridge, Mass., 1959).

[14] R. L. Christensen and I. Ames ; *Bull. Am. Phys. Soc.*, Series II, **4**, 139 (1959).

DISCUSSION

Questions from Mr. W. Steckelmacher

Question 1. I am not familiar with your work on quartz microbalance mentioned and would be interested to know of any special precaution to reduce (1) vibration sensitivity ; (2) electrostatic effects. Also, what is the maximum weight of samples which can be handled?

Answer. A detailed discussion of our microbalance technique is available in the following publications:

(a) *Phys. Rev.*, **108**, 1131–1136 (1957).

(b) *Semiconductor Products* (June 1959), pp. 36–41.

We find no need for elaborate precautions to eliminate vibration difficulties. Simple shock mounting of the table and isolation from the walls is adequate for our system. Electrostatic effects are eliminated by means of a ground contact to a conductive film on the balance. The capacity of the balance cited here is 1 gramme. Modification of the beam for greater loads but with decreased sensitivity is possible.

Question 2. A mass spectrum for the residual gases of an oil-pumped system was shown. Could you give details of the oil used and the type of pumps? Has any difference been found for different oils or pumps?

Answer. A single-stage oil diffusion pump (Consolidated Electrodynamics Corp.) with Octoil was used in our work. We have no experience using different pumps or pump oils.

Question from Mr. H. Gutbier

The unknown mass 19 you found in the mass spectrum could be H_3O^+. This ion radical appears always in ion sources in presence of H_2O and H_2.

Answer. The quantity of mass 19 present was much greater than the amount of H_3O^+ to be expected from the concentration of H_2O and H_2. Also, mass 19 was only observed in tubes with the getter, so that some relation between mass 19 and the getter seems apparent.

Residual Gases in Picture Tubes

J. C. FRANCKEN and J. VAN DER WAAL

Philips' Industries, Electronic Tube Division, Cathode-Ray Tube Development Department, Eindhoven, Netherlands

The omegatron, a small mass spectrometer, has been used to analyse the residual gas in television picture tubes.

First the principle of operation of the omegatron is briefly recalled, and a short description of the Philips execution is given. This instrument is mounted in a side arm connected to the bulb of a television tube, together with an ionisation gauge and the whole assembly is pumped simultaneously. Both completed tubes and partly processed bulbs have been prepared in this way.

The residual gas after seal-off has been analysed at different stages of processing, i.e. before and after flashing the getter, after drawing current with the ionisation gauge and during shelf-life.

The gas content after seal-off mainly consists of hydrogen, nitrogen and methane. Generally in the bulb blanks hydrogen is the main gas whereas in completed tubes nitrogen has the higher pressure. In all cases small traces of H_2O, CO *and* CO_2 *have been found.*

All these gases disappear almost completely after the getter has been flashed, but this operation produces an appreciable amount of hydrocarbons and some argon. Drawing current with the ionisation gauge or with the electron gun of a completed tube results in a break-down and a subsequent adsorption of the hydrocarbons. On shelf-life these gases are partly desorbed. Scanning the screens results in a very rapid decrease in pressure of the hydrocarbons.

Introduction

The residual gas content in sealed picture tubes has been examined with the aid of the omegatron, a small mass spectrometer. Early results of these investigations have already been published[1]. More thorough investigations have been carried out since then with the aid of an improved version of the omegatron, developed by A. Klopfer and his co-workers[2].

It may be recalled that the omegatron, invented by Hipple and co-workers[3] is a mass spectrometer analogous to the cyclotron. Ions formed in an electron beam are subjected to electric and magnetic forces due to a crossed high-frequency electric field and a magnetostatic field. A schematic diagram of the omegatron is given in Fig. 1.

The instrument is placed in a magnetic field in such a way that the electron beam is parallel to the lines of force. Ion paths, in general, are elliptical, circular or spiral, with a limited range. Only in cases where the frequency of the electric field approaches the resonance frequency

$$f_r = \frac{e}{2\pi M} B$$

(e = charge of the ion, M = mass of the ion, B = magnetic induction) the ions describe a spiral of uniformly increasing

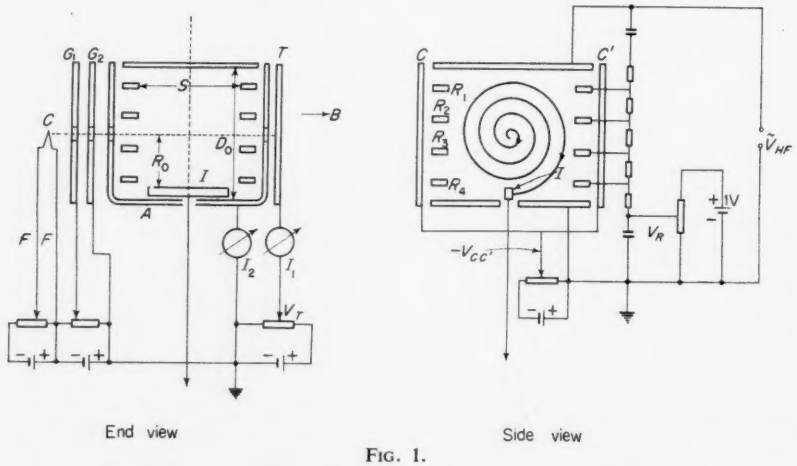

FIG. 1.

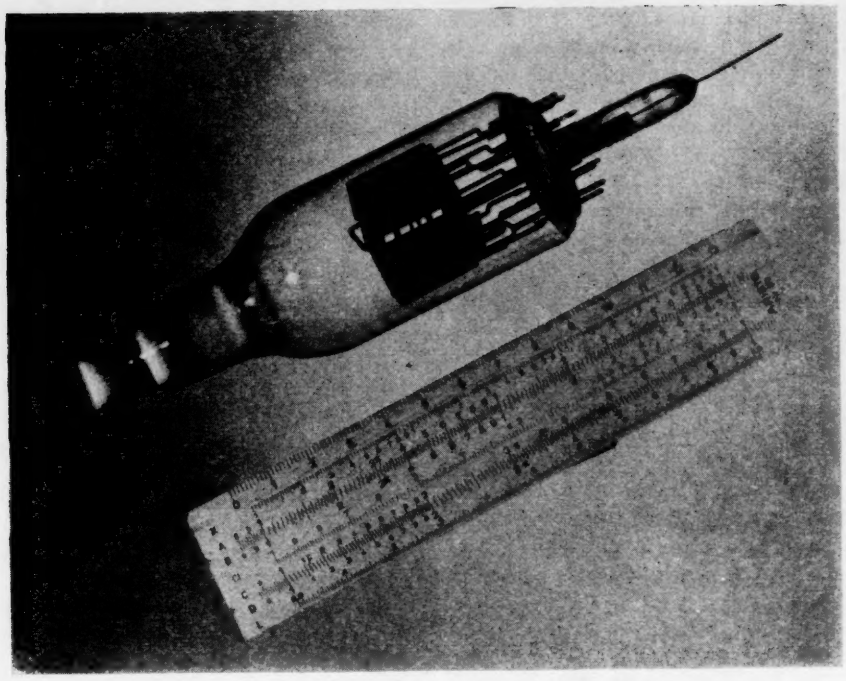

FIG. 2.

ol.
10
960

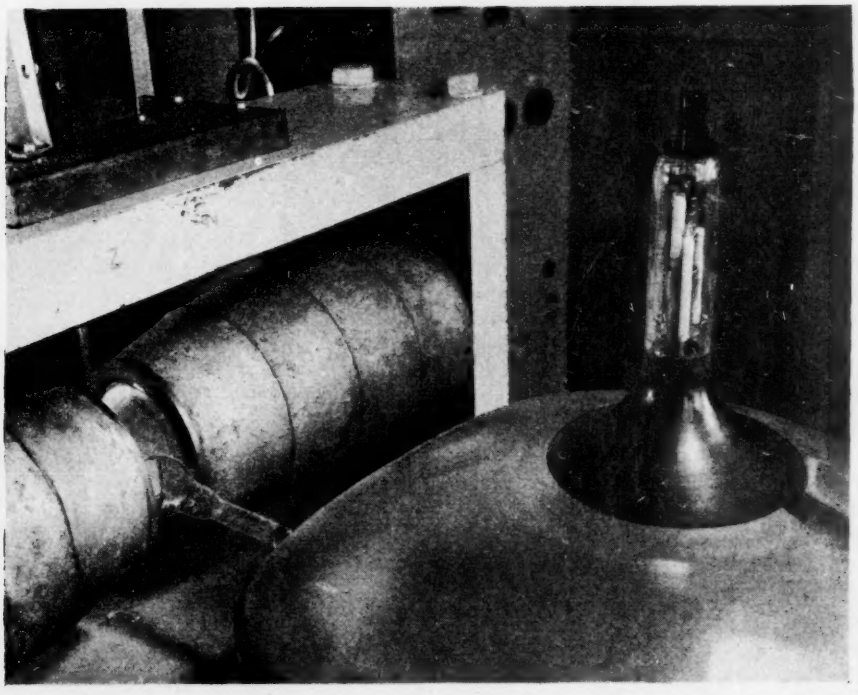

FIG. 3.

radius (Archimedes' spiral) and after making a certain number of revolutions are caught on the ion collector.

By changing the frequency of the electric field continuously a series of current peaks appear in the output of the ion collector which, after amplification, can be registered and measured. The Philips mode of the omegatron differs from previously published ones by having a pair of side plates added to the electrode configuration. As pointed out by Klopfer and co-workers[2], the electrostatic field in the omegatron is improved with these plates and a reproducible sensitivity can be obtained.

The omegatron, owing to its small size (Fig. 2) and high sensitivity, is very appropriate for use with sealed high-vacuum systems. Partial pressures between 10^{-9} and 10^{-5} mm can readily be measured. For pressures above 2.10^{-5} mm, however, qualitive measurements are hard to make. This is due to a loss of ions, resulting in a non-linear behaviour of the instrument.

Analysis of Residual Gases in Sealed Picture Tubes

In order to analyse residual gases in sealed picture tubes, the omegatron is mounted in a side arm connected to the bulb of such a tube (Fig. 3), together with an Alpert type of ionisation gauge.

A first series of measurements has been carried out on bulb blanks, using different types of barium getters. The gas composition was analysed at 6 different stages, i.e. :

(1) 20 hr after seal-off.
(2) After subsequent drawing of current with the ionisation gauge (i = 2.5 mA, t = 15 min.).
(3) After flashing the getter.
(4) After subsequent drawing of current with the ionisation gauge (i = 2.5 mA, t = 15 min.).
(5) After 24 hours' shelf-life.
(6) After 14 days' shelf-life.

In Fig. 4 the gas content of two typical bulbs, using two different makes of barium getter, is given. In the third column a typical case is shown where the barium getter has been degassed on the pump.

It can be seen that, after seal-off, the main residual gases are hydrogen, nitrogen and methane. With getter no. 1 there is also a considerable amount of ethane present. Pumping with the ionisation gauge reduces all pressures but some CO appears in two of the three cases.

This is in agreement with the scheme given by Klopfer and co-workers, since the cathode of the ionisation gauge is at a temperature between 1500° and 2000°C.[4]

After flashing the getter most of these gases disappear, but hydrocarbons and some argon appear instead. In the case where the getter has first been degassed on the pump the pressure of these gases is distinctly lower than in the other cases.

Pumping with the ionisation gauge results in a rapid decrease of pressure of ethane and propane, but methane is pumped at a much lower speed. During shelf-life some methane is usually desorbed. In the case of getter no. 1 some ethane also reappears.

The general composition of the residual gas does not change a great deal when the bulbs are processed and com-

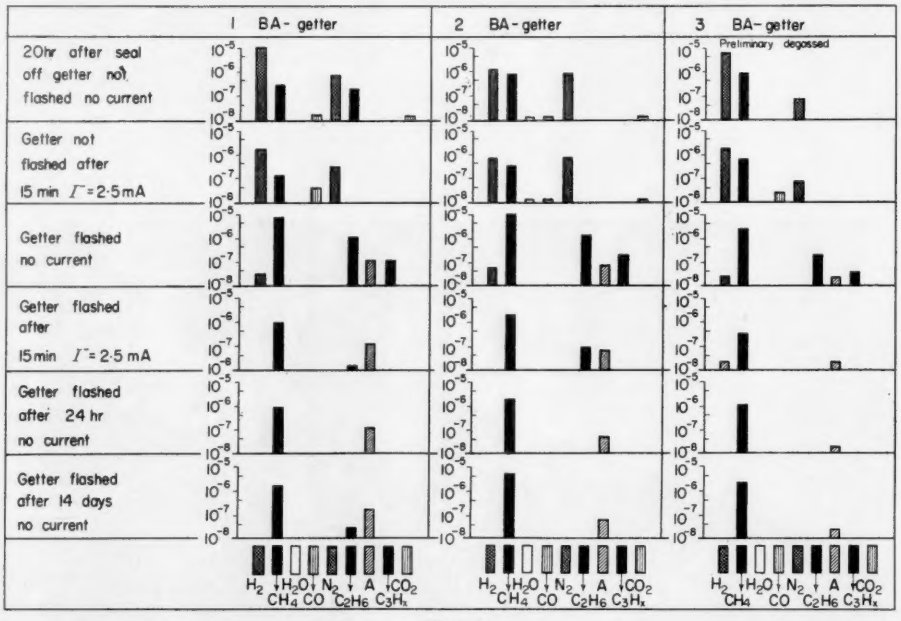
1 BA-getter
2 BA-getter
3 BA-getter
Preliminary degassed
20hr after seal off getter not flashed no current
Getter not flashed after 15 min I⁻=2·5mA
Getter flashed no current
Getter flashed after 15min I⁻=2·5mA
Getter flashed after 24 hr no current
Getter flashed after 14 days no current
H2 H2O CH4 CO N2 C2H6 A CO2 C3Hx

FIG. 4.

plete tubes are made. In Fig. 5 the gas content after seal-off is shown for :

(1) a bulb blank (cf. Fig. 1),
(2) a bulb with a sulphide screen only,
(3) a bulb with a complete, aluminized screen,
(4) a finished tube with completely processed bulb and electron gun.

It can be seen from this figure that, with a screen present, the hydrogen pressure is lower and the nitrogen pressure higher than without a screen. Presumably the screen adsorbs hydrogen and desorbs previously adsorbed nitrogen.

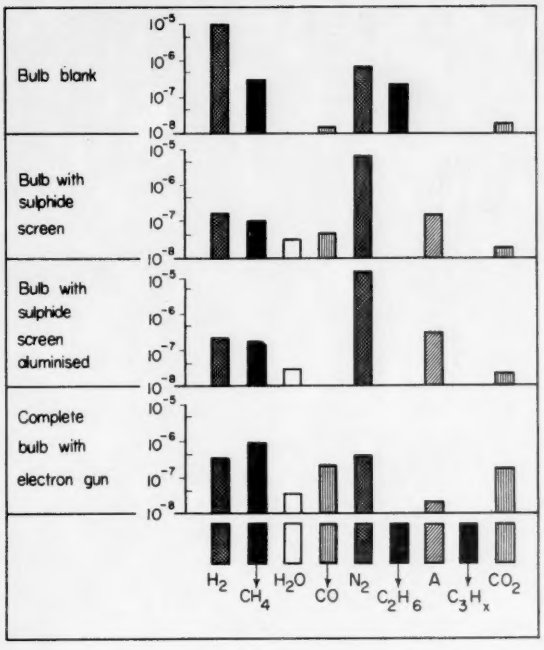

FIG. 5.

In the case where an electron gun is present more CO_2 is found. This gas is set free during the processing of the cathode on the pump prior to seal-off. In all cases the water content is higher than that in the blank.

The gas content after flashing the getter is the same as with bulb blanks : hydrocarbons and some argon are the only residual gases (Fig. 6). However, in the tube on the right

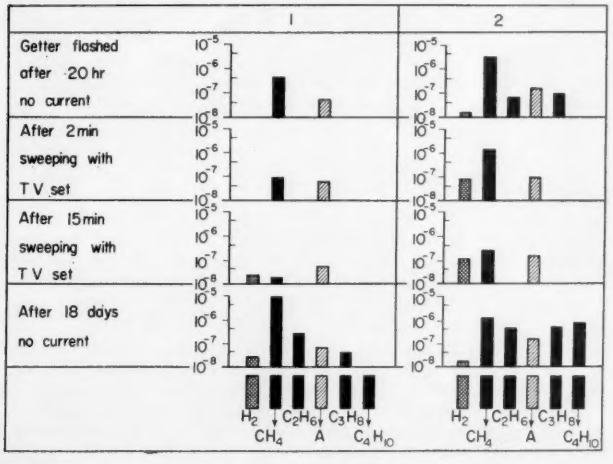

FIG. 6.

of this figure, the hydrocarbon content is greater and also there is an appreciable amount of some higher hydrocarbons.

In these experiments an omegatron only had been connected to the tube, the ionisation gauge having been omitted. A pumping effect could be obtained by sweeping the fluorescent screen with fast electrons (16 kV). It can be seen that hydrocarbons disappear but hydrogen is set free.

On shelf-life the hydrocarbons reappear ; in the case where higher hydrocarbons had been present there is a formation of even higher hydrocarbons. No doubt these gases are reaction products, probably resulting from gas-getter reactions as described by Klopfer[4].

It seems, therefore, that these reactions also take place at room temperature.

Pumping and desorption of hydrocarbons

As already stated, the pressure of residual hydrocarbons can be reduced by pumping with an ionisation gauge. Alternatively the electron gun of the tube can be used as an ion pump (Fig. 7).

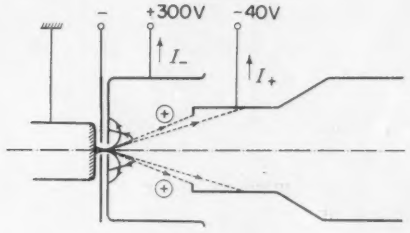

FIG. 7.

As a matter of fact, measuring residual gas pressure in picture tubes with the aid of the gun is common practice. During these measurements pumping occurs just as in the case of " normal " gauges.

In Fig. 8 the pumping effect on hydrocarbons is shown

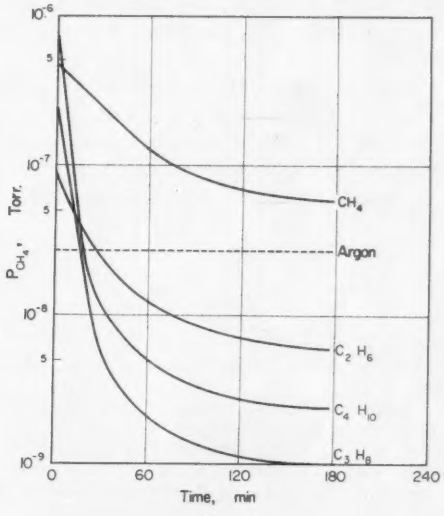

FIG. 8.

for a case where during shelf-life hydrocarbons up to butane had been desorbed and formed. In the beginning the pressure decreases exponentially, as is to be expected, but after $\frac{1}{2}$ hour saturation effects cause a decrease in pumping speed. Pumping can be looked at as a combined result of

(a) ionisation and subsequent adsorption of the ions ;

(b) dissociation at the cathode and other hot surfaces.

Initially the total pumping speed for methane is, in this case, of the order of 0.004 l per sec, using an ionisation

current of 400 μA. The heavier hydrocarbons disappear faster ; for butane the pumping rate is nearly 10 times as great as that for methane.

During shelf-life desorption and production of hydrocarbons lead to an increase in pressure. This is shown in Fig. 9 for methane and butane. The rate of increase is

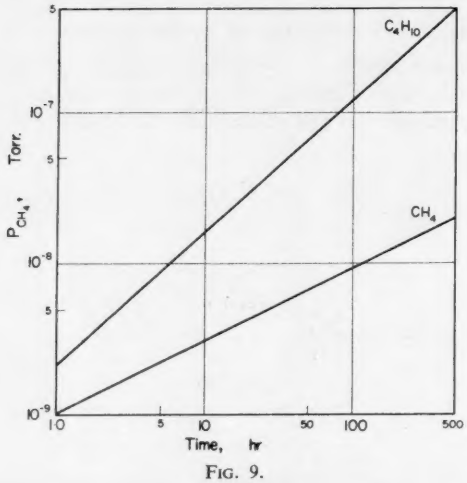

FIG. 9.

much greater for butane than that for methane. Those for ethane and propane are intermediate between these rates. The slope of the desorption curve for methane is about $\frac{1}{2}$. This suggests a diffusion process. The steeper slope for butane and the other hydrocarbons indicate another mechanism.

A much faster pumping of methane occurs when the screen of a picture tube is bombarded with fast electrons. In Fig. 10 results are given of a case where methane had deliberately been fed into a tube without a barium getter. The tube is operated at 16 kV and 200 μA with a raster

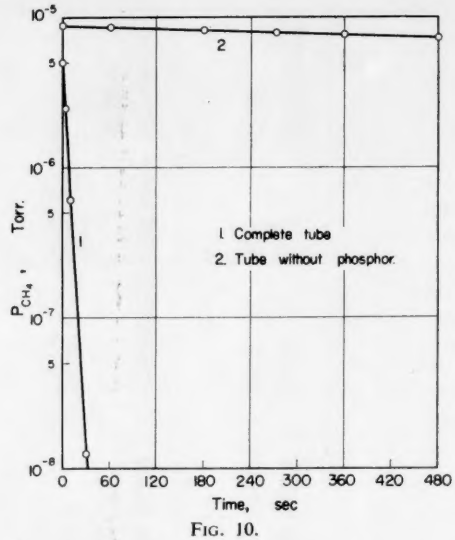

FIG. 10.

of 660 cm^2. The initial pumping speed is of the order of 2 l/sec. In a similar tube without phosphor operated in the same way, methane is pumped at an initial rate of 0.004 l/sec. This is the same as in the case of the ion pump effect described above.

It is not yet clear which mechanism causes the rapid pumping effect of hydrocarbons with screen bombardment.

References

[1] J. Peper ; ' Analysis of the Gaseous Contents of sealed Cathode-ray Tubes with the aid of the Omegatron ' (*Philips Technical Review*, vol. 19, 1957/1958, nos. 7–8, pp. 218–220).

[2] A. Klopfer ; ' Das Omegatron als Partialdruckmesser ' (*First International Congress on Vacuum Techniques, Namur*, 10–13 *June*, 1958).

[3] H. Sommer, H. A. Thomas, and J. A. Hipple ; ' The Measurement of e/M by Cyclotron Resonance ' (*Phys. Review* **82**, 697–702, 1951).

[4] A. Klopfer, S. Garbe, and W. Schmidt ; ' Residual Gases in Vacuum Systems ' (*International Symposium on Residual Gases in Electron Tubes, etc. Como, Sept.* 23–25, 1959).

DISCUSSION

Questions from Mr. F. A. Baker

Question 1. How do you account for the evolution of argon on firing your getters ?

Answer. Argon has evidently been absorbed by the getter, either during manufacture or packing. Even if no argon atmosphere is being used, it is conceivable that the argon originates from the atmosphere (see also Wagener ; *J. Appl. Phys.*, **28**, no. 9, pp. 1107–1013).

Question 2. What types of getters were used, and was argon always evolved ?

Answer. Three different well-known kinds of ring-getters as used in television tubes have been investigated. All these types evolved approximately the same amount of argon.

Question 3. Are partial pressure indications, due to presence of argon, observed at 20 a.m.u. as well as at 40 a.m.u. ?

Answer. Ion currents due to argon are always observed at 20 a.m.u. as well as at 40 a.m.u. The ion current at 20 a.m.u., due to double-charged argon ions, is about 10 per cent of that at 40 a.m.u.

Question from Mr. L. Holland

The high sorption measured for methane exposed to electron bombardment could arise from the formation of an unsaturated molecule which polymerises as a high molecular weight specie, and is condensed on the target on which it is formed. Electron bombardment of hydrocarbon vapours produces polymerised layers which continue to decompose while exposed to bombardment.

Answer. The probability of the formation of an unsaturated molecule by electron impact is far too small to account for the fast pumping of methane.

Evolution and Absorption of Gases in Electron Tubes

R. H. COLLINS and J. C. TURNBULL

Radio Corporation of America, Electron Tube Division, Lancaster, Pa., U.S.A.

Gas-evolution effects in vacuum tubes have been determined by use of the gas-collection method of Morrison, in which evolved gases in an operating tube are collected with a mercury pump, stored in its fore-vacuum system, and measured with a mass spectrometer after many hours of tube operation. The speed of absorption of the tube for various gases has also been determined by simultaneously leaking gases into the tube and using the same collection system, In this way the partial pressures of gases and their internal evolution and absorption rates in the operating tube were found.

These techniques were applied to a practical vacuum tube, the 21CYP22 *colour-television picture tube. Typical partial pressures of gases determined during electrical operation of the tube were : hydrogen,* 10^{-8} *Torr ; nitrogen (including a small fraction of carbon monoxide),* 10^{-9} *Torr ; and oxygen,* 2×10^{-11} *Torr. Oxygen is present only when the tube is scanned, and is evolved by non-metallic bulb surfaces which are bombarded with high-voltage electrons. Self-absorption of the tube for oxygen is very rapid (pumping speed is* 3000 *l./sec). Thus, oxygen partial pressure is maintained at such a low level during operation of this tube that there is no effect on performance of the oxide cathode.*

1. Introduction

Gases in vacuum tubes have long been a subject of interest to tube manufacturers because of the well-known effects of gases on the life of the oxide cathode. This interest has increased in recent years because of continuously increasing requirements for improved life and reliability. The work described in this paper was undertaken to determine the gas atmosphere existing in an electron tube during its normal operation, and over long periods of operating time. The method described by J. Morrison[1] and N. B. Hannay[2] of the Bell Telephone Laboratories was followed and applied to a practical tube made in factory production, the 21CYP22 colour-television picture tube. The results obtained on this tube, which operates at relatively high voltage, are generally applicable to other types of television picture tubes and to oscilloscopes.

2. Measurement of gases in tubes

The apparatus for analysing gases in tubes consists of (1) a gas-collection system for pumping gases from an operating tube and storing them for analysis, and (2) a mass spectrometer for determining quantities and concentrations of gases.

The gas-collection and analysis system is shown schematically in Fig. 1. The tube under test is attached to the vacuum system, which consists of a cold trap cooled with solid carbon dioxide and acetone, whose function is primarily to keep mercury vapour out of the tube, and a mercury diffusion pump. The high-pressure side of the pump contains a 1-litre storage volume and a mercury cutoff. When the mercury cutoff is closed the gases pumped from the tube are accumulated in the storage volume. With the system in this condition the tube may be operated for a number of hours so that a large-sized sample of gas is accumulated.

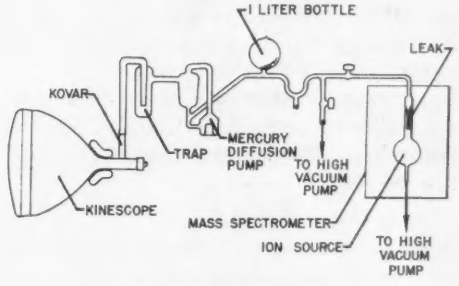

FIG. 1. Gas collection and analysis system.

For analysis of the accumulated sample the mercury cutoff is opened and the gas sample is allowed to expand through a capillary leak* into the mass spectrometer. The gas sample is pumped away slowly through the mass-spectrometer ion source ; during this time, the mass spectrum of the sample is scanned and the peak heights of the various gas components are determined. This gas-analysis system is conventional, and has been described by Inghram[3]. In the present work, the Model 21–610 and Model 21–620 mass spectrometers, supplied by the Consolidated Electrodynamics Corporation, have been used.

The gas-analysis system is calibrated by admitting a known quantity of a pure gas into the 1-litre storage volume, and

*This molecular-flow leak consists of a piece of precision-bore capillary tubing having a diameter of 0.040 in., a length of 4 in. and a conductance (for gas of molecular weight 28) of about 0.001 l./sec.

then determining the mass spectrum for this calibration quantity of gas by the same procedures described above for an unknown sample. The patterns of the individual gases are then used for calculating the composition of the unknown sample. Sensitivity of the equipment for the common gases is such that one litre-micron produces an ion current of about 10^{-12}A at the main ion peak.

The vacuum tube to be tested should preferably be a standard factory-made tube, exhausted and in good operating condition. The tube is attached to the vacuum-collection system without letting air into it by the method shown in Fig. 2. First, a hole, $\frac{1}{4}$ in. in diameter, is partially drilled through the tube neck by an ultrasonic impact grinder*, using a thin-wall tubular tool. A side tube of Kovar is then cemented to the tube by means of an epoxy cement†, and the hole is broken through the neck of the tube by impact with a magnetically controlled rod. The side tube is, of course, exhausted and properly outgassed before the hole is broken through.

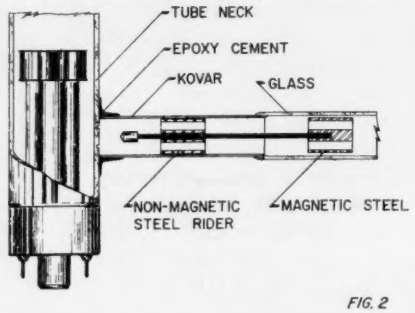

FIG. 2. Vacuum connection to kinescope neck.

The results obtained when the above procedure was applied to a standard television picture tube are given in Table I, which shows the rate of collection of gases observed when the tube was operated with high-voltage scanning (20-kV, 1-mA screen current) at various bulb temperatures. These data were obtained on a tube in which the getters were not flashed.

TABLE I

Gases from a kinescope with no getter flash

Operating conditions	Rate of collection of gases (litre-microns per hour)		
	H	CO + N_2‡	O_2
30 °C ambient temperature	0 to 0.05	0.003	0.0002
60 °C ambient temperature	0 to 0.05	0.008	0.0006
125 °C ambient temperature	0 to 0.05	0.040	0.0070

The data shown in Table I were taken over a period of tube operation of 16 hours, after the tube had been " broken in " by operation for a similar length of time. As indicated in the table, hydrogen occurs in variable amounts in the tube, and generally increases as the tube is operated over long periods of time. The levels of nitrogen, carbon monoxide and oxygen are more reproducible, and these gases increase as the bulb temperature is raised. Carbon dioxide, which is not shown in the table, is observed in some tubes at the higher bulb temperature of 125 °C, but is not seen at the lower bulb temperatures.

Gas background of the mass-analysis system is determined before the mercury cutoff is opened for the sample analysis. At this point the analysis system is being pumped at a slow rate through the mass-spectrometer ion source and the capillary leak, as shown in Fig. 1. A typical background analysis shows small peaks at mass 28 (carbon monoxide and nitrogen) and at mass 18 (water vapour). This background gas originates partly in the glass system attached to the spectrometer, which contains grease stopcocks, and partly in the spectrometer itself.

Gas background of the collection system, evaluated similarly by operation of the system for a period of time before the hole is broken through the neck of the tube, shows a higher peak at mass 28 with additional peaks at mass 30 (possibly nitric oxide) and at mass 44 (carbon dioxide). These gases originate mostly in the collection pump itself ; in order to minimise the pump background it must be well cleaned and filled with clean mercury. The outgassing of the system should be around 0.001 lμ/hr of mass 28, with substantially smaller amounts at masses 30 and 44. This gas background corresponds to an interference in the determination of partial pressures of gases in tubes, which is of the order of 10^{-9} Torr at mass 28, is substantially less at masses 30 and 44, and at other peaks (32, for example) is substantially less than 10^{-10} Torr.

This interference due to gas background is the chief factor which limits the usefulness of the storage method for determining very small outgassing rates in tubes. It is interesting to note that no change in background results from the presence of the epoxy cement used for attaching the tube to the vacuum system ; the same interference is found in systems which contain the epoxy cement as in all-glass systems which do not contain this material.

3. Partial pressure of gases in tubes

When an electron tube is operated various gas components are released by some surfaces and absorbed by others. Equilibrium partial pressures are thus established after a warm-up period when the absorption and desorption rates have become equal. For a tube operated on the pumping system, the quantity Q of a gas which is collected and stored in a time T is given by

$$Q = S \times p \times T, \qquad (1)$$

where S is the pumping speed of the system and p is the partial pressure of the gas in the tube. Q, the quantity determined from the peak heights in the mass spectrum,

* Raytheon Model 2–332 ultrasonic impact grinder.

† Stycast †2651 cement made by Emerson & Cuming, Inc.

‡ The sum of nitrogen and carbon monoxide (M/e = 28) is determined ; however, nitrogen is the predominant gas with not more than 10 per cent carbon monoxide present.

Vol. 10 196

is thus related to the partial pressure of the gas in the tube operated on the system.

In order to determine partial pressures by this method it is necessary to find the pumping speed S of the system. This speed is determined from equation (1) by measuring the pressure increase caused by the introduction of a gas at a constant rate into the high-vacuum side of the system. A constant small flow of a gas is admitted into the system through a capillary glass leak, while the corresponding increase in pressure is measured with an ion gauge. Argon gas is used to minimise pumping effects of the ion gauge. Fig. 3 shows how this method is used to measure the pumping

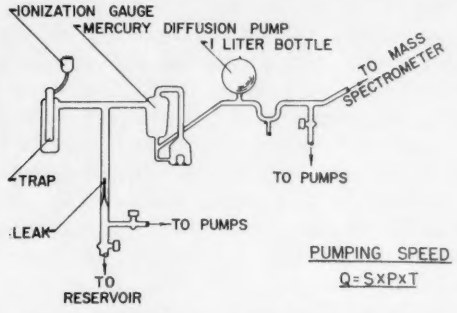

FIG. 3. System for measuring pumping speed.

speed of a pump with a cold trap attached. Table II shows values of pumping speed determined for a mercury pump

TABLE II

Pumping speed of a mercury pump and cold trap, Measured with Argon Gas

Leak rate into high vacuum side of pump	Pressure change in high-vacuum side	Pumping speed through cold trap
lmm/sec	Torr	l./sec
1.0×10^{-7}	1.1×10^{-7}	0.91
6.2×10^{-8}	7.5×10^{-8}	0.83
2.4×10^{-8}	2.9×10^{-8}	0.83
9.1×10^{-9}	1.1×10^{-8}	0.83
2.8×10^{-9}	3.0×10^{-9}	0.94

and cold trap, and for various values of leak rate and pressure. A satisfactory constant pumping speed is found over a wide range of low pressures for the collection system.

For the work described in this paper, the pumping speed of the system including the connection to the picture tube was 0.3 l./sec, measured for gases of molecular weight 28 (nitrogen). For this system, a collection rate of 1 lμ/hr would thus correspond to a partial pressure in the tube of 1×10^{-6} Torr. When this relation was used, and corrections were made for the effect of molecular weight of the various gases on pumping speeds, the partial pressures shown in Table III were found from Table I for the television picture tube under operating conditions.

TABLE III

Partial Pressure of Gases in a Colour Tube, Operated with Unflashed Getters

Operating conditions	Partial pressures of gases (Torr)		
	H	$N_2 + CO$	O_2
30 °C ambient temperature	0 to 1×10^{-8}	3×10^{-9}	2×10^{-10}
60 °C ambient temperature	0 to 1×10^{-8}	8×10^{-9}	6×10^{-10}
125 °C ambient temperature	0 to 1×10^{-8}	4×10^{-8}	7×10^{-9}

The figures in Table III show that the total pressure in the normally operated television picture tube, without flashed getters, and with the normal receiver ambient temperature of 40 °C, is about 10^{-8} Torr. Most of this pressure is accounted for by hydrogen.

4. Absorption and evolution of oxygen in the operating tube

Absorption. Absorption speed for oxygen was measured by providing a picture tube with two independent vacuum connections, as shown schematically in Fig. 4. These

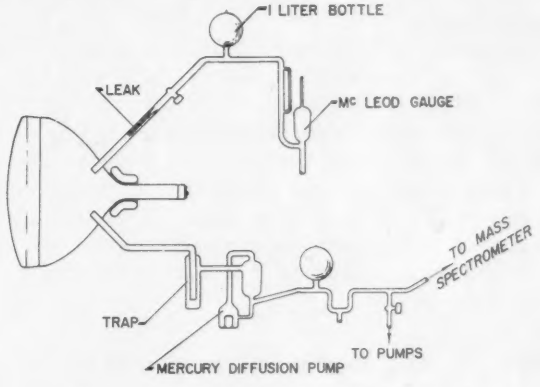

FIG. 4. System for measuring absorption speed.

connections were made to the funnel by means of tubulations inserted just above the neck, and breakseals were added consisting of glass bubbles which could be broken magnetically. These breakseal connections, of course, had to be applied to a specially made tube before it was processed through exhaust.

Absorption speed for oxygen, in a tube with unflashed getters, was then determined by leaking oxygen in through one connection at a known rate while the tube was operating. The other connection was used simultaneously to pump out gases for analysis. Absorption determined in this way occurred at a very high rate. As an example, if oxygen is leaked into the tube at a rate of 10 lμ/hr, the collection system pumps away only 0.001 lμ/hr ; that is, only 1 part in 10,000 of oxygen admitted to the tube is recovered by the mercury pumping system. This result indicates that the tube is pumping oxygen at a rate about 10,000 times faster than the speed of the vacuum pump. Since the latter was determined to have a speed of 0.3 l./sec, the absorption speed of the tube for oxygen admitted into the funnel is 3000 l./sec.

The graphite-silicate coating applied as a conductive layer to the large-area funnel of the television picture tube was

found to be mainly responsible for this rapid oxygen absorption. In this tube, the area of the coating is 3000 cm^2 ; the absorption speed of the coating is thus about 1 l./sec/cm^2. Absorption speed of the coating varies considerably with its composition.

Evolution. When the television picture tube is operated with no oxygen leaking into it, a small collection rate of oxygen of 0.0002 lμ/hr is found. The magnitude of the internal source of oxygen was determined by leaking oxygen into the operating tube at a rate which would double the measured amount of oxygen being pumped away. The oxygen admitted could then be assumed to be equal to the oxygen given off within the tube during operation. It was found in this way that the picture tube operating normally has an internal source of oxygen with a magnitude of 2 lμ/hr.

Evolution of oxygen has been found to occur during the electron bombardment of graphite-silicate coatings. Glass surfaces show a similar behaviour. These effects have been studied by Dr. B. J. Todd and his associates at the Corning Glass Works, and were the subject of a paper given on 21 May, 1959, at the ASTM Conference on Mass Spectrometry at Los Angeles.

In the present work the oxygen source is considered to be the conductive graphite-silicate coating itself, with minor contributions from glass surfaces not covered with this material. It is thought that the oxygen is evolved by these surfaces mainly due to bombardment by high-energy secondary electrons which are back-scattered from the directly scanned areas in the face of the tube. However, further work remains to be done on the oxygen effects, both absorption and evolution, in order to develop an understanding of the processes involved.

5. Effects of oxygen on emission and tube life

As stated above, a source of oxygen of considerable magnitude (2 lμ/hr) was found to be associated with operation and scanning of the television picture tube. Partial pressure of oxygen in tubes with unflashed getters was found to be reasonably low (2×10^{-10} Torr) due to rapid absorption of oxygen within the tube. It was found that flashing the barium getter in the neck of the tube further reduced oxygen partial pressure at the cathode by a factor of about 10 ; thus in the finished tube oxygen pressure is close to 10^{-11} Torr.

The cathode of a television picture tube, however, may be poisoned by exposure to small quantities of oxygen. Thus, if the absorptive processes were to become saturated through long operation of the tube, the cathode might be threatened with dangerously high partial pressures of oxygen. This possibility was examined by testing tubes for oxygen partial pressure after they were operated for extended times. No increase in oxygen partial pressure during extended operation has been found. It has thus been concluded, from these results and related work, that the small oxygen pressures in the television picture tube do not represent a practical limitation on the life of the tube.

6. Conclusions

The accumulation method of analysing gases in electron tubes during their operation was found to give satisfactory measurements on factory-made tubes. The method gives information on partial pressures of gases and on the internal evolution rates and absorption speeds of the tube for gases.

In the colour-television picture tubes, the predominant gas was found to be hydrogen, especially after long operation of the tube. During scanning of the tube, smaller quantities of nitrogen, carbon monoxide and oxygen were found. Oxygen was found to exist at sufficiently low partial pressure so that it does not affect the life of the tube.

A strong temperature dependence of oxygen partial pressure was found ; in general, increasing the bulb temperature by 30°C causes a threefold increase in oxygen pressure. Thus, in other tube types subjected to bulb bombardment oxygen poisoning of the cathode might be present, particularly if the tubes have high bulb temperatures.

7. Acknowledgement

The writers wish to acknowledge the aid received in discussion with Dr. B. J. Todd and Dr. John Sheldon, Corning Glass Works, as well as with Dr. L. Nergaard and Dr. R. Honig, Radio Corporation of America. Advice received from Mr. J. Morrison, Bell Telephone Laboratories, Inc., was particularly appreciated.

References

[1] J. Morrison ; *Trans. Vac. Symposium* (Pergamon Press, 1957).
[2] N. B. Hannay ; *CEC Recordings* **4** (No. 3), 9 (1950).
[3] M. G. Inghram, " Modern Mass Spectroscopy ", *Advances in Electronics*, vol. i, pp. 234–237 (Academic Press, Inc., 1948).

Vol. 10 196

SESSION II

Methods of Measuring Residual Gases during the Manufacture and Life of Tubes

An Electrostatic Mass Spectroscope

WERNER TRETNER

Fernseh G.m.b.H., Darmstadt, Germany

During the last few years, several methods have been known to analyse the residual gas of high vacuum devices by means of small mass spectrometer tubes. In these tubes which have a resolving power of about 20 or 30, the principle of mass separation by different times of flight is employed. Unfortunately, at pressure below 10^{-6} Torr, the signal currents generated by these tubes are so small that for the registration of the whole mass spectrum a comparably long time is required. In order to avoid this drawback a new mass spectrometer tube has been developed. Due to the high signal-output of this tube the whole mass spectrum, ranging from H^+ up to Hg^+, can be displayed on an oscilloscope at 50 Hz. Therefore, a practically continuous control of the residual gas can be achieved.

The signal of the mass spectrometer tube is generated by a cloud of charged particles of equal relative masses which oscillates along the axis of an electrostatic field with axial symmetry. This ion cloud consists of numerous superposed elementary clouds each of which being created by an electron beam in a strong accelerating field near one end of the tube. An electrode on the other end of the tube is used to pick up the displacement-current induced by the ion cloud. The ionizing electron beam is intensity-modulated with a variable frequency. Therefore, an ion cloud is built up only when the variable modulation frequency of the beam coincides with the oscillation frequency of any sort of ions. At frequencies other than those of the ions present in the residual gas, the elementary ion clouds cannot form one big cloud because practically no phase relation between them exists. The space-charge action of the elementary clouds explains that the functional dependence between mass intensity and partial pressure is not linear. A special tube having a resolving power $m/\Delta m \approx 20$ at all masses, is described which can be used at pressures below 5×10^{-5} Torr. This upper limit is set by the mean free path of the ions. The lower limit depends on the shot noise of the first amplifier stage. Thus, at a registration speed of 50 Hz, partial pressures in the order of 10^{-8} Torr can be detected. At still lower pressures a second operation method should be adopted which even permits the use of an electron multiplier.

ol.
10
960

DURING the last few years the measurement of partial pressures of the residual gas has been one of the aims of development in the technique of high vacuum. The scientific approach to this problem is based on the use of the well known mass spectrometer types. These devices have a high resolving power and a very good sensitivity. In the spectrogrammes of such devices the spectral lines of isotopes may easily be separated and coordinated to mass numbers. Even the Fein-Struktur may be investigated. On the other hand, considering the technical applications of high vacuum, such as the manufacture of vacuum tubes, the problems are set quite otherwise. Here, high resolution is not absolutely necessary because in most cases it is known what sorts of vapours and gases can be expected in the residual gas. In the first place one wants to know approximately the quantity of each gas. These informations should be given immediately. Furthermore, to meet the requirements of mass production, the spectrometer tube should be easy to outgas, and the control unit should be as compact as possible. Thus, resolving power and sensitivity may be neglected in favour of speed and simplicity of operation. Speed and simplicity of operation, these are the predominant features of the tube to be discussed now, the features mostly desired for technical work.

In order to give an introduction to the operation principle of the new tube, it seems favourable to proceed from the well known Omegatron. This tube is based on the principle of the Cyclotron and, therefore, requires a magnetic field. Unfortunately, even at the simplified Omegatron which is quite often used in the technique of high vacuum, this magnetic field has to be generated by a comparatively ponderous permanent magnet. Thus, a large scale application of the simplified Omegatron in the production of vacuum tubes presents some difficulties. For technical applications there is still another drawback which the Omegatron has in common with some other mass spectrometers. This is the relatively long time required to record the whole mass spectrum.

In view of these difficulties, when designing the new tube, we tried to avoid the use of a magnetic field by application of an electrostatic field. For this purpose, we replaced the almost circular motion of the ions in the Omegatron by

approximately linear oscillations in an electrostatic field. This principle shall be explained schematically in Fig. 1. The ion source is represented by an electron gun, the beam of which effects the ionization of the residual gas near one of the electrodes. For simplicity let us first consider only one sort of ions, for instance mercury ions. These ions,

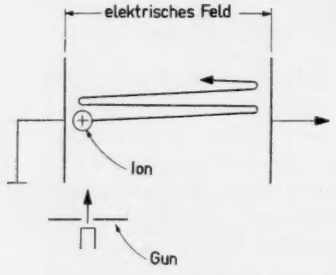

FIG. 1. The principle of the spectrometer tube.

one of which is represented in Fig. 1 near the electrode on the left hand side, are forced by an inhomogeneous electrostatic field to oscillate between the two plain electrodes. It is this periodic motion which replaces the circular motion of the ions in the Omegatron. If now, an electrical field is superimposed which alternates at the same frequency as the mercury ions oscillate, these ions may gain momentum and, therefore, may reach one of the field confining electrodes. This kind of operation is analogous to the operation of the Omegatron.

There is another mode of operation which is more practicable for technical applications than the Omegatron-like operation just described. Due to this mode of operation our tube will have an outstanding high output signal, naturally at the expense of resolution. It is this extremely high output signal which finally allows a high speed recording of the whole mass spectrum.

Considering again Fig. 1, let us suppose that not only mercury vapour is present in the residual gas but also some other gases. Then, we are able to select one sort of ions by modulating the ionizing electron beam with the same frequency as this sort of ions oscillates. During the first cycle, for instance, n ions may be generated. These move to and fro. During the second cycle n ions more are created, taking part on the discharge. Thus, at the beginning of each cycle, an elementary cloud of n ions joins the family of ions. Finally a big cloud of ions is formed consisting of numerous elementary clouds which are separated by phase differences of 2π. This cloud of charged particles of equal relative masses generates an output signal by inducing displacement currents to the confining electrodes. All ions with oscillation frequencies other than that applied to the control grid of the tube cannot form an ion cloud because the phase differences of their elementary clouds differ from 2π or a multiple of it.

The high frequency signal can be amplified without the difficulties encountered at dc-amplification. Furthermore, in order to measure all mass intensities practically at the same time, the modulation frequency of the ionizing electron beam may be sweeped periodically at mains frequency to cover the frequency band containing the oscillation frequencies of all masses to be investigated, for instance from mass 1 up to mass 300. The whole spectrum, therefore, may be recorded at 50 c.p.s.

Before going into details, let us first have a look on the configuration of the electrodes of an experimental tube. In Fig. 2 we see a cage consisting of several electrodes. The

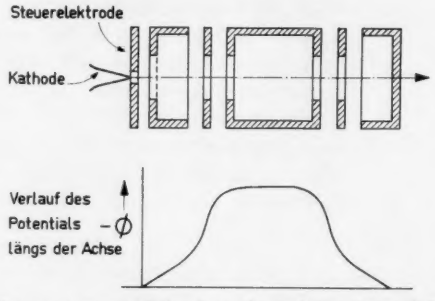

FIG. 2. The arrangement of the electrodes and the shape of the electric potential ϕ along the axis.

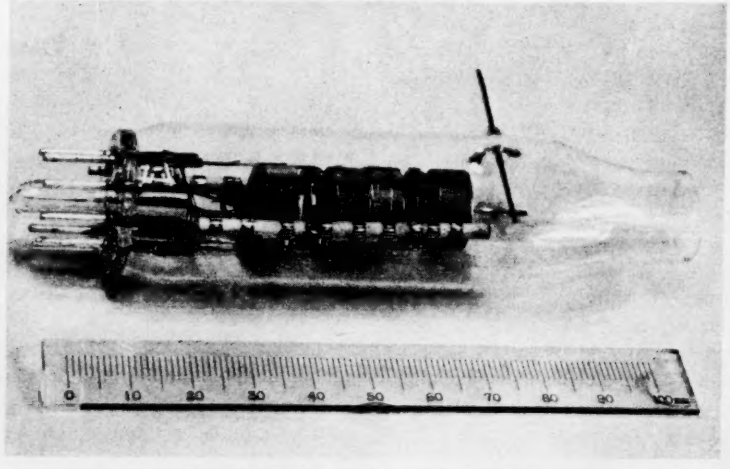

FIG. 3. An experimental spectrometer tube.

voltages applied to them are chosen so that an ion created at the left hand electrode of the cage is accelerated towards the centre of the tube. It then enters the decelerating field at the other end of the tube. Here it is repelled, and the whole process begins again. The ionizing electron beam originates from a tungsten wire cathode. The beam is accelerated by the following electrode of the cage, penetrates a fine mesh screen and enters the electrode cage. By the decelerating fields at both sides of the mesh, the electrons are forced to oscillate around the mesh wires. Thus, an electron either creates an ion or will be captured by the mesh screen without having produced an ion. Just in front of the cathode, the control grid is arranged by which the modulation of the ionizing beam is effected. By the end electrode at the opposite side of the tube the displacement current is picked up and fed to the first stage of the preamplifier.

The shape of the electrical field along the axis of the tube is shown below the electrodes. It is symmetric with respect to the centre of the cage. Each half of this ion-optical lens system is an immersion lens and, therefore, has a focussing action upon the ions.

An experimental tube designed according to the principles just described is shown in Fig. 3. The glass envelope has a length of 4 in. and a diameter of 1 in. The leads are strong enough to form a socket. The conductor of the signal electrode is arranged separately in order to avoid crosstalk from the modulated control grid.

The various elements of the control unit by which the tube is operated are shown in the following block diagram, Fig. 4. The upper box on the right side symbolizes the voltage

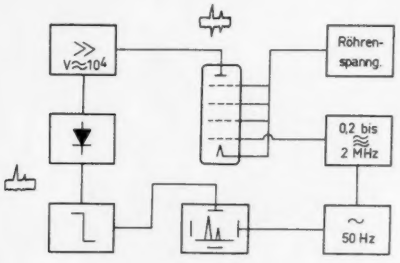

FIG. 4. Block-diagram of the control unit.

divider for the dc-voltages and the supply of the filament. Below this box we see the generator of the modulated, i.e. sweeped high frequency which is fed to the control grid. It is synchronized at mains frequency which also holds for the horizontal deflection of the oscilloscope. The output signal of the tube is fed to an ac-amplifier having a gain of about 10,000. The signal, after being rectified, passes a low pass filter in order to cut off the shot noise carried by the high frequencies, and then reaches the oscilloscope. Here, the mass spectrum may be observed in the co-ordinates of intensity and mass number.

A photograph of a mass spectrum taken in the manner just described is shown in Fig. 5. As indicated by the mass numbers the different lines correspond to the ions H_2^+, C^+, CH_4^+, H_2O^+, CO^+, CO_2^+, Hg^+, Hg^{++}. The spectrum was taken at a total pressure of 2.10^{-7} Torr on a mercury pumping system with liquid nitrogen on the mercury trap. The spectral lines at the mass numbers $7 = 28:4$ and $112 = 28 \times 4$ are ghost lines of mass 28. The line at mass number 7 is generated by higher harmonics contained in the alternating current induced by the ions of relative mass 28. Ghost masses at mass numbers higher than that of the original mass, i.e. at lower frequencies, occur when the phase difference of two consecutive elementary ion clouds is a multiple of 2π.

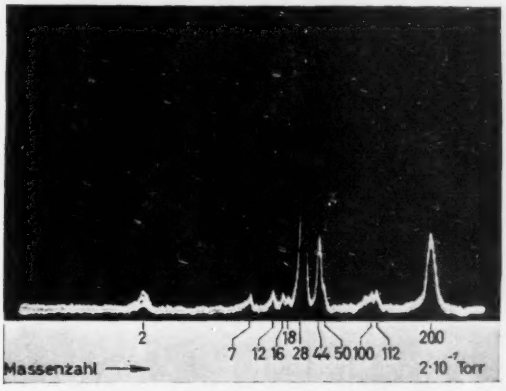

FIG. 5. A mass spectrum of the residual gas of a mercury-diffusion pumping system at a total pressure of 2×10^{-7} Torr.

Generally, only ghost lines of the first order occur, their intensities being less than 10 per cent than that of the main line. The resolving power visually estimated according to the recorded mass spectrum on the oscilloscope is about ten for all masses. The limiting resolving power amounts to approximately 20 and may be obtained by selecting a small frequency interval and spreading it over the horizontal scale of the oscilloscope. The limiting sensitivity corresponds to partial pressures of somewhat less than 10^{-8} Torr. The limiting factor for the sensitivity is the shot noise of the first amplifier stage. Therefore, still lower pressures may be detected by using a slower registration speed. This can be done by varying by hand the modulation frequency applied to the control grid. In this case, optimum resolving power is about 20 too. Towards higher pressures a limitation is set by the mean free paths of the ions. Therefore, the upper pressure limit should be between 1 and 5×10^{-5} Torr.

It is important to know that the heights of the spectral lines do not exactly represent the partial pressures of the corresponding gases. This is due to the fact that space charge effects play a dominating role for the signal generating mechanism. Nevertheless, in a rough approximation the heights of the spectral lines give a fair impression of the contribution of the partial pressures to the total pressure.

An interesting mode of operation of the tube at low pressures is possible by applying an electron multiplier in connection with the Omegatron-like operation principle. Fig. 6 shows how the tube construction then has to be modified. The former signal electrode should be perforated so that the ions which gained momentum by the alternating

electrical field may pass the holes and enter the multiplier structure.

Summarizing, it can be stated that this novel mass spectrometer tube, whose technical designation will be " Farvitron " may be applied with success in the technique of high vacuum. The Farvitron as described in this paper, may be used at pressures ranging from 5×10^{-5} Torr down to somewhat less than 10^{-8} Torr. Its optimum resolving power is about 20. Its main features are speed and simplicity of operation, which make it most suitable for supervising work.

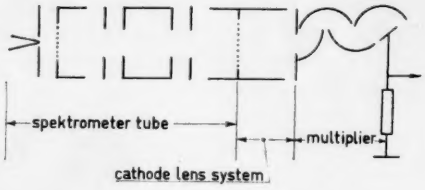

FIG. 6. Mass spectrometer tube with electron multiplier.

Vol.
10
1960

Analysis of Partial Pressures by Means of Omegatron and Farvitron

Comparative View of the Ranges of Application

G. REICH and F. FLECKEN

High Vacuum Research and Development Department, E. Leybold's Nachfolger, Köln-Bayental, Germany

The wide range of high vacuum technical problems, a solution of which may only be obtained by means of partial pressure analysis, is responsible for the fact that a variety of measuring methods becomes necessary. This applies in particular to sensitivity, pressure range, and rapid and comprehensive response. The two partial pressure gauges—the Omegatron and the Farvitron (see paper given by W. Tretner, Darmstadt)—dealt with in the present paper are matching each other in an ideal manner. While the Omegatron having high sensitivity and good resolving power allows only the subsequent measuring of single partial pressures, the Farvitron gives a complete survey of the composition of partial pressures on an oscillograph. For this reason the Farvitron having less resolving power and lower sensitivity is highly suitable for indicating partial pressures especially during rapidly varying processes in the pressure range between 10^{-8} *and* 10^{-5} *Torr.*

THE Omegatron has for many years now been used for analyzing partial pressures in studies carried out in the range of low pressures, and has proved to be an extremely reliable instrument. But its use as a control instrument, for example, in the manufacture of valves or in high vacuum plants, is impeded by several obstacles. In particular, there is the heavy magnet which restricts the use of the Omegatron. On the other hand, the required standard of resolution power and sensitivity for a mass spectrometer used in industry is appreciably lower because the course of a vacuum process is essentially known and only has to be controlled. Thus the required properties of a mass spectrometer are already broadly outlined—it must be possible to use it quickly, and its resolution power and sensitivity need not satisfy very high standards. The Farvitron features these properties to an extent which is adequate for the majority of purposes. Furthermore, both systems satisfy a most essential condition for carrying out reliable partial pressure analyses at low pressures, namely they are easy to bake out and have small inside surfaces. As a result, the respective mass spectrum obtained is only very slightly influenced by adsorption and desorption processes in the measuring system itself or in the lines leading to the system. The object of this paper is to outline the performance limits and thus the uses of these two instruments, the *Omegatron* and the *Farvitron*.

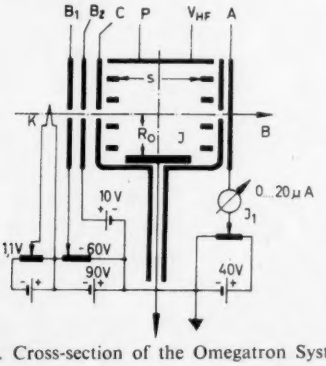

FIG. 1a. Cross-section of the Omegatron System.

K = hot cathode
B 1 and *B* 2 = focusing shields for the electron beam
C = screening box
A = Electron collector
P = high-frequency plate
I = Ion collector
Between the focusing shields a number of rings used as high-frequency voltage dividers for homogenizing the alternating field.

The Omegatron

The Omegatron tube, the properties of which will be discussed here, has a volume of approximately 50 cm^3. The electrodes are made of a platinum alloy. Fig. 1a shows a cross-section of the system. From left to right, we see the hot cathode *K*, the shields *B* 1 and *B* 2 for focusing the electron beam, the screening box *C* and the collector *A* for

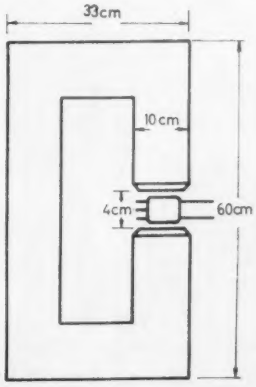

FIG. 1b. Permanent Magnet and Omegatron Tube.

the electrons. From top to bottom, we have the high-frequency plate *P*, a number of rings used as high-frequency voltage dividers for homogenizing the alternating field, and the ion collector *I*. Fig. 1b illustrates, to give a comparison of size, an example of the permanent magnet together with the Omegatron tube.

The results of the experiments conducted to study the properties of the instrument largely agree with the theoretical considerations, a fact which indicates the suitability of the Omegatron for quantitative measurements. The dependence of the ion current on the electron current for different gases

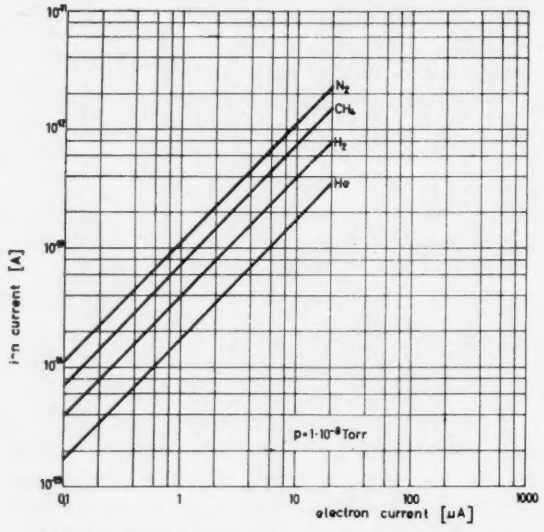

FIG. 2. Ion current as a function of electron current. The curves plotted are for hydrogen, nitrogen, methane and helium.

is illustrated in Fig. 2. The run of the curve is linear in the range of current from 1 to 20 microamperes.

Fig. 3 shows a calibration curve plotted for nitrogen for the masses 28 and 14. The electron current had a value of

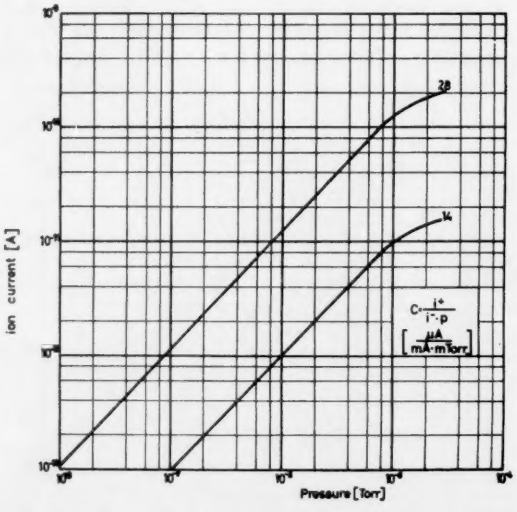

FIG. 3. Calibration curve plotted for nitrogen (masses 28 and 14) showing a sensitivity C equal to 11 (microampere per milliampere and millitorr).

1 microampere. This gives a sensitivity *C* equal to 11 microamperes/milliampere and millitorr, which corresponds to that of an ionization gauge. The curve starts to descend at a value above 1×10^{-5} Torr, the upper limit of the instrument's measuring range.

The limit of detection is largely determined by the amplifier, and is between several times 10^{-10} Torr and 1×10^{-9} Torr. This limit of sensitivity is not dependent on the total pressure within the measuring range. Fig. 4 provides data on the

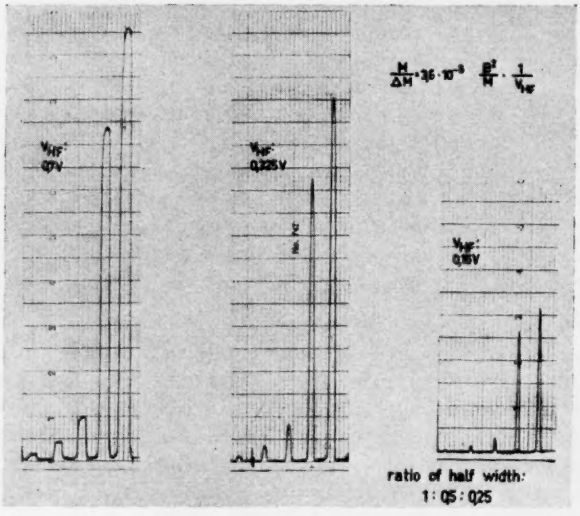

FIG. 4. Dependence of half-widths and high-frequency voltage. The curve has been plotted for the methane group, i.e. masses 12 to 16.

resolving power. The curve has been plotted for the methane group, in other words masses 12 to 16 at different high-frequency voltages. The voltages used are, from left to right, 0.7 V, 0.325 V and 0.15 V. Correspondingly, the half-widths are 1 : 0, 5 : 0, 25. The formula showing the relation between resolution power and high-frequency voltage is :

$$\frac{\Delta M}{M} = 3.6 \times 10^{-5} \frac{B^2}{M} \frac{1}{V_{HF}}$$

The field strength is 3.15 kGauss. Furthermore, it is noticed that the height of the lines decreases as the high-frequency voltage becomes less. But from a certain value, the height of the lines does not vary any more as the high-frequency amplitude increases. Fig. 5 illustrates this also for methane. It should also be pointed out that the influence on the residual gases also remains slight owing to the very small electron current.

The Farvitron

The working principle of the Farvitron mass spectrometer has already been described in the paper of Dr. Tretner, so that we can restrict our remarks to the uses of this instrument. In Fig. 6, the Farvitron tube is illustrated on the left. It has a volume of 45 cm³. All the control gear and the voltage supply equipment are incorporated in one housing which also holds the oscillograph tube for plotting the mass spectrum, as shown on the right. The instrument and the measuring tube are connected by a multiple cable. It is

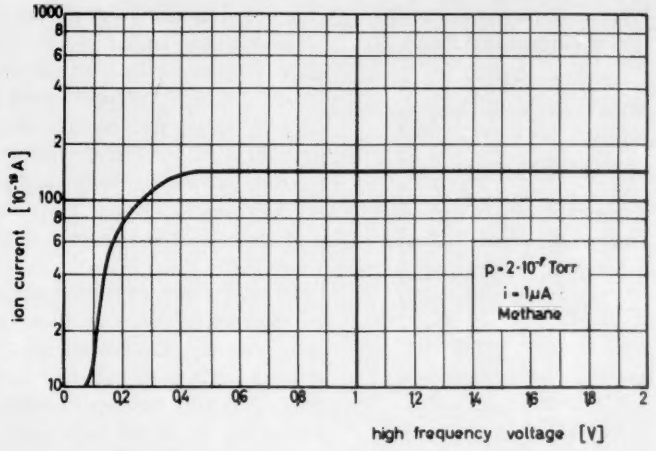

FIG. 5. Ion current as a function of high-frequency voltage for mass 16 (methane).

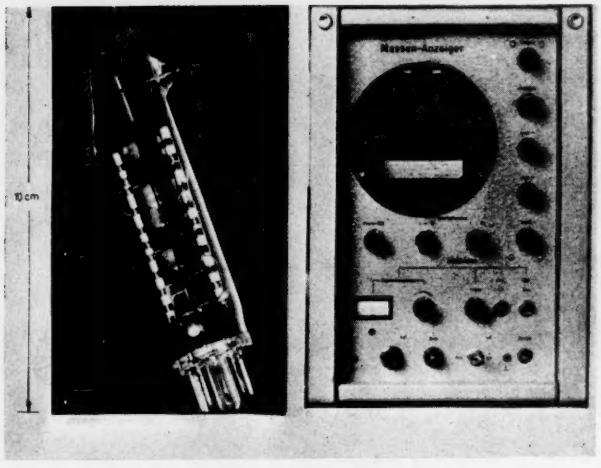

FIG. 6. Farvitron tube and control box.

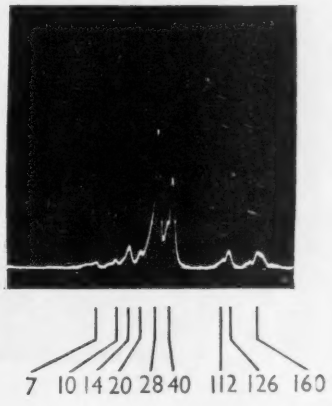

FIG. 7. Lines for masses 28 and 40. The scale is calibrated in units of mass.

thus possible by simple means to control several measuring points with only one instrument, for example to make spot checks in the manufacture of valves. It is merely necessary to fit a measuring tube on each packaged pump system involved. The control unit can be moved and connected in the shortest possible time, and is at once ready for instant operation.

The instrument is so designed that the residual gas spectrum is recorded for a range extending from mass 2 to mass 300. The mass lines appear on the screen at the same time, so that it is possible also to follow short processes qualitively. Fig. 7 shows such a screen with the masses 40 and 28 above a scale calibrated in unit of mass. Here, too, higher and lower harmonics appear as lines on the screen, just as they frequently do on some mass spectrometers. On the one hand, these are very useful for identifying the different masses but when a large number of residual gases are present, they may complicate the work. In this example, the lines are recognised for 7 and 112, which represent a quarter of, and four times 28, also mass 14 with the line 126, and lines 10, 20 and 160 which belong to mass 40. But as you see, the peaks of the harmonics are very small compared with the main peak.

The limit of detection for low pressures is 1×10^{-8} Torr, and limit in the upper section of the working range is at 1×10^{-5} Torr. Partial pressures of down to 1 per cent of the total pressure can be registered. Regarding the resolving power, experience has shown that $\Delta M = \sqrt{M}$, in other words the width of the mass line measured at 10 per cent of the intensity is equal to the square root of the mass. The optimal electron current varies according to the pressure range. Favourable values are shown in Fig. 8. In the upper section of the graph, the tube no longer operates at optimal efficiency due to space charge limitation, while in the lower part the sensitivity is too small.

The next slides illustrate a number of typical processes in high vacuum, which were followed on the screen. In Fig. 9, baking out a glass system, a rise of pressure will be observed which is essentially caused by the escape of water vapour. Section 1 shows the residual gas before baking out. The second section of the photograph was taken immediately after the start of the baking-out process. It is

noticed that the line for mass 18 has risen very considerably, and one also sees the upper and lower harmonics 4.5 and 72.

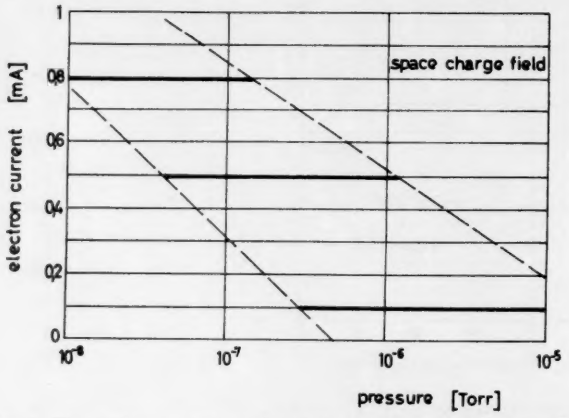

FIG. 8. The optimum setting of emission current according to the pressure range.

The only line visible for nitrogen is 28. After a long period of baking-out, the partial water vapour pressure drops again, as may be seen in the 3rd section of the photograph. Lines 7 and 14 now reappear alongside the main line 28. In Fig. 10, baking out the tube of an ionization gauge, there is very much CO. The two photographs, on the left and on the right, were taken before and after baking out, respectively. At first lines 7, 14 and 28 are seen, and later lines 7, 12, 16 and 28. It follows from this that 28 essentially represents CO.

In cases where at least 5 per cent of the ultimate pressure can be credited to a leak, then the Farvitron can be used as a leak detector. On coating the leak with alcohol or acetone, or spraying it with Freon or helium, the composition of the partial pressure changes in a characteristic manner. On the left of Fig. 11 we have the spectrum of the residual gas with masses 18 and 28. In the left section of the photograph, Freon has infiltrated into the system while being sprayed.

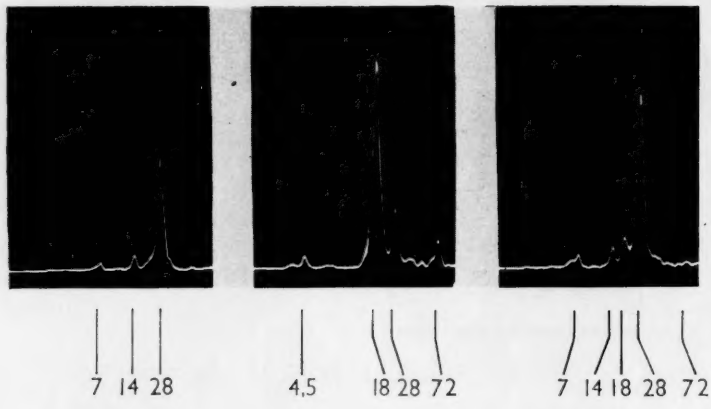

FIG. 9. Baking out of a glass system. The photographs were taken (from left to right) before baking out, immediately after baking out was started and after about 60 minutes.

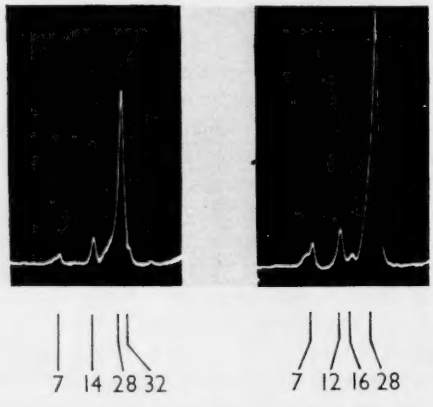

FIG. 10.
Degassing of metal electrodes of a manometer gauge.

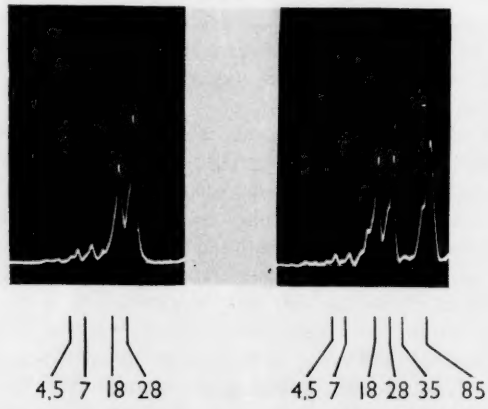

FIG. 11. Farvitron used as a leak-detector. First section: residual gas; second section: gas spectrum after Freon has infiltrated into the system.

New lines that have appeared are 35 and 85 which belong to Freon. It is clearly seen that the height of the nitrogen line has dropped in favour of the Freon line. The pressure was 1×10^{-7} Torr when this photograph was taken.

This brief report will no doubt have shown that greatly varying requirements have to be satisfied by a residual gas spectrometer. The two relatively simple instruments, the *Omegatron* and the *Farvitron*, supplement each other in a most purposeful manner so that we do have useful instruments at our disposal for dealing with the different tasks.

DISCUSSION

Question from Mr. Francken

When measuring with the Farvitron, mass 28 is connected with masses 7 and 112. Also mass 18 is connected with masses 4.5 and 72. On the other hand, mass 14 appears together with mass 126. Why does not mass 56 show up in this case?

Answer.

The amplification is not the same over the frequency range. Therefore the lower frequencies, i.e. higher mass lines, are preferred. In case of mass 14 : only 126 was seen over the noise level. For the same reason line 3.5 is not to be seen.

Vol.
10
1960

Emploi d'une Diode d'Essais comme Moyen de Controle des Materiaux de Construction des Tubes Electroniques

J. P. FREYTAG

Centre de Physique Electronique et Corpusculaire, Domaine de Corbeville, Orsay (S. et O.), France

Experience in the manufacture of high power microwave tubes (multi-MW range) has shown that the materials which constitute the tube are as much important as the materials which constitute the thermionic cathode itself. Indeed, where the oxide coated cathode is concerned, it has been recognized since the time of Wehnelt that the residual gas and the cathode performance are related. For a long time, the influence of the gas evolved of the electrodes and the tube envelope during operation, on cathode emission, has been recognized, too. All these phenomena have been designated " ambient phenomena " where " ambient " means the gases or vapours in the vicinity of the cathode and, in a wider sense, the sources of these gases and vapours which present the constructional parts of the tube. Since in the tube practice it is not always convenient to point out the nature of the ambient gases in function of the materials and the treatments they undergo, it has been found useful to examine the influence of the materials on an oxide coated cathode in a test diode, a technique which is in principle well known for controlling the cathode and tube materials of receiving tubes (" standard diodes "). The diode in question is adapted to the needs of pulsed tubes and allows—thanks to this fact and contrary to the usual standard diodes—to measure the cathode performance under the operating conditions except the anode voltage which is lowered. After a rapid description of this diode, it is shown that the influence of the ambients reveals three different behaviours of a $I^{2/3}$ *plot, where the available useful current (under space charge limitation) is limited either by apparition of the sparking phenomenon or by saturation. The influence of the operating conditions (d.c. or pulsed operation, pulse length, repetition frequency) on the current where the sparking occurs are demonstrated and the results obtained with certain anode materials are indicated ; that is : Iron, Kovar, Titanium, Molybdenum, Copper, Platinum and Nickel. The best anode materials were platinum and nickel ; in this latter case, in pulsed operation a current density of more than* 100 *A*/cm^2 *has been obtained, the limitation occurring not by saturation, but by sparking. Finally, the influence of the glass used as the diode envelope is shown. In conclusion, the diode reveals as a relatively simple control device. Nevertheless, when the nature of the ambients must be pointed out, more improved devices should be applied, such as the mass-spectrometer, a subject of the next paper.*

1. Introduction

Des expériences acquises pendant les dernières années dans la réalisation de tubes hyperfréquences à grande puissance (domaine des multimégawatts) ont montré que les matériaux constituant le tube sont aussi importants que ceux constituant la cathode thermoélectronique elle-même. En effet, on sait, depuis longtemps[1-4] que le gaz résiduel a une influence sur le comportement des cathodes.

Récemment l'influence de différents gaz sur l'émission a été chiffrée, par Wagener[5], pour la cathode à oxydes, et par Hashimoto et Uchida[6], pour une cathode *L*, Fig. 1. Dans cette figure, on a porté en abscisse les pressions partielles du gaz considéré et en ordonnée, le rapport entre le courant de saturation mesuré à la pression considérée et le courant de saturation mesuré lorsque la pression partielle est inférieure à 10^{-7} Torr, pour des températures de références données. On voit que pour la cathode à oxydes, à 800 °C, on n'obtient déjà plus la pleine émission pour des pressions partielles de CO et CO^2 inférieures à 10^{-7} Torr, et pour une pression partielle d'oxygène de quelques 10^{-7} Torr. Pour la cathode *L*, on n'obtient plus la pleine émission pour des pressions partielles d'oxygène voisines de 10^{-5} Torr, et pour des pressions partielles de gaz carbonique comprises entre 4.10^{-5} Torr et 10^{-4} Torr suivant la température.

Il est manifeste que la cathode *L* est moins sensible à l'empoisonnement que la cathode à oxydes, et ceci rejoint les vues de Plumlee[7] et de Nergaard[8] qui comparent une cathode à un réducteur chimique cédant ses électrons au vide, ce réducteur étant d'autant plus actif, donc d'autant plus facilement oxydable, que son travail de sortie est faible.

On sait aussi que des gaz peuvent être libérés par les électrodes ou par l'enveloppe lors du fonctionnement du tube. La diminution de l'émission, ou empoisonnement de la cathode, qui en découle est ce qu'on appelle le phénomène

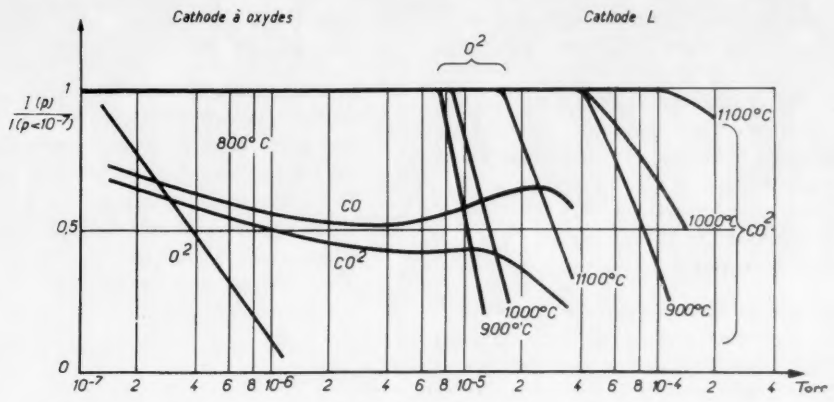

FIG. 1.

" d'ambiance ", le terme " ambiance " désignant les gaz ou vapeurs au voisinage de la cathode, et dans un sens plus large, les sources de ces gaz et vapeurs que constituent les pièces de construction du tube. Les gaz libérés peuvent provenir de gaz occlus dans les matériaux, ou de décomposition thermique ou de décomposition par bombardement électronique de composés chimiques[9, 10].

Comme il n'est pas toujours commode dans la pratique des tubes de déterminer la nature et la pression des gaz ambiants en fonction des matériaux et de leurs traitements préalables, il s'est avéré utile d'examiner l'influence des matériaux sur une cathode à oxydes dans une diode de contrôle.

Différentes diodes standards ont déjà été proposées, en particulier par l'American Society for Testing Materials. Citons celle décrite par McCormack en 1949[11], destinée à juger uniquement la qualité des matériaux de cathodes, et utilisant des éléments standards de lampes de réception, et celle décrite récemment par Misra[12] utilisant des éléments standards de tubes cathodiques. Ces diodes ne permettant pas de faire des mesures à un régime voisin du régime des tubes hyperfréquences à cause de la faible dissipation thermique de l'anode, une diode remplissant ces conditions, à l'exception toutefois de la tension anodique qui est réduite, a été développée.

2. Définition de la diode

Description de la diode

La Fig. 2 montre la structure de la diode. C'est une diode plane, d'environ 25 cm de longueur, ayant une anode circulaire de 40 mm de diamètre et de 2 mm d'épaisseur fixée sur un tube de kovar et pouvant être éventuellement refroidie par eau. La distance cathode anode est environ 1 mm, sa valeur précise étant mesurée pour chaque diode avec un cathétomètre. La cathode, entourée d'un anneau de garde en nickel, est une cathode type " tôle déployée " ayant une partie émissive de 4,5 mm de diamètre.

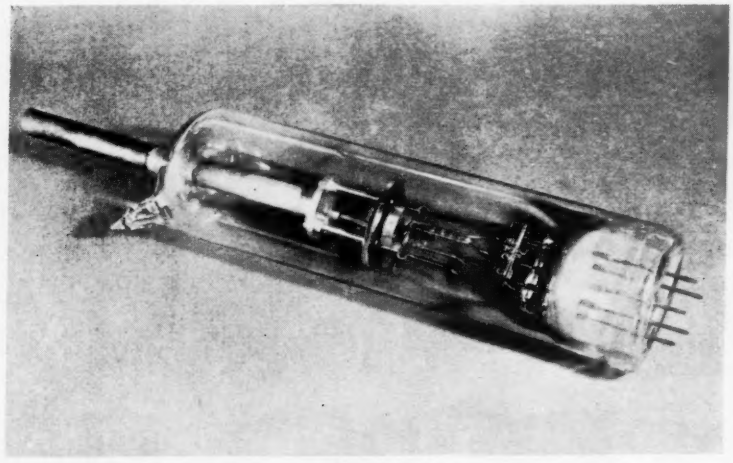

FIG. 2.

Une cathode type " tôle déployée "[13] est une cathode à oxydes ayant une réserve de matière émissive plus importante que les cathodes à oxydes habituelles. C'est une version technique de la cathode parcellée indiquée en 1954 par Huber et Charles[14]. La Fig. 3 est une microphotographie, au grandissement 40, indiquant les diverses étapes de la fabrication d'une telle cathode : Une feuille de tôle déployée

de nickel est soudée sur un boitier de nickel dans le but de former des alvéoles (3a). Ces alvéoles sont ensuite remplies de carbonates triples à raison de 15 mg/cm² (Fig. 3b). Une couche de carbonates est ensuite pulvérisée au pistolet sur la surface (Fig. 3c) à raison de 5 mg/cm². L'emploi de cette tôle permet d'utiliser une couche épaisse de carbonates ne se décollant pas du support.

Mentionnons que le nickel support et le nickel de la tôle sont du type actif au magnésium (0,07 pour cent).

Le getter est un getter à titane[15].

Traitement des différentes parties de la diode avant montage

Les traitements des différentes parties de la diode étant susceptibles d'influencer l'émission sont, sauf indications contraires, maintenus constants.

Nettoyage du kovar et de l'ampoule : Les opérations suivantes sont effectuées dans l'ordre :

— Nettoyage dans l'acide sulfurique dilué chaud pendant 2 min
— Nettoyage dans une solution de sulfo-chromique pendant 3 min
— Rinçage abondant à l'eau courante
— Rinçage à l'eau distillée
— Rinçage à l'alcool

Nettoyage des passages en molybdène :

— Electrolyse dans une solution de soude et de nitrite de soude
— Rinçage à l'eau courante
— Rinçage à l'eau distillée
— Rinçage à l'alcool

*Nettoyage des cathodes en nickel :**

— Dégraissage dans l'acétone
— Nettoyage pendant 5 min dans une solution bouillante de 1 litre d'eau distillée, 40 g de carbonate de sodium, 13 g d'hydroxyde de sodium
— Rinçage pendant 5 min dans l'eau distillée bouillante
— Rinçage dans l'acide acétique chaud à 5 pour cent
— Trois rinçages dans l'eau distillée bouillante
— Rinçage dans l'alcool.

Les pièces sont ensuite recuites sous hydrogène à 900°C pendant ½ heure.

Nettoyage des anodes :

Il est différent suivant le type d'anode employé. Les anodes sont toutes dégraissées dans l'acétone et sauf indications contraires recuites sous hydrogène (900°C).

Pompage

Après étuvage de la diode pendant 12 heures à 450°C, l'anode est dégazée à 950°C par induction haute fréquence, puis la transformation des carbonates est effectuée, l'anode étant chauffée à 900°C. Cette dernière opération a pour but de diminuer l'adsorption de gaz carbonique par l'anode[16] et de diminuer les dépôts formés par condensation de matériaux s'évaporant de la cathode. Avec ce procédé, on obtient, dans les diodes de référence, des cathodes donnant, sans activation notable, des densités de courant de l'ordre

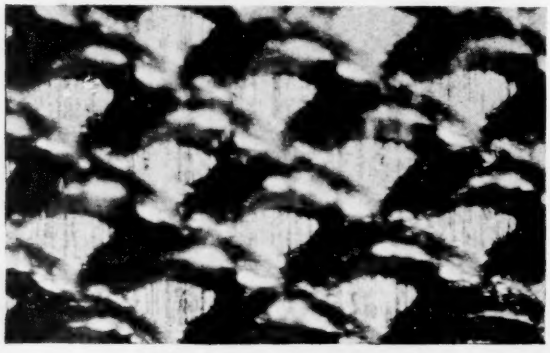

FIG. 3a.

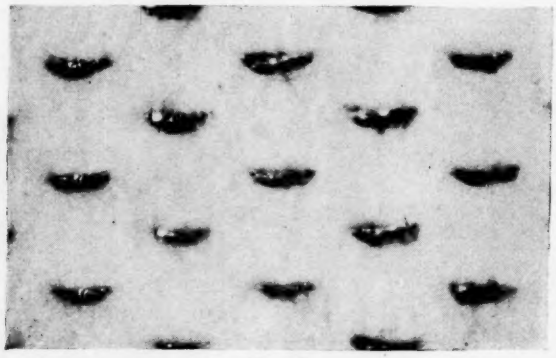

FIG. 3b.

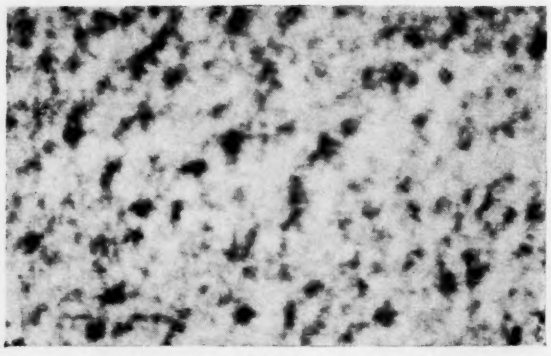

FIG. 3c.

* Inspiré par le " Tube Laboratory Manuel du M.I.T., 1956 ".

Vol. 10 1960

de 1 A/cm² en régime continu et d'une dizaine d'ampères par cm² en régime pulsé (1 μs 1000 c/s). Lorsque l'anode n'est pas chauffée pendant la transformation des carbonates, une activation est nécessaire et le temps pour obtenir ces densités de courant peut atteindre plusieurs heures.

3. Mesures de la qualité de la cathode

Les mesures ont été effectuées en régime pulsé, durée de l'impulsion $\tau = 1$ μs, fréquence de répétition $N = 1000$ c/s, la température de brillance de la cathode étant de 850° ou 900°C. Pour chaque diode on trace la caractéristique $I = f(V)$ avec une échelle $I^{2/3}$. La droite théorique de charge d'espace est donc une droite passant par l'origine (pour des tensions nulles, le courant dû à la vitesse initiale des électrons est négligeable sur l'échelle adoptée).

Allure des caractéristiques

L'expérience montre Fig. 4 que la caractéristique peut avoir trois allures :

(1) Une caractéristique suivant la droite théorique de charge d'espace et limitée par le sparking (courbe 1). Le sparking se traduisant sur l'oscillographe par des augmentations brutales du courant, pendant des fractions de la durée de l'impulsion et correspondant à l'apparition d'étincelles entre l'anode et la cathode.

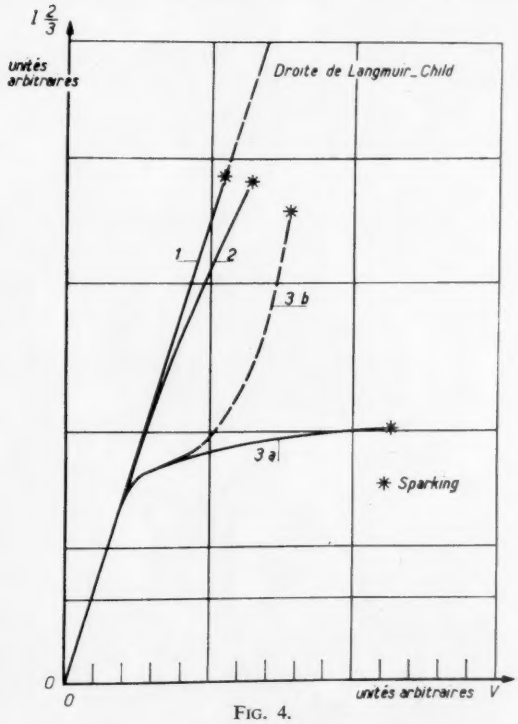

FIG. 4.

(2) Une caractéristique déviant de la droite théorique, mais ne présentant pas de saturation nette et étant limitée par le sparking (courbe 2). La différence entre la droite théorique et la caractéristique peut être interprétée, ou par la résistance de la couche émissive, ou par la saturation de certaines zones de la surface émissive.

Pour ces deux types de caractéristiques, la valeur du courant de sparking est en général reproductible ; le sparking n'empoisonnant pas la cathode, cette constatation est en accord avec les résultats de Nergaard[17].

(3) Une caractéristique saturée se terminant par le sparking (courbe 3a). La caractéristique peut présenter un effet Schottky anormal (courbe 3b).

Ces allures de caractéristique concordent avec celles indiquées par Coomes[18].

La Fig. 5 montre l'élévation de température de brillance moyenne de la couche, mesurée au moyen d'un pyromètre

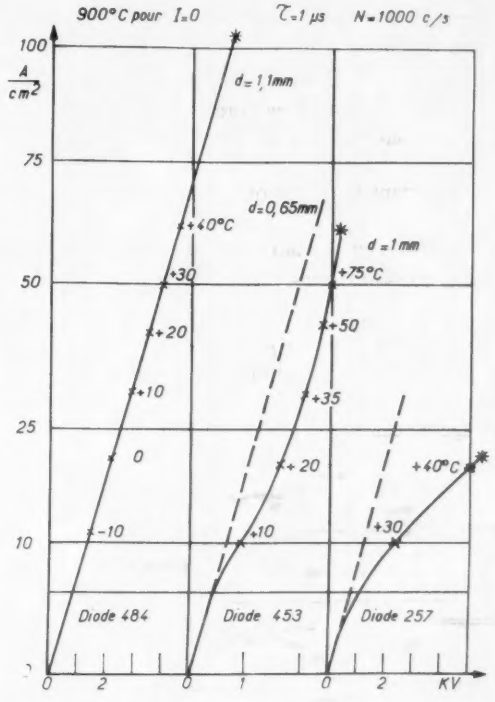

FIG. 5.

optique, lorsque la température du boitier est de 900°C en l'absence de courant émis, pour les trois types de caractéristiques. Pour un courant donné, l'élévation de température est plus faible pour la cathode dont la caractéristique suit la droite de charge d'espace que pour les deux autres, ce qui montre que la résistance de la couche est plus faible pour la cathode la plus émissive[19].

Le courant maximum utilisable est donc déterminé, ou par le sparking, ou par la saturation. C'est ce courant maximum que l'on prendra comme critère pour déterminer la qualité de la diode.

Considérations sur le sparking

Notons que le sparking peut être provoqué par les effets suivants :

— échauffement local de couche[20]
— rupture diélectrique de la couche interface[21]
— rupture diélectrique d'une zone appauvrie en donneurs d'électrons à la surface de la couche émissive (depletion layer[17]).

On constate que le sparking se produit, en général, à la fin de l'impulsion et que la valeur du courant de sparking augmente avec la température de la cathode.

La Fig. 6 montre la variation de la valeur du courant de sparking en fonction de la durée d'impulsion et de la fréquence de repétition.

DIODE	$\tau = 1\,\mu s$	$\tau = 4\,\mu s$	$\tau = 10\,\mu s$
166 ANODE Mo	50	27	-
231 ANODE Ni	105	55	45
252 ANODE Ni	120	80	> 45

$\tau N = 10^{-3}$ 850° c

DENSITÉ DU COURANT DE SPARKING EN A/cm^2 EN FONCTION DE LA DURÉE DE L'IMPULSION

DIODE	1 µs				4 µs	
	250 p/s	500 p/s	1000 p/s	2000 p/s	250 p/s	500 p/s
166 ANODE Mo	20	34	50	> 60	27	30
252 ANODE Ni	90	110	120	> 120	80	> 80

850 °c

DENSITÉ DU COURANT DE SPARKING EN A/cm^2 POUR 1 ET 4 µs ET DIFFÉRENTES FRÉQUENCES DE RÉPÉTITION

FIG. 6.

Dans le tableau du haut, on indique les densités de courant auxquelles le sparking se produit pour 3 diodes, à 850 °C, pour un duty cycle de 10^{-3} et pour $\tau = 1$, 4 et 10 μs. On voit que la valeur du courant de sparking diminue quand la durée de l'impulsion augmente[18].

Dans le tableau du bas, on indique les densités de courant auxquelles le sparking se produit pour 2 diodes, à 850 °C, pour $\tau = 1\ \mu$s et $N = 250$, 500, 1000 et 2000 c/s et pour $\tau = 4\ \mu$s et $N = 250$ et 500 c/s. On voit que la valeur du courant de sparking augmente avec la fréquence de repétition, pour une même durée de l'impulsion.

Cette dernière variation peut s'expliquer par l'augmentation de la température de la couche. On a mesuré, pour la diode 252 et pour 80 A/cm², que la température moyenne de la couche passe de 870 °C pour 1 μs–250 c/s à 900° pour 1 μs–2000 c/s (la température en l'absence de courant émis étant 850°).

Considérations sur le decay

Le decay de courant pendant l'impulsion peut provenir :
— ou de la couche émissive, par déplacement des donneurs d'électrons[17],
— ou de l'anode, par libération de gaz oxydants due au bombardement électronique[22, 23, 24].

Les expériences montrent que le decay augmente avec la durée de l'impulsion et avec la densité de courant et qu'il est, en général, plus faible pour une diode ayant fonctionné plusieurs dizaines d'heures que pour une diode venant d'être pompée. De plus la valeur du decay est liée à la forme de la caractéristique, le decay étant plus faible pour les diodes ayant des caractéristiques du type 1 et 2 que pour les diodes ayant des caractéristiques du type 3. En effet, pour des caractéristiques du type 1 et 2 la valeur du decay, à 900 °C et 20 A/cm², est de l'ordre de 5 pour cent pour des impulsions de 40 μs de durée. Pour des caractéristiques du type 3 et pour la même température de la cathode, la valeur du decay peut atteindre 40 pour cent, déjà pour des durées d'impulsions de 4 μs et des densités de courants de 10 A/cm² seulement.

4. Résultats

Les essais ont porté sur certains matériaux d'anode et sur quelques types de verre.

Essais avec différents matériaux d'anode

Essais avec des anodes non refroidies par eau

Métaux à haute perméabilité magnétique : Des essais ont été effectués avec des métaux à haute perméabilité magnétique en vue de les utiliser comme pièces polaires dans les tubes hyperfréquences, à savoir :
— le fer " Laxa " qui est un fer exempt de carbone
— " l'hyperm " CO50 de Krupp qui contient 50 pour cent de fer et 50 pour cent de cobalt
— le kovar qui est un fer-nickel-cobalt.

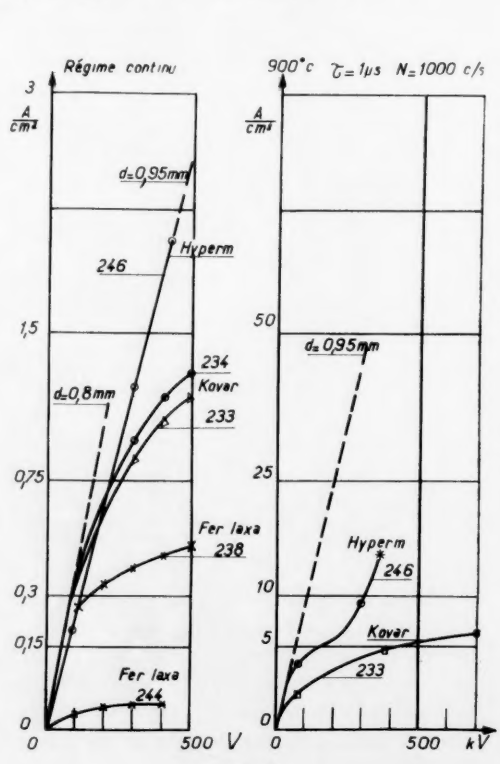

FIG. 7.

La Fig. 7 montre les caractéristiques, en régime continu et en régime pulsé, à 900 °C. On constate, en régime continu, que la saturation apparaît vers 15 mA/cm² et 0,3 A/cm² pour le fer et 0,45 A/cm² pour le kovar ; pour " l'hyperm ", la caractéristique suit la droite théorique jusqu'à 2,1 A/cm². En régime pulsé, la saturation apparaît pour des valeurs à peine plus élevées : 4 A/cm² pour " l'hyperm " et 1 A/cm² pour le kovar. Pour ces trois matériaux, l'émission obtenue est considérée comme faible.

Molybdène : Des diodes avec anode de molybdène ont été mesurées à la suite de déchets de tubes ayant des anodes constituées par ce matériau. On a trouvé dans des plaques de même provenance, deux qualités différentes qu'on appelle lot A et lot B pour les distinguer.

La Fig. 8 montre, pour les deux lots, en régime continu et en régime pulsé, une caractéristique type choisie parmi

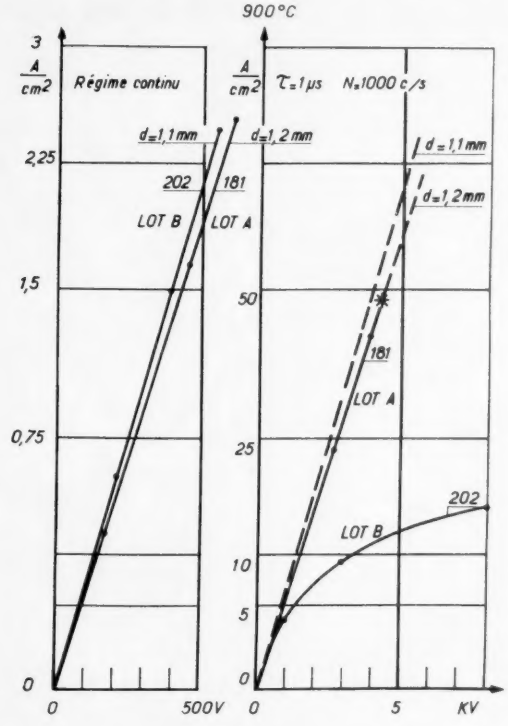

FIG. 8.

plusieurs essais. En régime continu, la caractéristique suit la droite théorique de charge d'espace jusqu'à 2,5 A/cm² pour les deux lots, mais en régime pulsé on obtient avec les anodes du lot A une caractéristique limitée par le sparking vers 50 A/cm² et pour le lot B une saturation vers 4 A/cm². On voit que des cathodes ayant des émissions identiques en régime continu (tout au moins jusqu'à 2,5 A/cm²), peuvent avoir des émissions différentes en régime pulsé[22]. Mentionnons qu'une analyse spectrographique des deux lots de molybdène n'a pas montré de différences signifiantes. Signalons aussi que différents traitements préalables : nettoyage chimique, recuits sous vide ou sous hydrogène même, à 1800 °C, n'ont pas influencé l'émission.

Titane : Des essais ont été effectués avec des anodes de titane ayant subi différents traitements avant montage.

La Fig. 9 montre les caractéristiques en régime continu et en régime pulsé pour trois diodes.

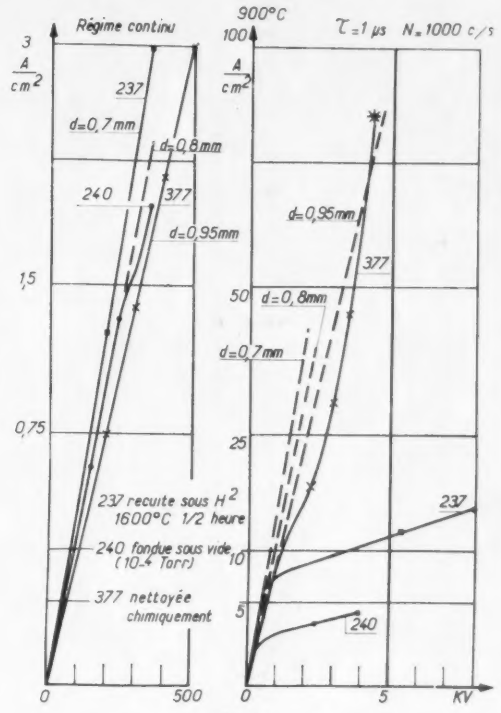

FIG. 9.

Le matériau de l'anode de la diode 240 avait été fondu sous vide (10^{-4} Torr) par bombardement électronique ; la caractéristique en régime continu marque un début de saturation vers 1,35 A/cm² et en régime pulsé vers 2 A/cm².

L'anode de la diode 237 a été recuite sous hydrogène sec à 1600 °C pendant ½ heure ; l'émission en régime continu atteint 3 A/cm², en régime pulsé la saturation apparaît vers 4 A/cm².

L'anode de la diode 377 a été nettoyée chimiquement (acide chlorhydrique : 9 vol. acide nitrique : 3 vol. acide fluorhydrique : 2 vol. eau distillée : l'émission en impulsions est plus importante, la saturation appraîssant vers 12 A/cm² et le sparking vers 80 A/cm².

L'émission la plus importante est donc obtenue avec l'anode n'ayant pas subi de traitements thermiques.

Nickel : De nombreux essais ont été effectués avec des anodes de nickel actif au magnésium, homologué pour cathodes. La Fig. 10 ne montre que les caractéristiques en régime pulsé pour 850 et 900°, les caractéristiques en régime continu atteignant toutes 3 A/cm². A 900 °C la caractéristique est limitée vers 115 A/cm² à cause de la puissance de sortie du modulateur. A 850 °C, après une légère déviation de la caractéristique vers 45 et 80 A/cm², le sparking apparaît au delà de 100 A/cm².

Platine : Des résultats identiques à ceux du nickel ont été observés avec des anodes en platine.

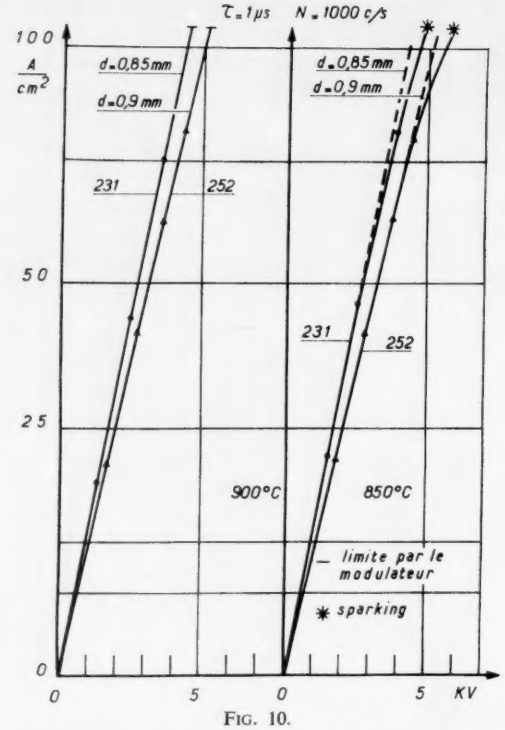

FIG. 10.

Essais avec des anodes de cuivre refroidies par eau

Trois types de cuivre ayant subi les mêmes traitements ont été comparés, à savoir :

cuivre OFHC (coulée 2233 TFM)
cuivre au tellure (0,5 pour cent de Te)
cuivre au phosphore (0,015 à 0,025 pour cent de P).

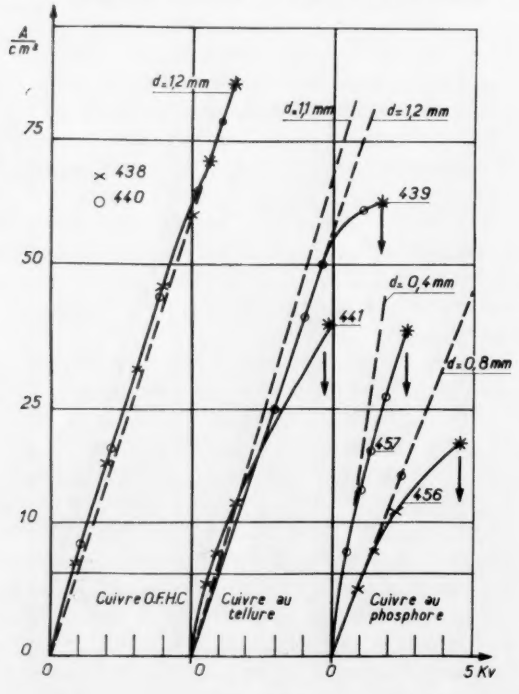

FIG. 11.

Ces anodes sont brasées sous hydrogène à un tube de kovar, puis dégazées sous vide à 700 °C. Après enrobage du tube de kovar, elles sont nettoyées dans un mélange d'acide sulfurique et nitrique. La Fig. 11 montre les caractéristiques en régime pulsé à 900 °C (les caractéristiques en régime continu sont identiques jusqu'à 3 A/cm² pour les trois types de cuivre).

Pour le cuivre OFHC les caractéristiques suivent la droite théorique de charge d'espace et sont limitées par le sparking à 70 et 85 A/cm².

Pour le cuivre au tellure, le sparking apparaît après un début de saturation à une valeur plus basse : 42 à 60 A/cm². Pour le cuivre au phosphore le début de saturation et le sparking ont lieu à une valeur encore plus basse : 33 à 12 A/cm².

Autre fait important, pour le cuivre au tellure et au phosphore : le sparking réduit fortement l'émission.

Le tableau Fig. 12 résume les valeurs de la densité du courant maximum obtenues avec tous ces différents matériaux d'anode.

MATÉRIAUX D'ANODES	DENSITÉ DE COURANT A/cm²	LIMITATION
FER LAXA	0,3	SATURATION
KOVAR	1	"
TITANE FONDU SOUS VIDE	2	"
HYPERM	4	"
MOLYBDÈNE lot B	4	"
TITANE RECUIT SOUS H^2	4	"
TITANE NETTOYÉ CHIMIQUEMENT	12	"
CUIVRE AU PHOSPHORE	15	"
CUIVRE AU TELLURE	50	"
MOLYBDÈNE lot A	50	SPARKING
CUIVRE O.F.H.C.	70-85	"
NICKEL HOMOLOGUÉ POUR CATHODE	> 100	"
PLATINE	> 100	"

DENSITÉ DE COURANT MAXIMUM À 1 µs 1000 c/s ET 900° c

FIG. 12.

On peut alors constater que la densité de courant maximum est limitée, soit par la saturation, vers les faibles valeurs, soit par le sparking, pour les valeurs supérieures à 50 A/cm².

Remarquons encore que ce n'est probablement pas l'élément métallique de l'anode qui est en cause, mais les gaz susceptibles d'être libérés par le matériau de l'anode.

Essais avec différents verres comme enveloppe

Les essais ont porté sur des diodes à anode de nickel et avec des verres suivants :

— deux lots A et B de verre Mo2 a ou S744.03, équivalent au verre Corning 7052

— un lot de verre Mo2 b ou S745.01, équivalent au verre Corning 7056
— un lot de verre B 40 ou S740.01.

Ce sont des borosilicates dont la composition donnée par le fournisseur est indiquée ci-dessous :

	SiO_2	Al_2O_3	B_2O_3	ZnO	MgO	CaO	K_2O	Na_2O
Mo2a	69.9	0.20	20.20	1.95			5.20	2.40
Mo2b	Verre d'essais de composition non communiquée, mais voisine de Mo2a							
B40	73.3	1.20	17.33		0.27	0.49	2.56	4.82

La Fig. 13 montre une caractéristique typique, prélevée

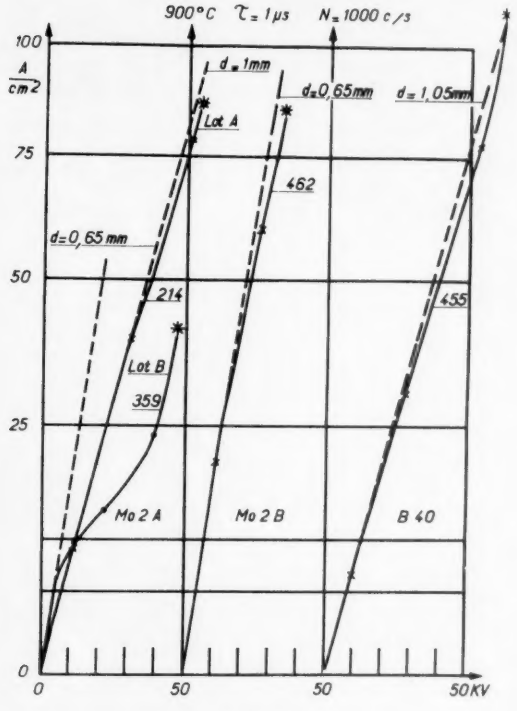

FIG. 13.

parmi plusieurs tests, pour chaque lot de verre, en régime pulsé 1 µs–1000 c/s à 900°.

Pour le lot A de Mo2 a, le Mo2 b et le B 40 la caractéristique est limitée par le sparking au delà de 80 A/cm². Pour le lot B de Mo2 a, la saturation apparaît vers 10 A/cm².

On retrouve donc pour deux lots d'un même type de verre, des différences analogues à celles déjà observées pour deux lots de molybdène employés comme anode.

La Fig. 14 montre le comportement en durée pour ces deux lots de verre. La durée est effectuée à un régime de 12 A/cm², 850°C et 1 µs 1000 c/s. Pour le lot B, la caractéristique se redresse lentement en fonction du temps et après 400 heures elle suit sensiblement la droite théorique de charge d'espace. La même caractéristique est encore

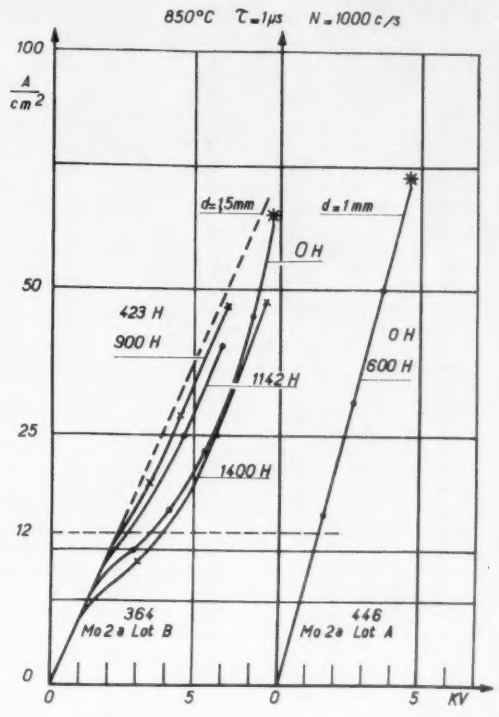

FIG. 14.

obtenue pour 900 heures, l'émission décroît ensuite.

Pour le lot A, la caractéristique au temps O suit la droite théorique de charge d'espace et est identique après 600 heures de durée.

La différence entre les lots A et B peut être attribuée à la présence de chlore qui peut être dégagé par le verre. (Comme on le sait[5] le chlore diminue l'émission d'une cathode à oxydes déjà à des pressions partielles de 10^{-8} Torr). En effet, on a observé avec le mauvais lot de verre des phénomènes de " ten volt effect " identiques à ceux décrits par Hamaker, Bruining et Aten[26]. On a mis en évidence, par micro analyse chimique, la présence de chlore dans la couche de carbonates lorsque les diodes, faites avec ce lot de verre, sont étuvées à une température supérieure à 400°C*.

D'autre part, d'après des renseignements du fournisseur, on sait que les verres Mo2 a et B 40 sont affinés avec des chlorures et des fluorures et le verre Mo2 b avec des antimoniures.

5. Conclusion

Ces résultats montrent que, non seulement l'émission maximum de la cathode à oxydes, mais aussi la forme du courant pendant l'impulsion (decay), dépendent fortement des matériaux constituant la diode, c'est-à-dire de l'ambiance. La diode se révèle donc comme un moyen de contrôle relativement simple. Néanmoins, lorsqu'on veut mettre en évidence la nature des gaz ou vapeurs ambiants elle ne dispense pas de mettre en jeu des moyens plus perfectionnés, tels que le spectromètre de masse, sujet de l'exposé suivant.

*Des analyses à l'aide de l'Omégatron, communication de M. Warnecke, Jr., ont confirmé la présence de chlore dans le lot B du verre Mo2a.

6. Remerciements

Ce travail a été excécuté sous la conduite de Mr. H. Huber. Je tiens à le remercier ici vivement.

Références

[1] Communication privée du Prof. Dr. F. Schröter, Ulm, Allemagne.
[2] I. Langmuir ; *The effect of space charge and residual gases on thermionic currents in high vacuum, Phy. Rev.* **2**, 11 (1913).
[3] J. O. Becker ; *Phenomena in oxide coated filaments, Phy. Rev.* **34**, 1323 (1929).
[4] G. Herrmann and O. Krieg ; *Der Einfluss von Gasen und Dämpfen auf die Emission von Oxydkathoden, Annalen der Physik* 6 *Folge, Bd* 4 (1949).
[5] S. Wagener ; *Reactions between oxide cathodes and gases at very low pressures, Proc. Phys. Soc.* **67**, 369–386 (1954).
[6] T. Hashimoto et M. Uchida ; *Reports of ECL, NTT*, 10, 3 April 1955.
[7] R. H. Plumlee ; *The electron donor centers in the oxide cathode, RCA Rev.* **17**, 231–274 (1956).
[8] L. S. Nergaard ; *The physics of the cathode, RCA Rev.* **17**, 486–511 (1957).
[9] G. H. Metson ; *Note on volt dependent poisoning effects in oxide cathode valves, Proc. Phys. Soc.* **62**, 589–591 (1949).
[10] D. A. Wright ; *Some effects of slow electron bombardment in thermionic valves, Brit. J. Appl. Phys.* **5**, 108–111 (1954).
[11] R. McCormack ; *A standard diode for electron tube oxide coated cathode core material approval tests, Proc. I.R.E.*, 683–687 (1949).
[12] R. P. Misra ; *Ultra-clean planar diode task force ASTM meeting held at Philco tube development lab., Landsale, Pa.*, 1 April, 1955. *La diode plane de référence de L'ASTM pour l'essai des matériaux de tubes électroniques et l'étude de leur traitement, Le vide* **77**, 256–263 (1958).
[13] H. Huber ; Microwave tube techniques in Europe. Fourth National Conférence on Tube Techniques, New York (Sept. 1958).
[13] H. Huber ; *Microwave tube techniques in Europe. Fourth National Conference on Tube Techniques, New York* (Sept. 1958).
[14] H. Huber et D. Charles ; *Exemples de réalisation de cathodes chaudes pour tubes hyperfréquences. Le Vide* **54**, 234–243 (1954).
[15] H. Huber et Monique Warnecke ; *La pompe à titane comme dispositif d'entretien du vide dans les tubes électroniques*, Congrès Intern. des Techniques du Vide, Namur, mai 1958.
[16] S. J. Stoll ; *Origin and analysis of gas in electron tubes, Brit. J. Appl. Phys.* **7**, 94–96 (1956).
[17] L. S. Nergaard ; *Studies of the oxide cathode, RCA Rev.* **12**, 464–545 (1952).
[18] E. A. Coomes ; *The pulsed properties of oxide cathodes, J. Appl. Phys.* **17**, 647–654 (1946).
[19] G. H. Metson ; *The conductivity of oxide cathodes, I.E.E.*, 316, Sept. 1957.
[20] Ch. Biguenet ; *Fonctionnement des cathodes à oxydes en régime transitoire, Le Vide* **22-23**, 661 (Juil.-Sept. 1949).
[21] D. A. Wright ; *Oxide cathodes. The effect of the coating core interface on conductivity and emission, Proc. Roy. Soc. A.* **190**, 394–417 (1947).
[22] S. Deb ; *Decay of emission from an oxide-coated cathode due to adsorption of matter liberated from the anode, J. Brit. Inst. Radio Engineers*, 157 (1954).
[23] G. R. Feaster ; *Pulse emission decay phenomena in oxide cathode, J. Appl. Phys.* **20**, 415 (1949).
[24] D. A. Wright ; *D.C. and pulsed emission from oxide cathode, Proc. Phys. Soc.* **62B**, 398 (1949).
[25] A. D. McQuillan and M. K. McQuillan ; *Titanium*, London, Butterworths Scientific Publications (1956).
[26] H. C. Mamaker, H. Bruining, and A. H. W. Aten, Jr. ; *Philips res. rep.* 2, 171–176 (1947).

Vol.
10
1960

Emploi du Spectrometre de Masse dans la Technologie des Tubes Electroniques

R. J. WARNECKE, Jr.

Centre de Physique Electronique et Corpusculaire, Domaine de Corbeville, Orsay (S. et O.), France

After mentioning the interest of using a mass spectrometer for the study of some fundamental problems raised by the technology of the electronic tubes, the author recalls and discusses the characteristics and performances required of the spectrometers to be used in the best conditions for the quantitative analysis of the residual gases, the study of their origin and influence (especially on the cathodes behavior). In order to have valid measurements, the inner structure of the analyzer tube must not modify the composition of the analyzed gas ; in other words, it must not have any internal residual gas. Therefore, the spectrometer must have reduced dimensions and the smallest possible surface effects, and it must be possible to outgas the tube energetically. These requirements usually exclude the use of classical sector field spectrometers and limit our choice to transit time spectrometers or radio frequency mass spectrometers. Two types of spectrometers which can be used with profit are described : the Omegatron and the Bennett type analyzer. The compared performances and characteristics of these two devices show that their qualities are complementary and that their simultaneous use can allow to perform the analysis concerned, both for static or rapidly varying phenomena, within a convenient range of pressure and mass.

ol.
10
960

1. Influence de l'ambiance sur le comportement des tubes

A l'image ancienne et bien insuffisante suivant laquelle un tube électronique n'est rien d'autre qu'un simple assemblage d'électrodes logées dans une enceinte sous vide, s'est substituée une représentation beaucoup plus conforme à la réalité et plus riche dans ses conséquences, qui fait d'un tube à vide un système chimique complexe dont tous les éléments sont en continuelle interaction par l'intermédiaire d'une phase gazeuse.

L'intérêt de cette conception vient de ce qu'elle met l'accent sur les phénomènes d'ambiance et leur influence, généralement néfaste, sur les caractéristiques des tubes, en particulier sur l'émission des cathodes. Se rappelant qu'une cathode est un émetteur d'électrons, c'est-à-dire au sens chimique du mot, un agent réducteur[1], baignant dans l'atmosphère résiduelle du tube, on conçoit que son comportement puisse être affecté par la présence, en quantités mêmes infimes, d'agents oxydants présents, à l'état gazeux, dans son voisinage. D'où la nécessité, non seulement d'abaisser suffisamment la pression dans un tube pour que les perturbations d'ordre électronique (ionisations, impacts ioniques, claquages, bruit, dispersion des faisceaux d'électrons) soient réduits à un minimum tolérable, mais encore d'éliminer du gaz résiduel les constituants oxydants responsables des perturbations d'ordre physico-chimique affectant le comportement de la cathode.

Comme la nature et les concentrations des gaz résiduels dépendent, pour une structure donnée, de la nature des matériaux entrant dans la constitution interne du tube et également de la manière dont ces matériaux ont été traités, c'est par le choix judicieux des matériaux dits " électroniques " et par l'emploi des méthodes de nettoyage et de dégazage appropriées que l'on peut espérer maîtriser les problèmes d'ambiance.

2. Nécessité de disposer de moyens d'analyse des gas residuels

Mais pour cela, il est souhaitable, voire nécessaire de disposer de moyens d'analyse permettant de connaître, à tout instant la nature et les pressions partielles des gaz évoluant dans les tubes, ceux-ci étant ou non en fonctionnement.

Si de tels moyens peuvent être mis en oeuvre, des solutions seront trouvées, non seulement à de nombreux problèmes de technologie, mais également à certaines questions encore mal élucidées, concernant la théorie du mécanisme interne des tubes, en particulier celles relatives aux cathodes à oxydes.

3. Conditions auxquelles doivent satisfaire les dispositifs d'analyse

Quels que soient les dispositifs susceptibles d'être utilisés pour l'analyse des gaz dans les tubes électroniques, ils doivent satisfaire à un certain nombre de conditions impératives qu'il convient de rappeler :

Comme de toute façon, l'analyseur doit être mis en communication directe avec le tube dont on veut étudier l'ambiance, il ne faut pas qu'il modifie la composition de cette dernière, autrement dit, le dispositif d'analyse ne doit pas avoir de résiduel propre, ou tout au moins, son résiduel doit être très petit et susceptible d'être connu. D'autre part, comme la pression globale dans un tube reste comprise

entre, disons 10^{-3} torr, lors des périodes de dégazage et parfois moins de 10^{-10} torr, une fois le tube scellé sous vide, l'analyseur doit être capable de mesurer des pressions partielles pouvant être inférieures à 10^{-11} torr ; c'est dire qu'une grande sensibilité est exigée, et ce, dans un domaine de masse compris entre 1 et 100 u.m.a. environ, l'expérience montrant que c'est dans cet intervalle que se situent les masses de la plupart des corps qui entrent dans la composition des gaz résiduels dans les tubes à vide.

Enfin, l'appareil doit permettre à la fois l'analyse de phénomènes évoluant lentement (comme par exemple la composition du gaz résiduel, à froid, pendant la période de pompage), et de phénomènes rapidement variables et parfois non reproductibles (parmi ceux-ci, citons l'absorption des gaz par un getter).

4. Les methodes d'analyse dont on dispose : micro-analyse chimique—spectromètre de masse

Ces exigences, en particulier celles relatives à l'analyse de phénomènes évoluant rapidement, excluent l'utilisation des *méthodes d'analyse microchimique* qui nécessitent généralement des mesures volumétriques, longues et délicates (puisqu'elles dépendent des conditions de température et de pression) et portant toujours sur des quantités de gaz relativement importantes[2].

Par contre, l'emploi des *méthodes d'analyse par spectrométrie de masse* s'avère beaucoup plus valable et parfois même le seul possible pour les mesures envisagées ici.

5. Les avantages de la spectrométrie de masse

Le spectromètre de masse est en effet un appareil spécialement conçu pour l'analyse des gaz sous faible pression et sa sensibilité élevée qui permet dans certains cas de mesurer des pressions partielles de l'ordre de 10^{-11} torr constitue du point de vue qui nous intéresse, une qualité fondamentale qui justifie à elle seule le choix de cette méthode d'analyse, encore qu'elle nécessite la mise en oeuvre d'un appareillage relativement complexe mais cependant assez commode à manipuler et ayant un temps de réponse pouvant être extrêmement court.

Pour que les analyses soient valables du point de vue quantitatif, il importe, comme nous l'avons dit, que le spectromètre ait un résiduel propre minimum : ceci impose que l'appareil soit de petites dimensions, que les effets de surface soient aussi réduits que possible et qu'il puisse être énergiquement dégazé.

Il est également souhaitable que le spectromètre ne nécessite pas obligatoirement l'utilisation d'un groupe de pompage autre que celui utilisé pour faire le vide dans le tube étudié, enfin que la cellule d'analyse puisse être éventuellement scellée sous vide avec le tube pour qu'il soit possible de suivre au cours du temps l'évolution de la pression et la composition du gaz résiduel, le tube étant ou non en fonctionnement.

6. Les types de spectromètre utilisables : l'Omégatron et le spectromètre de Bennett

Ces exigences excluent l'emploi des spectromètres classiques à champ secteur qui sont le plus souvent des appareils encombrants, présentant un résiduel non négligeable, et toujours associés à un dispositif de pompage qui leur est propre. Aussi, pour les analyses envisagées ici, leur préfère-t-on des appareils à performances plus réduites, surtout en ce qui concerne la valeur du pouvoir de résolution et l'étendue du domaine de masse exploitable, mais qui sont mieux adaptés aux conditions expérimentales précitées.

Parmi les divers types de spectromètres susceptibles d'être utilisés avec profit, nous retiendrons l'Omégatron qui se caractérise par une sensibilité très élevée aux basses pressions et le spectromètre de Bennett qui se distingue par le fait qu'il fonctionne correctement dans un intervalle de pression relativement étendu.

7. Caracteristiques de l'Omégatron

Comme l'on sait, l'Omégatron est un spectromètre de masse à résonance d'ions dont le principe énoncé par Sommer, Thomas et Hipple[3] présente de grandes analogies avec celui du cyclotron.

Il utilise un champ magnétique constant $\vec{B}$, généralement supérieur à 2000 oersteds, et, normalement à $\vec{B}$, un champ électrique alternatif $\vec{E}$ d'amplitude de l'ordre du volt et dont la fréquence f peut varier continuement entre quelques dizaines de kilocycles et quelques mégacycles.

Un faisceau très fin d'électrons, parallèle à la direction du champ magnétique et dont l'intensité n'excède pas une dizaine de microampères, ionise les molécules du gaz à analyser présent sous faible pression ($P<10^{-5}$ torr) dans la région où agissent les champs croisés $\vec{E}$ et $\vec{B}$ et sous l'action de la force électromagnétique $\vec{F} = e[\vec{E} + \vec{v} \wedge \vec{B}]$, les ions formés décrivent des trajectoires spirales dans des plans perpendiculaires au champ magnétique (Fig. 1).

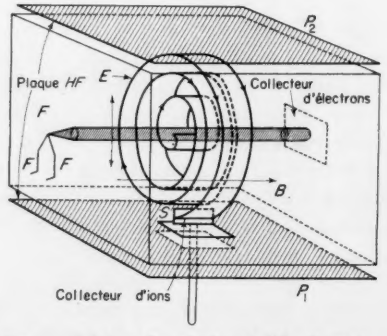

FIG. 1. Schéma de principe de l'Omégatron.

Parmi tous ces ions, seules les particules de charge e et de masse m dont la fréquence propre $F_o = \frac{1}{2\pi} \cdot \frac{eB}{m}$ est égale à la fréquence d'excitation f, reçoivent à chaque révolution un apport d'énergie emprunté au champ $\vec{E}$ et de ce fait, décrivent des spirales divergentes qui les amènent sur un collecteur situé à une distance déterminée R_o du faisceau d'électrons. Ces ions dits " résonnants " abandonnent leurs charges sur

le collecteur qui est inaccessible aux ions non résonnants de sorte que la mesure du courant ionique recueilli sur le collecteur S constitue une mesure de concentration en ions de masse m dans l'échantillon de gaz présent sous faible pression dans le spectromètre.

Par suite, en faisant varier la fréquence du champ électrique appliqué, on fait défiler sur le collecteur d'ions des particules de rapports $\frac{e}{m}$ différents. A chaque collection d'un groupe de même masse correspond ce qu'on appelle un " pic " qui se caractérise par son amplitude, proportionnelle au nombre d'ions collectés et sa largeur qui, pour un Omégatron donné, est une fonction de l'intensité des champs électrique et magnétique appliqués.

Fréquences et masses sont liées par la formule :

$$f_{kc/s} = 1{,}52 \frac{B_{gauss}}{m_{u.m.a.}}$$

Ainsi, les ions formés dans l'Omégatron sont séparés d'après leur masse, et la mesure des courants ioniques devrait indiquer leurs concentrations dans le gaz soumis à l'analyse.

Se rappelant que d'une manière générale le pouvoir séparateur d'un spectromètre de masse est défini par le rapport : $S = \frac{m}{\Delta m}$ de la masse de l'ion étudié au plus petit écart de masse décelable, on établit sans difficulté, dans le cas de l'Omégatron, la relation :

$$S = \frac{eB^2R_o}{2E_om}$$

qui montre que pour une valeur donnée de R_o, distance du collecteur d'ions à l'axe du faisceau d'électrons, le pouvoir de résolution est proportionnel au carré du champ magnétique et inversement proportionnel à l'amplitude E_o du champ électrique appliqué. On voit également que pour des valeurs données de ces champs, la résolution varie comme $\frac{1}{m}$.

Il n'est pas question dans le cadre de cet exposé de rappeler la théorie du fonctionnement de l'Omégatron, au sujet de laquelle on trouvera dans la littérature des informations détaillées[4-7]. Nous nous contenterons de résumer les performances essentielles de ce spectromètre et d'en discuter les avantages et les insuffisances, en nous basant sur les résultats expérimentaux obtenus avec un tube à enveloppe en verre et électrodes en platine, réalisé à la Compagnie Générale de T.S.F., et dont la figure ci-dessous montre la vue d'ensemble.

Sur la Figure 3 qui montre les détails de structure et de montage, on distingue en particulier :

— la chambre d'analyse B dans laquelle les ions sont formés et mis en mouvement sous l'action du champ magnétique $\vec{B}$, parallèle à l'axe $00'$ ou du champ électrique alternatif $\vec{E}$ normal à $\vec{B}$.

— les plaques HF, P_1 et P_6 et les anneaux de garde P_2, P_3, P_4 et P_5 entre lesquels on applique le champ électrique $\vec{E}$ et des tensions de polarisation destinées d'une part à extraire de la région centrale de la chambre d'analyse les ions non-résonnants qui ont tendance à s'accumuler au voisinage du faisceau d'électrons et d'autre part à améliorer le pouvoir de résolution en empêchant les ions qui ne sont pas exactement résonnants, d'atteindre le collecteur d'ions S.

— on voit également le filament F, le collecteur d'électrons C, le réflecteur d'électrons R et enfin la canalisation C qui conduit directement les gaz à analyser dans la chambre B.

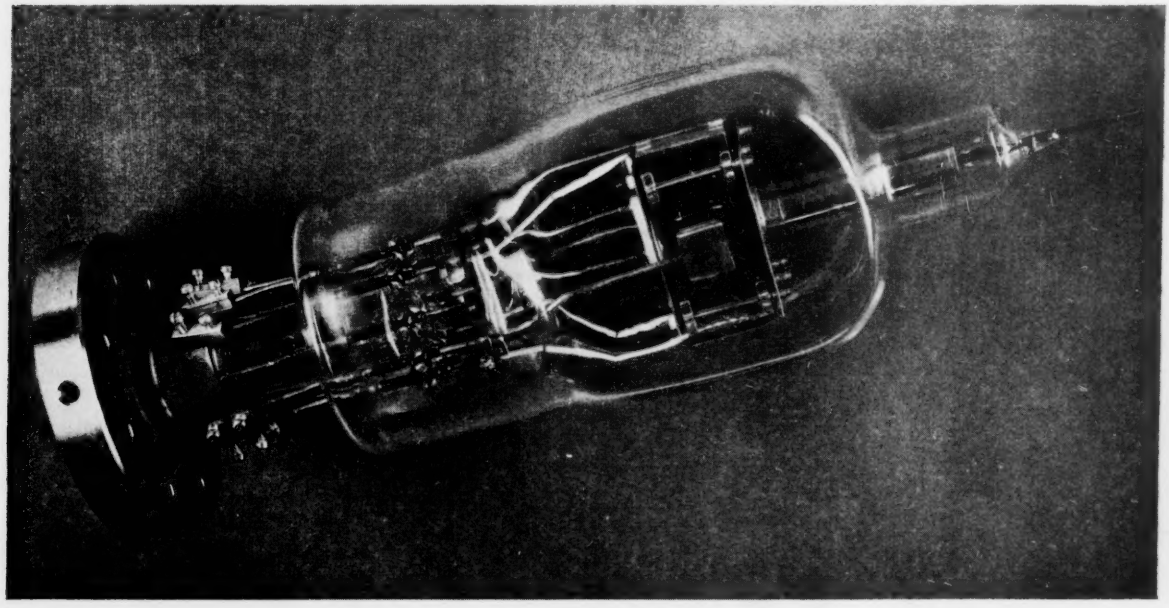

FIG. 2. Vue d'ensemble du tube Omégatron.

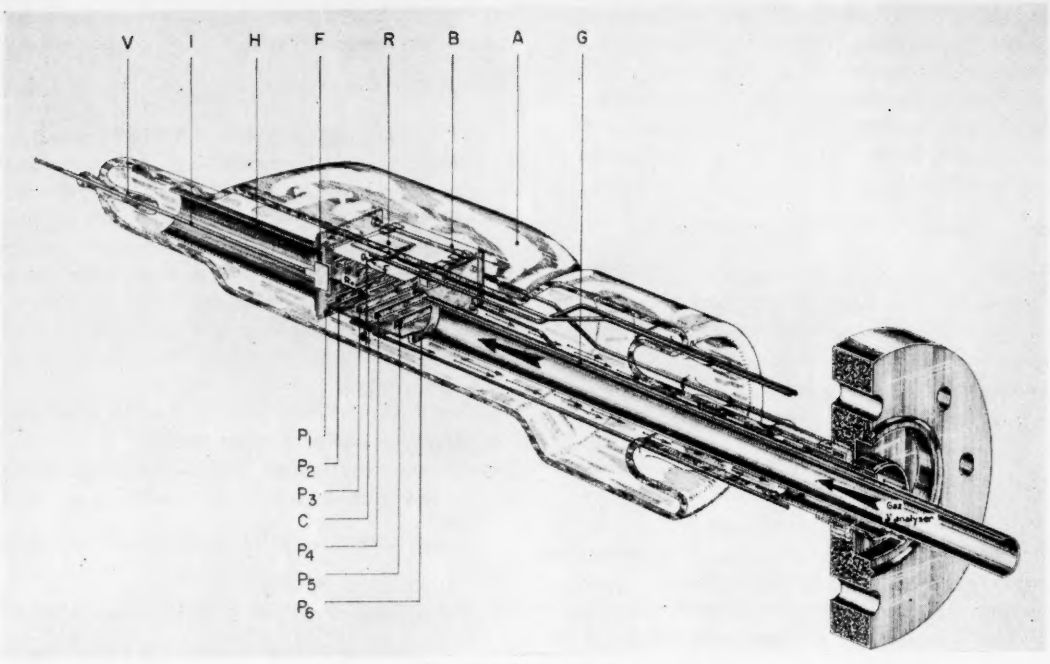

Fig. 3. Tube analyseur.

La jonction de la cellule, au groupe de pompage, au tube dont on veut analyser le gaz résiduel, et à l'organe de contrôle du vide (jauge Bayard-Alpert) est faite par l'intermédiaire d'un système à flasques et joints plats métalliques dont on voit une représentation schématique sur la partie supérieure de la Fig. 4. L'ensemble est étuvable jusqu'à 400 °C environ.

Pour réduire le plus possible les sources internes de gaz autres que celles provenant du tube soumis à l'analyse, le système de raccordement métallique peut être supprimé et l'Omégatron soudé directement sur le tube étudié (ainsi qu'il est indiqué sur la partie inférieure de la Fig. 4).

Avec ce dispositif et pour des conditions de pression telles que la longueur des trajectoires ioniques soit largement inférieure au libre parcours moyen des particules neutres à l'intérieur du spectromètre, on a pu vérifier expérimentalement :

(1) qu'à pression, courant électronique et tensions de polarisation constants, la loi de variation du pouvoir de résolution en fonction de l'amplitude du champ électrique $\vec{E}$ est très sensiblement celle prévue par la théorie, dans un intervalle compris entre 0,2 et 1 V/cm.

Avec un champ magnétique de 3000 Gauss et un champ électrique d'amplitude égale à 0,25 V/cm, le pouvoir de résolution est voisin de 45, ce qui signifie que l'on peut séparer toutes les masses des masses voisines jusqu'à $m = 45$. Dans ces conditions, le domaine de masse exploitable est compris entre $m = 1$ et $m = 100$ environ.

(2) que le courant d'ions collectés est approximativement proportionnel au courant ionisant, du moins tant que les effets de charge d'espace restent faibles, ce qui implique que le courant électronique n'excède pas une dizaine de μA.

(3) qu'il existe une stricte proportionnalité entre les

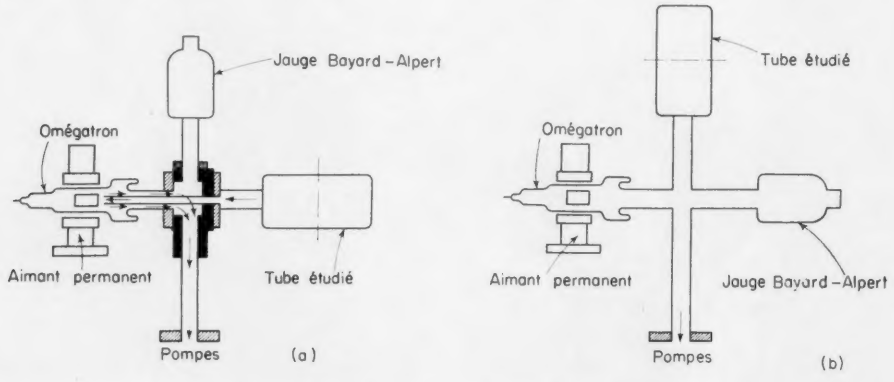

FIG. 4. Jonction de l'Omégatron au bâti de pompage.

pressions partielles et les amplitudes des pics correspondants, et ce, dans un intervalle de pression d'autant plus étendu (mais dont la limite supérieure n'excède pas 5.10^{-5} torr) que l'intensité du courant ionisant est plus faible.

(4) que le rendement de la source d'ions, c'est-à-dire le rapport du nombre d'ions collectés I_+ au nombre d'ions de même masse formés et soumis à l'action des champs croisés $\vec{E}$ et $\vec{B}$ reste compris entre 20 pour cent et 80 pour cent dans les conditions de sensibilité optimum.

(5) que le sensibilité du spectromètre, définie comme dans le cas d'une jauge à ionisation classique, par le rapport du courant d'ions collectés au produit du courant ionisant par la pression partielle correspondante, varie suivant les réglages adoptés et la nature du gaz étudié entre 1 et 10 $(\text{torr})^{-1}$.

Les plus petits courants mesurables au moyen de l'amplificateur à courant continu utilisé étant de l'ordre de 5.10^{-15}A, on déduit des résultats obtenus que dans les conditions les plus favorables et pour un courant ionisant de l'ordre de 10μA, les plus petites pressions partielles mesurables au moyen de l'omégatron sont de l'ordre de 5.10^{-11} torr. Ces résultats sont confirmés par d'autres expérimentateurs, en particulier Wagener et Marth[8].

(6) Enfin, on a vérifié que la précision que l'on peut obtenir dans la détermination des concentrations moléculaires, varie entre 2 et 7 pour cent, suivant que l'on compare ou non l'échantillon de gaz étudié à un standard de référence. La précision dépend d'ailleurs en grande partie de la stabilité de la pression dans la chambre d'analyse du spectromètre, pendant les mesures.

Ces quelques résultats extraits d'une étude systématique des différents paramètres agissant sur les caractéristiques de l'omégatron[7] montrent que ce spectromètre est très sensible et qu'il peut être valablement utilisé pour l'analyse, sous basse pression ($P<10^{-5}$ torr), de composés légers ($m<100$) dans la mesure où l'on n'exige pas une précision supérieure à quelques pour cent. C'est par ailleurs un spectromètre de dimensions réduites, facilement étuvable et susceptible d'être dégazé par chauffage *HF*. Enfin, compte tenu du fait que le temps de transit des ions, qui est indépendant de leurs masses, reste compris entre 10^{-4} et 10^{-3} seconde, le temps de réponse du spectromètre est négligeable devant les constantes de temps des circuits électroniques associés, de sorte que l'utilisation de l'omégatron jointe à celles des circuits de mesure à réponse rapide doivent permettre, sans difficulté particulière, l'observation de phénomènes évoluant très vite.

Toutefois, l'omégatron présente un certain nombre d'inconvénients qu'il convient de rappeler :

(1) tout d'abord, il nécessite l'emploi de champs électrique et magnétique croisés ; l'expérience montrant que l'orthogonalité de ces champs joue un rôle important à la fois sur la sensibilité et sur le pouvoir séparateur de l'appareil, le positionnement de l'aimant permanent par rapport à la cellule d'analyse est une opération délicate qui doit être refaite après chaque opération d'étuvage du spectromètre.

On obvie au moins partiellement à cet inconvénient en utilisant le dispositif de réglage visible sur la Fig. 5, qui permet grâce à un chariot muni de vis calantes et

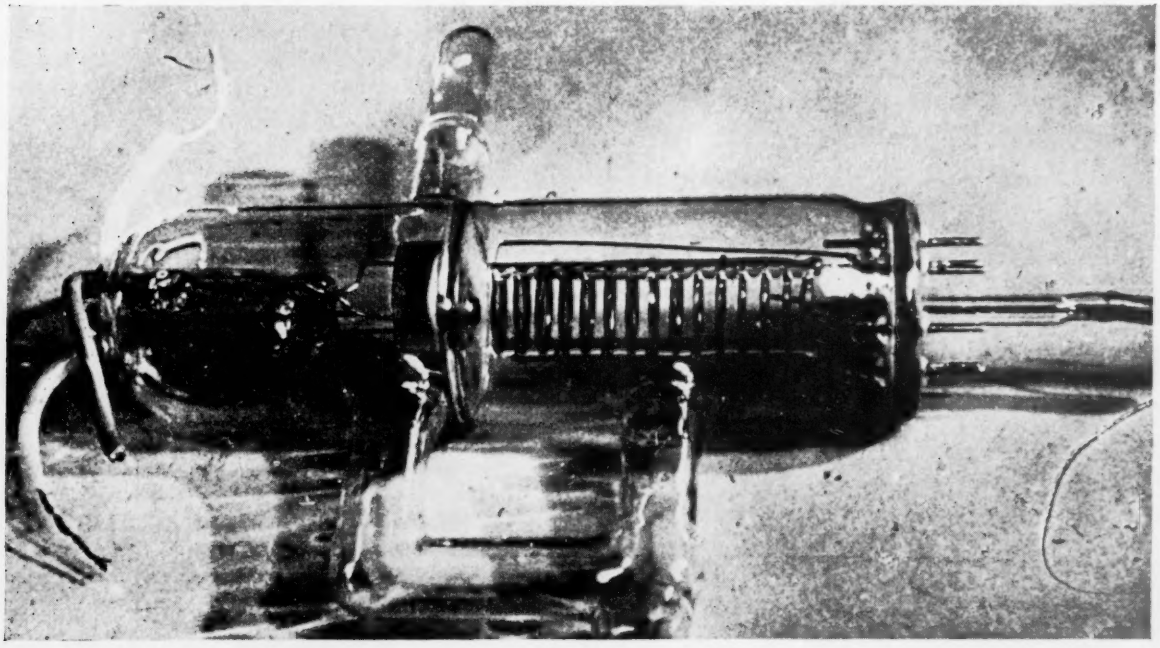

FIG. 5. Vue d'ensemble du dispositif d'analyse.

pivotant autour d'un axe solidaire de la platine portant le tube analyseur, d'assurer le positionnement précis de l'aimant par rapport au spectromètre, son effacement lors des périodes d'étuvage et sa mise en place exacte.

(2) d'autre part, l'expérience montre que les performances de l'Omégatron dépendent assez fortement des conditions de pression dans la chambre d'analyse ; plus précisément on observe qu'un fonctionnement correct de l'Omégatron nécessite que la pression dans le tube reste inférieure à 5.10^{-5} torr ; entre 5.10^{-5} et 5.10^{-7} torr, la sensibilité et le pouvoir de résolution sont encore sensiblement influencés par le facteur pression ; enfin, lorsque P est inférieur à 10^{-7} torr, cette influence devient négligeable.

(3) par ailleurs, il n'est pas possible, du moins avec la version de l'Omégatron présentée ici, de mesurer simultanément les pressions partielles des constituants du gaz analysé et la pression totale de ce gaz, ce qui est gênant pour l'étalonnage du spectromètre ; pour établir la correspondance entre les amplitudes des pics et les pressions partielles correspondantes, on doit mesurer la pression globale avec une jauge à ionisation et écrire, en tenant compte de la valeur des coefficients d'ionisation spécifique des différents constituants du mélange étudié, que la somme des pressions partielles mesurées avec l'Omégatron est égale à la pression globale indiquée par la jauge. Naturellement, cette méthode ne permet pas d'obtenir des résultats très précis.

(4) enfin, se manifestent parfois des effets de surface, difficiles à apprécier et que l'on ne peut pas toujours éliminer.

8. Caracteristiques du spectromètre de Bennett

En ce qui concerne le spectromètre de Bennett, rappelons qu'il s'agit d'un accélérateur linéaire miniature, dont la Fig. 6 donne le schéma de principe.

Le gaz à analyser est introduit, à travers une petite canalisation en verre, dans une chambre C_I où il est ionisé par des

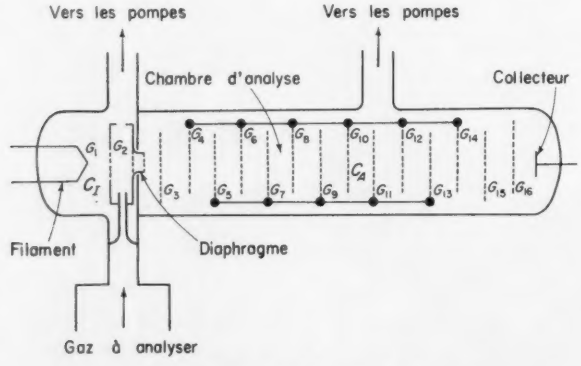

FIG. 6. Schéma de principe de l'analyseur de Bennett.

électrons issus d'un filament F et accélérés grâce à un système de grilles G_1 et G_2 portées à un potentiel positif d'environ 150 volts par rapport au filament.

Les ions positifs formés sont extraits de la source d'ions sous l'action d'un potentiel fortement négatif appliqué sur la grille G_3, et pénètrent dans une chambre d'analyse C_A où ils sont soumis à l'action d'un champ électrique alternatif $\vec{E}$ appliqué entre les grilles G_4, G_6, G_8, G_{10}, G_{12}, G_{14} d'une part, et G_5, G_7, G_9, G_{11} et G_{13} d'autre part.

Parmi tous les ions qui évoluent dans la chambre C_A, seules les particules de charge e et de masse m dont le rapport $\frac{e}{m}$ a une valeur déterminée, reçoivent en permanence de l'énergie empruntée au champ haute-fréquence et, après passage dans le filtre d'énergie constitué par les grilles G_{15}, fortement positive (150V environ) et G_{16}, à nouveau négative, peuvent atteindre le collecteur d'ions C qui est au potentiel zéro. Ce collecteur est inaccessible aux autres ions qui ne reçoivent pas suffisamment d'énergie pour vaincre la barrière de potentiel au niveau de la grille retardatrice G_{15}.

Ainsi, la mesure du courant ionique recueilli sur le collecteur C constitue une mesure de la concentration en ions de masse m dans l'échantillon de gaz présent sous faible pression dans le spectromètre, et par variation de la fréquence du champ HF ou, dans un intervalle étroit de masse, par variation de l'amplitude du champ, on fait défiler sur le collecteur d'ions les particules de rapports e/m différents.

Fréquences et masses sont liées par une relation de la forme :

$$m = K\frac{E_0}{f^2}$$

dans laquelle E_0 représente la tension d'accélération des ions (elle est de l'ordre de 20 volts) et K une constante de proportionnalité qui est fonction de la distance séparant les grilles sur lesquelles est appliqué le champ HF, et également du nombre de ces grilles.

La littérature fait état des possibilités intéressantes de ce spectromètre pour les analyses qui sont considérées ici ; on y trouvera en particulier des informations concernant une version du spectromètre de Bennett, développée dans les laboratoires Telefunken et dont la Fig. 7 montre une vue d'ensemble.

D'après les résultats mentionnés par le Dr. Schütze[9] il apparaît que :

(1) l'analyseur de Bennett, du moins dans cette version déjà ancienne, permet une exploration comprise entre $m = 1$ et $m = 100$, son pouvoir de résolution $S = \frac{m}{\Delta m}$ est de l'ordre de 25.

(2) en ce qui concerne la sensibilité, elle permet de déceler des pressions partielles de l'ordre de 10^{-7} torr.

(3) d'autre part, grâce à la séparation, par un diaphragme en verre, de la source d'ions et de la chambre d'analyse, également à l'application sur la grille G_3 d'une tension fortement négative, le spectromètre se prête à l'analyse de mélanges gazeux dont la pression varie beaucoup avec le temps; plus précisément, le pouvoir de résolution et la sensibilité gardent des valeurs sensiblement constantes dans un intervalle de pression compris entre 5.10^{-4} et environ 10^{-6} torr.

Vol. 10 196

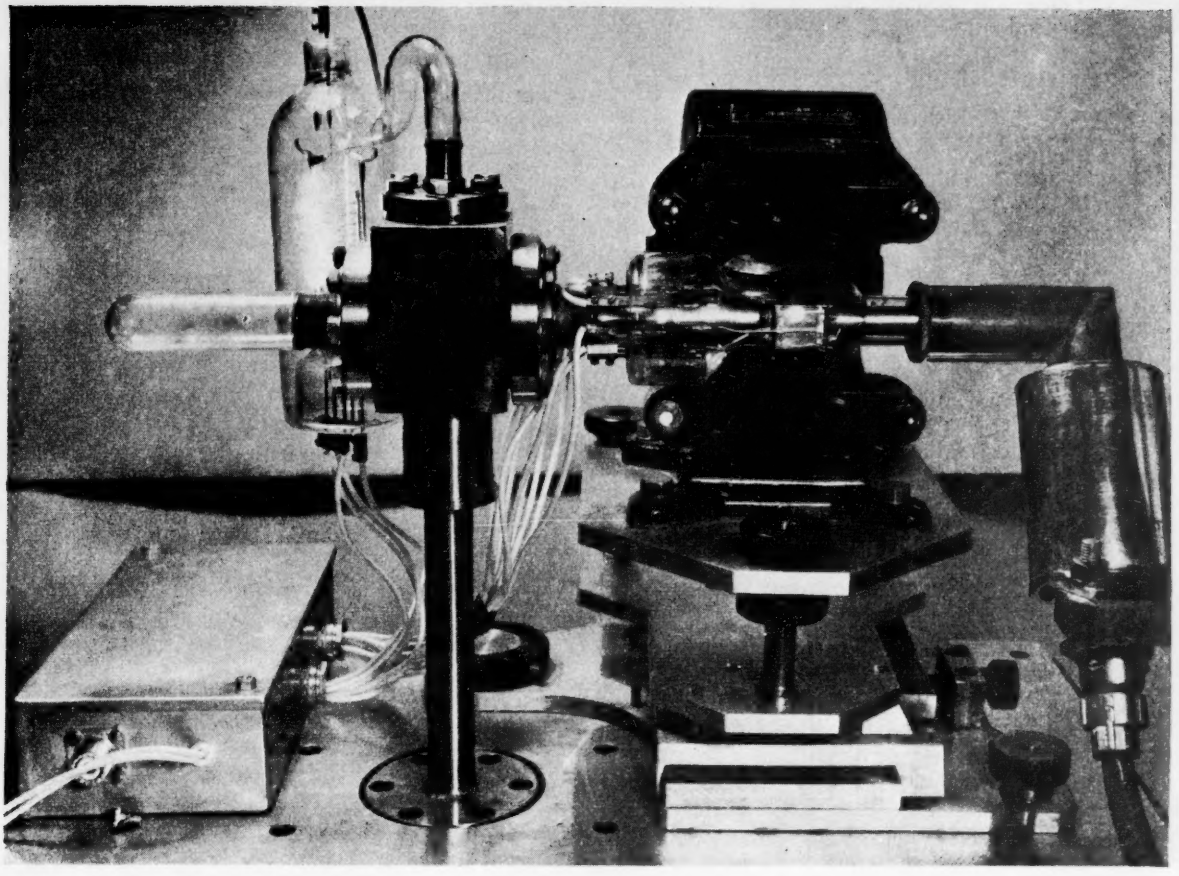

FIG. 7. Spectromètre de Bennett.

(4) une autre propriété importante de cet analyseur est qu'il permet de mesurer à la fois les pressions partielles et la pression globale du gaz dans la source d'ions ; cette dernière mesure s'effectue en appliquant une tension négative élevée sur la grille G_3 qui peut ainsi collecter toutes les particules ionisées issues de la source d'ions.

(5) la cellule d'analyse dont le volume n'excède pas 150 cm^3 est facilement étuvable et dégazable par chauffage *HF*. Enfin, en raison de la simplicité de sa structure interne les effets de surface sont très réduits.

Parmi les inconvénients à signaler, nous retiendrons les valeurs assez faibles de la sensibilité, du pouvoir de résolution et, associé à cela, le fait que le spectromètre n'est pas très bien adapté aux analyses à très basses pressions.

9. Comparaison des performances de l'Omégatron et de l'analyseur de Bennett

Le tableau suivant qui résume ce qui vient d'être dit, montre l'aspect complémentaire des performances de l'Omégatron et de l'analyseur de Bennett.

Performances	Omégatron	Spectromètre de Bennett
Domaine de *masse* exploitable (avec une résolution acceptable)	$1 < m < 100$	$1 < m < 100$
Pression maximum compatible avec un fonctionnement correct du tube	$P_{torr} < 10^{-5}$	$P_{torr} < 5.10^{-4}$
Sensibilité (plus petite pression partielle détectable)	5.10^{-11} torr	10^{-7} torr
Pouvoir de résolution (valeur moyenne)	$40 < S = \frac{m}{\Delta m} < 50$ (suivant la valeur du champ magnétique utilisé)	$9 < S < 25$
Précision	entre 3 et 10%	

10. Résultats expérimentaux

Avant de terminer, indiquons rapidement quelques résultats expérimentaux :

Lors de l'étude des diodes d'essai comme moyen de contrôle des matériaux électroniques, M. Freytag a montré l'influence sur le comportement des cathodes, de la nature des verres utilisés pour la fabrication des ampoules dans lesquelles sont montées ces diodes, et, parmi les produits de dégazage de certaines ampoules, a suspecté le chlore d'être responsable, au moins partiellement, des anomalies présentées par les caractéristiques d'émission. Pour vérifier cette hypothèse, nous avons étudié, au moyen de l'Omégatron, la composition du gaz dégagé par quelques-unes de ces ampoules, et ce, à différentes températures et pour deux sortes de verre français : le MO2A et le MO2B.

Les enregistrements suivants illustrent les résultats obtenus avec une ampoule de verre MO2A (ref. 280 49 31).

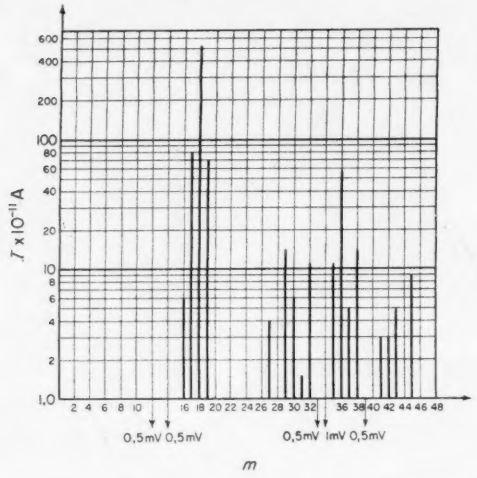

FIG. 8. Spectre du gaz résiduel à la température ambiante dans une ampoule de verre MO2A. Pression totale $P=3.10^{-6}$ torr.

La Fig. 8 montre le spectre du gaz résiduel dans l'ampoule, celle-ci ayant été pompée pendant une dizaine d'heures. On remarque en particulier l'existence des pics de masse 18

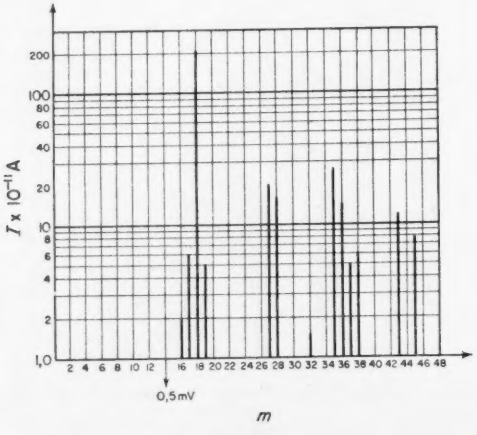

FIG. 9. Composition du gaz dégagé par une ampoule de verre MO2A après un palier d'étuvage à 200°C (durée 3 heures). Pression totale $P=1,6.10^{-6}$ torr.

(vapeur d'eau), 19 (fluor)*, 28 (oxyde de carbone), 32 (oxygène) 35 et 37 (chlore)*.

L'ampoule ayant été étuvée pendant trois heures à 200°C, un nouveau spectre fut enregistré qui montre, qu'exception faite pour le chlore, les pics ont maintenant des amplitudes plus faibles, en particulier celui de la vapeur d'eau (Fig. 9).

Enfin, on voit sur la Fig. 10 les résultats d'une autre analyse effectuée après un palier d'étuvage, d'une durée de

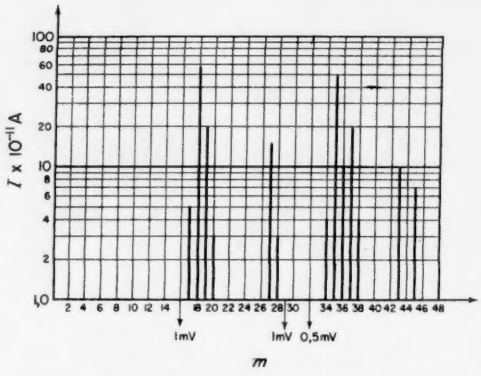

FIG. 10. Composition du gaz dégagé par une ampoule de verre MO2A après un palier d'étuvage à 450°C (durée 2 heures 30). Pression totale $P=1.10^{-6}$ torr.

deux heures et demie à 450°C. Les pics 35 et 37 ont encore augmenté, ce qui prouve qu'à cette température, assez voisine du point de ramollissement du verre, on n'a pas pu se débarrasser du chlore absorbé par l'ampoule.

D'une manière générale nous avons observé des spectres analogues pour le verre MO2B, à ceci près que les pics relatifs aux masses 13, 20, 35, 36 et 37 sont plus petits et tendent à disparaître lors des périodes d'étuvage.

Les perturbations relatives à l'émission des cathodes se manifestant beaucoup plus nettement lorsque l'on utilise des ampoules en verre MO2A, il semble bien qu'on puisse rendre le chlore et ses composés responsables des anomalies observées ; l'intérêt de l'emploi du verre MO2B devient alors évident ainsi que la nécessité d'un nettoyage chimique du verre MO2A (par exemple avec une solution de potasse) si l'on préfère pour des raisons technologiques l'emploi de ce verre à celui du MO2B.

Des analyses similaires ont été effectuées à l'aide du spectromètre de Bennett. Voici, à titre d'exemple, les spectres du

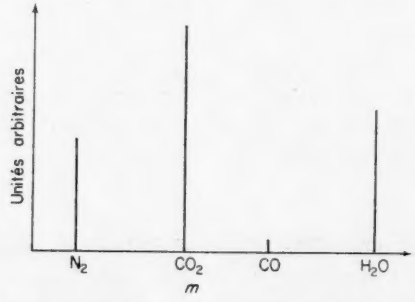

FIG. 11. Gaz dégagé par du verre fritté à 420°C.

* Il est à noter que ce verre est affiné à l'aide de chlorures ou de fluorures.

gaz dégagé par deux échantillons de verre fritté à 420°C[10] (Fig. 11 et 12) ; on voit que les principaux constituants de

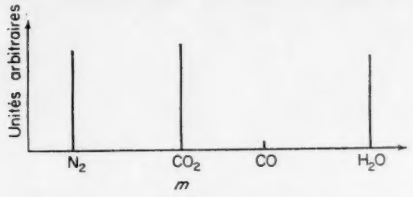

FIG. 12. Gaz dégagé par du verre fritté à 420°C.

ce gaz sont l'azote, la vapeur d'eau, l'oxyde de carbone et le gaz carbonique.

11. Conclusion

Bien d'autres mesures ont été faites à l'aide de l'Omégatron et du spectromètre de Bennett : les résultats obtenus et la comparaison des performances de ces deux appareils montrent qu'ils ont des qualités complémentaires et que leur emploi simultané doit permettre d'effectuer un grand nombre d'analyses, indispensables à la compréhension du mécanisme interne des tubes électroniques.

En raison de sa sensibilité élevée l'Omégatron sera utilisé préférentiellement pour la détermination de pressions partielles très faibles ; au contraire, lorsqu'il s'agira d'étudier des phénomènes associés à des fluctuations importantes de pression et nécessitant la mesure de pressions partielles relativement élevées, on devra utiliser le spectromètre de Bennett.

Associés à des circuits électroniques à réponse rapide, ces deux spectromètres peuvent être valablement utilisés pour l'observation de phénomènes évoluant rapidement, étant entendu qu'il faut adopter un compromis entre les exigences relatives d'une part, à la sensibilité des mesures et d'autre part, à la durée des enregistrements, l'une et l'autre variant en sens inverse.

Références

[1] L. S. Nergaard ; *Thermionic Emitters*, Fourth National Conference on Tube Technique, 10–12 Sept. 1958, New York.

[2] S. Dushman ; Vacuum Technique, *Analysis of gases in metals*, 648–653.

[3] H. Sommer, H. A. Thomas, and J. A. Hipple ; *The measurement of e/m by cyclotron resonance, Phys. Rev.* **82**, 97 (1951).

[4] J. Woodford and J. H. Gardner ; *Method for eliminating Omegatron radial field errors or for direct measurement of mass ratios, Rev. Sci. Instrum.* **25** (Jan. 1956).

[5] C. E. Berry ; *Trajectories in the Omegatron, J. Appl. Phys.* **25** (Jan. 1956).

[6] W. M. Brubaker and G. D. Perkins ; *Influence d'une distribution de champ électrique et magnétique dans le fonctionnement de l'omégatron, Rev. Sci. Instrum.* **27** (Sept. 1956).

[7] R. J. Warnecke, Jr. ; *Etude et réalisation d'un spectromètre de masse du type Omégatron. Application à la détection des fuites et à l'analyse des gaz sous faible pression, Annales de Radioélectricité* (Oct. 1959).

[8] J. S. Wagener and P. T. Marth ; *Analysis of gases at very low pressures by using the omegatron spectrometer, J. Appl. Phys.* **28**, (Sept. 1957).

[9] Communication privée.

[10] J. Ruf ; *Anwendung des HF-Massenspektrometers in Röhrenbau, NTG-Tagung, NW*, Hamburg (1958).

The Applicability of the Omegatron to Continuous Analysis of Residual Gases

FRANKLIN A. BAKER and TIZIANO A. GIORGI

The Polytechnic, 309 Regent Street, London, W.1
and
Northampton College of Advanced Technology, London, now at S.A.E.S. Getters, Via Gallarate 215, Milan, Italy

An experimental study is described in which residual gases were analysed by means of a cyclotron resonance mass spectrometer of the omegatron type. Analysis was continuous before, during and after both (a) ion pumping with a Bayard–Alpert pattern hot-cathode gauge and (b) the dispersal of a barium getter. Results are more extensive than any published hitherto and are presented both as mass spectra and the variation of gas constitution with time throughout each stage of the above operations. The study illustrates the potentialities of the omegatron as a tool for solving many problems existing in vacuum technology. In particular, by regarding the Bayard–Alpert pattern gauge as an electron tube, it is shown that the omegatron is well suited to the analysis of residual gases during the manufacture and life of tubes.

1. Introduction

Whatever the type of pump employed to produce a low gas pressure the relative abundance of gases in a mixture is inevitably altered during pumping. Consequently, it is true to say that most operations carried out *in vacuo* are in fact conducted in an unknown mixture of gases. For example, problems, such as those faced by getter manufacturers, are usually investigated in a series of known gases with as high a degree of purity as possible. Although this approach is in many respects desirable and is most likely to illustrate fundamental mechanisms it is unquestionably exceedingly difficult, in practice, to be sure of attaining the desired degree of purity. Further, it is frequently impossible to predict what will occur, in a given situation, when a mixture of gases is present, even if data is available for each of the individual constituents alone. It has, therefore, been suggested[1] that the mass spectrometer might be used to solve problems arising in high vacuum technology.

Unfortunately, the mass spectrometer is frequently a large vacuum system not readily adaptable to investigations involving individual vacuum tubes. In addition, the mass spectrometer can rarely be thoroughly degassed and is therefore likely to provide a mixture of gases which is different from that normally present in the tube under test.

From the time of its introduction[2] considerable interest has been shown in the omegatron. This is particularly due to its small size, relatively simple construction and the ease with which it may be degassed. In point of fact, two types of omegatron have been investigated.

(a) The more complicated structure, characterised by the use of guard rings, which follows most closely the original design ; and
(b) the simplified structure first used by Alpert and Buritz[3].

A number of investigators have set up and used omegatrons of both types. The results of these studies have, most frequently, been presented as a mass spectrogram of diffusion pump ultimate. Perhaps the most noteworthy exceptions are :

(i) the work of Garbe[4] and Wagener and Marth[5], each of which present a mass spectrogram over a barium getter, and
(ii) that of Diels[6] in which three mass spectrograms illustrate the changes in gas constitution during ion-getter (titanium) pumping.

The present work is characterised by the fact that all results have been taken by continuously scanning the atomic mass range. Thus a continuous record was made of the changes of gas constitution occurring, from diffusion pump ultimate, throughout the various operations that might be carried out during the manufacture and use of a special electron tube. By this means it is possible to determine not only the relative abundance of the more important gases present at any instant but also, from the variation of partial pressures with time, to assess the more important mechanisms involved in the sorption and desorption of gas.

2. Description of experimental apparatus

It was decided to use an omegatron of relatively simple construction in order to minimise the number of variables that would have to be dealt with during use. The omegatron actually used is of the type which has already been described by Reich and Nöller[7]. All the electrodes are of platinum and a relatively rigid construction is achieved by mounting one of the r.f. plates on the grounded shield which screens the lead which carries the resonating ion current.

The necessary r.f. potential was obtained from a video oscillator (Marconi Type TF885A/1). The stability of this instrument was checked, using a crystal controlled frequency

meter, and found to be perfectly satisfactory after an initial warming up period. Resonating ion current (from 10^{-7}A to 10^{-14}A) was measured by means of a vibrating reed electrometer (Ekco Type M572) and continuously registered on a potentiometer type pen recorder (Cambridge Inst.). This instrument was provided with a supplementary pen which enabled a frequency record to be made ; thus facilitating the identification of peaks.

Alcomax 111 alloy energising blocks are used in the construction of the permanent magnet (W. Jessop). The field across the 37 mm air gap was approximately 2600 oersted. Pole-pieces were of mild steel with a 75 mm diameter and were shaped so as to provide a relatively constant flux density in the interaction volume of the omegatron. The frequency range from 30 Kc/s to 5 Mc/s was found sufficient to cover the necessary mass range. Scanning of this range was achieved by means of a reversible d.c. motor coupled to the r.f. oscillator capacitor drive.

The Bayard–Alpert pattern ion gauge was normally operated by means of a standard stabilized electron emission unit (A.E.R.E. Harwell Type 1075B). Positive ion currents (from 4×10^{-4}A to 4×10^{-10}A) were measured by means of an electrometer unit of the type described by Allenden[8] and continuously registered on a small pen recorder.

Getters used in this study were " KIC " Size 6613 (Union Carbide Ltd.) which, on firing, evaporate pure barium. The barium-aluminium alloy is contained in an iron tube and supported by a nickel loop. In the present study the loop was cut so as to allow degassing and firing by the direct passage of current.

Electrical apparatus and all borosilicate glass vacuum system are illustrated (Fig. 1). The experimental tubes were

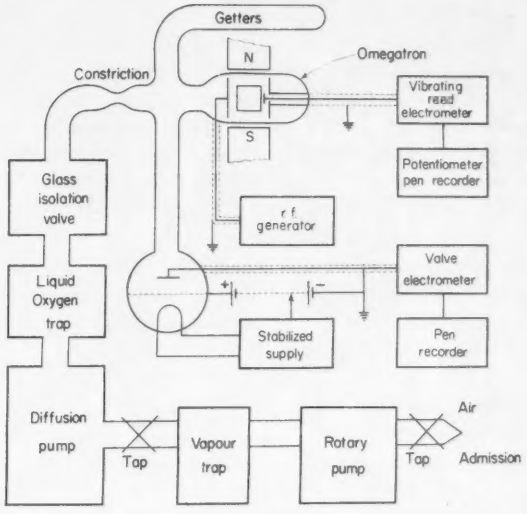

FIG. 1.

evacuated, through a 20 mm diameter ground glass isolation valve, by means of a two stage mercury diffusion pump. The isolation valve could be opened or closed at will by means of a small permanent magnet. A liquid oxygen trap was used to minimise the influence of mercury and other vapours on the pump ultimate.

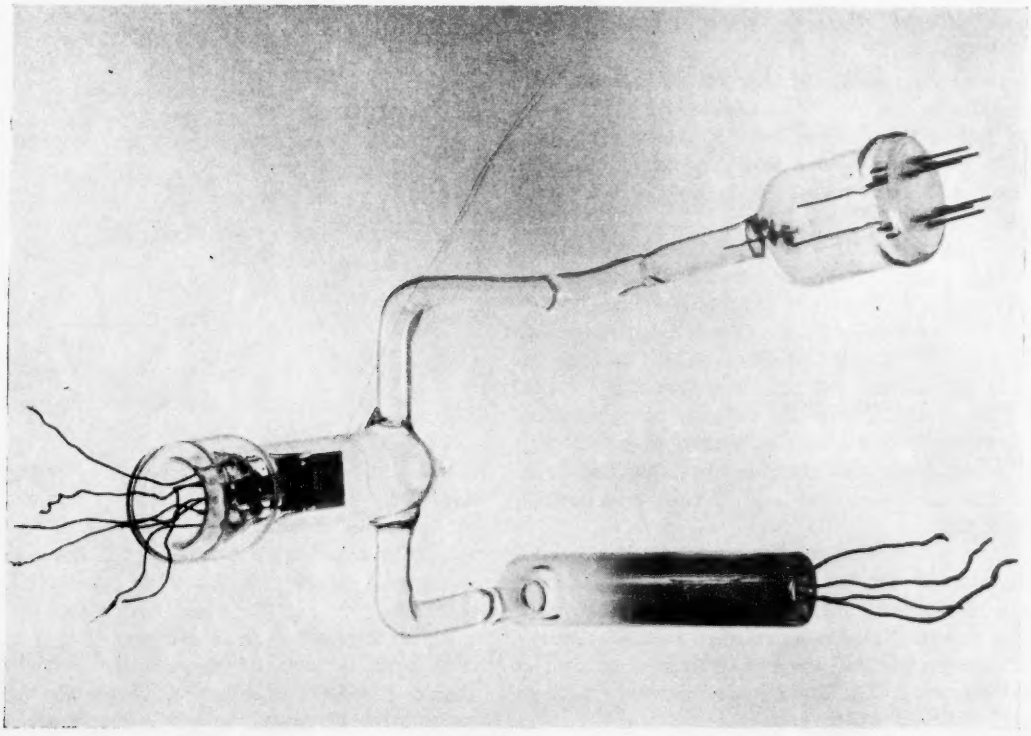

FIG. 2.

3. Experimental procedure

No experiment was conducted before the system was thoroughly degassed. This was accomplished by first baking for a few hours at from 400° to 450°C and second degassing, for approximately one hour, the getters and metal gauge structures. The latter was achieved primarily by electron bombardment in the Bayard–Alpert gauge and by radio frequency heating of the omegatron. This procedure was usually repeated two or three times after which no difficulty was encountered either over maintaining a pressure in the range from 1×10^{-7} torr to 8×10^{-10} torr, with the glass valve closed, or the consistency of results.

The speed at which the mass range was scanned was adjusted to provide adequate resolution coupled with sufficient speed to allow changes in gas constitution to be followed. (On average the range from 70 Kc/s to 450 Kc/s or 60 a.m.u. to 10 a.m.u. was covered in 100 sec.).

Experiments were conducted in two phases. In the first phase analyses were taken from the pump ultimate through degassing of the Bayard–Alpert gauge, during a period of ion-sorption pumping with the gauge isolated from the diffusion pump and, subsequently, with the ionisation gauge electron accelerating potential switched off.

In the second phase analyses were taken :

(i) throughout getter degassing, whilst pumping was continued with the diffusion pump ; and

(ii) before, during and after activation of the getter with the ion gauge sealed off (by glassblowing) from the diffusion pump (Fig. 2.).

4. Experimental results

The results of both phases of these experiments are presented in two ways :

(a) Composite mass spectra illustrate the gas constitution before and after some specific operation.

(b) Partial pressure indications, of the more abundant residuals, are plotted against time in order to illustrate the manner in which changes, shown in (a), have occurred.

Thus, Fig. 3 shows composite spectra of the diffusion pump ultimate and the gas constitution during degassing, i.e., the changes brought about by initiating degassing are illustrated. The most striking point here is the evolution of masses 28 and 32. Clearly, masses greater than about 44 a.m.u. are not resolved although their presence is to be observed. The precise form of the diffusion pump ultimate was found to vary in detail from experiment to experiment. These variations were attributed to slight variations in charging the liquid oxygen trap and in turn, very largely, to mercury vapour.

Fig. 4 shows the variation in gas constitution with time during degassing of the electrode structure (Bayard–Alpert gauge). The evolution of masses 28 and 32 was thought to be primarily due to the complex reaction between carbon, on the hot tungsten filament, and oxygen from water vapour to form carbon monoxide. This result confirms the findings of Blears[1].

At the start of ion pumping (Fig. 5) masses 28, 32 and some

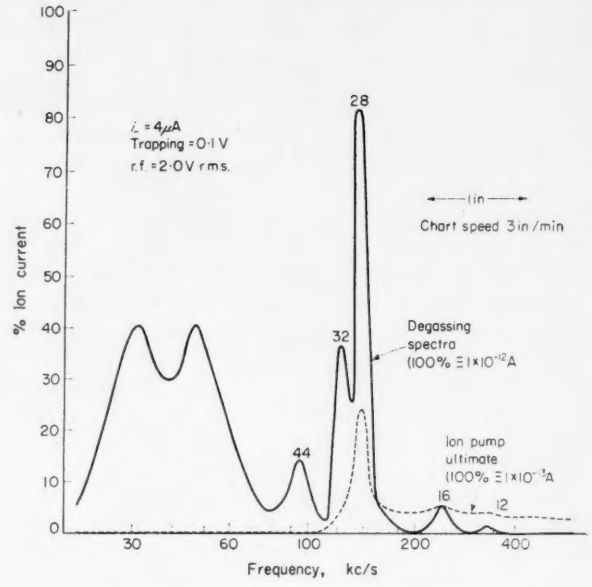

FIG. 3.

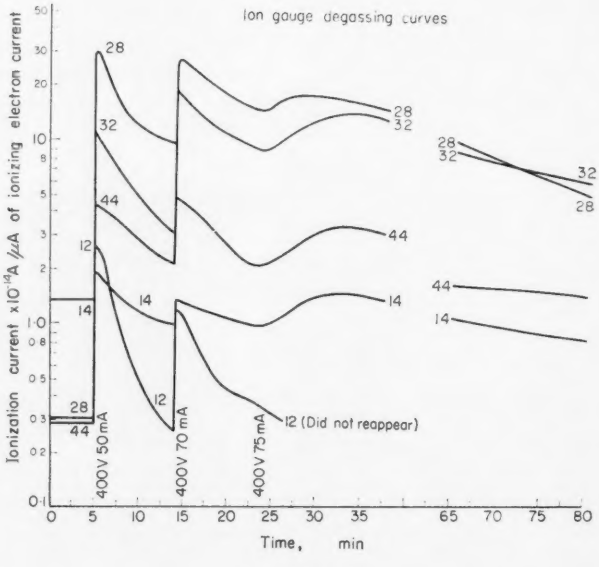

FIG. 4.

in excess of 44 are the most abundant. Pumping appears to remove the larger mass numbers more rapidly. Here it is important to consider the collision cross sections of the various masses for electrons, i.e. the illustrated variations of positive ion current with time do not reflect the true variations of partial gas pressures with time.

At the termination of ion pumping (Fig. 6) mass 28 is the only peak of any consequence. In order to terminate pumping, without causing a significant change in the temperature of the gauge, the grid potential was removed and the filament left operating (Fig. 7).

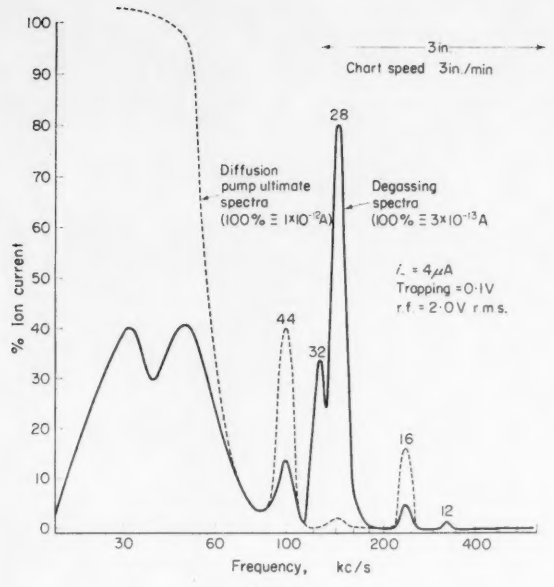

FIG. 5.

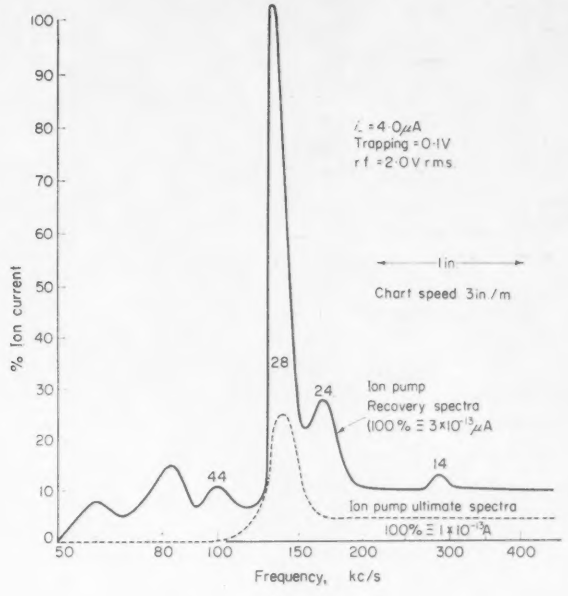

FIG. 7.

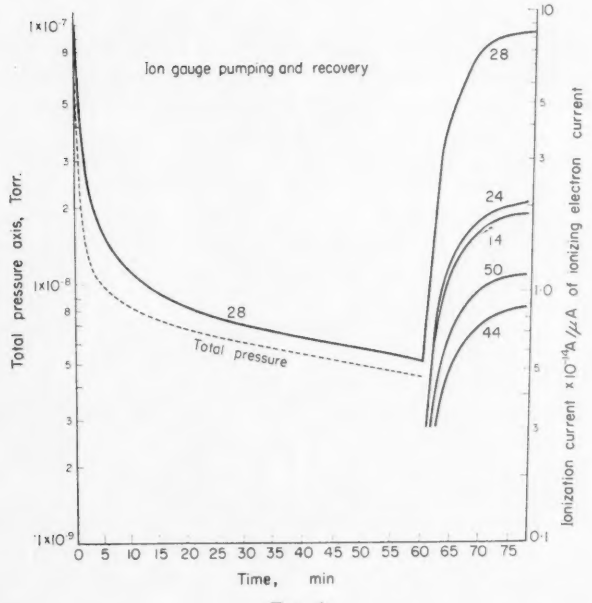
Ion gauge pumping and recovery
Total pressure axis, Torr.
Total pressure
Time, min
Ionization current × 10⁻¹⁴A/μA of ionizing electron current

FIG. 6.

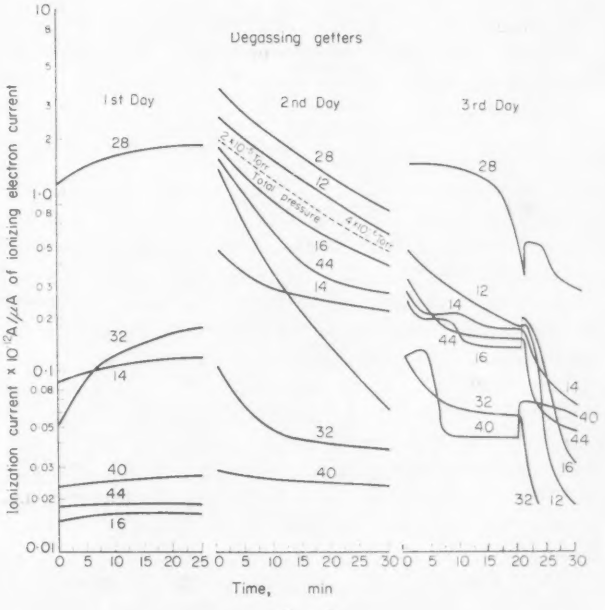

FIG. 8.

Recovery of gas under these conditions is primarily mass 28. A careful analysis of the cracking pattern obtained shows that this is almost entirely due to carbon monoxide. An interesting check is provided here by comparing the changes in total pressure, indicated by the Bayard–Alpert gauge, with the partial pressure recorded from the omegatron.

In the second phase of the experiments a number of small getters were mounted in a side tube (Fig. 8). Changes which occurred during degassing the metal gauge structure and getters differ from that illustrated in Fig. 4 only in detail, with the exception of the appearance of a significant quantity of mass 40. Again mass 28 is the most abundant gas present.

The final results were obtained with the gauges and getter tube sealed off from the pumps by glassblowing. No special precautions were taken over preheating the seal-off constriction and a relatively high total pressure resulted.

Fig. 9 illustrates the gas constitution before and after firing a getter. Clearly, masses 28, 14 and 44 predominate at seal-off whereas, after firing the getter, masses 40, 20 and 28 are of primary importance and masses 7, 14, 18 and 32 of secondary importance. Fig. 10 illustrates the changes occurring during and after firing the getter. It is important to note that the getters were fired relatively slowly by the direct passage of current, i.e. they were not " flashed ".

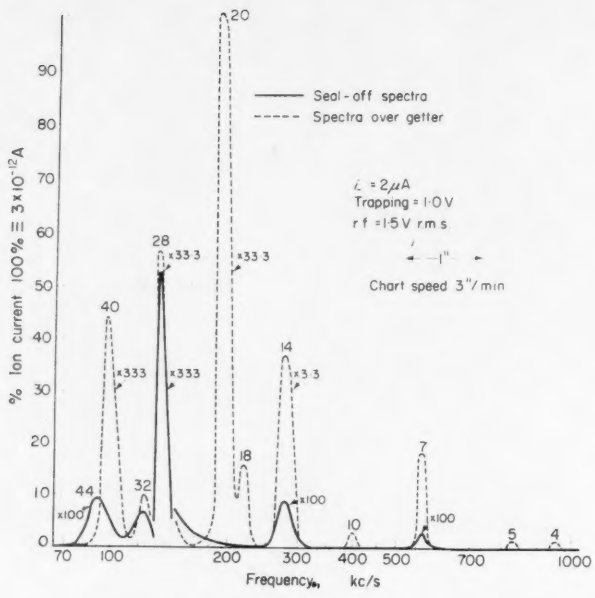

FIG. 9.

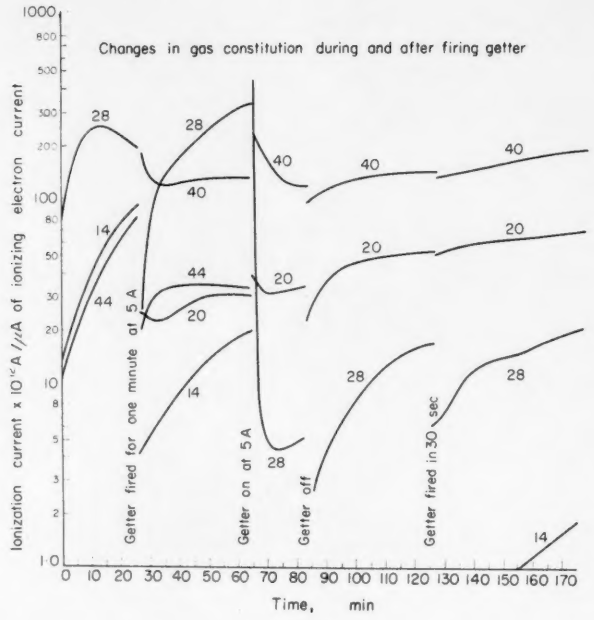
Changes in gas constitution during and after firing getter
Ionization current × 10⁻¹²A /μA of ionizing electron current
Getter fired for one minute at 5A
Getter on at 5A
Getter off
Getter fired in 30 sec
Time, min

FIG. 10.

This procedure was repeated and the results found to be consistent. The peaks at mass 40 and mass 20 were attributed to argon.

5. Conclusions

An experimental study, in which residual gases were analysed by means of a cyclotron resonance mass spectrometer of the omegatron type, has been described. In this study it is considered that the ionisation gauge may be regarded as a vacuum tube, with an electrode structure of tungsten and molybdenum. Thus, the omegatron is examined as a means of measuring residual gases during the manufacture and life of a vacuum tube.

It has been shown that a relatively simple version of the omegatron, where no special attention was given to attaining a high resolving power, is well suited to the study of this type of problem. Particularly important, in this type of work, is the relatively small size of the instrument and the ease with which it may be degassed.

The characteristic of this series of experiments is the way in which the mass range has been continuously scanned. This allows a record of partial pressure indications to be made against time in addition to the more usual mass spectrograms. One difficulty here is that the speed of scanning must be slow enough to provide adequate resolution in the record, i.e. the more rapid changes with time (transients) are not observed.

The technique employed ensured that a frequency scale was continuously marked off on the recorder chart with a supplementary pen. Scanning was alternately up and down the frequency scale. Thus by comparing peaks, on successive runs, against the frequency scale no difficulty was encountered over establishing the resonant frequency of any particular peak. However, it was observed that the resonant frequency for a particular mass number was apt to vary with the total pressure (never found to be in excess of 5 per cent of the resonant frequency at 100 Kc/s). So that some care was necessary over the identification of peaks. In point of fact, it is best to start by calibrating the instrument in a series of very pure known gases over as wide a range of pressures as possible. This allows a table of relative sensitivities to be drawn up and, under *ideal* conditions, it is then possible to work with true partial gas pressures. In this work very careful calibration was undertaken in an argon atmosphere and the sensitivity found to be $5\mu A/mA/\mu Hg$ under normal operating conditions (1.0 V r.m.s. ; 0.3 V trapping ; 0.5 μA electron current).

Throughout this work no difficulty has been encountered over the appearance of " ghost " peaks which Alpert and Buritz[3] regarded as a major difficulty to be encountered in using the instrument. We can only suggest that this may be connected with the cleanliness of the instrument.

It is very interesting to find carbon monoxide the most abundant residual during and after ion pumping with the Bayard–Alpert gauge. This result would indicate that the residuals and some carbon monoxide are removed more or less permanently. The typical total pressure curve with time[9] during pumping is therefore probably exhibiting a saturation characteristic due to the presence of carbon monoxide. However, this argument must only be applied to this particular mixture of gases. Again, it is curious that, although Blears[1] found carbon monoxide to be formed at a hot tungsten filament in the presence of water vapour, very little water vapour has been detected in these experiments.

Finally, the gas analysis over a barium getter differs from results previously presented. In particular, Wagener and Marth[5], using the same type of getter, did not observe any argon (40 a.m.u.) but did find a significant quantity of carbon dioxide (44 a.m.u.). Initially, this fact caused the present

Vol. 10 196

writers some uncertainty as to the identity of the principal peak. In point of fact, sufficient resolution was attained in these experiments to permit us to identify the peak as 40 a.m.u., i.e. a resonant frequency of 100 Kc/s as opposed to 90 Kc/s for 44 a.m.u. Ultimately, the most convincing evidence lies in an examination of the cracking patterns to be expected from the two gases.

Acknowledgements

The authors wish to thank Mr. F. Y. Poynton, Head of Department of Physics, Northampton College of Advanced Technology, for the facilities to carry out this work.

Thanks are also due to Mr. J. Yarwood, Head of the Physics Department, The Polytechnic, 309, Regent Street, London, W.1, for the interest he has shown.

References

[1] J. Blears ; *J. Sci. Inst.*, (Supplement No. 1), **28**, 36 (1951).
[2] H. Sommer, H. A. Thomas, and J. A. Hipple ; *Phys. Rev.* **82**, 697 (1951).
[3] D. Alpert and R. S. Buritz ; *J. Appl. Phys.* **25**, 202 (1954).
[4] S. Garbe ; *Vortrag Nr.* 32, *Philips*, Aachen (1958).
[5] J. S. Wagener and P. T. Marth, *J. Appl. Phys.* **28**, 1027 (1957).
[6] K. Diels ; *Vide*, No. 75 Mai-Juin, 143 (1958).
[7] G. Reich and H.-G. Nöller ; *Zeit. Phys. Nukl.* **9**, 617 (1957).
[8] D. Allenden ; *Electronic Eng.* **30**, 31 (1958).
[9] F. A. Baker and J. Yarwood ; *Vakuum-Technik* **6**, 147 (1957).

DISCUSSION

Question from Mr. S. P. Wolsky

What evidence do you have that the observed mass 32 was due to oxygen. It has been widely reported in the literature that oxygen reacts with the carbon present in tungsten filaments to produce CO. In our laboratory, the deliberate admission of oxygen in a similar system caused only a change in the CO peak.

Answer. The only peaks we have identified are as follows :

28 a.m.u.—carbon monoxide
40 a.m.u.—argon
44 a.m.u.—carbon dioxide.

In these cases identification was made after a careful examination of the respective craking patterns.

During this work peaks were frequently observed at 16 a.m.u. and 32 a.m.u. In the absence of other peaks, or evidence to the contrary, it was assumed that these were due to atomic and molecular oxygen respectively.

ol.
10
960

Double Pirani Bridge Leak Detector

G. CALVI

Centro Siciliano di Fisica Nucleare, Catania, Italy

For leak detecting in a vacuum system, a device has recently been suggested founded on the pressure drop in suction pipes.[1]

We wish to report the construction and testing of a device with variable sensitivity founded on the same principle.

In the tubes of a vacuum system, in operation the pressure drop depends on the resistance of the tubes to the flow of the gas.

But when a leakly vessel is connected to this system, the pressure drop is also a function of the size of the leak.

All this is evident if we look at the analogy existing between an electric circuit and a pumping system.

We consider an electric circuit constituted of a power supply with zero internal resistance and a wire of determined length and constant cross section.

If we represent with OA the length of the wire (Fig. 1)

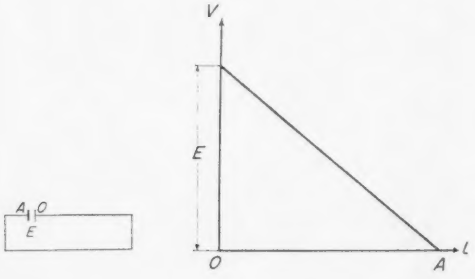

Fig. 1.

with OV the voltage E of the power supply, the line between V and A shows the variation of the voltage along the wire.

We consider now a circuit constituted by two or more parts of various cross sections, in such a way that the resistance per unit length is different in each part of the circuit (Fig. 2).

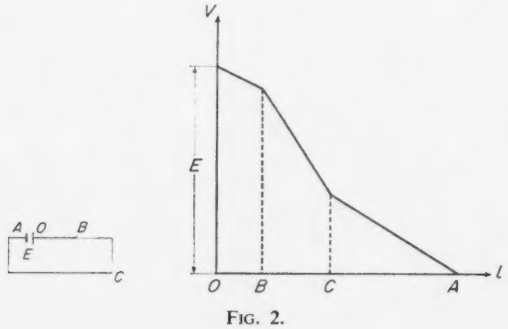

Fig. 2.

Between V and A there is not a straight line but a broken line because the voltage drop in each part of the circuit depends on its resistance.

The slope of each part of the broken line is a function of the applied voltage and the resistance per unit length.

We consider now a vacuum system made up of a diffusion pump and a rotary pump ; a vessel to be tested is connected to this system. For this circuit also we can trace a diagram similar to Fig. 2, marking along the abscissa the lengths of the parts of pipes and on the ordinate the pressures (Fig. 3).

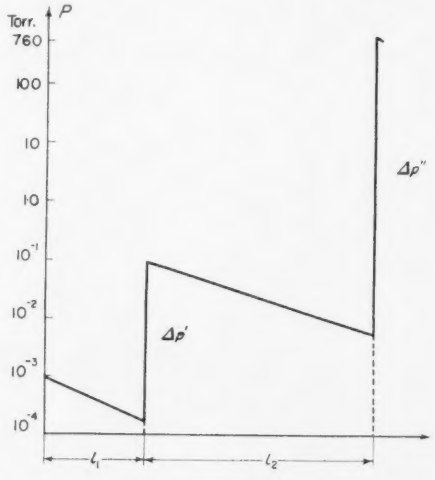

Fig. 3.

In this diagram l_1 is the equivalent length of the vessel and l_2 the length of the pipe between the diffusion and rotary pump ; $\Delta p'$ and $\Delta p''$ are the pressure drops in the diffusion and in the rotary pumps respectively.

As for the electric circuit, it is clear that the slope of the curve along each part is function of the size of the leak.

As before, moreover, neglecting the internal resistance of the pumps, which are equivalent to two power supplies, we assume the size of the pipes proportional to the slope of each part of the curve because the aerodynamics resistance of the pipe (molecular flow) is function of its size[2] :

$$R = K \frac{l}{d^3} \sqrt{\frac{\overline{M}}{T}}$$

where l is the length and d the diameter of the pipe, M the molecular weight and T the temperature of the gas flowing ; the pressure drop will be greater in the parts in which the size is smaller.

Thus, if in a part of the tube between the diffusion and the rotary pumps, we reduce the size of the pipes, the pressure drop between its ends will be greater than that with the larger pipe.

The diagram of Fig. 3 is changed as in Fig. 4. The part between *A* and *B* represent the size which has been reduced.

It is then clear that if we wish to utilize the pressure drop, it is better to make this in the part *AB* where the pressure drop is greater.

In mounting the above device we have made it in such a way that its sensitivity can be regulated by the size of the pipe and hence by the resistance of the part of pipe which is substituted when this device is inserted in a vacuum system.

We can do this, under the condition that the resistance of this part is not greater than the resistance of system.

In this way the limiting vacuum of the system is not altered by the insertion of the leak measuring device.

The leak detector has been built (Fig. 5) with a brass rod,

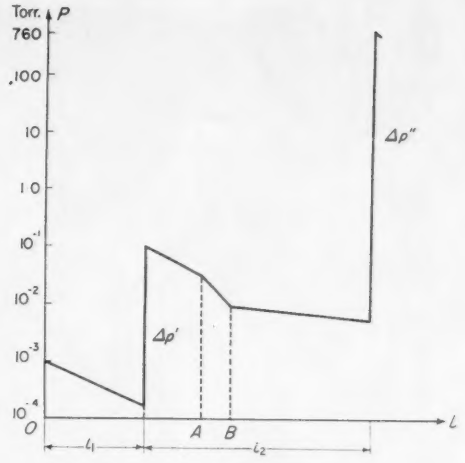

FIG. 4.

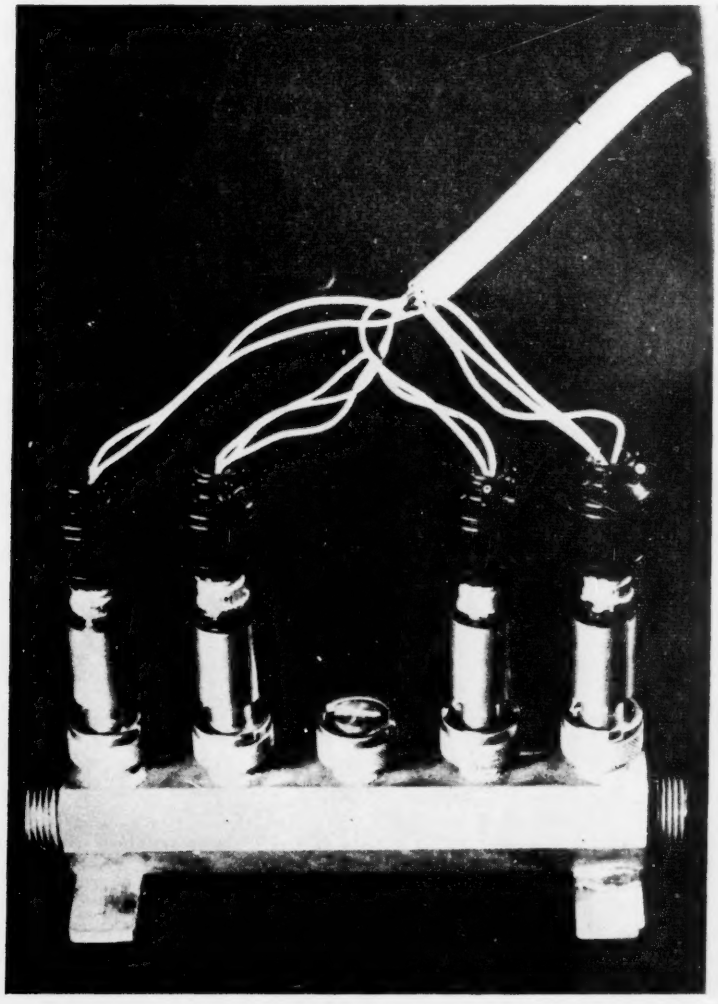

FIG. 5.

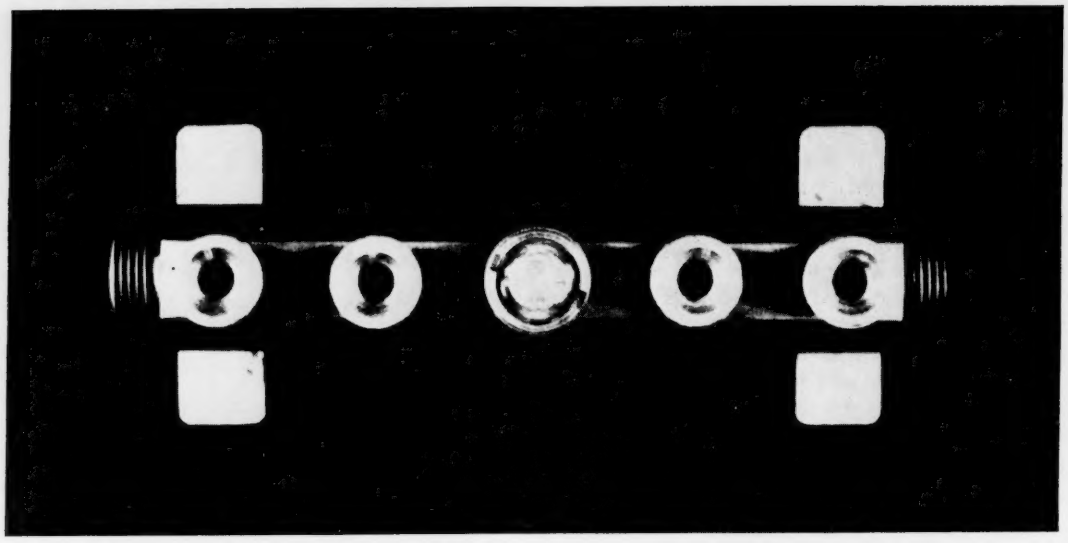

FIG. 6.

about 20 cm long, grooved along its axis and having at either end two unions, which make its mounting easy in a section of the vacuum system to be tested.

Two pairs of Pirani gauges are mounted in tubes connected perpendicularly to the 20 cm tube and equidistant from its ends (Fig. 6).

In the middle of this rod is inserted a throttle which is adjustable from the outside and which allows us to change the size of the tube. (The maximum diameter is 8 mm) (Fig. 7).

In such a way it is possible to change, within a wide range, the pressure drop between rod ends and therefore sensitivity of device as a leak detector.

The Pirani gauges mounted, as we have said, two by two on opposite sides of the throttle, are electrically connected as a Wheatstone bridge and in such a way that those placed on the same side in relation to the throttle form the opposite arms of the bridge (Fig. 8).

By so doing, even a little difference of pressure between two sides divided by the throttle, produces a corresponding change in the Pirani filaments resistance, and cause an unbalancing of the bridge.

The electrical circuit has been built inserting opportunely chosen resistances and potentiometers for balancing the bridge. The values of these have been chosen in such a way that the resistance of an arm of the bridge can change about 25 per cent by the mean value of the other arms.

The filaments of the Piranis are made of four cylindrical (minimignon) lamps 160 V—3 W whose bulbs have been opened.

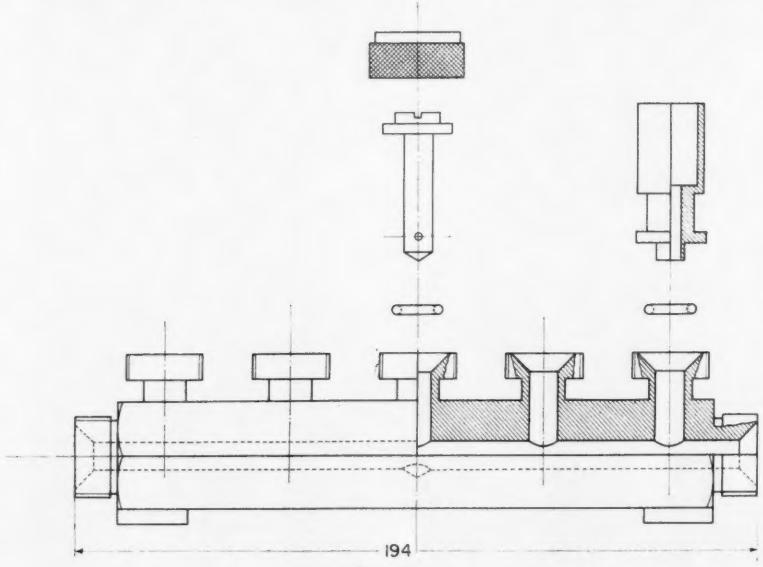

FIG. 7.

Vol. 10 1960

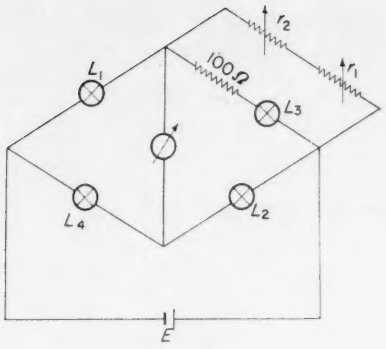

FIG. 8.

Such filaments have a cold resistance of 330Ω.

In order to bring such filaments to the Pirani working temperature, i.e. about 100 °C, the bridge must be fed by a constant d.d.p. of about 4 V. Under these conditions and in vacuum, the resistance of the filaments reaches 440Ω.

As a bridge null-point indicator a multiflex galvanometer was employed having a sensitivity of 1.2μV/mm.

The experimental results obtained have confirmed the hypothesis made.

The above device was connected to the pipe between diffusion and the rotary pumps of a pumping system to which was connected a vessel having a leak adjustable by a needle valve. The pressures in each part of this system have been measured, under various conditions.

It has been seen that the pressure drop between the two sides divided by the throttle, for constant size of this throttle, decreases with the decrease of the final pressure p_f of the vessel, and increases with the reduction of the throttle size.

With the maximum throttle size we have obtained a $\Delta p = 8\mu$Hg for $p_f = 1.1\mu$Hg, and a $\Delta p = 7\mu$Hg for $p_f = 0.8\mu$Hg. With the throttle size reduced to about $\frac{1}{4}$ of the maximum opening we have obtained :
for $p_f = 0.7\mu$Hg $\Delta p = 12\mu$Hg and for $p_f = 0.6\mu$Hg, $\Delta p = 11\mu$Hg.

Introducing, by the needle valve a leak into the vessel, for $p_f = 1\mu$Hg, $\Delta p_1 = 10\mu$Hg for maximum of the throttle size, and $\Delta p_2 = 14\mu$Hg for the above size reduced of about $\frac{1}{4}$, have been obtained.

When a little jet of H_2 was sprayed on the leak, another value for the Δp was obtained, and exactly :

$$\Delta p_1' = 11.5\mu\text{Hg} \quad \text{and} \quad \Delta p_2' = 16\mu\text{Hg}.$$

The change of the pressure drop in presence of the H_2, occurs because this gas, having a density less than that of air, enter the leak more readily than air.

The use of the device is as follows. After equilibrium pressure has been obtained in the vacuum system, the bridge is balanced with suitable potentiometers.

Then a very little jet of H_2 is sprayed on the surface of the vessel under test.

When this gas enters the vessel the bridge becomes unbalanced producing a deviation of the galvanometer index.

The sensitivity of this device is limited because any vacuum system suffers from unavoidable pressure fluctuations[3] which may amount to several per cent of the prevailing mean pressure. Those fluctuations cause, during the operation, an unstability in the null-point-indicator of about 6μV.

When the above device is set for maximum sensitivity, it can detect a leak of about 10^{-7} cc/s n.t.p.

This sensitivity should be compared with the average sensitivity of the mass spectrometry leak detectors (10^{-9} cc/s n.t.p.).

When we have large leaks the sensitivity is decreased in such a way that the instability produced by the pressure fluctuations, decrease suitably and the leak can be detected more easily.

The device has proved very useful for leak detecting the vacuum system of the 2 MeV Van de Graaff accelerator installed in this Centre.

References

[1] C. Minter-Clarke ; *Thermal Conductivity Leak Detector. Rev. Sci. Instrum.* **29**, 793 (1958).
[2] J. Yarwood ; *High Vacuum Technique*. Chapman & Hall Ltd., London.
[3] D. Clark ; D.S.I.R. Rep., 25 March 1945 and 20 April 1945.

DISCUSSION

Question from Mr. Steckelmacher

The full sensitivity obtainable with a Pirani leak detector can often not be realized because of lack of zero stability usually associated with the effect of unavoidable pressure fluctuations in the pumping system. It is therefore of interest to know how the leak detector described responds to changes in pressure and the short term stability of the zero reading found in practice. How does this effect limit the leak detection sensitivity obtainable in practice ?

How was the leak detection sensitivity quoted in the paper checked ?

Answer. After equilibrium pressure has been obtained in the vacuum system, it has been seen that an increase of pressure of about 2 per cent in the vessel under test produces a deflection of the galvanometer index of about 8 mm corresponding to about 10μV.

The zero instability of the galvanometer caused by the pressure fluctuations is of about 6μV.

The leak detection sensitivity was about of 10^{-7} cc/s n.t.p. ; and in practice, for the instability of the galvanometer, it is not possible to detect leaks smaller than this.

SESSION III

Origin of Residual Gases. Studies on the Conditions of Internal Surfaces of Tubes and their Gas Sorption and Desorption. Effects caused by Surface Alterations due to Gas Sorption.

Clean Surfaces and Sorption of Gases

A. NASINI, F. RICCA and G. SAINI

Istituto Chimico, Università di Torino, Italy

Chemisorption studies have progressively shown the importance of having available truly clean surfaces to obtain valuable results. To this end in the past few years extensive use has been made of evaporated films : however, recent trends seem to prefer the use of bulk materials (filaments, foils, tips) which can be degassed at high temperature. Such materials are much more versatile than films, and give a useful basis to the development of new techniques for the study of surface phenomena. These surfaces can be used any number of times ; they further permit the elimination of secondary phenomena, not strictly related to the surface, such as diffusion within the discontinuous structure of evaporated films. Techniques employing bulk materials are necessarily restricted to those metals which do not possess an appreciable vapour pressure at the degassing temperatures required. However, the results which have recently been obtained with this type of sorbent, by field emission microscopy, field ion microscopy and flash filament technique, are of great theoretical interest and can be applied to most of the other metals. We limit ourselves to quote the information obtained about the existence of : (a) various types of atoms on the metal surface, characterized by different sorption properties ; (b) different coefficients of surface diffusion for the different crystal faces ; (c) different states of the gas adsorbed on the metal. Concerning this latter point, useful information can be obtained from infrared spectroscopy of the adsorbed molecules. This complex picture of the observed phenomena is confirmed by our results for the adsorption of nitrogen and carbon monoxide on tungsten. The technique used to measure the velocity of adsorption, based on the flow of gas through a capillary of known conductance, is similar to that used in the field of getters ; the adsorbent is a tungsten lamina having a thickness of 0.0025 cm and a surface area of 27.5 cm^2 ; the measurements have been carried out in the pressure range of 10^{-7} to 10^{-8} Torr, and in the temperature interval between 90 and 480 °K. A problem of particular interest arises from the immeasurably low temperature coefficients and from the fact that the velocity of adsorption is initially independent of the surface coverage. The theoretical hypotheses put forward concerning this problem are briefly examined. The correct interpretation of such complex surface phenomena seems to be necessary even for the study of gas sorption by evaporated metal films.

Vol. 10 196

Introduction

In the last few years, the interest of researches in the field of heterogeneous catalysis has more and more tended towards the study of clean surfaces and their interactions with gaseous molecules, as a preliminary approach to the study of the very complicated phenomena involved in catalysis.

Clean surfaces, or surfaces contaminated in a controlled manner, present the only possible way of giving a basis to the theories on heterogeneous catalysis.

Most of the previous work, carried out on technical catalysts or on not properly clean surfaces, has been invalidated[1] : in fact the presence of preadsorbed gases on the surface may completely modify its adsorbing properties.

On the other hand recent knowledge in chemisorption appears to exclude that clean surface may be obtained by using metal powders as adsorbent, as often done in the past[2, 3].

However, it is quite easy to obtain very clean surfaces by using metal films, prepared by evaporation in vacuum. Hence the interest of workers in basic research on heterogeneous catalysis has been gradually converging towards problems and techniques which have many features in common with those presented by modern methods of production of high vacua.

Even on evaporated metal films, static measurements of the classical type were mainly performed[4], but a great deal

of new information about the mechanism of adsorption can obviously be obtained by kinetic measurements, which have to be carried out at much lower pressures if we want the process to last an appreciable interval of time.

So new techniques of measurement, based on the flow of gas in a capillary under Knudsen conditions, have been developed, partially utilising previous experience of researchers in the field of getters[5].

An example of systems employing this principle is given by the apparatus used in the present work for the study of

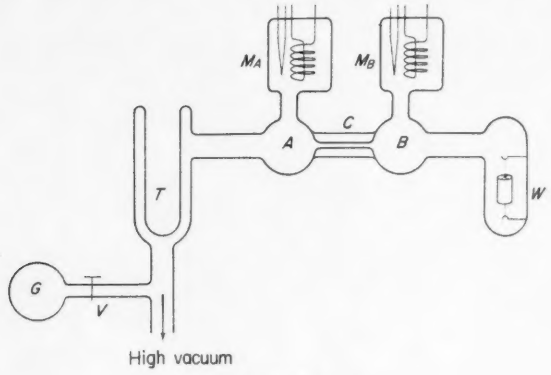

FIG. 1. Experimental apparatus.

sorption of gases on tungsten laminae, which will be described later in the experimental part (Fig. 1).

A second type of apparatus utilizing the same principle is the " flash filament cell "* of Becker and Hartman[6]. It is important to notice that in both these cases it is possible to make use of rather small adsorbing surfaces. Another technique utilising small adsorbing surfaces is that of Roberts[7–9] based upon the evaluation of the accommodation coefficient of neon on tungsten filaments. However the limits of such a method are clearly shown by its indirect approach and by its relatively small sensitivity.

It is interesting to note that the use of adsorbents of a small surface area, such as that of filaments, ribbons, laminae, and metal tips, has enabled the parallel development of new and important techniques for the study of surface phenomena such as the field emission microscopy, the field ion microscopy and the so-called technique of " ad-sorption spectra ".

The field emission microscope† shows the selectivity of the adsorption of gases on different crystal faces of the same adsorbing metal, and the surface diffusion of adsorbed films, in a large range of temperatures[10].

The field ion microscope‡ gives us useful information concerning the existence at the surface of the metal of atoms differently co-ordinated, and hence capable of different bonds for gaseous molecules[11].

Finally, the " ad-sorption spectra " technique§ gives us[11–16] good evidence for the existence of different states of the adsorbed film.

Such a result is confirmed for the case of carbon monoxide, by IR spectra of the adsorbed film, such as those obtained by Eischens[18].

*This apparatus consists of a bulb containing a tungsten filament as adsorbent, connected to an ion gauge. Gases can be introduced into this system at a controlled rate through a metal valve. The apparatus is connected to the pumping system through a movable glass plate with a small hole.

By operating the metal valve, a stationary pressure is reached, of the required value, then the tungsten filament is cleaned by heating, until the pressure again reaches its initial value.

After this, the filament is cooled ; the pressure rapidly falls to a lower value, due to the adsorption of gas by the tungsten surface.

At any time the filament can be " flashed " : the pressure will suddenly rise to a maximum value, and the variation in pressure enables us to calculate the quantity of adsorbed gas.

By repeating such operations at different times, adsorbed quantities can be plotted as a function of cold time.

†The field emission microscope utilizes the phenomenon of cold emission as follows : a wire etched to a very sharp point, whose radius varies from 10^{-5} to 10^{-4} cm, is placed in high vacuum and surrounded by a spherical anode, usually in the form of a fluorescent screen.

If a potential of the order of 10^4 volts is applied between tip and screen, cold emission occurs, since the field at the tip can reach values of 10^7–10^8 V/cm.

Electrons leave the tip, following paths parallel to the lines of force, and produce on the screen an electron emission map of the tip, with linear magnifications of the order of 10^5 to 10^6.

The different work functions characterizing the different crystal planes of a metal, bring to a neat individuation of these through their symmetry.

The presence of adsorbed molecules of gases produces an increase of the work function and a decrease of the emission and a darkening of the image of different crystal faces : hence it gives a direct visualization of the phenomena occurring at the surface.

‡The field ion microscope consists of an ordinary field emission tube containing gases at low pressure, where the tip is made anode and sufficiently high voltages are applied.

Ion patterns can thus be obtained, corresponding to the electron emission, but with greatly increased resolution.

Because of increasing field and image force effect, the probability of autoionization of gas atoms increases rapidly when they approach the metal surface. The ionization probability presents neat maxima above protruding atoms or lattice steps of the surface, depending on the local field enhancement ; it is such a probability distribution that produces the details in the ion image on the screen.

By operating the field ion microscope at a very low tip temperature (21 °K) and using helium (2.10^{-4} Torr) a resolution better than 3 Å can be obtained.

Such a resolution enables us to resolve the atomic lattice of tungsten.

§The so-called " ad-sorption spectra " are obtained with a typical flash filament cell, by recording the pressure variations during the flash of the filament, as a function of temperature.

In order to obtain this result, the metal filament employed as adsorbent is also used as a thermometer.

Variations in the resistance of the filament with temperature are transformed into currents and applied to the x-axis of an oscilloscope.

At the same time the ion current measuring the pressure in the cell, is applied to the y-axis.

Resulting traces on the screen are photographically recorded.

In many cases it is possible to see in this way a few maxima in the plots obtained for a single gas, corresponding to the temperatures for which different types of adsorbed molecules can be desorbed.

All these techniques, which resort to bulk materials, are based on the fact that the surfaces after adsorption can be brought back to their original conditions by high temperature degassing.

It is quite clear that the applicability of these methods is necessarily restricted to those metals having a low vapour pressure at the temperatures required for degassing, but of course, many of the conclusions obtained in these cases may be extended to a number of other metals.

From the results recently obtained by such methods, and in particular from the study of surface diffusion at very low temperatures, the following conclusions can be drawn :

(a) the surfaces of tungsten present, from the viewpoint of the adsorption of gases, a kind of heterogeneity depending on the characteristics of the different surface atoms ;
(b) in a given range of temperatures, the adsorbed film appears to be mobile, particularly on some faces of the crystal ;
(c) even at very low temperatures, true chemisorption appears to occur.

Experimental

The apparatus we used is illustrated in Fig. 1. The part of the system indicated by *A* is connected to the pumps and to the gas reservoir; gas admission is controlled by a needle valve.

The adsorbent is in the section *B*, which is connected to *A* through a capillary of known conductance.

In the pressure region employed (5×10^{-8} Torr) gas flow is governed by the laws of Knudsen, and so the flow is given by the product of the conductance of the capillary times the pressure difference existing between the two sections *A* and *B*, measured by the ionization gauges of Alpert type. The measurements were effected at constant pressure on the specimen. The adsorbent was a thin tungsten lamina, of a surface area of 27.5 cm². Hence we have a surface which can be cleaned by heating (by means of induced eddy currents) and whose surface area is considerably greater than that of ribbons and filaments used in the analogous techniques quoted above. In such a way satisfactory quantitative data concerning quantities adsorbed, could be obtained, as well as the adsorption velocities.

Measurements were carried out with nitrogen prepared from NaN_3, and with carbon monoxide prepared from Zn and $CaCO_3$.[19]

The purity of the gases was controlled mass spectrometrically.

Nitrogen adsorption[20]

In Fig. 2 we plot the experimental results of three different series of measurements, made in the same conditions of temperature and pressure. The pressure on the lamina was held constant throughout (5×10^{-8} Torr). The diagram demonstrates the good reproducibility of our measurements.

The curve here shown gives the variation of the adsorption velocity with time. The area under the curve allows a calculation of the total quantity of adsorbed gas.

By effecting such experiments at different pressures on the lamina in the range from 10^{-8} to 2×10^{-7} Torr, the velocity

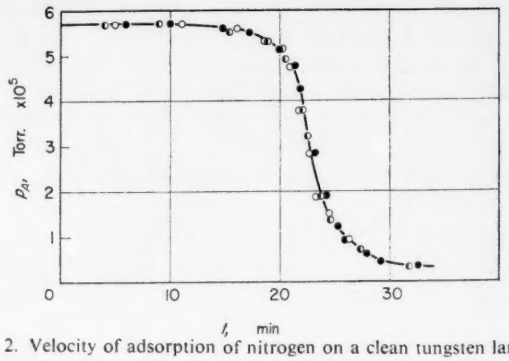

FIG. 2. Velocity of adsorption of nitrogen on a clean tungsten lamina.

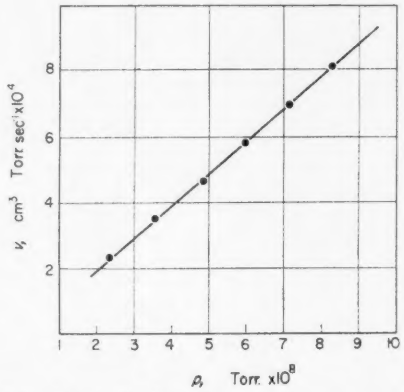

FIG. 3. Initial velocity of adsorption of nitrogen as a function of pressure.

increases linearly with pressure. This is shown in the graph of Fig. 3.

By increasing the constant pressure on the ribbon the time which is necessary to reduce the adsorption velocity to a negligible value, decreases ; the quantity of adsorbed gas is approximately constant in the range of pressures investigated, as shown in Fig. 4.

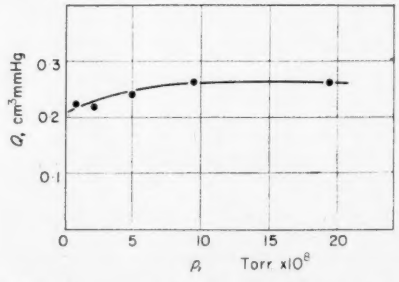

FIG. 4. Adsorbed quantity of nitrogen as a function of pressure.

The variation of adsorbed quantity in the range of temperatures investigated (from 90 to 481 °K) deserves particular interest.

The adsorption isobar is shown in Fig. 5 (solid curve). The plot shows that if measurements are performed at temperatures decreasing from 481 °K the line indicated by the ascending arrows is obtained. The adsorbed amount increases in a discontinuous way with decreasing temperature.

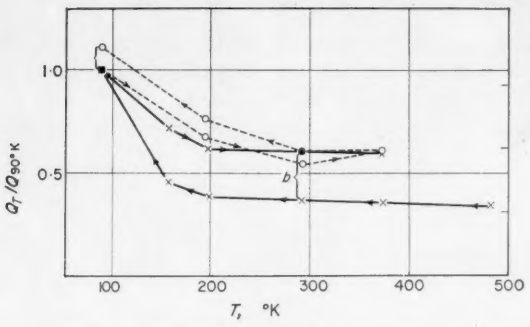

FIG. 5. Isobar of adsorption of nitrogen on tungsten.

If the isobar is followed in the reversed way, by increasing temperature from 90°K, the adsorbed quantity decreases, but the line does not follow the former one, indicating that the adsorbed quantity is higher than when the temperature is decreased.

Therefore it can be concluded that :

(1) the quantity of gas held on the surface of the solid at 298°K does not evaporate at higher temperatures in the range investigated (up to 481°K). This quantity, 0.25 cm^3 Torr, corresponds to 5.9×10^{14} adsorbed atoms/cm^2 of apparent area of the solid ;

(2) at 90°K the adsorbed quantity, 0.69 cm^3 Torr, corresponds to 16.2×10^{14} atoms/cm^2. By raising the temperature to 481°K, evaporation of 0.30 cm^3 Torr (7.0×10^{14} atoms/cm^2) occurs ; this evaporation is already almost completed at 198°K.

Therefore at 90°K, 9.2×10^{14} atoms/cm^2 are irreversibly held, *i.e.*, 3.3×10^{14} atoms/cm^2 are irreversibly adsorbed in addition to the 5.9×10^{14} irreversibly adsorbed at room temperature. This seems to suggest the existence of three different states of nitrogen adsorbed on the tungsten surface, corresponding to the irreversible fractions adsorbed respectively at 298 and 90°K, and to the reversible fraction adsorbed at low temperature.

In a paper work on the adsorption of nitrogen on evaporated tungsten films, Trapnell *et al.*[21] showed the substantial discontinuity of the isobar. They attributed this discontinuity to the existence of two different types of nitrogen adsorption :

(a) a weak adsorption which is reversible in the range of low temperatures, and negligible at room and higher temperatures ;

(b) a strong adsorption, irreversible in the range of temperatures studied by them (up to 400°K) and independent of pressure above room temperature.

The reversible fraction amounted to 42 per cent of the total adsorption. In our case the reversible portion is about 43 per cent of the total, at the same temperature. The main difference between the results of Trapnell and ours, consists in the fact that Trapnell was not able to distinguish between the two types of irreversible adsorption, shown by our experiments.

This difference comes directly from the more favourable experimental conditions characterizing our measurements. In fact we were able to clean the surface every time before the measurements at different temperatures, whilst Trapnell and co-workers were forced to bring the same film successively at the different temperatures, without cleaning ; besides this, the data for the Trapnell isobar had to be obtained beginning with the increasing temperatures part of the curve in order to reduce the slow absorption processes due to the diffusion into the interior of the film.

In the same Fig. 5 the dashed line represents the isobar obtained by Trapnell (for comparison purposes, in the ordinates we plotted not the absolute adsorbed quantities, but the ratios of adsorbed quantities at each temperature to the quantity adsorbed at 90°K). The diagram shows that the isobar obtained by these authors, if account is taken of the inner diffusion, substantially corresponds to the portion of our isobar which refers to increasing temperatures ; this precludes any possibility of detecting the complex character of low temperature adsorption.

Following the majority of authors we consider the nitrogen adsorbed at room temperature to be in the form of an atomic film.

However it is worthwhile to point out that, although the adsorption occurs with dissociation, the direct proportionality of adsorption velocity with pressure shows that the molecular adsorption is the rate determining step (Fig. 3).

Concerning the irreversible adsorption of nitrogen, it must be remarked that the lowest temperature investigated, besides 90°K, is that of melting ethyl ether.

Within this temperature region of about seventy degrees, we have no experimental data which enable us to define the shape of the isobar, but if account is taken of the small increase of adsorbed quantity between 198° and 160°K, and principally of the complete reversibility of this increase, it can be concluded that irreversible adsorption is limited to a small temperature region near 90°K : this seems to suggest that this type of adsorption requires a high surface concentration of adsorbed molecules, such as occurs at 90°K. This could be explained by supposing that the higher surface concentration of molecules could lead to a larger probability of filling some unfilled energy gaps.

This adsorbed quantity does not evaporate below 481°K, which is the upper temperature limit of our measurements : this suggests that the heat of adsorption is much higher than the usual heats of physisorption, and it seems to be concluded that a sort of chemisorption (though different from the chemisorption at room temperature) is involved. In the last few years, many authors have emphasized the role of the electronic factors in adsorption. Trapnell[21] and Ehrlich[15] suggest that groups of atoms of different types existing at the surface of the metal and having different electronic configurations could form strong covalent bonds with nitrogen atoms, or else weaker bonds with nitrogen molecules. The above quoted results of the recent work with the field emission microscope, and in particular the paper of Brock[22] concerning nitrogen adsorption on tungsten, shows the selective character of adsorption on the different regions of the surface ; new findings with the use of the field ion microscope show the existence of a relation between such a selectivity and the surface concentration of more " exposed " atoms of the surface, having a higher ability to bind the gas molecules or atoms.

These results, in the whole, seem to indicate that in the

surface there is a very limited number of types of atoms with different co-ordinating abilities, and to justify the existence of only a few types of adsorbed films. This could explain the formation of the atomic adsorbed film, as well as of molecular, reversible and irreversible films.

The picture of nitrogen adsorption could therefore be the following :

(a) an atomic irreversible film due to the adsorption on the most active sites, and corresponding to the adsorption occurring at room temperature and above ; this requires two atomic sites of the surface for each adsorbed molecule ;

(b) a molecular irreversible film, corresponding to the irreversible nitrogen adsorption at low temperature ; this would require one site for each adsorbed molecule ;

(c) a molecular reversible film, corresponding to the adsorption on less active sites or in a second layer. We assume as a working hypothesis the existence of a permanent site of the metal surface even for each reversibly adsorbed molecule.

Data concerning these three types of adsorbed nitrogen are collected in Table I.

TABLE I

ADSORPTION AT 298°K	ADSORPTION AT 90°K	
Irreversible from 298 to 481 °K	Irreversible from 90 to 481 °K	Irreversible at low temperatures
0.25 cm³ Torr	0.14 cm³ Torr	0.30 cm³ Torr
5.9×10^{14} atoms/cm²	3.3×10^{14} atoms/cm²	7.0×10^{14} atoms/cm²
a) *atomic irreversible adsorption*	(b) *molecular irreversible adsorption*	(c) *molecular reversible adsorption*
(two sites/molecule)	(one site/molecule)	(one site/molecule)
5.9×10^{14} sites/cm²	1.65×10^{14} sites/cm²	3.5×10^{14} sites/cm²

Total number of available sites : $\sim 11 \times 10^{14}$ *sites/cm²*

So we can calculate from our experiments the existence on the surface of 11×10^{14} sites/cm².

This figure compares well with the findings of other authors, and with the values which can be calculated from crystallographic data, as shown in Table II :

TABLE II

Authors	Nitrogen atoms adsorbed for cm² of tungsten surface (measurement temperature in brackets)	Adsorption sites per cm² of tungsten surface (crystal face in brackets)
Becker[1, 6]	$>5 \times 10^{14}$ (300 °K)	
Ehrlich[12, 15]	4×10^{14} (<373 °K)	
Eisinger[23, 24]	11×10^{14}	11.1×10^{14} (113)
Schlier[25, 26]	3.6×10^{14} (298 °K)	11×10^{14} (policr. surf.)
Kisliuk[26] *	3.4×10^{14} (>1000 °K)	
present work	5.9×10^{14} (298 °K) 16.2×10^{14} (90 °K)	11×10^{14}
Miller[9]		10.07×10^{14} (100) 14.24×10^{14} (110)

Adsorption of carbon monoxide on tungsten[28]

Other data which seem to be in agreement with our hypothesis come from measurements effected on the adsorption of carbon monoxide on the same tungsten surface.

Fig. 6 shows a typical experimental curve. The results of

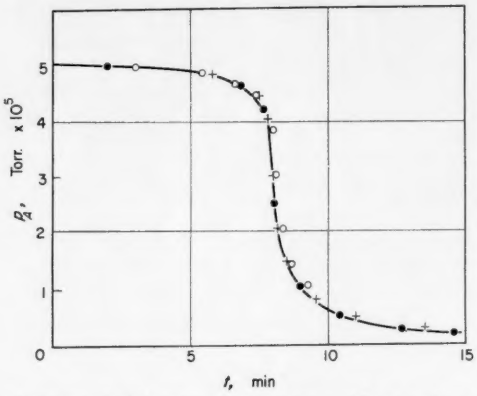

FIG. 6. Velocity of adsorption of carbon monoxide on a clean tungsten lamina.

three different measurements in the same experimental conditions show good agreement, and the general shape of the curve is similar to the curve obtained for nitrogen adsorption.

The isobar for the adsorption of carbon monoxide is shown in Fig. 7. Black dots represent the quantities of gas

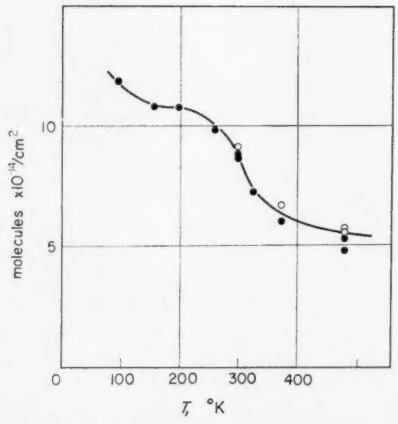

FIG. 7. Isobar of adsorption of carbon monoxide on tungsten.

adsorbed when individual measurements were made at different temperatures, white dots were obtained by performing the adsorption at a lower temperature, and then raising the temperature and waiting for equilibrium. The small differences between the two series of points do not seem to indicate the existence of an irreversible adsorption, if account is taken of the difficulty existing for obtaining a state of true equilibrium by working at very low pressures.

*In a paper, issued after this communication, concerning the nitrogen adsorption by tungsten ribbons at room temperature [*J. Chem. Phys.* **31**, 1605, (1959)], Kisliuk gives values ranging between 6 and 7×10^{14} atoms of nitrogen adsorbed per cm², in good agreement with ours.

The shape of the isobar clearly reveals the existence of two different adsorption processes, which can approximately be located below and above 200°K.

The technique of measurement does not permit us to work at pressures much higher than 6×10^{-8} Torr. In the range from 10^{-8} to 10^{-7} Torr the variation in the adsorbed quantity is not higher than some 20 per cent.

The adsorbed quantity corresponding to the flat portion of the curve is about 1×10^{15} molecules/cm^2 ; this figure agrees well with the number of sites which were calculated above for nitrogen.

The quantity of gas held on the surface at the upper limit of 481°K is about 6×10^{14} molecules/cm^2.

Therefore it corresponds to the " atomic " adsorption of nitrogen (5.9×10^{14} atoms/cm^2).

These comparisons suggest the hypothesis of a molecular adsorption of CO on the same sites on which nitrogen adsorption occurs.

The molecular nature of the CO adsorption on metals has been proved by infra-red absorption techniques as pointed out in the first part of this paper[18].

At 90°K there is a further increase in CO adsorption, whose nature appears rather difficult to elucidate.

It may be recalled that Rideal and Trapnell[29] found for the adsorption of CO on evaporated tungsten films and for temperatures from 80 to 293°K heats of adsorption ranging between 14.8 and 3.6 Kcal/mole ; these values suggest a weak chemisorption, overlapping the physisorption (whose heat of adsorption seem to be about 3–5 Kcal/mole).

Such weak chemisorption can be reversible even at low temperatures and some misunderstanding can arise between chemisorption and physisorption.

However it is worth while to remark that a fraction of CO evaporates very rapidly when the liquid air bath is removed from the adsorption cell, giving a sharp initial peak in the degassing curve, as shown in Fig. 8.

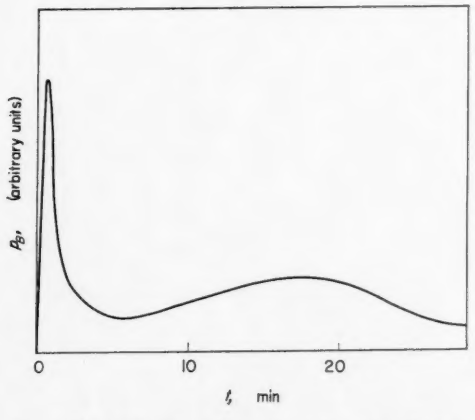

FIG. 8. Desorption with increasing temperature of carbon monoxide adsorbed on a tungsten lamina at 90°K.

This seems to give a qualitative support to the hypothesis of two different types of CO adsorption, at the temperature of 90°K.

Kinetics of adsorption

The following points concerning our experiments with nitrogen as well as with carbon monoxide must be considered :

(a) the adsorption velocity is largely independent of the degree of coverage at all temperatures ;
(b) the velocity is directly proportional to the pressure ;
(c) the initial value of the velocity is independent of temperature.

Whilst agreement exists between all the authors on the first two points, concerning the third our results are conflicting with recent work of Becker and Hartman who suggest the existence of a negative coefficient of temperature for the adsorption velocity of nitrogen on tungsten.

However, it must be recalled that in the experiments of Becker and Hartman the adsorption cell was held at constant temperature, while only the temperature of the adsorbent (a tungsten filament) was varied.

So, this experimental arrangement did not allow the attainment of a true thermal equilibrium.

In fact, the more recent work of Kisliuk[27] shows that, if the whole adsorption cell is held at the temperature of the adsorbing sample, the sticking probability, in the temperature range between 195 and 500°K, remains constant, in complete agreement with our findings in the temperature interval from 90° to 481°K.

The initial values of the sticking probabilities for nitrogen and carbon monoxide, as can be calculated from the data given in Figs. 2 and 6, are much smaller than the data reported by other authors, which, as a matter of fact, differ remarkably from each other.

Bearing in mind that in all these experiments the adsorbent surface was presumably clean, the disagreement seems to be due to some residual deficiencies involved in the method of measurement.

While our purpose is to investigate further this point, we may suggest the probable influence of two factors in the experimental measurement of the sticking probability.

The first is due to the existence of tubulations of limited conductance between the adsorption cell and ionization gauge ; this could give a drop of pressure between the two bulbs.

The only way to eliminate this drawback would be to introduce the electrodes of the ionization gauge directly in the adsorption cell.

However this arrangement could produce, besides thermal effect due to the hot filament, an activation due to the ionizing electron current. This effect was experimentally proved for hydrogen and oxygen[16], and could be possible even for nitrogen and carbon monoxide.

The effects produced by these factors depend upon many parameters, such as the relative arrangement of the cell and ionization gauge, the conductance of the tubulations, the surface area of the adsorbent, the temperature of the electron source, the intensity of the ionizing current, and the geometry of the electrodes.

All these parameters can vary appreciably for different apparatus, and therefore could explain the disagreement in the results of the different authors.

References

[1] J. A. Becker ; *Advances in Catalysis* **7**, 136 (1955).
[2] W. G. Frankenburg ; *J. Am. Chem. Soc.* **66**, 1827 (1944) ; **66**, 1838 (1944).
[3] R. T. Davis ; *J. Am. Chem. Soc.* **68**, 1395 (1946).
[4] B. M. W. Trapnell ; *Proc. Roy. Soc. A* **218**, 566 (1953).
[5] P. della Porta ; *Vacuum* **4**, 284 (1954).
[6] J. A. Beker and C. D. Hartman ; *J. Phys. Chem.* **57**, 157 (1953).
[7] J. K. Roberts ; *Proc. Roy. Soc. A* **152**, 445 (1935).
[8] W. C. Michels ; *Phys. Rev.* **52**, 1067 (1937).
[9] A. R. Miller ; *The Adsorption of Gases on Solids*, Cambridge University Press, p. 7 (1949).
[10] R. Gomer ; *Advances in Catalysis* **7**, 93 (1955).
[11] E. W. Müller ; *J. Appl. Phys.* **28**, 1 (1957).
[12] G. Ehrlich ; *J. Chem. Phys.* **23**, 1543 (1955).
[13] G. Ehrlich and T. W. Hickmott ; *Nature* **177**, 1045 (1956).
[14] G. Ehrlich ; *J. Chem. Phys.* **24**, 482 (1956).
[15] G. Ehrlich ; *J. Phys. Chem.* **60**, 1388 (1956).
[16] T. W. Hickmott and G. Ehrlich ; *J. Chem. Phys.* **24**, 1263 (1956).
[17] G. Ehrlich and T. W. Hickmott ; *J. Chem. Phys.* **26**, 219 (1957).
[18] R. P. Eischens and W. A. Pliskin ; *Advances in Catalysis* **10**, 1 (1958)
[19] S. Weinhouse ; *J. Am. Chem. Soc.* **70**, 442 (1948).
[20] G. Saini, F. Ricca, and A. Nasini ; *Ric. Sci.* **29**, 1523 (1959).
[21] E. Greenhalgh, N. Slack, and B. M. W. Trapnell ; *Trans. Faraday Soc.* **52**, 865 (1956).
[22] E. G. Brock ; *Advances in Catalysis* **9**, 452 (1957).
[23] J. Eisinger ; *J. Chem. Phys.* **28**, 165 (1958).
[24] J. Eisinger ; *J. Chem. Phys.* **30**, 412 (1959).
[25] R. E. Schlier ; *Bull. Am. Phys. Soc.*, Sez. II, **3**, 6 (1956).
[26] R. E. Schlier ; *J. Appl. Phys.* **29**, 1162 (1958).
[27] P. Kisliuk ; *J. Chem. Phys.* **30**, 174 (1959).
[28] F. Ricca, G. Saini, and A. Nasini ; *Acc. Sci. Torino* **93**, 557 (1958/59).
[29] E. K. Rideal and B. M. W. Trapnell ; *Proc. Roy. Soc. A* **205**, 409 (1951).

Vol.
10
1960

The Action of Molybdenum, Tungsten, Tantalum and Nickel on Residual Gases in a Vacuum System

N. W. ROBINSON

Mullard Research Laboratories, Salfords, Redhill, Surrey, England

The interaction between the above metals and residual gases in a vacuum system is studied by flash filament and mass spectrographic techniques. The chief action occurs with carbon monoxide and the metals molybdenum and tantalum. Critical flash temperatures are found below which residual carbon monoxide is diminished and above which it is increased. The effect of sputtered and evaporated films of the metals on glass is also described.

1. Introduction

The thermionic tube must operate in the presence of residual gases and it is important to investigate the kinds of gas and their reaction with the metals and glass forming the valve assembly. The tube does not always operate in an atmosphere in which the gas population remains constant in quantity or character and it is necessary to examine the consequences of any changes in environment or conditions which would affect its performance. The residual gases in a glass bulb alone are well known and are usually found to be a water vapour group (18), (17) carbon monoxide (28), methane CH_4 (16) and probably traces of N_2 (28), O_2 (32) and CO_2 (44).

Among the metals most commonly used in valve construction are Ni, Mo, W and Ta and it is proposed to describe experiments to show the effect of heating these metals in the form of filaments in residual gases in a glass envelope, and also to describe their action in the form of evaporated films.

2. Method

The general method of investigation was to attach a bulb containing a filament of the metal to the input of a mass spectrometer and measure the change in ion current at a particular mass number when the filament was heated to drive off any residual gas adsorbed.

The mass spectrometer was a Siri type instrument with a copper chamber. The background pressure could be reduced to 10^{-7} torr by continuous pumping. This to some extent limited the value of the quantitative results but allows some useful information to be obtained. At this pressure it was possible that the whole apparatus was covered with adsorbed layers of gas in dynamical equilibrium and would therefore take less part in any adsorption or desorption phenomena than if all parts had been rigorously clean.

The mass range which could be examined was from 16 to 60 a.m.u. The spectrometer chamber was baked to 100°C for 12 hr and the bulb containing the filament heated to 450°C also for 12 hr after which the filament was raised to a high temperature and allowed to cool in the residual gases. A mass spectrometer scan with the filament cold showed the presence of residual gases H_2O (18), CO (28), OH (17), CH_4 (16) in descending order of magnitude together with slight traces of O_2 (32) and CO_2 (44).

The filament was then flashed to a high temperature with the mass spectrometer set to detect each mass number in turn and any change in ion current was measured on a potentiometer recorder.

During the course of the experiments the temperature of the filament was measured with an optical pyrometer.

Molybdenum Filament

The molybdenum filament consisted of six sections each 6 cm long, 0.15 mm diameter bent into the form of a *V*, each leg being welded to 1 mm diameter Telcoseal pins.

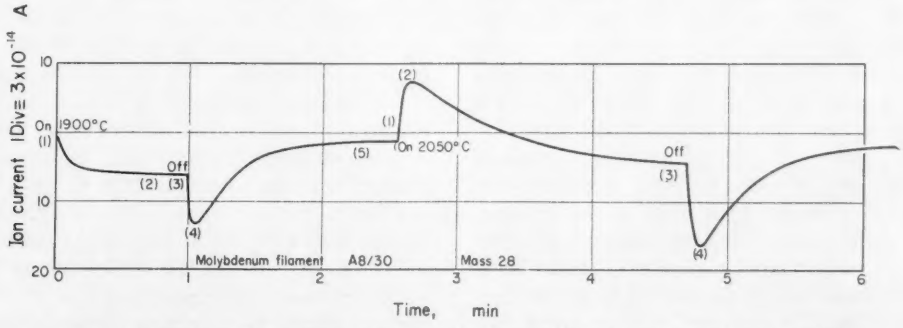

FIG. 1. Records of ion current when a molybdenum filament was heated and cooled.

On heating the molybdenum filament to high temperature >2000°C a slight reduction in ion current was detected at Mass 32 (O_2) after the filament had remained cold for an interval of 24 hr but this could not be repeated after shorter cold intervals. The only other response was obtained at Mass 28 (CO) and the remainder of the measurements were confined to this gas.

Fig. 1 shows typical traces obtained when the filament was heated at 1900°C cooled and then reflashed at 2050°C and again cooled. At the lower temperature there is a diminution of ion current while at the higher temperature there is an increase on heating the filament. A more systematic examination of the behaviour over a large temperature range was made and the results are summarised in Fig. 2. Curve (2)–(1) denotes the change in ion current at

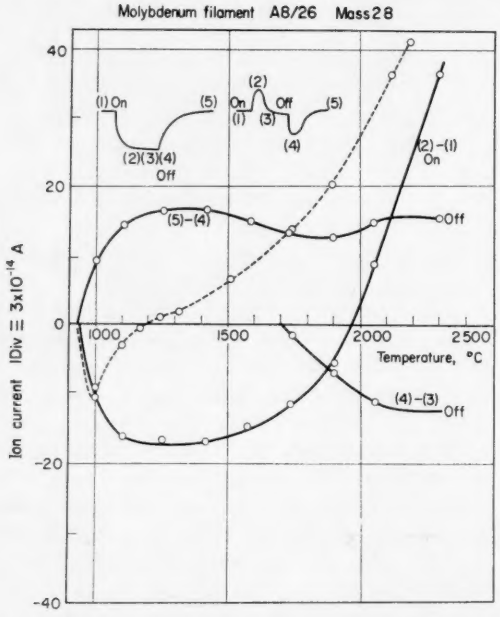

FIG. 2. Changes in ion current when a molybdenum filament is heated to various temperatures.

Curve (2)–(1)	Maximum changes on heating
Curve (4)–(3)	Maximum changes on cooling
Curve (5)–(4)	Final changes on cooling
Dotted curve	Changes in ion current on heating step by step

different temperatures. It is seen that no change occurred at temperatures below 950°C but above this temperature the ion current diminished to a minimum at 1200°C. Above this temperature it was apparent that a second action began which lessened the drop in ion current. At a temperature of 1940°C the two actions were equal and no change in ion current occurred. Above 1940°C there was an increase in ion current. The two actions occurred simultaneously when the filament reached its terminal temperature because the temperature gradient along its length would leave part of the filament at a temperature between 950°C and 1200°C even though the temperature at the centres of the filament loops was above 1200°C. Also the filament would pass through all the stages of temperature, from low temperature to the maximum when it was heated from cold. It was expected that the initial part of all traces would first show a depression of the ion current followed by an increase of the final temperature exceeded 1940°C, but when the appropriate voltage for high temperature heating was suddenly applied to the filament the rate of heating was too fast for the time constants of the inlet system and of the recorder and no depression was observed. In some experiments where the rate of heating was reduced slight depressions were found.

Curves (5)–(4) and (4)–(3) show the changes in ion current when the filament was switched off.

The intermediate stages during heating from room temperature could be eliminated by heating the filament step by step. Part of the records made under these conditions are shown in Fig. 3. They show a changeover in behaviour

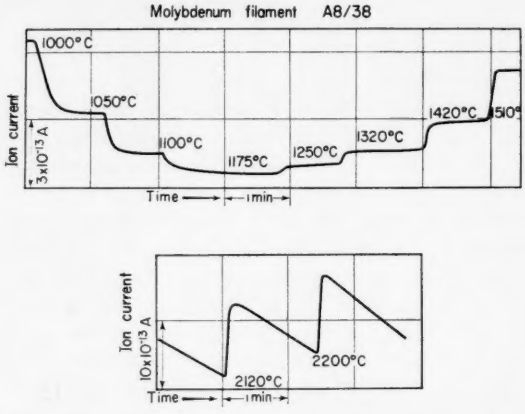

FIG. 3. Records of ion current when a molybdenum filament is heated step by step.
(a) Temperature range 1000°C to 1510°C
(b) ,, ,, 2000°C to 2200°C

from reduction of ion current to increase of ion current at temperatures between 1100°C and 1200°C and also show that when the temperature is about 2000°C a new reaction occurs which causes a rapid reduction in ion current after an initial peak.

The complete results are shown on the dotted curve on Fig. 2. Comparing the two sets of curves (2)–(1) for the initially cold filament and for the step by step heating, it is seen that the temperature for the first change in ion current is the same. Also the temperature at which the ion current does not change in the dotted curve is approximately the same as that at which the slope of the curve (2)–(1) passes through zero denoting that a second reaction is beginning.

The pumping action of the filament when heated to high temperature, as shown in the lower portion of Fig. 3, was investigated further by recording the ion current when the filament was maintained at 2050°C for about 20 min. It was found that the excess ion current above that of the residual ion current when the filament was cold, fell exponentially with time with a law $e^{-0.036t}$ for the first minute and thereafter with a law represented by $e^{-0.919t}$. Both of these rates were faster than the pumping rate of the diffusion pump through the system and hence may represent the rate at which chemical action was taking place.

Effect of Sputtered Molybdenum Films on Glass Bulbs

It is well known that gases dissolved from glass have a major influence on the kind of residual gases in a closed system. One of the methods which can be adopted to minimize this influence is to seal off the glass surface with an evaporated metallic film. Dr. Penning first showed that a molybdenum film performed this function very satisfactorily and as a result a whole range of stabiliser tubes has been produced.

In the following experiments two glass bulbs (Kodial glass) were fitted to separate inputs to the mass spectrometer. Each contained molybdenum disk electrodes. The two bulbs were heated from 20°C to 450°C and the outputs measured on the mass spectrometer at approximately equal temperature intervals. The outputs were similar and consisted of the residuals given previously. The bulbs were then cooled and neon admitted to one of them and a film of molybdenum sputtered uniformly over the inside of the bulb. The neon was then pumped out and the two bulbs were heated again to 450°C. On the second heating the output at mass 18 (H_2O) from the plain bulb was reduced to about 1/5th to 1/3rd over most of the temperature range whereas on the second heating of the sputtered bulb the output at mass number 18 (H_2O) was less than 1/500th over most of the temperature range. Similar results were obtained at mass numbers of 17 (OH) and 28 (CO).

The sputtered layer thus has the action of preventing gas being desorbed from the glass probably by a gettering action.

The molybdenum bulb was exposed to air for a short time and then reheated but here it was found that the water vapour output had increased considerably at temperatures of approximately 100°C and was more than that from the plain bulb. At higher temperatures of 300–450°C the output was less than from the plain bulb.

After a second heating to 450°C the efficiency of the molybdenum was almost completely restored.

The practical consequence of this behaviour of molybdenum may be considerable and will be dealt with later.

The Behaviour of Molybdenum Films in an Ion Gauge

The gettering effect of molybdenum was made use of in getter-ion pumping. Molybdenum from a molybdenum filament was evaporated on to the walls of an ion gauge.

A Bayard–Alpert type gauge was attached to the system and run at low electron currents to record the pressure.

Fig. 4 illustrates the history of the system which is taken from the continuous recording of the pressure with time. Initially the ion gauge filament was heated but the H.T. was not switched on. In the first part of the curve the molybdenum filament, which had not been degassed previously was heated in stages and the gas pressure rose as the temperature was increased. At a current of 9 Amps through the filament some molybdenum was evaporated and gettering action took place. The pressure was allowed to fall from 10^{-3} torr to 10^{-4} torr and the ion gauge HT was switched on. Pumping occurred and in a short time the pressure was reduced to 3×10^{-7} torr. Thereafter the HT was switched off and on many times and it is seen that each pumping was

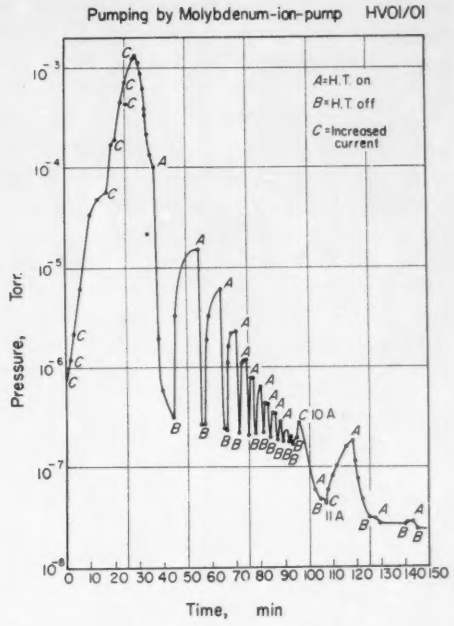

FIG. 4. Pressure records during the operation of an ion gauge with molybdenum evaporating from filament.

followed by incomplete recovery until both pumping and recovery were very small. The Mo filament was further heated and the gettering action was accelerated after a short burst of pressure. Further heating of the Mo filament released more gas which was ion pumped but switching off the HT did not release any gas. Repeated switching of HT on and off resulted in very little change in pressure.

It appeared that the molybdenum getter-pump pumps some gases very strongly and does not release them. In a short time it had pumped all the pumpable gases in the system and thereafter ceased to pump. The gases which were pumped were not released when ion pumping ceased and a residual gas was left which was inert to molybdenum. This was different from the behaviour of either titanion or zirconium which although they may pump more residual gas than molybdenum and therefore allow low ultimate pressures to be reached, nevertheless release hydrogen when the ion pump is switched off.

Molybdenum evaporated on to the walls of an ion gauge would therefore be good as a measuring gauge which could be run at high electron currents yet would not pump.

Summing up the properties of molybdenum it is found that there appears to be no reaction with residual gases on the hot filament below 950°C. Between 950 and 1200°C there is a reaction which results in a diminution of CO and above 1200°C a second action occurs which increases the CO in the system.

Molybdenum in the form of a film is excellent for gettering many residual gases and preventing gas desorbing from glass. It is possible that this property will be of great use where plastics or other substances have to be used in large nuclear machines where a thin film of molybdenum may be used to decrease the degassing of the plastic or non-metallic surfaces.

Molybdenum has the advantage over titanium and zirconium in getter ion pumps in that release of gas after pumping is virtually prevented.

Tantalum

Flash filament experiments were performed with tantalum. In this case the bulb containing the filament was mounted on the input to the mass spectrometer and various gases normally found as residual gases were introduced into the bulb. The gas adsorbed by the tantalum was measured by observing the gas desorbed on flashing. The background pressure of the mass spectrometer was about 3×10^{-7} torr and the pressure of introduced gas raised this to about 10^{-6} torr. Fig. 5 shows the results in which the change in ion current is expressed as a percentage of the original ion current.

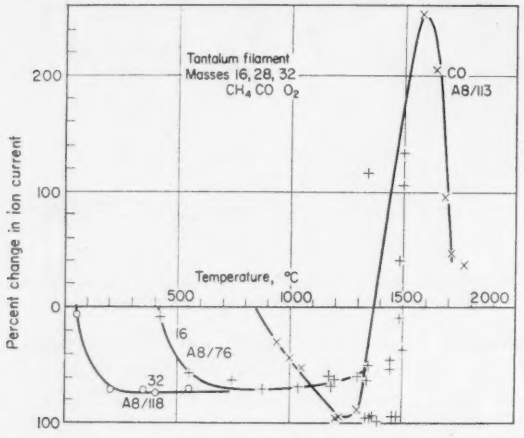

FIG. 5. Changes in ion current when a tantalum filament is heated in various gases.

Introduced gas pressure 10^{-6} torr
Background ,, ,, 10^{-7} torr
A8/113 ion current at mass 28 (CO) when heated in pure carbon monoxide (see Table I).
A8/116 ion current at mass 28 (CO) when heated in town gas (see Table I).

The gas (mass 32) was the residual oxygen when cylinder nitrogen was introduced into the bulb so that the partial pressure was low. Mass 16 CH_4 was derived from a sample of CO which contained about 3 per cent of methane.

From the slide it is seen that the ion current at mass 32 shows the first reaction at about 50°C, when there is a slight reduction. A similar reaction occurred by gradually increasing factors up to a temperature of 200°C and then remained constant up to at least 1350°C. It is possible therefore that the reaction was complete at 200°C.

With mass 16 CH_4 there was no reaction below 400°C and then the ion current was diminished by a factor which increased to a maximum of 70 per cent at 700°C. The action remained constant between 700°C and 1300°C at which temperature very erratic results were recorded. On one flash the ion current was diminished while on another it would increase. This region appeared to be unstable and was probably the result of reactions involving small quantities of residual gases of rapidly changing quantities.

With mass 28 CO there was no reaction below a temperature of 800°C but between 800°C and 1250°C the ion current diminishes by approximately 100 per cent. At 1350°C there was a change in reaction and above this temperature an increase in ion current was obtained. The magnitude of the increase reached a maximum at 1600°C and then fell rapidly at 1700°C.

A second set of experiments were performed with the carbon monoxide present in town gas. The general shape of the curve was the same in so far as the starting temperature for reaction was again 800°C, and the temperature at which the ion current increased was also the same but the magnitude of the increase at 1600°C was much less and the reaction continued up to a temperature of approximately 2000°C.

The difference in the two reactions with laboratory made CO and CO in town gas may be due to modified action in the presence of other gases. The compositions of the two samples of gas is given in Table I.

TABLE I

Percentage Composition of Gases Used in Curves A8/113 and and A8/116 on Fig. 5

Mass Number	16	17 & 18	24–27	28	29 & 30	37–43	44
Town Gas A8/113	27	8.2	14	27	3.3	10.9	9.6
Laboratory Carbon Monoxide A8/116	3.4	3.0		92	1.3		0.3

The effect of tantalum sputtered on to a glass bulb was to decrease the output of the usual standard gases from glass by approximately one third up to temperatures of 450°C. Thus a useful gain is made by covering a glass bulb with tantalum but the effect does not compare very favourably with molybdenum.

Tungsten

A tungsten filament in a glass bulb attached to a mass spectrometer behaved as shown in Fig. 6, when the filament was flashed. As with molybdenum no response was obtained at mass numbers of 18 and 32 but at mass (28) CO there was first an increase and then decrease of ion current when the flash temperature exceeded 1200°C. The peaks increased to a maximum at 1700°C and then tended to decrease. A more marked effect at the high temperatures was that the final current was less than the initial ion current.

On cooling the filament the response obtained was almost the reverse image of the trace on heating.

This is not the only reaction of residual gas with tungsten and it has been shown previously[2] that residual gas from tungsten may cause fluctuations in emission from an oxide cathode even though the peak pressure does not exceed 10^{-8} torr. It is thought that some of the fluctuations may be due to carbon monoxide which would tend to accelerate the reduction of the cathode and hence enhance the emission.

The fluctuations of cathode current took the form of enhancement and then depression of emission which may possibly be caused by different rates of reactions of CO and some poisoning gas.

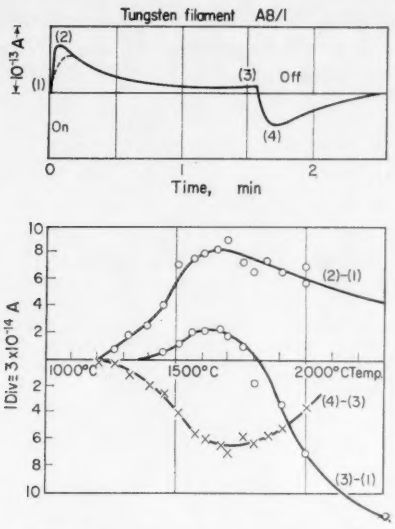

FIG. 6. Changes in ion current at mass 28 (CO) when a tungsten filament was heated in residual gases.

(2)–(1) Maximum changes on heating
(3)–(1) Final „ „ „
(4)–(3) Maximum „ „ cooling

Nickel

Nickel is a very important metal in thermionic tube manufacture and much is known of its properties at pressures of 10^{-5}–10^{-7} torr but when a nickel filament is flashed in a bulb at background pressures of 10^{-10} torr it was found that small quantities of gas are liberated at relatively low temperatures.

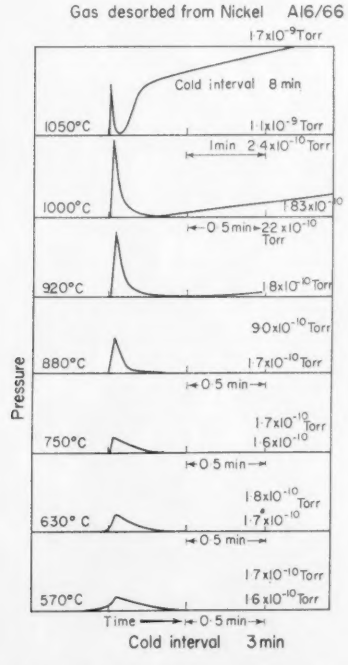

FIG. 7. Pressure changes when a nickel filament is heated to various temperatures in residual gases at ultra high vacuum.

Typical records are shown in Fig. 7 of the pressure produced in a glass bulb when the filament was flashed at various temperatures after a given cold interval. A small quantity of gas was desorbed at 570°C and rapidly adsorbed by the glass. The adsorption was complete in about 15 seconds. The quantity of gas increased slightly with increasing flash temperature. At 1000°C there was evidence of a second gas being desorbed.

Nickel sputtered on to glass had little effect on the water vapour output except at temperatures above 150°C where it caused a reduction to about 0.3. This improved at higher temperatures of 450°C to about .03. Mass 16 (CH_4) was reduced to about 0.2 over the temperature range 20–450°C. A sputtered nickel film causes a useful reduction gas output from glass particularly at high temperatures.

3. Summary

The experiments just described have shown the complexity of the problem of the reactions of gas and solids in vacuum devices. In operating a vacuum thermionic valve some metallic and other parts are raised to high temperatures either due to the hot cathode, electron current or electron bombardment. It is important to understand what happens to the residual gases in the vacuum envelopes and whether they have a deleterious effect on the oxide cathode or any other component in the tube. The results given here show that the gases may be transient, and disappear by adsorption in a very short interval after they are desorbed by the heated parts and may not be observed by steady state analysis by mass spectrometer.

It is also possible that the reactions described previously give only an incomplete picture of events since the history of only one component is measured, whereas the complete reaction may involve two or more gases. It is therefore required that an analysis should be made of all the gases simultaneously. In this way if CO is formed as a result of reaction with O_2 or with H_2O and carbon on the filament then, in a closed system, where only a small quantity of gas is available, the production of CO would be accompanied by a reduction of O_2 or H_2O.

A mass spectrometer for performing this rapid analysis would need :

(1) A rapid scan,
(2) A fast repetition rate,
(3) To operate at very low pressures,
(4) A high speed recording device.

Condition 1 requires that a multiplier would need to be used for detecting the small number of ions which would be available.

(2) Can be achieved by suitable electronics.
(3) This requires that the whole system should be bakeable.
(4) A C.R.O. and photographic recorder would need to be used.

There are other circumstances where transient gases may be important in the correct functioning of thermionic tubes.

Short bursts of gas driven off in warming up or in bombardment of metal parts may lead to breakdown in X-ray tubes, high voltage rectifiers and high duty transmitter tubes.

Transient gases may also cause fluctuations of cathode current which results in noise in microwave tubes and may also cause permanent poisoning.

DISCUSSION

Question from Mr. L. A. Petermann

Concerning the system Molybdenum–CO, you mention the existence of a slow pumping phenomenon above 1600°C. You attribute this to some chemical reaction between MO and CO. How did you rule out the ion-pumping effect of the pressure gauge itself?

Answer. There was no pressure gauge attached to the input side of the mass spectrometer when the molybdenum filament was flashed. The pumping effect could only be attributed to molybdenum at high temperatures. Below a temperature of 1600°C the ion current at mass 28 remains constant with time after the initial change but above this temperature the ion current decreases with time after the initial peak. The rate of decrease increases with temperature and results were shown at 2200°C where the rate was greatest.

Vol.
10
196

Some Reactions of Water in Electron Tubes

S. GARBE, A. KLOPFER and W. SCHMIDT

Allgemeine Deutsche Philips Ind.G.m.b.H., Zentrallaboratorium Aachen, Germany

During pumping of tubes a great part of the present gases is formed by water, which desorbs from the surfaces and is also evolved from various materials, especially from glass and mica. For a short outgassing time the evolution of water from the surface of the glass prevails, resulting in a decrease of the surface coverage with water. In sealed-off systems water vapour undergoes various reactions, as : adsorption on the surfaces ; reactions with the hot cathode, leading to formation of H_2, CO_2, CO and CH_4 ; and reactions at the barium getter mirror, giving H_2 and CH_4.

After flashing the getter an amount of 8×10^{-3} Torrl water had been introduced into a television picture tube, resulting in a far higher level of H_2, CH_4 and CO_2 than in normal processed tubes even after 180 hours life and operation. The H_2O pressure, however, had decreased from above 10^{-5} Torr to 4.10^{-9} Torr. Generally we may conclude, that an increased water evolution in tubes leads to a higher residual pressure of H_2, CH_4 and CO_2 during life.

01.
10
960

THE degassing of vacuum systems consists to a great part in the removal of water vapour, which is adsorbed on the surfaces and is also given off from various materials, especially from glass and mica.

1. The evolution of water from glass

On heat treatment of glasses *in vacuo* mainly water vapour and carbon dioxide are evolved.[1]

Water is included in the glass network in the form of OH-groups.[2] Up to now three different states of binding of the OH-groups to the glass network are known and there is also a close connexion between the amount of water in one of these states and the structure of a glass.

Apart from the desorption of an amount of physically and/or chemically bound water Q_0 from the surface, the evolution of water from glass is controlled by diffusion and the amount Q evolved after a time t is linear with respect to the square root of the time of beak-out :

$$Q = mt^{1/2} + Q_0.$$

The constant m is an exponential function of the reciprocal of the absolute beak-out temperature. For the diffusion from a slab, m is given by :

$$m = m_0 e^{-Q_m/RT} = 1.13\, C\, D_0^{1/2} e^{-Q_D/2RT}.$$

with $Q_m = Q_D/2$

C = uniform concentration of water in the glass (Torr l cm^{-3})

D = diffusion constant (cm^2 min^{-1})

With some glasses the value of m for constant temperature changes with time. In this case the plot of the initial value of log m against the reciprocal of the absolute temperature does not give a straight line (Fig. 1). In the example of a soda lime glass the evolution of water at temperatures below

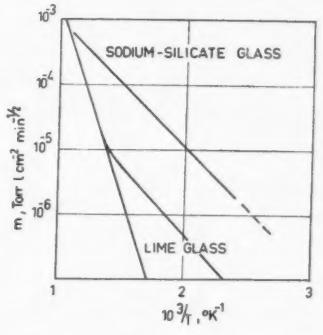

FIG. 1.

450 °C is in the initial stage governed by a much greater value of m than would result from linear extrapolation of the log m-$1/T$ plot above 450 °C. After 3 hr the value of m at 375 °C, e.g. changes from 3.6×10^{-6} Torr 1 cm^{-2}min$^{-1/2}$ to 1.3×10^{-6} Torr 1 cm^{-2}min$^{-1/2}$ (Fig. 2).

The change of m with degassing time is caused by a concentration gradient of the water in the glass. In this case the initial concentration of water near the surface is higher than in deeper layers. Such higher concentrations of water near the surface may have formed during processing of the glass and by the attack of the humid atmosphere while storing the glass. On normal outgassing procedure with temperatures up to 400 °C the amount of water given off from the surface layer exceeds by far the amount of water that has diffused to the surface from the interior of the glass. The high evolution rate during the first minutes of degassing at temperatures above 300 °C (Fig. 2) corresponds to water from the chemisorbed surface layer. The time which is needed to remove this " surface gas " depends on the temperature and the effective pumping speed.

The glass layer near the surface, which has a higher concentration of water than the interior, can be dissolved by a

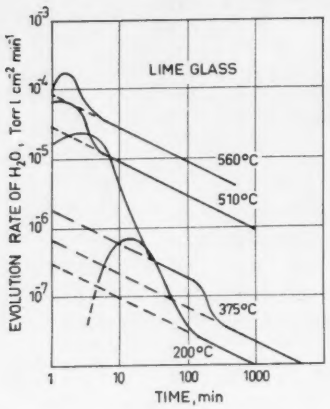

FIG. 2.

1 per cent HF wash. This results in a decreased amount of gas given-off by the surface and also the initial value of m decreases to that, which is given by the uniform concentration of water in the interior. As the chemisorbed surface layer of water forms slowly, also pre-degassed glass gives off a considerably lower amount of water from the surface, even if it has been exposed to the atmosphere for some hours (Fig. 3).

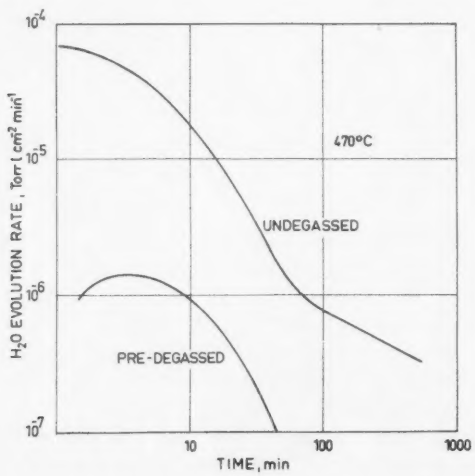

FIG. 3.

To give an example for the amount of water, released from the surface and the interior respectively, some figures are given for a soda-lime glass.

The amount of H_2O given off by the surface layer is 3×10^{-4} Torrlcm^{-2}, whereas it takes 45 hr at 420°C until the same amount has diffused to the surface from the interior.

Generally one may conclude that a relatively short bake-out of some minutes at temperatures up to 400°C only decreases the surface concentration of water on glass, whereas much longer time or a higher temperature is necessary to establish a concentration gradient near the surface.

As other sources of water evolution there may only be mentioned mica and ceramic structures of cathodes.

2. The interaction of water with surfaces

Apart from the evolution of water from different materials the pressure of water in a vacuum system is always influenced by the adsorption properties of the surfaces. If the evolution rate of water is to be neglected, the water pressure in a sealed-off system approaches an equilibrium pressure which is given by the covering of the surfaces with adsorbed water. If the temperature changes, also the adsorption equilibrium is altered. On a decrease of the temperature the partial pressure of water drops, until a new equilibrium has established. Fig. 4 gives the pressure change in an all-glass

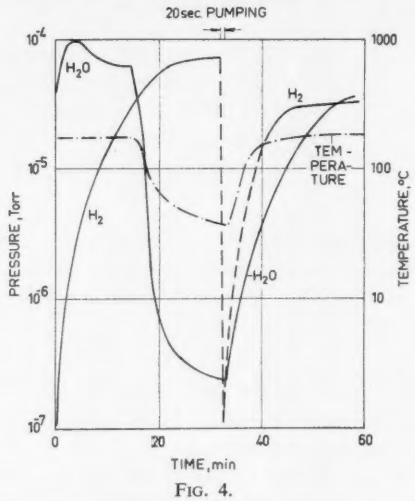

FIG. 4.

system with 0.3 l, when the temperature decreases from 180°C to 35°C. The partial pressure of water drops by two orders of magnitude, while a considerable amount of hydrogen is evolved. The measurement of partial pressures has been done by means of an omegatron with a directly heated oxide cathode. The greater part of the hydrogen is formed by the chemical reaction of the water with the hot cathode.

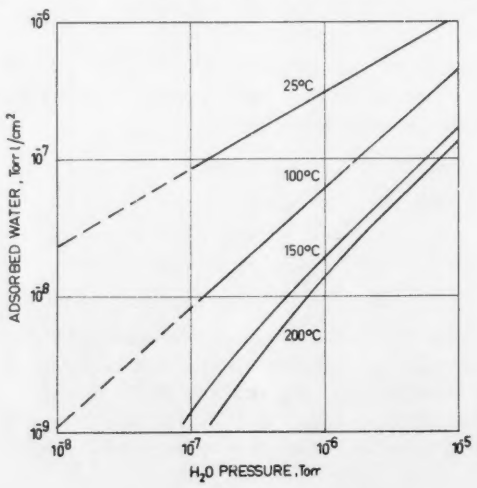

FIG. 5.

Moreover hydrogen is also desorbed in consequence of the chemical interaction of adsorbed water on glass, as has been seen in other experiments. The amount of water adsorbed on a borosilicate glass has been measured as a function of pressure and temperatures of the glass (Fig. 5). The adsorbed amount of water per cm^2 surface area is not related to the true but to the much smaller area, which is calculated from the dimensions of the glass system.

Below 10^{-5} Torr the adsorption of water on glass is not a simple physical adsorption. It is accompanied by a chemisorption of water on active sites of the glass surface. From the dependance of the pressure on the temperature at constant amount adsorbed, the mean heat of adsorption has been calculated (Fig. 6). It decreases with amount adsorbed.

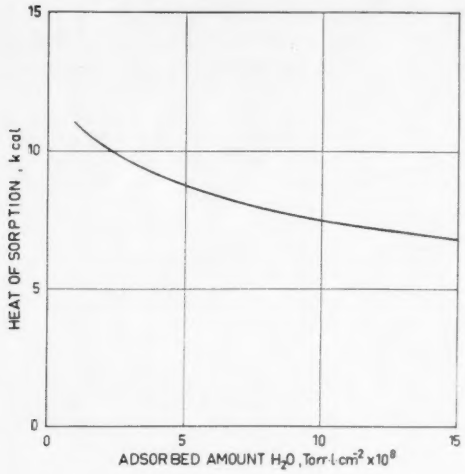

FIG. 6.

Giving a mean value higher than 10 kcal at an amount of adsorbed water below 10^{-8} Torrl cm^{-2} the adsorption heat decreases to 7 kcal for an adsorbed amount of 10^{-7} Torrl cm^{-2}.

Also from the dependance of time lag in setting up the steady state of flow on the temperature a mean adsorption heat of 6–7 kcal has been calculated. But the latter calculation gives only an approximate value as the calculation of the adsorption heat from the time-lag is based on the validity of Henrys Law which is no more suitable in the low pressure region at room temperature.

The decrease of the heat of sorption with increasing coverage indicates that at very low pressures the molecules are adsorbed at regions of higher adsorption energy. The physical adsorption is partly accompanied by chemisorption. Therefore the adsorption and desorption on temperature changes are also not fully reversible (Fig. 4). The equilibrium is slowly reached, whereas the greater part of the molecules is physically adsorbed and follows the temperature changes immediately. The strong adsorption of water brings about relatively long lifetimes of the molecules in the adsorbed state. The result is, that the steady state of molecular flow establishes with a considerable time lag. The pumping of water is also not only determined by the pumping speed and the conductance for free molecular flow but also by the lifetime of water in the adsorbed state and its dependance on temperature and pressure.[3]

Because of the adsorption phenomena and its reactions there cannot be a high water pressure in sealed-off electron tubes even if the getter is not yet evaporated. But hydrogen, formed by reactions of water, supplies always a considerable portion of the total pressure.

As an example we may mention the partial pressure measurement of a picture tube, in that an amount of 8.10^{-3} Torrl water had been let in. The getter had not been flashed. Ninety hours after the influx of water only 1 per cent of the quantity could yet be measured, but a considerable pressure of hydrogen had collected in the system, consisting of the TV tube and an omegatron. Probably the hydrogen had not only been formed by chemical reaction but also by exchange effect of water with previously adsorbed hydrogen.

There are a number of chemical reactions of water with hot cathodes, leading to the formation of H_2, CO, CO_2 and CH_4 and even higher hydrocarbons. The reaction rates depend on the kind of the cathode, its contaminants and the temperature of operation, but the reaction with the highest rate is the formation of hydrogen. The amount of hydrogen, formed per second is proportional to the water pressure. A H_2-formation rate of 3.10^{-1} Torr l/min Torr H_2O has been measured for a directly heated oxide cathode of about 1 cm^{-2} area at a temperature of 800 °C of the emitting surface.

If oxide cathodes are not heated they may take up a considerable amount of water, that is again given off when they are switched on (Fig. 7). In the shown experiment the

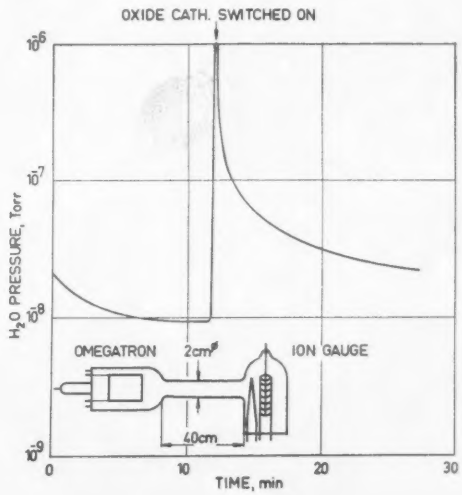

FIG. 7.

oxide cathode had been on room temperature for 15 hr in an not gettered vacuum system with a H_2O-pressure of 10^{-8} Torr. The increase of the H_2O pressure was measured by means of an omegatron which was connected to the switched cathode via a glass tube of 40 cm length and 2 cm diameter. The glass surfaces of the system were on room temperature. Therefore the amount of H_2O evolved from the cathode may

have been still higher because of the adsorption on the connecting tube. It is seen that the H_2O pressure rapidly decreases according to the adsorption.

Reactions of H_2O with the barium getter

The consumption of water by barium leads to the formation of $Ba(OH)_2$, at which reaction hydrogen is formed too. But as long as the getter is unsaturated the hydrogen is again taken up. At pressures below 10^{-5} Torr the hydrogen pressure above the getter is nearly as high as the water pressure.

There is a further reaction of water with carbon contaminants or carbide like constituents of the barium getter film, leading to the formation of hydrocarbons, especially CH_4, C_2H_6 and C_3H_8.[5] The rate of formation of CH_4, C_2H_6 and C_3H_8 is as 100 : 15 : 1. The hydrocarbons are formed by a chemical reaction and not by an exchange at the getter mirror, when water is taken up. A barium getter mirror of 10 cm^2 had been heated so that adsorbed hydrocarbons might desorb. The evolution rate of CH_4 was then below 2×10^{-11} Torrlmin^{-1} at a water pressure of 10^{-10} Torr. After the introduction of water into the experimental tube, again CH_4 was formed, with the same rate as function of the water pressure, as it was measured immediately after the evaporation of the getter (Fig. 8). The formation rate of

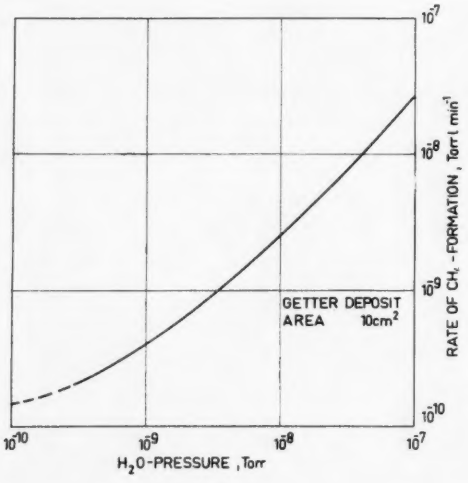

FIG. 8.

CH_4 is nearly proportional to the partial pressure of water. A barium getter which has been saturated at high temperatures quantitatively with CO, is converted to BaC_2, which forms C_2H_2 with water. But, as long as a getter is not yet consumed, the final gaseous products are always saturated hydrocarbons.

The rate of formation of CH_4 is nearly independent on the amount of CO, that the getter had previously taken up at room temperature. After a partial saturation of the getter with CO at room temperature, rates of formation of hydrocarbons had only been higher by a factor of 3 than immediately after evaporation of the barium getter. If water forms part of the residual gas of an electron tube with a barium getter, there will always be a formation of hydrocarbons, except the hydrocarbons are pumped in any way. If there is no pumping the rate of formation of CH_4 may be a measure of the prevailing water pressure.

3. The reactions of water in a television picture tube

Because of the adsorption of water at the surfaces the sensitivity of a direct measurement of the water pressure in an electron tube is limited by the increase in surface area, which is caused by the connection of the tube to a mass spectrometer. Even the use of an omegatron results in a considerable increase of the surface area of a small receiver tube, but in the case of a television picture tube the conditions are not markedly changed, if an omegatron is attached to it.

After flashing the getter an amount of water of 8.10^{-3} Torrl had been introduced into a TV tube via a metal tap. An omegatron was used to measure the pressure change in the tube on shelf life and operation (Fig. 9). The curves of the

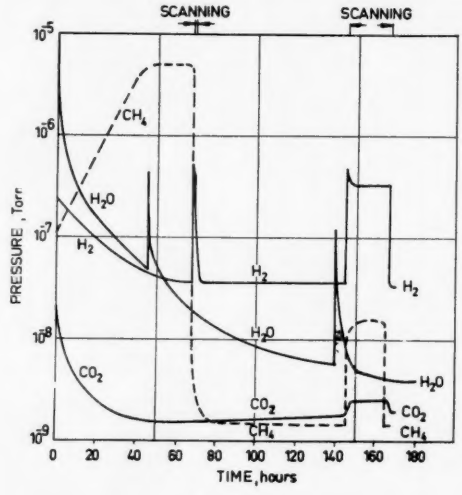

FIG. 9.

pressure of N_2, CO and A are omitted in Fig. 9 on account of better clearness, as the pressure of these gases is not essentially influenced by the introduction of water. After the water let-in has ceased the partial pressure of water quickly drops, because of getter action and adsorption at the surfaces. But later on the pressure decrease of water is not governed by the pumping speed of the getter but by the desorption rate of the adsorbed water and the lifetime in the adsorbed state, until a water molecule hits the getter mirror. After 170 hr life with 20 hr operation the partial pressure of water had again decreased to 4.10^{-9} Torr. The measured pressure in the omegatron, attached to the TV tube, is certainly not lower than the pressure in the tube, as the omegatron had the greatest distance to the getter mirror. The short peaks in the H_2O pressure correspond to the H_2O-evolution of the heated oxide cathode of an ionisation gauge.

The introduction of water into the TV tube results in an increased pressure of H_2, CH_4 and CO_2. These gases have

been formed by the reaction of water. Even after 20 hr scanning the level of these gases is much higher than in normal processed tubes, in which no water has been let in. Generally one may conclude that an increased evolution of water from tube elements as consequence of poor degassing results in a higher level of the residual gases of hydrogen, methane and carbon dioxide during life.

References

[1] J. Todd ; *J. Appl. Phys.* **26**, 1238 (1955).
[2] H. Scholze ; *Glastechn. Ber.* **32**, 81 u. 142 (1959).
[3] F. Kirchner ; *Z. angew. Phys.* **11**, 167 (1959).
[4] A. Klopfer, S. Garbe, and W. Schmidt ; *Symp. on Res. Gases in Electron Tubes, Como* (1959).
[5] F. H. R. Almer, H. J. R. Perdijk, and P. G. v. Zanten ; *1st Int. Congr. Vac. Techn. Namur* (1958).

01.
10
960

System Design and the Choice of Materials for the "Nimrod" Vacuum System

S. H. CROSS

A.E.R.E., Harwell, Berks, England

The backbone of a proton synchrotron is the massive electro-magnet which keeps the protons in orbit. Economy and utility in the design of this in conjunction with the beam dynamics of the machine decide many physical constants of the vacuum system if optimum performance is to be obtained, and the scattering effect of the residual gas molecules on the proton beam determines the pressure at which the system must work. The dimensions of the vacuum vessel are thus determined; calculations relating duct size to pumping speed and gas evolution rate have been carried out and the results of these are presented. Pumping units using 60 cm diameter oil vapour diffusion pumps have been designed and are now being produced. Tests of the first ones show that they are capable of attaining ultimate pressures (with no gas load) of 3×10^{-7} *torr. During investigations to discover the most suitable material with which to make the vacuum vessel, determinations of the gas evolution rates of various polymers have been carried out and certain of the epoxy resins with glass-fibre reinforcement are the best materials so far found, partly because of their high strength to volume ratio. Work has been done to show the effect that irradiation has on the mechanical strength and gas evolution rate of these materials. Techniques are being developed to produce laminates in the workshop which are free from voids that may cause leakage. The gas evolution rates obtained from these epoxy resins are higher than can be tolerated if the requisite operating pressure of* 10^{-6} *torr is to be maintained in the vacuum vessel and it is necessary to mask the surface exposed to the vacuum in order to reduce the amount of gas evolved, a technique which has already been applied in the "Saturn" proton synchrotron at Saclay using stainless steel strip, but the different design parameters of "Nimrod" calls for different techniques and considerable attention is being given to this.*

"NIMROD" is the 7 GeV proton synchrotron being built at Harwell for the National Institute for Research in Nuclear Science. The background and general structure of this machine have been described recently in a special series of articles.[1] It is sufficient to say here that the vacuum system for such a machine has certain special requirements. The vacuum vessel must work in an intense and varying magnetic field; to prevent distortion of this field and to avoid dissipation of a considerable amount of power the vessel must be substantially non-conducting; the walls of the vessel must be thin in order to utilise fully the magnet gap, and the operating pressure has to be kept low in order to minimise loss of protons due to scattering by residual gas molecules. The protons travel a distance of some 140,000 Km during the acceleration cycle, well beyond the mean free path attainable by present vacuum techniques and consideration of the scattering effect of residual gas molecules shows that a working pressure not exceeding 10^{-6} torr should keep the proton loss down to less than 10 per cent.[2] During machine operation very intense and penetrating radiation will be produced and the vacuum and mechanical properties of the materials used in the vacuum system must be chosen with this in mind.

Pumping units

The programme for building the machine necessitated that design of the pumping units and vacuum vessels should proceed simultaneously. The initial step was to relate the parameters of pumping speed, vessel dimensions and gas evolution rate at the required pressure. Since the vessel is in the form of a duct with a rectangular cross section of approximately 25 cm × 200 cm surrounding the circular machine of 45 m diameter, its pumping impedance has to be allowed for. Fig. 1 illustrates the relationship. For a given gas evolution rate from the surface of the vessel, the speed of pumping to maintain a length of vessel of fixed cross section at a mean pressure of 10^{-6} torr is shown by the dotted lines.

The length of vessel between pumps is, of course, inversely proportional to the total number of pumps used, and so a curve can be drawn which relates the total required pumping speed for a fixed length of vessel to the number and size of pumps. This is shown by the solid lines and illustrates clearly that, for a given gas evolution rate, because of the duct impedance the effect of increasing the size and decreasing the number of pumps employed beyond certain optimum values will increase the total pumping speed required, even

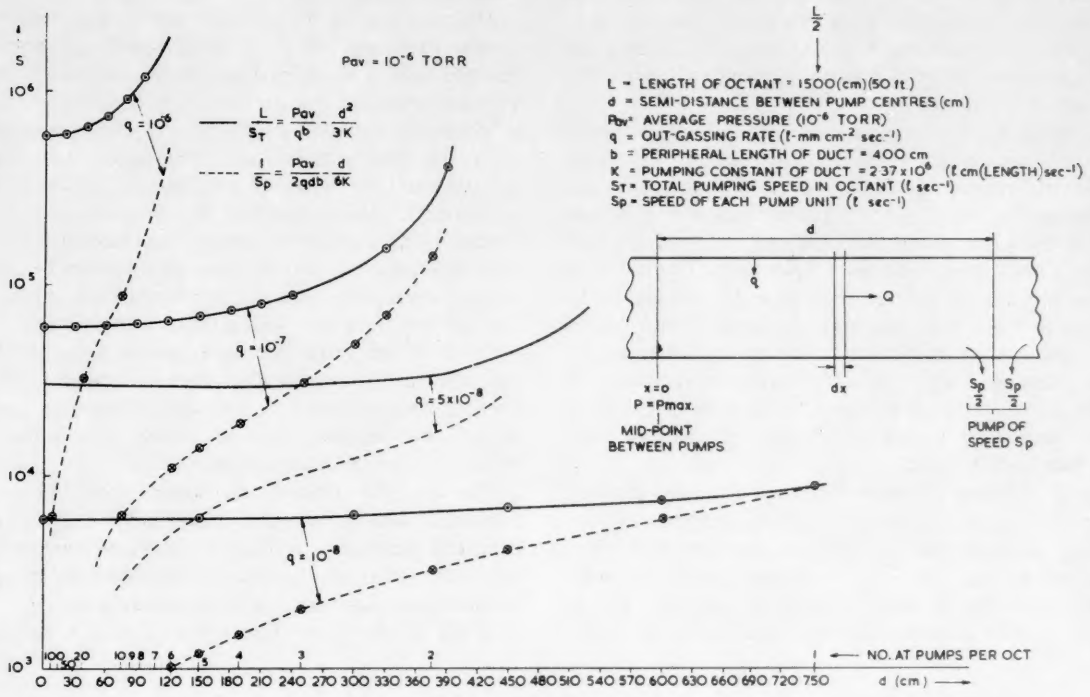
S
Pav = 10⁻⁶ TORR
q = 10⁻⁶
q = 10⁻⁷
q = 5x10⁻⁸
q = 10⁻⁸
L/S_T = Pav/q^b − d²/3K
1/S_p = Pav/2qdb − d/6K
L/2
L = LENGTH OF OCTANT = 1500(cm)(50 ft)
d = SEMI-DISTANCE BETWEEN PUMP CENTRES (cm)
Pav = AVERAGE PRESSURE (10⁻⁶ TORR)
q = OUT-GASSING RATE (l-mm cm⁻² sec⁻¹)
b = PERIPHERAL LENGTH OF DUCT = 400 cm
K = PUMPING CONSTANT OF DUCT = 2·37 x 10⁶ (l cm(LENGTH)sec⁻¹)
S_T = TOTAL PUMPING SPEED IN OCTANT (l sec⁻¹)
Sp = SPEED OF EACH PUMP UNIT (l sec⁻¹)
d
q
Q
dx
x=0
P=Pmax.
MID-POINT BETWEEN PUMPS
Sp/2
Sp/2
PUMP OF SPEED Sp
NO. AT PUMPS PER OCT
d (cm)

FIG. 1.

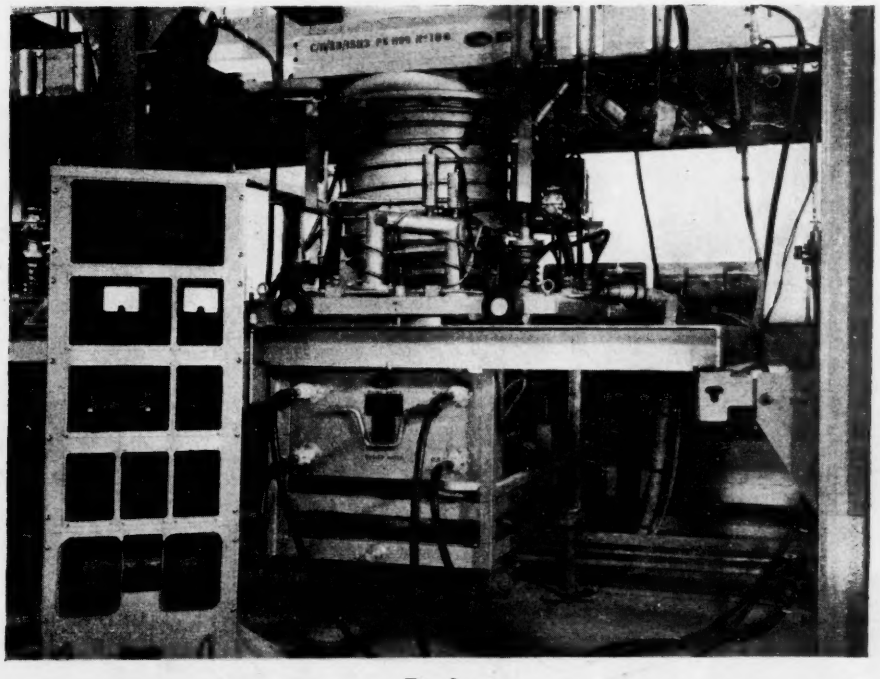

FIG. 2.

to a point where too few pumps can no longer give the required performance, no matter what their speed. Since the machine is divided into 8 similar parts, Fig. 1 has been plotted in terms of one octant. Appendix I gives the derivation of the curve.

The final choice of pumping equipment was for 40 pumping units, five to each octant of the machine (Fig. 2). Each unit is completely self contained and is readily removable for maintenance purposes. The diffusion pump is a 60 cm diameter fractionating and self purifying unit with a speed of some 12,000 l./sec, and uses Apiezon " C " oil. It is surmounted by a refrigerated chevron baffle to keep backstreaming to a low level, and by a sliding gate valve with a special slow opening device to limit the initial gas loan on the pumps. Backing is by a vapour booster pump and a small mechanical rotary pump, giving a compact unit, free from excessive noise and vibration. The baffled speed of each unit is 5000 to 6000 l./sec.

The control system is completely automatic. After pressing the " start " button the remainder of the sequence is controlled by pressure switches, timers and thermostats. The opening of the high vacuum valve is controlled separately, only being possible if all conditions are suitable. In the event of any fault occurring this valve is immediately closed.

Vacuum vessel

The magnetic field in which the vacuum vessel must operate rises from 300 G to 14 kG in 0.7 sec. During this time the field in the magnet gap must conform to extremely ac ate configurations, and the eddy currents which would be induced in a massive metal vacuum vessel would seriously affect the field gradient and thus impair the machine's performance. In addition the heating effect would be considerable, almost doubling the machine's losses with a corresponding increase in cooling requirements. The maximum amount of metal which can be introduced in the field without appreciably affecting the magnet design is stainless steel foil not more than 50 μ thick or its equivalent.

Ceramics are attractive materials in terms of vacuum and electrical properties, but their mechanical properties are such that a ceramic vessel would consume a great deal of valuable magnet aperture. Glass also suffers from similar mechanical disadvantages.

However, the recently developed epoxy resins when reinforced with woven glass cloth provide a very strong structural material which has a reasonably low outgassing rate, and a design has been evolved which utilises this material in such a way as to consume the minimum space.

It will be seen from Fig. 3 that a double walled vessel

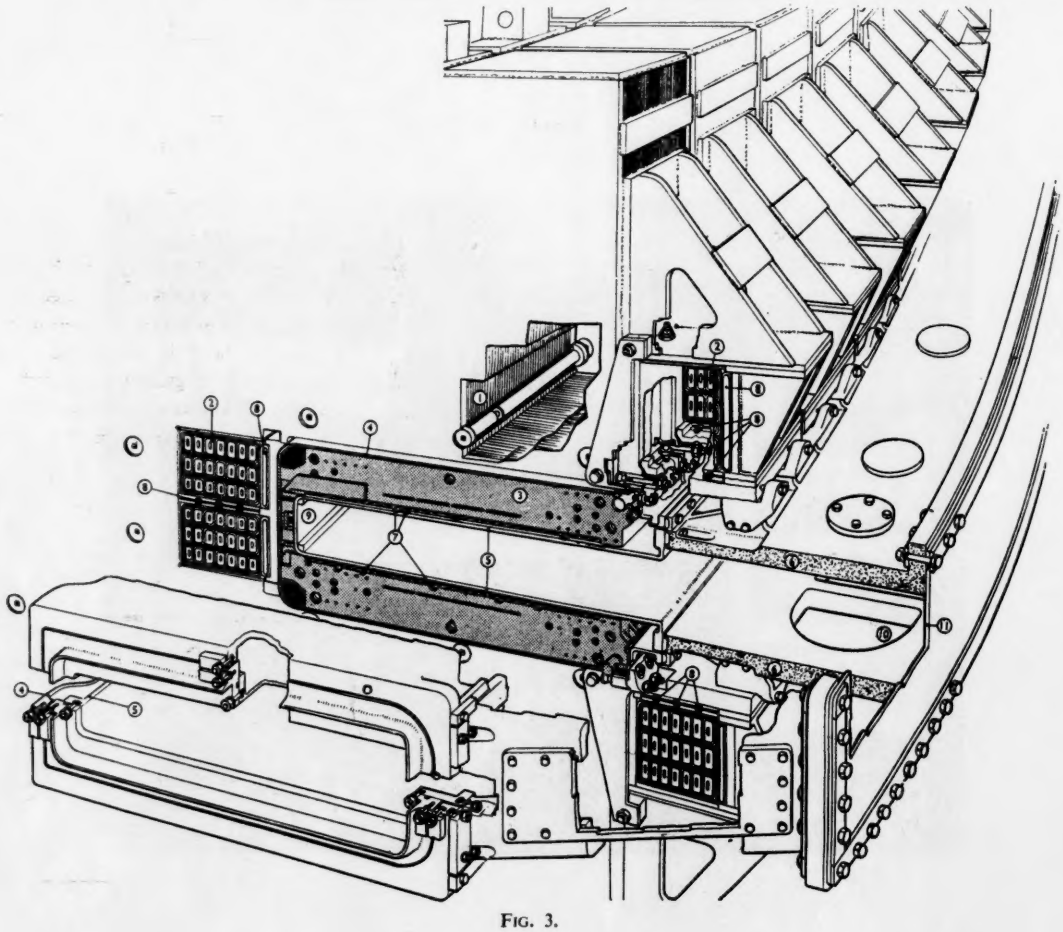

FIG. 3.

Vol. 10 196

system is used, the volume of the high vacuum space being some 80,000 l. The outer vessel contains the pole tips which, by being jacked apart at the back of the magnet throat and bolted to the magnet coil brackets through vacuum seals at the front provide the necessary support for this very thin (3 mm) vessel. The inner vessel, itself only 6 mm thick, is inserted between the pole tips and then the thick walled header vessel is brought up to the inner and outer vessel flanges. The header vessel is secured in place by integral webs which are secured to the coil brackets.

To accommodate manufacturing tolerances in these 15 m long vacuum vessels a specially moulded elastomer seal is necessary. Good sealing pressures are obtained by almost circular cross sections, joined by a web which bridges the gap between inner and outer vessels. The seal is mechanically balanced by having a similar section on either side of each row of bolts.

The inner vessel will be lined with thin stainless steel foil to mask the inner surface of the vacuum vessel and reduce the outgassing rate to the design figure. This lining also prevents the accumulation of electrostatic charges.

The considerable amount of gas which is evolved from all the surfaces contained in the outer vessel will be pumped away by a rotary pump, which ensures that the pressure in this space does not exceed 1 torr and so prevents the collapse of the inner vessel.

Epoxy resins

The resin received from the manufacturers is either a liquid or a solid thermoplastic, and will remain in this uncured condition for long periods, but by adding suitable polymerising agents (hardeners) a cure can be effected at will, the cured product being almost inert and within wide limits no longer thermoplastic. By using the resin in its liquid form to wet layers of glass cloth, the finally pressed and cured product possesses very good mechanical properties.

There is a considerable number of hardeners available and they have a profound influence on the characteristics of the cured product, which will vary in vacuum properties, radiation resistance and mechanical strength. They also affect the time and temperature needed to cure the resin and the ability of the mixture to wet out glass cloth and hence the feasibility of using any one particular manufacturing technique.

The hardener systems which have been investigated can be divided into three broad groups, the aliphatic amines, the aromatic amines and the anhydrides. The aliphatic amines are typical of the cold curing systems readily available but are inferior to the other two in vacuum and radiation resistance properties. The anhydrides have good vacuum and radiation resistance properties but need longer cure times ; the cure times can be reduced by using accelerating agents but these can sometimes have a deleterious effect on the final properties required.

The vacuum properties of these resins have been measured using the molecular effusion method described by Knudsen[3] with apparatus similar to that used by Power and Dennis.[4] Two forms of evaluation have been used. One involves temperature cycling the sample until all the absorbed vapours are removed, when the ultimate pressure-temperature relationship of the material can be determined. Since temperature cycling (except over a small temperature range) will not be possible on the finished product, the other test consists of measuring the variation of gas evolution rate with time under ambient or quasi-ambient conditions. Fig. 4 shows residual pressure versus reciprocal of absolute

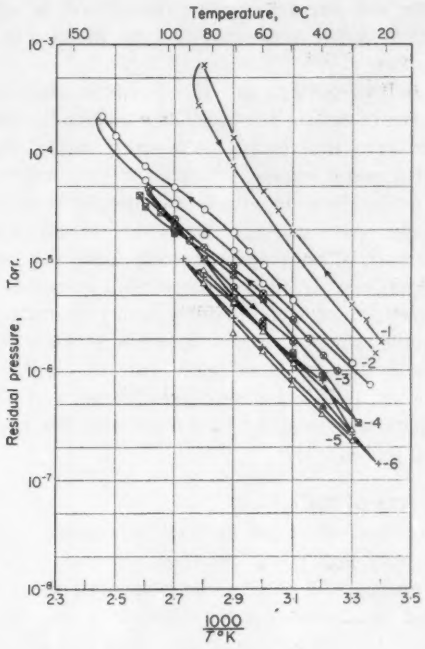

FIG. 4.

temperature for a number of temperature cycles of a typical plasticised epoxy resin polymerised with *p'p*-methylene dianiline. Further cycling shows no appreciable improvement over the lowest curve and this is taken to be typical of the vacuum behaviour of the resin when it has been degassed. Thin films are more readily degassed and satisfactory use of epoxy resins in sealed off devices has been reported.[5]

When effective degassing cannot be employed and the

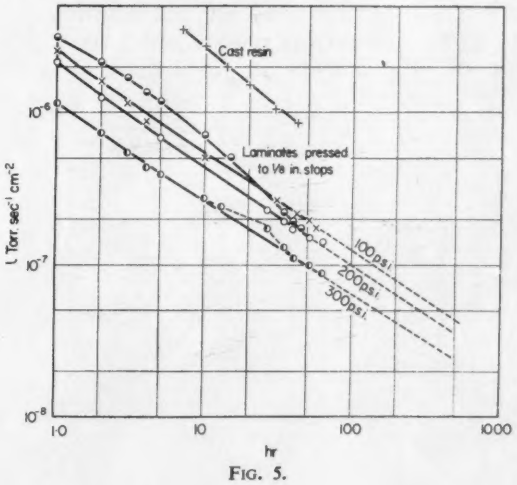

FIG. 5.

resin is frequently exposed to atmosphere the important parameter is the rate of desorption of previously absorbed gas. Fig. 5 shows the change of gas evolution rate in litre torr per second plotted against time for a typical unplasticised cast resin polymerised with *p'p*-methylene dianiline. Also shown on the same graph are curves for glass cloth reinforced laminates using the same resin system. An improvement in vacuum properties by the use of increased moulding pressures during the manufacture of the laminate can be noted and this is attributed to the increased ratio of glass to resin in the laminate.

Another interesting result which has been observed is that the addition of certain plasticisers can reduce the rate of gas evolution from the resin. Mass spectrometer tests[6] have shown that water vapour is the chief gas desorbed, so a possible explanation seems to be that the plasticiser is serving to block the epoxy lattice, reducing the amount of absorbed water vapour. The plasticiser itself does not appear to desorb readily provided it is not present in excess.

The tests on vacuum properties have been mainly carried out on samples with a total surface area of some 30 cm^2 but confirmatory tests on flat sheets with an exposed area of 1140 cm^2 and on a vessel with a surface area of 85,000 cm^2 gave results in substantial agreement with the tests on the smaller samples.

The effects of radiation

Certain areas of the machine will be exposed to bombardment by very high energy protons. Since a proton source of this energy will not be available until the machine is completed, irradiation tests have had to be carried out with other facilities. Experiments have been carried out in the Harwell 170 MeV proton cyclotron to relate damage due to proton bombardment to that obtained by neutron bombardment in a nuclear reactor,[7] and subsequent testing has been carried out by irradiating samples with reactor neutrons. Several samples are inserted simultaneously, a number being extracted at various intervals, the final ones having received doses in excess of 10^9 rads. Tests are then carried out to measure the gas evolution rate and flexural strength of the samples.

Fig. 6 shows the effect of radiation on the vacuum properties of a resin polymerised with *p'p*-methylene dianiline and Fig. 7 is for a resin polymerised with methyl " Nadic " anhydride. The latter sample has a lower gas evolution

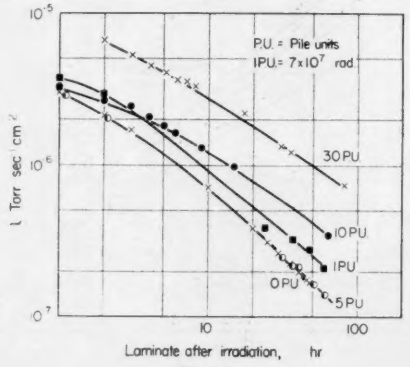

FIG. 6.

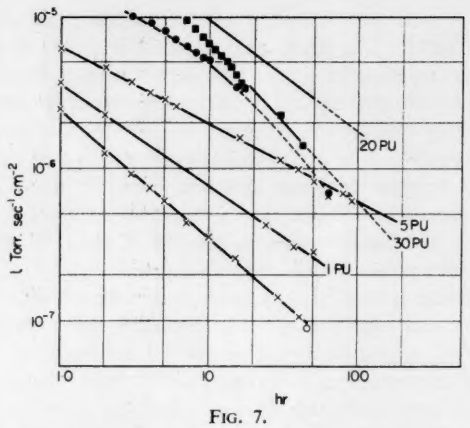

FIG. 7.

rate than the former when unirradiated but after both samples have been irradiated its gas evolution rate is worse, tests in all cases referring to fresh samples.

Fig. 8 shows the effect of radiation on the flexural strength of a number of polymers.

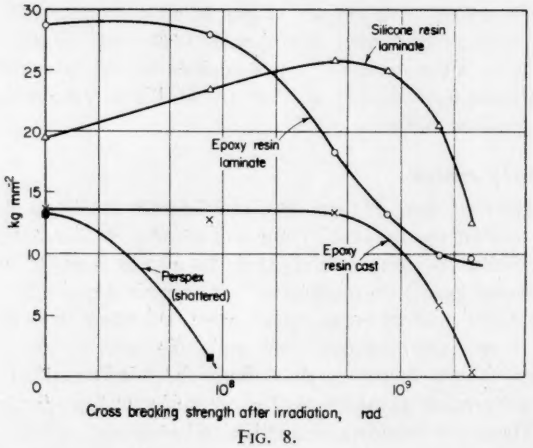

FIG. 8.

Acknowledgements

Acknowledgement is made to the Director of the Atomic Energy Research Establishment for permission to publish this paper, to the Director of the Rutherford High Energy Laboratory for encouraging its preparation and to R. J. B. Hadden and W. Spittle who have carried out much of this work.

References

1 T. G. Pickavance *et al.* ; *The 7 GeV Proton Synchrotron, Nuclear Engineering* (April 1959).

2 R. J. B. Hadden ; *Gas scattering in proton synchrotrons with variable rate of acceleration, U.K.A.E.A. report No. A.E.R.E. GP/R* 2189.

3 Martin Knudsen ; *The Kinetic Theory of Gases*, Methuen & Co. Ltd., Third Edn. (1950).

4 Private communication.

5 R. H. Collins and J. C. Turnbull ; *Evolution and absorption of gases in electron tubes, International Symposium on Residual Gases in Electron Tubes and Related High Vacuum Systems*, Section I (1959).

6 N. J. D. Prosser and A. H. Turnbull ; *Gas evolution from plastic materials in vacuum, U.K.A.E.A. report No. A.E.R.E. C/M* 362.

7 R. J. B. Hadden and W. Spittle ; *The effects of proton and neutron irradiations on an epoxy resin vacuum chamber proposed for the Harwell 7 GeV Proton Synchrotron, U.K.A.E.A. report A.E.R.E. A/R* 2690.

8 A. S. D. Barrett and C. H. Bosanquet ; *Resistance of ducts to molecular flow, I.C.I. Ltd. (Billingham Division) Report BR*-296 (November 1944).

APPENDIX

Symbols

Q	gas evolution rate	litre torr sec^{-1}
q	specific gas evolution rate	litre torr sec^{-1}cm^{-2}
b	peripheral length of duct	cm
K	conductance constant	litre cm sec^{-1}
P	pressure	torr
P_m	pressure (maximum)	torr
P_{av}	pressure (average)	torr
d	semi distance between pumps	cm
S	speed	litres sec^{-1}
S_p	pump speed	litres sec^{-1}
S_t	total speed	litres sec^{-1}
N	number of pumps	
L	length of octant	cm

From kinetic theory of gases:

$$Q_{(x)} = qxb = -K\frac{dp}{dx}$$

$$\therefore P = \frac{-qbx^2}{2K} + \text{const}$$

and since $P_{(x=0)} = Pm$

$$P = P_m - \frac{qbx^2}{2K}$$

Integrating for P_{av}.

$$P_{av} = \int_0^d \frac{(P_m - \frac{qbx^2}{2K})}{d}\,dx$$

$$= P_m - \frac{qbd^2}{6K}$$

and substituting for P_m, $(P_m = P + \frac{qbx^2}{2K})$

$$P_{av} = P + \frac{qbx^2}{2K} - \frac{qbd^2}{6K}$$

and $P = P_{av} + \frac{qb}{2K}(\frac{d^2}{3} - x^2)$

but $S_{(x)} = \frac{Q_{(x)}}{P_{(x)}}$

$$= \frac{qxb}{P_{(x)}}$$

$$= \frac{qxb}{P_{av} + \frac{qb}{2K}(\frac{d^2}{3} - x^2)}$$

when $x = d$, $S = \frac{S_p}{2}$

$$\therefore S_p = \frac{6qdbK}{3P_{av}}K - qbd^2$$

or $\frac{1}{S_p} = \frac{P_{av}}{qdb2} - \frac{d}{6K}$

but total pumping speed $S_t = NS_p$

and $d = \frac{L}{2N}$

$$\therefore N = \frac{L}{2d}$$

and we then have

$$\frac{L}{S_t} = \frac{P_{av}}{qb} - \frac{d^2}{3K}$$

Values of K taken from Barrett & Bosanquet[8].

Measurement of Gas Evolution and Absorption from Materials used in Vacuum Tubes

KAZUJI HASHIMOTO, HIDEO IWAYANAGI and HIROSHI FUKUSHIMA

Hitachi Mobara Plant, Mobara City, Chibaken, Japan

As a first step of their study on the gas-evolution from materials used in vacuum tubes, the writers took up three methods of measuring in common use, namely, the gas accumulation, the gas flow (differential Pirani gauge) method, and the flowmeter method. The writers, while reviewing the principles of these methods, discussed their sensitivities in relation to various gases, and mentioned difficulties in experimenting with low pressure gases, especially the outgas from the glass wall and other parts of the vacuum system as well as the reaction between the sample material and the gases evolved from it. On the basis of the experimental results, the writers have developed the gas evolution and adsorption gauges on the gas flow method, which record the measurement automatically. Some examples of the actual measurement of outgas characteristics of metal plates are given in this report. The characteristics of the gas absorption of titanium has many interesting problems and it suggests useful applications in the field of the vacuum tube production. The writers also carried out the experiment for studying the gas absorption rate of titanium for such gases as nitrogen, oxygen, carbon mon- and dioxide, at various temperatures. The pressure of the gas sealed in a vessel and contacted with the titanium surface decreased exponentially with time in the pressure range of this experiment, and then it is concluded that the absorption speed is nearly constant. From its dependence the activation energies of absorption for these gases were calculated. Moreover, some interesting phenomena such as the hysteresis effect of gas absorption and the jump of speed which occurred abruptly in the process of the carbon dioxide absorption were found.

1. Introduction

The gas evolution and absorption problem from the materials sealed in vacuum tubes is very important in the course of tube production. There are many reports[1, 2] about such problem, but on account of the complicated heat treatment of the metallic or non-metallic materials and of the difficulties of accurate quantitative measurement of gas pressure, we have had no systematic information about these subjects.

In vacuum tube engineering, the test of gas absorption and evolution from tube materials is so important in establishing the evacuation schedule of the tube that conventional gas evolution measuring techniques are desirable for tube makers. We can handle these gas problems in two ways as follows. In one case we want to know what amount or what kind of gases are evolved in the evacuation process, when the mounted electrodes are sealed in the glass tube, and then we can determine the optimum schedule of electrode cleaning by heating and/or evacuation. In the other case the investigation of gas evolution from the individual electrodes[3, 4] such as plate, mica, sleeve, etc., is also important to establish the quality control of the tube. Here we will describe the three types of the measuring methods. We will also report on the gas evolution from metal plates which are used in electrodes.

2. The measuring methods of gas evolution from materials

(a) *Accumulation method*

If we accumulate the evolved gas in a vessel of constant volume and measure its pressure, the quantity of gas evolved is measured directly. The volume of the evolved gas is calculated as follows :

$$Q = PV \tag{1}$$

Q : the volume of evolved gas ($1\text{-}\mu$)
P : the increased pressure of the vessel (μHg)
V : the volume of the vessel (1).

and the evolution speed at any time is obtained by differentiating equation (1).

$$S = V\frac{dP}{dt} \tag{2}$$

S : the evolution speed ($1\text{-}\mu$/sec).

(b) *Gas flow method*

When gas flows in a capillary tube, a difference of pressures appears along the capillary tube according to its resistance. In case of low pressures the differential Pirani gauge is usually employed.

(c) *Flowmeter method*

This method is reported by UEDA[3, 5, 6, 7]. When we place a plate, such as mica, in a stream of glowing gas, the

plate is rotated about its axis of suspension due to the force of impact of the molecules.

These methods a, b, and c, are shown in Figs, 1, 2, 4, 5 and 6.

The construction of the flowmeter is understood by Fig. 5 and 6. The thin vane is fixed to the fine tungsten wire and the weight is suspended in the oil (such as used for the diffusion pumps, for example) which acts as a damper. The angle of rotation is measured by the lamp and scale method, the reflecting mirror is fixed to the rotating axis of thin mica vane. We can measure the speed of gas evolution by this method, so the volume of gas evolved is calculated by integrating the speed of gas evolution.

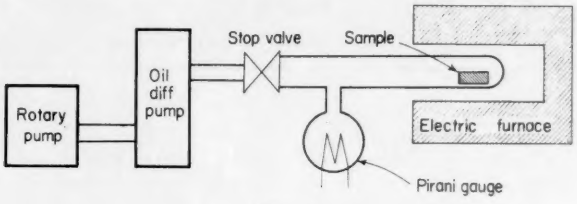

FIG. 1.

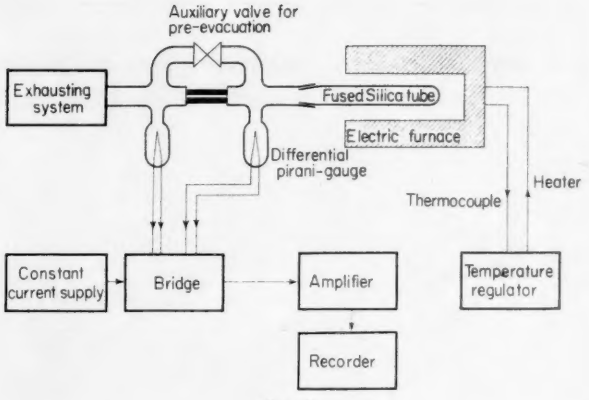

FIG. 2.

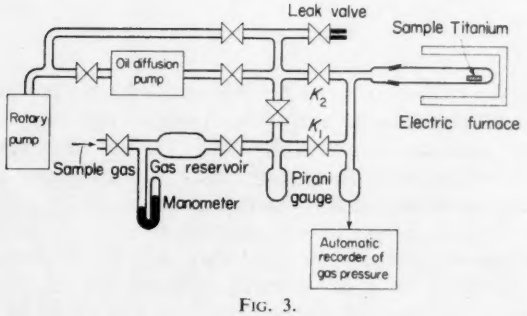

FIG. 3.

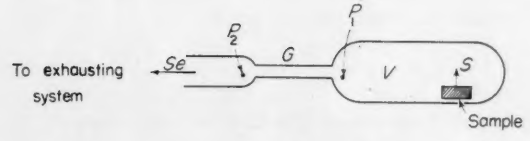

FIG. 4.

Fig. 3 shows the apparatus for measuring gas absorption of titanium which is mentioned in detail in the course of this paper.

If we use the notations in Fig. 4 as follows :

D : diameter of capillary (cm)
L : length of tube (cm)
R : gas constant (erg/°K Mol)
M : molecular weight of gas (g/Mol)
T : absolute temperature of gas (°K),

then the conductance of the capillary tube for molecular stream conditions is given by

$$G = \frac{1}{6}\frac{D^3}{L}\sqrt{\frac{2\pi RT}{M}} \times 10^{-3} \qquad (3)$$

let the pressures on each side of the capillary tube be P_1 and P_2 then the molecular stream condition for air is

$$\frac{P_1 + P_2}{2} \cdot D \leqq 15$$

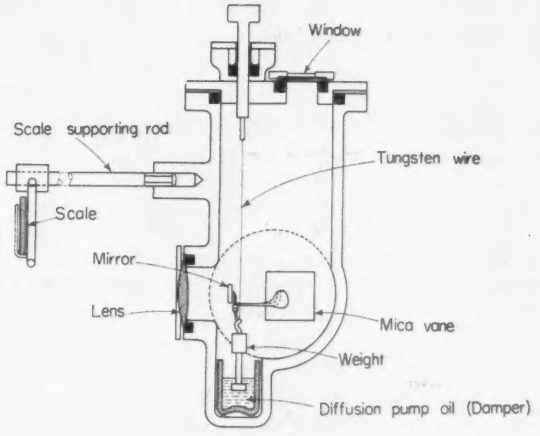

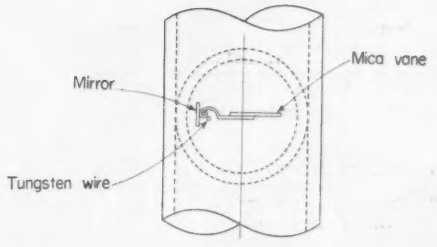

FIG. 5.

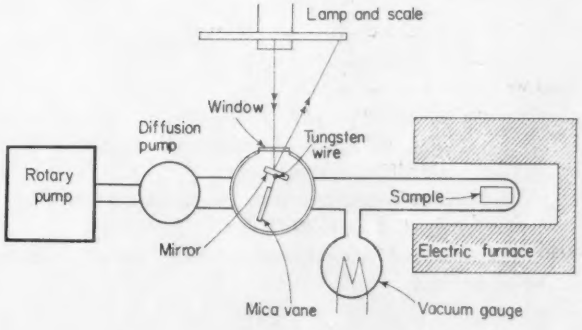

FIG. 6.

The quantity (Se) of gas flowing through the capillary is

$$Se = G(P_1 - P_2) \tag{4}$$

and the pressure P_1 at time t is expressed by

$$P_1 = \frac{1}{V}\int_0^t (S - Se)\, dt \tag{5}$$

From these equations the volume of gas Q evolved from the material is expressed as

$$Q = \int_0^t Sdt = G\int_0^t (P_1 - P_2)\, dt + VP_1 \tag{6}$$

then the total volume of gas evolved is obtained, under the condition that

$$\text{as } t \to \infty \quad P_1 \to 0$$

that is

$$Q_{tot} = G\int_0^\infty (P_1 - P_2)\, dt \tag{7}$$

The velocity of gas evolution will be obtained by differentiating equation (6)

$$S = G(P_1 - P_2) + V\frac{dP_1}{dt} \tag{8}$$

We can measure $\Delta P = P_1 - P_2$, considering $P_1 \gg P_2$ in most cases then equation (8) will be transformed to

$$S \doteqdot G\left[1 + \frac{V}{G}\frac{d}{dt}(\log \Delta P)\right] \Delta P \tag{9}$$

The writers have examined each method above mentioned. For the accumulation method, only the Pirani gauge sensitivities for each gases are important. The writers used the Hitachi V P H–62 Pirani gauge which has a platinum filament (filament current is 100 mA) and obtained the relative sensitivities for air, CO, H_2 and natural gas (metan). Table I shows the measured relative sensitivities and those calculated from the kinetic theory of gases.

TABLE I

Relative Sensitivities of Pirani Gauge

Gas		Air	CO	CO_2	H_2	Natural Gas
Relative	calculated	1.00	0.90	1.00	1.48	1.24
Sensitivities	observed	1.00	—	0.97	1.47	1.40

By the flow method the total volume Q is obtained from the equations (3) and (7)

$$Q = \frac{1}{r}\sqrt{\frac{29}{M}}\, G_0 \int_0^\infty \Delta P_0\, dt \tag{10}$$

where

r : specific sensitivity of the gauge for a gas of molecular weight M

G_0 : conductance for air

ΔP_0 : gauge pressure corrected to air (where molecular weight of air is 29).

From this equation, the relative sensitivity for any gauge will be given by

$$r\sqrt{\frac{M}{29}}$$

The force due to the impact of gas molecules which acts on the vane of the flowmeter is

$$F \propto \sqrt{M}.S \tag{11}$$

When the angle of rotation of the suspension is small, the relative sensitivity will be roughly

$$\sqrt{\frac{M}{29}}$$

Table II shows the relative sensitivities of the various measuring methods. Here we defined that the sensitivity of air should be 1.00, and those of CO, CO_2 and H_2 are calculated, a shown in Table II.

TABLE II

Relative Sensitivities of Various Measuring Methods

Gas		Air	CO	CO_2	H_2
Relative Sensitivities	Accumulation Method	1.00	0.09	0.97	1.47
	Flow Method	1.00	0.88	1.20	0.39
	Flowmeter	1.00	0.98	1.23	0.26

3. Sample chamber and exhausting system

Fig. 7 shows the sample chamber, and Fig. 2 and Fig. 3

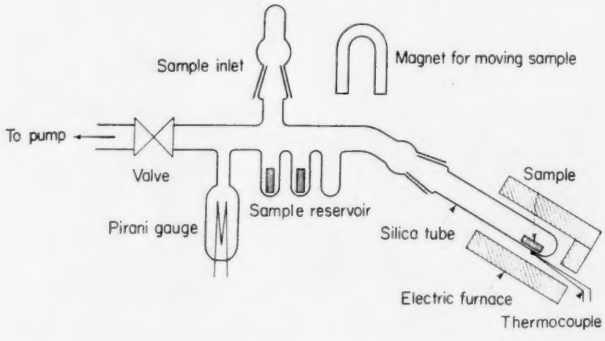

FIG. 7.

show the exhausting systems. We used a fused silica tube (16 mm inner diameter and 400 mm long). The volume of the gas accumulation vessel was 480 ± 3 cc and the capillary tube had an internal diameter of 1 mm, and was 50 mm long. The weights of the samples usually employed were 0.25 ~ 0.5g and the electric furnace was maintained to ±5°C of the experimental temperature. The unit of evolved gas was calculated per 100 g, for normal conditions (N.T.P.).

The conductance of the capillary tube was measured by the following method. If we put $s = o$ in the equation (5) and consider equation (4), we get

$$\log\frac{\Delta P}{\Delta P_0} = -\frac{G}{V}t \tag{12}$$

where ΔP_0 is the pressure difference ΔP at $t = o$ and

$$\Delta P \simeq .P_1 \ (P_1 \gg P_2)$$

$\Delta P - t$ curve is shown in Fig. 8 from which we get the conductance of the capillary for air 3.5×10^{-3} l/sec.

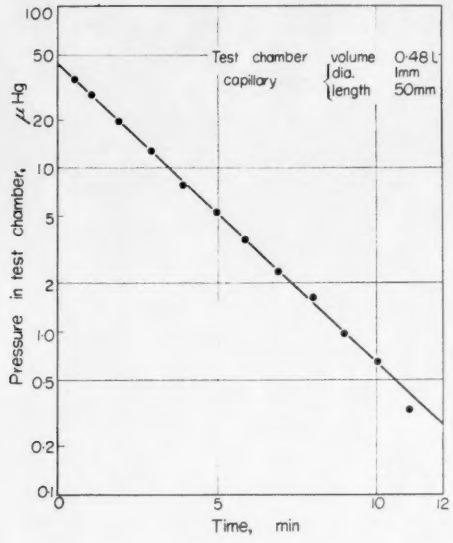

FIG. 8.

4. Experimental procedure

When the sample is heated in the closed vessel, a reaction between the sample and its own evolved gas may occur, or the gas evolution speed from the sample may be affected by the ambient gas pressure. By using the accumulation method we tried to measure the quantity of gas evolved from pure iron sheet (0.125 mm thick, 0.25 g in weight). Five samples were cleaned up and put into the sample chamber together. Samples No. 1, 2 and 3 using single pieces, and No. 4 double (0.05 g) were moved into the fused silica tube, using a magnet, in order to heat to a temperature of 850°C. Fig. 9 shows the results of these measurements for the evolution of gas from Fe plate by the accumulation method.

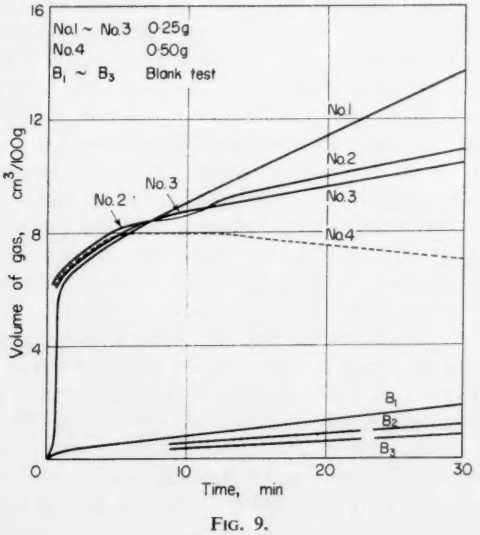

FIG. 9.

In Fig. 9, the curves B_1, B_2, and B_3 show the blank test before testing the samples. From these data it is known that in the first five minutes the quantities of gas evolved expressed in cc/100 g from No. 1 ~ No. 3 samples (0.25 g) and No. 4 sample (0.5 g) are nearly equal regardless of the weights of the sample. But after five min, the curves gradually change according to their own characteristics. We tried many experiments with many samples and obtained the following information.

(a) The gas evolution speed is not greatly affected by the ambient gas pressure.

(b) The changes of gas evolution after five minutes depend on the degassing treatment of the system. The discrepancy of curves No. 1, No. 2 at 20 ~ 30 min cannot be understood even if we take the blank test into consideration.

(c) The apparent speed of gas evolution at 20 ~ 30 min (see Fig. 9) is also affected by the accumulated gas pressure.

If we remove the samples from the furnace area to the sample chamber and somewhat decrease the temperature of the heater, the change of the accumulated gas pressure disappears. So it may be assumed that there occurs some reaction between the heated sample and the evolved gas or some gas included in the quartz wall. These phenomena are remarkable in tests carried out on nickel and iron sheets.

5. The result of gas evolution from several materials used in vacuum tubes

From the measured data the gas evolution volume and the evolution speed can be calculated using equations (7) and (8). We used the air coefficient. So the volume is calculated in terms of air. The total evolved volume differs according to the production process of the material even though the nature of the material is the same. At present tubes are usually evacuated by a fixed schedule empirically determined for normal electrode materials, so that the evolved gas affects the character and the life of the tube. Table III shows the volume of the gas evolved from various

TABLE III

Volume of Gas Evolved from Various Metal Plates[1]

Sample Number	Material	Gas Evolution[2] (cc/100g)		Note
		Washing	H_2 Firing[3]	
A	Nickel	5.96	2.68	Domestics
B	Nickel	4.06	2.42	,,
C	Pure Iron	8.46	0.15	,,
D	Ni Plated Iron	9.91	0.96	,,
E	Ni Plated Iron	16.3	6.6	Imports
F	Carbonized Nickel	3.8	0.83	Domestics
G	Carbonized Iron[4]	44.5	3.3	,,
H	Carbonized Iron[4]	—	29.7	,,
I	Carbonized Iron[4]	—	13.2	,,
J	Carbonized Iron[4]	—	14.3	,,
K	Carbonized Iron[4]	330	33.3	Imports

Note : [1] Thickness 0.12~0.13 mm.
[2] Test Condition : 850°C, 30 min.
[3] Firing Condition : 800°C, 10 min.
[4] These Materials are treated on the Surface only.

metal plates. These samples are 0.12 ± 0.01 mm thick, 0.125 g in weight, and they are experimented with in two ways. Namely, in one case the plate was only washed and in the other case it was heat-treated at 800 °C ; for 10 min in a hydrogen atmosphere and then kept for 24 hr in free air. After that the experiment was carried out in the furnace at a temperature of 850 °C for 30 min. We also measured the effect of the heat-treatment in a hydrogen atmosphere using samples of Ni or nickel-plated Fe. These samples were 0.125 mm thick. They were washed or heated at 600 °C, 800 °C ~ 1000 °C for 10 min in a hydrogen atmosphere before measuring the gas evolution at 850 °C for 20 min. Table IV shows the result of the experiments. From these

TABLE IV

Gas Evolution at Various Temperatures of Heat Treatment in Hydrogen Atmosphere

Treatment Temperature		(Washing)	600 °C	800 °C	1000 °C
Nickel	Evolution* (cc/100 g)	6.14	4.54	2.94	0.46
	Ratio	1.00	0.74	0.48	0.075
Ni Plated Iron	Evolution (cc/100 g)	10.2	4.18	0.92	0.64
	Ratio	1.00	0.41	0.090	0.063

Note : *Test Condition : 850 °C, 20 min.

experimental data we notice that there is some difference in the gas diffusion constant between Ni and Fe plates.

6. Relationship between gas evolution from titanium and its temperature

Gas evolution and absorption of titanium have useful applications in the field of vacuum tubes. A titanium plate was put into the sample chamber and heated at various temperatures in order to determine the volume of the evolved gas. The gas volume observably increased at a temperature of 400 °C, and at 700 °C the increasing rate of the evolved volume decreased. These data are shown in Fig. 10. In Fig. 10 the evolved gas volume Q is calculated per 100 g and normalized to N.T.P. Log Q is plotted as a function of the reciprocal of the absolute temperature (I/T). From these data (see Fig. 10) we can see that the relationship between gas evolution, log Q, from titanium and the temperature, (I/T), is given by a straight line which has a knee joint at the temperature 600 °C ~ 700 °C.

We can consider the activation energy for the mechanism of gas evolution. The activation energy is 1.7 eV for temperature lower than 600 °C, and 0.16 eV for temperature higher than 700 °C. From these experimental data we carried out further experiments to determine what kind of gas is evolved from titanium at various temperatures. We used as mass spectrograph (Hitachi RM-A). These data are shown in Table V. At 700 °C the CO gas is evolved, but at higher temperature only H_2 was observed.

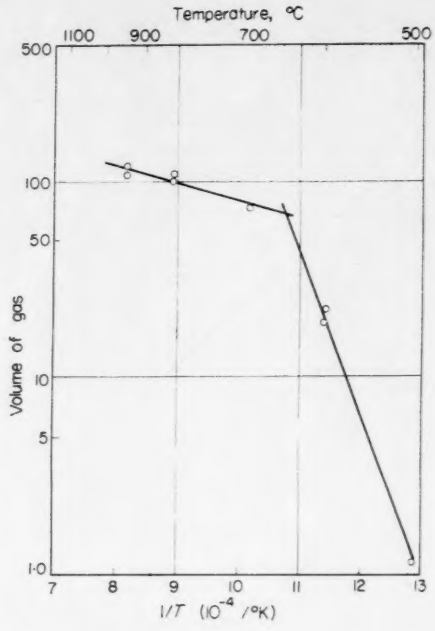

FIG. 10

TABLE V

Analysis of Gas Evolved from Titanium

Test Condition	H_2	CO	Others
900 °C 7 min.	99.5%	0.5%	
800 °C 7 min.	>99.5	<0.5	
700 °C 7 min.	78	20	about 2% of CO_2 and others

7. Gas absorption of titanium

After washing the titanium plate with benzine, we put it into the sample chamber, and evacuated all the vacuum system in the course of baking. In particular, the sample chamber was maintained at 1000 °C, for 60 min. When the pressure reached 10μHg and no more gas was evolved, we decreased the temperature of the sample chamber to the observing one and kept it in that condition. Then we inserted gas into the sample chamber, through the valve K (see Fig. 3). The valves K_1 and K_2 were closed during the measurement. The pressure change after gas insertion was observed automatically using the recording Pirani gauge system. We tried N_2, O_2, CO and CO_2, with the titanium plate of 3.5 cm^2 and 0.1 g. The initial gas pressure was 40μHg and the volume of the sample chamber was 500 cc. Figs. 11, 12, 13 and 14 show the experimental data. The gas pressure variation with time for N_2 (Fig. 11) shows a straight line if we plot log P on the vertical axis. In the case of O_2 the curves of log $P \sim t$ are somewhat complicated, but they appear to be a group of straight lines (Fig. 12). The knee points in the case of CO_2 (Fig. 14) are quite noticeable. Namely, curve (a) of Fig. 14 shows the experimental datum at a temperature of 700 °C. The absorption velocity

Vol. 10 1960

suddenly increased. This phenomenon may show that the absorption mechanism changes in the course of the absorption process.

If we repeat the experiment of absorption using the same sample, there sometimes occurs a difference of absorption ability of CO absorption on titanium in repeated tests. It is said that titanium retains every gas once absorbed except H_2 even if it is heated ; we experienced the same phenomenon. But by high temperature treatment the absorption ability is somewhat recovered. Fig. 16 shows the effect of heat treatment in vacuum on the O_2 absorption rate in the repeated tests. In this experiment we tried the absorption process twice at 600°C and twice at 500°C, making its absorption ability lower, and then treated the sample at 900°C in vacuum

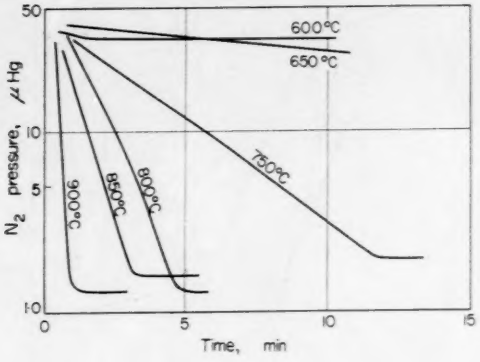

FIG. 11.

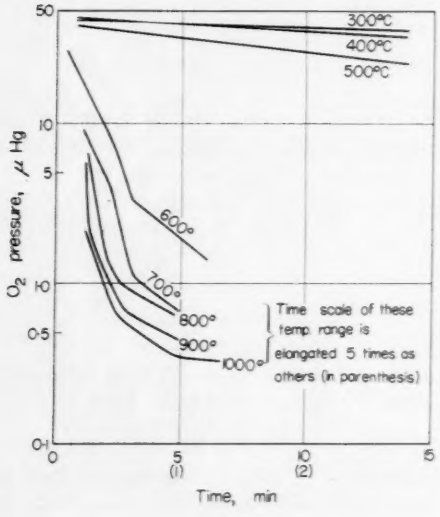

FIG. 12.

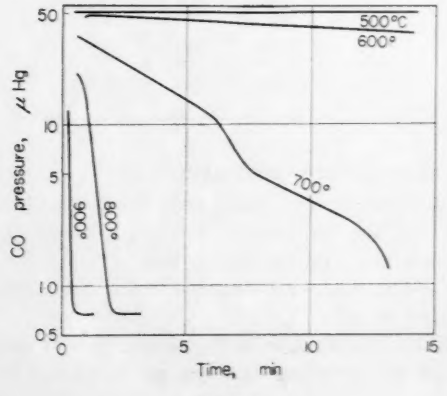

FIG. 13.

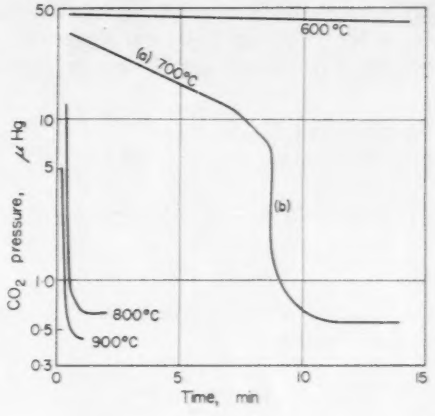

FIG. 14.

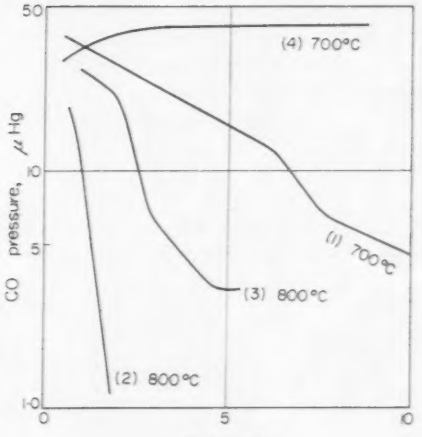

FIG. 15.

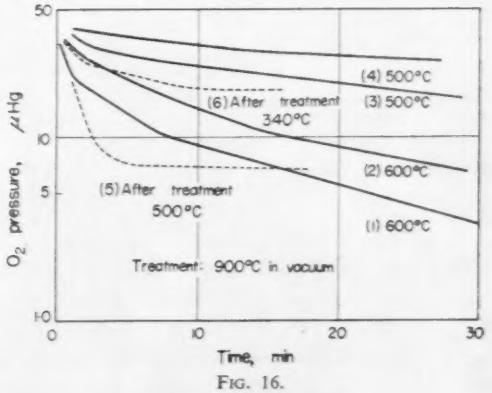

FIG. 16.

and carried out an absorption experiment at 500°C. In this case the ability recovered remarkably in the first five min. This phenomenon shows that the oxygen on the surface of the sample diffused into the sample, and the concentration of O_2 on the surface was lowered.

From the results of measuring the pressure changes caused by absorption, we can obtain the absorption velocity. According to the absorption mechanism we can consider many types of $P \sim t$ relationships, but in our experiment the pressure decreased exponentially with time especially in the case of N_2. The log $P \sim t$ curve seemed to be a straight line (Fig. 11). In this case if we use the following notations

P : pressure (μHg)
P_0 : the initial pressure ($t = 0$)
t : time
a : constant (the slope of log $P \sim t$ line)

then

$$P = P_0 e^{-at} \tag{13}$$

From this equation we can conclude that the absorption velocity should be constant.

$$D = \frac{Va}{A} \tag{14}$$

where

D : absorption speed (l/sec cm^2)
V : the volume of the vessel (l)
A : the surface area of titanium (cm^2)

and the volume of absorption Q is

$$Q = A D P \tag{15}$$

TABLE VI

Gas Absorption Rate of Titanium D (l/cm^2 sec)

Temperature	N_2	O_2	CO	CO_2
	$\times 10^{-3}$	$\times 10^{-3}$	$\times 10^{-3}$	$\times 10^{-3}$
300°C	—	0.023	—	—
400	—	0.039	—	—
500	—	0.057	~0	—
600	~0	1.72 1.57	0.047	0.006
650	0.1	—	—	—
700	—	17.7 18.3	0.47 0.52	(*a*) 0.42 (*b*) 7.9*
750	0.57	—	—	—
800	1.6	25 19	7.3	9.9
850	2.9	—	—	—
900	12	26 34	10	9.1
1000	—	34	—	—

Table 6 shows the gas absorption rate of titanium (D is in litre/cm^2 sec). The absorption velocity differs according to the temperature of the sample. If log D is plotted as a function of $1/T$, we obtain the results shown in Fig. 17.

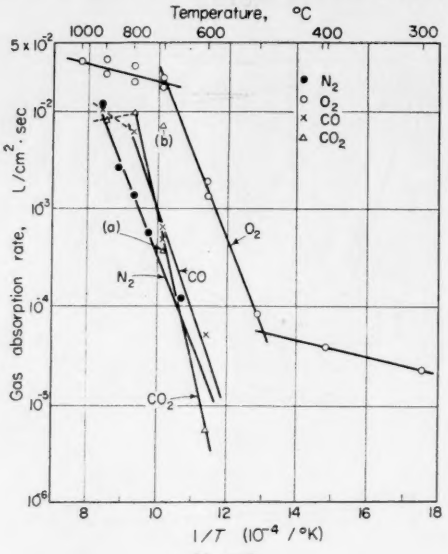

FIG. 17.

The N_2 line is nearly straight. O_2 consists of 3 straight lines the upper part of which is thought to come from measuring errors on account of its high absorption velocity.

If the absorption velocity D is defined as

$$D = D_0 e^{-\frac{E}{kT}} \tag{16}$$

where

K : Bolzman's constant
D_0 : E : const.

then E will be the activation energy, and we can obtain E for several types of gases as shown in Table 7.

TABLE VII

Activation Energy of Gas Absorption by Titanium

Gas	Temp. Range	E
N_2	600°C ~ 900°C	1.8 eV
O_2	300 ~ 500	0.17
	500 ~ 700	1.7
	700 ~1000	0.22
CO	600 ~ 800	2.0
CO_2	600 ~ 800	2.5

8. Gas absorption mechanism

Several writers[8, 9, 10] have considered the theory of absorption. Here we consider the simple model of monoatomic molecule. Let us assume that :

(1) The gas molecules are absorbed on the metal surface and diffused into it.
(2) The absorption point on the surface loses its absorption ability by absorbing only one gas atom, but when the

*The values of (*a*) and (*b*) correspond to the (*a*) and (*b*) region of the curve log $P \sim t$ at 700°C in the Fig. 14.

atom has diffused into the metal the point recovers its absorption ability.

(3) Two gas molecules cannot collide against one absorption point at the same time.

(4) The number of absorbed molecules depends on the rate of absorption of the surface, and the diffusion velocity into the metal depends on the density of the molecules on the surface.

(5) We consider the case of constant pressure of gas on the surface.

According to the above assumptions, if Na molecules are absorbed in unit time and unit area, and if Nd molecules diffuse into the metal, then

$$Na = Ka\,(1-\theta)\,n \tag{17}$$

$$Nd = Kd\,\mathrm{No}\;\theta \tag{18}$$

where

No : the number of absorption points (number/cm²)

θ : the rate at which a point loses its ability of absorbing and trapping a molecule.

Ka : the probability of capture of molecules which collide with the absorption point on the surface.

Kd : the diffusion probability of the molecules which is absorbed at the absorption point in unit time (1/sec).

n : the number of collision of molecules/unit time.

If we consider the absorption point (No, θ) which already has lost its absorption ability, and we differentiate for it with respect to time

$$\frac{d\theta}{dt} = \frac{1}{No}(Na - Nd) = Ka\,(I - \theta)\frac{n}{No} - Kd\,\theta \tag{19}$$

at the boundary conditions $t = o\ \theta = o, t = \infty \quad \frac{d\theta}{dt} = 0$

we get

$$\theta = \frac{Kan}{Kan + Kd\,No}\left[I - e^{-(Kan/No + Kd)t}\right] \tag{20}$$

From the kinetic theory of gases, n is given by

$$n = \frac{P}{\sqrt{2\pi mkT}} \tag{21}$$

where P : Pressure (dyne/cm²)

m : weight of one molecule (g)

also,

$$n_a = q/kT \tag{22}$$

q : the volume of gas absorbed per unit time and unit area (dyne/cm² sec).

then we obtain the velocity of absorption, D, using equations (17), (20), (21) and (22).

$$D = \frac{q}{p} = \sqrt{\frac{kT}{2m}} \cdot Ka\left[I - \frac{Ka'P}{Ka'P + Kd}\cdot\left(I - e^{-(Ka'P+Kd)t}\right)\right] \tag{23}$$

where

$$Ka' = \frac{Ka}{No\sqrt{2\pi\, mkT}}$$

When the gas pressure is high or the diffusion velocity is slow, namely $ka'P \gg kd$, we assume $(ka'P + Kd)\,t \gg 1$ in the equation (23).

In the case of constant volume the absorption volume q is given from the equation (23) and the obtained q is constant, namely

$$q = 7.5 \times 10^{-4}\, kTNoKd \tag{24}$$

So the pressure changes linearly with time. V. L. Stout and M. D. Gibbons[8] gave the results for a higher pressure (500μHg ~ 600μHg). If we consider No as the number of absorbing points in the equation (24), the average lifetime from absorption to diffusion on the surface ($1/Kd$) is shown in Table VIII. The lifetime is so short that our experimental

TABLE VIII

Mean Life Time of Gas Atoms Staying at Titanium Surface ($1/kd$)

Temp.	N	O	C
700°C	8 sec	0.3 sec	44 sec
800	4	0.03	4
900	2	—	2
1000	1	—	0.6
1100	2.5	—	0.2

Note : Calculated from Data of Stout & Gibbons.

data will be discussed in the case of low pressure in which the molecules are not supplied in sufficient quantity to the surface. In case of $ka'P \ll kd$, we can neglect the second term in the equation (23), then the absorption velocity D is constant. Then

$$D = 10^{-3}\sqrt{\frac{KT}{2\pi m}} \cdot Ka \tag{25}$$

In this case the change of pressure is obtained as shown in the equation (13), and our experimental data will also coincide. Stout obtained the same result for H_2 at relatively high pressure. We are considering that H_2 is only one gas that takes the absorption and evolution phenomena reversively, and the diffusion velocity is very large.

Conclusion

The gas absorption and evolution problems are very interesting and important in vacuum tube production. We tried many methods of measuring gas absorption and evolution. Titanium presents many interesting problems in the absorption and evolution phenomena. These problems are also considered theoretically.

In a titanium plate the absorption velocity observably increases at 500°C in case of oxygen, and other gases show the same phenomenon at 600°C ~ 700°C. At low pressures the absorption velocity is constant and it depends on the surface ability of metals, but not on the diffusion phenomenon. In case of polymolecular gas we may consider the mechanism of dissociation.

References

[1] Kinzokugakkai ; Report (*Showa* 25-29).
[2] Arizumi, Maekawa ; *J. Phys. Soc. Japan* **8**, 87 (1953).
[3, 4] Yamamoto ; *Hitachi Hyoron* **35**, 1343, 1759 (*Showa* 28).
[5, 6] Ueda ; *Oyobutsuri* **17**, 136, 370 (*Showa* 23).
[7] Ueda, Sugiura ; *J. Phys. Soc. Japan* **8**, 99 (1953).
[8] V. L. Stout and M. D. Gibbons ; *J. App. Phys.* **26**, 1488 (1955)
[9] Harashima ; *Shinkukan no Getter no Kansuru Kenkyu.*
[10] C. J. Smithells ; *Gases and Metals* (1937).

SESSION IV

Influence of Residual Gases on Tube Life

The Influence of Residual Gas on the Performance of the British Post Office Submarine Telephone Repeater Valve Type 6P12

R. W. LAWSON

Post Office Engineering Dept., London

The main source of gas in a pentode valve which has been pumped in accordance with the best modern practice has been found to be the occluded gas evolved from the valve components during the manufacture and life of the valve. The virtual elimination of this gas from certain of the valve components prior to valve assembly is one of the chief factors that have permitted the development of passive core valves suitable for use in submarine telephone schemes.

1. Introduction

The British Post Office has been concerned for a number of years with the development and production of thermionic valves for use in its submarine telephone schemes. One of the valves developed and discussed in this paper, the type 6P12, resembles an ordinary pentode receiving valve in many respects. The most important difference is the replacement of the active nickel core (which can give rise to valve failure due to interface growth) by one of pure platinum. Platinum was chosen for the cathode core because it was the only suitable cathode material available at the time with a sufficiently low silicon content to ensure absence of interface growth. The introduction of a passive core into the valve did not provide the immediate answer to improved valve life. In the absence of activators such as magnesium in the core, the oxide matrix proved difficult to activate and it soon became apparent that the production of satisfactory passive core valves was largely a gas problem.

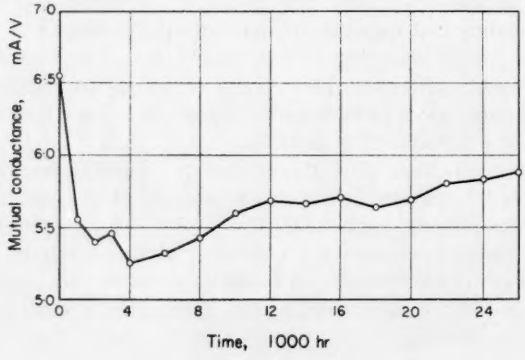

FIG. 1.

Life test conditions :—
anode = 90V
screen = 60V
anode current = 6·0mA
heater = 5·5V

Probably the most important parameter by which the suitability of a valve for use in submarine telephone schemes is judged is the stability of the mutual conductance. This in turn depends on the stability of the cathode activity. When an oxide cathode is subjected to a gas attack free barium is destroyed and the cathode activity declines. This deterioration is reflected in a fall in the mutual conductance. The mutual conductance trends during life for passive core 6P12 valves made under conditions that give rise to high gas pressures during pumping and subsequent life are illustrated in Fig. 1. Valves with characteristics such as these are clearly not acceptable and efforts were directed to locating the sources of gas that give rise to these characteristics.

In valves made with active nickel cores the loss of free barium due to gas attack is to some extent compensated for by the reducing action of the active constituents, magnesium and silicon. It is the absence of such activators in the platinum core that make it particularly important to remove the sources of gas.

2. Sources of gas in the valve

In a sealed-off working valve there are two sources of gas which can attack the oxide cathode. First there is the free gas that is left in the valve after the getters have been flashed and the valve sealed from the pump and aged. In this paper this is defined as the initial gas pressure, P_0. Secondly there is the gas evolved from the various components when the valve is operating under normal conditions. The magnitude of the initial gas pressure depends on the adequacy of the pumping techniques used, the efficiency of the getters and also on the amount of gas evolved from the valve components during pumping and ageing of the valves.

The repeater valves are pumped on high grade bench pumps capable of an ultimate vacuum of 2×10^{-7} Torr. A

brief description of the pumping schedule is as follows. After pumping down the valves are baked at 400 °C for 1½ hr. The anodes are then induction heated to about 900 °C, during this process the grid rods and the capacitance shields are raised to about the same temperature. The cathode carbonates are decomposed and the anodes are again induction heated. The cathode is activated by drawing current, under non-ionising conditions, to the various electrodes. The getter is then flashed and the valve sealed from the pump. The valves for which life characteristics are shown in Fig. 1, were pumped in this manner and as indicated earlier show clear signs of having suffered from a gas attack. The main source of gas in these valves was found to be the dissolved or occluded gas in the interior of the various components. The occluded gases are released when the components are raised to elevated temperatures to remove surface adsorbed layers of gas during the processing of the valve on the pump. The occluded gases can also be released during the life of the valve. All the materials used in valve manufacture, nickel, platinum, molybdenum tungsten, mica and glass, contain gas. The gases in the metals are occluded during manufacture. Mica, on the other hand, is a naturally occurring mineral containing hydroxyl groups and when raised to elevated temperatures can decompose and release large quantities of gas. The composition of the gas released from the various components is important but it so happens that oxygen and oxygen-containing compounds (water vapour and oxides of carbon) are among the most common gaseous contaminants of commercial materials and are also the most deleterious in their effects.

The rate of evolution of the occluded gas from the components, and hence the amount evolved during the pumping and ageing—and during life—is largely controlled by diffusion phenomena. The rate of evolution of gas depends therefore on the total quantity of gas in the component and on the temperature and dimensions of the component. The total quantity of gas evolved during the pumping and ageing is simply the time integral of the evolution rates of gas from the various components.

It is true that the whole purpose of induction heating the valve whilst on the pump is to degas the components but this results, when virtually unprocessed components are used, in so much gas being released that the cathode activity is impaired before the valve is sealed off. Even if this were not the case the duration of induction heating on the pump cannot be conveniently extended to ensure complete degassing of the components and hence no gas evolution during life. Thus the production of passive core valves is centred on the problem of reducing the total internal gas contents of the various components before the valve is assembled. The effects of reducing the gas contents of the components prior to valve assembly are threefold. First the total amount of gas evolved from the components during the pumping and ageing is reduced, thus enabling the cathode to be activated satisfactorily. Second, the initial gas pressure is reduced and finally a very low rate of gas evolution from the components during life is ensured.

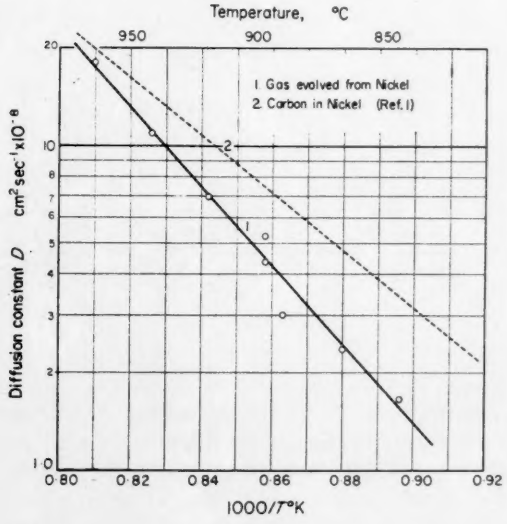

FIG. 2.

3. Elimination of gas prior to assembly of the valve

The components which have been found to require particular attention are the anode and capacitance shields both made from nickel sheet 0.15 mm thick, the grids consisting of fine molybdenum wire wound on nickel support rods 1 mm diameter and the cathode core. These are the components that reach the highest temperatures during the pump processing, ageing and during life.

All the components are first cleaned to remove surface contaminations. The removal of the dissolved gas in the materials is achieved in high temperature vacuum or hydrogen furnaces, the latter being generally used. The degassing time is controlled by diffusion processes and in general the higher the temperature used the shorter the time necessary to reduce the gas content of the material to a given level.

The outgassing properties of the various materials used in the valve have been studied and from them the various processing schedules necessary to degas the components have been derived. Nickel is probably the most common valve material and is used extensively in the repeater valves as sheet (for the anodes and shields) and as wire (for the support rods of the grids). The outgassing properties of nickel have been investigated in some detail and will be briefly considered here to show how the various degassing schedules have been derived.

The gas evolved from commercial grade nickel is largely carbon monoxide resulting from the reaction of carbon with the oxides of such impurities in the nickel as magnesium and silicon. The carbon concentration in the nickel investigated lies in the range 0.006 per cent to 0.05 per cent. Total gas quantities of between 2×10^{-3} and 20×10^{-3} l. Torr per gm. have been measured and the total quantity evolved is limited by the amount of oxygen present. In general, the total amount of gas evolved from wire is greater than that evolved from sheet material. The diffusion constant of the gas evolved has been measured in the temperature range 850–975 °C and is shown as a function of temperature in Fig. 2

where it is compared with the diffusion constant of carbon in nickel determined by Lander[1]. Since the evolution rate of gas is determined by the diffusion constant and since the two curves are in close agreement it is concluded that the evolution of carbon monoxide from nickel is largely controlled by the diffusion rate of carbon. From a knowledge of the diffusion constant, the degassing curve for wire or sheet can be calculated for any temperature. For sheet material of thickness x, the equation used is,

$$Q_R = \frac{8}{\pi^2} Q_0 \left(\exp - \frac{\pi^2 Dt}{x^2} + \frac{1}{9} \exp - \frac{9\pi^2 Dt}{x^2} + \frac{1}{25} \exp \frac{25\pi^2 Dt}{x^2} + \ldots \right)$$

where D is the diffusion constant, Q_R is the amount of gas remaining in the sheet after an outgassing time t and Q_0 is the initial gas content of the material assumed to be uniformly distributed.

For a wire of radius " a " the corresponding equation is

$$Q_R = 4Q_0 \left(\frac{1}{5.80} \exp - \frac{5.8Dt}{a^2} + \frac{1}{30.47} \exp - \frac{30.47Dt}{a^2} + \ldots \right)$$

In Fig. 3 the calculated degassing curve for 0.6 mm diameter nickel wire at 900°C (using the experimentally determined value of diffusion constant) is compared with an experiment where the nickel wire was outgassed in pure dry hydrogen at 900°C (Dew-point −60°C) for various times and the quantity of gas remaining in the wire, Q_R, was determined. It can be seen that experiment and calculations do not agree, the actual loss of gas from the wire proceeding at a greater rate initially than that calculated.

The reason for this discrepancy is that the oxides of the impurities such as magnesium and silicon are concentrated near the surface of the nickel and since the carbon is uniformly distributed throughout the wire the initial outgassing of the wire is governed by diffusion conditions more appropriate to a thin cylinder. The " skin " effect as it is called varies greatly from one sample of nickel to another depending on somewhat variable conditions of manufacture. The effect is usually more pronounced in the case of thin nickel sheet, and it is quite common to find that 80 per cent or more of the total gas content of sheet 0.150 mm thick is concentrated in a skin 10–15 μ thick.

Thermodynamic calculations predict that both magnesium and silicon can oxidise in a hydrogen atmosphere at 900°C if the partial pressure of water vapour is greater than 2×10^{-4} Torr, which corresponds to a Dew-point of nearly −90°C. Experience in the stoving of nickel sheet at 900°C in hydrogen at a Dew-point of −60°C support the calculations, a visible film of oxide being observed after 15 min treatment. However, nickel wire, of the same grade as the sheet, processed in a similar manner shows no such film. This difference of behaviour is believed to be associated with the different surface area to volume ratios of wire and sheet. Diffusion calculations and measured loss rates of carbon suggest that the arrival rate of carbon per unit area of surface is greater in the wire than in the sheet. Hence under the processing conditions considered, the balance between the oxidation of the magnesium and silicon by the water vapour in the hydrogen and the reduction of these oxides by carbon diffusing to the surface is such that for wire the oxides are reduced as quickly as they are formed but not for sheet. The practical implications are important in that commercial grade nickel sheet cannot be degassed in low temperature (900°C) hydrogen furnaces unless the Dew-point is below −90°C—a condition practically impossible to achieve.

It has been shown that nickel wire can be satisfactorily processed in hydrogen, of Dew-point −60°C at 900°C and the grids are given this treatment for 5 hr. This ensures that the wire used, of diameter 1 mm and less, and having gas contents in the range quoted, can be adequately outgassed. (The dissolved hydrogen in the nickel resulting from the process is removed during the 400°C bake of the valve on the pump.) Nickel sheet can be vacuum out-gassed at 900°C provided the vacuum is better than 10^{-4} torr at all stages during the process or it can be degassed in a hydrogen furnace of Dew-point −60°C at temperatures greater than 1100°C. When 80 per cent or more of the total gas content is concentrated in a skin 10–15 μ thick a simple chemical etch to remove the skin has proved to be an effective degassing process.

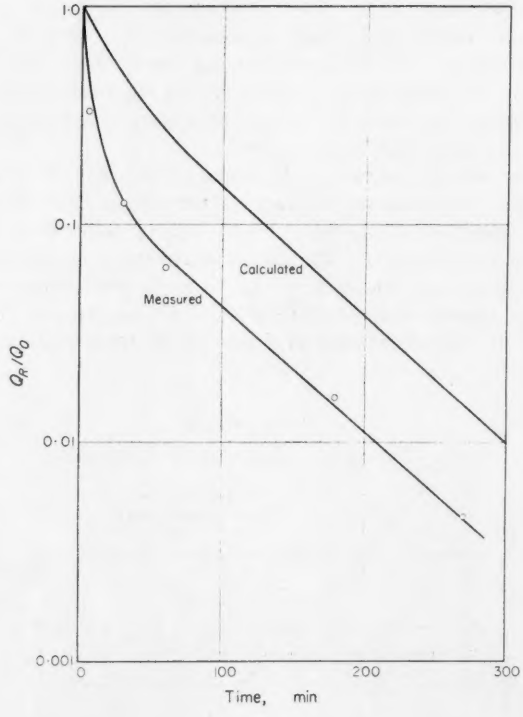

FIG. 3.

The materials are generally treated in their final component form and this limits the maximum temperature that can be used for outgassing because of the risk of mechanical damage and distortion. The minor dimension of the control and screen grids for example have to be held within a tolerance of ±15 μ and it is impossible to achieve this if an outgassing

Vol. 10 1960

temperature of 900 °C is exceeded. The processing schedules are designed to remove about 98 per cent of the initial gas content of some of the components—notably the grids. This is to be compared with the removal of some 10 per cent of the gas which is achieved by typical commercial practice.

TABLE I

Gas contents of 6P12 components before and after degassing

Component	Initial Gas Content (litre Torr × 10^{-3})	Gas Content after Degassing (litre Torr × 10^{-3})
Heater	0.5	0.5
Platinum Cathode	0.2	0.01
Control Grid	1.4	0.03
Screen Grid	0.9	0.02
Suppressor Grid	3.2	0.06
Anode	1.0	0.1
Capacitance Shields	1.2	0.12
Mica Spacers	Approx. 600	Approx. 600
Glass Bulb	Approx. 1000	Approx. 1000

Table I shows the initial gas contents of the components and the gas contents after processing prior to valve assembly. Surface adsorption of gas on the components is of course inevitable after they have been processed, indeed in some cases the quantity of surface absorbed gas is greater than that remaining in the body of the component. The storage time of processed components is kept to a minimum. They are stored in warm dry dust-free cabinets—this being preferable to vacuum containers where there is a risk of oil contamination.

Three of the components listed in Table I need further comment namely the heater, the mica spacers and the glass bulb. The mica and glass components contain relatively enormous amounts of gas which are not reduced by any processing treatment before valve assembly. Both materials are complex chemical compounds and the total quantities of gas quoted in the table are only released if the temperatures of the materials are raised to the point where chemical decomposition takes place. For ruby mica the decomposition temperature is in excess of 750 °C and glass has to be taken to the melting point to yield the quantity quoted. During pump processing and in normal running the temperature of neither of the materials approaches the temperature at which they decompose (except a small area of mica in contact with the cathode sleeve). The mica spacers are warmed by radiation from the anodes and shields when the valve is induction heated and can evolve some gas. Provided the induction heating is not too intensive the amount of gas evolved is small and is largely surface adsorbed gas—and the cathode activity is not impaired. The surface adsorbed layers of gas on the glass, which are readily released, are removed during the 400 °C bake before the cathode is decomposed and activated.

When the valve is running under normal conditions, the temperature of the mica spacers are low except in the region of the cathode locating slot which is in contact with the cathode operating at 730 °C. However, controlled experiments using fully degassed mica spacers have shown that during life neither mica nor glass contribute to the total gas evolution to an extent which influences the life characteristics. The reason for this is that during the normal running of the valve the temperature of both the mica spacers and the glass are such that the internal diffusion rate of the gases in the materials is very low. (This is a most fortunate circumstance as glass is not amenable to degassing and although ruby mica can be fully degassed it loses all its useful physical properties in the process and is no longer suitable for use in production valves.)

The heater consists of a tungsten helix coated with alumina, the alumina being fired on at about 1600–1700 °C. The porous alumina coating adsorbs gas readily when exposed to the atmosphere and hence cannot be effectively degassed. Higher firing temperatures which would sinter the alumina more effectively and so reduce the amount of gas adsorbed cause embrittlement of the tungsten and hence cannot be used. However during cathode decomposition the heater reaches temperatures of the order 1500 °K and it outgasses very rapidly at this temperature and loses most of its gas before the cathode is activated.

4. The effects of reducing gas contents of components on performance of valve

Initial parameters

The immediate effects of reducing the gas contents of the various components is an improvement in the initial activity of the cathodes. This is shown in Table II where the initial cathode activity and mutual conductance is shown for two groups of valves. The cathode activity of a pentode valve can be assessed in several ways and a convenient one is to measure the saturated emission at 700 °K with the control grid at +5 V. This is referred to as the Total Emission and the value in mA for the 6P12 cathode is roughly equivalent to the saturated emission in amps./cm² at the normal operating temperature of 1000 °K. The first group (Group I) had their components degassed on the lines indicated and the second group (Group II) had their components processed in accord with more normal commercial practice resulting in some 90 per cent of the gas being left in the components. Both sets of valves were given identical processing on high grade bench pumps and both contained barium flash getters.

TABLE II

Effect of degassing components on initial values of cathode activity and mutual conductance

	Cathode activity (T.E.) (mA)	*Mutual Conductance* mA/V
Group I	3.1	6.88
Group II	0.63	6.10

Life characteristics

The mutual conductance and cathode activity changes during life for the two groups of valves are shown in Fig. 4. It can be seen that the mutual conductance of the first group is stable after some few hundred hours life test as is the

cathode activity. The final level of cathode activity of the first group is considerably higher than the second group. The large fall in mutual conductance and the low level of cathode activity of the second group of valves is attributed to a higher initial gas pressure and to gas generated during life from some of the valve components. It will be seen that the second group of valves are recovering from the gas attack. This ability to recover from a gas attack once it has ceased is a typical characteristic of valves made with platinum cores. Group I valves have completed 7 years of life test and remain stable.

The results show that the use of rigorous pumping techniques and barium flash getters are not sufficient in themselves to reduce the residual gas in passive core valves to a level low enough to give satisfactory life characteristics. Thorough degassing of certain of the valve components prior to valve assembly is also necessary.

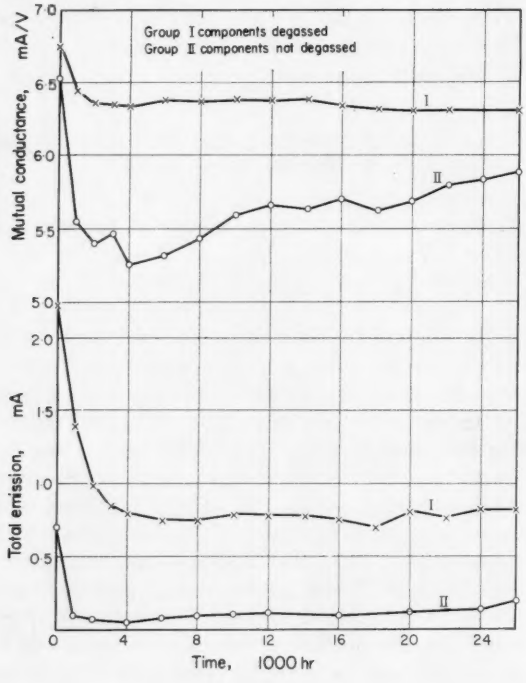

FIG. 4.

Life test conditions :—
anode = 90V
screen = 60V
anode current = 6·0mA
heater = 5·5V

5. Pressure variations in valve during life

The pressure in well processed (Group I) valves has been measured during pumping, ageing and life. Special assemblies were made for the measurements consisting of a normal pentode and a small Alpert ionisation gauge sealed into a common envelope. An alternative method used was to insert a molybdenum wire probe 75 μ diameter between the suppressor grid and the anode. The probe was primed at −9 V and collected positive ions generated by the electron

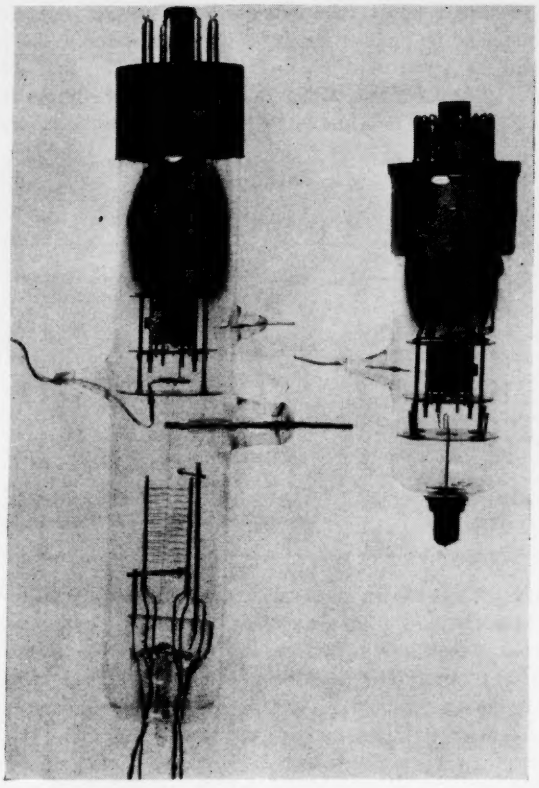

FIG. 5.

stream flowing to the anode. Due to the short ionising path of the electrons the sensitivity of the arrangement was rather low, about 0.20 μA/millitorr/mA and the probe current became insensitive to pressure changes below 7×10^{-9} Torr due to X-rays emitted from the anode. The results quoted below have been obtained on both types of assembly which are illustrated in Fig. 5.

The pressure in the valves just before getter flash is about 1×10^{-6} Torr. After the getter flash and seal-off the valve is given a low voltage ageing at the end of which the pressure approximates to 1×10^{-7} Torr.

The valve is then run as a pentode for 16 hr to stabilise before the "zero time" specification tests. The pressure at the end of the 16 hr run is about 1×10^{-8} Torr. During this preliminary run some 3.0×10^{-9} l Torr of gas has been dispersed some of which has attacked the cathode as can be seen from Fig. 6 which shows the cathode activity at the end of the 16 hr run as a function of the pressure at the beginning of the run. That most of the gas has been dispersed whilst the pentode has been running is shown by the fact that there is virtually no reduction in pressure if the valve is left inoperative, even for periods as long as 1000 hr.

After the specification tests the valve's life test begins and measurements show that the cathode activity, mutual conductance and pressure achieve stability at the same time. The time for achieving stability depends on the valve's running conditions and varies from a few hundred hours to about 3000 hr. The variation in pressure and cathode

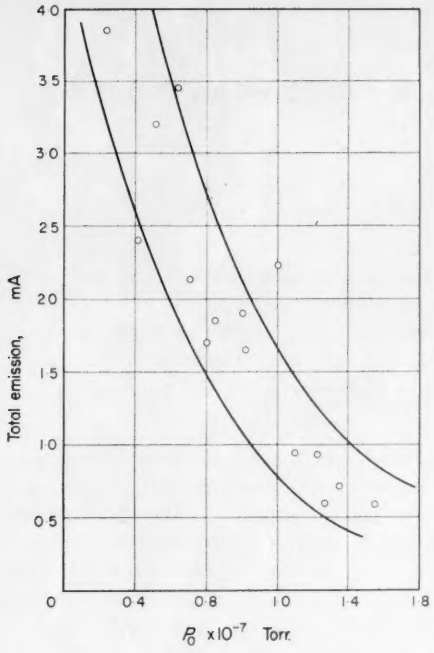

FIG. 6.

Life test conditions :—
anode = 90V
screen = 60V
anode current = 6·0mA
heater = 5·5V

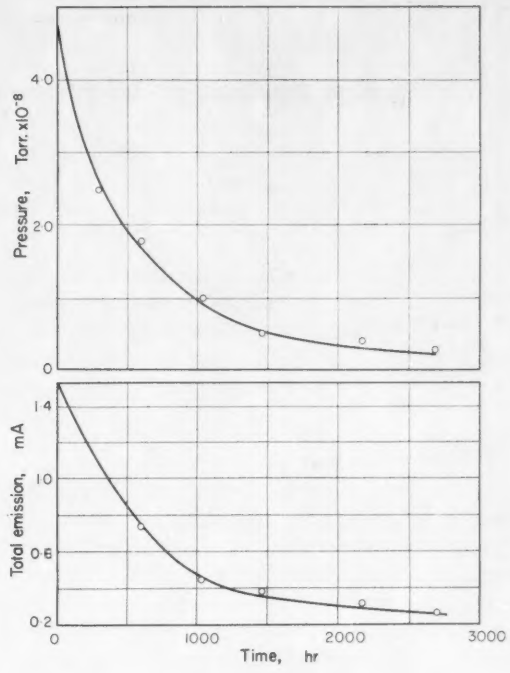

FIG. 7.

Life test conditions :—
anode = 90V
screen = 60V
anode current = 6·0mA
heater = 5·5V

activity during life for a pentode valve are shown in Fig. 7. The clean-up rate of the residual gas deduced from the curve is about 5×10^{-8} l.sec^{-1}, which is far below the rates quoted for barium getters.

Calculations based on diffusion data show that the evolution rate of gas from the components has either ceased or is steady at an extremely low level after the valve has run under normal conditions for about 100 hr. It is concluded from this and from the results just quoted that the fall in mutual conductance and cathode activity which occurs during the first few hundred hours life test is due to the adsorption by the oxide cathode of the whole or part of the initial residual gas. When all the residual gas has been adsorbed and in the absence of such gas generators as the components the cathode activity and mutual conductance become stable.

6. Conclusions

The main source of gas in a pentode which has been pumped in accordance with the best modern practice has been found to be the gas evolved from the valve components during the pumping and ageing of the valve. The virtual elimination of this gas prior to valve assembly has enabled passive core valves suitable for use in submarine telephony schemes to be produced.

In the submarine repeater valves currently being made by the British Post Office the passive platinum core has been superseded by a mildly active core of pure nickel containing 3½ per cent tungsten. Although cathodes using this material as a core are less susceptible to deactivation by gas attack, the degassing processes used for the platinum core valve have been retained, their virtues having been appreciated, and they give added insurance against valve failure.

Reference

1 J. J. Lander *et al.* ; *J. Appl. Phys.* **23**, No. 12 (1952).

DISCUSSION

Question from Mr. O. Pressel—Are the materials used in Post Office Valve specially processed, e.g., by vacuum metallurgy ?

Answer. No, the materials used in the 6P12 valve were not specially prepared. Commercial grade materials as normally supplied to the electronic valve industry were used. Valves currently being made at Dollis Hill use, wherever possible, high purity tungsten-nickel alloys made by the powder metallurgy process.

Question from Mr. O. Pressel

Is the glass used for the Post Office Valves predegassed ?

Answer.

No, it is not possible to predegas glass. Surface contaminations on the glass are removed by washing in detergent solution followed by thorough rinsing and oven baking in air at 400°C for one hour.

Noise Reduction in Microwave Tubes by Getter-Ion Pumping

N. W. W. SMITH

The Mullard Research Laboratories, Salfords, Redhill, Surrey, England

The problem of ion noise in microwave oscillators and amplifiers is explained. It is shown that residual gas pressures of approx. 10^{-9} Torr must be maintained in order to eliminate ion noise. A description is given of the construction of an ion getter pump which is built into a backward wave oscillator and designed to operate continuously while the oscillator is in use. The problems associated with maintaining low pressures in microwave valves are discussed.

Introduction

In recent years microwave oscillators and amplifiers have been used in applications demanding low levels of noise at frequencies very close to that of the fundamental microwave signal. It was discovered, however, that in certain devices the spectrum of the microwave output contained significant amounts of energy in unwanted, or spurious, signals and noise peaks clustered about the fundamental carrier signal. The devices in which this effect was most readily discernable were those employing long electron beams, namely the travelling wave amplifier and the backward wave oscillator.

Further investigation showed that these spurious effects were due principally to the presence of ionized residual gases within the electron beam[1].

Thus one method of eliminating these spurious effects is to reduce as far as possible the amount of residual gas within the vacuum envelope.

It was found that this solution to the problem necessitated maintaining residual gas pressures of approximately 10^{-9} Torr during the operation of the valve. Because of the construction of valves of this type, this proved to be a difficult target to attain.

This paper describes the construction and use of an ion getter pump built into a backward wave oscillator under the same glass envelope and designed to operate continuously while the oscillator is in use.

The characteristics of ion noise

Ion noise may conveniently be defined as those semi-random fluctuations occurring in an electron beam whose amplitude and spectral distribution can be affected by changes in the residual gas surrounding the beam. The region of the spectrum in which ion noise is apparent is between 10 Kcs and 10 Mc/s. It is in this region that the ion cyclotron and ion plasma resonant frequencies are to be found. This assumes that the electron beam is confined by a strong axially directed magnetic field and that ions formed are entrapped within the beam by space charge forces to form an ion core of density comparable with that of the electrons.

It is evident therefore that ion noise is not be found in the microwave region of the spectrum unless a strong microwave signal is present. If this is the case, however, the ion fluctuations in the beam of a microwave oscillator or amplifier modulate the microwave output of the device and then these fluctuations appear as modulation sidebands in the microwave spectrum. This has been conclusively demonstrated by experiment. An example of such a spectrum is shown in Fig. 1. Here it will be seen that two phenomena are to be

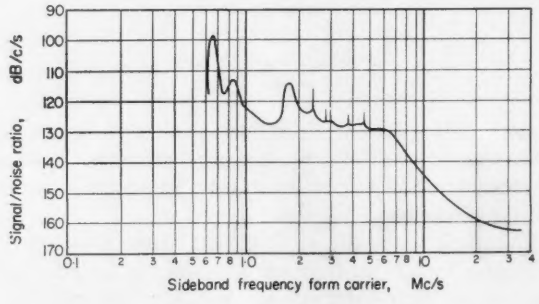

FIG. 1.

found, viz. ion noise peaks and discrete ion oscillations. These discrete oscillations are rarely found at residual gas pressures less than 10^{-7} Torr. It is believed that energy, which must be supplied to the system to sustain ion resonance, is derived from slow secondary electron emission caused by the impingement of a small amount of the primary electron beam upon the metallic walls of the device.[2]

The reduction of this type of noise as the residual gas pressure is decreased can be seen in Fig. 2 where, in this instance, measurements were made directly upon the electron beam.

From the foregoing discussion it will be appreciated that two other possible remedies exist for the elimination of ion noise. These are, firstly the removal of ions by electrostatic drainage and, secondly the reduction of secondary emission. Within the context of this paper it is sufficient to say that none of the remedies are absolute but that each is complementary to the others.

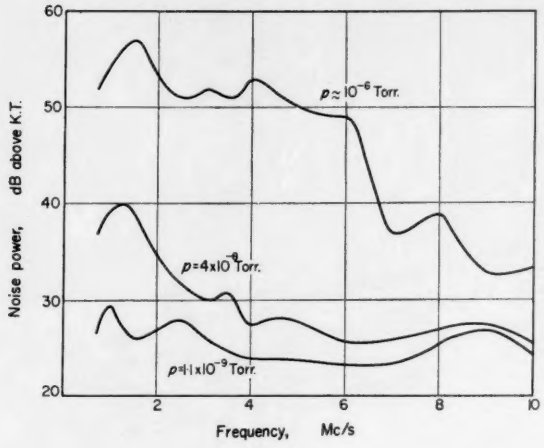

FIG. 2.

The construction of the backward wave oscillator

As a result of a number of experiments it was estimated that a pressure of less than 10^{-9} Torr would have to be maintained in the particular backward wave oscillator under consideration. This pressure would have to be maintained under all normal operating conditions despite localised heating and outgassing of metallic components caused by the moderately high powered electron beam (25 mA, 1500 V).

The processing of the valve during evacuation would become very important. In particular, a prolonged baking at the highest possible temperature would be of great benefit. However, with the existing valve construction, baking at temperatures greater than 420 °C was impossible. To increase the baking temperature significantly would have required a complete redesign of the valve. Consequently it was decided to attempt to reduce the residual gas pressure in a valve of the normal construction by using other means.

A diagram of the main components of the backward wave oscillator is shown in Fig. 3. The items most likely to prove

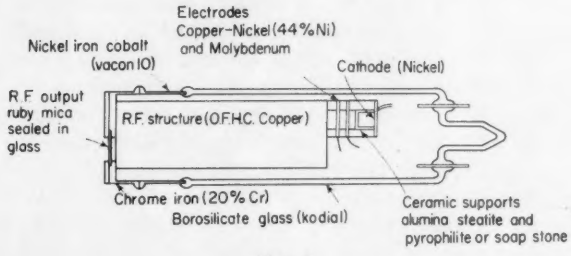

FIG. 3.

troublesome were the mica R.F. output " window " and the relatively large mass of copper. Mica spacers, etc., in the electron gun were replaced by ceramics and an improvement in the vacuum was noted but, from considerations of R.F. design, it was necessary to retain the mica window. Since this sheet was sealed at its edges by glass it was considered that the amount of gas coming from the mica cleavage planes would be small. For certain parts of the R.F. structure it was necessary to maintain the smallest possible dimensional tolerances, these parts were therefore made of OFHC.

Pressures obtained with the backward wave oscillator

A Bayard–Alpert ionisation gauge was attached to the pumping stem of a backward wave oscillator and both were baked at 420 °C for four days whilst being pumped with a three stage oil diffusion pump. During the subsequent processing the pressure was kept below 6×10^{-6} Torr by controlling the heating applied to the cathode and other electrodes. This was done in order to minimise recontamination of the cooler parts of the valve by the gases evolved from the hot cathode. Finally the valve and ionization gauge were sealed off from the diffusion pump and the barium getters fired. Immediately after seal-off the pressure was 2×10^{-8} Torr. This increased to 2.5×10^{-7} when the valve was operated. By operating the gauge as an ion pump at 10 mA emission current the pressure was eventually reduced to 6×10^{-8} Torr under operating conditions.

Although this was not a sufficiently low pressure to eliminate ion noise it was considered to be typical of the results obtainable by prolonged and careful processing.

The travelling wave tube

Similar noise phenomena have been observed in medium power and high power travelling wave tube amplifiers. It was not to be expected that ion noise would be found in low power amplifiers since a microwave signal output of at least one milliwatt would be required for the modulation sidebands to be detected. Also the electron density within the beam of a low power amplifier is very much less and consequently the ion trapping effects due to space charge forces are also greatly diminished.

The construction of a travelling wave tube differs from that of the backward wave oscillator. The total mass of metal within the vacuum envelope is much less but it is disposed uniformly within a long cylindrical glass envelope of small cross section. Although it is not very difficult to outgas portions of this metal by eddy current heating it is much more difficult to heat all of the metal simultaneously. Also, due to the shape of the envelope, it is difficult to remove rapidly gas which is evolved at the end of the tube which is remote from the pump. This gas is therefore able to contaminate clean components of the valve in passing towards the pump. With similar processing schedules, the operating pressure obtained in the travelling wave tube is approximately one order greater than that obtained in the backward wave oscillator.

The combined evapor-ion pump and backward wave oscillator

The completed backward wave oscillator is mounted in a close-fitting cylindrical magnet, it is possible, however, to provide additional space for an ion pump between the electron gun and the glass valve base by increasing the length of the cylindrical glass envelope. There remained the question of whether to use the Penning type of pump or the evapor-ion type. It was decided to use the latter type since the voltage required would correspond well with those already provided for the operation of the backward

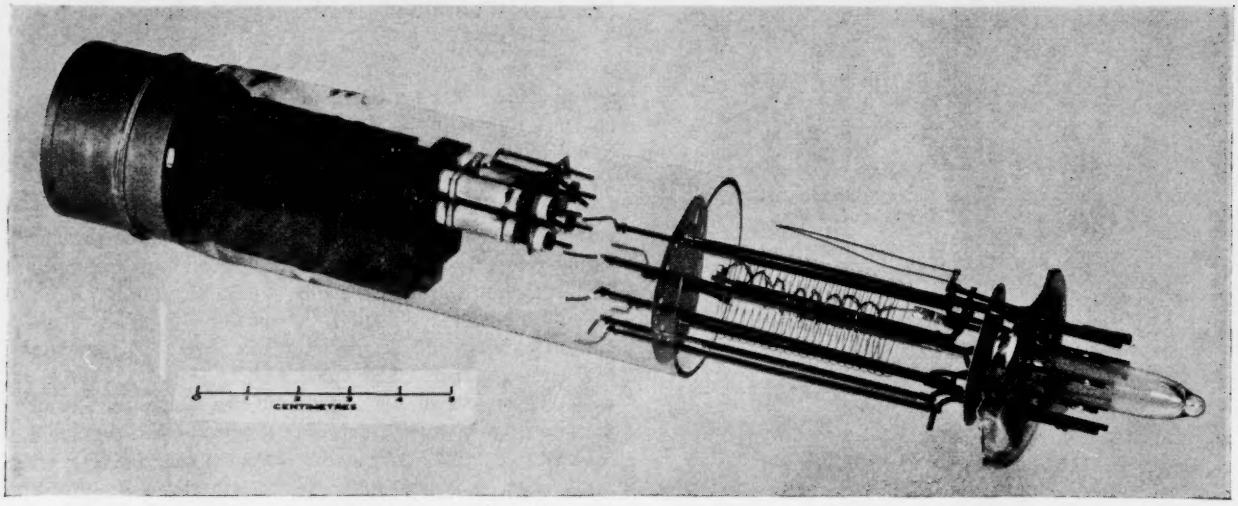

FIG. 4.

wave oscillator. It would thus be possible to connect together, for example, the anode of the backward wave oscillator with the grid of the evapor-ion pump.

A number of composite valves of this type were made each having small modifications in the construction of the pump. The final design is shown in Fig. 4. In the centre is a spiral of plaited tungsten and titanium wire which is electrically heated to evaporate a titanium film upon the glass envelope. Surrounding this is a molybdenum grid which provides the positive potential to draw electrons from the tungsten hairpin emitter upon the outside of the grid. Molybdenum shields are provided at the ends of the pump to mask the oscillator and the glass valve base from the evaporated titanium.

It is necessary to have the evaporator spiral in the centre of the pump in order to obtain a uniform thin film upon the glass envelope and to minimise localised heating. It would also appear to be advantageous either to combine the emitter and evaporator filaments, or to have the emitter filament also inside the grid. Neither of these schemes was found to be satisfactory for the following reasons :

(a) the much greater wattage required to produce the necessary electron emission from the evaporator also produced excessive heating of the glass envelope. This tended to nullify the pumping effect at very low pressures,
(b) with a separate emitter filament in close proximity to the evaporator it was found that the emitter filament would break after a few hours use. This it is believed is caused by the formation of a brittle tungsten-titanium alloy.

The pumping efficiency does not appear to be decreased by placing the emitter outside the grid since it is electrically connected to the evaporator and therefore electrons passing through the grid into the interior are repelled and pass again into the space between the grid and the glass envelope.

Results obtained with the evapor-ion pump

By the use of the evapor-ion pump it was found possible to operate backward wave oscillators at pressures between 1 and 4 $\times$ 10^{-9} Torr. In one instance a pressure of 8 $\times$ 10^{-10} Torr was reached under operating conditions. This was, in general, adequate to eliminate ion noise in the oscillator.

These pressures were not reached without considerable difficulty. Although it was found possible to decrease the length of time for which the valve was baked it was still necessary to process the valve with great care. It would be tedious to detail the stages of processing but the following general considerations emerge.

At pressures lower than 10^{-8} Torr a balance was rapidly being reached between ion pumping action and outgassing due to small increases in the temperature of the glass envelope. Thus it was necessary to employ forced air cooling particularly in the region of the cathode and pump emitter in order to keep the envelope temperature less than 35°C throughout.

The very small net pumping speed at the lowest pressures made it necessary to resort to outgassing the valve components for a second time and absorbing the gas evolved in the titanium film. For example, the cathode of the backward wave oscillator would be deliberately overheated and the electron beam would be defocused so as to impinge upon the copper R.F. structure. The resultant rise in pressure (to about 10^{-7} Torr) would then be rapidly diminished by the evapor-ion pump until, within a few minutes, the pressure returned to almost the original value. Upon the resumption of normal operation of the backward wave oscillator a further decrease in pressure would be observed.

The importance of careful initial outgassing of the components while the valve is still sealed to diffusion pump cannot be overstressed. This was carried out by direct current heating, R.F. eddy current heating and electron bombardment. The major difficulty in this respect is that of keeping the whole valve at an elevated temperature during outgassing of one particular component.

Immediately before sealing-off from the diffusion pump, the evaporator filament was heated sufficiently to start evaporation of the titanium. The wattage supplied to this filament was noted and care was taken not to exceed this

value during the subsequent operation of the ion pump. It was found that, unless this procedure was rigidly adhered to, the ultimate operating pressure could not be made less than 10^{-8} Torr.

It will be noted that the pressures quoted are those obtained under operating conditions (i.e. with a hot emitting cathode). The pressure obtained when the cathode is cold is generally one order less in spite of prolonged outgassing of the electron gun. This serves as an illustration of the difficulties encountered in maintaining a stable low pressure. Thus switching on the backward wave oscillator results in a change of pressure from 1×10^{-10} Torr to say 1.1×10^{-9} Torr. If, however, the residual gas pressure were 1×10^{-7} Torr in the inoperative valve and the same quantity of gas was liberated by heating the cathode then the pressure rise would be insignificant, namely from 1.0 to 1.01×10^{-7} Torr.

Conclusions

In performing this work one gains the impression of pursuing small quantities of gas from a hot surface to a cooler one with the object of entrapping as much of the gas as possible upon the getter surface during the transit. It is necessary therefore to obtain the highest possible pumping speeds in order to remove the gas liberated by heating before it contaminates the cooler surfaces. Ideally all the vacuum components (with the exception of the getter surface) should be heated simultaneously. There are, however, several practical considerations which limit the application of these principles. The use of glass for the vacuum envelope is a severe temperature limitation. For example, it was found necessary to reduce the baking temperature of the backward wave oscillator to 200°C during the initial outgassing of the filaments and electron gun otherwise localised softening of the glass caused the envelope to rupture.

In the lower pressure ranges when ion pumping is used it is advantageous to increase the bulb size of the pump section. This increases the area of getter surface and also assists in cooling the bulb. However, other considerations make this impossible.

Thus, under these limitations, it seems unlikely that pressures less than 10^{-9} Torr can be consistently maintained for this type of valve.

Acknowledgements

The author wishes to thank the Director of Mullard Research Laboratories and the Directors of Mullard Limited for permission to publish the paper. He also wishes to acknowledge the assistance of Messrs. Holman, Zelly and others of the laboratory staff in making these experiments.

References

[1] N. W. W. Smith ; *Proc. I.R.E.* **105**, Pt. B, *Suppl.* No. 11 (1958).
[2] K. G. Hernqvist ; *J. Appl. Phys.* **26**, No. 5 (1955).

Biographical information

N. W. W. Smith—leader of backward wave devices section of the Microwave Tubes Division at Mullard Research Laboratories, Redhill, England. At present working on low noise aspects of microwave oscillators and amplifiers. Formerly member of the scientific staff of the G.E.C. Research Laboratories, Wembley, England. Honours graduate in physics and associate of Institute of Physics.

ol.
10
960

A Pumping Schedule for a Power Travelling Wave Tube

J. R. TEW

Research Laboratories of The General Electric Company Limited, Wembley, England

A POWER travelling wave tube required in applications where a high signal to noise ratio is of importance has to be processed to ensure a residual pressure in the operating tube of a few times 10^{-9} Torr. This is a summary of a typical pumping schedule for such a tube, Fig. 1.

The tube consists essentially of a borosilicate glass envelope, an oxide cathode in a gun structure, a wire helix and a cooled collector, the whole dissipating 150 W, 75 mA at 2 kV.

These tubes are processed on a normal mercury-in-glass diffusion pump with two liquid nitrogen traps, one of which

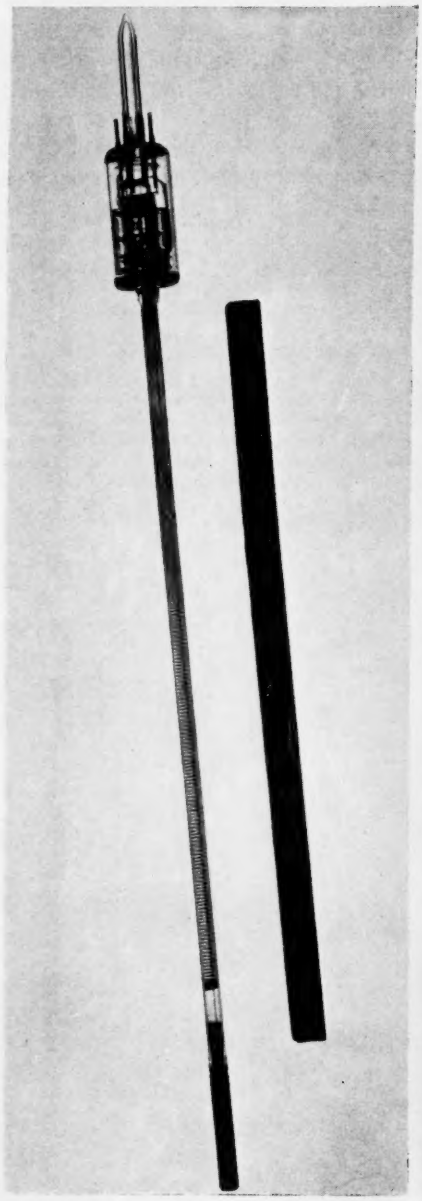

FIG. 1. A power travelling wave tube.

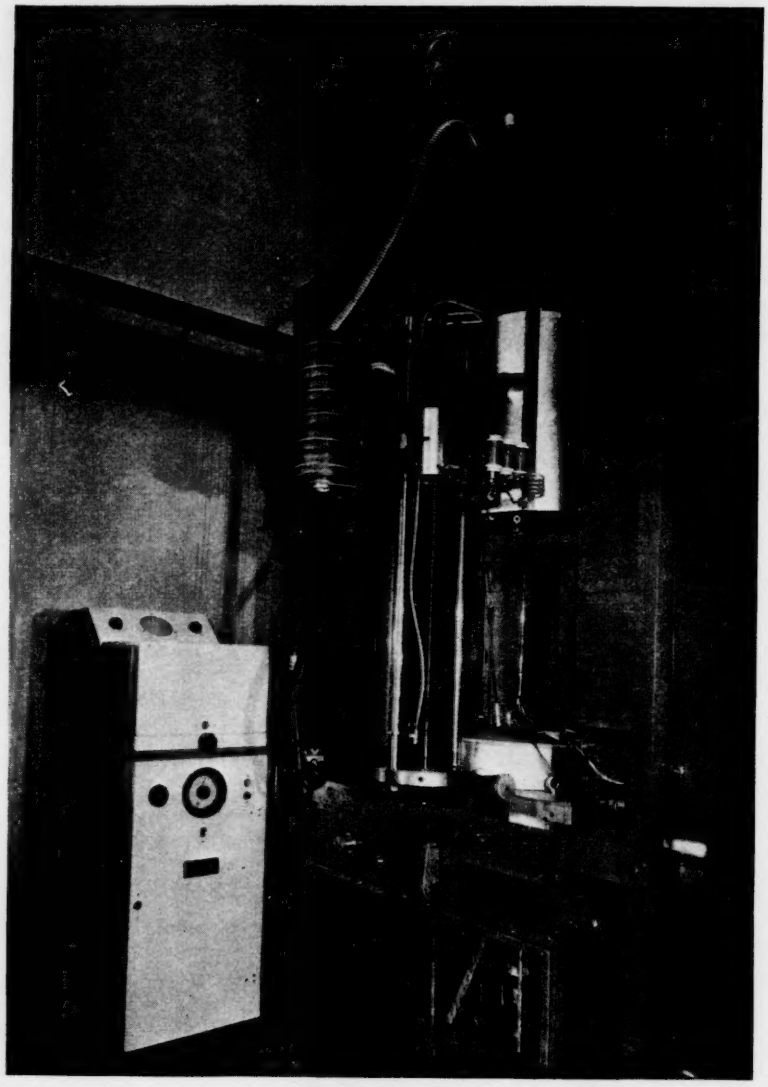

FIG. 2. Pumping station.

Vol.
10
196C

is baked with the tube. The pumping station is shown in Fig. 2. It incorporates besides the normal baking oven, an eddy current heating coil mounted to mechanically traverse the length of the tube and an adjustable electromagnet so that the tube may be operated on the pump.

Fig. 3 shows the pressure during processing. Commencing with sealing on, the tube is pumped down and baked at 400°C—section *B*, with the rate of rise of temperature controlled by the pressure.

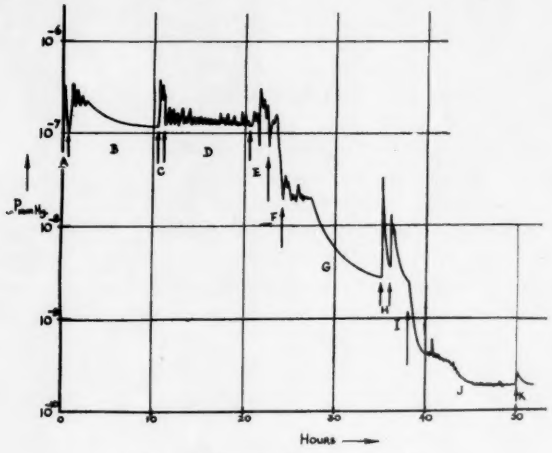

FIG. 3. Pressure during processing.

At *C*, the getter is outgassed with D.C. The oxide cathode is now activated—section *D*, again with a limit on the pressure, being completed in a period of 9 hr. The cathode heater voltage is reduced to its operating voltage and the oven is switched off.

The helix is now heated to 800°C by eddy current heating—section *E*, and by electron bombardment—section *F*.

When the pressure is below 10^{-7} Torr, the valve is slowly run up to slightly above its normal operating power, the various electrodes being bombarded in turn. It is left operating—section *G* until the pressure has fallen to a stable value.

The getter is now fired, only the cathode being operating, and the resulting gases removed by baking at 400°C for 2 hr.

The tube is run again until the pressure is stable at a few times 10^{-10} Torr. It is then sealed off, the total processing time being about 50 hr.

Due to the very stringent requirements regarding noise, it seems imperative that the pressure remains below a few times 10^{-9} Torr during operation. This has been found to be true so long as the wattage dissipations of the various electrodes attained on the pump are not exceeded.

I should like to stress that this is not the most economical way to process this type of tube, but it does show that good results can be obtained with long processing on a normal mercury-in-glass diffusion pump.

Effects of Continuous Gas Clean-up upon Cathodes Emission and Cathode Interface Impedance

THOMAS H. BRIGGS and STUART NADEAU

Briggs Associates, Inc., Norristown, Pa, U.S.A.

Emission capabilities of oxide cathodes have been studied for many years using techniques of increasing refinement. With the ASTM Standard diode it has been possible to detect significant differences between nickel base alloys and even between heats of these alloys. Results, however, have not been reproducible between laboratories, nor sufficiently sensitive for present-day needs. Study of data indicated the existence of an uncontrolled variable. This has been demonstrated to be gas which evolved slowly and in minute quantities. Gas accumulation in the cathode base metal has been measured. Gas liberation from grid and anode films has been shown to influence emission. Continuous clean-up of gas during tube operation has been shown beneficial. Experiments are being run with a variety of continuous getters, and with continuous pumping. In addition to longer electrical life, there is greater uniformity of cathode emission between readings. Important and unexpected influence upon cathode interface impedance has been found. It will be shown that several advances in tube performance, and simplifications in tube materials may be obtained through control of the micro-amounts of gas liberated continuously during tube life.

1. Introduction

Problems of cathode emission and of unwanted gas ions respect no geographical boundaries. So it is with a united front that so many of us from many countries gather in this conference to compare notes and to derive new ideas for controlling these problems encountered in electron tube production.

During my 30 years in the tube industry, I have been associated with many attempts to solve these problems. Major progress has been achieved. When magnesium getters first were replaced by barium, we saw gas currents drop by a factor of 100. Our early attempts to measure gas pressures in a tube, and to measure gas evolved from various materials with various processing were admittedly crude. Certainly, however, the problems were known to exist. So it is with pleasure that we hear today's papers disclosing new and refined techniques—so long and so seriously needed by the Tube Industry.

In the data which follow we wish to acknowledge support at various times from Superior Tube Company, Ronson Metals Corporation, and the United States Department of Defence.

2. Industry practice

The Radio Tube Industry has found it necessary to develop many cathode alloys and to test extensively each alloy and each heat of metal to insure compliance of performance characteristics with intended tube uses. I refer to the World-Wide Tube Industry, both in the U.S.A., in Western Europe, and in the U.S.S.R. Results are well documented in published literature.

Tests are run conventionally using production tube types. Generally one major critical type is selected for cathode and other material tests. Ultimately, the high cost and inconsistency of repeated tests cause a special tube structure to be selected for tests under optimally controlled conditions. Then new problems arise, how to adjust these data to production requirements.

Fig. 1 shows a variety of U.S.A. and European commercially available cathode alloys. Equivalent tables of U.S.S.R. standard alloys could have been illustrated equally well. A metallurgist doubts the sanity of an electron tube engineer when he attempts to state how some of these alloys differ !

When one considers that cathodes have several performance characteristics, then some degree of rationalization for alloy compositions can be found. We have defined these performance characteristics as : (1) rate of coating activation, (2) rate of sublimation, (3) rate of emission decay or length of emission life, (4) rate of interface impedance growth, (5) rate of free barium evaporation, as shown by grid emission, (6) rate of growth of heater-cathode leakage, (7) fundamental cathode operating temperature, and (8) hot bend strength.

Those of you who are research scientists will wish to define these characteristics in other terms. For the production engineer these have direct economic significance.

Some of these performance characteristics are relatively straightforward, easily measured, and relatively reproducible. Others, such as interface and longevity give erratic results. Still others, such as " emission reserve " (a combination of emission decay and free Ba evolution), and gas evolution need better test methods, and better test controls.

Alloy Type	. C	Cu	Fe	Mg	Mn	S	Si	Co	Ni + Co
German " A "	.05	.10	.10	.065	.05	.003	.02*	.50	Bal.
German " C "	.05	.10	.10	.065–.15	.05	.003	.02*	.50	Bal.
French Govt. Standard	.04	.10	.20	.10–.20	.08	.01	.05	?	Bal.
English " O "	.04	.10	.20	.07–.15	.15	.003	.01–.10	.85	99.5 Min.
U.S.—									
" Passive " (499)	.02*	.04	.05	0	.02	.005	.01	.8*	Bal.
" Normal " (220)	.02*	.20	.20	.03*	.20	.008	.01–.05	.8*	Bal.
" Active " (599)	.02*	.04	.05–.10	0	.10	.005	.15–.25	.8*	Bal.
(225)	.02*	.20	.20	.03*	.20	.008	.15–.25	.8*	Bal.
(699)	.02*	Tr	.05–.10	.05–.20	.04–.10	.005	.05–.15	.8*	Bal.

All figures are maxima unless shown as a range or are starred.
Carbon content in the cathode depends on size of material.

FIG. 1. Table of U.S.A. and European commercial cathode nickel analyses.

3. ASTM standard diode

The ASTM Standard Diode was evolved as a production and laboratory tool through cooperative efforts of a great many companies and their specialist engineers. This tube is shown in Fig. 2. The ASTM Reference Planar Diode

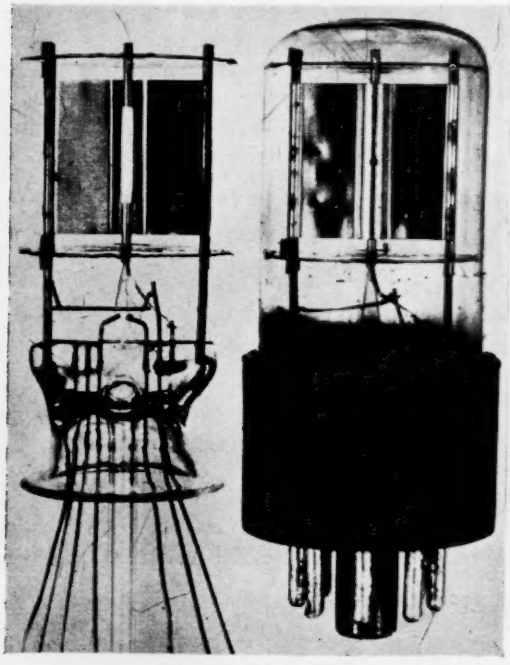

FIG. 2. A.S.T.M. standard diode tube used for cathode and gas investigations.

reported in a following paper by Dr. R. P. Misra is one of several efforts towards refinement.

From our work with both production tubes as well as with the ASTM Standard Diode, we can make the following statements :

1. Variability of results demonstrates existence of at least one major and uncontrolled variable.
2. Effects of cathode coating and tube processing are primary factors.
3. Effects of Cathode Alloys are secondary although this is NOT to say they are not of economic significance.
4. Variability between melts of the same cathode alloy have tertiary effects, and are believed to be susceptible of absolute control within economic limits.
5. Through control of the " unknown " variable in Item 1, influences of variables in Items 2, 3, 4 (coatings, alloys, melts) can be reduced significantly. Thus, (a) need for extensive materials testing can be reduced, with attendant significant savings of technical manpower and time, (b) proper materials can be selected for specific tube applications with greater confidence, (c) tube performance can be defined with assurance, (d) tube reliability and longevity will be increased significantly.

Certainly these are long over-due needs, and even more so if we are to compete successfully against our semi-conductor colleagues!

4. Test data

Over a period of time, we have amassed data which indicate that the uncontrolled variable is GAS. First, let us postulate that this gas is present in micro-amounts, too small to indicate as negative grid current, except by ultra-precise and special methods. Further, we postulate that this gas is being liberated continuously from the cathode and other tube parts even after excellent bake-out, bombardment, and pumping. Finally, we must remember the activated hot cathode is an excellent getter and located strategically so that it readily captures each positive gas ion.

Just a few gas ions combining with a few barium particles on the cathode will show no appreciable effect on emission. In fact, shortly a new barium supply will arrive, delivered by diffusion from the reaction of BaO and cathode core reducing agents, deep down at the interface level of this cathode assembly.

*Indicates values obtained from typical or averaged analyses.

Ultimately, depending upon many factors, the supply of reducing agents becomes depleted. The liberation of gas ions may continue unabated or may even increase. The struggle for chemical equilibrium becomes one sided. The cathode deteriorates and finally the tube is discarded.

What are the facts supporting this picture?

4a. Gas in cathodes

Fig. 3 shows the results of vacuum fusion gas analysis of cathode nickel. It may be noted that only oxygen and nitrogen determinations provide significant quantities present and significant changes with cathode processing and tube life. As bulk nickel tubes are drawn to finished cathode size, the gas content increases by a factor two. This is shown to be surface gas, since electropolish removal of 0.0001 in. layer of nickel brings back the original gas levels.

Cathode Nickel Gas Content—by Vacuum Fusion

Sample		$\%O_2$	$\%N_2$
2.0 in	OD raw stock	.0015	.0002
.045 in	OD surface etched off not coated	.0035	ND
.045 in	OD cathodes 0 hrs life from processed tubes	.01	.0004
.045 in	OD after 5000 hr life from ASTM standard diode tubes	.05	.0007

220 Grade Nickel—Various Processings

FIG. 3. Table of cathode nickel gas content for several processings—vacuum fusion analysis.

There is no significant increase in gas in cathodes removed from tubes before life. After 5000 hr life, nitrogen has about doubled in quantity. Oxygen has increased 14 fold. This latter is a value obtained by repeated tests and is clearly greater than the test method control limits.

Examination of cathodes at end of life over a considerable period of time, using different alloys, tube types, and made in different plants, showed cathode breakage upon bending. Breaks were characterized by the raggedness and brittleness associated with oxygen "diseased" nickel.

Specimens were prepared for metallographic examination by casting in plastic, sectioning, polishing, and etching in cyanide persulphate. Both longitudinal and transverse cathode sections were made.

Fig. 4 shows an active grade cathode alloy. In the unused state typical small grain structure is visible. After 1000 life hr at 850°C and with 120 ma/cm² cathode current drain, nickel grains have enlarged to equal the entire 0.002 in. wall thickness. There are heavy intergranular penetrations extending inward from the Ba-coated surface. In many instances penetration is complete. Sometimes, entire nickel grains can be "popped" free from the cathode. These intergranular penetrations never occur at the uncoated ends of the cathode. They never start on the inner cathode wall next to the heater. The degree of penetration is a function of cathode temperature, amount of coating reducing agent in the alloy, and time of cathode operation.

Fig. 5 is a cathode after-use photomicrograph (X250). It is similar to Fig. 4, but represents a passive (P50) grade cathode alloy. NO intergranular penetration is to be found.

FIG. 4. Longitudinal section of active grade cathode nickel (*above*) before and (*below*) after 1000 hr life.

FIG. 5. Longitudinal section of passive (P50) cathode nickel—after 1000 hr life.

Transverse micrographs are equally dramatic in demonstrating the percentage of cathode surface area covered by the thickness or width of these intergranular penetrations.

Identification of the material has not been made, beyond that of Fig. 3, showing that it is rich in oxygen.

From these data, this statement may be made :

There are three means for disposing of the end products of reactions between cathode base metals and alkaline earth oxide coatings.

1. Gaseous end product evolution into the envelope (e.g. carbon-monoxide, etc.).
2. Chemical compounds formed at the interface between sleeve and coating (e.g. barium orthosilicate).
3. Elements or compounds absorbed by the cathode base metal or penetrating grain boundaries of the base metal.

4b. Continuous gettering v. emission

The next experimental step was to compare BaAl flash getters, with CETO or CerAlloy 400* type continuous getters. It is assumed flash getters lose sorption ability after some hundreds of hours and are located relatively remote from the cathode. CA400 was used painted on anodes, end shields, or anode radiating fins. Diode, triode, and pentode tubes were employed in the study.

Fig. 6 compares ASTM Standard Diode Tubes which were laboratory processed with oil diffusion pumps. Characteristics plotted are (40v E_b) dc emission tested at rated (6.3 v) and about half rated (3.5 v) heater voltages. Also, there is shown at the bottom of the figure the total emission as measured by the low field method at $E_f = 2.0$ V and $E_b = 5.0$ V.

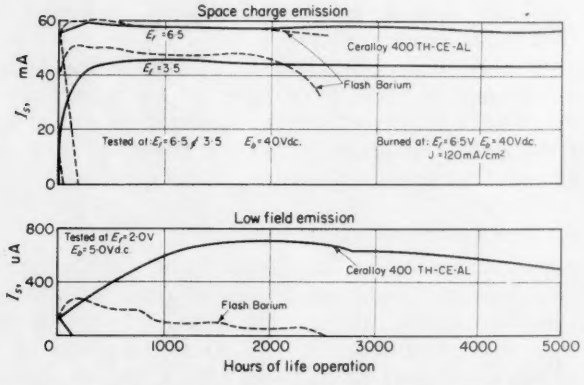

FIG. 6. A.S.T.M. standard diode life using ceralloy 400 continuous getter.

The CA400 getter tests happened to be run at a period when regular control diodes were afflicted with a poison epidemic. Thus, the direct control lot had less than 100 hr life before complete failure. These tubes are denoted in the graphs by long dashed lines. The CA400 gettered tubes not only overcome the poisoning but survived to double the normal age of any prior good diodes. The short dashed lines inserted represent the average of control lots typical of tubes before and after the poison epidemic. They differed from the CA400 gettered tubes only in use of BaAl flash getter, and time of processing.

Not only did CA400 tubes double life hours, but they gave the most uniform emission readings ever experienced during 10 years of standard diode work. Each tube reproduced its emission readings within 0.5 ma in 60 ma from one reading period to the next. Control tubes usually varied by 2–5 ma between readings.

A totally unexpected phenomenon appeared in low field emission data. Conventionally, both at Superior and at Raytheon, low field emission rose to a peak early in life (100–300 hr), then dropped to a low plateau, whose level appeared dictated by activity of the cathode alloy and quality of tube processing.

CA400 gettered diodes rose gradually to twice the low field value ever experienced and maintained this at almost the peak for 5000 hr.

These excellent emission results are interpreted as due to complete and continual clean-up of gas remnants throughout tube life by the special getter.

4c. Continuous gettering v. cathode interface impedance

Tests have been run in the BAI laboratory to study gas influences upon cathode interface impedance. The program contrasted 4 cathode alloys, 3 tube manufacturing plants, 3 cathode operating temperatures, and 3 cathode current drains, or a total of 108 life lot conditions. Results are evaluated statistically to insure a high degree of confidence in significance of results.

Subsidiary tests were run with vacuum melted and vacuum annealed nickel cathodes, electropolished cathodes, and substitution of CA400 getter in place of BaAl flash getter.

*Registered trade name of Ronson Metals Corp.

BAI-1 twin triode tubes of high Gm and Mu were used (similar to 6BX7 miniature tubes). Neither vacuum melted nickel, nor electropolished cathodes provided a statistically significant influence upon cathode interface.

Fig. 7 presents plots of interface resistance in ohms during 5000 hr of life. Interface was measured by the Wagner

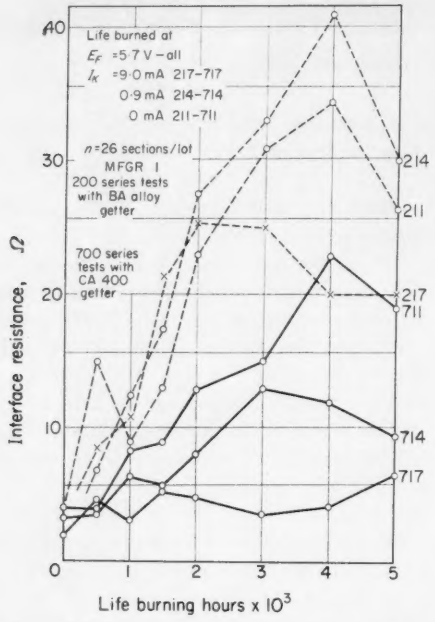

FIG. 7. Effect of continuous getter upon cathode interface resistance.

small signal sine wave method at two frequencies, 5 KC and 10 MC on equipment produced by CBC Electronics Company, Philadelphia. All tubes were made at one time from common mounts, and processed through sealex and aging in close sequence. Each of the 6 life lots plotted consisted of 13 tubes, or 26 triode sections. Lots may be identified as follows :

E_F	I_K	*Life Lot Numbers*	
		BaAl Flash Getter	CerAlloy 400 Getter
5.7 v	0.0 ma	211	711
5.7 v	0.9 ma	214	714
5.7 v	9.0 ma	217	717

All tubes were made by one manufacturer and from a single lot of 220 " normal " grade alloy cathodes. At 9.0 ma I_K the cathode current drain was about 68 ma/cm².

In general, Interface Resistance (Ri) for tubes with CA400 getter is about half that of the tubes with BaAl getter. There was less noticeable improvement in R_i when $I_K = 0$. This is believed due to lower getter temperature and hence less getter activity or gas sorptive qualities, since anode dissipation was essentially zero. Values of $-I_{c1}$, I_b, and Gm were also unusually consistent with the continuous gettered tubes.

From these tests, we believe strong evidence exists that traces of gas liberated continuously during tube life can be a significant cause for interface generation.

Wagener appears to present a somewhat different theory, based upon certain of his work. It is namely that the hydrogen atmosphere in tubes made without barium getters prevented the cathode interface from increasing its resistance by the collection of oxygen.

Wagener's theory is compatible with the low hydrogen sorption rate reported for CETO getters.

5. Future program

We are continuing investigations at BAI to reduce gas liberated during tube life and to determine whether this unwanted contaminant may be controlled so that reliability and longevity of tubes may be vastly improved. This work includes continuous getter tests, use of appendage pumps, and evaluation of more sensitive means for measuring tube characteristics.

Fig. 8 shows one of the new appendage pumps becoming available in the U.S.A. It is made by the ULTEK Cor-

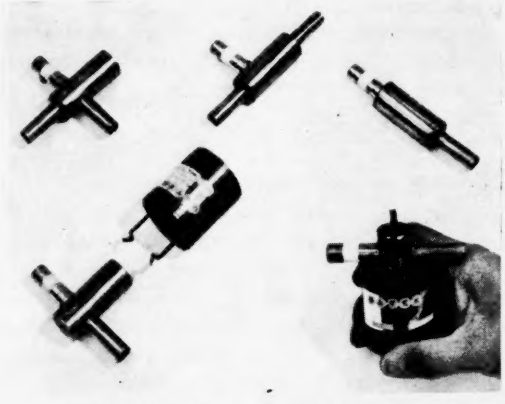

FIG. 8. Getter-ion appendage pump—ULTEK model.

poration, Palo Alto, California, and employs the getter-ion pump principle with magnetic field, such as has been published by Lewis Hall of ULTEK. It is unusually suitable for laboratory investigations, and practical application to large and expensive production tubes.

The more sensitive test methods will include Shot Noise, as described by Dahlke, a sensitive gas indicating method developed by O'Fallon, and an improved version of the retarding field temperature measuring method as refined at Cornell University.

6. Benefits to industry

The work which is being described at this Conference holds promise of major benefits to the Electron Tube Industries of all countries, and in turn to the users of tubes. From theoretical calculations and experimental data, it is but a step to practical utilization.

We are convinced that a major conservation of tube engineering effort may be made, once gas is controlled. More accurate data may be obtained on the mechanism of

Vol. 10 196

emission. Great progress will be made in controlling production quality and uniformity of tubes. Less time will be needed to test cathode materials.

We join with all attending this conference in believing that gas must be and can be controlled. Through such control, uses of tubes will expand, the net cost per thousand hours of tube usage will be reduced.

Our friends in the transistor industry will be aware then that they have real competition on their hands, that the tube industry is running a strong race!

References

[1] T. H. Briggs ; *Continuous Getters for Electron Tubes. Proceedings of the Third National Conference on Tube Techniques*, pp. 117–123 (Sept. 1959).

[2] T. H. Briggs, S. Nadeau, and R. B. Dickson ; *Interface Impedance—It can be Controlled. Proceedings of the Fourth National Conference on Tube Techniques*, pp. 231–237 (Sept. 1958).

[3] S. Wagener ; *Sorption of Gases at Very Low Pressures by Thorium Powder, Proc. Phys. Soc.* **B66**, 400 (1953).

[4] S. Wagener ; *The Use of Getters for the Production of Very High Vacua, Vacuum* **3**, 11 (1953).

[5] *Electrical, Chemical, Metallurgical Behaviour of Eight Commercia and Four Experimental Cathode Alloys in* 2000 *to* 5000 *hr Life Tests Electronics Laboratory Report*, 26 (Feb. 1952).

[6] L. D. Hall ; *Electronic Ultra-High Vacuum Pump, Rev. Sci. Instrum.* **29**, 367–370 (1958).

[7] Briggs Associates, Inc. ; *Summary of CerAlloy* 400 *Test and Performance Data, Bulletin* 2, Ronson Metals Corp. (April 1958).

[8] *A.S.T.M. Standard Diode Specification F270–52T, American Society for Testing Materials, Philadelphia.*

[9] A. M. Bounds, T. H. Briggs, and C. D. Richard ; *The Work of the American Society for Testing Materials on Specifications and Standards for Oxide Cathodes, Le Vide* **51**, 13–16 (May, 1954).

[10] A. M. Bounds, T. H. Briggs, and C. D. Richard ; *Development of New Cathode Nickels with Improved Performance, Le Vide* **51**, 18–21 (May 1954).

ol.
10
960

SESSION V

Methods employed in the Evacuation of the Tubes

On the Use of Metal–Oil Diffusion Pumps when operating with Discharge Tubes sensitive to Hydrocarbons

R. A. HAEFER

Balzers Aktiengesellschaft, Principality of Liechtenstein

In the stationary state the ultimate pressure in the recipient over a metal-oil diffusion pump having metal seals is defined, as well known, by the sum of the saturation vapour pressure of the oil and of the partial pressures of the thermal decomposition products (10^{-8} Torr equivalent N_2 pressure = 10^{-9} Torr true pressure). When operating with tubes sensitive to hydrocarbons it is however often desirable to attain even lower pressures. This is possible even without the use of deep cooling or Alpert traps by operating in a non-stationary state, i.e. immediately after the heating up of the valves. For the duration of the non-stationary state and for the magnitude of the pressure attainable in this state the adsorption characteristics of the oil molecules and the dimensions of the vacuum conduits are decisive. By the aid of a field electron microscope it has been proved that it is possible even with vacuum systems capable of being dismantled and provided with metal-oil diffusion pumps to attain completely clean surfaces, which in particular are free from oil molecules, and to keep them so over long periods. Consequences thereof for technological application have been pointed out.

Vol.
10
1960

THE developments in the field of the metal-oil diffusion pumps have led recently to a considerable lowering of the ultimate pressure attainable. While only 10 years ago a final pressure of 10^{-5} Torr only was attainable, nowadays values 3 orders of magnitude lower are attained even without deep cooling means. This progress has been made possible in that on the one hand the oil diffusion pumps were so built, that the effects of fractionating, purifying and careful heating of the working fluid, which determine the final pressure, have been realised in a favourable manner. On the other hand, in that oils of a particularly low vapour pressure and low decomposition rate have been developed[1, 2].

In these conditions the question arises, whether metal-oil diffusion pumps without deep cooling or Alpert traps can be used also in operations where extremely clean surfaces, particularly free from oil molecules, are decisive. In order to investigate this problem we used a field electron microscope which is better suitable than any other instrument to detect traces of contamination on surfaces. As is well known the operation of a field electron microscope presupposes an extraordinarily good vacuum. Hitherto one used to generate this vacuum with glass diffusion pumps which are in general filled with Hg and are provided with traps for liquid air. In order to suppress a back diffusion of light volatile hydrocarbons from the rotary pump to the high vacuum side, two diffusion pumps arranged in series are being used. On the high vacuum side glass joints capable of being dismantled are obviously not permissible[3, 4, 5].

The only feature of this arrangement which we have adopted in our pumping set (Fig. 1) capable of being dismantled and provided with metal-oil diffusion pumps is the series arrangement of two diffusion pumps[9]. All the sealing rings on the high vacuum side consist of aluminium. Over the three-stage oil diffusion pump Diff 170 (S = 170 l/s)* there are arranged in series : a water cooled baffle[6] which owing to its two structural features—a cap drawn down over the uppermost nozzle hat and angular profile baffle face—allows only a small back streaming of oil to pass. On top of this a test dome likewise capable of being water-cooled having a Bayard–Alpert gauge (high speed gauge[7]. Over a fused covar-glass seal a further Bayard–Alpert gauge (normal gauge) and the field electron microscope are connected. The glass tubes are heated up to 420 °C, the test dome and baffle to about 150 °C. While the furnace above the glass tubes is yet cooling down, the test dome and the baffle are connected to the cooling water. The driving medium in both diffusion pumps is Diffoil 71*. After the vacuum system has been operated for a long period for the purpose of conditioning, pressure-time graphs (Fig. 2) have been measured after differently long heating-up periods. For the pressure measurement the normal gauge is used. Before any test the complete system has been exposed to atmospheric pressure for 20 min. The diffusion pumps were switched on simultaneously with the heating up furnaces.

*The different types of pumps and oils referred to are products of the Balzers Aktiengesellschaft.

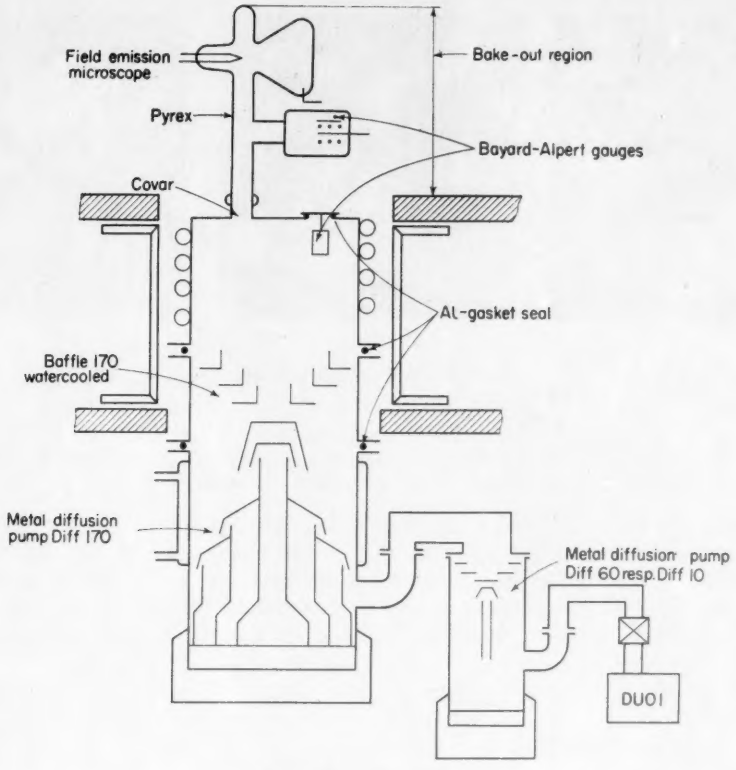

FIG. 1. Pumping system.

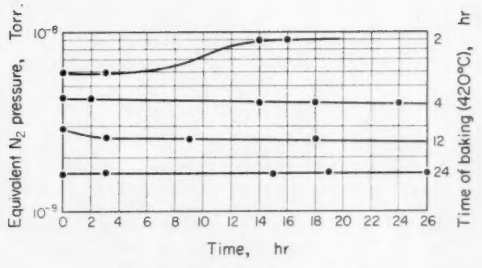

FIG. 2. Pressure-time curves.

In any case pressures lower than 10^{-8} Torr (equivalent N_2 values) were attained. After a heating-up for 24 hr a value of 2×10^{-9} Torr has been attained. This value has been maintained for more than 100 hours.

This result appears at first sight completely surprising if one considers that the vapour pressure of Diffoil 71 measured with the high speed gauge at a cooling water temperature of 10 °C is one order of magnitude higher, namely 2×10^{-8} Torr. This difference in the indications of the two tubes, which has been pointed out for the first time by Blears[7] exists only as regards the oil vapour pressures but not as regards the partial pressure of permanent gases, as could for example be easily ascertained by introducing argon. For the explanation of the effect we have to be aware that the high speed gauge measures the saturation vapour pressure of the oil, and that its indication corresponds to the stationary condition. In the normal gauge on the other hand prevails an unsaturated and non-stationary condition. The pumping action of the normal gauge cannot alone be made responsible for the unsaturation, as has been shown by tests to be reported elsewhere[8]. The explanation may, on the contrary, be that the glass tube, by which the normal gauge is connected, has a considerably lower coefficient of conduction for the molecular flow of oil molecules than for that of permanent gases, particularly during the " starting-up " period, which is required for setting up the stationary flow condition. According to Clausing[10] this starting-up period t_0 is determined by the time required for the formation of a mono-layer in the glass tube. The data* of our tests lead to $t_0 = 27$ hours.

In reality however the starting-up period is much longer (>100 hr), a fact which has recently been also observed by Kirchner[11] for the molecular flow of potassium. Kirchner's concept of a molecular flow combined with penetration into the wall seems however not to be applicable to oil molecules. Therefore it will be necessary to give up the basis of the theory of the non-stationary molecular flow (Langmuir's adsorption isotherme, monolayer = maximum coverage) in favour of an adsorption law valid for vapours, as recently formulated for example by Kraus[12] and which admits even the formation of multi-atomic layers. Investigations in this direction are on the way.

*Length and diameter of the glass tube : 10 cm and 1 cm respectively. Molecular weight $M = 450$, temperature $T = 293$ °K, pressure on the entry side $= 2 \times 10^{-9}$ Torr $= 0.1$ equivalent N_2 pressure. Average life time of an oil molecule in the adsorption state = 100 sec according to Frenkel's formula with $Q = 25$ k cal/Mol.

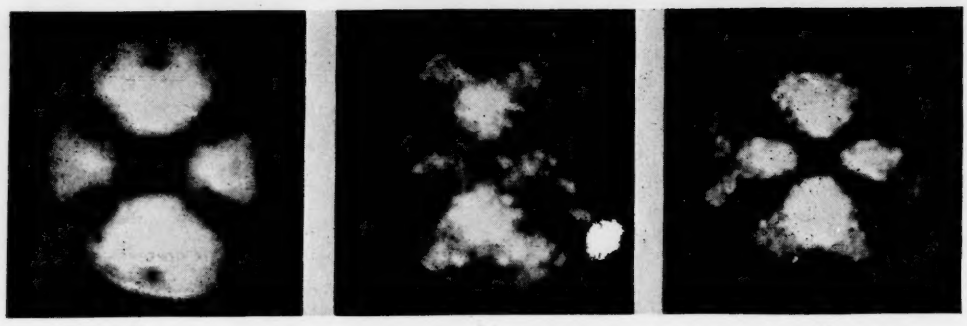

(a) (b) (c)

FIG. 3. Field emission patterns.

(*a*) clean tungsten, 1.9 kV for 1 μA emission.
(*b*) oil film on the tungsten tip, degree of coverage 0.3, formed within 1 hr,
(*c*) oil film on the tungsten tip, formed during a pumping period of 15 hr, 1.9 kV for 1 μA emission. Practically no change of work function within this period.

In the field electron microscope after thorough de-gassing of the tungsten tip the well known emission pattern of clean tungsten is obtained (Fig. 3a). Thereby the proof is established, that the vacuum system described succeeds in producing clean surfaces. On the other hand it is also possible to make the growing of oil layers on the point visible in the field electron microscope. After the lapse of one hour the slightly granulated pattern of Fig. 3b is obtained. The degree of coverage is 0.3. Fifteen hours later the emission pattern Fig. 3c is found. It equally shows a granular structure which is characteristic for adsorption films of comparatively large molecules. It is remarkable that neither the emission pattern nor the effective work function of the cold cathode tip did practically vary, not even in the course of a 15 hr pumping time.

With growing emission current the rate of decomposition of the oil molecules by electron impact* increases, and apparently these decomposition products express themselves in the form of bright doublets and occasionally even of quadruplet patterns such as are apparently characteristic for organic molecules[5, 13]. The field electron microscope has accordingly proved a useful instrument for studying the behaviour of oil molecules in vacuum systems. A more detailed description will be made in short elsewhere[14].

The practical useful application of the results obtained can be made in all cases where systems sensitive to contamination, particularly oil molecules are concerned, such as for example special electron and ion discharge tubes, with which the investigation or production period, respectively, lies within a stay down time of days.

References

[1] R. A. Haefer ; *Ergebnisse d. Hochvak. Technik u. d. Physik dünner Schichten*, 100–122, ed. M. Auwärter, Stuttgart (1957).
[2] R. A. Haefer and O. Winkler ; *Vakuum-Technik* **5**, 149 (1956).
[3] E. W. Müller ; *Z.S.f. Phys.* **102**, 734 (1936).
[4] R. A. Haefer ; *Z S.f. Phys.* **116**, 604 (1940).
[5] R. H. Good and E. W. Müller ; *Handbuch d. Physik* **XXI/1**, 176–231 (1956).
[6] G. Zinsmeister ; *First Int. Congress on Vacuum Technology, Namur* (1958).
[7] I. Blears ; *Proc. Roy. Soc. A* **188**, 62–76 (1946).
[8] R. A. Haefer and J. Hengevoss ; *Vakuum-Technik* (to be printed).
[9] E. A. Trendelenburg ; *Vakuum Symposium Transactions 1959* (to be printed).
[10] P. Clausing ; *Ann. d. Physik* (S.F.) **7**, 489 (1930).
[11] F. Kirchner ; *Z S.f. angew. Phys.* **11**, 167–169 (1959).
[12] Th. Kraus ; *Vakuum-Technik* **8**, 33 (1959).
[13] R. A. Haefer ; *Acta Physica Austriaca* **8**, 305–118 (1953).
[14] R. A. Haefer ; *Vakuum-Technik* (to be printed).

* or ion impact.

Vol. 10 196

Electron Tube Processing with Getter-Ion Pumps

L. MALTER and H. MANDOLI

Varian Associates, Palo Alto, California, U.S.A.

A description of the VacIon® getter-ion pump and of its physical processes is presented. Its performance and advantages over older pumping techniques are discussed. Particular attention is paid to the processing of electron tubes with VacIon pumps. Actual experience with thousands of tubes is presented, pointing out the very considerable benefits as regards performance and economic savings achieved by employing this technique. Brief mention is made of two other matters : (1) The use of sorption pumps to go from atmospheric pressure to the starting region of VacIon pumps. This completely eliminates the possibility of introducing contaminants into a system during processing. (2) The use of VacIon pumps as appendages of electron tubes so as to maintain the vacuum against the consequences of 1—inadequate processing, 2—outgassing during operation, and 3—leaks.

1. Introduction

Getter-ion pumps have been growing in promise and importance in recent years. A new pump in this category—the VacIon® pump was announced a little over a year ago. It is the purpose of this paper to cover briefly the design and pumping mechanism of the device and then to discuss its application to the processing of electron tubes and to the maintenance of vacuum in sealed-off tubes.

2. The major pumping mechanism

Shown in Fig. 1 is a cross-sectional side view of a single-cell pump. As in the Penning gauge, a cylindrical anode is

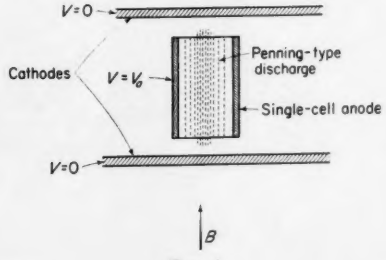

FIG. 1.

located between a pair of cathode plates. Upon application of suitable anode voltage and magnetic field, a cold-cathode electron discharge can be initiated and maintained down to very low pressures. Maintenance of the discharge arises from trapping electrons by an axial magnetic field.

One consequence of having electrons trapped in this fashion is that electron-ion pairs are produced through collisions between the trapped electrons and neutral gas molecules. Most of the newly produced electrons are also trapped. The positive ions go directly to the cathodes, causing some number of atoms of cathode material (titanium, for example) to be sputtered on to the anode. There the freshly sputtered atoms from the cathodes may combine chemically with active gases such as oxygen and nitrogen in the case when titanium is used as cathode material.

Studies to date indicate that with the single exception of hydrogen, the active gases are pumped primarily by getter action at the anode. Hydrogen, on the other hand, is cleaned up by gettering and subsequent solution at freshly exposed cathode surface. The exact mechanism for noble gas clean-up is still unknown but is believed to be primarily by ion burial.

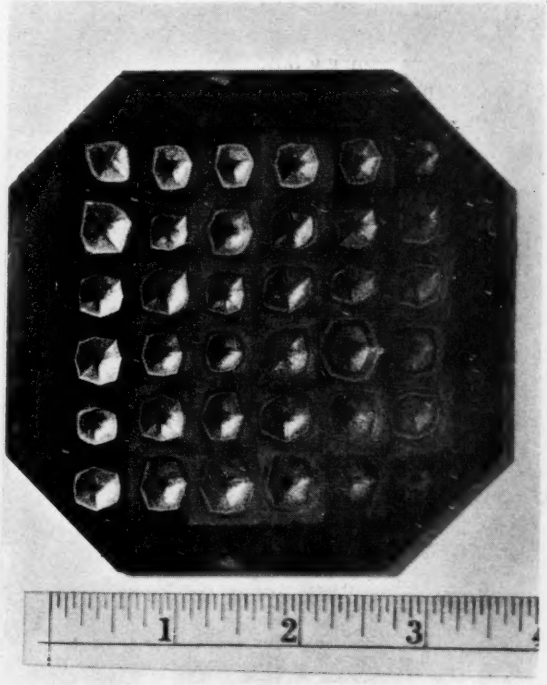

FIG. 2.

Fig. 2 indicates that quite significant quantities of titanium are removed from the cathodes by sputtering.

3. Experimental results

A basic objective of our present research program on VacIon pumps is to be able, starting from first principles of physics, to write down (via equations or curves) the dependence of current and speed on the parameters of importance—geometry (of which there are many facets), magnetic field, voltage, species of gas (including mixtures of gases), pressure, and cathode material.

As is often the case in formidable problems of this sort,

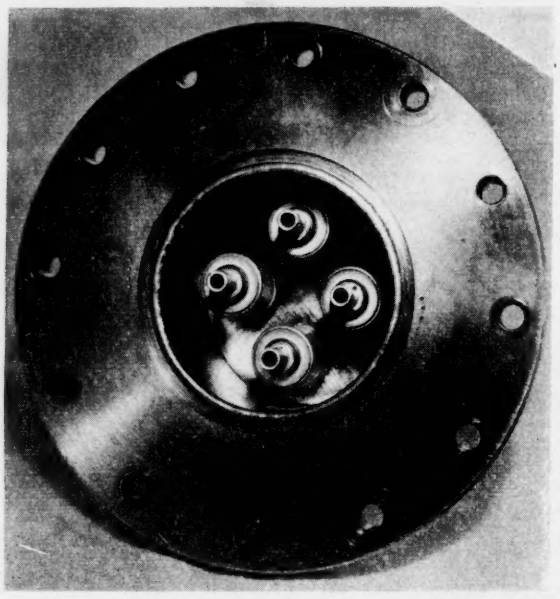

FIG. 3(a).

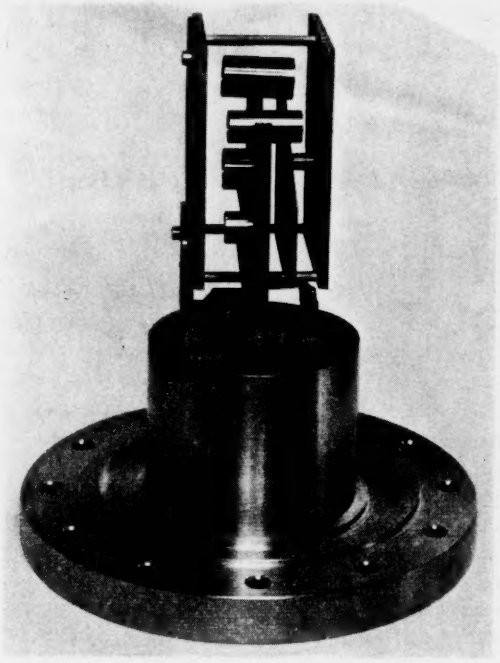

FIG. 3(b).

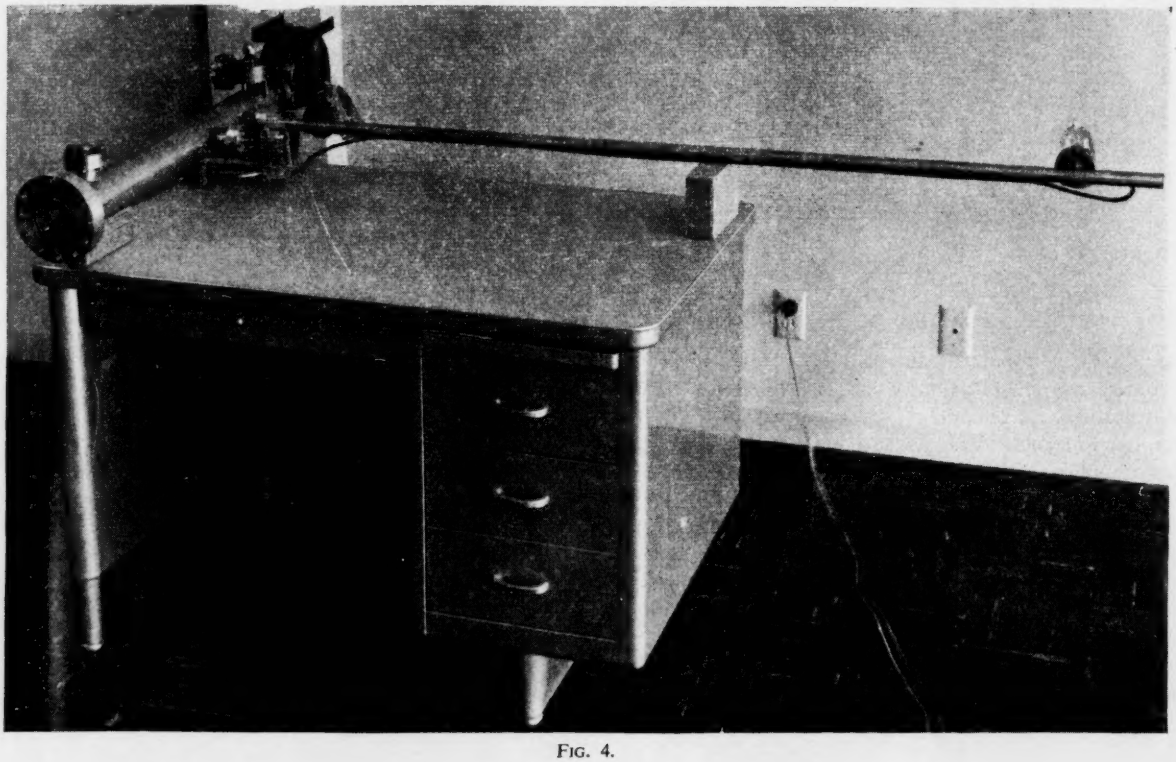

FIG. 4.

it is helpful, if not essential, to determine just *what* it is for which a theory must account. For this reason we are engaged in a rather extensive program of experimental investigation.

In one set of experiments, the dependence of speed and current on magnetic field, voltage, and geometry are being studied. Most of these experiments are being performed with single-cell anodes. As indicated in Figs. 3(a), 3(b) and 4, the test cathode-anode structures are fastened to a demountable flange. This flange is then attached to a two-gauge speed measuring apparatus. The portion of the apparatus surrounding the cathode-anode structures is placed between the pole-faces of an electro-magnet.

Although these experiments are far from complete, certain results warrant reporting at this time. Typical variations of speed with magnetic field are shown for two different anode voltages in Fig. 5.

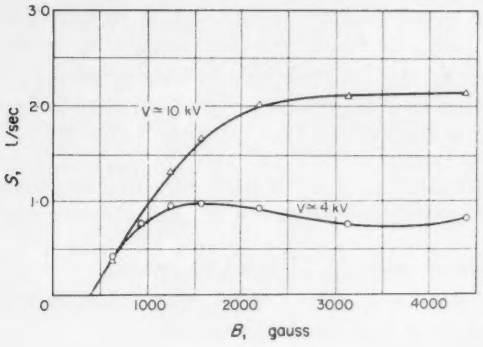

FIG. 5.

In another set of measurements, the dependence of speed and current on pressure and on species of gas were examined in some detail. Most of the data were taken on a medium-size, multi-cell pump (see Fig. 6) at nominally constant voltage and with fixed geometry and magnetic field.

One important result is that the speeds appear to be

TABLE I

Speeds for Various Gases for the VacIon Pump of Figure 7

Species of Gas	Speed l./sec
Hydrogen	850
Deuterium	590
Air	280
Nitrogen	260
Carbon Dioxide	230
Oxygen	155
Helium	30
Methane	780
Water Vapor	373
Ethyl Ether	380
Decane	310

Operating Conditions

Pressure Range = 5×10^{-8}—1×10^{-5} Torr
Anode Voltage = 3.5 kV

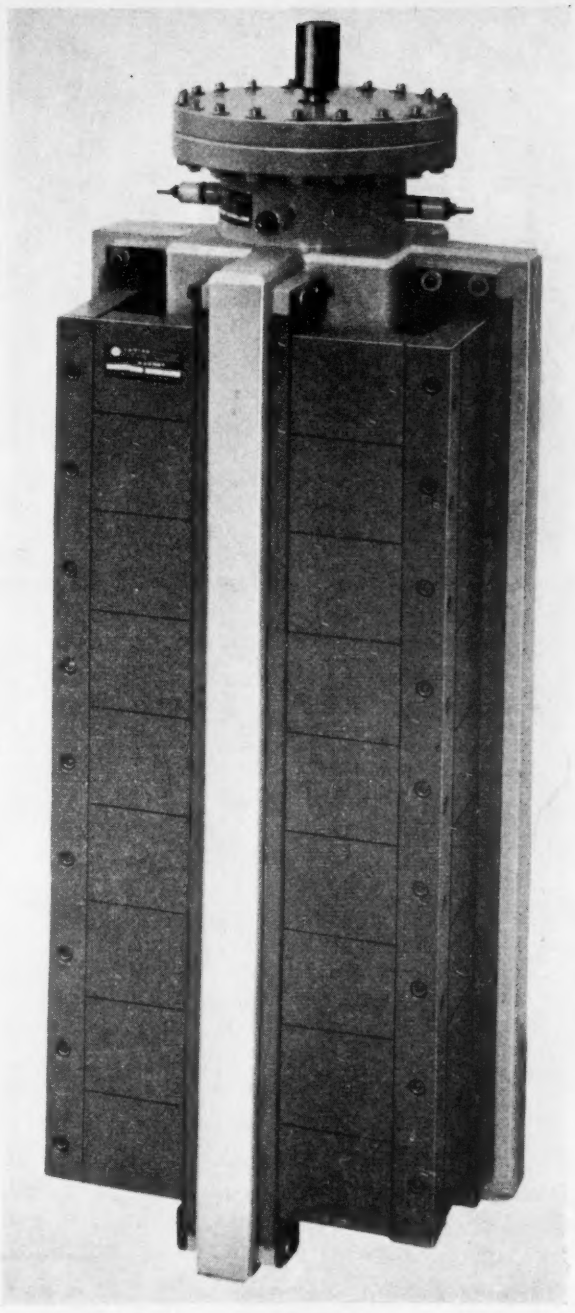

FIG. 6.

essentially independent of pressure over the range from about 2×10^{-8} to 10^{-5} Torr (see Fig. 7). As yet there is no compelling evidence that speed falls off significantly at the lower pressures, but the necessary measurements are still to be made. In the range from 10^{-5} to 10^{-4} Torr, the usual falling off of power supply voltage causes the speed to drop somewhat.

Pumping speeds for various gases for the particular pump studied are summarized in Table I.

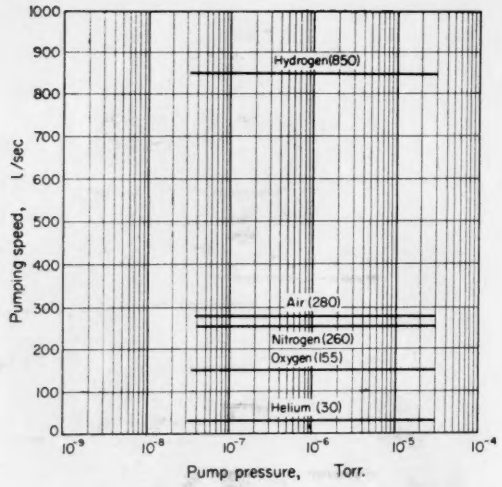

FIG. 7.

One other observation of importance is that, at constant voltage, the pump current is very nearly a linear function of

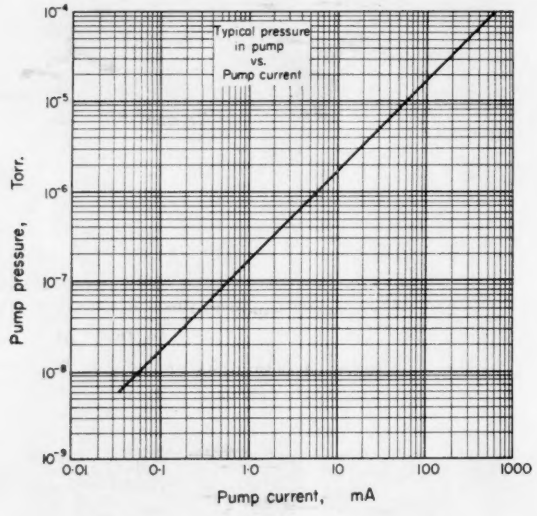

FIG. 8.

pressure over the range 10^{-8} to 10^{-4} Torr (see Fig. 8). Very possibly this linearity persists to much lower pressures.

4. Summary of characteristics

Getter-ion pumps in general have a number of attractive features which are presumably well-known. These include :

1. Fundamentally clean. No pump fluid involved ; hence no refrigerated baffle or trap needed.
2. No continuous forepumping required.
3. Usable with completely closed systems.
4. Power failures normally not serious. This is largely a consequence of items 1, 2, and 3 above. Stand-by power, therefore, is usually not required.

Certain types of getter-ion pumps possess such additional attractive features as :

5. Relatively portable.
6. Can be operated in any position.
7. Can withstand severe environmental conditions, such as shock, vibration, acceleration, and high temperature.

The VacIon pump in particular has, in addition to the foregoing, a number of further characteristics :

8. Fundamentally simple. No heaters, no hot filaments, and no moving parts.
9. Uniform pumping speed over a wide pressure range. Operable from 10^{-10} to 10^{-1} Torr, and possibly beyond.
10. Pump current provides a measure of pressure (hence no ion gauge required in many applications).
11. Power consumed by pump varies approximately linearly with pressure (hence very low power required at low pressures).
12. Major leaks not catastrophic. Abrupt exposure to atmospheric pressure usually causes no damage.
13. Speed can be conveniently voltage controlled.
14. Large amounts of titanium (or other cathode material) can be transported to the anode by sputtering. Titanium is efficiently used through inherent self-regulation. Hence, relatively long pump lives are achieved.
15. Valves normally not required between pump and system. (This arises chiefly as a consequence of items 1, 8, 12, and 13 above.)
16. Several of these features are attractive with regard to automation, automatic control, and remote control.

5. Tube processing with VacIon pumps

The application of the VacIon pump to the processing of electron tubes will now be considered.

Consider a system as shown in Fig. 9.

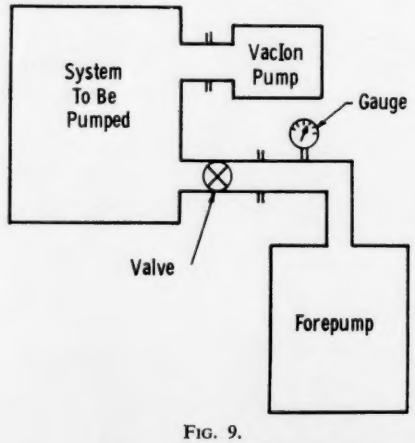

FIG. 9.

In operation, the pressure is first reduced to about 10^{-2} Torr by the roughing pump, voltage is applied to the VacIon pump, and a low-voltage, high current discharge occurs. Typically, the voltage across the pump is less than 500 V at this stage, with the current limited by the power supply.

The pumping which accompanies the low-voltage discharge is relatively slow and may for awhile be masked by gas evolution caused by the discharge. When it is apparent that net pumping by the VacIon pump is occurring, the roughing pump should be valved or pinched off from the rest of the system.

As the pressure falls, the power supply voltage rises. As a consequence the pumping speed increases. In a typical installation the power supply is so designed that in order to achieve reasonable speed below about 10^{-4} Torr, voltages of about 3 kV and above are generally desirable.

The length of time required to pump down from atmospheric pressure to some lower pressure depends upon many factors, such as size of pumps and size, materials, cleanliness, and previous history of the system. Clean, small systems, such as the one shown in Fig. 10 are often

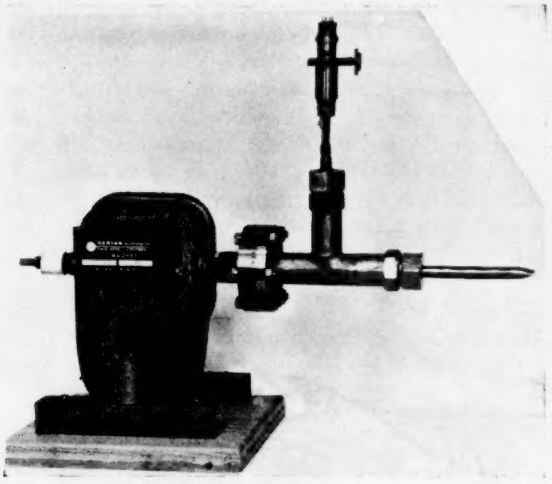

FIG. 10.

brought from atmospheric pressure to 10^{-5} Torr in less than 10 min. In that figure a small microwave tube is being pumped by means of a VacIon pump. In place of a valve to isolate the VacIon pump and tube a copper tube was pinched off following the completion of the rough pumping.

Tube processing by means of VacIon pumps enjoys the general advantages previously listed. However, it would be well to single out certain of these, as they apply to tube processing.

1. Lower limiting pressures are obtained. This results in improved life and lower noise output.
2. Considerable economies in capital investment are realized due to the elimination of valves and safety features necessary when diffusion pumps are employed. Since it is no longer necessary to combine fore-pumping, high vacuum exhaust, baking, cathode activation, RF processing and ageing into one complex and immovable structure considerable savings in equipment and in operating costs are possible. A single forepump on a rolling platform can serve many pumping stations.
3. Further very appreciable savings are possible due to the fact that liquid nitrogen is not needed. It has been found that this results in reduction in processing costs of the order of one dollar per tube.
4. Power failures which appear to be unavoidable in tube plants and which can and often do result in extensive losses, are now a matter of little concern.
5. The fact that the pump measures its own pressure means that no ionization gauge and power supply are needed. This can pay for the pump in smaller sizes.

6. Larger pumps

The photographs in the preceding section involved the processing of relatively small tubes with a VacIon pump of 5 l./sec capacity. For larger tubes or those with large oxide cathodes, it is desirable to use pumps of larger capacity. Fig. 11 shows a photograph of 3 pumps with capacities of

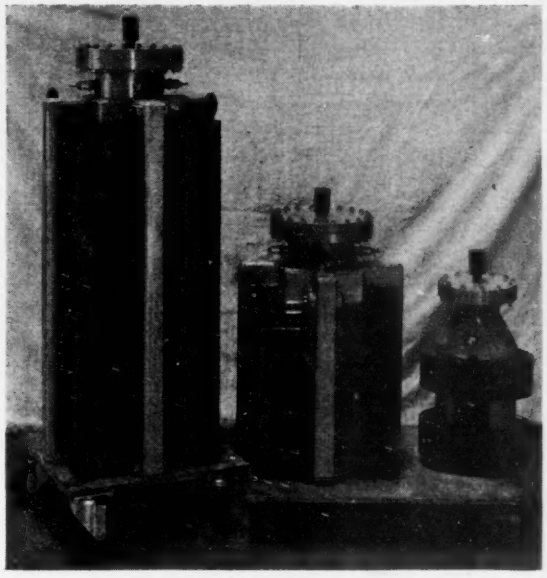

FIG. 11.

40, 140 and 280 l./sec. These have been used in processing of large klystrons with oxide cathodes up to 2.5 in. in diameter. In these sizes the pumps find other application, of course, as, for example, in evaporators, vacuum furnaces and particle accelerators. Analysis (and practice) indicate that there is no practical upper limit to the size of such pumps. Fig. 12 shows a 5000 l./sec pump which is being built for space chamber and hydrogen fusion applications.

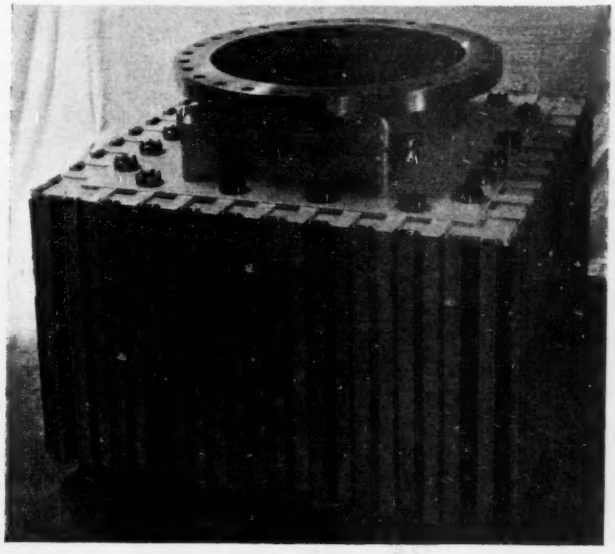

FIG. 12.

7. Sorption pumps

While this paper is concerned primarily with getter-ion pumps and their application to tube processing, it appears to be in order to mention briefly a technique for going from atmospheric to the very lowest pressures without any use of pumping fluids whatsoever, both in fore pumps and diffusion pumps. It has been found that by cooling activated charcoal or certain artificial zeolites (molecular sieve) one can reduce to the pressure in a system from atmospheric to the micron range where the VacIon pump can take over. This has been found to be of great value where extreme cleanliness is paramount, as for example, in the study of the physics of surfaces. Fig. 13 is a photograph of a system

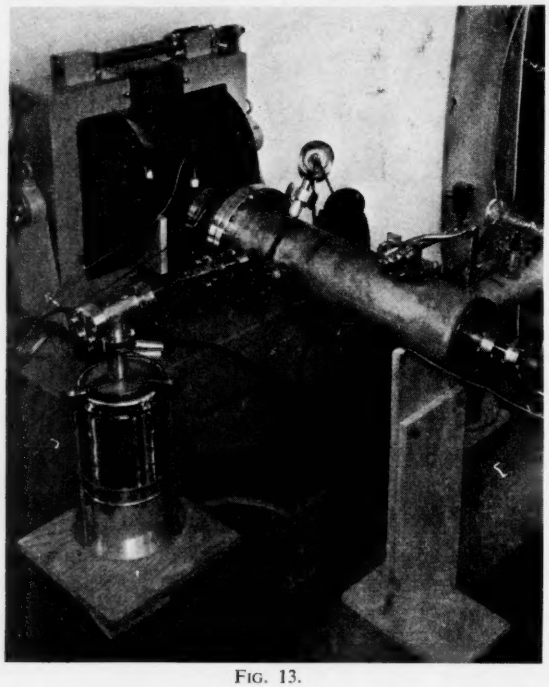

FIG. 13.

which was rough pumped with such a pump. These are now available under the designation of VacSorb* pumps.

8. Industrial experience

For the past two years VacIon pumps have been employed to an increasing extent in the processing of microwave tubes in the laboratories and factory of Varian Associates and of other electron tube manufacturers in the U.S.A. These have included, within Varian Associates, a total of over 6000 tubes with both oxide and Phillips cathodes. Results have been uniformly gratifying. No tube problems have ever been encountered which could be ascribed to the use of such pumps. Excellent life and lower noise are invariable results. In addition considerable savings in time and costs have been possible due to the elimination of liquid nitrogen and to the possibility of performing the various processing steps in separated locations.

In some cases after processing several hundred tubes, difficulty in starting is experienced as evidenced by a prolonged period in the micron range. This is ascribed either to the collection of condensibles in crevices of the pump and to their evolution during the pump heating which may occur during starting, or due to the flaking away of sputtered layers from the anode. Usually, complete restoration of easy starting can be effected by simply baking the pump in *air* for 2 hr at 400°C. This serves to completely oxidize the contained condensibles. Where this is not completely effective, a 10 min rinse with 2 per cent HF solution under supersonic vibration followed by a repeat of the air bake is generally effective. Studies have shown that the life of the pump is finite and is of the order of 4000 hr at 10^{-5} mm. Since life is inversely proportional to the pressure, life at pressures of 10^{-6} mm and less is measured in years. The end of life is arbitrary but is characterized by difficulties with flaking from the anode which result in gas bursts. While this condition can generally be remedied as described above, we choose to define the end of life in terms of the initial experience of this sort. Prolonged operation at high pressures will result in diffusion of titanium around the sputter shields onto the anode insulator with consequent leakage problems.

In practice the life of the small pumps is so great as to justify discarding it at the end of life. All pumps with speeds of 40 l./sec. or greater are designed so that replacement of the active electrodes is a simple matter taking only minutes.

FIG. 14.

* Trademark.

Vol.
10
196

9. Appendage pumping

Getter-ion pumps of the VacIon type are also finding extensive application to the maintenance of vacuum in sealed-off vacuum systems. They insure against the deficiencies of processing; against the inevitable outgassing during operation; and against amazingly large leaks.

Fig. 14 shows a 5 l./sec pump used in this manner on a super power klystron.

A leak which would result in a visible glow discharge in a few days can be held for years so that the pressure within the tube does not rise above 10^{-7} mm. This technique has been found useful not only in making possible the effective operation of tubes in the field where such would normally not be possible, but in permitting the completion of tests on experimental tubes. The time and economic gains have been appreciable.

10. Summary

A description of the VacIon getter-ion pump together with its physical principles was presented together with an analysis of its operating characteristics and advantages.

Particular attention was paid to the matter of processing electron tubes. Actual experience in this area was presented as a basis for the very considerable benefits to be derived from employing this technique.

Brief mention was made of two other matters:

1. The use of sorption pumps to go from atmospheric pressure to the starting region of the VacIon pump, thus completely eliminating the possibility of introducing contaminants into a vacuum tube or system, and,
2. The use of VacIon pumps as appendages to maintain the vacuum in a sealed-off system against the consequences of inadequate processing, outgassing during operation and leaks.

DISCUSSION

Question from Dr. S. H. Cross

What is the speed of the VacIon pump for Argon, and can Dr. Malter explain why the pumping speed he quotes for air is higher than that for nitrogen and oxygen?

Answer. The speed of the VacIon(R) pump for Argon is of the order of 1 per cent of that for air but exhibits cyclic variations so that if one is pumping against a constant Argon leak, the pressure in the system varies. This effect does not make itself felt under ordinary operating conditions when pumping air.

It is believed that the pumping speed for air exceeds that for oxygen and nitrogen due to the high sputtering ratio of Argon. The presence of even 1 per cent of Argon results in so great an increase in the sputtering of titanium that the gettering action for the oxygen and nitrogen is raised above its vaue for either of the active constituents when present alone.

Question from Mr. A. Schram

Is the end vacuum obtainable by your pump a function of the applied voltage, or is it independent? I fear that more and more trapped gas particles will be released when the bombarding ion energy rises.

Answer. The pumping speed of VacIon(R) pumps increases monotonically with increasing the applied voltage (see Fig. 5) and lowers the end vacuum obtainable. In an abrupt change to a considerably higher operating voltage one observes a transient increase of pressure. Within a matter of seconds the increased pumping speed more than compensates for any effect such as postulated by Mr. Schram.

Properties of a Small Titanium-Ion Pump

A. KLOPFER and W. ERMRICH

Deutsche Philips G.m.b.H. Zentrallaboratorium Aachen, Germany

A small getter-ion pump is described which has a capacity of several Torr liters for chemically active gases. The maximum pumping speed for CO is about 50 l/sec. The lowest pressure obtained with this pump is less than 10^{-10} Torr. The composition of the residual gases during the process of evacuation has been measured. The factors determining the lowest pressure that can be obtained are discussed.

Introduction

For many evacuation processes it is of advantage to have a small portable pump which maintains a low pressure for a long period and which can work without supervision. An example of a pump of this category is the combination of a getter mirror with either an Alpert ionization gauge or a Penning gauge.

Here we describe a pump in which getter material may be evaporated continuously or in steps over a limited period, during which time a Penning discharge is maintained in the vaporization chamber. This Penning getter pump is suitable, for example, to evacuate vacuum systems of moderate sizes up to that of a television picture tube.

Description

The electrode assembly is in principle the same as that of a simple Penning gauge. This system comprises an anode *A*, formed of a rectangular frame of molybdenum wire, and four cathodes K_1 . . . K_4. These latter contain the getter load. Perpendicular to the plane of the anode a magnetic field of 400 G is applied. The electrodes are mounted on a glass foot. The cylindrical pump housing, which is of glass, has a diameter of 34 mm and a length of 60 mm (Fig. 1). The pump weighs 40 g alone and 450 g with the permanent magnet. It is therefore easy to transport the unit.

To operate the pump a d.c. voltage of 2 kV is applied between its anode and its cathodes, one or more of the latter being heated by an a.c. current. The cathodes consist of twisted tungsten and titanium wires and are heated until the titanium starts to evaporate. The rate of evaporation is governed by the temperature and the number of cathodes heated thus. Part of the evaporating getter condenses immediately on the wall of the pump, gettering chemically active gases, while the rest helps to intensify the Penning discharge. At low pressures ($<10^{-4}$ Torr) it is only the evaporated getter that maintains the discharge. This can be confirmed from the reading given by a meter inserted between the cathode and the negative terminal of the power supply for the anode voltage; alternatively, it can be confirmed visually by using barium as the getter, for this metal shows a green colour in a discharge.

Via contact spring *F*, the potential of the getter mirror may be chosen as that one of the anode or negative with respect to the cathodes. In the latter case the mirror acts as an ion collector. In the former case, only physical adsorption is possible for chemically inactive atoms or molecules. Normally we give the getter mirror the same potential as the cathodes. The purpose of *S*, the circular molybdenum shield, as also of the " spats " marked *T*, is to prevent short circuits between anode and cathode by the condensed getter material. To provide electrical contact between spring *F* and the getter, a conducting layer is deposited on the inside of the wall of the pump. If it is desired to reach very low pressures with this pump, it is necessary to omit shield *S* and to weld the ends of the anode wire to two socket pins.

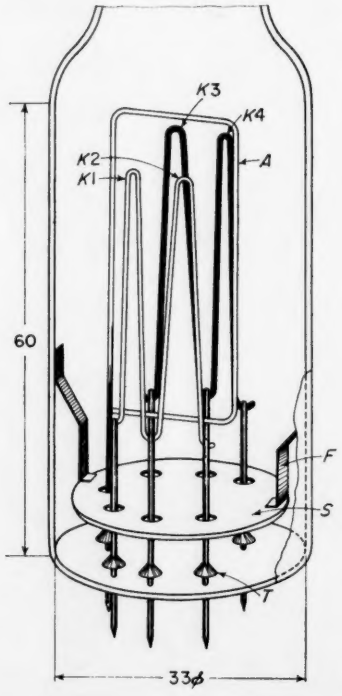

FIG. 1. Ti-Ion Pump with 4 hot cathodes (Ti–Pe *I*).

This makes it possible to heat all electrodes by passing a current through them.

The maximum electrical supply date are 2 kV at 2 mA for maintaining the discharge and 10 V at 10 A for heating the cathodes. The maximum power consumption of the pump is 100 W, at lower pressures this value is reduced to 20 W.

Properties of the titanium-Penning pump

The characteristic properties of a getter-ion pump are :

(a) initial operating pressure
(b) pumping capacity
(c) pumping speed
(d) ultimate pressure.

The initial operating pressure is governed by the applied method of evaporation. For the pump mentioned it is about 10^{-1} Torr. The pumping capacity, i.e. the total amount of chemically active gases that can be removed, is dependent on the amount of getter, the cathodes are loaded with. Usually each cathode contains 3 titanium wires 100 μ thick, which are twisted together with the carrier wire. The quantity of gas removed under optimum conditions with these 50 mg of getter amounts to 2.5 Torrl in the case of CO (this figure is based on a getter capacity of 5×10^{-2} Torrl/mg). Normally a mixture of various chemically active gases is present in a vacuum system, and consequently one cannot usually count on an average getter capacity of more than 1×10^{-2} Torrl/mg.

The pumping capacity can be increased to some extent by increasing the amount of getter in the cathodes. However, if a vacuum system evolves considerable quantities of gas for a long time, it must be possible to maintain a sufficient evaporation rate for this period. The pumping capacity can be increased by introducing certain modifications. On one side the hot cathodes are replaced by a cold cathode consisting of a solid plate of titanium. The anode frame is made of a massive titanium strip (see Fig. 2). Then the getter can be evaporated by three different methods, (a) heating " hot " cathodes K_2, K_3 and K_4 by passing current through them, (b) heating the anode by subjecting it to electron bombardment (without using a magnetic field), the necessary electrons being supplied by emission from the hot cathodes, and (c) by causing sputtering from the cold cathode. At low pressures one hot cathode must be used to maintain the discharge. With method (c), the starting pressure is allowed to be higher than with the other methods.

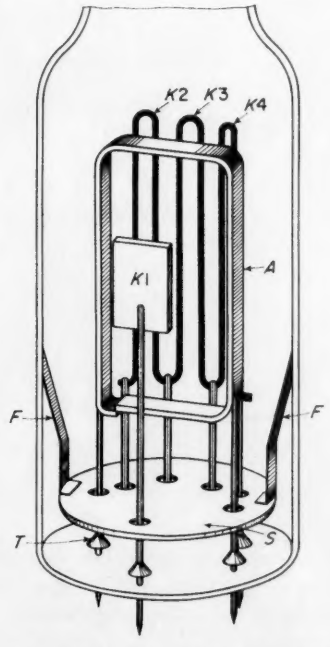

FIG. 2. Ti-Ion Pump with a cold and 2 hot cathodes (Ti-Pe *III*).

In the steady state the following relationship exists between the pumping speed S and dQ/dt, the quantity of chemically active gas that can be removed per second :

$$dQ/dt = C \times dM/dt = S \times p = \bar{s} \times p \times F \qquad (1)$$

dM/dt in the above equation means the amount of getter evaporating per time unit, C is the getter capacity, p the pressure at the mouth of the pump and S the pumping speed resulting from the gettering speed and the geometry of the pump housing. If F is the geometrical surface area of the getter mirror, a mean value s of the gettering rate may be stated, in the range where the pumping speed is not limited by the conductance of the pump mouth. Fig. 3 shows

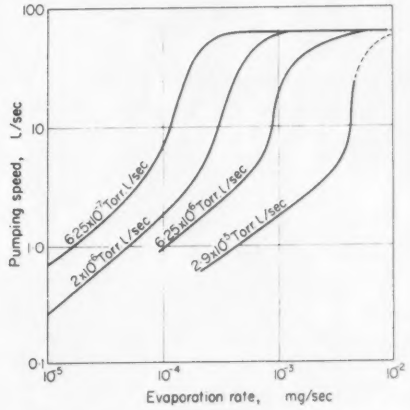

FIG. 3. Pumping speed of Ti-Pe *I* vs. evaporation rate of Ti for different rates of CO admitted.

measured values of S as a function of dM/dt, for different CO influxes. The maximum attainable pumping speed is 62 l/sec. The limitation results from the conductance of the pump mouth. Before the equation can be used, a relation must be found between the quantities C and S or s. Pairs of values for C and S or $\bar{s}$ have been calculated from the curves of Fig. 3 and are shown in Fig. 4. The upper abscissa indicates getter capacity in Torrl/mg ; the values of the lower abscissa represent the ratio between the number of CO molecules absorbed and titanium atoms striking the wall. Except in the part of the curve where S is limited by the diameter of the mouth, S and C are clearly interdependent : a given pumping speed fixes the getter capacity and *vice versa*. The steep rise of the curves in Figs. 3 and 4 means that the sticking probability of CO on Ti increases

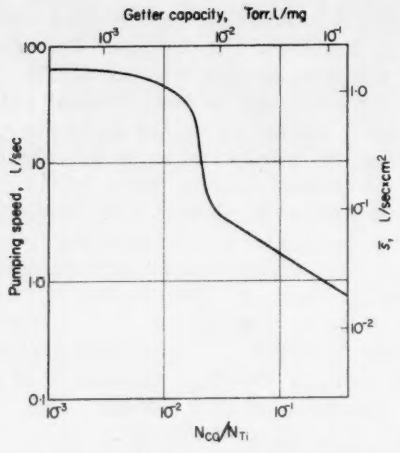

FIG. 4. Pumping speed of Ti–Pe *I* vs. getter capacity for CO.

rapidly when the surface coverage of the getter mirror is very low ; alternatively, it may be that the reactivation of an occupied getter place is only possible by several titanium atoms.

A constant pumping speed, independent on the gas influx, can be maintained, if the evaporation rate is varied proportional to the pressure on the pump. From equation (1) follows

$$\frac{dM}{dt} = \frac{S}{C} \times p \qquad (2)$$

For some fixed pumping speeds the linear relationship of equation (2) is shown in Fig. 5. Other values of the ratio

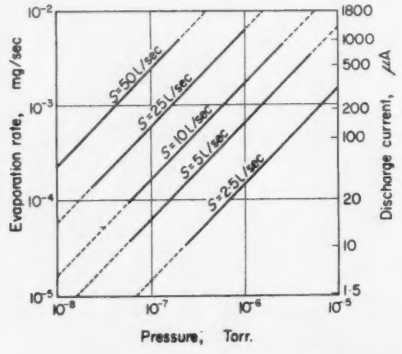

FIG. 5. Evaporation rate of Ti as a function of CO pressure on the mouth of Ti–Pe *I* for S = const.

S/C can be deduced from the curve of Fig. 4 and put into equation (2). By subtracting the discharge current with cathodes cold from that with hot cathodes one obtains a fairly good value for the steady rate at which the hot cathodes evaporate getter material (Figs. 6 and 7).

It will be clear from the foregoing that the discharge current from the hot cathode is not a measure of the gas pressure. The pump can however, be used as a pressure gauge when the cathodes are cold (Fig. 7). The pressure curves are appropriate to N_2 and CO for a magnetic field of 400 G, anode voltages of 1 kV and 2 kV, and a series resistor of 1 MΩ.

Pumping speeds have not yet been measured for other chemically active gases. For chemically inactive gases like methane and the noble gases the pumping speeds were found to be much lower (see Table I).

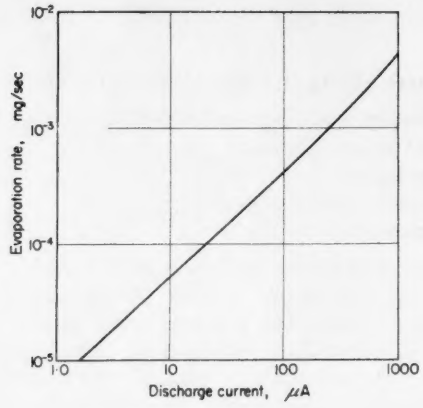

FIG. 6. Evaporation rate of Ti as a function of the discharge current in Ti–Pe *I*.

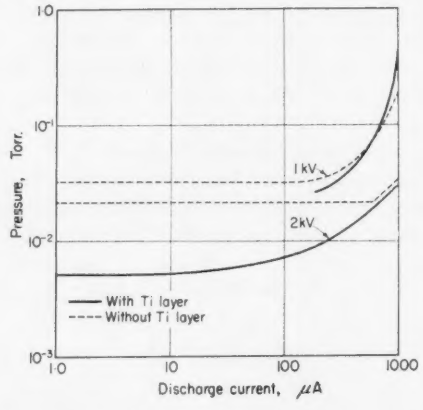

FIG. 7. Discharge Current as a function of the pressure in Ti–Pe *I* with cold cathodes. H = 400 G, V_A = 1 kV and 2 kV.

TABLE I

Pumping speeds for various chemically inactive gases

Gas	Discharge Current, μA	S l/sec	p Torr
He	100–1000	2×10^{-3}	1×10^{-5}–3×10^{-5}
Ne	500	5.5×10^{-3}	1×10^{-3}
A	100	3.5×10^{-3}	1×10^{-3}
	500	7.5×10^{-3}	1×10^{-3}
CH_4	100	7.4×10^{-2}	1×10^{-3}
	500	2.1×10^{-1}	1×10^{-3}

Ultimate pressures

The ultimate pressure attainable with getter-ion pumps depends to a very great extent on the speed of the ion pump, on the method of degassing and the purity of the getter material employed.

When evacuating a small vacuum system which had a volume of 0.5 l, and which consisted of an omegatron, a Bayard–Alpert ionization gauge and a Penning titanium pump, partial pressures were measured by means of the omegatron. We investigated four such systems in different states of degassing.

After the getter was evaporated, a system without any vacuum heat treatment mainly contains water, carbon dioxide and hydrocarbons. The partial pressures of H_2O and CO_2 are determined by the rates of desorption from glass surfaces and by the pumping speed that is effective in the omegatron. The presence of hydrocarbons may be attributed to two different reactions. Firstly, the hydrogen present as an impurity in the getter load may react during the evaporation of the latter with carbon impurities, forming hydrocarbons with 1 to 5 carbon atoms. The temperatures and H_2 pressure conditions necessary for the reaction are present in a system of this kind. Secondly, even at room temperature water reacts with the carbon impurities in the getter mirror to form hydrocarbons. In consequence of the desorption and the reactions just mentioned, in such a completely undegassed system the ultimate pressure is about 10^{-7} to 10^{-8} Torr[1].

If the system is subjected to moderate degassing in advance, the desorption rate of H_2O and CO_2 is very much less. The evacuation time and the ultimate pressure attained are then governed by the pumping speed of the ion pump and by the amount of hydrocarbons formed from H_2 and carbon impurities. Evacuation time diminishes as the degassing of the vacuum system and the getter material are improved. Moderate degassing allows pressures of about 1×10^{-9} Torr to be attained. The residual gases mainly consist of CH_4, CO and H_2. Very low pressures can be attained by applying a degassing method like that described by Alpert[2] to the vacuum system. The lowest pressure obtained with the pump described was below the X-ray limit of the ionization gauge ($<2 \times 10^{-10}$ Torr).

Fig. 8 shows pump-down curves for the system at various states of degassing, and Fig. 9 shows the composition of the residual gases in systems which had undergone moderate

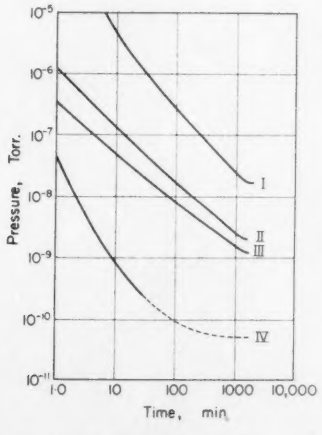

FIG. 8. Time of evacuation of small glass systems (0.5 l) by Ti–Pe *I*
I. No bake-out.
II, III. Short bake-out.
IV. Rigorous bake-out.

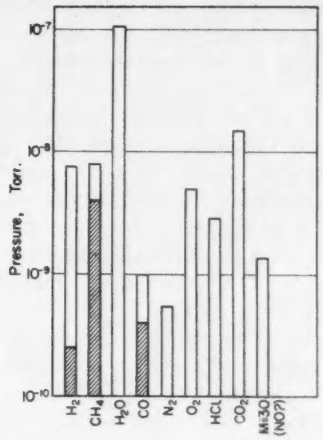

FIG. 9. Residual gases in a undegassed glass system after pumping for 200 min with Ti–Pe *I*. (Hatched parts give residual gases of a baked-out system.)

preliminary degassing and no degassing at all. The peak at mass 30 could not be identified. A value of the ionization sensitivity equal to that of N_2 was used to calculate the partial pressures of HCl and the unknown gas (which may have been NO).

We shall now discuss the factors that may limit the lowest obtainable pressure when the getter is evaporated continuously. During the degassing process, Cl and H_2 impurities in particular must be removed from the ultra-high vacuum system with a good auxiliary pump by firing the getter to a temperature close to its melting point. The pressure must not exceed 10^{-6} Torr at the end of the degassing period. Chlorine impurities tend to react with hydrogen to form HCl. Mention has already been made of hydrocarbon formation. In addition, between H_2 and titanium there is an equilibrium pressure which depends on temperature and H_2 concentration.

A certain amount of hydrocarbon formation takes place even after thorough preliminary degassing and it is therefore necessary to incorporate an ion pump that is very effective for CH_4. An ion pump with a hot cathode removes methan by electrical clean-up and by thermal dissociation. Heating of the getter mirror caused by the hot cathode increases the production of CH_4 and raises the partial pressure of H_2. Therefore it is necessary to cool the getter mirror. Blower cooling is generally sufficient.

Chemically inactive gases sticking on the surface of the getter mirror may be liberated by chemically active gas molecules due to a displacement reaction. Similar exchanges take place as a result of ion bombardment[3, 4]. We made certain of this effect by means of a titanium-ion pump. The getter mirror was bombarded with helium ions (energy 1250 eV). The quantity of helium adsorbed resulted in a surface coverage corresponding to a quarter of one monolayer. Towards the end of the evacuation process the pumping speed had decreased appreciably. Then the ion pump was switched off and neutral nitrogen admitted to the pump. A rise in the partial pressure of helium was observed

considerably greater than when no N_2 was introduced. The displacement ratio was 1 : 300, i.e. one helium atom was liberated by one N_2 molecule among 300 gettered.

Displacement reactions of this kind also accompany the evaporation of the getter when chemically inactive gases adhere to the condensation surfaces. During evaporation the ion-collecting surface is struck by titanium particles as well as by particles of chemically active gases present as impurities in the getter load. Therefore it may be better in many cases not to evaporate the getter continuously, provided that the mirror is still unsaturated and there is no evidence of saturation by noble gases.

If on account of saturation by noble gases a limiting pressure has been established, it is possible to " bury " atoms of noble gases by " plastering " with getter material. However, only particles captured in deeper layers are effectively treated in this way.

The exchange reactions are particularly pronounced with helium. Owing to the fact that glass is permeable to helium[2] it is likely that this gas will be present in ultra-high vacuum systems. The permeation rate of glass depends on the content of glass formers therein[5]. The quantity of helium permeating into a vacuum system per unit time is given by

$$q = \frac{K \times F}{d} \times \Delta p \qquad (3)$$

where K = permeability, F = surface area, d = thickness of the glass wall and Δp = difference between helium pressures on inside and outside of glass. The ultimate pressure attainable for helium is accordingly given by

$$p_e = q/S_{He} \qquad (4)$$

where S_{He} is the pumping speed for helium.

For borosilicate glass used in the pump described, the permeability K is 1.5×10^{-13} l mm cm^{-2} sec^{-1} and the pumping speed $S_{He} = 2 \times 10^{-3}$ l/sec. For a vacuum system whose surface area is 500 cm^2 and whose glass walls are 1.5 mm thick, the obtainable ultimate pressure may be calculated to 1×10^{-10} Torr. By using alumino-silicate glasses or other types whose content of glass formers is low, the permeability of helium can be decreased by a factor of 100 to 1000. Accordingly, very great attention must be paid to the choice of glass types if very low pressures (below 10^{-10} Torr) are to be attained.

From these studies we must draw the following conclusions : If pressures in the ultra-high vacuum range are to be obtained with a titanium-ion pump in which the getter material evaporates continuously, it is necessary to diminish the formation rate of hydrocarbons, the permeation rate of helium and the hydrogen content of the system.

References

[1] G. Reich and H. G. Nöller ; *Vac. Tech. Trans.* p. 97 (1957).
[2] D. Alpert and R. S. Buritz ; *J. Appl. Phys.* **25**, 202 (1954).
[3] E. Brown and J. H. Leck ; *Brit. J. Appl. Phys.* **6**, 161 (1955).
[4] L. J. Varnerin and H. J. Carmichael ; *J. Appl. Phys.* **28**, 913 (1957).
[5] F. Norton ; *J. Appl. Phys.* **28**, 34 (1957).

Vol. 10 196

The Gas Sorption Characteristics of Penning Pumps and Titanium Films

L. HOLLAND and A. HARTE

Research Laboratory, Edwards High Vacuum Ltd., Crawley, England

The gas sorption characteristics of evaporated Ti-films about 100 Å thick and of a Penning pump with titanium electrodes have been studied and compared. The Penning pump also served as an ion-source with the Ti-films. The sorption apparatus consisted of a bakable stainless steel getter chamber of 1400 cm² area and a Penning pump of 75 mm diameter. The vacuum seals were made with metal gaskets and the pressure measured with a hot filament ion-gauge. The gas to be sorbed was admitted to the getter chamber from a reservoir via a calibrated leak. Sorption rates were measured in the pressure interval 0.001–1μ Hg. The pumping speed of an evaporated Ti-film alone was negligible (<0.1 l./sec), but greatly enhanced when the Penning ion-source was in operation as previously found by Gale. Inert gases were only sorbed by the Penning pump. Instantaneous speeds measured at 10^{-6} Torr for fresh Ti-films with the ion-source in operation were, in l./sec., as follows: Air, 56; N_2, 56; O_2, 56; H_2, 234.

When the sorption rates of either the Penning pump alone or the Penning pump with a Ti-film were plotted in terms of mass sorption rates (litre microns/sec) as a function of pressure it was found that the resultant curves were parallel to the ionization current/pressure curve of the Penning discharge, i.e. the mass sorption rate at a given pressure was directly proportional to the discharge current at that pressure. *The sorption characteristics of mixed gases were studied to find the effect of one molecular type on the clean up of another. It is shown that the sorption rate of hydrogen is reduced by the presence of organic vapours, e.g. methane. Sorption rates were also measured for gas mixtures of argon/hydrogen, and nitrogen/" Calor " gas (butane). Measurements were rendered difficult when using hydrocarbon/gas mixtures due to the uncertainty in determining the sensitivity factor to be used with the ion-gauge. The role of ionization in enhancing the gas sorption rate is discussed by Holland in an appendix. The increase in the rate of clean up by titanium was not due to ions flowing to the film because the getter chamber was at a positive potential. The high sorption rate of H_2, O_2, and N_2 when ionized was attributed to their atomization in the Penning discharge. Thin films of titanium are composed of densely packed grains and the enhanced rate of clean up is attributed to the atomic gas being able to penetrate the interstices between the grains and reaction products on the porous film.*

1. Introduction

A simple getter-ion pump can be made with an evaporation chamber in which the chemically active metal is evaporated to form a thin film with facilities for ionizing the residual gas such as a hot cathode ionization gauge or Penning gauge. Alternatively one may use a Penning ionization system with cathode electrodes which sputter chemically active material on to the container walls ; such an apparatus will be termed here *Penning Pump*. Numerous types of getter-ion pumps based on these principles have been evolved for pumping sealed-off electronic tubes and Holland[1] has recently reviewed the literature on the subject. Titanium has been extensively used as a getter material in such devices because it sorbs a wide range of gases and small quantities of the metal can be evaporated from tungsten spirals or sputtered from cathode electrodes. Barium films are extensively used for gettering in sealed-off glass envelopes, but they form thick oxide and carbonate layers which peel and contaminate the vacuum apparatus if exposed to atmosphere, whereas the less active titanium deposits superficially oxidize but remain stable when exposed to the atmosphere.

Gale[2] has used a combined titanium evaporation chamber and Penning ionization source for exhausting X-ray tubes. Gurewitsch and Westendorp[3] have increased the rate of gas sorption of a Penning pump by using either titanium or carbon electrodes, and Hall[4] has described a Penning pump of about 10 l./sec made with titanium electrodes which is suitable for pumping magnetrons, etc. Reikhrudel *et al.*[5] have measured the pumping speed of a Penning pump as a function of applied voltage, magnetic field strength and gas pressure, but it is not clear whether tantalum or titanium was used for the cathode electrodes. Jepson[8] has recently reported the pumping speed of a Penning pump for various gases. However the foregoing reports give little information on the pumping speeds which can be obtained with a particular combination exhausting the mixed gases present in a

normal vacuum system and even less appears to be known about the mechanism of gas sorption. Experiments have therefore been made to find the sorption characteristics of evaporated titanium films in the presence of different ionized gases and of a Penning pump fitted with titanium electrodes. The results obtained are of practical value and throw interesting light on the effects of gaseous impurities on the pumping speeds of specific gases.

2. Experimental apparatus and procedure

General

The apparatus used consisted of two stainless steel chambers in which were housed the evaporation and ionization facilities as shown in Fig. 1. The getter chambers were evacuated through an isolation valve by a 10 l./sec diffusion pump charged with Silicone 703 and backed by a 30 l./min rotary pump. The isolation valve was of the all metal type with a copper to steel valve seating and a soldered metal bellows shaft seal. All of the vacuum seals above the diffusion pump flange were bakeable and made with either aluminium[6] or copper[7] gaskets which have been described elsewhere. With the exception of the isolation valve the getter vessel and its contents could be baked at 300 °C for accelerating degassing.

Evaporation chamber and titanium vapour source

The evaporation chamber was 15 cm diameter and 21 cm high with welded stainless steel flanges for connection to the Penning ionization system and baseplate. Glass to metal lead-in electrodes were welded into the baseplate for carrying the L.T. power to the evaporation filaments. Copper rods 10 cm high and 12 mm diameter were screwed on to each of the lead-in electrodes and terminated with filament clamps made of copper bar. The filaments were made of three tungsten wires of 0.5 mm diameter twisted together and wound with four turns spaced 12 mm apart on a 6 mm diameter mandrel. On each of the filament turns was suspended hairpin shaped pieces of titanium wire of 12 mm length and 1 mm diameter. The filaments were heated by a 12 volt 60 amps L.T. supply with a variable transformer controlling the output voltage. The titanium evaporated on the inner walls of the vessel had an estimated deposit area of 1370 cm^2.

Penning pump and ionization source

The electrodes of the Penning ionization system were mounted inside a stainless steel tube of 7.6 cm diameter as shown in Fig. 1. The anode consisted of a short tube made of titanium sheet 3.2 cm wide welded to form a 7.6 cm diameter tube which was sprung inside the main vessel. The cathodes consisted of two plates shaped to follow the contour of the tubular vessel and 7.6 cm long and 5.1 cm wide. The two cathodes were connected to a glass to metal lead-in electrode.

The magnetic field was provided by a permanent magnet with a field strength of 400 oersted. The h.t. power was supplied by a high reactance transformer with a full-wave rectifier giving a maximum output of 3 kV at 50 mA. The output voltage of the supply was controlled by a " Variac " in the input to the transformer. It is not essential to use a d.c. supply because of the rectifying properties of the Penning electrode system, but it is more convenient for precise measurement. A graph of the h.t. current as a function of pressure with a constant voltage of 3 kV applied to the Penning electrodes is shown in Fig. 2. It can be seen that

Vol. 10 1960

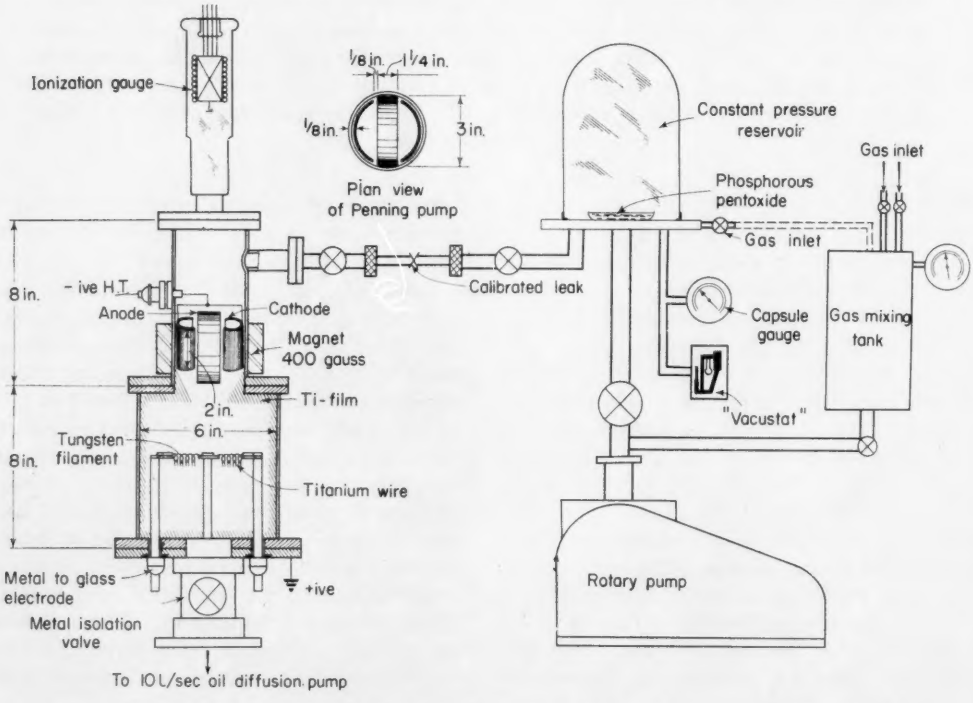

FIG. 1. General arrangement of getter-ion pumping system and pumping speed measuring apparatus.

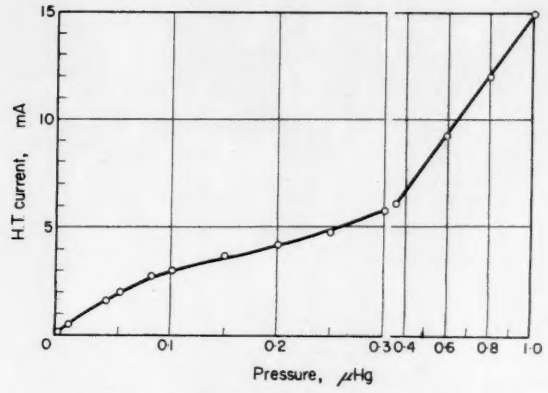

FIG. 2. Variation of h.t. current with air pressure for Penning pump.

the slope of the current/pressure curve is fairly constant, but for pressures below 0.1μ Hg the curve is no longer a straight line.

If the h.t. current is directly proportional to pressure then this should result in a Penning pump having a constant volumetric speed (S l./sec) independent of pressure P and a mass sorption rate (SP l.μ/sec) which decreases linearly with pressure. This is because the number of molecules sorbed (i.e. the mass of gas exhausted) depends on the intensity of the ionization and the rate of sputtering both of which directly depend on the current flowing to the electrodes. Inspection of the data of Reikhrudel *et al.* shows that their Penning pump had a constant speed S over a wide pressure range when the magnetic field was above 1000 oersted. Such a high magnetic field requires the use of a large magnet assembly which negates the compactness of the pump electrodes. Jepsen has also reported a constant speed for a Penning type pump operated between 10^{-5}–10^{-8} Torr and with field strengths of about 1000 gauss.

The Penning ionization system described here was used in combination with evaporated titanium films or as a pump in its own right.

Measurement of pumping speed

The gas pressure in the getter vessel was measured by a hot cathode ionization gauge in a glass envelope connected to the stainless steel vessel by a glass to metal seal of 25 mm bore. Gas was admitted to the getter system through a fixed leak made by crushing a metal capillary tube. The leak was calibrated by holding the pressure constant in the reservoir chamber at a value between 1–20 Torr and measuring the rate of pressure rise in the getter vessel which had previously been evacuated to a low pressure (0.01 Torr) by the diffusion pump and then isolated. Curves were then plotted for a number of gases relating the reservoir pressure to the mass flow rate through the leak. When gettering tests were made the volumetric speed S could be found at any instant by dividing the mass flow rate by the *instantaneous* pressure.

The speed of the leak and the calibration factors used for the ionization gauge with different gases is shown in Table I. Values of the leak rate for the respective gases have also been calculated from their molecular weight and the measured leak rate for air assuming that the leak was in the molecular

TABLE I

Leakage Rates and Ionization Gauge Calibration Factors for Different Gases

Gas	Gauge Factor	Mol. wt.	LEAK RATE		
			Measured (cc/s)	Corrected for Gauge Sens. (cc/s)	Calculated from air measurement (cc/s)
Air	1	28.8	0.039	0.039	0.039
N_2	1	28	0.04	0.04	0.04
O_2	0.8	32	0.035	0.043	0.037
H_2	0.4	2	0.048	0.12	0.15
A	1.33	39.9	0.037	0.028	0.033
"Calor"*	4.6†	55	0.085	0.019	(0.028)
Coal‡	1.25§	—	0.04	0.032	—

flow range. Some sorption experiments were made using hydrocarbon gases with the approximate contents given in Table I. The calibration factor of the gauge changed with time as hydrocarbon decomposition products were formed in the gauge head and the sorption rates measured for the organic gases should be considered as only indicative of the true rate. The sensitivity factors of the ion-gauge for "Calor" and coal gas relative to air were independently determined by Mr. Ellsworth of this laboratory and his values are given in the table.

Experimental procedure

The getter apparatus was initially evacuated by the diffusion pump to a pressure below 10^{-5} Torr and then baked at 300°C until the combined leakage and desorption rates were about 0.5 cc μ/sec. The titanium getters were outgassed by heating the metal just below its melting point and as the films were deposited the pressure in the getter vessel fell to below 10^{-7} Torr with the isolation valve closed. When the pumping speed of the Penning pump was measured the apparatus was treated as above but titanium was not evaporated.

3. Experimental results

Penning pump

Pumping speed. Shown in the lower curves of Figs. 3, 4 and 5 are the pumping speeds of the Penning pump measured as a function of pressure for various gases. These readings were taken with the pressure rising and falling and there was no observable hysteresis in the speed curve over the pressure range measured. The pumping effect shows itself when the pressure in the Penning head has been sufficiently reduced

*Fuel gas commercially available containing approximately by volume: 51–20 per cent propane; 78–84 per cent butane (in ratio 40 parts *iso*-butane 60 parts normal butane); 1–2 per cent butene.

†Measured against Mcleod reading.

‡Coal gas has the typical volumetric composition: 47 per cent H_2; 36 per cent CH_4; 8 per cent CO; 2 per cent CO_2; 3 per cent N_2; together with various hydrocarbons 4 per cent.

§Measured against Mcleod reading.

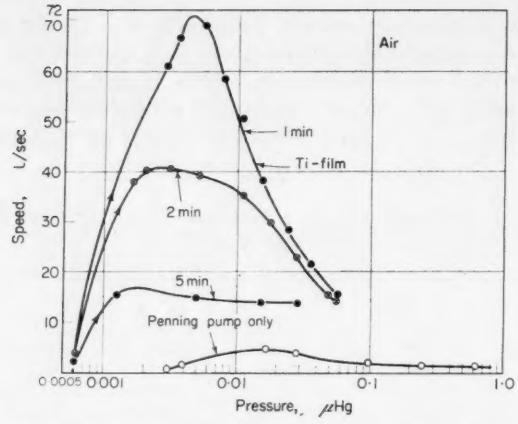

FIG. 3. Pumping speed of Penning pump with and without evaporated titanium film for air. Pumping speed of titanium films measured over 1, 2 and 5 min intervals with progressive increase of pressure. New film deposited for each series of measurements.

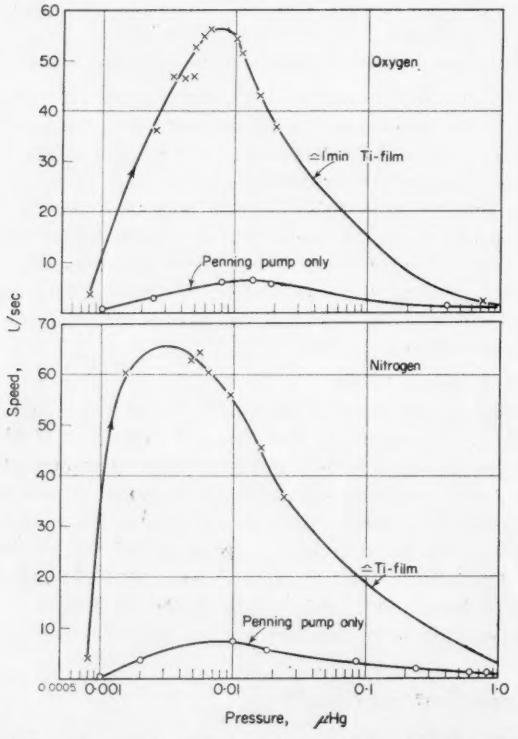

FIG. 4. Pumping speed of Penning pump with and without evaporated titanium films for oxygen and nitrogen.

for the sputtered material to escape from the cathode electrodes which corresponds to a pressure of 100μHg and an applied voltage higher than 300 V.

It is of interest to consider why the pumping speed of the Penning pump is not completely constant with pressure. If one replots the sorption rates in terms of the mass sorption rate (l.μ/sec) as shown in Fig. 9 for the Penning pump alone then it can be seen that the sorption curve does not contain a maximum but only slightly departs from being a linear function of pressure. As explained earlier the mass sorption

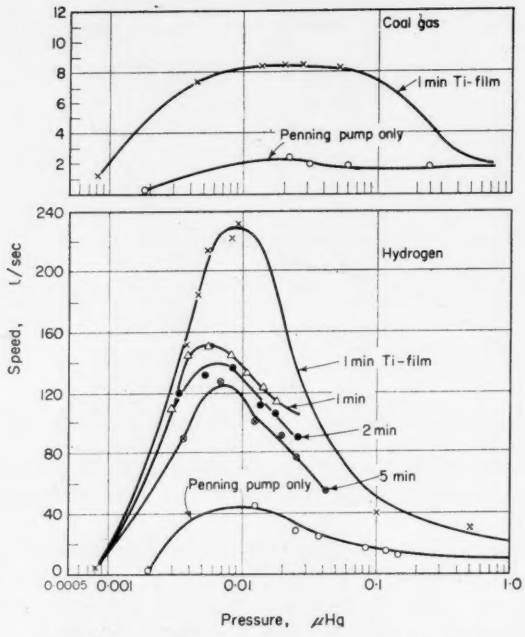

FIG. 5. Pumping speed of Penning pump with and without evaporated titanium films for hydrogen and coal gas. Sorption rate of titanium films for hydrogen determined over different time intervals with progressive increase of pressure and a fresh film deposited for each series of measurements.

rate of a Penning pump should be a direct function of the current flowing in the Penning head and Fig. 2 shows that at low pressures the current curve bends in the same direction as the mass sorption curve in Fig. 9. Presumably when the Penning pump is operated at high magnetic field strengths the h.t. current becomes a completely linear function of the pressure and this accounts for the constant speed curves (l./sec) measured by other workers.

Argon. Inert gases, unlike chemically active gases, cannot combine with the sputtered deposit so that they are pumped slowly as is shown for argon in Fig. 6. It is of interest

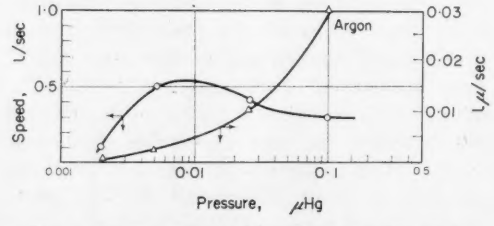

FIG. 6. Pumping speed of Penning pump for argon.

to conjecture how the inert atoms are sorbed in a Penning pump. If the argon ions bombarding the cathode are trapped in the metal then sputtering must continuously expose the previously sorbed gas so that an equilibrium value would be reached at which the rate of absorption is equal to the rate of desorption. It is possible that the neutral argon atoms are physically adsorbed for short periods to the walls on which the sputtered deposit settles and thus become trapped in the deposit.

Vol. 10 1960

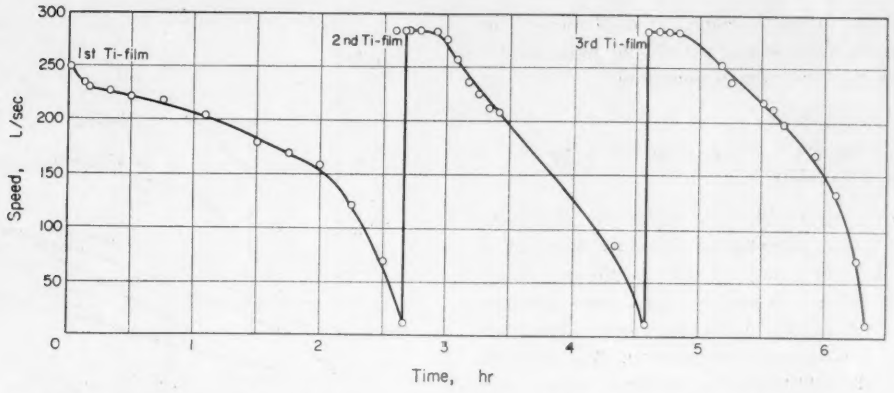

FIG. 7. Pumping speed of renewed titanium film measured at 8×10^{-6} Torr with Penning ion-source in operation.

[*Note added to Manuscript.—Since this work was done it has been found that the pumping speed of the Penning pump decreased to much lower values than those reported here. It is believed that the pump electrodes initially absorb gas, and time is required to attain equilibrium. The equilibrium values are in l./sec : air, 1 ; N_2, 1·2 ; O_2, 0·8 ; H_2, 0·9 ; Coal gas, 0·85 ; A, 0·2.*]

Sorption of gases by titanium films

Pumping speeds for various gases. The sorption rates of evaporated titanium films of about 50–100Å thickness are plotted in volumetric terms (litres per second) in Figs. 3 and 4 for air, oxygen and nitrogen with the Penning pump in operation and operated at a constant voltage of 3 kV. The sorption rates of the Ti-films without the ion-source were less than 0.1 l./sec and could not be measured accurately with the existing leak. The presence of ionization due to the hot filament ion-gauge used for pressure measurement did not appear to influence the sorption rates. The speed curves were measured with the gas pressure being raised. The reservoir pressure was held constant over a given time interval whilst each speed measurement was made. Thus the speed curves for air in Fig. 3 were made with a new film for each series of tests and the *instantaneous* pressure in the getter chamber measured at the end of 1, 2 and 5 min intervals. By this means it is possible to see the effect of gas saturation of the deposit. Plotted in Fig. 5 is the sorption rate of hydrogen and coal gas in terms of l./sec and these curves show that the high sorption rate of hydrogen is not maintained when hydrogen/hydrocarbon gas mixtures are sorbed. Pure hydrogen is sorbed for long periods by a titanium deposit and the sorption rate can be restored by evaporating a fresh film as shown by the pumping speeds measured at constant pressure and given in Fig. 7. It is interesting to observe that the clean up rates of the Ti-films for the gases used follow the sorption curves of the Penning pump and this is discussed further below.

Mass sorption rates and ionization. When the volumetric sorption rates of the titanium films in Figs. 3, 4 and 5 are replotted in terms of mass sorption rates (litre/microns per second) as shown in Figs. 8 and 9 it can be seen that the clean up rates become almost linear functions of pressure and these curves are also parallel to those for the mass

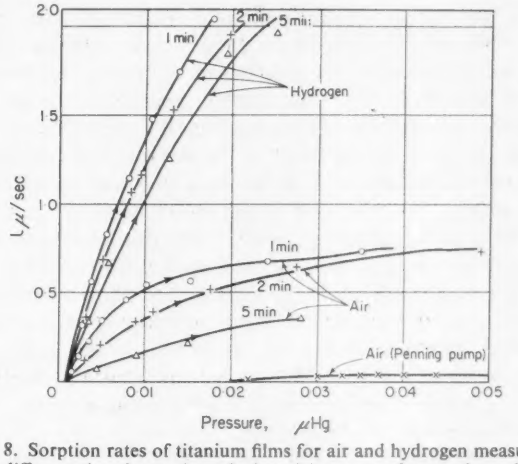

FIG. 8. Sorption rates of titanium films for air and hydrogen measured over different time intervals and plotted in terms of mass throughput (l.μ/sec) at different pressures ; Penning ion-source in operation throughout tests.

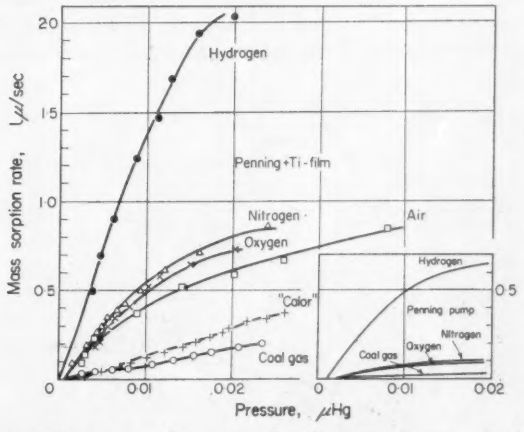

FIG. 9. Maximum sorption rates of various gases measured within 1 min intervals and plotted in terms of mass throughput (l.μ/sec) at different pressures ; Penning ion-source in operation throughout tests.

sorption rates of the Penning pump. If the Penning pump is activating the gas being sorbed and increasing its clean up by the Ti-film then one would expect the mass sorption rate of the film to vary with pressure in a similar way to the

discharge current curve in Fig. 2, which in fact it does. The effects of ionization on the sorption rate of the getter film is discussed further in the appendix by Holland.

The sorption of gas mixtures

We shall consider the effect of pumping a mixture of say two gases A and B as follows :

Case (i). Consider A is an inert gas and B is a chemically active one. Gas A is not pumped by the getter film and is only removed by the ion pump. There is the possibility that the chemically active gas and inert gas may interfere with the sorption of one another by the ion pump. However in the simplest case one can consider that gas A is removed from the mixture at the rate measured for the ion pump with the pure gas and gas B is removed at a rate measured for the getter film with the pure gas. Thus the lower mass sorption rate of air compared with oxygen and nitrogen in Fig. 9 can principally be accounted for by the presence of one per cent of argon in the air which is removed very slowly by the ion pump and produces a high partial pressure in the getter chamber. A similar effect occurs in the pumping of air by a getter-ion pump with a continuously evaporating titanium source, as shown by Holland and Laurenson[9].

Case (ii). Consider both A and B are chemically active. In this case the pumping speed of the gas mixture is not likely to be derived from the individual speeds of the pure gases, because one of the two gases may be preferentially sorbed, e.g. form a chemical compound in preference to the other, or sorbed in such a way as to prevent the other gas from being taken up. Thus oxygen is known to form a dense oxide on solid titanium and prevent the absorption of hydrogen at normal temperatures.

To find whether there is any validity in these theories measurements have been made of the sorption rates of argon/hydrogen and " Calor " gas/nitrogen mixtures. The sorption rates in mass terms have been plotted as a function of pressure in Figs. 10 and 11. It is to be noted that the mass sorption rates of the mixed gases have been derived

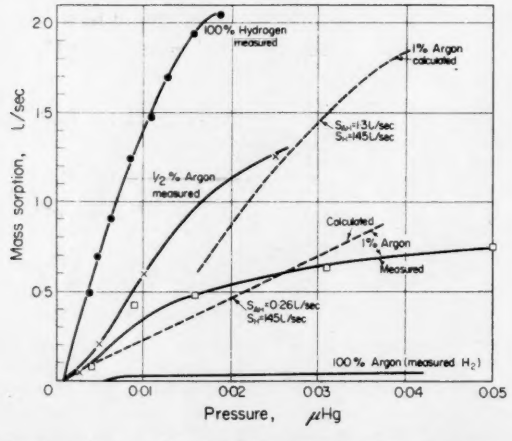

FIG. 10. Pumping speed of titanium film and Penning pump for hydrogen/argon mixtures. All calculations have been made assuming that the leak rate and ion-gauge calibration factors are those for hydrogen so that the sorption rate curve for pure argon is the equivalent hydrogen rate.

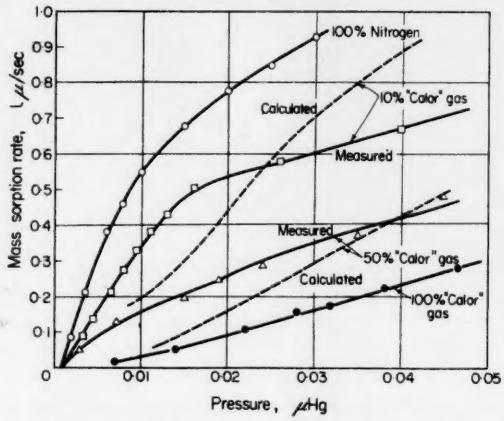

FIG. 11. Pumping speed of titanium film and Penning pump for nitrogen/" Calor " gas mixtures. All calculations have been made assuming that the leak rate and ion-gauge calibration factors are those for nitrogen, so that the sorption rate curve for " Calor " gas is the equivalent nitrogen rate.

by assuming that the leakage rate from the reservoir and the calibration factor of the ionization gauge for a particular mixture is that of one of the pair of gases. Thus the values for hydrogen were used for the hydrogen/argon mixtures and those for nitrogen for the nitrogen/" Calor " gas mixtures. This method was employed because the exact proportion of each type of gas in the getter chamber was not known since it depended on the rate at which they were individually removed from the mixture. However if the mass sorption rates of say argon are expressed in terms of the *equivalent hydrogen* rates then the sorption rates for a given gas mixture can be derived from those for the pure gases. The calculated curve for a mixture can then be compared with the measured curve and if they agree then this should indicate that each gas has been sorbed independently of the other.

Thus the mass throughput for pure argon is plotted as $M_A L_H / L_A$, where M_A is the true throughput and L_H and L_A are the leakage rates for hydrogen and argon given in Table I. Likewise the argon pressure P_A is multiplied by (1.33/0.4) to give the equivalent hydrogen pressure. When one measures the mass sorption rate of the hydrogen gas mixture the ion-gauge current I is converted to that for hydrogen $I/0.4 = P_T$, but since there is a mixture of gases present one is really reading $P_T = 1.33/0.4\ P_A + P_H$, where P_A and P_H are the partial pressures of argon and hydrogen respectively. Likewise the mass sorption rates measured for the mixed gas are

$$M_m = \frac{L_H}{L_A}(M_A) + M_H$$

It can be shown that the relation between the true pumping speed S_A of argon and its hydrogen equivalent S_{AH} is given by

$$S_{AH} = S_A \frac{0{\cdot}4 L_H}{1{\cdot}33 L_A}$$

From these expressions it is possible to derive a sorption rate for the gas mixture from the sorption rate of the pure

gases assuming that there is no interaction between the gases when each is present. Such a theory would normally apply to the pumping performance of a diffusion pump.

The results of doing this for hydrogen/argon mixtures are shown in Fig. 10. The measured values show that the introduction of $\frac{1}{2}$ and 1 per cent of argon in hydrogen greatly lowers the sorption rate. The effect is even more pronounced when one appreciates that the concentration of argon in the gas is reduced to 0.11 per cent and 0.23 per cent after flowing through the leak from the reservoir. The calculated mass sorption values in Fig. 10 are based on the argon pumping speed given in Fig. 6, *i.e.*, $S_A \simeq 1$ l./sec. Recent work shows that the equilibrium speed for pure argon is 0·2 l./sec. and when this value in terms of its hydrogen equivalent is used, almost perfect matching is obtained between the measured and calculated curves.

Calculations have been made for nitrogen/" Calor " gas mixtures on similar lines to those described above. In this case both " Calor " gas and nitrogen are sorbed by the getter film and the Penning pump. The results for the gas mixtures show that the sorption rate of nitrogen is lowered by the presence of " Calor " gas but not to an extent which suggests there is any interaction between the two gases. " Calor " gas is mainly made up of saturated hydrocarbons which may be decomposed in the Penning discharge or chemisorbed to the Ti-film by a catalytic process. Experiments are now being made with initially unsaturated hydrocarbons to find whether their surface adsorption reduces the clean up of other gases.

4. Acknowledgements

Acknowledgements are made to Mr. W. A. Sheraton who made some of the measurements on the pumping speeds of the organic gases and to Edwards High Vacuum for permission to publish this report.

References

1 L. Holland ; *J. Sci. Instrum.* **36**, 105 (1959).
2 A. J. Gale ; *C.V.T. Vacuum Symposium Trans.*, p. 12, Pergamon Press (London 1956).
3 A. M. Gurewitsch and W. F. Westendorp ; *Rev. Sci. Instrum.* **25**, 389 (1954).
4 L. D. Hall ; *Rev. Sci. Instrum.* **29**, 367 (1958).
5 E. M. Reikhrudel, G. V. Smirnitskaya, and A. I. Borisenko ; *Radiotekhnika i Elektronika*, 281 (1956).
6 J. Holden, L. Holland, and L. Laurenson ; *J. Sci. Instrum.* **36**, 281 (1959).
7 R. Brymner and W. Steckelmacher ; *J. Sci. Instrum.* **36**, 278 (1959).
8 R. L. Jepsen ; *Le Vide* **14**, 80 (1959).
9 L. Holland and L. Laurenson ; *Le Vide* (1959) to be published.

ol.
10
960

APPENDIX

The Effects of Ionization on the Gas Sorption Characteristics of Titanium Films

L. HOLLAND

It is of interest to consider the manner in which ionization of the gas being sorbed enhances its clean up by a titanium deposit as shown in the previous report.

The getter film is at the anode potential so that positive ions formed in the Penning head could not be attracted to the metal deposit. If in fact the ionization of the gas to be sorbed is truly responsible for the rise in the sorption rate then this must occur by the creation of unusual species such as dissociated molecules. It is well known that the sorption of hydrogen by metals is greatly enhanced if it is in atomic form. Thus Reimann[1] found that magnesium sorbed hydrogen more quickly in the presence of an ionizing electron stream because atomic hydrogen was formed during neutralization of the H_2^+ ion.

When oxygen is cleaned up it is initially chemisorbed to the metal surface and finally forms a dense oxide layer. Thus after the first rapid sorption of gas the oxygen removal should be at a slow rate as diffusion proceeds across an oxide layer. The curves relating the mass sorption rate of oxygen to pressure show that the clean up increases with pressure and consequent increase in the ionizing current. Thus there is a direct relation between activation of the gas and the current flowing in the Penning discharge. The writer at first considered that the activation effect arose from the presence of impurities in the oxygen, e.g. inert gases such as argon, which were removed only by the Penning pump. This would make the sorption of oxygen appear to depend on the ion-current. However, when the source of the tank gas was checked it was found to be produced by electrolysis with the approximate composition given in Table II. Thus

Table II

Typical Volumetric Composition of Commercial Tank Gases used for Sorption Experiments

Gas	Nitrogen	Oxygen*	Hydrogen*
N_2	99.9–.95%	0	0.05%
O_2	0.5%	99.65%	0.05%
H_2	50 p.p.m.	0.3%	99.9%
H_2O†	200 p.p.m.	200 p.p.m.	200 p.p.m.
CO	5 p.p.m.	0	5 p.p.m.
CO_2	10 p.p.m.	200 p.p.m.	10 p.p.m.
A	5–10 p.p.m.	0	0
Ne + He	0.08% (max.)	0	0
Carbon products	—	4 p.p.m.	20 p.p.m.

*These gases were obtained by electrolysis.
†Water vapour was removed by the drying agent in the reservoir.

one is forced to the conclusion that ionization of oxygen in the Penning head activates it and increases its rate of sorption by titanium.

Thin films of metals of fairly high melting point (>1500°C) are known to have a structure of densely packed fine grains and a large interior area. Thus the effect of the ionization could be to produce atomic oxygen which more easily diffuse or migrate into the interstices between the grains in the titanium deposit. It is of interest to note that Bloomer[2] found that an ionizing discharge had little influence on the rate of clean up of oxygen by barium, but that the gettering rate of a used film could be increased if the gas molecules collided with a heated tungsten filament. Atomic oxygen is produced in a cold cathode glow discharge and will therefore most likely be produced in a Penning discharge. It is not at all clear to what degree atomic oxygen is produced in the conventional grid/ionizing system used by Bloomer but such an ion-source is not so productive of ions as a Penning discharge. The hot tungsten filament used by Bloomer would have dissociated the impacting oxygen molecules producing atomic oxygen ; this strengthens the contention that atomizing the gas raises its sorption rate.

The energy of dissociation of molecular oxygen is higher than that of hydrogen, but in the Penning cold cathode discharge the ion current flowing at a given pressure is higher for oxygen than that for hydrogen. Even so the sorption rate of the activated hydrogen is greater than that of the activated oxygen, which is obviously due to the more easy diffusion of the small hydrogen atom between the grain boundaries.

It is to be noted that ionization in the hot filament ion-gauge used in the experiments described in the foregoing report did not influence (within the experimental error) the sorption rate of the Ti-films. This could easily be due to the low level of the ion current compared with that flowing in the Penning discharge rather than to the absence of atomic oxygen. However we have the report by Wagener[3], who used a hot cathode ion-system, that sorption of oxygen by barium is not influenced by the activation of the gas and the contrary report of Cloud *et al.*[4] that the sorption rate of thick barium layers for oxygen is increased by activation with a Penning gauge. Unlike titanium, barium deposits of comparable thickness are less compact and the oxide which forms on their surface is loosely packed. Thus oxygen would more freely enter their structure than with titanium and the effect of using atomic oxygen would only show itself later in the film life, when reaction products had formed.

References

[1] A. L. Reimann ; *Phil. Mag.* **16**, 673 (1933).
[2] R. N. Bloomer ; *Brit. J. Appl. Phys.* **8**, 40 (1957).
[3] S. Wagener ; *Nature* (London), **173**, 684 (1954).
[4] R. W. Cloud, L. Beckman, and J. G. Trump ; *Rev. Sci. Instrum.* **28**, 889 (1957).

Vol
10
196

Method for Ageing of Electron Valves

O. PRESSEL

The Mullard Radio Valve Co. Ltd., Croydon, England

It is desirable to exhaust valves under conditions which simulate the ratings at which the valve is used when operated during its life. To do this with a conventional pump unit may be very difficult for many types of valves and indeed often impossible because a diffusion pump would not produce pressure low enough to maintain the high voltage-gradients used for instance in X-Ray-Tubes, High Tension Rectifiers and some types of Microwave Valves. Exhausting such devices on a conventional pumping system has to be followed by a conditioning process to make the valve suitable to operate at its desired ratings. This conditioning process can be a very long and hazardous operation requiring skilled personnel.

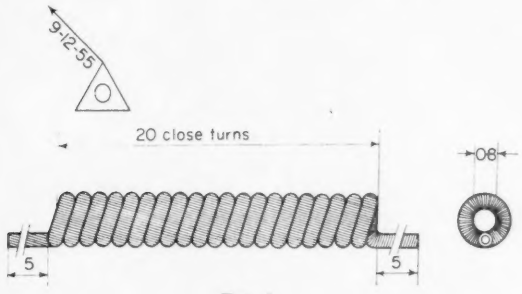

Fig. 1.

For some time we have employed at the Mullard Radio Valve Co. a method which uses a diffusion and rotary-pump only for exhaust during baking and the simplest degassing operations like filament heating. The valve is sealed off the pump with a getter ion pump attached and operated at gradually increased ratings up to and above the desired operating conditions. The Getter Ion Pump not only absorbs and adsorbs much of the gases and vapours produced during the conditioning process but is also used to measure the pressure. This is useful for determining the rate of increase of loads applied.

The results we achieved are really most encouraging. It was my intention to present some quantitative information and also say something of the economics of the system. But for various reasons I was unable to complete the survey.

I would, however, like to sketch very briefly the Getter Ion Pump used.

This is a cheap device and is only used once for the processing of a single special valve or a number of valves on a common manifold. The Ion Pump consists of a triode system similar to the arrangement used in the Bayard and Alpert Gauge. For pumping 10 MA at 200 V are used for ionisation of the gas. Simultaneously pressure readings down to 10^{-10} Torr can be made. A Getter mirror is produced from a Zirconium wire supported by Tungsten in the following way :

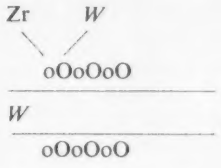

Spacing of the wire by a second *W* wire makes it possible to control the temperature accurately well above the melting point of the Zr.

Fig. 2.

The triode and the getter spiral are sealed in a glass bulb approx. 60 mm in dia. and 100 mm long connected by a glass tube of approx. 15 mm dia. to the valve to be pumped. For operating it is possible to use either a heavy mirror on the glass and the pump with the triode only or it is also possible to run the getter continuously and evaporating slowly. In the latter case it is advantageous to cool the glass bulb to counteract the heating by the getter spiral in order to prevent the release of gases which are only adsorbed on the surface of the mirror. The Getter Spiral, at temperatures above 1000 °C, not only contributes to the pumping process by producing the Zirconium Vapour, but is itself a very powerful getter for a number of gases which will be removed by a chemical action with the Zr.

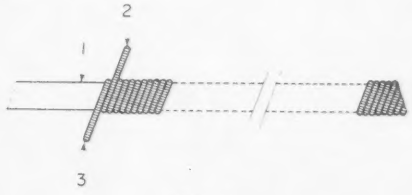

Fig. 3.

This getter has been mentioned in the recently published book " Materials and Processes of Electron Devices " by Knoll. He quotes Espersen who used the getter only following exhaust by a standard 20 l/sec Diffusion Pump.

Espersen found at pressures of the order of 10^{-6} the getter spiral three times as effective as the Diffusion Pump. Espersen, who is a member of an associated company of Mullard, used our getters for his experiments. The getter is a standard component used for about 20 years in a number of sealed off devices, sometimes continuously glowing in series with the heater. With our getter ion pump, attached to a volume of approx. 1 l., it is possible to reduce the seal off pressure from about 10^{-6} to about 10^{-8} in a few minutes. During conditioning the pressure may momentarily rise to 10^{-4}. Considering the finite conductance and the inertia of the meter reading it can be assumed that the pressure in the vicinity of the applied load will be considerably higher.

To reach pressures below 10^{-8} Torr, considerably longer times are necessary and developments are in hand to improve the performance as far as pumping speed and capacity is concerned with a device which is inexpensive to produce and also simple to operate.

Vol.
10
1960

SESSION VI

The Function of the Getters during the Manufacture and Life of the Tubes

Les Getters au Baryum dans les Tubes Electroniques de Reception

J. BAILLEUL LANGLAIS

La Radiotechnique, 51 Rue Carnot, Suresnes (Seine), France

Les deux rôles que l'on prête traditionnellement aux getters sont examinés en étudiant les variations de pression au sein d'un tube : 1—au cours du flash ; 2—au cours du traitement et de la vie de celui-ci. On montre la très grande importance du dégazage des getters sur pompe avant coupe et flash, ainsi que l'influence du chauffage, du débit et des périodes de stock sur l'évolution de la pression. Après avoir rappelé les divers modes d'absorption des gaz à chaud et à froid, quelques cas " pathologiques " accidentels sont étudiés. On indique en particulier, comment l'examen de la couleur de dépôts anormaux de baryum peut aider dans la recherche des causes de défectuosité. Quelques conclusions très pratiques sont tirées de cette étude.

1. Evolution de la pression dans un tube électronique

1. *Ce que nous demandons au getter*

Nous attendons d'un getter idéal une rétention rapide et définitive de tous les gaz susceptibles d'occuper les espaces interélectrodes d'un tube au cours de sa vie depuis le moment où il constitue un système isolé jusqu'à sa mort. Ceci, parce qu'il ne suffit pas que, dans un tube à cathode à oxydes, le libre parcours moyen des electrons soit grand en égard aux distances interélectrodes, mais parce que bon nombre de gaz sont très nocifs pour la cathode.

Notre fait est de savoir dans quelle mesure et dans quelles circonstances les getters au baryum (stabilisés à l'aluminium) satisfont à cette exigence. Tout d'abord pour mieux dégager le rôle qu'ils jouent, examinons ce qui se passerait, sans eux, dans un tube.

2. *Ce qui se passe dans un tube sans getter*

Dans le graphique ci-dessous (Fig. 1) nous montrons l'évolution de la pression au sein d'un tube dans lequel le getter n'a pas été flashé. Le pompage s'est effectué normalement et après coupe la pression est classiquement voisine de 3 ou 4.10^{-3} Torr. Elle s'abaisse légèrement en stock. Au cours de la première phase du traitement la pression croît jusqu'à devenir supérieure à 10^{-2} Torr par suite du bombardement électronique des électrodes ; néanmoins, pendant ce temps l'émission du tube croît. Par contre lors de la deuxième phase du traitement, bien que la pression s'améliore, l'émission du tube chute considérablement. Il est vraisemblable que le baryum de la cathode entre autres, sert alors de getter, ceci au détriment de l'émission. On voit ensuite que la pression dans le tube laissé en stock 200 heures environ croît : la vitesse de désorption des divers matériaux internes (verre, électrodes) devient plus grande que la vitesse d'adsorption de la cathode.

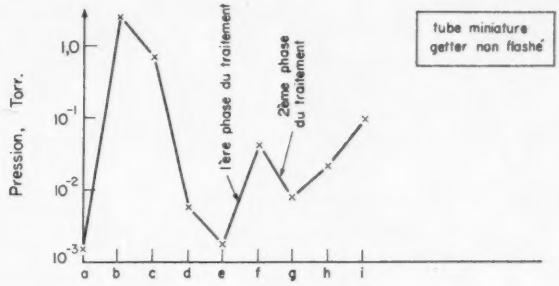

Stade a : pression dans le tube sur pompe
Stade b : pression maximum lors du chauffage haute fréquence
Stade c : pression maximum lors de la décomposition
Stade d : pression dans le tube après coupe
Stade e : pression dans le tube après 2 heures de stock
Stade f : pression maximum au cours du traitement
Stade g : pression après traitement
Stade h : pression après 190 heures de stock
Stade i : pression après 3 heures de fonctionnement.

FIG. 1.

Contrairement à ce que nous verrons par la suite avec des tubes à getter flashé, la mise en fonctionnement du tube accélère la montée en pression. L'expérience s'arrête à ce stade car le tube est d'ores et déjà hors d'usage.

3. *Description et critique de la technique de mesure de la pression*

La mesure de la pression au sein d'un tube est toujours délicate car il s'agit de choisir un instrument qui perturbe le moins possible le milieu dans lequel on l'introduit.

Nous avons utilisé le micromanomètre à thermocouple parce qu'il a pu être réalisé dans un volume réduit, parce que sa plage de fonctionnement va de quelques Torrs à 10^{-4} Torr, que le phénomène d'ionisation est exclu, et

qu'il permet de faire des mesures d'une façon continue.

Toutefois, les indications d'un tel manomètre dépendent de la nature du gaz. Bien que l'avancement des recherches permette d'avoir quelques idées sur la composition de l'atmosphère résiduelle, celle-ci n'est pas toujours la même. Nous avons préféré exprimer nos résultats avec les chiffres lus directement sur l'appareil étalonné pour l'air, sans apporter des corrections dont nous ne serions pas sûrs.

D'autre part, le schéma des montages que nous donnons ci-dessous (Fig. 2) montre que les valeurs de pression trouvées

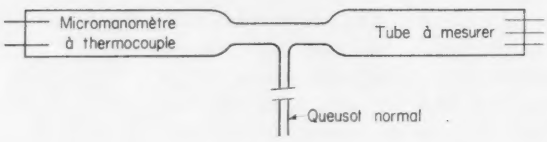

FIG. 2.

sont très certainement trop fortes car un seul getter doit assurer un bon vide dans un espace plus grand que de coutume.

Pour toutes ces raisons, nous demandons au lecteur de bien vouloir considérer que les chiffres donnés ne représentent pas des valeurs absolues de pression.

4. *Ce qui se passe au moment du flash*

Le graphique de la Fig. 3 illustre l'évolution de la pression

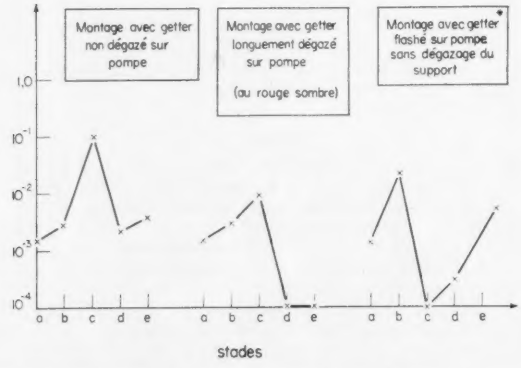

Stade a : pression dans le tube sur pompe avant flash
Stade b : pression dans le tube après coupe
Stade c : pression maximum dans le tube au moment du flash (sans bombardement)
Stade d : pression dans le tube après flash
Stade e : pression dans le tube après 120 heures de stock.

*un dégazage du support minimise la remontée de pression en stock.

FIG. 3.

au moment des flashes d'un getter dégazé sur pompe, d'un getter non dégazé sur pompe et enfin d'un getter flashé sur pompe. (Tous nos montages comportent un étuvage préalable d'une heure à 400°C du micromanomètre).

Les enseignements suivants se dégagent :

(a) Il est très profitable de dégazer (vers 650°C environ) le getter sur pompe, sinon il arrive que la pression après flash soit supérieure à la pression avant flash.

(b) L'absorption d'un getter même bien dégazé est considérablement moindre que ce que l'on croit habituellement. Elle est dans bien des cas inexistante. Le baryum à l'état de vapeur n'absorbe pratiquement que la gaz dégagé par le getter lui-même.

5. *Ce qui se passe au moment du traitement*

Nous avons schématisé dans le graphique de la Fig. 4

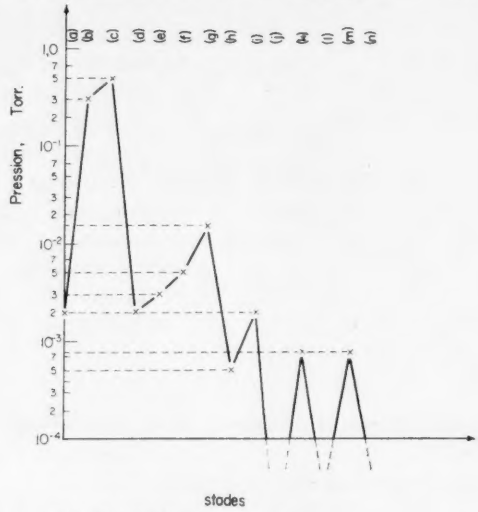

(a) *P.* sur pompe
(b) *P.* max. pendant dégazage HF
(c) *P.* max. pendant la décomposition
(d) *P.* avant coupe
(e) *P.* après coupe
(f) *P.* au bout de 20 h de stock environ
(g) *P.* max. pendant flash
(h) *P.* après flash
(i) *P.* au bout de 100 h de stock environ
(j) *P.* après traitement (Saturation et durcissage)
(k) *P.* après stock (30 heures environ)
(l) *P.* après stabilisation (200 heures)
(m) *P.* après stock (200 heures environ)
(n) *P.* après fonctionnement

FIG. 4.

l'évolution de la pression dans un tube au cours du traitement, des périodes de stock et du fonctionnement du tube. Nous pouvons tirer les conclusions ci-après :

(a) Presque toujours une période de stock amène une montée de pression. Apparemment, bien que nos expériences ne soient pas complètement terminées, ces montées de pression se manifestent de façon moins sensible au fur et à mesure que le tube a fonctionné plus longtemps.
En absence d'ionisation ou d'excitation des molécules, faut-il dire que le getter n'absorbe pas les gaz, qui adsorbés par la surface des matériaux seraient restitués même à froid ? Cette vue est sans doute trop simpliste et nous verrons dans la suite de l'exposé, quand nous ferons un rappel de l'origine des gaz résiduels que le getter peut jouer le rôle d'échangeur de gaz (voir formation des hydrocarbures parag. II, 1).

(b) Par contre, dès que le tube est mis en fonctionnement (et même lorsque le filament seul est allumé) on assiste à une descente brutale de la pression. Nous savons pourtant que les surfaces des électrodes quand elles

Vol. 10 196

sont chauffées et mieux encore quand elles sont bombardées, dégazent comme nous l'avons montré dans l'étude des tubes sans getter. L'absorption par un getter des molécules de gaz qui viennent le frapper est donc considérablement accrue quand ces dernières sont excitées ou partiellement dissociées.

2. l'Absorption des gaz par le baryum

Pour mieux comprendre les phénomènes que nous venons de décrire globalement, il est nécessaire de séparer les différents paramètres et pour celà d'étudier l'absorption des différents gaz par le baryum.

1. *Nature et origine des gaz residuels*

— Leur détermination a été entreprise relativement souvent, à l'aide d'un spectrographe de masse ou d'un omégatron, et en général, on est d'accord pour attribuer une prédominance aux hydrocarbures et à l'oxyde de carbone.

— Les hydrocarbures (méthane, acétylène...) doivent leur formation à l'action de la vapeur d'eau sur le carbone et les carbures, ou bien dans certaines conditions de température et de concentration à l'action de l'hydrogène sur le carbone.

Rappelons en particulier le processus possible de formation de l'acétylène dans un tube :

(α) $3\,Ba + 2\,CO \rightarrow BaC_2 + 2BaO$

(β) $BaC_2 + H_2O \rightarrow BaO + C_2H_2\uparrow$

SMITHELLS et RANSLEY[20] montrèrent que CO est continuellement émis à partir des éléments en Ni. Le carbone diffuse de l'intérieur du nickel à la surface et réagit alors avec de l'oxygène[11]. De semblables réactions se produiront chaque fois que de l'oxygène libre entrera en contact avec du carbone[13-18] à une température suffisamment élevée. (L'oxygène peut provenir de la décomposition d'oxydes par bombardement électronique).

— En présence de H_2, CO_2 mal évacué peut donner H_2O + CO.[15]

— CO et dans une plus faible mesure CO_2 peuvent être dus au choc des électrons sur des restes minimes de nitrocellulose qui a servi de support aux carbonates et qui a été ensuite éliminée par chauffage.

— L'hydrogène et l'argon ont été aussi détectés en proportions importantes.

— On trouve encore de l'azote (pièces en molybdène-verre) et du gaz carbonique (carbonates de baryum, de tungstène, de molybdène).

2. *Propriétés communes à tous les gaz vis-à-vis du baryum*

(α) Les quantités de gaz retenues sont supérieures à celles qui recouvriraient la surface " macroscopique " d'adsorption d'une couche monomoléculaire (V. Fig. 5).

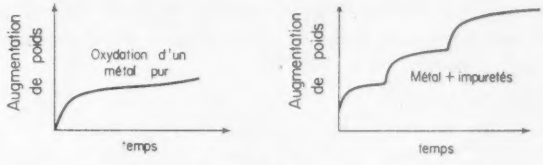

FIG. 5.

Ba Poids mol. 137,4 Vol. mol. 38 cm³	Nature des gaz	Type de courbe $Q\,f(t)$	Q (t, 20 °C) en $cm^3.\mu_{Hg}.cm^{-2}$	Nombre de couches mono-moléculaires	Composés probables : Nature	Densité	Poids moléculaire g	Volume moléculaire cm^3	Coefficient d'expansion
	CO	*I* (même allure que courbe de l'oxydation du Cr, Al, Si)	270 220[11] 624[15]	18 15 41 34[18]	Ba C_2	3,75	161,4	43	1,13
	CO_2	*I*	1 632[1] 600[15]	102 38	CO_3 Ba	4,43	197,4	44,5	1,17
			$cm^3.\mu_{Hg}.mg^{-1}$						
	H_2O	*II*	35 000[15]	436	Ba $(OH)^2$	4,5	171,4	38	1
	H_2	*III*	30 à 45 000[15]		Ba (H_2)	4,21	139,4	33	0,87
	O_2	*IV*	50 000[15]		BaO	5,72	153,4	27	0,71
			$cm^3.{}_{Hg}.mg^{-1}$						
	N_2	*III*	3 740[1] 330[15]	234 20	$Ba_3\,N_2$ ou $Ba(N_3)^2$ [15]			23[15] 76[15]	0,60 2
	$C_2\,H_2$ CH_4		Σ Σ	(sauf si décomposé par points chauds ou par électrons) (sauf si le tube est traversé par un flux électronique[22])					
	Gaz nobles (argon..)		Σ	(sauf si les atomes sont activés[21])					

NOTA : Les chiffres entre parenthèses correspondent aux références bibliographiques.

FIG. 5 (tableau).

(β) Le phénomène de pompage est *irreversible* : de nombreux essais de désorption ont été tentés sans succès[11, 12, 16]. Il ne s'agit donc pas seulement d'une physiadsorption, mais plutôt d'une chemisorption ou d'une solution du gaz absorbé dans le baryum.

(γ) Une élévation de la température du dépôt de getter conduit toujours à une augmentation de la vitesse, de la puissance d'aspiration et de la quantité totale absorbée.

3. *Essai de classification des gaz suivant leurs propriétés vis-à-vis du baryum*

Ce sont les propriétés communes α et γ qui vont nous le permettre. Il résulte de ces propriétés que : ou bien la surface " microscopique " réelle d'adsorption est plus grande que la surface apparente, ou bien il y a diffusion dans la masse du dépôt de baryum, déjà à la température ordinaire, puisqu'elle existe vraisemblablement à une température plus élevée. Le graphique 6 rassemble les types de courbes le plus souvent trouvées donnant la puissance d'aspiration Q en fonction du temps d'un dépôt de baryum aussi pur que possible vis-à-vis de différents gaz. Pour ces mêmes gaz, nous groupons dans le tableau (Fig. 5) quelques données. (La méthode de mesure du pompage d'un getter a été examinée dans une communication du 1er Congrès des Techniques du Vide à Namur en juin 1958).

(α) *Groupe CO–CO_2*

Leur courbe $Qf(t)$ est du type I (Voir graphique de la Fig. 6) : La puissance d'aspiration assez élevée au départ

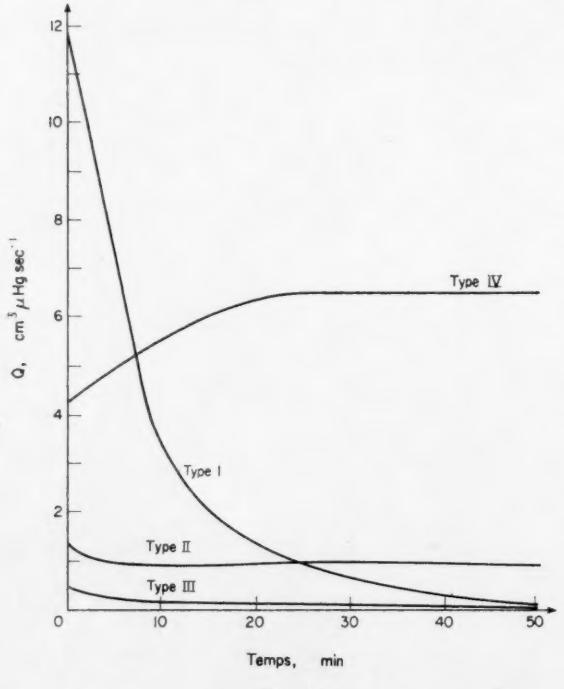

FIG. 6.

décroît rapidement pour s'annuler après une durée d'adsorption d'environ 1 heure. Cette courbe a même allure que les courbes d'oxydation de Cr, Al, et de Si. Ces résultats conduisent à l'hypothèse suivante : le composé formé " empoisonne " le getter en donnant une couche superficielle, imperméable aux gaz (aux oxydes en question et également aux gaz d'autre nature). Le fait que les composés probables présentent un coefficient d'expansion supérieur à 1 étaye cette hypothèse. Malgré cela, il n'est pas étonnant que l'adsorption totale représente plusieurs couches monomoléculaires : on sait qu'à l'échelle submicroscopique, la moindre rugosité rend la surface réelle des dizaines et même des centaines de fois supérieure à la surface apparente. Une très intéressante étude des surfaces de dépôt de getter, à l'aide d'un microscope électronique, a été menée par J. J. B. Fransen et H. J. R. Perdijk[3]. Ces auteurs ont montré que la surface du getter est constituée par un assemblage de grains ayant un diamètre d'environ $5/100\mu$.

(β) *Groupe H_2O, H_2, O_2*

Leur courbe $Qf(t)$ est du type II, III, IV. La partie horizontale de ces courbes est caractéristique des couches poreuses. Le pompage peut durer plusieurs heures sans qu'il y ait d'effet d'empoisonnement du getter. Il est remarquable qu'alors le coefficient d'expansion des composés probables est inférieur ou égal à 1. Les molécules de gaz frappant le dépôt peuvent pénétrer plus facilement à l'intérieur de ce dernier. La quantité totale de gaz retenu est très élevée.

(γ) *L'azote*

Les résultats trouvés ne sont guère reproductibles. Peut-être y a t-il plusieurs composés possibles. Il n'est du reste pas certain que de nouveuax composés soient formés, l'absorption peut être due à une solubilité du gaz dans le réseau de Ba.

Dans tous les cas, sans qu'il y ait " empoisonnement ", la vitesse est très faible. D'après Wagener, ce gaz serait adsorbé sous forme atomique alors que CO le serait sous forme moléculaire[12-bis].

(δ) *Les hydrocarbures* (surtout l'acétylène) ont la réputation de ne pas être retenus par le baryum, sauf s'ils sont décomposés par un courant électrique ou par des points chauds dans le tube.

(ε) *Les gaz rares*

L'absorption de l'argon est réputée négligeable à moins que les atomes soient activés[22].

La classification ci-dessus est encore valable si l'on compare la faculté de condensation de ces gaz vis-à-vis de la probabilité de condensation calculée pour chacun d'eux, sachant que le nombre de molécules frappant une surface d'un cm² par seconde est :

$$\gamma = \tfrac{1}{4} n\, Vm$$

Avec n : nombre de molécules contenues dans 1 cm³ de gaz à la pression p.

Vm : vitesse moyenne des molécules correspondant à leur température T.

Si S est la vitesse d'aspiration, le nombre de molécules adsorbées est $S.n$.

Si toutes les molécules frappant la surface étaient retenues, on devrait avoir :

$$Sn = \tfrac{1}{4} n\, Vm \quad \text{ou} \quad S = \tfrac{1}{4} Vm = \tfrac{1}{4}\sqrt{\frac{8RT}{M}} = 3630\sqrt{\frac{T}{M}}$$

Vol. 10 196

d'où le tableau suivant si l'on prend $T = 300°K$ (Fig. 7). (On remarquera que la vitesse initiale théorique est indépendante de la pression, qu'elle dépend de la température et de la nature du gaz).

Gaz	*Sc* vitesse initiale théorique calculée	*Sm* vitesse initiale mesurée (12)	$\frac{Sm}{Sc}$
CO	11 850	5 000	0,4
CO_2	9 500	5 000	0,6
O_2	11 100	300	0,02
H_2	44 500	50	0,001
N_2	11 850	1	0,0003

FIG. 7.

les valeurs de l'absorption totale à diverses températures. Ces chiffres nous permettent de classer les gaz comme précédemment.

D'une part, les gaz " empoisonneurs " du getter à la température ordinaire diffusent à l'intérieur du dépôt et l'absorption totale croît considérablement. D'après Bloomer[23] l'empoisonnement cesse pour CO à partir de 80°C. D'autre part, les gaz du groupe H_2O–H_2–O_2 ont une absorption qui croît dans des proportions tout à fait comparables à celles dans lesquelles croissent les valeurs de probabilité de chocs en fonction de la racine carrée de la température comme nous l'avons vu plus haut.

L'azote se distingue encore par l'anarchie dans les différents résultats.

Nature du gaz	$\frac{Q(t,100°C)}{Q(t,\ 20°C)}$	$\frac{Q(t,200°C)}{Q(t,\ 20°C)}$	$\frac{Q(t,300°C)}{Q(t,\ 20°C)}$	$\frac{Q(t,400°C)}{Q(t,\ 20°C)}$	Couleur du dépôt	
					Absorption à 20°C	Absorption à plus de 300°C
CO[16]	5,5	6,1	12,5	13,9	inchangé	Brun[16, 13]
" [12]	2	7	30			
CO_2[16]	3,3	5,5	9,7	11	inchangé	Brun rosé
" [1]				5,6		
H_2O[16]			2		inchangé	Rouge brun transparent
H_2[16]		1,22	2	2,2		Brun très transparent[16]
O_2[16]			1,14			Blanc laiteux
N_2[16]	1,45	10,3	15	15,5	inchangé (couche légèrement plus transparente)	Brique
" [12] bis		6				
" [1]				1,5		
Valeurs calculées d'après la probabilité de chocs	1,16	1,27	1,4	1,51		

FIG. 8.

Si l'on considère la relation d'Arrhenius qui permet de définir l'énergie d'activation E d'une réaction

$$Sm = exp. - \frac{E}{RT}$$

(*Sm* étant la vitesse réelle de la réaction dans des conditions données, c'est en quelque sorte un facteur de probabilité

R est la constante des gaz parfaits

T est la température absolue).

On voit que l'on trouve des valeurs de *E* particulièrement élevées pour H_2 et N_2, ce qui nous incline à penser que H_2 et N_2 sont absorbés sous forme atomique (une partie de l'énergie d'activation nécessaire à la réaction étant utilisée pour dissocier les molécules).

4. *Influence de la temperature*

(*a*) Le tableau ci-dessus (Fig. 8) donne les rapports entre

Nous avons également porté dans ce tableau un certain nombre de couleurs de dépôts caractéristiques illustrées par les photographies des Figs. 9, 10, 11.

La photographie de la Fig. 10 nous permet de comparer une éprouvette provenant d'un essai quantitatif d'absorption d'azote par le baryum à chaud (300°C) et un tube présentant un flash anormal de même couleur brique.

La photographie 11 nous donne avec le tube de plus grande taille un getter flashé vraisemblablement en présence d'oxygène.

Le tube de petite taille semble ne pas avoir été flashé. Or ce tube après avoir terminé ces essais de durée (1100 h) était parfaitement bon : il est probable dans ce cas que l'hydrogène ait été le principal constituant de l'atmosphère résiduelle.

La photographie de la Fig. 9 montre une comparaison intéressante entre une éprouvette qui a servi à des essais quantitatifs d'absorption de CO^2 par le baryum à chaud

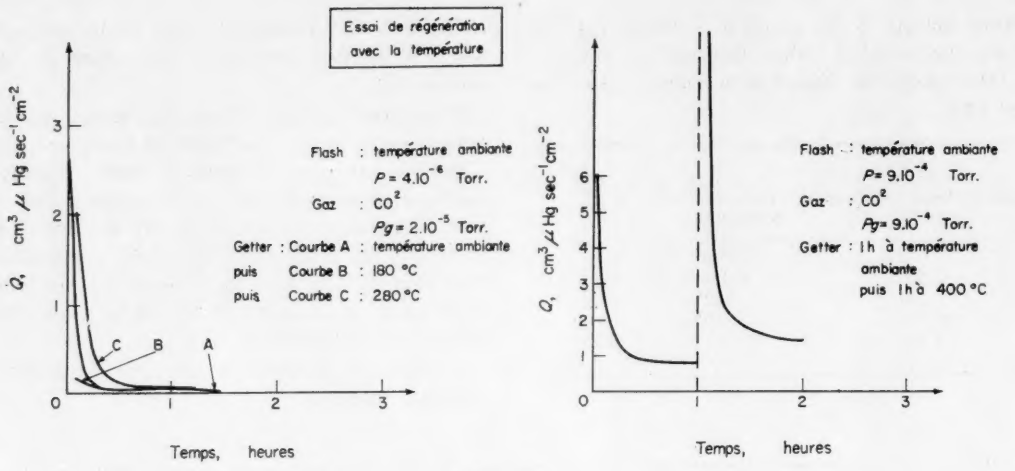
Essai de régénération avec la température
Flash : température ambiante
P = 4.10⁻⁶ Torr.
Gaz : CO²
Pg = 2.10⁻⁵ Torr.
Getter : Courbe A : température ambiante
puis Courbe B : 180 °C
puis Courbe C : 280 °C
Q, cm³ μ Hg sec⁻¹ cm⁻²
C
B
A
Temps, heures
Flash : température ambiante
P = 9.10⁻⁴ Torr.
Gaz : CO²
Pg = 9.10⁻⁴ Torr.
Getter : 1h à température ambiante
puis 1h à 400 °C
Q, cm³ μ Hg sec⁻¹ cm⁻²
Temps, heures

FIG. 12.

(300 °C) et un tube présentant un flash accidentellement défectueux.

(β) Essai de régénération d'un dépôt de Ba par élévation de la température

Le graphique de la Fig. 12 donne deux exemples de régénération de la puissance d'aspiration du gaz carbonique d'un getter, dans des conditions très différentes. Cette régénération apparaît d'autant plus spectaculaire que la température est plus élevée (jusqu'à 400 °C).

3. Consequences pratiques

1. *Flasher le plus rapidement possible après coupe*

Nous avons vu (paragraphe 1, 2) qu'entre la coupe et le flash, la pression s'abaisse le plus souvent en début de stock. La cathode, déjà quelque peu formée sur pompe, absorbe probablement une large partie des gaz disparaissant. A l'exception de quelques cas particuliers mal expliqués, il est meilleur de flasher dès que possible à la sortie de pompe.

2. *Attendre pour flasher que les ampoules soient froides*

Refroidir les dômes d'ampoules par un jet d'air soufflé au moment du flash. Si un tube ne désorbe que des gaz qui n'empoisonnent pas le getter, celui-ci va jouer son rôle très longtemps, nous n'en voulons pour preuve que l'exemple de ce tube qui, après 1100 heures de durée, avait presque perdu la trace de son getter mais qui était parfaitement bon.

Néanmoins, comment absorber au mieux les empoisonneurs ?

Leur absorption étant un phénomène de surface, il y a intérêt à ce que la surface du dépôt exposée aux gaz soit la plus grande possible : la surface apparente du dépôt étant imposée, il faut une surface réelle très importante.

Fransen et Perdijk[3] pensent qu'il est impossible de dégazer complètement le support du getter et qu'en conséquence le baryum ne peut s'échapper sous sa forme atomique, mais qu'il constitue plutôt une brume composée de fines gouttelettes qui se condensent sous forme de petits grains sur le verre. Ces grains s'agglomèrent d'autant moins pour donner une surface réelle d'autant plus grande que la température du verre de l'ampoule est plus basse. Ces auteurs ont montré également qu'un dépôt extrêmement fin et divisé donne une absorption totale pour CO très élevée. Une application de ce fait est très connue : c'est le flash sous une pression d'argon de quelques Torrs pour obtenir un dépôt très absorbant à surface " microscopique " élevée[2, 3]. Le dépôt dans ce cas est noir mat alors qu'il est brillant quand le getter est flashé sous bon vide[4, 9, 11].

3. *Adopter un temps de flash aussi court que possible*

Cela évitera au dépôt de trop s'échauffer, au support de baryum de trop dégazer et même de se volatiliser, ce qui est un défaut assez fréquent. La photographie de la Fig. 13 nous montre comment se manifeste ce défaut. Une entrée d'air pratiquée dans un tube a fait que le dépôt de baryum s'est oxydé comme de coutume, mais que la partie inférieure du dépôt (que rien ne distinguait à l'oeil avant l'entrée d'air) demeure parfaitement noire indéfiniment. Un examen microscopique montre que ce dépôt tout en s'atténuant descend bas le long du tube. Ceci est tout à fait défavorable du point de vue des isolements dans le tube. La photographie 14 prouve que ce défaut peut être prononcé à un tel point qu'il empêche le getter de " blanchir " lorsque celui-ci a été mis à l'air. Il s'est formé une espèce de couche imperméable aux gaz même à la pression atmosphérique.

Sous vide, le getter était complètement empoisonné par cette couche métallique. Des macrographies (empreintes obtenues par voie chimique) ont révélé la présence de fer (matériau support du getter).

Un autre aspect que peut prendre le dépôt du getter flashé trop fort nous est indiqué par la Fig. 15. Le dépôt est bleu métallique (alliage fer-baryum vraisemblablement). Dans ce cas le support du getter a l'aspect photographié (Fig. 16).

4. *Disposer le getter aussi loin que possible du verre de l'ampoule*

Ceci évitera une augmentation trop importante de la température du verre, provoquée par le rayonnement des pièces chauffées par induction.

Vol. 10 1960

FIG. 9

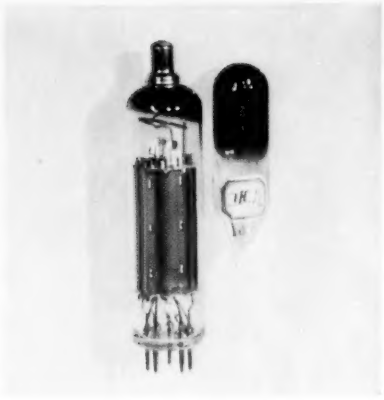

FIG. 10.

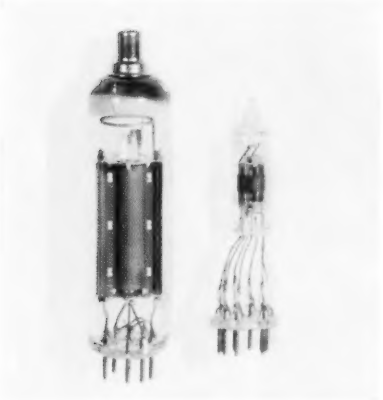

FIG. 11.

ol.
10
960

FIG. 13.

FIG. 14.

FIG. 15.

FIG. 16

Vol.
10
1960

5. *Disposer le getter aussi loin que possible des pièces pouvant être le siège d'une induction lors du flash*

Ceci évitera de dégazer dangereusement ces pièces.

Ce n'est pas une bonne chose en particulier de monter un getter sur un écran. Chaque fois que l'on pourra le faire, il sera préférable de le placer sur une tige. Toutefois, il existe des cas où ce n'est pas possible d'agir ainsi : on est alors obligé de flasher sur pompe.

6. *Traiter le tube le plus rapidement possible après flash*

Nous avons dit qu'une période de stock amenait presque toujours une montée de la pression même après flash et que l'ionisation et l'excitation thermique des molécules mettaient en oeuvre le getter. Il y a donc intérêt pour ne pas empoisonner la cathode à traiter le tube immédiatement après flash afin que le getter " absorbe ".

7. *Ménager le plus possible de grands trous dans les micas supérieurs* pour laisser libre passage aux gaz.

8. *Conserver le getter dans une boîte bien fermée* plutôt que sous vide, sans *précautions spéciales* : le pompage produisant une détente qui condense la vapeur d'eau.

9. *Ne pas toucher avec les doigts* tous les getters comportant dans leur support des éléments en fer. Le chlorure de fer formé sera évaporé pendant le flash, ce qui conduit à une précipitation du fer sur l'ampoule aussi bien que sur le mica supérieur.

10. *Peut-on régénérer un getter empoisonné dans un tube ?*

— On peut reflasher le getter : celà conduit souvent à des résultats satisfaisants si l'on ne va pas jusqu'à couper le getter.

— La régénération par chauffage du getter dans un tube conduit très rarement à un bon résultat (nous avons eu en Laboratoire une réussite sur 10 environ) car il est très difficile de chauffer seul le getter : une amélioration du vide dans le tube ne peut se produire que si le tube est " bien pompé ". Or, deux causes (concomitantes ou non) font qu'un tube est " mal pompé " :

(1) pompage insuffisant

(2) mauvais dégazage des électrodes et des isolants.

Rappelons ici que lorsque le volume des anodes est faible par rapport à la grandeur du tube, leur chauffage ne suffit pas pour dégazer correctement les micas ; il faut compenser par un étuvage plus soigné de ceux-ci.

11. *Remarque*

Du fait de l'existence de gaz qui empoisonnent un getter, celui-ci peut se révéler efficace ou non suivant l'ordre de désorption des gaz à partir des électrodes d'un tube ; par exemple : si un gaz " empoisonneur " se désorbe le premier ou a été mal pompé lors de la fabrication du tube, le getter sera vite hors de service. Le fait qu'en fonctionnement l'ampoule d'un tube soit à une température élevée (150 °C par exemple) est favorable du point de vue du getter.

4. Conclusion et perspectives d'avenir

Chacun sait qu'actuellement, on emploie, lors de la fabrication des getters, non pas du baryum, mais un alliage de baryum-aluminium stable à l'air : le $BaAl_4$. Lors de la volatilisation, seul le baryum s'échappe, l'aluminium s'alliant au métal support.

Nous avons vu que la structure du film de baryum est une structure granuleuse et que l'aptitude à l'absorption d'un getter est d'autant plus grande que la surface réelle du dépôt est plus grande, autrement dit que les imperfections du réseau cristallin (lacunes, joints de grains) sont plus grandes.

Nous pouvons donc imaginer le parti à tirer de l'adjonction d'impuretés ou d'additions bien choisies.

Certaines impuretés sont des véhiculeurs de gaz. Le soufre, le phosphore, l'antimoine dans les aciers par exemple véhiculent l'hydrogène, celui-ci n'étant pas soluble dans les métaux sous forme moléculaire : il se forme un hydrure capable de diffuser.

On connait aussi le cas d'impuretés causes de " claquages " dans certains phénomènes d'oxydation à couche d'oxyde protecteur.

La " corrosion " (ce mot étant pris dans son sens le plus large comme étant le phénomène général de l'altération de tout matériau) physico-chimique que nous recherchons dans l'utilisation des getters pourrait être fortement préparée par une corrosion purement métallurgique tant sont liés les phénomènes de corrosion physico-chimique et ceux de cohésion des grains métalliques.

Expliquons-nous :

Les métallurgistes savent combien dangereuse peut être une ségrégation anormale des impuretés aux joints des grains : une précipitation de composés à partir d'une solution solide provoquant une véritable " décohésion " des grains. Or, toute imperfection de structure ouvre une large porte à la corrosion physico-chimique.

Il n'est donc pas impensable de posséder un jour un getter dont le dépôt suffisamment divisé ne connaitra plus de gaz " empoisonneurs ".

Bibliographie

[1] J. Bailleul-Langlais ; *Essais quantitatifs de getters, Congrès de Namur* 1958.

[2] J. Morisson and R. Zetterstrom ; *Barium getters in Carbon Monoxide, J.O.A.P.*, 437–442 (Avril 1955).

[3] J. J. B. Fransen and H. J. R. Perdijk ; *Barium Getters Films, Philips Tech. Rev.* **19**, 290–300 (1957/8).

[4] S. Wagener ; *A Method for Measuring the Efficiency of Getters at Low Pressures, Brit. J. Appl. Phys.*, 225–231 (1950).

[5] A. Klopfer, S. Garbe, and W. Schmidt ; *Residual Gases in Vacuum Systems*, Communication au Symposium de Côme (Septembre 1959).

[6] J. A. Becker ; *Use of Getters for Ultra High Vacua, 11th Annual Conference on Physical Electronics*, (29-30-31 Mars 1951-MIT).

[7] R. Wild ; *Les Getters et Leur Emploi, Le Vide*, 252–257 (Mai 1947).

[8] S. Wagener ; *Efficiency and Mechanism of Barium Getters at Low Pressures, Brit. J. Appl. Phys.*, 132–138 (1951).

[9] S. Wagener ; *The Production of Very High Vacua by the Use of Getters, Proc. Inst. Electr. Engrs.* Part III G.B., **99**, 135–147, (1952).

[10] S. Wagener ; *Influence of Electronic impact on the Rate of Sorption of Gases on to Getter Materials, Nature* **173**, No. 4 (1954).

[11] S. Wagener ; *The Use of Getters for the Production of Very High Vacua, Vacuum* **3**, 11–23 (1953 paru 1954).

[12] S. Wagener ; *Adsorption Measurements at Very Low Pressures*, I, *J. Phys. Chem. U.S.A.* **60**, 567 (1956 ; II, **61**, 267–271 (1957).

[13] R. N. Bloomer ; *Barium Getters and Carbon Monoxide, Brit. J. Appl. Phys.* **8**, 352–355 (1957).

[14] R. N. Bloomer ; *Absorption of Oxygen and Carbon Monoxide by Barium Alloy Getters, Nature* **178**, No. 4540, 1000–1001 (1956).

[15] P. della Porta ; *Performance Characteristics of Barium Getters, Vacuum*, **4**, No. 3 (July 1954).

[16] P. della Porta ; *Performance Characteristics of Barium Getters at Elevated Working Temperature of the Valves, Vacuum* **4**, No. 4 (Oct. 1954).
[17] R. N. Bloomer ; *Barium Getters and Oxygen, Brit. J. Appl. Phys.* **8**, 40–43 (1957).
[18] H. J. R. Perdijk ; *Miroirs de Getter de Baryum, Rev. Tech. Philips*, No. 10, 328–339.
[19] R. N. Bloomer and M. E. Hame ; *The Electronic Clean-up of Gases in Sealed-off Vacuum Systems, Vacuum* **3**, 128–135 (Avril 1953).
[20] Smithells and Ransley ; *Degassing of Ni and the Diffusion of CO through Ni, Proc. Roy. Soc. A* **155**, 195–212 (1936).
[21] J. Peper ; *Analyse à l'Aide de l'Omégatron des Gaz Contenus dans des Tubes Cathodiques Scellés, Rev. Tech. Philips* **19**, 275–277 (1957–8).
[22] A. W. Cloud, L. Beckman, and J. G. Trump ; *Barium Absorption Pumps for High-Vacuum Systems, Rev. Sci. Instrum.* **28**, 889 (Nov. 1957).
[23] R. N. Bloomer ; *Reaction of Carbon Monoxide with Evaporated Barium Film, Nature*, 249–250 (August 3, 1957).
[24] S. J. Stoll ; *Origin and Analysis of Gas in Electron Tubes, Brit. J. Appl. Phys.* **7**, No. 3 (1956).
[25] I. Arizumi and S. Kotani ; *On the Oxidation of the Evaporated Barium Film, J. Phys. Soc. Japan* **5**, 70–75 (1950).
— *Absorption of Carbon Monoxide by the Barium Getters, J. Phys. Soc. Japan.*
[26] Part I, *Experiments at Low Temperature*, **7**, 152–158 (1952).
[27] Part II, *Theory of Absorption*, **7**, 158–163 (1952).
[28] Part III, *Lattice Imperfections*, **7**, 163–166 (1952).
[29] Part IV, *Absorption Experiments in the Temperature Range between 0 °C and 250 °C*, **7**, 415–420 (1952).
[30] Part V, *Theory of Absorption*, **7**, 422–426 (1952).
[31] I. Arizumi and S. Kotani ; *Gettering Process of Barium—Sorption Properties of Oxygen to Barium, J. Phys. Soc. Japan* **7**, 300–307 (1952).
[32] Y. Mizushima, Z. Oda, and O. Ochi ; *The Structure of Evaporated Barium Films, J. Phys. Soc. Japan* **12**, 355–368 (April 1957).
[33] Z. Oda ; *Kinetic Study of Gas Adsorption on Evaporated Metal Films, Elect. Communic. Lab. Japan* **6**, 71–77 (March 1958).
[34] R. Gomer ; *Surface Diffusion of CO on W, J. Chem. Phys. U.S.A.* **28**, 168 (1958).
[35] L. Beckman ; *Investigation of a Barium Vacuum Getter Pump, Ark. Fys. Sverige* **13**, 255–256 (1958).
[36] L. Holland ; *The Effect of Gettering on the Reflectivity of Aluminium Films, Brit. J. Appl. Phys.* **9**, 336–337 (1958).
[37] Y. Tuzi and H. Okamoto ; *Surface Area Variation of Evaporated Barium Film by Oxidation, J. Phys. Soc. Japan* **13**, 225 (1958).
[38] G. Ehrlich, T. W. Hickmott, and E. B. Hudda ; *On the Low Temperature Chemisorption of N_2 and CO, J. Chem. Phys. U.S.A.* **28**, 506–507 (1958).
[39] J. A. Becker ; *Some Adsorption and Field Emission Effects for Oxygen on Tungsten*, Field Emission Symposium S.I.N.D.—27.5/21.4.
[40] M. J. D. Low ; *Enhanced Surface Reactions—Oxygen Adsorption on Several Metals, J. Electrochem. Soc. U.S.A.* **105**, 103–105 (1958).
[41] J. Benard, J. Moreau, F. Gronlund ; *Nouvelles Recherches sur la Microstructure des Surfaces Métalliques dans les Atmosphères Faiblement Oxydantes*, Colloque national sur la chimie des hautes températures, Paris 1957—CNRS 1957, 27/22, p. 10–11.
[42] J. Eisinger ; *Electrical Properties of Nitrogen Adsorbed on Tungsten, J. Chem. Phys. U.S.A.* **28**, 165–166 (1958).
[43] P. della Porta ; *The Gettering Process in Modern Receiving Valve Manufacture, Vacuum* **6-8**, 41–58 (1956–1958).
[44] T. H. Briggs ; *Continuous Getters for Electron Tubes, Proc. of the Third National Conf. Tubes Techniques*, p. 117–123 (Sept. 1956).
[45] Rehkopf ; *Measurements of Gas Evolution or Sorption of Anode Materials under Simulated Life Conditions, Sylvania Tech.* **9**, 114–116 (Oct. 1958).
[46] K. Blodgett ; *Clean-up of Atomic Hydrogen, J. Chem. Phys.* **29**, (July 1958).
[47] L. S. Nergaard ; *Thermionic Emitters, R.C.A. Review*, 199–204 (June 1959).
[48] N. W. Robinson ; *Some Vacuum Problems in the Valve Industry, Vacuum* **6-8**, 21–40 (1956–1958).

Vol.
10
1960

On the Use of Getters in TV Cathode-ray Tubes

ELIE BIOLLEY

Le Cathoscope Français, Lyon, France

Since some years, to increase the pictures brightness, the Kinescopes have been aluminized. But the unavoidable heavy aluminium thickness in the centre of the screen is visible, as dark centre, at low ultor voltage. For this reason, the minimum operating voltage is indicated on each type data. It is however easy for the Kinescopes manufacturer to remain in the allowed limits taking account that the Getter Baryum layer, which has a higher atomic mass, is more opacious than the aluminium film and can increase the defect occasioned by the bad uniformity of this one, affecting the colour uniformity of the screen at low ultor voltage. It appears convenient to direct, during the getter flash the Baryum molecules, in order to see they deposit out of the screen area. A good solution has been found by the S.A.E.S. who supply a ring getter with very efficient deflector. The rational use of this getter introduces special cautions, otherwise the new getter type will be worse than the old one. During this communication, some test results will be given illustrating perfectly this theory.

Les difficultés rencontrées au cours de la recherche d'une meilleure uniformité de couleur des écrans de tubes cathodiques de Télévision dans le cas de l'utilisation à tension d'alimentation réduite, ont amené Le Cathoscope Français à étudier particulièrement l'influence du dépôt métallique provenant de la vaporisation du baryum getter.

Sans que cela paraisse absolument nécessaire pour la majorité de l'auditoire, nous rappellerons que la couche mince et poreuse d'aluminium déposée sur la face interne de l'écran, dans le but d'en accroître sensiblement sa brillance (70 pour cent environ), est opaque aux ions à cause de leur volume, et opaque à certains électrons dont la vitesse est insuffisante pour assurer leur pénétration.

Ce film d'aluminium obtenu par vaporisation sous vide protège la matière luminescente de l'écran contre les brûlures ioniques qui ne manquent pas d'apparaître, après de nombreuses heures de fonctionnement sur les écrans de tubes non aluminisés et même munis de " piège à ions ". L'opacité de cette couche d'aluminium (poids atomique = 27) est, pour une tension anodique d'accélération donnée, fonction de son épaisseur. Mais, dans un type de tube cathodique déterminé, muni d'un canon droit, sans " piège à ions ", alimenté sous 16 KV par exemple, si cette couche est suffisante pour arrêter les ions négatifs accélérés électrostatiquement, elle risque d'être trop épaisse, arrêtant de ce fait une partie des électrons devant exciter le luminophore.

En conséquence, il convient de lui donner une épaisseur convenable dont la mesure, à travers l'épaisseur de la dalle de verre supportant l'écran, est facile. Ceci est aisé à obtenir en production de série par arrêt automatique de la vaporisation.

Or, si l'on est certain de pouvoir contrôler le phénomène en un point de l'écran (au centre généralement), il est difficile d'obtenir la même épaisseur dans les angles. En effet, le vide est suffisant pour que le libre parcours moyen des molécules d'aluminium soit assez grand et que leur déplacement ait lieu en ligne droite, et il est malaisé d'obtenir une excellente répartition du film d'aluminium ; ceci conduit généralement les Fabricants à surcharger, malgré l'utilisation de caches répartiteurs, le centre de l'écran afin que les angles soient suffisamment protégés, compte tenu de la transformation dans les angles d'une partie de cette couche au cours des traitements de recuisson effectués sur l'ampoule. Au cours de ces traitements, une partie du film d'aluminium se transforme en silico-aluminate non détectable puisque transparent et non conducteur. Dans le but d'illustrer ce qui précède, nous avons reporté dans le tableau ci-dessous quelques résultats de mesures effectuées au Cathoscope Français à Lyon.

Type d'Ampouie	Epaisseur de la Couche d'Aluminium après Vaporisation		Epaisseur de la Couche d'Aluminium après Recuisson	
	Au Centre	Dans les Angles	Au Centre	Dans les Angles
21″ 90°	1.800 A°	750 A°	1.800 A°	700 A°
17″ 90°	1.400 A°	730 A°	1.400 A°	670 A°
21″ 110°	2.000 A°	700 A°	2.000 A°	650 A°
17″ 110°	2.400 A°	700 A°	2.400 A°	650 A°

De la lecture du tableau ci-dessus, il ressort que la couche d'aluminium est toujours plus épaisse au centre de l'écran que dans les angles, en particulier sur les tubes à grand angle de déflexion et principalement sur ceux de faibles dimensions, le point de vaporisation se trouvant nécessairement en dehors du col et par conséquent peu éloigné de la face.

Cette imperfection est visible à tension anodique réduite, la zone de surépaisseur apparaissant plus sombre que le

reste de l'écran. La quantité d'électrons parvenant à traverser la couche centrale d'aluminium pour exciter le luminophore se trouve nécessairement réduite. Ceci étant admis, il convient simplement que la zone centrale sombre n'apparaisse qu'en dessous d'une certaine valeur de la tension anodique fixée au titre de limite inférieure pour l'utilisation du tube cathodique.

Cette limite étant fixée compte tenu des exigences d'utilisation et de fabrication, il y a lieu pour y satisfaire de s'assurer d'une bonne répartition du baryum getter.

En effet, le baryum métal vaporisé par chauffage haute-fréquence de l'alliage Baryum-Aluminium devant, pour être efficace, recouvrir la plus grande surface possible de l'enceinte vidée, viendra, si aucune précaution particulière n'est prise, se déposer surtout sur la face de l'écran. L'épaisseur du dépôt sera maximum au centre, car l'anneau getter étant situé plus bas dans le col de l'ampoule que ne l'était la source d'aluminium au moment de la préparation de l'écran, les parois du col réduisent l'angle de vaporisation.

Or, ce dépôt de baryum (poids atomique = 137), dont on peut mesurer l'épaisseur, est très opaque au passage des électrons et vient accentuer, à tension anodique réduite, l'assombrissement de la zone centrale de l'écran. La meilleure façon d'apprécier l'influence de ce dépôt, en complément de la mesure de son épaisseur, consiste à noter la valeur de la tension anodique pour laquelle on commence à apercevoir le centre sombre de l'écran.

Nous indiquons, ci-dessous, les valeurs de cette tension pour différents types de tubes cathodiques de Télévision relevées avant et après vaporisation du baryum.

Type de Tube	Tension d'Apparition de Centre Sombre		Epaisseur de la Couche de Ba au Centre
	Avant Vaporisation du Getter	Après Vaporisation du Getter SAES Ø = 18 mm sans déflecteur	
21″ 90°	7,5 kV	8,5 kV	200 A°
17″ 90°	6,5 kV	8 kV	300 A°
21″ 110°	8 kV	9,5 kV	300 A°
17″ 110°	9 kV	12 kV	600 A°

Ces chiffres montrent combien la présence du dépôt métallique de baryum sur l'écran vient accentuer l'effet de la mauvaise répartition du film d'aluminium.

Le Fabricant de tubes cathodiques se voit donc contraint de diriger la vaporisation par l'emploi d'un déflecteur placé au-dessus de l'anneau de getter et laissant libre le passage du pinceau électronique durant sa déviation verticale et horizontale. Cette dernière condition rend la fabrication et la mise en place d'un tel dispositif assez délicate. Aussi, la S.A.E.S. très au courant de ce problème a-t-elle eu l'idée de réaliser un type de getter annulaire avec déflecteur donnant sur ce point entière satisfaction, comme le montrent les chiffres indiqués dans le tableau ci-dessous.

Type de Tube	Tension d'Apparition du Centre Sombre		Epaisseur de la Couche de Ba au Centre
	Avant Vaporisation du Getter	Après Vaporisation du Getter SAES Ø = 18 mm avec déflecteur interne	
21″ 90°	7,5 kV	7,5 kV	0
17″ 90°	6,5 kV	7 kV	100 A°
21″ 110°	8 kV	8,5 kV	100 A°
17″ 110°	9 kV	11,5 kV	500 A°

On notera l'avantage de l'utilisation du getter avec déflecteur, qui doit toutefois être employé avec prudence. En effet, la présence du déflecteur dirigeant la vaporisation de telle façon que la majeure partie du dépôt de baryum prenne place sur la partie conique de l'ampoule, favorisera la turbulance et une faible partie du baryum ne manquera pas de pénétrer à l'intérieur du canon accédant ainsi aux isolateurs sur lesquels sont fixées les différentes électrodes qui sont à des potentiels très différents. Comme entre les deux groupes d'électrodes constituant la lentille de concentration apparait intégralement la haute tension reportée entre leurs points de fixation assez rapprochés sur les isolateurs—en particulier dans les canons utilisés dans la fabrication des tubes cathodiques de Télévision à col très court—on notera l'apparition d'arcs en cours de fonctionnement et de conductibilités donnant généralement naissance à une émission parasite vagabonde du fait qu'elle prend naissance au-delà de l'électride de contrôle.

Le Fabricant de tubes cathodiques dispose de moyens d'étincelage valables pour détruire ces dépôts inattendus de baryum qu'il est parfois fort difficile d'éviter. Néanmoins, préfère-t-il généralement s'en protéger en adaptant la forme, la dimension des ouvertures et la disposition des électrodes de concentration afin d'éviter que le baryum n'aille se déposer sur les barrettes d'assemblages sous l'action du déflecteur indispensable.

Nous pensons avoir ainsi montré que la solution au problème ardu de l'emploi d'un getter dans les tubes cathodiques de Télévision est suffisamment malaisée pour que l'on puisse, au cours de ce Symposium International, y consacrer quelques instants afin d'attirer l'attention des participants que je remercie d'avoir bien voulu me suivre au cours de ces exposé.

Vol. 10 196

Clean Up of Gases in TV Picture Tubes by Barium Getters

HISAO TAKAYAMA and HIDEKI KOBAYASHI

Electron Tube Division, Nippon Electric Co. Ltd., Tokyo, Japan

In this brief communication the authors present the comparative results obtained in television tubes where getters of Japanese and Italian production have been used. The measurements are carried out using the electron gun of the tube as an ionization gauge and applying the well known "gas ratio" technique normally used for pressure measurements in picture tubes. The various types of gases employed are introduced into the tube by breaking an ampoule containing a known quantity of the gas in question, which has been placed within the tube prior to its sealing. Data is given about the influence of the various gases employed on the emission from the cathode, as well as on the behaviour of the barium film after sorption of the different gases.

1. Introduction

Gettering actions have been studied by the constant volume method for the practical evaluation of barium getters in TV picture tubes. The quality of a getter is usually expressed by its gettering rate and absorption capacity. But the valve manufacturer is interested in the practical use of a getter inside, for example, TV picture tubes.

2. Experimental procedures

The authors attempted to get some information on the practical performance of barium getters, evaporated in the picture tube, type 14RP4A. Two types of barium getters were used, one of which (hereinafter called *A*) is a barium-aluminium alloy and contains more than 85 mg of barium, the other (hereinafter called *B*) is type St15/0/22 manufactured in Italy.

In order to simulate the evolution of gas in the tube after the manufacturing process, an ampoule containing a known quantity of a certain gas was brought into the tube inserted in the hollow at the top of the electron gun mount in the manner shown in Fig. 1.

Ampoules having volumes of both 33.0 cc and 2.65 cc were used according to the quantity of the gas to be contained, large and small, respectively. The inner volume of the TV tube was 7,950 cc. The varieties and quantities of gases contained in the ampoules in these experiments are listed in the Table I.

TABLE I

The varieties and quantities of gases

Gas	Quantity of Gas (in mmHg cc)
Dry Air	265, 400, 600
Nitrogen	230, 337, 675
Oxygen	265, 1000, 2000
Carbon Dioxide	185, 560, 1320
Hydrogen	159, 1300
Carbon Monoxide	100

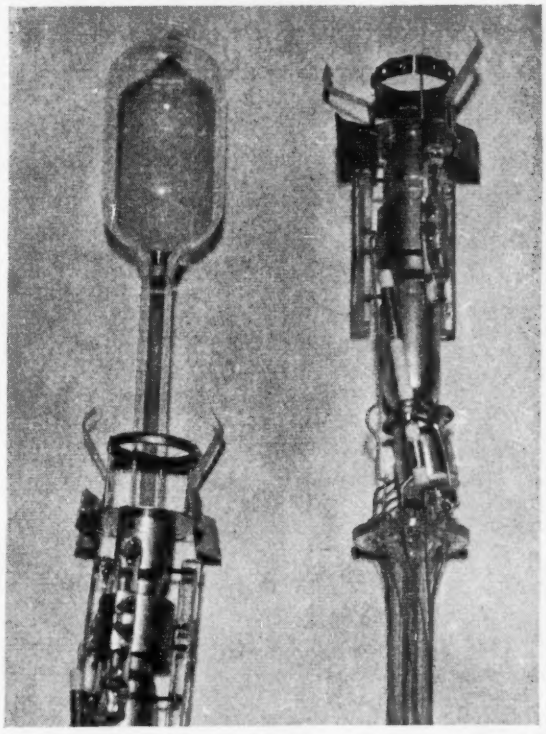

FIG. 1.

After the sealing-in process of gun mount and ampoule, the tube to be tested was evacuated to 1×10^{-5} to 1×10^{-6} Torr. The cathode was activated, the getter flashed, and the ageing procedure applied, following the standard schedule. During all these processes, care was taken to keep the screen of the tube under test facing upwards. At the beginning of the measurement, the TV tube is turned abruptly upside-down, so that the ampoule falls off from the electron gun

mount on to the fluorescent screen and is broken, thereby liberating the gas contained inside.

Starting immediately after the ampoule has been broken, the change of pressure in the test tube is measured in terms of the " gas ratio " which is generally accepted as a measure of the pressure in cathode ray tubes. The authors are supposing in their experiments that the pressure in the tube for a gas ratio of $= 1$ corresponds to a pressure of about 5×10^{-5} Torr for dry air. Having been held at room temperature for a few days, the test tube was operated for about 24 hr, scanning the whole fluorescent screen by the electron beam at an energy of some 14 KV (i.e. raster ageing), and the change of pressure was recorded at each stage.

3. Results of measurements

The reproducibility of the measurement was fairly good, excepting few examples shown in Fig. 4. In Fig. 2, Fig. 3, and Fig. 4, each curve represents average results taken from data of 3 test tubes with the exceptions mentioned above. The quantity of the gas absorbed by the getter before the ampoule was broken is assumed to be negligibly small.

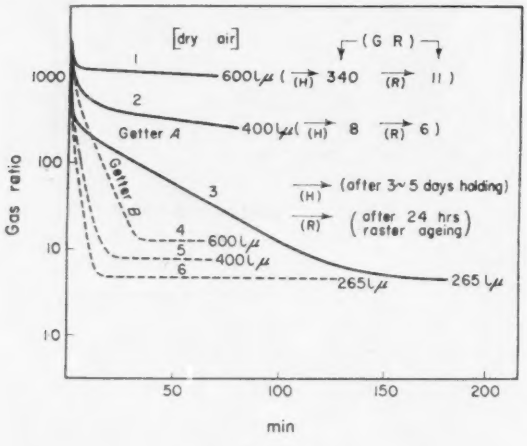

FIG. 2.

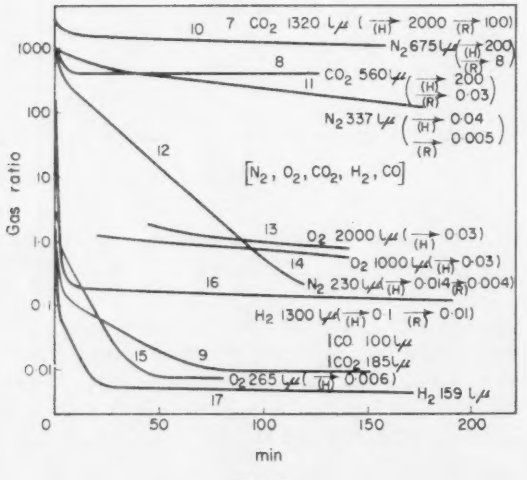

FIG. 3.

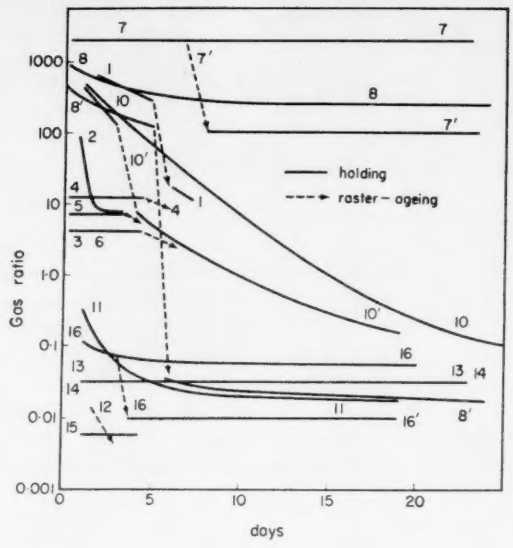

FIG. 4.

The evaporation of barium is partially affected by the presence of the ampoule, as some of the barium is deposited on the external surface of the ampoule during the evaporation, instead of on the inner wall of the TV tube. But the conditions of evaporation may be assumed to be similar from tube to tube.

(a) The changes in pressure (expressed in terms of gas ratio) with time are shown in Fig. 2, Fig. 3 and Fig. 4, with the quantities of various gases as parameters, in semi-logarithmic scale. As for the change of pressure in general, there is a rapid fall in the first stage followed by a slow fall which seems to be almost linear in the graph plotted. It might be said that the gettering rate is nearly independent of the pressure around the getter in the latter stage.

(b) For dry air, getter *B* shows a gettering rate at least ten times greater than getter *A* in the linear region, as shown in Fig. 2. For example, in the case of 400 1μ of dry air, the gettering rate of getter *A* is 0.2 cc/sec in contrast with that of 20 to 50 cc/sec of getter *B*. In other words, getter *A* requires one day to reach its final vacuum, whereas getter *B* reaches the same vacuum in 20 min in the above case.

With getter *A* and getter *B* the same final vacuum is obtained provided equal quantities of dry air are absorbed, as explained in Table II in greater detail.

TABLE II

Final vacuums with dry air

Quantities of dry air		Final Vacuum	
in mmHg cc	in GR (calc)	getter *A*	getter *B*
265	1100	2.5	2.5
363	1510	4	4
400	1670	6	6
600	2500	11	10

Vol. 10 1960

The fact described above could be explained by the existence of 0.93 per cent of argon in dry air which would remain in the tube and not be taken up by the getter.

(c) The absorption curves of getter *A* for various gases are shown in Fig. 3 and Fig. 4, in a short and long time range, respectively. Getter *A* has absorbed as much as 1,300 1μ of carbon dioxide, 675 1μ of nitrogen, at least 2,000 1μ of oxygen, 1,300 1μ of hydrogen and 100 1μ of carbon monoxide until the last stage.

(d) Referring to the plots of Figs. 2, 3 and 4, there are noticeable differences between the absorption curves for dry air and nitrogen compared with those for carbon dioxide and hydrogen. The former continue to fall gradually for many hours after the rapid falls at the initial stage. The latter remain nearly constant for a long time after the rapid falls at the initial stage. These phenomena seem to be easily explained by the well-known fact that the absorption of carbon dioxide and hydrogen by the barium deposit is a surface phenomenon and the absorption capacity is determined by the surface area of the deposit. On the contrary, dry air and nitrogen are absorbed through the surface little by little.

The absorption curves of oxygen seem to be difficult to characterize, but the getter absorbs oxygen very rapidly compared with other gases, except hydrogen. The barium film becomes semi-transparent and seems to be nearly used up when it has absorbed a large amount of oxygen, say 2,000 1μ. On the other hand, it does not alter appreciably when the tube has contained nitrogen, hydrogen or carbon dioxide.

(e) The effect of raster ageing on the final vacuum of the tube is remarkable as shown in Fig. 4 for nitrogen, carbon dioxide, hydrogen and dry air. It is not yet certain in this experiment whether raster ageing is also effective for oxygen or not.

Concerning the effect of raster ageing in general, the manufacturer of TV picture tubes experiences that it definitely improves the final vacuum of TV picture tubes in the manufacturing process. The authors could not answer conclusively the question whether the effect of raster ageing is due to the so-called discharge gettering or is to be attributed to a temperature effect. But the practice of ageing the tube without applying high tension to the ultor electrodes does not sufficiently improve the final vacuum of TV picture tubes.

(f) For oxygen and carbon dioxide, an emission slump takes place immediately after the evolution of gas. With 265 1μ of oxygen, the emission recovers after a period of the order of 10 min, but with 1,000 or 2,000 1μ of oxygen it is reduced to almost zero, and cannot be recovered by any treatment. In the latter case an appreciable reduction in cathode temperature and oxidation of the other electrodes is also caused.

The emission is gradually restored in the case of 560 1μ of carbon dioxide with the gradual recovery of vacuum during the raster ageing process, but the emission did not recover with 1,320 1μ of carbon dioxide. In the case of carbon dioxide, the emission is low when the pressure in the tube becomes about 5×10^{-3} Torr, and recovers almost completely when the pressure is better than 1×10^{-5} Torr.

On the contrary, for nitrogen, dry air and hydrogen, the cathode current increases probably owing to the effect of space charge neutralization. Of course, the cathodes are severely destroyed by ion bombardment when raster ageing has been continued for more than 10 hr with a gas ratio greater than 10.

4. Conclusions

Although some results are obtained as mentioned above, the change of pressure in the initial stages of this equipment was too rapid to be followed and the important characteristics of gettering action in this region could not be investigated. The constant volume method is simple but not fully analytical as is well-known, and as is shown up above. Being unsatisfied by the results obtained, the authors are compelled to undertake more complex experiments. It is intended to investigate the method of keeping a constant pressure on the getter film during the measurements as described by Dr. P. della Porta[1] in his paper in *Vacuum*.

The authors are expecting and hoping to get more information about gettering actions in easily accessible forms for manufacturers of TV picture tubes who are taking an interest in the relation between final vacuum and tube life.

Reference

[1] P. della Porta ; *Performance Characteristics of Barium Getters with Particular Reference to their Application in Thermionic Valves, Vacuum* 4, 284 (July 1954).

Some Barium Getter Problems on the Vacuum Tubes

KAZUJI HASHIMOTO and KENJI KITAGAWA

Hitachi Mobara Plant Mobara City, Chibaken, Japan

The writers have carried out experiments on the action and behaviour of getters as used in the actual production of, for example, receiving tubes, power tubes, cathode ray tubes, mercury rectifiers and X-ray tubes. Initially the results obtained from the study of the flashing conditions of the getter and the effect of these conditions on the sorption of gases are presented. Results are given for the quantity of the gas sorbed during the first minute, the following four minutes and the successive 10 min, for getters which have been evaporated for 10 and 60 sec. The difference in the quantity of gas initially sorbed when using different times of flashing are quite remarkable in the case of N_2 and H_2. Due to this the quantity of gas sorbed can nearly be doubled by a rapid firing of the getter. This difference is less marked for O_2 and negligibly small for CO and CO_2. Similar studies have been made using rare gases ; these studies have been helped by using the electron microscope to study the surface of the getter film. Studies have also been made on the influence of the distance between getter and condensing wall and hence of the condensing area of barium film. By examining cathode ray tubes, the dependance of the tube pressure and life on the conditions of flashing of the getter have been studied. In non aluminized picture tubes data are presented giving the most favourable angle of connection of the getter assembly to the electron gun. The modifications made to the cathode structure of X-ray tubes in order to obtain the most favourable conditions when using the getter are reported. Data on the pressure obtained under such circumstances are also presented. Subsequently a study is given of the gas sorption by barium, magnesium and titanium, in mercury vapour tubes. Finally there is a study of the influence of the getter on the emission from the oxide cathodes employed in mercury rectifiers made with an apposite apparatus.

Vol.
10
196

1. Introduction

Many authors have reported on the gas absorption ability, its influence on the final pressure measurement and the mechanism of gas absorption of barium getters.

In our factory the writers have carried out experiments on the getters action and behaviour when it is used in vacuum tube production, for example, of receiving tubes, power tubes, cathode ray tubes, mercury rectifiers and X-ray tubes from the viewpoint of actual procedure.

Here we want to present some results concerning the type of getter used in these tubes.

2. The effect of flashing conditions on the gas absorption characteristics

The so-called barium getter used is actually an alloy of aluminium and barium. So in this paper by barium getter we mean a barium-aluminium alloy getter.

The gas absorption ability of a getter film in a vacuum tube is chiefly affected by its flashing conditions which are controlled by heating, time interval and gas pressure and the distance between the getter and the glass wall. The getter is heated by the passage of an electric current and the heating time is variable. These results are shown in Table I. CO and CO_2 have larger initial gas absorption velocities than other gases. The mean free path of a barium atom is so small in CO and CO_2 that collisions with these molecules may be

TABLE I

Gettering Rate of Barium for Various Gases

Gas	Flashing Condition		Gettering Rate* (cc/min)		
	Heating Current	Heating Time	0~1′	1′~5′	5′~15′
O_2	10A	60″	504	155	58
	12	10	778	274	56
N_2	10	60	176	65	51
	12	10	385	234	60
CO	10	60	1331	96	32
	12	10	1390	151	31
CO_2	10	60	1232	132	42
	12	10	1232	179	46
H_2	10	60	671	127	32
	12	10	1062	180	47

**Note* : Gettering Rate : Showing Mean Value during Time Division for Measurement.

frequent. Molecules of CO and CO_2 are rapidly absorbed due to their large polarity ; they react more easily with barium atoms than would monoatomic molecules, such as O_2, N_2, H_2. The more speedily the getter is flashed at high temperature, the larger is the absorption ability. We experimented under a number of conditions with a constant volume of a nitrogen (containing vessel 1100 cc) and measured the pressure at one hour after flashing. Fig. 1 shows how effective the flashing times and temperatures are. In these experiments the quantity of evaporated barium should be considered, but it was found to be independent of heating conditions. Further experiments on the getters absorption ability were carried out in rare gases ; He, Ar, Xe, as shown in Fig. 2. The results show that this ability is much larger

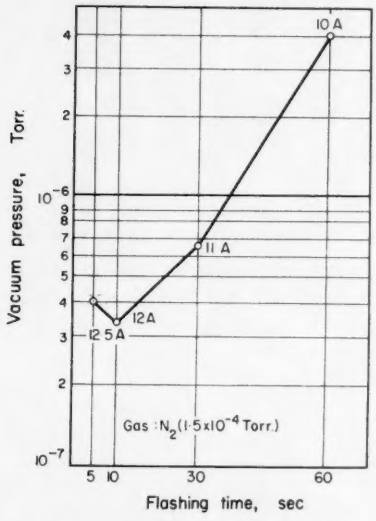

FIG. 1.

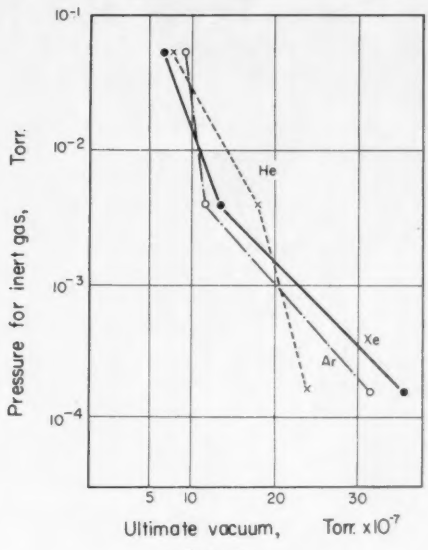

FIG. 2.

in a low vacuum rather than in a high vacuum. But the absorption ability is independent of the type of rare gas. We tried to observe the surface of the getter films which were flashed in rare gases, by using the Hitachi Electron Microscope (SiO replica method). The surface of the film becomes somewhat rough depending on the pressure (Fig. 3).

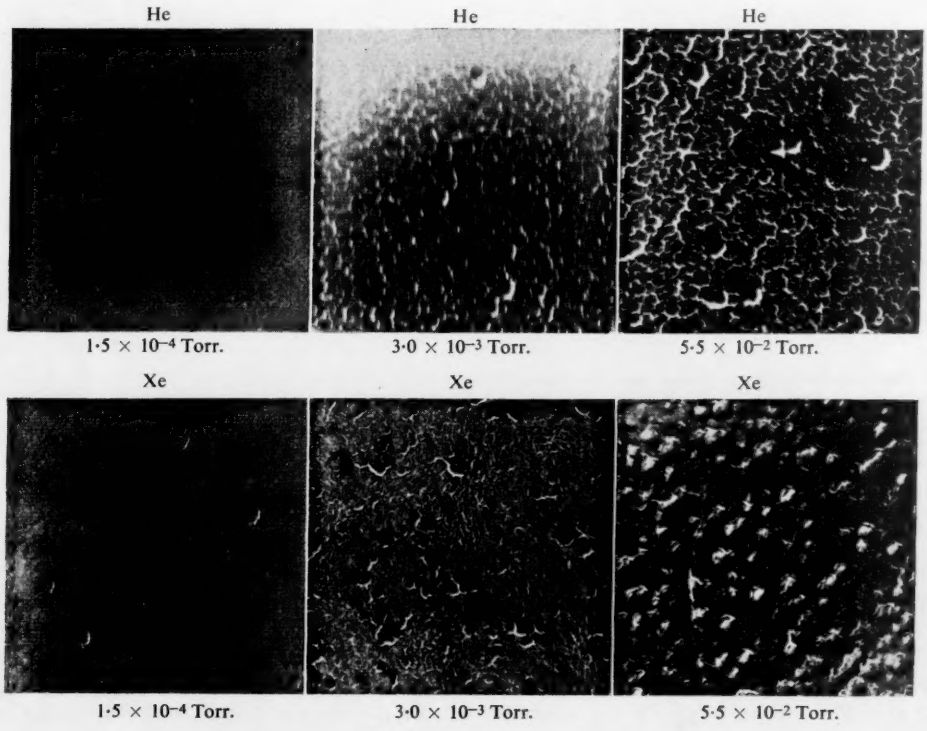

FIG. 3.

The result of experiments on the effect of the distance between the getter and the glass wall is shown in Fig. 4. When the distance between the getter and the glass wall is large, the flashed film area is also large, and the initial gas absorption ability is strong. The gas absorption ability is weakened by repeated gas admision, but when the distance is small the ability is maintained longer in spite of the small area of the film.

We tried to apply these experimental facts to the various getters used in different vacuum tubes.

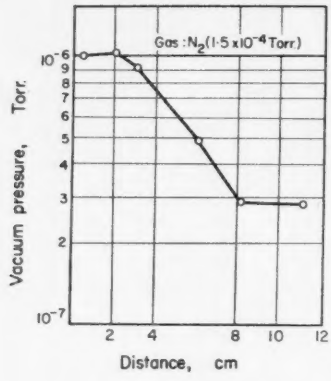

FIG. 4.

3. Getter effect on life test in kinescope

The life of electron tubes is mainly affected by their residual pressure. In kinescopes the order of pressure (GR) is represented by the ratio of ion current to the electron beam current after five minutes' heat run. (We identify this value 5GR.) Table II shows the relationship between the value of

TABLE II

Relation between Vacuum coefficient (5GR) and Percentage Life of Television Picture Tube

Tube Type	5GR				
	0.1	0.2	0.3	0.4	0.5
Non Aluminized Tube	98%	90%	85%	80%	73%
Aluminized Tube	100%	100%	94%	81%	84%

5GR and the life of the tubes. From this result the pressure in kinescopes is very important in order to make their life long. To get a good vacuum in kinescopes the flashing condition of the getter and its area are also very important. In actual production we must consider and watch the behaviour of the getter film so that it does not flash to the fluorescent screen or to the neck of the tube near the gun assembly. After many experiments we obtained the conditions on the angle of mounting the getters, as shown in Fig. 5. If the getter is flashed to the kinescope screen, there appears unevenness on the center and at the edges of the kinescope screen. So we can measure how the getter film is contamined, by studying the unevenness of brightness on the screen, as shown in Fig. 5.

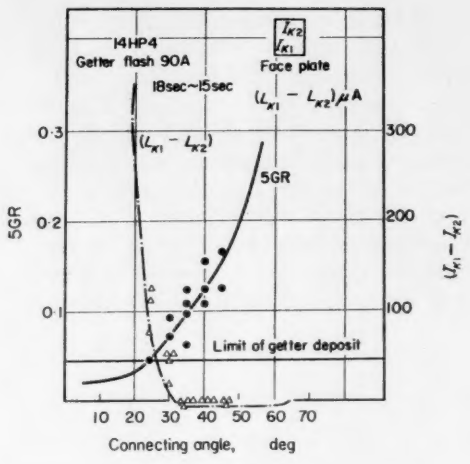

FIG. 5.

4. The application of getters to X-ray tubes

We have changed the design of the cathode assembly of the X-ray tube, as shown in Fig. 6, in order to obtain easier getter flashing. The barium getter is flashed by the passage of an electric current.

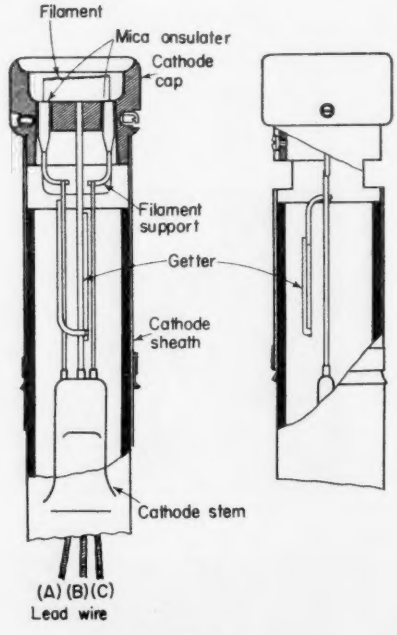

FIG. 6.

Usually in X-ray tubes the cathode is constructed in such a way that the filament is insulated on one side from the cathode cap. In our case both sides of the filament are insulated from the cathode cap, and the getter wire is mounted between the lead wire which is at the centre of the stem and the cathode cap. If we apply a voltage between the two lead wires (in Fig. 6, A & B), the getter will be flashed. After the getter is burned off, we can measure the pressure in the

X-ray tube (see Fig. 7) by using it as an ionization gauge, since we can apply the positive and negative voltages to the cathode cap and anode respectively. Table III shows the

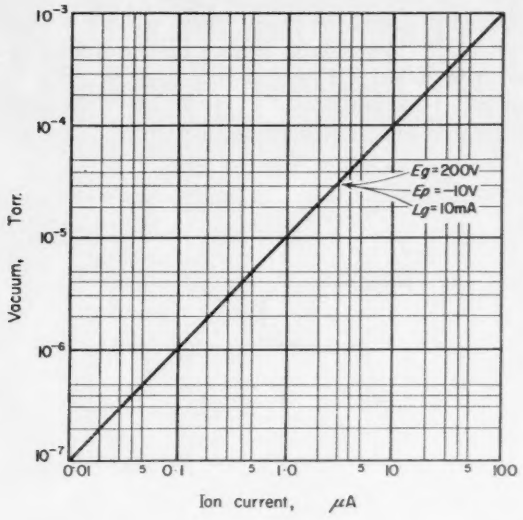

FIG. 7.

TABLE III

Effect of Getter on Vacuum of X-ray Tube

Barium Getter	Vacuum Pressure (Torr)		
	Before Operating	After Operating	After Life Testing
with	(1∼5) × 10^{-7}	(1∼5) × 10^{-7}	(3∼4) × 10^{-7}
without	4 × 10^{-5}	2 × 10^{-5}	(2∼0.8) × 10^{-4}

effect of the getter on the X-ray tube. From this table it is understood that if we use a getter in an X-ray tube we can obtain a high vacuum, of the order of 10^{-7} Torr, and this vacuum is maintained after the maximum load test or the life test. If we do not use the getter, as usual, the pressure gradually changes.

5. Gas absorption of a getter in mercury vapour

In mercury vapour rectifiers with a hot cathode, an Mg or Mg–Ba getter is usually employed. But in this case the getter film amalgamates and evolves some gas. In high vacuum tubes without mercury vapour, the getter action is so strong that the so-called pre-heat treatment of the getter is not really necessary. But when there exists mercury vapour in the vacuum vessel, the getter action is remarkably affected by whether or not pre-heating of the getter is carried out. If we do not pre-heat the getter it acts as a source of gas. Generally the gas evolved from the getter mainly consists of H_2 and the volume of this gas and its composition are nearly equal to those present before the getter is flashed. Table IV and Fig. 8 show how pre-heating of the getter

TABLE IV

Influence of Pre-Heat Treatment on Gas Evaluation after Flashing Ba and Mg Getter in Mercury Vapour

	Getter		
	Ba	Ba	Mg
Pre-Heat Treatment	with	without	without
Gas Evolution	(4∼12) × 10^{-4}cc	(1.2∼2.8) × 10^{-2}cc	(9∼24) × 10^{-3}cc

Note : (1) Pre-Heat Treatment : 800°C, 20″.

(2) Ba Getter : Ba content = 1.5 mg, Deposit Quantity = (0.6 ∼ 1.2) mg.

Mg Getter : Mg content = 13 mg, Deposit Quantity = (6 ∼ 9) mg.

affects its absorption ability in mercury vapour. In this experiment we used a 900 cc vessel and the weight of vaporized

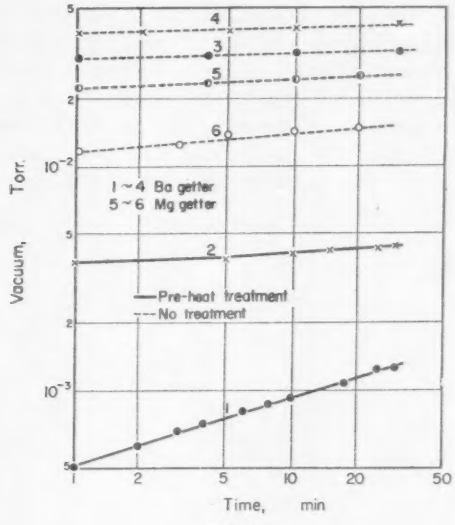

FIG. 8.

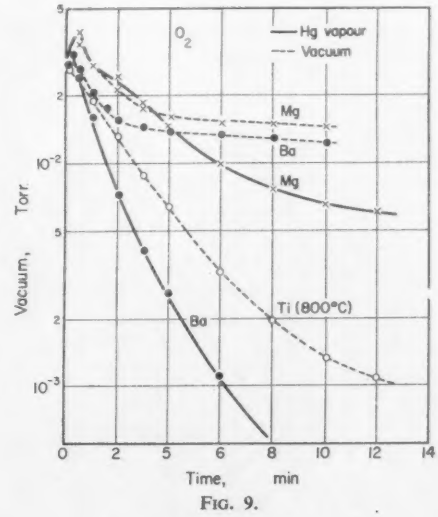

FIG. 9.

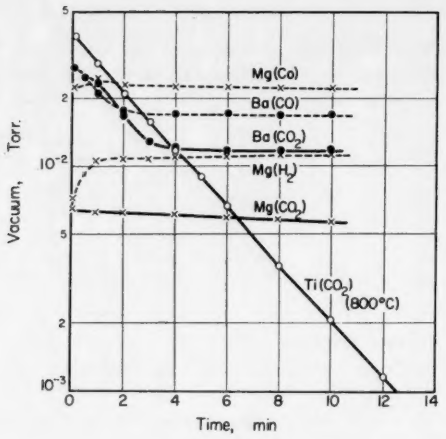

FIG. 10.

Ba and Mg were 0.6～1.2 mg and 6～9 mg per type of getter respectively. Since the vaporized volume of the Mg getter is larger than that of Ba, the gas evolution for the Mg amalgam will be smaller than that of Ba according to their ability in forming amalgam. From these experimental facts the absorption ability of Mg or Ba getters in mercury vapour is much weaker than that in vacuum. We also tested the absorption ability of the getter for O_2, H_2, CO_2 and CO in the presence of Hg vapour, and show the experimental results in Fig. 9 and 10. These experiments were carried out by measuring the change of vacuum with time when introducing several kinds of gases into the vessel after flashing the getter. In order to know the velocity of creation of the amalgam we tried to maintain the getter film in mercury vapour and measured the change of the pressure with time. Fig. 11, 12, 13, 14 and Table V show the experimental data. From these results we realized that Mg, Ba getter films evolve gas in the presence of mercury vapour, Ba evolving more gas than Mg under similar conditions.

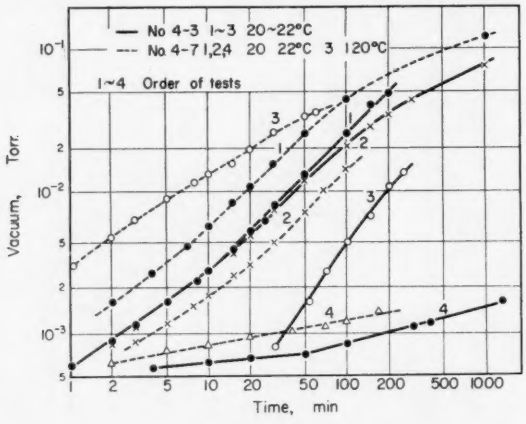

FIG. 11.

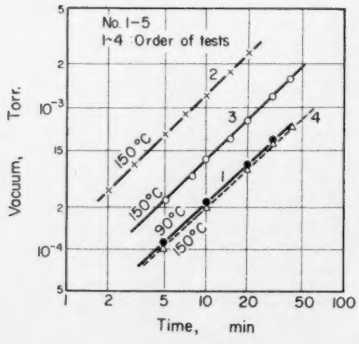

FIG. 12.

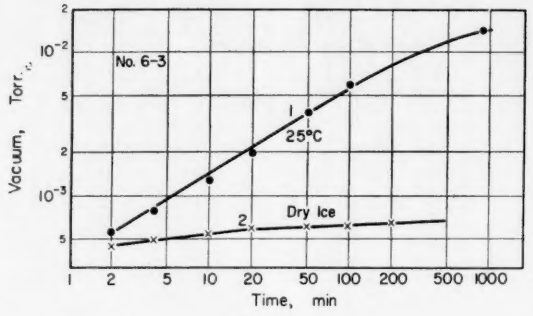

FIG. 13.

TABLE V

Gas Evolution from a Getter Mirror in Mercury Vapour

Kind of Getter	No. of Lot	Keeping Condition		Gas Evolution (cc)	
		Getter Bulb Wall Temp. (°C)	Time (min)	After Flashing Getter	After Keeping Getter Mirror During All Night
Ba	4–3	20	30	1.3×10^{-3}	1.9×10^{-4}
		,,	200	7×10^{-3}	2.4×10^{-3}
		,,	1000	1.8×10^{-2}	
,,	4–7	25	30	2×10^{-3}	1×10^{-3}
		,,	100	7×10^{-3}	3×10^{-3}
		,,	2500	7×10^{-2}	
,,	6–3	,,	30	1.5×10^{-3}	4×10^{-4}
		,,	200	1.3×10^{-2}	8×10^{-4}
		,,	1000		1.8×10^{-3}
Mg	12–27	40	30	4.1×10^{-4}	1.2×10^{-4}
		,,	860	1.2×10^{-3}	
,,	5–5	20	30	6×10^{-4}	6×10^{-4}
		,,	200	1.2×10^{-3}	1×10^{-3}
		,,	1000	2.6×10^{-3}	
,,	5–13	,,	30	6×10^{-4}	1.8×10^{-4}
		,,	200	2.4×10^{-3}	3.5×10^{-4}

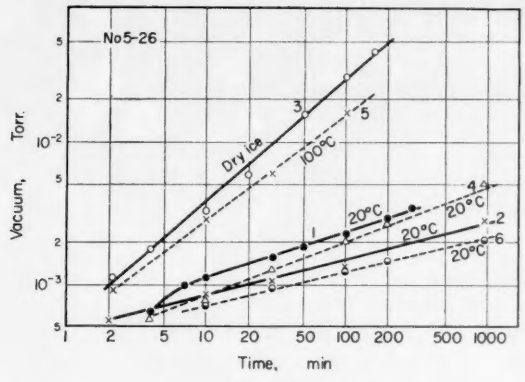

FIG. 14.

Generally when the getter mirror on the glass wall is heated to higher temperatures the velocity of gas evolution is greater. We also know that the gettering action is affected by the previous history of the film.

6. The effects of the getter on the electron emission from oxide cathodes in mercury rectifiers

Generally Mg and Mg–Ba alloys have been in common use as getters in mercury rectifiers having oxide cathodes. These metals form amalgam by reaction with mercury, and this amalgam evolves gas. If the gas exists freely in the oxide cathode vacuum tube, a decrease in emission will occur. We sealed a test diode structure to the mercury rectifier valve 1H16 which has an oxide cathode. (See Fig. 15.) This

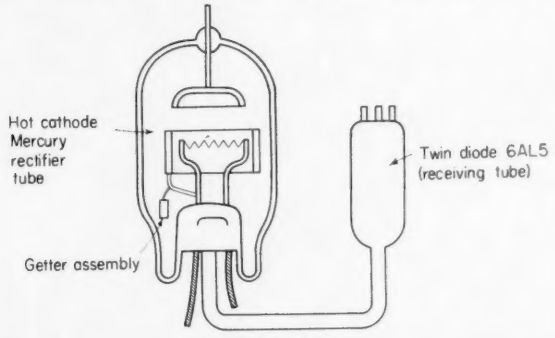

FIG. 15.

diode is operated in the region of the initial velocity current. The change of the emission level is known from the value of the heating current of the cathode, Ifs, which should give a constant emission current of 1μA when the anode voltage is 4.0v. Fig. 16 and Fig. 17 show the value of the voltage drop in the mercury rectifier or the value of Ifs of the test diode before or after getter flash, since there is a relationship between Ifs and the emission as already mentioned. If gases exist in this vacuum tube which damage the oxide cathode, then we must increase the heating current of the cathode to give a higher emission. In Fig. 16 and Fig. 17 we

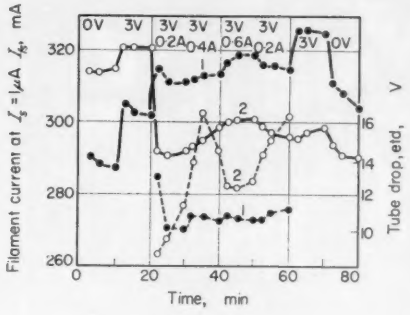

FIG. 16.

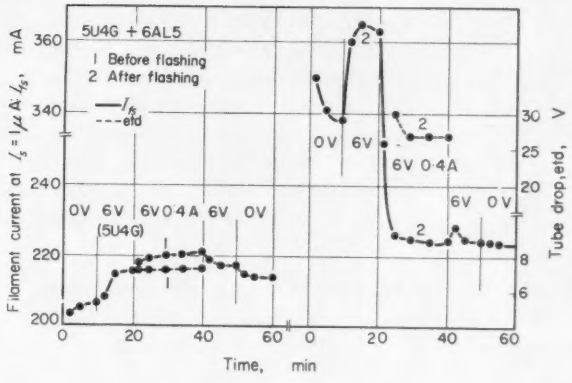

FIG. 17.

can see that flashing a Mg getter produces a poor vacuum.

If the anode current flown into the mercury rectifier, the Ifs suddenly decreases. This special case shows that H_2 is evolved in the bulb. This effect is also shown by the drop in voltage across the rectifier. We tried many experiments. Fig. 18 shows the relationship between Ifs and the drop of voltage in the mercury rectifier. In Fig. 18 a dotted line shows the results obtained by admitting H_2 and CO_2 into the bulb.

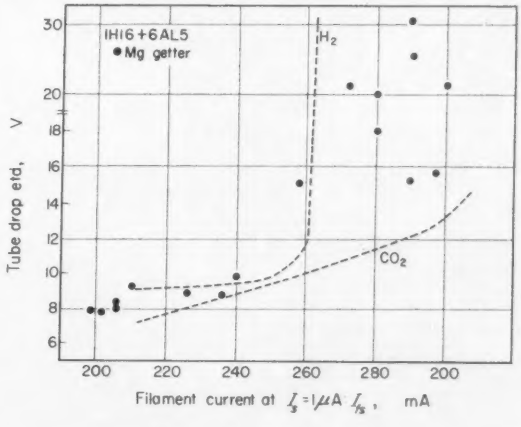

FIG. 18.

Use of Zirconium Sintered Getters

J. M. SOURDILLON

C.I.F.T.E. Courbevoie (Seine), France

The statement concerns the general conditions of elaboration and some examples of application of a getter obtained by sintering of a mixture of powders of zirconium hydride (80 per cent in weight) and of aluminium (20 per cent in weight). The getter holder (preferably in a circular form) is made of nickel pressed or of molybdenum embossed. A cold compression of the powder directly on its holder is proceeded. The sintering operation is made under high vacuum at about 1050°C. Some tests of application of those getters have been made with HT tubes EY81 and 6AX2N, and with the 21B6 and 5725 tubes. The results are very good after 500 hr life. Tests made with power valves of 12 kW with graphite anode (type 3T12000A5) with getters of large dimensions, show that the output was now in good condition during working. In general meaning, the getter being not volatilized, but only heated at high temperature, we do not observe metallic settling on the inner surface of the bulbs so that risks of leakage on cold inner surface or of nocious capacitances reduce considerably. We notice a very steady work.

Emploi de getters frittes à base de zirconium

Parmi les getters couramment utilisés dans les tubes électroniques, on peut distinguer les dégazeurs en capsule que l'on vaporise sur les parois internes des tubes (flash-getters)—par exemple, getters au baryum stabilisé—et les dégazeurs en dépôt (coating getters) qui sont généralement déposés sur une pièce des tubes avant montage.

Dans cet exposé, nous allons examiner un dégazeur appartenant à cette seconde catégorie et constitué d'une poudre à base de zirconium fritté sur un support métallique. Après avoir décrit les conditions générales d'élaboration de ce getter, nous donnerons quelques exemples d'application.

Procédé de fabrication

Les getters étudiés se présentent sous la forme de petites coupelles remplies d'une substance active frittée et ont été mis au point par M. Patriarche, Ingénieur du Centre d'Etudes et de Recherches de la Cifte.

Le procédé de fabrication comprend essentiellement les opérations suivantes :

— Préparation du support,
— Préparation du mélange de poudres actives,
— Compression à froid,
— Frittage sous vide,
— Contrôle.

Préparation des supports

La Fig. 1 représente trois types de supports expérimentaux, dont les profils ont été étudiés de façon à permettre la compression et le frittage de la substance active directement sur ces supports.

Les supports A et B sont destinés aux tubes miniatures et subminiatures, le support C à des tubes d'émission de grande puissance.

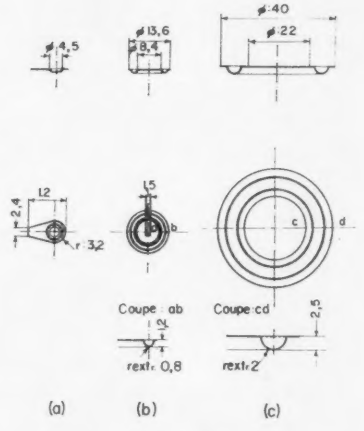

FIG. 1.

Le support A est obtenu par emboutissage d'une bande de nickel de 0,12 mm d'épaisseur : la languette de nickel permet d'assurer la fixation de la pièce à l'intérieur du tube.

Le support en forme de cuiller est destiné à recevoir environ 20 mg de substance active : le support annulaire contient environ 80 mg de ce produit et cette disposition en anneau permet de chauffer la pièce par HF au moment des traitements de dégazage ou d'activation du getter dans de bonnes conditions.

La Fig. C représente une coupelle de plus grandes dimensions pour des getters mis en oeuvre dans des tubes d'émission à refroidissement naturel d'une puissance utile de 12 kW. Cette coupelle peut contenir 1 g de matière active. Dans ce cas, et pour des raisons de technologie propres à ces tubes, les pièces sont réalisées par repoussage d'une tôle de molybdène de 0,25 mm d'épaisseur.

On procède évidemment à des dégraissages soignés au bain de trichloréthylène chaud suivi d'un rinçage à l'alcool dénaturé.

Préparation de la poudre

Pour des raisons de sécurité de manipulation, on utilise naturellement non pas le zirconium mais l'hydrure de zirconium.

Pour la confection des getters, on utilise un mélange d'hydrure de zirconium pulvérulent passé au tamis 325 mailles (44μ) et de poudre d'aluminium : l'addition d'aluminium a, en effet, un double objet :

(1) Constituer au moment de la compression à froid du mélange, une sorte de liant pour la poudre d'hydrure de zirconium qui est dure et peu malléable. On parvient ainsi à augmenter la cohésion du comprimé et son adhérence au support.
(2) Favoriser, lors du frittage, la réalisation d'un produit poreux, par suite de l'évaporation partielle de l'aluminium.

Les essais que nous allons décrire concernent un mélange constitué de 80 pour cent d'hydrure de zirconium et de 20 pour cent d'aluminium en poids. La poudre est soigneusement desséchée dans une étuve à rayonnement infrarouge portée à 70 °C pour éliminer toute trace d'humidité qui conduirait à des produits défectueux.

Compression à froid

Comme le produit cherché doit présenter la surface maximale pour un volume minimal, il n'est pas nécessaire de réaliser avant frittage un comprimé très dense, aussi une simple compression à froid sous une faible charge (2 T/cm^2) permet-elle d'obtenir des pièces poreuses et présentant une résistance suffisante aux manipulations indispensables avant frittage : les pièces sont moulées directement dans leurs coupelles.

Les divers grains d'hydrure de zirconium et d'aluminium, intimement mêlés, viennent au contact les uns des autres : les films gazeux ou les faibles couches d'oxydes qui se trouvent ordinairement à leur surface sont partiellement rompus et les métaux se trouvant directement en contact en certains points, ont tendance à offrir une certain cohésion par soudure à froid. Du reste l'imbrication mécanique mutuelle des divers grains assure également une cohésion suffisante.

Frittage

Les opérations de frittage sont réalisées sous vide par chauffage par induction HF dans les conditions suivantes :

— on dispose dans un récipient en molybdène en forme de tonneau, un certain nombre de pièces comprimées à froid dans leur coupelle,
— on commence par chauffer l'ensemble progressivement sous vide à une température relativement basse (300 ou 400 °C) : on observe des dégagements gazeux assez abondants correspondant à une phase de dégazage des divers matériaux et à une première libération de l'hydrogène retenu par le zirconium.

Lorsque les dégagements observés paraissent pratiquement terminés, on chauffe par paliers de 15 min. jusqu'à 900 °C. Au cours de ce chauffage, les barrières d'alumine, que peuvent présenter les grains d'aluminium, se fragmentent car elles n'ont aucune plasticité et lorsqu'on atteint une température voisine de 658 °C, les grains d'aluminium fondent en augmentant leur volume de 5 à 6 pour cent, ce qui a pour effet de produire un léger gonflement du mélange.

— on poursuit le chauffage jusqu'à 940 °C, température à laquelle l'hydrure de zirconium achève de se décomposer.

Au cours de ce chauffage, on observe une volatilisation partielle de l'aluminium qui forment dans la substance des cavités et lui confère une structure poreuse. On laisse refroidir l'ensemble sous vide jusqu'à la température ambiante.

Le cycle des traitements dure ainsi 3 h. environ.

Dans le cas des getters de grandes dimensions à support en molybdène, il est commode de disposer régulièrement les pièces les unes au-dessus des autres, autour d'un cylindre commun. On observe qu'étant donné les grandes dimensions de la partie frittée, il est prudent de chauffer très progressivement l'ensemble sinon des décollements inacceptables de la substance active peuvent se produire.

Utilisation

En vue de déterminer les conditions optima d'utilisation de ce type de getter, nous avons entrepris une étude de l'absorption des gaz par les getters Zr–Al à l'aide d'un appareil réalisé suivant les indications du Dr. Della Porta.

Le dispositif permet de mesurer la vitesse volumétrique de pompage du getter à pressions stationnaires. Le flux de gaz s'écoule à travers un tube capillaire de conductance C et se trouve mesuré par la lecture des pressions en amont Pm et en aval Pg, à l'aide de deux jauges à ionisation, la pression en amont du tube capillaire étant ajustée par une fuite réglable et une pompe à diffusion.

La capacité instantanée, $Q = C(Pm–Pg)$ est déterminée à Pg constant.

$$Pg = 5.10^{-5} \text{ Torr}$$

La vitesse volumétrique de pompage est donnée par la relation :

$$v = C\frac{Pm-Pg}{Pg}$$

Les mesures ont été effectuées avec de l'air sec.

Le processus expérimental comportait les opérations suivantes :

(1) Mise sous vide de l'appareil—étuvage à 425 °C pendant 5 h.
(2) Dégazage du getter par chauffage par induction HF (1 min. à 900 °C et 2 min. à 1000 °C).
(3) Réglage de la pression Pg dans la chambre du getter à une valeur constante

$$Pg = 5.10^{-5} \text{ Torr}$$

(4) Chauffage permanent du getter à une température constante par induction HF et lectures de la pression Pm pour Pg constant en fonction du temps.

La Fig. 2 représente différents isothermes obtenus pour des températures de 900–750–600 °C et 20 °C.

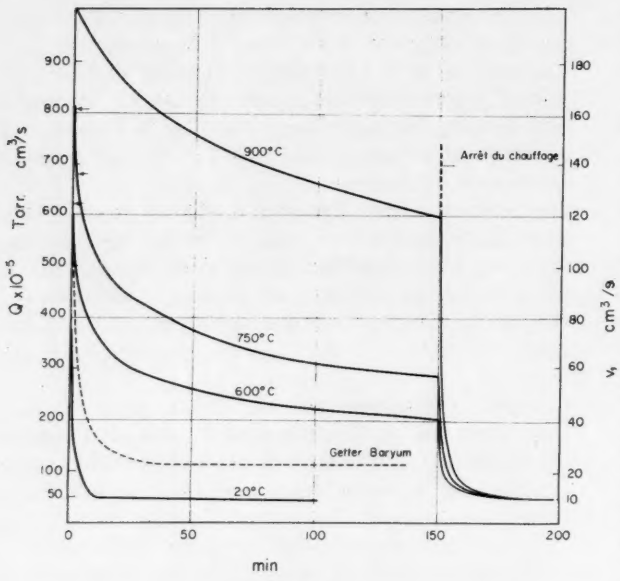

FIG. 2.

A titre d'éléments de comparaison, on a tracé également la courbe obtenue par flash d'un getter au baryum (getter comprenant 20 mg de baryum, surface du miroir 4 cm²) pour $Pg = Cte = 5.10^{-5}$ Torr. Ces courbes montrent que le getter Zr–Al est d'autant plus efficace que la température à laquelle il est porté est plus élevée. On a donc intérêt à le fixer dans une zone chaude du tube.

Les getters ainsi réalisés sont montés dans les tubes électroniques en lieu et place des getters ordinairement utilisés.

Au cours du pompage des tubes, on procède à un dégazage de la substance active en la chauffant par induction HF (ou éventuellement par effet Joule) à une température de l'ordre de 1000°C–1100°C, puis après la coupe du queusot, on porte la pièce à 1000°C environ pendant quelques secondes.

L'efficacité du getter résulte alors des différents mécanismes d'absorption susceptibles de se produire. Etant donnée la grande surface de contact de la substance active, l'absorption par contact des gaz résiduels avec le getter semble se produire dans de bonnes conditions, cette absorption étant d'ailleurs nettement influencée par la température à laquelle le getter se trouve porté, au moment de son activation et également au cours de la vie du tube.

Essais d'application

Des essais d'application de ces getters ont été entrepris sur plusieurs types de tubes, en particulier sur les valves THT 6AX2N—sur des tubes 21B6—5725 et 5654, enfin sur des tubes d'émission du type 3T12.000.A5.

Valves 6AX2N

Le valve 6AX2N est un tube redresseur à très haute tension qui fonctionne dans les conditions maximales suivantes :

Tension inverse de crête	22.000 v.
Tension inverse de crête pour un courant redressé nul	24.000 v.
Courant redressé	1 mA.
Courant anodique de pointe	40 mA.

la champ maximal réalisé étant de 100.000 v/cm environ (distance cathode-anode : 2,5 mm).

Le fait que le tube fonctionne à très haute tension impose un isolement interélectrode particulièrement soigné.

Dans la fabrication courante, on relevait assez souvent avec des getters au baryum, des fuites électriques qui amorçaient des arcs et qui étaient dus vraisemblablement à des projections métalliques sur les parois ou sur les entretoises en mica lors du flash du getter. De plus, au-delà de 22.000 v, on voyait apparaître assez fréquemment le long de l'enveloppe en verre, une luminescence due à l'action de rayons X mous. Cette luminescence s'accompagnait généralement d'une transformation du verre qui se trouvait parfois complètement attaqué.

Aussi était-il intéressant de se rendre compte si l'emploi d'un getter au zirconium, étant activé par chauffage par induction HF sans donner lieu à des vaporisations métalliques, pouvait apporter des améliorations à la fabrication de ces tubes.

Les premiers essais ont consisté à remplacer le getter au baryum traditionnel par un getter Zr–Al du type " pastille " monté sur sa coupelle en nickel et contenant 20 mg de substance active. Les tubes étaient pompés sur une machine automatique à 36 positions. Au cours du cycle de pompage, les opérations de dégazage et d'activation du getter par chauffage HF à 1000°C étaient réalisées à l'aide d'un concentreur de champ. Aussitôt le tube passait en position de coupe du queusot.

On a observé à ce moment sur certains tubes que le vide réalisé était médiocre. Il suffisait alors de réchauffer par induction HF le getter pendant quelques secondes à 1000°C pour obtenir un vide correct. Ce défaut était dû notamment au fait que le getter, se refroidissant rapidement lors du passage de la position " chauffage du getter " à la position " coupe du queusot ", ne se trouvait plus à la température optimale pour éliminer les gaz résiduels. Pour éviter ces difficultés, on a réalisé le getter annulaire à 80 mg de Zr–Al dont l'inertie thermique est nettement plus grande. De plus, le chauffage par induction se fait nettement plus facilement (une simple inductance à 1 spire suffit).

En définitive, on a observé que ces tubes étaient capables de fonctionner dans des conditions en général supérieures à celles exigées par le cahier des charges (notamment au cours des essais d'arcs). De plus, le phénomène de luminescence a paru nettement plus faible que dans le cas des tubes monté avec d'autres types de getter.

Les essais de durée ont été absolument comparables aux essais réalisés avec des tubes comportant des getters au baryum stabilisés (120.000 tubes ont été fabriqués ainsi et ont donné toute satisfaction).

Tubes 21B6

Des essais ont été réalisés sur ces tubes. Il s'agit de pentodes de sortie pour " balayage lignes " de postes récepteurs de télévision.

Les tubes fonctionnent suivant les valeurs maximales suivantes de ces différentes caractéristiques :

Tension d'anode	250 v.
Tension d'anode pour un courant d'anode nul	550 v.

Vol. 10 196

Tension de grille-écran (No. 2) pour un courant de grille No. 2 nul	550 v.
Tension de grille-écran	250 v.
Tension de grille de contrôle pour un courant de grille No. 1 de 0,3μA	−1,3 v.
Dissipation d'anode	8 w.
Dissipation grille-écran	4,5 w.

Les tubes essayés étaient équipés de 2 getters Zr–Al annulaires. Le premier était rendu actif juste après pompage et scellement du tube. Le second après les traitements d'activation.

Ainsi, on obtenait à ce moment un vide correct correspondant à un courant inverse de grille inférieur à 1μA.

Les tubes ont été mis en essais de durée sur poste de télévision.

La Fig. 3 donne les valeurs du courant inverse de grille qui caractérise la qualité de vide en fonction du temps. On

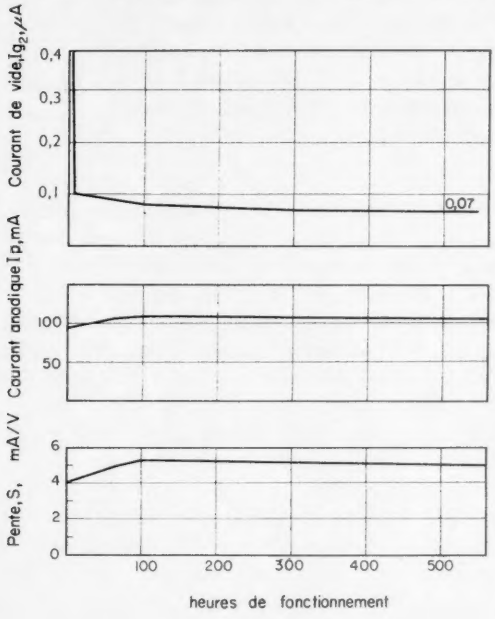

FIG. 3.

voit qu'après 500 h de fonctionnement, le courant ne dépasse pas 0,07μA. A titre indicatif, on a représenté les courants moyens anodiques en mA et la pente exprimée en mA/v. On voit que l'émission reste constante pendant la durée des essais.

Tubes 5725

Des essais ont également été réalisés sur les tubes miniatures 5725, pentodes à pente variable conçues pour résister spécialement aux chocs et aux vibrations.

Les conditions maximales d'utilisation sont résumées ci-après :

Tension d'anode	180 v.
Tension de grille No. 2	140 v.
Tension de grille No. 3	27 v.
Puissance dissipée sur l'anode	1,7 w.
Puissance dissipée sur la grille No. 2	0,75 w.
Courant de cathode	18 mA
Tension filament-cathode	90 v.

Les tubes étant équipés de getters circulaires Zr–Al ont été pompés dans les conditions standard, le getter soigneusement degazé à 1050°C avant coupe du queuseot est ensuite activé à 950°C.

Les essais de durée ont montré que le courant inverse de grille reste pratiquement constant. Après 500 h de fonctionnement, sa valeur moyenne est de 0,01μA. Les diverses caractéristiques ne se distinguent en aucune façon des caractéristiques des tubes de fabrication courante à getter baryum.

Tubes 3T12.000.A5

Les getters de grandes dimensions ont été introduits dans des tubes d'émission de grande puissance (type 3T12.000.A5 fournissant une puissance utile de 12 kW en régime permanent et de 100 kW en régime intermittent (15 secondes de travail pour 4 min de repos).

L'expérimentation étant encore trop récente, il ne nous est pas possible de donner de statistiques, cependant nous avons pu faire deux constatations intéressantes :

— d'une part, on gagne sur le temps de pompage de façon appréciable,

— d'autre part, lorsque les tubes ont subi des surcharges assez importantes pour provoquer des remontées de pression, il est possible de rétablir la pression initiale en réactivant le getter à haute température, cette opération étant suivie naturellement d'une réactivation de la cathode.

En résumé

Les opérations de frittage des getters Zr–Al décrites permettent d'obtenir une substance poreuse particulièrement active à haute température. Le getter n'étant pas volatilisé, mais seulement chauffé quelques secondes à 950°–1000°C, ne provoque pas de métallisation sur les parois froides du tube, ce qui diminue considérablement les risques de fuites électriques et de capacités parasites.

Lorsque des dégagements gazeux apparaissent après pompage, on constate qu'il est généralement possible d'absorber ces gaz par un simple chauffage de la substance active du getter par induction HF.

Enfin, au cours de la vie des tubes essayés, on a observé que le fonctionnement de ces getters était très stable.

Test of Use of Titanium as Getter

J. M. SOURDILLON

C.I.F.T.E. Courbevoie (Seine), France

It seems interesting to do some absorption tests of residual gas in replacing in the tubes with oxide cathode, the getters ordinarily used by titanium pieces of simple form. The described tests concern 2 special types of tubes : a miniature 3B4, with beam tetrode whence the realization (setting up and pumping) is rather difficult, taking into account of the imposed performances ; an experimental oscillator miniature tube chosen, particularly, in reason of its small volume. The metal used was pure titanium. In a first series of tests, we eliminated completely barium getters and the fixation of residual gas has been assured by the presence of titanium anode instead of conventional nickel anode. In a second series of tests, we searched to replace the barium getter by one simple piece of small dimensions in pure titanium ; small disc of titanium sheet or rings in titanium wire of 1 mm in diameter. These pieces were heated by R.F. after exhausting and tip off. These diverse tests permitted to notice the efficiency of the titanium used directly as getter : the ageing process is very soft and does not make any metallic projection on the inner side of the bulb, that eliminated some possible defects (inter-electrode leakage, noxious capacitances).

Essais d'utilisation du titane comme fixateur de gaz

Parmi les métaux susceptibles de fixer les gaz résiduels des tubes électroniques, les plus couramment utilisés comme getters, non flashés sont :

— le zirconium,
— le tantale,
— le colombium ou le thorium, et
— le cérium,

employés en feuilles minces, en fils ou sous forme de poudre frittée sur un support.

Chacun de ces métaux est généralement actif surtout dans certaines gammes de températures propres à chacun d'eux et fixe sélectivement les gaz.

Aussi le choix technologique du getter à employer dans un tube déterminé est-il parfois relativement délicat à faire.

Devant les intéressantes propriétés du titane, on peut se demander quelles sont les possibilités de ce métal lorsqu'on l'introduit directement comme getter dans un tube électronique. Les essais très simples que nous allons décrire nous permettront de faire quelques remarques à ce sujet.

Rappelons, en premier lieu, brièvement, quelques-unes des propriétés de ce métal qui attirent particulièrement l'attention.

(1) L'affinité du titane est remarquable pour de nombreux gaz, notamment pour l'oxygène, l'azote, l'hydrogène, l'oxyde de carbone, le bioxyde de carbone etc., tous gaz que l'on rencontre couramment dans les tubes.

Ces gaz donnent non seulement des combinaisons chimiques en surface, mais ils pénètrent par solubilité dans le réseau du métal.

Ainsi à la température ordinaire, le titane se présente sous la forme de cristaux dont le réseau est du type hexagonal compact constituant la phase α. Au-dessus de 882°C, cette phase α se transforme en une phase β ayant un réseau cristallin du type cubique centré. Ces deux phases possèdent des propriétés physico-chimiques très particulières à l'égard des impuretés car elles ont des pouvoirs dissolvants en général très différents.

La phase α par exemple dissout en quantité appréciable l'azote et l'oxygène ainsi que 4 autres éléments (le bore, le cérium, le carbone et l'aluminium).

La phase β dissout l'hydrogène (ainsi que le molybdène, le tantale, le zirconium) et elle est facilement oxydable à haute température.

Ce qui du reste, nous intéresse surtout, c'est que les réactions chimiques qui peuvent intervenir sont le plus souvent irréversibles : ainsi les gaz, une fois fixés, ne sont généralement plus dégagés par la suite (exception faite toutefois pour l'hydrogène dans certaines conditions).

(2) Il est important de se souvenir également que la tension de vapeur du titane à haute température est très voisine de celle du nickel, mais nettement plus importante que celle du zirconium.

(3) Au point de vue des propriétés électriques, on remarque que la valeur de la résistivité dépend beaucoup de la présence d'impuretés dans le métal. Cependant, à la température ambiante, cette résistivité est voisine de 50 microohms/cm et atteint environ 150 microohms/cm au point de transformation allotropique. Le métal étant relativement résistant, on peut envisager de le chauffer par effet Joule sans difficulté, ce qui peut présenter un intérêt dans certains cas.

(4) Corrélativement, la conductivité thermique est faible ($-0{,}045$ cal/cm²/cm/S/°C à 20°) par rapport aux métaux

Vol.
10
1960

couramment utilisés, ce qui peut être gênant lorsqu'il s'agit de faire évacuer des calories, mais ce qui peut être utile lorsqu'on désire maintenir le métal à une certaine température.

(5) Le titane offre d'autre part, des propriétés mécaniques assez remarquables : sa mise en forme ne présente pas de grandes difficultés.

La phase α a un réseau cristallin hexagonal aplati qui possède 5 systèmes de plans de déformations possibles (2 systèmes de plans de glissement—3 systèmes de plans de mâcle) ce qui lui assure une grande ductilité.

La phase β stable au-dessus de 882°C est plastique et rend possible également d'importantes déformations.

Naturellement si le métal renferme des impuretés, les propriétés mécaniques peuvent être très perturbées. Par exemple, les éléments solubles dans la phase α font perdre généralement à celle-ci une partie de sa ductilité en la rendant fragile.

En fait, le titane s'emboutit et se forge plus facilement que la plupart des aciers, il se courbe sans difficulté, mais comme il est relativement élastique, des rayons de courbure déterminés paraissent cependant assez difficiles à obtenir avec des feuilles minces.

Dans nos essais, nous avons utilisé du titane commercialement pur, des Aciéries Electriques d'Ugine. Des nuances non alliées, fabriquées par ce fournisseur, nous avons choisi la nuance UT40 parce qu'elle est la plus ductile et qu'on peut facilement la mettre en forme à basse température. Nous disposions ainsi de plaques de titane de 0,4 mm d'épaisseur et de fil de 1 mm de diamètre. Pour les essais que nous envisagions, il était nécessaire de réaliser des pièces en tôle de titane de 0,15 à 0,12 mm d'épaisseur. Nous avons donc procédé à un laminage de la tôle de 0,4 mm afin de ramener son épaisseur aux valeurs désirées : le métal, fort écroui après ces opérations, était devenue fragile (faible allongement) et ne supportait plus que difficilement les déformations. On a donc cherché à restaurer ces tôles par des traitements de recuit. On sait que les recuits de ce genre doivent être réalisés en atmosphère d'argon ou sous vide et c'est cette dernière méthode que nous avons mise en oeuvre.

Divers essais nous ont montré que la température de recuit la plus avantageuse était de l'ordre de 700°C, la durée de l'opération étant de 30 min.

Nous avons remarqué que des températures supérieures à 800–850°C provoquaient une recristallisation rapide du métal en gros grains. Il était donc nécessaire de limiter la température du traitement pour conserver au métal une granulation fine qui rendait seule possible les fortes déformations ultérieures. D'autre part, on constatait qu'il n'était pas souhaitable de prolonger trop la durée du recuit, sinon la croissance des grains se manifestait également. En définitive, on a obtenu l'épaisseur voulue en deux séries de passes du laminoir suivies chacune d'un recuit sous vide de 30 min, à 700°C.

Avec ces tôles minces, nous avons réalisé des pièces présentant des nervures et fortement cambrées. Ajoutons que le soudage électrique des pièces se faisait très facilement par points.

Pour observer l'effet getter du titane, nous avons songé à remplacer dans des tubes de fabrication courante, le getter ordinairement utilisé (en l'occurence getter flash au baryum stabilisé) par une pièce en titane appropriée.

Le tube miniature tétrode 3B4 a été choisi pour ces essais pour des raisons simples : ce tube, par suite de ses caractéristiques poussées, était très sensible à une altération du vide en cours de fonctionnement ; d'autre part, des essais de fonctionnement du tube 3B4 standard étaient en cours, à l'époque où nous avons entrepris cette étude : il était donc relativement facile de suivre les résultats en fabrication.

Essais

Tubes 3B4 a anodes en titane

Les tubes 3B4 sont des tétrodes à faisceau dirigé dont les caractéristiques d'emploi en amplificateur de puissance HF et en oscillateur classe C télégraphie à modulation de fréquence sont résumées ci-dessous.

Tension d'anode	150 v. max
Tension de grille No. 1	−75 v.
Tension de grille No. 2	135 v.
Résistance en circuit-grille	100,000 ohms
Courant d'anode	25 mA
Courant grille No. 1	1,5 mA
Puissance appliquée à l'anode	3,75 w.
Puissance dissipée sur l'anode	3 w.
Puissance dissipée sur l'écran	1,1 w.

Les premiers essais ont consisté à équiper les tubes d'anode en titane, à les monter sans getter baryum, la présence du titane seule devant assurer l'élimination des gaz résiduels.

Les tubes expérimentés ont été pompés dans les conditions standard, puis après la coupe du queusot, on a chauffé par induction HF, les anodes à 950°C pendant 5 secondes, de façon à rendre actif le titane et à absorber ainsi les gaz résiduels.

On a procédé ensuite à la stabilisation d'émission dans les conditions ordinaires, puis les tubes ont été mis en essais de durée et on a relevé périodiquement les différentes caractéristiques.

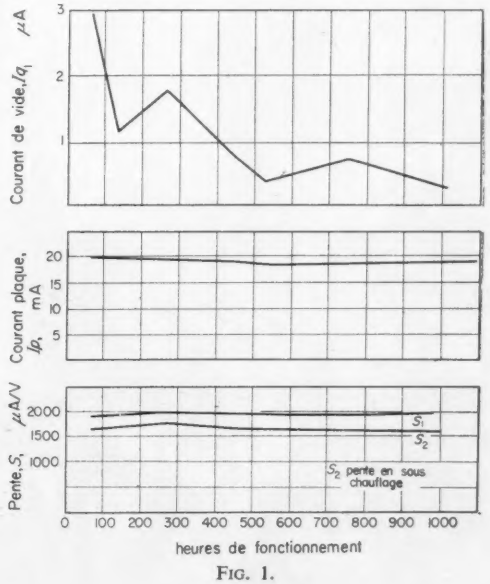

FIG. 1.

On trouve sur la Fig. 1 les valeurs du courant moyen de vide (courant inverse de grille) relevé sur une série de 15 tubes en fonction du temps. On remarque que le courant de vide a primitivement une valeur élevée, puis décroît avec quelques irrégularités jusqu'à 0,2μA—ce qui demeure une valeur acceptable mais relativement élevée. (Dans les tubes de fabrication courante, la valeur limite tolérée est de 1μA après 500 h de fonctionnement, mais la valeur moyenne est généralement très inférieure).

On observe que le courant plaque demeure constant au cours des essais.

Les pentes exprimées en μA/V :

S1, pente en chauffage normal,

S2, pente en sous-chauffage,

restent remarquablement stables, ce qui indique qu'au cours des 1000 h d'essais, l'émission est demeurée constante. D'ailleurs, ces pentes ont pratiquement les mêmes valeurs que celles des tubes standard.

Ainsi, on remarque que pour une émission bonne en durée, le courant de vide est relativement important, ce qui laisse supposer que les gaz résiduels, non absorbés dans ce cas, n'ont pas d'action néfaste sur la cathode. Et, en fonctionnement, les tubes n'ont pas évolué différemment des tubes standard.

Anneaux en titane

Le fait d'employer des anodes en titane permettrait assurément d'obtenir des tubes corrects en émission sans intervention d'autre getter, mais la réalisation de ces anodes serait assez délicate comme nous l'avons vu. Aussi, dans une seconde série d'essais, avons-nous cherché à remplacer les getters au baryum par une pièce en titane de forme plus simple. En particulier, nous avons réalisé des anneaux de 10 mm de diamètre environ avec du fil de titane UT40 de 1 mm de diamètre. Ces anneaux ont été préalablement dégazés sous vide (1200 °C) puis montés sur 3B4 à la place des getters au baryum.

Pendant le pompage de chacun des tubes, l'anneau a été dégazé à 1050 °C, puis après coupe du queusot, on a effectué un chauffage par induction HF à 900–950 °C (15 sec). Après les opérations de stabilisation de l'émission, les tubes ont été mis en essai de durée.

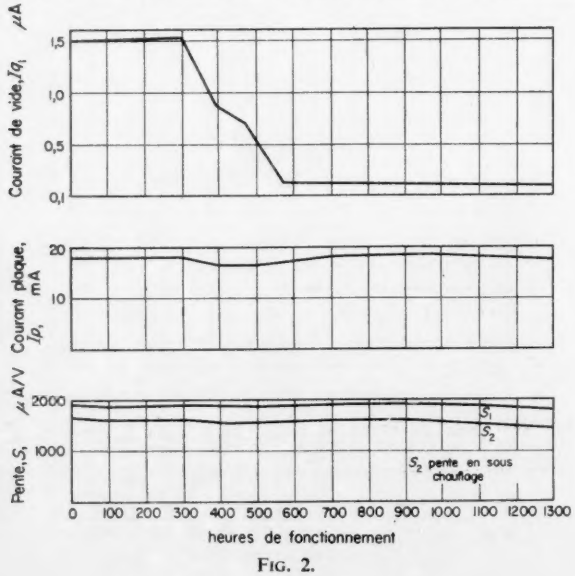

FIG. 2.

La Fig. 2 représente l'évolution du courant de vide, du courant anodique et des pentes S1 et S2 (normales et en sous-chauffage) obtenues en fonction du temps de fonctionnement. On observe que le courant de vide reste pratiquement constant pendant les premières heures de fonctionnement, puis décroît régulièrement, se fixe enfin aux environs de 0,1μA sans jamais s'annuler. Les diverses caractéristiques montrent, par ailleurs, que l'émission des tubes essayés demeure sensiblement constante et analogue à celle des tubes normaux. Ces résultats indiquent que les anneaux de titane permettent d'obtenir un vide suffisant pour que le fonctionnement des tubes 3B4 soit assuré.

Des essais de même nature ont été entrepris non pas avec des anneaux en fils de titane, mais avec de petits disques en tôle de 0,15 mm d'épaisseur et 10 mm de diamètre. Les résultats étaient tout à fait analogues.

Tubes oscillateurs subminiatures

A la suite des résultats précédents, nous avons cherché à utiliser le titane comme getter dans un tube oscillateur subminiature expérimental. Il s'agissait d'un tube de très petit volume à caractéristiques particulières qui devait notamment résister à des accélérations de 20.000 g. L'extrême réduction du volume de ces tubes rendait délicate la volatilisation d'un getter flash (fuites électriques, capacité parasite et décollement du miroir de baryum étaient à craindre). Les conditions de fonctionnement imposaient, par conséquent, une structure particulièrement robuste et rigide.

Les tubes ont été équipés d'anode en titane et montés sans aucun autre getter. Au cours du pompage, on a procédé à un dégazage des anodes par chauffage induction HF à 950 °C, puis après la coupe du queusot, on a chauffé à nouveau les anodes 10 secondes à 900 °C pour obtenir le meilleur vide. Après stabilisation, les mesures de vide ont montré que le courant inverse de grille ne dépassait pas 0,02μA. En fonctionnement, les tubes ont donné pleinement satisfaction.

Conclusion

En définitive, les essais mentionnés suggèrent les remarques suivantes :

En premier lieu, le titane présente des qualités qui autorisent son emploi comme getter sous les formes que nous venons de décrire :

— une tenue mécanique satisfaisante aux températures d'utilisation (rigidité),

— des propriétés électriques, magnétiques, thermiques intéressantes conduisant à un procédé d'activation du getter par chauffage par induction HF particulièrement souple,

— une tension de vapeur acceptable jusqu'à des températures relativement élevées, si bien que l'activation du getter ne provoque pas de projections métalliques sur les parois froides du tube ou sur les entretoises isolantes,

— les gaz résiduels paraissent fixés de manière généralement irréversible jusqu'aux températures de fonctionnement des tubes,

Vol. 10 196

— enfin, il est possible d'absorber des fuites virtuelles apparues en cours de fonctionnement des tubes par un simple chauffage de quelques secondes.

Par contre, l'emploi de ce métal paraît onéreux :

— le métal lui-même est relativement coûteux,
— comme il est oxydable à basse température, il convient de le protéger pendant les opérations de scellement des tubes électroniques par des insufflations d'argon, ce qui est coûteux,
— la mise en forme et l'emploi de ce métal réclament des traitements de dégazage et de recuit sous vide particulièrement soignés,
— enfin, on remarque dans les tubes essayés, un reliquat gazeux qui ne parait pas nocif pour la cathode, mais qui peut être gênant dans certaines applications.

En conclusion, on peut avancer qu'il n'est pas exclu d'utiliser le titane directement comme dégazeur sous les formes indiquées ; ces applications paraissent néanmoins se limiter à quelques cas spéciaux pour lesquels le métal peut présenter alors un intérêt technologique réel.

Bibliographie

[1] V. L. Stout and M. D. Gibbons ; *Gettering of Gas by Titanium, J. Appl. Phys.* **26**, No. 12 (1955).
[2] J. E. Beggs ; *The Use of Titanium in Vacuum Devices Transactions*, **3**, No. 2 (1956).
[3] R. de Vitry ; *Le Titane, Revue de Métallurgie* (Déc. 1956).
[4] F. Fourment ; *Quelques Généralités sur le Titane et sa Métallurgie, Soc. des Ingénieurs Civils de France* (Fév. 1957).
[5] A. D. MacQuillan and M. K. MacQuillan ; *Titanium*, Butterworths Scientific Publications (London) (1956).
[6] J. L. Everhart ; *Titanium, Metals in Design Engineering* **46**, No. 5 (1957).
[7] E. Pruvot ; *L'industrie de quelques métaux nouveaux, Société Française des Electriciens* No. 97 (Janv. 1959).

ol.
10
960

The Ceto Getter—its Chemical Structure and Hydrogen Gettering Properties

J. H. N. VAN VUCHT

Philips Research Laboratories, N.V. Philips' Gloeilampenfabrieken, Eindhoven, Netherlands

Ceto, which is an alloy of thorium, mischmetall and aluminium is used as a non-evaporating getter. In the course of an elaborate investigation of the ternary system Th–Ce–Al, it has been proved that its crystallographic structure is of the $CuAl_2$ type, just like the closely related binary compound Th_2Al. The properties of the Th_2Al, Ceto and intermediate compounds with regard to hydrogen were studied. X-ray and neutron diffraction, supplemented by nuclear magnetic resonance measurements, each at liquid nitrogen temperature, and room temperature, gave information about the structure of the reaction products. Hydrogen equilibrium-pressure measurements at temperatures from 250°C up to 700°C gave thermodynamic information and enabled to calculate the equilibrium pressures at lower temperatures. A kinetic study, based on a simple model, of an autocatalytic sorption is reported.

Introduction

For some time the non-evaporating getter Ceto[1] has been the subject of an elaborate fundamental investigation in our laboratories. This getter has excellent properties and it was hoped that some of them, as well as the role which was played by each constituent, could be understood on the grounds of its chemical structure.

The structure of Ceto

The getter consists of a quaternary alloy. It is made by

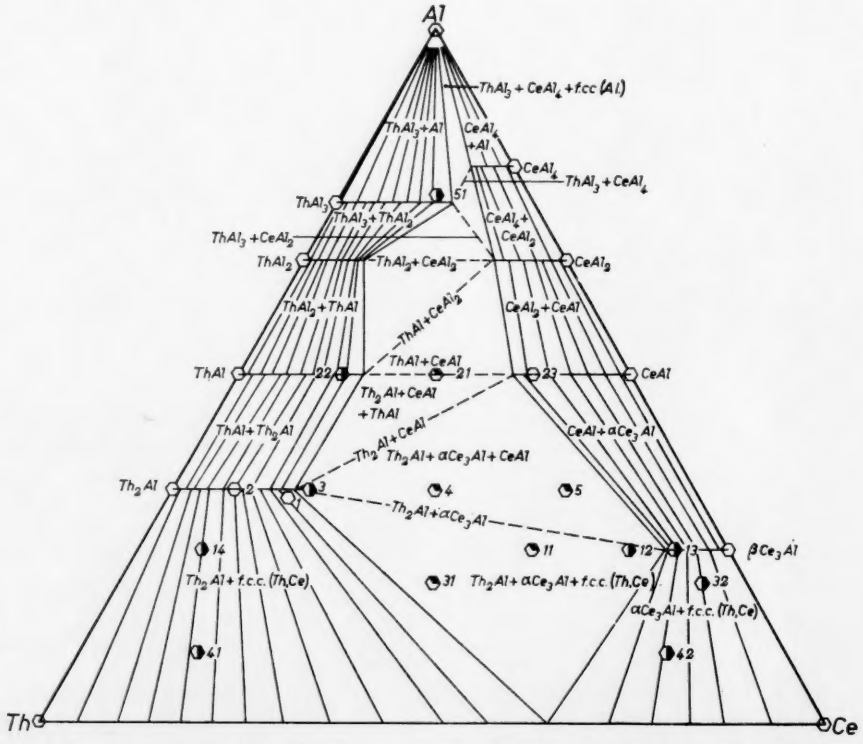

FIG. 1. Ternary system Th–Ce–Al. Tentative diagram at 500°C. For the range of stability of α and βCe_3Al see van Vucht 1960 (to be published).

sintering a mixture of thorium powder and a powdered alloy called *Ceral* at 900°C in vacuum. This *Ceral* consists of Cermischmetall (80 per cent cerium, 20 per cent lanthanum) and aluminium, and has the chemical composition $(Ce,La)Al_2$. The total getter composition (in atoms) is about

10 Th, 2.5 Ce, 0.5 La, 6 Al.

A possible determination of the chemical structure meant the examination of the quaternary system Th–Ce–La–Al. It proved, however, a great simplification that a getter with exactly the same properties could be obtained if the mischmetall was replaced by pure cerium. So the quaternary system could be reduced to a ternary one :

Th–Ce–Al.

With the help of X-ray analysis and metallographical and thermo-analytical methods it was possible to determine most of the phases in this system. The results with respect to the binary systems have been published before and were confirmed by the work of others[2–7]. The total result is, briefly, given by Fig. 1. Here the Ceto composition has got the number 1. It is seen that its structure, practically for 95 per cent, is isomorphous with that of Th_2Al, the neighbouring binary compound. Th_2Al is tetragonal with $a = 7.616$ Å and $c = 5.861$ Å. So is Ceto with $a = 7.606$ Å and $c = 5.860$ Å. The structure of both compounds is of the $CuAl_2$-type. The only difference between the two atomic structures is that the thorium atoms in Th_2Al are replaced by a very probably random mixture of thorium and cerium atoms (in a ratio of about 10 : 3).

The system Th_2Al–H_2 ; introduction

Most of the work in connexion with the hydrogen gettering properties was done on the binary compound Th_2Al, as it is the simpler and better defined one. At several points, however, the influence of substituting thorium by increasing amounts of cerium has been checked. It was found that the behaviour of the getter did not change essentially by this substitution. Therefore in this report our communications will be confined to results of the system Th_2Al–H_2. They concern the reaction products of hydrogen with the metal, the conduct of hydrogen in the metal and finally the reaction from the kinetic point of view. The techniques used in our work shall not be described extensively here. A fully detailed report will appear elsewhere in the near future.

The atomic structure of Th_2Al

As is commonly known hydrogen often forms interstitial solutions or compounds with metals. Therefore it will be worthwhile to study the packing of atoms in the Th_2Al structure. Fig. 2 shows, next to a basal plane projection, the configuration of the thorium atoms in perspective. From this picture it is easily seen that the places where the hydrogen atoms are most likely to be located can be divided in two kinds of tetrahedral holes. Per unit cell, that is per Th_8Al_4 there are sixteen sites of one kind (crystallographically equivalent). They are located in tetrahedra that are coupled two and two together by joining their base (" double holes ").

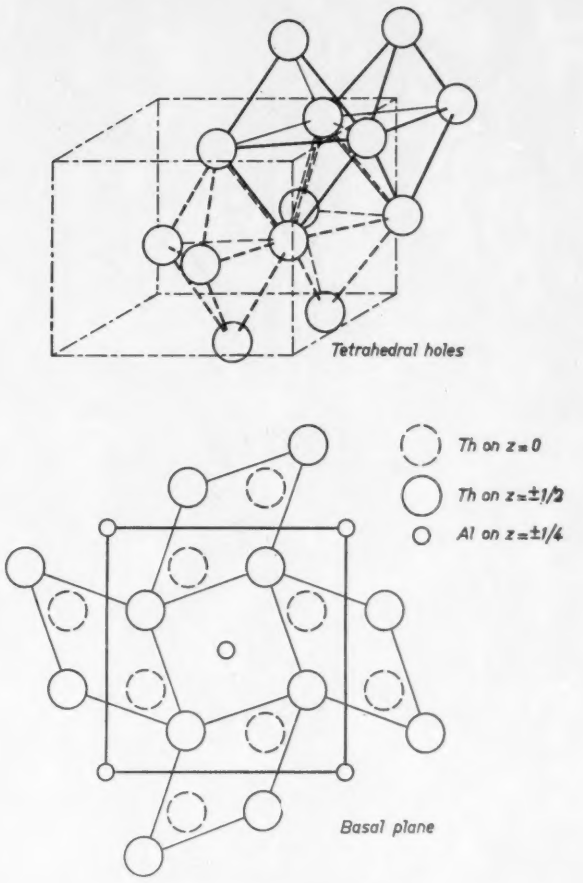

FIG. 2. Crystal structure of Th_2Al.

Their position is $(x, \frac{1}{2}+x, \pm z)$, $(\frac{1}{2}+x, \bar{x}, \pm z)$, $(\bar{x}, \frac{1}{2}-x, \pm z)$ $(\frac{1}{2}-x, x, \pm z)$ $(\frac{1}{2}+x, x, \frac{1}{2}\pm z)$, $(x, \frac{1}{2}-x, \frac{1}{2}\pm z)$, $(\frac{1}{2}-x, \bar{x}, \frac{1}{2}\pm z)$, $(\bar{x}, \frac{1}{2}+x, \frac{1}{2}\pm z)$.

Furthermore we notice 4 tetrahedral holes

$\pm(\frac{1}{2}, 0, \frac{1}{4})$ and $\pm(0, \frac{1}{2}, \frac{1}{4})$.

With the thoriums in their proper positions (Fig. 2 is somewhat idealized), they are rather narrow, compared to the sixteen holes first mentioned.

Hydrogen equilibrium pressure isotherms

One of the techniques used for determining which compounds are formed and how stable the reaction products are is the technique, already applied by Sieverts, of measuring equilibrium pressure isotherms. In our case a very simple apparatus was used with a volume of ca 1.5 l. In this volume the hydrogen equilibrium pressure was measured with the help of a Pirani manometer above 200 mg of finely crushed (grain size $< 35\ \mu$)Th_2Al powder. The isotherms obtained are shown in Fig. 3. There are several remarkable points in this figure. First of all we find as an ultimate H content of the metal a number very near to sixteen H atoms per unit cell. Near to this value the equilibrium pressures rise very rapidly to values that exceed one atmosphere. Secondly the isotherms have no plateau. This is an indication that—at these temperatures—no two phase region exists. On the

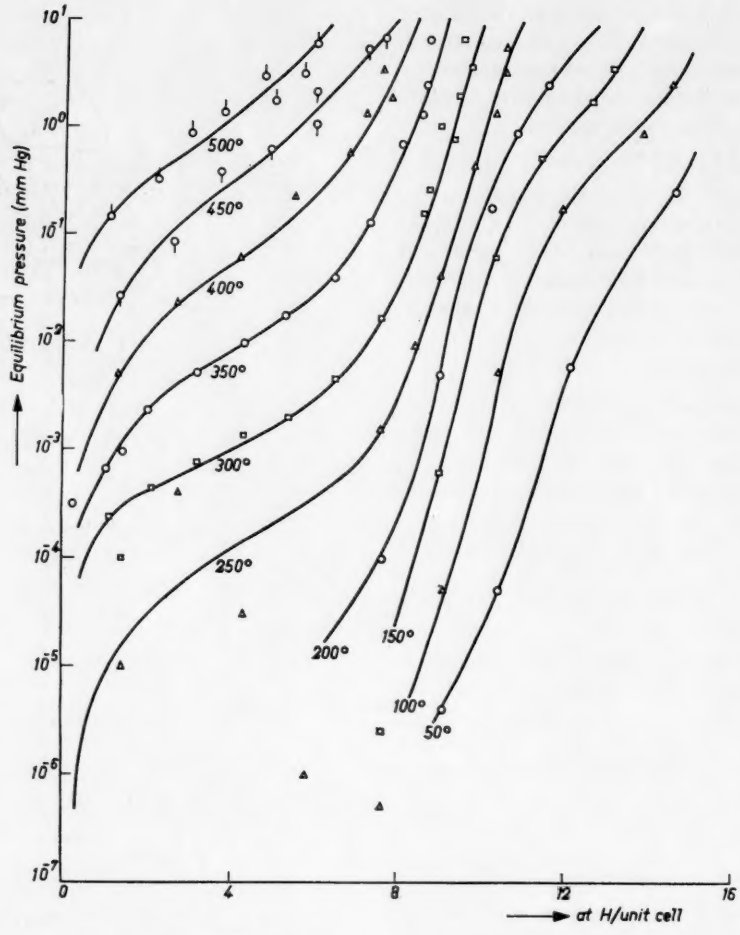

FIG. 3. Isotherms of the equilibrium pressure of hydrogen above Th_2Al.

contrary, up to an H content of ca. 4 per unit cell the behaviour of hydrogen in the metal must be very ideal for the pressure isotherms follow the law

$$C_H = K\sqrt{p_{H_2}}$$

where C_H is the hydrogen concentration in the getter metal. For the 400 °C isotherm this is shown in Fig. 4. The existence, however, of the point of inflexion in the isotherms at the concentration of about $4H$/unit cell might be an indication that at lower temperatures a two phase region occurs. A similar point of inflexion is seen at the composition $Th_8Al_4H_{12}$.

The set of isotherms can give us thermodynamical data as well. In Fig. 5 $\ln p$ has been plotted versus $1/T$ for three different H concentrations. The slopes of the lines give the heat of solution of one mole H_2 into the metal (at constant H content). Apparently the heat of solution increases with hydrogen content. Again this is an indication that at lower temperatures a two-phase region may appear. Furthermore it is possible from these lines to determine the equilibrium hydrogen pressure (in the thermodynamical sense). Thus an extrapolation to room temperature of the line for $Th_8Al_4H_4$ leads to an equilibrium pressure of 10^{-13} Torr. This pressure will never be reached however, mainly because of inhibiting effects of preferentially adsorbed surface-deteriorating gases.

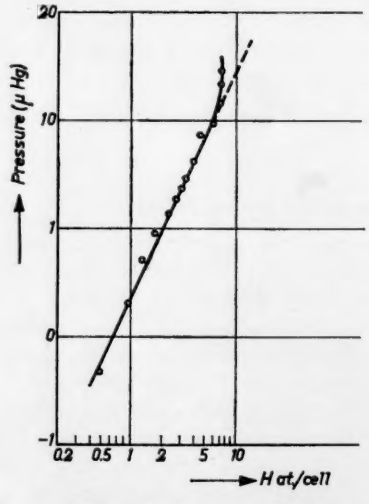

FIG. 4. The 400 °C isotherm on a log-log scale.

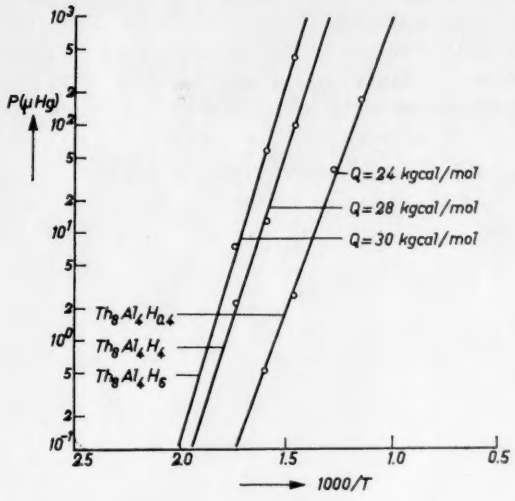

FIG. 5. Equilibrium pressures (logarithmic) versus 1000/T in the system Th_2Al–H_2.

X-ray investigations

Powder specimens of Th_2Al, loaded with increasing amounts of hydrogen were investigated with X-rays. The specimens weighed 500 mg and were carefully homogenized after the hydrogen was sorbed. Then they were protected by coating them with a solution of acetyl cellulose in dried acetone, without exposing them to air. After that the powder was taken out of the sorption apparatus and prepared in the normal way for room temperature X-ray diffraction on a Philips Diffractometer. The diagrams obtained were quite satisfactory and could easily be indexed. Most of them showed one phase. Only between the concentrations H_0 and H_6 two phases were found, isostructural (with respect to Th and Al) but differing in lattice parameters. In this two-phase region an increase of the H content of the specimen resulted only in a diminution of the H_0-phase lines and an amplification of the H_6-phase lines. The results of the X-ray work are compiled in Fig. 6. Obviously one of the two-phase regions, which were presumed on the grounds of the isotherm measurements, does exist at room temp. The critical temperature must lie between room temperature and 250°C. The point of inflexion in the curves at H_4 (Fig. 3) above this temperature thus proves to be a reliable indication.

The second remarkable point in Fig. 6 is the anomality in the distortion of the tetragonal unit cell in the *a* direction, occurring exactly at the composition H_8. It is intriguing that exactly the half-filled cell should have the longest *a*-axis. One might think of an ordering of H atoms. Certainly it is a new valuable indication for the existence of a second phase, having the ideal composition $Th_8Al_4H_8$ and showing a widening region of homogeneity at rising temperatures.

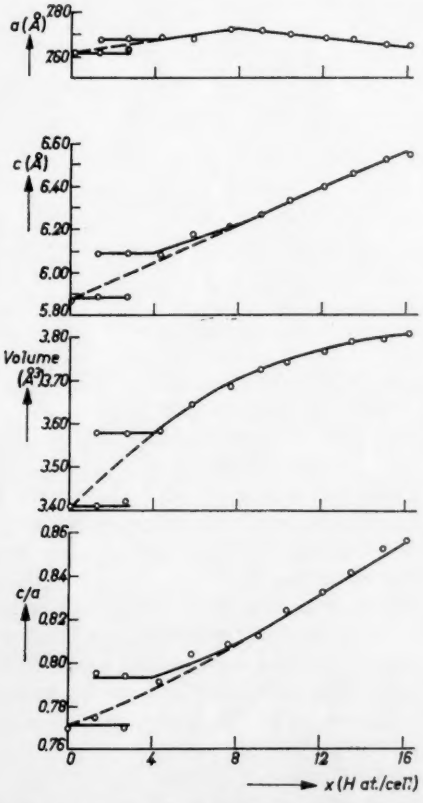

FIG. 6. Cell dimensions as a function of hydrogen content of Th_2Al at room temperature.

Neutron diffraction experiments

Since with X-ray diffraction it is impossible to locate exactly the hydrogen atoms in our metal powders, neutron diffraction was used in an attempt to solve this problem. Because hydrogen scatters neutrons incoherently we made specimens containing deuterium. The diffraction measurements were carried out in Kjeller (Norway) at the J.E.E.P. reactor in co-operation with J. A. Goedkoop, B. Loopstra and J. Bergsma. Before long a detailed report of this work will be published, but in the meantime a short survey of the results is given here.

The powder specimens used weighed about 25 grams and were of the compositions $Th_8Al_4D_8$, $Th_8Al_4D_{12}$ and $Th_8Al_4D_{16}$, lying each in the single-phase region at room temperature. The diagrams obtained are shown in Fig. 8. For comparison the X-ray diagrams for the corresponding H compositions are given in Fig. 7 It is seen clearly that in the X-ray diagrams the increase in hydrogen only effects a line shift due to the lattice expansion. The intensities of the reflections are unchanged. In the neutron diffraction diagrams, however, there is not only a line shift but (more important) a big change in intensity, due to the scattering power of the deuterium atoms. These observed intensities agreed fairly well with the calculated ones for a random distribution of the deuterons over the sixteen positions in the " coupled tetrahedra " (in $Th_8Al_4D_{16}$ all positions are occupied).

On the one hand this result concurred with our experience that sixteen was the maximum number of hydrogen atoms sorbed per cell. On the other hand a random distribution of protons in the half-filled interstitial lattice could not explain the behaviour of the *a* dimension of the unit cell.

However there are a few types of partial order that are not distinguishable from total randomness by diffraction, e.g. the situation that each double hole contains one proton, but this proton has equal chances to be in the upper or the lower part, or the situation that doubly filled " double holes " and totally empty " double holes " are mixed at random. These partial order types give only rise to weak effects in the diffuse background. Moreover a short range order is not detectable in this way as well.

In order to make a possible order grow more distinct a diffraction diagram of $Th_8Al_4D_8$ at $-190°C$ was taken. This diagram differed only in minor details from the one taken at room temperature, and left no room for configurations otherwise than random with the restrictions mentioned before.

Nuclear magnetic resonance

More information we tried to get from nuclear magnetic resonance measurements. This work was done in co-operation with D. Kroon and C. v. d. Stolpe[8]. Because of the expected skin effect our powder specimens of about 10 grams were diluted with fine dry quartz powder, thus isolating the metal grains from each other.

At room temperature the resonance lines of the compositions $Th_8Al_4H_8$ and $Th_8Al_4H_{12}$ were very narrow. This may be explained by a " motional narrowing " effect.

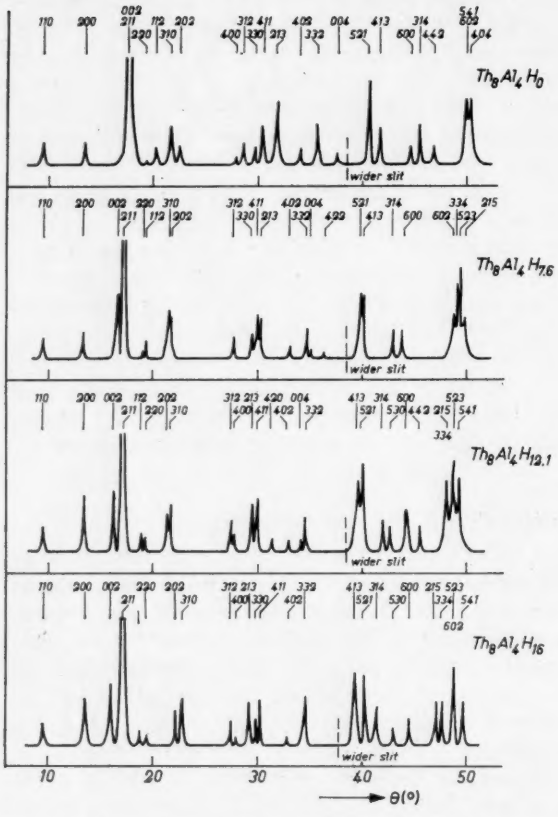

FIG. 7. X-ray diagrams of Th_2Al and three different hydrogen containing compositions.

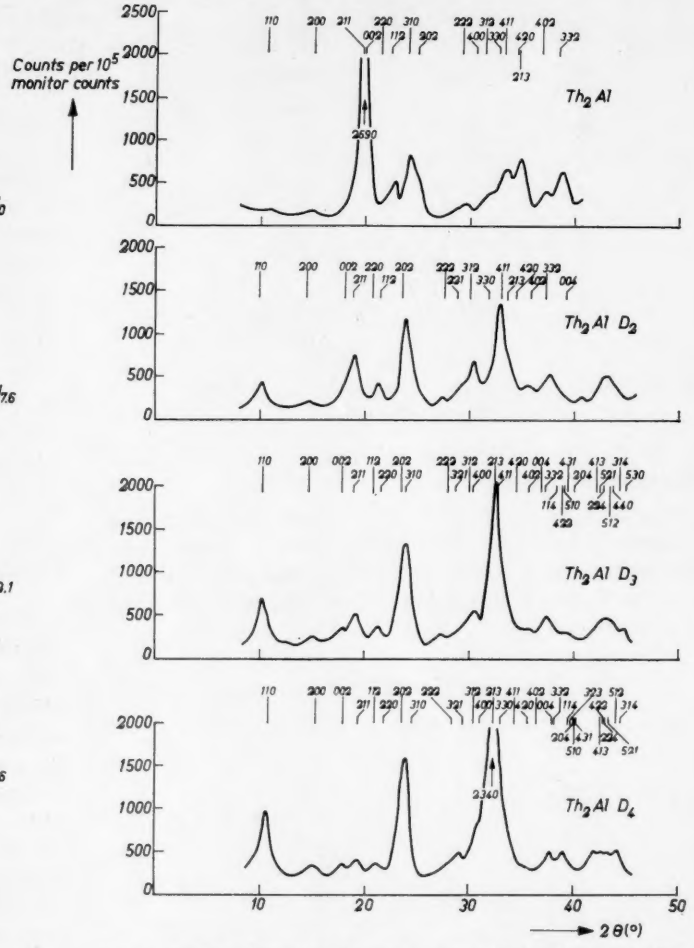

FIG. 8. Neutron-diffraction diagrams of Th_2Al and the corresponding deuterium containing compositions of Fig. 7.

The protons are moving from interstice to interstice in a time short compared to the characteristic time for the spin-spin magnetic interaction in this substance. By reducing the number of " interstitial vacancies ", as is done by saturation of the metal with hydrogen in $Th_8Al_4H_{16}$, or with a mixture of equal amounts of hydrogen and deuterium in $Th_8Al_4H_8D_8$, we are able to restrain the translations. Consequently a broadened resonance line is observed at room temperature for these compositions. The measured second moments S_2 (the mean square widths) of these lines agreed well with the calculated ones, if we used the positions found by neutron diffraction for $Th_8Al_4D_{16}$. The second moment of $Th_8Al_4H_8D_8$ agreed with the assumption of a random mixture of protons and deuterons.

Going to low temperatures the mobility of protons can be reduced even in partially filled lattices. This is shown in Fig. 9 for $Th_8Al_4H_8$. A similar behaviour was found for

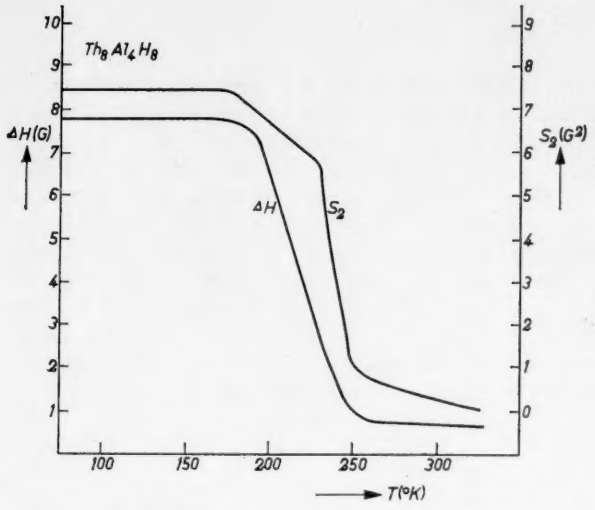

FIG. 9. Nuclear magnetic resonance. Line width ΔH and second moment S_2 versus temperature for $Th_8Al_4H_8$.

$Th_8Al_4H_{12}$. However, there was a difference. In the case of $Th_8Al_4H_8$ the high-temperature narrow line gradually broadened when the temperature was lowered, whereas in the case of $Th_8Al_4H_{12}$ the intensity of the narrow line decreased, while at the same time a broad line appeared (see Fig. 10).

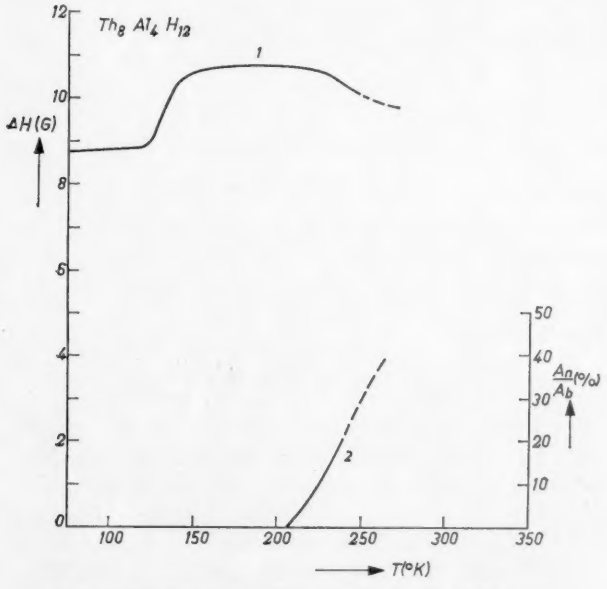

FIG. 10. Nuclear magnetic resonance for $Th_8Al_4H_{12}$.

1. Line width ΔH versus temperature.
2. Ratio of the integrated areas of the narrow (A_n) and broad (A_b) lines versus temperature.

Apparently $Th_8Al_4H_{12}$ was segregating at this temperature, splitting up in two phases, one with the broad line and one with the slowly widening line. These might be the phases $Th_8Al_4H_8$ and $Th_8Al_4H_{16}$, which is a reasonable supposition in view of the observed points of inflexion in the isotherms. We tried to confirm this by low-temperature (−190°C) X-ray diffraction, but we did not find a new two-phase region.

The resonance line of $Th_8Al_4H_8$ started to broaden at 250°K (Fig. 9). Below 230°K the second moment of the line changed slowly from 5 Gauss^2 to about 8 Gauss^2 at 170°K. Below 170°K the lines showed a remarkable flat top. This line shape is characteristic for resonance of a two-proton system or may be for a four-proton system. Anyhow this should mean that, at 170°K and lower some kind of order is present. The value of S_2 does not agree with a configuration where " double holes " are doubly filled. So all what can be said is that the nuclear magnetic resonance results for $Th_8Al_4H_8$ and $Th_8Al_4H_{12}$ at lower temperatures are not in accordance with the conclusions drawn from low temperature diffraction work on $Th_8Al_4D_8$ with neutrons and on $Th_8Al_4H_{12}$ with X-rays. There is, however, not necessarily a contradiction between them, for we have to bear in mind that the proton resonance method only gives short-range information, whereas diffraction work typically gives long-range information. In fact we might see this as a demonstration of how the two methods are supplementary to each other.

Kinetics of the reaction Th_2Al–H_2; autocatalysis

Besides the work, which substantially concerned static problems, kinetic experiments were done. An interesting phenomenon was the autocatalytic sorption of hydrogen.

The crushed Th_2Al as such generally is inactive at room temperature. This is quite naturally, for, unless very strong precautions have been taken, the surface of the getter particles will be covered by a protecting layer of e.g. the very stable oxides. The getter can be activated by heating it in vacuo at about 900°C. After subsequent cooling, a 200 mg powder specimen sorbs more than 20 Torr litre hydrogen within half a minute at room temperature. This activity can be destroyed very easily by deteriorating the surface with " poisoning " gases, as there are oxygen, water vapour, CO_2, CO and nitrogen.

If an activated specimen of Th_2Al is deliberately de-

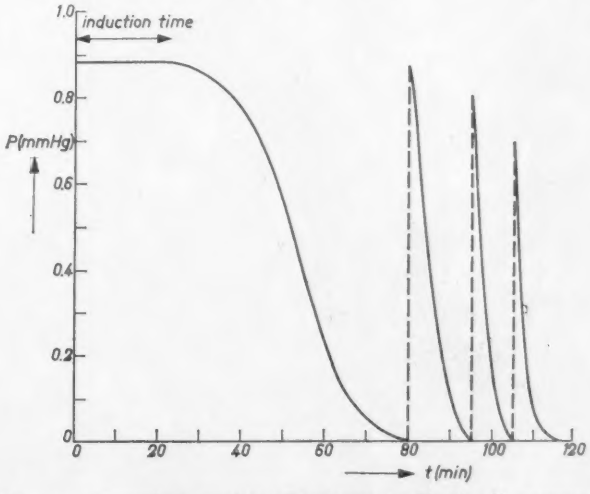

FIG. 11. Autocatalytic sorption of hydrogen by Th_2Al. H_2-pressure in a constant volume versus time.

activated by exposing it to 5 mm of oxygen at room temperature during 10 min, the sorption rate of hydrogen (after removing the oxygen) has become immeasurably small. After about 30 min, however, a slow sorption sets in, its rate growing until about half of the gas is sorbed. Then it slows down again. This behaviour is shown in Fig. 11. Here p_{H_2} (in a constant volume) is plotted against time. A new amount of hydrogen admitted is sorbed much quicker. This can be repeated several times.

This phenomenon might be explained in the following way. The deliberately caused inactivity is due to a surface layer of oxide. The layer is very thin (of the order of a few monolayers). The hydrogen can only pass through it very slowly (whether because of imperfections as microcracks, or because of the atomic structure). If some hydrogen gets through, however, the underlying metal expands (in our case anisotropically). The protecting skin is stretched until cracks arise. Then the hydrogen is able to pour through these cracks, causing the metal to expand at a greater rate and thus the skin to produce more failures. In this way a self-accelerating sorption results. The reaction has to slow down in the end by lack of hydrogen, which indicates a certain pressure dependence.

On the basis of this model we tried to analyse the series of sorption curves of Fig. 11. In our picture

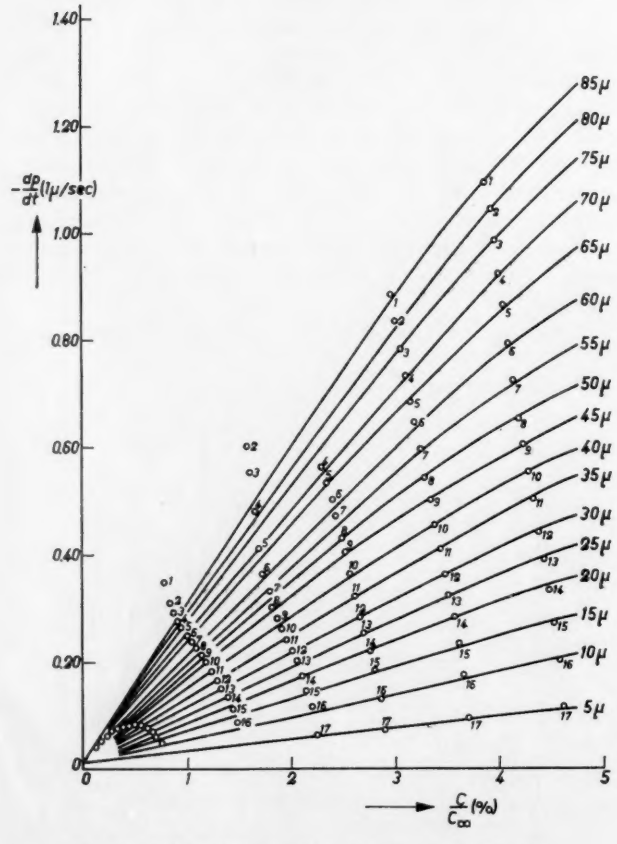

FIG. 12. Autocatalytic sorption of hydrogen by Th_2Al. $-dp/dt$ versus c/c_∞ at various pressure values.

$$-\frac{dp}{dt} = f(\omega) \cdot f'(p)$$

where ω is the active surface area, which is a function of the amount of hydrogen already sorbed at time t. We can take $-dp/dt$ for constant pressure values in a series of sorption curves such as in Fig. 11 and plot them against the amount of hydrogen taken up already. Thus we get a bundle of lines, coming from one point on the $-dp/dt$ axis (Fig. 12). By looking in this figure at a constant hydrogen concentration in the metal and plotting the $-dp/dt$ values versus the corresponding p values on a log–log scale (Fig. 13) we find that the hydrogen sorption rate is linearly dependent on the pressure above the getter. This result is not surprising and makes the model used more acceptable.

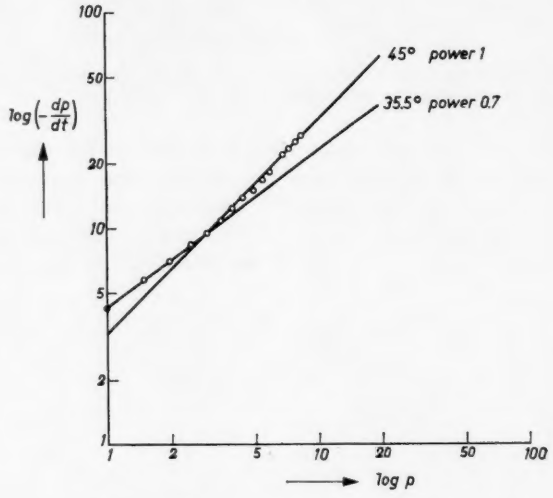

FIG. 13. Autocatalytic sorption of hydrogen by Th_2Al. $-dp/dt$ versus pressure at $c/c_\infty = 3.6$ per cent.

Conclusion

Summarizing our results concerning the behaviour of hydrogen in Th_2Al we can state the following. At temperatures of 300 °C and higher and at concentrations up to 4H/unit cell the dissolved hydrogen atoms behave ideally. Yet there exists a slight attraction between them, which results in a two phase region at room temperature between $Th_8Al_4H_0$ and $Th_8Al_4H_8$. There are indications that $Th_8Al_4H_8$ is a separate compound next to $Th_8Al_4H_{16}$, the maximum hydrogen containing composition. At room temperature where protons move very rapidly in the lattice they form an uninterrupted series of solid solutions. At lower temperatures nuclear magnetic resonance experiments give reason to believe that on a very small scale two phases are mixed. Moreover they give arguments for an ordering of H atoms in the interstitial lattice to pairs or quartets at lower temperature. This could not be confirmed with neutron diffraction on deuterium compounds.

We are trying now to complete this picture by measuring the specific heats of the various compositions, going from

liquid nitrogen temperature to room temperature, and by measuring their paramagnetic susceptibility. The results of these investigations will be reported in due time.

Acknowledgement

I want to express my thanks to all who have co-operated in this work and especially to my assistants P. Colijn, J. Pegels and J. M. Bogaard.

References

1 W. Espe, M. Knoll, and M. P. Wilder ; *Electronics* **23**, 80 (1950).
2 P. B. Braun and J. H. N. van Vucht ; *Acta Cryst.* **8**, 117 (1955).
3 P. B. Braun and J. H. N. van Vucht ; *Acta Cryst.* **8**, 246 (1955).
4 J. R. Murray ; *J. Inst. Metals* **84**, 92–96 (1955).
5 J. H. N. van Vucht ; *Z. Metallk.* **48**, 253–258 (1957).
6 J. H. N. van Vucht ; *Philips Res. Rep.* **12**, 351–354 (1957).
7 R. T. Weiner, W. E. Freeth, and G. V. Raynor ; *J. Inst. Metals* **86**, 185–188 (1957).
8 D. J. Kroon, C. v. d. Stolpe, and J. H. N. van Vucht ; *Archives des Sciences, Genève* **12**, fasc. spéc., 156–160 (1959).

ol.
10
960

Gettering Activity of Zr, Ti and Ba for Oxygen Gas under the Mercury Vapour

S. FUKAGAWA

Japan Radio Co. Ltd., Mitaka, Tokyo, Japan

The absorbability of oxygen gas in barium, titanium and zirconium is known, but when mercury vapour is simultaneously present this influences seriously the absorbability of oxygen gas in Mercury Vapour Hot Cathode Tubes containing mercury vapour. An easy method for the measuring of getter activity in oxygen gas under mercury vapour is to measure the electrical conductivity of the oxide layer of the oxide cathode. This is that the oxide cathode itself is a semiconductor of excess Ba metal type, and the comparison relation with the pressure of its exterior oxygen (in this case oxygen inside the tube) has been utilized. For this purpose, an oxide part has been coated over the pure nickel sleeve, and over this a pure nickel wire is wound as a probe. The electrical conductivity of these two poles is measured at a regulated temperature. The mixed oxygen and mercury vapour inside the tube is measured by the increase-decrease of oxygen. By this method, the absorbability of oxygen has no change in titanium and zirconium even in presence of mercury vapour, but in regard to barium, in presence of mercury vapour, this latter amalgamates with mercury vapour and thus the previously absorbed oxygen is freed.

Vol. 10 1960

THE life of mercury vapour hot cathode electron tube is greatly shortened by even an exceedingly small amount of residual gases. The reason is due to the fact that the oxide cathode is deactivated by mainly oxygen and other gases.

Therefore, it is desirable to use a getter which will absorb oxygen and other gases in case of the mercury vapour being used. We have conducted many experiments for this purpose, by measuring the gettering actions of barium, titanium and zirconium metals against oxygen gas. These experiments were performed a few years ago[1], but as I believe that the measuring methods adopted in that test have much interest even now, I have decided to explain it again.

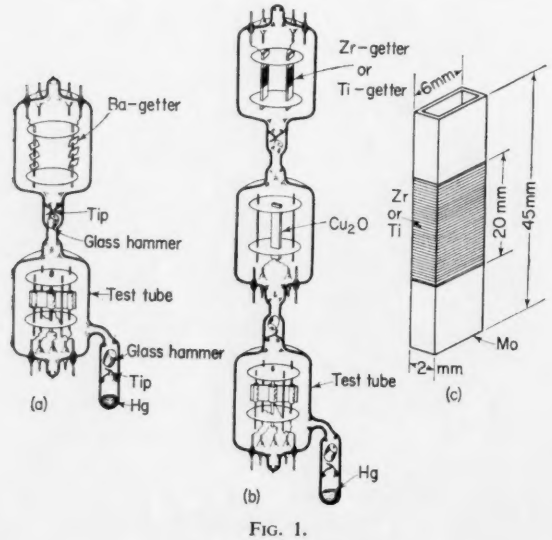

FIG. 1.

Experimental test tubes are shown in Fig. 1. They are assembled in 3 chambers including each mercury, oxide cathode and gettering metal, and constructed so that chambers can be mutually connected by breaking the partition walls as required. Also, a chamber having Cu_2O is assembled-in so that oxygen gas can be inserted. In Fig. 1, (a) is in the case of Ba-getter, (b) is in the case of Zr- and Ti-getter. In this case Zr and Ti are coated on the surface of molybdenum rectangular tube shown in (c) and these temperatures are controlled by a filament inserted in the tube. In Fig. 2, geometrical dimensions of oxide cathode inside of cathode probe tubes have been entered. The chamber with mercury is heated or cooled from the exterior and thus the temperature of mercury is kept at desired degrees, while the exterior surroundings of test tube as a whole are kept at 100°C during the measurements. The cathode oxide paste is made from the ordinary triple carbonate $(Ba\text{–}Si\text{–}Ca)(CO_3)_2$ and is coated on the pure nickel sleeve. On the surface, a same quality pure nickel wire (dia. 0.02 mm) is wound as a probe. The electrical conductivity of the oxide cathode is measured by the electric current when cathode temperature is kept at 970°K and a voltage of + 5V is applied to the probe on the cathode. In the exterior of the cathode, a cylindrical anode for current ageing was arranged.

As the oxide paste is a semi-conductor, the electrical conductivity should change according to degree of activity and temperature of cathode. The cathode emissivity change greatly, proportional to the amount of oxygen gas, and reversible, and simultaneously the emissivity is followed by the change of electical conductivity of its oxide layer. We

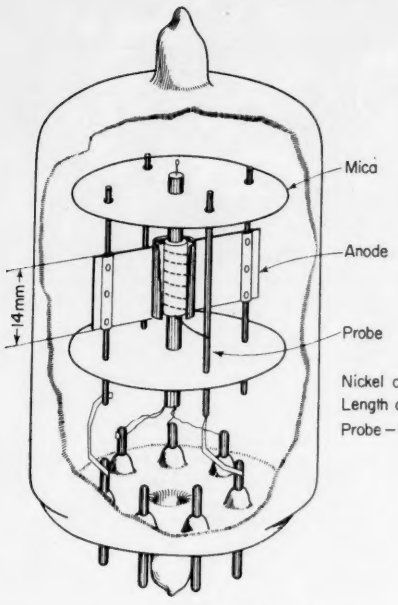

FIG. 2.

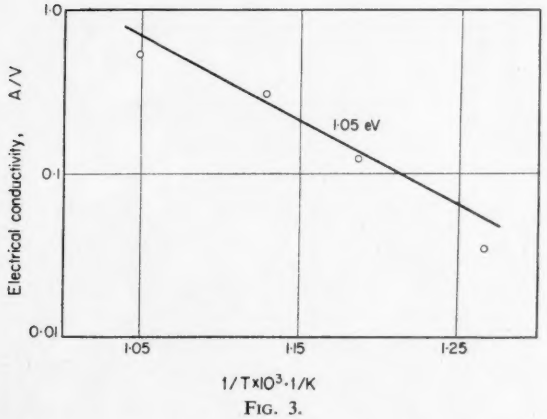

FIG. 3.

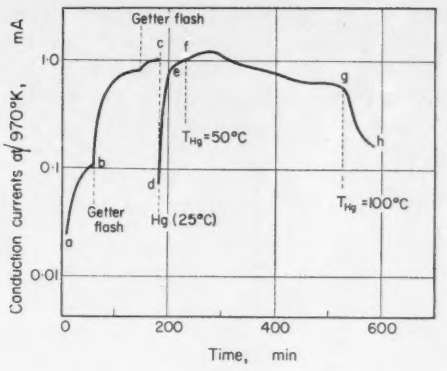

FIG. 4.

to the penetration of residual gases along with mercury vapour from the mercury chamber. But conductivity is soon restored, thus *d–e* curve is recorded. When mercury is heated to 50°C saturated vapour (2.5×10^{-3} Torr), the conductivity is decreased and it is observed that Ba-getter mirror is turned white from the rim.

If mercury is heated to 100°C at *g* point, it becomes mercury vapour of 0.25 Torr and at the same time conductivity is decreased more rapidly (curve *g–h*).

(b) Fig. 5 shows the course observed when mercury

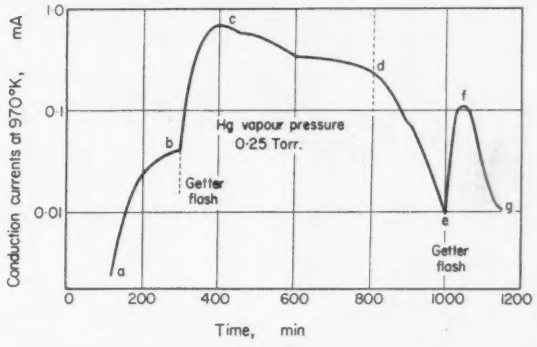

FIG. 5.

have shown in Fig. 3 as an example of our experiments the characteristic changes of the electrical conductivity of cathode against temperature. According to our several measurements by this method, the activation energy for conductivity were 1.9–0.98eV for 800–950°C. These values are the same as experimented by Dr. R. Loosjes[2] and Dr. D. A. Wright[3].

(1) *Barium Getter under the Mercury Vapour*

(a) The course of oxide layer being activated by the thermal activation in the high vacuum is shown as the conductivity curve *a–b* in Fig. 4. At the point *b* this curve is nearly saturated and it shows that cathode activity is in state of equilibrium with residual gases in the tube.

At this point the partition wall to a getter room flashed with Ba-getter is broken. Then residual gases are absorbed by Ba-getter deposited and conductivity is increased and at a certain point this increasing stops. And when Ba-getter is flashed once more, the curve *b–c* is obtained. At this *c* point the partition wall to the mercury chamber is broken and the conductivity of oxide layer is decreased instantly due vapour of 0.25 Torr is included from the first. Thermal activation is imposed at first and the curve *a–b* is obtained. At *b* point Ba-getter is flashed. Conductivity rises up to *c* point and then it begins to drop. At *d* point cathode temperature is reduced to 1000°K and AC voltage is applied to anode through its mean current of 56 mA/cm², and then conductivity is decreased more and more rapidly. When Ba-getter is flashed again at *e* point, conductivity rises temporarily up to *f* point, but soon drops as *f–g*. It is supposed that amalgam with Ba-getter mirror has been made more actively due to the existence of mercury ions and metastable excited mercury atoms resulted from discharging at *d–e* and also *f–g* curves.

And in both cases, Ba-getter mirror amalgamated with mercury gradually releases oxygen which was absorbed once. Namely, under the existence of mercury vapour barium cannot keep its activity as " getter ". Even if at the moment of flashing the activity is extremely high, oxygen is released gradually as amalgamation proceeds, when Ba is exposed to mercury vapour for long time.

(2) *Titanium and Zirconium under the Mercury Vapour*

The absorption characteristics of the titanium and zirconium for many kinds of gases are shown in Fig. 6[4] and Fig. 7[5]. They show that for oxygen the physical absorption

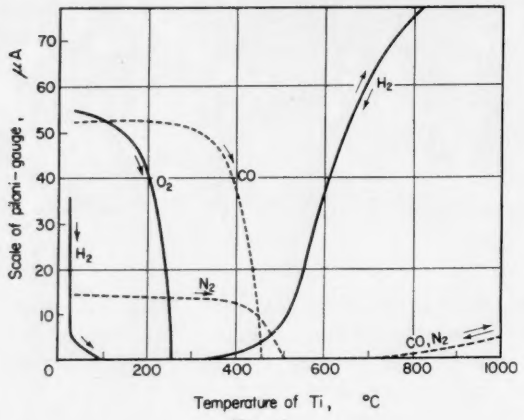

FIG. 6.

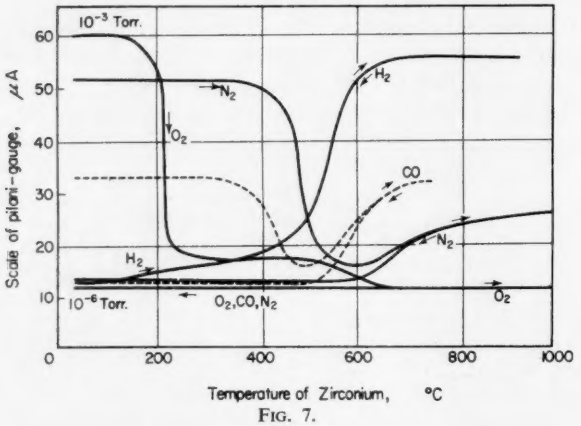

FIG. 7.

of one or two atomic layers on the surface appears within the temperature range of less than 180°C. But beyond this temperature, the diffusion of the oxygen atoms into the metals occurs, and such activities become stronger as the temperature rises higher. Differing with any other gases such as H_2, CO or N_2, oxygen which was absorbed once cannot be released at any temperature.

A problem arises whether any change in the character would be observed under the mercury vapour. The results of the experiments are shown in Fig. 8 and Fig. 9. If the pressure of mercury vapour is kept at 0.25 Torr and the cathode temperature is 1220°K, the electric conductivity increases as shown *a–b* just the same as in case of barium. At *b* point the partition wall to the chamber of Cu_2O is broken and two chambers are connected together, and then the electric conductivity becomes deteriorated temporarily due to the residual gases in the Cu_2O chamber and recovers gradually up to *c* point. Heating the Cu_2O then and oxygen is introduced gradually, deterioration of the electric conductivity of the oxide layer could be observed as shown by the curve *c–d*. By breaking a partition wall to the titanium chamber at *d* point, the conductivity rises in accordance with the absorption of the oxygen gas by titanium. Two Ti-

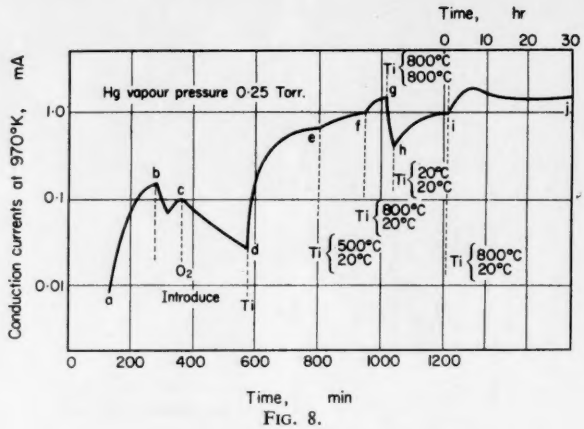

FIG. 8.

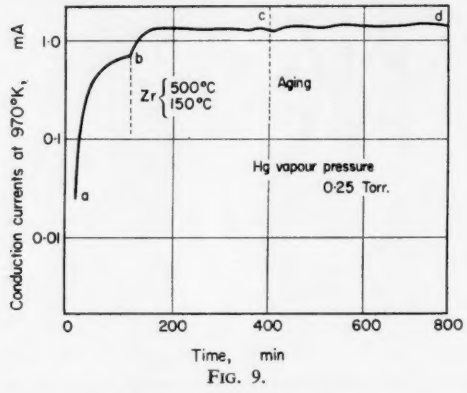

FIG. 9.

getters are contained in the chamber and the curves *d–e*, *e–f* and *f–g* show respectively the results of the experiments when one of the getters was always kept in room temperature and another to be in room temperature, 500°C and 800°C. When both getters are heated to 800°C, as shown at *g* point, the conductivity was decreased as curve *g–h* because many kinds of gases other than oxygen such as N_2, H_2, CO etc. were exhausted from Ti-getters. At *h* point the heating current of one Ti-getter is cut off in order to drop its temperature to the room temperature, then the conductivity increase was observed as *h–i*, due to re-absorption of the residual gases. Under the condition of the cathode temperature at 1000°K, and the anode mean current 56 mA/cm², the change of conductivity *i–j* was obtained and the conductivity was regained perfectly just same as in *g* point.

Quite the same tendency was observed about the zirconium, one example of which is shown in Fig. 9.

As above mentioned, getter activity of titanium and zirconium is never deteriorated under the circumstances even in mercury vapour, however, barium and probably magnesium getters may not be ones which can be left alone in the mercury vapour for a long time.

References

1 S. Fukagawa, M. Hiraoka, and H. Adachi ; *Elec. Comm. Japan*, No. 34, 351 (1952).
2 R. Loosjes and H. J. Vinks ; *Philips Res. Rep.* **4**, 6, 449 (1949).
3 D. A. Wright ; *Nature* **164**, 4173, 714 (1949).
4 S. Fukagawa and Y. Nambo ; *I.R.E. (Japan)* (1940 Oct.).
5 S. Fukagawa ; *Technique of Materials for Electron Tubes and Ultra-High Vacuum.* (Japanese) Ohm-sha Tokyo (1956).

Vol. 10 1960

SESSION VII

Techniques for measuring Getter Activity

Apparatus and Techniques for Measurements of the Adsorption of Gases by Evaporated Getters

P. DELLA PORTA

S.A.E.S. Getters, Milan, Italy

The present work describes the apparatus and techniques used at the S.A.E.S. Research Laboratories to study the gettering action of evaporated barium films on different gases. During the past few years the sorption of gases by getters (evaporated or not) has been increasingly studied from a kinetic approach, by techniques capable of giving a direct measurement of the velocity of sorption. Kinetic measurements can be effected either by measuring the fall of pressure with time in a sealed container of known volume, or by estimating the gas flow through a capillary of known conductance. The latter method can be applied by keeping the manifold pressure constant and allowing the getter pressure to vary with time, but more useful results can be obtained when the pressure on the getter is kept constant. Measurements at constant p_m are by us usually confined to preliminary large scale investigations. For such measurements suitable apparatus and automatic pressure recordings are used, which enable us to carry out more than one test at the same time. For sorption studies at very low pressures, the normal apparatus is attached to an ultra high vacuum system. The experimental results obtained by measuring the gas flow at constant p_g, when suitably interpreted, allow us to study the complex sorption mechanism, showing the existence of diffusion phenomena, giving useful indications about the mobility of molecules on the surface and within the film and permitting the evaluation of the activation energy of different processes. Suitable apparatus enables us to study the influence of hot filaments and ionizing electron currents in the vicinity of the getter. A knowledge of these effects is in fact necessary for a correct evaluation of the data obtained for sorption velocities by using ionization gauges and permits these effects to be kept at a minimum in the experimental procedure. Furhter suitable apparatus is employed to study other parameters which may effect the activity of barium getters, such as the time of flashing, the pressure immediately preceding the firing of the getter, the distance and temperature of the surface on which the film is formed. In particular such devices permit the study, by electron microscopy, of the structure of the barium films obtained under various conditions. Finally, the recent introduction of mass spectrometers of reduced dimensions and able to measure very low partial pressures (e.g. the omegatron), enable us to confirm the eventual chemical processes occurring on the barium film (catalytic reactions) and also it opens a way to the study of getter action on gaseous mixtures.

Introduction

The activities of the S.A.E.S. Research Laboratory, which has now been in existence for eight years, can be subdivided into three main periods.

During the first period, 1951 to 1955, the work of the laboratory was entirely devoted to the development of the new types of ring getters. To this end new alloys were investigated and produced having properties which were a compromise of : large sorption capacity, stability to air, easy handling and reliability.

This period ended with the introduction of the now regularly produced types of getters of Italian origin. Their production, which started in 1954, has continuously increased and can now cover most of the world's demand.

The second period, 1955 to 1957, was devoted to general studies of the gettering properties of the getters produced, in order to give as near a complete picture as possible of their behaviour under actual industrial conditions. The result of these researches were published in two articles which appeared in *Vacuum*[1, 2].

Some of the results published in these articles have now been modified and amplified, in view of the deeper knowledge obtained using more suitable apparatus and refined techniques. Further, consideration has been given to parameters which were then neglected.

Research work in this direction began in 1958. Since then we have accumulated a great number of data concerning the kinetics of sorption under the most varied conditions.

A number of difficulties were encountered, in particular the disturbing effects of hot filaments and ionizing electron currents. We have investigated these effects[3] and in some cases we have been able to reduce their influence on sorption measurements.

The new results obtained have enabled us to individuate the various phenomena comprising the gettering action. It has been possible to estimate the activation energies connected with these phenomena and to identify and separate them when they overlap, as is usually the case.

The results of these researches will be presented by us in subsequent papers[3–6]. The primary object of this paper is to illustrate the apparatus and techniques used, and also to convey the line of our future researches.

Apparatus employed to measure gas sorption by getters

Sorption by getters can be investigated using either static or dynamic techniques. Normally the latter produce far more indicative results and are based on the flow of gas, under Knudsen conditions[7], through a capillary.

In sorption studies it is of the highest importance to obtain reproducible results, hence it is essential to minimize or to eliminate the effects of the background pressure of the system.

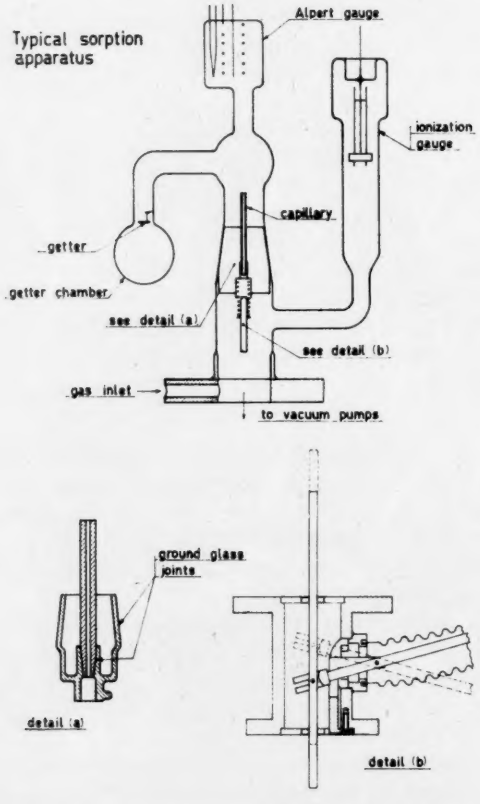

FIG. 1. Manifold employed in sorption studies showing the method of introducing and changing capillaries.

Usually our measurements are carried out in the pressure range 10^{-5} to 10^{-4} Torr. It is therefore essential to produce ultimate system pressures of at least two orders of magnitude lower. In order to do this the pumping system and experimental apparatus must fulfil the standard conceptions used in the attainment of very high vacuum[8], i.e. pyrex construction, grease free joints, degasable by extended periods of baking up to temperatures of 450 °C.

The manifold part of the apparatus by us normally employed is shown in Figs. 1 and 2. The remainder of the

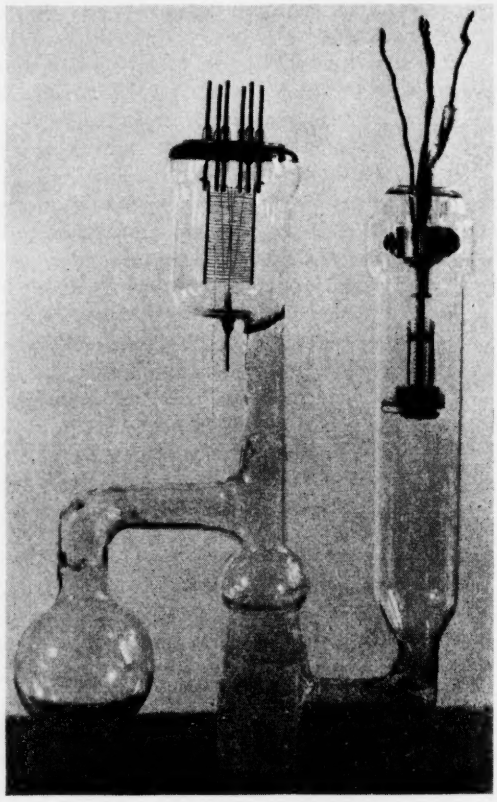

FIG. 2. Photograph of manifold.

system comprises a three-stage fractionating oil diffusion pump, liquid air trap, etc. The two flanges above the liquid air trap are joined, using the aluminium gasket technique described recently by Holden, Holland and Laurenson[9].

The cone, shown in detail (a) of Fig. 1, by means of which the capillary is introduced between the getter chamber and the pumping line, is raised or lowered by means of the mechanism shown in detail (b) of Fig. 1.

The position of the getter chamber is such as to facilitate its immersion in thermostatically controlled baths. The position of mounting of the getter is such as to produce, when evaporated, as near a uniform film thickness as possible.

Those appliances are by us normally employed operating at a constant p_g, a method whose advantages have been previously enunciated[10]. The less satisfactory method at constant p_m[11] is by us only used for large scale preliminary research.

Vol. 10 196

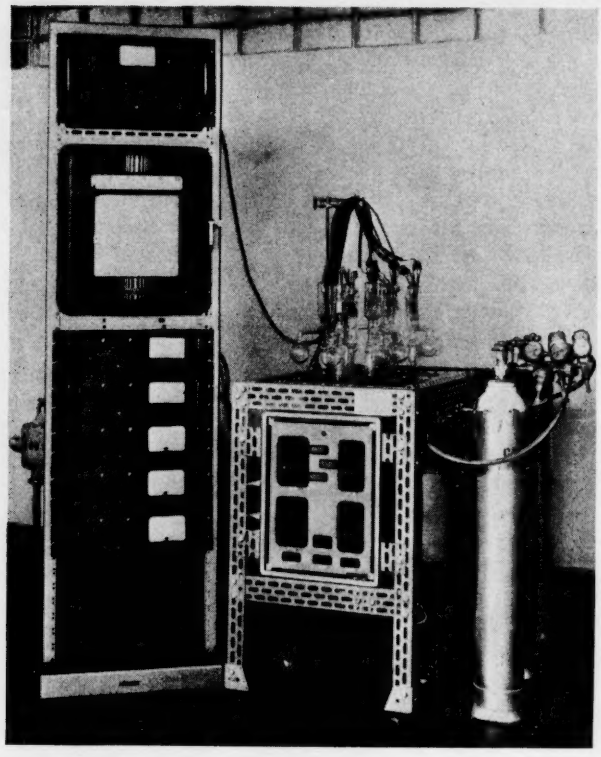

FIG. 3. Multiple heads automatic sorption apparatus, working at constant p_m.

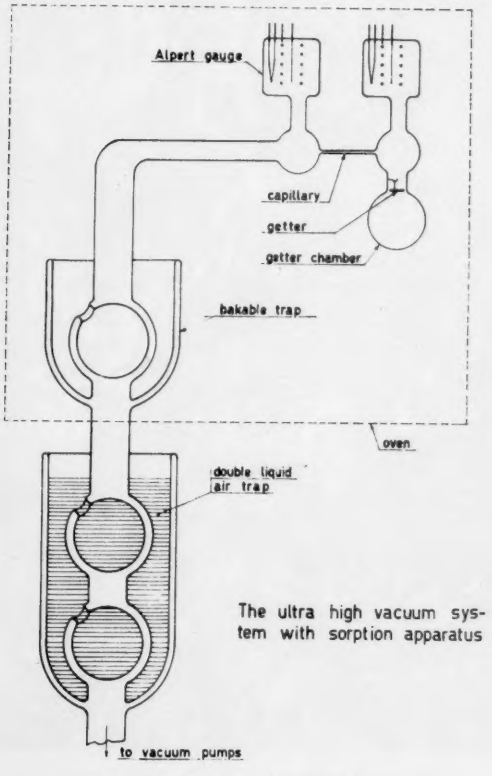

FIG. 4. Ultra-high vacuum system.

This method is more easily applicable to a semi-automatic instrument on which a number of simultaneous experiments can be carried out.

A practical realization of this apparatus, which has been developed by us is shown in Fig. 3. At the centre of this photograph two such five head manifolds are shown. They comprise five getter chambers with respective ionization gauges registering p_g and a central gauge which indicates the constant p_m value. These gauges are controlled by the instruments shown on the left hand of the picture. The output from each amplifier is recorded automatically on a six point recorder. This, of course, facilitates subsequent comparison of results.

Ultra-high vacuum apparatus

The scope of our research is not purely on technological problems, but since we are also trying to explain the fundamental gettering phenomena, we have been obliged to carry out a series of measurements in pressure regions where the ultimate of the system must be in the ultra high vacuum range (below 10^{-9} Torr).

With this in view we have constructed the system shown in Fig. 4 which is similar to that recently described by Venema[12]. This, although utilizing the usual pumping techniques, is comprised of an all glass system (see Fig. 5) containing no

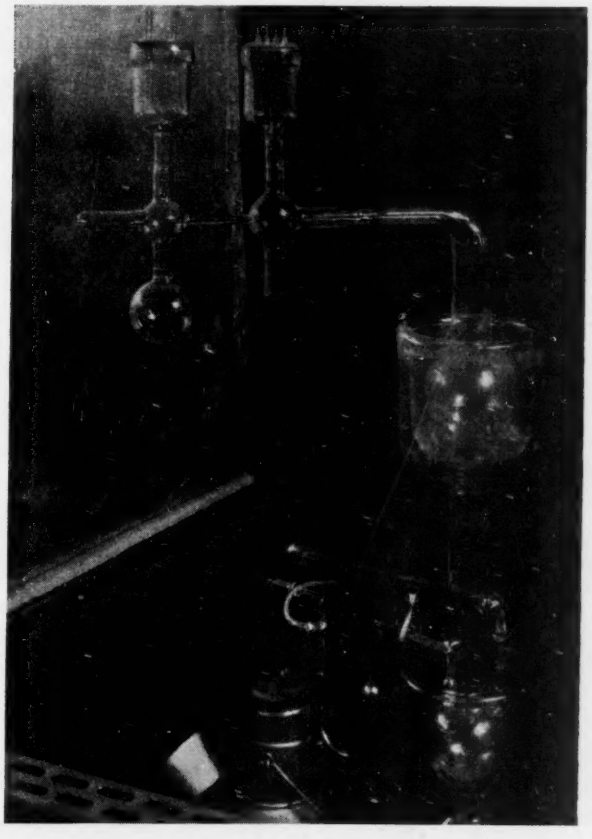

FIG. 5. Ultra high-vacuum system also showing method of controlling liquid air level.

movable parts ; a fixed capillary is employed. The lower double trap is always filled with liquid air whose level is kept at a constant value by the arrangement of Venema. Whilst this is the case the upper part of the system is being baked and subsequently liquid air is also introduced in the upper trap. The two ionization gauges are of the Alpert type for obvious reasons, and are used at reduced emissions.

The problems of the hot filaments and ionizing electron currents

In all the apparatus previously described we necessarily have had to employ ionization gauges for our measurements. It is well known that the presence in these gauges of hot filaments and ionizing electron currents may give misleading indications concerning the sorption of various gases by the evaporated getter films. It is therefore necessary to know the exact nature of their effect in order to minimize or eliminate it and so permit a better knowledge of the effective kinetics of sorption by the getter.

This effect has therefore been studied by us[3], in the pressure range of interest, for the temperatures and fields usually employed in the ionization gauges.

In order to do this special tubes have been used. The schematic arrangement of the manifold now reads as in Fig. 6. The special tubes, which can be any of those in details *a*, *b*, *c*, and *d* of Fig. 6, are situated at *X*. The distance between *X* and the getter chamber is variable and the electrodes of tube *X* may so be located in the getter chamber.

All the filaments of the tubes employed except where otherwise stated are of tungsten.

By employing the simple diode shown in detail (*a*) of Fig. 6, we can study the influence of an electron ionizing current on the normal manner of sorption by the getter.

The effect of the influence of the hot surface area is studied by employing the multi-filament tube shown in detail (*b*).

The tube shown in detail (*c*) is a double grid ionization gauge which enables us to study the effect of the ionizing current and the temperature of the hot filament independently. This is done by using the external grid as a control grid.

The tube shown in detail (*d*) can either contain two tungsten filaments having different emitting surfaces, or one filament of tungsten and one of thoriated tungsten.

Using this type of tube it is possible to visualize the effect of temperature on the pumping of different gases.

Recent trends in our research work

The studies up to now carried out have given us a general indication of the manner in which individual gases are sorbed by getters.

For a more detailed study of the gettering processes we are now directing our efforts to sorption studies on gas mixtures, and to the study of the actual surface of the getter film. In order to do this, more sophisticated methods of research are necessary.

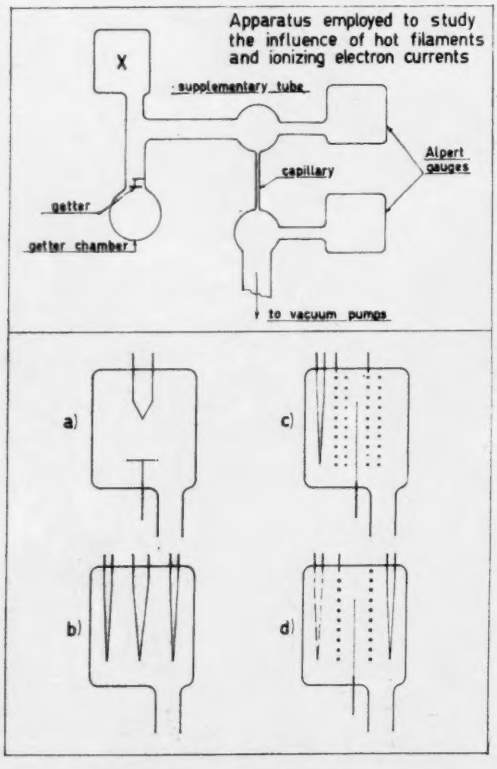

FIG. 6. Schematic arrangement of manifold when studying the effects of the hot filament and ionizing electron current. The details show the various heads which can be employed and which are situated at *X*.

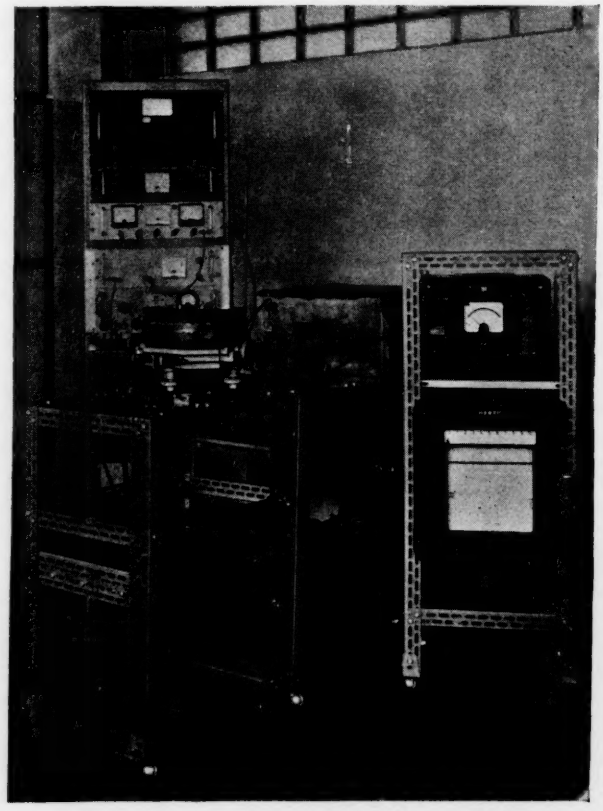

FIG. 7. The Omegatron and auxiliary equipment.

Hence, our recent endeavours have been directed towards mass spectrometric methods of analysis and electron microscopic studies of the getter surface.

In order to fulfil this first requirement we have turned to the omegatron mass spectrometer and will in due course consider other types of spectrometers which in merit of their simplicity, size, ease of degassing, etc. are particularly suitable for these studies. These instruments besides allowing us to work with gas mixtures, will also enable us to study pump ultimates, gases evolved during degassing, gases released by electron impact or ion bombardment, etc.

The instrumentation and vacuum apparatus developed by us for the omegatron is shown in Fig. 7. Since at this symposium a number of communications are presented illustrating the omegatron, we will describe the apparatus in general terms. The actual omegatron head now employed, is of all-platinum construction, and of the type originally described by Bell[13]. Other designs are under study.

On the extreme left of the photograph shown in Fig. 6 are the various control units. Reading from top to bottom they are: control unit for the ionization gauge reading manifold pressure, display unit for getter chamber pressure, omegatron head control panel, radio frequency amplifier, and the radio frequency oscillator.

In the foreground can be seen the magnet, field 3,900 oersted, on its own individual mounting which enables us to use it on the various stations which are fitted with omegatrons. The system of mounting is such that it gives complete three dimensional freedom of movement.

For obvious reasons the magnet is not shown in position nor is the electrostatic screening cover, visible on the far end of the pumping system platform.

On the extreme left is shown a vibron electrometer whose output feeds the high speed chart recorder shown. Shortly, employing an electromechanical system, in its final stages of construction and unfortunately not shown in the photograph, it will be possible to continuously scan and record the mass range 1 to 150 a.m.u. or any particular portion of such range, in times which may be varied at will from 30 sec. to 12 min.

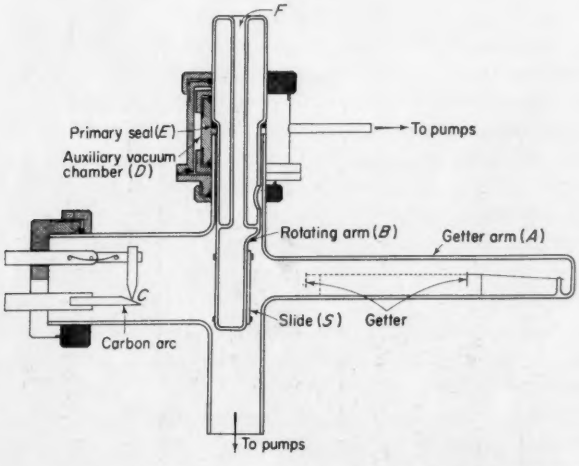

FIG. 8. Apparatus employed to obtain carbon replicas of getter film surfaces for the electron microscope.

To study the structure of the barium films we have begun, with Prof. Ostacoli of the Chemical Institute of the University of Turin, a series of investigations with the electron microscope and will in due course also employ other techniques, such as electron diffraction, etc.

We shall try to consider all the well-known parameters affecting this structure, the main ones being:

(a) the distance of the condensing wall from the source,
(b) time of evaporation,
(c) pressure during evaporation,
(d) nature of residual gases during evaporation,
(e) alloy from which the barium is evaporated,
(f) the temperature of the condensing wall.

The influence of each of these parameters on the structure of the film can, as previously mentioned, be studied using the electron microscope. In order to obtain the necessary replicas for this work we have developed the system shown in Fig. 8.

The getter is placed in the right hand arm *A*. The distance of the getter from the slide (*S*) on which the evaporated barium condenses is variable. Slide *S* is mounted on the rotating arm *B*. Once the barium film has been deposited,

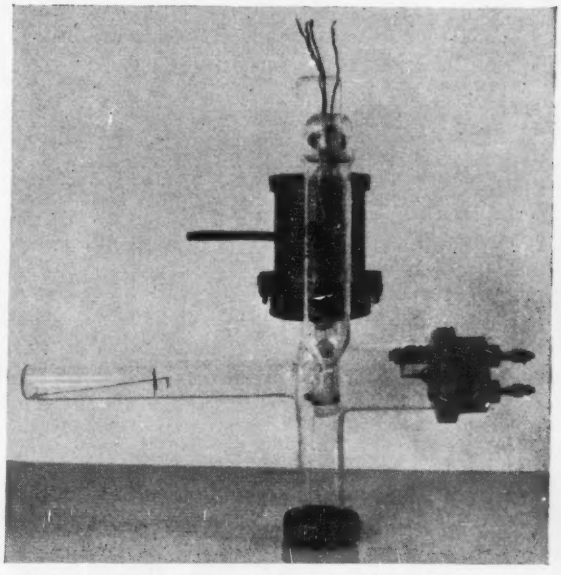

FIG. 9. Practical realization of Fig. 8.

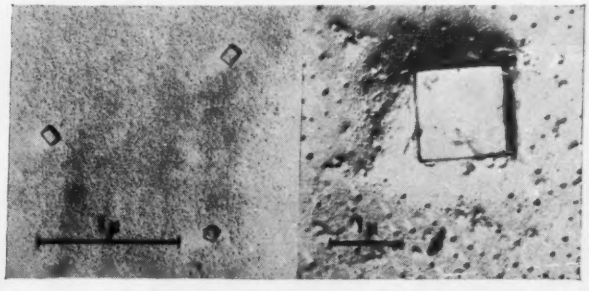

FIG. 10. Crystal growths in a barium film observed using the electron microscope.

the slide is rotated through 180° and graphite is deposited on it from the carbon arc *C*. When rotating the arm *B*, leaks in the seal *E* are prevented by the vacuum existing in chamber *D*. Through *F*, thermostatically controlled baths can be introduced so that the barium film can be deposited on surfaces at different temperatures.

The practical realization of this apparatus is shown in Fig. 9.

An illustrative example of the type of results obtained by this technique is shown in Fig. 10.

These are graphite replicas, platinum shadowed, of barium films which present some interesting crystalline formations.

Manipulation of the results obtained in the study of sorption by getters

To facilitate the interpretation of subsequent papers, the methods used to analyze the experimentally obtained data, will be briefly summarized.

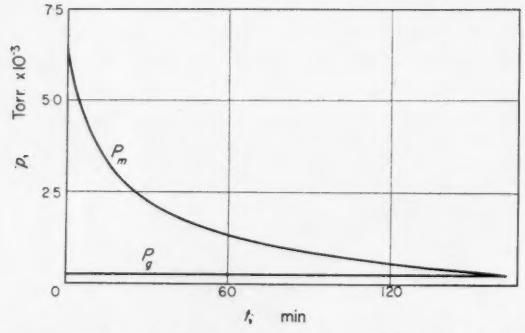

FIG. 11. Dependence of p_m on time at constant p_g, for hydrogen.

In Fig. 11 is shown a typical curve, for hydrogen obtained at a constant value of p_g. The curve shows how p_m changes with time.

Utilizing this curve we can construct the graph shown in Fig. 12. This shows the velocity of sorption (in $cm^3\ sec^{-1}$), as a function of the quantity Q_t of gas sorbed at time t.

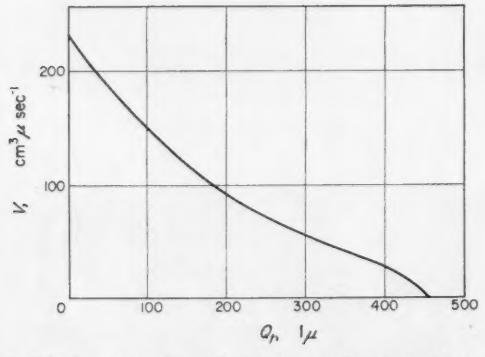

FIG. 12. Velocity of sorption of hydrogen as a function of the quantity of hydrogen sorbed.

This graph is indicative of the type of phenomena occurring, it gives the total quantity of gas sorbed and enables us to calculate the activation energy associated with the initial sorption phenomena. From the initial velocity of sorption it is also possible to estimate the sticking probability of the various gases on the barium film.

From Fig. 12 we can through a series of calculations construct the graph shown in Fig. 13. This shows the quantity of gas sorbed at the time t, as a function of the square root of t.

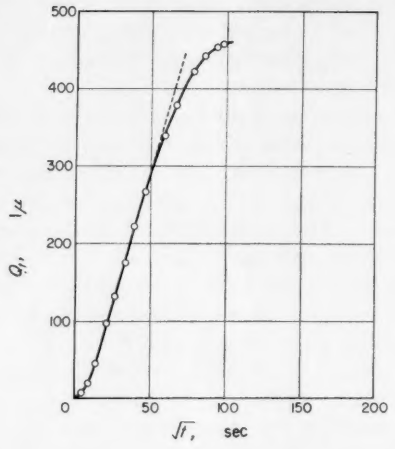

FIG. 13. Quantity sorbed as a function of the square root of time for hydrogen, showing the existence of diffusion phenomena.

It is to be noted that, the linear portion of this graph corresponds to a diffusion phenomenon.

In our previous communications to the Fifth National Symposium of the American Vacuum Society at San Francisco[14], the theoretical considerations which enable us to calculate the energy of activation for the various diffusion phenomenon were given.

The deviations from linearity which are quite noticeable in this case, are indicative of the processes which throughout the life of the getter, control the sorption of the gas in question.

Conclusions

Some doubts may exist concerning the practical value of the information obtainable from this type of study, but we think that the knowledge we are obtaining is fundamental for an understanding of the sorption mechanism in getters.

The disagreement between workers on the behaviour of films be it in the laboratory or in actual tubes, and the empirical methods in which solutions are taken, show that the gettering action is still not completely clarified.

In fact, the nature of sorption is really complex and results from various distinct phenomena often superimposed on each other.

During recent years our research work has expanded rapidly and we have always had new and more difficult problems to overcome.

However, the connections between the behaviour of various gases on barium films are emerging, the result obtainable by different techniques begin to agree, and several contradictory points begin to be explainable.

Vol. 10 196

References

[1] P. della Porta ; *Vacuum* **4**, 284 (1954).
[2] P. della Porta ; *Vacuum* **4**, 464 (1954).
[3] P. della Porta, S. Origlio, and E. Argano ; this volume, p. 194.
[4] F. Ricca, and P. della Porta ; this volume, p. 215.
[5] P. della Porta, and E. Argano ; this volume, p. 223.
[6] P. della Porta, and S. Origlio ; this volume, p. 227.
[7] M. Knudsen; *The Kinetic Theory of Gases*, Third Edition, Methuen's Monographs, London (1953).
[8] D. Alpert ; *J. Appl. Phys.* **24**, 860 (1953).
[9] J. Holden, L. Holland, and L. Laurenson ; *J. Sci. Instrum.* **36**, 281 (1959).
[10] P. della Porta, and F. Ricca ; *Communication to the First International Congress on Vacuum Techniques*, Namur (June 1958).
[11] S. Wagener ; *Brit. J. Appl. Phys.* **1**, 225 (1950).
[12] A. Venema and M. Bandringa ; *Philips Techn. Rev.* **20**, 145 (1958–59).
[13] R. L. Bell ; *J. Sci. Instrum.* **11**, 269 (1956).
[14] P. della Porta, and F. Ricca ; *Transactions of the Fifth National Symposium of A.V.S., Boston*, 1958, Pergamon Press (1959), p. 25.

ol.
10
960

Use of the A.S.T.M. Reference Planar Diode for Studying Getter Properties

R. P. MISRA

Tung-Sol Electric, Inc., Bloomfield, N.J., U.S.A.

A SHORT description of the A.S.T.M. Reference Planar Diode will be presented even though detailed description is available in Le Vide Number 77, September-October, 1958. Particular points of importance about this diode which make it suitable for using it to study life properties of the cathode when different getters are used will be discussed.

Some data will be presented indicating the gases inside tubes as measured by a special mass spectrograph tube and procedures pointed out whereby quantitative use of this tube may be made to study the effect on cathode life.

Curves indicating the use of the tube itself as an ion gauge for residual gas pressure will be presented. Finally the availability of the parts for this reference diode to laboratories in Europe will be pointed out and mechanisms sought whereby communication on data between European investigators and the A.S.T.M. Group in the United States may be facilitated.

Editor's note : The author regrets that the complete article cannot be published as the original material was unfortunately destroyed.

Vol.
10
196

An Automatic Apparatus for the Testing of Getter Adsorption

M. G. CHARLTON, D. NEWSON and P. J. WHITCHURCH

The Mullard Radio Valve Co. Ltd., Material Research Laboratory, Mitcham Junction, Surrey, England

Routine testing of getter films has in the past been carried out using dosing methods, which require the constant attention of an operator. An apparatus has therefore been developed which operates automatically, recording the uptake of gas and at the same time maintaining the gas pressure over the getter constant. The principle of operation is as follows. Pulses of gas enter the getter chamber from a reservoir through a special magnetic valve which is continuously and rapidly opened and closed. The ratio of time open to time closed is automatically controlled so as to maintain a constant pressure in the getter chamber. Control is exerted by a special switching circuit which continuously varies the ratio of interval on to interval off, according to the input signal. This signal is provided by the voltage across the meter in the getter chamber Pirani gauge circuit. With a Pirani gauge attached to the gas reservoir, a continuous record of pressure drop against time can be obtained with a potentiometer recorder. If a capillary tube and high pressure Pirani gauge are interposed between the getter chamber and the magnetic valve, the signal from this Pirani gauge may be used to obtain a direct record of gettering rate against time. The apparatus has been used with carbon monoxide and hydrogen at getter chamber pressures of about 1μ. There is no limit with regard to the use of higher pressures, but with the present control circuit the use of lower pressures would lead to less satisfactory control, which at 1 micron pressure was never worse than ±10 per cent, and generally much better.

1. Introduction

Routine testing of the activity of getter films has in the past been carried out by dosing methods, which have the disadvantage that the test requires the constant attention of an operator. Whilst it was not possible to reduce the time taken for the test, it did seem possible and desirable to reduce the time that the operator needed to devote to the test, by designing an apparatus that would function automatically.

The objective, therefore, was to devise a method whereby a continuous record of the uptake of gas over a period of time could be obtained, whilst the pressure over the getter film was automatically maintained constant. Constancy of the pressure over the getter was considered a very desirable and important feature of any testing method, because of the greater ease of interpretation of gas adsorption curves obtained under these conditions. The aim, therefore, was to achieve this at pressures down to 0.001 torr.

2. General principle of the method

A diagram of the apparatus is shown in Fig. 1. In the form shown it may be employed in two different ways: (a) to obtain a record of uptake of gas in the form of reservoir pressure/time curves, or (b) to obtain a direct record of adsorption rate against time.

For the purpose of illustration we shall at first confine our attention to the first application, in which case the capillary and tap *T*.1 may be ignored.

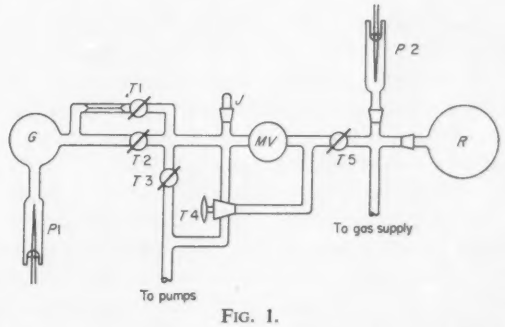

FIG. 1.

Essentially the system consists of a getter chamber *G*, with a Pirani gauge *P*.1 attached, which is connected to a gas reservoir *R* through a special magnetic valve *M.V.* A second Pirani gauge *P*.2, suitable for use at hydrogen pressures up to 1–2 torr, is attached to the reservoir. The system is pumped through taps *T*.3 and *T*.4.

The magnetic valve opens and closes continuously with a complete cycle period (time open plus time closed) of about ¼ sec. The rate of flow of gas from the reservoir to the getter is determined by the ratio of period open to period closed, which is controlled by an electronic circuit in accordance with the signal derived from the Pirani gauge (*P*.1) unit. The error signal is quite small compared with the total signal and so the integrated gas flow rate is maintained very close to the rate of adsorption and hence the pressure in the getter chamber is kept substantially constant (about ±2 per cent).

A continuous record of the reservoir pressure during the course of the run is obtained by using a potentiometer recorder in association with the high pressure Pirani gauge (*P*.2).

3. Details of the apparatus

The Magnetic Valve

Fig. 2 shows a sectional drawing of the valve. Gas enters the valve through the lower side tube and then passes through

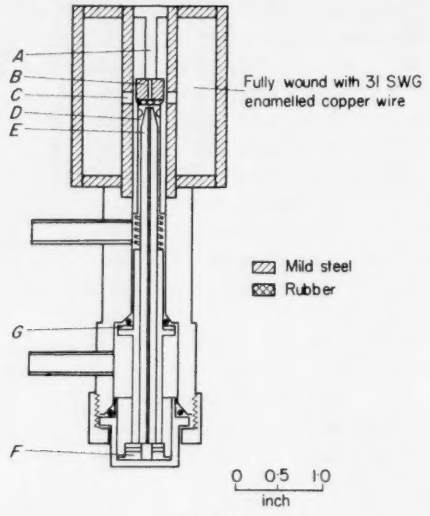

FIG. 2.

holes round the periphery of block *F* and thence up the capillary tube *E*. When the valve is open the gas escapes from the capillary, passes out through holes in the wall of tube *D* and finally leaves through the upper side tube.

The moving part of the valve, which closes the capillary, consists of a thin-walled brass tube (*D*) which is attached to a mild steel block (*B*) and at the end of which is jammed a thin disc of silicone rubber. The tube slides closely but very easily on the capillary tube and rests upon a very light spring. The magnet coil is wound on a mild steel bobbin and enclosed in a mild steel case. The magnetic circuit is broken by a brass ring (*C*), which is hard soldered to the mild steel sections of the bobbin.

The upward movement of the iron block *B* is restricted by the stop *A*. When the block is pulled down by the field it should almost cover the gap in the magnetic circuit, the total movement being about 1 mm. Some adjustment in the position of the assembly is made possible by the use of a set of thin washers for placing beneath the block *F* and the washer *G*. The clearance between the steel block (*B*) and the steel tube is made as small as possible, consistent with there being no risk of their actually touching.

A 10 cm length of 0.5 mm diameter stainless steel capillary tube was used, this diameter being found suitable for most experiments. The tube was tapered at the top end to a diameter of about 2 mm, and the tip was made square to the axis and polished.

It was originally intended that this valve should be energised by connecting the coil directly into the switching circuit (cf. following section) but this was not satisfactory, for the voltage developed across it was too low. The coil (100Ω resistance) was therefore run on a separate 12 V supply which was switched by a relay in the control circuit.

The closing force of the valve is not great and so a perfect seal could not be expected. However, the leak rate was sufficiently low, being about 0.001 l.μ hydrogen/sec with a pressure difference of 300μ, under which conditions the flow-rate through the open valve was about 0.2 l.μ/sec. Obviously, the apparatus ceases to operate properly when the adsorption rate of the getter falls below the leak rate of the closed valve.

The Control Circuit

The signal for the switching circuit was taken from across the meter in the Pirani gauge (*P*.1) unit. This was a 100Ω meter and the voltage developed across it at a hydrogen pressure of 1μ was about 6 mV.

The function of the control circuit was to maintain the pressure at a constant given value by varying the on/off time ratio of the magnetic valve in accordance with the deviations in the meter voltage from the value corresponding to the required pressure.

Because the signal voltage was low, a transistor circuit was used. This is shown in Fig. 3 and consists of a two-stage

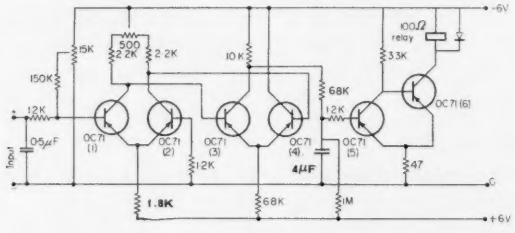

FIG. 3.

balanced amplifier followed by a voltage controlled oscillator. The current produced by the input voltage through the 1.2 K resistor is backed off by that produced by the 15 K potentiometer and 150 K resistor, the residual current—in effect the error signal—flowing into the base of transistor (1). Thus the setting of the 15 K potentiometer determines the value of the input signal at which control takes place and hence the value at which the pressure is maintained constant. With the circuit as shown the pressure may be controlled up to a value corresponding to a voltage of 40 mV across the meter. The upper limit may be increased by reducing the 150 K resistor. Connecting this circuit across the meter increased the pressure reading, at 1μ, by about 10 per cent, for which allowance was made.

Transistors (1) and (2) form a balanced pair, selected to have approximately equal collector leakage currents and equal gains. They are mounted together in a metal block to prevent temperature differences occurring. Exact balancing of these transistors is achieved with the 500 ohm potentiometer. With the input terminals shorted and the 15 K potentiometer set at the minimum position the 500Ω potentiometer is adjusted until the oscillator starts to operate.

The matching of the second pair of transistors (3 and 4), which provides a further stage of amplification, is less critical.

The final pair of transistors (5 and 6) constitutes the oscillator, which provides the required pulses for the relay which switches the magnetic valve. These are connected to form a bistable circuit, in which either one or the other transistor, but never both, can be fully conducting at a given instant. The switching characteristics of this circuit are determined by the signal from the collector of transistor (3), and the resistance-capacity circuit connected to the base of transistor (5).

The diode across the relay coil prevents high voltage pulses arising at the collector of transistor (6), which could quickly damage the transistor. The condenser across the input circuit is not essential to the operation of the circuit, but was included to reduce electrical interference from other equipment.

Deviation from 6 V for the supply lines is permissible, but would necessitate some adjustment in the values of the common emitter resistor (1.8 K) and the collector resistors (2.2 K). Under operating conditions the collectors of transistors (1) and (2) should be about 1 V negative with respect to the zero line.

Recording of Results

The adsorption process is followed by means of the pressure change in the reservoir. A high pressure Pirani gauge is used for this purpose, with the filament maintained at constant temperature by an automatic feed-back circuit. This type of gauge has, over a fairly wide pressure range, a pressure-current relationship of the type

$$p = K(I^2 - I_0^2)$$

where I_0 is the bridge current at zero pressure. This gives a rather inconvenient scale on the recorder chart. However, this difficulty is largely avoided by the use of a thermal junction which gives a voltage output that is approximately proportional to the square of the current input.

Operating Parameters

To obtain the best performance from the apparatus, as assessed by the constancy of the pressure over the getter, it is necessary to decide on certain operating parameters, and to do this it is necessary to know of what order are the adsorptive capacity and maximum adsorption rate of the getter.

Thus the reservoir pressure and valve conductance (i.e. capillary diameter) together determine the maximum gas flow rate obtainable. Also, for a getter of given capacity, the percentage change in the reservoir pressure during the course of an experiment is determined by the quantity of gas in the reservoir and hence by the reservoir pressure and volume.

The valve conductance may be changed by having interchangeable capillaries, or by inserting wires of different diameters into the one capillary.

4. Direct measurement of adsorption rate

For this application the Pirani gauge *P*.2 is transferred to the ground joint *J* and the capillary and tap *T*.1 are brought into use, the tap *T*.2 being shut-off after pumping the getter chamber. The operation of the apparatus is the same as before except that the gas now passes through the capillary interposed between the getter chamber and magnetic valve, and the Pirani gauge *P*.2 provides a record of the pressure on the high pressure side of this capillary. This pressure, provided conditions are such that the gas flow is molecular, provides a direct measure of the adsorption rate, as in the well known capillary method of Wagener.

A number of capillaries of different diameter may be placed in parallel, each with a tap in series, so as to provide a number of ranges. An automatic method for changing the sensitivity once during the course of a run has been successfully applied. The experiment was started with two capillaries of different diameter both in use, the larger of the two being incorporated in the device shown in Fig. 4. By

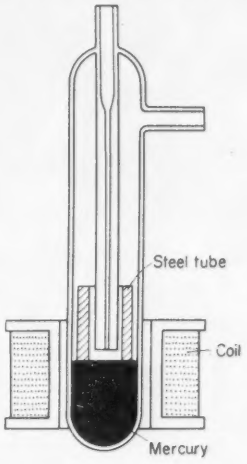

FIG. 4.

means of an adjustable contact on the potentiometer recorder it was arranged that the solenoid was energised, and the coarser capillary thereby blocked, when the deflection fell to a fraction of the full scale.

The usefulness of the method for direct recording of adsorption rates is, however, seriously limited by the fact that the correct choice of values for the operating parameters is much more critical ; thus any considerable departure from the optimum conditions leads to marked oscillations in the pressure recorded by gauge *P*.2. Moreover, extra operating parameters are introduced, namely the capillary diameter and the pressure on the high pressure side, and these two variables together must satisfy the conditions for molecular flow.

5. Performance of the apparatus

Figs. 5–7 show the records from typical runs. Figs. 5 and 6 show the change in reservoir pressure with time for experiments with hydrogen and carbon monoxide respectively. The discontinuity in the curve of Fig. 5 is due to switching the Pirani gauge to a more sensitive range. Fig. 7 shows a record obtained when the method was used for direct measurement of adsorption rate. The curves shown in Figs. 5 and 7 were obtained, using a thermal junction as described previously.

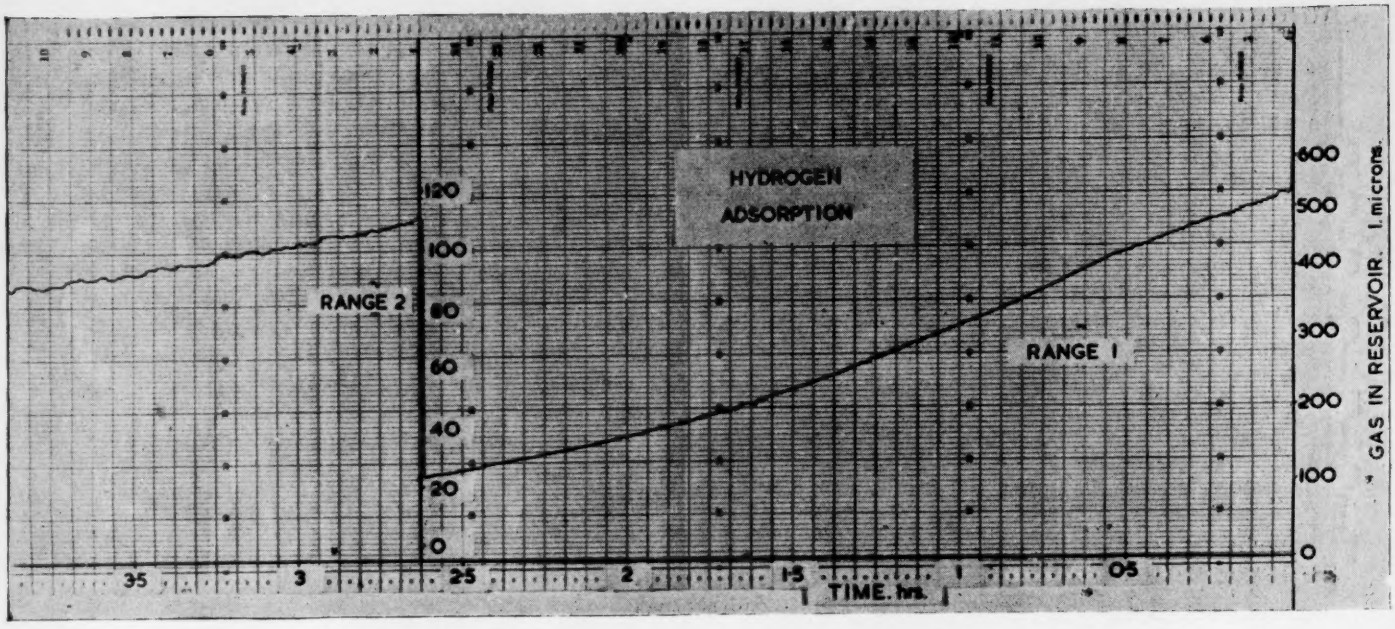

FIG. 5.

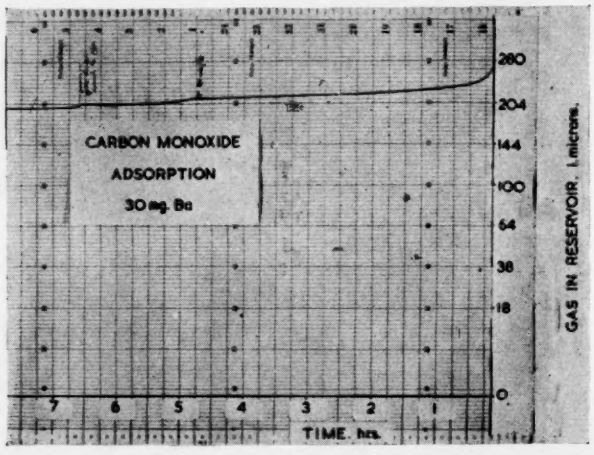

FIG. 6.

FIG. 7.

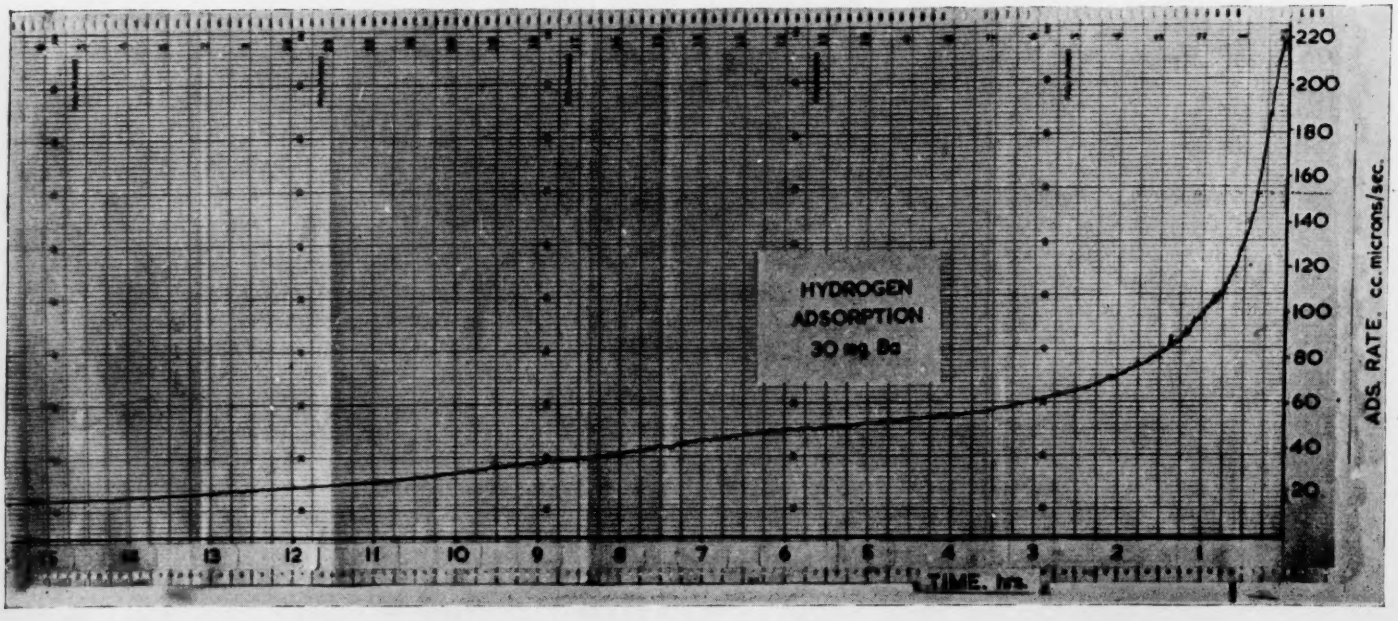

6. Conclusions

The method described can be successfully used for obtaining a continuous record of the uptake of gas by a barium film at a constant pressure, without the continual attention of an operator being required. The control unit is not sufficiently sensitive to give satisfactory control of the getter chamber pressure if this is substantially below 1 micron ; any higher pressure may be used, however.

It is possible to use the apparatus for the direct recording of adsorption rates, but it is likely to be of value for this application only under certain circumstances.

Acknowledgements

We wish to thank Dr. J. A. M. van Moll, Head of the Material Research Laboratory, and the Directors of The Mullard Radio Valve Co., Ltd., for permission to publish this paper.

Vol.
10
1960

SESSION VIII

Getter Activity on Various Gases and Gas Mixtures. Parameters of Concern

The Influence of Ionizing Electron Currents and Hot Filaments on the Gas Adsorption by Barium Films

P. DELLA PORTA, S. ORIGLIO and E. ARGANO

S.A.E.S. Getters, Milan, Italy

In studying the effect of ionizing electron currents on the sorption of gases by getters, it is necessary to distinguish between : (a) the pumping action of the hot filament and of the ionizing current, and the sorption by the getter ; (b) the gettering of activated particles and usual gettering of gaseous molecules. Bloomer has pointed out how the activating action of the ionizing electron current is to be added to the normal gettering by barium films. This criterion has been applied in all our work on the various phenomena mentioned previously : normal gettering, electrical clean-up, pumping effect of the hot filament and gettering of activated particles. By using an analogous additive principle, it is still possible to employ an ionization gauge of the Alpert type to measure the pressure, even when studying the effects of an ionizing electron current, by falling back on supplementary electrodes and tubes for a study of the other parameters. The measurements have been carried out employing the capillary technique at constant pressure on the getter. The apparatus used in these experiments is obtained by simple modifications of devices already described in previous communications. Such modifications introduce, on the getter side of the capillary, supplementary tubes with the required electrodes. With such devices we have carried out a number of tests to compare the velocity of pumping with and without getters, in various gases, when altering temperature and size of the surface and the intensity and energy of the ionizing electron beam.

Vol.
10
1960

Introduction

It has been known for a long time that ionizing discharges can produce a lowering of pressure and that there are many complex mechanisms whose effects bring about this result.[1]

It is also known that a similar effect is found in particular in hot cathode devices such as ionization gauges operated under high vacuum conditions.[2]

The molecules striking the hot cathode may often split up into atoms which are easily chemisorbed on the walls of the container.

On the other hand the positively charged molecule-ions produced by the electron current may be easily neutralized and trapped on these same walls which are negatively charged by the electron flow.[3, 4]

Even noble gases, ionized by the electron current, may be trapped on the metal evaporated during the degassing of the electrodes.[5, 6]

Finally it is known that it is just the very pumping effect of ionization gauges which produces ultra-high vacuum in containers of limited volume.[2]

However, it is more difficult to evaluate the action of the hot cathode and the ionizing electron current when there is a getter or any other metal surface active in the chemisorption of gases.

The critical importance of this problem immediately becomes evident when we consider the recent spread of getter-ion pumps for the production of ultra-high vacuum.[7]

It is even more obvious when we consider that a normal electron tube represents precisely a system of this kind.

On the other hand this problem has a great importance from the point of view of the theoretical study of the gettering of gases by evaporated metal films, and, in a more general way, of the chemisorption of gases by metals.

This is so since the defining of a possible activating action of the electron discharge may clarify the nature of the phenomenon, and also since many of the more recent and interesting results obtained in this field have been produced by means of ionization gauges which might be themselves a source of misinterpretation.

In order to clarify these basic problems further data are required. This is the reason why our Laboratory has begun systematic fundamental research on the influence of hot cathodes and ionizing electron currents on the sorption of various gases by getter films.

In studying the effect of ionizing electron currents on the sorption of gases by getters, it is necessary to distinguish between :

(a) the pumping action of hot filament and of ionizing electron current, and the sorption by the getter,
(b) the gettering, by the metal film, of the usual gaseous molecules and of the molecules activated by the ionizing electron current.

Bloomer[8] has pointed out how the activating action of the ionizing electron current is to be added to the normal gettering by barium films.

Here we extend this additive principle by assuming that :

(a) the activating actions of two ionizing electron currents can be added,

(b) the activating action of an ionizing electron current is itself the summation of various phenomena, i.e. electrical clean-up, pumping effect of the hot filament and gettering of activated particles.

Hence, from (a) we can still employ an ionization gauge for pressure measurements, when studying the effects of an ionizing electron current with supplementary electrodes and tubes ; and from (b) we can individually investigate the influence of the different phenomena previously mentioned.

Due to these principles we have begun the construction of the experimental apparatus described in another communication.[9]

The measurements have been carried out employing the capillary technique at constant pressure on the getter. The apparatus used in these experiments is obtained by simple modifications of devices already described in previous communications. Such modifications introduce, on the getters side of the capillary, supplementary tubes with the required electrodes.

With such devices we have carried out a number of tests to compare the velocity of pumping with and without getters, in various gases, when altering temperatures and size of the surfaces and the intensity and energy of the ionizing electron current.

Results and discussion

Nitrogen

The graphs shown in Fig. 1 relate to nitrogen sorption on barium films of 2 mg at a pressure of 3×10^{-4} Torr, and were obtained by employing a supplementary diode with an electron ionizing current of 5 mA.

It is possible to show this effect by establishing the ionizing electron current in the getter chamber and by measuring the increase of p_m necessary to maintain p_g at a constant value.

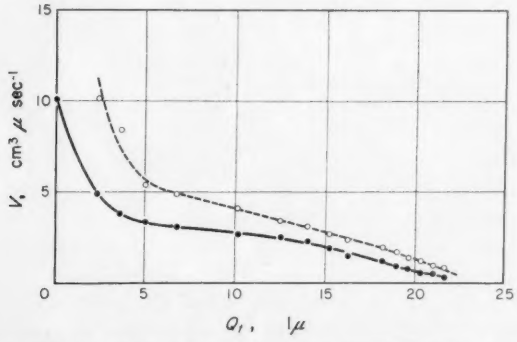

FIG. 1. Velocity of nitrogen sorption as a function of the quantity sorbed showing the effect of the ionizing electron current.
○ In the absence of ionizing electron current.
● In the presence of an ionizing electron current of 5 mA.
Weight of evaporated barium = 2 mg
Apparent surface area of film = 100 cm²
Sorption temperature = 298 °K
Pressure (p_g) = 3×10^{-4} Torr.

The continuous line is a typical sorption curve where the velocity is shown as a function of the quantity sorbed. The dashed line shows the sorption velocity when the supplementary diode is operating.

Whilst the continuously decreasing velocities are effectively shown by the lower curve, the upper curve shows only relative values, since it has been constructed from experimental points determined by establishing, at intervals and for brief periods, the ionizing electron current.

The influence of the temperature of the hot filament is illustrated by the results shown in Fig. 2.

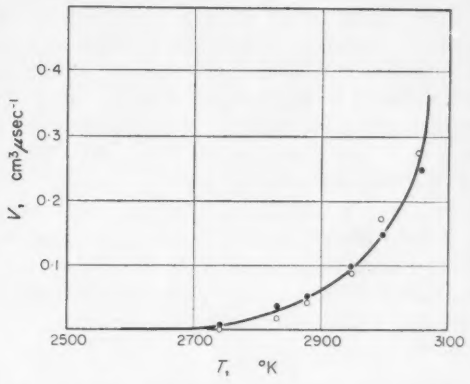

FIG. 2. Pumping effect, for nitrogen, of a hot surface as a function of temperature.
○ In the absence of a getter film.
● In the presence of a getter film.
Bulb temperature = 298 °K
Pressure (p_g) = 5×10^{-5} Torr
Weight of evaporated barium = 2 mg
Apparent surface area of film = 100 cm².

The points shown with solid circles are for results obtained with a barium film of 2 mg on a surface of 100 cm², from which have been deducted the gettering velocities due only to the barium film in the absence of any supplementary filament.

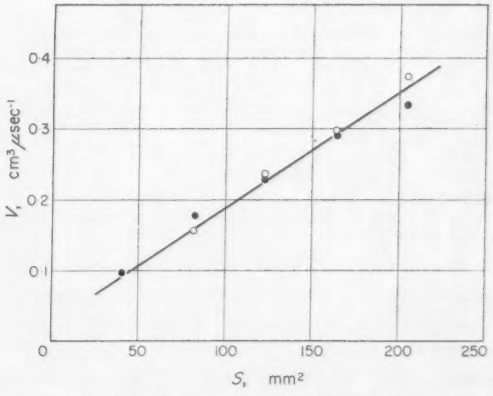

FIG. 3. Pumping effect, for nitrogen, of a hot surface as a function of its area.
○ In the absence of the getter film.
● In the presence of a getter film.
Bulb temperature = 298 °K
Surface temperature = 2,950 °K
Pressure (p_g) = 5×10^{-5} Torr
Weight of evaporated barium = 2 mg
Apparent surface area of film = 100 cm².

From these results it is found that the hot filament itself exhibits a certain pumping action regardless of the presence of the getter film.

This pumping effect only occurs for relatively high temperatures of the order of 2,700 °K and more, in agreement with previously reported results.[10]

It is therefore obvious that this effect does not influence the data in Fig. 1, since in this case the temperature of the filament in the diode was about 2000 °K.

To study the influence of the hot surface area we have employed the tube containing a number of filaments, all of the same area, which has been previously illustrated.[9]

This influence is shown in Fig. 3. The solid circles correspond to readings obtained in the presence of a barium film of 2 mg deposited on a surface area of 100 cm². The open circles are for measurements carried out in the absence of the barium film. The successive points correspond to the switching on of the filaments one after the other. The relationship shown is practically linear.

Some experiments carried out using an ionization gauge head with two different filaments having the same surface area but one being of tungsten, and the other of thoriated tungsten, have confirmed that the pumping of nitrogen is not dependent on temperature within the limits of practical interest of the latter, Fig. 4.

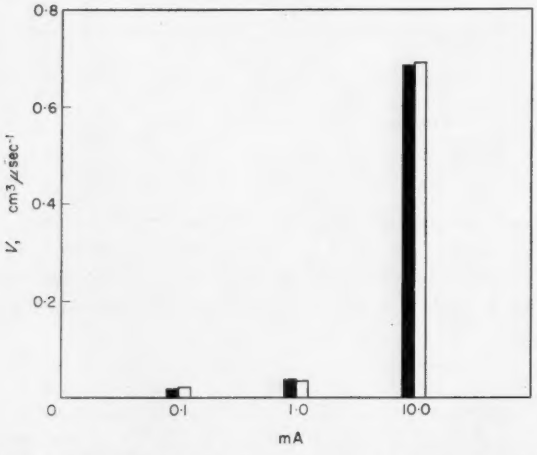

FIG. 4. Pumping effect, for nitrogen, of ionizing electron currents from filaments having different emittivities.

■ Tungsten filament.
□ Thoriated tungsten filament.
Pressure (p_g) = 5×10^{-5} Torr
Both filaments have equal emitting surface areas of 46.5 mm².

The different values for the velocity of pumping by the gauge head were obtained by maintaining constant the various applied potentials*, and the pressure within the getter chamber (5×10^{-5} Torr). Only the temperatures of the filament were altered to obtain the desired emission.

If the pumping action of the ionization gauge were dependent on temperature, one should obtain a difference between the pumping action of the two filaments, which, due to their difference in emittivities, must reach different temperatures to produce the same electron emission.

Hydrogen

In the case of hydrogen too, the presence of an ionization gauge has an appreciable influence on the sorption velocity.

The influence of temperature is already well known from the early and brilliant work of Langmuir[11]. Therefore, the problem is to show the influence of the ionizing electron current, in the absence of parasitic temperature effects.

To this end we have made use of the double grid ionization gauge[9], of the type employed by Robinson and Berz[12] to study the initial pumping and recovery of ionization gauges.

This special tube was of course used as an auxiliary tube, a conventional Alpert type gauge being employed to record pressures.

The two grids are employed to vary the ionizing electron current, without variations of filament temperature and accelerating voltage but simply by controlling the electron flow by means of the supplementary outer grid. (We therefore produce electrons having the same energy, from a cathode at constant temperature, but we are able to vary the intensity of the ionizing electron current.)

These refinements have enabled us to obtain the curve shown in Fig. 5, at a constant filament temperature of 1700 °K.

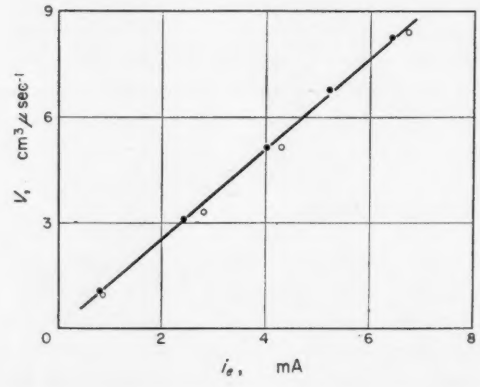

FIG. 5. Pumping effect, for hydrogen, of the ionizing electron current. (The effect due to the hot filament having been deducted).

○ In the absence of a getter film.
● In the presence of a getter film.
Bulb temperature = 298 °K
Pressure (p_g) = 5×10^{-5} Torr
Weight of evaporated barium = 2 mg
Apparent surface area = 100 cm².

The two types of points are for measurements at a pressure of 5×10^{-5} Torr in the presence (solid circles) and in the absence (open circles) of a barium film.

In order to obtain the velocity values merely due to the ionizing electron current, we have measured (be it in the presence as well as in the absence of the getter film) the increase in velocity when the required potentials were applied to the two grids, the filament been kept at the required constant temperature throughout the experiment.

By employing the same system we have obtained exactly similar results for various filament temperatures.

* Ion collector potential = 0, filament potential = 80 V, grid potential = 250 V.

Vol. 10 196

From Fig. 5 it is evident that the appreciable effect due to the ionizing electron current, in the case of hydrogen, is due to ion pumping and not to an increased getter activity.

Carbon Monoxide

It is well known that Bloomer[13], in the case of carbon monoxide, found a limited effect due to the electron current, without giving particular attention to the effect of temperature.

Preliminary measurements have in actual fact shown that temperatures of the order of 2600 °K are necessary to produce a noticeable increase in the pumping speed.

In these temperature regions, be it in the present case of carbon monoxide as well as in that of nitrogen previously referred to, the pumping effect of the hot filament may probably be attributed to chemical pumping, due to interactions on the hot surface of the tungsten filament, as well as gettering due to the small quantities of tungsten which can evaporate from the filament and condense on the enclosing walls.

In the temperature region of practical interest a study of the influence due to ionizing electron currents, confirms the findings of Bloomer[13], at least for the decreasing part of the velocity curve.

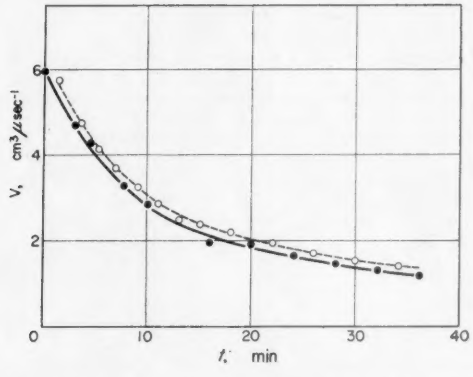

FIG. 6. Velocity of carbon monoxide sorption as a function of time showing the pumping effect of the ionizing electron current for the decreasing part of the velocity of sorption curve.

● In the absence of the ionizing electron current.
○ In the presence of the ionizing electron current (5 mA).
Weight of evaporated barium = 2 mg
Apparent surface area of film = 100 cm²
Sorption temperature = 298 °K
Pressure (p_g) = 5×10^{-6} Torr.

This is shown in Fig. 6, for measurements carried out on a film of 2 mg of barium, having a surface area of 100 cm², at room temperature and at a pressure of 5×10^{-6} Torr.

The dotted curve (relating to sorption velocities in the presence of ionizing electron currents), was constructed using points, obtained in the manner described when discussing Fig. 1. The electron ionizing current is 5 mA.

In the initial horizontal part of the velocity of sorption curve it was not possible to reveal any effects of this nature, probably due to the small entities involved, which are overshadowed by the high initial sorption velocities.

Oxygen

It is found that in the case of oxygen, temperature has an appreciable effect on the velocity of sorption, in particular in that part of the curve showing a decrease in sorption velocity. This type of result is shown in Fig. 7.

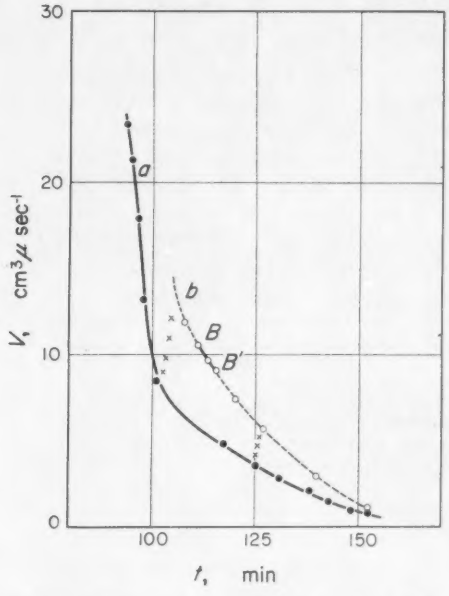

FIG. 7. Velocity of sorption for oxygen as a function of time showing the pumping effect of the filament.

● In the absence of the hot filament.
○ In the presence of the hot filament (1950 °K).
Weight of evaporated barium = 2 mg
Apparent surface area of film = 100 cm²
Sorption temperature = 298 °K
Pressure (p_g) = 1.7×10^{-5} Torr.

This figure refers to oxygen sorption (at a constant pressure of 1.7×10^{-5} Torr and at a temperature of 298 °K) on a film of 2 mg of barium deposited on an area of 100 cm². Curve (a) shows the sorption velocity when the filament in the supplementary tube is cold ; curve (b) was constructed using points (following the same procedure as when constructing Figs. 1 and 6) and shows the sorption velocity in the presence of the hot filaments (temperature about 1950 °K), except for the tract *B–B'* corresponding to measurements continuously carried out in the presence of the hot filament. The crosses indicate the variations of velocity with temperature.

Naturally when the velocities of gettering become smaller, the increase in velocity due to the hot filament, also diminishes.

This result is in good agreement with that found by Bloomer[8], that is, whilst in the initial tract the hot filament had no influence on the velocity of sorption, in the decreasing part of the curve it was possible to show a small increase in pumping.

Carbon Dioxide

In Fig. 8 is illustrated how, in the case of carbon dioxide, it was impossible to show any increase of sorption velocity due to the hot filament and ionizing electron currents, during the whole of the sorption process.

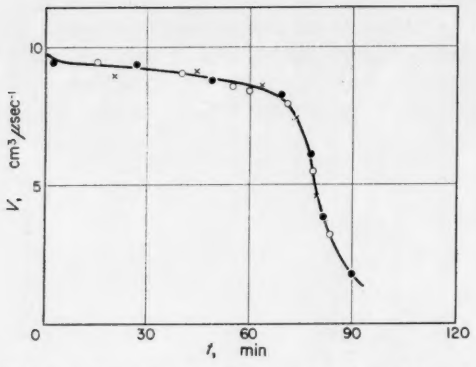

FIG. 8. Velocity of sorption for CO_2 as a function of time showing that there is no effective pumping due to the ionizing electron current as well as the hot filament.

- ● In the absence of hot filament and ionizing electron current.
- ○ In the presence of hot filament (2300°K) and absence of ionizing electron current.
- × In the presence of hot filament and ionizing electron current (5 mA).

Weight of evaporated barium	= 2 mg
Apparent surface area of film	= 100 cm²
Sorption temperature	= 298°K
Pressure (p_0)	= 5×10^{-6} Torr.

In this graph the solid circles relate to experimental values of the sorption velocity of carbon dioxide by the getter, when the auxiliary tube is not used. The open circles indicate values relating to the presence of a tungsten filament at a temperature of about 2300°K, and the crosses to values obtained when employing an electron ionizing current of 5 mA.

Conclusions

From the results mentioned, as well as from numerous other experimental data obtained by us concerning the influence of hot filaments and ionizing electron currents on the gettering of various gases by barium films, it appears that we must report for some gases a considerable effect due to the two factors mentioned.

Generally it appears that the thermal effect can be directly related to the action of the filament, and not to an influence on the sorption of the gaseous species by the film.

The ionizing electron current, on the other hand, produces, in certain cases, in particular for nitrogen, besides the expected ion pumping, independent of the presence of the getter, an effective increase in the gettering.

This can result from various phenomena : ionization, dissociation, activation, etc. Due to the complexity in behaviour, previously related, and to the differences existing between each gas, the involved picture of such phenomena should be separately investigated for each individual gas.

A program of such a nature has been in course in our Laboratory for some time, and the results when completed will be published and discussed for each gas in the near future.

References

1 J. Plücker ; *Pogg. Annal.* **103**, 91 (1958).
2 D. Alpert ; *J. Appl. Phys.* **24**, 860 (1953).
3 H. Schwarz ; *Z. Phys.* **122**, 437 (1943).
4 H. Schwarz ; *Z. Phys.* **117**, 23 (1940).
5 L. J. Varnerin and J. H. Carmichael ; *J. Appl. Phys.* **28**, 913 (1957).
6 J. H. Carmichael and T. S. Knoll; *Transactions of the Fifth National Symposium A.V.S., San Francisco* (1958), Pergamon Press (1959), p. 18.
7 L. Holland ; *J. Sci. Instrum.* **36**, 105 (1959).
8 R. N. Bloomer ; *Brit. J. Appl. Phys.* **8**, 40 (1957).
9 P. della Porta ; this volume, p. 181
10 M. Farber and A. J. Darnell ; *J. Chem. Phys.* **21**, 172 (1953).
11 I. Langmuir ; *J. Am. Chem. Soc.* **37**, 417 (1915).
12 N. W. Robinson and F. Berz ; *Vacuum* **9**, 48 (1959).
13 R. N. Bloomer ; *Brit. J. Appl. Phys.* **8**, 352 (1957).

DISCUSSION

Question from Mr. L. Holland

Your results for nitrogen are in agreement with those of Cloud, Beckman & Trump who found that thick barium films sorbed nitrogen (and oxygen) faster with a Penning ion source in operation. As in your results, they found that activation of hydrogen by ionization did not influence the sorption rate of barium. Since the sorption occurs by diffusion through reaction products and between the film crystallites the results suggest that only atomic nitrogen and possibly atomic oxygen can penetrate the pores of the film and be sorbed rapidly once the reaction has proceeded.

On the other hand, the form of the crystallites and the reaction products do not block the passage of hydrogen and there is no improvement by dissociation. This is not the case with for example titanium where the film structure is initially compact and the surface layers, such as the oxides, are free from pores. In this case activation (dissociation) appears to be essential for rapid sorption. Probably the atomic gas more readily penetrates the interstices between the film grains.

In conclusion have you considered using a Penning-ion-source because a hot filament would not be present and the yield of active gases would be higher.

Answer. Our Laboratory is carrying out a set of tests with much higher ionizing currents, using a Penning ion-source.

Up till now we were interested in separating the phenomena, possibly caused by the ionization gauge, and therefore we limited our researches to the currents present in these tubes.

The Absorption of Gases by Barium Getter Films applied as a Tool

J. J. B. FRANSEN and H. J. R. PERDIJK

Electronic Valve Laboratory, N.V. Philips' Gloeilampenfabrieken, Eindhoven, Netherlands

Some means will be discussed by which all barium-alloy getter types may be compared. Both the " melting-curve " and " yield-curve " of a getter type will give full information on its properties during flashing. From them the reliability of the getter may be read. Further a hydrogen- and/or oxygen-capacity measurement can be used to check for contamination in the barium film produced. An additional investigation on the CO-capacity will inform on the active area of the film, which usually will be larger than the area of the surface covered by barium. The method will be explained by applying it both to a radio-valve getter and to a television-getter.

1. General

Gas absorption measurements by getter films may be performed with two definitely different aims.

One aim may be to do these measurements to gather more information on the behaviour of various gases in the presence of the absorbing substance. Then in this case we are interested in the vacuum conditions : the rate of clean up, the ultimate vacuum obtainable.

The other point of view may be to use gas absorption as a tool to obtain some more knowledge on the gettering substance itself. For instance on the compounds formed or on the structure of the getter material.

Both starting points may lead to experiments which may be similar. However the interpretation of the results will be different.

There will be a correlation between the two types of investigations, that is, the clean up will depend on the state of the getter film.

It turned out to be possible to decide upon clean up ability from film structure differences.

In the following we will indicate how gas absorption measurements may be applied to obtain information on the barium getter mirror evaporated from alloy getters by a high frequency heat treatment. So we will use the gas absorption as a tool. Some time ago this had led to the hypothesis that a barium getter film normally consists of a large number of tiny droplets more or less sintered together.[1,2]

The ultimate state of the fresh film will first of all depend on the getter design. Furthermore it can be influenced by the conditions during the evaporation.

Means will be dealt with, by which some properties of alloy getters of various origin and shape can easily be compared.

The mounting of the getter has always been chosen in such a way that a thin but non transparent barium layer will be formed.

2. Getter design

The getter design can find expression in two curves : the " melting-curve " and the " yield-curve ". From these can be derived how the getter type under investigation can best be evaporated.

As an example a home-made ring-shaped radio-valve getter will be discussed. The experiments have been performed in the envelope drawn in Fig. 1. The getter is

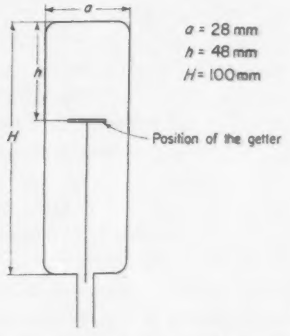

FIG. 1. Radiovalve getters may be checked in the envelope drawn. By adjusting the mounting position of the getter the barium film can be made non-transparent.

mounted as indicated in the figure. The getter film will cover the top of the envelope over the getter.

The tube is connected to a pump. It is heated at 400 °C for 10 min. Then it is allowed to cool down to room temperature. Now, by h.f. heating of the getter holder, barium can be evaporated. However, various h.f. energies may be applied for the purpose. We will have to select a suitable energy.

The behaviour of the getter in dependence on various h.f. heat treatments can be expressed in a graph (Fig. 2) by plotting along the axes the time of the start of barium evaporation and the total heating time. The start of barium evaporation depends on the energy applied. The cross indicates a treatment due to which barium starts to evaporate 7 sec after switching on, whereas the heat treatment was stopped at 10 sec.

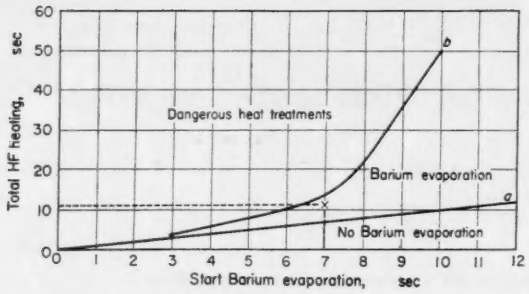

FIG. 2. Curve *b* is the " melting-curve ". It can be obtained by heating a number of getters of the same type, when applying various energies. Both the time elapsed until barium evaporation starts and the time where fusion of the container will occur have to be observed. Each treatment can be indicated in the figure by a point fixed by the times observed. All points should be found over curve *b*. Points under curve *b* indicate safe treatments only.

Curve *b* separates two regions. Over curve *b* all treatments will be found which might lead to fusion of the container. Under curve *b* no melting will occur.

Curve *a* connects the points belonging to treatments where just no barium evaporation will take place. In between curve *a* and *b* more or less barium evaporation will be obtained. We can choose out of these treatments.

Curve *b* is an important one. It has been obtained by the following considerations : Each item of the getter batch will have its own " melting-curve ", due to slight variations in structure. However only one point of each of these curves can be measured, for each getter can only be used once. If all " melting-curves " of the getters in the batch lie close together, it will be sufficient to measure the points of some samples, applying various energies. Then these few points will define curve *b* very well as the envelope of the " melting-curves " of all the items. In this case the getter batch will be a reliable one on evaporation and it will be the more reliable the steeper curve *b*.

If on the other hand the points measured are scattered over the field a large number of getters have to be flashed and the points which get off worst will decide the shape of curve *b*. Such a batch will be unreliable. The irregularities in the positions of the points indicate failures in the getter batch or even a failing of the getter design.

If in Fig. 2 we choose a high frequency energy, where barium starts to evaporate for instance after 7 sec heating, then by titration the yield can be investigated as a function of the total heating time, which may be 8, 9, 10 sec. So

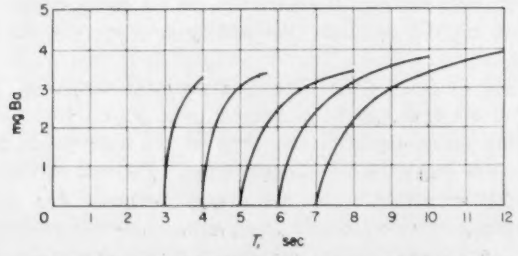

FIG. 3. The " yield-curve " indicates the amount of barium evaporated as a function of time. For five high frequency energies yield-curves have been given. The start of barium evaporation (point of intersection on the horizontal axis) is a measure of the energy applied.

" yield-curves " can be made for various h.f. energies applied. In Fig. 3 five " yield-curves " have been plotted, each of them belonging to one and the same h.f. adjustment. The total heating time has been varied only.

From the graph can be derived how long has the getter to be heated in each case to obtain for instance a yield of 3 mg. Now for the getter type under investigation some well defined possibilities of making a getter film containing 3 mg of barium are known.

For practical applications we can choose out of them the one which best meets our requirements. Besides that we are able to compare various getter types if their curves are known, of course only as far as it concerns their behaviour during flashing.

3. Purity of the getter film

It proves to be possible by means of a simple gas absorption experiment to check the barium film for contamination.

Hydrogen can be used for the purpose. Well dosed amounts of hydrogen are allowed to be absorbed by the barium film (at room temperature), until no further absorption is observed. During this treatment the shiny getter film will gradually turn into a transparent layer[3] if the barium has not been contaminated (Fig. 4).

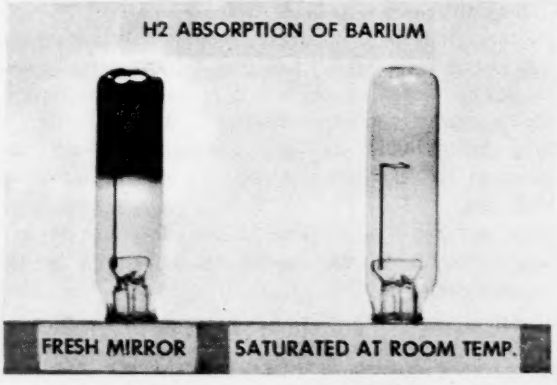

FIG. 4. If at room temperature hydrogen is allowed to be absorbed a pure barium film will turn into a completely transparent film by formation of BaH_2. A stain on the wall indicates an impurity in the film.

The amount of hydrogen, absorbed by the amount of barium present in the film (the latter found by titration) will by division give the absorption per mg getter material. In this figure we have another means to check on the completeness of the hydride formation by comparing it with the theoretical value.

If the hydride formation cannot be completed a stain on the wall of the glass envelope will be visible. Mostly this stain will be the key to find the source of the contamination.

Also a thin layer of evaporated material not being barium, if present, can easily be detected.

For the same purpose an oxygen capacity measurement can be applied. Here also a transparent layer[3] will be obtained at room temperature if the barium film has not been contaminated (Fig. 5).

It has to be noted that not all investigators agree with these observations. Della Porta[4] states that only a superficial reaction between barium and hydrogen exists.

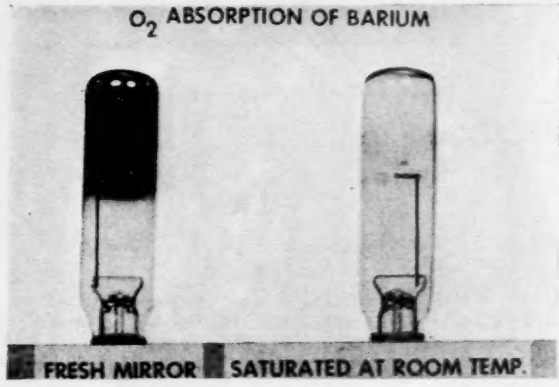

FIG. 5. Oxygen may be used to obtain information on impurities in the barium film as well. A pure barium film will be transparent when at room temperature the oxidation has been completed.

4. Microscopic area

Now let us suppose to have obtained satisfactory results on purity. We know how to flash the getter to obtain 3 mg of barium and we know that the barium film has not been spoiled during the formation. Then the next step may be to find the actual active getter area, which usually will be larger than the glass surface covered by the film. This area will be named the microscopic area. A large microscopic area will be of interest since the absorption rate for all gases and the absorption capacity for superficially absorbed gases may be supposed to increase with increased microscopic area.

Since CO is a gas which at room temperature is absorbed superficially by barium[3] (Fig. 6) we apply this gas as a measure for the microscopic area. The higher the CO absorption capacity per mg barium, the larger the microscopic area will be and the better the getter type will behave in practice.

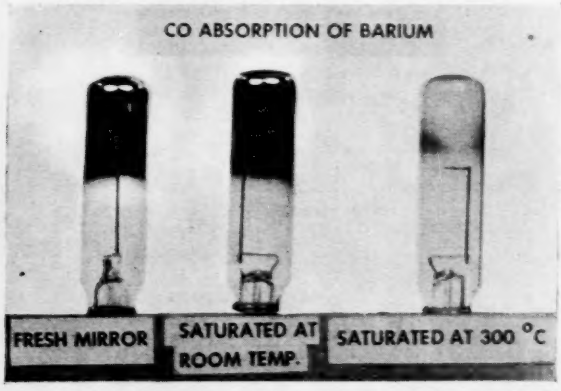

FIG. 6. The CO-absorption by a barium film cannot be completed at room temperature, since only a superficial reaction will take place. The film scarcely changes in appearance. The absorption capacity of CO at room temperature is a measure of the microscopic area of the film. At higher temperatures (over 150°) the film will change to transparent reaction products, being barium oxide and barium carbide.

At higher temperatures (over 150 °C) all barium will react with CO to form BaC_2 and BaO.[5]

Again it has to be noted that no agreement exists on this point. Bloomer[6] states that barium and CO react to form BaO and free carbon, which is in contradiction with the results of our experiments.

When heated, the layer will turn transparent like during the absorption of hydrogen and oxygen at room temperature (Fig. 6).

According to the reaction: $3\,Ba + 2\,CO \rightarrow 2\,BaO + BaC_2$ 81.9 l.μ CO/mg Ba can be absorbed.

Experimentally we obtained: 81 ± 7 l.μ CO/mg Ba.

The CO-absorption capacities per mg barium, measured at ambient temperature may depend on the getter type and various other factors, one of the latter being the flashing conditions.

For the home-made ring-shaped radio-valve getter under investigation we obtained a higher CO-absorption capacity at room temperature if the getter (having a yield of 3 mg) is more quickly flashed. The curve indicates a rise from 12 up to 20 l.μ/mg (Fig. 7).

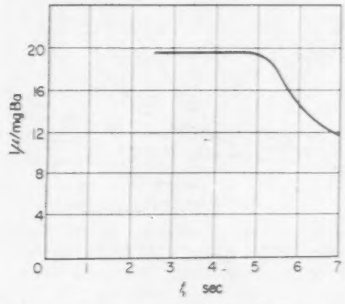

FIG. 7. The CO-absorption capacity, measured at room temperature, of a ring getter ("melting-curve" in Fig. 2, "yield-curves" in Fig. 3) proves to be dependent on the flashing conditions. The more energy applied during the evaporation of barium (indicated by the start of barium evaporation on the horizontal axis in the figure), i.e. the more rapid barium starts to evaporate, the higher the CO-absorption capacity per mg evaporated barium proves to be.

The quicker the getter is flashed the larger the microscopic area will be and the better the getter will behave in practice as well.

5. Television getters

The same holds for television getters. Here a larger bulb has to be used (Fig. 8).

In Fig. 9 the "melting-curves" of ring getters of various origin for TV-tubes with 110° deflection have been plotted. As can be seen in the figure large differences in behaviour during the h.f. heat treatment can be obtained. The curve on the right describes the behaviour of an unreliable getter. The left-hand curve is the best of all. This getter type will further be discussed (Fig. 10).

Its good "melting-curve" indicates the possibility of rapid evaporation.

Again the yields as a function of the total heating time now for four different h.f. energies have been plotted (Fig. 11).

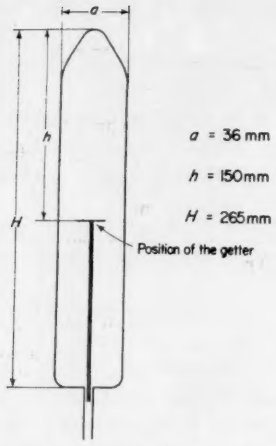

FIG. 8. Getters for TV-tubes have to be evaporated in larger envelopes to obtain not too thick a layer. Here also the barium film should be non-transparent.

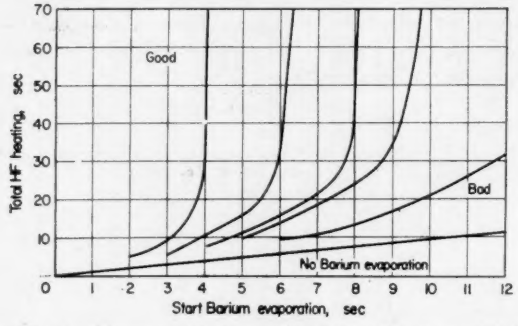

FIG. 9. The "melting-curves" of some ring getters of various origin have been drawn in this figure. Large differences exist in their properties during the evaporation. The steeper the curve the more reliable the getter type will be.

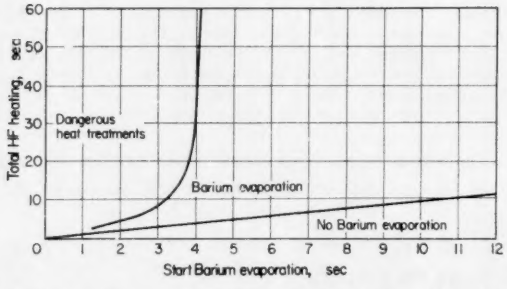

FIG. 10. The "melting-curve" of the best getter, already shown in Fig. 9. The getter can be heated rapidly. It will yield 28 mg of barium in 20 sec (start evaporation : 4 sec).

28 mg of barium can easily be obtained from this getter. The mark on the left-hand curve indicates the time at which it will be likely that the getter trough fuses. The heat treatment indicated by the next curve is already completely safe if 28 mg of barium are required ; 20 sec heating will be sufficient.

The CO-capacities per mg barium (measured at room temperature) as a function of the h.f. energy applied (indicated by the time at which Ba starts to evaporate) have been represented in Fig. 12.

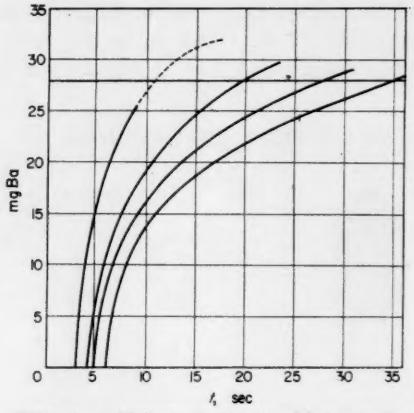

FIG. 11. The TV-getter, which possesses a "melting-curve" as drawn in Fig. 10, yields 28 mg of barium. Four "yield-curves" have been shown in the figure, corresponding to four high frequency energies applied. If barium starts to evaporate at 3 sec it is likely that the getter container will fuse before 28 mg have been obtained (indicated by the dotted part of the curve). If barium starts to evaporate at 4 sec, then the heat treatment will be completely safe. In 20 sec 28 mg will have been evaporated.

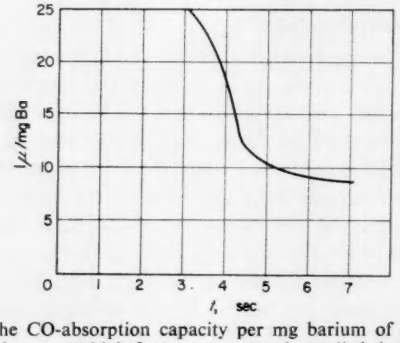

FIG. 12. The CO-absorption capacity per mg barium of a TV-getter increases when more high frequency energy is applied during flashing (see also the "melting-curve" in Fig. 10 and the "yield-curve" in Fig. 11). A high energy corresponds to a rapid start of the evaporation (short time on the horizontal axis).

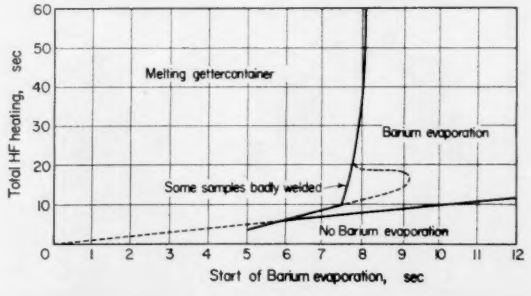

FIG. 13. A rectangular getter, containing four welds in the circuit, proved to have the properties as indicated by the "melting-curve" drawn in the figure. However some samples in the batch were badly welded and fused already for treatments in the region where no melting must occur (indicated by the dotted line). This is a defect of the batch. The "melting-curve" cuts the no-barium borderline (at 6 sec on the horizontal axis). This means that more rapid evaporation will lead to fusion of the container before barium starts to evaporate. This is a defect of the getter design.

Here a rise from 10 to 25 l μ/mg has been observed, when the getter is flashed more quickly.

Vol. 10 196

So again quick evaporation will be an advantage (c.f. radio-valve getter results (Fig. 8.)

If the bulb had been much larger, as in fact in TV-tubes will occur, then the CO-absorption capacity per mg barium, so the microscopic area of the film as well, will be much larger too.

In Fig. 13, as an example the " melting-curve " of a getter batch, now out of date, containing some defective getters is shown. This getter is a rectangular getter having four welds in the circuit. One of these welds proved to be bad obviously due to a failure of the machine which made them. Such a batch will be unreliable and ought to be discarded for practical applications and for experimental purposes as well.

The " melting-curve " cuts the no-barium line at 6 sec on the horizontal axis. This means that quick heating of the getter will lead to fusion before barium has had the chance to evaporate. This is a defect of the getter design and means a limitation of its applicability.

In Fig. 14 the gas absorption results have been tabulated for the loop getter R1 679 51. In all experiments the gas absorption was supposed to be completed when within ten minutes no further decrease in pressure was observed.

Absorption of various gases by a Bariumfilm in $l_{\mu t}$(0°C)/mg Ba

Gas	Absorption experimentally							Absorption theoretically	According formula
	Temp.film during absorption in °C								
	25	50	100	150	200	250	300		
H_2	128±7							123 →	BaH_2
O_2	69±9							62 →	BaO
CO	12	12	25	67	81	81	81±7	81·9 →	$BaO + BaC_2$
								Bloomer: 123 →	BaO + C

Gettertype: R16795I
Flashing conditions: Start Barium evaporation: 7sec
Total HF heating time: 11sec

FIG. 14. The gas absorption results, which have been discussed, tabulated. The experimentally obtained absorption capacities for hydrogen, oxygen and carbon monoxide may be compared with the values calculated from the compounds which might have been formed. The capacity for CO at higher temperatures proves to be in agreement with the formation of barium oxide and -carbide. According to the reaction proposed by Bloomer much more gas should have been absorbed.

References

[1] J. J. B. Fransen and H. J. R. Perdijk ; *Philips Techn. Rev.* **19**, 290 (1957).
See also : Y. Mizushima, Z. Oda, and O. Ochi, *J. Phys. Soc. Japan* **12**, 355 (1957).
[2] H. J. R. Perdijk ; *Lecture Internat. Symposium on Residual Gases in Electron Tubes*, Como (Sept. 1959).
[3] S. Wagener ; *Vacuum* **3**, 11 (1953).
[4] P. della Porta ; *Vacuum* **6**, 41 (1959).
[5] F. H. R. Almer, H. J. R. Perdijk and P. G. van Zanten ; *Lecture First International Congress on Vacuum Techniques, Namur*, Pergamon Press (1958).
[6] R. N. Bloomer ; *Brit. J. Appl. Phys.* **8**, 352 (1957).

Structure of Barium Getter Films

H. J. R. PERDIJK

Electronic Valve Laboratory, N.V. Philips' Gloeilampenfabrieken, Eindhoven, Netherlands

The structure of barium getter films, made by means of barium aluminium alloy getters, has proved to be of granular nature. A hypothesis is advanced in which it is stated that, during the heat treatment of a getter, barium mainly will be sputtered instead of evaporated. Various facts to support this hypothesis will be discussed.

1. Situation

Nowadays the getter normally used in electronic tubes is barium evaporated from a barium aluminium alloy. This alloy is stable in the air and can be handled as a powder. The alloy may be packed in holders of various shapes and sizes. Metal powders may be added to improve the evaporation of barium. For this purpose metal powders have been applied in pellet getters since about 1950.

In the getters the quality of the materials used by the supplier will play an important role with respect to the absorption ability of the barium film, evaporated from them.

Besides that the film structure depends on the getter design as well, so the gas absorbing properties of various types of getters of one supplier will generally be different.

Usually a getter will be heated by high frequency energy to obtain the deposit. Each getter type has its own peculiar behaviour during this heat treatment. The h.f. heating ought to be adapted to this behaviour to obtain the most favourable state of the barium film.

The most suitable heat treatment may be derived both from the " melting-curve " and the " yield-curve "[1]. Then it still has to be investigated whether this heat treatment will fit in the manufacturing process of the valve in which it is intended to use the getter.

Furthermore there are many other circumstances, which may influence the absorption ability of the film as there are : the temperature of the envelope during flashing, the dimensions of the surface covered by barium which determines the thickness of the layer, whether the getter is flashed on- or off- the pump, the presence of gases during flashing and the types of these gases, the gas evolution of the getter itself previous to the start of barium evaporation and so on.

2. Hypothesis

A useful hypothesis on the barium evolution has proved to be the following :

(a) During the heating of the getter such a large amount of barium per unit of time is formed that barium is mainly sputtered instead of evaporated. The droplets fly to the wall and stick.

(b) On the glass wall the droplets may sinter together. This sintering will depend on the temperature of the droplets when they arrive and on that of the wall itself. Sintering diminishes the active area.

(c) The absorption of, for instance, CO (at room temperature) is proportional to the microscopic area of the getter film. Then the capacity for CO, measured at room temperature, is a measure of this area. (A barium layer with a thickness of $9.10^{-3}\mu$ is converted.)

(d) The absorption ability of a getter film will largely depend on the microscopic area.

3. Some facts

To support the hypothesis the following facts may be advanced :

(a) By means of three getter types all of similar construction, only differing in yield, six getter films have been made. From Fig. 1 it can be concluded that the variations made had little effect on the microscopic area, nevertheless the thickness of the film was varied by a factor ten. This is in accordance with the hypothesis (details in ref. 2). Only in the thinner film the sintering has been less and in the thicker film the sintering has been more pronounced. A slightly sintered layer will show the structure of Fig. 2*. A strongly sintered layer a structure like in Fig. 3.

(b) It will be clear that evaporation of a small getter in a large envelope will work against sintering. The CO-absorption capacity at room temperature will rise. A value of 57 $l\mu$ CO/mg Ba has been observed[2] (Fig. 4). This value proved to be insensitive to variations in temperature of the bulb during flashing, which indicates that all droplets were practically completely separated ; no sintering could occur.

(c) Evaporation of a getter in an argon atmosphere resulted in an absorption capacity of CO at room temperature of 70 $l\mu$ CO/mg Ba (Fig. 4). When CH_4 is used as the gas atmosphere during the evaporation 60 $l\mu$ CO/mg Ba has been obtained. This suggests that there is no essential difference when evaporating a getter in a large envelope or in an inactive gas, which works as a cooling

*The photographs have been made on an electron-microscope by Mr. H. B. Haanstra of Philips Physical Laboratory.

Gettertype	mg Barium evaporated	Distance getter to top bulb in mm	CO absorption at room temp. in $l\mu$/mg
R I 679 50	3·5	6	8
		40	12
R I 679 51	2·6	6	12
		40	12
R I 679 82	0·9	6	12
		40	18

FIG. 1. Three similar types of barium alloy getters, varying in yield, have been mounted in envelopes as drawn on the right in Fig. 4. A thicker and a thinner film can be made by varying the area of the glass surface covered by barium. The CO-absorption capacity in $l\mu$/mg barium (measured at room temperature) proves to be independent on the film thickness within wide limits. Flashing conditions : high frequency heating during 11 sec, start barium evaporation at 7 sec.

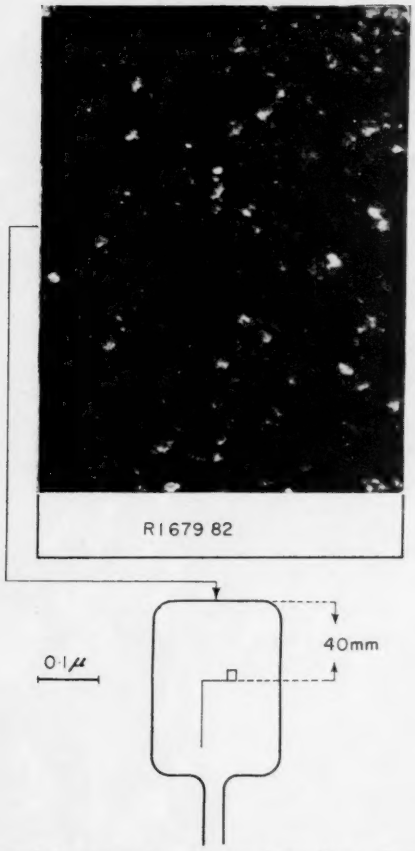

FIG. 2. Granular structure in a barium getter film. Grain diameter 0.04μ approximately.

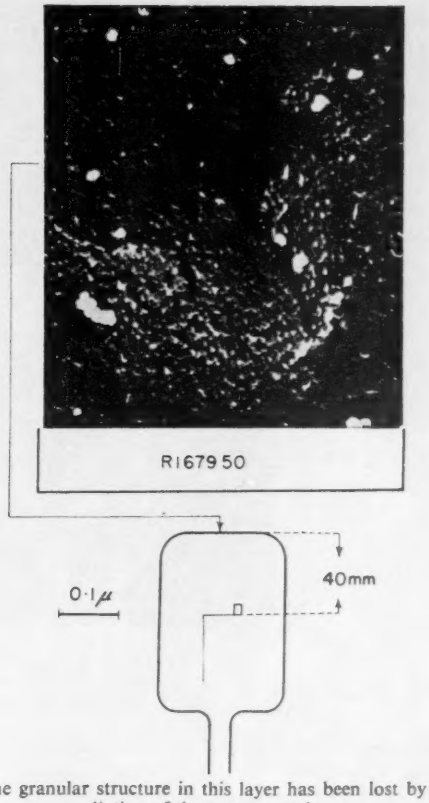

FIG. 3. The granular structure in this layer has been lost by the heat radiation of the getter container.

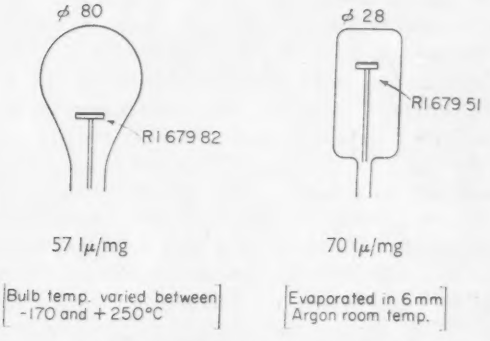

FIG. 4. A small getter R1 679 82 (0.9 mg barium) evaporated in a large envelope absorbs 57 $l\mu$ CO/mg at room temperature. Varying the glass temperature, between −170 °C and +250 °C during flashing, does not influence the CO-absorption capacity ; when measured at ambient temperature. Evaporation of a 2.6 mg getter (R1 679 51) in an argon atmosphere at ambient temperature results in a barium film capable to absorb 70 $l\mu$ CO/mg. Obviously the structures of the various films are similar. These results may be explained by sputtering of barium during flashing.

medium. This again may be interpreted as being in accordance with the hypotheses.

(d) When the barium droplets come into contact with each other on a heated glass surface during the evaporation then the CO-absorption capacity per mg barium (measured at room temperature) decreases the higher the temperature of the glass[2]. For a completely sintered layer the CO-absorption capacity at ambient temperature will no longer be proportional to the amount of barium evaporated but it will be proportional to the macroscopic area. Such a crystallised film (Fig. 5) proved to have an absorption capacity of 0.3 $l\mu$/cm^2 approximately.

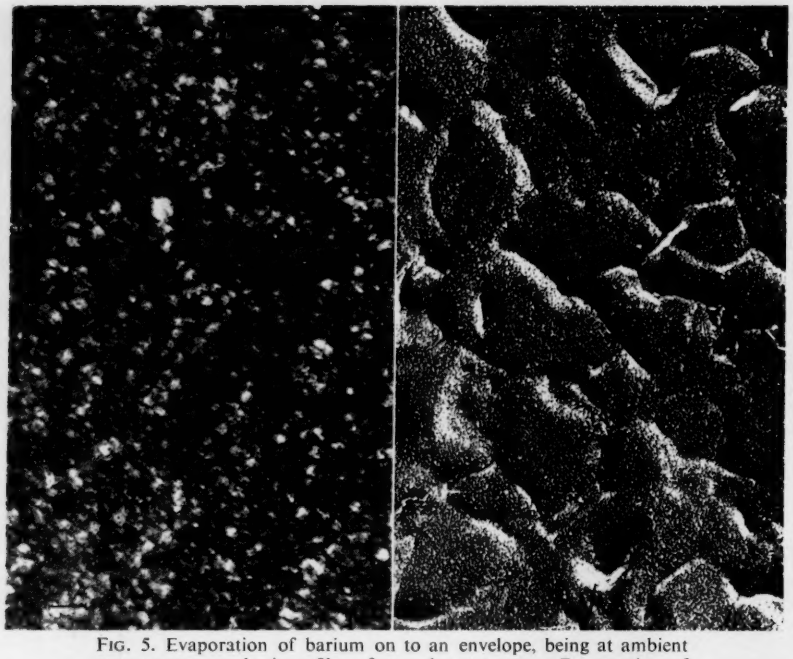

FIG. 5. Evaporation of barium on to an envelope, being at ambient temperature, results in a film of granular structure. Evaporation of barium from the same getter type on to an envelope, being at 340 °C, will result in a layer, crystallized on the wall (see also Fig. 12).

(e) The reaction of CO and barium leads to carbide and oxide formation (Fig. 6). There are arguments[3] to suppose that also at room temperature this reaction will hold*

$$3\,Ba + 2\,CO \rightarrow BaC_2 + 2\,BaO.$$

The Ba–CO reaction can be used when estimating the grain size in the barium film. From the absorption of a fully sintered layer (0.3 1μ CO/cm^2) and the reaction formula of Ba and CO can be derived that 3.6×10^{-3} mg barium will react per cm^2. This means that a layer of 9 mμ has been converted[2]. For spherical barium grains, also reacting until a thickness of 9 mμ has been used up, the diameter of the grains can be calculated to be 0.05μ (Fig. 7). This is in good agreement with the diameters visible on the photographs made by means of the electron microscope. So the CO-absorption can be used as a measure for the microscopic area indeed.

$$3Ba + 2CO \rightarrow 2BaO + BaC_2$$

[Theoretically : 81·9 1μ CO/mg Ba
experimentally : 81 ± 7 1μ CO/mg Ba]

$$BaC_2 + H_2O \rightarrow BaO + C_2H_2$$

FIG. 6. Barium and carbon monoxide react to form barium oxide and barium carbide. This reaction is in agreement with the CO-absorption capacity at 300 °C. At this temperature all barium will be converted. A subsequent reaction with water vapour results in acetylene production. If the barium-CO-reaction has not been completed (at temperatures lower than 150 °C) a water vapour reaction may result in the formation of methane and higher hydrocarbons.

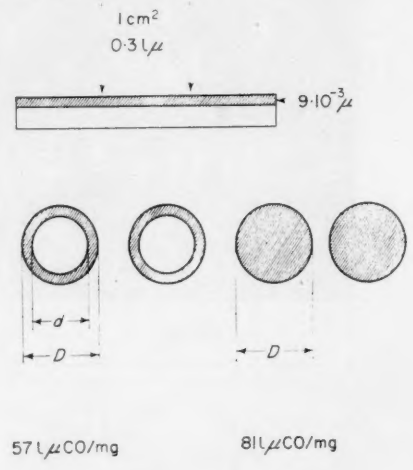

$$\frac{1/6\pi d^3}{1/6\pi D^3} = \frac{24}{81} \qquad D - d = 18 \times 10^{-3}$$

$$D = 0{\cdot}05\mu$$

FIG. 7. At room temperature a sintered barium film will react with CO until a layer having a thickness of $9.10^{-3}\mu$ has been converted. A grainy barium layer (all grains separated) absorbs 57 1μ CO/mg. For spherical particles it is assumed that the thickness of the converted layer is $9.10^{-3}\mu$ as well. A completely converted grainy film absorbs 81 1μ CO/mg. From these data the grain diameter can be calculated (0.05μ). This result is in accordance with the photographs made on an electron microscope, where the grains are of comparable size.

* Bloomer[4] states that BaO and C will be formed.

(f) Holland[5] remarks that, as a general rule during the evaporation of metal films, deposited in vacuum, the film will be less granular the more rapid its formation has been. However in barium films just the opposite effect has been observed : the quicker the film is formed the more granular it proved to be. So we can conclude that, from alloy getters, barium mainly does not evaporate. This again supports the hypothesis of sputtering (Fig. 8).

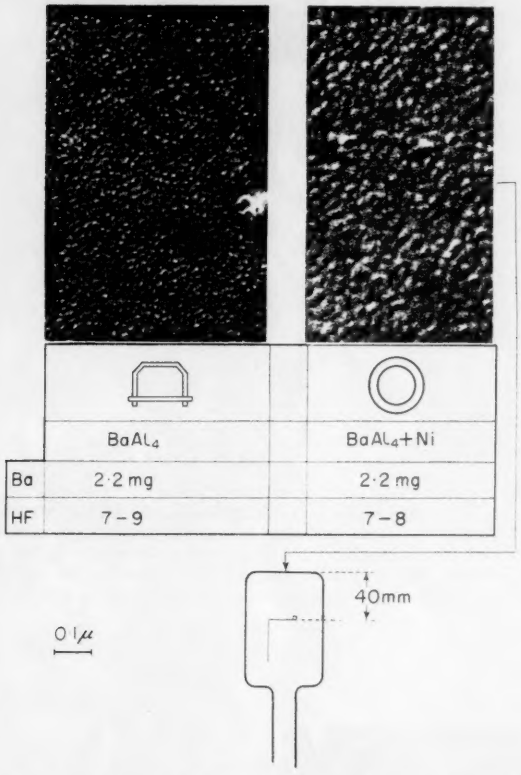

FIG. 8. The structure of a barium film depends on the getter design. The getter, containing $BaAl_4$ only, evolves the smaller grains, whereas the getter containing $BaAl_4$ and a nickel addition, which will evaporate more rapidly, yields the larger grains.

(g) The temperature of the bar of a loop getter R1 679 51 has been measured as a function of time during the evaporation of barium (Fig. 9). This experiment has been performed with the aid of a photo-transistor pyrometer[6]. The temperature at which barium evaporates turned out to be between 1125°C and 1300°C. The rate of evaporation of barium from 1 mm length of the getter bar will be approximately 0.07 mg/sec. Taking in account the slit-width in the bar (0.3 mm) the evaporation rate proves to be over 0.02 gr/sec cm². From this, the vapour pressure over the slit can be calculated[7], since :

$$p_{mm} = 17.14\,G\sqrt{\frac{T}{M}}$$

where : p_{mm} = vapour pressure of barium in mm.
G = rate of evaporation in gr/sec cm².
T = absolute temperature.
M = molecular weight of barium.

Here a pressure of 1 mm approximately will be obtained for $T = 1500$°K.

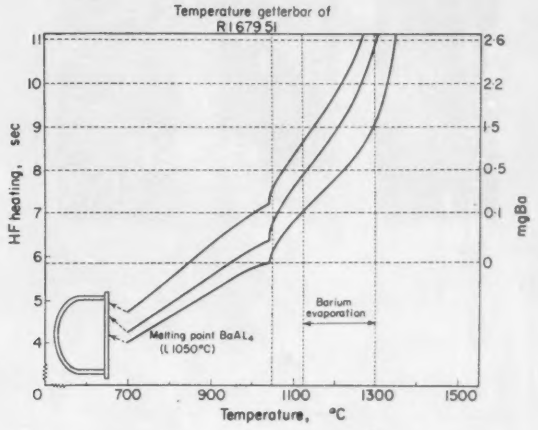

FIG. 9. During flashing the increase in temperature of the getter bar, containing the barium-aluminium alloy, has been observed. Flashing conditions : high frequency heating 11 sec, start barium evaporation 7 sec. A temperature gradient exists along the getter bar. The curves in the figure correspond with three places on the getter bar, as indicated. Near 1050°C, where the alloy melts[9], the temperature rise ceases for a while. At 1125°C barium starts to evaporate in an appreciable amount. Most of the barium has been evolved from a length of 8 mm of the getter container, when the temperature exceeds 1300°C.

Now Dushman[8] states that when during the evaporation the vapour pressure is much in excess of about 10μ, i.e. 0.01 mm, there is danger of excessive sputtering, often due to gas evolution. Furthermore evaporation in the presence of residual traces of gases, having a pressure of a few microns or more, will make the deposit diffuse and non-adherent.

Both circumstances are more or less realized when evaporating a getter, since getters will usually not be degassed and, even when this has been done, the degassing cannot have been completed.

So I think it to be likely that sputtering will take place.

4. Further experimental results

In Fig. 8 it can be seen that the grain size depends on the getter design. A getter only containing $BaAl_4$ will make smaller grains than a getter with a nickel addition. The latter will evaporate more explosively.

Also the grain size in subsequent layers of the same getter need not to be the same (Fig. 10). The grain size of the getter, containing $BaAl_4$ only, proves to be larger at the end of the evaporation. The grain size in the film of an explosive getter does not show this effect (Fig. 11). If this getter film is heated too much, for instance by radiation of the getter holder, then the grains sinter together and the microscopic area decreases (Fig. 11).

If the getter has been evaporated on to a hot bulb wall then it will crystallize (Fig. 12).

The hypothesis has also proved to be very useful, when applied in practice.

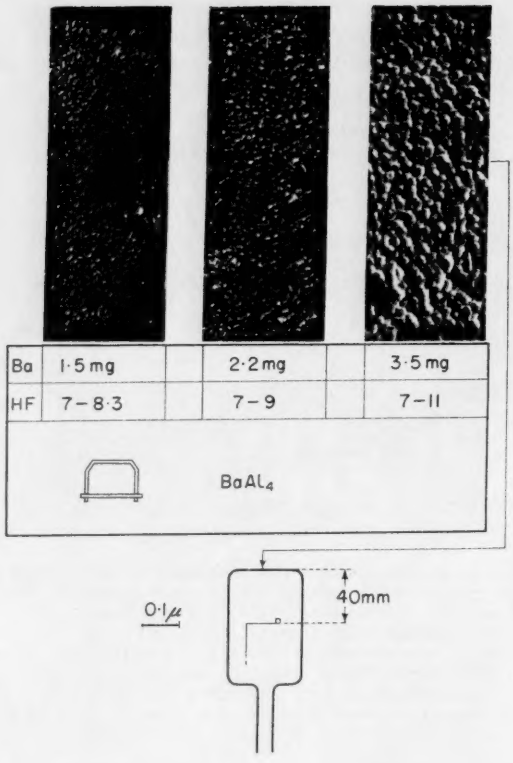

FIG. 10. This getter contains $BaAl_4$ only (see Fig. 8). During the high frequency heating barium starts to evaporate slowly. In the thinner film the grains may be small and fused by simultaneous barium evaporation originating from the ends of the getter bar, where the temperature is lower (compare Fig. 9). At higher temperatures (at the end of the heat treatment) sputtering dominates.

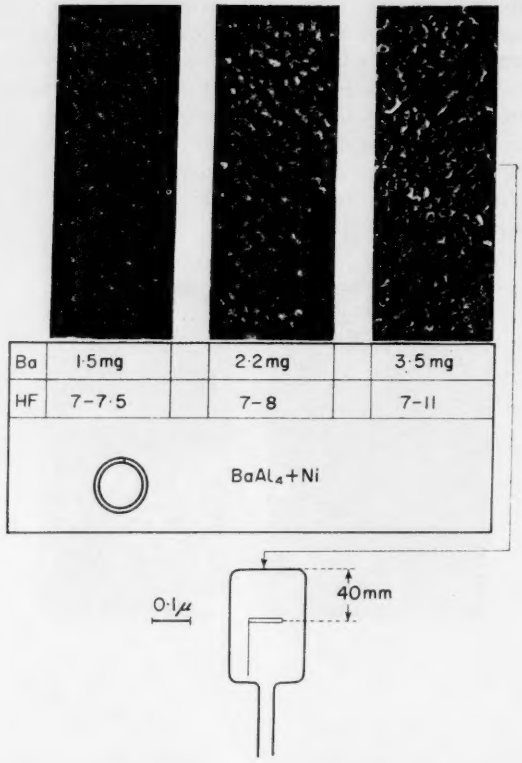

FIG. 11. This getter contains $BaAl_4$ and a nickel addition (see Fig. 8). When flashed the temperature throughout the getter ring rises rapidly, partly due to the exothermic formation of a nickel-aluminium alloy. Here barium will mainly be sputtered. The heat radiation of the container, when lasting too long, may sinter and fuse the granular film.

Vol.
10
1960

FIG. 12. A barium film evaporated on to a hot envelope (340°C) will recrystallize. Barium crystals are clearly visible in the photograph, now made on an electron microscope when applying a smaller magnification.

References

[1] J. J. B. Fransen and H. J. R. Perdijk ; *Lecture International Symposium on Residual Gases in Electron Tubes*, Como (1959).
[2] J. J. B. Fransen and H. J. R. Perdijk ; *Philips Techn. Rev.* **19**, 290 (1957).
[3] F. H. R. Almer, H. J. R. Perdijk, and P. G. van Zanten ; *Lecture First Intern. Congress on Vac. Techn., Namur*, Pergamon Press (1958).
[4] R. N. Bloomer ; *Brit. J. Appl. Phys.* **8**, 352 (1957).
[5] F. H. R. Almer and P. G. van Zanten ; *Philips Techn. Rev.* **20**, 89 (1958–59).
[6] L. Holland ; *Vacuum Deposition of Thin Films*, Ch. 7, p. 209, Chapman & Hall, London (1956).
[7] S. Dushman ; *Vacuum Technique*, Ch. 1, p. 20, John Wiley & Sons, New York (1949).
[8] S. Dushman ; *Vacuum Technique*, Ch. 11, p. 758, John Wiley & Sons, New York (1949).
[9] Dilip K. Das and Douglas T. Pitman ; *J. Metals*, 1175 (Oct. 1957).

DISCUSSION

Question from Mr. Holland

It has been stated that the grain structure is not always small when barium is rapidly evaporated. This may be true if other factors such as the support temperature is not controlled. Thus barium has a fairly low melting point and thus a high atomic mobility at low temperatures. Rapid deposition could result in a rise in the temperature of the outer barium layers due to the liberation of the latent heat of evaporation.

Heat radiation from the vapour source is not so important as the heat of the condensation, because as the barium film grows it tends to reflect the heat radiation.

You have stated that the evaporation temperature could attain 1200 °C. At this temperature aluminium in the getter alloy could evaporate.

Do you know the aluminium content of the film ?

Answer.

Indeed there are indications that the heat radiation from the source only plays an important role in extreme cases where the source is placed close to the film.

The aluminium content of barium films from alloy getters has always been found to be less than 1 per cent by weight.

ol.
10
960

Study of the Surface Structure of Barium Getter Deposited Film by an Electron Microscope

K. M. YAZAWA*

Tokyo Shibaura Electric Co., Ltd., Transistor Plant, Kawasaki City, Japan

The rate of gas sorption of the flash-getter depends especially on whether the structure of the deposited film is in an amorphous state or not. Therefore, if we observe the surface structure of the deposited film and also measure the saturated value of sorption or electrical resistivity of the deposited film, this may help to clarify the mechanism of sorption and develop an interesting method to study getters. The preparation of specimens suitable for the electron microscope and some of the results obtained are described.

1. Preparation of the specimens

The specimens for the electron microscope were made by applying the "silicon monoxide first replica method", and it was possible to observe the surface structure of many active materials, such as deposited barium films, oxide coated cathodes, etc.

Initially, in a high vacuum, the "SiO" was flashed and deposited on the surface of the "barium film" previously produced.

Next, some pure argon was carefully introduced into the vessel to increase its pressure to atmospherics.

The specimen was then rapidly soaked in ethyl alcohol

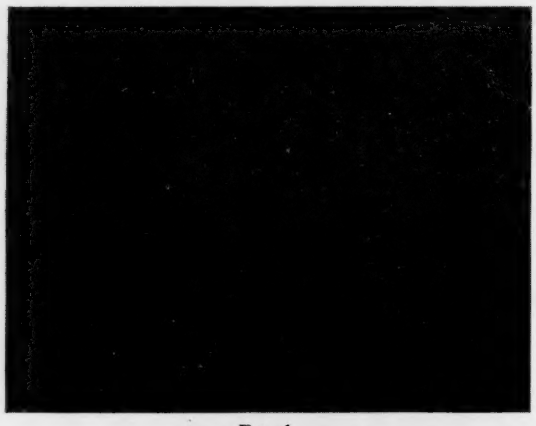

FIG. 1.

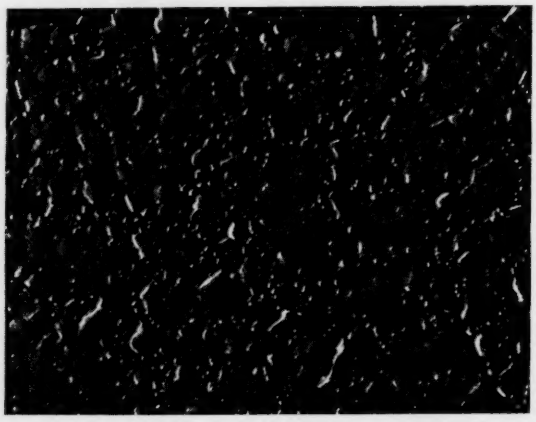

FIG. 2.

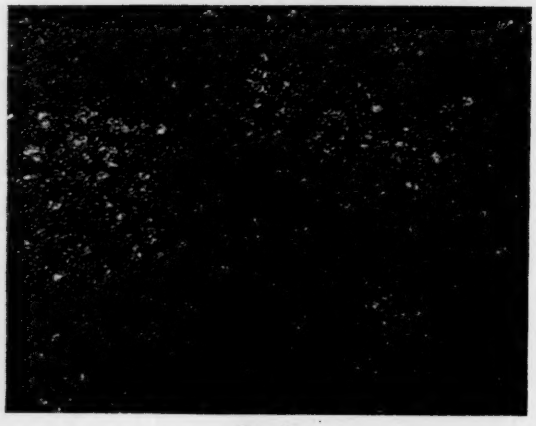

FIG. 3.

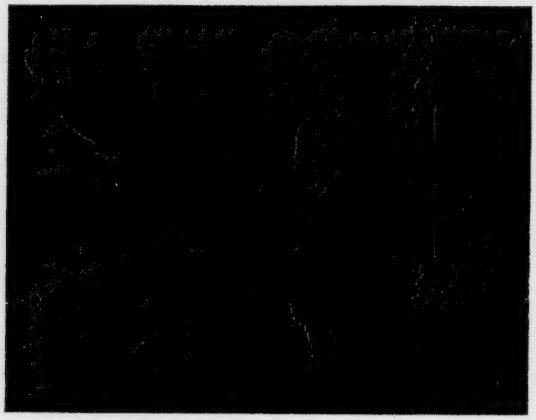

FIG. 4.

* Formerly at Matsuda Research Laboratory, Tokyo Shibaura Electric Co., Ltd.

Vol.
10
196

FIG. 5.

FIG. 6.

for protection of the active material, such as a barium film.

Next, drops of water were slowly and successively added to the alcohol. However, in the case of a barium film, a dilute solution of 10 per cent HCL is preferable to water. In the case of a barium film, it reacts slowly with the acid and the water. The " SiO " film, i.e. the replica of the active material, peels off and remains suspended in the liquid.

The " SiO " film is removed from the liquid and dried in a hot chamber, then examined with the electron microscope.

2. Results and discussions

The preceding photographs give some examples of our experiments.

Fig. 1 shows the surface of an evaporated barium film obtained in the usual manner, and having a good gettering action.

Fig 2 represents the surface of an evaporated barium film. condensed on a surface at 370°C, and having a poor performance.

Fig. 3 shows the surface of a barium film formed on a heated wall, indicating that recrystallization has partially commenced.

Fig. 4 represents the surface of a barium deposit formed in argon gas (10^{-2} torr), indicating the presence of many folds and having an excellent performance.

Figs. 5 and 6 show the surface of a barium deposit which has adsorbed a small quantity of air. It can be seen that there are many swellings which are usually associated with splits of the film.

This suggests that the reaction occurs initially at some lattice points on the surface, so called " nuclei ", and the reaction then propagates to the surrounding lattice points.

After the thin compound layer is formed, the gas molecules diffuse into the barium deposit through the split. And then, it was recognized that the rate of reaction parallel to the surface is larger than that in a vertical direction in the absence of thermal diffusion.

The Adsorption of Methane by Barium Films in the Presence of a Thermionic Current

M. G. CHARLTON and F. H. SOUTHAM

The Mullard Radio Valve Co. Ltd., Material Research Laboratory, Mitcham Junction, Surrey, England

The adsorption of methane at pressures of 7×10^{-7} to 7×10^{-6} torr has been studied both in the presence and absence of a thermionic current drawn from a tungsten filament, using the capillary flow method of Wagener, and maintaining the pressure over the barium film constant. The pumping speeds of barium films covering up to 160 cm² and up to 20 mg in weight under normal conditions were very small and were less than 5 cc/sec at 1.5×10^{-6} torr. The presence of an incandescent tungsten filament caused a slight increase in pumping speed of the barium films of about 10–20 cc/sec. Drawing an emission current from the filament appreciably increased the pumping speed of the getter, the increase amounting to 70–100 cc/sec at 1.5×10^{-6} torr with a current of 5 mA. The pumping speed was independent of the area and weight of barium film but was approximately proportional to the thermionic current; it was almost independent of the pressure, up to 7×10^{-6} torr, and hence the adsorption rate (pumping speed $\times$ pressure) was roughly proportional to pressure. The results show that the adsorption rate on barium films of methane activated by electron impact is determined entirely by the frequency of electron-gas molecule collisions. It is not known whether the active species consists entirely of ions or whether non-ionized radicals and molecules resulting from the decomposition of methane are involved.

Vol. 10 1960

1. Introduction

In recent years it has gradually become evident that methane is a frequent, and sometimes major, constituent of the residual gas in vacuum systems and devices at very low pressures. Thus methane has been found in the residual gas of getter ion pumps,[1, 2] and in vacuum tubes and cathode ray tubes,[3, 4, 5] where, apparently, it is not adsorbed to any appreciable extent by the barium getter. Indeed, there is evidence that the getter may be responsible, at least partly, for the presence of this gas in valves and cathode ray tubes, for Fransen and Perdijk[4] have reported that it is formed when water vapour comes into contact with a barium film saturated with carbon monoxide.

It therefore seemed of some interest to know to what extent methane, at low pressures, was adsorbed on barium deposits, particularly in the presence of a thermionic current, this possibly being of some importance in the actual behaviour of the getter in valves and cathode ray tubes.

2. Experimental details

Principle of the Method and Apparatus

The now well known capillary flow method of Wagener[6] was used, this being most suited to the measurement of adsorption rates at low pressures. A diagram of the apparatus is shown in Fig. 1. The getter chamber A was connected to a manifold through a removable capillary leak C of known conductance. Gas was allowed to flow through the manifold, and the flow controlled so as to maintain the pressure over the getter at a constant value. The pressure on the manifold side of the leak, p_m, was measured with the ionization gauge $G.2$, and the getter chamber pressure, p_G, with the gauge $G.1$. The pumping speed, G, of the getter is given by

$$G = \frac{(p_m - p_G)}{p_G} U$$

where U is the conductance of the capillary.

The capillary leak, which had a conductance of 20 cc/sec, could be removed by means of a magnet so as to facilitate pumping out of the getter chamber. The gas flowing to the getter chamber had to pass through the electrode assembly

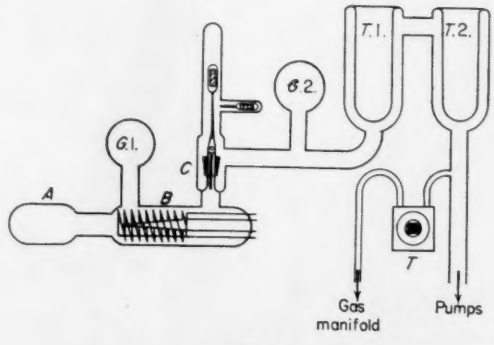

FIG. 1.

at *B*. This comprised an anode, in the form of a molybdenum wire helix spaced 1–2 mm from the glass, with a hairpin tungsten filament (the cathode) mounted axially. The distance between this assembly and the getter chamber was kept as short as possible. The whole of the apparatus shown in the diagram could be baked under a hood at 400 °C.

The methane used was supplied in sealed glass bulbs, and mass-spectrometric examination of the gas showed that there was less than 0.1 per cent impurity present.

At first a Knudsen gauge was used to measure the getter chamber pressure so as to avoid any possible activation of the gas that might occur if an ion gauge were used. It was found, however, that even after prolonged baking of the whole gauge the degassing rate of the gauge while operating was still too high, in comparison with the low adsorption rates of methane, for satisfactory measurements to be made. It was therefore replaced by an ion gauge, which, together with the other ion gauge, was operated with an electron current of 0.2 mA, at which value the pumping speed was very low.

Experimental Procedure

The system was baked and pumped overnight, and then the gauges and the molybdenum helix were degassed by electron bombardment and the getter by high frequency heating. The trap T_2 was then filled and a pressure of about 10^{-9} torr obtained. The capillary leak was dropped in position and blank measurements were made of the pumping speed for methane with (a) the hot tungsten filament only, and (b) the hot filament with an emission current being drawn.

The capillary was then removed, the getter fired, and trap T_1 filled and the capillary then replaced. Pumping rates were then measured (*a*) for the barium deposit alone, (*b*) with the filament hot (ca 1800 °C), and (*c*) with the filament hot and an emission current drawn.

3. Results

All experiments were carried out with getter chamber pressures of about 1.5×10^{-6} torr, except in one case when the effect of this as a variable was studied.

Fig. 2 shows the results obtained in a typical experiment. " LT on " indicates when the filament was raised to temperature and " HT on " indicates when the emission current was started. Two curves are shown, one for the blank experiment, and one for the experiment with the barium deposit. Obviously the pumping speed of the barium film at any stage is given by the difference between the two curves. The pumping speed of the barium deposit alone was too small to be determined, and it can only be stated, on the basis of a number of experiments, that it must be less than 5 cc/sec for a film area of about 140 cm^2.

Accurate determination of the effect of the hot filament on adsorption by the barium was not possible because of gas evolution from the filament. This was unavoidable because before being raised to temperature, the filament had already been exposed, cold, to a methane pressure of about 10^{-6} torr. With a barium film and a hot filament pumping speeds from 20 to 30 cc/sec were obtained. The hot filament alone gave rather variable results, but the highest pumping speed was 15 cc/sec. Thus the barium deposits, in the presence of a hot filament, must have had minimum pumping speeds of 5–15 cc/sec.

The results obtained on the influence of an electron current were more satisfactory, for the pumping speeds were appreciably greater than those mentioned so far. A number of experiments were carried out, with an emission current of 5 mA and an anode voltage of 120 V. Overall pumping speeds of 90 to 120 cc/sec were obtained, which, after making the necessary blank correction for electronic pumping alone, corresponded to pumping speeds of 60–80 cc/sec for the barium deposits.

The pumping speed of a barium film in the presence of an emission current was found to be independent of the weight and area of barium deposit, essentially the same result being obtained for 1 and 20 mg deposits covering 150 cm^2, and for 1 mg deposit covering 4 and 140 cm^2. It was possible to account for this observation in two ways. Firstly, the activated molecules responsible for the enhanced adsorption might be adsorbed as fast as they were formed. Secondly, if the activated molecules were deactivated on collision with the walls of the system, then the area of film available for adsorption would, because of the geometry of the system, have been constant and independent of the total film area.

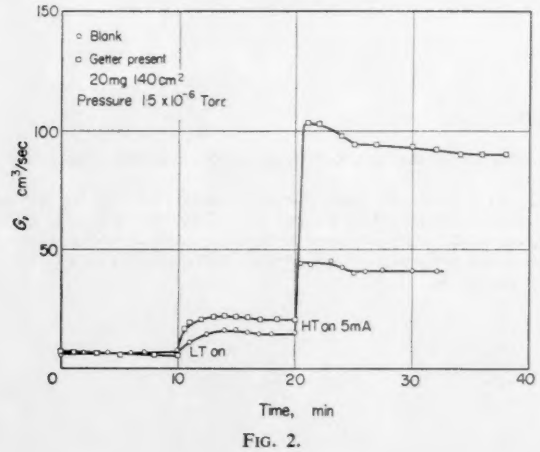

FIG. 2.

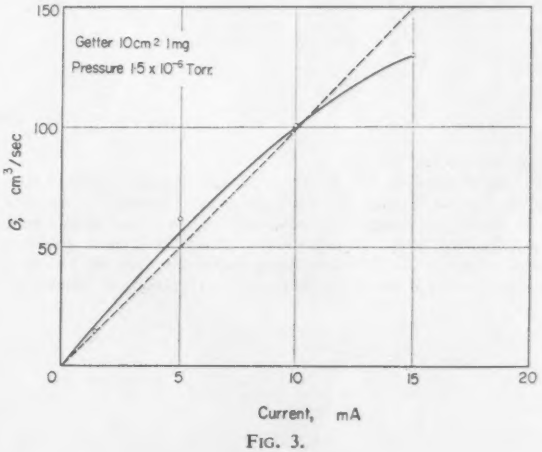

FIG. 3.

This was so because the surface of the getter chamber wall in line of sight of the ionizing assembly was coincident with, and of similar area to that of the smallest film used. An experiment was therefore carried out to test this latter hypothesis, by firing the getter into the extremity of a limb mounted at right angles to the axis of the ionizing assembly, thereby making it impossible for any particle to reach the deposit without undergoing at least one collision with the walls of the system. The results were, in fact, similar to those obtained previously, whereas if the hypothesis had been correct, adsorption by the barium film would have been greatly reduced.

It therefore appeared that the rate determining factor was probably the electron/methane molecule collision frequency. This hypothesis was tested by carrying out an experiment in which the electron current was varied and one in which the getter chamber pressure was varied. An approximately linear relationship was observed between the pumping speed and electron current, for currents of 1.5–15 mA (Fig. 3). There was also a linear relationship between adsorption rate (pumping speed X pressure) and pressure, up to about 4×10^{-6} torr, with some departure from linearity from 4×10^{-6} to 7×10^{-6} torr (Fig. 4).

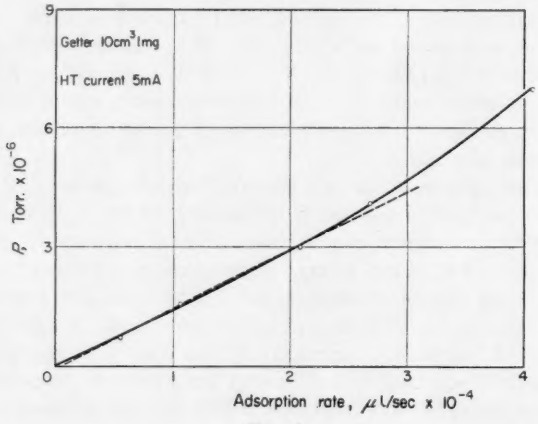

FIG. 4.

4. Discussion

The results provide strong evidence that in the enhanced adsorption of methane by barium deposits at low pressures, in the presence of a thermionic current, the rate determining process is the rate of collision of methane molecules with electrons. This implies that there is no accumulation of the active species in the system and that they are removed by the getter very rapidly. We do not know, however, what the active species is. Experiments in which a potential could be applied to the barium deposit, but which we, unfortunately, have not yet done, would show if an ionized species were involved. The detailed mechanism of the adsorption process is likely to prove rather complex, however, when we consider that the mass spectrum for methane shows that the following species are formed in the approximate percentage shown : 40 per cent CH_4^+, 20 per cent CH_3^+, 35 per cent H^+, 5 per cent CH_2^+, CH^+, C^+, H_2^+.

It is possible to calculate very approximately the number of electron/gas molecule collisions that will occur. Thus the fraction of electrons colliding with gas molecules having a mean free path L_G, in travelling a distance l is given by l/L_e, where L_e, the mean free path of an electron, is much greater than l and is equal to $5.65\,L_G$. Calculation gives a value of about 2 for the ratio of the number of molecules adsorbed to the number undergoing collision. This calculation, however, is based on a very much over-simplified theory of electron collisions, which will only give a very approximate result, on which it would be dangerous to base any conclusions as to whether non-ionized activated molecules are involved in the adsorption process.

Acknowledgements

We wish to thank Dr. J. A. M. van Moll, Head of the Material Research Laboratory, and the Directors of The Mullard Radio Valve Co., Ltd., for permission to publish this paper.

References

[1] J. C. Swartz ; *Vacuum Symposium Transactions*, p. 83, London, Pergamon Press (1955).
[2] G. Reich and H. G. Nöller ; *Vac. Symposium Transactions*, p. 97 (1957).
[3] N. D. Morgulis ; *Zhur. Tekh. Fiz.* **25**, 1667 (1955).
[4] J. J. B. Fransen and H. J. R. Perdijk ; *Philips Tech. Rev.* **19**, 300 (1957–58).
[5] J. S. Wagener and P. T. Marth ; *J. Appl. Phys.* **28**, 1027 (1957).
[6] S. Wagener ; *Brit. J. Appl. Phys.* **1**, 225 (1950).

DISCUSSION

Question from Mr. Holland

The poor agreement of the sorption rate with the collision formula probably arises because the methane is decomposed on the electron target where it is temporarily adsorbed. Thus if one admits methane or similar hydrocarbons to a glow discharge a layer of polymerized hydrocarbons is formed on surfaces facing the cathode, i.e. on faces exposed to high electron bombardment. Hydrogen is released in the desaturation of the adsorbed hydrocarbon and this is taken by the barium.

Answer. I entirely agree that this might very well be the case. Activation or decomposition of the gas in the adsorbed state by electron collision would probably occur with a far greater degree of probability than in the gas phase. Your experimental observations are, I think, very interesting.

Carbon Monoxide Sorption by Barium Films

F. RICCA
Istituto Chimico, Università di Torino
and P. DELLA PORTA
S.A.E.S. Getters, Milan, Italy

A number of workers have in the past few years studied carbon monoxide sorption by barium films, often obtaining diverging results. The complex nature of the problem, which cannot be considered as a simple surface adsorption, is shown by the work of ARIZUMI *and* KOTANI, *who propose a model based on the existence of lattice imperfections in the barium film and also by the work of* BLOOMER *who applies to this phenomenon the* MOTT-CABRERA *theory for oxidation of metals. The problem is here considered in view of the results obtained by the capillary technique at constant pressure on the getter. The experiments have been carried out in the temperature region between 195°K and 473°K. The kinetics of sorption may be studied and an analysis of the mechanism of the process may be undertaken from the obtained data. The initial velocity of the adsorption is approximately the same at the various temperatures at which the experiments were carried out, and remains nearly constant for an interval of time which increases with increase in temperature. The decreasing part of the sorption velocity curve can be interpreted as due to a diffusion phenomenon. The initial part of the curve at constant velocity, which is characteristic of carbon monoxide sorption by barium, had been often misinterpreted and attributed to the limited conductance of the capillary, and so considered non relevant to an explanation of the phenomenon. In agreement with the work of the previously mentioned Japanese authors, we recognized the value of this result, which depends on the fact that various processes are involved in the phenomenon, each one rate determining according to the pressure and temperature prevailing and according to the quantity of gas already sorbed by the getter. The whole phenomenon is thought to be due to an initial adsorption on the surface and to a subsequent surface diffusion having a low activation energy or, at sufficiently high temperatures, to a bulk diffusion, which is characterized by a higher activation energy. The end of the constant velocity portion of the curve is thought to be related to the instant when the diffusion becomes slower than the surface adsorption. The evaluation of the energy of activation for the diffusion phenomenon reveals the existence of a critical temperature in the neighbourhood of 373°K.*

Introduction

The phenomena which can occur in carbon monoxide sorption by barium films are numerous and they can be included in at least three distinct types of processes :

(a) adsorption of the gas on the surface of the barium film, or on the surface of the reaction product already formed,
(b) diffusion processes to fresh barium atoms*,
(c) chemical reaction between carbon monoxide and the metal.†

* Diffusion phenomena have been recognized by the proposal advanced by Morrison and Zetterstrom[1] to verify which of the laws concerning the oxidation of metals are characteristic of gettering of CO by barium, as well as by the model put forward by Bloomer[2] for the application of the Mott–Cabrera theory and finally are implicitly present in the model used by Fransen and Perdijk[3] of a barium film of granular structure, with a layer made up of the oxide and carbide of barium, which covers all of the granular structure of the film.

The possible diffusion phenomena are in themselves numerous and complicated : surface diffusion of the species physically adsorbed or chemisorbed above the metal surface or above the products of a reaction, diffusion in the interspaces of the film due to its granular structure, diffusion of gases in the discontinuities of layers continuously formed by the reaction occurring, diffusion of gas into the structure of the reaction product or into the structure of the metal, finally diffusion of the reaction products within the barium or *vice versa*.

† Concerning the reactions of CO on Ba Morrison and Zetterstrom[1] consider the following possibilities :

(1) $Ba + CO \rightarrow Ba O + C$ (2) $3Ba + 2CO \rightarrow Ba C_2 + 2Ba O$ (3) $Ba + 2CO \rightarrow Ba (CO)_2$

but lacking experimental results a choice between the three cannot be made.

Fransen and Perdijk[3, 4, 5] hold that the most probable occurring is the second, due to the finding of acetylene which may be formed by the action of water on the product of reaction between CO and Ba. As a result of the formation of barium carbide such a reaction is in fact possible :

$$BaC_2 + H_2O \rightarrow BaO + C_2H_2.$$

These workers claim the second reaction can occur at room temperature and above.

The first of the three reactions is considered by Bloomer[2] since it explains some of the characteristics of the sorption kinetics experimentally obtained by him with the action of the free carbon atoms contained in the layer of barium oxide.

Reactions of the third type probably account for the initial phases of chemisorption.

Finally, the hypothesis of still other reactions with a catalytic process giving rise to CO_2, is advanced by Arizumi and Kotani[6], to justify certain particular characteristics of CO sorption at room temperature.

It is clear that depending on the temperature and pressure conditions, as well as the structure of the film, or according to the stage of sorption reached, either of the process mentioned above may be the rate determining phenomenon.

It is therefore always necessary to bear in mind these points when we attempt to review the problem.

It is also very important to have available a technique really capable of giving the correct picture of the kinetics of sorption.

The technique employed in this work is the well known one based on the Knudsen flow of gas through a capillary of given conductance.

Concerning this technique, we have already emphasized in a previous communication[7] the importance of carrying out the measurements at constant pressure on the getter. At the same time we have shown the advantages which can be derived from expressing the experimental results in terms of the velocity of sorption.

Velocity of sorption curves

The velocity of carbon monoxide sorption on barium films remains initially constant for a more or less extended interval of time at all the experimental temperatures employed; it then decreases, in certain cases very rapidly.

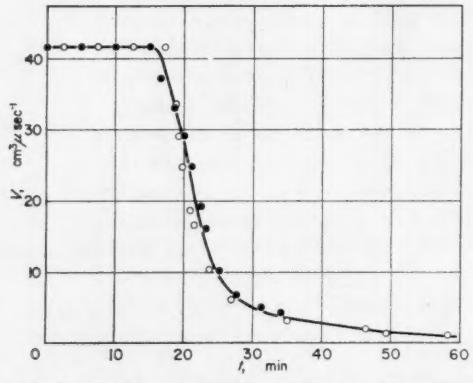

FIG. 1. Velocity of carbon monoxide sorption as a function of time.
Weight of evaporated barium = 2 mg
Apparent surface area = 100 cm²
Sorption temperature = 298 °K
Pressure (p_g) = 1.2×10^{-5} Torr.

Fig. 1 shows the experimental results for the velocity of sorption as a function of time for carbon monoxide on a barium film of about 2 mg having an apparent surface area of 100 cm², at room temperature and at a pressure of 1.2×10^{-5} Torr on the getter.

The two different types of points correspond to two different experiments, on two different barium films, carried out under similar conditions, and are therefore indicative of the reproducibility of our experiments.

Similar curves have been obtained by all previous workers.

Their essential characteristic is the initial horizontal tract, concerning which a few words may be appropriate.

An incorrect interpretation of this behaviour has in fact been put forward by Morrison and Zetterstrom[1] and subsequently accepted by Bloomer for the oxidation of barium films.[8]

These workers have considered the initial constant velocity as due to the limited conductance of the capillary, which sets an upper limit to the velocity of sorption by the barium film.

Therefore, due to this, they have placed no value on the initial part of the velocity of sorption curve, considering that only in the decreasing part of the curve is a true indication of gettering given.

In fact for a given p_m (manifold pressure) the capillary certainly influences the velocity of sorption ; but its conductance only determines the value of p_g (pressure on the getter) for which the flow through the capillary equals the velocity of sorption by the getter.

So, really, the pressure on the getter is the limiting factor, and, at a given pressure, the velocity of sorption curve perfectly describes the gettering ability of the metal film.

Such a fact becomes even more strikingly evident when measuring at constant p_g.

It is interesting to note that Arizumi and Kotani had realized in 1952 the physical importance of this fact, and on this basis had formulated their theory on the influence of lattice imperfections.[9]

Surface adsorption

If we recognize the validity of the indication given by the initial horizontal tract of the velocity of sorption curves the problem of its interpretation immediately draws our attention.

It is evident that, it is impossible to explain the tract at constant velocity, on the basis of theories of the Mott–Cabrera type for the oxidation of metals, which Bloomer had tried to apply in this case and which we will reconsider later.

On the other hand, it is equally impossible to consider such a behaviour as due to a normal chemisorption on the surface of the barium film : in such a case, we should have an appreciable dependence of the velocity on the degree of coverage of the surface (we should have in this case $v \propto (1 - \theta)$ or $v \propto (1 - \theta)^2$ according to whether the adsorbed molecules occupy one or two sites of the surface). Further, the quantity of gas sorbed in the interval of time during which the velocity remains constant is greatly superior to that required for the formation of a mono-layer.

It would seem more probable that the initial surface phase is characterized by a large mobility.

This could account for the fact that the velocity of sorption is independent of the degree of coverage of the surface, but it would be contrary to the strong interaction which would be expected to occur between carbon monoxide and barium.

A way out of this difficulty exists. It is to admit the formation at the surface of the film of a preliminary weakly bound physisorbed phase, having a high mobility.

It is difficult to say whether this " precursor " is constituted by a phase physisorbed on the barium, before the molecules have time to react chemically with the metal, or if it is in fact carbon monoxide adsorbed on the barium oxide already formed, or again if another mechanism is to be applied to its formation. Any hypothesis concerning it can only be tentative, until the actual existence of such a precursor has received a more direct experimental proof.

Vol. 10 196

However, it is interesting to note that the initial constant value for the velocity of adsorption has recently been found to appear in a number of other cases, such as the adsorption of carbon monoxide and nitrogen on tungsten.[10, 11, 12] Even in these cases, it was found necessary to propose, be it in a slightly modified manner, the hypothesis of a precursor which justified the particular kinetics of the phenomenon.[13]

Considering now Fig. 2, we have a linear dependence of

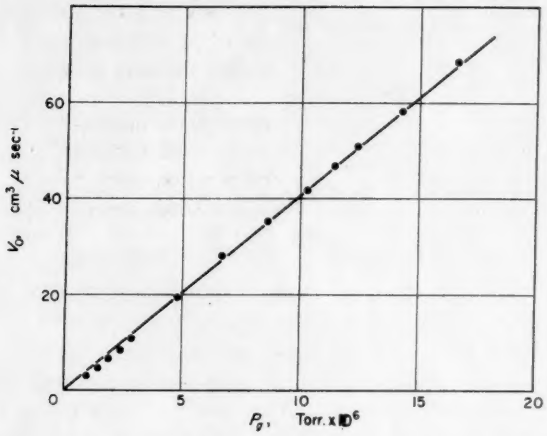

FIG. 2. Initial velocity of carbon monoxide sorption as a function of pressure on the getter (p_g).
Weight of evaporated barium = 2 mg
Apparent surface area = 100 cm²
Sorption temperature = 298 °K.

the initial sorption velocity on the pressure existing on the getter.

At the low pressures at which measurements are carried out, a precursor which is physically adsorbed, and so possesses a low activation energy for desorption, should present a low concentration on the surface.

This could explain the proportionality existing between the velocity and the pressure on the getter in the tract of the curve showing constant velocity, since we would be in a zone where the surface concentration of the adsorbed phase is almost linearly dependent on pressure.

Resuming, according to the hypothesis put forward, we should have a preliminary adsorption characterized by a high mobility of the phase formed, which would then allow the molecules adsorbed to quickly reach and react with the free barium atoms. The second stage would, according to this model, consist of diffusion processes.

Diffusion processes

In a previous paper[14] we have underlined the role of diffusion on the gettering of nitrogen.

If we consider gas diffusion into the film as a diffusion in a linear semi-infinite medium, and assume that throughout the process the gas concentration on the film surface remains constant, it can easily be shown that the quantity of diffused gas, Q_t, is proportional to the square root of time.

Even Santeler, applying his " vacuum process evaluation " to the data previously published by one of us,[15, 16] has shown the existence of diffusion phenomena [17, 18]

Now, if we plot, for carbon monoxide, Q_t as a function of the square root of time, we obtain curves of the type shown in Fig. 3. The two curves correspond to measurements carried out at two different temperatures, all other parameters being kept constant.

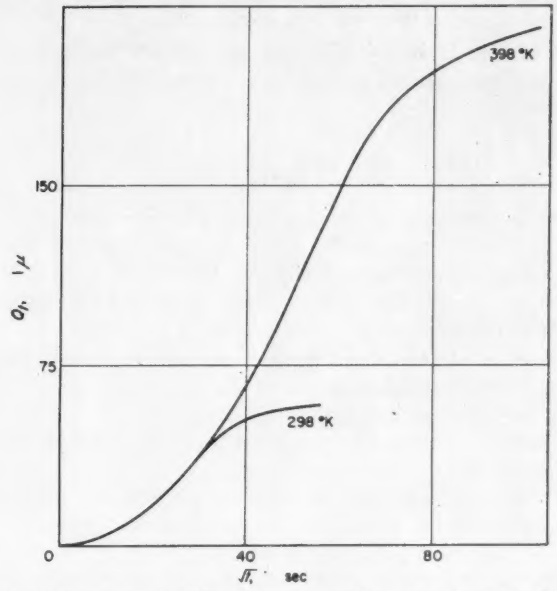

FIG. 3. Quantity of carbon monoxide sorbed as a function of the square root of time.
Weight of evaporated barium = 2 mg
Apparent surface area = 100 cm²
Pressure (p_g) = 1.2×10^{-5} Torr.

Fig. 3 clearly shows that :

(a) the first portion of the curves is obviously parabolic, since we have seen that the initial sorption velocity remains constant for a certain interval of time,
(b) although a certain portion of the curve is linear, large deviations from linearity exist towards the end of the curves,
(c) at different temperatures, deviations from linearity set in at different values of the quantity sorbed.

Already in the case of nitrogen,[14] we had found that deviations from linearity were present at the beginning and end of the curve, in particular we had advanced the hypothesis that the latter deviation was due to the very limited thickness of the barium films.

In fact if we consider Fig. 4, it is clear that, in the case of

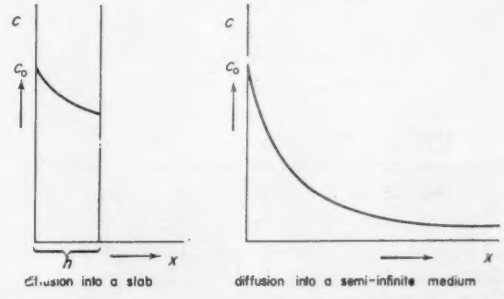

FIG. 4. Dependence of diffusion on limited film thickness.

diffusion into a medium of limited thickness the absolute value of the concentration gradient at $x = 0$ decreases much more rapidly than in the classical case of the semi-infinite medium.

Since $Q_t = \int_0^t (J_t)_{x=0}\, dt$, where $(J_t)_{x=0}$ represents the flow of the diffusing species through the defining surfaces between the gaseous and metallic phases, at time t, and is given by

$$(J_t)_{x=0} = -SD\left(\frac{\partial c}{\partial x}\right)_{x=0}$$

We have that Q_t will increase less rapidly with time.

The linear relationship between Q_t and $\sqrt{t}$ is only true for a semi-infinite medium, and therefore we must expect a deviation towards lower values, just as shown by the experimental curves.*

Therefore, it would appear that the non linearity of the experimentally obtained curve of Q_t versus $\sqrt{t}$ does not indicate that we are not dealing with a diffusion phenomenon, but purely shows the influence of the thickness of the barium film on diffusion.

Leaving aside, for the moment, the problem of diffusion in a finite medium, we shall consider as confirmed the presence of rate determining diffusion phenomenon.

We can therefore state that, initially, the preliminary adsorption of the gas at the surface of the getter is the slowest phenomenon occurring and so rate determining. Since we operate at constant pressure on the getter, the velocity of sorption is constant for all the time during which the highly mobile " precursor " can rapidly diffuse away from the exposed surface.

However, the diffusion processes are slowing down with time, hence the diffusion velocity will become, at a given time, less than the adsorption velocity on the surface.

From that time onwards the diffusion becomes the slowest process and will be rate determining, and so the sorption of gas will follow the diffusion laws.

A schematic representation of the overlapping of the two phenomena is shown in Fig. 5.

Evidently the point of intersection between the two curves depends on the structure of the film. In fact, a more porous film will present less difficulty to diffusion than a compact film, and this will therefore retard the time when diffusion processes become rate determining.

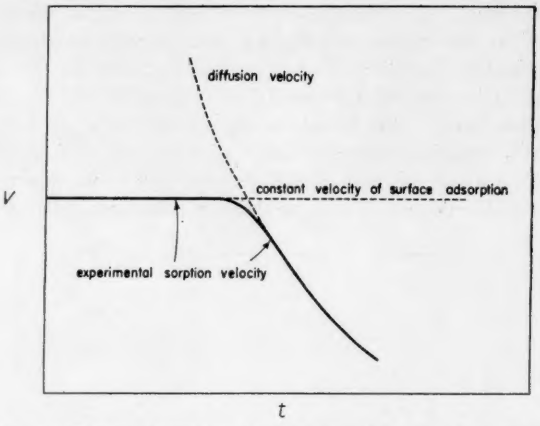

FIG. 5. Kinetics of sorption of carbon monoxide on barium films. On the basis of the necessary coexistence of the surface adsorption and the diffusion within the film, the diagram shows schematically their successive predominance as rate determining processes.

At this point it is interesting to recall the experimental findings of Morrison and Zetterstrom[1] concerning the recrystallization of barium films and the evaporation of getters in an argon atmosphere.

The recrystallization obtained by heating the film before introducing CO, produced much shorter horizontal tracts in the velocity of sorption curve.

On the other hand, flashing the getter in argon, while still giving the same velocity of adsorption, was found to extend the horizontal tract of the curve by a factor of two or three.

Since the recrystallization at high temperatures reduces the real surfaces and the flashing of the getter in argon produces a film of higher porosity, these results of Morrison and Zetterstrom are in complete agreement with the arguments proposed by us.

Concerning the point of intersection of the curves previously mentioned (Fig. 5), it is evident that the temperature at which sorption takes place will be of paramount importance.

Temperature influence

Velocity of sorption measurements for carbon monoxide

* In the case of a semi-infinite medium, we have for the distribution of the concentrations along the diffusing direction, the following equation :

$$C = C_o\left(1 - \operatorname{erf}\frac{x}{2\sqrt{Dt}}\right)$$

where :

$$\operatorname{erf}\frac{x}{2\sqrt{Dt}} = \frac{2}{\sqrt{\pi}}\int_0^{\frac{x}{2\sqrt{Dt}}} \exp(-\xi^2)\, d\xi.$$

But in the case of thin slab of thickness h we have the equation :

$$C = C_o\left\{1 - \frac{4}{\pi}\sum_{\nu=0}^{\infty}\frac{1}{2\nu+1}\sin\frac{(2\nu+1)\pi x}{h}\exp\left[-\left(\frac{(2\nu+1)\pi\sqrt{Dt}}{h}\right)\right]\right\}$$

(see for example W. Jost ; " Diffusion in solids, liquids and gases ". Academic Press, New York, 1952), for which, for t sufficiently large, a gradient of concentration smaller than in the first case can be calculated.

by evaporated barium films have been carried out in the temperature range of 195 to 473°K.

The results thus obtained are shown in Fig. 6. In this diagram the velocity of sorption is not given as usual in terms of time, but as a function of the quantity of gas sorbed up to the time considered. This permits a more direct comparison between the velocities of sorption at the different temperatures.

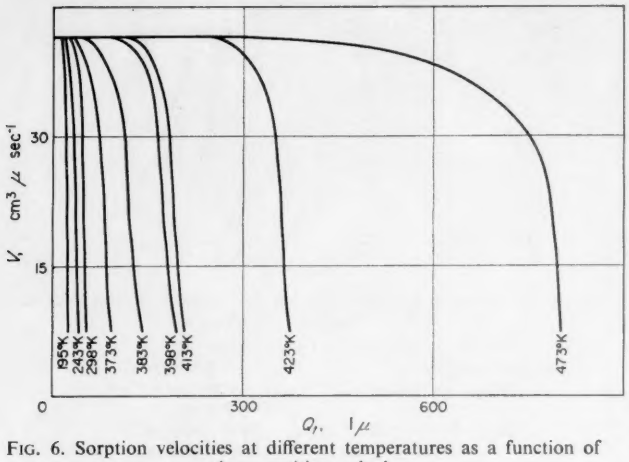

FIG. 6. Sorption velocities at different temperatures as a function of the quantities sorbed.

Apparent surface area = 100 cm².

The quantities of evaporated barium are 2 mg for all curves except for those at temperatures of 423°K and 473°K where 5 mg and 8.5 mg were evaporated respectively.

All measurements have been carried out under pressure conditions which allow, at all the temperatures, the same number of molecules to strike unit area in unit time.

All measurements have been carried out under pressure conditions which allow, at all the temperatures, the same number of molecules to strike unit area in unit time.*

With reference to Fig. 6 let us consider the fact that the initial velocity of adsorption remains constant with variations of temperature.

This fact seems to indicate further that the phase which was considered as a "precursor" of the sorption process is a physisorbed phase, whose formation does not require any activation energy.

A second consideration which can be advanced on Fig. 6 concerns the increase in length, with temperature, of the horizontal part of the curve, and so the increase of the quantity of gas sorbed at nearly constant velocity.

Since the constant velocity of surface adsorption is the same at different temperatures, whilst the diffusion velocity obviously increases with temperature (we have in fact $D = D_0 \exp \frac{-E}{RT}$), the intersection of the two curves varies when the temperature changes and the interval of time during which the velocity of sorption remains constant, increases with increasing temperature.

Hence, from the curve in Fig. 6 it should be possible to calculate the energy of activation for the diffusion processes which have occurred in the barium film.

It is difficult to fix the quantity sorbed, corresponding to which we can say that diffusion processes become evident and rate controlling.

Considering, as an approximation, a point where the velocity of adsorption has decreased by 2.5 per cent with respect to its initial value, one can plot the data as in Fig. 7.

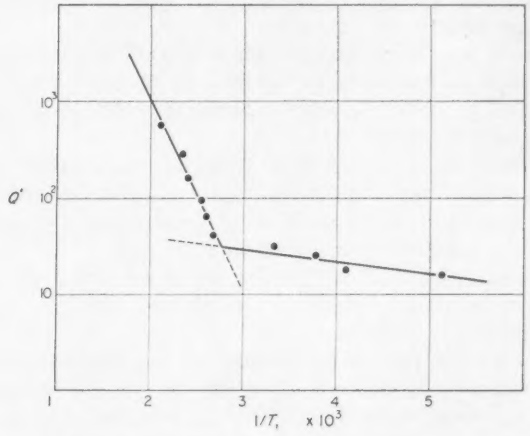

FIG. 7. Temperature dependence of carbon monoxide diffusion in barium films.

From Fig. 7 it is seen that the experimental points fall on two straight lines which intersect in the proximity of 363°K.

The linearity of the points confirms the applicability of the model adopted, and partially supports the validity of the

* Under Knudsen flow conditions, the relation between the pressure p_g' measured by the gauge M_g' at a temperature T_G' to the actual pressure p_g on the getter at a temperature T_G, is

$$\frac{p_g'}{p_g} = \sqrt{\frac{T_G'}{T_G}} \qquad (1)$$

(See, for example, Dushmann). Hence to retain a constant p_g at the various temperatures one should vary p_g as given by equation (1).

In order to obtain interesting indications concerning the kinetics of the phenomenon at the various temperatures, it is however, preferable to operate under conditions which result in a constant number of molecules striking the surface of the getter in a given time.

The number of molecules which in one second strike one cm² of the surface of the getter at a pressure p_g and a temperature T_g is given by,

$$n_g = \frac{3.513 \times 10^{22}}{\sqrt{M}} \cdot \frac{p_g}{\sqrt{T_g}} \qquad (2)$$

where M is the molecular weight of the gas and p_g is in Torr. From equation (1) and (2) we have :

$$n_g = \frac{3.513 \times 10^{22}}{\sqrt{M\,T_g'}}\, p_g' \qquad (3)$$

Hence if T_g' is constant (temperature at which the gauge M_g' is operated) in order to have a constant n_g at various temperatures, one must in all experiments maintain a constant value of p_g'.

method used to calculate the activation energy which depends on the beginning of a decrease in the sorption velocity.

On the other hand, the two distinct straight lines show the existence of two energies of activation, respectively below 1000 cal/mole and about 9000 cal/mole, and therefore two distinct diffusion processes, respectively predominant below and above the critical temperature.

The existence of two energies of activation and so of two distinct diffusion processes, entailing the existence of a critical temperature, can be considered as a fact. However, the numerical values here quoted for the activation energies are subject to revision, since the calculations have been carried out with the approximation previously stated.

The applicability of the Mott-Cabrera theory to the gettering of CO

The importance of examining the applicability of Mott's theory to the sorption of gases by metal films is obvious if we bear in mind the fact that Bloomer considers it applicable to the cases of oxygen and carbon monoxide,[2, 8] and that recently Roberts and Tompkins[19] have tried to apply it to nitrogen sorption on calcium.*

Let us now briefly compare the results of the theoretical and experimental work carried out by Bloomer applying Mott's theory to the sorption of carbon monoxide by barium films, with our results.

There exists, according to Bloomer, a critical temperature of about 80 °C below which the quantity of gas sorbed should be independent of the thickness of the evaporated barium film and dependent on the temperature.

Above this temperature the quantity of gas sorbed should be proportional to the thickness of the metal film and independent of temperature.

On the one hand we can remark on the relatively good agreement between the critical temperature found by Bloomer and that found by us (~373 °K) whilst in the other we have to report that the phenomena occurring above and below this temperature are not those experimentally found by us.

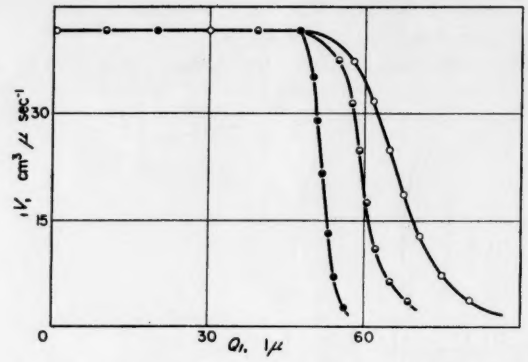

FIG. 8. Velocities of sorption showing the influence of film thickness below the critical temperature.

Sorption temperature = 343 °K
Pressure (p_g) = 1.2×10^{-5} Torr
Apparent surface area = 100 cm²
Weight of evaporated barium = 4.2 mg ○ / 2 mg ◒ / 0.6 mg ●

In fact, the quantities sorbed below the critical temperature are appreciably dependent on the thickness of the barium film, as shown in Fig. 8.

In this figure are plotted the sorption velocity curves obtained at a temperature of 343 °K and a pressure of 1.2×10^{-5} Torr on three different barium films, having all the same apparent surface area (100 cm²) but different thickness (0.6, 2.0, 4.2 mg). These curves show, not only the dependence of the sorbed quantity on thickness, but also the differences existing in diffusion velocities, which have been previously mentioned when discussing the influence of the thickness of the film on the diffusion process.

Besides this, the quantities sorbed below the critical temperature are found to be greatly dependent on the

* Mott put forward successively different hypotheses concerning metal oxidation, in the case of the formation of compact and homogeneous oxide layers (in particular in the case of the oxidation of aluminium).[20–23]

He assumes that, excepting the very initial phase of oxygen surface adsorption, the oxidation is due to the diffusion of the metal through the already formed oxide layer up to the surface exposed to the gas. After some preliminary hypotheses,[20, 21] subsequently criticized by the theoretical and experimental work of Cabrera,[24, 25, 26] the essential points of Mott's latest theory[22, 23] can be summarized in the following manner.

Metal diffusion through the oxide layer is made up of electron diffusion and metal ion diffusion.

The work function for the passage of electrons from metal to oxide is very low and the electrons always pass easily through the oxide layer to fill the free energy levels of the oxygen adsorbed at the surface. So the passage of electrons through the oxide cannot be considered the rate determining process in metal diffusion towards the surface.

The flow of electrons goes on until their energy level reaches that of the Fermi distribution in the metal ; at this point a well determined difference of potential is established between the metal surface and the external surface of the oxide which influences the migration of the metal ions.

In the movement of ions we must distinguish between the passage of ions from metal to oxide and the migration of ions within the oxide under the action of the field.

If the temperature is high, the field has no appreciable influence on the passage of ions from metal to oxide and the migration of the ions within the oxide layer is the rate determining process.

If the temperature is low, the influence of the field on the passage of the ions from metal to oxide is essential, and such a passage will be the rate determining process.

The results of Mott's theory in terms which are familiar in the field of getters can be summarized in the following way :—

There is a critical temperature T_c. Above the critical temperature,

(a) The getter capacity is limited only by the thickness of the barium film and increases proportionally with thickness.

(b) The sorption velocity is inversely proportional to the quantity of gas sorbed.

Below the critical temperature,

(a′) The capacity of the getter is independent of the barium film thickness (provided this is greater than the final thickness of the protective layer) and when the temperature changes it increases according to the relation $Q = K\left(1 - \frac{T}{T_c}\right)^{-1}$.

(b′) The sorption velocity changes exponentially as the reciprocal of the sorbed quantity.

Since, for the application of Mott's theory, the stationary state of the adsorbed layer must be granted the velocity of sorption does not change with pressure.

Vol. 10 196

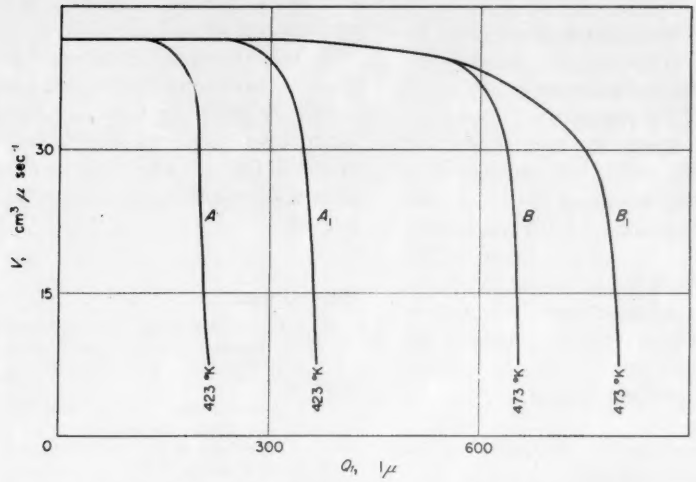

FIG. 9. Velocities of sorption as a function of quantities sorbed at temperatures above the critical temperature and for different film thicknesses.

Sorption pressure = 1.2×10^{-5} Torr
Apparent surface area = 100 cm².
A Sorption temp. = 423 °K weight of evaporated barium = 2 mg
A_1 " " = 423 °K " " " " = 5 "
B " " = 473 °K " " " " = 5.4 "
B_1 " " = 473 °K " " " " = 8.5 "
The metallic character of the film only disappeared for curves *A* and *B*.

structure of the barium film (depending for instance on the temperature of condensing surfaces during getter evaporation, or on subsequent recrystallization processes).

The quantities sorbed above the critical temperature are also found to be dependent on temperature. In particular, the disappearance of the metallic character of the film, does not necessarily take place : it only occurs if the thickness of the film is such that diffusion can maintain throughout the film an appreciable velocity.

This is clearly shown in Fig. 9. In this figure are shown the curves obtained at two temperatures greatly in excess of the critical temperature, at the usual pressure of 1.2×10^{-5} Torr with barium films of different thickness.

Curve *A* was obtained at 423 °K on a barium film of 2 mg, at the end of this experiment the film was totally exhausted. However, in the case of curve A_1 still obtained at 423 °K, but on a barium film of 5 mg, the metallic character of the getter film did not disappear.

Exactly similar differences were found in the behaviour of two films (respectively of 5.4 and 8.5 mg) at 473 °K, as illustrated by curves *B* and B_1 of Fig. 9.

However, the fundamental objection which can be put forward regarding the applicability of the Mott's theory to carbon monoxide gettering, concerns the initial phase of sorption at constant velocity, and more generally the dependence of the sorption velocity on pressure.

Concerning the dependence on pressure, first of all we must underline the fact that Mott's theory was worked out for the oxidation of metal surfaces when subjected to atmospheric pressure. In this theory the very initial phase of surface adsorption is never considered as rate determining.

If the adsorption velocity on the oxide surface were less than the flow of ions through the oxide layer, all the typical Mott treatment would be inconsistent.

Besides this, the difference of potential between the metal surface and the external surface of the oxide, is implicitly justified by the saturation of the adsorbed surface layer.

So Mott's theory seems to have a limit of applicability, that is, to those pressures which can guarantee a saturation of the surface and so a constant difference of potential ; and it cannot explain the linear dependence of the sorption velocity on pressure which is found experimentally (Fig. 2).*

* It was recently proposed in the previously mentioned paper of Roberts and Tompkins,[19] applying Mott's theory to the nitridation of calcium, that such a linear dependence could be explained by considering the adsorption of gas on the surface of the reaction product (nitride in this case instead of oxide) as a " spots " adsorption.

For each spot, the surface concentration of the adsorbed molecules would be the same, and hence the field at each spot would be constant. Pressure would only affect the number of spots present on the surface.

It remains to be seen, however, even for this very interesting point of view which limits of pressure and temperatures are required for its applicability.

In particular, bearing in mind the necessarily high mobility of the adsorbed species (otherwise we would have a chaotic surface distribution and not spots), the spots can only be justified, either on the basis of groups of " active sites " of adsorption, related to the microscopic structure of the surface or on the basis of cooperative phenomena capable of leading to the formation of surface clusters.

Whilst for the first hypothesis we would again be confronted with the gradual saturation of active-sites and hence with the problem of the dependence on pressure, the second hypothesis should be examined particularly from the point of view of its applicability to a number of gases, since it seems improbable that such an explanation could be widely applicable.

Finally, such a complex hypothesis could reasonably be taken into consideration to explain the linear dependence of sorption velocity on pressure, only if the other experimental data showed a doubtless correspondence to Mott's theory. This does not seem to be so in our case.

Conclusions

The picture obtained for carbon monoxide sorption by barium films is based on the identification, by kinetic considerations, of at least two distinct phenomena : the first of which is surface adsorption and the second is diffusion.

For the first of these phenomena we have shown the absence of a temperature coefficient, i.e. of any activation energy, and have suggested that this phase of the process should be considered as a " precursor " for the true chemisorption, probably consisting of physical adsorption on the layer of the products of reaction at the surface of the metal.

For the second phenomenon we have been able to show the existence of two distinct diffusion processes, characterized by two very different activation energies, the first of which is so low as to indicate almost certainly that we are dealing with surface diffusion.

These results, bearing in mind the information given by other authors on the granular structure of barium films, allow us to distinguish diffusion through the discontinuities in the film, i.e. on the surface of the granules which compose it and diffusion through the layer of the reaction product already formed.

This picture is very similar to that obtained in the case of nitrogen and we think that, due to the very different appearance in the behaviour of the two gases, this similarity is relevant.

The study of these processes has enabled the identification of a critical temperature (about 373 °K).

However the identification of such a critical temperature should not be held to mean that two distinct zones of action sharply divide the two phenomena.

Our definition has been reached from a kinetic point of view, and by considering only which effect could occur to bring to an end the initially constant velocity of sorption.

In spite of this, a contemporary existence of the second type of diffusion should not be excluded. It would merely have a supplementary and secondary function.

It is therefore probable that the attenuated indications given by the curves shown in Fig. 6, for temperatures greater than 363 °K, are due to the initial but nevertheless appreciable phenomenon of surface diffusion.

On the other hand, even below 363 °K, the bulk diffusion phenomenon becomes ever more important with time, as the surface is gradually covered. In such circumstances two factors contribute : the diminishing size of the free surface available for gas adsorption and the increase in covered surface, from which the gas can, be it slowly, diffuse to the interior.

References

[1] J. Morrison and R. B. Zetterstrom ; *J. Appl. Phys.* **26**, 437 (1955).
[2] R. N. Bloomer ; *Brit. J. Appl. Phys.* **8**, 352 (1957).
[3] J. J. B. Fransen and H. J. R. Perdijk ; *Philips Tech. Rev.* **19**, 290 (1957–58).
[4] J. J. B. Fransen and H. J. R. Perdijk ; this volume, p. 199.
[5] H. J. R. Perdijk ; this volume, p. 204.
[6] T. Arizumi and S. Kotani ; *J. Phys. Soc. Japan* **7**, 492 (1952).
[7] P. della Porta and F. Ricca ; *Communication to the First International Congress on Vacuum Techniques, Namur* (June 1958).
[8] R. N. Bloomer ; *Brit. J. Appl. Phys.* **8**, 321 (1957).
[9] T. Arizumi and S. Kotani ; *J. Phys. Soc. Japan* **7**, 152 (1952) ; **7**, 158 (1952) ; **7**, 163 (1952).
[10] J. A. Becker and C. D. Hartman ; *J. Chem. Phys.* **57**, 157 (1953).
[11] G. Saini, F. Ricca, and A. Nasini ; *La Ricerca Scientifica* **29**, 1523 (1959).
[12] F. Ricca, G. Saini, and A. Nasini ; *Atti Acad. Sci. Torino* **93**, 557 (1958–59).
[13] G. Ehrlich ; *J. Phys. Chem.* **60**, 1388 (1956).
[14] P. della Porta and F. Ricca ; *Fifth National Symposium A.V.S., San Francisco* (1958), Pergamon Press (1959), p. 25.
[15] P. della Porta ; *Vacuum* **4**, 284 (1954).
[16] P. della Porta ; *Vacuum* **4**, 464 (1954).
[17] D. J. Santeler ; *General Electric, General Engineering Laboratory, Report No.* 58GL146 (May 1958).
[18] D. J. Santeler ; *General Electric, General Engineering Laboratory, Report No.* 58GL303 (Nov. 1958).
[19] M. W. Roberts and F. C. Tompkins ; *Proc. Phys. Soc. A*, **251**, 369 (1959).
[20] N. F. Mott ; *Trans. Faraday Soc.* **35**, 1175 (1939).
[21] N. F. Mott ; *Trans. Faraday Soc.* **39**, 472 (1940).
[22] N. F. Mott ; *Trans. Faraday Soc.* **43**, 429 (1947).
[23] N. Cabrera and N. F. Mott ; *Rep. Progr. Phys.* **12**, 163 (1948).
[24] N. Cabrera ; *C.R. Acad. Sci.* **220**, 111 (1945).
[25] N. Cabrera, J. Terrien, and J. Hamon ; *C.R. Acad. Sci.* **224**, 1558 (1947).
[26] N. Cabrera and J. Hamon ; *C.R. Acad. Sci.* **224**, 1713 (1947).

Nitrogen Sorption by Barium Films

P. DELLA PORTA and E. ARGANO

S.A.E.S. Research Laboratory, Milan, Italy

In previous communications nitrogen sorption on barium films having a mean thickness of 0.02 mg/cm², has been reported. This thickness had in fact been adopted to facilitate the reproducibility of results. The study of the sorption by the capillary method under Knudsen flow conditions and at constant pressure on the getter, has enabled the identification of an initial adsorption on the getter surface directly exposed to the gas, and of subsequent diffusion processes within the film, which are characterized by two different activation energies, below and above 413°K. The present work tends to prove the applicability of such a model in the case of film thicknesses encountered in the manufacture of electron tubes (about 0.2 mg/cm²). Still looking at the problem from the tubes manufactures point of view, the influence of the time of flashing of the getter on the sorption velocity for nitrogen is examined. The time of flashing is varied, in this series of experiments, from 4 to 40 sec. The influence of the residual pressure previous to the flashing of the getter is also examined in the pressure range from 10^{-6} to 10^{-3} Torr. Finally it should be noted that examining the data obtained for the sorption of nitrogen on films of different thickness, as well as from the comparison of such data with similar results for carbon monoxide and hydrogen previously reported, it would appear that parallel mechanisms may be identified in the sorption of a number of gases by barium films.

Introduction

In a communication to the Fifth National Symposium of the American Vacuum Society[1], a detailed picture of the processes involved in the sorption of nitrogen by evaporated barium films was presented. It was in fact possible to evaluate the activation energy for the initial phase of surface sorption, and to individuate the existence of two distinct phenomena of diffusion within the film, one of which was considered to be superficial and could be attributed to the granular structure of the film.

Those indications were all obtained using films, resulting from the evaporation of 2 mg of barium, and having an apparent surface area of 100 cm². So the film thickness, if it were perfectly continuous, compact and uniform, would be 5.7×10^{-6} cm. However, the real thickness of such films may vary between 600 and 1000 Å.

Such thicknesses are decidedly smaller than those usually found in electron tubes, and were employed because they furnished better reproducibility of results, a condition which is essential in a study which is almost entirely dedicated to isolating the sorption mechanisms.

It has seemed opportune to ascertain to which degree the scheme just mentioned can be applied to the processes of nitrogen sorption by films which have thicknesses comparable to those normally found in industrial electron tubes. It has also been thought opportune to investigate the influence of some other parameters (more directly related to actual techniques) on the sorption of nitrogen by barium films.

For this new series of experiments the experimental apparatus is similar to that already described in previous articles, except for the obvious fact that the dimensions of the bulb on which the evaporated barium condenses are varied.

The getters employed for the present series of experiments are of Italian production type ST2/7 × 7.

The barium was evaporated using eddy current induction heating. The time of firing of the getter, except where otherwise stated, was 15 sec.

Results and discussion

The influence of temperature on the initial value of the sorption velocity

In Fig. 1 the logarithm of the initial sorption velocity (in terms of unit area of apparent surface and unit pressure) is given as a function of the reciprocal of the absolute temperature T.

The two types of points correspond to barium films of 2 mg having apparent surface areas of 100 and 17 cm².

The pressure is 5×10^{-6} Torr for the experiments with surfaces of 100 cm², and 5×10^{-5} for the other surface area.

The following facts emerge from the data illustrated in Fig. 1 :

(a) the initial velocity of sorption is directly proportional to the gaseous pressure ;

(b) the initial velocity of sorption is directly proportional to the geometrical surface area of the film ;

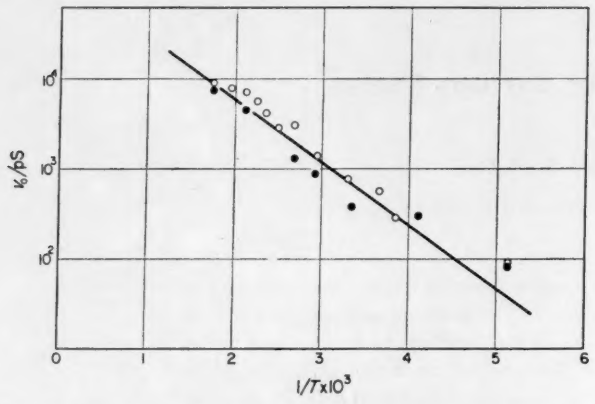

FIG. 1. Temperature dependence of the sorption velocities of nitrogen in $cm^3 \mu sec.^{-1}$/Torr cm^2, by barium films having different surface areas.

Weight of evaporated barium	= 2 mg
● Apparent surface area	= 17 cm^2
Pressure (p_g)	= 5×10^{-5} Torr
○ Apparent surface area	= 100 cm^2
Pressure (p_g)	= 5×10^{-6} Torr.

(c) the same type of adsorption occurs throughout the temperature range investigated (from 175 to 573 °K) and for both film thicknesses.

Finally the activation energy, which can be found from the slope of the straight line, is approximately 3000 cals/mole, a value which had been previously established.

It should be noted that at the lowest temperatures employed a certain departure from linearity exists. In fact in some experiments carried out at liquid air temperature, the initial velocity of sorption has been found to be almost the same as that found at 175 °K.

The most probable hypothesis with respect to this is that, at such low temperatures physical adsorption of the gas is to be added to the normal surface phenomenon (activated adsorption, probably chemisorption accompanied by dissociation of the nitrogen molecules). Probably such physical adsorption occurs on the reaction product itself.

This phenomenon would always be present, but would only assume a certain importance at these low temperatures.

An hypothesis of this type had already been put forward by us in our previous communication due to the fact that the total quantity of nitrogen sorbed was under some circumstances greater than the corresponding stoichiometric value expected for the formation of barium nitride.

An analogous behaviour has also been observed for the sorption of carbon monoxide and hydrogen.

Experimental evidence of diffusion phenomena

Fig. 2 shows the curve obtained, for a barium film of 2 mg and having an apparent surface area of 17 cm^2, at a temperature of 373 °K and a pressure of 5×10^{-5} Torr, when the quantity of gas sorbed is plotted as a function of the square root of time.

From this it can be seen that, except for the initial part of the curve, the relation is approximately linear. In previous communications we have shown that this corresponds to a rate determining diffusion process.

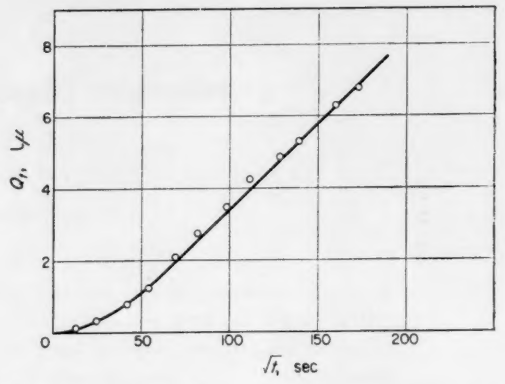

FIG. 2. Time dependence of the quantity of nitrogen sorbed by a barium film.

Weight of evaporated barium	= 2 mg
Apparent surface area	= 17 cm^2
Sorption temperature	= 373 °K
Pressure (p_g)	= 5×10^{-5} Torr.

Hence, even in this case the characteristics of films having a technical thickness show the same behaviour previously found for thinner films.

It should be noted that in this case the linearity persists for longer periods of time. This is probably due to the fact that an increased film thickness brings us nearer to the conditions assumed in deriving the diffusion laws.

It should in fact, not be forgotten that, the linearity between Q_t and $\sqrt{t}$ only applies when considering a medium of infinite extent.

Concerning the two distinct types of diffusion processes, we have analogous indications to those obtained using films of 0.02 mg/cm^2. Further, the activation energy seems to be of the same order of magnitude to those previously calculated : about 2 Kcal for surface diffusion, and 10 Kcal for bulk-diffusion.

However, the accuracy in experiments with smaller surface areas is less, due to the slow evolution of the process.

Influence of the conditions of evaporation of the getter on the sorption of nitrogen

The conditions in which the barium film is evaporated greatly influence its subsequent gettering properties.

These conditions are : preliminary heating of the getter prior to its evaporation, residual pressure in the getter chamber at the instant of evaporation, time of evaporation, distance between getter and condensing surface (and hence film thickness), temperature of the walls on which the film is formed, etc.

In the work previously referred to, the influence of the last two mentioned parameters had been studied. To facilitate comparison these results are again reproduced in Figs. 3 and 4.

Let us now consider two other parameters which are of great interest from a practical viewpoint : the residual pressure in the getter chamber at the instant of evaporation, and the time of firing of the getter.

In Fig. 5 the influence of the former on the sorption velocity for nitrogen, at room temperature is shown.

Vol. 10 196

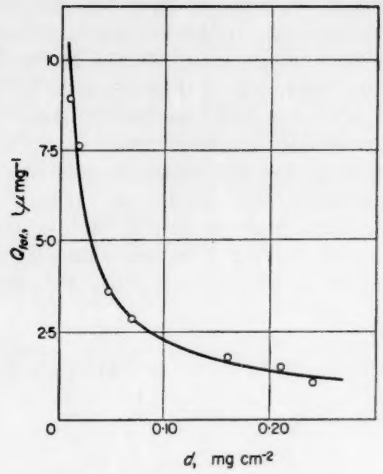

FIG. 3. Total amount of sorbed nitrogen as a function of the thickness of the barium film.

Apparent surface area	= 100 cm^2
Sorption temperature	= 298 °K
Pressure (p_g)	= 5 × 10^{-4} Torr.

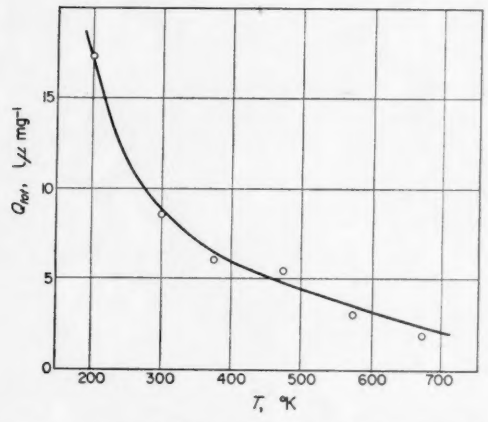

FIG. 4. Total amount of nitrogen sorbed by barium films as a function of the temperature of condensation of the film.

Weight of evaporated barium	= 2 mg
Apparent surface area	= 100 cm^2
Pressure (p_g)	= 5 × 10^{-4} Torr.

In this figure by plotting the sorption velocity as a function of the quantity of gas sorbed three very different curves are obtained. They correspond to residual pressure values in the getter chamber of 5 × 10^{-5}, 5.5 × 10^{-4} and 2 × 10^{-3} Torr respectively.

These values correspond to pressures in the getter chamber, prior to getter evaporation, when the pumping line between getter chamber and manifold has been reduced to the capillary, used to measure the sorption velocity, having a conductance of about 2 cm^{3}sec^{-1} for nitrogen.

From this figure it is seen that, in the pressure range between 10^{-5} and 10^{-3} Torr, which is that of practical interest, an increase in the residual pressure appreciably decreases the sorption velocity.

At first sight this result could appear contradictory when

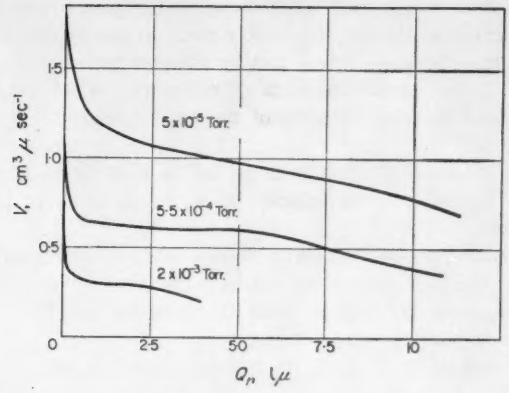

FIG. 5. Sorption velocities as a function of the quantity of gas sorbed for films evaporated at different residual pressures.

Weight of evaporated barium	= 2 mg
Apparent surface area	= 17 cm^2
Sorption temperature	= 298 °K
Pressure (p_g)	= 5 × 10^{-5} Torr.

compared to the well known increase in gettering velocity obtainable by evaporating barium in an argon atmosphere.

In actual fact this is not so : argon, at pressures greater than those considered here, promotes the formation of particularly porous films and thus their permeability to gases, increasing in this way both surface adsorption and diffusion to the interior. However, argon itself, being inert, does not remain on the barium surfaces in high concentrations (at least at temperatures of practical interest) and even then it is only held in a weakly bound physisorbed phase.

The gas mixture present in the getter chamber, which determines the residual pressure when the getter evaporates, is only partially constituted by inert gases.

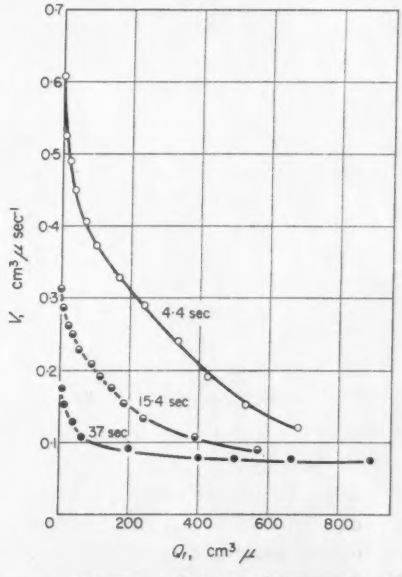

FIG. 6. Sorption velocities as a function of the quantity of gas sorbed for different times of flashing of the getter.

Weight of evaporated barium	= 2 mg
Apparent surface area	= 17 cm^2
Sorption temperature	= 298 °K
Pressure (p_g)	= 5 × 10^{-5} Torr.

So that, whilst the residual pressures (which are still relatively low) do not appreciably influence the structure of the films, the gases which can be chemisorbed in a stable phase on their surface, produce a " poisoning " which reduces the initial sorption velocity of the gas subsequently introduced.

Fig. 6 shows the influence of the time of firing of the getter on its sorption velocity for nitrogen, at room temperature.

In this figure by plotting sorption velocity as a function of the quantity of gas sorbed, we have obtained three distinct curves, corresponding to times of firing of 4.4, 15.4 and 37 sec respectively.

In each of these cases, the evaporation of the getter was carried out when the getter chamber was still directly connected to the manifold, so that the different times of firing would not present a significant influence on the pressure in the getter chamber during firing of the getter.

From this figure it can be seen that the greatest gettering velocity is obtained for the most rapidly fired getters.

This is probably due to the more disordered state of the film obtained under such conditions. In fact, a certain amount of sputtering can accentuate the granular structure of the film, and the rapid condensation can reduce the crystal growth as well as increase lattice imperfections.

Reference

[1] P. della Porta and F. Ricca ; *Trans. Fifth National Symposium A.V.S., San Francisco* (1958), Pergamon Press (1959), p. 25.

Vol.
10
196

Hydrogen Sorption by Barium Films

P. DELLA PORTA and S. ORIGLIO

S.A.E.S. Research Laboratory, Milan, Italy

The capillary method, under Knudsen flow conditions and at constant pressure on the sorbent, is in this work applied to the study of hydrogen sorption on evaporated barium films. Particular precautions have been taken to reduce to a minimum the influence of the hot filament and electron current of the ionization gauge (Alpert type) on the measurement of the sorption velocity. To this end, thoriated tungsten filaments have been employed and very low ionizing electron currents (0.01 mA) have been used. The experimental results have been obtained in the temperature range between 195 and 473°K, on barium films of approximately 2 mg, evaporated from a stabilized barium-aluminium alloy and having an apparent surface area of 100 cm². A preliminary investigation of the curves giving velocity of sorption as a function of time, shows that the shape of such curves is dependent on the pressure range in which they are obtained. At the higher pressures the kinetics of adsorption follows very closely the diffusion laws, as is shown by the nearly linear relation existing between quantity sorbed and square root of time. On the other hand at lower pressures, the graphs show an almost horizontal portion, corresponding to a constant velocity of sorption lasting a considerable period of time. These differences in behaviour show that for hydrogen, as for other gases, the sorption by barium films is made up of a number of phenomena superimposed on each other. The different appearance of the various phenomena for different gases can, with all probabilities, be attributed to the different coefficients of diffusion of the gases and the relative activation energies.

ol.
10
960

Introduction and experimental procedure

Previous experiments carried out by us on the sorption of hydrogen by evaporated barium films, had shown a picture filled with difficulties.[1, 2] This was due to the poor reproducibility of results and the evident action of factors which escaped totally or partially from our control.

The progress recently made in the understanding of the sorption mechanism of various gases by getters, and the preliminary study of the action of electron ionizing currents and hot filaments,[3] have now enabled us to investigate the problem more deeply.

The experimental method employed is the already well known one of gas flow, under Knudsen conditions, through a capillary.

The experimental set up is the usual one, which has already been employed in our Laboratory for a number of years in the systematic study of gettering of various gases by evaporated barium films.

We have of course employed capillaries of reduced diameter which are more suitable to measure the flow of hydrogen.

Particular attention has been paid to reduce to a minimum the secondary pumping ; due to the Alpert type ionization gauge which is employed to measure the hydrogen pressure on the getter.

To this end we have used very low electron ionizing currents (0.01 mA), for which the gauge gives an ion current of only 48 μA per Torr hydrogen pressure on the getter. To record such low ion currents we have employed an amplifier capable of measuring currents of the order of 10^{-11} A.

Further, we have replaced one of the tungsten filaments of the Alpert ionization gauge by a thoriated tungsten one. Employing an electron accelerating potential of 150 V, the temperature of the filament, in order to obtain an electron current of 0.01 mA, is never greater than 1400°K. So that, the pumping effect due to the dissociation of hydrogen molecules on the hot filament is negligible compared to the velocity of sorption by the getter.

The experiments have been carried out on films of 2 mg of barium, having an apparent surface area of 100 cm², in the temperature interval between 195 and 473°K.

Results and discussion

One of the major causes of confusion in the data previously obtained by us on the sorption of hydrogen, besides the poor reproducibility of results from a quantitative point of view, was due to the disconcerting fact that, at times, when pressure and temperature were altered, the shape of the sorption curve changed in an alarming manner.

Bearing in mind the experiments carried out with CO and N_2, we have tried to establish if for hydrogen the various processes of surface adsorption and diffusion within the film, could alternatively be predominant on the kinetics of the gettering phenomenon, according to temperature and pressure conditions.

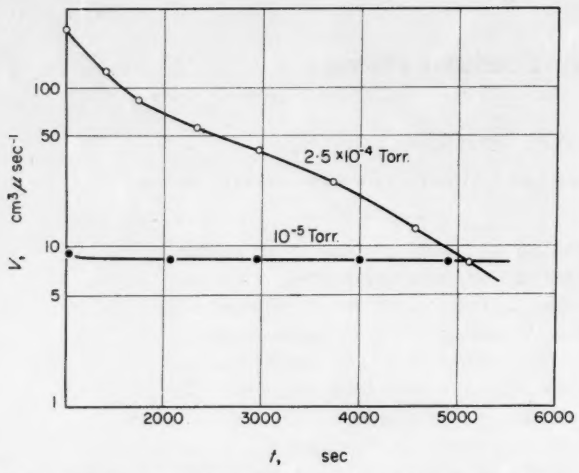

FIG. 1. Velocity of sorption as a function of time at two different pressures.
Weight of evaporated barium = 2 mg
Apparent area of film = 100 cm²
Temperature of bulb = 473 °K.

In Fig. 1 is plotted, on a logarithmic scale, the velocity of sorption as a function of time, at a temperature of 473 °K and at pressures of 2.5×10^{-4} and 1×10^{-5} Torr.

It is obvious from this graph that, except for a minute initial decrease, the velocity of sorption at the lower pressure remains constant for a considerable time.

However, for the sorption curve obtained at the higher pressure, there results a sharp decrease with time. But it is still possible, even in this case, to perceive an initially greater slope in the curve.

We are therefore confronted with two phenomena possessing different rate determining processes.

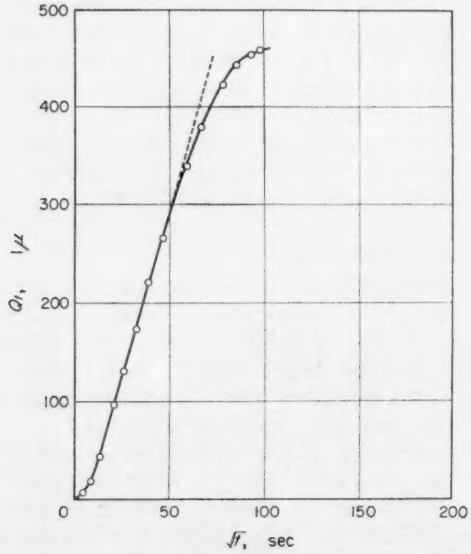

FIG. 2. Time dependence of the quantity of hydrogen sorbed by a barium film.
Weight of evaporated barium = 2 mg
Apparent surface area = 100 cm²
Sorption temperature = 473 °K
Pressure = 2.5×10^{-4} Torr.

Whilst in the process occurring at the lower pressure the velocity is limited by the pressure itself, and therefore remains constant under the experimental conditions employed (p_g constant), in the case of the higher pressure we have a decrease of velocity with time which can be directly attributed to a slowing down of the diffusion of hydrogen within the film.

This viewpoint is confirmed by the curve shown in Fig. 2, based on the experimental data used in Fig. 1, for the curve at a pressure of 2.5×10^{-4} Torr.

It is even more evident if we consider that the two curves in Fig. 1 intersect. After a given time the velocity of the phenomenon at the higher pressure becomes smaller than the one at the lower pressure, in spite of the fact that the quantity of gas arriving at the surface remains 25 times greater.

Evidently the concentration of hydrogen within the film is already so high that diffusion is greatly reduced. On the other hand, in the case of the getter at the lower pressure, the quantity of gas diffused within the film at the time when the curves intersect is small, so that the velocity of diffusion can still be greater than the rate at which gas strikes the surface, hence the latter continues to be the rate determining process, and the velocity retains its initial value.

In Fig. 3 the logarithms of the initial velocity of adsorption (surface phenomenon), expressed in cm³ micron sec^{-1} and referred to a pressure of 1 Torr, are plotted as a function of the reciprocal of temperature.

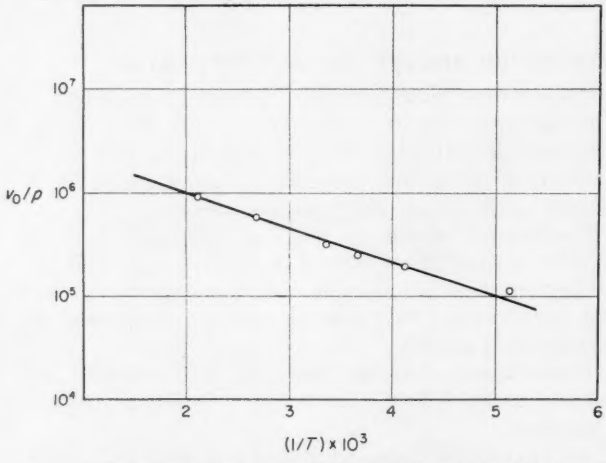

FIG. 3. Temperature dependence of the sorption velocity of hydrogen on barium films.
Weight of evaporated barium = 2 mg
Apparent surface area = 100 cm²
Pressure = 2.5×10^{-4} Torr.

The relationship between these two variables is linear. From the slope of this line the energy of activation is found to be approximately 1500 calories.

This is a relatively low value of the activation energy, such as one usually obtains for a surface chemisorption phenomenon. However, it is left undecided whether this value of activation energy is related to a direct chemisorption of the hydrogen on the metallic barium or to a further adsorption of gas on the superficial hydride layer formed. It is not to be excluded that the short initial decrease in velocity, pointed out in Fig. 1, is to be associated with a

gradual change in the nature of the surface on which the gas is adsorbed.

For diffusion, a typical picture of the influence of temperature, is given in Fig. 4.

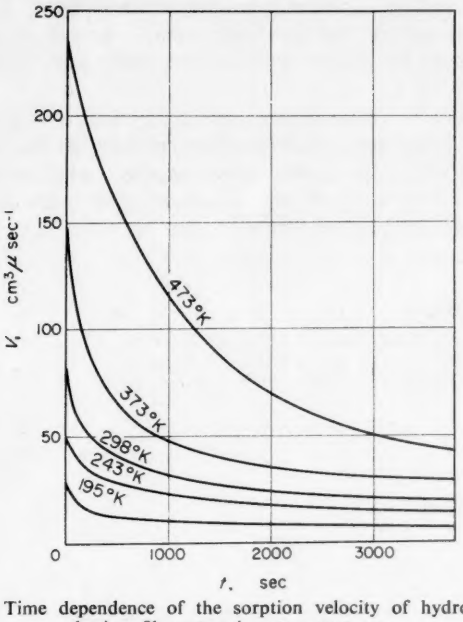

FIG. 4. Time dependence of the sorption velocity of hydrogen by barium films at various temperatures.
Weight of evaporated barium = 2 mg
Apparent surface area = 100 cm²
Pressure = 2.5×10^{-4} Torr.

All the curves are for measurements carried out at a pressure of 2.5×10^{-4} Torr, so that at all the temperatures employed the phenomenon followed the diffusion laws.

If these same data are plotted as in Fig. 2, and if, of the curves thus obtained only the linear portions are considered, the diagram shown in Fig. 5 is obtained.

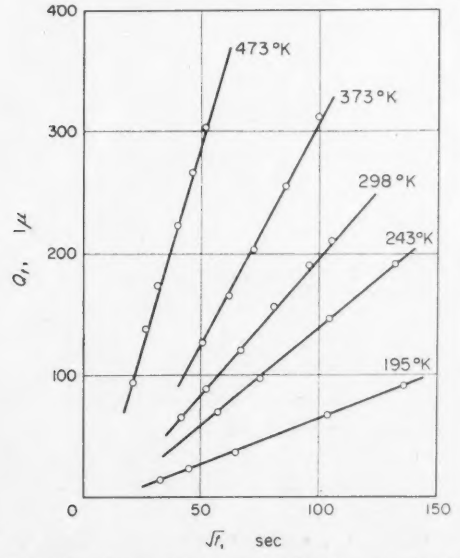

FIG. 5. Time dependence of the quantity of hydrogen sorbed by barium films at various temperatures.
Weight of evaporated barium = 2 mg
Apparent surface area = 100 cm²
Pressure = 2.5×10^{-4} Torr.

From the angular coefficient of the straight lines in Fig. 5 it is then very easy to calculate the activation energy associated with the diffusion process.

In Fig. 6 the logarithms of these angular coefficients are plotted as a function of the reciprocal of temperature.

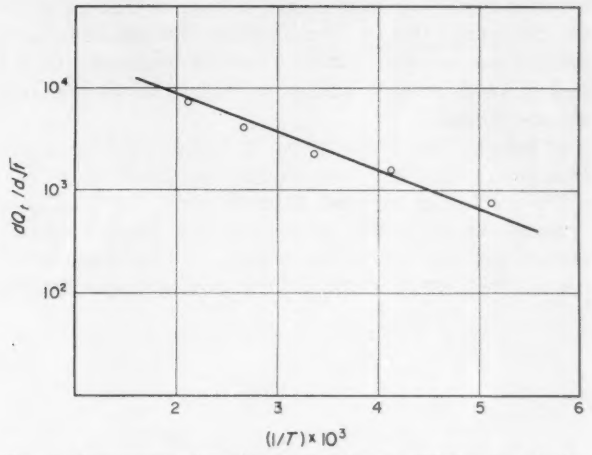

FIG. 6. Temperature dependence of hydrogen diffusion into barium films.
Weight of evaporated barium = 2 mg
Apparent surface area = 100 cm²
Pressure = 2.5×10^{-4} Torr.

The relation is still linear, and the energy of activation has a value of about 3000 calories.

This value is decidedly smaller than that obtained for N_2 and CO, as was to be supposed to be the case for hydrogen.

In the case of hydrogen, we do not find any evidence for the existence of two distinct types of diffusion, which were found to exist in the case of the other gases studied.

This is due, with all probability, to the fact that the lower value of activation energy required for bulk-diffusion of hydrogen, makes of this the predominant phenomenon even at temperatures which are much smaller than those of technical interest.

An investigation on the existence of a surface diffusion phenomenon, should be carried out in the liquid air temperature region.

On the basis of this result it would appear reasonable to expect that, since the temperatures of practical interest are always above an eventual critical temperature (corresponding to the transition from surface to bulk-diffusion), the sorption process should continue until the film is completely destroyed.

Naturally, however, the velocity of diffusion is decreasing with time, and if temperature and pressure are not very high, the life of the getter ceases, from a practical point of view, long before the complete utilization of the barium film.

Hence, even for the case of hydrogen, one cannot simply evaluate the actual capacity of sorption of the getter on the basis of the quantity of barium evaporated, but one must give the proper weight to those factors which introduce the surface and the structure of the film.

Conclusions

The study of hydrogen sorption by evaporated barium films, enables us to distinguish two different processes :

(a) a surface adsorption process, which is rate determining at high temperatures and low pressures,

(b) an internal diffusion process, which is rate determining at low temperatures and high pressures.

In the first of these processes, it appears that an initial phase, probably due to direct chemisorption on the metallic barium, can be distinguished from the remainder of the process which probably occurs on the hydride surface layer already formed.

In general hydrogen sorption by barium films is strictly analogous to the sorption of nitrogen and carbon monoxide.

The absence, in the temperature interval considered, of a " critical temperature " associated to the diffusion phenomenon, such as found for other gases, can be attributed to the fact that, for hydrogen, the energy of activation for the diffusion process within the reaction product is much lower.

We can therefore state that, the most interesting and promising result of our researches is given by the almost uniform behaviour in the mechanism of sorption of gases so dissimilar such as nitrogen, carbon monoxide and hydrogen.

This result is very significant since it emerges from the analysis of behaviours which at first sight appear entirely different.

The researches on other gases, at the moment in progress in our Laboratories, will ascertain whether in fact we are dealing with a mechanism which can be applied generally. If such is the case the progress made in the understanding of the gettering action would be quite considerable.

References

[1] P. della Porta ; *Vacuum* **4**, 284–302 (1954).
[2] P. della Porta ; *Vacuum* **4**, 464–475 (1954).
[3] P. della Porta, S. Origlio and E. Argano ; this vol., p. 194.

Vol.
10
196

Selective Getters

ING. J. HEJZLAR and ING. V. HORÀČEK

Vuvet, Praha-Hloubětín, Nademlýnská 600, Czechoslovakia

Studies of the emission stability of oxide cathodes with tungsten core have shown that the presence of hydrogen in the residual atmosphere is of great significance for the stability of the emission properties of the cathode. A number of experiments was therefore carried out in order to ascertain the effect of hydrogen on the work function and the conductivity of the oxide layer with nickel and tungsten support. To obtain practical results we had to increase the partial hydrogen pressure in the bulb which was accomplished by using a getter with selective effect for hydrogen. The above mentioned getter was prepared and its properties in radio-tubes investigated.

The effect of hydrogen on oxide cathodes

A short review is given of investigations concerning the influence of hydrogen on oxide cathodes.

Wagener[1] studied the effect of hydrogen in the pressure range from 10^{-7} to 10^{-5} Torr and found a small increase in emission with increasing hydrogen pressure. According to theoretical studies of Rittner[2] hydrogen is a moderate activator for pressures of 1 ata. Wagener[3] believes that the hydrogen protects the interface layer of the cathode from deactivating influences of oxygen. Plumlee[4] has reported that hydrogen causes the rise of the principal donors in the cathode. Moore and Allison[5] found during their studies of the cathode on a ceramic support a reductive effect of the atomic hydrogen.

Our first investigations had the purpose to study the short-termed effect of hydrogen on oxide cathodes after a life of about 1000 hr. These experiments were carried out with the help of a system consisting of a diode, an ionisation gauge and a hydrogen source. The hydrogen source was an electrically heated titanium strip saturated with hydrogen. Experiments were made with usual cathodes as well as with cathodes with artificially produced interface layers and with BN and moulded cathodes. We obtained similar results in all these cases. For example, an indirectly heated cathode with passive nickel showed an increase of the saturation current of 40 per cent after the treatment of the cathode with hydrogen for a short period. The effect of hydrogen on a cathode which had artificially deposited interface layer Ba_3WO_6 20μ thick was very evident. The work function of the cathode decreased by 0.12 eV and the resistance by 35 per cent. Another cathode, however, whose interface layer of Ba_2SiO_4 was produced quite similarly, was only slightly affected by the short-termed influence of hydrogen. The effect of hydrogen is particularly obvious on cathodes which have a small emission current such as on a cathode with an artificial interface layer of Ba_3WO_6 (Table I). Measurements with long pulses (pulse width 1 ms) have shown that the increase of the partial hydrogen pressure (pressure range 10^{-7}–10^{-6} Torr) leads to a decrease of the current decay during the pulse.

TABLE I

Cathode	$I_e\left(\frac{mA}{cm^2}\right)$ before H_2 exposure	$I_e\left(\frac{mA}{cm^2}\right)$ after H_2 exposure	ΔeV	%
Ni/(BaSrCa)O	960	1460	−0, 03	
Ni/Ba_2SiO_4/(BaSrCa)O	1600	1920	−0, 02	−10
W/(BaSrCa)O	1600	1760	−0, 01	− 1
W/Ba_3WO_6/(BaSrCa)O	112	376	−0, 12	−35
Ni/(BaSrCa)O + Cu/	930	1320	−0, 03	−77

Mechanism of the oxide cathode

Before discussing the selective getters we would like to mention some newer aspects of the mechanism of the oxide cathode.

(a) According to the classical theory the cathode emission is due to the presence of the excess barium in the oxide layer. The barium produces donors which were determined by various physical methods.

(b) Moore, Wooten and Morrison[6] have shown that no correlation has been found between the emission and the concentration of the excess barium. Such a relation, should it exist, could be only assumed in areas of low concentrations of barium which cannot be detected with existing analytical methods.

(c) According to Plumlee[4] the principal donor is probably produced by OH^-.e, -which originates in the cathode in the presence of hydrogen and water vapours contained in the residual atmosphere.

(d) As to the emission of the oxide cathode, Moore and Allison[5] hold, that other factors than the content of the excess barium are much more important. These authors believe that the presence of the metallic support is no necessary condition for the emission of the oxide layer.

Generally it can be said that the optimum performance of the oxide cathode can be obtained under suitably chosen equilibrium conditions. One of the possibilities to realise

these conditions is the use of the activating and stabilising properties of hydrogen. This method is practicable by the application of selective getters.

Selective getters

The expression "selective getters", introduced by Wagener,[3] refers to materials which enable to bind various gases and to produce and maintain simultaneously the atmosphere of another certain gas in a closed volume. Hydrogen belongs to the group of gases which influence the cathode favourably and have an activating effect. As to selective getters, thorium hydride can be mentioned as an example (Wagener). The equilibrium pressure of hydrogen is a function of the temperature of the metal and of the content of the dissolved hydrogen and is given by the equation

$$p_{H_2} = K \,.\, q \,.\, \exp \frac{H}{R\,T} \qquad (1)$$

where

K = constant,

q = hydrogen content in l.μ/mg,

H = heat of solution (kcal/mol),

R = gas constant.

The application of selective getters used by Wagener, which were prepared from thorium hydride, showed a considerable decrease of the interface-layer resistance after many thousand hours when compared with barium getters. There exist other groups of metals having similar properties to thorium, i.e. a considerable ability to solve hydrogen.

Composition of the selective getter

Significant for the technical application is the so-called Mischmetall which contains principally cer and lanthan and small quantities of other metals of the rare earths. During the development of a suitable getter we had to keep in mind that the usual technology of radiotubes had not be affected, i.e. :

(a) the getter had to react with the residual gases which deteriorate the oxide cathode,

(b) the getter had to enable the maintaining of a hydrogen pressure of 10^{-7} to 10^{-5} Torr in the tube,

(c) the above mentioned properties should hold good in the temperature range of 50–200 °C,

(d) the getter must be stable during the assembling of the system of the tube and during the storage,

(e) it must be possible to activate the getter during the pumping of the tube,

(f) the getter should be available also in powder form to enable the preparation of pellets and sintered layers,

(g) the getter must have a low vapour pressure.

The stability of the Mischmetall in the atmosphere, especially in powder form, is very unsufficient and therefore it is necessary to alloy it with suitable metals. A number of experiments to ensure the necessary stability has been carried out in our institute and the following technique was employed :

The Mischmetall was molten in vacuum to remove the oxides and the stabilisation was then accomplished by alloying it in vacuum with Cu and Al, i.e. with metals whose gas solubility is very small. The alloying results in a small decrease of the hydrogen solubility. When using iron for the alloying process we obtain a coarse crystalline structure which facilitates the pulverisation of the ingot.

The stability of the alloy in powder form as well as in solid form was investigated, in the case of the powder (grain size 120μ) by determining its weight increase. The properties of the alloy containing hydrogen are very different. This leads to the conclusion that the activation of the getter in the tube could be carried out during the pumping process.

Practically the selective getter in radiotubes was activated by heating the pellet, which contained a mixture of the getter alloy and titanium hydride powder. This leads at temperatures above 400 °C to a desorption of titanium hydride and to the solution of hydrogen in the alloy. The hydrogen set free during the desorption gets partially absorbed by the alloy and partially it is pumped away. The hydrogen content in the alloy depends on the temperature and the heating time of the getter. After a prolonged heating of the getter the hydrogen which was temporarily absorbed by the alloy is again set free. It is important not to exceed the maximum temperature of about 800 °C to preserve the changes in the lattice caused by the absorption of hydrogen.

Investigations concerning the pumping speed of the getter were carried out only informatively for carbon dioxide and air. The pumping speed was measured with the help of a method described by Wagener.[7] The diagrams of pumping speed for CO_2 and air see [8].

Further studies were made to investigate if the elementary hydrogen from the getter can be desorbed with other residual gases such as oxygen or carbon dioxide, which can be expressed by the relation

$$MeHx + 1/2\,O_2 \rightleftharpoons MeO + 1/2\,.\,x\,.\,H_2 \qquad (2)$$

or if the reaction follows exclusively the equation

$$2\,MeHx + \left(\frac{x}{2} + 1\right)\,.\,O_2 \rightleftharpoons 2\,MeO + x.H_2O \qquad (3)$$

We have found that the reaction (2) affects to a certain extent the value of the partial pressure of hydrogen or in other words, that the hydrogen is expelled by other gases which form within given limits stable compounds with metals of the rare earths.

Application of the selective getter

A number of radiotubes containing selective getters was manufactured. In all cases a pellet weighing 50 mg (the titanium hydride content being 20 per cent) was used. The pumping process as well as the heating of the pellet were the same as is used with barium getters of the FeBa and SAES type.

We also carried out experiments in a different way : we heated the getter after the tube had been sealed off. In this case the hydrogen after having been desorbed from the titanium hydride was readsorbed during the activation

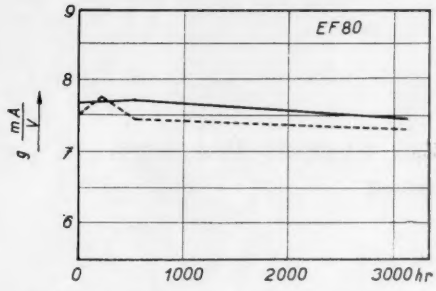

FIG. 1a. Variation of the transconductance during life test of the tube EF 80.
————selective getters — — — — barium getters.

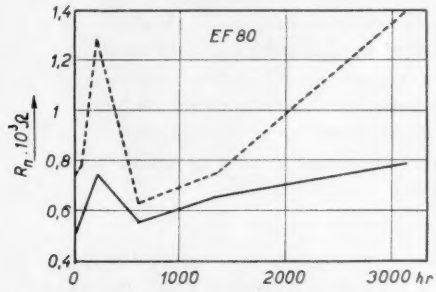

FIG. 1b. Variation of equivalent noise resistance (R_n) of electron tubes EF 80 during life test.
————tubes with selective getters
— — — — tubes with barium getters.

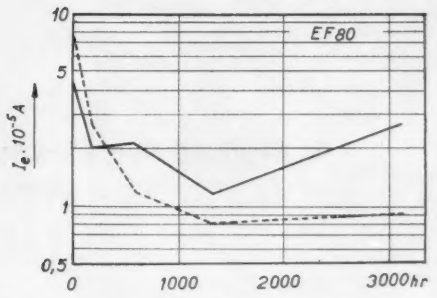

FIG. 1c. Variation of temperature limited emission current (measured at low cathode temperature—heater voltage 2 V) during life test of the tube EF 80.
————selective getters — — — —barium getters.

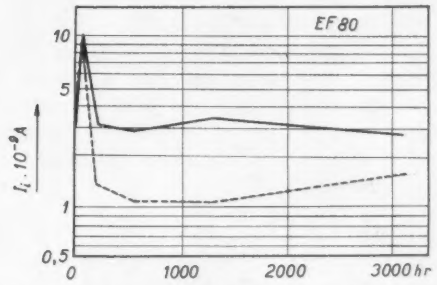

FIG. 1d. Variation of ion current during life test of the tube EF 80 with plate as a ion collector.
————selective getters — — — —barium getters.

process. The hydrogen pressure in the tube was at the beginning of the activation about 10^{-3} Torr and towards the end of the process it had the required values.

Figs. 1a, 1b, 1c and 1d show the life-tests characteristics of radiotubes EF 80 containing barium getters and selective getters.

References

[1] S. Wagener ; *Reactions between Oxide Cathodes and Gases at Very Low Pressures, Proc. Phys. Soc.* **67B**, 369–386 (1954).

[2] E. S. Rittner ; *A Theoretical Study of the Chemistry of the Oxide Cathode, Philips Res. Rep.* **8**, 184–238 (1953).

[3] S. Wagener ; *The Use of Getters for the Production of Very High Vacua, Vacuum* **3** (Jan. 1953).

[4] R. H. Plumlee ; *The Electron Donor Centers in the Oxide Cathode, RCA Rev.*, 231–274 (June 1956).

[5] G. E. Moore and H. W. Allison ; *Emission of Oxide Cathodes Supported on a Ceramic, J. Appl. Phys.* **27**, No. 1.

[6] G. E. Moore, L. A. Wooten, and J. Morrison ; *Excess Ba Content of Practical Oxide Cathodes and Thermionic Emission, Appl. Phys.* **26**, 943 (1955).

[7] S. Wagener ; *The Production of Very High Vacua by the Use of Getters, Proc. IEE* **99**, 135–147 (1952).

[8] J. Hejzlar ; *Das Selektive Getter, Abstracts, Symposium in Como* (1959).

SESSION IX
Various

A Method for Measuring of Caesium Vapour Pressure in Photoelectric Tubes

S. JERIČ AND E. KANSKY

Ljubljana, Yugoslavia

A simple method for determination of caesium vapour pressure (P_{Cs}) in the 10^{-4} to 10^{-15} Torr range based on the surface ionization of caesium on hot tungsten has been described and its theory and accuracy have been discussed. The continuous ion current method allows the determination of P_{Cs} in the (10^{-4}–10^{-9}) Torr range whilst the discontinuous flashing method extends this range from 10^{-9} down to 10^{-15} Torr. The latter method enables the determination of very low residual P_{Cs} in photoelectric tubes. Construction details of various photocells and 11-stage photomultipliers with built-in ionization diodes and electrical circuits used are given. Usefulness of the method is illustrated by following the process of caesium bonding by antimony and silver oxide surfaces and of the adsorption of caesium on glass.

We have applied well known phenomenon of surface ionisation of caesium on tungsten to the measurements of very low pressures of caesium in the photoelectric tubes. So we have been able to follow various processes during the manufacture and life of these tubes. Caesium is the unavoidable component of the photoelectric compounds, but causes also many troubles. We can hope that by the extensive compiling of the results of these measurements several important thermodynamical and kinetical conclusions will be made and so the technology of the photoelectric tubes at least concerning caesium will be based on less empirical foundations.

Following equations define the degree of ionisation α and the coefficient of ionisation β :

$$\alpha = \frac{n_+}{n_0 - n_+} \qquad \beta = \frac{n_+}{n_0}$$

β can be expressed by α :

$$\beta = \frac{\alpha}{1 + \alpha}$$

n_+ number of evaporated Cs^+
n_0 number of Cs atoms striking unit area of the emitter per second.

In the absence of the electric field the degree of ionisation α_0 depends on work function φ, ionisation potential of caesium atom V and temperature as Langmuir and Kingdon have shown :

$$\alpha_0 = A \cdot e^{\frac{\phi - V}{kT}}$$

Both A and φ are functions of the surface covering θ. The lower θ is, the greater are A and φ and thus α_0 tends to very great values and β according to the equation to 1. At very low pressures the value of β is less problematical than at higher pressures. When we measure the steady ion current from the hot tungsten emitter in a very low caesium pressure, there is no danger for θ to surpass the limiting value with which β becomes less than 1. But when we measure the velocity of the adsorption on the cold emitter by measuring electric charge of the flashed up ions, β might become less than unity if the time of adsorbing is too long.

Combining some simple equations of the kinetic theory of gases :

$$n_0 = \frac{nv}{4} = \frac{n_+}{\beta} = \frac{1}{\beta} \cdot \frac{i}{e_0}$$

$$n = \frac{P}{kT}$$

$$v = \sqrt{\frac{8kT}{\pi m}}, \text{ where denote :}$$

n_+ number of evaporated Cs ions
n_0 number of Cs atoms striking unit area of the emitter per sec
n number of Cs atoms per unit volume
i current density,

we obtain two following equations to calculate caesium pressure P_{Cs} :

$$P_{Cs} = 2.08 \cdot 10^{-7} \cdot \frac{1}{S} \cdot \frac{de}{dt} \sqrt{T} \text{ Torr}$$

$$P_{Cs} = 2.08 \cdot 10^{-7} \cdot i \cdot \sqrt{T} \text{ Torr}$$

We can use the first equation when the charge e of the evaporated Cs ions is known and the second one when we measure the steady ion current.

In the Fig. 1 we see the charge of evaporated ions (measured by deflections of the ballistic galvanometer) against

Vol. 10 1960

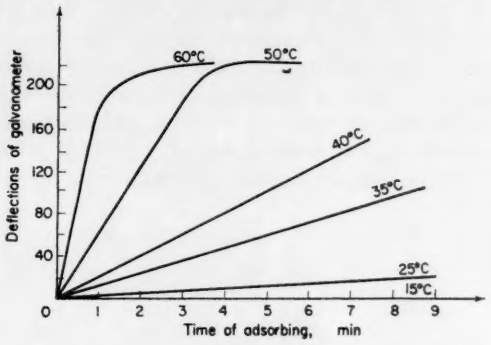

FIG. 1.

the time of caesium adsorbing in minutes. Because the curves tend linearly towards zero we can suppose that β is constant and because of above mentioned grounds unity. Only at the top of the first two curves when the pressure was higher because of the higher temperatures, we can see, that the charge of evaporated Cs ions becomes independent of the time and this because of the adsorption and evaporation of *Cs* atoms.

In the Fig. 2 we see the ranges of caesium pressure we have

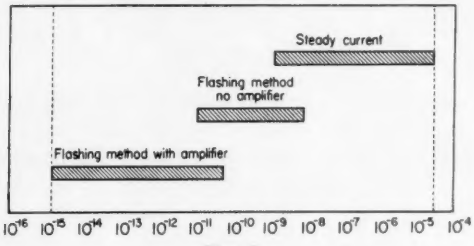

FIG. 2.

been able to cover by this method : by measuring steady ion current the range from 5×10^{-5} to 10^{-9} Torr ; by flashing method without amplification the range from 10^{-9} to 10^{-11}, with amplification the range 10^{-10} to 10^{-15} Torr. The upper limit is given by the electric discharge in caesium vapour, the lower limit by laboratory equipment and background currents.

If caesium pressure is very low the ion current is low too and difficult to measure. In this case it is better to let *Cs* adsorb during known time on the cold surface of the emitter, then flash it up and measure its electric charge. In the

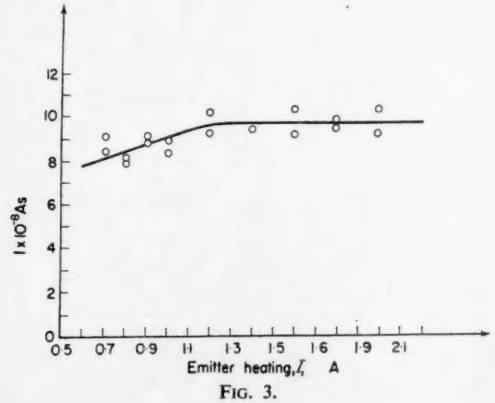

FIG. 3.

Fig. 3 we see the electric charge of the evaporated ions against heating current of the emitter. The charge is generally independent of the heating of the emitter. The scattering of the results is remarkable about 10 per cent.

In the next Fig. 4 the dependence of the electron and

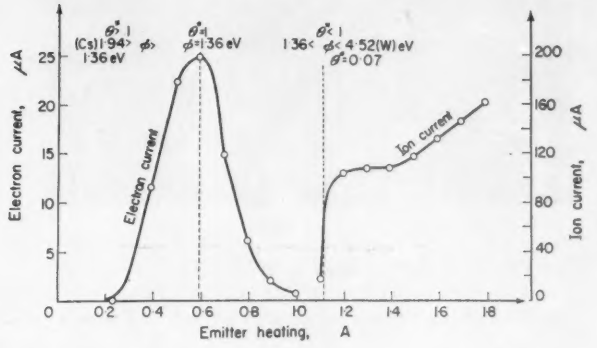

FIG. 4.

caesium ion current on the heating current of the emitter is shown. The caesium pressure in the tube was rather high about 10^{-6} Torr. At the low temperatures the covering of the surface is high : θ is greater than unity ; work function in this range lies between 1.94 eV (for metallic caesium) and 1.36 eV (at the maximum when θ is 1). Right from this range θ becomes less than unity, whereas work function increases. At $\theta = 0.07$ the difference $\varphi - V$ becomes great enough, that the ion current can begin. (The data as for θ and φ are by Becker.)

Fig. 5 is the photograph of the caesium evaporation

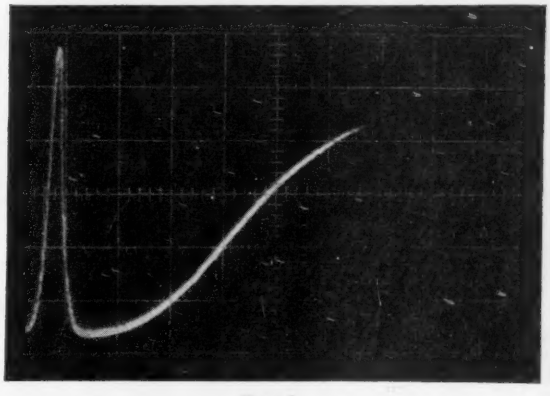

FIG. 5.

impulse on the screen of an oscillograph. The heating current was 1.1 *A*, the time of the adsorption 1.5 min. One square of the net on the screen had the value 2.5×10^{-8} As. By planimetring the area of the impulse and putting the value of the charge into the equation mentioned at the beginning of the discussion we can obtain the pressure.

Also in the Fig. 6 we see the photograph of an evaporation impulse. The heating current was lower than that of the former picture. One can observe, that after the main maximum a very low and unexpressive one appears. We

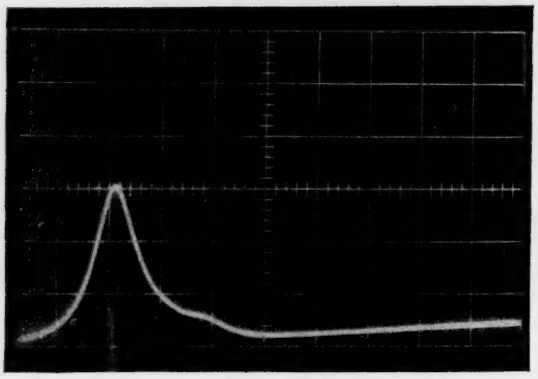

FIG. 6.

have tried to explain it by hypothesis that *Cs* is bound to the surface of tungsten by two different energies.

Fig. 7. We put before the emitter a photocell which was

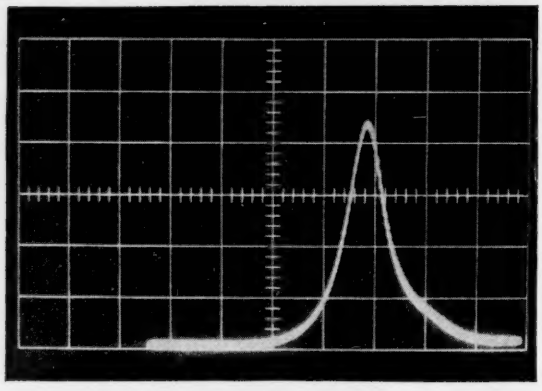

FIG. 7.

sensitive in near infrared. Photocell began to signal when the temperature of the emitter was about 800°C. In the figure we see the photocurrent to which the caesium impulse is added against the time of emitter heating. Thus we have been able to estimate the temperature of the evaporating of caesium.

The time of adsorption has to be determined very accurately. If the adsorption of caesium is shorter than one minute it is difficult to define the time of adsorption because of thermical perseverance of the emitter.

The Fig. 8 represents a photocell with ionisation diode

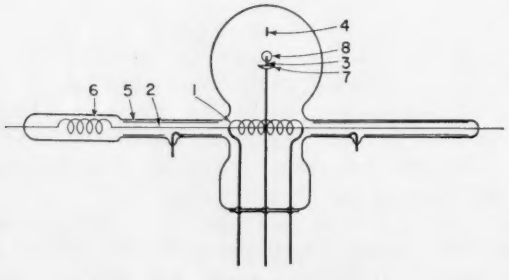

FIG. 8.

built in. The number 2 denotes the emitter, 1 collector, 5 silver-coating, 6 spiral made of tungsten wire to stretch the emitter. The effective surface of the emitter has to be well defined. Therefore the edges of the collector and of the silver-coating are very near and the collector and the silver-coating on the same potential. The photograph (Fig. 9) shows such a photocell with the ionisation diode.

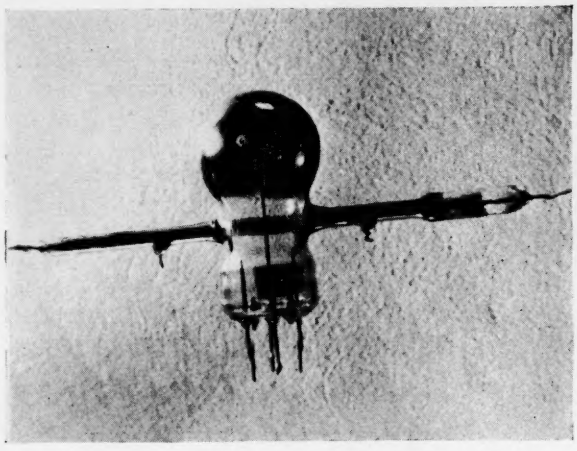

FIG. 9.

When we are interested only in changes of caesium pressure and not in its absolute value we can use a very simple form of the caesium diode. We can see such a diode in the Fig. 10. The loop formed collector with two bent leaflets

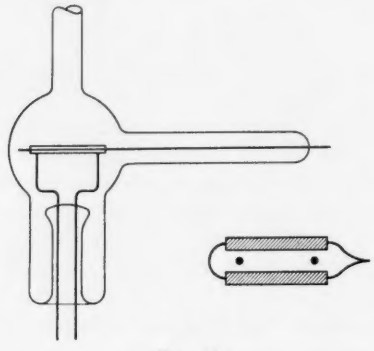

FIG. 10.

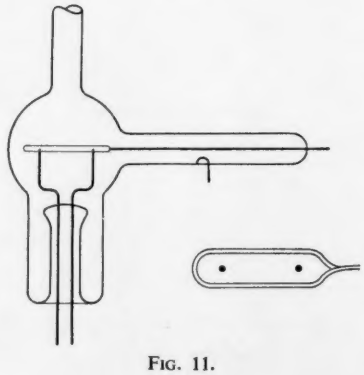

FIG. 11.

Vol.
10
196

is mounted through the side tube. To follow with such an ionisation diode the changes of caesium pressure outside of the ionisation diode it is necessary that the emitter stands in the beam of caesium atoms and that the walls of the bulb have a strong gettering action on caesium atoms, so we can neglect the pressure of caesium in the ionisation diode. Fig. 11 shows the same tube. The collector is only a loop

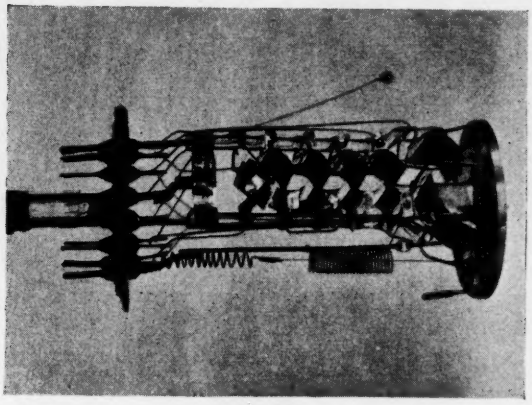

FIG. 12.

In the following discussion we shall review shortly some results we got studying the kinetics of the reactions : silver-oxyde-caesium, antimony-caesium and glass-caesium.

The flow of caesium Q to the studied layer at the pressure P can be obtained by measuring the pressure drop after the shutting a valve in the way of caesium. The time at the shutting of the valve and corresponding quantities are denoted by O.

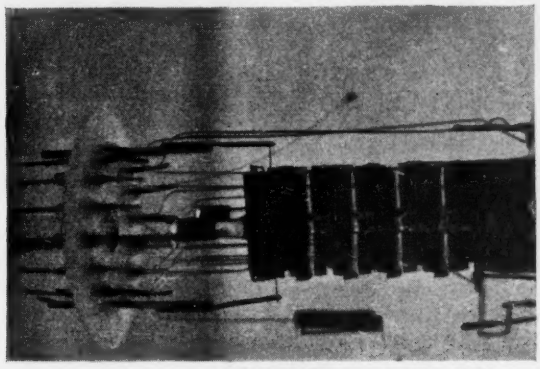

FIG. 13.

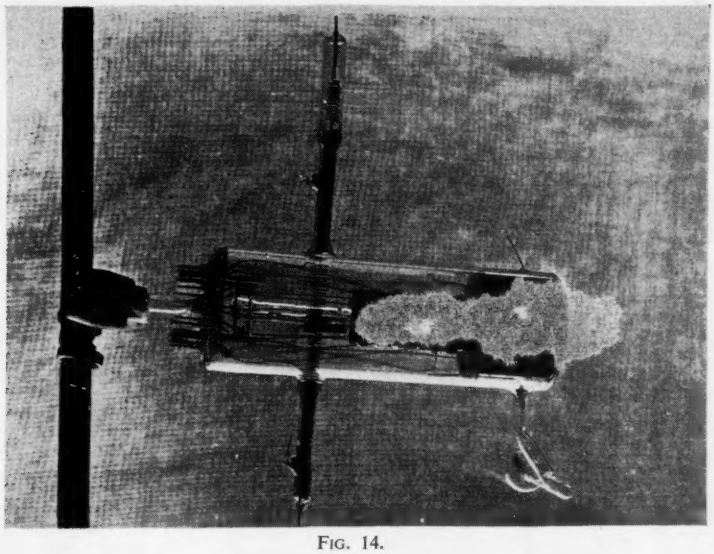

FIG. 14.

about the emitter. The emitter is made of tungsten wire 10 mm long, φ 0.1 mm.

In the next three figures some photomultiplier tubes with ionisation diodes are represented. (Fig. 12) : Diode built at the side of the dynode-system. (Fig. 13) : The emitter built in the space of the anode and last dynode. (Fig. 14) : A photomultiplier tube with a complete ionisation diode.

The electrical circuit used may be represented by Fig. 15. In the right side there is the photocell, in the left side the caesium diode. When the pressure is measured the photocathode has the positive potential against collector. Operating voltage between the collector and the emitter is 120 V from a battery. The heating current of the emitter is taken from an accumulator.

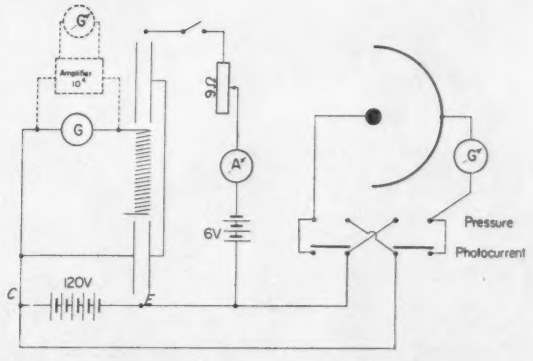

FIG. 15.

$$Q = \left(\frac{dP}{dt}\right)_{t=0} . V = (P_0 - P_f) . c_0$$

V volume of the bulb
P_f final pressure (defined as the pressure at $Q = O$)
c_0 caesium binding velocity of the reacting layer in ml/min.

As the drop of the pressure follows the exponential law we can write more generally :

$$\frac{dP}{dt} = \frac{c}{V} . (P - P_f)$$

with $\frac{c}{V} = k$:

$$\frac{dP}{dt} = k(P - P_f)$$

k velocity constant

From these equations we can calculate the velocity constant k and c (or c_0) caesium binding velocity if the flow of caesium upon layer and correspondent difference $P - P_f$ are known.

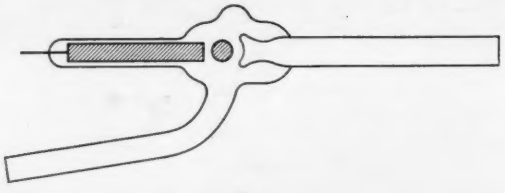

FIG. 16.

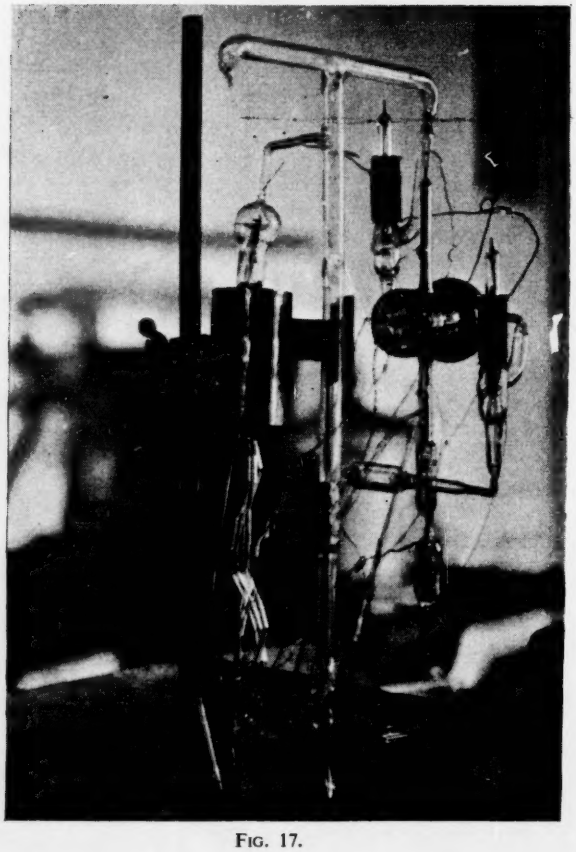

FIG. 17.

Fig. 16 represents the magnetic valve to shut the flow of Cs to the photocell. The iron pellet which is attracted by the iron rod lies on the polished layer. The photograph (Fig. 17) shows a photocell with ionisation diode and two valves just mentioned put in the caesium side tube and in the pumping side tube.

To this day we have made a lot of such measurements. But for the present it is impossible to make any more or less general conclusions because of many factors which take part in : (1) the inner surface of the bulb is not given only by measured layer but also by glass and by some metallic parts ; (2) we have observed that velocity constant depends on the speed of introducing Cs ; (3) after a longer break of introducing Cs (during this time the layer was at room temperature) we always observed a rather great diminution of velocity constant ; (4) the dependency of k on temperature ; (5) it is very probable that residual gases have influence on these reactions. The pressure of residual gases at our measurements was 2–5 $\times$ 10^{-7} Torr.

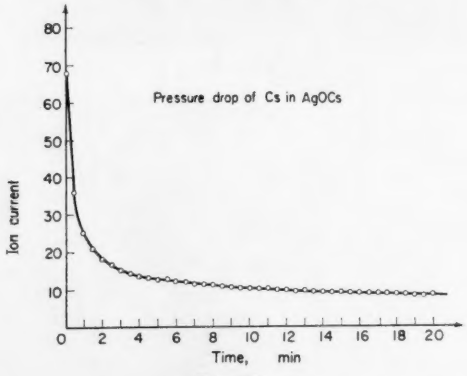

FIG. 18.

We give here only one example of the pressure drop measurements. Fig. 18 shows the pressure drop of Cs above growing AgOCs layer.

In the Table I we see the Cs binding velocities in ml/min

TABLE I

No.	$c = Vk$ (ml/min), AgOCs, 110 °C								
1	44								
2	50								
3	42								
4	35								
5	37								
6	25								
7	13,7	—13,0	—10,0	—10,0	— 9,7				
8	22,0	— 10,3	—12,7	— 9,7	—11,8				
9	23,0	— 13,3	— 9,8	— 9,1	— 9,2	8,8	9,8	9,4	—9,0
10	16,3	— 18,5	—13,7	—10,7	—10,7	—10,3	9,2	—8,6	—8,0
11	22,5	— 17,7	—14,6	—14,4	—10,3	— 8,7	—8,6	—8,6	—8,5
12	13,5	—14,8	—10,4	—11,1	—10,3	— 7,4	—10,0		
13	7,3	— 6,0	— 5,3	— 4,3	— 4,4	— 5,9			
14	10,0	— 7,0	— 7,4	— 5,6	— 4,0	— 5,2	—5,7		
15	9,0	— 9,3	— 7,6	— 6,4	— 4,6	— 5,4	—5,5		
16	8,4	— 7,2	— 7,0	— 6,8	— 5,4	— 6,0			

of thin silver-oxide layer at 110°C. The numbers in the first column indicate the subsequent shuttings of the valve. In the horizontal rows there are values of c obtained along the same pressure drop curve. Some first values of c which do not obey the exponential law are separated from others by dotted line. The upper part of the values was obtained by flashing method, the lower part by steady ion current measurements. Between 12 and 13 measurement we can see a diminution of c. The course of the reaction was here stopped during the night. It seems that reactivity of the layer was diminished because of some recrystallisation process.

References

[1] E. Kansky and S. Jerič ; *International Congr. Vac. Science and Techn.* (Pergamon Press, London).
[2] F. H. De Boer ; *Elektronenemission und Adsorptions-erscheinungen*, Verl. Barth, Leipzig (1937).
[3] J. A. Becker ; *Phys. Rev.* **28**, 341 (1926).
[4] J. B. Taylor and I. Langmuir ; *Phys. Rev.* **44**, 423 (1933).
[5] J. B. Taylor and I. Langmuir ; *Phys. Rev.*, 753 (1937).
[6] K. H. Kingdon and I. Langmuir ; *Proc. Roy. Soc. A*, **107**, 61 (1925).

Vol.
10
1960

Some Results of the Measurement of Caesium Vapour Pressure in Photoelectric Tubes during their Manufacture and Life

E. KANSKY and S. JERIČ

Ljubljana, Yugoslavia

Residual caesium pressure (P_{Cs}) *in phototubes with Ag–O–Cs and* Cs_3Sb *cathodes have been determined by using the method described in the previous paper and compared to the calculated values.* P_{Cs} *in a* Cs_3Sb *cell at room temperature is about* 10^{-14} *Torr, and in a Ag–O–Cs cell about a hundred times lower. We observed an appreciable increasing of* P_{Cs} *in* Cs_3Sb *photocells during the operation. " Current activation " of* Cs_3Sb *photocathodes can be explained by this effect.* P_{Cs} *data for different photocathode activation processes of photocells and photomultipliers are given. Sensibilization of photocathodes with minute quantities of oxygen lowers the* P_{Cs}. *Relations between* P_{Cs} *and photomultiplier dark current are discussed.*

THE measurements of the Cs vapour pressure (P_{Cs}) are very interesting from the theoretical point of view, as they give us the possibility to follow the kinetics and the thermodynamics of the chemical reactions which take part at the formation of Cs compounds in thin layers. From the practical point of view these measurements enable us to get objective and quantitative ideas about the activation process of photocathodes in photocells, photomultipliers and similar photoelectric tubes which are based so far exclusively on the empirical data and on the skill of the experimentator. These measurements give us entirely new possibilities to follow the dynamics of Cs in photoelectric tubes during their working period.

The first problem to be discussed is the residual Cs vapour pressure in photocells. Caesium vapour pressure in Cs–Sb cells can be estimated as follows. After a long working period of a photocell with a semitransparent cathode we can notice on the red Cs_3Sb layer a yellowish spot (Fig. 1) which is due to the electrolysis. It is very probable that the composition of this spot is CsSb. The P_{Cs} of Cs_3Sb is higher than that of CsSb. There is a tendency therefore to equalise the composition of both layers and to make disappear the yellowish spot. The present cell has a cathode thick about 200 Å, and the yellowish spot has existed unchanged for 6 years. On the base of simple gas kinetics calculations we can conclude that the P_{Cs} in this cell has to be below 10^{-13} Torr.

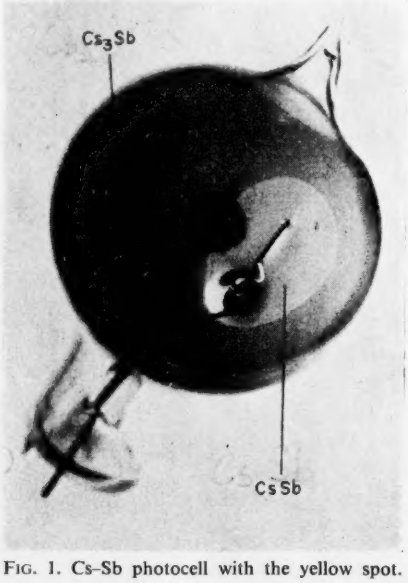

FIG. 1. Cs–Sb photocell with the yellow spot.

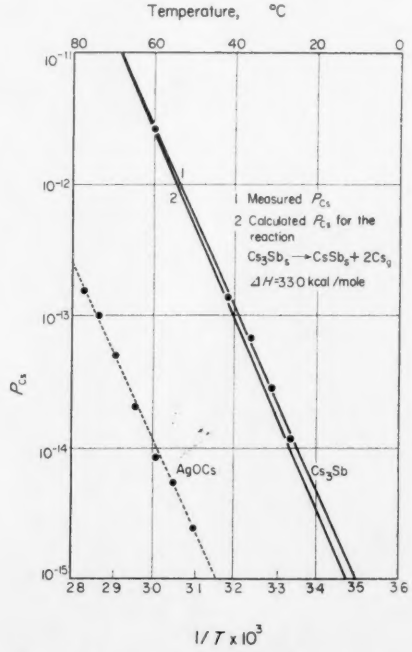

FIG. 2. P_{Cs}-temperature relationship in Cs–Sb cell.

The temperature dependence of the residual P_{Cs} in sealed cells, previously described[1, 2], was measured with the flashing method using an amplifier. The temperature range was from 20 to 60°C and the cell was kept in a conventional water thermostat. The temperature of the photocathode was believed to be constant within two degrees. The relationship between P_{Cs} and temperature is shown in Fig. 2. Line No. 1 represents the measured values. The line No. 2 gives the values calculated for the reaction :

$$Cs_3\,Sb_s \rightarrow Cs\,Sb_s + 2\,Cs_g$$

The P_{Cs} at the room temperature is about 10^{-14} Torr. The P_{Cs} in a Ag–O–Cs cell which is represented by the dotted line is lower for about two orders of magnitude. Table I shows the ΔH[3] and ΔS values used in the calculations. The calculated P_{Cs} is given by the equation :

$$\log P_{Cs} = \frac{-7230}{T} + 10{,}1$$

TABLE I

	ΔH (kcal)	ΔS (cal/deg)
Cs_3Sb	—46,6	54,8
CsSb	—18,1	26,1
Cs gas	18,8	42,6
Reaction	66,1	56,5

The mentioned P_{Cs} has been found for exactly stoichiometric compound Cs_3Sb. It is known that this compound has a homogeneity range with an excess of Cs[4, 5]. The P_{Cs} in this range is given by Henry's law. Therefore we find in the actual cells with good emission P_{Cs} in a broad interval (Fig. 3) the lower limit of which is the Cs pressure

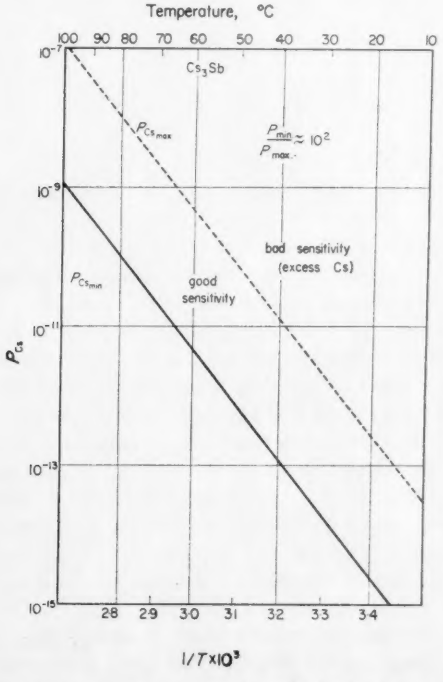

FIG. 3. P_{Cs} interval for good sensitivity in Cs–Sb cell.

of the stoichiometric compound. The upper limit is not exactly defined we suppose, however, on experimental grounds that the ratio P max/P min is about hundred.

The Fig. 4 shows the temperature dependence of P_{Cs}

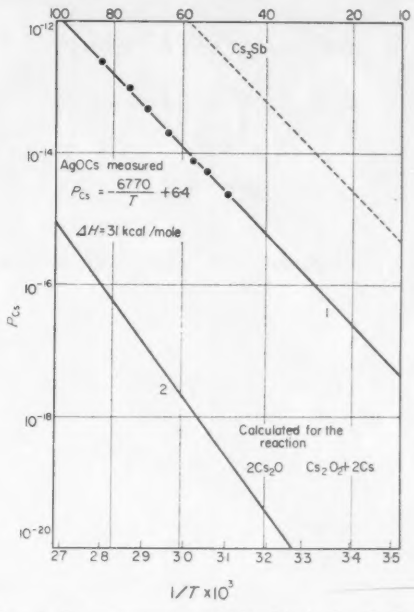

FIG. 4. P_{Cs}-temperature relationship in Ag–O–Cs cell.

in a cell with a semitransparent Ag–O–Cs cathode. Its value is about 10^{-16} Torr at the room temperature. It is well known that the basic compound of this cathode is Cs_2O[6]. The dissociation of the oxide after the following equation :

$$2\,Cs_2O \rightarrow Cs_2O_2 + 2\,Cs$$

is thermodynamically possible[7]. On this way calculated P_{Cs} is represented by the line No. 2. There is no agreement between these two lines. We can state therefore that the residual P_{Cs} is not influenced by the dissociation of the Cs_2O. The measured enthalpy of evaporation is much lower than the calculated one. We can thus conclude that Cs which evaporates is much weaker bonded than Cs in the oxide lattice. The low entropy change experimentally found also denies the dissociation of Cs_2O and supports the assumption about the evaporation of Cs atoms from privileged sites, that means atoms ad- or absorbed in localised centres.

An interesting phenomenon is the increase of P_{Cs} which we observed in Cs–Sb cells during operation (Fig. 5). We measured P_{Cs} in a dark cell. In a certain moment we let to pass a photocurrent through the cell illuminating the cathode. Immediately we noticed an increase of P_{Cs}. At constant photocurrent the P_{Cs} is constant too and drops to its initial value immediately after switching off the illumination. In the figure P_0 is the initial Cs pressure which has the value 3×10^{-14} Torr while P_2, P_5 and P_{10} are Cs pressures at photocurrents 2, 5, and 10μA respectively. The ratio P_{1L}/P_0 shows that P_{Cs} increase 25 times at 10μA photocurrent. It has been established that the increasing of

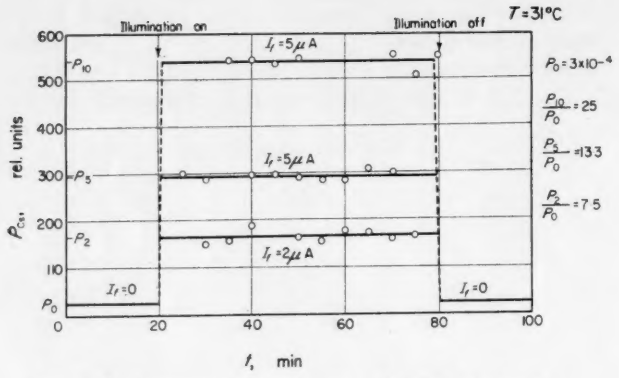

FIG. 5. P_{Cs} increase during the work of Cs–Sb photocell.

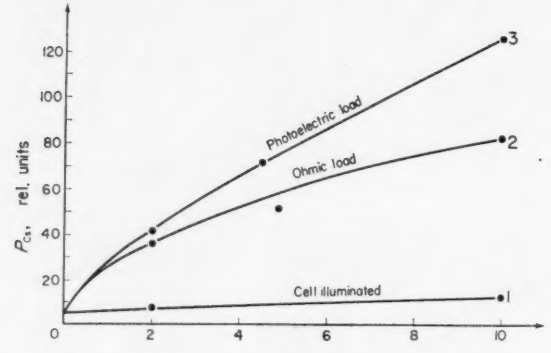

FIG. 6. Factors causing the increase of P_{Cs}.

P_{Cs} is due to at least two causes as shown in Fig. 6 : the illumination and the conduction current. It is very likely to be due to the heating of the cathode by Joule effect. A third cause could be the photodesorption which was not established with certainty in our experiments. The effect of the illumination represented by the curve No. 1 is rather small. Much bigger is the effect of the conduction current (curve No. 2). The photocathode was provided with two silver lacquer covered contacts 15 mm apart through which the d.c. current passed. During the measurements the cell was in darkness. The curve No. 3 represents the increasing of P_{Cs} caused by the photocurrent.

If we introduce during the activation process an excess of Cs into the photoelectric tube the cathode sensitivity drops. We can restore the high sensitivity by eliminating the adsorbed caesium from the cathode. One possibility is to pass a comparatively high photocurrent, for instance 5μA/cm², through the cell. We observe a slow increasing in sensitivity which reaches a constant value after a certain period as shown in Fig. 7. We called this effect " current activation " and believed to be due to electrolytic phenomena. The P_{Cs} measurements, however, showed that the excessive caesium evaporates from the cathode surface.

The photocathode activation processes.—There are two essentially different activation methods (Fig. 8). First we may produce the alkali-metal—in our case caesium—in the tube. The excess of caesium has to be removed by evaporation or absorption in the glass envelope and metal parts or by a suitable caesium getter. The P_{Cs} change is diagram-

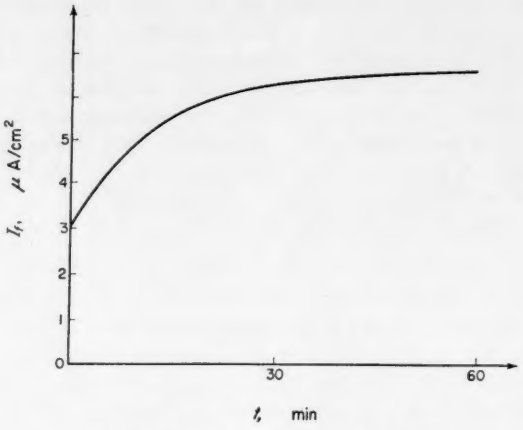

FIG. 7. " Current activation " of a Cs–Sb cell.

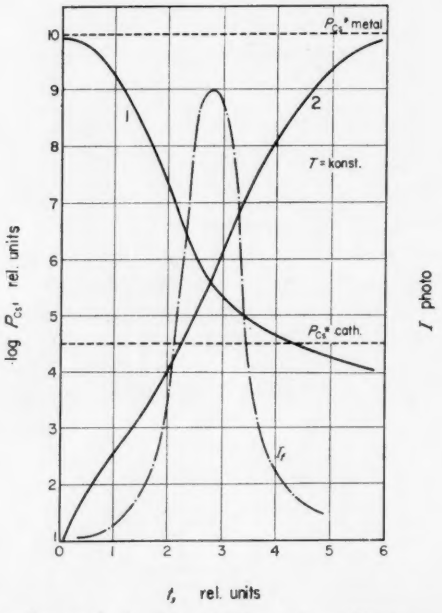

FIG. 8. P_{Cs} changes during the activation process (diagrammatically).

matically presented by the curve No. 1. We start with a relatively high pressure, close to the caesium metal equilibrium pressure which diminishes during the activation process towards the cathode equilibrium pressure. In the second method (curve No. 2) the caesium vapour is introduced from a side tube. At the beginning P_{Cs} is practically zero and increases towards the cathode equilibrium pressure, and further towards the caesium metal equilibrium pressure when a larger amount of excessive caesium is introduced. The dotted curve in Fig. 8 represents the photosensitivity. In both cases the activation has to be stopped at maximum sensitivity.

Examples.—Fig. 9 represents a diagram of the activation process of a photocell with Cs–Sb photocathode. Caesium is introduced from a side tube at a relatively high rate. The activation temperature is 140°C. The curve P_{Cs} represents the Cs pressure change, while the curve I_f, the sensitivity

Vol. 10 1960

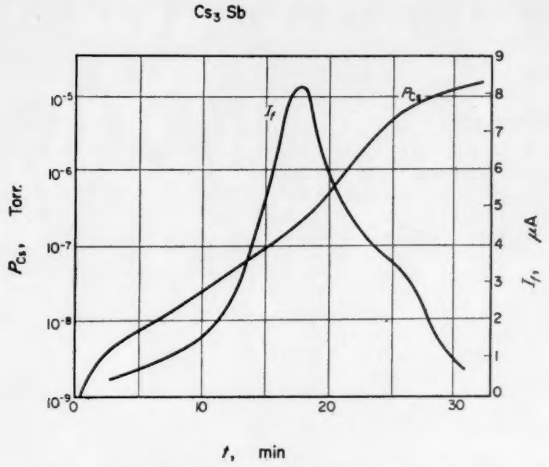

FIG. 9. P_{Cs} change during the activation process in Cs–Sb cell. Caesium was introduced from the side tube.

of the cathode. The maximum sensitivity is reached at the Cs pressure 10^{-7} Torr. At 10^{-5} Torr we have practically no sensitivity, while the insulation currents are remarkable.

Fig. 10 shows the activation process of a photomultiplier

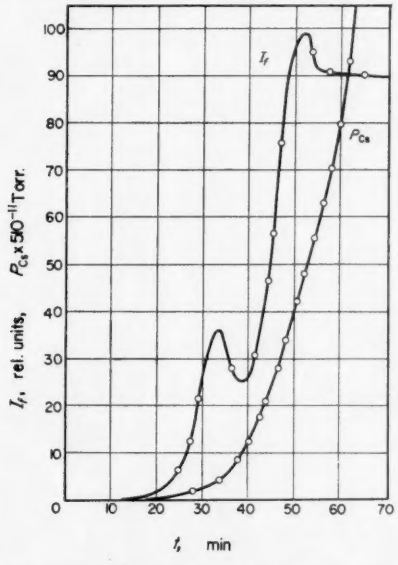

FIG. 10. P_{Cs} change during the activation process in multiplier with Cs–Sb cathode (caesium was introduced from the side tube).

with transparent Cs–Sb cathode and Ag–Mg dynodes. Caesium is again introduced from a side tube into the cathode space. The temperature is 150°C. The rate of Cs introduction is rather small, and we detect it from the pronounced minimum of sensitivity. We stopped the activation process at 10^{-9} Torr. After cooling the tube down to room temperature the caesium pressure dropped below 10^{-12} Torr.

Fig. 11 shows the activation process of a photomultiplier of the same type in which caesium was produced from a pellet fixed in the tube. The temperature was 110°C. We started with a pressure 10^{-5} Torr and stopped the activation at 10^{-9} Torr.

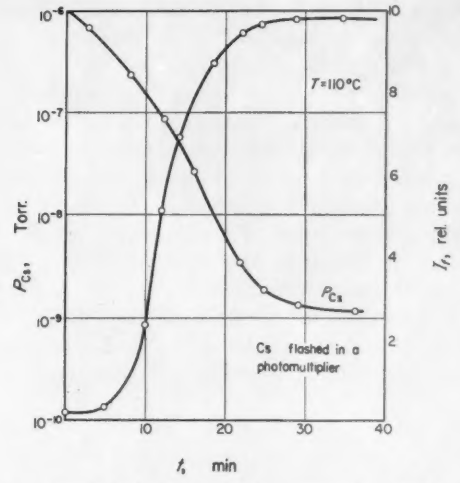

FIG. 11. P_{Cs} change during the activation process in a multiplier with Cs–Sb cathode (caesium was flashed in the tube).

Whilst in a photocell the residual Cs pressure may vary in a broad interval (Fig. 3), this cannot be true of a photomultiplier. Caesium absorbed on dynodes causes fluctuating high dark currents, originated by the field emission. As an example can be mentioned the photomultiplier which had the P_{Cs} about 10^{-12} Torr in the dynodes space. At a voltage over 1000 V the tube was useless because of extremely high dark currents. To get a useful multiplier the caesium pressure in the dynode space must be about 10^{-14} Torr. There are two possibilities to eliminate adsorbed caesium from dynodes and to get a low pressure : prolonged heating or treatment of a tube with small amounts of oxygen.

The treatment of photocathodes with minute quantities of oxygen, called sensibilisation, is very often used. We notice after each sensibilisation a remarkable reduction of P_{Cs}

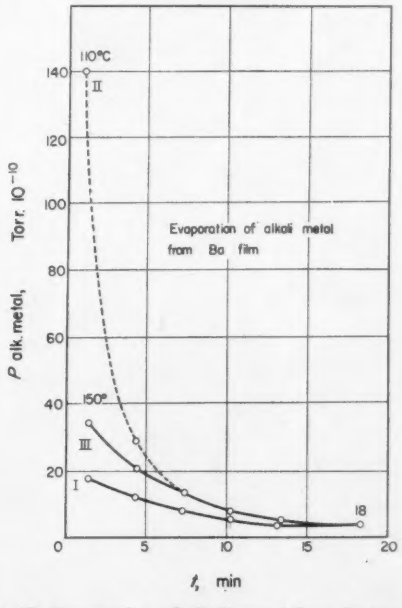

FIG. 12. Evaporation of alkali metal from barium film.

sometimes for several orders of magnitude. In many cases the increasing of sensitivity after sensibilisation can be explained by the reduction of P_{Cs}.

In some multipliers we flashed a barium getter before activating the cathode. Immediately after the flashing we noticed an ion current in our ionisation diode. The reason, quite certainly, is the evaporation of alkali metal contained as contamination in the barium getter. Fig. 12 shows an example of evaporation of alkali metal from barium film. Curve No. 1 represents the dropping of the alkali metal pressure at room temperature just after flashing. After 18 min we raised the temperature to 110°C. The alkali metal pressure is given by the curve No. 2. The curve No. 3 gives the pressure drop at 150°C. After cooling the cell down to the room temperature we could detect no ion current any more.

References

[1] E. Kansky and S. Jerič ; *International Congress Vac. Science and Techn.*, Pergamon Press, London.
[2] S. Jerič and E. Kansky ; *Symp. on Residual Gases in Electron Tubes*, Como (1959).
[3] E. Kansky ; to be published.
[4] V. S. Hlebnikov ; *J. Techn. Phys. USSR*, Moscow, 17–333 (1947).
[5] K. H. Jack and H. H. Wachtel ; *Proc. Roy. Soc. A*, **239**, 1216–46 (1957).
[6] H. De Boer ; *Elektronenemission und Adsorptionserscheinungen*, Verl. Barth, Leipzig (1937).
[7] Gmelin's Handbuch der Anorg. Chemie, Verl. Chemie, Weinheim, Band 25, Caesium (1937).

Vol.
10
196

VACUUM

An Ampoule Freeze-Dryer for Microbiological Research

J. D. MELLOR and D. F. OHYE

Commonwealth Scientific and Industrial Research Organization, Division of Food Preservation and Transport, Homebush, New South Wales, Australia.

(*Received 28 August 1959*)

The construction and operation of an ampoule freeze-dryer for drying suspensions of micro-organisms in 72 tubes at controlled temperatures in the range −50° to 20°C are described. In the apparatus the suspensions can be frozen in situ *by placing the tube holder in thermal contact with the condenser. Means of obtaining reasonably uniform temperatures in different suspending fluids in the same experiment, and of maintaining constant low temperatures in slow drying suspensions are discussed.*

1. Introduction

Many types of dryer for investigations into the freeze-drying of micro-organisms have been described[1] but all of them fall short of the requirements for precise study of the effects of the physical conditions during drying[2]. The apparatus described here was designed for freeze-drying of suspensions of micro-organisms in glass tubes under conditions which can be measured and controlled. In particular, provision was made for prefreezing of the specimens *in situ* by conduction of heat to the condenser block, and for precise control of the temperature of them during drying. The rate of freezing may be varied by simple means and the specimen temperature may be controlled at any desired value in the range from −50° to 20°C.

A capacity of 72 tubes was chosen to provide a suitable number of replicate specimens for the experimental work for which the dryer was to be used. Efforts were made to obtain simplicity in the construction and operation of the apparatus.

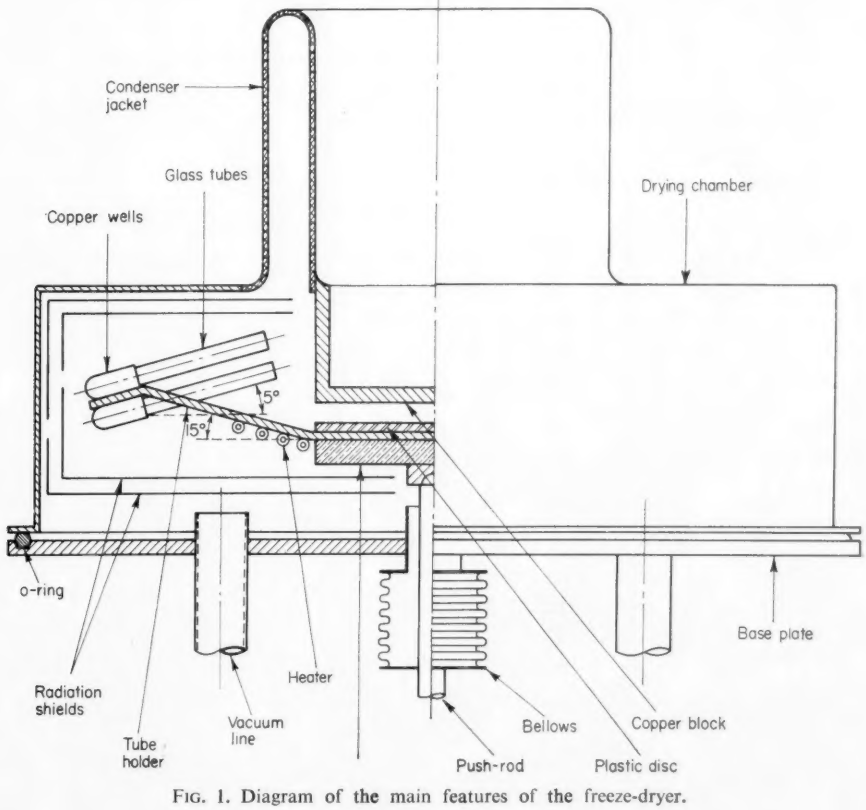

FIG. 1. Diagram of the main features of the freeze-dryer.

2. Description of apparatus

The main features of the freeze-dryer are shown in Fig. 1. The drying chamber consists of a brass base plate 16½ in. *dia.* × ¼ in. thick with an 8 S.W.G. brass cover 15 in. *dia.* × 6 in. high with the condenser well forming the central part of it. An 8 S.W.G. × ¾ in. wide brass flange around the base of the cover seals against a ¼ in. *dia.* O–ring neoprene gasket in a machined V–groove near the edge of the base plate.

The condenser consists of a 20 S.W.G. stainless steel jacket, 5 in. inside *dia.* ; 7 in. outside *dia.* × 3¼ in. high with the inside flanged edge hard soldered to a hollow copper block, 4 $\frac{5}{16}$ in. outside *dia.*, 4 in. inside *dia.* × 4 in. high. The outer flanged edge of the jacket is hard soldered to the brass cover of the drying chamber. The condenser is normally cooled with 5 lb of dry ice-alcohol refrigerant, enough for 8 hr running of the apparatus. Stainless steel was chosen for the jacket because of its relatively low thermal conductivity. The dimensions are such that the mechanical strength is quite adequate while the quantity of heat conducted from the cover to the refrigerant is satisfactorily small. Under normal working conditions frosting of the exposed surface does not extend beyond the top of the jacket, and the cover of the drying chamber remains dry.

The evaporator is essentially a tube holder consisting of a spun copper disk 13 in. *dia.* × 10 S.W.G. shaped as shown in Fig. 1 to which are soldered 72 copper wells 28 S.W.G. × 1 in. deep in two layers radially spaced around the periphery. The wells provide a snug fit for the glass tubes which have nominal dimensions ⅜ in. *dia.* × 3½ in. long, and position them at an angle of 5° to the horizontal, with their mouths pointing toward the centre. Holes are drilled in the disk to allow the passage of the lower layer of tubes. A 40 W 'Pyrotenax' heater is soldered to the tube holder as shown in Fig. 1.

Through the base plate 3, 1 in. *dia.* brass tubes are screwed and soldered to ensure vacuum tightness. One of these is connected to a vacuum pump type 1S50 (Edwards High Vacuum Ltd.) by a flexible coupling, and it has a side arm to which are attached an air admittance valve type RS1A and an adjustable needle valve type OS1C (Edwards High Vacuum Ltd.). The other two tubes are fitted with demountable O–ring seals in order to connect a thermocouple vacuum gauge type 1946 (Radio Corporation of America) to one, and an electrical lead-in for 22 wires to the other. The electrical lead-in consists of heavy gauge bare wires, two being heater leads and the rest for thermocouples. They are held in position by a fibre-board former and the whole bonded with 'Araldite' type I resin to a hollow brass cylindrical block.

A common difficulty in small freeze-dryers is that radiation of heat from the warm walls of the drying chamber to the specimens being dried is relatively large, so that, it is impossible to maintain the specimen at a constant low temperature when supplying heat at a minimum rate electrically. This difficulty is avoided in the present design by surrounding the tubes and tube holder by an envelope of two concentric radiation shields. The shields are spun 26 S.W.G. aluminium with polished surfaces and are attached to the top and bottom of the chamber with insulated spacers.

3. Operation

Method of cooling.

Specimens consisting of approximately 0.2 ml of suspension in each tube are frozen *in situ* before the chamber is evacuated, in order to avoid frothing and the formation of surface films which occur when methods of evaporative freezing are used. The former method has certain advantages since the rate of freezing can be controlled as well as varied. Fairly rapid cooling and freezing is achieved by raising the tube holder into contact with the bottom of the cold condenser so that cooling takes place by conduction along the metal. The tube holder is raised by means of a push-rod shown in Fig. 1 which is actuated by an external wheel through a gearing system. The connexion between the push-rod and platform carrying the tube holder is through a universal joint to ensure good thermal contact between the flat surfaces of the condenser and tube holder. The platform carrying the tube holder is made of nylon to restrict conduction of heat along the push-rod. The rate of cooling may be reduced when desired by inserting a plastic disk of perspex of suitable thickness on the central portion of the tube holder where it acts as a thermal resistance between the base of the condenser and the tube holder.

Measurement and control of temperatures.

The temperatures of the specimens in 6 tubes, the tube holder and the condenser are measured with thermocouples. These, and a short-circuited lead, are connected through a uniselector switch which may be operated manually by a push-button or automatically by means of an electronic interval timer for use with a potentiometer or recorder. In order to minimize errors due to thermal conduction along the wires and to permit precise placing of the junctions at the deepest part of the layer of suspension in the tube, 40 S.W.G. enamelled copper-constantan thermocouple wires are used in conjunction with heavier 26 S.W.G. lead wires. The placing of junctions is important so as to determine the end-point of sublimation from the measurements.

The temperatures of the specimens are controlled indirectly by controlling the temperature of the tube holder to ±1 °C. The output of a thermocouple with its hot junction in thermal contact with the tube holder is amplified through a fast acting and sensitive electronic controller to operate an on-off relay in the heater circuit. During the sublimation phase the temperature of the specimens are generally below that of the tube holder. This is due to the evaporative cooling effect which is a function of the residual air pressure in the drying chamber and of the properties of the suspension. Fairly close control of the amount of evaporative cooling was found feasible by manual adjustment of the leak valve on the vacuum line. Control of the specimen temperature within the required operating limits could then be effected by heating the tube holder to maintain a constant temperature difference between it and the specimens.

4. Performance

Typical temperature histories during cooling and freezing of 0.2 ml of suspension in 0.5 M NaCl in tubes in the apparatus are shown in Fig. 2. The curves show no plateaux at the

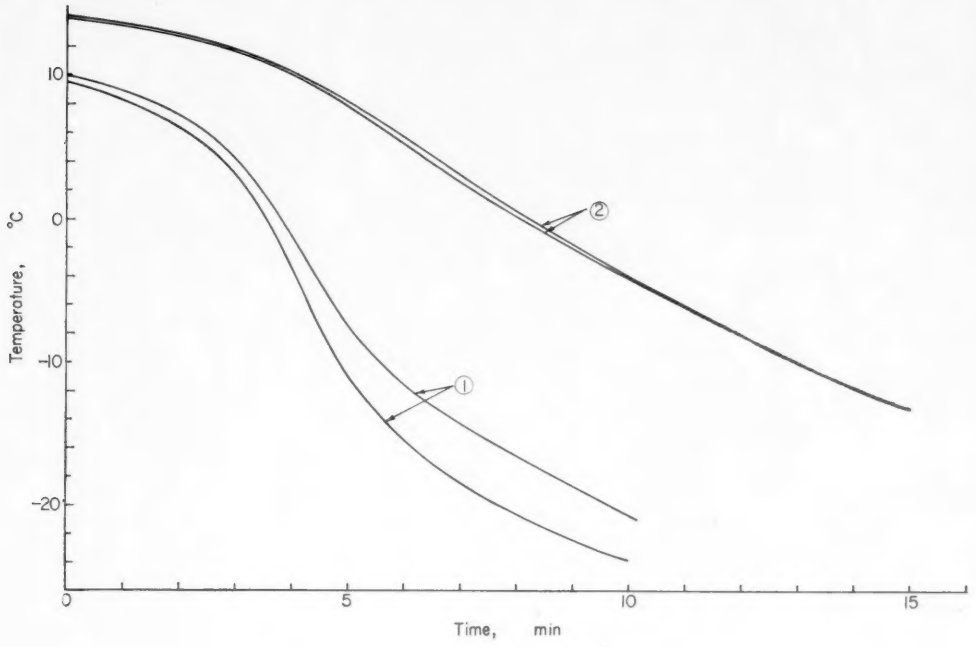

FIG. 2. Typical freezing curves for 0.2 ml of suspension in 0.5 M NaCl with condenser temperature less than −70°C. (1) Tube holder in contact with condenser. (2) Tube holder in contact with condenser through plastic disk $\frac{1}{16}$ in. thick.

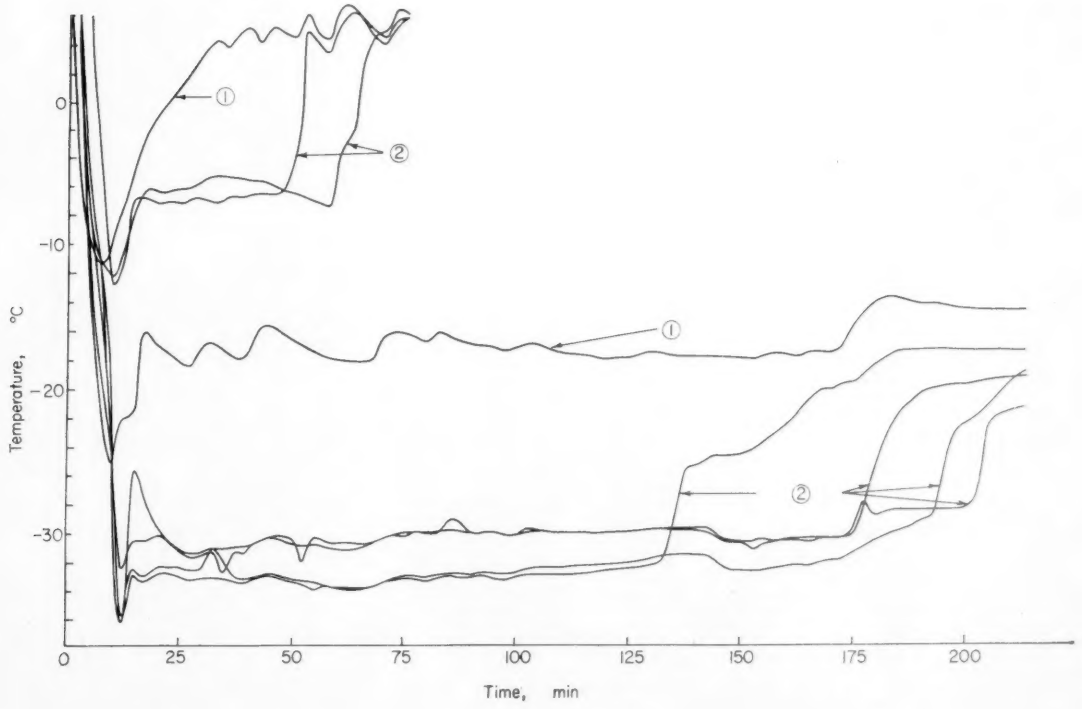

FIG. 3. Typical temperature histories for 0.2 ml of suspension in 0.5 M NaCl in two drying experiments with condenser temperature less than −70°C and total pressure adjusted. (1) Temperature of tube holder. (2) Temperature of specimens.

freezing point of the solution, no doubt because the thermal capacity of the system is large compared with the heat of fusion of the liquid. It is evident from these curves that fairly rapid freezing can be achieved, and that substantial reductions in the rate of freezing can be obtained by inserting suitable disks of plastic material between the tube holder and the condenser.

In Fig. 3 are shown typical temperature histories during drying of 0.2 ml suspension in 0.5 M NaCl at two widely different temperatures, −6° and −33°C. It will be seen that in both experiments there was a very satisfactory control of the specimen temperature during the sublimation phase of drying. The rise in the temperature at the end of this phase was quite sharp in the experiment at −6°C. This type of curve has been found to be characteristic for drying of most types of suspension in this apparatus whatever the temperature. At both temperatures there were substantial variations in the apparent times to complete the sublimation phase. Much of this variation was probably due to differences in the positions of the thermocouples rather than to real differences in the drying time between tubes.

The curves for the −30° to −33°C experiment in Fig. 3 fall into two groups which are 3–4°C apart in the sublimation phase. Those showing the higher temperatures were in tubes which fitted tightly in the tube holders and the lower temperatures were in loosely fitting tubes. Loosely fitting tubes are generally used.

It will be seen from Fig. 3 that the specimen temperatures tend to be well below the temperature of the tube holder during active sublimation. The extent of this evaporative cooling varies greatly between different suspending fluids, suspensions in water tending to cool many degrees whereas those in 0.75 M sucrose cool only a little. These differences of about 23°C are, presumably, due to differing resistances to the flow of water vapour within the specimens being dried, and the large thermal resistance, about 1 B.t.u./ft²hr°F between the wells and the tubes at high vacuum. It is desirable to be able to dry suspensions in different fluids at approximately the same temperature in one experiment. Two methods are available with this apparatus to help achieve this ideal. Firstly, the thermal resistance may be reduced about thirty-fold by providing a film of a suitable oil between the wells and the tubes. It will be seen from the temperature curves in Fig. 4 that this method reduces the difference in drying temperatures between suspensions in water and 0.75 M sucrose when operating at a total pressure of 0.01 Torr to about 15°C. This method alone is not enough to reduce the temperature differences sufficiently. The second measure available is increasing the pressure of the residual air in the chamber. It will be seen from Fig. 4 that increasing the total pressure from 0.01 to approximately 0.1 Torr reduced this temperature difference by a factor of about 5. Increasing the pressure reduces the rate of drying so that the most satisfactory compromise will not be the same under all circumstances.

When drying suspensions with a very high internal resistance to the flow of water vapour it appears that radiation of heat from the walls of the dryer can, despite the radiation shields be too great to allow the drying to proceed at −25°C or lower. This difficulty may be overcome by raising the

Vol. 10 1960

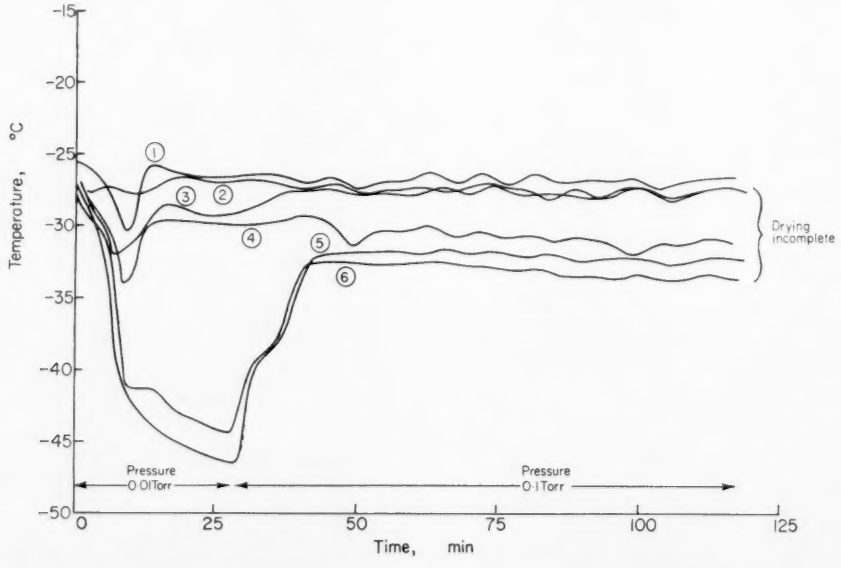

FIG. 4. Temperatures during drying of 0.2 ml of suspension in different suspending fluids with an oil film between the wells and the tubes, condenser temperature less than −70°C and total pressure adjusted. (1) Temperature of tube holder. (2), (3) Temperature of 0.75 M mannitol specimens. (4) Temperature of 0.75 M sucrose specimen. (5), (6) Temperature of water specimens.

tube holder so that it makes light contact, presumably through a layer of snow, with the condenser.

This dryer has been used to study the effects of drying on the survival of micro-organisms dried under various conditions of solute concentration and temperature[3, 4]. Also, it has been found suitable for drying suspensions at controlled temperatures above 0°C.

Acknowledgements

The apparatus described was constructed in the laboratories of the Division of Food Preservation and Transport of the Commonwealth Scientific and Industrial Research Organization, Australia. We wish to thank Dr. W. J. Scott for his active interest and encouragement, Mr. E. W. Hicks for his valuable contributions to the design and Mr. M. C. Taylor for assistance with the electronic circuitry.

References

[1] R. M. Fry; The Preservation of Bacteria, in ' Biological Applications of Freezing and Drying ' (Edited by R. J. C. Harris), 217–231, Academic Press, New York (1954).

[2] D. Greiff and H. Pinkerton, The Effects on Biological materials of Freezing and Drying by Vacuum Sublimation. I. Development and Testing of Apparatus, *J. Exp. Med.* **100**, 81 (1954).

[3] R. H. Leach and W. J. Scott, The influence of rehydration on the viability of dried micro-organisms, *J. Gen. Microbiol.* Vol. 21, Oct. 1959.

[4] R. H. Leach, D. F. Ohye, and W. J. Scott, The death of micro-organisms during drying in relation to solute concentration and drying temperature, *J. Gen. Microbiol.* Vol. 21, Dec. 1959.

ol.
10
960

The Theoretical Development of the Vapour Vacuum Pump

N. A. FLORESCU

School of Applied Physics, University of New South Wales, Sydney, Australia

(Received 30 November 1959)

The empirical development of the vapour pump led to the rejection of such phenomena as diffusion or condensation as the only processes involved in the function of this instrument. Further theoretical attempts which ignored the action of the vapour jet in producing a high vacuum have failed to correctly interpret the experimental results. By considering the removal of the gas molecules by the vapour stream as the basic process, a satisfactory theory of the vapour pump has been obtained. The theoretical conclusions were able to describe the working mechanism of the pump, to explain a large variety of experimental results, and to indicate the proper way of achieving design improvements.

1. Introduction

An ideal vacuum producing device possesses, as an essential part, an aperture having a side connected with the container to be evacuated, while on the other side a perfect vacuum is maintained. Due to molecular agitation, gas from the container will expand through the aperture into the exhausted space. A steady pumping process will take place provided that the molecules coming through the aperture are continually removed into the atmosphere. Thus, the pumping action is nothing else than the removal of molecules from a lower to a higher concentration. A vacuum pump, therefore, is a device able to maintain a pressure difference and to remove gas molecules against this pressure gradient. The efficiency of the vacuum pump depends on the rate of gas removal.

As an outstanding practical example consider the vapour pump* shown schematically in Fig. 1. The gap (*A*) between the edge of the nozzle (*B*) and the walls of the casing (*G*) represents the pumping aperture. A vapour jet leaving the nozzle maintains a high vacuum below the gap by removing the gas molecules diffusing into the jet towards the forepressure outlet. From here the gas molecules are taken to the atmosphere by the forepump. Cooling of the casing is provided in order to maintain a steady distribution of vapour concentration along the pump.

The vapour pump is still the most used vacuum producing device. For more than 40 years this instrument has had no serious rival because of its simplicity, robustness and economy. The physical phenomena which take place during its function, however, were not correctly understood until recently. The various theoretical results were followed by some improvements in the practical design, such that with the same material and mechanical construction it is possible to make more efficient vapour pumps today than 20 years ago.

The purpose of this article is to present the theoretical aspect of the vapour pump as a device able to achieve extreme vacuum. The ejector pump† is not included in this treatment, although its working action is similar. This latter type is efficient at moderately low pressures in a relatively small range. In any practical design a vapour pump is associated with an ejector pump for economical reasons. Such a compound pump does work against higher forepressures which usually are obtained by means of mechanical pumps.

2. Phenomenological description of the vapour pump

As a final experimental result from a number of investigations so far available[4, 5, 6, 7], the following description of the processes taking place in the vapour pump may be presented.

The basic condition for obtaining a relatively tight seal across the pump casing, in order to prevent gas molecules from escaping from the forepressure side towards the pumping aperture, is the ability of producing a vapour jet of certain molecular concentration, which is able to spread after leaving the nozzle. Since the jet spreading occurs only at low pressures, the vapour pump does function efficiently below a limit of the gaseous pressure, about 0.05 Torr in a proper design for air, which will be called critical forepressure. Such a device, therefore, should preferably be named a vapour spread pump or a jet spreading pump.

A pump having a narrow aperture would not require a large vapour spreading. However, this will greatly limit the pump speed. A ratio between the area of the expanded jet and the nozzle opening from 5 to 10 is necessary in order to have a good performance. Using a denser jet to achieve a larger gas compression, the pump would work against higher forepressures. However, the pumping efficiency is

* Also known as " diffusion pump "[1] and " condensation pump "[2].

† The behaviour of the De Laval nozzle in such a pump was investigated from the view point of gas dynamics.[3]

Vol.
10
196

very poor at low pressures, if the jet becomes denser than a normal value.

Suppose that the forepressure is equal to the critical value. The vapour jet leaving the nozzle at speeds, usually higher than the average molecular speed, spreads and produces a shock wave. Because of the continuous flow of vapour molecules, suitable cooling of the casing is necessary to achieve condensation of the vapour at a certain rate in order to maintain the steady state. Any gas molecule present in the blast is entrained by the vapour molecules and removed over the shock boundary, which like a dam maintains the abrupt pressure difference between the forepressure and the lower partial pressure of the gas in the vapour. The gas molecules at a concentration below that corresponding to the forepressure passing through the aperture and then entering the blast will have the same fate. Thus, a pumping effect will result which is indicated by a certain pump speed.

Under the above conditions (Fig. 1c) the shock boundary is quite close to the nozzle's opening. Because of such a small distance, which is called effective length of the pump, some leakage may occur and therefore, a residual gas pressure would be present in the blast. This backwards escape gas obviously affects the rate of gas removal. In the static state, the lowest pressure produced by the pump is equal to this partial gas pressure.

If the forepressure is higher than the critical value (Fig. 1d) no tightness by the vapour barrier can be achieved and therefore no pumping action would result.

As the forepressure is decreased (Fig. 1b) the effective length increases, even if the density and the speed of the jet remain constant. By this change, the leakage across the shock boundary is greatly reduced, thus the pumping action shows an improved efficiency.

At forepressures lower than about 0.01 Torr the shock boundary disappears (Fig. 1a). The jet maintains now a gradient of increasing pressure until the value of the forepressure is reached at a distance which gives the effective length of the pump. In final state, i.e. when no gas molecules are removed by the jet, the ultimate vacuum obtainable in the vapour pump may be measured at the inlet.

3. Failure of earlier theories

Gaede's original idea[1] was that the pumping action in the vapour pump is produced by the diffusion of the gas into a streaming vapour. He suggested that by this means very high exhaustions might be achieved, provided that the vapour is gas free. He even gave the criterion of obtaining the optimum rate of diffusion, which is expressed as a function a of the mean free path of the gas molecules in the vapour and the diameter of the pumping aperture. The optimum condition $a=1$, however, required a very small value for the diameter. Introduction of the Langmuir's design[2], as well as the construction of vapour pumps of high speeds has demonstrated that Gaede's assumption was incorrect.

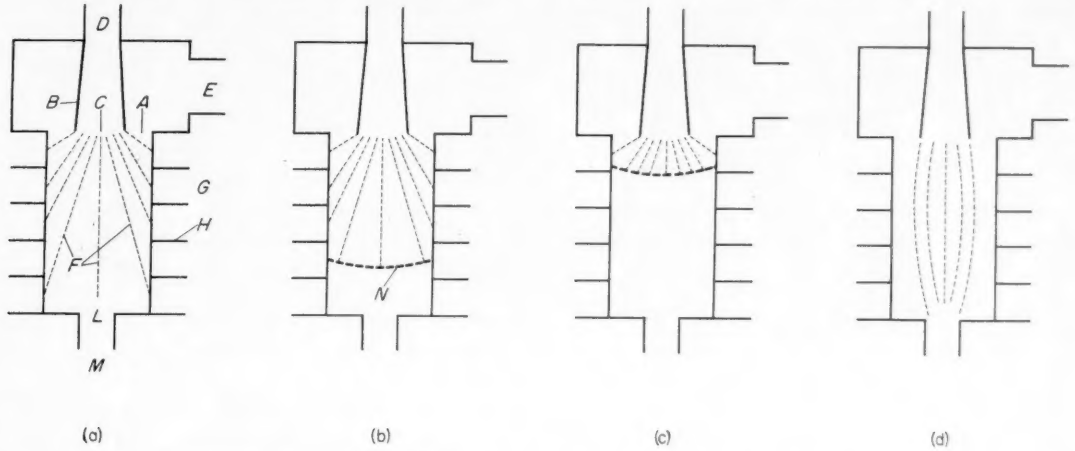

FIG. 1. Schematical illustration of operation of the vapour pump. *A*—pumping aperture ; *B*—nozzle ; *C*—nozzle aperture ; *D*—vapour inlet ; *E*—gas inlet ; *F*—vapour jet ; *G*—pump casing ; *H*—water or air cooling ; *L*—fore-pressure outlet ; *M*—to forepump ; *N*—shock wave.

a. Forepressure about 0.001 Torr *b*. Forepressure about 0.02 Torr
c. Forepressure about 0.04 Torr *d*. Forepressure about 0.1 Torr

Gaede was aware of the fact that the gas diffused into the vapour and carried away by the stream had to be discharged at a higher pressure. He, therefore, suggested that the vapour stream may not be able to remove all gas molecules which diffused into it, as well as the possibility of backward diffusion of the molecules against the stream.

The number of gas molecules which passed through an aperture into a space filled with mercury vapour was calculated by taking into consideration the vapour molecules streaming in the opposite direction. Supposing that in the vapour space there is some gas at partial pressure p_0, the following expression for the specific pump speed was obtained

$$s = \frac{\bar{v}}{4}(ka - p_0/p) \qquad (1)$$

where $\bar{v}$ is the average molecular speed of the gas entering the aperture at pressure p. The constant $k<1$ expresses the ratio of gas molecules driven away by the vapour to the total number diffused into the vapour. The validity of this formula has already been discussed by the writer[8] who

demonstrated that k characterizes the geometry of the pump inlet, not the operating conditions. Gaede assumed $k = 0.08$. Then, even for the optimum condition $a = 1$, a specific pump speed of 1 l/s cannot be obtained. This result, however, is strongly in disagreement with experimental findings.

Considering that all gas molecules entering the jet are removed at the stream speed, i.e. $s.p = U.p'$, in which U is the speed of the jet, and p and p' the gas pressures on both sides of the pumping aperture, the following expression of the maximum specific pump speed

$$s = \frac{\bar{v}}{4} \frac{1}{1 + \bar{v}/4U}$$

was obtained.[9] It will be seen in section 7 that this formula is unable to interpret the experimental results.*

In order to calculate the limiting pressure, Gaede used Stefan's formula which gives the gradient of partial pressure created by opposite streaming of two gases. He considered the special case when a vapour streams at high speed while a gas is at rest, and deduced the resulting drop in the gas pressure along the stream. Thus, the ratio r of the gas pressure p_0 at the diffusion aperture to the pressure at the end of the stream, i.e. the forepressure pf, is given by

$$r = \frac{p_0}{pf} = \exp\left(-\frac{PUl}{760 \cdot D}\right) \qquad (2)$$

where l is the distance between the aperture and the forepressure outlet, P and U the pressure and the speed of the vapour, respectively, and D is the coefficient of gas diffusion referred at atmospheric pressure.

In calculating the ultimate vacuum obtainable in the vapour pump the following assumption was also considered on many occasions[10, 11, 9]. The vapour molecules impart their speed to the gas molecules which have diffused into the jet. During the operation of the pump two processes take place at the same time : the flow of gas molecules having the same speed as the vapour jet, and the backwards diffusion of gas molecules. The ultimate pressure is reached when the rates of these processes become balanced. Since the rate of the backward diffusing gas molecules increases with decreasing pressure, this process has to be limited in order to obtain the steady state. This means that the lowest pressure cannot be decreased below a relatively high value. The theoretical formulation based on the above assumption leads to a formula similar to (2).

The numerical values obtained with this formula are in total disagreement with the experimental measurements. For instance, the calculated ultimate vacuum was found to be 1.2×10^{-3} Torr, while the measured value with a pump operating under the same conditions was 4×10^{-7} Torr.[6] Pressures as low as 10^{-12} Torr would be impossible to be obtained if the vapour pump works in accordance with the diffusion theory. However, in recent years such experimental achievements[12, 13] have been reported.

From (2) an important conclusion is that the equilibrium pressure p_0 would be higher for lighter gases because D is larger. However, considering the pressure as a function of the pumping speed

$$p = \frac{Q}{S} + \left(P - \frac{Q}{S}\right) \exp\left(-\frac{St}{V}\right)$$

(the ordinary exhaustion process formula in which S is the pumping speed, Q is the rate of gas desorption, V is the volume of the vessel, and P is the initial pressure) a contradictory result is obtained, since S is larger for lighter gases.

Another doubtful result of this theory is that concerning the nature of the vapour used. Calculation by means of equation (2) shows that vapour molecules of small mass would produce a more effective pumping action than those of large mass, i.e. Apiezon oils.

4. Gas removal by the vapour jet

Consideration of the ultimate vacuum in the vapour pump as a result of the equilibrium between the gas carried by the vapour stream and the opposite gas diffusion has failed to agree with any experimental measurements. A different view is necessary in order to arrive at the correct description of the processes occurring during the function of this type of pump.

A few years ago the writer[14, 15] attempted to develop the theory of the vapour pump based on the assumption that the pumping effect is the result of the gas removal due to collisions between vapour molecules and the gas molecules present in the jet. This is in agreement with the pumping principle outlined in section 1. The vapour stream accomplishes two actions through the continuous impacts of the vapour molecules against the gas molecules at the same time. Firstly, a gradient of gas concentration is maintained, increasing in the direction of the stream. Secondly, gas molecules entering the jet are continuously removed towards the forepressure outlet. The efficiency of the former action is determined by the ultimate pressure attained, and that of the latter by the specific pump speed.

The mathematical formulation has led to satisfactory results, which have not been invalidated by any experimental and theoretical investigations since reported. On the contrary, as a result of certain reliable experimental results it has been possible to make some refinement to this theory.

Experimental evidence of the removal action in the vapour pump is required at this stage, before proceeding with the mathematical development.

The action of the vapour molecules for producing the pumping effect was first mentioned by Jones and Russel[16]. By reasoning that the pump speed would be directly proportional to the quantity of the mercury vapour passing through the pump, they stated that a definite number of mercury atoms are required to remove a single gas molecule. They experimentally found that 1.1×10^4 mercury atoms are necessary to direct the motion of an air molecule, the gas pressure being 10^{-4} Torr, whereas at 1.5×10^{-3} Torr only 10^3 mercury atoms are required for the same effect. These values, however, should be corrected in accordance with more recent experimental evidence.

* Nöller[3] believes that $p = p'$ during the operation of the pump. This conclusion, however, is erroneous since in this case the above formula gives $s = 0$.

Measurements by Jacobs and Kapff[17] on the trajectories of several commercial pump oils in air at about 10^{-3} Torr pressure have indicated that the oil molecules are only slightly deflected when they collided with air molecules. The vapour oil jet was able to traverse distances of many times the mean free path of the oil molecules without being appreciably deflected. This experimental result gives a direct justification to the assumption of the removal action by the vapour molecules.

Indication of course of the gas pressure along the pump casing has given a perfect illustration of the actual action by the vapour jet. This is shown in Fig. 2. The gas pressures

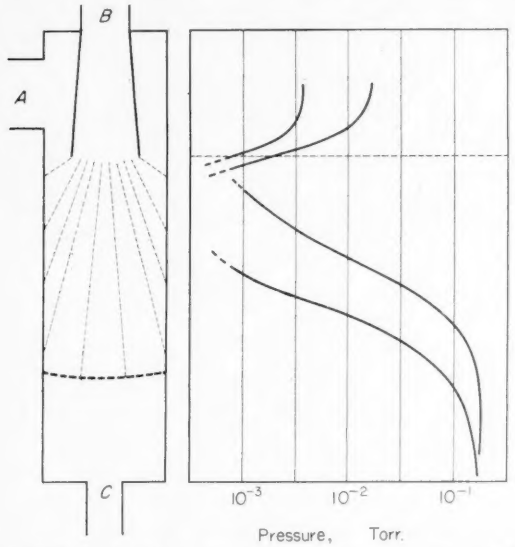

FIG. 2. Distribution of the gas pressure in the vapour pump (deduced from Alexander's[4] measurements) for two different heat inputs.
A—gas inlet ; *B*—vapour inlet ; *C*—forepressure outlet.

have been deduced from experimental results available.[4] The sudden decrease of the gas pressure at the level of the nozzle proves that the gas molecules entering the vapour jet are swept away at high speed. This direct evidence of the gas removal is the most important experimental result supporting the present theory of the vapour pump.

5. Theoretical expression of the ultimate pressure

Consider the case when the pump inlet is closed. The only action of the vapour jet after reaching the steady state is to maintain along the pump an invariable gradient of gas concentration. On both sides of the pumping aperture a gas concentration n_0 corresponding to the ultimate pressure will be present. Experimental evidence shows that this description is correct provided that the actual forepressure is much lower than the critical forepressure. This condition, however, does not mean a limitation of the theoretical considerations. A low forepressure is necessary in order to obtain the ultimate pressure unaffected by any backwards escape gas. Practically, this may always be accomplished by adding booster or ejector stages as in multi-stage pumps.

Let N_v and U be the molecular concentration and the speed of the gas free jet, respectively, immediately after leaving the nozzle. Following the transfer of energy of the jet by collisions with the gas molecules and the cooled walls, a uniform decrease in the number of vapour molecules along the pump casing may be considered. At a distance l corresponding to the effective length of the pump, the action of the jet collapses. The vapour is practically condensed and the gas has reached the forepressure with molecular concentration n_f. We further assume that the gas molecules do not spread towards the pump axis, and therefore the isobars are plane surfaces parallel to the pump aperture.

Consider two isobars separated by a small distance dx at a distance x from the nozzle. Since the gas concentration uniformly increases with x, the pressure difference between the isobars considered is given by

$$\frac{1}{3}\, mv^2 dn \tag{3}$$

where dn is the increase in gas concentration from one isobar to the other, v is the square root of the mean square speed, and m is the mass of the gas molecule.

In a small volume limited by the two isobars and intercepting an area of one cm^2 on each surface there are Ndx vapour molecules, if N is the vapour concentration at distance x from the nozzle. The number or gas molecules collided with per second is then $NZdx$, where

$$Z = \sqrt{\pi}\, \varrho^2 n \hat{v} \frac{\psi(\alpha)}{\alpha} = \sqrt{\frac{2\pi}{3}}\, \varrho^2 n v \frac{\psi(\alpha)}{\alpha} \tag{4}$$

is the rate of collisions[18] effected by a vapour molecule. The factor α is equal to $v_v/\hat{v}$, the ratio of the square root of the mean square speed of vapour molecules to the most probable speed of gas molecules, and ϱ is the radius of the vapour molecule. The function $\psi(\alpha)$ which is dimensionless can be found in tables[18].

If MU is the momentum of a vapour molecule, it follows that the pressure exerted by the jet against the isobar considered is given by $NZMUdx$, which in the steady state is balanced by the opposite action due to the pressure gradient. Thus

$$NZMUdx = \frac{1}{3}\, mv^2 dn \tag{5}$$

In accordance with the previous assumption we may write

$$N = N_v \left(1 - \frac{x}{l}\right) \tag{6}$$

From (4), (5) and (6) it follows

$$\sqrt{\frac{2\pi}{3}}\, \varrho^2 M N_v n v U \frac{\psi(\alpha)}{\alpha} \left(1 - \frac{x}{l}\right) dx = \frac{1}{3}\, mv^2 dn$$

which by integration with respect to x from 0 to l, and to n from n_0 to n_f, gives the final formula

$$r = \frac{n_0}{n_f} = \frac{p_0}{p_f} = \exp\left(-\sqrt{\frac{3\pi}{2}}\, \varrho^2 N_v \frac{MU}{mv} \frac{\psi(\alpha)}{\alpha} l\right) \tag{7}$$

By means of this expression the ultimate pressure p_0 reached in the vapour pump may be appreciated by taking for the various factors values close to those found experimentally.

The calculated values of r for different gases are too small to have a physical meaning. The acceptable conclusion is, therefore, that the vapour pump would be able to produce the perfect vacuum. This result seems to be the first quantitative evidence for the earlier suggestion by Gaede[1] and Langmuir[2] that there is no limit to the vacuum obtained with the vapour pump. The above formula cannot be subjected to any experimental test. The fundamental theoretical outcome that p_0 is extremely low, is sufficient to confirm the correctness of the view advanced about the pumping action occurring in the vapour pump.

6. The rate of gas removal

The efficiency of the pumping action is given by the net rate of gaseous molecules removed towards the forepressure outlet. In calculating the theoretical value of this rate the following assumptions are made :

(a) The vapour stream is uniformly distributed over the cross-sectional area of the pump casing.

(b) The concentration N_v of the vapour is constant throughout the effective length 1.

(c) The gas molecules do not spread towards the centre of the pump.

(d) No gas molecules escape across the shock boundary from the forepressure.

These restrictions will simplify the mathematical treatment without affecting appreciably the actual description of the various processes occurring in the pump.

A volume whose base of unit area is perpendicular to the pump axis, and whose length is l contains $N_v l$ vapour molecules. The total number of gas molecules colliding with the vapour molecules per unit time will be $N_v Z l$, the factor Z being given by (4). Since a fraction of the gas molecules diffusing into the jet is knocked back by collisions with the vapour molecules, the gas entering the jet has not the same concentration as at the inlet of the pumping aperture. This will be $n_1 < n$. If n_0 is the concentration of the gas when the ultimate pressure is attained, only

$$\sqrt{\frac{2\pi}{3}}\varrho^2 N_v (n_1 - n_0)\, vl\, \frac{\psi(a)}{a}$$

gas molecules will be able to be removed towards the forepressure outlet. The number of gas molecules which pass through unit area of the shock boundary per unit time is then given by

$$v = \sqrt{\frac{2\pi}{3}}\beta\varrho^2 N_v (n_1 - n_0)\, vl\, \frac{\psi(a)}{a} \qquad (8)$$

where β expresses the removing efficiency of the jet, i.e. the fraction of the gas molecules directed toward the forepressure outlet after being collided with by vapour molecules.

Further, from the law of the equipartition of energy

$$mv^2 = Mv_v^2$$

it follows

$$v = v_v \sqrt{\frac{M}{m}} \qquad (9)$$

where M and m are the masses of the vapour and gas molecules, respectively.

The vapour molecules moving more or less on parallel paths, v_v is actually the speed U of the jet. Since the gas molecules enter the jet through the annular gap of area a, the volumetric rate of gas removal will then be given by

$$R = \frac{va}{n_1} = \sqrt{\frac{2\pi}{3}}\beta\varrho^2 N_v Ula \sqrt{\frac{M}{m}}\,\frac{\psi(a)}{a}\,\frac{n_1 - n_0}{n_1} \qquad (10)$$

or

$$R = \sqrt{\frac{2\pi}{3}}\beta\varrho^2 N_v Ula \sqrt{\frac{M}{m}}\,\frac{\psi(a)}{a}\left(1 - \frac{p_0}{p_1}\right) \qquad (10a)$$

p_1 and p_0 being the pressures corresponding to n_1 and n_0, respectively.

We have seen that p_0 has an extremely low value unless a secondary process occurs, such as leaking or degassing. Even for the lowest pressure so far obtained, p is still considerably larger than p_0, and therefore p_0/p_1 may be neglected. The rate of gas removal R may thus be considered as being independent of the intake pressure.

Formula (10) contains also the important conclusion that the rate of gas removal depends both upon the driving vapour and the gas to be pumped by the quantity

$$\beta\varrho^2 Ul \sqrt{\frac{M}{m}}\,\frac{\psi(a)}{a}$$

No comparative study of the influence of the type of vapour upon R was reported so far. It is only known that the vapour pumps available working with high molecular mass oils (350–500) show a better efficiency than when using mercury (200). A slightly increase in the performance was reported[19] when Silicone oil (molecular mass 500) replaced Apiezon B oil (350). Alexander[20], however, measured a larger speed with a vapour pump at lower pressures, when mercury (200) was replaced by glycerol (90). At higher pressures no difference was obtained. It is to be expected that R would be somewhat affected, since the speed of the jet is higher for vapour of smaller molecular mass. The radius of the vapour molecule also has to be taken into account.

Regarding the dependence of R on the molecular mass of the gas, the theoretical conclusion is in agreement with the experimental result that for the same working conditions the pump can be efficient for various gases.

7. Role of the concentration and speed of the vapour jet

From formulae (7) and (10) the importance of both the jet concentration and its speed is at once apparent. The performance of the gas removal may therefore be controlled by these two factors, which usually are altered by changing the heat input.

Some authors still persist in the belief that the essential factor in pump speed would be only the speed of the jet. This was emphasized by Langmuir, and later Crawford[21] used a divergent nozzle in order to increase the jet speed.

In agreement with formulae (7) and (10) reliable experimental evidence shows that both factors mentioned are

essential in the pumping action, however their contribution to the pump efficiency needs to be discussed.

If the pumping effect is considered as resulting from the gas removal action by the vapour, the correct conclusion appears obviously. The speed of the jet plays the same role in the whole range of intake pressures. The gas removal should be carried out at a speed as high as possible irrespective of the rate of gas diffused into the vapour. When this speed is lower than the average speed of the gas molecules entering the jet, a gas concentration larger than n_0 may be present in front of the nozzle, if at the same time N_v is not able to maintain ν given by (8) at the required value. Supposing an upper limit[16] for β of about 10^{-3}, a lower limit for N_v is obvious. This also suggests that the vapour concentration has to be larger at higher intake pressures.

In order to make a distinction between the contribution of the jet intensity to the gas removal from that due to the jet speed, both the heat input HI and the nozzle aperture NA have to be adjusted. The vapour concentration in front of the nozzle may be increased by enlarging the nozzle aperture, in which case the speed of the jet will be relatively low. The opposite would occur if the aperture is diminished. Therefore, with only two sets of values HI and NA the decisive test can be obtained.

A number of experimental data[4] are presented in Table I where T is the absolute temperature of the vapour, U is the speed of the jet, Q is the rate of mercury vapour streaming through the nozzle aperture, and KN_v is obtained from the obvious relation $Q = KN_vU$. The pump speed* in each case as a function of the intake pressure is shown in Fig. 3. Curve 4 clearly illustrates the disastrous effect of the re-

TABLE I

Curve Fig. 3	NA cm²	HI W	T °K	Q g/sec	$U\times10^{-4}$ cm/sec	KN_v
1	1.80	1100	443	2.16	3.6	0.60
2	1.80	2100	462	5.27	4.7	1.12
3	7.02	2100	445	6.53	2.6	2.50
4	7.02	4100	465	14.04	2.9	4.84

bounding of gas molecules by a too-dense jet, particularly at very low pressures, while curve 1 indicates the low removal efficiency by a jet of small concentration in the range of higher intake pressures. These results, therefore, prove that the speed of the jet is the dominant factor at lower pressures, whilst its concentration is essential at higher pressures. The maxima of the curves are regularly displaced with the increasing rate of vapour passing through the nozzle, but not with the increasing jet speed. This experimental evidence confirms the correctness of the formula (10), which asserts that the rate of gas removal R is proportional to the product N_vU.

The set of curves also shows that by varying the nozzle aperture and the heat input of the pump, it is possible to obtain a high pumping performance in a large range of pressures.

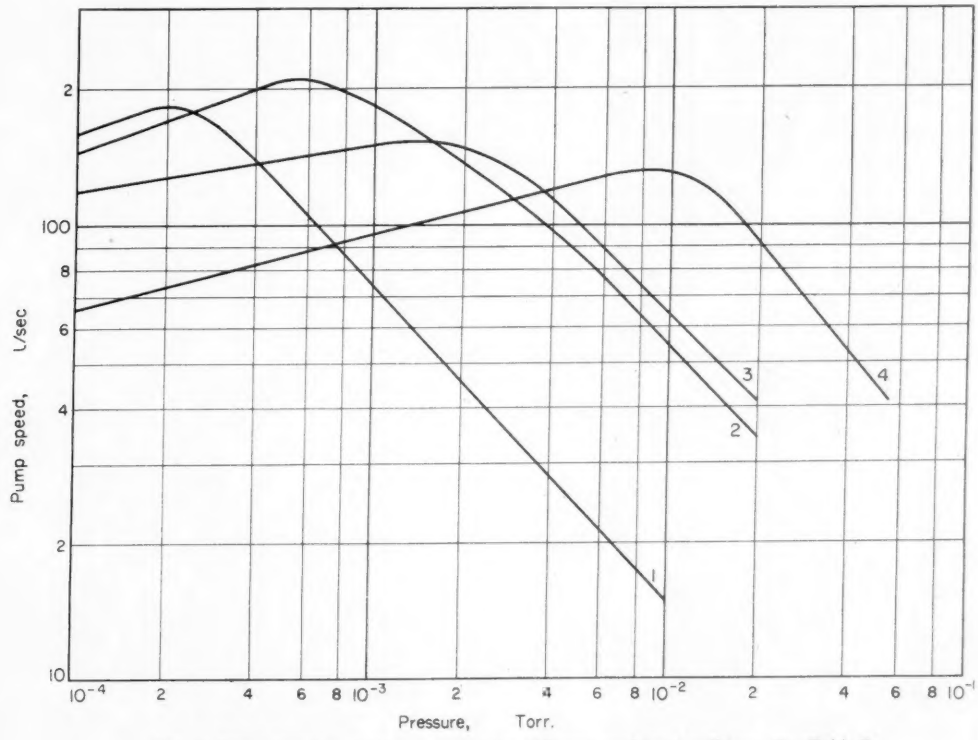

FIG. 3. Pump speed vs. intake pressure[4] for different working conditions (See Table I).

* In these experiments the pump speed was limited by the rate of gas removal.

8. Gas removal at higher intake pressures

In the ideal pump the vapour jet is able to remove at high speed all gas molecules diffusing into the vapour, such that at any time the gas concentration between the nozzle and the shock boundary is equal to that corresponding to the ultimate pressure, provided that the jet concentration is able to give the necessary impact to the gas molecules. Both these requirements are not met in a practical design.

The pump inability to sweep at high speed all molecules entering the jet towards the forepressure outlet, has as a result that the lowest gas concentration n' (corresponding to pressure p') within the effective length of the pump may be higher than the concentration of the ultimate pressure n_0. This latter is reached in or near the static regime, when the gas throughput is relatively small. Thus, the actual rate of gas removal in the upper range of pressures should rather be expressed by

$$R^1 = \sqrt{\frac{2\pi}{3}}\,\beta\varrho^2 N_v U l a \sqrt{\frac{M}{m}}\,\frac{\psi(a)}{a}\,\frac{n_1 - n^1}{n_1} \qquad (11)$$

or

$$R^1 = \sqrt{\frac{2\pi}{3}}\,\beta\varrho^2 N_v U l a \sqrt{\frac{M}{m}}\,\frac{\psi(a)}{a}\left(1 - \frac{p^1}{p_1}\right) \qquad (11a)$$

The steady residual gas at concentration n' at the outlet of the pumping aperture will diffuse toward the centre of the jet. Such an increase in the gas pressure in front of the nozzle for large intake rates could experimentally be proved.[8]

A special design of the vapour pump was used in order to be able to measure simultaneously the gas pressure p at the pump inlet and the partial pressure p' of the gas at the level of the nozzle orifice. The opening of the cylindrical nozzle was large, while the annular gap narrow. In such an arrangement the gas removal by the jet would take place at the jet periphery, and therefore its centre would remain gasfree. If, however, in the working conditions considered, the pressure measured p' is higher than the ultimate pressure p_0, it means that the gas molecules not removed penetrate the vapour blast reaching even its central part. Fig. 4 shows that the residual gas pressure in the jet increases with the gas throughput. Fig. 5 shows that this increase greatly depends on the heat input, i.e. the jet concentration.

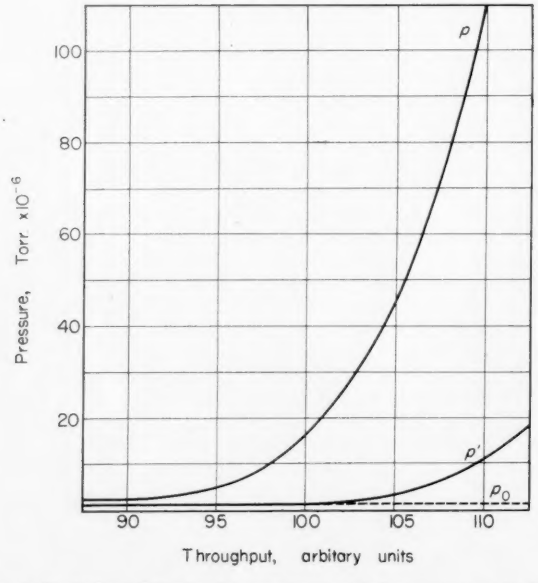

FIG. 4. Variation of the intake pressure p and the pressure p' in front of the nozzle with the gas throughput (heat input 55 W).

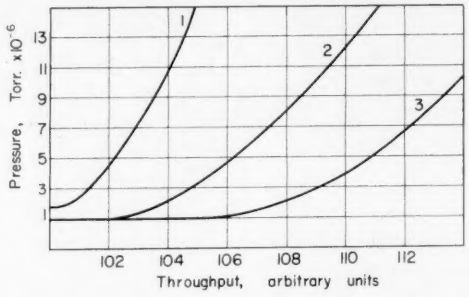

FIG. 5. Variation of p' with the gas throughput for different heat inputs. Curve 1—52 W ; Curve 2—55 W ; Curve 3—58 W.

These experimental results show that if the gas throughput increases, the vapour is unable to remove all incoming molecules, and therefore the residual gas pressure p' in the jet would have an appreciable value. This means, in accordance with (11), that the gas removal is affected. Even with an experimental design better than any practical vapour pump, the ultimate pressure in the centre of the nozzle aperture could be maintained only in the range of lower intake pressures. The increase in the gas content in the jet did not originate from the forepressure side, because gas was admitted into the pump at such a rate that any small increase measured in the forepressure did not exceed the value which affected the ultimate pressure.

9. Speed of the vapour pump

The speed of the vapour pump being defined as the volume of the gas passing through the aperture of area a per unit time can easily be calculated. The molecular concentration of the gas on both sides of the aperture being n and n_0, respectively, the net rate of passing molecules is then expressed by

$$v_1 = \frac{av}{4}(n - n_0) = a\sqrt{\frac{kT}{2\pi m}}(n - n_0) = c(n - n_0) \qquad (12)$$

where v is the average molecular speed, and C is the conductance of the aperture. The pump speed is then

$$S = \frac{v_1}{n} = c\,\frac{n - n_0}{n} \qquad (13)$$

This value, however, can never be attained in an actual vapour pump because of the impossibility of the perfect practical construction, and occurrence of various secondary processes.

Firstly, the pumping aperture has always a certain thickness, and therefore, the actual conductance C' is different from C.

Secondly, following the rebounding of gas molecules by vapour molecules, the net rate of gas molecules passing through the aperture is smaller than that given by formula

Vol. 10 1960

(12). This means that the geometrical conductance C' is affected, and therefore, will have a value of $\gamma C'$, where $\gamma<1$.

Thirdly, as already mentioned, the gas removal might be poor because of inadequate vapour jet. In such a case, gas molecules at a concentration $n'>n_0$ may be present at the aperture outlet.

Thus, the net rate of gas molecules passing through the aperture would be

$$\nu^1 = \gamma C^1 (n - n^1)$$

The actual speed of the pump will then be

$$S^1 = \frac{\nu^1}{n} = \gamma C^1 \frac{n - n^1}{n} = \gamma C^1 (1 - \frac{p^1}{p}) \qquad (14)$$

Under normal working conditions the vapour concentration and the jet speed should have such values that the rate of gas removal be equal to the rate of gas entering the jet

$$S = R \qquad (15)$$

This condition is not totally independent of the gas, however, the fact that both sides contain the factor $1/\sqrt{m}$ is an undoubted test of this theory.

In practice, in accordance with the above discussion, the following condition is required

$$S^1 \leqslant R^1$$

Even if the efficiency of the gas removal can be increased the pump speed cannot be increased above S^1, since the jet is not able to remove more gas molecules than enter the pump.

Reasonable numerical values for various factors in (11) taken within the ranges experimentally permissible, give acceptable evaluation for R^1. In Table II it is shown that R is able to be larger than S, and this condition should be met by any well-designed vapour pump.

Generally, any measured value in the range of low pressures smaller than the calculated speed S^1 indicates rather that the gas was partially prevented from reaching the vapour blast, than the inefficiency of the jet in removing the gas which is able to enter the pump. The process of gas diffusion into the vapour jet, as already mentioned, was the initial problem in the development of the vapour pump. The rebounding of gas molecules by collisions with the vapour molecules was considered by Gaede in expressing the pump speed. A considerable amount of experimental evidence has shown that this effect is mainly controlled by the vapour jet, and not by the size of the pumping aperture. This view has led to an improvement of the pumping performance.

10. Improvement of the rate of gas entering the jet

When the jet having a certain concentration and speed is able to remove all gas molecules available, any increase in the jet speed will not improve the pumping performance. As the rate of diffusing molecules increases, a denser vapour stream is required to maintain the performance. However, the increase in the jet concentration is accompanied by a too extensive expansion, such that some vapour spreads backwards. This latter effect increases considerably the rate of rebounding of the gas molecules, and therefore reduces the pump speed.*

This serious drawback takes place in all practical designs of the vapour pump. Despite numerous efforts, the vapour backspreading could not be appreciably reduced until the writer[22] suggested an improvement of the nozzle.

The basic idea was to obtain a divergent vapour jet able to maintain the gas concentration at a very small value within the effective length of the pump, to offer little chance to the gas molecules of being rebounded, and to have little tendency of backspreading.

These requirements would be met by a jet having a high speed at the periphery, and whose concentration increases from the periphery to the central region. Such a jet could be obtained by means of a modified nozzle.

The new arrangement is shown in Fig. 6. In a divergent nozzle (C) an open thin-walled tube (D) is placed coaxially and kept in position by two supports (E). Only a small fraction of the vapour coming from the boiler passes through the narrow annular gap between the nozzle and the inlet of the coaxial tube. This space forms, therefore, an annular nozzle of De Laval type. The annular jet after leaving this nozzle at high speed has a small vapour concentration. On the contrary, the vapour streaming through the cylindrical tube has a large concentration. Thus, after leaving the nozzle the whole jet has a larger concentration in the central region than at the periphery, where the vapour speed is higher than in the centre.

The intense stream leaving the cylindrical tube spreads out and at a certain distance from the nozzle opening the vapour

TABLE II

Theoretical values of R *and* S *in the mercury vapour pump calculated from equations* (10) *and* (13), *respectively.*

β	M g	ρ cm	Nv	U cm/sec	l cm	Gas	$\frac{M}{m}$	$\frac{\psi(\alpha)}{\alpha}$	R l/sec	S l/sec
10^{-3}	200	1.75×10^{-8}	1.65×10^{16}	3.6×10^{4}	10	Air	6.94	2.15	$16.25a(1-\frac{p_0}{p_1})$	$11.67a(1-\frac{p_0}{p})$
						Hydrogen	100	2.01	$57.50a(1-\frac{p_0}{p_1})$	$43.65a(1-\frac{p_0}{p})$

* In Gaede's design the vapour stream had a very low speed and therefore, an appreciable tendency to spread backwards. This explains why his pump operated with only relatively small vapour concentrations.

will become transversally homogeneous. However, this diverging jet being surrounded by vapour at high speed, and not by vacuum, the backspreading is greatly reduced.

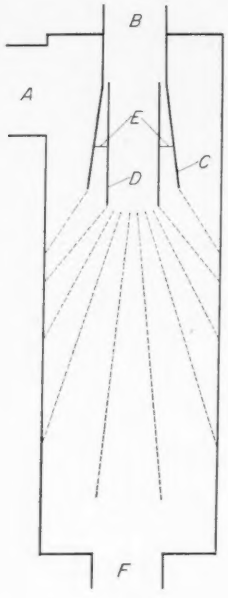

FIG. 6. The modified nozzle.

The behaviour of such a modified nozzle was experimentally investigated[22] and found to be in agreement with the above reasoning. The vapour backspreading was appreciably diminished, and therefore, the speed of the pump increased with increasing the heat input above the normal value, a result which was oppxoite to that indicated by a conventional vapour pump of the same dimensions and working in the same conditions. Thus, the concentration at the jet periphery is the factor which limits the gas diffusion into the vapour.

The possibility of increasing the pump speed without enlarging the number of vapour molecules available, proves that the jet is able to remove gas at a larger rate than that passing through the pumping aperture. This latter rate, therefore, limits the maximum speed of the pump.

This improvement in the performance of the pump shows that the processes in the pump take place in agreement with the theory described.

11. Conclusions

A great delay in understanding the operation of the vapour pump, and thus achieving improvements in its practical design has been caused by ignorance of the pumping principle. In this paper it is emphasized that the pumping effect results from the removing action of the vapour jet.

Experimental evidence of this action taking place in the vapour pump is mentioned.

The theoretical considerations developed here are concerned only with the type of vapour pump able to produce very low pressures. Since this device is based on the spreading of the vapour leaving the nozzle, it may be called a jet spreading pump.

The expression of the ultimate pressure obtainable in such a pump was formulated by assuming that the time rate of momentum of the vapour molecules imparted to the gas molecules is in equilibrium with the pressure resulting from the gradient of increasing concentration of the gas. Calculation shows that very low values can be obtained, thus giving an acceptable justification to the general assumption that there is theoretically no limit, except that set up by leakage and desorption to the lowest pressure which can be attained by operation of the vapour pump.

Next, taking into account the driving action of the vapour jet which collides with the gas molecules that have diffused into it, a formula was obtained expressing the rate of gas removal. Since the pumping action results from the transfer of jet momentum to the gas molecules, the rate of this removal increases with decreasing molecular mass of the gas pumped.

The two formulae (7) and (10) show that the performance of the vapour pump depends on both, the concentration and the speed of the jet after its expansion from the nozzle. However, it is pointed out that the pumping performance is affected if the magnitude of these factors is taken arbitrarily, even when their product is maintained constant. Measurements have indicated that by suitable choice of their magnitude the pump would be highly efficient over the whole range of working pressures.

As the upper limit of the pump speed is determined by the conductance of the pumping aperture, the rate of gas removal has to be at least of the same order of magnitude. Calculation shows that the pumping efficiency of the jet is able to meet this requirement. Therefore, in a well designed vapour pump, the pump speed is limited by the net rate of gas passing through the pumping aperture.

The vapour backspreading was mentioned as the major cause which affects the rate of gas entering the jet, particularly in the lower range of pressures. This drawback can be reduced by the use of a modified type of nozzle. Experiments carried out with such an improved nozzle have shown that low speed and high concentration of the vapour molecules, at the stream periphery, are responsible for the diminution of the pump speed.

Although the contribution of the vapour pump in science and industry is well-known, its particular use in production of the extreme vacuum needs to be emphasized. That the vapour pump maintains a high performance even in the range of lowest pressures so far measured, may be demonstrated by the following simple experiment. A mercury vapour pump provided with a dry ice trap and two liquid air traps, all connected in series, was able to maintain in a glass system of about 2 l. containing an ionization gauge and some other electrodes a pressure of about 10^{-10} Torr, following a moderately degassing treatment. However, after the system was sealed off, the pumping of the ionization gauge alone could not maintain a pressure below 10^{-9} Torr. The pumping speed of the vapour pump was, therefore, considerably larger than that of the clean-up pump.

The theoretical development outlined in this paper is

Vol.
10
1960

applied to the single stage vapour pump in the range of gaseous pressures up to about 0.05 Torr. This upper limit for the pump of optimum efficiency is set by the inability of the vapour jet both to spread within the pump casing and to build up an effective pump length of reasonable magnitude. The above requirements are essential in order to obstruct any backwards escape of the gas molecules. If these are only partly met the efficiency of the pump may greatly be affected.

The relatively low critical forepressure would mean a great limitation in the use of the vapour pump. However, in practical designs the vapour pump is backed by one or two stages, these latter being suitable modifications of the vapour pump in order to be able to work against higher forepressures, but, of course, these are not efficient any more in the range of very low pressures.

Regarding the operation of the actual vapour pump, the following conclusions should be mentioned : the performance of the practical design is limited by the impurities evolved from the driving vapour and the pumping effectiveness by the rate of vapour molecules escaping into the vacuum system.

References

[1] W. Gaede ; *Ann. der Phys.* **46**, 357–392 (1915).
W. Gaede, *Z. techn. Phys.* **4**, 337–369 (1923).
[2] I. Langmuir ; *Phys. Rev.* **8**, 48–51 (1916).
[3] H. G. Nöller ; *Z. angew. Phys.* **7**, 218–229 (1955).
H. Kutscher ; *Z. angew. Phys.* **7**, 229–240 (1955).
[4] P. Alexander ; *J. Sci. Instrum.* **23**, 11–16, (1946).
[5] B. B. Dayton ; *Rev. Sci. Instrum.* **19**, 793–804 (1948).
[6] N. A. Florescu ; *Vacuum*, **4**, 30–39 (1954) (Published 1956).
[7] R. Jaeckel, H. G. Nöller, and H. Kutscher ; *Vakuum-Techn.* **3**, 1–15 (1954).
[8] N. A. Florescu ; *Investig. Phys.* Nr. 2, 7 (1955).
[9] R. Jaeckel ; *Z. Naturforschg.* **2a**, 666–677 (1947).
[10] L. Wertenstein ; *Proc. Camb. Phil. Soc.* **23**, 578–583 (1927).
[11] M. Matricon ; *J. Phys. Rad.* **3**, 127–144 (1932).
[12] H. D. Hagstrum ; *Rev. Sci. Instrum.* **24**, 1122–1142 (1953).
[13] D. Alpert ; *Science* **122**, 729–733 (1955).
[14] N. A. Florescu ; *Investig. Phys.* Nr. 2, 20 (1952).
[15] N. A. Florescu ; *Investig. Phys.* Nr. 1, 16 (1953).
[16] L. T. Jones and H. O. Russel ; *Phys. Rev.* **10**, 301–304 (1917).
[17] R. B. Jacobs and S. F. Kapff ; *Ind. Engng. Chem.* **40**, 842–846 (1948).
[18] L. B. Loeb ; *The Kinetic Theory of Gases*, p. 101 (McGraw Book Co. 1934).
[19] J. R. Davy ; *Industrial High Vacuum*, p. 10 (Pitman & Sons, London, 1951).
[20] P. Alexander ; *J. Sci. Instrum.* **25**, 313–314 (1948).
[21] W. W. Crawford ; *Phys. Rev.* **10**, 557–563 (1917).
[22] N. A. Florescu ; *Austral. J. Appl. Sci.* **8**, 305–316 (1957).

ol.
10
960

On the General Principles of Chemical and Ionic Pumping*

R. N. BLOOMER

Research Laboratory, Siemens Edison Swan Ltd., Harlow, Essex
(*Received 10 December 1959*)

As a start some differences between physical and chemical adsorption are emphasised. The distinction between chemical and ionic pumping is defined and discussed, and examples quoted, both recent and historical. Since in getter-ion pumps different kinds of gases have to be handled simultaneously, examples are mentioned where the presence of some gases is known to greatly influence the kinetics of adsorption of other particular gases. In any case, the interpretation of the readings obtained when checking pump performance is hazardous when gases of differing condensation coefficient are present together. A simple test that measurements are well-founded is described. Some surface reactions that can limit the performance of getters, and ways of possible improvement, are suggested.

1. Introduction

As an introduction to the various types of pumps described in following papers, and to illustrate the general principles of chemical and ionic pumping, it is useful to consider some details of the ways in which gas molecules may be held bound by metal deposits. At the start some contrasts between physical adsorption and chemisorption must be emphasised. In physical adsorption the energy of binding by Van der Waals' forces is some tenth or so of an electron volt. No potential energy barrier occurs between the free and bound states, and hence such binding is common and takes place readily. In chemisorption the energy of binding may be as much as a few electron volts, and an activation energy may be required, as in the process of dissociating the incident molecule into atoms for taking up by the metal. Because of these requirements, chemisorption is specific to some metal surfaces only.

It is necessary to define the meaning of the terms chemical and ionic in the title. The word "chemical" is used to describe exchanges of electrons between reacting atoms that have only thermal energies : the word "ionic" is used to describe the removal from the vapour phase of ionized or otherwise excited molecular fragments which have acquired energy, as in an electron discharge. In other words, chemical clean-up of gases follows natural affinities : but ionic clean-up has to be induced.

It might be thought that unnatural chemical reactions also would be induced, or the probability of natural ones increased, by the running of ionizing discharges near active materials as a means of supplying any activation energy needed. However, both these possibilities are unlikely to happen commonly, for these reasons. Firstly, the physical processes in chemical and ionic clean-up are quite different. Thus some ion clean-up can occur because ions are smaller than atoms, and so can be shot into traps in materials, like interstitial lattice positions near the surface, from which they cannot move after trapping an electron ; but in chemisorption any ion formation is in passing at the electronic surface of the metal (the image plane in electrostatics). Secondly, the condensation coefficient for molecules (the fraction of molecules incident in unit time, that stick to a surface) and the energy of binding in chemisorption are independent of each other. For example, oxygen and barium react exothermally, but barium films can be prepared that do not take up oxygen until after an induction period of about 15 min.[1]

A notable exception to the common lack of influence of ionizing discharge upon chemical binding of gases is the case of nitrogen. This gas can be excited to a metastable state that is relatively long-lived, and in which about 8 eV of energy is bound. Lukirsky and Ptizyn[2] discovered that the taking up of nitrogen by magnesium films only begins when the energy of electrons passing through the gas is raised to about 8 eV. (Positive ions of nitrogen are formed only when the energy of bombarding electrons is raised above about 17 eV). A similar result is also found when the Lukirsky and Ptizyn experiments are repeated with barium films, using for these measurements Pirani gauges, like those described by Riemann[3], at pressures down to 10^{-6} torr. The action of the metastable nitrogen is also revealed by an increased of pumping speed in proportion with the electron current in a nearby ionization gauge.

It is known from the work of Hagstrum and Tate[4] that activated (particularly metastable) forms of oxygen can enter into chemical combination with residual impurities on the walls of vacuum systems ; but there is no evidence that these forms are ordinarily important in the removal of oxygen by chemically active materials like barium[1]. This is reminiscent of the earlier work of Rodebush and Nichols[5] on molecular beam detection.

*This paper was presented at a one-day symposium held at the Institute of Physics, London on 17 April 1959.

Vol. 10 196

2. Comments upon some difficulties with mixtures of gases, and with some complicated gases

When two or more kinds of gas molecules together impinge on a metal surface, on which they would singly adsorb by different processes, say physically and chemically, the binding of either of them may be greatly influenced by the presence of the other kind. An example is the influence of traces of the noble gas neon upon the adsorption of chemically active gases on tungsten, as investigated by Roberts[6]. In a getter-ion pump the evaporated metal must act as a sink for many kinds of gas simultaneously, and so the results of precise studies, like those of Roberts, cannot be applied directly in interpretation of performance measurements. But they do warn of the difficulties that could occur in service.

Moreover, with complicated molecules of which only a part can be chemisorbed, false impressions of the performance of a getter-ion pump may be obtained from measurements of pressures. Stout and Gibbons[7] found that titanium films remove carbon from impinging methane molecules, at a pressure of a few microns Hg, and release hydrogen. Measurements in this laboratory have shown that a similar behaviour occurs with benzene and toluene, at a pressure of order 10^{-6} torr, such as might occur in unbaked demountable vacuum apparatus. Thus the gettering of hydrocarbon molecules can cause a rise of pressure, that increases integrally with the number of hydrogen molecules released (sometimes, from solution in the metal).

Apart from real effects like those just mentioned, false indications of the pumping of active gases can be obtained when there is a trace of a relatively inert gas in the system. The usual method of measuring the pumping speed of getter ion pumps (or the condensation coefficient of gases upon getter films) is to compare the speed of the pump with the calculated, or measured, conductance of an aperture, or pipe, by means of pressure readings, as introduced by Wagener[8]. But Wagener[9] has shown that the observed speed of pumping, S_{obs}, deduced from measurements of the pressure ratio across a constriction of known conductance K, placed between a source of gas and a getter, will be less than the true speed, S_T, according to the relation $S_{obs} = S_T/(1 + S_T f/K)$ . . . (1), when there is a fraction f of inert impurity in the gas supply. Numerically small values of f have a large influence upon the value of S_{obs}/S_T, since measuring apparatus is usually designed so that K/S_T is small also, for the sake of accuracy.

A common case of practical importance when assessing the performance of a getter ion pump can arise from the 1 per cent of argon in air entering through leaks. But if something like this is spoiling direct measurements of getter ion pump performance, it can be demonstrated by doing experiments with a range of area of getter film, and allowances made in the way now described. From the Kinetic theory of gases $S_T = c\ (kT/2\pi m)^{\frac{1}{2}}A$, where c (the condensation coefficient) is the fraction of incident molecules of mass m, and average thermal energy $(3/2)kT$ at absolute temperature T (k is Boltzmann's constant), that are bound on unit area of a getter film having a total surface area A. By substituting in (1) it is seen that a plot of $1/S_{obs}$ against $1/A$ values will be linear and of slope $\tan^{-1}\ 1/c(kT/2\pi m)^{\frac{1}{2}}$, from which c may be computed, if the pressure measurements in the experiments are well founded. The intercept of such a plot, at $1/A = 0$, is f/K, whence f also may be computed.

3. Details of some surface reactions that can occur in getter ion pumps

It is the detailed mechanisms of surface reactions between metals and gases that control the performance of getter ion pumps, and so comment on these details is appropriate here. Some general patterns of behaviour are becoming discernible from recent work : but specific exceptions do occur and can be practically disturbing. A well-known exception is the evolution of hydrogen from titanium when the pressure or temperature equilibrium is disturbed. Weinman and Cameron[10] have exploited this when pumping a hydrogen ion source with a titanium getter ion pump. However, as general examples it is convenient to take the reaction of oxygen with evaporated films of titanium and barium, since both metals are commonly used in getter ion pumps (see Davis and Divatia[11] and Cloud, Beckman and Trump[12].)

Some measurements of the adsorption of oxygen by titanium and barium films kept near room temperature, as in service in getter ion pumps, have shown differences between these metals that are significant for their use in practical pumps. In the case of titanium and oxygen the first monolayer or so is taken up relatively quickly : then the speed of pumping (proportional to condensation coefficient) falls off rapidly. In all about 4 monolayers of oxygen are taken up, assuming for simplicity a close packing of gas molecules upon the apparent surface area of a patch of titanium film evaporated slowly *in vacuo* (pressure less than 10^{-7} torr). But with barium and oxygen about 30 monolayers are taken up, at a constant condensation coefficient, to form a protective layer of oxide[13].

With titanium and oxygen the behaviour is reminiscent of that of oxygen on tungsten, investigated by Becker[14], using field emission microscopy. Becker found that there is a high heat of adsorption (energy of binding about 4 eV), typical of chemisorption, whilst the first monolayer is forming (with first valence bonds). But the energy of binding decreases rapidly as more oxygen is held on the surface and for which only second (2 eV) or 3rd valence bonds with the metal are possible. The kinetics of the building up of the oxygen concentration at the surface are probably like those that have been further investigated by Gomer[15] for various gases upon tungsten. In a particular range of low temperatures (approximately 30–70 °K for oxygen or tungsten) physical and chemisorption co-operate in adding oxygen. At such temperatures the chemisorbed oxygen is held fixed to particular lattice sites. But any oxygen physically adsorbed on to that already chemisorbed is mobile, and moves to the edge of the raft of chemisorbed oxygen, there to be itself chemisorbed. If the temperature is too low the physically adsorbed gas is immobile : if too high the gas evaporates before it can move to the edge where growth of the chemisorbed layer takes place. At much higher temperatures (approximately 500 °C) growth of a chemisorbed layer occurs

by a process of migration (radially rather than at a straight edge) from one trap (chemisorption site) to the next, needing an activation energy, of about 1 eV, which decreases slightly as the traps all fill. (A radial growth process like this provides a simple explanation of the variation of condensation coefficient of oxygen on barium, at room temperature, during the deposition of the first monolayer[13].) Support for the idea that studies of a well defined system like oxygen on tungsten are significant for titanium as well comes from the measurements of Wagener[16] who has found that elements near the centre of the periodic table (like tungsten and titanium) behave similarly as getters.

By contrast, with barium, the mechanism of oxidation can be understood following first Mott[17] for metals in electrolytic baths, and later Mott and Cabrera[18], for oxidation of thin films generally. Barium ions move through the growing oxide via interstitial lattice positions, until the thickness increases so much that the potential gradient across the oxide (oxygen is electronegative) is too weak for electron transfer by field emission (i.e. tunnel effect).

4. Some possible ways of improving the performance of getter ion pumps

In order to increase the capacity of titanium for taking up oxygen, and so make a nice balance between metal and gas arrival rates less important than in present continuous evaporation pumps, it would seem to be advantageous to cool the deposited metal to low temperatures. (Alternatively, titanium deposits could be heated to high temperatures, when chemisorption may proceed unaided by physical adsorption). By contrast, films of barium need be heated only a little above room temperature (40 °C or above), so that thermionic emission of electrons can occur across otherwise thin (approximately 100 Å) protective layers of oxide so allowing further growth. Moreover, since barium ions move interstitially it is beneficial to have numerous lattice defects. Therefore, it should help if some differently sized foreign atoms are evaporated with the barium. Certainly, for very thin deposits, the condensation coefficient can be increased by choosing a substrate with a high density of lattice defects.

Suggestions like these follow atomic details in the mechanisms of gas reactions with metals. In practical getter pumps, barium for example, is probably evaporated so rapidly that globules are deposited, not individual atoms, as established by Fransen and Perdijk[19] for routine firing of getters in electronic tubes. Such geometrical details have some influence upon the performance of getter ion pumps. But such influences are relatively unimportant compared with, say, the details of energetics and kinetics, that determine whether or not the evaporating metal forms stronger bonds with underlying metal already deposited than with gas adsorbed on the surface. With knowledge of these details it can be foretold whether or not it will be worthwhile overcoming technical difficulties to increase metal evaporation rates. Again, with so-called ion pumps of the Penning gauge type, it is detail that must be studied. In these, for example, is the metal of electrodes (usually titanium) useful because after being sputtered to the walls it can take up gas ; or does gas react with those metal electrodes that are kept clean by sputtering off oxide layers, and the like ? Some abrasion pump experiments have shown that merely exposing fresh titanium by scratching causes reductions in gas pressure above the metal[20].

References

1 R. N. Bloomer ; *Brit. J. Appl. Phys.* **8**, 40 (1957).
2 P. I. Lukirsky and S. W. Ptizyn ; *Z. f. Physik*, **71**, 339 (1931).
3 A. L. Reimann ; *Phil. Mag.* **16**, 673 (1933).
4 H. D. Hagstrum and J. T. Tate ; *Phys. Rev.* **59**, 509 (1941).
5 W. H. Rodebush and W. A. Nichols ; *J. Amer. Chem. Soc.* **52**, 3864 (1930).
6 J. K. Roberts ; *Some Problems in Adsorption*, Cambridge University Press (1939).
7 V. L. Stout and M. D. Gibbons ; *J. Appl. Phys.* **26**, 1488 (1955).
8 S. Wagener ; *Brit. J. Appl. Phys.* **1**, 225 (1950).
9 S. Wagener ; *J. Phys. Chem.* **60**, 567 (1956).
10 J. A. Weinman and J. R. Cameron ; *Rev. Sci. Inst.* **27**, 288 (1956).
11 R. H. Davis & A. S. Divatia ; *Rev. Sci. Inst.* **25**, 1193 (1954).
12 R. W. Cloud, L. Beckman, and J. G. Trump ; *Rev. Sci. Inst.* **28**, 889 (1957).
13 R. N. Bloomer ; *Brit. J. Appl. Phys.* **8**, 321 (1957).
14 J. A. Becker ; See, for example, *Advances in Catalysis*, **8** (New York Academic Press Inc. 1955).
15 R. Gomer ; *Second International Conference on Surface Activity*, **2**, 236 (London, Butterworths Scientific Publications 1957).
16 S. Wagener ; *J. Phys. Chem.* **61**, 267 (1957).
17 N. F. Mott ; *Trans. Faraday Soc.* **35**, 1175 (1939).
18 N. F. Mott and N. Cabrera ; *Rep. Prog. Phys.* **12**, 163 (1948).
19 J. J. B. Fransen and H. J. R. Perdijk ; *Philips Tech. Rev.* **19**, 290 (1958).
20 M. E. Haine, E. W. R. Francis, and R. N. Bloomer ; *Nature*, **182**, 931 (1958).

Vol. 10 1960

Carbon Contamination of Glassware used for Vacuum Purposes

H. BATEY

G.P.O. Research Station, Dollis Hill, London, N.W.2

(Received 12 January 1960)

The report deals with the detection, elimination, and some properties of a film of carbonaceous matter which exists on glass pinches and envelopes as used in normal receiving valves. The film is resistant to conventional washing methods, and probably originates either from lubricating oil used on glass forming machines or from the cathode binder. It is indirectly identified by the deposition of a layer of carbon on the surface of the oxide cathode resulting from heating the glass envelope at a certain stage in the vacuum processing of the valve. Some effects on valve performance resulting from this form of contamination are implied, and some methods by means of which the film can be eliminated are described.

1. Introduction

In the course of experimental work at Dollis Hill on thermionic valves it has been observed that an oxide cathode can, under appropriate circumstances, receive a thin surface layer of carbon during its vacuum processing.

The report shows that within the conventional receiving valve there are at least two relatively massive sources of carbon. One source is the organic binder which is used in the technique of spraying the alkali earth carbonates on to the cathode core; the other is a strongly adherent film of carbonaceous matter on the surface of the common forms of glassware used in valve manufacture. The two sources are separated and examined independently but with special emphasis on the glassware aspects.

2. Experimental work

(a) *Method of Detection*

The method used for detection will be readily appreciated by a valve engineer. A cathode core is coated with barium strontium carbonates by the usual spraying technique using an organic binder. The coated core is fitted with an insulated heater, mounted on a valve "pinch", and sealed into the conventional valve envelope. The assembly is then mounted on a bench pump, evacuated, and the cathode carbonates converted thermally to the oxides. At this stage the activated oxide cathode is set at 650°C and the glass envelope raised in temperature to 400°C. As the glassware temperature rises it is observed that a grey film is forming on the oxide surface, and the intensity of the film may increase to a jet black. Fig. 1(a) illustrates a typical example of a blackened cathode. Fig. 1(c) shows a blackened cathode which has had part of the surface scraped to expose the white underlay of the oxide.

The activated oxide cathode is incidental to the investigation, and is only employed as a reaction indicator.

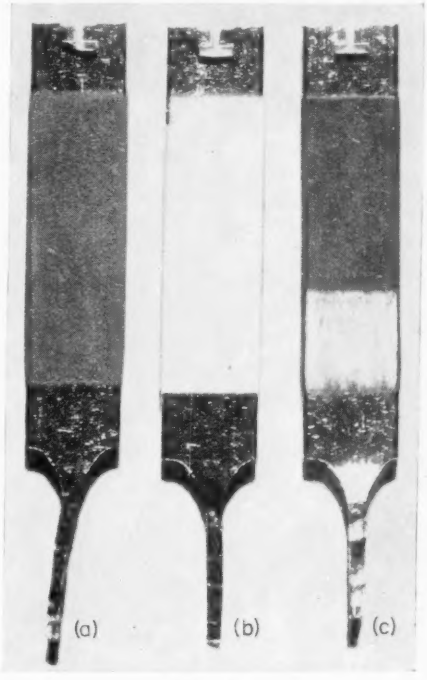

FIG. 1.

(b) *Separation of the Carbon Sources*

The first experimental step is to separate the carbon sources by elimination of the organic binder used in the carbonate spraying technique. A convenient method is to use a spray with a methacrylate binder, and then to bake out the volatile depolymerized methacrylate at 400°C before mounting the cathode on the pinch. If platinum cores are used the bake out of the binder can be effected in air without oxidation of the core metal.

If the experiment of 2(a) is now repeated, using a cathode

which has been cleared of binder, the result is still a carbon-blackened oxide surface. This carbon is therefore thought to originate from the surface of the heated glassware, passing across in some volatile form to the hot oxide cathode surface where it decomposes.

(c) *Elimination of the Glassware Film*

The next experimental step is to eliminate the suspected film of carbonaceous matter on the glassware. One method is to attempt to oxidize the film by the action of chromic acid. Valve pinches and envelopes are therefore completely immersed in chromic acid for some minutes, rinsed in distilled water and dried in a low temperature oven before mounting of the cathodes.

The experiment of 2(a) is now repeated using a cathode which has been cleared of binder, and glassware which has been treated with chromic acid. The result is still a carbon-blackened oxide surface, but the intensity of the carbon layer is appreciably less than that produced on the cathode in the previous experiment. Evidently the chromic acid has had some effect but it is inadequate to oxidize the film of carbonaceous matter on the glassware completely. An improved type of chromic acid is now used to " clean " the glassware. It is prepared by stirring concentrated sulphuric acid with an excess of chromium trioxide crystals. The resulting mixture has a mustard-yellow colour with a heavy sludge of the same tint—in marked contrast to the crimson colour of the conventional fluid.

The experiment is repeated using glassware which has been treated with the improved chromic acid mixture. The result is now a " white cathode " as shown by Fig. 1(b). Now that the glassware is free from carbonaceous matter and the cathode cleared of binder, both sources of carbon are eliminated and no reaction occurs at the surface of the oxide cathode when the glass is heated.

(d) *Organic Binder Reaction*

The final experimental step is to retain the organic binder in the cathode, and eliminate the carbonaceous film from the glass, leaving the cathode as the only source of carbon.

The experiment of 2(a) is again repeated, using a cathode containing an organic binder, and glassware which has been treated with the chromic acid mixture. The result is a carbon-blackened cathode. In this instance the carbon must originate from the cathode binder which is probably volatilized during the initial heating of the cathode to condense on to the cool glass envelope. The glass becomes contaminated with an organic film which decomposes on the surface of the hot activated oxide cathode when the envelope is subsequently heated.

3. Some properties of the film

(a) *Effect of Preliminary Glass Bake*

The intensity of the carbon film deposited on the surface of the oxide cathode has been observed to be influenced by the glass bake conditions. Assemblies using cathodes which contain a methacrylate binder, and glassware which is known to be contaminated with a film of carbonaceous matter, are evacuated and glass baked before the thermal breakdown of the cathode carbonates. Each assembly is individually baked at a different temperature for a different time. The cathode carbonates are then decomposed to the oxides, and the activated cathode is set at 650 °C. The glassware is then re-heated to 400 °C as in 2(a). Each experiment produces a cathode with a different degree of greyness. From the results graphs are produced (Fig. 2) showing how the

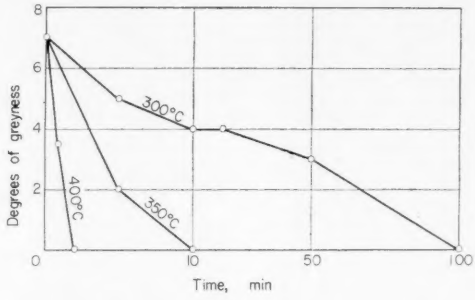

FIG. 2.

pre-decomposition glass bake influences the intensity of the carbon film deposited on the oxide cathode. From the graphs it is seen that two minutes bake at 400 °C is sufficient to clear the volatile carbon compounds completely, whilst at 300 °C one and a half hours appear necessary.

(b) *Cathode Temperature Dependence*

The intensity of the carbon film deposited on the surface of the oxide cathode is also known to be influenced by the temperature of the cathode at the time of heating the glass.

The experiment of 2(a) is repeated with a batch of assemblies whose cathodes are set at different temperatures. From the results a curve is produced of carbon film intensity for various values of cathode temperature (Fig. 3). The curve

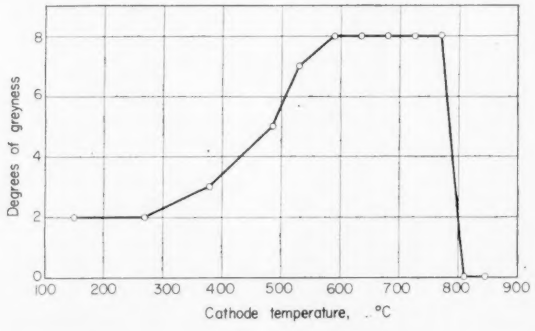

FIG. 3.

shows that the maximum intensity extends over the temperature range of 580 °C to 770 °C. Above 800 °C the reaction is not evident, and below 580 °C the intensity steadily declines.

(c) *Influence of the Carbon Film on the Cathode Temperature*

Temperature measurements of a cathode are made before and after the carbon film is deposited on the surface of the oxide cathode using a direct reading pyrometer and a 13 per cent Pt/Pt Rh. thermocouple welded to the cathode core. A drastic reduction of the cathode temperature is observed as shown by Fig. 4.

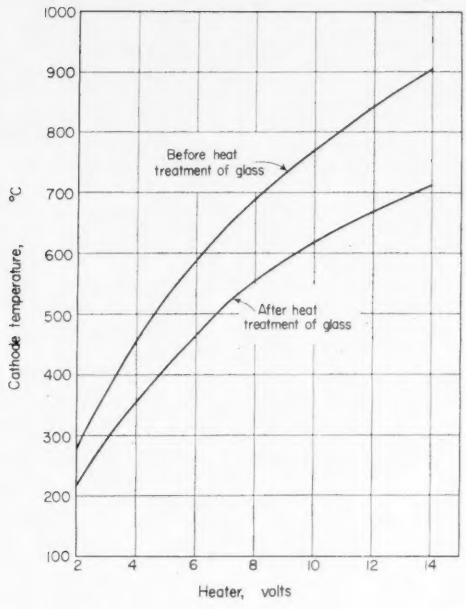

FIG. 4.

4. Possible implications in valve manufacture

(a) *Effects on Valve Performance*

Carbon deposits of the magnitude indicated above are clearly undesirable in most vacuum devices and especially in thermionic valves where the oxide cathode is necessarily used. A surface layer of carbon on the oxide cathode increases the thermal emissivity of the cathode which causes a reduction of thermionic emission. The carbon compounds which produce the cathode film may themselves lead to carbon contamination of the valve components, resulting in capacitances and electrical leakages. An increase in gas level in vacuum tubes may also occur due to the release of carbon compounds into the valve atmosphere.

(b) *Suggested Sources of the Glassware Contamination*

The carbonaceous matter exists on the glass pinches and envelopes as received from the manufacturer. Contamination, therefore, occurs most probably during the forming of the glassware. Glass forming machines are lubricated with oil, and in some cases the mould used for forming valve envelopes has a cork lining which is impregnated with an organic lubricant. On contact with the hot glass the lubricant is vaporised and eventually condenses on the cooling glass envelope to form a strongly adherent film of carbonaceous matter. Compressed air is also used for glassworking and traces of oil from the compressor may condense on the glass.

Conclusions

It is established that an unidentified carbonaceous film exists on the surface of the common forms of glassware used for vacuum purposes. This film may be removed by washing in a suitable chromic-sulphuric acid fluid or by baking in vacua for a few minutes at 400 °C. If the film is left on the inner surface of a thermionic valve envelope it may under appropriate conditions decompose on the surface of the oxide cathode with undesirable consequences.

Acknowledgement

Acknowledgement is made to the Engineer-in-Chief of the Post Office for permission to make use of the information contained in the paper.

Letters to the Editor

Note on Vacuum and Condensing Temperature Requirements for the Freeze-Drying of Tissue

CLAIMS have been made by various authors[1-3] that the time taken for the freeze-drying of tissue may be cut down from the usual three-four days required to times of the order of 12 h by making certain modifications to the traditional methods of freeze-drying. These modifications include (a) lowering the pressure within the system to about 10^{-5} torr instead of the usual 10^{-2}–10^{-3} torr and (b) condensing the water vapour given off on a surface cooled by liquid N_2.

It was decided to investigate these claims using an Edwards' TD2 tissue dryer. Experiments on the drying time were therefore carried out utilising an oil diffusion in addition to the usual mechanical pump and substituting liquid N_2 for the drikold–CO_2 mixture in the water condenser in certain cases.

For comparative purposes, it was necessary to have specimens for drying with similar exposed surface areas. Preliminary work was therefore done on the drying of 5 per cent gelatine solutions. A known volume of the liquid (0.2 ml) was injected into a small brass cup and allowed to solidify before placing in the tissue holder in the freeze-drying apparatus. By this means a constant surface area of exposure was obtained for different experiments.

The results obtained on drying times of gelatine samples at temperatures of −30°C to −40°C may be summarised as follows : (a) the drying time appeared to be independent of the pressure in the system between the limits of 10^{-2} torr (mechanical pump) and 10^{-5} torr (mechanical pump + oil diffusion pump), and (b) it was not affected by replacing the drikold-acetone mixture with liquid N_2. Similar results were indicated when rat liver was freeze-dried, although there was some difficulty here with regard to comparing surface areas of specimens. However, the drying time of about three days could not be cut down by modifying pressure or condensing temperature.

Discussion of results

The initial theoretical argument for lowering the pressure in the system[1] appears to be based on the assumption that the rate of evaporation of water molecules would be proportional to $(P_T - P_A)$ where P_T = the vapour pressure of water at the particular temperature of drying and P_A = the pressure in the system. This is, however, not true : the rate of evaporation will be proportional to $(P_T - P)$ where P = the partial pressure of water in the space above the evaporating surface. The important factor for rapid freeze-drying should therefore be the rate of removal of evaporated water molecules by condensation. With regard to the condensing temperature, the partial pressure of water at −78°C (drikold-acetone temperature) is so low that this temperature should be perfectly adequate for condensation.

Stephenson[4] has given a theoretical analysis of the process of freeze-drying which indicates that the most important rate-determining stage is the diffusion of water molecules from the interior of the tissue to the surface, and that an air pressure in the system of less than 10^{-2} torr should not normally be necessary. Similar conclusions have been reached by Jansen[5].

On the basis of this evidence there seems little hope then that substantial decreases in drying time will be obtained by modifying the design of equipment already in use with regard to vacuum or condensing temperature.

The author would like to express his gratitude to Edwards Hivac Co. Ltd., Crawley, Sussex, for granting him facilities and apparatus to carry out this work, and to Mr. T. Rowe for helpful suggestions and discussion.

[1] B. G. Malmstrom ; *Exptl. Cell Res.* **2**, 688 (1951).
[2] D. Glick and B. G. Malmstrom ; *ibid.* **3**, 125 (1952).
[3] G. Moberger, B. Lindstrom, and L. Andersson ; *ibid.* **6**, 228 (1954).
[4] J. L. Stephenson ; *Bull. Math. Biophysics* **15**, 411 (1953) ; **16**, 23 (1954).
[5] M. T. Jansen ; *Exptl. Cell Res.* **7**, 318 (1954).

S. COTSON*

*Courtauld Inst. of Biochemistry, Middlesex Hospital, London, W.*1.

* Present Address : *Dept. Chemistry, Borough Polytechnic, London, S.E.*1.

Calibration Factors of Ionization Gauges for Hydrocarbon Gas Mixtures

DURING recent work in this laboratory with getter-ion pumps it became necessary to measure the calibration factors of ionization gauges for certain gases containing hydrocarbon molecules viz. : (1) " Calor " gas which consists by volume of, propane 15–20 per cent, butane 78–84 per cent (in ratio 40 parts *iso*-butane 60 parts *normal* butane), Butene 1–2 per cent, and (2) coal gas, typical composition, H_2 47 per cent ; CH_4 36 per cent ; CO 8 per cent ; CO_2 2 per cent ; N_2 3 per cent and (C_2H_3, C_2H_4, C_6H_6) 4 per cent. Calibration factors for the more common gases O_2, N_2, H_2, A, etc. have been reported but values were not available for the foregoing mixed hydrocarbon gases.

Three types of ionization gauge heads were calibrated, these were, a conventional hot filament ion-gauge ; an Alpert type

	Ion Gauge Type	Alpert Type	Penning Type
Filament power	2.5 A at 10 V	2.5 A at 10 V	—
Collector	−22 V d.c. to filament	−22 V d.c. to filament	−2 kV
Grid	+100 V d.c. to filament	+100 V d.c. to filament	—
Grid Current	1 mA	1 mA	—
Magnetic Field	—	—	500 G

ion-gauge and a cold cathode gauge of the Penning type. The ion-gauges were operated under the following conditions.

Both of the ion-gauge heads had thorium treated tungsten filaments which operated at about 1200°C. The Penning gauge had a tubular cathode which was squashed to make two flat electrode surfaces with a ring anode mounted between the flattened faces. The electrodes were made of stainless steel and the assembly was mounted in a magnetic field of 500 G.

The ionization gauges were calibrated in the 10^{-4} torr range using a McLeod gauge. The vacuum system consisted of a 2 in. silicone oil diffusion pump on which was mounted a small chamber and a flange to which the gauge heads were connected. Air was taken as a standard and the calibration factors were measured by pumping the system down to its ultimate, about 10^{-5} torr, and observing the pressure readings for both gauges. The desired gas was then admitted and the pressure increased to different levels while readings on both gauges were observed. The ultimate for the McLeod was then subtracted from all the McLeod readings and the ultimate for the ionization gauge subtracted from all the ionization gauge readings. The pressure differences measured with the McLeod gauge were plotted against the pressure differences for the ionization gauge and the slope of the resultant curve taken.

The calibration factors with respect to air were as follows:—

Gas	Conventional ion-gauge	Alpert ion-gauge type	Cold cathode Penning Gauge
" Calor " gas	4.6	3.7	5.4
Coal gas	1.25	—	—

The calibration values for " Calor " gas agree quite well with those measured by H. Moesta and R. Renn[1] who used a conventional ion-gauge with propane, *normal* and *iso*-butane and reported factors of 4.606, 4.972, and 4.713 respectively.

Acknowledgements are made to Mr. L. Holland who suggested the foregoing work and to Edwards High Vacuum Ltd. for permission to publish this account.

[1] H. Moesta and R. Renn ; Bestimmung von Erichfaktoren für Ionisationsmanometer. *Vakuum Technik* **6**, 35 (April 1957).

L. Elsworth

Vacuum Deposition Research Laboratory,
Edwards High Vacuum Limited.

ol.
10
960

Book Reviews

PROCEEDINGS OF THE FOURTH NATIONAL CONFERENCE ON TUBE TECHNIQUES. New York University Press, New York, 1959. 270 pp. Price $7.50.

THIS paper-backed volume contains a wealth of specialized information on recent work in the field of electron tube manufacture and testing. The subject matter of the papers included is given in the following list. Where the actual title of the paper is quoted it is in inverted commas. For the sake of brevity, authors' names are omitted.

1. An up-to-date account of flash and bulk getters (35 refs.).
2. The development of cold field-emission cathodes and the ultra high vacuum techniques employed (chiefly, titanium gettering) (5 refs.).
3. Electroformed ceramic-to-metal seals for an external circuit travelling-wave tube (1 ref.).

4a and 4b. Abstracts of papers on ceramic-metal sealing.

5. A quasi-optical seal for the open funnel end of a large (up to 36 in.) television cathode ray tube.
6. Improving glass-to-metal seal resistance to high humidity deterioration.
7. " A UHF metal-ceramic planar tetrode ".
8. " Temperature limitation of planar grids ".
9. The reduction of grid emission.
10. Coolants for high power tubes.
11. Brazing tungsten to molybdenum.
12. " Brazing by diffusion-controlled formation of a liquid intermediate phase " ; the object being to perform the braze at as low a temperature as possible.
13. A shaker for component evaluation of electron tubes.
14. An adjustable chuck for a glass-blowing lathe.
15. An optical system for the production of phosphor screens for colour television cathode ray tubes.
16. A review of European microwave tube techniques, including aspects of vacuum technology (118 refs.).
17. The production of fine complicated patterns by vacuum deposition methods in the development of the vidicon—a colour television pick-up tube.
18. Electron guns for travelling wave tubes.
19. Use of infra-red photography to measure cathode temperature.
20. Practical studies of sublimation from electron tube cathodes (2 refs.).
21. " The R.F. modulated field emission cathode as a harmonic generator ".
22. The use of the field-emission cathode in a two-cavity microwave amplifier.
23. " A noise display machine for studying cathode properties ".
24. Properties of the primary electron emitter consisting of a layer of porous magnesium oxide on a nickel base at room temperature.
25. " Secondary emission from MgO films and crystals " (7 refs.).
26. Production of the new materials, copper-base Aliron and copper-cored Aliron, for tube anodes.
27. " Surface resistivity of metals and dielectric-metal joints ", especially in relation to the problem of providing a vacuum tight aperture for microwave power generators through which energy is conveyed from inside the tube to the external transmission system.
28. Critical review of properties of pure rhenium, tungsten-rhenium and molybdenum-rhenium alloys and their uses in electron tubes (12 refs.).
29. Effect of nuclear radiation (neutrons, gamma-rays etc.) on glass (6 refs.).
30. " Means of reducing sublimation from base metals ".
31. " The effect of exhaust procedures upon the thermionic-emission qualities of nickel cathode alloys ".
32. Account of dispenser cathodes, defined as cathodes that gain " electron emissive power by virtue of material dispensed on " their surfaces (31 refs.).
33. " Thorium impregnated matrix cathode ".
34. Abstract of paper on refractory matrix cathode.
35. " The effect of calcium in thoriated-tungsten filaments on emission " ; a higher calcium content improves the drawing properties of the wire but causes slumped emission during life.
36. Relation between performance of a thermionic emitter and ambient gases surrounding it.
37. " Dynamic equilibrium processes in oxide-coated cathodes " ; a study of the factors which contribute to the production and destruction of donors (6 refs.).
38. Measurement of cathode interface impedance by pulse and sine-wave techniques.
39. Determination of the resistance and capacitance of an oxide coating on a thermionic cathode by ultra-high frequency measurements (3 refs.).
40. " Interface resistance—it can be controlled " !
41. Abstract of paper on the measurement of cathode interface impedance.
42. " Field emission in image tube ".
43. " Determination of vacuum-tube catastrophic and wear-out failure properties from life-testing data ".
44. An all-quartz microbalance for use in vacuum to study mass changes in electron tube electrodes which occur, e.g. due to cathode sublimation, gas sorption (2 refs.).
45. Measurement of motion of grid wires in UHF planar triodes.
46. Grid emission in power tubes (abstract).

The text is well printed, most of the line drawings are excellent, the photographic illustrations are generally good considering that they are within the text and not on selected paper. The high technical level of the papers cannot be doubted. Some of them exhibit the staccato style popular in America ; unfortunately, it does not lead to smooth reading ; one or two papers exhort the reader to follow the practice recommended to such an extent that they read almost like electioneering propaganda ! However, this no doubt indicates the outstanding vigour of the American electron tube industry.

J. YARWOOD

Vacuum Notes

International Organization for Vacuum Science and Technology

READERS will be familiar with the activities of the International Organization for Vacuum Science and Technology either directly as members or from the article contributed in a previous issue of *Vacuum* by Professor E. Thomas, the President.

The Bulletin of the Organization is now a well established and valuable service but a strain on its, as yet, slender revenue. Having in mind the important role which IOVST has to play in the advancement of Vacuum Science and Technology, with which this journal is also concerned, the Publishers believe that they could serve these interests and also its readers by offering to devote a section of *Vacuum* to the publication of the IOVST Bulletin and to donate to the Secretariat of the Organization at Brussels, preprints for distribution to the membership in the usual way.

This offer has been gratefully accepted by the President on behalf of the Organization and the next issue of the Bulletin will appear in the forthcoming issue of *Vacuum*.

It is important to remember that all communications concerning the Bulletin should be addressed directly to the Secretariat in Brussels and not to the Publishers of *Vacuum*.

ol.
10
960

LIFE HONORARY MEMBERS

THE Executive and Advisory Committees of the International Organization for Vacuum Science and Technology (IOVST), created at the First International Congress on Vacuum Techniques held in Namur in June 1958, are happy to announce that at their Joint Meeting held in Brussels on 1 February, 1960, it was unanimously decided to nominate and appoint as Life Honorary Members Prof. Dr. Louis DUNOYER (France) and Prof. Dr. Marcello PIRANI (Germany), both eminent pioneers of vacuum techniques.

This acknowledgement of the admiration and great esteem of IOVST for these two prominent and well-known scientists will, it is felt sure, be appreciated by all vacuum specialists and also by those who realize the increasing importance of vacuum science and techniques.

Classified Abstracts

Classification System

I. General Vacuum Science and Engineering

(Books, review articles, bibliographies, summaries, general techniques, articles on basic vacuum physics)

10. Vacuum Technology

11. Production of Low Pressures

12. Measurement of Low Pressures

13. Vacuum Applications

14. Kinetic Theory of Gases (transport phenomena, diffusion through vapors, molecular flow of gases, etc.)

15. Fluid Dynamics (turbulent and viscous flow of gases, flow through nozzles, boundary layer flow, etc.)

16. Gases and Solids (sorption, diffusion through solids, permeation, etc.)

17. Thermodynamics (compression, temperature, reactions, vaporization, dissociation, vapor pressure, cryogenics, etc.)

18. Gaseous Electronics (ionization, discharges, plasma, emission, etc.)

19. Radiation (light, heat, X-rays, microwave radiation, etc.)

II. Vacuum Apparatus and Auxiliaries

(Design, testing, operation, performance and techniques of using individual apparatus for the production, measurement, and control of low pressures)

20. Pumping Systems (plant)

21. Pumps and Pump Fluids (mechanical pumps, vapor pumps, getter-ion pumps, cryopumps, etc.)

22. Gauges (including mass spectrometer types)

23. Plumbing (joints, pipe, gaskets, fittings, flanges, glass-to-metal seals, shaft seals, etc.)

24. Valves (stopcocks, variable leaks, gas introducing devices, needle valves, etc.)

25. Baffles, Traps, and Refrigeration Equipment

26. Automatic Protective and Control Equipment (cut-offs, switches, liquid level controls, manostats, etc.)

27. Leak Detectors and Leak Detection

28. Heating Equipment (ovens, resistance heating units, induction heating units, etc.)

29. Miscellaneous

III. Vacuum Applications

30. Evaporation and Sputtering (to form solid coatings)

31. Evacuation and Sealing (electronic tubes, switches, lamps, vacuum insulation, gas-filled devices)

32. Nucleonics (particle accelerators, counters, plasma machines, isotope separation, etc.)

33. General Physics and Electronics (electron tube physics, electron microscopy, diffraction camera, field emission microscope, spectroscopes, X-ray tubes, low temperature physics, etc.)

34. High Altitude and Space Technology (test chambers, ion propulsion, etc.)

35. Impregnation and Potting

36. Drying, Degassing and Concentration (including freeze-drying, glass processing, evaporation of solvents, etc.)

37. Metallurgy, Inorganic Chemistry, Analytical Chemistry (production and analysis of metals and inorganic chemicals, melting, casting, annealing, sintering, degassing in molten state, vacuum fusion gas analysis, mass spectrometer analysis of inorganic materials, etc).

38. Distillation, Organic Chemistry, Isotopic Gas Analysis

39. Miscellaneous Applications (fumigation, etching, forming, surface area measurement, etc.)

IV. Materials and Techniques Used in Vacuum Technology

(Properties, composition, purification and use of materials ; fabrication and processing techniques)

Vol. 10 196

40. Gases and Vapors

41. Metals and Alloys (including mercury)

42. Glass and Ceramics

43. Plastics and Elastomers

44. Waxes, Lubricants, Cements, Lacquers, Paints, Oils

45. Soldering, Welding, Brazing

46. Glass Blowing, Glass-to-metal and Ceramic-to-metal Sealing Techniques

47. Outgassing Data, Vapor Pressure Data, Gettering Data

48. Heating, Refrigeration, Ultrasonics, Centrifuging

49. Miscellaneous Materials and Techniques

V. Basic Science and Engineering
(For cross reference purposes)

50. Mathematics

51. Physics, Astronomy, Geophysics

52. Physical Chemistry

53. Metallurgy, Ceramics, Inorganic Chemistry

54. Biology, Biochemistry, Pharmaceutics, Toxicology, Organic Chemistry

55. Chemical Engineering

56. Electrical Engineering, Electronic Circuits

57. Mechanical Engineering

58. Nucleonics

59. Miscellaneous

ol.
10
960

Abstracts

General Vacuum Science and Engineering

11. Production of Low Pressures

11 : 21

1. Molecular Pumping.
United States. A vacuum pump is described by which the molecular pumping principle may be extended to very low pressures. The system is entirely self contained and is free of lubricated bearings. In addition, the system may be made of glass or metal and lends itself to bake-out. A suspended steel rotor is suspended within a vacuum tight glass chamber by an axial magnetic field provided by a solenoid above the chamber. A sensing coil fixes the field and the suspension of the rotor. The rotor is spun by a rotating magnetic field produced by drive coils located at the periphery of the rotor and outside of the chamber. The pumping action is between the rotor and a grooved plate below it. Clearances are 0.05 cm or less. The grooved plate is sealed by an aluminium washer and a glass cylinder. The latter provides take-up for differential expansion. Peripheral rotor speed may be twice average molecular velocity. With the high pressure side at 10^{-9} Torr the pump will produce a differential of 10^{4} with a resulting low pressure value of 10^{-13}. Further reduction in pressure may be accomplished by series or parallel arrangement of two or more such pumps. Pumping speed may be made quite high. In addition to glass the chamber may be made of non magnetic metals. L. E. P.

J. W. Beams, *Science*, **130**, No. 3386, 1406–1407, Nov. 1959.

14. Kinetic Theory of Gases

14

2. Gas-Kinetic Collision Diameters of the Halomethanes.
United States. The Knudsen-gage radiometer technique has been used to measure gas-kinetic collision diameters for 17 halomethanes with a probable error of ± 1 per cent. at 340, 415, 512 and 610°K. These results together with literature data for five additional halomethanes have been fitted with Lennard-Jones (12–6) potential constants using Hirschfelder's method. Calculated viscosities are listed for the 22 halomethanes at the four temperatures. The derived L–J force constants are found to be well correlated with the molecular polarizabilities. Necessary parameters are tabulated from which values of the collision diameters for the remaining 47 halomethanes may be predicted with an estimated uncertainty of less than $\pm 2\%$. (Author)

George A. Miller and Richard B. Bernstein, *J. Phys. Chem.* **63**, 710–713, May 1959.

14 : 51

3. Calcium Atomic Beam Source and Interference Beyond Two Meter Retardation.
K. W. Meissner and Victor Kaufman, *J. Opt. Soc. Amer.* **29**, No. 10, 943–944, Oct. 1959.

15. Fluid Dynamics

15

4. Transitional Correction to the Drag of a Sphere in Free Molecule Flow.
United States. The mechanics of collisions between molecules in front of a sphere moving at hypervelocity through a rarefied atmosphere are analyzed. The study is concerned with the "transitional" regime in which molecules emitted by the surface begin to shield the body from the oncoming Newtonian stream and the net drag decreases from its free-molecular value. It is found that a simplified but physically significant model can be formulated, and that it leads to a dependence of the drag coefficient on two transition parameters. These can be interpreted as the Reynolds number and the surface-to-free stream temperature ratio. The predictions of this theory agree qualitatively and in order of magnitude with observations.

R. M. L. Baker, Jr., and A. F. Charwat, *Physics of Fluids*, **1**, 73–82, March-April 1958.

15

5. Laminar Steady-State Magnetohydrodynamic Flow in an Annular Channel.
Samuel Globe, *Physics of Fluids* **2**, 404–408, July-August 1959.

15

6. Magnetohydrodynamic Flow in a Shock Tube.
M. Mitchner, *Physics of Fluids*, **2**, 62–72, Jan.-Feb. 1959.

15

7. Some Exact Solutions of the Navier-Stokes and the Hydromagnetic Equations.
William C. Meecham, *Physics of Fluids*, **2**, 121–125, March-April 1959.

15

8. Laminar Flow in the Entrance Region of a Porous Pipe.
Harold L. Weissberg, *Physics of Fluids*, **2**, 510–517, Sept.-Oct. 1959.

15

9. Integration Theory for One-Dimensional Viscous Flow.
Gerald Rosen, *Physics of Fluids*, **2**, 517–521, Sept.-Oct. 1959.

15 : 17 : 30

10. Evaporation into a Boundary Layer. II. Dissociation in Evaporation.
Letter by Ernest Bauer and Martin Zlotnick, *Physics of Fluids*, **2**, 236, March-April 1959.

15

11. Vacuum Type Gas Flow Calibrator.
A vacuum-type gas-flow calibrator was designed and constructed for making accurate calibrations of flowmeters needed for the investigation of high-pressure flames. This calibrator operates by automatically measuring the time required to pressurize a known volume from a near vacuum to 1 atmosphere pressure. The gas volume flow rate is obtained by dividing the calibration volume by the pressurization time and applying corrections from PVT data. This apparatus has been successfully used to calibrate flowmeters for use with hydrogen, oxygen, nitrogen, air, methane, nitric oxide, carbon monoxide, and various homogeneous nonexplosive gas mixtures.

William A. Strauss and Rudolf Edse, *Rev. Sci. Instrum.*, **30**, 258.

Vol. 10 1960

16. Gases and Solids

16 : 30 : 33

12. Secondary Positive Ion Emission from Metal Surfaces.
Secondary positive ions ejected from surfaces of Mo, Ta, and Pt under bombardment by inert gas ions of low energy (<1000 ev) have been studied in high vacuum ($\lesssim 10^{-8}$ torr of background gases) using a 60° sector field mass spectrometer with a 6-in. radius of curvature, the object being to explore this as a technique for investigating solid surfaces in general. Ion species characteristic of the base metal, of surface compounds, and of a few bulk impurities were found. Quantitative analyses based on abundance ratios of the ions are unreliable, however owing to the enormous and essentially unknown differences in ionization efficiencies for the various species. Application of the technique to the investigation of surface kinetics seems highly promising, and as an illustration certain observations on the formation of PtO_3 on a Pt surface and its desorption at high temperatures are presented. Another possible application is to the study of sputtering, although some of the properties of secondary ions are shown to be quite different from those of sputtered particles in general. The secondary ions characteristic of the base metal comprise only a small fraction (0.01 per cent for Pt) of the total sputtering yield, are principally singly charged and monatomic, have a low average energy (4–5 ev) and energy spread, and may result either from physical sputtering of the base metal or from the dissociation of surface compounds or both.

Richard C. Bradley, *J. Appl. Phys.*, **30**, 1–8, Jan. 1959.

16

13. Alkane Adsorption on Silica, Alumina and Silica-Alumina Catalysts.
D. S. MacIver, P. H. Emmett and H. S. Frank, *J. Phys. Chem.*, **62**, 935–942, Aug. 1958.

16

14. Effects of Interparticle Condensation on Heats of Adsorption and Isotherms of Powder Samples.
C. Pierce, *J. Phys. Chem.*, **63**, 1076–1079, July 1959.

16

15. Model Calculation of the Temperature Dependence of Small Molecule Diffusion in High Polymers.
W. W. Brandt, *J. Phys. Chem.*, **63**, 1080–1084, July 1959.

16 : 41

16. Surface Properties of Germanium.
Y. L. Sandler and M. Gazith, *J. Phys. Chem.*, **63**, 1095–1102, July 1959.

16

17. The Slow Step in Chemisorption. The Possible Role of the Solid Adsorbent. II.
G. Parravano, H. G. Friedrick and M. Boudart, *J. Phys. Chem.*, **63**, 1144–1146, July 1959.

16

18. Adsorption of Inert Gases by Modified Carbons.
W. F. Wolff and P. Hill, *J. Phys. Chem.*, **63**, 1161–1164, July 1959.

16

19. Effects of Interparticle Condensation on Heats of Adsorption and Isotherms of Powder Samples.
C. Pierce, *J. Phys. Chem.*, **63**, 1076–1079, July 1959.

16

20. Model Calculation of the Temperature Dependence of Small Molecule Diffusion in High Polymers.
W. W. Brandt, *J. Phys. Chem.*, **63**, 1080–1084, July 1959.

16

21. The Slow Step in Chemisorption. The Possible Role of the Solid Adsorbent. II.
G. Parravano, H. G. Friedrick and M. Boudart, *J. Phys. Chem.* **63**, 1144–1146, July 1959.

16

22. Adsorption of Inert Gases by Modified Carbons.
W. F. Wolff and P. Hill, *J. Phys. Chem.*, **63**, 1161–1164, July 1959.

16

23. The Sorption of Hydrocarbon Vapors by Silica Gel.
D. W. McKee, *J. Phys. Chem.*, **63**, 1256–1259, Aug. 1959.

16

24. The Determination of Surface Areas from Krypton Adsorption Isotherms.
Note by P. J. Malden and J. D. F. Marsh, *J. Phys. Chem.*, **63**, 1309–1310, Aug. 1959.

16

25. The Rates of Adsorption of Water and Carbon Monoxide by Zinc Oxide.
Note by M. J. D. Low and H. A. Taylor, *J. Phys. Chem.*, **63**, 1317–1318, Aug. 1959.

16

26. Heat of Adsorption of Parahydrogen and Orthodeuterium on Graphon.
E. L. Pace and A. R. Siebert, *J. Phys. Chem.*, **63**, 1398–1400, Sept. 1959.

16

27. Effect of Poisoning on the Infrared Spectrum of Carbon Monoxide Adsorbed on Nickel.
C. W. Garland, *J. Phys. Chem.*, **63**, 1423–1425, Sept. 1959.

16

28. Infrared Spectra of Hydrocarbons Adsorbed on Silica Supported Metal Oxides.
L. H. Little, *J. Phys. Chem.*, **63**, 1616–1622, Oct. 1959.

16

29. Sorption and Magnetic Susceptibility Studies on Nitric Oxide-Silica Gel Systems at a Number of Temperatures.
A. Solbakkën and L. H. Reyerson, *J. Phys. Chem.*, **63**, 1622–1625, Oct. 1959.

16

30. Adsorption Studies on Metals. VIII. Monofunctional Organic Molecules on Reduced Oxide-Coated Nickel and Copper.
Y.-F. Yu, J. J. Chessick and A. C. Zettlemoyer, *J. Phys. Chem.*, **63**, 1626–1630, Oct. 1959.

16

31. Thermal Aging of Silica Gels.
Note by A. C. Makrides, *J. Phys. Chem.*, **63**, 1789–1791, Oct. 1959.

16 : 30

32. The Adsorption of Some Gases on Evaporated Metal Films and on Oxidized Films of Nickel.
United States. Low pressure adsorption isotherms at 76.8 and 90.2°K are reported for krypton, methane and ethane on copper and oriented nickel evaporated films, and on an oriented oxidized film of nickel. The krypton and methane isotherms on nickel oxide and the krypton isotherms on nickel follow the Langmuir equation. The methane isotherm at 76.8°K on nickel is s-shaped, the low pressure region following the Langmuir equation. The ethane isotherms on copper, nickel and nickel oxide are all s-shaped. The ethane isotherm on nickel oxide shows a first-order phase change. The nature of the adsorbed phase, the variation of the calculated heat of adsorption is discussed from the point of view of the van der Waals two-dimensional equation, the entropy of adsorption and the effect of the polarizing field of the adsorbent on the van der Waals attraction. Proof is given for the orientation of ethane in the adsorbed phase, and a method for the preparation of oriented films of nickel oxide is described. (Author)

J. L. Shereshefsky and B. R. Mazumder, *J. Phys. Chem.*, **63**, 1630–1638, Oct. 1959.

16

33. Acid-Base Interaction in the Adsorption of Olefins on Aluminum Kaolinite.

United States. The interaction of n-butane, trans-butane-2, 1-chloroethylene and trans-1, 2-dichloroethylene with Na-, Ca- and Al-saturated kaolinite was investigated using adsorption and desorption techniques. Al-kaolinite was observed to chemisorb both butene-2 and 1-chloroethylene. The data support the contention that adsorbed aluminum is the site of surface acidity. Varying the degassing temperature of Al-kaolinite from 25 to 315° indicated an intimate relation between surface acidity and the moisture associated with the clay surface. Calculations suggest that the interaction with trans-butene-2 involves an acid-catalyzed polymerization. (Author)

J. J. Jurinak and D. H. Volman, *J. Phys. Chem.*, **63**, 1373–1376, Sept. 1959.

16

34. A Precision Adsorption Apparatus for the Study of the Interactions Between Gas Atoms and Surfaces.

United States. A precision apparatus for the study of the interactions between gas atoms and surfaces of low specific area is described. A low temperature adiabatic calorimeter is used as the sample cryostat and the precise techniques of gas thermometry are used for pressure measurement. The gas is metered into the system with an accurate gas transfer apparatus. Data for the measurement of known volumes, and of the apparent volume of a vessel containing a low specific area, highly graphitized carbon black, are given. These measurements, made with different rare gases at various temperatures, indicate a precision of between 1 and 2 parts per 10,000. The apparent volume data are converted to the usual quantity of adsorbed volume to give room temperature adsorption isotherms at coverages of less than 2 per cent of the monolayer. (Author)

G. Constabaris, J. H. Singleton and G. D. Halsey, Jr., *J. Phys. Chem.*, **63**, 1350–1355, Sept. 1959.

16 : 52

35. The Time Lag in Diffusion. IV.

United States. Certain aspects of " non-Fickian " diffusion are discussed and a classification of " non-Fickian " (as well as Fickian) diffusion is obtained according as the diffusion current is (or is not) derivable from a gradient of a scalar function, the potential of diffusion. In the former instance an expression for generalized time lag for permeation rate experiments with n-dimensional spherical symmetry is obtained. Finally we comment shortly on memory effects and frame of reference corrections. (Author)

H. L. Frisch, *J. Phys. Chem.*, **63**, 1249–1252, Aug. 1959.

16

36. The Sorptive Properties of a Zeolite Containing a Preadsorbed Phase.

United States. It is shown that when a degassed zeolitic substrate is saturated with respect to a given sorbate, not even the largest channels or pores are necessarily physically filled. By examining the adsorption of a second sorbate on a zeolite already saturated with respect to another vapor, information may be gained as to the positions of molecules in the preadsorbed layer with respect to the substrate structure. Even a non-dipolar species such as CCl_2F_2 appears to form clusters around the charge-compensating cations, comparable with the " hydration sheaths " of coordinated water suggested by others to explain the diffusion of water in zeolitic channels. (Author)

P. Cannon and C. P. Rutkowski, *J. Phys. Chem.*, **63**, 1292–1296, Aug. 1959.

16

37. Adsorption and Diffusion of Argon on Tungsten.

United States. A field emission method for studying the adsorption and diffusion of A on W is described. It is found that the first adsorbed layer decreases the work function of W by 0.8 V. Multilayer adsorption is observed by the decrease in emission caused by layers beyond the first. Estimates for the heat of adsorption and the activation energy of diffusion in the first layer are obtained. The behavior of the multilayer adsorbate is discussed in terms of its physical and electrical properties. (Author)

Robert Gomer, *J. Phys. Chem.*, **63**, 468–472, April 1959.

16 : 30

38. The Interaction of Krypton with Metals. An Appraisal of Several Interaction Theories.

United States. Adsorption data for the interaction of krypton with evaporated films of iron, copper, sodium and tungsten at 75°K have been obtained. Krypton isotherms on sodium films treated with oxygen and water vapor are reported. Interaction energies are determined and compared with those predicted by several dispersion force theories. It is found that the-Kirkwood-Muller equation is the most suitable of the theories considered and that it yields semi-quantitative agreement with experiment for both metallic and non-metallic adsorbents. It is possible to predict the general form of isotherms of the rare gases on homogeneous surfaces by using Kirkwood-Muller energies in an isotherm equation developed by Singleton and Halsey. (Author)

R. A. Pierotti and G. D. Halsey, Jr., *J. Phys. Chem.*, **63**, 680–686, May 1959.

16

39. The Influence of a Chemisorbed Layer of Carbon Monoxide on Subsequent Physical Adsorption.

United States. Experiments reported in this paper show that, on cobalt catalysts, a part of the carbon monoxide chemisorbed at liquid nitrogen temperature is removed by evacuation at −78°. Thus two types of chemisorption of CO are visualized, one resisting desorption at −78° and the other desorbing at −78°. The former type suppresses the subsequent low temperature physisorption of nitrogen and carbon monoxide whilst the latter does not. The suppression is attributed to the positive charge gained by the metal surface as a result of CO chemisorption. These observations also show that low temperature CO chemisorption methods cannot be used, in all cases, to determine the extent of metal surface. (Author)

M. V. C. Sastri, T. S. Viswanathan and T. S. Nagarjunan, *J. Phys. Chem.*, **63**, 518–521, April 1959.

16

40. The Exchange of Deuterium Gas with the Hydrogen Associated with Solid Catalysts. I. The Model Tantalum-Hydrogen System.

United States. A study of the kinetics of the exchange reaction between pure deuterium gas and tantalum initially containing interstitial hydrogen has been made with a view to establishing the feasibility of the method for studies of the nature of the hydrogen content of solids, both with regard to the amount of hydrogen initially held by the solid, and also as to the energetics of the exchange reaction. The tantalum-hydrogen system was selected as a " model system " because the interstitial hydrogen occupies sites of equivalent energy approximating a model required for a simple, theoretical treatment ; also, the exchange takes place at relatively high temperatures, minimizing the isotope effect. The kinetic experiments were made using both constant temperature and continuously rising temperature techniques. The results were found to be in good agreement, indicating that the rising temperature technique can be used advantageously to obtain the parameters of interest, the principal advantages being a large saving of time. From the isothermal data, it was possible to determine the true activation energy for the underlying rate process. The same data showed that the apparent activation energy and the true activation energy differed approximately by the heat of solution of hydrogen in

Vol. 10 1960

tantalum. It is of interest to note that the true activation energy for the underlying rate process probably sets an upper limit on the activation energy for diffusion of hydrogen through the tantalum lattice. The results obtained in this investigation should serve to establish a criterion by which results obtained from systems of catalytic interest can be compared. (Author)

Francis J. Cheselske, W. E. Wallace and W. Keith Hall, *J. Phys. Chem.*, **63**, 505–512, April, 1959.

16

41. The Chemisorption of Oxygen on Silver.
United States. The silver-oxygen system has been studied by measuring the change in surface potential of a silver surface produced by oxygen chemisorption, and by measuring the paramagnetism of a silver surface after oxygen chemisorption. The change in surface potential was obtained by measuring the current flow into or out of a condenser consisting of gold and silver plates at ~220° when oxygen is admitted to the system. The change in surface potential is negative ~0.2 V. The surface paramagnetism was measured by ortho-para hydrogen conversion, and the surface after oxygen chemisorption is slightly paramagnetic, corresponding to one unpaired electron per 150 Å². (Author)

J. T. Kummer, *J. Phys. Chem.*, **63**, 460–463, April 1959.

16

42. Relations Between Different Definitions of Physical Adsorption.
United States. The conventional two dimensional definition, a mechanical (or " bound " molecule) definition, and the correct Gibbs (surface excess) definition of physical adsorption are compared in the Henry's law region in terms of " effective " solid-gas molecule potentials. The differences are considerable. Also, the Gibbs definition is put in the form of an exact " two dimensional " virial expansion (surface pressure expanded in powers of excess surface density) and compared with the approximate virial expansion according to the two dimensional definition. The exact " two dimensional " treatment does not lead to a law of corresponding states or a pair-wise additive intermolecular potential as usually assumed. (Author)

T. L. Hill, *J. Phys. Chem.*, **63**, 456–460, April 1959.

16

43. An Infrared Study of the Water-Silica Gel System.
United States. An infrared study of bound and adsorbed water in silica gel has been made. It was found that hydrogen in silica gel could be completely replaced by deuterium upon treatment with D_2O at room temperature. Deuteration of silica gel allowed unambiguous differentiation between absorption bands arising from silica itself and those arising from atomic groupings that contain hydrogen. It was found that " bound water " in silica gel consists entirely of SiOH groups located on the surface. The infrared spectrum of physically adsorbed water closely resembles that of liquid water. Dehydration of silica gel at high temperatures removes surface SiOH groups ; these can be reconstructed by reaction with adsorbed water at room temperature. (Author)

H. A. Benesi and A. C. Jones, *J. Phys. Chem.*, **63**, 179–182, Feb. 1959.

16 : 47

44. The Structure of Gas-Adsorbent Carbons.
United States. Irregularly shaped and layer-type pore structures have both been proposed for gas-adsorbent carbons. In an attempt to distinguish between these structures, the penetration by liquids with different molecular shapes into the pore systems of these carbons has been studied. Conventional nitrogen-adsorption and analytical methods have been applied to the calculation of structural dimensions. The evidence favors a layer-type structure, with a micropore system consisting of molecular-size fissures between relatively large graphitic planes. (Author)

W. F. Wolff, *J. Phys. Chem.*, **62**, 829–833, July 1958.

16 : 30 : 52

45. Surface Reactions on Evaporated Palladium Films.
United States. A study was made of a number of surface reactions on evaporated palladium films at 0°. The method used was to allow a monolayer of adsorbed gas to react with a second gas, added in small doses, and to follow reaction volumetrically and by analysis of the gas phase. In this way, extent of reaction, products and course of the reaction could be followed. The systems used were : Pd-O_2 + CO, Pd-CO + O_2, Pd-O_2 + H_2, Pd-H_2 + O_2, Pd-O_2 + C_2H_4, and Pd-C_2H_4 + O_2. Extensive reaction was found in each case. (Author)

S. J. Stephens, *J. Phys. Chem.*, **63**, 188–194, Feb. 1959.

16

46. The Adsorption of Krypton on Germanium.
A. J. Rosenberg, *J. Phys. Chem.*, **62**, 1112–1119, Sept. 1958.

16

47. The Adsorption of Water Vapor on Quartz and Calcite.
N. Hackerman and A. C. Hall, *J. Phys. Chem.*, **62**, 1212–1214, Oct. 1958.

16

48. A Useful Adsorption Isotherm.
Note by O. Redlich and D. L. Peterson, *J. Phys. Chem.*, **63**, 1024, June 1959.

16

49. Adsorption of Fluorinated Methanes by Linde Molecular Sieves.
Peter Cannon, *J. Phys. Chem.*, **63**, 160–165, Feb. 1959.

16

50. Infrared Studies of Physically Adsorbed Polar Molecules and of the Surface of a Silica Adsorbent Containing Hydroxyl Groups.
M. Folman and D. J. C. Yates, *J. Phys. Chem.*, **63**, 183–187, Feb. 1959.

16

51. Adsorption and Catalysis.
P. H. Emmett, *J. Phys. Chem.*, **63**, 449–456, April 1959.

16 : 30

52. Theory of Permeation Through Metal Coated Polymer Films.
W. Prins and J. J. Hermans, *J. Phys. Chem.*, **63**, 716–719, May 1959.

16 : 32

53. Oxygen Sorption and Electrical Conductivity of Copper Oxide Films.
A. W. Smith and H. Wieder, *J. Phys. Chem.*, **63**, 2013–2016, Dec. 1959.

16

54. The Time Lag in Diffusion. III.
Note by H. O. Pollak and H. L. Frisch, *J. Phys. Chem.*, **63**, 1022, June 1959.

17. Thermodynamics

17

55. The Dissociation Pressure of Aluminum Carbide.
United States. The vapor pressure of Al_4C_3 has been measured in the region from 1500 to 1800°K by means of the Knudsen effusion method and of a torsion method. ΔH^0 at 1600°K was calculated for the reaction $Al_4C_3(s) \longrightarrow 4\ Al(g) + 3\ C(s)$ by means of the second law and the third law, and respective values of 89 (+3) kcal./mole Al and 87 (+3) kcal./mole Al were obtained. The results indicate carbon content of no more than 2 per cent in the vapor when aluminum carbide is dissociated at 1600°K. (Author)

D. J. Meschi and A. W. Searcy, *J. Phys. Chem.*, **63**, 1175–1178, July 1959.

17

56. A Mass Spectrometric Study of the Vaporization of Ferrous Bromide.

United States. A mass spectrometer has been used to analyze the vapors effusing from a Knudsen cell containing $FeBr_2(s)$. In the temperature interval 620–665°K, the monomer is the predominant vapor species ; but at the melting point the dimer concentration becomes significant. Thermochemical data have been determined for the reactions : $2FeBr_2(s) = Fe_2Br_4(g)$, $\Delta H^0_{640} = 59.5 \pm$ kcal./mole dimer ; $Fe_2Br_4(g) = 2FeBr_2(g)$, $\Delta H^0_{640} = 34.7 \pm 4$ kcal./mole dimer. (Author)

Richard F. Porter and Richard C. Schoonmaker, *J. Phys. Chem.*, **63**, 626–628, April 1959.

17

57. Oxygen Dissociation Pressures Over Uranium Oxides.

United States. Oxygen dissociation pressures over the uranium oxides, $UO_{2\cdot0}$ to $UO_{2\cdot6}$, were measured between 950 and 1150° by the Knudsen effusion method. In this temperature and composition range there are three stable uranium oxides : UO_2 in which the solubility of oxygen increases with temperature, U_4O_9 with a narrow homogeneity range, and U_5O_{13} in which oxygen dissolves. A phase diagram of the uranium-oxygen system was constructed and thermodynamics values were derived. (Author)

P. E. Blackburn, *J. Phys. Chem.*, **62**, 897–902, Aug. 1958.

17 : 34

58. High-Altitude Atmospheric Density.

United States. Atmospheric density values obtained from the motion of artificial earth satellites, at altitudes between 186 and 656 kilometers, are discussed. There is some doubt about the reliability of densities from satellites because of the effects of ionization and, in the case of nonspherical satellites, because of their orientation. Densities inferred from satellites are higher than for the ARDC model of the atmosphere. These densities are about ten times higher than densities inferred from rocket-borne ionization gauges between 186 and 230 km. The inference of atmospheric density from rocket-borne ionization gauges is discussed critically, and densities so obtained are considered to be inferior in reliability to the satellite densities. The satellite densities suggest molecular scale temperatures higher than those of the ARDC model in one or more regions of altitude above 80 km.

Theodore E. Sterne, *Physics of Fluids*, **1**, 165–171, May-June 1958.

17 : 34

59. Comparison of High-Altitude Rocket and Satellite Density Measurements.

United States. Atmospheric density measurements obtained with rocket-borne ionization gauges are compared with U.S.A. and U.S.S.R. satellite-drag density measurements. There is no significant disagreement between the results obtained by the two methods once atmospheric variations are taken into account.

H. E. LaGow and R. Horowitz, *Physics of Fluids*, **1**, 478–479, Nov.-Dec. 1958.

17

60. Approximate Formula for the Thermal Conductivity of Gas Mixtures.

United States. An approximate formula for the thermal conductivity of multi-component gas mixtures is derived from rigorous kinetic theory by well-defined approximations. Numerical calculations with the formula are relatively simple, and the only data needed are the molecular weights, thermal conductivities, and either viscosities or heat capacities of the pure components at the same temperature as the mixture. The form of the formula is quite similar to the earlier empirical Lindsay-Bromley equation. The formula is tested by comparison with experimental results on a number of binary and ternary mixtures involving both monatomic and polatomic nonpolar gases. Agreement is satisfactory, and is nearly as good as obtained with the full rigorous theory.

E. A. Mason and S. C. Saxena, *Physics of Fluids*, **1**, 361–370, Sept.-Oct. 1958.

17 : 47

61. Dissociation Pressure and Stability of Beryllium Carbide.

United States. Equilibrium pressures for the reaction $1/2Be_2C(s) = Be(g) + 1/2C(s)$ were measured in the temperature range 1430–1669°K. by the Knudsen technique. The dissociation pressure in this temperature range is given by the equation $\log P$ (atm) $= 7.026 + 0.347-(19,\ 720 + 537)/T$. The heat and free energy of formation of beryllium carbide were derived from the above equation in combination with the literature vapor pressure data for solid beryllium. (Author)

B. D. Pollock, *J. Phys. Chem.*, **63**, 587–589, April 1959.

17

62. Kinetic Theory of Moderately Dense Gases.

R. F. Snider and C. F. Curtiss, *Physics of Fluids*, **1**, 122–139, March-April 1958.

17

63. Condensation of an Imperfect Boson Gas.

Robert H. Kraichnan, *Physics of Fluids*, **2**, 463–466, July-August 1959.

17 : 47

64. The Vaporization of Molybdenum and Tungsten Oxides.

P. E. Blackburn, M. Hoch and H. L. Johnston, *J. Phys. Chem.*, **62**, 769–773, July 1958.

17

65. Applicability of the Knudsen Effusion Method to the Study of Decomposition Reactions. The Decomposition of Magnesium Hydroxide.

E. Kay and N. W. Gregory, *J. Phys. Chem.*, **62**, 1079–1083, Sept. 1958.

17 : 18

66. Thermodynamics of Electrically Conducting Fluids.

Boa-Teh Chu, *Physics of Fluids*, **2**, 473–485, Sept.-Oct. 1959.

17

67. Compressibility and Intermolecular Forces in Gases : Methane.

H. W. Schamp, Jr., E. A. Mason, A. C. B. Richardson, and A. Altman, *Physics of Fluids*, **1**, 329–338, July-Aug. 1958.

17 : 30

68. Evaporation into a Boundary Layer.

Ernest Bauer and Martin Zlotnick, *Physics of Fluids*, **1**, 355–357, July-Aug. 1958.

17

69. Heat Transfer to a Sphere at the Transition from Free Molecule Flow.

Letter by P. Hammerling and B. Kivel, *Physics of Fluids*, **1**, 357, July-Aug. 1958.

17 : 15 : 30

Evaporation into a Boundary Layer. II. Dissociation in Evaporation. See Abstract No. 10.

18. Gaseous Electronics

18

70. Electron Acceleration against an Opposing Field in a Vacuum Electromagnetic Discharge.

Letter by Joseph Slepian, *Physics of Fluids*, **1**, 547, Nov.-Dec. 1958.

Vol. 10 196

18 : 33

71. The Stellarator Concept.
United States. The basic concepts of the controlled thermonuclear program at Project Matterhorn, Princeton University, are discussed. In particular, the theory of confinement of a fully ionized gas in the magnetic configuration of the stellarator is given, the theories of heating are outlined, and the bearing of observational results on these theories is described. Magnetic confinement in the stellarator is based on a strong magnetic field produced by solenoidal coils encircling a toroidal tube. The configuration is characterized by a "rotational transform", such that a single line of magnetic force, followed around the system, intersects a cross-sectional plane in points which successively rotate about the magnetic axis. A theorem by Kruskal is used to prove that each line of force in such a system generates a toroidal surface ; ideally the wall is such a surface. A rotational transform may be generated either by a solenoidal field in a twisted, or figure-eight shaped, tube, or by the use of an additional transverse multipolar helical field, with helical symmetry. Plasma confinement in a stellarator is analyzed from both the macroscopic and the microscopic points of view. The macroscopic equations, derived with certain simplifying assumptions, are used to show the existence of an equilibrium situation, and to discuss the limitations on material pressure in these solutions. The single-particle, or microscopic, picture shows that particles moving along the lines of force remain inside the stellarator tube to the same approximation as do the lines of force. Other particles are presumably confined by the action of the radial electric field that may be anticipated. Theory predicts and observation confirms that initial breakdown, complete ionization, and heating of a hydrogen or helium gas to about 10^6 degrees K are possible by means of a current parallel to the magnetic field (ohmic heating). Flow of impurities from the tube walls into the heated gas, during the discharge, may be sharply reduced by use of an ultra-high vacuum system ; some improvement is also obtained with a divertor, which diverts the outer shell of magnetic flux away from the discharge. Experiments with ohmic heating verify the presence of a hydromagnetic instability predicted by Kruskal for plasma currents greater than a certain critical value and also indicate the presence of other cooperative phenomena. Heating to very much higher temperatures can be achieved by use of a pulsating magnetic field. Heating at the positive-ion cyclotron resonance frequency has been proposed theoretically and confirmed observationally by Stix. In addition, an appreciable energy input to the positive ions should be possible, in principle, if the pulsation period is near the time between ion-ion collisions or the time required for a positive ion to pass through the heating section (magnetic pumping). (Author)

Lyman Spitzer, Jr., *Physics of Fluids*, **1**, 253–265, July-Aug. 1958.

18

72. Electrical Breakdown between Close Electrodes in Air.
Prebreakdown electron current between electrodes closing at voltages below the minimum which can give breakdown by successive ionization of air molecules has been measured by two different methods. This field emission current varies widely in successive experiments, increasing in general with decreasing voltage, with maximum values of the order of 10^{-7} amp. At the small electrode separations characteristic of breakdown at voltages below 300, it is shown that the ions necessary for breakdown come from the anode surface. The number of ions in the space at one time is so small that they cannot cooperate to enhance the gross field at the cathode, which is a conclusion having important consequences for the theory of breakdown.

L. H. Germer, *J. Appl. Phys.*, **30**, 45–51, Jan. 1959.

18

73. On the Research and Development of Electron Emitting Substances for Gas Discharges.
Criteria for the stability and chemical behavior of electron emitting substances in gas discharges are obtained by means of thermodynamics. Theoretical analysis is supplemented by means of experimental methods intended for the study of processes at elevated temperatures, such as thermogravimetry and differential thermal analysis. The application of the above permits some insight into the processes of formation, activation, and detrition of electron emitting compositions, guiding the development of a number of improved cathodes. (Author)

D. M. Speros, *J. Electrochem. Soc.*, **106**, 791–799, Sept. 1959.

18

74. Supersonic Motion of Vacuum Spark Plasmas along Magnetic Fields.
D. Finkelstein, G. A. Sawyer, and T. F. Stratton, *Physics of Fluids*, **1**, 188–193, May-June 1958.

18

75. Response of Electrostatic Probes to Ionized Gas Flows in a Shock Tube.
Letter by Robert G. Jahn and Fred A. Grossee, *Physics of Fluids*, **2**, 469, July-Aug. 1959.

18

76. Absorption of Gases in the Low Pressure Arc.
E. Ia. Pumper, *Sov. Phys. Tech. Phys.*, **3** : 10 (Transl.), 2088.

18

77. Micro-discharges and Pre-discharge Currents between Metal Electrodes in High Vacuum.
L. I. Pivovar and V. I. Gordienko, *Sov. Phys. Tech. Phys.*, **3** : 10 (Transl.), 2101.

18

78. Automatic Cloud Chamber for Gas Discharge Studies.
K. R. Allen and K. Phillips, *Rev. Sci. Instrum.*, **30**, 230.

18

79. Design and Performance of a Hot Cathode Magnetically Collimated Arc Discharge Ion Source.
Manlio Abele and Wolfgang Mechbach, *Rev. Sci. Instrum.*, **30**, 335.

18

80. Cold Cathode Electric Discharge at Low Pressures in a Magnetic Field.
G. V. Smirnitskaya and E. M. Reikhrudel, *Sov. Phys. Tech. Phys.*, **4** : 2 (Transl.), 131.

18

81. Anode Region in a Low Pressure Gas Discharge,
N. A. Neremina and B. N. Klyarfeld, *Sov. Phys. Tech. Phys.*, **4** : 1 (Transl.), 13.

18 : 17

Thermodynamics of Electrically Conducting Fluids. See Abstract No. 66.

19. Radiation

19 : 51

82. Design of High-Resolution Monochromator for the Vacuum Ultra-violet. An Application of Off-Plane Eagle Mounting.
T. Namioka, *J. Opt. Soc. Amer.*, **49**, 961–966, Oct. 1959.

19 : 51

83. Phase Changes on Reflection from Evaporated Chromium Films.
C. Weaver, R. M. Hill, J. E. S. Macleod, *J. Opt. Soc. Amer.*, **49**, 992–997, Oct. 1959.

19 : 51

84. The Theory of the High Frequency Brush Discharge.
R. Grigorovici and G. Crustecu, *Optitsu I Spekstroskopiia*, **VI**, 2, Feb. 1959.

19 : 30

85. Preparation of Phase Diffraction Gratings by Vacuum Evaporation.

A. E. Ennos, *J. Opt. Soc. Amer.*, **50**, 14–17, Jan. 1960.

19 : 30

86. Method for Obtaining Uniform Evaporated Layers.

Martin V. Schneider, *J. Opt. Soc. Amer.*, **50**, 18–20, Jan. 1960.

19

87. On the Measurement of the Temperatures of Unenclosed Objects by Radiation Methods.

The functional relationships between apparent temperature and true temperature for the total radiation pyrometer, the optical pyrometer, the two-color pyrometer, and the two-temperature pyrometer are developed and discussed. It is shown that it is impossible to measure the temperature of an unenclosed object in the range 2000°–4000°K with accuracy greater than about 10 per cent without prior knowledge of the emissivity. If the emissivity is known within 20 per cent, the temperature can be determined within 1 or 2 per cent by means of an optical pyrometer, particularly if the instrument is operated at the blue end of the spectrum. The accuracy obtainable with the other instruments under equivalent conditions is significantly lower.

(Author)

A. G. Emslie and H. H. Blau, Jr., *J. Electrochem. Soc.*, **106**, 877–880, Oct. 1959.

Vol.
10
1960

Vacuum Apparatus and Auxiliaries

21. Pumps and Pump Fluids

21

88. Improvements in or Relating to Vapour Operated Vacuum Pumps.
United States. One of the disadvantages of vapour operated pumps is that the liquid or pump fluid is usually an organic material which is readily oxidized or otherwise deteriorated when exposed to the atmosphere at the temperature required for operation. For this reason precautions must be taken against exposing hot pump fluid to air at pressures substantially higher than the operating pressure of the pump if damage to the pumping fluid is to be avoided. Where rapid pump down cycles are required some operators prefer to use valveless systems and take the precaution of cooling the pump fluid from its operating temperature to a safe temperature before exposure to atmosphere. This reduction in pump fluid temperature has been achieved by turning off the boiler heating element and waiting for the pump fluid to cool or by providing cooling coils around the exterior of the pump casing in the vicinity of the boiler. Pump fluid is then cooled by circulating a cooling fluid such as water to the external coil. The advantage of these methods is the time required for re-heating the pump fluid to its operating temperature. This patent describes a vapour operated pump in which the fluid is cooled rapidly by internal cooling coils which are arranged to cool only the upper portion of the pool of pump fluid which is the only part exposed to the atmosphere. The advantage of this method is that only a portion of the fluid is cooled so that it may be quickly re-heated for cycling operations. This provides a vapour operated pump with an extremely short heating cycle time. A full description of the apparatus is given. A quench coil is situated internally at the top of the boiler and when water is circulated is capable of cooling the surface of the fluid very rapidly. The normal operating temperature of a typical pump fluid is 200°C and by circulating tap water through a quench coil of the type described the temperature of the pump fluid was lowered from 200°C to 180°C in 20 sec, this temperature being considered the maximum safe value for the type of fluid. Thus atmospheric pressure may be admitted to the pump within 20 sec after cooling has started but in practice a safety factor is provided by passing cooling water through the quench coil for approximately 80 sec thus cooling the pump fluid to about 155°C. A curve of pressure against time shows how quickly the pump can be restored to operation after the fluid is cooled with the quench coil. Starting with a pressure of about 0.5 Torr the cooling water is blown out of the quench coil with air and the heating elements are turned on. Within $3\frac{1}{2}$ min the pump is operating and has reduced the pressure to between 1.5 and 1×10^{-4} Torr. A similar curve shows the length of time required by the same pump without the internal cooling coil and it is shown that this pump requires nearly 9 min to achieve the same pressure as is possible when the quench coil is used. Thus the invention provides means for achieving a substantial reduction in the cycle time of a vapour operated pump. The position of the quench coil is not critical and rapid quenching of the fluid at the surface has been obtained with the quench coil located from about $\frac{1}{4}$ inch above to about $\frac{1}{4}$ in. below the normal operating level of the pool.

Patent Specification by G. T. Gerow and R. J. Weeks, *Brit. Pat. Spec.* No. 809, 379, Feb. 25th, 1959.

21

89. Improvements in or Relating to Vapour Vacuum Pumps.
United Kingdom. In any kind of batch vacuum process it is desirable that the system should be capable of being rapidly brought up to atmospheric pressure and rapidly revacuated. If the vacuum system is being pumped by a vapour vacuum pump it is undesirable that the pump boiler should be exposed to air at atmospheric pressure whilst the fluid is hot. When the vapour pump is connected directly to the system being pumped it is necessary before bringing the system up to atmospheric pressure to interrupt the heating of the boiler of the pump and allow the boiler to cool before emitting air to the system. The disadvantage of this technique is that the boiler cooling and heating times make rapid vacuum cycles impossible. Thus many vacuum pumping systems have an isolation valve between the vapour pump and the system being pumped, together with a valve controlled by-pass duct from the system to the roughing pump. Such isolation valves may severely restrict the speed of the vapour pump. This patent describes a vacuum vapour pump which can be connected directly to the system to be evacuated and can be operated to produce rapid exhausting cycles from atmospheric pressure without dangerous exposure of the pump fluid to air. This pump is provided with a valve for isolating the boiler of the pump from the main duct supplying vapour to the jets. During the time that the boiler is isolated from the main duct, that is, during the idle period of the pump, a means of condensing the vapour is provided. Thus, the temperature gradients associated with the heat flow into the boiler and the pressure in the boiler respectively are maintained at predetermined controlled values so that upon reconnecting the boiler with the jet system the pump enters immediately into effective operation. The boiler pressure and the temperature gradient from the heater to the boiler shell are the same as the normal operating conditions of the boiler so that at the end of an idle period the pump attains its full pumping capacity instantaneously. It is also possible to permit the boiler pressure and temperature to rise by a predetermined controlled amount during the idle period so that upon restoring communication of the boiler with the main vapour duct the maximum mass throughput and the maximum backing pressure against which the pump will operate are temporarily increased and gradually return to normal as pump down proceeds.

Patent Specification by B. D. Power, *Brit. Pat. Spec.* No. 806788, Dec. 31st, 1958.

21

90. Annular Jet Pump.
Werner H. Haak and Frederick Vratny, *Rev. Sci. Instrum.*, **30**, 296.

21

91. Rough Pumping with Activated Charcoal.
R. L. Jepsen, S. L. Mercer and M. J. Callaghan, *Rev. Sci. Instrum.*, **30**, 377.

21 : 11

Molecular Pumping. See Abstract No. 1.

22. Gauges

22

92. Small, Lightweight Ionization Gauge Control Circuit.
H. B. Benton, *Rev. Sci. Instrum.*, **30**, 887.

22

93. Principle of a Semiconductor Manometer in the Pressure Range of 1 mm to 10^{-6} mm Hg.
M. Varieak and B. Saftie, *Rev. Sci. Instrum.*, **30**, 891.

23. Plumbing

23

94. Improvements in and Relating to Vacuum Vessels.
United Kingdom. A method of sealing together two parts of a vacuum vessel is described. The parts are metallized in the

vicinity of the sealing surfaces, and when held together a low melting point solder is applied to the seal. A smooth junction is obtained over the sealing surfaces.

Brit. Pat., 799,277, 6 Aug. 1958.

23

95. Inflatable Gasket for the 72 in. Bubble Chamber.
Luther R. Lucas and H. Paul Hernandez, *Rev. Sci. Instrum.*, **30**, 941.

24. Valves

24

96. Metal Bakeout Valve for Ultrahigh Vacuum.
Carsten M. Haaland, *Rev. Sci. Instrum.*, **30**, 947.

24

97. New Techniques with Attainment of High Vacua.
Robert A. Rapp, *Rev. Sci. Instrum.*, **30**, 839.

24

98. Ultrahigh Vacuum Valve.
Norman H. Axelrod, *Rev. Sci. Instrum.*, **30**, 944.

24

99. Large Ultrahigh Vacuum Valve.
W. J. Lange, *Rev. Sci. Instrum.*, **30**, 602.

27. Leak Detectors and Leak Detection

27

100. This Simple Method Finds Vacuum Leaks.
Note by R. W. Naylor, *Chem. Eng.*, **66**, 1959, Sept. 1959.

27

101. A New Mass Spectrometer Leak Detector for General Use.
A small portable mass spectrometer for table mounting adjustable for use with searcher gases of different masses such as H_2, He, Ar, CO, O_2, C_2, H_2, Butane, Freon, Town gas etc., may be used for vacuum as well as pressurized systems. The details of construction is described. One part of He in 10^6 parts of air may be detected. The resolution of the standard equipment is about 15 (defined as $\Delta M/M$) where M = mass of a singly charged ion.

Hans-Weber Drawien and Kurt Kronenberger, *Z. Instrkde*, **67**, 157–161, 1959.

Vol.
10
196

Vacuum Applications

30. Evaporation and Sputtering

30 : 52

102. Diffusion of Silver in Silver Sulfide.
United States. Diffusion of radioactive Ag-110 in silver sulfide was measured in polycrystalline specimens. Disk shaped specimens were cut from a rod of vacuum melted and annealed silver sulfide. In the first experiments the radioactive tracer, Ag-110, was evaporated on to the disks from a tantalum ribbon *in vacuo*. In later experiments, the tracer was applied by treating the disk with active silver nitrate solution. The coated specimen was placed between two sheets of platinum foil in a vessel evacuated to less than 10^{-5} Torr, filled with helium, and then raised quickly to the desired temperature in a bath of Wood's metal. B. B. D.

R. L. Allen and W. J. Moore, *J. Phys. Chem.*, **63**, 223–226, Feb. 1959.

30 : 52

103. Heterogeneous Reaction Studies by Infrared Absorption.
United States. An experimental apparatus and procedure were developed for obtaining the infrared spectra of substances which are adsorbed on the surface of freshly evaporated metal surfaces. In addition, this equipment may be used either to observe changes in the reflectivity of the metal surfaces or to observe changes in gaseous components while a reaction is taking place. The basis of the equipment is the use of a multiple reflection cell whose front surfaced mirrors are covered by freshly evaporated catalyst metal. When ethylene is added in excess to new rhodium mirrors, it is adsorbed with dissociation to produce ethane and an adsorbed substance. Evidence was obtained which indicates this substance is composed of paired carbon atoms which probably are present on the catalyst surface. This adsorbed substance may be hydrogenated to ethane at room temperature and at hydrogen pressures of less than 1 mm. No direct evidence was found for hydrogen-carbon bonds in the adsorbed molecules. The ethylene adsorption is accompanied by a small decrease in film reflecting power while the hydrogenation step is accompanied by a similar increase in reflectivity. When the CO pressure over new rhodium mirrors is 1 mm, an infrared absorption band at 4.854μ is observed. A band of increased reflectivity is also observed at 4.785μ. Upon evacuation, the absorption band shifts to 4.914μ, whereas the band of increased reflectivity remains unchanged. When CO is added to new nickel mirrors, a large infrared absorption band is observed at 4.859μ, corresponding to gaseous nickel carbonyl. However, no other nickel carbonyl bands are observed. The 4.859μ band disappears upon evacuation. These results show that the CO is more strongly adsorbed on the rhodium catalyst than on the nickel catalyst. The positions of the infrared absorption bands suggest that the CO is chemisorbed as single linear molecules. When hydrogen is added to new rhodium mirrors, a decrease in film reflecting power occurs. Only a fractional recovery in reflectivity occurs upon evacuation. As many as 23 absorption bands are observed which may be attributed to hydrogen on the rhodium surface. (Author)

Harold L. Pickering and Hartley C. Eckstrom, *J. Phys. Chem.*, **63**, 512–517, April 1959.

30 : 52

104. Physical Techniques in the Study of Silver Catalysts for Ethylene Oxidation,
United States. To investigate whether different crystal planes of silver give different results in the catalytic oxidation of ethylene to ethylene oxide with air, several types of evaporated silver film were used. By evaporating *in vacuo* or in 1 mm of nitrogen or hydrogen, films containing crystals randomly oriented or with the 110 plane parallel to the glass support were obtained. Both types were about equally active and selective. Most significantly, it was found that use of an oriented film for ethylene oxidation at 250–280° caused recrystallization to randomly oriented material in 2–4 hr. Thus, unusual crystal faces would not be expected to persist in use. Disorientation did not occur when similar films were heated in air at 250°. Detection of volatile impurities in silver catalysts were done by heating to near-fusion temperature in a small chamber connected to the inlet reservoir of a mass spectrometer. Appreciable amounts of carbon, oxygen, hydrogen and sulfur compounds were shown to be present in silver made by reduction of the oxide or by chemical deposition from solution. Fractional monolayers could be detected on catalysts with surface areas of 0.2 m^2/g. Another measurement of possible utility was that of surface potential relative to a gold electrode in air. Values for powdered silver catalysts held in a flat tray ranged from −500 to +500 mv and were reproducible to about 10 mv. Chemisorption of phosphorus, sulfur or chlorine compounds made the values more negative. (Author)

J. N. Wilson, H. H. Voge, D. P. Stevenson, A. E. Smith and L. T. Atkins, *J. Phys. Chem.*, **63**, 463–468, April 1959.

30 : 34

105. Temperature Stabilization of Highly Reflecting Spherical Satellites.
G. Hass, L. F. Drummeter, Jr., M. Schach, *J. Opt. Soc. Amer.*, **49**, 918–924, Sept. 1959.

30 : 52

106. Calculation of the Performance of a High-Vacuum Thermionic Energy Converter.
The performance of a high-vacuum thermionic energy converter has been evaluated from Langmuir's 1923 paper on the thermionic diode. The results are presented in the form of a generalized set of curves which show output voltage as a function of current drawn from the device. These general curves have then been applied to a few specific cases to determine what cathode-anode spacings, and cathode and anode properties will be required to produce a practical energy converter.

H. F. Webster, *J. Appl. Phys.*, **30**, 488–493, April 1959.

30 : 52

107. Selective Delineation of Screw Dislocations by Cathodic Sputtering.
A method of revealing screw component dislocations involving low-energy cathodic sputtering with argon ions is presented. It is observed that hillocks having the shape of truncated cones with a spiral pattern on their tops form at the sites of intersection of screw dislocations with the surface. The hillocks probably form by mobile surface atoms attaching themselves to the step provided at the intersection of a screw dislocation with the surface. It is shown that the density of screw dislocations on a given plane depends on the orientation of the plane with respect to the crystal growth axis.

B. B. Meckel and R. A. Swalin, *J. Appl. Phys.*, **30**, 89–94, Jan. 1959.

30

108. Improvements in or relating to the Deposition of Metals and the like Substances on Webs by Evaporation *in vacuo*.
West Germany. This invention relates to the deposition of metals and other materials on for example webs of synthetic materials by evaporation *in vacuo*. The patent describes how the fibrous surface of the web material may be sealed by impregnation with a resin, for example an *iso*-cyanate modified polyester resin.

Brit. Pat., 800,093, 20 Aug. 1958.

30

109. A Method of Applying Films by Deposition in Vacua and Electrical Impedances when Made by the Method.
United States. This patent describes a method of applying films of predetermined thickness with precise and continuous control. The method is applicable to the deposition of a number of materials including metals, their oxides and suitable semiconducting or intermetallic substances. Deposition of vitreous materials, such as silica for the purpose of protection or electrical insulation, is also possible. A typical vacuum chamber is described, pumped by conventional methods. Inside the vacuum chamber are situated the vapour sources, the workholder which carries the substrata on which the vapour is to be deposited, and a light source and photo-electric cell for determining the optical transmittance of films deposited on a transparent monitor plate. The workholder consists of a circular plate with a series of holes around the periphery. These holes are designed to hold the work and the transparent monitor plate. The sources are situated underneath the workholder and as the plate rotates, each hole is brought into line with one of the sources or the photocell device. Thus with each revolution of the workholder, a film is progressively deposited on the work. Similarly the optical transmittance of the monitor plate is measured by the photocell once during each revolution. The repeated exposures are continued until the film on the transparent support reaches a given value of optical transmittance. This also gives an accurate indication of the electrical resistance of the film if empirical constants which establish the relationship between electrical resistance and optical transmittance are first obtained for each particular material. This method of monitoring is considered accurate in view of the fact that the process usually employs three to four hundred treatment cycles. The apparatus has been designed particularly for making resistance elements protected by a vitreous evaporated layer or for making capacitors by the deposition of conducting films on both sides of a dielectric plate, made for example from barium titanate.

Brit. Pat. 801 030, 3 Sept. 1958.

30

110. Substrate Damage in Film Thickness Measurement by Beam Interferometry.
Canada. Letter by G. D. Scott, *Nature*, **184**, Suppl. No. 6, p. 354–355, 1 Aug. 1959.

111. Interferometric Studies of Synthetic Diamonds.
United Kingdom. S. Tolansky and I. Sunagawa, *Nature*, **185**, No. 4708, 203–204, 23 Jan. 1960.

30

112. Investigation of Thin Films Produced by Evaporating Indium Antimonide in Vacuum.
G. A. Kurov and Z. G. Pinsker, *Sov. Phys. Tech. Phys.*, **3** : 10 (Transl.), 1958.

30

113. Control of the Thickness of Evaporated Layers During Evaporation.
G. Papp, *Rev. Sci. Instrum.*, **30**, 911.

30 : 15 : 17

Evaporation into a Boundary Layer. II. Dissociation in Evaporation. See Abstract No. 10.

30 : 16 : 33

Secondary Positive Ion Emission from Metal Surfaces. See Abstract No. 12.

30 : 16

The Adsorption of Some Gases on Evaporated Metal Films and on Oxidized Films of Nickel. See Abstract No. 32.

30 : 16

The Interaction of Krypton with Metals. An Appraisal of Several Interaction Theories. See Abstract No. 38.

30 : 16 : 52

Surface Reactions on Evaporated Palladium Films. See Abstract No. 45.

30 : 16

Theory of Permeation Through Metal Coated Polymer Films. See Abstract No. 52.

30 : 17

Evaporation into a Boundary Layer. See Abstract No. 68.

30 : 19

Preparation of Phase Diffraction Gratings by Vacuum Evaporation. See Abstract No. 85.

30 : 19

Method for Obtaining Uniform Evaporated Layers. See Abstract No. 86.

32. Nucleonics

32

114. New Electrostatic Accelerator.
Considering the proposition that the maximum usable voltage of most electrostatic accelerators is limited by the breakdown and electrical discharges in the accelerating tube, the authors have designed and constructed a new machine operating at potential gradients of 1400 Kv/foot. It was assumed by the authors that the breakdown of the tube was associated with films of organic contaminants on the tube surfaces. Consequently, the entire accelerating tube and vacuum system were constructed of bakeable materials. The pumps used are evaporion type and the system reaches pressures of a few times 10^{-8} mm Hg. All gaskets, valves, gauges, and other vacuum accessories are designed to have low vapor pressure, even at bakeout temperature. C. L. G.

Irving Michael, *et al.*, *Rev. Sci. Instrum.*, **30**, 855.

32

115. 22 MeV Electron Linear Accelerator.
N. A. Austin and S. C. Fultz, *Rev. Sci. Instrum.*, **30**, 284.

32

116. Duo Plasmatron Ion Source for Use in Accelerators.
C. D. Moak, *et al.*, *Rev. Sci. Instrum.*, **30**, 694.

32

117. Zero Gradient Synchrotron at the Argonne National Laboratory.
Engineer, **208**, 5413, 492, Oct. 1959.

32 : 16

Oxygen Sorption and Electrical Conductivity of Copper Oxide Films. See Abstract No. 53.

33. General Physics and Electronics

33

118. Recombination of Atoms at Surfaces.
J. C. Greaves and J. W. Linnett, *Trans. Faraday Soc.*, Part 4, **55**, 1338–1345, Aug. 1959. Part 5, **55**, 1346–1354, Aug. 1959.

33

119. Theory and Application of Molecular Beam Techniques for the Design of Collision Free Sampling Systems. Part 1. Molecular Beam Formation by Multiple Aperture Collimating Systems.

C. W. Nutt, J. S. M. Botterill, G. Thorpe, and G. W. Penmore, *Trans. Faraday Soc.*, **55**, 1500–1515, Sept. 1959.

Part 2. Molecular Beam Formation by Adiabatic Expansion of Gas through Apertures in Thin Diaphragms.

C. W. Nutt, G. W. Penmore, and A. J. Biddlestone, *Trans. Faraday Soc.*, **55**, 1516–1523, Sept. 1959.

33

120. Emission of Relatively High-Energy Ions from Low-Voltage Arcs.

United Kingdom. Some interesting effects have been observed with low-voltage arcs for which so far no completely satisfactory explanations have been found. The principal effect observed is the emission of luminous rays consisting of ions of the cathode material at energies much greater than the total potential difference across the arc. (Author)

E. R. Harrison, *Nature*, **184**, 245–246, 25 July, 1959.

33

121. Improvements in or Relating to Methods of Forming Luminescent Screens Coated with Thin Films of Organic Material.

United Kingdom. In the preparation of luminescent screens for example for cathode ray tubes or for electron microscopes it is necessary for the phosphor layer to be coated with a thin film of organic material such as nitrocellulose. This organic layer is used as a temporary substrate for a vacuum deposited coating. The problem is to prevent the film of organic material from penetrating between the grains of the luminescent screen. It is common practice to fill up the cavities between the grains with a liquid for example water and to remove it after the film has been formed by evaporation. This layer of water is known as the liquid bed. The object of this invention is to avoid the loss of time resulting from the renewed introduction of a liquid bed after the phosphor settling bed has been decanted. A method is described of forming a luminescent screen coated with a thin coherent film of organic material. This method includes the steps of settling a luminescent material from an aqueous alkaline suspension having a pH value greater than 9.5 and containing in solution potassium or sodium silicate and at least one other alkaline compound. After the luminescent material has settled, an amount of acidifying agent is added to reduce the pH value of the liquid to a value between 5 and 8.5 thus providing on the phosphor settling bed a solution of the organic material with a specific gravity lower than that of the settling bed. During the course of the experimental work extensive tests have revealed that the unsatisfactory formation of film when using the settling bed itself as the liquid bed in providing the film is due to the alkalinity of the settling bed. In order to obtain satisfactory adhesion of the luminescent material it is necessary to use an amount of silicate such that the liquid has a pH value higher than 9.5. If a solution of the organic film-forming material is provided on the settling bed giving the alkaline reaction described then an emulsion occurs on the separating surfaces of the liquids resulting in a very irregular film having a streaky dull appearance. This formation is avoided by reducing the pH value in accordance with the invention. The pH value may be reduced in a very simple way by adding to the settling bed an amount of acid for example phosphoric acid or by adding acid reacting salts for example sodium dihydrogen phosphate. The materials already known may be used for the organic films. Among these materials nitro cellulose is particularly useful although satisfactory films may also be formed with esters of polymethacrylic acid. A complete method is described for forming a luminescent screen coated with an organic film in a cathode ray tube 22 cm diameter.

Brit. Pat. Spec. No. 801067, 10 Sept., 1959.

33

122. A Comparison of Charges on the Electron, Proton, and Neutron.

United Kingdom. Letter by H. Bondi and R. A. Lyttleton, *Nature*, **184**, Suppl. No. 13, 974, 26 Sept. 1959.

33

123. Field Effects on Chemisorbed Films in Electron Emission Microscopy.

United Kingdom. Letter by R. J. Hill and P. W. M. Jacobs, *Nature*, **184**, Suppl. No. 12, 895–896, 19 Sept. 1959.

33

124. Ionization Phenomena in Gases.

Sweden. Report of the fourth International Conference on Ionization Phenomena in Gases, which took place at Uppsala, Sweden, in August, 1959. The very wide programme included sections on plasma physics as well as on fundamental processes and other applications of electric discharges, and attracted a representative gathering of about 800 scientists from research organizations active in this field in 25 different countries. (Author)

Report by J. Dutton, D. Harcombe, and E. Jones, *Nature*, **184**, No. 4696, 1353–1358, 31 Oct. 1959.

33

125. Tensile Strength of Liquid Argon, Helium, Nitrogen, and Oxygen.

J. W. Beams, *Physics of Fluids*, **2**, 1–5, Jan.-Feb. 1959.

33

126. Precision Thermometer System for Liquid Helium Range.

B. J. Sandlin and J. C. Thompson, *Rev. Sci. Instrum.*, **30**, 659.

33

127. Precooling Device for Liquid Helium Transfer Tube.

H. H. M. Zerbst, *Rev. Sci. Instrum.*, **30**, 601.

33

128. Strong Focussing Ion Source for Mass Spectrometers.

Clayton F. Giese, *Rev. Sci. Instrum.*, **30**, 260.

33

129. Ion Optics for the V-Type Surface Ionization Filament Used in Mass Spectrometry.

Leonard A. Dietz, *Rev. Sci. Instrum.*, **30**, 235.

33

130. A New Method of Comparing the Mass of Bodies in a Vacuum.

The masses to be compared (weights and samples of arbitrary shape) are inserted under an evacuated belljar, so that on substitution the effect of the identical belljar does not have to be taken into account. Changes in air density are compensated by the use of an equivalent belljar on the other scale pan which remains permanently evacuated and contains the balance weights.

C. De Vreese, *Z. Instrkd.*, **67**, 25–28, 159 Nr. 2, 1959.

33 : 42

131. Interferometric Calibration of Quartz End-Measuring Rods.

The vacuum wavelength interferometer used in the calibration of quartz end-measuring rods is described in detail.

E. Engelhard, *Z. Instrkde.*, **67**, 59–65, Nr. 3, 1959.

33 : 16 : 30

Secondary Positive Ion Emission from Metal Surfaces. See Abstract No. 12.

33 : 18

The Stellarator Concept. See Abstract No. 71.

34. High Altitude and Space Technology

34

132. Change of Cosmic Rays in Space.
United States. H. V. Neher, *Nature*, **184**, No. 4684, 423–425, 8 Aug. 1959.

34

133. Air Density in the Upper Atmosphere from Satellite Orbit Observations.
United Kingdom. Letter by G. V. Groves, *Nature*, **184**, Suppl. No. 4, 178, 18 July 1959.

34 : 51

134. Dissipation of Planetary Atmospheres.
United Kingdom. The author analyzes Jeans expression for an atmosphere in isothermal equilibrium, and points out with L. Spitzer that this does not apply to real planetary atmospheres because the isothermal assumption does not hold. The tenuous atmosphere of the moon is especially considered. Conditions which influence dissipation at the escape level are considered. It is pointed out that gas density at escape level for small planetary gravity conditions will be reached at greater height. This critical density will not be the same for different values of gravity. The critical pressure p is proportional to g. For the moon, on this basis, dissipation rate, computed as per Jeans, is 6 times too high. Ionization at escape level is considered. It is shown that this will result in increased molecular density through the increased number of free charged particles. This causes the effective escape level to rise and rate of escape to drop. The corresponding drop in mean molecular weight will counteract the above charge mechanism. The plasma condition will result in charged layers and an electrophorous effect and the escape layer will be bound to the lower layers and its density thus increased, this also resulting in a well defined exophere boundary. The effect of interplanetary gas density (10^3/cm^3) is next considered. This later gas density (γ) may be a decisive influence in the escape level for thin atmospheres. As the escape level molecular density approaches γ, dissipation becomes impossible and the atmosphere of a sufficiently small body becomes indestructible. Asteroids may retain, in this way, a considerable, although tenuous, gaseous envelope. Calculations from this show that the ground density of lunar air is about 10^{-12} of the earth's sea level pressure. Additive effects of adsorption and absorption, as well as radioactive assay and physiochemical processes could alter this figure considerably. L. E. P.

V. A. Firsoff, *Science*, **130**, 1337–1338, 13 Nov. 1959.

34 : 17

High-Altitude Atmospheric Density. See Abstract No. 58.

34 : 17

Comparison of High-Altitude Rocket and Satellite Density Measurements. See Abstract No. 59.

34 : 30

Temperature Stabilization of Highly Reflecting Spherical Satellites. See Abstract No. 105.

35. Impregnation and Potting

35 : 42

135. Low-Melting Inorganic Glasses with High Melt Fluidities below 400°C.
The ternary and quaternary interactions of the elements arsenic, thallium, sulfur, and selenium were studied with the aim to synthesize glasses which exhibit high fluidities at temperatures below 400°C. The ternary systems As–Tl–S, As–Tl–Se, and As–Se–S were found to satisfy this condition. These glasses are chemically durable, exhibit extremely low water solubility, and have shown no tendency toward devitrification. Their electrical resistivities fall into the range from 10^{12} to 10^{16} ohm.cm, and their dielectric constants vary from 4 to 20.

(These glasses are available from Baker and Adamson, 40 Rector St., New York 6, N.Y. in powder form or as preforms pressed from powder, but can also be produced by vacuum deposition as thin films on the order of 0.001 in. thick. Semiconductor devices can be hermetically sealed by these glasses.) Note added by abstractor. W. H. K.

S. S. Flaschen, A. D. Pearson, and W. R. Northover, *J. Amer. Ceram. Soc.*, **42**, 450, Sept. 1959.

35

136. Impregnants for Castings.
This article discusses the various methods of impregnating castings and the types of impregnants available. Included are polyesters, sodium silicate, metal powders, phenolics, sal ammonia, tung oil and styrene monomer. A. G.

Robert J. Fabian, *Materials in Design Engineering*, **50**, 102–106, Oct. 1959.

36. Drying, Degassing and Concentration

36 : 41

137. Processing Techniques Used in Degassing during Casting of Rolling and Forging Steels based on the Vacuum Lift Process.
In the vacuum-lift process a part of the melt is lifted out of the filled casting ladle into an evacuated vessel and returned into the ladle after vacuum treatment. These partial treatments are repeated until the whole contents of the ladle shows the desired degree of adgassing. The various principles and parameters of the process are discussed including: minimum quantity, suction pipe, mixing time, temperature losses, etc.

Fritz Harders, Helmut Knuppel, and Karl Britzmann, *Stahl und Eisen*, **79**, 267–272, Nr. 5, 1959.

36 : 41

138. Vacuum Degassing of Low Carbon Unkilled Steel during Casting or during Solidification into Block Form. I. Degassing of Unkilled Soft Steel under Vacuum.
Soft steel for deep drawing applications may be much improved by a vacuum treatment (casting by steam degassing; melting steel at a reduced pressure).

Georg Henke and Walter Hess, *Stahl und Eisen*, **79**, 405–407, Nr. 7, 1959.

36 : 41

139. Vacuum Degassing of Low Carbon Unkilled Steel during Casting or during Solidification into Block Form. II. Casting by Stream Degassing of Unkilled Soft Steel.
Effective degassing is achieved if the steel is poured from the ladle directly into a mould in a vacuum so that only on solidification does it again come into contact with atmospheric air. Furthermore the low pressure paths (e.g. the vacuum tunnel) should be kept as short as possible. A steam jet ejector was used as the vacuum pump.

Hubert Hoff, Herman-Josef Kopineck und Gustav Opfer, *Stahl und Eisen*, **79**, 408–410, 1959.

36 : 41

140. Methods of Heating for Large Scale Industrial Degassing of Molten Steel.
It is recommended either to preheat the vessel at low power or to apply heat at large power only during the vacuum treatment or to use both methods. A further effective reduction in temperature losses is achieved using arc melting methods.

Helmut Knippel, Karl Brotzmann, Karl Rüttiger, und Arnulf Dcener, *Stahl und Eisen*, **79**, 272–273, 1959.

36 : 41

141. Steel degassing Based on the Circulating Degassing Process.
In principle molten steel is circulated through a degassing vessel. The steel is lifted continuously from the ladle through a suction pipe into an evacuated degassing vessel and is returned by a second pipe back into the ladle. The many possible applications of this process in steelmaking could so far not be completely evaluated (present application only for heavy steel forgings).

Herbert Thielemann und Hermann Maas, *Stahl und Eisen*, **79**, 276–282, 1959.

36 : 41

142. Measurements and Control during the Vacuum Degassing of Molten Steel.
The quantities to be measured are as follows :—
The quantity, pressure and composition of the gases removed in the vacuum lift process (using a gasometer, pressure recorder and gas analysis system) are measured as well as the level changes with time of the molten steel in the lower bath using a float device.
In this way data are obtained on the oxygen and hydrogen content as well as the flow velocity of steel from the upper vacuum chamber to the lower bath.

Karl Brotzmann, Karl Rüttiger, Klaus Förster, und Robert Hentrich, *Stahl und Eisen*, **79**, 410–414, 1959.

36 : 41

143. The Removal of Oxygen in the Treatment of Steel Melts in Vacuum.
The degassing of steel is based on the fact that at lower pressures the solubility of gases in steel is reduced. From this a number of reactions may be considered of which the carbon–oxygen reaction is the most important one for the removal of oxygen from the steel. This is the subject of the above paper. It is necessary to know the degree of outgassing and the time of degassing. If the exposed surfaces are sufficiently large, degassing will be accelerated to the point where the greater part of the oxygen content is removed if the steel is exposed to the vacuum for only 0.4 minutes. (Vacuum lift process, Vacuum induction furnace).

Helmut Knüppel, Albrecht Drevermann und Franz Oeters, *Stahl und Eisen*, **79**, 414–419, 1959.

37. Metallurgy, Inorganic Chemistry and Analytical Chemistry

37

144. Production Mass Spectrometer.
Engineer, **208**, 5403, 78, 14 Aug. 1959.

37 : 49

145. Oxidation of Silicon Carbide in the Temperature Range 1200 to 1500°.
Note by Robert F. Adamsky, *J. Phys. Chem.*, **63**, 305–307, Feb. 1959.

37

146. The Fractionation of Oxygen Isotopes between Water and Sulfur Dioxide.
L. L. Brown and J. S. Drury, *J. Phys. Chem.*, **63**, 1885–1886, Nov. 1959.

37

147. New Vacuum-Melting Furnace.
This note gives some of the pertinent features of a full-scale, pilot consumable-electrode vacuum-melting furnace.
Note by D. Freiday, *Mech. Eng.*, **81**, 73, Nov. 1959.

37

148. High-Temperature Pressure-Vacuum Furnace.
William Ladding and Laurence Hammell, *Rev. Sci. Instrum.*, **30**, 885.

37

149. High Temperature Laboratory Vacuum Furnace.
E. V. Komelsen and J. O. Weeks, *Rev. Sci. Instrum.*, **30**, 290.

37

150. Vacuum Degassing in Ladle—A New Technique in Steelmaking.
Hydrogen and other gases are removed from molten steel while it is in the ladle. By purging with helium while the vacuum is being drawn, hydrogen is reduced to less than 2 ppm in about 15 min. This new technique permits steel from one heat to be poured into several ingots. (Author)

Anon., *Metal Progress*, **76**, 111–114, Sept. 1959.

37

151. Mechanical Testing with a 3000°F Radiant Heat Furnace.
A radiant heat furnace which operates up to 3000°F is powered by quartz pencil lamps. The test chamber is designed to use any atmosphere—air, vacuum, partial pressure, pressure or inert gases. A. G.

J. K. Hoy, *Metal Progress*, **76**, 81–83, Sept. 1959.

37

152. A New Tool for Case Carbon Evaluation.
A direct reading vacuum spectrograph can be used to determine the carbon gradient in steel. This method is compared with analyses of carbon by combustion. (Author)

Alan Goldblatt, *Metal Progress*, **76**, 87–88, Sept. 1959.

37

153. Degassing and Vacuum Refining Furnace.
Engineer, **208**, 5415, 569, 6 Nov. 1959.

Materials and Techniques used in Vacuum Technology

39. Miscellaneous Applications

39

154. Synthesis of Boron Phosphide and Nitride.
United Kingdom. Letter by R. C. Vickery, *Nature*, **184**, Suppl. No. 5, 268, 25 July 1959.

40. Gases and Vapours

40

155. Non-Equilibrium Properties of Rare Gases.
Note by M. P. Madan, *J. Phys. Chem.*, **62**, 893–894, July 1958.

40

156. Heating by Electron Bombardment.
United Kingdom. This is a report of the symposium on " Electron Bombardment Floating-Zone Melting and Allied Electron Bombardment Techniques ", held at the Services Electronics Research Laboratory, Baldock, Herts, on 10 March 1959.

A. Calverley, *Nature*, **184**, No. 4687, 692–693, 29 Aug. 1959.

40

157. Effect of Argon and Helium on the Thermal Conductivity of the N_2O_4 $2NO_2$ System.

Kenneth P. Coffin, *J. Chem. Phys.*, **31**, 1290–1297, Nov. 1959.

40

158. Adsorption Diffusion and Evaporation of Carbon Monoxide on Tungsten.
Ralph Klein, *J. Chem. Phys.*, **31**, 1306–1313, Nov. 1959.

40

159. Molecular Ions.
Robert N. Varney, *J. Chem. Phys.*, **31**, 1314–1316, Nov. 1959.

40

160. Probability of Double Ionization by Electron Impact for Neon, Argon and Xenon.
J. D. Morrison and A. J. C. Nicholson, *J. Chem. Phys.*, **31**, 1320–1323, Nov. 1959.

40

161. Diffusion Coefficient of Atomic Hydrogen through Multicomponent Mixtures.
Note by Henry Wise, *J. Chem. Phys.*, **31**, 1414–1415, Nov. 1959.

40

162. Effect of Water Vapor on the Dissociation of Hydrogen in an Electrical Discharge.
Note by Thomas N. Shaw, *J. Chem. Phys.*, **31**, 1142–1143, Oct. 1959.

40

163. Molecular Dissociation and Reconstitution on Solids.
Gert Ehrlich, *J. Chem. Phys.*, **31**, 1111–1126, Oct. 1959.

40

164. On the Velocity Distribution in a Chemically Reacting Gas.
The departure of the velocity distribution function from the Maxwellian form and the corresponding correction to the reaction-rate formula have been calculated for a gas undergoing a slow bimolecular reaction. Kinetic theory methods based on the Boltzmann transport equation have been used. The calculations take into account the effect of the reaction in depleting the tail of the Maxwell distribution, but do not take into account the effects of the heat of reaction. It is found that when kT is one-fifth the activation energy, the reaction rate is 8 per cent less than that predicted by the conventional simple collision theory. A. G.

R. D. Present, *J. Chem. Phys.*, **31**, 747–750, Sept. 1959.

41. Metals and Alloys

41

165. Measuring the Thermal Emissivity of Strip Materials.
To determine the total thermal emissivity of metallic strip materials used in the construction of electron tube components, a method is described which permits making such measurements in less than 10 min. with a reproducibility of one to two per cent in air up to temperatures of about 350°C. A square sample, $\frac{1}{2}$ in. on its side, to which a 0.002-in.-dia. chromel-alumel wire has been welded at the center, is supported by thin invar or " Kovar " wires within a box. Facing the sample are three partitions provided with apertures slightly larger in dia. than that of the sample. The radiation from an infrared heat lamp, mounted outside the box, impinges on the sample surface which has been uniformly blackened over an oxygen-free gas flame. By comparing the temperature readings, T_1 and T_2, obtained first with one side of the sample blackened and then with both sides blackened while the energy input and the temperature in the box are held constant at 43.2°C (for convenience, because $T_2^4 = 10 \times 10^9$°K). The emissivity of the unblackened surface is obtained from applying Stefan–Boltzmann's equation to the two cases, i.e.

$$\frac{\epsilon_2}{\epsilon_1} = e = \frac{2(T_1^4 - T_2^4) - (T_2^4 - T_0^4)}{T_2^4 - T_0^4} \qquad (\text{for } \epsilon_1 \sim 1)$$

" Carbonized surfaces with a loose-powder type of carbon deposit will measure from 93 to 98 per cent that of a true black body. Carbonized surfaces that have been polished will vary from 80 to 90 per cent depending upon the degree of polish. Aluminum-clad or aluminized surfaces vary from 88 to 93 per cent, depending on the type of transformation process used in manufacturing. Monocarb surfaces may vary from 70 to 88 per cent, depending on the control of carbon removal or brushing. Nickel-plated surfaces ordinarily used for tube plate parts may vary from 60 to 75 per cent ". W. H. K.

D. R. Kerstetter, *Sylvania Technol.*, **12**, 118–120, Oct. 1959.

41

166. Spectral Emittance of Ceramic-Coated and Uncoated Specimens of Inconel and Stainless Steel.
The normal spectral emittance of Inconel and type 321 stainless steel specimens with six different surface treatments, including application of National Bureau of Standards ceramic coatings A-418 and N-143, was determined at 900°, 1200°, 1500°, and 1800°F over the wave-length range 1.5 to 15γ. The specimens with different surface treatments had markedly different spectral emittance curves. The bare polished specimens had the lowest spectral emittance at all wave lengths, and the specimens coated with A-418 had the highest spectral emittance over most of the range 5 to 15γ. The spectral emittance of all specimens increased with temperature at all wave lengths. (Author)

J. C. Richmond and J. E. Stewart, *J. Amer. Ceram. Soc.*, **42**, 633–640, Dec. 1959.

41

167. The Behavior of Rhenium in Electron Tube Environments.
Rhenium, tungsten, and rhenium-coated tungsten have been exposed to carburizing atmospheres and to water-cycle attack, rhenium and tungsten to aluminum oxide at 1750°C for 7000 hr,

and rhenium to boron-containing atmospheres. It was confirmed that rhenium, unlike most other refractory metals, does not form a carbide. Rhenium forms a boride, which forms a eutectic with another boride or with rhenium, and melts under 2250°C. Thoriated rhenium maintains microstructural and mechanical integrity after long exposure in vacuum at 1750°C in contact with alumina. Rhenium and rhenium-coated tungsten are highly resistant to water-cycle effects. (Author)

G. B. Gaines, C. T. Sims, and Robert I. Jaffee, *J. Electrochem. Soc.*, **106**, 881–885, Oct. 1959.

41 : 16

Surface Properties of Germanium. See Abstract No. 16.

41 : 36

Processing Techniques Used in Degassing during Casting of Rolling and Forging Steels based on the Vacuum Lift Process. See Abstract No. 137.

41 : 36

Vacuum Degassing of Low Carbon Unkilled Steel during Casting or during Solidification into Block Form. I. Degassing of Unkilled Soft Steel Under Vacuum. See Abstract No. 138.

41 : 36

Vacuum Degassing of Low Carbon Unkilled Steel during Casting or during Solidification into Block Form. II. Casting by Stream Degassing of Unkilled Soft Steel. See Abstract No. 139.

41 : 36

Methods of Heating for Large Scale Industrial Degassing of Molten Steel. See Abstract No. 140.

41 : 36

Steel Degassing Based on the Circulating Degassing Process. See Abstract No. 141.

41 : 36

Measurements and Control during the Vacuum Degassing of Molten Steel. See Abstract No. 142.

41 : 36

The Removal of Oxygen in the Treatment of Steel Melts in Vacuum. See Abstract No. 143.

42. Glass and Ceramics

42

168. Precipitation in Microscopic Cracks.
It is shown that precipitation occurs in Griffith-type surface cracks in solids from solutions or from vapors under conditions in which a plane surface would be dissolved or vaporized. A reduction in the equilibrium vapor pressure at the crack tip from that of a plane surface is produced by the driving force to reduce the surface energy of the crack. An equation is derived relating vapor pressure at the tip of the crack to vapor pressure over an infinite plane. This relation is used in deriving an expression for the fill-up of cracks with time. Experimental data on the measurement of the retreat of the crack edge with time appear to be in good agreement with the derived expression. A discussion of the effect of such crack healing on the mechanical properties of the solids is included. (Author)

G. R. Pulliam, *J. Amer. Ceram. Soc.*, **42**, 477–482, Oct. 1959.

42

169. Breaking Stress of Glass Determined from Dimensions of Fracture Mirrors.
Relations previously have been shown between the size of the fracture mirror and the nominal breaking stress. In the present paper, this relation is derived analytically involving one unknown quantity which must be determined experimentally. This quantity is $\sigma_m\sqrt{\rho}$, where σ_m is the intrinsic strength of the glass and ρ the effective radius of the crack tip. Tests on glass rods indicated that the breaking stress could be determined from the radius of the fracture mirror. For 80 per cent of the specimens the values obtained were within 8 per cent of those obtained from the test loads. (Author)

E. B. Shand, *J. Amer. Ceram. Soc.*, **42**, 474–477, Oct. 1959.

42 : 53

170. Strength of Synthetic Single Crystal Sapphire and Ruby as a Function of Temperature and Orientation.
The modulus of rupture of sapphire single crystals was determined as a function of temperature for specimens with orientations favoring plastic deformation and for specimens with unfavorable orientations. From 600°C to 1000°C, the strength of both types increased with increasing temperature, but the increase was more pronounced for the former. Ruby specimens oriented favorably for plastic deformation also showed a large increase in strength. It is conjectured that the increase in strength results from stress relief by microscopic plastic deformation. (Author)

J. B. Wachtman, Jr., and L. H. Maxwell, *J. Amer. Ceram. Soc.*, **42**, 432–433, Sept. 1959.

42 : 53

171. Internal Stresses in Model Ceramic Systems.
Model ceramic systems of crystals and glass fabricated by vacuum hot compaction were used to study methods of detection of internal stress on the crystalline phase. Effects of the volume fraction of the glass, compaction temperature and time, and crystal particle size in modifying induced internal stress are presented. These effects, together with X-ray diffraction and wetting studies, indicate that internal stress development is closely connected to setting of the crystal by the glass and the formation of a second crystalline phase. Limited results regarding influence of internal stress on strength of ceramic bodies indicate that increasing internal stress on the crystal phase decreases the modulus of rupture when the particle size of the crystal component remains constant. The results of this work indicate that the full potential of ceramic systems may not be realized with the presence of internal stress. (Author)

R. M. Fulrath, *J. Amer. Ceram. Soc.*, **42**, 423–429, Sept. 1959.

42

172. The Dielectric Behavior of Solids Embedded in a Homogeneous Medium.
Dielectric constant and tan δ of powdered crystal phases of alumina, quarts, and wollastonite were determined. Since it is very difficult to obtain dielectric measurements of very fine (powdered) crystals, a technique of embedding the solids in a homogeneous medium was used. The relationship between particle shape and volume present in the composite to the dielectric properties of such fine powders was in accord with that indicated by Niesel's theory. (Author)

Barlane R. Eichbaum, *J. Electrochem. Soc.*, **106**, 804–809, Sept. 1959.

42

173. Improved Apparatus for Rapid Measurement of Viscosity of Glass at High Temperatures.
An apparatus is described for measuring the viscosity of glass in the range 6.5 to 13,000 poises. About 15 min/point are required to establish a viscosity-versus-temperature curve. About 75 gm of glass are required for a determination. Precision is good, repair is simple, and maintenance is low. The apparatus is suitable for either research or control purposes. (Author)

R. L. Tiede, *J. Amer. Ceram. Soc.*, **42**, 537–541, Nov. 1959.

42

174. Strength and Static Fatigue of Abraded Glass under Controlled Ambient Conditions. I. General Concepts and Apparatus.
An extensive experimental study of the factors affecting the tensile strength and static fatigue of bulk glass has been conducted. To minimize the effects of past history of the specimens, all specimens were subjected to a controlled, reproducible surface abrasion. Time, temperature, and chemical environment were subject to control and systematic variation during the period from abrasion to test and during the strength test itself. Specimens consisted of flat laths tested in cross bending with the abraded spot in the center of the tension face. An electronically controlled electromagnetic tester permitted applications of pulse loads or constantly increasing loads with controllable durations from about 0.0025 sec up to any desired value. The apparatus and methods for producing the abrasions, controlling the environment, and performing the tests are described in this paper. A brief review of the experimental background on the strength of glass is also presented as an introduction to the aims and concepts of this study. (Author)

R. E. Mould and R. D. Southwick, *J. Amer. Ceram. Soc.*, **42**, 542–547, Nov. 1959.

42

175. Strength and Static Fatigue of Abraded Glass under Controlled Ambient Conditions. II. Effect of Various Abrasions and the Universal Fatigue Curve.
A controlled grit blast was found to be a reproducible method of producing standardized damage to a glass surface. The effects of grit size, blast pressure, and amount of grit on the strength of the resulting specimens are reported. Static fatigue curves (strength vs. load duration) were obtained for specimens immersed in room-temperature distilled water and in liquid nitrogen (77°K) after the specimens had been subjected to various abrasion treatments. The low-temperature strength was independent of load duration, and for surface damage of simple geometry it was inversely proportional to the square root of the initial crack depth, consistent with the Griffith theory. Abrasions of different geometry produced differing static fatigue curves at room temperature, and in one case curves actually crossed. If, however, the strength values for each abrasion were divided by the low-temperature strength for that abrasion and plotted vs. a reduced time coordinate, all the data could be fitted to a single " universal fatigue curve." This analysis led to a clear distinction between " linear " and " point " flaws, the former being flaws (such as emery scratches) which have an extension in a direction perpendicular to the applied stress and the latter being of a more localized character. Linear flaws fatigue more rapidly than point flaws by a factor of fifty and for each type of damage the fatigue rate is inversely proportional to the exponential of the initial flaw depth. A detailed analysis of the data in terms of several static fatigue theories from the literature shows that none of them provides a complete and adequate explanation of these results. (Author)

R. E. Mould and R. D. Southwick, *J. Amer. Ceram. Soc.*, **42**, 582–592, Dec. 1959.

42

176. Effect of Fluorides on Infrared Transmittance of Certain Silicate Glasses.
Relatively large amounts of fluorides can be incorporated into silicate glasses without producing opalescence or turbidity if certain oxides, such as La_2O_3 or Ta_2O_5, are included in the glass composition. In most cases, the fluorides reduce the absorption at the 2.75-μ water band, thus improving the glasses for use as infrared material. The fluorides also decrease the refractive index values of the glasses. Striae are produced in the glasses when the fluoride content is more than about 4 mole per cent. (Author)

G. W. Cleek and T. G. Scuderi, *J. Amer. Ceram. Soc.*, **42**, 599–603, Dec. 1959.

42

177. Thermal Conductivity. XIV. Conductivity of Multicomponent Systems.
The thermal conductivity of a number of multicomponent systems has been determined as a function of composition and temperature. There were silicate glasses, MgO–NiO, Al_2O_3–Cr_2O_3, UO_2–UO_{2+x}–ThO_2, ZrO_2–HfO_2–CaO, MgO–Mg_2–SiO_4, MgO–BeO, Al_2O_3-mullite, MgO–$MgAl_2O_4$, Al_2O_3–ZrO_2, Al_2O_3-glass, and Si–SiC. Analyses of these results indicate that a second component in solid solution markedly lowers the thermal conductivity. The second-component scattering mean free path is inversely proportional to concentration at low concentrations and independent of temperature at the temperatures studied (above room temperature). The conductivity of each polyphase ceramics can be predicted if the conductivity of each phase, amount of each phase, and phase distribution (including pore phase) are known. (Author)

W. D. Kingery, *J. Amer. Ceram. Soc.*, **42**, 617–627, Dec. 1959.

42

178. Fifth International Glass Congress Organised by the International Commission for Glass in Munich.
Short reports are given of the lectures given in the period 29.6 to 4.7.1959 based on the summaries prepared by the German glass technical society. The lectures are considered in the following divisions : Technical Scientific lectures including the physics and chemistry of glasses (thermal expansion), and lectures concerning the history and formation of glass.

Glas. Email, **92**, 399–401, 421, 447–451, 1959.

42 : 43

179. " Araldite." An Artificial Resin for Preparing Working Models in the Ceramics Industry.
Araldite glues (ethoxyline resins) are used for joining various materials (light metals, steel, ceramics, glass, vulcanised rubber, hardened plastic, cork, leather, textiles, etc.). Applications and fabrication are reported on.

K. Leutner, *Glas. Email*, **92**, 377–378, 1959.

42 : 33

Interferometric Calibration of Quartz End-Measuring Rods. See Abstract No. 131.

42 : 35

Low-Melting Inorganic Glasses with High Melt Fluidities below 400°C. See Abstract No. 135.

43. Plastics and Elastomers

43

180. Cleaning Techniques for Rubber O-Rings Used in Vacuum Systems.
J. R. Young, *Rev. Sci. Instrum.*, **30**, 291.

43 : 52

181. Irradiation of Polyethylene. IV. Oxidation Effects.
H. Matsuo and M. Dole, *J. Phys. Chem.*, **63**, 837–843, June 1959.

43 : 42

" Araldite ". An Artificial Resin for Preparing Working Models in the Ceramics Industry. See Abstract No. 178.

44. Waxes, Lubricants, Cements, Lacquers, Paints, Oils

44

182. When to Consider Automatic Spray Equipment.
Warren Beach, *Metal Finishing*, **57**, No. 10, 69–71, Oct. 1959.

Vol. 10 196

44

183. Applying Decorative Effects to Molded Plastics.
W. H. Rohr, *Industrial Finishing*, 22–42, Nov. 1959.

44

184. The Oscicator, a New Flow Coater.
An entirely new concept of flow coating. Low solvent loss and any part or piece that can be power machine washed can be flow coated. Old flow coaters may be converted to the new type with a conversion package. Color changes are simple and fast.

E. A. Zahn, *Industrial Finishing*, Oct. 1959.

45. Soldering, Welding and Brazing

45

185. Copper Welding for Maximum RF Conductivity.
E. F. McLaughlin, *Rev. Sci. Instrum.*, **30**, 372.

46. Glass Blowing, Glass-to-metal and Ceramic-to-metal Sealing Techniques

46

186. Metal-Glass Vacuum Seal for Use at Low Temperatures.
N. de Haas, *Rev. Sci. Instrum.*, **30**, 594.

47. Outgassing Data, Vapor Pressure Data, Gettering Data

47

187. Titanium as a Gettering Material.
United States. It was found that barium getters would not hold a cathode ray tube at a pressure much lower than 10^{-6} torr. An investigation of titanium metal as a getter material was carried out. An ion pump was first used. This pump consisted essentially of an electron emitting tungsten source, an accelerating grid and a negatively charged titanium coating which could trap and absorb positively charged particles. The titanium film was evaporated from a heavy tungsten filament. However it was found that a comparable pumping action could be obtained merely by the use of a wall coating of titanium metal without the use of the ion-forming system (pressures were measured using a Penning gauge). The superior gettering power of titanium was demonstrated by making two identical tubes of "Pyrex" each containing one getter material. Each tube was connected to an ion gauge. After outgassing for 1 hr at 350°C the system was sealed off at 5×10^{-5} torr. The tube containing barium was fired and the pressure fell to 6×10^{-7} torr but the tube containing titanium fell to 2×10^{-8} torr (probably limited by the gauge). The ion gauge was in operation during the experiments and its pumping action was an embarrassment to accurate measurement. A second series of experiments were carried out using gauges of the Alpert type. Two tubes complete with electron gun and phosphor screen one containing a conventional barium getter, the other containing a titanium getter were given identical treatment. They were sealed and disconnected from a common pumping system at a pressure of 3×10^{-5} torr after a short outgassing period at 325°C. After 30 days the pressures were measured and the getters were fired. The pressure measurements were recorded on a diagram which shows pressure against time for the two tubes. The results show a marked superiority of the titanium except when a very large amount of gas was liberated by strongly over running the cathode filament. In this case similar results were obtained. As a result of this work two important points have been determined.
(i) Oil vapour seems to poison titanium films to a greater extent than barium films.
(ii) It is desirable to flash the getter quickly in order to deposit a porous layer.
It is concluded that the use of titanium as a flash getter gives significantly lower residual pressures in most sealed off vacuum envelopes.

Letter by R. L. Stow, *Nature*, **184**, Suppl. No. 8, 542–543, 15 Aug. 1959.

47

188. Vapor Pressure of Thorium Tetrafluoride.
Note by A. J. Darnell and F. J. Keneshea, Jr., *J. Phys. Chem.*, **62**, 1143–1145, Sept. 1958.

47

189. Vapor Pressures and Molecular Composition of Vapors of the RbF-ZrF_4 and LiF-ZrF_4 systems.
K. A. Sense and R. W. Stone, *J. Phys. Chem.*, **62**, 1411–1418, Nov. 1958.

47

190. Vaporization Characteristics of p-Dibromobenzene.
United States. Vapor pressures of *p*-dibromobenzene have been measured in the temperature range −45 to 74° using effusion, gas saturation and static techniques : log $Patm = -3850T^{-1} + 8.80$. Condensation coefficients, estimated from effusion pressure dependence on cell geometry, range from near unity at the lowest temperatures to *ca.* 0.025 at 13°. (Author)

J. H. Stern and N. W. Gregory, *J. Phys. Chem.*, **63**, 556–559, April 1959.

47

191. Method for Rapid Determination of Vacuum Outgassing Rates.
Ivory P. S. Fish, *Rev. Sci. Instrum.*, **30**, 889.

47

192. An Investigation of Some Vaccum Properties of Epoxy Resins.
E. A. Kolenko and V. G. Iurev, *Sov. Phys. Tech. Phys.*, **3** (Transl.), 2073.

47 : 16

The Structure of Gas-Adsorbent Carbons. See Abstract No. 44.

47 : 17

Dissociation Pressure and Stability of Beryllium Carbide. See Abstract No. 61.

47 : 17

The Vaporization of Molybdenum and Tungsten Oxides. See Abstract No. 64.

49. Miscellaneous Materials and Techniques

49

193. Translucent Phosphor Coatings in High-Pressure Mercury-Vapor Lamps.
C. H. Haake, *J. Electrochem. Soc.*, **106**, 866–870, Oct. 1959.

49

194. Molybdenum Disulfide of High Surface Area.
Note by F. T. Eggertsen and R. M. Roberts, *J. Phys. Chem.*, **63**, 1981–1982, Nov. 1959.

49

195. Electrical Conductivity of Single Crystals of MgO.
The electrical conductivity of magnesium oxide at temperatures in the region of 1300°C is observed to depend upon the partial pressure of oxygen surrounding the sample. The conductivity increases at oxygen pressures both higher and lower than 10^{-5}

atmospheres. At this pressure the conductivity is a minimum. This effect is increased as the iron content is increased and is almost absent in the purest samples.

The conductivity is electronic rather than ionic and the number of charge carriers is controlled by the number of lattice vacancies. The dependence of conductivity on oxygen pressure may be satisfactorily explained by changes in stoichiometry and thus lattice defects in magnesium oxide. These changes in stoichiometry are larger when the magnesium oxide is contaminated with a variable valence impurity like iron than when it is pure. (Author)

S. P. Mitoff, *J. Chem. Phys.*, **31**, 1261–1269, Nov. 1959.

49 : 37

Oxidation of Silicon Carbide in the Temperature Range 1200 to 1500°. See Abstract No. 145.

Vol.
10
1960

Basic Science and Engineering

51. Physics, Astronomy and Geophysics

51 : 14
Calcium Atomic Beam Source and Interference Beyond Two Meter Retardation. See Abstract No. 3.

51 : 19
Design of High-Resolution Monochromator for the Vacuum Ultra-violet. An Application of Off-Plane Eagle Mounting. See Abstract No. 82.

51 : 19
Phase Changes on Reflection from Evaporated Chromium Films. See Abstract No. 83.

51 : 19
The Theory of the High Frequency Brush Discharge. See Abstract No. 84.

51 : 34
Dissipation of Planetary Atmospheres. See Abstract No. 134.

52. Physical Chemistry

52
196. Surface Functionality of Amorphous Silica by Infrared Spectroscopy.
R. S. McDonald, *J. Phys. Chem.*, **62**, 1168–1178, Oct. 1958.

52
197. The Molecular Composition of Sodium Iodide Vapor from Molecular Weight Measurements.
United States. A technique has been developed for the determination of the molecular weight of vapors at high temperatures, by measurement of the pressure at constant vapor density, the pressure measuring device being a molten gold manometer. For the dissociation of Na_2I_2 into NaI measurements from 1175 to 1350°K indicate a ΔE° of 40.2 kcal. mole^{-1} and a ΔS° of 27.0 e.u. at 1260°K. (Author)

S. Datz and W. T. Smith, Jr., *J. Phys. Chem.*, **63**, 938–940, June 1959.

52
198. Ion-Molecule Reactions of 1, 3-Butadiene, of Acetylene and of Acetylene-Methane Mixtures.
United States. The reactions with molecules of positive ions formed in the electron bombardment of 1, 3-butadiene, of acetylene and of acetylene-methane mixtures in the ionization chamber of the mass spectrometer have been investigated. Appearance potentials of the more important primary ions of 1, 3-butadiene have been measured as well as the appearance potentials of all secondary ions. The heats and cross-sections of ion-molecule reactions have been calculated. (Author)

R. Barker, W. H. Hamill, and R. R. Williams, Jr., *J. Phys. Chem.*, **63**, 825–828, June 1959.

52
199. Interaction of Oxygen with Titanium Dioxide.
United States. Reversible oxygen adsorption has been measured on commercial grade titanium dioxide powder at 500, 700 and 900° as a function of the ambient pressure by a weighing technique. No oxygen adsorption is detectable in highly purified TiO_2 in the same temperature range. Mass losses have been recorded in a dynamic high vacuum as a function of temperature for highly purified TiO_2 " bulk " and also for purified TiO_2 containing various quantities of BaO, TiF_4 and Na_2O. Details of the techniques employed for carrying out the measurements are discussed. Interpretation of the mass changes observed in the bulk material indicates that " dehydration " of TiO_2 is complete at 800° and that incipient decomposition of bulk TiO_2 occurs at 875° in a dynamic vacuum of 10^{-6} mm. The reversible oxygen adsorption is believed to occur at surface impurity centers. (Author)

A. W. Czanderna and J. M. Honig, *J. Phys. Chem.*, **63**, 620–626, April 1959.

52
200. Chemical Effects of Low Energy Electrons.
R. R. Williams, Jr., *J. Phys. Chem.*, **63**, 776–780, June 1959.

52
201. Dissociation of C_2H_5T and 1, 2-$C_2H_4BrBr^{82}$ by β-Decay.
S. Wexler and D. C. Hess, *J. Phys. Chem.*, **62**, 1382–1389, Nov. 1958.

52 : 16
The Time Lag in Diffusion IV. See Abstract No. 35.

52 : 16 : 30
Surface Reactions on Evaporated Palladium Films. See Abstract No. 45.

52 : 30
Diffusion of Silver in Silver Sulfide. See Abstract No. 102.

52 : 30
Heterogeneous Reaction Studies by Infrared Absorption. See Abstract No. 103.

52 : 30
Physical Techniques in the Study of Silver Catalysts for Ethylene Oxidation. See Abstract No. 104.

52 : 30
Calculation of the Performance of a High-Vacuum Thermionic Energy Converter. See Abstract No. 106.

52 : 30
Selective Delineation of Screw Dislocations by Cathodic Sputtering. See Abstract No. 107.

52 : 43
Irradiation of Polyethylene. IV. Oxidation Effects. See Abstract No. 180.

53. Metallurgy, Ceramics and Inorganic Chemistry

53
202. Magnetic Ceramics. VI. Evaluation of Some Methods of Nickel Ferrite Formation.
The extent of nickel ferrite formation, as affected by four preparatory techniques, was investigated by determining the magnetic moment of the reacted powder with a vibrating-coil magnetometer. The oxide, carbonate, hydroxide, and oxalate methods were used. At low temperatures the hydroxide and oxalate techniques were found to give the greatest yield of ferrospinel. The hydroxide method yielded a magnetic material by precipitation. Weight-loss measurements were correlated to the magnetic data. (Author)

George Economos, *J. Amer. Ceram. Soc.*, **42**, 628–632, Dec. 1959.

53

203. Corrosion Research at the National Bureau of Standards. To provide science and industry with solutions to some of the practical engineering problems encountered to-day, the National Bureau of Standards is investigating the primary processes of corrosion. Large, single metal crystals are employed in some of the research to correlate corrosion with the arrangement of atoms in the crystal lattice. The parts played by electrical phenomena and cathodic protection comprise a phase of the programme. One study deals with the nature and mechanism of formation of oxide films on metal surfaces. The effect of illumination on the corrosion reaction has also been studied. By attacking the problem from different directions, the Bureau's corrosion research staff hopes to improve the present methods of combating corrosion. (Author)

Engineer, **208**, 5410, 371, 2 Oct. 1959.

53 : 42

Strength of Synthetic Single Crystal Sapphire and Ruby as a Function of Temperature and Orientation. See Abstract No. 169.

53 : 42

Internal Stresses in Model Ceramic Systems. See Abstract No. 170.

54. Biology, Biochemistry, Pharmaceutics, Toxicology, Organic Chemistry

54

204. Mass Spectrometer for Respiratory Studies.
Engineer, **208**, 5413, 485, 23 Oct. 1959.

59. Miscellaneous

59

205. Spectral Study of a Visible, Short-Duration Afterglow in Nitrogen.
G. E. Beale, Jr., and H. P. Broida, *J. Chem. Phys.*, **31**, 1030–1034, Oct. 1959.

59

206. On the Trapping of Free Radicals of Oxygen and Chlorine.
Sidney W. Benson and Kenneth H. Anderson, *J. Chem. Phys.*, **31**, 1082–1085, Oct. 1959.

Vol.
10
196

VACUUM

Ein Partialdruckvakuummeter nach dem Prinzip des elektrischen Massenfilters

KARL-GEORG GÜNTHER

Laboratorium ZW|LS der Siemens-Schuckertwerke A.G., Nürnberg, Deutschland

A Partial Pressure Vacuum Gauge working according to the Principle of the Electrical Mass Filter

KARL-GEORG GÜNTHER

Laboratorium ZW|LS der Siemens-Schuckertwerke A.G., Nuremberg, Germany

01.
10
960

1. Einleitung

In jüngster Zeit werden zahlreiche Arbeiten bekannt, die sich mit der Untersuchung der Gaszusammensetzung in evakuierten Behältern befassen. Ziel dieser Arbeiten ist einserseits die Erforschung des Ultrahochvakuums sowie der zu seiner Erzeugung bestehenden Möglichkeiten. Andererseits machen die mannigfachen und zunehmend angewandten Methoden der Vakuumverfahrenstechnik eine Aufklärung und messende Kontrolle der hierbei ablaufenden Prozesse wünschenswert, wie sie durch Aussagen über die Art und Menge der freiwerdenden Gase und Dämpfe möglich sind. Beispielsweise wird die sinngemässe Steuerung einer Metallentgasung wesentlich erleichtert, wenn die Art und der zeitliche Verlauf der hierbei freigesetzten Gase und Dämpfe bekannt sind. Das gleiche gilt von den zahlreichen Anwendungsgebieten der Vakuumtrocknung.

Unter den verschiedenen für die Partialdruckmessung verwendeten Methoden haben die massenspektrometrischen Verfahren bisher die zuverlässigsten Angaben geliefert. Die Anforderungen an ein Gerät nach diesem Prinzip sind dabei wesentlich anders als in der üblichen Massenspektroskopie : Es wird eine Anordnung bevorzugt, die bei mässigem Aufwand und einfacher Bauweise wenig störanfällig ist ; insbesondere soll durch ein kleines Volumen der Messzelle der eigentliche Vakuumprozess nicht oder nur wenig beeinflusst werden. Von grosser Bedeutung ist eine eindeutige und reproduzierbare Beziehung zwischen Ionenstrom und

1. Introduction

In very recent times a number of papers have been published dealing with investigations on the composition of gases in evacuated vessels. The aim of this work was, on the one hand, research into problems of ultra high vacuum and the possibility of achieving the same. On the other hand, the varied and growing number of applications of new methods in vacuum processing techniques make it desirable to understand, measure and control the processes. This is made possible by determining the type and quantity of gases and vapours released. For example, the control of a metal degassing process is considerably simplified if the nature and variations in time, of the gases and vapours given off during the process, are known. The same applies to the numerous applications of vacuum drying.

Of the many methods of measuring partial pressures those based on mass spectrometrical devices have to date given the most reliable results. The requirements of a mass spectrometer for this application are, however, essentially different to the requirements of the usual mass spectroscopy ; an arrangement is favoured which should be fairly simple in construction, reasonably cheap and not liable to give trouble in use ; it is desirable that the measuring cell should have a small volume so that the vacuum process proper is influenced very little, or not at all. Of very great importance is a definite and reproducible relationship between ion current and partial pressure. On the other hand, in most cases a

Partialdruck. Demgegenüber genügt in den meisten Fällen ein Auflösungsvermögen von $m/\Delta m = 40$ bis 60 und ein damit erfassbarer Massenbereich, der sich etwa bis zur Masse 70 erstreckt. Die in den letzten Jahren auf diesem Gebiet vorgenommenen Untersuchungen haben im wesentlichen zur Ausbildung von drei auf dem Prinzip des Massenspektrometers beruhenden Haupttypen von Partialdruckmessern geführt. (Bild 1).

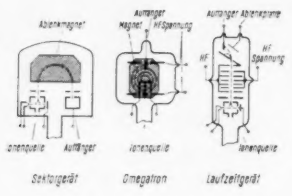

BILD 1. Verschiedene Massenspektrometer mit Eignung zur Partialdruckmessung.

Die erste Type stellt ein vereinfachtes Sektormassenspektrometer konventioneller Bauart dar, d.h., die aus der Ionenquelle mit homogener Geschwindigkeit austretenden Ionen werden in einem magnetischen Sektorfeld gemäss ihrer verschiedenen Massen voneinander getrennt[1].

Die zweite Type, das sogenannte Omegatron arbeitet nach Art eines Miniaturzyklotrons, in dem die unter Einfluss eines elektrischen Hochfrequenzfeldes der Frequenz ω und eines Magnetfeldes B aufgespulten Ionen nur dann den Auffänger erreichen, wenn sie der Zyklotronresonanzbedingung genügen[2, 3].

$$m = \frac{e \cdot B}{\omega} \tag{1}$$

Die dritte Type, das sogenannte Laufzeitmassenspektrometer erreicht die Massentrennung auf rein elektrischem Weg. Hierzu werden die unterschiedlichen Laufzeiten der homogen eingeschossenen Ionen verschiedener Massen ausgenutzt, die zum Durcheilen definierter Strecken notwendig sind[4, 5].

Sämtliche der genannten Geräte haben sich auf verschiedenen Gebieten des sauberen Hoch- und Ultrahochvakuums bewährt und interessante Aussagen möglich gemacht. Eine Anwendung an industriellen Anlagen wird hingegen durch den empfindlichen Aufbau, die Störanfälligkeit gegenüber verschiedenen Dämpfen und vor allem das Versagen bei höheren Drucken, d.h. im Gebiet oberhalb 10^{-5} bezw. 10^{-4} Torr erschwert.

Vor einigen Jahren wurde von Paul und Steinwedel ein neuartiges Verfahren zur Massentrennung beschrieben—das sogenannte elektrische Massenfilter[6]—welches gemäss seiner Wirkungsweise als Partialdruckmesser besonders geeignet ist und für verschiedene Anwendungszwecke den obengenannten Typen überlegen ist.

resolving power of $m/\Delta m = 40$–60 should be sufficient to cover a mass range up to about mass 70.

Investigations in the last years in this field have essentially led to the development of three main types of partial pressure measuring instruments working according to the principle of the mass spectrometer (see Fig. 1).

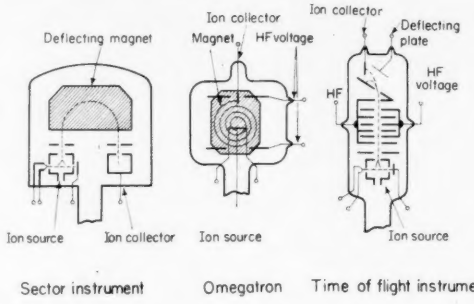

FIG. 1. Different mass spectrometers suitable for measuring partial pressure.

The first type is a simplified Sector Mass Spectrometer of conventional construction, i.e. the ions leaving the ion source with a homogeneous velocity are separated in the magnetic sector field according to their different masses[1].

The second type, the so-called Omegatron, works according to the principle of a miniature cyclotron in which, under the influence of an electrical high frequency field of frequency ω and a magnetic field B, certain ions will only reach the sector if they satisfy the cyclotron resonance condition[2, 3].

$$m = \frac{e \cdot B}{\omega} \tag{1}$$

The third type, the so-called Time of Flight Mass Spectrometer, achieves mass separation by purely electrical means. In this device the differing times of flight of homogeneously injected ions of different masses, which are necessary to cover a fixed distance[4, 5] is employed.

All of the devices mentioned have found useful application in the different fields of clean high and ultra high vacuum and made it possible to obtain interesting results. Application to industrial plant has, however, been very difficult. This is due to their delicate construction, their liability to be affected by the presence of certain vapours and especially due to their failure to operate at higher pressures, i.e. in the range above 10^{-5} Torr.

A few years ago a new method of mass separation was described by Paul and Steinwedel, the so-called electrical mass filter[6] which due to its method of operation is specially suited to measure partial pressures and for many applications is superior to the types mentioned above.

Vol. 10 196

2. Prinzip des elektrischen Massenfilters

Eine Anordnung nach dem Prinzip des elektrischen Massenfilters ist schematisch in Bild 2 dargestellt.

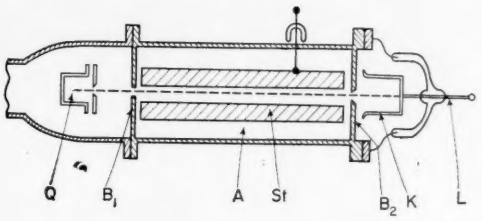

BILD 2. Prinzipieller Aufbau eines elektrischen Massenfilters.

Der in der Ionenquelle aus dem zu untersuchenden Gas gebildete Ionenstrahl tritt nach Durchlaufen einer Beschleunigungsspannung U_B durch die Einschussblende B_1 in den Analysatorraum A ein. Dieser wird im wesentlichen von einem elektrischen Quadrupolfeld erfüllt, zu dessen Erzeugung vier parallele Zylinderstäbe S mit Kreisquerschnitt vorgesehen sind. Durch Beaufschlagen der Feldstäbe S mit einer Hochfrequenzspannung der Form V . cos wt und einer überlagerten Gleichspannung U entsteht in der Nähe der Systemachse ein hyperpolisches, elektrisches Feld, das sich in erster Näherung von einem Potential der Form

$$\varphi(x, y, z, t) = \frac{U + V\cos wt}{2}\left(\frac{x^2-y^2}{r_0^2}\right) \qquad (2)$$

ableitet. Darin bedeuten x und y die Koordinaten senkrecht zur Systemachse und $2r_0$ den Abstand der Feldstäbe. Die Bahnen der in ein solches Feld eingeschossenen Ionen der Masse m und der Ladunge werden durch Bewegungsgleichungen beschrieben*, die leicht in die sogenannten Mathieu'schen Differentialgleichungen

$$\frac{\delta^2 x}{\delta\xi^2} + \left\{a - 2q\cos(2\xi+\pi)\right\} x = 0;\ \frac{\delta^2 y}{\delta\xi^2} = \ldots;\ \frac{\delta^2 z}{\delta\xi^2} = \ldots \qquad (3)$$

mit bekannten Lösungseigenschaften umgeformt werden können. Die hierzu eingeführten Grössen a, q und ξ drücken sich dabei wie folgt aus

$$a = \frac{4eU}{mw^2r_0^2};\ q = \frac{2e\,V}{mw^2r_0^2};\ \xi = \frac{wt}{2} \qquad (4)$$

Betrachtet man Gl. (3) für beide Raumkoordinaten x, y, so folgt aus der Theorie der Mathieu'schen Differentialgleichungen ein Bereich stabiler Lösungen $x(\xi)$; $y(\xi)$ der nur von den Parametern a und q abhängt und etwa das in Bild 3 dargestellte Gebiet überdeckt.

Mit stabilen Lösungen sind dabei ' beschränkte ' periodische Funktionen $x(t)$; $y(t)$ der Raumkoordinaten gemeint, während im instabilen Bereich x, y mit der Zeit t gegen ∞ wachsen. Für die eingeschossenen Ionen bedeutet dies im erstgenannten Fall ein stabiles Schwingen um die Feldachse x, $y = 0$, während im Bereich der instabilen

*$m\ddot{x} + e(U + V\cos wt)\,x/r_0^2 = 0$
$m\ddot{y} - e(U + V\cos wt)\,y/r_0^2 = 0$
$m\ddot{z} = 0$

2. Principle of the electrical mass filter

An arrangement showing the principle of the electrical mass filter is given diagrammatically in Fig. 2.

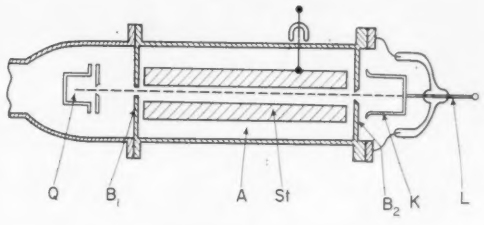

FIG. 2. Principle arrangement of an electrical mass filter.

The gas to be investigated is formed into an ion beam within the ion source. The ion beam is accelerated by the voltage U_B and injected through the diaphragm B_1 into the analysing space A. Analysis is essentially carried out by an electrical quadrupole field, obtained by four parallel cylindrical rods S having circular cross section. By energizing these rods S with a high frequency field of the form V. coswt and using a superimposed steady voltage U one obtains in the vicinity of the axis of the system a hyperbolic electrical field from which to a first approximation a potential of the form

$$\varphi(x, y, z, t) = \frac{U + V\cos wt}{2}\left(\frac{x^2-y^2}{r_0^2}\right) \qquad (2)$$

can be derived. In this x and y are co-ordinates perpendicular to the axis of the system and $2r_0$ is the distance between the field rods. The trajectory of ions with mass m and charge e injected into such a field are described by equations* of motion, which can easily be transposed into the so-called Mathieu's differential equation with well known properties of solution.

$$\frac{\delta^2 x}{\delta\xi^2} + \left\{a - 2q\cos(2\xi+\pi)\right\} x = 0;\ \frac{\delta^2 y}{\delta\xi^2} = \ldots;\ \frac{\delta^2 z}{\delta\xi^2} = \ldots \qquad (3)$$

The quantities a, q, and ξ here introduced, are expressed as follows.

$$a = \frac{4eU}{mw^2r_0^2};\ q = \frac{2e\,V}{mw^2r_0^2};\ \xi = \frac{wt}{2} \qquad (4)$$

Consider equation (3) for the two space co-ordinates x and y. Then it follows from the theory of Mathieu's differential equations, that there is a range of stable solutions $x(\xi)$, $y(\xi)$ which depends only on the parameters a and q, and covers a region shown approximately in Fig. 3.

By stable solution, a solution involving a " limited " periodic function $x(t)$; $y(t)$ of the space co-ordinates is meant, whereas in the unstable region z and y increase to infinity with the time t.

In the first case this means that the injected ions oscillate in a stable manner about the axis of the field x, $y = 0$, while in the second case in the region of unstable solutions the ions suffer ever increasing oscillations until they finally touch the

*$m\ddot{x} + e(U + V\cos wt)\,x/r_0^2 = 0$
$m\ddot{y} - e(U + V\cos wt)\,y/r_0^2 = 0$
$m\ddot{z} = 0$

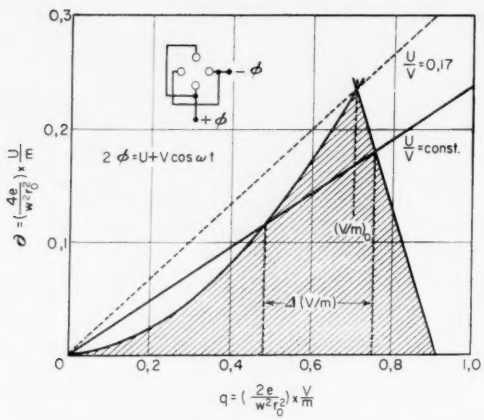

BILD 3. Zur Theorie der Mathieu'schen Differentialgleichungen.

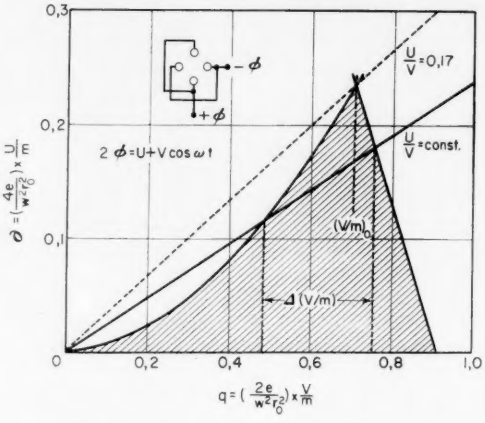

FIG. 3. The theory of the Mathieu's differential equations.

Lösungen die Ionen bis zur Berührung der Feldstäbe aufgeschaukelt und dort entladen werden. Durch Wahl der Parameter a ; q, *d.h.* durch die Grössen $U/w^2.m$ und V/w^2m ist es also möglich, entweder die eingeschossenen Ionen das Feld passieren zu lassen oder durch Aufschaukeln und Entladen an den Feldstäben auszufiltern.

Möchte man schliesslich nur Ionen eines bestimmten Massenbereiches durch die Austrittsblende B_2 gelangen lassen, so kann man die Gleichspannung U mit der Hochfrequenz-Amplitude V durch eine lineare Beziehung verknüpfen ;

$$U = \lambda . V \tag{5}$$

und damit eine Arbeitsgerade im stabilen Lösungsbereich der Parameter a und q festlegen (vergl. Bild 3). Für einen Wert $\lambda_0 \approx 0{,}17$ berührt diese Gerade nur noch die Spitze des stabilen Bereiches, d.h. es werden nur noch Ionen der einzigen Masse m das Feld durchsetzen können, wobei m lediglich von der Geometrie des Feldes, der gewählten Frequenz w und der Amplitude V abhängt :

$$m = \frac{2\,eV}{q_0 w^2 r_0^2} = \frac{2{,}85\,eV}{w^2 r_0^2} \tag{6}$$

Theoretisch würde in diesem Falle eine Auflösung $m/\Delta m = \infty$ erreicht. Gleichzeitig ist jedoch die Intensität des austretenden Ionenstrahls 0. Man wird daher einen λ–Wert dicht unterhalb λ_0 wählen, d.h. die Arbeitsgerade wird den stabilen Bereich dicht unterhalb der oberen Spitze durchsetzen. Weiterhin ist es notwendig, dass die Ionen im Analysatorfeld so lange verbleiben, dass die gewünschte Abtrennung der instabilen Teilchen, d.h. das Ausfschaukeln bis zur Berührung der Feldstäbe auch tatsächlich erfolgt. Die hierzi erforderliche Mindestzahl von Schwingungen n mit

$$n \approx 3{,}5\ (m/\Delta m)^{1/2} \tag{7}$$

legt die zulässige Beschleunigungsspannung U_B der eingeschossenen Ionen auf Werte unterhalb

$$U_B \approx 4{,}2\ .\ 10^{-14}\ L^2 v^2 \left(m\,\frac{\Delta m}{m}\right) \text{V} \tag{8}$$

fest. Mit Ausnahme dieses Maximalwertes ist die Ionenenergie völlig unkritisch[7].

rod electrodes where they give up their charge. By selecting the parameters a, q, i.e. the quantities U/W^2m and V/W^2m it is therefore possible to arrange that injected ions either pass through the field or are excited to unstable oscillations so that they are discharged at the rod electrodes and thereby filtered out.

Finally if it is desired to allow only ions of a certain mass range to leave the exit aperture B_2 then one can arrange to establish a linear relationship between the constant voltage U with the high frequency amplitude V of the form

$$U = \lambda . V \tag{5}$$

In this way an operating line is established in the region of stable solutions of the parameters a and q (compare with Fig. 3). For a certain value $\lambda_0 \approx 01.17$ this line touches only the peak of the stable region, i.e. under this condition, ions of the single mass m will be able to pass through the field, where m depends only on the geometry of the field and the frequency ω and amplitude V chosen. m is given by :

$$m = \frac{2\,eV}{q_0 w^2 r_0^2} = \frac{2{,}85\,eV}{w^2 r_0^2} \tag{6}$$

Theoretically, this would mean that a resolution $m/\Delta m = \infty$ had been achieved. However, at the same time the intensity of the emitted ion beam would be 0.

One therefore selects a value of λ close to λ_0, i.e. such that the operating line cuts the stable region very near to the top peak.

It is furthermore necessary that the ions should remain for a sufficiently long time in the analysis field to ensure the desired separation of the unstable particles, i.e. that there should be enough time for their excitation to run away oscillations until they touch the field electrodes. For this condition a minimum number of oscillations n is required, where

$$n \approx 3{,}5\ (m/\Delta m)^{\frac{1}{2}} \tag{7}$$

and therefore the accelerating voltage U_B of the injected ions is required to be less than

$$U_B \approx 4{,}2\ .\ 10^{-14}\ L^2 v^2 \left(m\,\frac{\Delta m}{m}\right) \text{V} \tag{8}$$

The energy of the ions is otherwise not at all critical apart from this condition of a maximum value[7].

Vol. 10 1960

3. Verhalten als Partialdruckvakuummeter

Aus dem beschriebenen Prinzip der Massentrennung folgen Eigenschaften, die das elektrische Massenfilter für eine Verwendung als Partialdruckvakuummeter besonders geeignet machen. Zunächst erlaubt die genannte Freizügigkeit bezüglich der Ionenenergie die Verwendung von Ionenquellen, die einfach und robust gebaut sein können. Insbesondere sind Konstruktionen möglich, die auf hohe Ergiebigkeit und besonders gewählte Druckabhängigkeit des extrahierten Ionenstromes abgestimmt sind, ohne die Einschränkungen die bei definierten Ionenenergien zwangsweise vorliegen. Aus dem gleichen Grunde sind mit einem solchen Gerät keine ' Geister-Linien ' zu erwarten, wie sie sonst durch Energieverlust und Umladungen insbesondere bei höheren Restgasdrucken auftreten.

Die Benützung bei relativ hohen Drucken wird schliesslich dadurch erleichtert, dass die stabilen Ionen längs ihres gesamten Flugweges durch den Analysatorraum fokussierenden Kräften unterliegen. Restgasstösse werden also in weit geringerem Masse als bei konventionellen Sektorspektrometern zu Linienverbreiterung und Intensitätsminderung führen.

Die beim Omegatron so gefürchteten Fremdschichten mit der Folge von Potentialverschiebungen auf den Elektroden fallen beim Massenfilter wegen der hohen Betriebsspannungen (vergl. Gl. 6) weit weniger ins Gewicht. Auch hierdurch wird die Verwendung im Bereich hoher Drucke und an dampfverseuchten Rezipienten erleichtert. Schliesslich kommen der einfache Aufbau des rein elektrisch arbeitenden Analysators, das hierdurch bedingte geringe Gewicht und die Möglichkeit kleiner Volumina der Messzelle den Forderungen entgegen, die man an ein Partialdruckvakuummeter stellt.

Aufgrund dieser Eigenschaften ist zu erwarten, dass eine vorteilhafte Partialdruckmessung mit dem elektrischen Massenfilter vor allem im Bereich relativ hoher Drucke, d.h. in Verbindung mit den zahlreichen Aufgaben der industriellen, Fein- und Hochvakuumtechnik möglich ist, also gerade dort, wo die eingangs genannten Spektrometertypen ihre Brauchbarkeit verlieren.

Auf diesen Anwendungsbereich sind die nachstenend beschriebenen Untersuchungen daher vornehmlich ausgerichtet. Darüberhinaus macht jedoch die Möglichkeit der Anwendung besonders ergiebiger Ionenquellen die Erzielung einer hohen Ionenstrahl-Intensität, d.h. einer hohen Empfindlichkeit denkbar. Damit würde gleichfalls der Bereich kleinster Drucke erfasst sowie eine Verwendung als empfindlicher Lecksucher nahegelegt.

Versuchsgerät und Auflösung

Die in erster Linie für die technische Anwendung gedachte Versuchsmesszelle des elektrischen Massenfilters wurde in Metallausführung gebaut. Analysatorteil, Ionenquelle und das Hüllrohr der Messzelle sind in sich geschlossene, leicht demontable Bauelemente. Über einen Verbindungsstutzen mit Flansch ist der unmittelbare Anschluss der Röhre an den Rezipienten vorgesehen, in welchem Partialdruckmessungen oder Gasanalysen durchgeführt werden sollen.

Der Analysatorteil wurde so dimensioniert, dass ein

3. Behaviour as a partial pressure vacuum gauge

From the principle of mass separation just described follow properties which make the electrical mass filter especially suitable for partial pressure vacuum meter applications. Firstly the freedom in selection of ion energies already mentioned allows the use of simple and robustly constructed ion sources. Thus constructions are possible adjusted to give a high yield and result in a specially chosen pressure dependence of the extracted ion current without the limitations when well defined ion energies have to be imposed. For the same reasons no " ghost-lines " are to be expected in such devices as may occur in other devices as a result of energy losses or recharging phenomena especially at higher residual pressures.

Finally, the application of this device at higher pressures is facilitated because the stable ions are subjected to focusing forces along their whole path length throughout the analysis space.

Hence, the line-width broadening and intensity reduction suffered by conventional sector type spectrometers as a result of collisions with residual gas, occurs to a much reduced extent.

In the case of the omegatron the greatly feared effect of contaminating layers leading to potential shifts at the electrodes are of much less importance when operating at high potentials (see equation 6). This again facilitates the application of the device in a higher pressure range and in connection with vapour contaminated equipment.

Finally the requirement for a partial pressure vacuum gauge is met by an analysis system of simple construction operating purely electrically and therefore having a measuring cell of light weight and small volume.

On account of these properties it is expected that particularly advantageous partial pressure measurements are possible with the electrical mass filter at relatively higher pressures, i.e. in connection with the numerous tasks of the industrial medium and high vacuum techniques, which is just the range where the other types of spectrometers mentioned above show a loss in usefulness.

The investigations described below are therefore particularly aimed at applications covering this range. Furthermore the possibility of employing special high yield ion sources makes it feasible to obtain a high ion beam intensity, i.e. a high sensitivity. In this way the region of lowest pressures would be covered as well as an application to a sensitive form of leak detector.

Experimental apparatus and resolution

The experimental cell of the mass-filter was built in a metal construction for mainly technical applications in the first place. The analysis part, in source and surrounding envelope of the measuring cell were made as self contained and easily demountable parts. A connecting stub terminating in a flange serves for the direct connection of the tube to the vacuum system in which the partial pressure measurements or the gas analysis are to be carried out.

The analysis part was dimensioned so that a mass range up to ion-mass $M = 80$ could be covered and at the same time be able to resolve mass units within this range. The

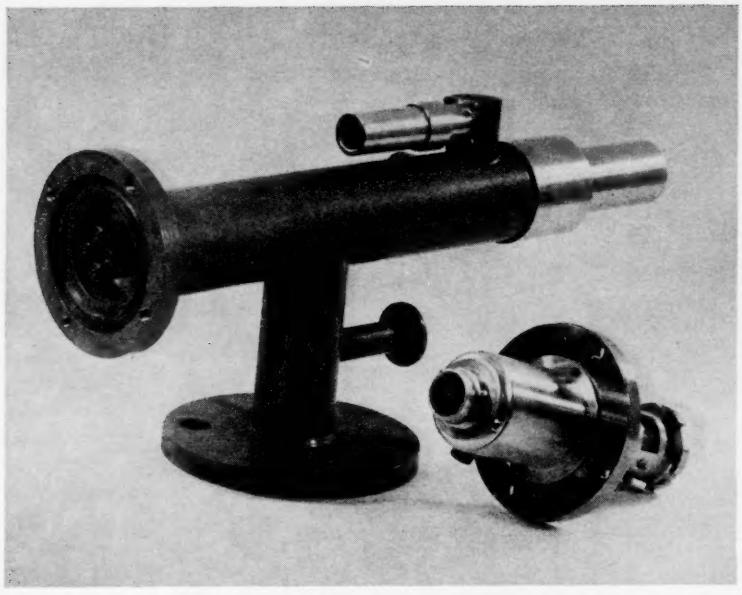

BILD 4. Versuchsausführung.

Bereich bis zur Ionenmasse $M = 80$ erfasst werden kann und gleichzeitig ein Auflösungsvermögen möglich ist, welches die Trennung der Masseneinheit innerhalb dieses Massenbereiches gestattet. Die so ausgeführte Messzelle hat eine Gesamtlänge von lediglich 35 cm bei einem Rohrdurchmesser von ca. 5 cm (Bild 4).

measuring cell designed along these lines had a total length of only 35 cm with a diameter of about 5 cm (Fig. 4).

The associated high frequency generator could then be limited to a maximum power of 20 W. The variation of the masses to be separated out was obtained by changing the high frequency amplitude V superimposed on a similarly

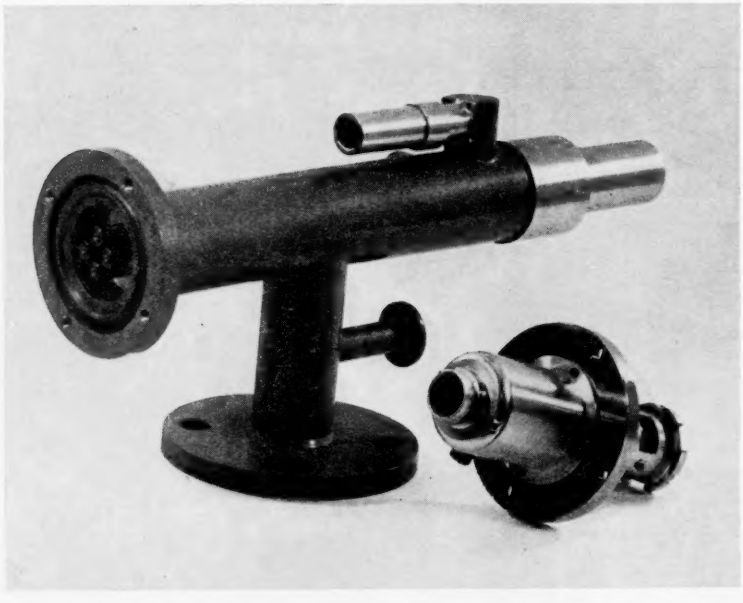

FIG. 4. Experimental arrangement.

Der zugehörige Hochfrequenzgenerator konnte damit auf eine Hochfrequenzleistung von max. 20 W beschränkt werden. Die Variation der ausgefilterten Masse erfolgt durch Veränderung der Hochfrequenzamplitude V, welcher eine analog veränderliche Gleichspannung U überlagert ist. Durch Regelung von U, V und ω wird das Verhältnis U/V innerhalb des gesamten Massenbereiches annähernd konstant gehalten. Durch Wahl kleiner Ioneneinschussblenden

varying direct voltage U by regulating U, V and W the ratio U/V could be held almost constant throughout the whole mass range to be covered. On the other hand, by choosing a small ion injection aperture a high ion current transmission* is aimed at, so that a constant resolution is obtained with

*Transmission = ratio J_2/J_1 of transmitted ion beam intensity to injected ion beam intensity of a stable i.e. a focused mass.

wird andererseits eine hohe Ionenstromtransmission* angestrebt, so dass ein konstantes Auflösungsvermögen sowie eine intensitätsproportionale Wiedergabe der einzelnen Massen innerhalb des gesamten Massenbereiches resultieren.

Bild 5 zeigt ein Massenspektrum wie es nach Einlass eines Luft-Benzingemisches in die Messzelle aufgenommem wurde. Der Totaldruck lag bei 1.10^{-4} Torr.

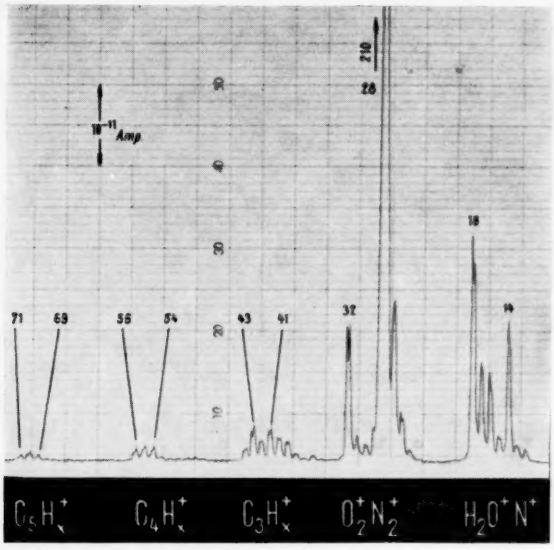

BILD 5. Massenspektrum mit dem elektrischen Massenfilter.

Bezieht man auf die Halbwertsbreite der Massenlinien, so zeigt sich, dass Massen mit dem Abstand Δm einer Masseneinheit noch gut voneinander getrennt werden. Das gilt sowohl im Bereich der Masse 10 wie auch der Masse 80. Das Auflösungsvermögen steigt also mit der Massenzahl an und erreicht einen Maximalwert von $m/\Delta m \approx 80$. Die Forderung $\Delta m = 1$ ist demnach im gesamten Massenbereich erfüllt.

Gleichzeitig ergibt sich, das zur Beurteilung des Trennvermögens mehr als das Auflösungsvermögen $m/\Delta m$ die trennbare Massendifferenz Δm geeignet ist. Das liegt an der Wahl der Betriebsdaten und den Aussagen der Gl. 8 :

Neben der Exaktheit und Konstanz der Feldgrössen r_0 ; V und ω sowie des Verhältnisses $\lambda = U/V$ ist die Wahl der maximalen Ionenbeschleunigungs- oder Extraktionsspannung U_B für die erzielbare Massentrennung entscheidend. Aus Intensitätsgründen wird man U_B möglichst hoch wählen. Sind nun die Feldstäbe exakt justiert und ausserdem die Grössen ω ; V durch die Regelautomatik des Senders ausreichend stabilisiert, so wird nach entsprechender Einstellung von λ die Massentrennung nur noch von U_B abhängen. Dann ist aber gemäss Gl. 8 die trennbare Massendifferenz Δm vorgegeben und nicht die Grösse $m/\Delta m$. Neben U_B ist auch $\lambda = U/V$ für die ausgefilterte Ionenstrahlintensität massgebend. Man wird daher λ möglichst klein wählen und auf einen solchen Wert λ_0 einstellen, dass

*Transmission = Verhältnis J_2/J_1 von durchgelassener und eingeschossener Ionenstrahlintensität einer stabilen, d.h. fokussierten, Masse.

an intensity proportional reproduction of different masses throughout the whole mass range. In Fig. 5 is reproduced a mass spectrum taken when an air-benzene mixture was admitted to the measuring cell. The total pressure was about 1×10^{-4} Torr.

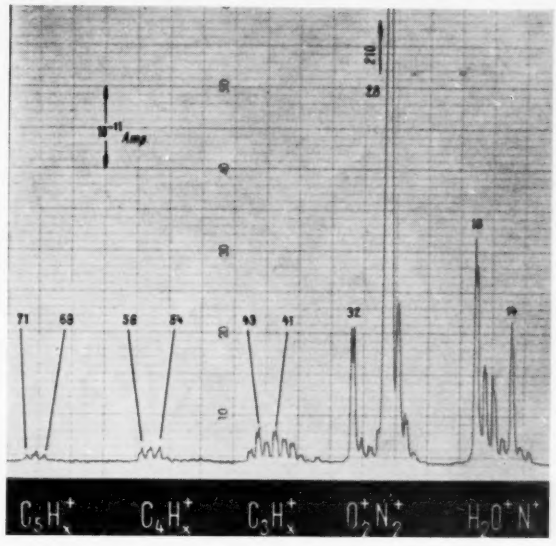

FIG. 5. Mass spectrum obtained with the electric mass filter.

Referring to the half value width of the mass lines it is seen that masses with the separation Δm of one mass unit are still well separated. This is the case around mass 10 as well as at mass 80. The resolution therefore, increased with mass number and reached a maximum of $m/\Delta m$ 80. The requirement $\Delta m = 1$ is, therefore, fulfilled over the whole mass range.

At the same time it is evident that the power to separate adjacent mass number is judged better from the smallest separable mass differences Δm than from the resolution $m/\Delta m$. This is due to the choice of operating conditions and the results of equation 8.

Apart from the accuracy and constancy of the field parameters λ_0, V and W as well as the ratio $\lambda = U/V$ the achievable mass separation is decided by the choice of the maximum ion accelerating and extraction voltage U_B.

For intensity reasons U_B will be taken as high as possible. If the field-rods are positioned precisely and also the quantities W ; V are stabilized sufficiently by automatic control at the signal generator, then after the corresponding adjustment of λ the mass separation depends only on U_B. Then, however, the separable mass difference Δm is pre-determined and not the quantity $m/\Delta m$. The ion beam intensity filtered out is determined both by U_B and the ratio $\lambda = U/V$. Hence, λ is taken to be as small as possible and adjusted to such a value λ_0 that the required degree of resolution is just obtained ; in the case considered here with $\Delta m = 1$; $m_{max} = 80$, i.e. $(m/\Delta m)$ max $= 80$. Following from equation 8 a further increase in λ is of no advantage but only has the disadvantage of giving smaller ion intensities. In any case, with $\lambda = \lambda_0$ about 30–50 per cent of the injected

die an das Auflösungsvermögen gestellten Forderungen gerade noch erfüllt werden ; im vorgegebenen Fall mit $\Delta m = 1$; $m_{max} = 80$ also $(m/\Delta m)_{max} = 80$. Eine weitere Steigerung von λ bringt wegen Gl. 8 keine Vorteile sondern nur den Nachteil kleinerer Intensität. Immerhin konnten mit $\lambda = \lambda_0$ noch 30–50 prozent der eingeschossenen stabilen Ionen ausgefiltert, die Transmission T also auf einen Wert von 0,3–0,5 gebracht werden.

Senkt man λ und damit die maximale Auflösung $m/\Delta m$ ab, so steight T weiter an und erreicht im vorliegenden Fall für $m/\Delta m \approx 20$ den Wert 1, erkenntlich an dem abgeflachten Maximum der Massenlinien (Bild 6).

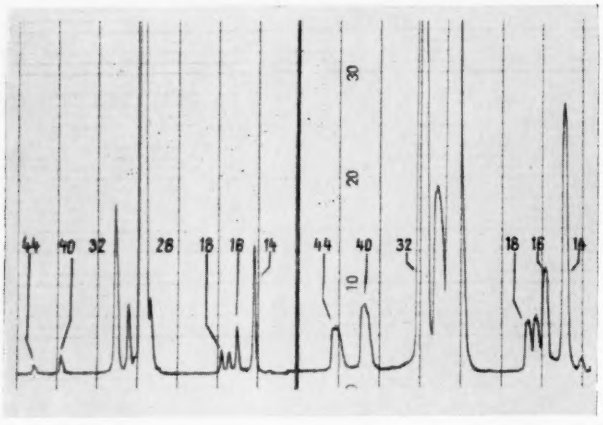

BILD 6. Massenspektren mit verschiedenen Transmissionen.

Ein weiteres Absenken von λ bringt keine zusätzliche Intensitätssteigerung und ist daher nicht sinnvoll.

$\lambda = U/V$ kann durch Drehen eines Potentiometerknopfes beliebig eingestellt werden. Es ist also möglich, Auflösungsvermögen und Intensität des Massenfilters in weiten Grenzen leicht zu verändern und damit während der Messung den jeweiligen Gegebenheiten anzupassen. Darin liegt ein weiterer Vorteil dieser Anordnung zur Partialdruckmessung.

Die Form der einzelnen Massenpeaks (Bild 6) zeigt den für das elektrische Massenfilter typischen, unsymmetrischen Charakter, d.h. die der kleineren Masse zugewendete Flanke ist weniger steil als die gegenüberliegende und ausserdem am unteren Ende etwas geschweift ausgebildet. Ein evtl. geringer Untergrund rührt also vornehmlich von derartigen Ausläufern besonders intensiver Massen her. Die Ursache für diese Peak-Form liegt in der entsprechend unsymmetrischen Begrenzung des stabilen Lösungsbereiches der zugeordneten Bewegungsleichungen (vergl. Bild 3).

Eine genauere Untersuchung zeigt, dass die Form der Massenlinien und damit das erzielte Auflösungsvermögen bis zu Drucken von 10^{-3} Torr nahezu unverändert bleibt. Damit ist gemeint, dass der genannte Druck die ganze Messzelle, einschliesslich des Analysators gleichmässig erfüllt. Das Fehlen der Stossverbreiterung ist also wieder eine Folge der auf dem gesamten Flugweg wirksamen fokussierenden Kräfte. Erst bei Drucken von mehreren 10^{-3} Torr zeigt sich eine zunehmende Linienverbreiterung. Immerhin können an der oberen Bereichsgrenze von ca. 10^{-2} Torr z.B. noch die Massen 14 und 16 getrennt werden.

ions were filtered out, i.e. the transmission was as high as 0.3–0.5.

If λ is reduced, the maximum resolution $m/\Delta m$ is decreased and T is further increased giving, in the above instance, for $m/\Delta m \approx 20$ the value 1, as seen from the flattened maximum of the mass lines (Fig. 6).

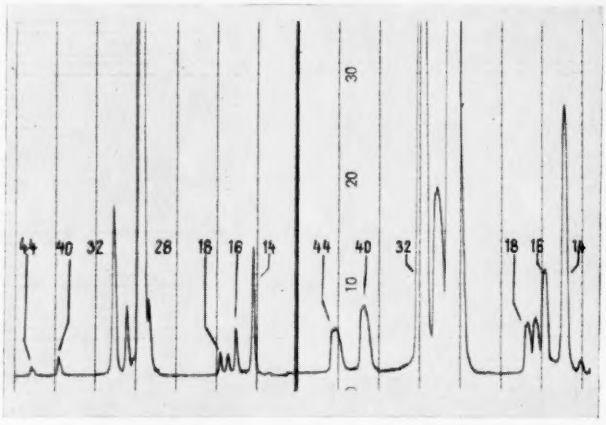

FIG. 6. Mass spectrum for different values of resolution and transmission T.

A further reduction of λ gives no further increase in intensity and is therefore of no advantage.

The value of $\lambda = U/V$ can be adjusted to any value by turning the knob of a potentiometer. It is, therefore, possible to adjust in a simple manner the resolution and intensity of the mass filter within wide limits to suit the required conditions. Therein lies a further advantage of this arrangement for partial pressure measurements. The form of individual mass peaks for the electrical mass filter (Fig. 6) shows the typically unsymmetrical character, i.e. the side facing the smaller masses is not as steep as the opposing side and is also curved at the bottom. Hence, any possible background is associated with such off-shoots of any high intensity masses. The reason for this peak form lies in the corresponding unsymmetrical limitation of the domain of solutions of the associated equations of motion (see Fig. 3).

A more detailed investigation shows that the form of the mass lines and hence the achievable resolution is virtually unchanged up to pressures of 10^{-3} Torr. This pressure condition refers to a uniform pressure throughout the whole measuring cell including the analyser. Hence, the absence of any broadening by collision forces is again a consequence of the focusing forces being effective over the whole flight path. Only at pressures of several 10^{-3} Torr a progressive line broadening takes place. Thus at an upper pressure limit of about 10^{-2} Torr for example, masses 14 and 16 are still separable. With a fixed value of ion accelerating potential the above mentioned properties are given merely by the injection aperture and the analyser system and are independent of the type of ion source used. However, the ion source construction principles have a decisive effect on the operating range of the measuring cell especially the pressure interval over which it operates and the absolute value of the ion beam intensity, i.e. the sensitivity obtained.

Vol
10
196

Die vorgenannten Eigenschaften sind bei gleicher Ionenbeschleunigungsspannung allein durch die Einsschussblenden und das Analysatorsystem gegeben und von der Art der benutzten Ionenquelle unabhängig. Das Prinzip und die Ausführung der Ionenquelle bestimmen aber entscheidend den Arbeitsbereich der Messzelle, insbesondere das Druckintervall und den Absolutwert der Ionenstrahlintensität, d.h. die Empfindlichkeit. Reproduzierbarkeit der Messung und Störanfälligkeit des gesamten Systems sind gleichfalls stark von der Ionenquelle abhängig und für die praktische Anwendung von besonderem Interesse.

Verhalten mit Glühkathoden-Ionenquelle

In der Massenspektrometrie wird bisher fast ausschliesslich die Gasionisierung mit Hilfe von Elektronenstossionenquellen durchgeführt, wobei als Elektronenquelle eine Glühkathode dient[8].

Wegen der geringen Gasdrücke (10^{-6} bis einige 10^{-4} Torr) führt ein Elektron auf seinem Flugweg praktisch nicht mehr als einen Ionisierungsakt aus. Bei gegebener Beschleunigungsspannung liegt für die Ionisierung also stets eine homogene Elektronenenergie vor, die man mit 70 bis 100 eV üblicherweise in das Maximum der sogen. differentiellen Ionisierung legt. Diese Ionenquelle hat den Vorzug, dass sich bei den gewählten Drucken die Ionenintensitäten der verschiedenen Gase nahezu ungestört überlagern und ausser vom Partialdruck nur von der Höhe der differentiellen Ionisierung abhängen. Bei der Verwendung im elektrischen Massenfilter entfällt mit der Notwendigkeit homogener Ionenenergie die sonst gültige Forderung nach Ionisierung an Orten gleichen elektrischen Potentials. Statt eines scharf ausgeblendeten und senkrecht zum Ionenstrahl orientierten Elektronenstrahls kann man also ein breites Elektronenbündel und eine beliebige Orientierung desselben wählen, die ausschliesslich auf optimale Ionenausbeute abgestimmt werden kann.

Die zunächst hier benutzte einfache Ionenquelle wurde so ausgeführt, dass der ionisierende Elektronenstrahl wahlweise longitudinal oder transversal das Ionisierungsvolumen durchsetzt. Der Ionenstrahl wird stets longitudinal d.h. in der Systemachse abgesaugt. Dabei ist die Extraktionsspannung in ihrem Betrag völlig unkritisch, solange sie nicht den durch Gleichung 8 vorgegebenen Höchstwert überschreitet.

In Bild 7 sind die Ionenausbeuten als Funktion des Druckes

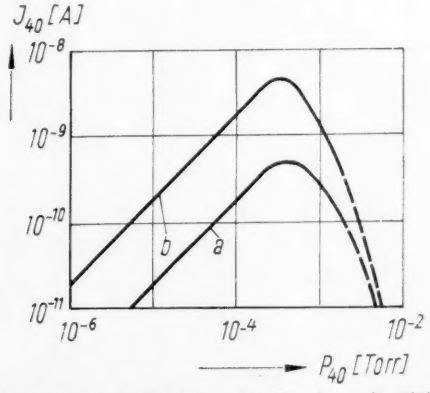

BILD 7. Ionenstrom als Funktion des Druckes mit Glühkathoden-Ionenquelle Elektronenstrahl transversal (a) und longitudinal (b).

Reproducibility of measurements and any liability of breakdown of the whole system are also strongly dependent on the ion source and its constructional details are therefore of special interest for any practical application.

Behaviour with thermionic cathode ion source

The gas ionization in mass-spectrometry to date is carried out almost exclusively with the help of electron collision type ion sources where a thermionic cathode serves as the source of electrons (8).

Due to the low gas pressure (10^{-6} to some 10^{-4} Torr) an electron may carry out rarely more than one act of ionization on its trajectory. At a given accelerating voltage a homogeneous electron energy is generally available usually of the order of 70–100 eV which corresponds to the maximum of the so-called differential ionization. This ion source has the advantage that at a given pressure the ion intensity of different gases is superimposed almost undisturbed depending, apart from the partial pressure, only on the value of the differential ionization.

In the application of the electric mass filter there is no need for homogeneous ion energies and hence, also there is no need for the usual requirement of ionization at points of equal electric potentials. Instead of a sharply defined narrow beam of ions at right angles to the electron beam one can choose a wide bundle oriented in any direction to the electron beam which is merely adjusted for optimum yield of ions.

The simple ion source used here at first was so arranged that the ionizing electron beam could be arranged to pass through the ionization space either in a longitudinal or transverse direction. The ion beam is always withdrawn longitudinally, i.e. in the direction of the axis of the system.

The value of the extraction voltage used in this application was quite uncritical as long as it did not exceed the maximum value given by equation 8.

In Fig. 7 the ion-yield is plotted as a function of pressure, both for the longitudinal and transversely oriented electron beam, as obtained after admitting pure argon gas. Apart from the higher intensities obtained with the longitudinally extracted ion currents, both curves show the same behaviour with pressure, i.e. for pressures, up to 2×10^{-4} Torr the ion

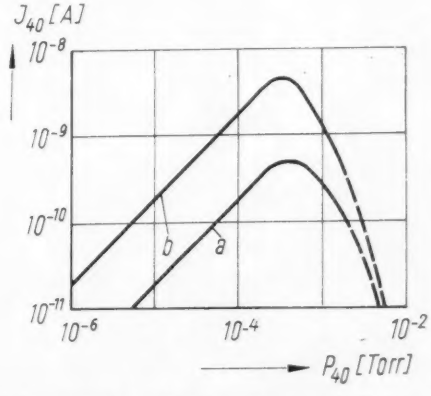

FIG. 7. Ion current as a function of pressure in the case of thermionic cathode ion sources.
Electron beam transversal (a) and longitudinal (b).

dargestellt wie sie für die beiden Fälle des longitudinal bezw. transversal orientierten Elektronenstrahls bei Einlass von reinem Argon erhalten wurden. Abgesehen von der höheren Intensität der mit longitudinaler Extraktion gemessenen Ionenströme zeigen beide Kurven den gleichen Druckverlauf ; d.h. bis zu Werten von etwa 2.10^{-4} Torr steigt der Ionenstrom am Auffänger linear mit dem Druck an.

Dann setzt eine Abkrümmung ein, die vermutlich auf Raumladungserscheinungen innerhalb der Ionenquelle zurückzuführen ist. Stossverluste längs der Ionenlaufstrecke sind bei diesen Drucken allein wegen der mittleren freien Weglänge (ca. 50 cm) und der fokussierenden Kräfte im Analysator noch nicht zu erwarten. Nach Überschreiten eines Maximums bei 3.10^{-4} Torr sinkt die Intensität ab und erreicht für Drucke oberhalb 3.10^{-3} Torr den Wert 0. Die Lage des Maximums verschiebt sich gemäss Bild 8 in der Reihenfolge N_2^+, O_2^+, N^+, O^+, in Richtung höherer Drucke und liegt für O^+ z.B. bei etwa 1.10^{-3} Torr. Ein Nachweis ist in diesem Falle noch bis zu Werten von ca. 1.10^{-2} Torr möglich. In diesem Bereich ist die mittlere freie Weglänge mit $\Lambda \approx 1$ cm so weit abgesunken, dass der rapide Intensitätsabfall bereits durch Stossverluste längs der Ionenlaufstrecke zu erwarten ist. Der Vergleich der gaskinetischen Stossradien mit dem Verlauf der verschiedenen Kurven in Bild 8 zeigt jedoch, dass im Druckbereich bis 10^{-3} Torr die oben erwähnten Raumladungserscheinungen die Form der Eichkurve bestimmen.

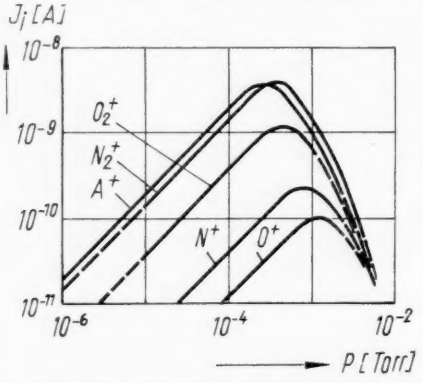

BILD 8. Ionenstrom als Funktion des Druckes für verschiedene Gasanteile.

Bild 8 lässt gleichfalls erkennen, dass für Argon eine Empfindlichkeit von ca. 3.10^{-5} A/Torr erreicht wird. Nimmt man als kleinsten bequem nachweisbaren Auffängerstrom einen Wert von 10^{-14} A an, so führt dies zu einer unteren Grenze von $p_{min} = 3.10^{-10}$ Torr für den niedrigsten noch nachweisbaren Partialdruck. Eine Empfindlichkeitssteigerung durch Vergrössern der Einschussblende ist kaum möglich, da zur Erzielung gleicher Auflösung die Transmission notwendigerweise absinken müsste. Durch erhöhte Ionenextraktion an der Ionenquelle sowie durch elektrische Abbildung des Ionenstrahls auf die Einschussblende kann jedoch im Bedarfsfall eine weitere Intensitätssteigerung erzielt werden. Betrachtet man die obere Bereichsgrenze, so ist eine unmittelbare Partialdruckmessung über $p_i = c_i \cdot A_i$* current at the collector increases linearly with pressure.

At higher pressure there is a decrease in current presumably due to space charge effects within the ion source. At these pressures collision losses along the ion path, within the analyser, are not to be expected because of the relatively long mean free path (approx. 50 cm) and also the continuous focusing action within the analyser.

The intensity reaches a maximum value at 3×10^{-4} Torr and then decreases and is reduced to zero at pressures above 3×10^{-3} Torr. The position of the maximum is displaced in the sequence N_2+,O_2+, $N+$,$O+$, in the direction of higher pressures as shown in Fig. 8 and e.g. for $O+$ the maximum lies at about 1×10^{-3} Torr. Hence in this case detection is possible up to pressures of about 1×10^{-2} Torr. In this pressure range the mean free path $\lambda \approx 1$ cm is reduced to such low values that rapid intensity reduction is to be expected due to collision losses along the ion path length.

Comparison of the gaskinetic collision radii with the curves given in Fig. 8 shows, however, that in the pressure range up to 10^{-3} Torr the form of the curves is largely determined by the space charge effects mentioned above.

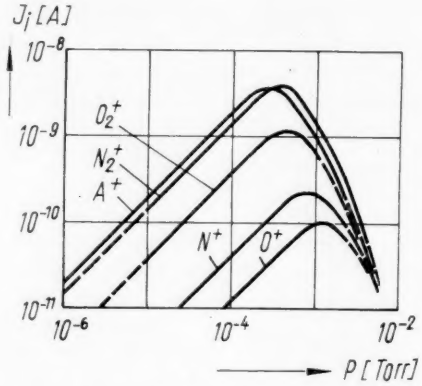

FIG. 8. Ion current as a function of pressure for different partial pressures.

It is also seen from Fig. 8 that for Argon a sensitivity of about 3×10^{-5} A/Torr is achieved. If the smallest detectable collector current is taken to be 10^{-14} A, then the lower partial pressure limit which can be detected is $p_{min} = 3 \times 10^{-10}$ Torr.

The sensitivity can hardly be improved by increasing the injection aperture because the same resolution could only be achieved at the expense of transmission. However, by increasing the extraction of ions at the source, and electrical imaging of the ion beam on to the injection aperture, it may be possible to increase the intensity if required.

Considering the upper limit, a direct measurement of partial pressures is possible using the relation $pi = Ci\,Ai$* up to the departure from linearity of the calibration curve, i.e. up to a pressure of about 2 to 5×10^{-4} Torr. Above this pressure it is necessary to consider carefully all the

*Partialdruck p_i.
Ausschlag A_i ; Eichfaktor c_i des betreffenden Gases.

*Partial pressure *Pi*.
Indicated current *Ai*.
Calibration factor for the particular gas *Ci*.

bis zur Abkrümmung der Eichkurve, d.h. bis zu einem Druck von 2 bis 5.10^{-4} Torr möglich. Darüberhinaus ist eine sorgfältige Berücksichtigung sämtlicher der für die verschiedenen Gase gültigen Eichkurven sowie des Totaldruckes notwendig. Die Partialdruckangabe wird dadurch wesentlich erschwert, wenn nicht unmöglich gemacht. Die verkürzte Lebensdauer der Glühkathode sowie deren Beeinträchtigung durch vorhandene Dämpfe und Zersetzungsprodukte sind ebenfalls von Nachteil und lassen im Druckbereich oberhalb von etwa 10^{-4} Torr die Verwendung einer kalten Ionenquelle zweckmässig erscheinen.

Verhalten mit Kaltkathoden-Ionenquelle

Die Verwendung einer Kaltkathoden-Ionenquelle wird in Verbindung mit dem elektrischen Massenfilter dadurch erleichtert, dass die Ionenenergie bis auf die Festlegung einer oberen Grenze beliebige Beträge annehmen kann. Diese Grenze liegt jedoch bei der hier gewählten Ausführung unterhalb von 150 V und kann nur unter Beeinträchtigung der trennbaren Massendifferenz überschritten werden. Eine Hochfrequenz-Ionenquelle mit ihrer hohen Energie-dispersion ist daher schlecht geeignet.

Anders verhält es sich mit der Penning-Ionenquelle. Die Brennspannungen liegen zwar auch hier bei mehreren 100 bis 1000 V, doch kann bei geeigneter Anordnung der Elektroden eine ausreichende Abschirmung erfolgen. Das Prinzip entspricht dem eines Penning-Vakuummeters: (Bild 9). Die zwischen zwei Kathodenplatten und einer ringförmigen Anode beschleunigten Elektronen werden durch ein Magnetfeld derart abgelenkt, dass sie bis zum Erreichen der Anode eine hohe Zahl von Schwingungen ausführen. Die damit verbundene Verlängerung der effektiven Weglänge reicht aus, um auch bei Drucken von 10^{-5} Torr und darunter noch so viele Stossprozesse auszuführen, wie sie zum Aufrechterhalten einer elektrischen Entladung notwendig sind.

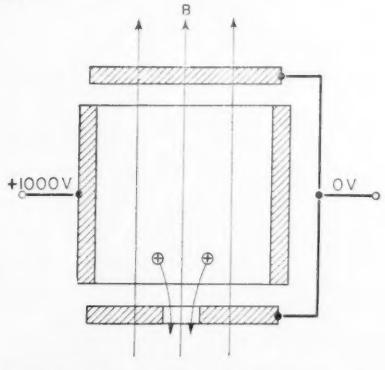

Bild 9. Prinzip einer Penning-Ionenquelle.

Die gebildeten Ionen sorgen ihrerseits durch Elektronenbefreiung beim Aufprall auf die Kathode für die notwendige Elektronenzahl. Wegen ihrer grossen Masse werden sie nur geringfügig vom Magnetfeld abgelenkt und erreichen die Kathode ungestört. Ein quasineutrales Plasma kann sich also erst bei höheren Drucken ($\geqslant 10^{-3}$ Torr) ausbilden.

Die Ionisierungsbedingungen sind zunächst viel unübersichtlicher als bei der Glühkathoden-Ionenquelle. Die stossenden Elektronen können jede Energie zwischen 0 und

calibration curves of the gases involved as well as the total pressure. Hence, the partial pressure indication becomes very difficult or almost impossible to carry out.

In the pressure range above 10^{-4} Torr, the shortened working life of the thermionic cathode as well as their deterioration through any vapours and decomposition products which may be present is also a disadvantage and makes it expedient to consider a cold cathode ion source.

Behaviour with cold cathode ion source

In the electrical mass filter the use of a cold cathode ion source is considerably simplified because the energy of the ions can take on any arbitrary value provided it does not exceed a certain upper limit. This limit lies, however, in the particular construction chosen here, below about 150 V and larger values can only be used at the expense of the mass difference to be separated. A high frequency ion source with its high dispersion of energies is, therefore, not very suitable. The matter is different in the case of Penning ion sources. Although the discharge voltages are, in this case, several 100 up to 1000 V, it is possible with a suitable arrangement of electrodes to obtain sufficient screening. The principle corresponds to that of a Penning vacuum gauge (Fig. 9). Electrons accelerated between two cathode plates and a ring anode are deflected by a magnetic field in such a manner that they perform a large number of oscillations before they reach the anode. The increase in effective path length achieved in this way ensures that at pressures as low as 10^{-5} Torr and below enough collisions can take place as are necessary for the electrical discharge to be maintained.

The ions formed collide with the cathodes and thereby ensure the release of a sufficient number of electrons to

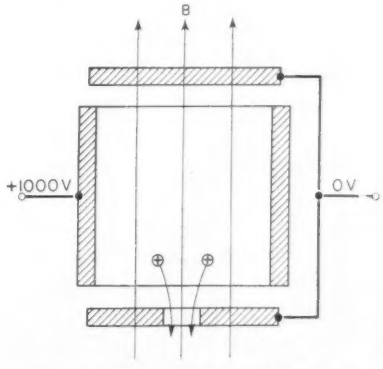

Fig. 9. Principle of a Penning ion source.

maintain the required numbers of electrons. Because of their great mass the ions are only deflected a very small amount by the magnetic field and, therefore, reach the cathode undisturbed. An almost neutral plasma is only formed at higher pressures (greater than about 10^{-3} Torr).

The conditions for ionization are not as easy to visualize as in the case of the thermionic cathode ion source. The colliding electrons can have any energy between 0 and the full discharge voltage. Also the electrons set free in the act of ionization can take part in further ionization. The electron current is, therefore, dependent on the gas pressure.

dem durch die volle Brennspannung vorgegebenen Wert besitzen. Ebenso sind die beim Ionisierungsakt befreiten Elektronen an der Ionisierung beteiligt. Der Elektronenstrom ist also vom Druck abhängig. Das gleiche gilt von der Brennspannung, da der zur Stabilisierung der Entladungsstrecke übliche Vorwiderstand einen druckabhängigen Spannungsabfall aufnimmt.

Es ist daher notwendig, durch zusätzliche Massnahmen eine gewisse Anpassung der Penning-Ionenquelle an den vorgesehenen Zweck zu bewirken. Zunächst muss die Geometrie der Elektroden so gewählt werden, dass im wesentlichen nur Ionen mit Energien unter 100 eV die Extraktionsöffnung erreichen. Mit einer gesondert angelegten Extraktionsspannung U_B ist dann die Feineinstellung der maximalen Ionenenergie und der optimalen Ionenausbeute möglich. Zur Erzielung eines gleichmässigen Ionenstrahls mit reproduzierbarer Verknüpfung von Intensität und Gasdruck ist es unbedingt notwendig, das Entladungsplasma sowohl zeitlich wie räumlich zu fixieren. Auch diese Forderung kann durch Anpassen von Elektrodenform und-stärke sowie Verlauf des Magnetfeldes innerhalb eines weiten Druckbereiches befriedigend erfüllt werden.

Bild 10, Kurve A^+ zeigt die Charakteristik $J_{40} = f(p_A)$, wie sie mit einter Penningionenquelle genannter Bauart bei Einlass von reinem Argon erhalten wurde.

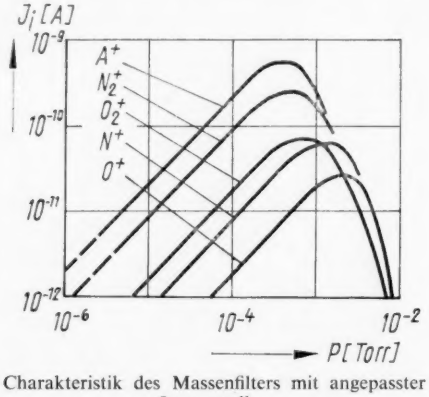

BILD 10. Charakteristik des Massenfilters mit angepasster Penning-Ionenquelle.

J_{40} bedeutet darin die Intensität des ausgefilterten Ionenstrahls der Masse 40. (Die übrigen der eingezeichneten Kurven wurden bei Einlass von Normalluft gemessen). Der Auffängerstrom J_{40} steigt mit dem Gasdruck monoton und vor allem reproduzierbar an und erreicht bei Drucken zwischen 5.10^{-4} und 8.10^{-4} Torr ein Maximum. Die Lage des Maximums hängt von der Ionenart ab und verschiebt sich in der Reihenfolge A^+, N_2^+, O_2^+, N^+, O^+ in Richtung höherer Drucke. So liegt das Maximum z.B. für O^+ bereits bei etwa $2{,}5.10^{-3}$ Torr. Dieses Verhalten entspricht demjenigen der Glühkathodenionenquelle, nur mit dem Unterschied, dass hier die Maxima in Richtung höherer Drucke verschoben sind. Lage und Ionenabhängigkeit der Maxima deuten auf Raumladungseffekte innerhalb der Ionenquelle hin. Hierfür spricht auch die Möglichkeit, durch Abänderung der Elektrodenform die Lage des Maximums zu verschieben. In Bild 11 sind zwei derartige Kurven gegenübergestellt wiederum ermittelt bei Einlass von reinem Argon.

The same holds for the discharge voltage because with the usual series resistance necessary to stabilize the discharge, a pressure dependent voltage drop is obtained.

It is, therefore, necessary to take additional measures before the Penning ion source can be used for this purpose. Firstly, the geometry of the electrodes must be so chosen that essentially only ions having energies less than 100 eV reach the extraction aperture. With an extraction voltage U_B specially applied the fine regulation of the maximum ion energy and the optimum ion yield is possible. To achieve a uniform ion beam with reproducible interrelation of intensity of gas pressure, it is definitely essential to fix the discharge plasma in space as well as in time. This condition can also be satisfactorily achieved for a wide range of pressures by suitable choice of electrode forms and adjusting the strength as well as the configuration of the magnetic field.

Fig. 10, curve A^+ shows the characteristics for $J_{40} = f(p_A)$ obtained with a Penning ion source of the type mentioned after admitting pure argon.

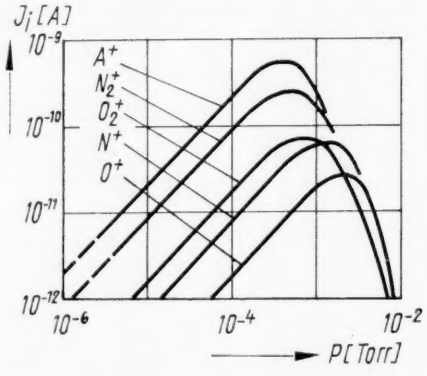

FIG. 10. Ion current as a function of pressure obtained with a modified Penning ion source.

The intensity of the filtered ion beam of mass 40 is here denoted by J_{40}. (The other curves shown in the figure were obtained by admitting ordinary air). The calculated current J_{40} rose steadily with gas pressure in a reproducible manner achieving, at a pressure between 5×10^{-4} and 8×10^{-4} Torr, a maximum. The position of the maximum depends on the type of ion and is displaced in the sequence A^+, N_2^+, O_2^+, N^+, O^+ in the direction of higher pressures. Thus the maximum of, e.g. O^+ lies at about 2.5×10^{-3} Torr. This condition corresponds to that obtained with a thermionic cathode ion source, the only difference being that here the maximum is displaced in the direction of higher pressures. The position and dependence of the maxima on the ions in question indicate a space charge effected within the ion source. This is confirmed by the possibility that the maximum can be displaced by changing the form of the electrodes. Fig. 11 shows two such curves obtained again by the admission of pure argon.

Whereas Curve I corresponds to Curve A^+ in Fig. 10 and can be reproduced in all its parts, Curve II shows a curve reproducible only at pressures above 10^{-4} Torr.

Vol.
10
196

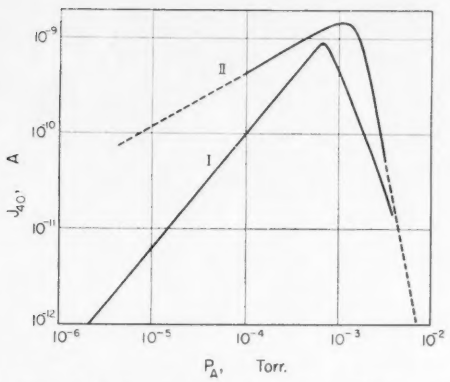

BILD 11. Charakteristiken bei verschiedener Ausführung der Penning-Ionenquelle.

Während Kurve I der Kurve A^+ in Bild 10 entspricht und in allen Teilen reproduziert werden kann, zeigt Kurve II einen reproduzierbaren Verlauf nur für Drucke oberhalb 10^{-4} Torr. Demgegenüber ist es durch Änderung der Elektrodenform gelungen, Intensität und Maximumsdruck auf etwa das Doppelte zu erhöhen.

Die beiden Ionenquellen-Typen ermöglichen es also, entweder im Druckbereich zwischen 1.10^{-4} und etwa 1.10^{-3} Torr oder im Bereich 1.10^{-6} Torr . . . 5.10^{-4} Torr Messungen des Partialdruckes p_i durchzuführen :

$$p_i = f(p_0) \cdot J_i$$

Die Verknüpfung $f(p_0)$ von Partialdruck p_i und dem Auffängerstrom J_i wird hierbei durch Eichung gewonnen. Für Gesamtdrucke p_0 unterhalb des Maximums ist $f(p_0) \approx C_i$ annähernd eine von der Gasart abhängige Konstante (Bild 10 und 11).

Ist die Art der zu erwartenden Gase bekannt und ausserdem sichergestellt, dass ihre Massen sämtlich innerhalb des erfassten Massenbereiches liegen, so kann der Partialdruck p_i auch nach

$$p_i = p_0 \frac{c_i \, J_i}{\sum_{\kappa} c_k \, J_k}$$

bestimmt werden. Hierzu muss das gesamte Spektrum durchfahren und jede auftretende Linie erfasst werden. Dafür entfällt die Notwendigkeit einer Eichung. Der Totaldruck p_0 ergibt sich aus dem Entladungsstrom der Ionenquelle.

Voraussetzung für sämtliche dieser Messungen ist allerdings, dass die für die jeweiligen Gase gültigen Werte c_i echte, von der Gaszusammensetzung unabhängige Konstanten sind.

Eine Überprüfung wurde für die Gase N_2, A, H_2O durch Einlass definierter N_2–H_2O und A-H_2O-Gemische durchgeführt. Der Wasserdampfanteil bewegte sich zwischen 20 und 80 prozent. Die ermittelten Ionenströme J_1 ($M = 18$) ; J_2 ($M = 28$)* und J_2 ($M = 40$) zeigten sich in guter Näherung den eingestellten Partialdrucken verhältnisgleich :

$$\frac{J_1}{J_2} = c_{12} \frac{P_1}{P_2} ; \quad \frac{J_1}{J_3} = c_{13} \frac{P_1}{P_3}$$

*Der Anteil der atomaren Stickstoffionen beträgt in allen Fällen nur etwa 5 prozent der Stickstoff-Molekülionen und kann hier also in 1. Näherung vernachlässigt werden. Analoges gilt von den verschiedenen, möglichen Ionen des Wassermoleküls, sowie der Argonatome.

The change in form of the electrodes has on the other hand resulted in increasing the intensity as well as the maximum pressure by a factor of two.

The two types of ion sources therefore allow to measure partial pressure, *Pi* either in the pressure range between

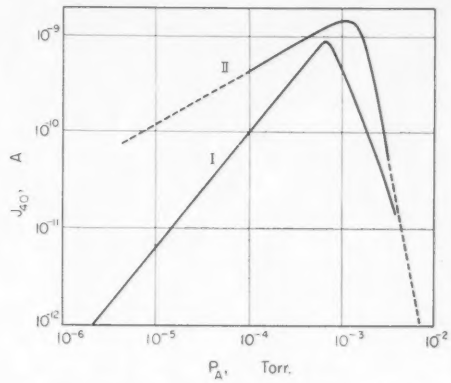

FIG. 11. Ion current against pressure curves obtained for different Penning ion sources.

1×10^{-4} and about 1×10^{-3} Torr or in the range 1×10^{-6} Torr . . . 5×10^{-4} Torr. Where

$$Pi = f(Po). \quad Ji$$

and the connection of $f(Po)$ with the partial pressure *Pi* and the collector current *Ji* is obtained by calibration. For total pressures *Po* below the maximum $f(Po) \approx Ci$ and is approximately a constant depending only on the gas in question (Fig. 10 and Fig. 11).

If the gases to be expected are known and it has been ascertained that their mass range lies within the total range covered, then the partial pressure may also be determined from the relation

$$p_i = p_0 \frac{c_i \, J_i}{\sum_{\kappa} c_k \, J_k}$$

This is carried out by sweeping over the whole spectrum to cover every line which may occur. Calibration is then not necessary. The total pressure *Po* is noted from the discharge current within the ion source.

All these measurements assume, however, that the values *Ci* for each gas should be true constants independent of gas composition.

This was tested experimentally for the gases N_2, A, H_2O by admitting measured quantities of N_2–H_2O and A–H_2O mixtures. The water vapour proportion varied between 20 and 80 per cent. It was shown that the ion currents $J_2(M = 18)$; $J_2(M = 28^*)$ and $J_2(M = 40)$ were proportional to the partial pressure ratios to a good approximation :

$$\frac{J_1}{J_2} = c_{12} \frac{P_1}{P_2} ; \quad \frac{J_1}{J_2} = c_{13} \frac{P_1}{P_2}$$

*The proportion of atomic nitrogen ions was in all cases about 5 per cent of the nitrogen molecular ions and can therefore be neglected to a first approximation. Similar remarks hold for the various possible ions of the water molecule as well as the argon atom.

Die Grössen c_{12} und c_{13} mit

$$c_{12} = 1{,}65 \pm 0{,}25\ ;\ c_{13} = 1{,}15 \pm 0{,}15$$

entsprechend dem Verhältnis c_i/c_k der in der Ionenquelle gültigen Ionisierungswahrscheinlichkeiten der verschiedenen Gase und gelten im Druckbereich unterhalb des Maximums der erwähnten Eichkurven.

Dieses Ergebnis ist trotz der bereits erwähnten, komplexen Ionisierungsbedingungen nicht erstaunlich und auch allgemein zu erwarten : Gemäss der grossen freien Weglängen von Ionen und Elektronen im Entladungsplasma und zufolge der durch die Elektrodenform und die Brennspannung vorgegebenen Feldstärken kann man bis herauf zu Drucken von einigen 10^{-3} Torr Ionisierungsenergien annehmen, die im Mittel weit über den Appearence-Werten sämtlicher Gase liegen. Für Beträge oberhalb von 70 eV ist ausserdem die differentielle Ionisierung nur schwach vom konkreten Wert der Elektronenenergie abhängig. Eine bevorzugte Ionisierung des Gasanteils mit kleiner Ionisierungsarbeit tritt erst dann ein, wenn sich das Plasma dem thermischen Gleichgewicht nähert. Dies ist innerhalb des interessierenden Druckbereiches nicht der Fall.

Drucke oberhalb des Maximums der Eichkurve bis nahe 10^{-2} Torr lassen sich noch erfassen, wenn die Art der in dem zu untersuchenden Gemisch enthaltenen Gase sowie deren spezielle Eichkurven bekannt sind. Dieser Fall liegt bei zahlreichen Prozessen der Vakuumverfahrenstechnik vor.

Verzichtet man auf die unmittelbare Verbindung von Rezipient und Messzelle sondern schafft durch Verwendung einer Hilfspumpe und einer Drosselstelle ein Druckgefälle zwischen beiden, so kann man selbstverständlich Vorgänge bei beliebig hohen Drucken untersuchen. Durch entsprechende Dimensionierung des Drosselelementes hat man es dann in der Hand, den günstigsten Arbeitsdruck innerhalb des Messgerätes bezw. der Ionenquelle einzustellen. Die gemessene Empfindlichkeit von ca. 2.10^{-6} A/Torr liegt nicht wesentlich unter derjenigen der Glühkathoden-Ionenquelle. Ebenso ist die Stabilität des extrahierten Ionenstromes durchaus mit derjenigen der Glühkathoden-Ionenquelle vergleichbar. Das gleiche gilt von der Ansprechgeschwindigkeit bei Einlass eines Testgases. Erinnerungseffekte, d.h. zeitlich nachklingende Ionenemissionen nach Abpumpen der zugeordneten Gaskomponente wurden ebenfalls in dem untersuchten Druckbereich 10^{-5} . . . 10^{-2} Torr nicht beobachtet.

Damit steht die modifizierte Penning-Ionenquelle derjenigen mit Glühkathode bezüglich Empfindlichkeit und Genauigkeit nicht wesentlich nach. Darüberhinaus hat sie jedoch beachtliche Vorteile, die sie vor allem für den Einsatz an technischen Anlagen geeignet macht.

Der Aufbau ist robust und wenigstöranfällig. Insbesondere sind plötzliche Lufteinbrüche ohne schädliche Wirkung. Aggresive Dämpfe beeinträchtigen Funktion und Lebensdauer nur geringfügig. Die Möglichkeit eines Dauerbetriebes der Quelle bis herauf zu Drucken von 10^{-2} torr erweitert den Messbereich des Massenfilters in Richtung hoher Drucke und macht damit erst einen der Hauptvorteile des Trennprinzips nutzbar. Schliesslich kann der Entladungsstrom der Ionenquelle auf einfache Weise zur Anzeige des Totaldruckes ausgewertet werden.

The quantities C_{12} and C_{13} were found to be

$$c_{12} = 1.65 \pm 0.25\ ;\ c_{13} = 1.15 \pm 0.15$$

corresponding to the ratio Ci/Ck of the ionization probability of the different gases applicable to this particular ion source and were shown to correspond to the values given in the calibration curves mentioned above for the pressure range below the maximum.

In spite of the complex ionization conditions this result is not unexpected : due to the large mean free path of ions and electrons in the discharge plasma and due to the strength of field determined by the form of the electrodes and the discharge voltage, one can assume ionization energies whose mean value lies far above the appearance potentials of most gases, for pressures up to several 10^{-3} Torr. Furthermore, the differential ionization is only weakly dependent on the value of the electron energy when voltages are above 70 eV. Preferred ionization of any particular gas requiring small ionization energy only occurs when the plasma approaches thermal equilibrium conditions. This is not the case in the pressure range of interest.

Pressures up toal most 10^{-2} Torr above the maximum of the calibration curve can still be dealt with provided it is known which gases occur in the mixture to be investigated and what are their calibration curves. This is a condition frequently met with in applications to vacuum processing techniques.

Dispensing with the direct connection between the reaction chamber and the measuring chamber by the use of an auxiliary pump and throttle to create a pressure drop between the two, it is evident that phenomena may be investigated at any desired higher pressure. By suitable sizing of throttling element it is possible to adjust the pressure in the measuring apparatus, i.e. the ion source to the best operating conditions.

The measured sensitivity of about 2×10^{-6} A/Torr lies not very much below that of the thermionic cathode ion source. Also the stability of the extracted ion current is quite comparable with that of the thermionic source. The same applies to the response time on admitting a test gas. Any memory effect, i.e. any ion emission persisting after evacuating a certain gas component was not observed in the pressure range 10^{-5} . . . 10^{-2} Torr investigated.

Hence the modified Penning ion source is not much inferior to the thermionic cathode with respect to sensitivity or accuracy, but on the contrary it shows notable advantages making it specially suitable for application to technical plants.

The construction is robust and not liable to be damaged, especially when sudden admission of air should occur. They are little affected in operation and life by reactive vapours. The possibility of continuous operation of the source at pressures up to 10^{-2} Torr enlarges the measuring range of the mass filter in the direction of higher pressures so that one of the main advantages of this method of mass separation may be utilised. Finally, the discharge current in the ion source is a simple means of indicating the total pressure.

Therefore, while the electrical mass filter with thermionic cathode ion source of suitable construction is chiefly suitable for proving the presence of the smallest partial pressures,

Während also das elektrische Massenfilter mit Glühkathodenionenquelle angepasster Bauart vor allem zum Nachweis kleinster Partialdrucke geeignet ist, ergibt sich durch Einbau der Penning-Ionenquelle ein besonders robustes Partialdruckvakuummeter für den technischen Hoch- und Feinvakuumbereich.

4. Anwendung

Als konkretes Beispiel für eine zweckentsprechende Anwendung des elektrischen Massenfilters möge die Vakuumtrocknung von elektrischen Isolationspapieren dienen. Neben Luft und den Dämpfen der Tränköle treten hier vornehmlich Wasserdampf und CO_2 bezw. CO als Zersetzungsprodukte des Papiers im Trocknungsbehälter auf, deren Überwachung zur Beurteilung des Trocknungsprozesses geeignet ist. Erreicht der Arbeitsdruck während des Verfahrens Werte unterhalb 10^{-2} Torr, so kann das Massenfilter unmittelbar auf den Trocknungsbehälter aufgesetzt werden. Die Ausführung mit kalter Kathode besitzt hierbei sowohl ausreichende Empfindlichkeit und Messgenauigkeit wie auch die für Langzeitmessungen motwendige geringe Störanfälligkeit. Bild 12 zeigt den Verlauf der Partialdrucke p_{18} und p_{28} als Funktion der Zeit bei Ablauf einer Modelltrocknung einer geringen Papiermenge. Eine besondere Beheizung des Trocknungsgutes war nicht vorgesehen.

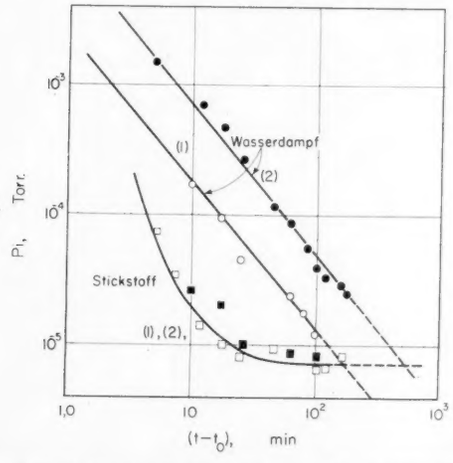

BILD 12. Partialdruckverlauf p_{18} und p_{28} während einer Modelltrocknung (1) mit Leerkessel (2) mit eingelegtem Kondensatorpapier.

Man erkennt den während der Beobachtungszeit annähernd inearen Abfall des Wasserdampfdruckes, während der Stickstoffpartialdruck einem Sättigungswert zustrebt. Dieser Wert entspricht dem Eindringen atmosphärischer Luft durch zufällige Undichtigkeiten des Trocknungsbehälters.

Wird hingegen eine an sich übliche Beheizung des zu trocknenden Papieres durchgeführt ($T = 100$–$130\,^\circ C$), so treten mit zunehmender Trocknungszeit neben $m = 18$ und 28 sowie Massenanteilen des Tränköls die Masse $m = 44$ mit ansteigender Intensität auf. Der zeitliche Verlauf, sowie ein Vergleich der Massen 14, 16, 28 und 32 lassen die Deutung zu, dass mit $m = 44$ der Teildruck von CO_2 und mit $m = 28$ nach längerer Trocknungszeit fast ausschliesslich der Teil-

the provision of a Penning ion source leads to a robust partial pressure vacuum gauge specially adapted for the technical high and fine vacuum range.

4. Applications

Consider the vacuum drying of electrical insulating paper as a concrete example for a suitable application of the electrical mass filter. Apart from air and vapours arising from the impregnating oils the main constituents occurring in the drying chamber are water vapour and CO_2, or CO from decomposition products of the paper, and their measurement serves to supervise the drying process. If during the process the operating pressure falls below 10^{-2} Torr the mass filter may be connected right on to the process chamber. The construction based on the cold cathode has in this case the required sensitivity as well as being suited for long period measurements.

Fig. 12 shows the change of partial pressures P_{18} and P_{28} with time for an experimental run using a small quantity of paper. There was no special provision for heating the substances to be dried.

It is seen that during the period under observation an approximately linear decrease in water vapour pressure

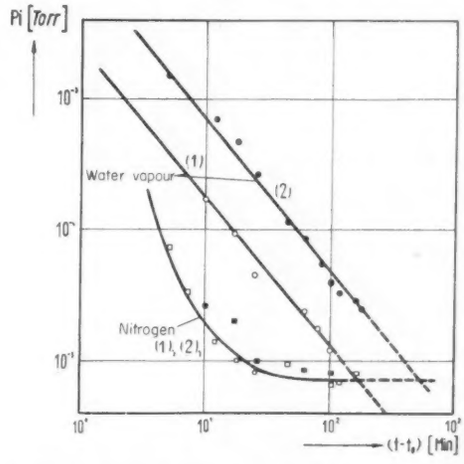

FIG. 12. Partial pressure changes for P_{18} and P_{28} during a trial run (1) with empty chamber (2) with condenser paper inserted.

occurs while the nitrogen partial pressure tends to a saturation value. This value corresponds to accidental leakage of atmospheric air into the process chamber.

If on the other hand the usual practice is followed whereby the paper to be dried is also heated ($T = 100$–$130\,^\circ C$) then with increasing time of drying apart from masses $m = 18$ and 28 one also obtains increasing partial pressures due to the impregnating oil $m = 44$. The behaviour of indicated masses with time as well as a comparison of masses 14, 16, 28 and 32 admit of the interpretation that after a lengthy drying period with $m = 44$ the partial pressure of CO_2 and with $m = 28$ almost exclusively a partial pressure of CO

druck von CO angezeigt wird. Betrachtet man das Verhältnis der Gasanteile CO, CO_2, H_2O untereinander, so erkennt man, wie dieses einem Grenzwert zustrebt. (Bild 13).

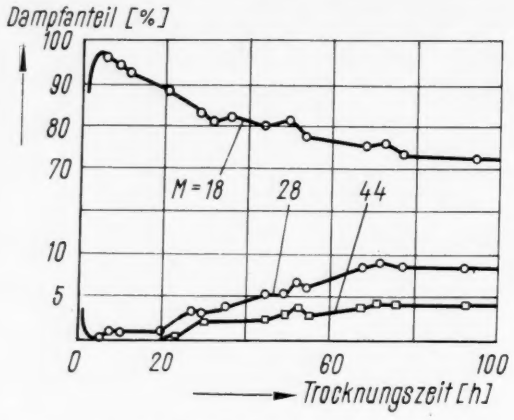

BILD 13. Dampfanteile der Massen 18, 28 und 44 in der Trocknungsatmosphäre.

Man kann vermuten, dass dieser Grenzwert der Zersetzungsgeschwindigkeit des zu trocknenden Papieres mit Freisetzung der Gase H_2O, CO, CO_2 entspricht. Die Abspaltung dieser Gase ist bereits in der Literatur mehrfach angegeben und untersucht worden[9, 10]. Eine weitere über die Annäherung an den Grenzwert hinausgehende Papiertrocknung würde also lediglich die Schädigung des Papieres fortsetzen, ohne zu einer Verbesserung der elektrischen Eigenschaften durch Wasserentzug führen zu können*).

5. Zusammenfassung

Es wird ein Partialdruckvakuummeter beschrieben, welches auf einem neuartigen massenspektrometrischen Prinzip, dem sogenannten elektrischen Massenfilter nach Paul[6] beruht. Die Massentrennung erfolgtrein elektrisch mit Hilfe eines hyperpolischen Hochfrequenzfeldes. Die Auswahl der verschiedenen Massen ist durch Variation der Hochfrequenzamplitude möglich. Das Auflösungsvermögen wird durch Einregeln einer der Hochfrequenzspannung überlagerten Gleichspannung eingestellt und kann während des Betriebes innerhalb wieter Grenzen verändert werden.

Das verwendete Trennprinzip erlaubt eine Anwendung des Gerätes auch bei relativ hohen Totaldrucken im Bereich des Hoch- und Feinvakuums. Es wird daher zunächst eine Messzelle beschrieben, die für den Einsatz an technischen Vakuumanlagen gedacht ist. Bei einer Gesamtlänge von 35 cm lassen sich mit dieser Anordnung Massen innerhalb des gesamten Bereiches $m = 2$ bis 85 erfassen und bei einem Auflösungsvermögen von max. 80 in ausreichender Weise voneinander trennen. Durch die besondere Ausführung von Ionenquelle und Analysatorteil ist eine Partialdruckanzeige im Druckbereich zwischen 5.10^{-6} und 5.10^{-3} Torr möglich. Die Empfindlichkeit der Anordnung bewegt sich zwischen 10^{-6} und 10^{-5} A/Torr.

*Eine ausführliche Mitteilung über diese Untersuchungen ist demnächst an anderer Stelle vorgesehen.

is indicated. If the interrelation of gases CO, CO_2, H_2O is compared it is seen that they approach a limiting value (Fig. 13).

It may be assumed that this limit corresponds to the rate of decomposition of the paper being dried resulting in evolution

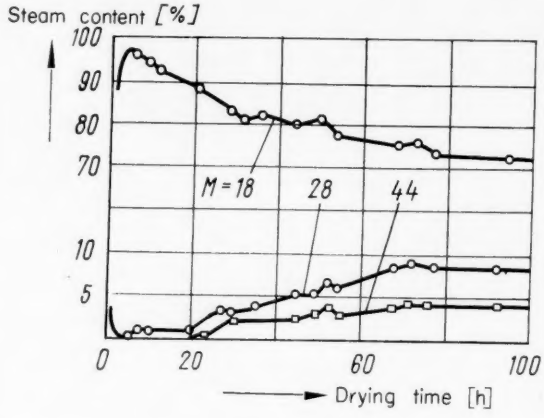

FIG. 13. Vapour constituents of masses 18, 28 and 44 in the drying atmosphere.

of the gases H_2O, CO, CO_2. The appearance of these gases has been mentioned and investigated several times in the literature[9, 10].

It is concluded therefore that a further period of drying beyond the limit would merely continue to damage the paper without leading to any improvement in its electrical properties by moisture removal.*

5. Conclusion

A partial pressure vacuum gauge is described operating according to a new mass spectrometrical principle, the so-called electrical mass filter by Paul[6]. The mass separation is carried out purely electrically by means of a hyperbolic high frequency field. Selection of different masses is possible by variation of the high frequency amplitude. The resolution is adjusted by the steady voltage superimposed on to the high frequency voltage and can be varied within wide limits during operation.

This method of mass separation allows for the use of the instrument at relatively high total pressures in the range of high- and fine-vacuum. Hence, a measuring cell is described intended in the first place for application to technical vacuum plant. The arrangement has a total length of about 35 cm for covering adequate separation of the whole mass range $m = 2$ to 85 with a maximum resolution of 80. By a special construction of the ion source attached to the analysis part it is possible to obtain a partial pressure indication covering the pressure range between 5×10^{-6} and 5×10^{-3} Torr. The sensitivity of the arrangement lies between 10^{-6} and 10^{-5} A/Torr.

*A detailed communication on these investigations is intended in some other place.

Vol. 10 196

Als Anwendungsbeispiel wird die messende Kontrolle bei der technischen Trocknung von elektrischen Isolationspapieren beschrieben. Die Analyse zeigt, dass neben dem Partialdruck von Wasserdampf der Anteil der Gase CO und CO_2 wichtige Aufschlüss über den Verlauf der Trocknung erbringt.

6. Dank

Für die Möglichkeit zur Durchführung dieser Arbeit sowie für wertvolle Diskussionen sei Herrn Dir. Dr. A. Siemens und Herrn Dr. W. Hänlein herzlich gedankt.

Gleicher Dank gebührt Frau L. Denk für die Durchführung zahlreicher Messungen.

Schrifttum

[1] G. D. Perkins und D. E. Charpentier; 4. *Nat. Symp. on Vacuum Technology Transactions.* S.125–128. Pergamon Press, London (1957).
[2] H. Sommer, H. A. Thomas und J. H. Hipple; *Phys. Rev.* **82**, 697 (1951).
[3] A. Klopfer; *Advances in Vacuum Sci. and Techn. I.* Pergamon Press, London, 397–400, (1960).
[4] W. H. Bennet; *J. Appl. Phys.* **21**, 143 (1950).
[5] P. F. Váradi, L. G. Sebestyén, und E. Rieger; *Vakuumtechnik* **7**, 13–16 und 46–51 (1958).
[6] W. Paul und H. Steinwedel; *ZS. Naturforschung* **8***a*, 448 (1953).
[7] W. Paul, H. P. Reinhard, und U. v. Zahn; *ZS. f. Physik.* **152**, 143–182 (1958).
[8] H. Ewald und H. Hintenberger; *Methoden und Anwendungen der Massenspektroskopie*, Verlag Chemie G.m.b.H., Weinheim/Bergstrasse, 39 u.f. 23–51 (1953).
[9] H. Veith; *Kolloid-Zeitschr*, 1950, 67–72 (1957).
[10] E. J. Murphy; *Trans. Electrochem. Soc.* **83**, 161–174 (1943).

As an example of the application the measured control during a technical drying process of electrical insulating papers is described. Analysis shows that important conclusions on the drying process are obtained by observing the presence of the gases CO and CO_2 in addition to the partial pressure of water vapour.

Acknowledgements

Acknowledgements are extended to Director Dr. A. Siemens and Dr. W. Hanlein for facilities to carry out this work as well as for valuable discussions. Thanks are also due to Mrs. L. Denk for carrying out a large number of measurements.

References

[1] G. D. Perkins and D. E. Charpentier; 4. *Nat. Symp. on Vacuum Technology Transactions.* S.125–128. Pergamon Press, London (1957).
[2] H. Sommer, H. A. Thomas and J. H. Hipple; *Phys. Rev.* **82**, 697 (1951).
[3] A. Klopfer; *Advances in Vaccuum Sci. and Techn. I.* Pergamon Press, London, 397—400, (1960).
[4] W. H. Bennet; *J. Appl. Phys.* **21**, 143 (1950).
[5] P. F. Váradi, L. G. Sebestyén, and E. Rieger; *Vakuumtechnik* 7, 13–16 and 46–51 (1958).
[6] W. Paul and H. Steinwedel; *ZS. Naturforschung* **8**a, 448 (1953).
[7] W. Paul, H. P. Reinhard, and U. v. Zahn; *ZS. f. Physik.* **152**, 143–182 (1958).
[8] H. Ewald und H. Hintenberger; *Methoden und Anwendungen der Massenspektroskopie*, Verlag Chemie G.m.b.H., Weinheim/Bergstrasse, 39 u.f. 23–51 (1953).
[9] H. Veith; *Kolloid-Zeitschr*, 1950, 67–72 (1957).
[10] E. J. Murphy; *Trans. Electrochem. Soc.* **83**, 161–174 (1943).

Vacuum as an Insulator*

R. HAWLEY

Department of Electrical Engineering, King's College, University of Durham

(*Received 2 February 1960*)

This article reviews the properties of vacuum when it behaves as an electrical insulator, the factors which determine breakdown, and the hypotheses advanced to account for the breakdown. Conclusions are drawn which suggest the direction which future developments might take.

1. Introduction

Vacuum is finding increasing applications as an insulator but its usefulness is limited by the occurrence of a heavy current arc when the electrical stress is increased beyond the critical value. Although it is an excellent insulator at small separations, as the gap is increased the stress required to cause breakdown decreases. Vacuum breakdown was first noted in 1676 and the first description of the vaucum arc was given in 1897. More recently much work on the breakdown aspect has been carried out in America, France, Great Britain and Soviet Russia. Owing to the diversity of experimental techniques there are many parameters which appear to affect the mechanism of breakdown and the object of the present article is to present a résumé of all previous work relating to vacuum as an insulator.

2. Properties of vacuum insulation

If a sufficiently high potential is applied to metallic electrodes separated by an insulating medium, breakdown is said to occur when a spark passes between them. This spark marks the transition from one more-or-less stable electrical condition to another. Although first observed by Harris in 1834, it was shown by Paschen in 1889, that when the insulating medium is gaseous, the potential necessary to produce a spark is nearly a linear function of the number of molecules encountered by an ion or an electron in traversing the gap. In other words, it is proportional to the gas pressure, p, and the electrode separation, d. For large values of $(p.d.)$, the breakdown voltage, V, is characteristic of the gas and nearly independent of electrode material. For values of $(p.d.)$ less than about 10 Torr cm the contribution of secondary effects at the electrodes ceases to be negligible and there is a minimum value of sparking potential which depends not only on the gas but also on the material and the surface condition of the electrodes[56]. At pressures below 10^{-4} Torr, that is below the glow-discharge region, the breakdown is no longer dependent on the pressure or the nature of the intervening gas. It is in this region that the vacuum arc is observed.

At these pressures the mean free path of the molecules is large compared with the system dimensions and a charged particle drawn from one electrode to the other is unlikely to collide with residual gas molecules. As the potential across a pair of plane, parallel, smooth-surface electrodes in a vacuum is increased, a very small current due to field or auto-electronic emission may begin to flow. Under certain circumstances it is generally supposed that by secondary effects, these electrons produce further charged particles at the anode and these in turn may produce enhanced electron emission on striking the cathode. In some cases pulses of current arise or electrode material may be transferred. As

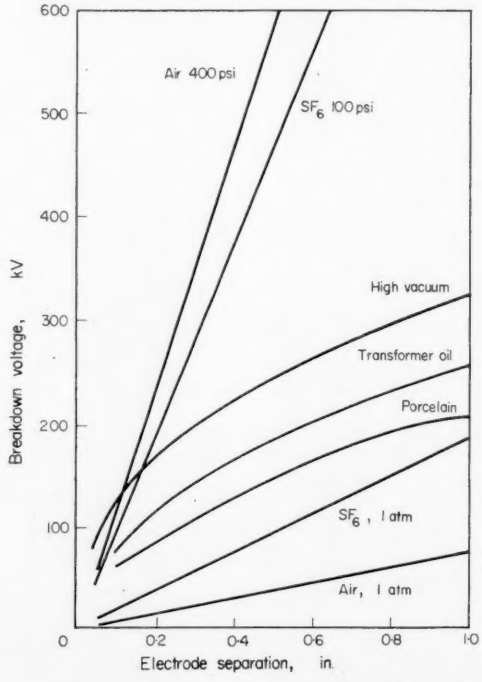

FIG. 1. Direct current breakdown strength of typical solid, liquid, gaseous and vacuum insulation in a uniform field (Trump[79]).

[Reproduced with the kind permission of the Massachusetts Institute of Technology. Figure taken from *Dielectric Materials and their Applications* by A. R. von Hippel, John Wiley & Sons Inc. and the Technology Press of M.I.T.]

*Paper presented before the North Eastern Graduate and Student Section of the Institution of Electrical Engineers.

Vol. 10 1960

TABLE I

Insulation Spectrum

Dielectric	Typical Examples	Typical Applications	Power Factor cos θ	Relative Permittivity ϵr	Specific Resistance ohm-m ρ
Compressed solids	Pressboard	Slot liners in machines	0.013	3.1	10^7
Solids	Porcelain	Sealing ends	—	5–7	10^9–10^{12}
	Mica (Muscovite)	Capacitor dielectrics	0.0003	4.5–7	10^{10}–10^{14}
Semi fluid compounds	Bitumen compound	Termination disconnecting boxes	0.03–0.04 (20 °C–60 °C)	3.5	10^{11}
	Gum rosin	Cables	0.001	2.6	10^{15}
Liquids	Mineral insulating oils	Switchgear	0.0002	2.0–2.5	10^{10}–10^{12}
	Chlorinated diphenyl and trichlorbenzene	Capacitors	0.003	4.2	10^9–10^{11}
Compressed gases	Nitrogen	H.V. cables	→0	→1	→Infinity
	Sulphur hexafluoride	Switchgear	→0	→1	→Infinity
Gases	Air	Overhead lines	→0	→1	→Infinity
	Carbon dioxide		→0	→1	→Infinity
Gases at reduced pressure	Argon	Gas filled photo electric cells (0.2 torr) gas filled lamps (100 torr)	→0	→1	→Infinity
Medium high vacuum (Soft vacuum 1–10^{-3} torr)	—		0	1	Infinity
High vacuum (10^{-3}–10^{-7} torr)	—	Vacuum switches	0	1	Infinity
Very high vacuum (Hard vacuum)	—	Electron tubes	0	1	Infinity

Unless otherwise stated all measurements taken at 20 °C and are average values.

the voltage is increased above a critical value instability is produced and a heavy current arc flows. It is generally accepted that this occurs in vapours released at the electrodes. The current in the arc is limited almost solely by the characteristics of the supply circuit.

The position of vacuum in an insulation " spectrum " is shown in Table I and its voltage holding, as obtained by Trump, is compared with other typical dielectrics in Fig. 1. Table II shows some of the applications where vacuum is called upon to act as an insulator.

TABLE II

Examples of Applications of Vacuum Insulation

Application	Degree of Vacuum Torr
Vacuum switches and current switching devices	10^{-4}–5×10^{-4}
Electron tubes, photocells, etc.	10^{-10}–10^{-3}
Low loss H.F. capacitor	10^{-7}
Electrostatic voltmeter	10^{-5}
Particle accelerators	2×10^{-6}–10^{-4}
Experimental fusion devices	10^{-9}–10^{-5}

3. Breakdown parameters

In the next few sections are discussed the various factors upon which breakdown of a vacuum gap appears to depend. Vacuum alone could be regarded as the perfect dielectric, but its use as such requires metallic electrodes. Hence it is really the combination of these two which forms the subject of all that follows.

(*a*) *Conditioning effect*

During some early experiments, Anderson observed that while bombardment of steel electrodes with electrons, for a time prior to testing, produced very little effect on the breakdown voltage, a combination of sparking the electrodes first in an atmosphere of hydrogen and then in vacuum, resulted in a final breakdown voltage of more than double the value at which the first spark occurred.[5] It was first shown by Millikan and Sawyer and has since been confirmed by others that if the gap is continually sparking over, even in vacuum only, the breakdown voltage increases until it reaches a " plateau ". Results obtained in the plateau region still vary within fairly wide limits. However, if " reproducible " data are required the electrodes must first be conditioned in some such way. For hydrogen conditioned electrodes the

number of sparks required to reach a plateau is about 10 otherwise it can be as many as 10,000[5, 25, 32, 34, 45, 59, 72, 78]. In some cases it has been observed that the conditioning is not permanent and if the voltage is removed for a time or the electrodes exposed to the atmosphere then the next breakdown value will be much lower, but the re-conditioning process will then take place much more quickly. Conditioning has also been noted at high frequencies[31, 41, 48, 59, 76], and during tests on accelerator tubes.

(*b*) *Electrode spacing*

Anderson also showed that as the separation between a pair of plane-parallel electrodes was increased the breakdown voltage did not increase at an equal rate. That is to say the average potential gradient, or stress, at which breakdown occurred was reduced with increased spacing. This has been termed the " Total Voltage Effect "[5, 78, 82]. These experiments also showed that the stresses were inadequate, at the larger spacings, to provide an explanation of breakdown in terms of high field emission.

Cranberg, supported by independent workers, observed that there appeared to exist an extremely simple relationship between the electrode spacing and the most probable sparking voltage, for spark conditioned electrodes in either static or continuously pumped vacuum.

This relationship can be written :—

$$VE = C \qquad (1)$$

where V = total applied voltage

E = gross surface gradient

and C = a constant, depending on the electrode material and its surface condition.

In the case of plane-parallel electrodes the relationship becomes :—

$$V = k\sqrt{d} \qquad (2)$$

on substituting $E = V/d$ in equation (1).

Thus $$V = K d^{\alpha} \qquad (3)$$

where $\alpha = \frac{1}{2}$

The criterion [equation (3)] has been applied in a modified form to the design of accelerator tubes[29]. Most of the experimental results obtained to date when plotted to a log-log scale approximate to straight lines with slopes of about one half and recent precise investigations are in close agreement[3, 45, 67]. Other hypotheses give different values for α, for example, Slivkov quotes 0.625 and it is possible that the relationship does not hold for small gaps, say less than 1 mm[73]. Cranberg's work suggests a dependence of breakdown on total voltage between the electrodes and the potential gradient at their surfaces. It has been thought that the use of r.f. voltages has resolved their respective roles.[50] Fig. 2 shows a section of results plotted in straight line form. Note that as the gap is increased by a factor of 10^7 the stress for breakdown is reduced by a factor of 600.

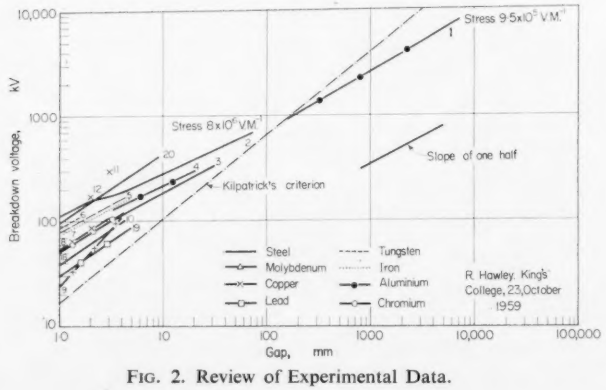

FIG. 2. Review of Experimental Data.

(*c*) *Material of electrodes*

As will be seen from Fig. 2 the material of the electrodes appears to exert a strong influence on the breakdown voltage for a given separation[5, 12, 25, 45, 60, 73].

Table III shows a list of materials in order of diminishing voltage-holding, but variations in position have been reported. With a 1 mm gap and conditioned electrodes, Trump showed that stainless steel held about 120 kV d.c. whereas copper would only hold approximately 40 kV d.c.[5, 45]. The threshold voltage for the so-called " Micro-discharges " and the voltage at which a continuous current appears in the gap have also been shown to be dependent on the electrode material[7, 45, 68].

TABLE III

Material
Stainless steel
Case hardened steel
Nickel
Cupalloy
Tantalum
Aluminum
Lead
Copper
Carbon
Silver

The amount of damage due to sparking varies for each material. For use in high power vacuum spark gap switches it is reported that brass is the best electrode material because it resists corrosion by the arc. That is to say the surface remains smooth after a few sparks. Any roughness of the electrode would enhance field emission which would lower the maximum hold off voltage. However, the superior corrosive properties of brass were not noted in straightforward breakdown tests[37, 38, 41].

The anode material appears to play the major role in determining the breakdown voltage which in turn seems to be proportional to the tensile strength of the anode material. Should extreme differences exist in the physical properties of the cathode and anode the breakdown voltage, according to Heard, may be lower than that for the poorest electrode material in the gap[45, 46, 67, 72, 73].

(*d*) *Electrode configuration*

The majority of experiments performed so far have been with either electrodes designed to give a uniform field distribution or spheres with gaps small compared to the sphere radius which gave in effect uniform fields. A pertinent piece of evidence showing the effects of electrode configuration

Vol. 10 1960

has been published by Leader. Using impulse voltages he has shown that higher breakdown strengths for a given gap were obtained with the extreme geometry of a point opposite a plane. The breakdown strength increased as the point diameter decreased. For a given gap, and electrode configuration of a point opposite a plane, the voltage holding was higher when the point was the anode. The actual breakdown voltage of a given gap as quoted by Leader appears to be on the low side. Electrode configuration has been shown to have an effect on the threshold voltage of the micro-discharges and the appearance of a continuous current in the gap[2, 40, 51, 68, 73].

(*e*) *Electrode temperature*

A direct investigation of the effects of the electrode temperature was recently carried out by Slivkov. For nickel and iron electrodes the strength remained unchanged for temperatures as high as 500 °C thus leading to the conclusion that gases and vapours of organic compounds adsorbed on the surface of the electrodes did not substantially influence the occurrence of breakdown. This is said to follow from the fact that adsorbed gases, and especially the quantity of vapours of organic compounds, undergo a large decrease upon heating from ambient temperature to 450–500 °C. Other characteristics obtained on heating are used by Slivkov to support his hypothesis of breakdown[73, 74]. Variations in sparking rate at 14 Mc/s have been reported but X-ray intensity background does not appear to be markedly affected[21, 48].

(*f*) *Frequency of applied voltage*

While quite an amount of work has been carried out using different types of voltage, namely impulse, direct and alternating (50 c/s) no real comparison can be made between them due to the fact that the various experimenters used different techniques and electrode materials. However it was thought that a given gap should stand a higher impulse than it would with static voltage. This fact was confirmed by Denholm, in tests on steel electrodes with a gap of 0.5 mm. The breakdown voltages are shown in Table IV. The divergence increased as the gap increased[25].

TABLE IV

Type of Voltage	Breakdown Voltage kV
Impulse	72
Alternating (50 c/s)	62
Direct	54

The first investigation showing the effect of using high frequency voltage appears to be that of Halpern who succeeded in maintaining 2×10^6 V across a 5 cm copper gap at a frequency of 2800 Mc/s. This was about a factor of four higher than had ever been obtained with direct voltage across outgassed copper. An extensive report has been issued on the subject of spark damage and high voltage breakdown of metals at 14 Mc/s. Formative time lags have been observed of the order of 10^{-7}–10^{-8} seconds for a 1 mm gap[21, 25, 34, 39, 44, 51, 62, 75].

(*g*) *Magnetic field in the gap*

A magnetic field in the gap will markedly change the nature of the breakdown phenomena and the degree of damage to the electrodes. For example, breakdown has been shown, by Redhead, to occur at about 1 kV between concentric cylinders 8.5 mm apart in a vacuum of 10^{-8} Torr with an axial magnetic field of 1000 G in the gap. The problem of breakdown under perpendicular electric and magnetic fields is of increasing importance, for example in Z.E.T.A., and work is at present being carried out on this aspect[4, 22, 36, 69].

(*h*) *External circuit*

Once breakdown occurs, the current in the arc is limited by the external circuit. It has been shown that if this limited current is below a critical value between 0.25 and 1.00 amps then a stable discharge will not be maintained. This is in line with values deduced for glow-arc transition[32, 51, 70, 71]. The value of the internal resistance of the voltage source and of the capacitance in parallel with the discharge gap, has an effect on the amount of charge transferred in a single micro-discharge. The amount of stored energy released in the arc will affect the amount of damage occurring at the electrode surface and hence the amount of pre-breakdown current. According to Denholm if a large follow current is allowed to flow this will smooth the roughened parts of the electrodes and hence increase, rather than lower, the breakdown voltage[8, 25, 45, 68].

(*i*) *Pressure*

Increase in local pressure during breakdown has been observed and such gas released decreased as conditioning progressed[43, 48, 51, 60, 66]. Whilst in general breakdown below 10^{-3} Torr is not dependent on pressure this is not so in particle accelerators for here the mean free paths of the gas particles are comparable with the dimensions of the apparatus. Observations have been reported where the breakdown voltage rose with increasing pressure, for example from 130 kV at 5×10^{-5} Torr to 500 kV at 25×10^{-5} Torr, with a 40 cm air gap. Leece has examined possible reasons for this[52]. Breakdown has been reported as being dependent on the type of residual gas in the system[29].

(*j*) *Electron current component*

Experiments performed by Pivovar using a magnetic field in the gap are said to show that the electron current component plays a large part in the development of breakdown and other work tends to support this view, at least for accelerating voltages greater than 80 kV[25, 41].

(*k*) *Nature of electrode surfaces*

Early workers, who believed that breakdown was initiated by field emission from microscopic points on the cathode, were of the opinion that higher breakdown strengths could be obtained the smoother the cathode surface. The conditioning effect was assumed to be due to the removal of micro-projections by spark-over. The results of Anderson and Leader tended to show however, that there was a condition beyond which further improvement in quality of surface finish, had no connection with the breakdown. Hadden showed that there was no great difference in voltage holding for copper between acid dipped surfaces, unpolished

surfaces smoothed with 00-emery under water, and electrolytically polished surfaces. Substantial evidence to the contrary has however, been provided by Trump. He has shown that if the electrodes are buffed to a high polish or a mirror finish with a minimum of scratches and the residual buffing compounds removed by solvents and detergent washing then the breakdown voltage for aluminium is so much improved that it gives a better performance than steel or even stainless steel[5, 35, 51, 79, 80].

Direct studies of clean surfaces are complicated by the fact that oxidation takes place, organic vapours are generally present which may give rise to carbon on the electrodes and also that the action of polishing is to form a fudge of oxide, metal and abrasives. This will be so even after special care is taken in cleaning the surface. The growth of a molecular layer of oxide on copper at a presusre of 10^{-4} Torr of oxygen has been shown to be almost instantaneous and the estimated time for a layer of oxygen molecules to cover a surface is 0.06 sec at a pressure of 10^{-5} Torr of oxygen. Once the arc has been struck it appears to move over preferential areas on the surface[9, 30, 84, 85].

(l) Insulator in the gap

If the electrodes in a vacuum are separated by insulating material, in the form of a rod, it is known that breakdown over the rod takes place without its puncture at a lower voltage than in a simple vacuum gap. If the rod is fused into the cathode or fitted into a groove in the cathode, Gleichauf reports that the breakdown strength is considerably increased[32, 33].

While the conditioning effect was observed when the electrodes were separated by a glass or quartz insulator, variations in the electrode material appeared to have no effect on the breakdown voltage. However, the material of the insulator and its surface condition exerted a strong influence on the value of breakdown voltage.

The problem of flashover along insulating materials in vacuum is of interest and will be of increasing importance as high power vacuum devices are developed. Oil vapour deposited on an insulator surface can become carbonised and cause trouble[12, 29].

4. Criterion for vacuum breakdown

In the design of high-voltage equipment it is not so much the breakdown voltage of electrodes conditioned by multi-sparkover that is of importance, but the voltage at which the first spark will occur. This is particularly true of experimental fusion devices where it may well be impossible to condition such large structures. An empirical criterion for minimum sparking voltage that covers a large range of surface gradients, gaps and frequencies, has been put forward by Kilpatrick[49].

Currents, due to field emission and energetic ions are considered necessary to initiate sparking and consideration of these effects leads to the expression :

$$W E^2 (\text{exp. } -K_1 E) = K_2 \qquad (4)$$

where W = maximum possible energy of a particle at the electrode surface, prior to a spark, in eV.

E = cathode gradient, V/cm

$K_1 = 1.7 \times 10^5$

$K_2 = 1.8 \times 10^{14}$

Kilpatrick presents graphs for the determination of W in the r.f. case which takes into account transit time and phasing effects. The criterion fits experimental data in the ranges :—

$10^{-5} <$ gap < 10 cm

$30 <$ voltage $< 1.2 \times 10^6$ V

$9 \times 10^4 <$ surface gradient $< 8 \times 10^7$ V/cm

d.c. $<$ frequency < 3000 Mc/s

and is valid for metal electrodes not specially prepared. It is relatively insensitive to the kind of metal or the kind of vacuum system and applies to electrodes covered in oil. Fig. 3 shows the equation (4) plotted in an approximate straight line form with a slope of about 0.7.

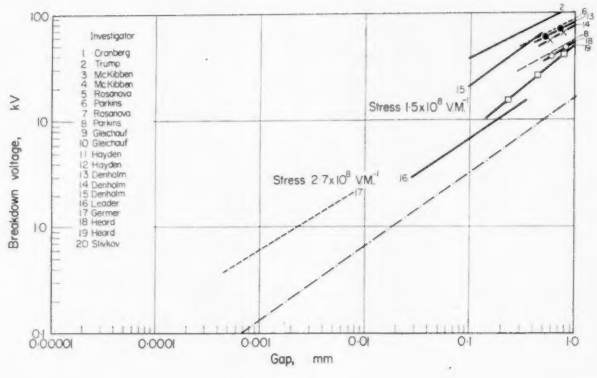

FIG. 3.

5. Pre-breakdown conduction

The currents between electrodes with ultra clean surfaces in excellent static vacuum have generally been shown to be due to field emission, when a field intensifying factor has been taken into account. The reason for this factor is that many observations have been made where the field strengths in the gap were several magnitudes less than that required theoretically to give appreciable emission. Hence it was assumed that the field at the surface of the cathode was intensified by small projections. Values chosen for the intensifying factor appear to be rather high and other mechanisms of enhanced emission at these lower fields have been proposed. It has been suggested that such results could better be interpreted in terms of thermionic Schottky emission. At the other end of the scale at field strengths of the order of 7×10^7 V/cm, departures from the Fowler–Nordheim law have been attributed to space charge effects or failure of the image law and non-uniformity of the work function of the metal.*

*26, 27, 31, 41, 53, 55, 56, 63.

In the field of continuously pumped systems and unoutgassed electrodes the phenomena of pre-breakdown seems to be different. Again, currents flow at values of field strengths considerably less than those which are required for field emission. The basic portion of such currents appear to be made up of electrons. Many workers have noted cases where the current is not a direct function of voltage but that self-extinguishing pulses of current are produced. The threshold voltage for such micro-discharges shows a conditioning effect, is independent of the electron component of the pre-breakdown current, and dependent on the condition of the electrodes, the pressure, and nature of the gas in the tube, the electrode material, the pumping fluid, and to some extent the electrode separation. Various explanations have been put forward of which the most reasonable seems to be that of Mansfield and Fortescue.† The postulated mechanism considers that a positive ion is produced in the gap, or at the electrodes, by some process such as the ejection of a positive ion by an electron. Then, provided that the surfaces of the electrodes are covered with a suitable contaminating layer of hydrocarbons, this positive ion will more than regenerate itself by the production of negative ions at the cathode which release further positive ions at the anode. Measurements of secondary emission coefficients support the general theory advanced. In systems having voltage sources with high internal-impedance, i.e. accelerator tubes in electrostatic generators, the quenching effect is due to a fall in voltage across the gap, however for other systems, while Arnal postulates a clean up of adsorbed hydrogen on the metal surface, Mansfield suggests that a modification of the surface layer takes place[6, 58]. A suggestion by Calvert, that field emission plays an important role has been shown not to apply to gaps greater than 1.5 mm[68].

6. Vacuum breakdown hypotheses

Hypotheses which have been put forward to explain the mechanism of vacuum breakdown can be split broadly into three different classes :—

(*a*) those postulating an interchange of elementary particles, i.e. electrons, positive ions, etc.,

(*b*) those assuming surface effects at the electrodes, i.e. resistive heating of projections, evaporation of microscopic areas, instability of surface, etc.,

(*c*) those postulating a clump-type mechanism.

Class (*a*)

Under the first classification comes the Positive Ion Hypothesis. This was first proposed to explain certain phenomena experienced in a high-voltage vacuum discharge tube[5, 78, 82]. Experimental evidence indicated that the discharge within the tube was due to ionisation at the electrode surfaces as a consequence of the impact of ions, electrons and photons. A quantitative explanation of the mechanism is as follows :—

Let A = Average number of positive ions produced by one electron.

B = Average number of secondary electrons produced by one of these positive ions.

C = Number of photons produced by one electron.

D = Number of secondary electrons produced by an average photon.

An electron in the interelectrode space is accelerated towards the anode and on impact liberates A positive ions and C photons which travel to the cathode. On arrival each ion will liberate B electrons and each photon D electrons, so that the number of electrons in the gap is $(AB + CD)$. Then when the condition :—

$$(AB + CD) \geqslant 1 \tag{5}$$

is realized, the interchange becomes cumulative and breakdown occurs.

Experiments have been devised to determine the magnitude of the coefficients A and B. The coefficient A was measured as a function of electron energy for the case of an outgassed parallel plane steel gap and was found to increase sharply near the breakdown voltage to about 2×10^{-3}. Thus for the AB mechanism to be important the value of B would have to be of the order of several hundreds. B was shown to have energy values of 2 to 20, the value increasing with incident ion energy. Hence the mechanisms as envisaged would appear to be non-cumulative although it has been suggested by Borovik that the electron current would be focussed by the positive ions and that this would tend to increase the coefficient A[1, 12, 13, 80]. A similar type which considers the effect of negative ions is the Positive-Ion Negative-Ion Hypothesis[60]. A positive ion produced at the anode is accelerated by the electric field in the gap towards the cathode, where it produces B electrons and E negative ions. Both these types of negatively charged particles are accelerated to the anode where one electron striking the anode produces A positive ions, and one negative ion produces F positive ions. Breakdown is assumed to occur when :—

$$(AB + EF) \geqslant 1 \tag{6}$$

Class (*b*)

Under the second classification comes a hypothesis which arose from work concerned with the development of a new type of field emitter[28]. Using very clean, electrolytically etched cathodes, very high static vacuum and advanced techniques, it was shown that as the voltage between a sharply pointed cathode and a flat anode, was increased, the field current density was consistent with the value predicted by the wave mechanical field emission theory, when space charge effects were taken into account. This was so up to the order of 10^8 amp/cm^2 when observations were terminated by an explosive arc. Breakdown was shown to be due to resistive heating at the cathode point.

Under practical conditions, at which residual gas pressure is of the order of 10^{-5} Torr, the above conditions do not apply. Ahearn in 1936, and Denholm, in 1958, assumed

†6, 10, 11, 12, 14, 17, 18, 20, 23, 25, 32, 47, 49, 56, 57, 61, 64, 67, 81.

that prior to breakdown, field emission currents flow from the cathode from small surface projections where the local fields and mechanical forces are the greatest. Local resistive heating takes place depending on the size and geometry of these projections and on their thermal contact with the body of the cathode. As the field is increased a rupture occurs at the projection where conditions of mechanical force, resistive heating and tensile strength are most favourable and breakdown follows[2, 25].

A slightly different hypothesis has been put forward by Chambers who postulated that the field emission electrons emitted from the cathode strike the anode and produce positive ions by secondary emission. These positive ions are accelerated in the gap and bombard the cathode, and rupture of the cathode is assumed to occur when the potential and the number of positive ions are large enough, and breakdown follows[19].

The hypotheses of Semenov, Meyers and Raatz and Arnal are similar[7, 8, 11, 16, 65]. The electrons are assumed to heat relatively small sections of the anode on colliding with it and to give rise to intense evaporation of the material or liberation of quantities of absorbed gas. The arc develops in the streams formed by the vapour of the anode material or in those of the gas. These ideas have been further developed to account for the breakdown of very small gaps[15]. Parkins went a stage further when he assumed that quanta as well as metal vapour were released from the anode. The quanta arrive at the cathode and release photo-electrons which in turn arrive at the anode and give rise to further quanta and vapour. The vapour forms a local high pressure region and ionisation due to the electrons, takes place in this region. The released ions bombard the cathode giving rise to molecules and electrons. Breakdown occurs when the process becomes cumulative[66]. It is debatable whether the presence of absorbed gases is necessary for breakdown[12, 74].

A hypothesis which provides a satisfactory explanation of what happens when the cathode is mercury, has been put forward by Tonks who showed that even under the combined effects of gravity and surface tension a mercury surface could no longer be stable in an electric field when the stress reached a value of 53 kV/cm. At this stress instability is produced and breakdown follows[77, 83].

Class (c)

There are finally, those discharges assumed to be initiated by actual transfer of electrode material. According to Cranberg, local regions of high temperature may be formed on an electrode as a result of the impact of particles of matter which carry a charge and therefore are capable of acceleration by the field in the gap. It was assumed that on the surface of each electrode there would always be weakly attached particles of conducting material which would be detached by the electric field forces[24]. These clumps of material would traverse the gap and experimental data was deemed to support the view that these could produce local temperatures in excess of metallic boiling points. It was assumed that such a situation would lead very quickly to the development of full breakdown.

The Slivkov hypothesis presents a somewhat different mechanism of clump breakdown. It assumes that even for small voltages, particles begin to be detached from both electrodes. When the voltage is sufficiently high they collide with the opposite electrode and adhere to the surface and only become free again on the application of a higher stress. When the kinetic energy of a micro-particle at the moment of its collision with an electrode is sufficiently large, the particle vapourises to a gas cloud in which the discharge commences. Thus this clump theory postulates the evaporation of the article and not of the electrode[73]. Evidence supporting a clump type theory in terms of material transfer across the gap has been reported but doubts have been expressed about the validity of the experimental techniques employed[5, 17, 42, 67].

7. Conclusions

It is important that the properties of vacuum as an insulator should be most carefully reconsidered and if possible improved. At the present time it seems that the breakdown voltage of a given gap can be increased by :—

(*a*) changing the electrode material
(*b*) conditioning
(*c*) introducing a non-uniform field
(*d*) increasing the frequency
(*e*) polishing the electrode.

Should a way be found that enables vacuum to support the same gradients at high gap spacings as it does at the lower gaps then not only will this result in a decrease in size of equipment already using vacuum insulation but vacuum will be able to challenge the compressed gases which at the moment are far superior in their performance at larger spacings.

A theory applicable to the whole field of vacuum breakdown and pre-breakdown effects is clearly a desirable possibility. Alternatively hypotheses selected from those already advanced might be chosen for the particular regimes and situations for which they appear to be valid. Once the exact mechanism of breakdown is ascertained then methods of increasing the voltage holding of a given gap may be evolved. It seems most likely that in order to determine this exact mechanism of breakdown, surface effects at the electrodes will have to be studied as the stress is increased from zero to the breakdown value.

Acknowledgements

The author is indebted to Dr. C. A. Walley and P. Powers for extremely helpful discussions and gratefully acknowledges the award of the Ferranti Scholarship by the Institution of Electrical Engineers. The work was carried out in the Department of Electrical Engineering, King's College, Newcastle upon Tyne and the author also wishes to thank Professor R. L. Russell for his interest.

References

[1] B. Arset, R. W. Cloud, and J. G. Trump; Electron Emission from Metals under High-Energy Hydrogen Ion Bombardment, *J. Appl. Phys.* **25**, 1365 (1954).

Vol. 10 196

[2] A. J. Ahearn; The Effect of Temperature, Degree of Thoriation and Breakdown on Field Current from Tungsten and Thoriated Tungsten, *Phys. Rev.* **50**, 238 (1936).

[3] D. D. Aleksandrov, N. F. Olenzkaia, and S. V. Ptitsyn; Electrical Strength of High Voltage Tube, *Soviet Phy. Tech. Phy.* **3**, **4**, 836 (1958).

[4] N. L. Allen; The Threshold Gas Pressure required to sustain a Stable Arc in a Magnetic Field, *Proc. Phys. Soc.* **B**, **65**, 697 (1952).

[5] H. W. Anderson; Effect of Total Voltage on Breakdown in Vacuum, *Elec. Eng.* **54**, 1315 (1935).

[6] R. Arnal; Influence of the Superficial Concentration of Hydrogen on the Threshold of Electrical Micro-Discharges in Vacuum, *Comptes Rendus* **240**, 610 (1956).

[7] R. Arnal; On the Initiation of Electrical Discharge in a Vacuum, *Comptes Rendus* **238**, 132 (1954).

[8] R. Arnal; On the Condition of Breakdown of Metallic Surface in a Vacuum in Terms of Electrical Supply, *Comptes Rendus* **23**, 2402 (1954).

[9] F. Ashworth; Field Emission Microscopy, *Advances in Electronics* **3**, 35 (1951).

[10] F. Bertain; On a Statistical Phenomena of Discharge between Electrodes in Vacuum, *Comptes Rendus* **222**, 64 (1946).

[11] J. P. Blewett; Electron Loading in Ion Accelerating Tubes, *Phys. Rev.* **81**, 305 (1951).

[12] E. S. Borovik and B. P. Batrakov; Investigation of Breakdown in Vacuum, *Soviet Phy. Tech. Phys.* **3**, 1811 (1958).

[13] H. C. Bourne, R. W. Cloud, and J. G. Trump, Role of Positive Ions in High-Voltage Breakdown in Vacuum, *J. Appl. Phys.* **26**, 596 (1955).

[14] H. C. Bourne; Composition of the Interelectrode pre-breakdown Current in High Vacuum, *J. Appl. Phys.* **26**, 625 (1955).

[15] W. S. Boyle, P. Kisliuk, and L. H. Germer; Electrical Breakdown in High Vacuum, *J. Appl. Phys.* **26**, 720 (1955).

[16] S. M. Bragine, A. V. Valter, and N. N. Semenov; Theory and Practice of Dielectrics, *Moscow* (1929).

[17] P. F. Brown; The Transfer of Metal between Electrodes in a High Vacuum on Application of a High Electric Field, *Proc. Phys. Soc.* **B**, **68**, 564 (1955).

[18] W. J. R. Calvert; Pre-Breakdown Current and Vacuum Breakdown, *Proc. Phys. Soc.* **B**, **69**, 651 (1956).

[19] C. C. Chambers; Emission of Electrons from Cold Metal Surfaces, *J. Franklin Inst.* **218**, 463 (1934).

[20] D. R. Chick, S. E. Hunt, W. M. Jones, and D. P. R. Petries; A Van De Graaff Accelerator Tube of very Low Retrograde Electron Current, *Nuclear Inst. & Methods* **5**, 205 (1959).

[21] W. W. Chupp and H. G. Heard; Spark Damage and High Voltage Breakdown of Metals in Vacuum at 14 Megacycles, *U.S.A.E.C., U.C.R.L.* 1962 (1954).

[22] W. W. Chupp, H. G. Heard, and E. J. Lauer; The Behavior of Electrode Materials subjected to Energetic High Vacuum R.F. Sparking in the Megavolt Range, *U.S.A.E.C., U.C.R.L.* 2099, (1954).

[23] D. S. Clifford, R. L. Fortescue, and J. Roberts; Failure of Vacuum Insulation at Low Field Strengths, *Nature* **170**, 503 (1952).

[24] L. Cranberg; The Initiation of Electrical Breakdown in Vacuum, *J. Appl. Phys.* **23**, 518 (1952).

[25] A. S. Denholm; The Electrical Breakdown of Small Gaps in Vacuum, *Canad. J. Phys.* **36**, 476 (1958).

[26] W. P. Dyke; Field Emission : Large Current Densities, Space Charge and the Vacuum Arc, *Phys. Rev.* **89**, 799 (1953).

[27] W. P. Dyke, J. K. Trolan, E. E. Martin, and J. P. Babour; The Field Emission Initiated Vacuum Arc. (1) Experiments on Arc Initiation ; (2) The Resistively Heated Emitter, *Phys. Rev.* **91**, 1043 (1953).

[28] W. P. Dyke and W. W. Dolan; Field Emission, *Advances in Electronics & Electron Phys.* **8** (1946).

[29] R. N. Edwards and J. F. Lawyer; Design Criteria for Accelerator Vacuum Systems, *Fourth National Symposium on Vacuum Technology* **73** (1957).

[30] F. Garforth; Private Communication.

[31] V. N. Glazanov; Breakdown in Vacuum, *Elektrichestro* **3**, 40 (1958).

[32] P. H. Gleichauf; Electrical Breakdown over Insulators in High Vacuum, *J. Appl. Phys.* **22**, 535 (1951).

[33] P. H. Gleichauf; Electrical Breakdown over Insulators in High Vacuum, *J. Appl. Phys.* **22**, 766 (1951).

[34] B. S. Gossling; Flash Arc in High Power Valves, *J. Inst. Elect. Engrs.* **72**, 460 (1932).

[35] R. J. B. Hadden; The Effect of Surface Treatment on Electric Breakdown between Copper Electrodes at 50 cycles at Very Low Pressure, *A.E.R.E.* G/M92 (1951).

[36] R. Haefer; The Breakdown Voltage of Gaseous Discharges in Transverse Magnetic Fields, for the Range of Pressure 10 to 10^{-8} mm Hg, *Acta Phys. Austriaca* **7**, 52 (1953).

[37] D. C. Hagerman and A. H. Williams; High Power Vacuum Spark Gap, *Rev. Sci. Instrum.* **30**, 182 (1959).

[38] D. C. Hagerman; Private Communication.

[39] J. Halpern, E. Everhart, R. A. Rapuano, and J. C. Slater; Preliminary Studies on the Design of a Microwave Linear Accelerator, *Phys. Rev.* **69**, 688A (1946).

[40] K. Hashimoto; The Figures on the Surface of Metal Electrodes Produced by the Breakdown in High Vacuum, *J. Appl. Soc. Japan* **2**, 70 (1947).

[41] R. Hawley; Electrical Breakdown in Vacuum, *Tech. Rep. Elect. Eng. Dept. University of Durham.*

[42] H. G. Heard and E. J. Lauer; Transfer of Anode Metal in D.C. Non-sparking Discharge in High Vacuum, *U.S.A.E.C., U.C.R.L.* 1622 (1952).

[43] H. G. Heard; D.C. Drain and Breakdown Phenomena for Unoutgassed Metals, *U.S.A.E.C., U.C.R.L* 1697 (1952).

[44] H. G. Heard; Formative Time Delay of High Vacuum Sparks, *U.S.A.E.C., U.C.R.L.* 2251 (1953).

[45] H. G. Heard; Electron Loading and High Voltage Sparking of Metals in Vacuum, *U.S.A.E.C., U.C.R.L.* 2252 (1953).

[46] J. Imachi; High Voltage Spark in High Vacuum, *Rev. Phys. Chem., Japan*, **18**, 119 (1944).

[47] J. W. Kennedy, E. A. Bryant, P. V. Murphy, U. Merton, and E. K. Storms; Some Experiments on Electrical Conduction in Vacuum, *U.S.A.E.C., A.E.C.U.* 3989 (1957).

[48] W. D. Kilpatrick; Sparking and X-ray in a Mercury Pumped Vacuum System, *U.S.A.E.C., U.C.R.L.* 1907 (1952).

[49] W. D. Kilpatrick; Criterion for Vacuum Sparking Designed to Include both r.f. and d.c., *Rev. Sci. Instrum.* **28**, 824 (1957).

[50] W. D. Kilpatrick; Private Communication.

[51] D. Leader; Electrical Breakdown in Vacuum, *Proc. Inst. Elect. Engrs.* **2**, A, 100, 138 (1953).

[52] J. W. Leech; Electrical Breakdown at Very Low Gas Pressures, *Brit. J. Appl. Phys.* **6**, 107 (1955).

[53] T. J. Lewis; High Field Electron Emission from Irregular Cathode Surfaces, *J. Appl. Phys.* **26**, 1405 (1955).

[54] T. J. Lewis; Some Factors Influencing Field Emission and the Fowler–Nordheim Law, *Proc. Phys. Soc.* **B**, **68**, 938 (1955).

[55] T. J. Lewis; Theoretical Interpretation of Field Emission Experiments, *Phys. Rev.* **101**, 1694 (1956).

[56] F. Llewellyn-Jones; Ionization and Breakdown in Gases, Methuen (1957).

[57] W. K. Mansfield; Pre-breakdown Conduction between Electrodes in Continuously Pumped Vacuum System, *Brit. J. Appl. Phys.* **8**, 73 (1957).

[58] W. K. Mansfield; Private Communications.

[59] R. A. Millikan and R. A. Sawyer; Extreme Ultra-Violet Spectra of Hot Sparks in High Vacua, *Phys. Rev.* **12**, 167 (1918).

[60] J. L. McKibben and R. K. Beauchamp; Insulation Flashover Tests in Vacuum and Pressure, *U.S.A.E.C., A.E.C.D.* 2039 (1948).

[61] J. L. McKibben and K. Boyer; Current Loading in Ion Acceleration Tubes, *Phys. Rev.* **82**, 315 (1951).

[62] F. J. Miranda; The Time Lag of Breakdown of Vacuum and Pressure Gaps, *A.E.I. Report* A292 (1954).

[63] M. J. Morant; Interpretation of Experiments on Electron Emission in Spark Gaps, *Proc. Phys. Soc.* **B**, **68**, 513 (1955).

[64] L. B. Mullett, R. E. Clay, and R. J. B. Hadden; Multipactor Effect in Linear Accelerators and other Evacuated R.F. Systems and a New Cold Cathode Valve, *A.E.R.E.* GP/B 1076.

[65] O. E. Meyers and W. A. Raatz; Vacuum Sparking, *U.S.A.E.C., L.R.L.* 158.

[66] W. Parkins; Vacuum Sparking Potentials under Surge Conditions, *U.S.A.E.C., M.D.D.C.* 858 (1946).

[67] L. I. Pivovar, V. M. Tubaev, and V. I. Gordienko; The Effect of the Electron Current Component on Development of Electrical Breakdown in High Vacuum, *Soviet Phys. Tech. Phys.* **2**, 5, 909 (1957).

[68] L. I. Pivovar and V. I. Gordienko; Micro-Discharge and Pre-Discharge Currents between Metal Electrodes in High Vacuum, *Zh. tekh. Fiz.* **28**, 10, 2289 (1958).

[69] P. A. Redhead; The Townsend Discharge in a Coaxial Diode with Axial Magnetic Field, *Canad. J. Phys.* **36**, 255 (1958).

[70] M. P. Reece; The Vacuum Switch and its Application to Power Switching, *J. Inst. Elect. Engrs.* **275** (May, 1959).

[71] J. W. Rittenhouse; The Role of the Vacuum Switch in Power Applications, *Elect. Eng.* **76**, 202 (1957).

[72] N. B. Rosanova and V. L. Granovskii; On the Initiation of Electrical Breakdown of a High Vacuum Gap, *Soviet Phys. Tech. Phys.* **1**, 3, 471 (1957).

[73] I. N. Slivkov; Mechanism for Electrical Discharge in Vacuum, *Soviet Phys. Tech. Phys.* **2**, 9, 1919 (1957).
[74] I. N. Slivkov; The Influence of the Electrode Temperature on the Electrical Breakdown Strength of a Vacuum Gap, *Soviet Phys. Tech. Phys.* **3**, 4, 708 (1958).
[75] L. B. Snoddy; Vacuum Spark Discharge, *Phys. Rev.* **37**, 1678 (1931).
[76] R. W. Sorenson; The Power Application Vacuum Switch, *Elec. Eng.* Page 150 (1958).
[77] L. Tonks; A Theory of Liquid Surface Rupture by a Uniform Electric Field, *Phys. Rev.* **48**, 562 (1935).
[78] J. G. Trump, and R. J. Van de Graaff; The Insulation of High Voltage in Vacuum, *J. Appl. Phys.* **18**, 327 (1947).
[79] J. G. Trump; Private Communication.
[80] J. G. Trump; Insulation Strength of High Pressure Gases and of Vacuum, *Dielectric Material & Applications* (1954).
[81] C. M. Turner; Electron Loading in Ion Acceleration Tubes, *Phys. Rev.* **81**, 305 (1951).
[82] L. C. Van Atta, R. J. Van de Graaff, and H. A. Barton; A New Design for a High Voltage Discharge Tube, *Phys. Rev.* **43**, 158 (1933).
[83] M. Warmoltz; The Time Lag in Starting a Low Pressure Arc on a Mercury or Gallium Cathode in Connection with Field Emission and Surface Deformation, *Phillips Res. Rep.* **2**, 426 (1947).
[84] H. Wroe; Vacuum Arcs, on Tungsten Cathodes, *Nature* **182**, 338 (1958).
[85] H. Wroe and R. H. Anderson; An Effect of Oxide Layers on the Behaviour of Vacuum Arc Cathode Spots, *Nature* **183**, 1544 (1959).

Vol.
10
196

Physical Processes in Small Titanium Ion Pumps

R. O. JENKINS and W. G. TRODDEN

Research Laboratories of The General Electric Company Limited, Wembley, England

(Received 13 May 1960)

Experiments with small ion pumps in which titanium is continuously deposited are described. Two types were investigated, the first being a conventional thermionic ionisation gauge with titanium evaporating from a directly heated source in the envelope and the second a Penning type of discharge tube in which titanium was sputtered from the end plates. In the first type all the gases and vapours tested were pumped by ion burial and all except argon were also pumped by adsorption onto the already deposited titanium film and then covered by the arriving titanium. In addition the hot tungsten could combine chemically with oxygen and also convert hydrogen into the atomic form which was then able to diffuse into the titanium. Water vapour and organic vapours were also decomposed by the hot tungsten. In the Penning discharge pump the speed of pumping was constant for each gas over a wide range of pressures, and depended on the titanium sputtering rate and rate of adsorption of the various gases. It was found that appreciable desorption of pumped gases took place in the sputter-ion pump but could be made negligible in the evaporation-ion pump.

1. Introduction

The clean up of ionized gases is a phenomenon which has been known since the very early days of research on vacua. It is however only relatively recently that the use of ion pumps to replace diffusion pumps has been contemplated. The work of Alpert[1] showed that ionization gauges themselves could achieve ultra high vacua in small isolated systems if the quantity of gas to be cleaned up on the walls of the gauge was small. Any attempt to clean up large quantities of gas and still achieve a good ultimate vacuum clearly requires that simultaneously with the ionization, a continuously renewed clean surface must be provided on which to adsorb the gas. Such a surface should itself be sufficiently active to adsorb and preferably combine chemically with most gases likely to be present in a vacuum system. While active metal getters such as barium[2] can be used as a pump by a slow continuous evaporation, with or without ionization, the technique is rather inconvenient, and has limitations. The alternative is to use one of the somewhat less active metals, such as titanium or zirconium, generally employed as non-dispersed getters. The "Evaporation" pump of Herb[3] was the first application of this principle on a large scale. Very high pumping speeds were achieved by evaporating titanium from a continuously fed wire on to the inside of a large bore tube, with a discharge operating simultaneously. More recently an improved method of evaporating the titanium from a continuously fed wire has been developed by Holland[4, 5], and described in a review of ion pumps[6].

Pumps consisting essentially of a thermionic ionization gauge with a static source of evaporating titanium have also been developed, and larger types employing this principle, and having a construction similar to a transmitting valve have been described by Huber and Warnecke[7].

The Penning discharge can also be used for ion-pumping. In this discharge the high energy gas ions sputter material from the cathode plates and this is then deposited on to the anode and walls of the tube. Hall[8], has described a pump with titanium cathode plates and a multiple anode in the form of an "egg box" which gives 36 separate discharge spaces. Further developments of this type of pump have been described by Jepsen[9].

The experiments described below were made on small pumps with glass envelopes using sputtering and evaporation of titanium. In particular, the physical mechanisms have been identified by varying operating parameters and observing their effect on pumping speed. At the same time, as the main contemplated use of these small pumps was for attachment to sealed off devices processed originally on conventional vacuum systems, the rate of re-evolution of gas when the pumps were not operating was also studied.

2. Experimental technique

Apparatus

Measurements were made on a vacuum system shown diagrammatically in Fig. 1. This was constructed of Wl borosilicate glass, and the upper part could be baked at temperatures up to 500 °C. In this part the ion pump being investigated was coupled closely with a Bayard-Alpert ionization gauge which could thus measure the pressure at the ion pump. This section of the vacuum system could be isolated from the diffusion pumps and gas inlet by a magnetically operated cut-off containing indium (m.p. 155 °C).

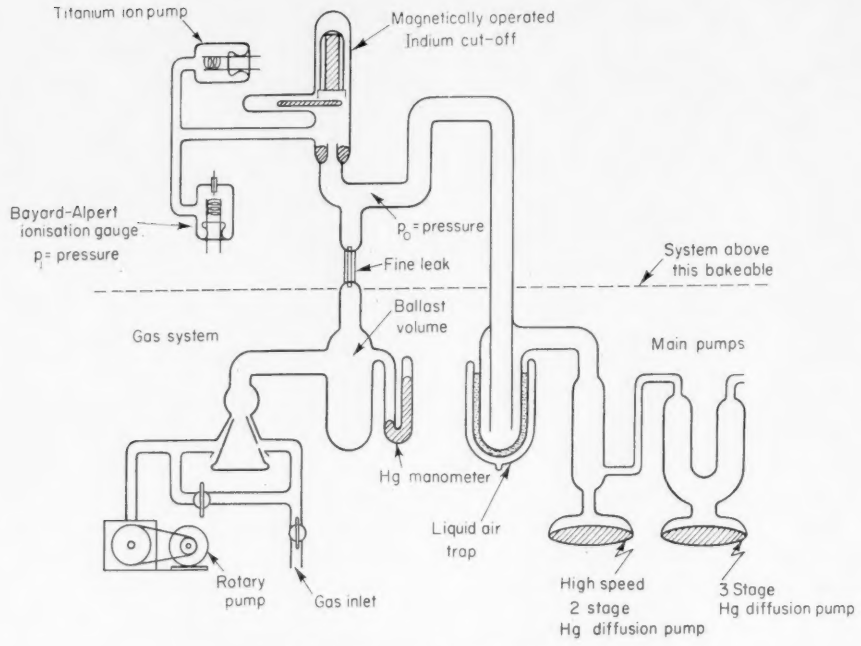

FIG. 1. Diagram of vacuum system.

Gas could be admitted to the diffusion pump side of the cut-off through a small leak consisting of a length of nickel wire sealed into a Wl glass capillary tube. The high pressure side of the leak was connected to a ballast volume in which the pressure was indicated by a mercury manometer. This volume could either be evacuated by a rotary pump or filled with gas or vapour under test. By adjusting the pressure in the ballast volume it was possible to control the pressure at the diffusion pump side of the cut-off over the range of $<10^{-7}$ Torr to $>10^{-3}$ Torr.

The evaporation-ion pump

This pump (Fig. 2) contained an electron-accelerating grid and two filaments, one to produce electrons for ionization and the other to give a supply of evaporating titanium. The grid was a 30 mm diameter helix of 0.2 mm diameter molybdenum wire, of height 40 mm, with a pitch of 10 turns/in. This helix was spot welded to two 1 mm diameter tantalum support rods. The electron emitting filament was a standard 12 V, 42 W tungsten lamp filament of length 6 mm and helix diameter 1 mm. The titanium source filament consisted of a 0.2 mm diameter titanium wire closely wound on a 0.2 mm diameter tungsten wire, over a length of 25 mm. An improved source used on later tubes was one 0.2 mm titanium and two 0.2 mm tungsten wires twisted together, the titanium being subsequently melted to fill the interstices between the tungsten wires. The titanium wire was drawn down from a larger size obtainable commercially. A molybdenum plate shielded the pinch from the evaporating titanium. The Wl glass envelope had a short tungsten rod sealed through the wall. A small area of "Aquadag" suspension had been applied on the inner wall surrounding the rod. This ensured good electrical contact between the rod and the film of titanium deposited on the wall subsequently. The area of the titanium film was about 80 cm^2.

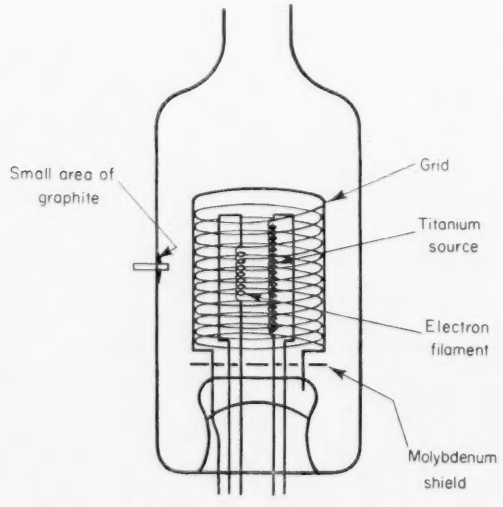

FIG. 2. The evaporation-ion pump.

The sputter ion pump

The sputter ion pump (Fig. 3) was considerably simpler in construction than the evaporation-ion type, being similar to a conventional Penning cold cathode ionization gauge. The anode was a cylinder 19 mm in diameter and 16 mm long, made of 0.2 mm thick molybdenum sheet. The cathodes were in the form of squares of 19 mm side, made of titanium sheet 1 mm thick. The separation between cathodes and anode was about 1.5 mm. These electrodes were mounted on 1 mm diameter tantalum support wires. The pinch had one lead-through wire set apart from the other wires, and this was used for the anode connexion. A glass tube

Vol.
10
1960

was positioned over this connexion near the pinch. This reduced to a negligible value any electrical leakage between

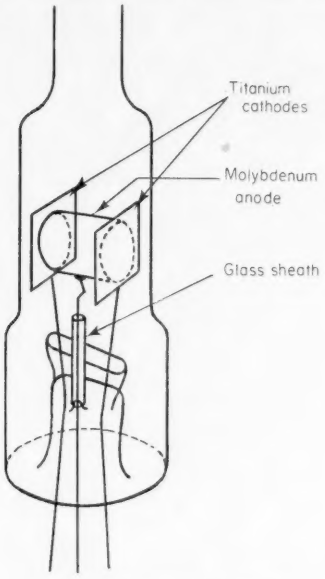

FIG. 3. The sputter ion pump.

the cathode and anode connexions due to sputtered titanium. The glass envelope, again of WI, was shaped to fit between the pole pieces of a magnet, which were 3.2 cm apart. The electrode structure was thus immersed symmetrically in the magnetic field, generally 2600 G, the field being in the direction of the axis of the cylinder.

In the operation the cathodes were connected together electrically, and a potential difference, usually 3–5 kV, applied between cathode and anode, through a resistor of 2.2 megohms.

Experimental procedure

The experimental procedure with each type of pump was as follows. The main system and the gas system were evacuated by their respective pumps and then the main system was baked, usually overnight, at about 475 °C, with the cut-off in the open position as shown in Fig. 1. After baking the ionization gauge and ion pump were outgassed. The evaporation-ion pump grid was outgassed by bombardment, while at the same time the titanium source was gradually heated up to 1400 °C. With the sputter-ion pump outgassing was much easier. It was only necessary to eddy current heat the electrodes to a temperature of about 1000 °C for about 15 min initially, and in the later experiments this outgassing time could be reduced to a few minutes.

In measuring pressure an electron current of 0.2 mA was used in the Bayard–Alpert gauge. This low value reduced the ion pumping action of the gauge to a negligible amount. In general the pumping speed of the pump was measured as follows. With the ion pump switched off the gas under test was admitted at a suitable pressure, p_0, to the diffusion pump side of the open cut-off by introducing the appropriate pressure into the ballast volume. In the absence of pumping action the pressure at the ionization gauge would also be p_0. The pump was then switched on, and after the resultant drop in pressure had reached an equilibrium, the new lower pressure p_1 was noted. If the conductance of the system between the ion pump and the diffusion pump side of the cut-off is L l./sec., the pumping speed of the ion pump at pressure p_1 is given by

$$s = \frac{p_0 - p_1}{p_1} L \text{ l./sec.} \tag{1}$$

This assumes that the pumping speed of the ionization gauge is much less than L. In the particular case of oxygen this assumption was found not to hold, and p_0 had to be found by fitting a second ionization gauge at the diffusion pump side of the cut-off. If now the first Bayard–Alpert gauge reads p_2 with the ion pump off, its own pumping speed is

$$s_{gauge} = \frac{p_0 - p_2}{p_2} L \text{ l./sec.} \tag{2}$$

If the equilibrium pressure at the gauge next to the ion pump after switching on the ion pump is p_1, the speed of the pump is given by

$$s = \frac{p_2 - p_1}{p_1} (L + s_{gauge}) \tag{3}$$

The value of L in (2) and (3) was estimated from the dimensions of the connecting tubes and was 0.4 l./sec.

In measuring pumping speeds very much less than L a different method was adopted since the error in the measurement of the difference $(p_0 - p_1)$ in equation (1) would have been of the same order as $(p_0 - p_1)$ itself. A pressure p_0 was established in the system. The cut-off was then closed by heating the indium to its melting point and magnetically lowering the glass bell into the molten indium. The time constant of the resulting exponential pressure decay, τ seconds, was then observed. If the cut-off volume is V l., the pumping speed is

$$s = \frac{V}{\tau} \text{ l./sec.} \tag{4}$$

It was found in practice that the preliminary outgassing of the titanium source in the evaporation pump had deposited an active film on the envelope which would act temporarily as a pump. Speeds of the order of 0.3 l./sec. for gases other than argon were observed before switching the pump on. To eliminate this transient effect it was usual to admit the gas under test to a pressure of about 10^{-3}–10^{-4} Torr for a few minutes to saturate the surface layer before making measurements. The outgassing procedure for the sputtering pump left the surfaces covered by an adsorbed film and no appreciable pumping occurred before switching on.

Desorption was usually measured as follows. After the ion pump had been working at some relatively high pressure for several minutes, the cut-off was closed and the cut-off volume was pumped down to a low pressure. The pump was then switched off and the resulting rise of pressure with time noted. If Δp microns is the rise in pressure in time Δt seconds, and V was the cut-off volume in litres, the rate of desorption is

$$D = \frac{\Delta p}{\Delta t} V \text{ l./}\mu\text{/sec.} \tag{5}$$

In cases where D was very small the rate was measured by switching off both pump and gauge for a long time, usually several hours, after which the gauge was switched on the measure Δp.

3. The experimental results

Evaporation-ion pump

Nitrogen. The pumping speeds in nitrogen in the pressure range 10^{-7} to 10^{-4} Torr are shown in Fig.4 for various rates

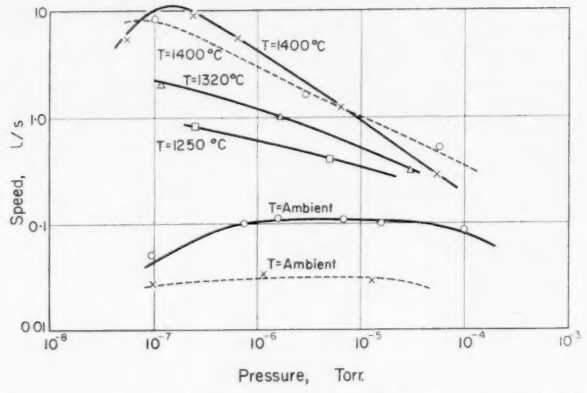

FIG. 4. Pumping speeds of nitrogen and carbon monoxide with the evaporation-ion pump.

of titanium evaporation. Here fixed ionization conditions were used during the measurements, the electron current being 3.5 mA at a grid potential of 170 V, with the collector at −51 V. It was found that the pumping speeds were considerably lower until a visible film had been deposited on the bulb. No pumping occurred with the tungsten filament hot, but without electron current. Thus in the absence of titanium evaporation the pumping is achieved by ionization of the gas molecules, the ions being collected on the envelope. A high titanium evaporation rates the pumping is mainly the result of molecules being adsorbed and trapped on the wall film by arriving titanium atoms. At these evaporation rates the electron current could be switched off without noticeably affecting the pumping speeds. The results taken with air under the same conditions were indistinguishable from those with nitrogen. With the high evaporation rate at 1400 °C the fall off in speed below 3×10^{-7} Torr was probably due to small amounts of gas still being released from the titanium source.

It was found that at pressures of 10^{-5}–10^{-7} Torr the pumping speed due to ion pumping was proportional to the electron current if the grid and collector voltages were held constant, and no titanium was being evaporated. If the electron current and collector voltages were constant, there was a grid voltage about 300 V at which the pumping speed was a maximum. These results are shown in Figs. 5 and 6.

Carbon monoxide. With carbon monoxide the behaviour was similar to that with nitrogen except that the speeds, shown in Fig. 4, were lower. Again, the speed of ion pumping was proportional to electron current, and varied with grid voltage in a manner similar to that with nitrogen. This is also shown in Figs. 5 and 6.

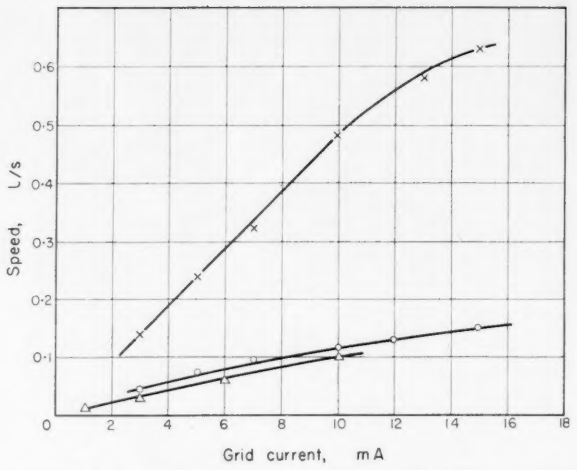

FIG. 5. Evaporation-ion pump pumping speed/electron current characteristics.

Argon. The pumping speed with argon was considerably lower than that for nitrogen, and in the pressure range 10^{-7} to 10^{-4} torr was constant and independent of whether or not titanium was evaporating. Furthermore, it was independent of whether or not a thick film of titanium had been deposited on the envelope. Speed was again proportional to electron current, and variation of speed with grid voltage was similar to that for carbon monoxide. These characteristics are shown in Figs. 5 and 6. All these observations indicate that the pumping is entirely ionic.

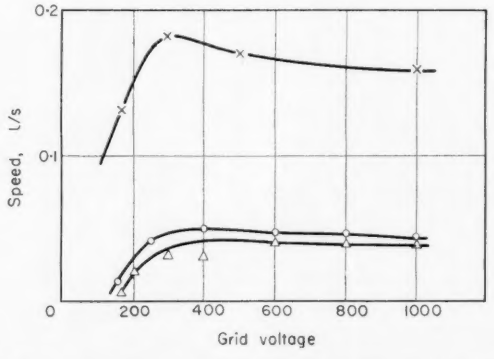

FIG. 6. Evaporation-ion pump pumping speed/grid voltage characteristics.

Although the pumping would take place without titanium being evaporated, in continuous use the film would probably need to be supplied with fresh titanium, to prevent too high a concentration of argon being built up, resulting in desorption.

Oxygen. With oxygen the Bayard–Alpert ionization gauge contributed an appreciable pumping speed by the formation of an oxide of tungsten at the filament surface. This oxide was driven on to the surrounding electrodes and the envelope, where it stayed as a stable compound. To determine the magnitude of this effect, an experiment was made with a second ionization gauge on the diffusion pump side of the cut-off, as described in Section 2.4. Its speed

Vol. 10 196

was found to be independent of filament temperatures above 1800 °C but fell off at temperatures below this.

Having determined the pumping speed due to the ionization gauge, the speed of the pump was obtained as described in Section 2.4, using equation (3). The results are shown in Fig. 7. At low titanium evaporation rates the pumping

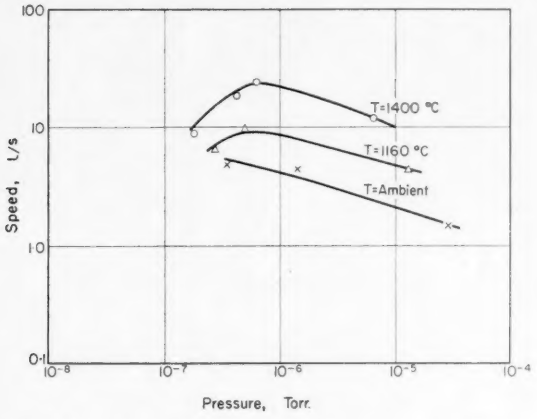

FIG. 7. Pumping speeds of oxygen with the evaporation-ion pump.

action was shown to be mainly in the formation of tungsten oxide, as the electron current had an almost negligible effect on the speed. It is probable that the ionic pumping speed would be rather similar to that for nitrogen. The evaporation of titanium had a greater pumping effect than that for nitrogen and carbon monoxide.

Hydrogen. When only the filament of the ion pump was operated there was an appreciable pumping speed. At any particular pressure this speed became constant when the temperature of the tungsten exceeded about 1500 °C. This pumping is due to the effect originally shown by Langmuir[10] that atomic hydrogen is formed at the surface of hot tungsten. This atomic hydrogen can then diffuse directly into the titanium film on the wall, as it is well known that hydrogen diffuses through metals in the atomic state. The extra pumping due to ionization is relatively small as shown in Fig. 8. Evaporation of titanium causes a considerable increase in the rate of pumping as for other gases. The speed again increases as the pressure is lowered, until out-

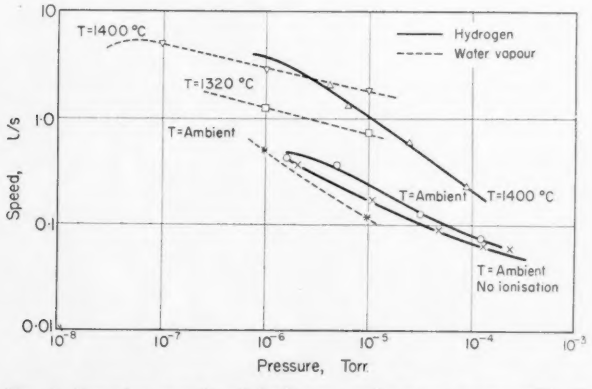

FIG. 8. Pumping speeds of hydrogen and water vapour with the evaporation-ion pump.

gassing from the titanium offsets this increase. This is very difficult to avoid when hydrogen has been present just previously in the system.

Water vapour. The curves for water vapour pumping are also shown in Fig. 8. It will be seen that the hot tungsten filament causes some pumping while the ionization increases it slightly. The hot filament reacts with the water vapour, combining with the oxygen, and evidently giving some atomic hydrogen which is absorbed by the titanium, resulting in a net pumping effect. The deposition of titanium increases the speed considerably as in the other gases.

Benzene vapour. The organic vapour chosen was benzene (C_6H_6). An unusual feature is noticeable in the pumping curves shown in Fig. 9. With the hot tungsten filament

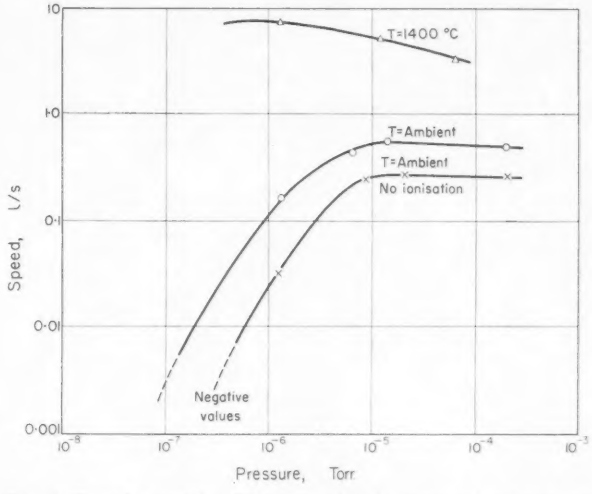

FIG. 9. Pumping speeds of benzene with the evaporation-ion pump.

only, at high pressures a positive pumping action is found, but it becomes negative below about 10^{-6} mm. Ionization increases the positive pumping speed, while the deposition of titanium has its usual effect. The negative pumping speed with the hot filament is probably caused as follows. The benzene vapour combines with the tungsten, carburising it, releasing hydrogen, and possibly other hydrocarbons. It is clearly possible for the complete breakdown of a molecule of benzene to give three molecules of hydrogen. If this happens, the pressure rises when the tungsten filament is heated, giving an apparent negative pumping speed.

Desorption in the evaporation-ion pump. The desorption of gas which had been previously pumped was in general small except for argon, but depended on the amount of relatively gas-free titanium which had been deposited during the final evacuation prior to measuring the desorption. With the permanent gases studied, after operating the pump at pressures of about 10^{-4} Torr for 10 min and then pumping down the cut-off volume for a few minutes with the filament source evaporating at 1400 °C the subsequent desorption rate over hours was 10^{-10} lusecs or less. With argon, however, the rate was about 10^{-7} lusecs.

If, however, the amount of titanium deposited during the pump-down was less, the desorption was greater. A

series of curves showing the rise of pressure of nitrogen in the cut-off volume after various pump-down procedures is shown in Fig. 10. In each case the pump had operated for

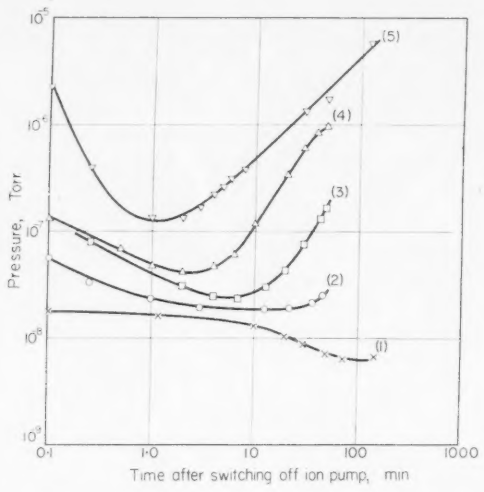

FIG. 10. Desorption in the evaporation-ion pump.

10 min at a pressure of 10^{-4} Torr before the cut-off was closed. No desorption was noted when the high rate of titanium evaporation was maintained during the pump-down (Curve 1). A lower rate of evaporation resulted in some desorption (Curves 2, 3 and 4) which was however less when ionization had also been present (cf. Curves 3 and 4). The desorption rate was highest of all (3.5×10^{-7} lusecs) when the pump-down was by ionization only (Curve 5).

Ultimate vacuum obtainable with the evaporation-ion pump. To produce ultra-high vacua, the following procedure was adopted. After baking overnight the pump was outgassed for an hour as described in 2.4, and the gauge outgassed simultaneously by bombardment. Then the power supplies were switched off and the cut-off closed. The ionization gauge was then operated normally, with an electron current of 1 mA, and the pump with an electron current of 10 mA, the grid and collector voltages being 500 and −51 V respectively. The titanium was heated to about 1160°C. After 1 hr the pressure had reached 2×10^{-10} torr. This could not be reduced further by altering the titanium evaporation rate or the electron current. Increases in these caused a greater residual outgassing rate thus offsetting the increased pumping speed.

If, after outgassing, the pump was operated at pressures higher than about 10^{-6} torr, the ultimate pressure on pumping down a closed volume was appreciably higher than 2×10^{-10} Torr.

Sputter-ion pump

Pumping speed with various gases. The pumping action was measured for the same gases over a range of pressures similar to that investigated with the evaporation pump. These tests were made with a field of 2600 G and a potential of 3 kV applied through a 2.2 MΩ resistor. In addition the effect of variation of the potential with this magnetic field was investigated for nitrogen.

It was found with all the gases that a high pumping speed was observed when the pump was first switched on after previous outgassing. This high rate decayed to a lower equilibrium value in a time inversely proportional to the pressure, corresponding to the clean-up of a certain quantity of gas. The initial rate of pumping for nitrogen was about 3 l./sec. and the total quantity of gas pumped during the period of enhanced speed was about 3.6 lμ. The equilibrium pump speeds are shown in Fig. 11 for the various gases.

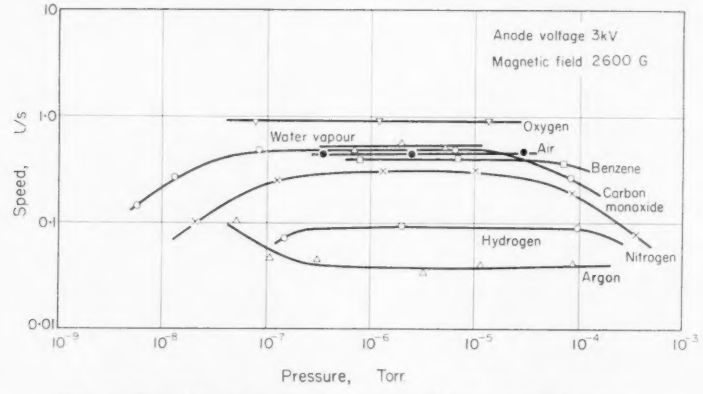

FIG. 11. Pumping speeds of various gases with the sputter ion pump.

It will be seen that the speeds are sensibly independent of pressure over a wide range with a falling off at high and low pressures.

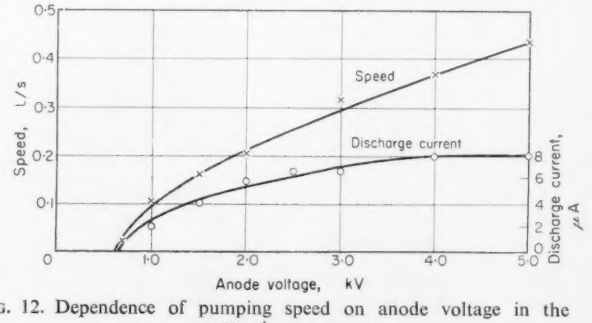

FIG. 12. Dependence of pumping speed on anode voltage in the sputter ion pump.

Vol. 10 1960

The effect of potential on the pumping speed and discharge current for nitrogen is shown in Fig. 12.

Desorption and ultimate vacuum. The ultimate vacuum attainable and the subsequent desorption were measured as follows. After operation at a certain pressure for 5 min, the cut-off was closed and the system pumped down to the ultimate vacuum. Then desorption was measured as described before. It was found that both the ultimate pressure achieved and the subsequent desorption rates were approximately proportional to the starting pressure before operating the cut-off. The rates of desorption for various gases are given in the Table. In this table is given also the starting pressure before operating the cut-off.

TABLE

Gas	Starting Pressure torr	Rate of Desorption, lusecs
Nitrogen	1×10^{-3}	8.0×10^{-7}
	1×10^{-4}	1.0×10^{-7}
	1×10^{-6}	1.3×10^{-10}
Carbon monoxide	2×10^{-4}	6.7×10^{-7}
Argon	1×10^{-4}	1.6×10^{-7}
Oxygen	2×10^{-3}	5×10^{-6}
Hydrogen	2×10^{-4}	4.2×10^{-6}

The best vacuum was obtained by vigorously outgassing the ionization gauge and pump, then closing the cut-off and pumping down at an anode voltage of 4.5 kV. After 2 hr the discharge current had reached a value of 2.5×10^{-10} amps. Previous experiments with nitrogen showed that in the range 10^{-9} to 10^{-4} Torr the discharge current was proportional to pressure, and the sensitivity was 10 amps/Torr. For a current of 2.5×10^{-10} amps the pressure obtained by extrapolating was 2.5×10^{-11} Torr.

It was found difficult to make the sputter-ion pump strike at pressures below 10^{-10} Torr and this difficulty increased with lower applied voltages. When the discharge had been struck it could persist down to the lowest pressures observed. Superimposed on the discharge current were stray currents due to leakage and field emission. Their value was found by removing the magnet, which resulted in the discharge extinguishing.

The observed ultimate pressure of 2.5×10^{-11} Torr was about four orders lower than the starting pressure. If the ion pump was allowed to pump for some time at about 10^{-4} Torr the ultimate pressure which could be achieved subsequently without outgassing the metal parts was about 10^{-8} Torr, which again was about four orders below the starting pressure. It seems fairly certain that the ultimate pressure is limited by the rate of desorption of gas which has been previously pumped.

4. Discussion of physical processes

The various experimental observations can be correlated with the physical processes taking place in the pumps, and some approximate calculations can be made to see how theory and practice agree. Each of the various processes will be examined in turn.

True ion pumping in the evaporation-ion pump

In this process the gas is ionized by the electrons from the filament as in an ionization gauge. The ions are then accelerated by the negative potential applied to the titanium film and driven into the film where they are held. Provided the film is renewed at a rate adequate to combine chemically with the gases, chemical forces will bind most of the gas firmly, except the rare gases such as argon where only the very much smaller physical forces are present. This accounts for the fact that desorption of argon was much greater than other gases. It would be expected that nearly all ions striking a fresh film of titanium would be retained and by measuring the efficiency of the tube as an ionization gauge a theoretical value of the pump speed could be derived. The maximum measured efficiency of ionization was about 100μA ion current/μ pressure/mA of electron current for nitrogen (rather higher than most conventional ionization gauges due to the larger electrode spacings). Assuming all the ions are adsorbed this corresponds for an electron current of 10 mA to an ion pumping speed for nitrogen of about 0.2 l./sec. independent of pressure which is somewhat lower than the observed value. The variation of pumping speed with electron voltage (Fig. 6) shows the maximum corresponding to the usual maximum efficiency of ionization as observed in an ionization gauge although the voltage is slightly higher than normal probably due to the different geometry. The slower pumping speeds for argon and carbon monoxide under the same conditions were found to be very close to the theoretical value.

Titanium evaporation pumping

The evaporation pumping takes place as follows. The gas molecules striking the titanium film can be adsorbed on its surface. In most cases, excluding the rare gases, there is an appreciable chance of a molecule being adsorbed, and the rate of their arrival is such that even with the highest rate of deposition of titanium used, the surface will remain covered with an appreciable fraction of a monomolecular layer of gas. The arriving titanium atoms are continuously covering the layer and so trapping the gas molecules which are thus " pumped ". The titanium can hold firmly only its chemical equivalent of gas. On this basis the maximum pumping speed in l./sec. will be proportional to the evaporation rate of the titanium and inversely proportional to the pressure. This effect can be seen qualitatively from Fig. 4 for nitrogen. The higher speeds observed for the evaporation pumping of oxygen (Fig. 7) are probably due to the fact that the possible compounds are either TiO_2 or TiO_3 and TiN respectively.

The absence of evaporation pumping for argon is due to the fact that surface adsorption forces are purely physical and are insufficient to hold many argon atoms on the titanium surface, particularly under ion bombardment.

It is possible to make a rough estimate of theoretical evaporation pumping speeds for N_2. Assuming a titanium temperature of about 1400°C the rate of evaporation of titanium can be calculated and thus the rate of its chemical

combination with the N_2 molecules, and hence the maximum possible pumping speed. This speed comes to be approximately $10^{-5}/p$ l./sec. where p is the pressure in Torr. From Fig. 4 at a pressure of 10^{-6} Torr the observed speed was 6 l./sec. compared with the calculated value of 10. This suggests that at this pressure the titanium film is always covered by an appreciable fraction of a monolayer of gas as further titanium is being deposited. With a very high evaporation rate particularly at low pressure the speed will be limited by the rate at which the gas can reach the titanium surface and be adsorbed and only a small fraction of the chemical equivalent may be trapped. This appears to be the case in the pump of Holland and Laurenson[5].

Oxygen combination with hot tungsten

Oxygen combines chemically with tungsten at high temperatures to form compounds usually in the range WO_2 to WO_3. These are relatively volatile and evaporate and recondense on the walls of the tube. From the experimental results, the observed pumping speeds, with the temperature of the tungsten above 1800 °C, were about 4 l./sec., decreasing somewhat at higher pressures. From kinetic theory the rate at which molecules strike a surface corresponds to about 10 l./sec./cm^2. As the effective area of the tungsten filament was about $\frac{1}{3}$ cm^2, it appears that almost all the molecules striking the hot tungsten combine with it at the lower pressures.

This agrees well with the recent observations of Schlier[11]. Early results of Langmuir[12] give a lower figure, which may possibly be due to the ease with which the tungsten surface becomes carburized. The oxygen then decarburizes it, forming carbon monoxide as follows

$$2W_2C + O_2 \rightarrow 2CO + 4W$$

This results in each reacting oxygen molecule giving two carbon monoxide molecules, and thus considerably decreasing the apparent clean up rate.

Formation of atomic hydrogen by hot tungsten

The fraction of hydrogen molecules striking hot tungsten which are dissociated can be calculated from the data of Langmuir[10]. From these, above a tungsten temperature of 1500 °C with pressures of $<10^{-4}$ Torr, more than 90 per cent of the hydrogen molecules striking the tungsten are dissociated, so that further increases in temperature should have only a small effect. The experimental observations were in good agreement with this prediction. The pumping speed due to the permeation of the atomic hydrogen into the titanium was about 0.3 l./sec., whereas the hydrogen would have been dissociated by the filament at about 12 l./sec. There is thus about a 2.5 per cent probability of the atomic hydrogen diffusing into the titanium before recombination on the surface. The drop in speed at higher pressures is probably due to a greater relative increase in recombination which is proportional to the square of the surface concentration.

Other reactions with hot tungsten

The cyclic reaction between water vapour and hot tungsten, resulting in continuous transfer of tungsten to the walls, is a well known phenomenon in tungsten lamps, and accounts for the pumping action observed in these experiments with the hot filament only. The following reaction takes place at the surface of the hot tungsten

$$W + 2H_2O \rightarrow WO_2 + 2H_2$$

The tungsten oxide evaporates and condenses on the envelope while the hydrogen is dissociated by the hot tungsten and can diffuse into the titanium film. From the fact that at a pressure of about 10^{-6} torr the pumping speed is the same as for hydrogen it appears that at this pressure, practically all the water vapour molecules striking the tungsten take part in the oxidation reaction, and all the hydrogen thus formed is dissociated. The drop in pumping speed as the pressure is increased (Fig. 8) may again be due to increased recombination of atomic hydrogen. The cyclic reaction in a tungsten lamp is caused by the atomic hydrogen reducing the tungsten oxide on the walls to reform water vapour, which continues the process.

The reactions between benzene and hot tungsten are more complex. One possible reaction is the carburization of tungsten and the release of hydrogen. As three molecules of hydrogen are produced for each molecule of benzene decomposed such a reaction would make a negative contribution to the pumping speed. This evidently outweighs any positive pumping action at low pressures (Fig. 9). The positive pumping speed at higher pressures suggests that two or more molecules of benzene are taking part in a reaction which results in the formation of fewer gaseous molecules, but further study would be required to understand the process fully.

Sputter-ion pumping

The pumping action of the sputter-ion pump appears from the experimental evidence to take place as follows. When the pump is first switched on after outgassing, the high energy positive ions formed by the Penning discharge are driven into the titanium cathode plates and buried. At the same time some of the titanium surface atoms are removed by the impact of the positive ions and recondense, mainly on the inside of the anode. Immediately after the pump has been outgassed, the sputtered material will be pure titanium which, when it condenses on the anode will adsorb gas. At the same time all the positive ions arriving at the cathode are likely to be buried. The number of ions striking the cathode per second can be calculated from the fact that the current they carry is 10 amps/mm pressure. Assuming all the ions are retained, this corresponds to a pumping speed of about 2 l./sec. independent of pressure, which is slightly less than the observed value of about 3 l./sec. The extra gas pumped will be that adsorbed on the titanium deposited on the anode.

As this process continues, the immediate surface layer of the cathode will accumulate a high concentration of gas, as the ions are unable to penetrate very far, and the sputtered material will consist then of titanium and the previously adsorbed gas. When this layer has reached equilibrium, as much gas is released by sputtering as is absorbed by ion burial. The pumping action is then only by adsorption of gas on the titanium covered anode and burial by the titanium being deposited by sputtering. The amount of gas contained

Vol. 10 196

in the equilibrium surface layer and entering during the period of enhanced pumping speed is, in the case of nitrogen, about 3.6 $l\mu$ which corresponds to about twenty atomic layers in the cathode surface.

At present it seems uncertain whether, when pumping a chemically active gas, the material sputtered from the cathode is the compound, or the gas and titanium separately. In either case it would be expected that the maximum amount of gas that can be pumped will be approximately the chemical equivalent of the titanium removed from the cathode. The rate of sputtering is proportional to the ion current which in turn is proportional to the pressure, and thus the rate of removal of gas molecules from the system is proportional to pressure. This means that the pumping speed should be independent of pressure, which is in fact observed experimentally, both in these experiments (Fig. 11) and by Hall[8] and Jepsen[9].

The rate of sputtering was sufficiently slow in these experiments for it to be assumed that the titanium deposit on the anode was always covered by a gas monolayer and approximately the chemical equivalent will have been held by the arriving titanium. From the measured pumping speed of nitrogen, and the value of the ion current for 3 kV calculation shows that approximately one titanium atom must be sputtered from the cathode for six arriving nitrogen ions. Fig. 12 shows that the pumping speed increases more rapidly than the ion current with increasing voltage. This is due to an increase in sputtering efficiency as the energy of the positive ion increases. It is known that the efficiency of sputtering also increases with the mass of the ion. Thus the lower pumping speed for hydrogen is probably due mainly to the lower sputtering efficiency. The higher pumping speed for oxygen is probably accounted for by each titanium atom retaining more oxygen molecules, as the sputtering rate will not be very different from that for nitrogen. A similar effect was seen in the evaporation pump.

The finite pumping speed of argon may probably be explainable as follows. Although the sputtering rate is high, due to the large ion mass, evidence from the evaporation-ion pump suggests that the physical adsorption of argon on to the surface of titanium is so small that the rate of pumping by the usual adsorption mechanism could not account for the speed. It is possible that pumping may be due to a leakage of positive ions from the electrode system and burial in the glass walls which is known to happen in other discharge devices. The observed pumping speeds for air are consistent with the assumption that the various constituents are pumped independently at their usual speeds, and this also applied to the evaporation pump.

The general fall-off in speed at higher pressures is probably due mainly to the drop in the discharge voltage caused by the series resistance, but loss of energy of the ions by collision with neutral atoms within the discharge space may also contribute to the effect. The decreases in speed at low pressures are mainly due to desorption of gas previously pumped, as explained in the next section.

Desorption of gas

The experiments with nitrogen on the evaporation pump show that when pumping is carried out with ionization only or with only a relatively slow rate of titanium deposition, the surface layer contains loosely held gas which is subquently desorbed. This gas, which must be held by physical adsorption only will be desorbed at a rate probably proportional to its concentration. It is thus clearly possible to reduce this desorption to a very low level by continuing to deposit titanium after a good final vacuum has been achieved, so that a clean titanium layer is left. The ultimate pressure achieved is therefore a function of outgassing of other parts of the pump and system. In practice the titanium source and the other hot components are the chief sources of gas and long outgassing schedules are necessary to achieve ultra high vacua.

In the sputtering pump conditions are somewhat different in that the rate of deposition of titanium cannot be varied independently but is always proportional to pressure. This prevents the deposition of a thick titanium layer with low gas content during the pump-down from higher pressures, unless this is a protracted operation due to a slowly decreasing outgassing rate in the system. The relatively slow rate of sputtering means that the titanium layer is generally covered with a monolayer of gas, a proportion of which is only loosely held when covered by the arriving titanium.

As the pumping speed is theoretically independent of pressure, the ultimate pressure achieved will be proportional to the rate of desorption of this loosely held gas, other sources of gas being negligible in this pump. The desorption rate will vary as the concentration of physically adsorbed gas which in turn will be proportional to the pressure at which the pump was operating immediately prior to pump-down. If the pump-down is quick, as in these experiments, the extra amount of titanium deposited is small and has little effect on the desorption. Thus both the desorption rate and ultimate pressure achieved are approximately proportional to the previous operating pressure, as observed experimentally.

5. Conclusion

It has been possible from the experiments described, to assess the contribution of various physical processes to the operation of small titanium ion pumps. While many of these results may be applicable by extrapolation to larger devices, other factors may also have to be taken into account. In pumps with a high rate of titanium evaporation or sputtering the speed may be limited by the actual area of the titanium film or the ease of access of the gas to the film, rather than by the actual rate of evaporation. The performance of evaporation pumps will also probably be limited at low pressure by the gas released by the evaporated titanium, until titanium with a very low gas content is available. It appears certain, however, from the results published in the literature so far that the ion pumps will take their place with diffusion pumps as means of obtaining high vacua, although at present it is somewhat early to assess accurately their final scope of use.

Acknowledgement

In conclusion, the authors wish to thank the M.-O. Valve

Company Limited, on whose behalf much of this work was carried out, for permission to publish this paper.

References

[1] D. Alpert; *J. Appl. Phys.* **24**, 860 (1953).
[2] R. W. Cloud, L. Beckman, and J. G. Trump; *Rev. Sci. Instrum.* **28**, 889 (1957).
[3] R. G. Herb, R. H. Davis, A. S. Divatia, and D. Saxon; *Phys. Rev.* **89**, 857 (1953).
[4] L. Holland, L. Laurenson, and J. T. Holden; *Nature, Lond.* **182**, 851 (1958).
[5] L. Holland and L. Laurenson; *Le Vide* **81**, 141 (1959).
[6] L. Holland; *J. Sci. Inst.* **36**, 105 (1959).
[7] H. Huber and M. Warnecke; *1st International Conference on Vacuum Techniques.* Pergamon Press, London (1958).
[8] L. D. Hall; *Rev. Sci. Instrum.* **29**, 367 (1958).
[9] R. L. Jepsen; *Le Vide* **81**, 80 (1959).
[10] I. Langmuir; *J. Amer. chem. Soc.* **37**, 417 (1915).
[11] R. E. Schlier; *J. Appl. Phys.* **29**, 1162 (1958).
[12] I. Langmuir; *J. Amer. chem. Soc.* **37**, 1139 (1915).

Vol.
10
1960

Letters to the Editor

The Formation of Luminescent Films by Evaporation

EVAPORATED films of some phosphors may retain their luminescence if the components volatilize without separation, or are made to diffuse into the correct lattice position by baking[1]. Evaporated phosphor films are grainless and non-scattering, therefore halation is reduced and high definition can be achieved[2]. Smooth evaporated films have a low light output because, apart from other causes, the light produced in the film can only be emitted at incident angles less than the critical angle. Studer and Cusano[3] found that emitted light lost from the edge of the film was not more than fifty per cent of the total. The formation of transparent films has been carried out by several workers. Feldman and O'Hara[1, 2] have produced films by the vacuum evaporation technique, while Studer and Cusano[3, 4] have developed the vapour phase process.

We were interested in producing films of zinc sulphide phosphors but the films produced by voalatilization appeared to require lengthy evaporations and special substrates for post firing[1]. It was believed that phosphors might exist which could be directly evaporated to form luminescent films without undue component separation and some experiments were made using a standard vacuum evaporation plant fitted with an 18 in. diameter metal bell jar, which could be exhausted to 10^{-5} Torr. Only a limited amount of work was done but because of the general lack of knowledge of this subject it was thought worth while to publish this short letter. The phosphors viz., ZnS (Ag), ZnS (Cu, Pb) and ZnS (Mn)* were obtained commercially and evaporated from a crucible by radiation from a flat spiral filament made of tungsten, on to soda lime lantern slides.

The manganese activated zinc sulphide phosphor produced films showing a weak orange luminescence when evaporated normally without baking the substrate or post firing, but luminescent films were not obtained when the other materials were evaporated. Further work was therefore carried out with the ZnS (Mn) phosphor. When a mixture of zinc sulphide and manganese were evaporated they did not produce a luminescent film, which showed that the commercial phosphor contained other substances of importance as co-activators. Some of the luminescent films were more yellow than the original phosphor which indicated that chlorine, which promoted yellow luminescence, was an important additional activator. It was established that yellow films having a small excess of chlorine, gave a higher light output than those films showing an orange fluorescence.

The evaporated phosphor films were coated with aluminium to prevent accumulation of electric charge when they were exposed to the electron stream from an electron gun assembly at 5kv in a 6 in. diam. vacuum chamber. The thickness of the phosphors was measured by multiple beam interferometry. There was an optimum value for the film thickness of about 1–1.3 microns to obtain maximum luminescence, so that raising the thickness above this value did not increase brightness. With a film of 1–1.3 microns thick the best brightness obtained without post firing, was about thirty per cent of the value for the powdered phosphor.

Thick zinc sulphide films are hygroscopic and absorb water vapour from the atmosphere. It has been shown that durable zinc sulphide films can be obtained by baking[5]. However, when the phosphor material was evaporated on to a hot substrate luminescence was not obtained, probably due to the chlorine being re-evaporated.

Badly adhering films could be overcome by using magnesium fluoride phosphors. Magnesium fluoride is easier to evaporate and in powder form when containing zinc fluoride (10–20 per cent) and manganese fluoride (0.5–3.0 per cent), gives a higher brightness than a powdered zinc sulphide phosphor. Thus mixtures of MgF_2, ZnF and MnF were pelleted and evaporated from a molybdenum boat. A luminescent magnesium fluoride phosphor film obtained with 10 per cent ZnF and 3 per cent MnF, had a brightness comparable to a film produced with the manganese activated zinc sulphide phosphor.

A few final tests of ZnS (Mn) without post firing were made on cathode ray tube face plates, assembled with an electron gun and tested under running conditions. The brightness obtained seemed promising. There was little or no after glow and an extremely fine spot could be obtained on a black background as also found by Feldman[2] and Studer[3]. The phosphor layer appeared to be fairly robust under electron bombardment, because the electron beam could be left stationary for some time without damaging the phosphor.

With present technique the successful production of an evaporated phosphor is still much a question of chance, as the activator or activators must arrive at the substrate in the required concentration and occupy the necessary lattice positions in the film. The reconstruction of a phosphor in film form cannot easily be controlled because the composition and structure of a deposit depends on many variable factors, such as : rate of evaporation, substrate temperature, activator concentration in the evaporant and its volatility and condensation characteristics.

Acknowledgements are made to Mr. L. Holland, who suggested the foregoing work, and to Edwards High Vacuum for permission to publish this letter.

1 C. Feldman and M. O'Hara; *J. Opt. Soc. Amer.* **47**, 300 (1957).
2 C. Feldman; *J. Soc. Motion Pic. Tele. Engrs.* **67**, 455 (1958).
3 F. J. Studer and D. A. Cusano; *J. Opt. Soc. Amer.* **45**, 493 (1955).
4 F. J. Studer; *J. Soc. Motion Pic. Tele. Engrs.* **65**, 197 (1956).
5 L. Holland and S. K. Bateman; *Brit. J. Appl. Phys.* (to be published).

S. K. BATEMAN.

Vacuum Deposition Research Division,
Edwards High Vacuum Limited.

* ZnS (Mn) was supplied by Levy West Laboratories, Wembley, Middlesex.

Improvement in Operation with McLeod Gauge

THE MOST convenient method for controlling the mercury in the short form of the McLeod gauge requires the evacuation of the mercury reservoir. To read the pressure the mercury is raised by admitting atmospheric air into the reservoir. With such an arrangement, however, the evacuation of the gauge from atmospheric pressure, as well as the reverse operation,

requires great care. Since the gauge is isolated from the reservoir by a mercury column, their evacuation has to be carried out simultaneously, otherwise the mercury will rise, thus trapping gas at a relatively high pressure in the compression chamber, if the pressure is lowered in the gauge only, or gas may bubble through the mercury in the reservoir, if this latter is evacuated more quickly than the gauge.

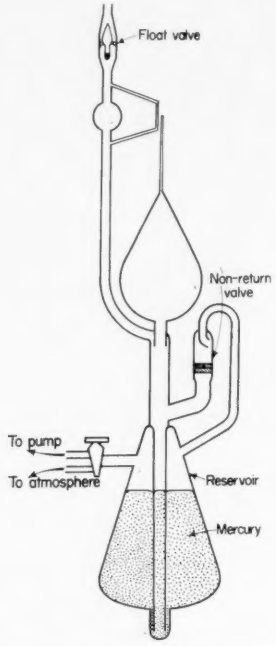

FIG. 1. McLeod gauge provided with a non-return valve.

Since no suggestion has been made for avoiding this drawback, we will describe in the present note a simple procedure which has been used satisfactorily in our laboratory. As shown in the accompanying sketch, a by-pass containing a non-return valve was added between the vertical tube leading to the compression chamber and the part of the reservoir above the mercury. This valve is made of a sintered glass disk of No. 4 porosity, about 15 mm in diameter, sealed horizontally into an enlarged portion of the by-pass glass tube. When the sintered disk is covered by a pool of mercury about 2 mm in depth, the arrangement forms a non-return valve, i.e. gas may pass through it only in an upward direction. The valve is connected in such a manner that gas is able to flow from the gauge into the reservoir.

For evacuating the system, the vacuum pump connected to the reservoir is started first. The pressure will decrease in both the gauge and the reservoir. After a while the main pump may be started to further lower the pressure in the system. When the gauge needs to be disconnected or the system altered, the air which is admitted will pass through the valve, thus the pressure in the reservoir will increase at the same rate as in the gauge.

It is worthy of note that the portion of the by-pass tube below the non-return valve, should not be smaller than 10 mm in diameter, so that no mercury will remain trapped in it.

N. A. FLORESCU.

School of Applied Physics,
The University of New South Wales,
Sydney Kensington Australia.

Vol.
10
196

A Tetrode Ionization Gauge

Introduction

Pressures between 10^{-3} and 10^{-8} torr are conveniently measured by means of an ionization gauge. The usual form for these gauges is that of a triode electron tube. In the normal mode of operation, a potential of 200 or 300 V is applied to the grid which may thus accelerate electrons from the cathode. At this energy, electrons readily ionize gaseous molecules, so that if the plate is given a potential of -20 to -50 V all the ions formed are collected. The ion current measured in the plate circuit is directly proportional to the molecular concentration in the region of the electrodes, provided the current of accelerated electrons is held constant. With changing pressure however, a number of factors cause this current to change by an order of magnitude over the operating range of the gauge. Since in many applications it is convenient to have a directly reading pressure gauge, a number of electrical and electronic schemes have been devised to keep the electron current constant. As the electron energy must be kept constant as well, all these devices operate by means of filament temperature control.

Already in 1938 C. G. and D. D. Montgomery realized that the electron current could be controlled by means of an additional grid. One of the most important features of this gauge is that the filament temperature is essentially constant, and thus the pressure in the system being measured is constantly proportional to the molecular concentration of gas in the gauge. This type of tube is referred to as a tetrode gauge, and due to the similarity of ionization gauges with electron tubes, it is convenient for the purpose of discussion, to give geometrically similar electrodes identical names, even though their functions may be different in the two cases.

The tetrode gauge allows us to accelerate electrons from the cathode by means of applying a positive potential to the screen, and to collect ions, as in the case of the triode, by means of the plate.

The grid now lends itself to a simple voltage feedback system to control the electron current. In the simplest case, the current through a cathode resistor R_K provides the bias voltage for grid and plate, changes in which may be used directly as corrective signals on the grid, as is shown in Fig. 1. The grid

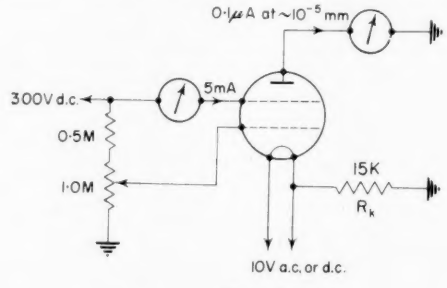

FIG. 1.

also permits amplified feedback, to give almost perfect screen current stability. For most practical indicative uses however, the stability afforded by the simple voltage feedback system is sufficient, if the parameters are correctly chosen. It can be shown that best stabilization is obtained for a large value of R_K and a high mutual conductance for the grid-screen section of the tube.

The gauge described by Montgomery[1] made use of a standard type 47 electron tube. However this and most other tubes incorporate oxide coated filaments, whose operational life at pressures of the order of 10^{-5} Torr may only be 30 min. Hence it was found useful to develop a gauge, whose construction is described below, which not only has a robust filament, but which also allows rapid degassing of the electrode system.

Construction

The gauge electrodes are entirely of tungtsen, and consist of three concentric, equally pitched, cylindrical spirals of 1 mm wire acting as grid, screen and plate, as is shown in Fig. 2.

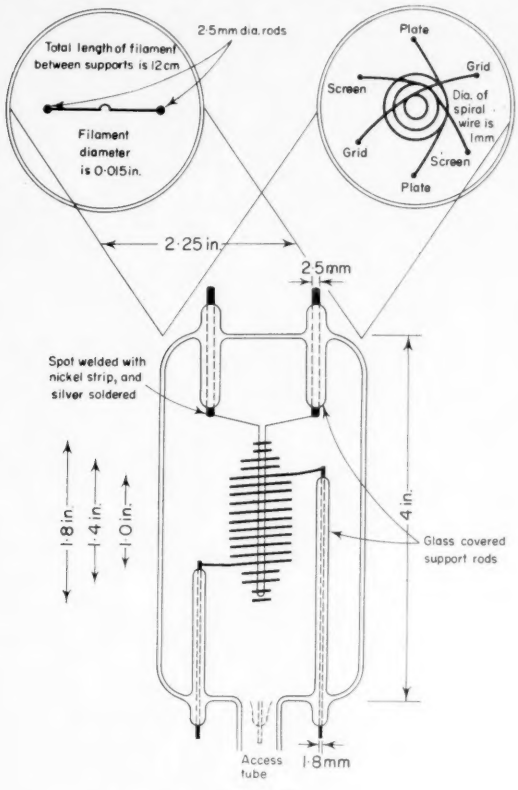

FIG. 2.

The filament, in the form of a hairpin, is of 0.015 in. tungsten wire, and draws 10 amps at 10 V ; a long life is to be expected from such a filament. All the electrodes have an electrical connection to each end, enabling the passage of a heating current for rapid degassing, as well as ensuring a rigid electrode mounting. An all tungsten system was chosen, as this metal remains essentially rigid, even at red heat. The pitch of the spirals is 10 per in.; they were wound on to solid brass formers to ensure uniformity in their geometry. The formers held one end of the tungsten wire in a diametric hole, and were turned by means of a slow speed lathe. The wire was held with even tension and heated with an oxygen-gas torch, to prevent splitting as it rolled on to the former. After removal from the formers, the spirals were cut to the appropriate lengths, and spot welded by means of an interposed nickel ribbon, to 1.8 mm tungsten rods, glass covered except at the ends, and previously set into a glass base. The filament however requires 2.5 mm rods, due to the large current. The spot welds were then silver soldered over, since it is difficult to obtain durable mechanical rigidity and satisfactory electrical conduction through a spot welded tungsten joint, which is nevertheless necessary because even high melting point silver solder becomes soft during the final glass blowing process of providing the electrode structure with a glass envelope and access tube. The plate consists of 10 turns on a 0.75 in. diameter former ; the screen, 14 turns on a 0.5 in. ; and the grid, 18 turns on a 0.25 in. former. The guiding spiral grooves of the formers have a depth of about 0.02 in. The reason for the difference in lengths of the spirals, is to prevent electrons from reaching the screen, without first passing through the grid. Due to the filament being supported at one end only, in operation the tube must be mounted vertically, with the filament hanging down.

Operation

When the gauge is connected as shown in Fig. 1, with the screen at 300 V, and a 15,000 Ω cathode resistor, a fractional change of 3.5 per cent in the electron current takes place when the operating pressure is changed from 10^{-5} to 10^{-4} Torr.

At 10^{-5} Torr the ion current is about 0.1 μA, a current which is easily measured on a high impedance voltmeter, as the plate-cathode resistance is of the order of 10^{9} Ω.

Simple and compact control units are possible for a tetrode ion gauge, which, compared with those for triode gauges, are economical in terms of both space and cost.

Acknowledgements

The author wishes to acknowledge the glass blowing of D. Ellis, and the receipt of a Melbourne University Research Grant, which supported this work.

[1] C. G. and D. D. Montgomery; *R.S.I.* **9**, 58 (1938).

PETER SCHWERDTFEGER

Present Address : *Physics Dept.,*
McGill University, Montreal,
Canada.

(*Received* 7 *April* 1960)

Vol.
10
1960

Organisation internationale pour la Science et la Technique du Vide

International Organization for Vacuum Science and Technology

Internationale Organisation für Vakuum-Physik und -Technik

ASSOCIATION SCIENTIFIQUE

30, avenue de la Renaissance, Bruxelles 4, Belgique

Président :
Prof. Dr. E. Thomas

Secrétaire administrative:
Mme A. De Henau

2e année	**BULLETIN D'INFORMATION No. 7**	**Juillet**
2nd year	**NEWS BULLETIN No. 7**	**July 1960**
2. Jahrgang	**INFORMATIONSBLATT Nr. 7**	**Juli**

ol.
10
960

SOMMAIRE — SUMMARY — INHALT

Editorial—Leitartikel 335

1. Comptes rendus du Premier Congrès International des Techniques du Vide (Namur, juin 1958)
Proceedings of the First International Congress on Vacuum Techniques (Namur, June 1958)
Berichte über den Ersten Internationalen Kongress für Vakuumtechnik (Namur, Juni 1958) 335

2. Comités nationaux de l'OISTV .. ..
IOVST National Committees .. ..
Nationale Ausschüsse der IOVPT 336

3. Comité de normalisation .. ..
Vacuum Standardization Committee .. ..
Normungs-Komitee 336

4. Comité pour la formation des spécialistes .. ..
Committee for the formation of specialists .. ..
Komitee für die Ausbildung von Spezialisten 337

5. Liste des nouveaux membres de l'OISTV .. ..
List of IOVST new Members .. ..
Liste der neuen Mitglieder der IOVPT 337

6. Réunions—Meetings—Tagungen 338

7. Résumés des communications présentées par des membres de l'OISTV au Symposium de Côme (sept. 1959) (*suite*) .. ..
Abstracts of the Proceedings communicated by the IOVST's members to the Como Symposium (Sept. 1959) (*continuation*) .. ..
Zusammenfassende Auszüge aus den durch die Mitglieder der IOVPT bei der Zusammenkunft in Como (Sept. 1959) vorgetragenen Berichten und Mitteilungen (*Fortsetzung*) 339

8. Photocopies—Photokopien 339

Nous renouvelons l'appel lancé dans le numéro précédent :
We wish to renew the call appearing in our former number :
Wir erneuern die in unserer vorhergehenden Nummer erlassene Aufforderung :

*
* *

Deux bulletins d'adhésion sont joints au présent numéro : l'un destiné aux membres fondateurs collectifs (sociétés et associations), l'autre destiné aux membres fondateurs individuels (personnes).

L'OISTV vous saurait gré de l'aider dans son action, en remettant ces bulletins à des sociétés et à des personnes intéressées à la science et à la technique du vide.

*
* *

Vol.
10
196

Two application forms are attached to the present number : one is meant for Associate Founder Members (societies and associations), the other is meant for Individual Founder Members (persons).

The IOVST would appreciate your co-operation by transmitting these forms to societies and persons interested in vacuum science and technology.

*
* *

Dem vorliegendem Bericht sind zwei Beitrittsformulare beigelegt : eines ist für Kollektiv-Gründermitglieder (Gesellschaften und Körperschaften) bestimmt und das zweite für individuelle Gründermitglieder (Personen).

Die IOVPT wäre Ihnen verbunden, wenn Sie sie in ihrer Tätigkeit unterstützen würden, indem Sie diese Beitrittsformulare an die an der Vakuum-Physik und -Technik interessierten Gesellschaften und Personen weiterleiten.

2e année | BULLETIN D'INFORMATION No. 7 | Juillet
2nd year | NEWS BULLETIN No. 7 | July 1960
2. Jahrgang | INFORMATIONSBLATT Nr. 7 | Juli

EDITORIAL — LEITARTIKEL

Nous sommes très heureux de souligner l'aide importante qu'un de nos premiers membres fondateurs collectifs a bien voulu nous apporter et qui entraîne une réduction sensible de nos dépenses.

La firme PERGAMON PRESS, qui publie la revue VACUUM, nous a en effet proposé d'y insérer, dorénavant, notre bulletin gratuitement et sans conditions. Elle met également à notre disposition les tirages à part destinés à nos membres.

Nous exprimons toute notre reconnaissance à PERGAMON PRESS dont le geste généreux assure une diffusion plus grande ainsi qu'une présentation meilleure à notre bulletin.

Nos membres constateront avec plaisir que notre action ne cesse de se développer. Les groupes nationaux du vide de la République Fédérale Allemande et du Japon ainsi que la Communauté Européenne de l'Energie Atomique viennent d'adhérer à l'OISTV.

Que tous nos nouveaux membres sachent combien leur collaboration nous sera utile.

*
* *

We are very pleased to record the important assistance which one of our first associate founder members has been kind enough to give and which brings with it an appreciable reduction of our expenses.

PERGAMON PRESS, which publishes "VACUUM" has offered to include the bulletin in the international journal free of charge. It will also supply gratis reprints for distribution to our members.

We express our appreciation to PERGAMON PRESS whose generous gesture ensures a larger distribution as well as an improved presentation of our bulletin.

Our members will notice with pleasure that our action is unceasingly developing. The national vacuum groups of the German Federal Republic and of Japan as well as the European Community of Atomic Energy have just adhered to the IOVST.

May all our new members realize how useful their co-operation will be to us.

*
* *

Es freut uns ausserordentlich von der bedeutenden Hilfe Mitteilung machen zu können, welche uns seitens eines unserer Kollektiv-Gründermitglieder zuteil wurde und wodurch eine fühlbare Herabminderung unserer Ausgaben zu verzeichnen sein wird.

Die Firma PERGAMON PRESS, welche die Zeitschrift VACUUM herausgibt, hat uns den Vorschlag gemacht, von heute ab in derselben unser Informationsblatt kosten- und bedingungslos zum Abdruck zu bringen. Sie stellt gleicherweise die Auflage, ausser der für unsere Mitglieder benötigten Exemplare, zu unserer Verfügung.

Wir drücken der PERGAMON PRESS für ihr Entgegenkommen, welches uns eine grössere Verbreitung wie auch eine bessere Aufmachung unserer Informations-Blätter sichert, unseren besten Dank aus.

Unsere Mitglieder werden mit Genugtuung feststellen können, dass sich unser Tätigkeitsfeld ohne Unterlass weiter entwickelt. Die nationale Vakuum-Gruppe der Bundesrepublik Deutschland und diejenige von Japan sowie die Europäische Atomgemeinschaft treten der IOVPT bei.

Unsere neuen Mitglieder können davon überzeugt sein, dass uns ihre Mitarbeit die wertwollsten Dienste leistet.

*
* *

1. Comptes rendus du Premier Congrès international des Techniques du Vide (Namur, juin 1958)

Proceedings of the First International Congress on Vacuum Techniques (Namur, June 1958)

Berichte über den Ersten Internationalen Kongress für Vakuumtechnik (Namur, Juni 1958)

Nos membres auront vraisemblablement été informés par PERGAMON PRESS de la publication de ces comptes rendus en deux volumes sous le titre général

ADVANCES IN VACUUM SCIENCE AND TECHNOLOGY

Le volume I (approx. 508 p. $11\frac{1}{4} \times 8\frac{3}{4}$ in.) comprend 9 conférences données en séance d'ouverture et en séances plénières ainsi que 80 communications consacrées aux problèmes de base des techniques du vide et à l'ultra-haut vide.

Le volume II (approx. 376 p. $11\frac{1}{4} \times 8\frac{3}{4}$ in.) comprend 75 communications relatives aux utilisations des techniques du vide.

Cet ouvrage, à la publication duquel PERGAMON PRESS a apporté ses meilleurs soins, sera de la plus grande utilité à tous ceux qui s'intéressent à la science et à la technique du vide.

*
* *

Our members will probably have been informed by

PERGAMON PRESS of the publication of these proceedings in two volumes under the general title

ADVANCES IN VACUUM SCIENCE AND TECHNOLOGY

— Volume I (approximately 508 p. $11\frac{1}{4} \times 8\frac{3}{4}$ in.) consists of 9 lectures given in the opening session and in the plenary sessions as well as 80 communications assigned to the fundamental problems in vacuum techniques and to ultra-high vacuum.

— Volume II (approximately 376 p. $11\frac{1}{4} \times 8\frac{3}{4}$ in.) consists of 75 communications relative to the vacuum systems applications in various sciences and techniques.

This work, to which PERGAMON PRESS has given its best attention, will be of the greatest use to all those who are interested in vacuum science and technology.

*
* *

Unsere Mitglieder wurden wahrscheinlicherweise durch die PERGAMON PRESS von der Herausgabe der zwei Bände mit unseren Berichten unter dem allgemeinen Titel

ADVANCES IN VACUUM SCIENCE AND TECHNOLOGY

unterrichtet.

— Der erste Band (beiläufig 508 S. $11\frac{1}{4} \times 8\frac{3}{4}$ in.) beinhaltet 9 in der Eröffnungssitzung und in den Plenarsitzungen gehaltenen Vorträge wie 80 Mitteilungen gewidmet den Grundproblemen der Vakuum- und Höchstvakuum-Techniken.

— Der zweite Band (beiläufig 376 S. $11\frac{1}{4} \times 8\frac{3}{4}$ in.) beinhaltet 75 Mitteilungen bezüglich der Benutzung der Vakuumtechnik.

Dieses Werk, welchem die PERGAMON PRESS ihre besondere Sorgfalt angedeihen liess, wird für alle welche sich für die Vakuum-Physik und -Technik interessieren, von grösstem Nutzen sein.

*
* *

2. Comités Nationaux de l'OISTV — IOVST national committees—Nationale Ausschüsse der IOVPT

Le Deutsches nationales Komitee für Vakuum, présidé par le Prof. Dr. R. JAECKEL, s'est inscrit comme membre fondateur collectif et est devenu ainsi le comité national de la République Fédérale Allemande au sein de l'OISTV.

La Vacuum Society of Japan, présidée par Mr. S. ASAO, a également adhéré à l'OISTV en qualité de membre fondateur collectif et est devenue comité national japonais.

Enfin, précisons que c'est la Physikalische Gesellschaft in der Deutschen Demokratischen Republik qui constitue le groupe national du vide de l'Allemagne de l'Est et non la " Sektion Vakuumtechnik " de cette société, comme nous l'avions annoncé erronément dans notre bulletin no. 5 (p. 10).

*
* *

The Deutsches nationales Komitee für Vakuum, presided by Prof. Dr. R. JAECKEL, has registered itself as associate founder member and has in this way become the national committee of the Federal German Republic in the midst of the IOVST.

The Vacuum Society of Japan, presided by Mr. S. ASAO, has also adhered to the IOVST in the capacity of associate founder member and has become the Japanese national committee.

Finally, let us bring out that it is the Physikalisches Gesellschaft in der Deutschen Demokratischen Republik which constitutes the national vacuum group of Eastern Germany and not the " Sektion Vakuumtechnik " of this company, as we have erroneously published in our bulletin no. 5 (p. 11).

*
* *

Das Deutsche nationale Komitee für Vakuum, dessen Vorstand Prof. Dr. R. JAECKEL ist, trug sich als Kollektiv-Gründermitglied ein und wurde derart der nationale Ausschuss der Bundesrepublik Deutschland im Schosse der IOVPT.

Die Vacuum Society of Japan, dessen Vorstand Herr S. ASAO ist, trat gleicherweise der IOVPT als Kollektiv-Gründermitglied bei, und wurde derart der nationale Ausschuss Japans.

Es ist festzustellen, dass die Physikalische Gesellschaft in der Deutschen Demokratischen Republik die nationale Vakuum-Gruppe von Ost-Deutschland darstellt und nicht die " Sektion Vakuumtechnik " dieser Gesellschaft, wie dies irrigerweise in unserem Informationsblatt Nr. 5 (Seite 11) veröffentlicht wurde.

*
* *

3. Comité de Normalisation—Vacuum Standardization Committee—Normungs-Komitee

Un contact a été établi et sera maintenu avec l'Organisation Internationale de Normalisation ISO.

La British Standards Institution a nommé Mr. A. S. D. BARRETT comme représentant anglais.

D'autres pays désigneront prochainement leurs délégués.

*
* *

A contact has been established and will be maintained with the International Organization for Standardization ISO.

The British Standards Institution has nominated Mr. A. S. D. BARRETT as the English representative.

Other countries will shortly designate their delegates.

*
* *

Die Verbindung mit der International Organization for Standardization (ISO) wurde aufgenommen und wird weiter aufrecht erhalten werden.

Die " British Standards Institution " hat Herrn A. S. D. BARRETT als englischen Vertreter aufgestellt.

Die anderen Länder werden in Kürze ihre Delegierten ernennen.

*
* *

Vol. 10 1960

4. Comité pour la formation des spécialistes— Committee for the formation of specialists— Komitee für die Ausbildung von Spezialisten

Les travaux de ce comité se poursuivent également. Le Prof. Dr. J. M. DUNOYER a pu obtenir les locaux et les moyens matériels nécessaires au bon fonctionnement et au succès des cours de Science et de Technique du Vide qu'il organisera en France en juillet 1961.

*
* *

The work of this committee is also continuing. Prof. Dr. J. M. DUNOYER has been able to obtain the premises and the necessary material means for the good functioning and for the success of the Vacuum Science and Technology courses which he will organize in France in July 1961.

*
* *

Die Arbeiten dieses Komitees nehmen ihren Fortlauf. Herr Prof. Dr. J. M. DUNOYER konnte sowohl die Lokale wie das nötige Material für die erfolgreiche Abhaltung der Kurse über Vakuum-Physik und -Technik, welche er im Juli 1961 in Frankreich organisieren wird, erhalten.

*
* *

5. Liste des nouveaux membres fondateurs de l'OISTV allant du 16 avril au 15 juillet 1960

List of the new founder members of the IOVST, as from April 16 to July 15, 1960

Liste der neuen Gründer-Mitglieder der IOVPT vom 16. April bis 15. Juli 1960

La liste suivante comprend les noms des nouveaux membres fondateurs classés selon le pays où ils résident :

The following list contains the names of the new founder members who are classified according to their present residing State :

Die nachfolgende Liste umfasst die Namen der neuen Gründer-Mitglieder, eingeteilt nach dem Lande ihres gegenwärtigen Wohnsitzes :

MEMBRES FONDATEURS COLLECTIFS
ASSOCIATE FOUNDER MEMBERS
KOLLEKTIVE GRÜNDER-MITGLIEDER

Allemagne (Rép. Féd.) — Germany (Fed. Rep.) — Deutschland (Bundesrepublik)

Deutsches nationales Komitee für Vakuum,
(Délégué et suppléants : Prof. Dr. E. JAECKEL, Prof. Dr. K. DIELS, Dr. W. PUPP, Prof. Dr. H. EBERT, Dr. W. HÄNLEIN, Dr. H. MIESSNER, Dipl. Ing. W. NERGE, Dr. H. BRETSCHNEIDER, Dr. BEHRENS).

Etats-Unis — U.S.A. — V.S. von Nordamerika

Central Scientific Company, Chicago 13, Ill.
(Delegate : Mr. Robert G. PICARD, Vice-President).

Japon — Japan

Vacuum Society of Japan.
Tokuda Seisakusho, Ltd., Tokyo.
(Delegate : Mr. Tokichi TOKUDA, President).

Liechtenstein

Balzers Aktiengesellschaft für Hochvakuumtechnik und Dünne Schichten.

Organisations européennes — European organisations — Europäische Organisationen

Communauté Européenne de l'Energie Atomique—Europäische Atomgemeinschaft — Comunità Europea dell'Energia Atomica—Europese Gemeenschap voor Atoomenergie (EURATOM).
(Délégué : M. J. GUÉRON, Directeur Général, div. Recherche et Enseignement).

MEMBRES FONDATEURS INDIVIDUELS
INDIVIDUAL FOUNDER MEMBERS
INDIVIDUELLE GRÜNDER-MITGLIEDER

Allemagne (Rép. Féd.) — Germany (Fed. Rep.) — Deutschland (Bundesrepublik)

Hans-Joachim FORTH, Dr. Ing., Köln-Sülz.
Heinz HOCH, Dr. rer. nat., Brauweiler, Landkreis Köln.
Gottfried SCHIEFFER, Cand.-Phys., Köln-Riehl.

Belgique — Belgium — Belgien

André DE HENAU, Physicien, Wemmel.
Eric RUTTIENS, Techn. Electromécanique, Bruxelles 15.

Etats-Unis — U.S.A. — V.S. von Nordamerika

Hugh S. CHRISTIAN, Chief Eng., Lancaster, Ohio.
Sydney M. ELLIS, Ind. Prod. Manager, Erie, Pennsylvania.
Robert E. FISCHER, Technician, Albany 6, California.
R. FRANK, Chem. Eng., Los Angeles 43, California.
Max GARBER, Director, Rochester 3, N.Y.
William R. MEOLI, Asst. Sales Manager, New Hyde Park, L.I., N.Y.
Pete MUNCH, Sales Manager, Berkeley 3, California.
Edward W. PERKINS, Manager, Rochester 3, N.Y.
John L. PETERS, Manager, Hempstead, L.I., N.Y.
George H. TIMMINGS, Director & President, Chicago 25, Illinois.

France — Frankreich

Robert D'AUTEUIL, Ing., Wissous (S. & O.).

Inde — India — Indien

S. C. DASGUPTA, M.Sc., Manager, Bombay.

Japon — Japan

Yata KASUO, Researcher, Tokyo.
Hiroshi NAKAGAWA, Chief Res. Lab., Tokyo.

Norvège — Norway — Norwegen

Erling ILLØKEN, Elect. Eng., Bergen.

Royaume-Uni — United Kingdom — Grossbritannien

John Radford BAILEY, B.Sc., Aldermaston, Berks.
H. G. MCOWAN, London, S.W.19.

Suisse — Switzerland — Schweiz

Konrad BUOB, Food-technologist, Genève.
Peter STOLL, Prof. Dr. sc. nat., Zürich 48.

Misprint — Erratum

Bull. no. 3—p. 11—Harold Baier (instead of Harol Baier).

Nouvelles Adresses — New Addresses — Neue Adressen

James S. Hetherington, Free lance eng., Boston, Mass.
Cambey, B.Sc., Hamilton, Ontario.

Addendum (Associate Founder Members)

Mr. Douglas Latham, B.Sc., a Director of Edwards High Vacuum Ltd., Crawley (U.K.), has been nominated as the delegate of this company.

*
* *

TABLEAU RÉCAPITULATIF — GENERAL TABLE
ZUSAMMENFASSENDE TABELLE

Pays — Countries — Länder	Membres fondateurs collectifs Associate founder members Kollektive Gründer-Mitglieder	Membres fondateurs individuels Individual founder members Individuelle Gründer-Mitglieder
Org. europ.—Europ. Org.	1	2
Allemagne—Germany—Deutschland :		
Rép. Dém.—Dem. Rep.	1	2
Rép. Féd.—Fed. Rep.—Bundesrep.	6	34
Argentine—Argentinien		2
Australie—Australia—Australien		9
Autriche—Austria—Österreich		1
Belgique—Belgium—Belgien	14	51
Brésil—Brazil—Brasilien		2
Canada		9
Espagne—Spain—Spanien	1	5
Etats-Unis—U.S.A.—V.S. von Amerika	13	290
France—Frankreich	1	12
Hongrie—Hungary—Ungarn		4
Inde—India—Indien		1
Israël		1
Italie—Italy—Italien	2	5
Japon—Japan	3	5
Liechtenstein	1	4
Norvège—Norway—Norwegen		2
Pays-Bas—Netherlands—Niederlande	1	7
Philippines—Philippinen		1
Pologne—Poland—Polen		1
Royaume-Uni—U.K.—Grossbritannien	3	28
Suède—Sweden—Schweden		3
Suisse—Switzerland—Schweiz		11
Tchécoslovaquie—Czecho-Slovakia—Tschechoslowakei		2
Union Sud-Africaine—Un. of S. Africa—Südafrikanische Union		1
Yougoslavie—Yugoslavia—Yugoslavien		3
	47	498

Nous saurions gré aux membres changeant d'adresse ou de fonction de bien vouloir nous en aviser le plus rapidement possible. Ils faciliteront ainsi la tâche du Secrétariat.

*
* *

We would be obliged if the members changing their address or function would kindly advise us of same as quickly as possible. They will in this way facilitate the task of the Secretariat.

*
* *

Wir wären denjenigen Mitgliedern, welche ihre Adresse oder Funktion ändern verbunden, wenn sie uns hiervon so schnell wie möglich verständigen würden ; hierdurch wären die Arbeiten des Sekretariats wesentlich erleichtert.

*
* *

6. Réunions — Meetings — Tagungen

Dans cette rubrique, nous annonçons les réunions consacrées à la science et à la technique du vide.

Ne pouvant reproduire ici toutes les informations relatives à ces manifestations, nous prions nos membres de demander de plus amples renseignements aux organisateurs.

*
* *

Under this heading, we announce the symposia being held in connection with vacuum science and technology.

It being impossible to reproduce here all the information relating to these symposia, we request our members to enquire more details from the organizers.

*
* *

In dieser Spalte zeigen wir die der Vakuum-Physik und -Technik gewidmeten Tagungen an.

Da wir nicht sämtliche Auskünfte und Nachrichten dieselben betreffend abdrucken können, bitten wir unsere Mitglieder sich wegen umfassenderer Informationen an die Organisatoren zu wenden.

*
* *

a) Prof. Dr. R. JAECKEL weist darauf hin, dass die Deutsche Arbeitsgemeinschaft Vakuum im Oktober dieses Jahres zwei Geschäftssitzungen abhalten wird und zwar 1. am 5.10 in Mannheim im Anschluss an eine Vortragstagung der Verfahrenstechnischen Gesellschaft im VDI und 2. zwischen dem 17. und 21.10 in Wiesbaden anlässlich der Tagung des Verbandes Deutscher Physikalischer Gesellschaften.

*
* *

b) Mr. A. S. D. BARRETT has kindly drawn our attention to the following notice which appeared in the June number of the " Chartered Mechanical Engineer " page 305 :

" *User Experience of large scale Industrial Vacuum Plant*

" A symposium of some six papers on aspects of user experience of large scale industrial vacuum plant is now being arranged by the Institution. It will be held in London on 1st March 1961.

" The meeting's main objective will be to provide an opportunity for designers and users of vacuum plant to get together for the mutual exchange of experience and discussion of problems.

" It is planned to include in the Symposium contributions reviewing experience, problems and techniques in the food and metal industries ; on the fabrication of large vessels, including welding and testing techniques, and on vacuum seals. The Symposium is the outcome of a recommendation made by the Joint British Committee for Vacuum Science and Technology on which the Institution is represented.

" Further details of the arrangements will be announced in due course."

*
* *

7. Résumés des communications présentées par des membres de l'OISTV au Symposium de Côme, 23-25 septembre 1959

Abstracts of the Proceedings communicated by the IOVST's members to the Como Symposium, 23-25 September 1959

Zusammenfassende Auszüge aus den durch die Mitglieder der IOVPT bei der Zusammenkunft in Como (23.-25. September 1959) vorgetragenen Berichten und Mitteilungen

Dans les numéros 4 et 6 de notre bulletin, nous avons publié deux listes de résumés des communications présentées par des membres de notre organisation à l' " International Symposium on Residual Gases in Electron Tubes and Related High Vacuum Systems ".

Les communications ayant été publiées in extenso dans le numéro 1/2 février/avril 1960, Volume 10 de la revue Vacuum, il n'est plus nécessaire de faire paraître dans ce bulletin les résumés des communications suivantes :

*
* *

In numbers 4 and 6 of our bulletin, we have published two lists of abstracts of the communications presented by members of our organization at the " International Symposium on Residual Gases in Electron Tubes and Related High Vacuum Systems ".

The communications having been published in extenso in number 1/2 February/April 1960, Volume 10 of " Vacuum ", it is not necessary to publish in this bulletin the abstracts of the following communications :

*
* *

In den Nummern 4 und 6 unseres Informationsblattes haben wir zwei Listen der durch die Mitglieder unserer Organisation über das " International Symposium on Residual Gases in Electron Tubes and Related High Vacuum Systems " vorgetragenen zusammenfassenden Berichte veröffentlicht.

Da die Mitteilungen in extenso in den Nummern 1/2 Februar/April 1960, Band 10 der Vacuum-Zeitschrift veröffentlicht wurden, ist es nicht mehr nötig in diesem Informationsblatt die folgenden Mitteilungsauszüge erscheinen zu lassen :

*
* *

— R. RICCA (Torino) and P. DELLA PORTA (Milano).—Carbon Monoxide sorption by Barium Films.
— P. DELLA PORTA and E. ARGANO (Milano).—Nitrogen Sorption by Barium Films.
— P. DELLA PORTA and S. ORIGLIO (Milano).—Hydrogen Sorption by Barium Films.
— S. JERIČ and E. KANSKY (Ljubljana).—A Method for Measuring of Caesium Vapour Pressure in Photoelectric Tubes.
— E. KANSKY and S. JERIČ (Ljubljana).—Some Results of the Measurement of Caesium Vapour Pressure in Photoelectric Tubes during their Manufacture and Life.

*
* *

8. Photocopies — Photokopien

Nous tenons à préciser que c'est la firme The Alloyd Corporation, organisatrice du First Symposium on Electron-Beam Melting, tenu le 20 mars 1959 à Boston, Mass., qui nous a autorisés à envoyer à nos membres la photocopie des communications présentées à ce symposium.

Conformément à l'accord conclu récemment avec la firme précitée, notre Organisation ne peut fournir que la photocopie de toutes les communications (prix des 96 pages de photocopie : 720 francs belges).

Rappelons que la liste complète des communications a paru dans le bulletin no. 6.

*
* *

We wish to point out that it is the firm The Alloyd Corporation, organiser of the First Symposium on Electron-Beam Melting, held on the 20th March, 1959, at Boston, Mass., who has authorized us to send to our members the photocopy of the communications presented at this symposium.

In terms of the agreement recently concluded with the above-mentioned firm, our Organisation can only furnish the photocopy of all the communications (price of the 96 pages of the photocopy : 720 Belgian Francs).

Let us remind that the complete list of the communications has appeared in Bulletin no. 6.

*
* *

Wir möchten feststellen, dass es die Firma The Alloyd Corporation, Organisatorin der First Symposium on Electron-Beam Melting, abgehalten am 20. März 1959 in Boston, Mass., ist, welche erlaubt, an unsere Mitglieder die Photokopien der bei dieser Berichterstattung abgegebenen Berichte zu senden.

Zufolge dem mit dieser Firma letzhin abgeschlossenen Uebereinkommens, kann unsere Organisation nur die Photokopie der Gesamtheit dieser Berichte zum Preise von bfrcs. 720.—für 96 Seiten Photokopien liefern.

Wir erinnern an die vollständige Liste der Berichte, welche in unserem Informationsblatt Nr. 6 erschien.

Vol.
10
1960

Abstracts

General Vacuum Science and Engineering

10. Vacuum Technology

10 : 20 : 27 : 32 : 33

207. Summarized Proceedings of a Symposium on Current Developments in the Production of High Vacua—London, April 1959.

United Kingdom. The symposium was organized by the Institute of Physics and held in London on 17th April, 1959. The first session was devoted to getter-ion and ion-sorption pumps and two opening papers were read. The first dealt with " General principles of chemical and ionic pumping in vacuum systems ", and was by R. N. Bloomer, Siemens Edison Swan Ltd., Harlow, Essex. The difference between " chemical " and " ionic " pumping was discussed. Chemical reactions between gases, and active metals and gases were mentioned and so was the effect that ions can be driven into electrodes that are otherwise inert chemically. It has been customary for the performance of getter-ion pumps to be studied for particular gases singly, but it was pointed out in this paper that the presence of some other gas can greatly modify the kinetics of the absorption of particular gases. The importance of the study of surface reactions on getters, their performance limits, ways of improvement and nature of the metal films deposited in pumps were stressed. The second paper was on " The design and use of getter-ion pumps ", and was read by L. Holland, Edwards High Vacuum Ltd., Crawley, Sussex. Two principal types of getter-ion pumps were mentioned : Evapor-ion pump in which the getter film is replenished and Penning pump in which the getter film (Ti or Ba) is deposited by cathodic sputtering. Novel vapour source arrangements were described and emphasis was given to the design of pumps with metal gaskets for baking. The pumping performances were mentioned and also factors limiting the ultimate pressure. The combination of getter-ion pumps with conventional pumps is useful for high gas throughputs at pressures below 10^{-6} Torr. The short opening contributions to the Discussion were the following : (i) " The use of getter-ion pumps in the maintenance of high vacua in electron tubes ", by N. W. Robinson, Mullard Research Laboratories, Salfords, Surrey. Methods were described by which electron tubes may be pumped to pressures of 10^{-10} Torr under production conditions. (ii) " Some recent results in the development of getter-ion pumps ", by R. L. Jepsen, Varian Associates, Polo Alto, California, included basic operation of the VacIon pump, the description of the firm's research program and characteristics and design considerations of the pumps. (iii) " The dual sorption modes of Boyard–Alpert ionization gauges ", by C. Carter, University of Liverpool, described two distinct sorption characteristics with the ratio of pumping speed of five to one. The effect was ascribed to changes in the electrical potential of the inner surface of the glass envelope. (iv) " The sorption by titanium of oxygen and nitrogen at low pressures ", by L. G. Carpenter and W. N. Mair, Royal Aircraft Establishment, Farnborough, Hampshire. The rate of sorption of oxygen had been measured and the probability per impact for α and β-titanium determined. The reaction probability was also measured for the titanium nitrogen reaction. The second session was opened with a paper on " Problems in the production of high vacua in large equipment ", by J. Blears, Metropolitan-Vickers Electrical Co. Ltd., Manchester, dealing with problems in the design of vacuum systems. Factors of importance are various materials, different characteristics and the required condition of surfaces, ultimate pressure, convenience and available capital. The degassing of surfaces, bakable systems and the use of mercury diffusion pumps where the formation of deposits on the surface adversely affects the operation of equipment were described. Application of getter and ion pumps as well as refrigerated baffles was also mentioned. The second opening paper to this session was on " The vacuum system of the 7GeV Accelerator ", and was read by S. H. Cross, U.K.A.E.A., A.E.R.E., Harwell, Berkshire. Details of the work on the vacuum and radiation stability of the glass fibre reinforced epoxy resins were given. Problems peculiar to the design of this vacuum system and the resulting pumping units were described. As short opening contributions to the Discussion two brief papers were read. " Characteristics of some pumps and experimental results ", by B. D. Power, Edwards High Vacuum Ltd., Crawley, Sussex. Characteristics of oil vapour pumping groups were contrasted with those of mercury vapour pumping groups. " Some results of vacuum studies relating to large machines ", by R. S. Barton, U.K.A.E.A., A.E.R.E., Harwell, Berkshire. Results were discussed obtained on an apparatus set up for the measurement of the outgassing rate, vapour, pressure and gas permeability. The third session was opened with four short papers on the analysis of residual gases in kinetic vacuum systems. (i) " The role of the omegatron in diffusion pump development ", by N. T. Gallagher, Leybold Vacuum Sales Ltd., London. The relative efficiencies of working fluids were determined by using an omegatron for partial pressure measurement. Mechanically cooled baffles cannot prevent the passage of the more volatile hydrocarbons. (ii) " The application of miniature mass spectrometers to leak detection and analysis ", by A. O. Edmunds, 20th Century Electronics Ltd., Croydon, Surrey. Two instruments were described, the first of them being designed for leak detection but is useful for gases with mass numbers up to about 40. The second instrument has been employed for the process control on an isotope separation plant. (iii) " The study of high vacua with a small mass spectrometer ", by B. N. Green, Metropolitan Vickers Electrical Co. Ltd., Manchester, described a 2 in. radius 180° bakable mass spectrometer and typical figures obtained for the partial pressures of residual gases. (iv) " The influence of evaporated metal films on the residual gases in glass envelopes " by N. W. Robinson, Mullard Research Laboratories, Salfords, Surrey. Some films reduce the output of water vapour from plain bulbs to about 1/100, at temperatures up to 450° C. This is attributed to gettering and sealing of the surface. Molybdenum, magnesium and aluminium were found most effective.

Conference Report, *Brit. J. Appl. Phys.*, **10**, 383–391, Sept. 1959.

12. Measurement of Low Pressures

12

208. Forced Periodic Changes of Kinetic Energy of Gas Molecules as a Means of Vacuum Measurement.

Helmut Schwarz, *Rev. Sci. Instrum.*, **31** : 4, 433–438.

13. Vacuum Applications

13 : 39 : 42

209. Methods of Cleaning Glass by Vapour Degreasing and Ultrasonically Agitated Solvents.
United Kingdom. The production of clean glass surfaces for vacuum evaporation purposes has been studied, using a number of different chemical cleaning techniques. The principal cleaning methods investigated were vapour degreasing, using a range of solvents, and high- and low-frequency ultrasonic agitation of an *iso*propyl alcohol bath. The cleanliness of glass surfaces after treatment was assessed from their coefficient of friction, wetting properties and adherence to vacuum deposited coatings. In terms of these properties vapour degreasing in pure *iso*propyl alcohol produced the cleanest surface. However, low-frequency ultrasonic agitation was the most effective method of removing gross surface contamination. The cleaning of intricately shaped components is briefly discussed and it is shown that the gas pressure above the cleaning medium must be initially reduced to allow the solvent to enter cavities and thus provide maximum irradiation of the surface. Ultrasonic cleaning was found to be most effective when operated at low frequency 25 kc/s with an undegassed fluid under atmospheric pressure.

T. Punter, *Brit. J. Appl. Phys.*, **10**, 332–336, July 1959.

14. Kinetic Theory of Gases

210. Torsion Balance Measurements with Molecular Beams.
United Kingdom. A torsion balance is described for measuring the momentum carried by the molecules in a molecular beam with an intensity of about 10^{12} mol/s or more. The beam struck a vane suspended on a platinum fibre 3μ in diameter. The balance could be used at elevated temperatures. At room temperature, measurements of the balance deflexion were made to 1 part in 500, under favourable conditions. An investigation was made of the intensity of a molecular beam of carbon dioxide formed by a fairly simple molecular-beam generator, which is described. Deviations of gas flow from molecular flow and attenuation of the beam by scattering were important factors.

D. W. Bassett and A. J. B. Robertson, *Brit. J. Appl. Phys.*, **10**, 534–538, Dec. 1959.

16. Gases and Solids

16

211. The Chemisorption of Gases on Chromia Surfaces at Low Temperatures.
D. S. MacIver and H. H. Tobin, *J. Phys. Chem.*, **64**, 451–457, April 1960.

16

212. Physical Adsorption on Chemisorbed Films.
Note by D. S. MacIver and H. H. Tobin, *J. Phys. Chem.*, **64**, 683–686, May 1960.

16

213. The Diffusion of Hydrocarbons in Polyisobutylene.
Note by G. Blyholder and S. Prager, *J. Phys. Chem.*, **64**, 702–703, May 1960.

16

214. Successive Differential Absorptions of Vapors by Glassy Polymers.
Akira Kishimoto, Hiroshi Fujita, Hisashi Odani, Michio Kurata and Mikio Tamura, *J. Phys. Chem.*, **64**, 594–598, May 1960.

16

215. The Theory of Diffusion Controlled Absorption Kinetics with Accompanying Evaporation.
R. S. Hansen, *J. Phys. Chem.*, **64**, 637–641, May 1960.

16 : 17

216. Coefficients of Evaporation and Condensation.
United States. A model is developed for crystal growth and evaporation which invokes the Kossel concept of a crystal surface being composed of low index facets, of low binding energy for adsorbed atoms, separated by ledges of higher binding energy. The treatment indicates that surface diffusion kinetics are important in most instances of crystal growth and evaporation. Prior kinetic treatments, such as those involving limitations of crystal growth because of entropy effects or diffusion in the vapor phase, are modified to include surface diffusion effects. Values for evaporation and condensation coefficient predicted by the kinetic treatment are compared with experimentally determined values. (Author)

J. P. Hirth and G. M. Pound, *J. Phys. Chem.*, **64**, 619–626, May 1960.

16

217. Diffusion of Hydrogen in Thorium.
United States. The diffusivity of hydrogen in thorium was measured from 300 to 900°. Over this temperature range, $D = 2.92 \times 10^{-3} \exp(-9750/RT)$. The diffusivity increased with concentration above 600° but did not vary significantly with purity, grain size or cold working. Two different methods of determining diffusion constants were used and gave similar values. (Author)

D. T. Peterson and D. G. Westlake, *J. Phys. Chem.*, **64**, 649–651, May 1960.

16 : 52

218. The Oxidation of Evaporated Barium Films (Getters).
Note by S. J. Gregg and W. B. Jepson, *Brit. J. Appl. Phys.*, **9**, 417–418, Oct. 1958.

16 : 33 : 47

219. Properties of Getters in Electronic Tubes.
United States. In the first part of the paper flash getters are discussed, whose active part is a thin metal film obtained by evaporation from a getter assembly. The properties of the getter assembly which are compared for different getters are subdivided into : pre-flashing properties (resistance to air and moisture, and freedom from particles), flashing properties (flashing temperature and time, yield of active metal, directional vaporization and gas content) and post-flashing properties (freedom from particles and—for some special types of getters—freedom from magnetism). As for the properties of the getter film, two of these, adherence and volatility, do not concern adsorption. The adsorption properties as such are determined by gettering rate and getter capacity. Methods of measuring the adsorption properties at very low pressures are discussed, and values of initial getter rates and of capacities are given for different getter materials and gases. As for the capacity of the getter, it is assumed that this has reached its final value when the rate has fallen to a figure which is equal to the adsorption rate of the cathode in the tube. The capacity depends on temperature in two aspects : it increases with operating temperature, but it is reduced by intermediately heating the getter film above the operating temperature. A discussion of desorption shows that none of the common gases can be desorbed from barium getter films at moderate temperatures. The preparation and activation of bulk getters, which are getters made from powder, sheet or wire, is discussed in the second part, and rate and capacity values for such getters are given. The capacity values show a strong increase with temperature owing to which the bulk getters become superior to flash getters of equal area at temperatures above about 500°C. As for desorption, only hydrogen so far, has been found desorbable at temperatures up to 900°C. (Author)

J. S. Wagener, *Proc. 4th National Conf. on Tube Techniques*, p. 1. New York University Press, New York 1959.

Vol. 10 1960

16

220. The Submonolayer Adsorption of Argon and Krypton on Molybdenum Disulfide ; Phenomenological Comparison with Studies on Graphite.

United States. The adsorption isotherms of argon and krypton in the submonolayer coverage region on samples of hexagonal molybdenum disulfide are reported. Extensive experimental detail is given, since this constitutes the first such report. Two different temperatures for degassing lead to different results, since oxide contamination is volatile at an intermediate temperature. A comparison of the results with those published for graphitic substrates points out the conditions necessary for MoS_2 to behave as a homogeneous surface. (Author)

P. Cannon, *J. Phys. Chem.*, **64**, 858–861, July 1960.

16

221. New Technique for Measurement of Low Dissolved-Air Content of Water.

United Kingdom. A method is described to measure the dissolved-air content of water enclosed in a vessel. This method uses an air bubble and is very suitable for the measurement of the air content of undersaturated samples. Tests have been made of typical specimens and the limitations of the technique are discussed.

D. M. J. P. Manley, *Brit. J. Appl. Phys.*, **11**, 228–229, June 1960.

16 : 18

222. Evaporation and Diffusion Rate Measurements on Cathodes of Sintered Nickel Containing Alkaline-Earth Oxides.

United Kingdom. The evaporation rate of barium from a sintered nickel cathode and the diffusion rate of barium through it have been measured using ^{140}Ba and tracer techniques. Confirmation of the evaporation rates thus determined have been obtained by comparison with measurements made by a method due to Becker. The activation energy of evaporation is 2.2 to 2.5 eV. Two diffusion processes operate, one predominant in the range 875 to 1020°C and one below 875°C. The activation energies are 2.5 and 0.5 eV respectively. The mechanism of diffusion at the higher temperatures appears to be Knudsen flow following evaporation from the inner surfaces, and that for the lower temperatures probably by surface diffusion.

J. F. Richardson and F. A. Vick, *Brit. J. Appl. Phys.*, **11**, 73–77, Feb. 1960.

16

223. Adsorption on Porous Solids.

Note by B. H. Clampitt and D. E. German, *J. Phys. Chem.*, **64**, 284–286, Feb. 1960.

16 : 39

224. The Quantum Mechanical Correction for the High Temperature Van der Waals Interaction of Light Gases and Surfaces. A New Method of Determining Surface Area.

M. P. Freeman, *J. Phys. Chem.*, **64**, 32–37, Jan. 1960.

16

225. Reactions of Titanium and Zirconium with Oxygen, Air, Nitrogen and Carbon Dioxide.

Japan. There are many reports concerning the reaction rates of titanium and zirconium with oxygen and air, but they are only limited to the cases when the large quantity of oxygen react. In a case when the oxidation quantity is low, the condition should be different. The author investigated the reaction rates at high temperature in a relatively low vacuum (10–30 Torr) by a special microbalance which has the sensitivity of 1.3μg/0.01 mm and the reaction products were also examined with X-ray analysis. This work extended to the investigation of reactions with nitrogen and carbon dioxide. The reactions of titanium and zirconium with 15 Torr oxygen followed parabolic rate law at the temperature between 350–700°C, and the activation energies were 39,600 and 34,200 cal/mol respectively, and the products were ZiO_2 and TiO_2 in a monoclinic system. The reaction of zirconium with air also followed parabolic rate law, but the activation energy was 42,200 cal/mol. In the reaction of zirconium with nitrogen often the rate determining process was the diffusion rate of minute content of oxygen in nitrogen, but in the case of titanium this process did not affect so much. Both followed parabolic rate law and activation energies were 35,000 cal/mol. In the reactions of titanium and zirconium with carbon dioxide, the process followed parabolic law at first, then linear process followed. The activation energies were 69,000 cal/mol and 65,000 cal/mol respectively, the diffusion and dissolving rate of carbide in oxide seemed determining the whole rate. H. N.

M. Someno, *J. Vacuum Soc. Japan*, **3**, 55–61 (1960).

17. Thermodynamics

17 : 37

226. Viscosity and Thermal Conductivity of Liquid Boron Trifluoride.

United Kingdom. The normal liquid range of boron trifluoride is −100 to −127°C. Conventional methods have been adapted to measure viscosity and thermal conductivity throughout this range of temperature, and experimental results are presented.

A. N. Spencer and M. C. J. Todd, *Brit. J. Appl. Phys.*, **11**, 60–64, Feb. 1960.

17 : 52

227. The Dissociation Pressure of CdSb.

Note by V. J. Silvestri, *J. Phys. Chem.*, **64**, 826–827, June 1960.

17 : 52

228. Sublimation Pressures of Solid Solutions. I. The Systems Tin (IV), Bromide-Tin (IV), Iodide and Tin (IV), Bromide-Titanium (IV). The System Tin (IV), Bromide-Tin (IV), Iodide-Carbon Tetrachloride.

United States. A manometer has been designed for measuring vapor pressures of materials the vapor of which slowly interacts with or dissolves in the manometric liquid. It was used to measure the sublimation pressures of pure $SnBr_4$ and $TiBr_4$, of solid solutions of $SnBr_4$ in SnI_4 over a small range of temperature, and of solid solutions of $SnBr_4$ in $TiBr_4$ at 22°. Marked negative deviations from Raoult's law were found in the system $SnBr_4$–SnI_4, interpreted as a tendency toward the formation of mixed halides in the solid state. A supplementary study of the solid–liquid equilibria in the system $SnBr_4$–SnI_4–CCl_4 at 12° was undertaken to examine the distribution of $SnBr_4$ and SnI_4 between solid and saturated liquid solution. The distribution is of Type II in the Roozeboom classification, although it gives some evidence of compound formation. Measurement of the sublimitation pressures in the system $SnBr_4$–$TiBr_4$ proved very difficult, and the results, although erratic, showed positive deviations from Raoult's law. (Author)

J. J. Keavney and N. O. Smith, *J. Phys. Chem.*, **64**, 737–742, June 1960.

17

229. Dewar System for Low Temperature Experiments.

A special system of glass Dewars for experiments at low temperatures is described in which the liquid nitrogen shield consists of two separate parts, one dipping into the other. The upper shield is constructed with three walls rather than the usual two, since it must be open at the bottom. The liquid helium Dewar fits fairly closely inside this extra wall, with a thin air space between the two, and extends downward into the lower shield. The upper shield thus is mechanically isolated from the liquid helium Dewar. Access to a cold spot of the liquid helium flash is provided by a tube passing upward through the bottom of the lower shield and coupled to the liquid helium flask by means of a spherical ground glass joint. Various advantages of this system and possible modifications thereof are discussed. (Author)

C. T. Zahn, *Rev. Sci. Instrum.*, **31** : 3, 328–330.

17 : 16

Coefficients of Evaporation and Condensation. See Abstract No. 216.

18. Gaseous Electronics

18

230. Noise Propagation on Uniformly Accelerated Multivelocity Electron Beams.
W. M. Mueller and M. R. Currie, *J. Appl. Phys.*, 1876–1880, Dec. 1959.

18

231. Propagation Characteristics of Detonation-Generated Plasmas.
Melvin A. Cook, Robert T. Keyes and Lex L. Udy, *J. Appl. Phys.*, 1881–1892, Dec. 1959.

18

232. Charge Localization on the Surfaces of Oxide-Coated Cathodes.
United Kingdom. Anomalous results obtained while using the Kelvin method of determining contact potential differences between oxide-coated cathodes and an evaporated gold film reference surface in an atmosphere of hydrogen have been investigated. Very high contact potential differences have been associated with a separation of charge from ionized gas on the passage of a discharge current. This charge, either positive ions or electrons, remains on the surface of the oxide cathode for periods (sometimes as long as several days) dependent on the conductivity of the oxide coating. This in turn depends upon the nature of the oxide material, its state of activation and its temperature. Experiments are also described on the behaviour of probe cathodes in hydrogen.

B. J. Hopkins and F. A. Vick, *Brit. J. Appl. Phys.*, **11**, 223–227, June 1960.

18 : 33

233. Anode Surface Effects in Diodes Containing Oxide-Coated Cathodes.
United Kingdom. Two types of experimental tube have been built to study the behaviour of thin films deposited on the anode by evaporation during the breakdown and activation of calcium and barium oxide coated cathodes. First, with diodes of cylindrical symmetry, a contact-potential-difference method has been used to follow the changes in anode work function during activation of the cathode at several anode potentials. Emission-poisoning effects have been related to changes in the anode work function and it appears that there are two separate contaminating films on the anode surface : a very tightly held electropositive layer and a loosely bound electronegative layer. The emission decay process by the decomposition of compounds on the anode does not explain the results adequately. The second tube contained a movable glass electrode upon which a gold film could be deposited by evaporation. The results from these tubes confirmed those from the cylindrical diodes and also the validity of the contact-potential-difference method.

B. J. Hopkins, *Brit. J. Appl. Phys.*, **11**, 124–128, March 1960.

18

234. Cathode Work Function, Sparking Potentials and Secondary Ionization Coefficients for Oxide-coated Cathodes in Hydrogen.
United Kingdom. The Kelvin vibrating electrode technique has been applied to measure the contact potential difference between oxide-coated cathodes and a gold reference surface in the presence of hydrogen. Special high vacuum (Alpert) techniques were used to ensure high gas purity. By the use of both calcium oxide and barium oxide cathodes, in various states of activation, it was possible to obtain a range of work function from 1.4 to 3.6 eV. Paschen curves were plotted for each of these oxide cathodes at room temperature, and minimum sparking potentials and secondary ionization coefficients were determined. A linear relation was found between the cathode work function and the minimum sparking potential. The slope of this line indicated that a 1 eV change in work function corresponded to a change of 55 V in the minimum sparking potential. The slope of the line was confirmed by independent work function measurements using the graph of the Richardson thermionic equation. The curves (ω/α) v (E/p) showed a rapid increase in ω/α with decreasing values of E/p at $E/p < 100$ V/cm mmHg.

D. E. Davies and B. J. Hopkins, *Brit. J. Appl. Phys.*, **10**, 498–501, Nov. 1959.

18

235. Influence of the Cathode Work Function on the Sparking Potential in Hydrogen.
United Kingdom. The Kelvin or vibrating electrode method of measuring contact potential differences has been used to follow changes in work function of evaporated metallic films in a parallel plate electrode system in hydrogen at about 10 mmHg pressure. A reduction in cathode work function of the order of 0.3 eV was effected by passing a current of 10^{-7} A for 10 s. After about 30 min the cathode work function returned to its original value. Similar treatment caused a reduction in the sparking potential of 30 V, which also returned to its original pre-discharge value in times of the order of 30 min. This, together with other experimental data, is consistent with the fact that positive ions from the discharge current remained on the cathode surface for periods up to 30 min after the current was switched off. It has been possible to demonstrate that, while these positive ions are being neutralized, there is a relationship between the work function of a cathode and its sparking potential in hydrogen.

D. E. Davies and R. K. Fitch, *Brit. J. Appl. Phys.*, **10**, 502–505, Nov. 1959.

18

236. Glow Discharge Characteristics of Helium-Neon Mixtures.
United Kingdom. The maintaining and breakdown potentials for a number of helium-neon mixtures have been determined over a pressure × distance (pd) range of 1 to 75 cm mmHg. The normal cathode fall and the minimum breakdown potential were higher for mixtures containing from 1 to 5 per cent neon, than for either of the pure gases. At higher pd values the breakdown potential was lower for mixtures of the order of 50 per cent helium-50 per cent neon, than for the pure gases. These results suggest reactions between the two gases affecting the ionization coefficients. Charge exchange processes, detected by Oskam in the afterglow of such mixtures, are consistent with the emission spectra of the glow discharge, and are the probable cause of the variations.

G. F. Weston, *Brit. J. Appl. Phys.*, **10**, 523–526, Dec. 1959.

18 : 33 : 56

237. Deuterium-Filled Thyratrons.
Note by K. G. Cook and G. G. Isaacs, *Brit. J. Appl. Phys.*, **9**, 497–498, Dec. 1958.

18 : 33 : 56

238. Deuterium as a Filling for High-Voltage Thyratrons.
Note by R. J. Armstrong and N. S. Nicholls, *Brit. J. Appl. Phys.*, **9**, 498–499, Dec. 1958.

18

239. The Grid Emitting Properties of Titanium.
United Kingdom. Experiments are described in which the emission from thin films of barium and barium oxide deposited on titanium is compared with that from similar deposits on tungsten. With deposits of both barium and barium oxide the emission from titanium is very much less than that from tungsten throughout the temperature range investigated (700–1000°C). Above about 900°C the evaporation of titanium will poison the emission of an adjacent oxide cathode, but it is

Vol. 10 1960

concluded that from 700°C up to this temperature titanium would possess good grid emission suppression properties. This could enable titanium to be used as a screen grid winding wire in the place of carbonized molybdenum wire in a number of receiving valves, and as an electrode material in other electronic devices where hot electrodes become contaminated with cathode material.

J. A. Champion, *Brit. J. Appl. Phys.*, **9**, 491–495, Dec. 1958.

18

240. The Magnetic Stabilization of Low Pressure D.C. Arcs.
United Kingdom. Self-sustaining d.c. arc discharges between solid metal electrodes at pressures down to 10^{-4} Torr have been investigated. At pressures below a few millimeters of mercury, arcs on both refractory and non-refractory metals behaved like "cold cathode" arcs. "Spot-splitting" and "reverse driving" of the cathode spot were observed and a form of instability is described. Reverse driving of the cathode spot or spots by the magnetic field set up by the current in the electrodes themselves is suggested as the cause of the instability. A magnetic method of stabilizing the discharge is described, requiring an axial magnetic field of at least 500 G. A marked constriction of the positive column was caused with this value of field. The magnetically stabilised discharge has been used experimentally to produce short welds on $\frac{1}{8}$in. thick mild steel plate at 1μ of mercury pressure using about 40 A at 30 V.

H. Wroe, *Brit. J. Appl. Phys.*, **9**, 488–491, Dec. 1958.

18

241. The Cleaning of Glass in a Glow Discharge.
United Kingdom. An investigation into the glow discharge cleaning of glass in kinetic vacuum systems is described. The cleanliness of the treated glasses is assessed by their coefficient of friction μ, freedom from optical absorption and wetting characteristics. Glasses bombarded by high energy electrones from the cathode dark space in the presence of hydrocarbon vapours are coated with organic layers, whereas glasses bombarded in the positive column are cleaned. Deposits formed in hydrocarbon vapours have a value of $\mu = 0.3$ and cannot be wetted, whereas those formed in silicone vapour are wettable and have a value of $\mu = 0.6$. An electrode system is described for use in evaporation plant in which the high energy electrons traversing the cathode dark space are prevented from bombarding the glass. Random bombardment by positive ions and neutral molecules in air, A, N_2, H_2 and O_2 produces clean glass with $\mu = 0.7$–0.9. The contamination of the cleaned surfaces by hydrocarbon and silicone molecules is discussed. Freshly deposited silica films and glass surfaces prepared by fracture *in vacuo* become contaminated by strongly adsorbed silicone molecules, whereas clean aged surfaces of glass and silica are not contaminated because the cations are screened by OH-ions.

L. Holland, *Brit. J. Appl. Phys.*, **9**, 410–415, Oct. 1958.

18 : 33

242. Thermionic and Related Properties of Calcium Oxide.
United Kingdom. Using probe diodes, changes in thermionic emission and conductivity of cathodes of calcium oxide on nickel have been followed during activation and poisoning. The effects of material liberated from the anode have been studied. The mean nominal thermionic work function is 1.69 eV for the fully activated cathode from the slope of a Richardson line, with an estimated temperature coefficient of 1.1 mV/°K. Three regions of conductivity have been found; the activation energies for the two at the lowest temperatures are 1.3 eV and 0.81 eV. The current-voltage characteristics between the cathode base and probe show two types of curvature, one dominant above 625°K and the other below this temperature. A linear relation extending over four orders of magnitude between the logarithms of emission and of the conductivity has been observed during activation. Assuming that semi-conductor theory may be applied the mean value of the surface work function is calculated to be 0.7 eV.

B. J. Hopkins and F. A. Vick, *Brit. J. Appl. Phys.*, **9**, 257–263, July 1958.

18

243. Cathode Emission Measurements in Low Pressure Discharges.
United Kingdom. A method described in an earlier paper for measuring the zero field emission from hot cathodes in discharges is compared with that of the probe methods described by C. G. Found. Good agreement is obtained, thus supporting the interpretation of the measured characteristics. It is shown how this method may be applied to measure the emission from cathodes in ordinary long discharge tubes, such as fluorescent lamps, without the necessity for inserting probes or interfering with the construction of the tubes or electrodes in any way.

Miss A. D. Forster-Brown and M. A. Cayless, *Brit. J. Appl. Phys.*, **10**, 409–411, Sept. 1959.

18

244. Reversible Poisoning by Sulphur, Oxygen and Other Gases of Oxide-Coated Cathodes at High Temperatures.
United Kingdom. A simple mass spectrometer has been used to select and study the behaviour of the negative ions of sulphur and oxygen emitted by oxide-coated cathodes on recovery from the poisoning of their electron emission by these agents over the temperature range 1075–1300°K. Only the atomic ions were observed, and the behaviour of the $^{32}S^-$ ion emitted on recovery from sulphur poisoning was similar to that of the $^{16}O^-$ ion emitted on recovery from oxygen poisoning. The ion $^{13}CH^-$ also had a slight poisoning effect. Measurements of the energy distributions of these ions shows that, during recovery, many more of them were sputtered off the top surface of the cathode than were evaporated from its pores. These results support the hypothesis that high-temperature reversible poisoning is caused by the adsorption of negative ions on the internal and external surfaces of the porous oxide-coating.

N. A. Surplice, *Brit. J. Appl. Phys.*, **10**, 359–364, Aug. 1959.

18 : 40

245. Microwave Method of Investigating the Afterglow of Pulsed Gaseous Discharges.
United Kingdom. An apparatus suitable for recording the decrease of electron density in the afterglows of pulsed microwave discharges at 3 and 10 cm wavelengths is described. This employs the well-known method of measuring the frequency shift induced in a resonant cavity by the presence of free electrons, but a new method of detecting the resonant reflexions using a hybrid T-junction is employed. Modifications to the frequency-modulation method of probing the afterglow, which are particularly suitable for the analysis of slowly decaying plasmas, are described. An account is also given of a vacuum system suitable for handling high purity gases.

M. C. Sexton, J. J. Lennon and M. J. Mulcahy, *Brit. J. Appl. Phys.*, **10**, 356–359, Aug. 1959.

18

246. First Ionization Coefficients in Hydrogen, Neon, and Argon.
United Kingdom. Values of the first ionization coefficient η in hydrogen have been determined in the range $40 < E/p_0 < 500$ V cm^{-1} mm^{-1} of mercury at 0°C to $\pm$ 2 per cent (where E is field strength and p_0 the gas pressure at 0°C). Evaporated metal film electrode tubes have been developed so that rigorous outgassing procedures could be adopted, and an analysis has been used whereby the values of η can be correctly calculated from the current-voltage data. Preliminary results have also been obtained for neon and argon (commercial spectroscopically pure) using the same techniques.

D. E. Davies, *Brit. J. Appl. Phys.*, **10**, 301–305, July 1959.

18

247. Excitation and Ionization Rates of Mercury in Discharge Plasmas.
United Kingdom. Excitation and ionization rates of mercury by inelastic electron collisions in gas discharge plasmas with Maxwellian electron energy distribution have been calculated from the collision cross-section data for electron temperatures between 5000 and 54,000°K. Published cross-section data have been used where available, and estimates have been made in several cases of interest for which no data are known.

M. A. Cayless, *Brit. J. Appl. Phys.*, **10**, 186–190, April 1959.

18 : 33

248. Production of X-ray During a Low-Pressure Gas Discharge.
United Kingdom. The impulse breakdown of several gases at pressures of a few microns of mercury has been investigated. During the first stage of the discharge, a microsecond burst of X-rays is emitted from a spot of about 8 mm diameter on the anode electrode. If the initial voltage applied to the tube is 600 kV, a single X-ray pulse will produce a legible radiograph through about 5 cm of steel. The mechanism of the discharge has been studied and high speed photographs of the visible discharge show a luminous column moving from cathode to anode. Steenbeck's theory has been extended to show qualitatively the probable sequence of events during the discharge.

R. F. Thumwood, *Brit. J. Appl. Phys.*, **10**, 147–151, March 1959.

18 : 31

249. Thermionic Properties of Thorium Deposits on Control Grid Materials.
United Kingdom. Experiments are described in which the emission is measured from thin films of thorium deposited on different platinum-molybdenum phases of approximate composition Pt, Pt_3Mo, Pt_2Mo, Pt_3Mo_2 and Mo. The emission from all the platinum phases is considerably lower than that from pure molybdenum. The lowest emission was observed with the Pt_3Mo phase. The emission from thorium deposited on to the Pt_3Mo_2 phase decays rapidly at temperatures of 1300°C and above, whereas that from similar deposits on molybdenum does not. The emission from thin films of thorium deposited on to titanium and tungsten has also been studied. The emission from a layer on titanium that had been thoroughly pre-cleaned was found to be much less than that from a similar layer on tungsten. The application of these results to the suppression of grid emission in the presence of thoriated tungsten cathodes in transmitting valves is discussed.

J. A. Champion, *Brit. J. Appl. Phys.*, **10**, 71–74, Feb. 1959.

18

250. Evaporation of Thorium from Carburized Thoriated Tungsten Cathodes.
United Kingdom. The evaporation of thorium from carburized thoriated tungsten cathodes is shown experimentally to be approximately the same as that from similar uncarburized cathodes at the same temperature. The thorium in a carburized cathode is, however, produced continuously at an adequate rate at the operating temperature of 2000°K by reduction of the thoria by the tungsten carbide. The uncarburized cathode operates on a reserve of thorium built up by flashing at 2800°K at which temperature the tungsten reduces some of the thoria. These reactions have been examined by thermochemistry and it is shown that thorium diffuses to the surface of both types of cathode by a mechanism relatively insensitive to temperature.

R. O. Jenkins and W. G. Trodden, *Brit. J. Appl. Phys.*, **10**, 10–15, Jan. 1959.

18

251. Studies of Cold Cathode Discharges in Magnetic Fields.
United States. Some experimental studies of a cold cathode discharge in a strong magnetic field are described. Current densities of the order of half an ampere per square centimeter in various gases were used. For such a discharge, the current to the cathodes is about 75 per cent ionic. Positive ions leaving the discharge by moving across the magnetic field were observed with a mass spectrometer and showed a temperature of about 1 V. Fast electrons from the cathode escape from the discharge across the magnetic field without losing the greater part of their energy. By considering the rate of ion production it is shown that the slow electrons in the discharge have a temperature less than about three volts. Fluctuations in charge densities must play a very important role in the mechanism of the discharge.

John Backus, *J. Appl. Phys.*, 1866–1869, Dec. 1959.

18 : 16

Evaporation and Diffusion Rate Measurements on Cathodes of Sintered Nickel Containing Alkaline-Earth Oxides. See Abstract No. 222.

19. Radiation

19 : 33 : 37 : 38

252. Summarized Proceedings of a Conference on Electron Microscopy, Exeter, July 1959.
United Kingdom. The annual conference of the Electron Microscopy Group of the Institute of Physics was held in the Washington Singer Laboratory, University of Exeter, from 7 to 10 July 1959. The papers presented are summarized in this report.

Conference Report, *Brit. J. Appl. Phys.*, **11**, 22–32, Jan. 1960.

19 : 32 : 33

253. Absolute Intensity Measurements of the Carbon and Aluminium X-Ray K-Lines with a Proportional Counter.
United Kingdom. The efficiencies (quanta per electron per unit solid angle) of thick target carbon and aluminium X-ray K-line production, as a function of accelerating voltage, have been measured and plotted in the region below 10 kV. The construction and performance of the proportional counter with which the measurements were made is also described.

R. M. Dolby, *Brit. J. Appl. Phys.*, **11**, 64–68, Feb. 1960.

19

254. Some Developments and Applications of Microfocus X-Ray Diffraction Techniques.
United Kingdom. This paper describes a low angle X-ray scattering camera, a microbeam camera and an electron gun for a microfocus X-ray tube. In the low angle scattering camera which can resolve a spacing of 1000 Å using CuK radiation, the X-ray beam is totally reflected by two crossed bent glass plates, which focus the relatively intense beam on to a small spot on the film. Provision is made for accurately positioning a selected area of the specimen in the path of the beam. This facility is also provided in the microbeam camera for transmission and back reflexion work. In the electron gun, focusing is facilitated by independent adjustment of the positions of the filament and grid cylinder, while the tube is in operation.

A. Franks, *Brit. J. Appl. Phys.*, **9**, 349–352, Sept. 1958.

19

255. Summarized Proceedings of a Colloquium on X-Ray Fluorescence Analysis, London, February and April 1958.
United Kingdom. X-ray fluorescence as an analytical technique was the subject of a joint meeting of the Applied Spectroscopy and X-ray Analysis Groups of The Institute of Physics held in London on 21 February 1958 (and repeated on 1 April). A summarized account of the papers read by the principal speakers and the ensuing discussions at the two meetings is given below.

Conference Report, *Brit. J. Appl. Phys.*, **10**, 105–116, March 1959

Vol 10 196

19

256. Summarized Proceedings of a Conference on X-Ray Analysis, Manchester, April 1958.

United Kingdom. The annual Spring Conference of the X-ray Analysis Group of The Institute of Physics was held at the Manchester College of Science and Technology on 18 and 19 April 1958. The papers and discussions ranged over a wide field including structural studies, apparatus and techniques of analysis.

Conference Report, *Brit. J. Appl. Phys.*, **10**, 116–123, March 1959.

19

257. Apparent Loss of Efficiency in Multilayer Cathodoluminescent Films.

Charles Feldman, Letters to the Editor, *J. Opt. Soc. Amer.*, **50**, 628–629, June 1960.

19

258. Reflectance-Increasing Coatings for the Vacuum Ultraviolet and Their Applications.

P. H. Berning, G. Hass, and R. P. Madden, *J. Opt. Soc. Amer.*, **50**, 587–597, June 1960.

19

259. Selective Modulation of Radiation by Periodical Variation of Gas Temperature.

A. O. Sall, *Optics and Spectroscopy*, **VII**, 355–356, Oct. 1959.

19 : 51

260. Effect of Foreign Gases on The Absorption of Infrared Radiation by Water Vapors in the Region of an Individual Line in Band 2.7μ.

K. P. Vasilevsky and B. S. Neporent, *Optics and Spectroscopy*, **VII**, 353–354, Oct. 1959.

19 : 51

261. Candoluminescence and Surface Recombination Luminescence of Phosphors in the Atmosphere of Activated Gas.

A. N. Gorban and V. A. Sokolov, *Optics and Spectroscopy*, **VII**, 350–351, Oct. 1959.

19 : 51

262. Thin Film Optics. V. The Properties of Silicon.

M. P. Lisitsa and N. G. Tsvelykh, *Optics and Spectroscopy*, **VII**, 341, 344, Oct. 1959.

19 : 51

263. Optical Properties of Metal Films in the Region of Anomalous Skin-Effect.

Van-Si-Fe, V. P. Silin, and E. P. Fetisov, *Optics and Spectroscopy*, **VII**, 339–341, Oct. 1959.

19

264. Investigation of the Thermal Activation Energy of Photostimulated Flashes in Zns:Cu:Pb Phosphors.

V. L. Levshin and B. M. Orlov, *Optics and Spectroscopy*, **VII**, 330–334, Oct. 1959.

19

265. Initial Stages of The Rise of Luminescence in Phosphors with Levels of Several Kinds.

V. V. Antonov-Romanovskii, *Optics and Spectroscopy*, **VII**, 327–330, Oct. 1959.

19

266. Study of The Absorption Spectrum of Zinc Sulfide.

N. A. Vlasenko, *Optics and Spectroscopy*, **VII**, 320–324, Oct. 1959.

19

267. On The Temperature Dependence of The Intensities of Vibrational Absorption Bands of Gases in The Case of Fermi Resonance.

M. P. Lisitsa and V. L. Strizhevskii, *Optics and Spectroscopy*, **VII**, 305–307, Oct. 1959.

19

268. Study of The Temperature Dependence of the Intensity of Infrared Absorption Bands in Solutions.

V. N. Smirnov, *Optics and Spectroscopy*, **VII**, 302–305, Oct. 1959.

Vol. 10 1960

Vacuum Apparatus and Auxiliaries

20. Pumping Systems

20

269. Vacuum Pumping Set.
Description of commercial equipment.
Engineer, **209**, 5430, 309, Feb. 1960.

20

270. Vacuum Pump Selection.
Digest of " Selection of Pumping Systems for Vacuum Metallurgical Processes ".
A. S. D. Barrett and M. E. Harper, *J. Inst. Metals*, **87**, 1958–59, 227–234. *Metal Progress*, **77**, 192–196, June 1960.

20 : 27 : 32 : 33 : 10

Summarized Proceedings of a Symposium on Current Developments in the Prdouction of High Vacua. See Abstract No. 207.

21. Pumps and Pump Fluids

21

271. Centripetal Air-Pump Operated Electromagnetically.
Letter by B. Popper and M. Reiner, *Brit. J. Appl. Phys.*, **10**, 54–55, Jan. 1959.

21

272. Studies on the Construction of a Mechanical Booster Pump.
Japan. The authors manufactured the mechanical booster pump for trial. This is called as type PMB–010, and operating items are : Free Displacement : 10.2 L/revolution ; theoretical pumping speed : 18.26 m^3/min. The observed pumping speed was about 80–60 per cent of the theoretical pumping speed. In the case of pumping hydrogen, the pumping speed decreases by about 50 per cent of that for the air. H. N.

S. Kashu and C. Hayashi, *J. Vacuum Soc., Japan*, **3**, 184–188, 1960.

21

273. Performance of the Booster Pump of Multi Nozzle Type (1).
Japan. The characteristics for multi nozzle booster pump is investigated. Inlet diameter of the pump is 100 mmϕ, and the number of convergent-divergent type nozzles attached in two lines on the conical chimney can be changed. The operating oil is di-Butyle-phthalate, and oil temperature is changed from 185°C to 200°C. With 10 nozzles on the upper chimney and 20 on the lower chimney the maximum pumping speed is 240 l/sec at 5×10^{-4} mmHg. With 10 on the upper and 12 on the lower, the maximum pumping speed is 240 l/sec at 2×10^{-3} mmHg. With 8 and 20, the M.P.S. is 230 l/sec at 5×10^{-4}, with 8 and 13, the M.P.S. is 280 l/sec at 2×10^{-4} mmHg. The critical back pressure is 2–3 $\times 10^{-1}$ mmHg. H. N.

K. Ishikawa and T. Tanaka, *J. Vacuum Soc. Japan*, **3**, 151–154, 1960.

21

274. Selection of Pumping Fluid which can be Safely Used in Oil Rotary Pump and Oil Ejector.
Japan. In some cases, the vapor or the mist of the operating oil of ejector goes to the rotary pump. If both the pumping fluids of pumps are the same one, we can neglect this trouble. The authors recommend the spindle oil, and tri-chlor-diphenyl.

Note by H. Ishi and K. Akiyama, *J. Vacuum Soc. Japan*, **3**, 1888–189, 1960.

22. Gauges

22

275. Bistable Behaviour of the Bayard-Alpert Ionization Gauge.
United Kingdom. It has been observed that the Bayard-Alpert ionization gauge can possess either of two completely independent and stable modes of operation. The difference appears as variations in the pressure sensitivity of the gauge and complementary changes in the electrical adsorption characteristics of different gases. The bistable behaviour has been consistently observed on three different gauges and is attributed to the electrical charging of the inner surfaces of the gauges as a result of secondary-emission processes. Confirmation of this hypothesis has been made with a metal-screened gauge in which it was possible to control the discharge.

G. Carter and J. H. Leck, *Brit. J. Appl. Phys.*, **10**, 364–367, Aug. 1959.

22

276. The Sub-Standard Ionization Gauge, its Characteristics and Utility.
Japan. The Vacuum Society of Japan is endeavouring to determine the standards of vacuum measurement. Already the standard McLeod gauge was installed at Electro-technical Laboratory of Industrial Ministry. Intent is to distribute the sub-standard ionization valves calibrated by this McLeod gauge to the accuracy of $\pm$ 3 per cent. Collector is nickel cylinder, 27.5 mm diameter, 30 mm high, grid is made of 0.3 mm diameter tungsten, winded 10 mm diameter, 30 mm high, pitch 4 mm, filament is hair-pin type 0.2 mm diameter tungsten, length is about 70 mm. Electrodes are mounted on button stem and envelope is made of coval 45 mm diameter, 100 mm length, succeeded coval pipe of 15 mm of inner diameter and 110 mm of length. The operating condition is prescribed as follows : grid potential is $+125 \pm 0.5$ V d.c., collector potential is -25 ± 0.26 V d.c., emission current is 2 ± 0.085 mA. Thus the sensitivity has kept the accuracy of $\pm$ 3 per cent over the pressure range from 3×10^{-6} Torr to 1×10^{-4} Torr. H. N.

H. Ishi and K. Nakayama, *J. Vacuum Soc. Japan*, **3**, 77–81, 1960.

22

277. High Speed Ionization Gauge.
Japan. The pressure measured by " high speed ionization gauge ", in which the electrodes are mounted directly in a vacuum system, is apt to show much less reading compared to that by an ordinary ionization gauge. To find out the reason why this tendency arises, the authors measured the difference between readings of these two gauges in many cases, especially concerning the oil diffusion pump, and found that the difference is caused chiefly by the condensable vapour which can be eliminated by cold trap. Further, the mechanism from which these vapours seem to originate is assumed. The decomposition of pumping oil, and the adsorption of oil vapour to the glass envelope, are sure to cause these differences. H. N.

G. Horikoshi and A. Miyahara, *J. Vacuum Soc. Japan*, **3**, 13–18, 1960.

22

278. An Ultra-High Vacuum Mass Spectrometer.
Japan. To analyse a very small quantity of gas, and to investigate the adsorption phenomena in ultra-high vacuum, the authors constructed a metal mass spectrometer which is operated in ultra-high vacuum. The difficulties which are experienced in constructing all metal ultra-high vacuum equipments are more serious in this case. A large amount of outgas difficulties of

Vol. 10 196

vacuum tight joints and flanges, should be more sensitive to the performance of the mass spectrometer than usual ultra-high vacuum equipment. The noticeable features of this mass spectrometer are as follows : (1) The analyzing tube is made of stainless steel, and all analyzing parts including tube are set in electric oven, enabling them to be baked up to 350°C ; (2) The gaskets of the tube are oxygen free copper ; (3) The trap which contains oxygen free copper foil is equipped ; (4) Vac-Ion type ultra-high vacuum pump is equipped ; (5) Sample inlet system is also enabled to be evacuated to ultra-high vacuum. The analyzing tube is 60° type single focusing, and radius of ion orbit is 15 cm, and it can identify components with mass range between 1 and 200 a.m.u. The system can be evacuated up to 1–2 $\times$ 10^{-8} Torr, and best operating condition was in 1.4 $\times$ 10^{-8} Torr. The magnet is 1000 G electromagnet, and resolving power was 150. Minimum enquire sample quantity was 10^{-6} cc/N.T.P. By this mass spectrometer, the authors investigated the residual gas in an analyzing tube. Before baking up, the main component of residual gas is H_2O with small quantities of CO, N_2, Ar, CO_2, and hydrocarbons. After baking up and under 1 $\times$ 10^{-6} Torr vacuum CO or N_2 was identified as a main component. Under 1 $\times$ 10^{-7} mm Hg the gas of M/e = 28 are still main component, but the composition of CO was estimated as 40 per cent, and under 1 $\times$ 10^{-8} Torr the CO occupies 80 per cent. H. N.

K. Kawasaki, T. Sugita, A. Fujinaga, M. Goto, and J. Kai, *J. Vacuum Soc., Japan*, **3**, 96–103, 1960.

23. Plumbing

23

279. Leak-proof Joint for High Vacuum Work.
Note by V. N. Schrodt, *Chem. Eng.*, **67**, 128, 1960.

23

280. Method for Sealing Stainless Steel to Glass.
J. E. Benbenek and R. E. Honig, *Rev. Sci. Instrum.*, **31** : 4, 460.

23

281. Platinum to Pyrex Tubular Housekeeper Seals.
B. B. Graves, *Rev. Sci. Instrum.*, **31** : 3, 349.

23

282. Plastic-to-Metal Vacuum Seal for Rotating Targets.
H. Toffer and R. L. Amrein, *Rev. Sci. Instrum.*, **31** : 3, 348.

23

283. Metallic Valve Seals.
Short note in *Engineer*, **209**, 5442, 829, May 1960.

24. Valves

24

284. Magnetically Driven Fast-Acting Valve for Gas Injection into High Vacua.
In order to admit a variety of cold gases in short bursts to study plasma effects in high vacua, the leak valve operating period must be on the order of 100μ secs. or less. The authors describe completely the construction and geometry of such a valve. This valve is fitted with a spring disc assembly, a teflon seat and a copper ribbon field coil soldered to the valve body. The valve will seal at vacua of approximately 10^{-7} Torr with pressures of from 1–4 atmospheres on the gas inlet side.

B. Gorowitz, K. Moses, and P. Gloersen, *Rev. Sci. Instrum.*, **31** : 2, 146–148.

24

285. Mercury Float Valve.
Zlatko Knor, *Rev. Sci. Instrum.*, **31** : 3, 351.

25. Baffles, Traps and Refrigeration Equipment

286. Principles of Thermoelectric Devices.
United Kingdom. In recent years, the use of semiconductor thermojunctions has improved the efficiency of generation by means of the Seebeck effect and has made thermoelectric refrigeration a practical possibility. By using semiconducting compounds of high mean atomic weight, Seebeck coefficients of about 200μ V/°C have been obtained without the ratio of electrical to thermal conductivity departing too far from the value given by the Wiedemann-Franz law for metals. The most favourable semiconductors have been improved still further by alloying with isomorphous metals. Different devices employing the thermoelectric effect are discussed among which a thermo-electrically cooled vacuum baffle.

H. J. Goldsmid, *Brit. J. Appl. Phys.*, **11**, 209–217, June 1960.

27. Leak Detectors and Leak Detection

27

287. One Year Operating Experience with CEC Helium Leak Detector, Type 24–210.
Japan. The features of the CEC Type 24–210 Leak Detector were described from a user's point of view. Diary of operation and repair was attached. (Author)

H. Nakagawa, *J. Vacuum Soc. Japan*, **3**, 178–183, 1960.

27

288. Vacuum Testing of Tube Elements for Steam-Raising Units.
A high-vacuum process for the testing of tube elements for the steam-raising units at the Hunterston nuclear power station is described. The test is designed to ensure that the maximum leakage of water into the coolant circuits of each reactor shall be well within the capacity of the CO_2 drying plant—in this case 6 lb of water per hour. The charcoal-Pirani gauge method, which depends on preferential absorption, was chosen because it is reliable, simple and suitable for use in a works. (Author)

M. S. Hayward, *Engineer*, **209**, 5440, 732–735, April 1960.

27 : 32 : 33 : 10 : 20

Summarized Proceedings of a Symposium on Current Developments in the Production of High Vacua. See Abstract No. 207.

28. Heating Equipment

28 : 37

289. Resistance-Heated High Vacuum Furnace for Temperature to 1400°C.
An experimental high vacuum furnace with a platinum-rhodium resistance heating element is described ; it is operable also in oxygen or other gases up to pressures of at least 10^{-3} Torr. The furnace is assembled from readily obtainable equipment, and knife-edge vacuum seals are used throughout. The uniform hot-zone is approximately $1\frac{9}{32}$ in. in dia. and 2 in. long. The power required for 1400°C, the maximum safe operating temperature, is about 1 kw ; at this temperature the pressure is $\sim 10^{-8}$ Torr. This furnace is suitable for electrical conduction studies as well as for heat treatment, etc.

Julius Cohen, *Rev. Sci. Instrum.*, **31** : 3, 267–270.

28

290. Apparatus for the Measurement of Specific Heats of Metals.
Great Britain. This apparatus allows measurement of specific heats to be made *in vacuo* up to at least 500°C. The specimen in the form of a flat cylinder has its temperature steadily increased by a metered amount of electrical energy supplied by an internal heater. Radiative heat losses are eliminated by means of an adiabatic screen which surrounds the specimen and which is kept at the same temperature by auxiliary heaters. The rate of temperature rise can be controlled by the energy input, enabling the specific heat to be investigated over small temperature ranges. The specimen and guard assembly are enclosed in a steel vacuum jacket which carries an external heater. Thermocouple and

heater leads are brought out through rubber seals. Determinations can be made up to 900°C and accuracy of ±3 per cent has been obtained up to 500°C. (Author, modified)

W. H. Martin and J. Rixon, *J. Sci. Instrum.*, **36**, 179–182, April 1959.

28

291. Linear Voltage Temperature Furnace for Thermal Analysis. *Great Britain.* A furnace which may be operated in vacuum or an inert atmosphere and which was developed for thermal analysis studies of Be and its alloys. Extremely rapid heating or cooling rates may be employed if required, or with slow heating and cooling rates, a linear variation in voltage with time will produce a correspondingly near-linear variation in temperature. The furnace assembly is enclosed by a glass bell-jar 18 in. in diameter by 24 in. high and is evacuated by a 4 in. oil diffusion pump to give 1.10^{-4} mmHg at 1000°C. The maximum temperature quoted is 1300°C. The heating element is made of tantalum and slow rates of temperature change (2–5°C/min is mentioned) are obtained by using a motor-driven variable transformer. (Author, modified)

A. J. Martin and K. L. Edwards, *J. Sci. Instrum.*, **36**, 170–172, April 1959.

29. Miscellaneous

29

292. Thermoplastic Recording.
United States. A new method is described for recording electrical signals. Information is written at extremely high density by means of an electron beam on a film consisting of a low melting thermoplastic material. This can be projected as a full color image, or can be converted to an electrical signal. The tape, which is processed by quick heating, can be readily erased and re-used.

W. E. Glenn, *J. Appl. Phys.*, **00**, 1870–1873, Dec. 1959.

Vol.
10
196

Vacuum Applications

30. Evaporation and Sputtering

30

293. Vacuum Evaporator for Copper.
Japan. The vacuum evaporator which evaporates the large quantity of copper downwards is described. Differing from the ordinary evaporator which the substance evaporates to the upward direction, there are many difficult problems. The heater is composed of three molybdenum plates, one as a cover, and the others form a side plate of a triangle container and the tails of side plates form a narrow gap as an extended funnel. 3 g. of copper is heated by 620 A current and evaporates during 80 sec. The mean evaporating rate is 4.17 mg/sec.cm^2 and the thickness of the condensed copper is 20μ, then the mean condensing rate is 0.25μ/sec. In the case of 4 g. copper evaporated by 720 A, the figures change as 4.04 mg/sec.cm^2, 26.8μ, and 0.244μ/sec. respectively. H. N.

K. Asano, *J. Vacuum Soc., Japan*, **3**, 19–24, 1960.

30

294. Low Cost Coatings for Metal Products.
This article discusses various methods of coating metal products and includes properties and costs of the finished product. The material covered includes : selected organic coatings, hot dip coatings, immersion coatings, vacuum metallized coatings, chemical conversion coatings and rust preventives. A. G.

Robert J. Fabian, *Mat. Design Eng.*, **51**, 114–116, March 1960.

30

295. Studies on the Manufacturing Process of Selenium Photocell.
Japan. The most important factor affecting the photovoltaic characteristics of a selenium photocell is the condition of vacuum evaporation process. The best process described is : vacuum evaporate selenium over base to the thickness of 10^{-3} cm under pressure of 10^{-5} Torr, anneal in open air about an hour at the temperature 180–200°C, then vacuum spatter cadmium metal to cover selenium under the pressure of 10^{-2}–10^{-3} Torr of 1 : 1 argon and oxygen. The content ratio of argon and oxygen must be varied according to the temperature of selenium plate, and the fact that the characteristics of cadmium film chiefly affect the photovoltaic property photocell was ascertained. H. N.

Y. Sakai and A. Kunioka, *Vacuum Chem., Japan*, **8**, 1–7, 1960.

30

296. Annealing Silicon Monoxide Films on Aluminium Mirrors.
United Kingdom. It was observed that the silica coatings produced by thermal evaporation of silicon monoxide in a vacuum could be scratched and particles removed in form of fine dust. This is due to the highly stressed and brittle state of the evaporated film, and heat treatment was therefore used to remove stress and defects in the film structure. The evaporation system and the method of testing wear resistance is briefly described. The experiments showed that baking at 200°C or above is required for annealing while 180°C is not sufficient for the purpose. The rate of cooling did not have any effect, but burnishing of the annealed silicon monoxide films with a soft cloth improved their wear resistance. It is best to anneal the silicon monoxide film after its deposition and avoid undue temperature rise of the substrate during coating. If aluminium is deposited on to a hot substrate, mirrors with a brownish tinted reflection are obtained and also if the aluminium is heated after deposition but before evaporation of the silicon monoxide, films with a diffuse reflectance are produced. These effects are due to oxidation and grain growth in the deposit. Thick and stable monoxide films (approximately 1μ) were prepared by annealing.

Note by L. Holland, T. Putner and R. Ball, *Brit. J. Appl. Phys.*, **11**, 167–168, April 1960.

30

297. The Effect of Gettering on the Reflectivity of Aluminium Films.
United Kingdom. Aluminium films evaporated on glass from a single vapour source are more optically absorbing at high angles of vapour incidence if the films are slowly deposited or prepared in a poor vacuum. The rise in the optical absorption with vapour incidence angle is attributed to the degree of gas contamination of the growing film increasing as the deposition becomes more oblique. Such an effect could arise from a greater ratio of the number of gas molecules to vapour atoms combining at the receiver in regions of low vapour intensity. The reflectivities of aluminium films prepared at different gas pressures and rates of deposition show qualitative agreement with the hypothesis when plotted as a function of vapour incidence angle. The simple theory advanced is not applicable at gas pressures above 1μ mercury because the vapour atoms are scattered by gas molecules before striking the receiver.

L. Holland, *Brit. J. Appl. Phys.*, **9**, 336–337, Aug. 1958.

30 : 56

298. Preparation of Metal Film Resistors on Laminated Plastics.
United Kingdom. Some properties of metal resistance films on resin-bonded glass cloth have been investigated. Plastics laminates bonded with different polymers were coated with films of nickel-chromium alloy by vacuum evaporation and with sandwich films of gold between bismuth oxide layers deposited by sputtering. Glow discharge cleaning was essential before evaporation to make adherent films. Silicone resin bonded laminates were unsuitable for preparing stable resistors, because they had a large number of surface defects produced by strains arising during the curing process. Melamine bonded laminates were decomposed by ion bombardment during discharge cleaning or sputtering. The resistors were tested under a load of 1 W/in.^{2} of film area over a period of 3 months. Resistors which became non-conducting during the test were found to break down invariably along surface scratches in the base material. The most stable resistors on plastics bases were produced with epoxy or polyester resin bonded laminates, and with the metal films protected by a melamine lacquer. Nickel-chromium films up to 800Ω/square and gold films up to 50Ω/square reached a stable resistance value after an ageing period of about eight weeks.

G. Siddal and G. Smith, *Brit. J. Appl. Phys.*, **10**, 35–39, Jan. 1959.

30 : 32

299. Deposition by Thermal Evaporation of Thin Films of Titanium and Zirconium for Tritium Targets.
United Kingdom. Equipment and procedure are described for applying thin films of titanium and zirconium as tritium carriers to backings of copper, gold and platinum. A large proportion of the coatings prepared absorbed high atom ratios of tritium, titanium being more satisfactory in this respect than zirconium. It is suggested that defects in the coating arise mainly from the undesirable reaction of the metals with residual gases, particularly oxygen, during evaporation in the vacuum chamber. Firstly, this causes stress, brittleness, and owing to lack of adhesion, blistering of the deposit ; secondly absorption of tritium is inhibited by the oxide film on the metal surface, and

the total amount absorbed reduced as a result of there being fewer lattice sites available for the tritium. All electron diffraction examinations showed that although the deposits appeared bright and metallic, a thin protective oxide film was present on the evaporated titanium and zirconium.

V. D. Scott, L. W. Owen, *Brit. J. Appl. Phys.*, **10**, 91–93, Feb. 1959.

30 : 33

300. Technique for Preparing Thin Films of α-iron.
United Kingdom. A technique is described for preparing foils of α-iron which are suitable for direct-transmission examination in an electron microscope. While there is no guarantee that a particular point on the foil will be thin enough for examination, results show that the technique produces foils enabling localized effects to be observed.

D. G. Brandon and J. Nutting, *Brit. J. Appl. Phys.*, **10**, 255–256, June 1959.

30 : 56

301. Superconducting Computer Elements
United Kingdom. A survey is made of the present status of superconducting circuit components, including both active elements of the " cryotron " type and passive elements such as persistent current memory cells. The factors which affect the speed of operation of these devices are discussed, and the future shown to be closely linked with developments in the technology of thin metallic films.

E. H. Rhoderick, *Brit. J. Appl. Phys.*, **10**, 193–198, May 1959.

30 : 32

302. Simple Evaporator for Radioactive Metals.
Great Britain. This note describes a set-up in which the active material is evaporated from the bottom of an alumina crucible 2.5 cm high and 1.5 cm diameter, the bell-jar, etc., being shielded by a glass tube having two small holes to allow the wire of the filament to pass. The top of the shield is closed by a cover glass. Note by L. W. Barr and D. A. Blackburn, *J. Sci. Instrum.*, **36**, 197, April 1959.

31. Evacuation and Sealing

31

303. Progress in Electric Lamps.
H. G. Jenkins, *Engineer*, **209**, 5443, 857–861, May 1960.

31

304. Discharge Lamp Production Development.
Engineer, **209**, 5441, 774–775, May 1960.

31 : 40 : 41 : 42

305. Absorption of Sodium and Argon by Glass.
United Kingdom. Methods are described for measuring the absorption of both sodium and argon by glasses. The rate of absorption of sodium increases rapidly with temperature and is linear with time at a constant temperature. Ionization of the sodium does not change the rate of absorption. Micro-sections show that the absorbed sodium forms a layer of apparently uniform sodium concentration which advances through the glass with a sharp front. The concentration of sodium in this layer was found to be as high as 2×10^{22} atoms cm^{-3} in one case. Argon is only absorbed when ionized and the rate of absorption is more or less independent of temperature below 300°C. The argon does not diffuse through the glass and is partially evolved when heated to over 350°C.

J. W. Wheeldon, *Brit. J. Appl. Phys.*, **10**, 295–298, June 1959.

31 : 46

306. On the High Temperature Reaction of Silica Glass with Copper and Copper Oxide.
Japan. Silica-glass is more recommended material for electron tube or other insulating envelope. But in manufacturing silica-glass electron tube, it is in serious difficulty to joint metals with silica-glass. The authors investigated on the high temperature reaction of silica-glass and Cu and CuO_2, and observed the contact angle between molten Cu and silica-glass is varied by the Cu_2O content in the mixed liquid of Cu and SiO_2. To make the contact angle below 90°, it must contain Cu_2O, and this should be a key point to make Cu–SiO_2 seal. H. N.

H. Okamoto and Y. Murakami, *J. Vacuum Soc., Japan*, **3**, 228–232, 1960.

31

307. Analysis of the Residual Gases in Several Types of High-Vacuum Evaporators.
United States. A mass spectrometer study is made of the residual gases in several types of vacuum evaporators. The spectrometer (which employs a diatron 20 tube) and its operation are described in detail. In conventional evaporators the major constituent of the residual gas is water vapor. Furthermore, hydrogen, nitrogen and hydrocarbons were detected. The results of several operational methods and improvements of the evaporators are discussed, for instance—effects of a mild bake-out, cracking of heavier oil molecules on hot filaments, effects of internal liquid nitrogen traps (water vapor and CO_2 are preferably adsorbed, furthermore heavier hydrocarbons, CO, and hydrogen), effects of a titanium getter (reducing the oxygen pressure, but releasing large quantities of hydrogen, if not thoroughly outgassed), outgassing of a tantalum boat or a tungsten wire (hydrogen), gettering of a NiFe film (hydrogen), outgassing characteristics of different gasket materials. In an ultra-high vacuum system, where no oil or mercury pumps were used and which was thoroughly baked out, the residual atmosphere consisted only of nitrogen and hydrogen. All other gases were not detectable, i.e. their vapor pressures were lower than 10^{-10} Torr. For thin film deposition the importance of thorough outgassing of the source materials is pointed out. The paper contains many graphs and tables. K. H. B.

H. L. Caswell, *IBM J. Res. Develop.*, **4**, 130–142, 1960.

31

308. Sublimatography.
Japan. The new concept called " Sublimatography " is introduced. The vapourized material under vacuum will condense at the particular temperature, so called as V.C.P. (Vacuum Condensing Point), so if this vapour enters into the column which has a decided temperature gradient, it will condense at the particular point. This V.C.P. can be used as a physical property of substances similar as melting point or boiling point. Samples are sealed in an upper part of a long glass tube, and evacuated to the pressure of 10^{-5} Torr, and then heated by conventional means. The lower part of the tube is inserted into the special furnace, in which the temperature is kept higher at the top of the furnace and lower at the bottom, and this temperature gradient is strictly controlled. The vapour comes down from the top of the glass tube while it is cooled gradually, and then condenses at the appropriate zone according to the nature of the sample. If the sample is a mixture, the components are condensed separately, and we can recognize its components and composition. By this means, the author investigated the V.C.Ps. of many substances and recognized the impurities contained in many analytical reagents, the minute components in a natural substance (i.e. caffeine in tea), and oily material in a natural substance (i.e. nicotine in tobacco). This method is also extended to the new technique to investigate metals and alloys and the chemistry of molecular compounds. Sublimatographic diagnosis can be performed by the analysis of urine and blood by this method. H. N.

F. L. E. Shibata, *Vacuum Chemistry, Japan*, **8**, 8–15, 1960.

Vol. 10 196

31

309. Some Properties of a Graded Vacuum Spark Gap.
J. W. Mathers and A. H. Williams, *Rev. Sci. Instrum.*, **31** : 3, 297–303.

31 : 18

Thermionic Properties of Thorium Deposits on Control Grid Materials. See Abstract No. 249.

32. Nucleonics

32

310. Cern Proton Synchrotron.
Engineer, **209**, 5429, 277–278, Feb. 1960 ; **209**, 5430, 315–318, Feb. 1960.

32

311. Large Double-Focusing Mass Spectrometer.
Engineer, **209**, 5435, 547–548, March 1960.

32 : 33 : 10 : 20 : 27

Summarized Proceedings of a Symposium on Current Developments in the Production of High Vacua. See Abstract No. 207.

32 : 33 : 19

Absolute Intensity Measurements of the Carbon and Aluminium X-Ray K-Lines with a Proportional Counter. See Abstract No. 253.

32 : 30

Deposition by Thermal Evaporation of Thin Films of Titanium and Zirconium for Tritium Targets. See Abstract No. 299.

32 : 30

Simple Evaporator for Radioactive Metals. See Abstract No. 302.

33. General Physics and Electronics

33

312. Method for Size-Distribution Determination of Non-Volatile Droplets by Electron Microscopy.
United Kingdom. The droplets are sampled on a thin wet film of gelatin solution and washed away when the gelatin has set. Replicas are taken of the impressions left by the spread out droplets. The replica diameters are converted to droplet diameters by the application of a spread factor which although determined for larger droplets by light microscopy may be reliably applied to droplets in the electron microscope size range.

W. J. Harris, *Brit. J. Appl. Phys.*, **10**, 139–140, Mar. 1959.

33

313. Summarized Proceedings of a Conference on Electron Microscopy, Bangor, September 1957.
United Kingdom. The Annual Conference of the Electron Microscopy Group of The Institute of Physics was held in the Department of Botany, University College of North Wales, Bangor, from 10 to 12 September 1957. The papers presented, and discussion on them, are summarized in this report.

Report on the Conference on Electron Microscopy, Sept. 1957, *Brit. J. Appl. Phys.*, **9**, 306–311, Aug. 1958.

33

314. Reflexion Electron Microscopy Using Diffracted Electrons.
United Kingdom. Crystalline surfaces have been examined in the reflexion electron microscope with the angles of illumination and viewing adjusted so that diffracted electrons contributed to the images. In this way, the size and distribution of the diffracting regions have been determined. A resolution of 80 Å has been obtained, which is at least four times better than that obtained in normal reflexion micrographs.

J. S. Halliday, *Brit. J. Appl. Phys.*, **11**, 158–162, April 1960.

33

315. Accuracy of Selected-Area Microdiffraction in the Electron Microscope.
United Kingdom. Because of the spherical aberration at the objective lens, the area of an object defined by the selector aperture for microdiffraction experiments does not exactly correspond to the actual parts of the specimen contributing to the pattern. Further errors may arise through incorrect lens settings. The magnitude of the possible errors and the electron-optical explanation are discussed. The theoretical results are in reasonable agreement with the experimentally observed errors. It is concluded that especial care is required in studies of thin metal foils where mis-orientations between grains are being measured.

A. W. Agar, *Brit. J. Appl. Phys.*, **11**, 185–189, May 1960.

33

316. Selected Area Microdiffraction in the Electron Microscope. Note by A. W. Agar, *Brit. J. Appl. Phys.*, **9**, 419, Oct. 1958.

33

317. The Theory of Ballast Tubes or Barretters.
United Kingdom. The theory is based on a simple graphical method of solving the equation of thermal equilibrium of an electrically heated wire in a gas-filled enclosure. The results account for the main operating characteristics and have accurately predicted the ratings of various low voltage barretters. It is also shown why, in practice, barretters have always consisted of an iron wire in hydrogen.

R. O. Jenkins, *Brit. J. Appl. Phys.*, **9**, 391–394, Oct. 1958.

33 : 37

318. Heat-Reflecting Windows Using Gold and Bismuth Oxide Films.
United Kingdom. Thin gold films sandwiched between certain metal oxide layers possess a high electrical conductivity and high optical transparency. They also have a high infra-red reflectance and may be used as transparent heat-reflecting coatings if their yellowish tinted colour in transmitted light can be tolerated. The observation window of an enclosure exposed to infra-red radiation was coated with different film combinations, and their effectiveness in reducing the internal temperature rise determined. The reflectance and transmittance of the coatings were measured at $\lambda = 0.56\mu$ and in the infra-red region using a photometer with a broad bandwidth ($0.8–2\mu$). Results are given for the following : plain glass ; a high reflecting bismuth oxide film on glass ; gold film on glass ; and gold films sandwiched between bismuth oxide and silicon monoxide coatings. Optimum performance was obtained with a $Bi_2O_3/Au/Bi_2O_3$ multi-layer of 450/130/450 A thickness which had a transmittance of 73 per cent for green light and a reflectance of 74 per cent in the near infra-red region, compared with values of 55 and 35 per cent respectively for a gold film of the same thickness without the oxide layers.

L. Holland and G. Siddall, *Brit. J. Appl. Phys.*, **9**, 359–361, Sept. 1958.

33

319. The Ageing of Vacuum Standard Lamps on a.c. and d.c.
United Kingdom. A comparison is made of the rates of fall of luminous intensity and current, at constant voltage and colour temperatures 2390°K approximately, of 100 V 30 W vacuum photometric standard lamps, on a.c. and d.c. supplies. The rate for intensity is considerably higher on d.c. than on a.c., while the rate for current is lower. These specific effects of d.c. operation can be accounted for simply by changes in filament emissivity. There is no necessity to postulate a migration of tungsten along the surface of the filament, as in the authors' previous work on gas-filled lamps. The effects are shown to be almost fully reversible, after many hours of burning, by suitable application of reversed d.c., and a.c., supplies. As for gas-filled

lamps, the usefully smaller rate of depreciation characteristic of a.c. operation may be fully retained on d.c. by reversal of polarity at regular convenient intervals, so that the use of a.c. becomes legitimate for the normal preliminary ageing tests.

W. Barnett, R. G. Berry and J. S. Preston, *Brit. J. Appl. Phys.*, **9**, 317–318, Aug. 1958.

33 : 37

320. The X-Ray Scanning Microanalyser.

United Kingdom. The chemical microanalysis of a surface by the Castaing technique is carried out by exciting characteristic X-ray emission from a selected point, located optically under a stationary electron beam about 1μ in diameter. In many cases, the speed of working is greatly increased by the use of a scanning technique, which enables the surface distribution of a given element to be presented visually as an image on a cathode-ray tube screen. For quantitative analysis of a selected feature, accurate positioning of the beam may be carried out by reference to this image, or to a similar image showing topographical detail. The method has been applied to elements of atomic number 12 and above, in metallurgical, biological and mineralogical specimens. The paper deals with the principle, theory and design of an X-ray scanning microanalyser, and typical applications are illustrated by two examples.

P. Duncumb, *Brit. J. Appl. Phys.*, **10**, 420–427, Sept. 1959.

33 : 37

321. New Method for the Determination of Grain or Crystallite Size from Spotty Diffraction Rings.

United Kingdom. In contrast to previously proposed methods for determining grain size from X-ray diffraction rings which employed back-reflexion photographs, the new method uses transmission photographs. The specimen is also oscillated through a known angle. Possible confusion between Laüe and Debye-Scherrer spots is therefore avoided, and adjustment of experimental conditions to give a suitable number of spots enables a wide range of grain sizes to be covered. The angular divergence of the X-ray beam can be eliminated and the volume of specimen irradiated accurately estimated. The effects of grain-size distribution on visibility and blackening of spots are considered and a graphical method is proposed which takes account of grains at the surface and within a specimen.

K. W. Andrews, *Brit. J. Appl. Phys.*, **10**, 321–325, July 1959.

33 : 37

322. High-Resolution Shadow-Casting Technique for the Electron Microscope Using the Simultaneous Evaporation of Platinum and Carbon.

United Kingdom. Conventional shadowcasting techniques using heavy metals as shadowing materials suffer from a limited resolution imposed by the granulation of the metal. The paper describes a method for the simultaneous evaporation of platinum and carbon. This produces a deposit which does not granulate but at the same time has the high electron scattering power required for shadowing purposes. The properties of the deposit relating to its suitability as a shadowing material are fully discussed. The method is illustrated by means of various applications, one of which, the cleavage face of a sucrose crystal, exhibits monomolecular steps 11 Å high.

D. E. Bradley, *Brit. J. Appl. Phys.*, **10**, 198–203, May 1959.

33 : 37

323. Analysis of the Lighter Elements by Total Reflexion of Their Characteristic X-ray Wavelengths.

United Kingdom. The analysis of characteristic X-ray wavelengths in the region of 10 Å has been achieved by a technique employing total external reflexion.

A. Franks and R. F. Braybrook, *Brit. J. Appl. Phys.*, **10**, 190–191, April 1959.

33

324. New Method for Increasing the X-ray Reflection Power of Lithium Fluoride Crystals.

United Kingdom. Bending and quenching methods for increasing the dislocation density and hence the X-ray reflection power of lithium fluoride have been found ineffective when applied to certain crystals of British origin. An ultrasonic treatment is described which, with abrasion of the surface, gave a gain in reflection intensity of up to 3½ times at 2.0 Å and 7 times at 0.6 Å.

E. F. Pristley, *Brit. J. Appl. Phys.*, **10**, 141–142, March 1959.

33

325. Recent Techniques in Ultra High Vacuum.

United States. The vacuum requirements for attainment of stable field emission currents are considerably more demanding than those which are generally encountered in other electronic devices. A necessary adjunct to the development of useful field emission has therefore been the development of vacuum techniques capable of meeting these requirements. Through a suitable choice of envelope material and the use of thoroughly degassed refractory metal electrodes it has been possible to hold the rate of change of field emission current emitted for a fixed applied voltage to a few per cent per 100 hours of operation at useful current levels. This performance implies that the partial pressure of neither chemically active nor inert gas exceeded 10^{-12} mm Hg during the test. An ideal envelope material for use in ultra high vacuum work should be impervious to atmospheric gases and should withstand high power loadings without itself becoming a source of gas. The lead glasses and other dense soft glasses meet the former requirement well but release undesirable amounts of gas at moderate ambient temperatures. Hard glasses having high silica content, such as the borosilicate glasses, perform well at high temperatures but are excessively permeable to atmospheric helium. Glasses of the alumino-silicate group exhibit characteristics which make them an excellent compromise between these extremes, as their permeation rate of helium is less than 10^{-4} times that of 7740 Pyrex, and their rate of release of gases when heated is comparable to that of 96 per cent silica glass. Techniques are outlined which have been found useful in the adaptation of the two most readily available glasses of this type, Corning 1720 and 1710, to the fabrication of experimental high vacuum electronic devices.
(Author)

E. E. Martin and F. M. Collins, *Proc. 4th National Conf. on Tube Techniques*, 21, New York University Press, New York, 1959.

33 : 40

326. A Vacuum Microbalance and its Use in Studies of Electron Tube Materials.

United States. A very sensitive balance is a useful tool for a study of those processes occurring in electron tubes which involve minute changes of mass. A vacuum microbalance has been set up to study some of these processes. A few of the more important features of this balance and certain steps involved in its use will be described. The sublimation rates for nickel containing 0.1 per cent magnesium and nickel containing 0.1 per cent aluminium have been studied, temperature being a parameter. The results obtained for the Ni–Mg samples check quite well with those which one can predict on the basis of quoted values for diffusion constant and vapor pressure. Variations in cleaning and processing schedules did not affect the results. On the other hand, the results obtained for the Ni–Al samples were not those which one might have expected. There was no clear cut indication that any aluminum had been lost even at temperatures approaching 1000°C. Again it was found that variations in cleaning and processing schedules did not affect the experimental results. Other samples of nickel alloy, also

the change in mass of a sleeve coated with barium and strontium carbonates are to be studied. Any interesting results will be reported. (Author)

G. F. Rouse, *Proc. 4th National Conf. on Tube Techniques*, 262, New York University Press, New York, 1959.

33 : 10 : 20 : 27 : 31

Summarized Proceedings of a Symposium on Current Developments in the Production of High Vacua. See Abstract No. 207.

33 : 47 : 16

Properties of Getters in Electronic Tubes. See Abstract No. 219.

33 : 18

Anode Surface Effects in Diodes Containing Oxide-Coated Cathodes. See Abstract No. 233.

33 : 56 : 18

Deuterium-Filled Thyratrons. See Abstract No. 237.

33 : 56 : 18

Deuterium as a Filling for High-Voltage Thyratrons. See Abstract No. 238.

33 : 18

Thermionic and Related Properties of Calcium Oxide. See Abstract No. 242.

33 : 18

Production of X-Ray during a Low Pressure Gas Discharge. See Abstract No. 248.

33 : 37 : 38 : 19

Summarized Proceedings of a Conference on Electron Microscopy. See Abstract No. 252.

33 : 19 : 32

Absolute Intensity Measurements of the Carbon and Aluminium X-Ray K-Lines with a Proportional Counter. See Abstract No. 253.

33 : 30

Technique for Preparing Thin Films of α-iron. See Abstract No. 300.

37. Metallurgy, Inorganic Chemistry, Analytical Chemistry

37

327. Brazing in Vacuum by Induction Heating.
Prolonged heating of unstabilized austenitic alloys during brazing may precipitate carbides at grain boundaries. Induction heating restricts the heat application to the joint to be brazed and shortens the brazing time. The use of this method for joining stainless steel caps and shells to make hermetically sealed canisters is described briefly. A. G.

Note by Richard E. Paret, *Metal Progress*, **76**, 127, Dec. 1959.

37

328. Vacuum Treatment of Molten Steel in Germany.
Developed by Dortmund-Hörder Hütten-Union, this process is applicable to vacuum furnaces, openhearth and oxygen converter production. It operates on the basic principle of forcing successive portions of liquid steel into a vacuum vessel by atmospheric pressure. A variety of controlled alloy additions can be made late in the degassing cycle. This feature, combined with a major reduction of oxygen content, leads to improved cleanliness and increased product yield. (Author)

P. J. Wooding and W. Sieckman, *Metal Progress*, **77**, 116–122, Jan. 1960.

37

329. Steel Vacuum Degassed in the Ladle.
Note by Anon., *Mat. Design Eng.*, **51**, 12, Feb. 1960.

37

330. Missiles Boost Vacuum Melting.
This note briefly discusses the impact of the missile programs on the vacuum melting field. The trend is to bigger furnaces and bigger ingots. Specific examples are given of large furnaces in operation or being planned together with some details of their capacities. A. G.

Note by G. J. McManus, *Iron Age*, **185**, 87, March 1960.

37

331. World's Largest Vacuum Induction Furnace.
The furnace has a three-chamber design to permit semi-continuous casting. Every size of ingot between 200 and 5000 pounds can be poured and both molds and tundishes can be rotated when pouring. Several engineering innovations designed to make the installation versatile are described. A. G.

J. W. Byrne, *Metal Progress*, **77**, 83–86, April 1960.

37

332. Levitation—New Tool for Metallurgy.
Note by Anon., *Metal Progress*, **77**, 127–128, April 1960.

37

333. Vacuum Furnace Brazes Parts at Temperatures to 4500°F.
A new resistance-type furnace designed for sintering, brazing, heat treating, and annealing is described. It operates at temperatures up to 4500°F with pressures in the 0.1 micron range. It has been used to determine interstitial elements (O_2, N_2, H_2) in refractory metals and their alloys, to vacuum anneal fusion-welded joints of refractory metals and their alloys and to sinter various exotic metals and their alloys. A. G.

Mel Schwartz, *Iron Age*, **185**, 68–70, June 1960.

37

334. New Furnace Permits Recovery of Reactive Metal Scrap.
A new vacuum melting furnace, primarily intended for titanium scrap recovery, is described. It combines the features of skull melting by permanent electrode with vacuum melting by consumable electrode. A. G.

Iron Age, **185**, 108–109, June 1960.

335. Vacuum Furnace for Creep-Rupture Testing.
A creep and stress-rupture testing chamber is described which can operate up to 2700°F under a high vacuum. Principal design features are low power requirement, ease of test assembly, and adaptability to conventional creep and stress-rupture testing machines. (Author)

T. F. Hengstenberg and E. F. Vandergrift, *Metal Progress*, **77**, 94–97, June 1960.

336. Air Hardening Grade and Vacuum Degassed Offer New Possibilities.
Note by Charles T. Evans, Jr., *Metal Progress*, **77**, 105–106, May 1960.

37

337. Welding Processes.
Various welding processes are discussed including : ultrasonic, high-frequency resistance, foil seam, magnetic-force, percussion, friction, thermo-pressure, diffusion-bond, electroslag and electron beam. A. G.

John J. Chyle, *Mech. Eng.*, **82**, May 1960.

37

338. Vacuum Furnace.
Engineer, **209**, 5445, 944, June 1960.

37

339. 4 MeV Linear Accelerator for Radiographic Examination of Welds.
Engineer, **209**, 5438, 657, April 1960.

37

340. Preparation of High Purity Single Crystal Silicon.
The effect on crystal conductivity of the presence of impurity atoms is considered and a relationship derived between the electrical conductivity and the concentration of impurities. Crystal pulling from a melt in a crucible of pure transparent fused quartz imposes a limit on crystal purity by the small traces of undesirable impurity elements in even the purest fused quartz. Zone melting by means of a h.f. field is one of the methods used to overcome this contamination. The author describes a high vacuum floating zone refiner and stresses its importance both in ensuring the supply of consistently good crystals for device material and in the solution of certain research problems. (Author)
J. L. Parmee, *Engineer*, **209**, 5446, 979–982, June 1960.

37 : 17

Viscosity and Thermal Conductivity of Liquid Boron Trifluoride. See Abstract No. 226.

37 : 38 : 19 : 33

Summarized Proceedings of a Conference on Electron Microscopy. See Abstract No. 252.

37 : 28

Resistance-Heated High Vacuum Furnace for Temperature to 1400°C. See Abstract No. 289.

37 : 33

Heat-Reflecting Windows Using Gold and Bismuth Oxide Films. See Abstract No. 318.

37 : 33

The X-Ray Scanning Microanalyser. See Abstract No. 320.

37 : 33

New Method for the Determination of Grain or Crystallite Size from Spotty Diffraction Rings. See Abstract No. 321.

37 : 33

High-Resolution Shadow-Casting Technique for the Electron Microscope Using the simultaneous Evaporation of Platinum and Carbon. See Abstract No. 322.

37 : 33

Analysis of the Lighter Elements by Total Reflexion of their Characteristic X-Ray Wavelengths. See Abstract No. 323.

38. Distillation, Organic Chemistry, Isotopic Gas Analysis

38 : 19 : 33 : 37

Summarized Proceedings of a Conference on Electron Microscopy. See Abstract. No. 252.

39. Miscellaneous Applications

39

341. The Vernier Effect in the Interferometric Measurement of the Thickness of Thick Layers.
I. N. Shklyarevskii, E. T. Verkhovtseva, and G. N. Polyakova, *Optics and Spectroscopy*, **VII**, 4, 349–350, Oct. 1959.

39 : 42 : 13

Methods of Cleaning Glass by Vapour Degreasing and Ultrasonically Agitated Solvents. See Abstract No. 209.

39 : 16

The Quantum Mechanical Correction for the High Temperature Van der Waals Interaction of Light Gases and Surfaces. A New Method of Determining Surface Area. See Abstract No. 224.

Vol. 10 1960

Materials and Techniques used in Vacuum Technology

40. Gases and Vapours

40

342. Calorimetric Heat of Adsorption—Nitrogen on Tungsten.
P. Kislink, *J. Chem. Phys.*, **31**, 1605–1611, Dec. 1959.

40

343. Total Collision Cross Sections for the Interaction of Atomic Beams of Alkali Metals with Gases.
Erhard W. Rothe and Richard B. Bernstein, *J. Chem. Phys.*, **31**, 1619–1627, Dec. 1959.

40

344. Studies of the Evaporation of Condensates Containing Nitrogen Atoms.
The products of an electrodeless discharge in nitrogen or mixtures of nitrogen in neon or argon were condensed at 4.2°K. The products evolved from this condensate when it was allowed to warm up slowly were continuously analyzed by means of a mass spectrometer having a lower detection limit of 2×10^{-8} mm of nitrogen atoms. Experimental evidence is presented for the presence of nitrogen atoms in the warm-up products. It was estimated that less than 10^{-3} per cent of the nitrogen atoms originally condensed could be recovered. (Author)

John T. Herron and Vernon H. Dibeler, *J. Chem. Phys.*, **31**, 1662–1665, Dec. 1959.

40

345. On Chemical Reactions in Free Molecule Flow.
This paper deals with heterogeneous chemical reactions within systems in which the relevant geometric dimensions are small compared with the mean free path of gas molecules. A typical example can be found in a surface reaction occurring at moderate pressures inside the pore of a catalyst with a radius of several angstroms. Specific problems of this type have in the past been formulated, subject to the well-known limitations of ordinary diffusion theory, in terms of differential equations for the species concentrations. This in turn supposes that the reaction pattern is dependent on local conditions. A more general and exact formulation given in the following shows that the concentration of a molecular species at a point is determined by the concentration distributions of all species stemming from the entire system. Thus one is led to a formulation in terms of integral equations. In an application of the theory the validity of the conventional differential equation approach is investigated and is found to yield satisfactory results only under certain limiting conditions. (Author)

Paul L. Chambre, *J. Chem. Phys.*, **32**, 24–27, Jan. 1960.

40

346. Negative Ion Formation in NO_2 by Electron Attachment.
R. E. Fox, *J. Chem. Phys.*, **32**, 285–287, Jan. 1960.

40

347. Pressure Induced Shifts of HCl Lines Due to Foreign Gases.
Note by D. H. Rank, W. B. Birtlay, D. P. Eastman, and T. A. Wiggins, *J. Chem. Phys.*, **32**, 296–297, Jan. 1960.

40

348. Pressure Induced Shifts of HCl Lines Due to Foreign Gases.
Note by M. A. Hirshfeld, J. H. Jaffe, and S. Kimel, *J. Chem. Phys.*, **32**, 297–298, Jan. 1960.

40

349. Pressure Shifting of Spectrum Lines : Some Empirical Generalizations.
Note by D. H. Rank, W. B. Birtley, D. P. Eastman, and T. A. Wiggins, *J. Chem. Phys.*, **32**, 298–299, Jan. 1960.

40

350. Threshold Ionization of HCl by Electron Impact.
R. E. Fox, *J. Chem. Phys.*, **32**, 385–386, Feb. 1960.

40

351. Thermal Conductivity of Binary Mixtures of Diatomic and Monatomic Gases.
B. N. Srivastava and A. K. Barua, *J. Chem. Phys.*, **32**, 427–435, Feb. 1960.

40

352. Molecular Diffusion Studies in Gases at High Temperature. IV. Results and Interpretations of the CO_2–O_2, CH–O_2, H_2–O_2, CO–O_2 and H_2O–O_2 Systems.
R. E. Walker and A. A. Westenberg, *J. Chem. Phys.*, **32**, 436–442, Feb. 1960.

40

353. Infrared Emission Spectra of Gaseous B_2O_3 and B_2O_2.
David White, David E. Mann, Patrick N. Walsh, and Armin Sommer, *J. Chem. Phys.*, **32**, 481–487, Feb. 1960.

40

354. Infrared Emission Spectrum of Gaseous HBO_2.
David White, David E. Mann, Patrick N. Walsh, and Armin Sommer, *J. Chem. Phys.*, **32**, 488–492, Feb. 1960.

40

355. Excitation of the Auroral Green Line in Nitrogen Afterglows.
R. A. Young and K. C. Clark, *J. Chem. Phys.*, **32**, 607–611, Feb. 1960.

356. Vibrational Distribution in Late Nitrogen Afterglows.
R. A. Young and K. C. Clark, *J. Chem. Phys.*, **32**, 604–604, Feb. 1960.

40

357. Formation of Excited NO and N_2 by Wall Catalysis.
Note by Robert R. Reeves, Gene Mannella and Paul Harteck, *J. Chem. Phys.*, **32**, 946–947, March 1960.

40

358. Use of Constant-Boiling Systems in Calibration of Mass Spectrometers and other Molecular Beam Instruments.
Note by Alan W. Searcy, Wendell S. Williams, and Paul O. Schissel, *J. Chem. Phys.*, **32**, 957–958, March 1960.

40

359. Thermal Conductivity of Condensed Films : Methane.
A new method of determining the thermal conductivity of condensed films at low temperature has been developed. It is based on determining the surface temperature of a film of known area and thickness by measuring its equilibrium vapor pressure. The thermal conductivity (K) of the film is calculated by measuring the increase in surface temperature as the film thickness is increased when a known heat flux is flowing across the film. For methane at 85°K, $K = 3.5 \times 10^{-3}$ $w/cm°K$. (Author)

John T. Clarke and Ralph Gorden, Jr., *J. Chem. Phys.*, **32**, 705–707, March 1960.

40

360. Interaction of Hydrogen with Tungsten.
Measurements have been made under ultra-high vacuum conditions of the rates and isotherms for the adsorption of hydrogen on tungsten, the rate of desorption of hydrogen from tungsten,

and the rate of formation of atomic hydrogen by an incandescent tungsten filament. For pressures below 10^{-7} mm and filament temperatures above 1475°K, the fraction of molecules striking the filament surface that is dissociated is constant and at least 0.05. Values of surface coverage and the rate of formation of atomic hydrogen as a function of filament temperature and hydrogen pressure are derived from experimental data. A. G.

T. W. Hickmott, *J. Chem. Phys.*, **32**, 810–823, March 1960.

40

361. Surface Migration of Nitrogen on Tungsten.
Gert Ehrlich and F. G. Hudda, *J. Chem. Phys.*, **32**, 942–943, March 1960.

40

362. On the Mechanism of the Lewis-Rayleigh Nitrogen Afterglow.
K. D. Bayes and G. B. Kistiakowsky, *J. Chem. Phys.*, **32**, 992–1000, April 1960.

40

363. Emission Spectra of N_2, O_2, and NO Molecules Trapped in Solid Matrices.
H. P. Broida and M. Peyron, *J. Chem. Phys.*, **32**, 1068–1071, April 1960.

364. Collision of a Gas Atom with a Cold Surface.
The collisional transfer of kinetic energy from a gas atom to a cold solid is investigated in a simple model. In two limiting cases the combined equations of motion of the atoms and the lattice are solved exactly. The efficiency of energy transfer obtained from these calculations is much higher than that which is predicted from Lennard-Jones' single phonon approximation. (Author)

Robert W. Zwanzig, *J. Chem. Phys.*, **32**, 1173–1177, April 1960.

40

365. Electron Capture by Neutral Molecules.
R. E. Stantan, *J. Chem. Phys.*, **32**, 1348–1350, May 1960.

40

366. Thermal Conductivity of Helium and Hydrogen at High Temperatures.
A steady-state hot wire method for measuring the thermal conductivity of light gases in the temperature range 1200° to 2100°K is described. In contrast to other methods, free convection currents and large temperature gradients exist ; convection effects are shown to be negligible, and the experimental procedure for eliminating the large gradient effects is described. The thermal conductivity of helium is found to follow the equation $\lambda \times 10^6 = 991 + 0.678\ (T - 1200)$ ca/sec. cm deg. over the temperature range covered. That for hydrogen is $\lambda \times 10^6 = 1434 + 1.257\ (T - 1200)$ cal/sec. cm deg. (Author)

Normand C. Blais and Joseph B. Mann, *J. Chem. Phys.*, **32**, 1459–1465, May 1960.

40

367. Interactions between Molecules Adsorbed on a Surface.
Oktay Sinanoglu and Kenneth S. Pitzer, *J. Chem. Phys.*, **32**, 1279–1288, May 1960.

40

368. Measurements of Multicomponent Diffusion Coefficients for the CO_2–He–N_2 System using the Point Source Technique.
R. E. Walker, N. DeHaas, and A. A. Westenberg, *J. Chem. Phys.*, **32**, 1314–1316, May 1960.

40

369. Chemisorption of CO on Ni using a Radioactive Tracer.
A method is described for measuring the amount of chemisorbed CO on Ni. After cleaning the Ni specimen is put in a vacuum system and the pressure reduced to about 5×10^{-9} Torr. Outgassing is carried out by induction heating. The total absorption was found to vary from 2 to 3×10^{-14} absorbed molecules/cm² of geometric area. A. G.

A. D. Crowell, *J. Chem. Phys.*, **32**, 1576–1577, May 1960.

40

370. Ionization Potential of Fluorine.
Note by John T. Herron and Vernon H. Dibeler, *J. Chem. Phys.*, **32**, 1884–1885, June 1960.

40

371. Transport in Dilute Gases and Chemical Forces.
Richard K. Osborn, *J. Chem. Phys.*, **32**, 1817–1820, June 1960.

40 : 18

Microwave Method of Investigating the Afterglow of Pulsed Gaseous Discharges. See Abstract No. 245.

40 : 41 : 42 : 31

Absorption of Sodium and Argon by Glass. See Abstract No. 305.

40 : 33

A Vacuum Microbalance and its use in Studies of Electron Tube Materials. See Abstract No. 326.

41. Metals and Alloys

41

372. The Heat Capacity and Thermodynamic Functions of Uranium from 5 to 350°K.
H. E. Flotow and H. R. Lohr, *J. Phys. Chem.*, **64**, 904–906, July 1960.

41

373. The Volatility of Actinium.
Note by K. W. Foster and L. G. Fauble, *J. Phys. Chem.*, **64**, 958–960, July 1960.

41 : 47

374. Vapor Pressure of Thorium.
United States. The vapor pressure of solid thorium was determined over the temperature interval 1757 to 1956°K by the vacuum evaporation method of Langmuir. Special purification of the thorium was necessary since traces of ThO_2 react with thorium to give ThO(g). Thorium also reacts with residual gaseous oxygen in the vacuum system to form ThO(g). The latter effect was found to be negligible at residual oxygen pressures of less than 2×10^{-8} mm. The vapor pressure equation for Th(s) ⟶ Th(g) is $\log P_{atm} = -28{,}780 \pm 620/T°K + 5.991 \pm 0.333$. These results yield values of $\Delta H^0_{29.8(subl)}$ of 137.3 ± 2.8 kcal/mole and 136.6 ± 0.5 kcal/mole from a slope and third law determination, respectively. From an estimate of the pressure of ThO(g) over Th(s) containing ThO_2(s), D_0^0 (ThO) = 196 kcal/mole. (Author)

A. J. Darnell, W. A. McCollum and T. A. Milne, *J. Phys. Chem.*, **64**, 341–346, March 1960.

41

375. Thermionic Properties of Uranium.
Thermionic measurements were made on uranium metal in the form of drawn wire and on films of uranium deposited on tungsten by evaporation in ultra-high vacuum. Measurements of the emission current as a function of accelerating potential and of the work function of the bulk material indicated that the surface was never completely freed of oxide. Measurements of the work function and emission constant A as a function of the thickness of the evaporated films showed both ϕ and A to increase with increasing depth of deposit up to 15 atom layers and to reach constant values of 3.47 ± 0.03 eV and 114 ± 12 amp cm^{-2} deg^{-2}, respectively, for deposits 15–200 atom layers

Vol. 10 1960

deep. Qualitative measurements of the ionization potential of uranium by means of surface ionization showed the positive ion current to increase with increasing temperature indicating the ionization potential to be greater than 4.53 eV. The magnitude of the positive ion currents suggested an ionization potential of 4.5–5.0 V. (Author)

E. G. Rauh and R. J. Thorn, *J. Chem. Phys.*, **31**, 1481–1485, Dec. 1959.

41

376. Materials Below −100°F.
The properties of various metals and alloys at low temperatures are discussed. Included are copper, aluminum, austenitic stainless steels, iron and steel, low-alloy steel, nickel-steel alloys, cast iron and various solders. A. G.

O. A. Hansen, *Mech. Eng.*, **82**, 60–62, April 1960.

41 : 47

377. The Measurement of the Heats of Sublimation of Zinc and Cadmium with the Mass Spectrometer.
K. H. Mann and A. W. Tickner, *J. Phys. Chem.*, **64**, 251–253, Feb. 1960.

41

378. Extended Theory of Sputtering.
Don E. Harrison, Jr., *J. Chem. Phys.*, **32**, 1336–1341, May 1960.

41

379. Sputtering of Silver by Light Ions with Energies from 2 to 12 keV.
Finn Gronlund and Walter J. Moore, *J. Chem. Phys.*, **32**, 1540–1545, May 1960.

41 : 42 : 31 : 40

Absorption of Sodium and Argon by Glass. See Abstract No. 305.

42. Glass and Ceramics

42 : 13 : 39

Methods of Cleaning Glass by Vapour Degreasing and Ultrasonically Agitated Solvents. See Abstract No. 209.

42 : 31 : 40 : 41

Absorption of Sodium and Argon by Glass. See Abstract No. 305.

43. Plastics and Elastomers

43

380. Rubber Developments—1957–1959.
This is a review of the literature and covers many new rubbers and adhesives. A comprehensive list of references is included. A. G.

Leora E. Straka, *Mech. Eng.*, **82**, 71–77, April 1960.

44. Waxes, Lubricants, Cements, Lacquers, Paints and Oils

44

381. Lacquering Techniques for Vacuum Metallizing on Metals and Thermosetting Plastics.
The advantages of vacuum metallizing as opposed to chrome plating. Some of the advances made in the industry and some problems involved in the process are discussed. R. H.

M. A. Self, *Metal Finishing*, **58**, 40–43, May 1960.

45. Soldering, Welding, Brazing

45

382. New Alloy Points Up Advantages of Electron Beam Melting.
The electron beam melting technique has been used to produce a new alloy containing 90 per cent tantalum and 10 per cent tungsten which has a wide useful temperature range—from −200° to +5200°F. The triple-melt cycle used and the furnace set-up are described. A. G.

D. F. Mastick, *Iron Age*, **185**, 98–99, April 1960.

45

383. Which Copper-Base Alloy for a Brazed Part?
E. Belkin, *Materials Design Eng.*, **51**, 114–116, March 1960.

45

384. Electron-Beam Welding—Machining.
Note by D. Freiday, Assistant Editor, *Mech. Eng.*, **82**, 78, March 1960.

46. Glass Blowing, Glass-to-metal and Ceramic-to-metal Sealing Techniques

46

385. A Method of Improving the Glass-to-Metal Seal Resistance to High Humidity Deterioration in Electron Tubes.
United States. A serious problem exists wherein power tubes employing powdered glass seals become gassy when exposed to high humidity conditions. Spectrographic analysis of these tubes indicates that initially there is hydrogen and possibly water vapor present and, as the process continues, the tube eventually becomes filled with air. This leakage may be due to the fact there is poor adherence between the oxide and the metal in a conventional tungsten seal. There is also the possibility that all tubes may be limited in life, though not so noticeably, when stored under tropical conditions. Following humidity tests on several types of power tubes with tungsten and kovar leads, which indicated a failure rate of 80 per cent, 18 diodes of Geissler-type design were constructed with conventional seals. Nine of these diodes were made with beaded tungsten seals and nine with powdered glass tungsten seals. One of the beaded tungsten seal diodes (11 per cent) and seven of the powdered glass seal diodes (78 per cent) became gassy following high temperature, high humidity tests. Spectrographic analysis of the gas in these diodes indicated that there was either water vapor or hydrogen present. Twenty-two diodes were next constructed using chromium-plated tungsten leads to investigate an improved sealing technique. Nine of these were the leaded tungsten seal type and thirteen of the powdered glass tungsten seal type. No failures occurred for the beaded seals, and a five-to-one improvement resulted for the powdered glass seal type. (Author)
G. C. Fincke, Jr. and G. W. Taylor, *Proc. 4th National Conf. on Tube Techniques*, 34, New York University Press, New York, 1959.

46

386. Electroformed Ceramic-to-Metal Seal for Vacuum Tubes.
United States. This process of electroforming ceramic-to-metal seals was conceived for the purpose of fabricating a multiple-seal structure. It avoids the high probability of failure encountered in brazing a large number of seals simultaneously. One advantage of the electroformed seal is the simplicity of the required jigging. Other advantages are the lack of mechanical stress due to processing at room temperature and the minimized use of materials and brazing alloys with undesirable mechanical and thermal characteristics. This advantage particularly applies to sealing of structures which contain glass windows that will not withstand mechanical and thermal shock or high temperatures. The method has the same advantages offered by the conventional ceramic-to-metal structures, such as high mechanical strength, thermal-shock resistance and the ability to withstand high temperatures. This paper outlines the procedures used in making the structure mentioned above. It includes the mechanical design, the metallizing procedure, the electroforming process and information on heat cycling tests and gassing characteristics. Also discussed are the advantages of electroforming certain types of vacuum joints normally made by brazing. It would

seem that further development of this process could lead to the more economical production of tubes that now use complicated brazed joints, expensive materials or highly-skilled personnel. (Author)

M. D. Hare, R. F. Keller, and H. A. Meneses, *Proc. 4th National Conf. on Tube Techniques*, 25, New York University Press, New York, 1959.

46

387. A High Temperature Ceramic-Metal Seal Made with Low Vapor Pressure Materials.

United States. The ceramic-metal sealing techniques commonly used in industry make use of such braze materials as BT, silver or copper. These seals cannot be heated above the temperature limit fixed by the melting points or the vapor pressures of these materials. Hence, a ceramic-metal seal that would permit one to make electron tubes which could be taken to higher temperatures than those fixed by these materials would be indeed useful. Such a ceramic-metal seal has been developed. It extends this temperature limit by several hundred degrees. Details on the materials and method used in making the seal as well as the times, temperatures, and atmospheres for sintering the metallizing to ceramic and bonding the ceramic to metal are given in this paper. Tubes made with this seal have been heated to temperatures above 1000°C without contamination from the seal materials and without deleterious effect on seal strength or vacuum tightness of the seal. (Author)

P. R. Pondy, *Proc. 4th National Conf. on Tube Techniques*, 29, New York University Press, New York, 1959.

46 : 31

On the High Temperature Reaction of Silica Glass with Copper and Copper Oxide. See Abstract No. 306.

47. Outgassing Data, Vapor Pressure Data, Gettering Data

47

388. Vapor Pressures of $FeCl_2$, $FeBr_2$ and FeI_2 by the Torsion Effusion Method.

R. J. Sime and N. W. Gregory, *J. Phys. Chem.*, **64**, 86–89, Jan. 1960.

47

389. Molecular Sieves in Atmosphere Control.

These synthetic crystalline compounds, now being widely used in atmosphere generators, have a great affinity for water and other polar compounds, and can separate gases and liquids with remarkable selectivity according to their molecular sizes, polarity and carbon bond saturation. Specific applications are in gas drying, air drying and gas separation. (Author)

Herbert W. Westeren, *Metal Prog.*, **77**, 75–78, Feb. 1960.

47 : 16 : 33

Properties of Getters in Electronic Tubes. See Abstract No. 219.

47 : 41

Vapour Pressure of Thorium. See Abstract No. 374.

47 : 41

The Measurement of the Heats of Sublimation of Zinc and Cadmium with the Mass Spectrometer. See Abstract No. 377.

49. Miscellaneous Materials and Techniques

49

390. Low Friction of Metals in Reciprocating Sliding.

Yasukatsu Tamai, *J. Appl. Phys.*, 1874–1875, Dec. 1959.

49

391. Kinetics of Strontium Oxide on Tungsten.

J. A. Cape and E. A. Coomes, *J. Chem. Phys.*, **32**, 210–214, Jan. 1960.

49

392. Mass Spectrometric Investigation of the Sublimation of Molybdenum Dioxide.

R. P. Burns, G. DeMaria, J. Drowart, and R. T. Grimley *J. Chem. Phys.*, **32**, 1363–1366, May 1960.

49

393. Check for Vacuum Producers.

Sometimes, in operating a vacuum process, the absolute pressure in the system will begin to rise or to cycle erratically. An arrangement is described which makes it possible to check whether the system has developed a leak or whether the vacuum producer is malfunctioning. The test is described for a steam ejector but is applicable to other vacuum producers. A. G.

Note by E. F. Harp, *Chem. Eng.*, **67**, 162, May 1960.

49

394. The New Welding Process.

This article reviews a number of welding processes, some still in the experimental stage and others widely used in production. Included is the electron beam welding process. The advantages and disadvantages of this method, as well as possible applications, are discussed. A. G.

Jack C. Merriam, *Materials Design Eng.*, **51**, 105–120, Jan. 1960

Basic Science and Engineering

51. Physics, Astronomy, Geophysics

51

395. Study of Electroluminescence of Zns–Cu Single Crystals.

V. E. Oranovskii and B. A. Khmelinin, *Optics and Spectroscopy*, **VII**, 336–338, Oct. 1959.

51

396. The Influence of an Activator on the Stability of F-Centers.

I. A. Parfianovich and E. I. Shuraleva, *Optics and Spectroscopy*, **VII**, 324–327, Oct. 1959.

51 : 19

Effect of Foreign Gases on the Absorption of Infrared Radiation by Water Vapours in the Region of a Individial Line in Band 2.7μ. See Abstract No. 260.

51 : 19

Candoluminescence and Surface Recombination Luminescence of Phosphors in the Atmosphere of Activated Gas. See Abstract No. 261.

51 : 19

Thin Film Optics. V. The Properties of Silicon. See Abstract No. 262.

51 : 19

Optical Properties of Metal Films in the Region of Anomalous Skin-Effect. See Abstract No. 263.

52. Physical Chemistry

52 : 16

The Oxidation of Evaporated Barium Films. See Abstract No. 218.

52 : 17

The Dissociation Pressure of CdSb. See Abstract No. 227.

52 : 17

Sublimation Pressures of Solid Solutions. I. See Abstract No. 228.

56. Electrical Engineering, Electronic Circuits

56 : 18 : 33

Deuterium-Filled Thyrations. See Abstract No. 237.

56 : 18 : 33

Deuterium as a Filling for High-Voltage Thyratrons. See Abstract No. 238.

56 : 30

Preparation of Metal Film Resistors on Laminated Plastics. See Abstract No. 298.

56 : 30

Superconducting Computer Elements. See Abstract No. 301.

ol.
10
960

ERRATUM

Vacuum Vol. 10. Nos. 1 and 2. J. BAILLEUL LANGLAIS p. 147, equation following fig. 8

for $Sm = exp. -\frac{E}{RT}$ read $Sm = Sc\ exp. -\frac{E}{RT}$

Vol.
10
1960

VACUUM

An Omegatron Mass Spectrometer and its Characteristics

A. KLOPFER and W. SCHMIDT

An omegatron with noble-metal electrodes is described, which can be given a constant sensitivity to within 10 per cent by the application of a suitable electrostatic field. The sensitivity is not even affected by the action of corrosive gases and vapours, such as H_2O, CO_2 and CH_4, over long periods, and is reproducible from omegatron to omegatron as long as the dimensions are kept constant. A comparison of the ionization probability given in the literature with that calculated from the calibration curve of the omegatron shows that nearly all the resonance ions formed by the electron beam reach the ion collector. The adjustment of the operating data, needed to achieve this condition is in general independent of the mass. Some characteristics of the omegatron are described.

01.
10
960

1. Introduction

In recent years omegatrons were developed in a number of laboratories for gas analysis in high-vacuum and ultra-high vacuum systems.

The original device, described by Sommer and co-workers[1] in 1951, was modified by Alpert and Buritz[2] to give a simpler design. Their 1954 publication describing this model also pointed out the suitability of the instrument for gas analysis in ultra-high vacuum systems. This type of omegatron has been widely used since then, and several further modifications have also been described, e.g., Brubaker and Perkins[3] designed an omegatron in which the sensitivity is increased by use of suitable electrostatic fields.

The theory of the idealized omegatron (neglecting electrostatic fields and space-charge effects) was worked out by Sommer *et al.*,[1] who gave expressions for the resolving power, time of flight, path length and the final energy of the ions. The equations of motion of the ions in an idealized omegatron were derived and discussed by Berry.[4] A number of omegatron characteristics, such as the influence of the adjustment on the ion current and the resolving power, were determined experimentally by Edwards.[5]

The Philips laboratories started to carry out qualitative analysis of the residual gases in television tubes with the aid of omegatrons in 1953.[6] Research also has been going on concerning the suitability of the omegatron for measuring partial pressures, so that it can also be used for the quantitative analysis of residual gases. A suitable type has now been designed, and its construction and properties are described in this paper.

2. Principle of the omegatron

The principle of operation of the omegatron has been described in detail in the publications cited in the introduction, so only the main action will be given here.

The omegatron works on the same principle as a cyclotron. In a homogeneous static magnetic field, ions moving perpendicular to the magnetic field describe circles whose radius is given by the equation :

$$r = \frac{m}{e} \times \frac{v_0}{B} \qquad (1)$$

where m = mass of the ion, e = charge of the ion, v_0 = component of velocity perpendicular to the magnetic field and B = magnetic field strength.

The angular frequency of these ions is :

$$\omega_c = \frac{e}{m} \times B \qquad (2)$$

A *rf* field $E_{rf} = E_0 \sin \omega t$ applied perpendicular to the magnetic field will accelerate or retard the circulating ions. If the frequency $\omega/2\pi$ of the alternating electric field is equal to the frequency of revolution of the ion, $\omega_0/2\pi$, then the ion picks up the same amount of energy each revolution, and its path becomes an Archimedes' spiral. At resonance, the ions are finally trapped by a suitably placed collector, and they can be detected by means of a sensitive amplifier. The nonresonant ions describe spiral paths with pulsing radii, the maximum values of which are limited, and therefore they do not reach the ion collector. The ions are formed by collision of the residual gas molecules with electrons moving parallel to the magnetic field.

3. Measurement of partial pressures with the omegatron

In order to measure partial pressures with the omegatron, the frequency of the alternating electric field is altered either continuously or in suitable steps. The e/m ratios for the various ions present may be derived from the frequencies at which a resonant ion current appears, using equation (2). This usually presents no difficulties as long as the mass of the ion is not too great. The usual mass-spectrometric methods must now be used in order to deduce the nature of the original gas from the detected ions. The electron

impact not only produces singly charged gas molecules but also doubly charged ones, and also fragment ions. It is possible to determine the nature of the gas from the intensities at various mass numbers by comparison with the known ion-patterns of various gases. The ion-patterns must be determined for each gas by calibration.

The partial pressures of the various components of the gas mixture can be determined from the ion current. If the ionization probability is σ, then the ion current i_0^+, formed by the electron beam with a path length s, is at a partial pressure p :

$$i_0^+ = s\,\sigma\,p\,i^- \tag{3}$$

where i^- is the electron current.

The current reaching the ion collector will then be :

$$i^+ = a i_0^+ e^{-L/\lambda} = a\,s\,\sigma\,p\,i^-\,e^{-L/\lambda} \tag{4}$$

where L is the path length for the resonant ions and λ is the mean free path. The factor a represents the collection efficiency, if the mean free path is large in comparison to the path length of the ions, while the term $e^{-L/\lambda}$ takes into account the losses due to collision of the circulating ions with the molecules of the residual gas. An equation of the form of (4) must hold for each component of the gas mixture and also for each fragment of such a component.

If the omegatron is to be used as a measuring instrument, the sensitivity, that means the value of a, must be constant. The presence of other gases must also have no effect on a. The latter condition is especially important if the nature of the gases is to be deduced from the intensities of the fragment ions.

In an idealized omegatron, in which no electrostatic fields are found, a will have the value 1. In a real omegatron, however, such fields are always present, e.g. because a small positive field must be applied to prevent the drift of the ions in the direction of the magnetic field due to thermal energy. Components of the field strength perpendicular to the magnetic field are therefore present in the middle of the omegatron, which causes ions to move on cycloidal paths along the equipotential lines. Surface layers on the electrodes of the omegatron, which can be charged, alter the electrostatic field and thus the motion of the ions. All the effects mentioned above cause a change of a with time and also from tube to tube. Since the applied electrostatic potentials in the omegatron are of the same order of magnitude as those arising from the effects mentioned above, a is normally found to vary over the whole range from 0 to 1. Under these conditions the omegatron is only suitable for use as a qualitative gas analyzer, but not as a partial pressure measuring device.

4. Omegatron with side plates

In the course of our investigations to use the omegatron for the measurement of partial pressures we have developed a tube which gives a constant sensitivity, and an a-value of 1, when adjusted properly. The main features of the tube are shown in the schematic drawing of Fig. 1. The view perpendicular to the direction of the magnetic field is exactly the same as for the tube designed by Sommer *et al.*[1] The first electrode G_1 can be used to stabilize the electron current, which is drawn from a directly heated barium oxide coated cathode. This type of cathode is used to minimize the rates of reactions with reactive gases. The electrode G_2 has about the same potential as the electron collector T. The position of the omegatron in the magnetic field must be so adjusted that no electrons reach the electrode A, i.e. the meter J_2 may not indicate any current, otherwise the sensitivity of the tube will be considerably altered by secondary

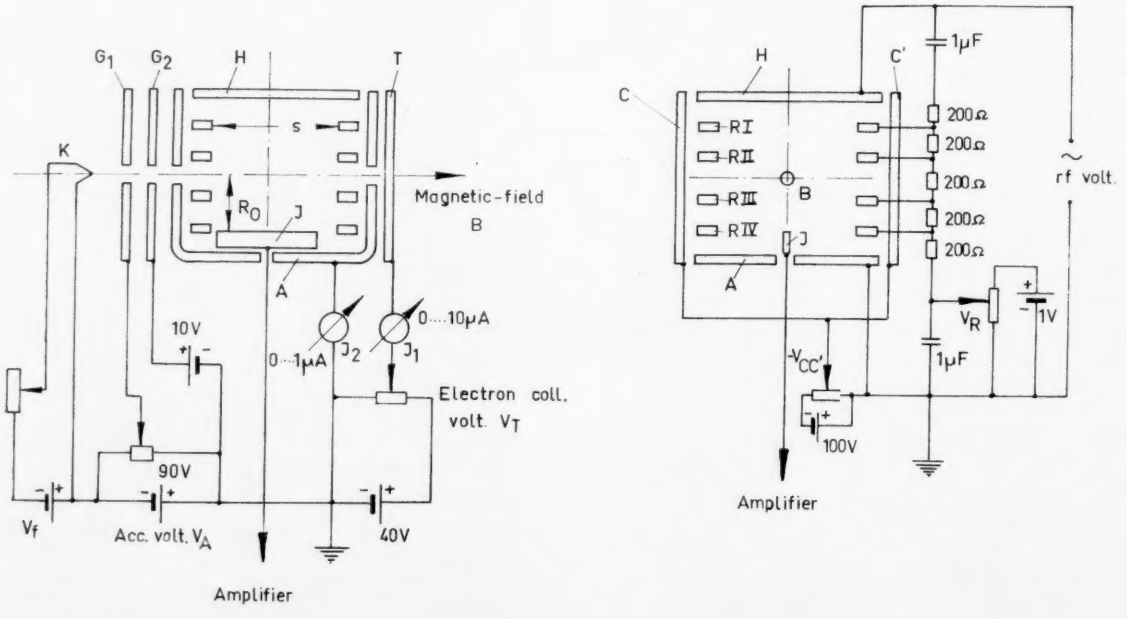

FIG. 1.

electron effects. The *rf* voltage is applied to electrodes *H* and *A*. The *rf* field is homogenized by the guard rings *R* and the voltage divider, which are given a slight positive electrostatic voltage to prevent the ions from drifting in the direction of the magnetic field. In addition to the arrangement described by Sommer *et al.*, the model described here has two side plates *C* and *C'*. If a negative voltage is applied to these plates an electrostatic field is produced which gives the tube a reproducible sensitivity. The value of the negative voltage $V_{CC'}$ needed to obtain a maximum ion current depends on the number of guard rings due to the field penetration and also on the positive voltage V_R. With four guard rings, the optimal value of the ratio of V_R to $V_{CC'}$ was found by experiment to be about 1 : 100. V_R is usually + 0.1 to 0.4 V.

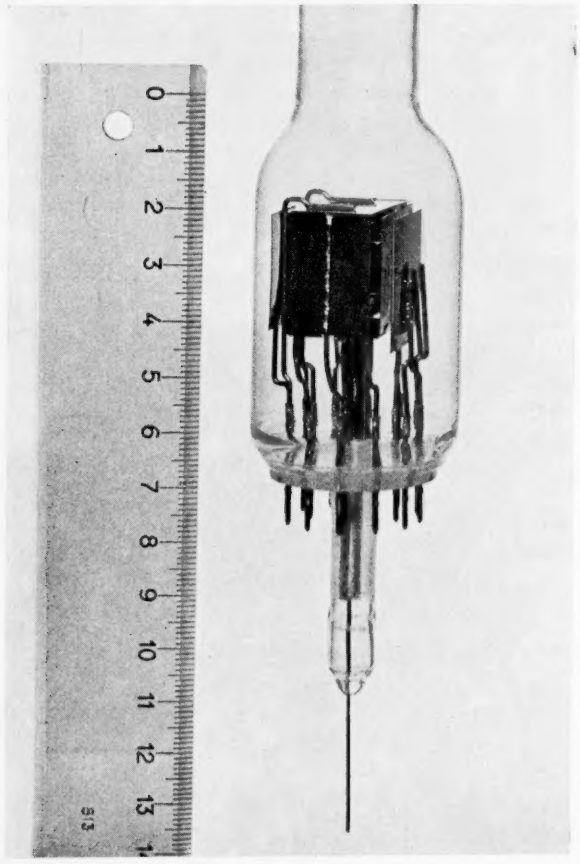

FIG 2.

The overall dimensions of the omegatron tube are shown in Fig. 2. The electrode assembly forms a cube of about 2.5 cm on edge. The electrodes are mounted directly on a glass base without the use of ceramics or mica, and are surrounded by a glass bulb. The tube as a whole can be degassed in an electric oven at 400 °C, and the metal electrodes can be degassed at 900 °C by induction heating. These high temperatures are sometimes found to be necessary in order to remove troublesome layers from the surfaces of the electrodes. If the omegatron is not heat-treated, the choice of the metal for the electrodes is unimportant, as long as the electrodes are thoroughly cleaned beforehand. Heat treatment is definitely necessary, however, if the evolution of gas from the electrodes is to be minimized. We use noble metals for the electrodes, in order to prevent the formation of oxide layers during the degassing. A platinum-iridium alloy has proved to be the best for this purpose.

In order to produce a magnetic field of 5000 G we use permanent magnets or electromagnets, with homogeneous or inhomogeneous fields. Homogeneous fields (homogeneity up to 0.2 per cent) have the advantage that the position of the omegatron between the poles of the magnet is not critical, and that sharp peaks are obtained. Inhomogeneous fields with a field strength decreasing radially away from the centre cause a focussing of the ions in the direction of the magnetic field. The peak is broadened at the foot, however, and the omegatron must be carefully placed in the magnetic field, because the guiding centre of the ion orbit drifts along a path normal to the field gradient.[7] However, the lower weight of a magnet with an inhomogeneous field (2 per cent inhomogeneity in the space of the analysis chamber) makes us prefer this type to the type with greater homogeneity.

In order to produce the *rf*-field, any commercial signal generator can be used, which supplies an output voltage independent of the frequency up to a few volts r.m.s.

The lowest detectable partial pressure is determined by the sensitivity of the d.c. amplifier ; vibrating reed amplifiers, therefore, are to be preferred to electrometer-type amplifiers. The connection lead from the ion collector of the omegatron to the input of the amplifier must be well shielded.

The stabilization of the ionizing electron current proved to be necessary, all the standard methods of electron beam control used with mass spectrometers being able to be applied to the omegatron shown in Fig. 1. The emission current can be stabilized by means of a cathode resistor at constant potential of G_1, or by controlling the potential of G_1 by the voltage drop along a resistor caused by the electron current to *T* or by regulation of the cathode heating current.

The mass spectrum may be simply displayed on the screen of an oscilloscope or written with a recorder as described by Peper[6].

5. The action of the omegatron with side plates

A detailed mathematical treatment of the motion of the ions will be given in a following paper, so only a brief description of the action of the omegatron with side plates is given here.

The potential distribution in the plane through the middle of the omegatron and perpendicular to the magnetic field was measured with the aid of an electrolytic tank. The measurements have shown that there is a small negative potential of a few tenths of a volt up to a few volts over the whole of the plane in question with respect to the electrodes *A*, *H* and *I*, except in the outer region around the guard rings *R*. Some electrostatic equipotential lines in this plane

are shown in the schematic drawing of Fig. 3 for a simplified model of an omegatron without guard rings. The *rf* field and the space-charge effects being neglected for the moment positive ions move in cycloidal paths along the equipotential lines in one of the two directions shown, depending on the place they are formed, away from the middle of the omegatron. In order to prevent the ions from moving upwards away from the collector, the positions of the ion source *O* and the electric centre *M* must be as shown in Fig. 3. A certain separation of these two points is already brought about by the asymmetry caused by the ion collector, and a complete separation may be achieved by suitable placing of the electrode *H*.

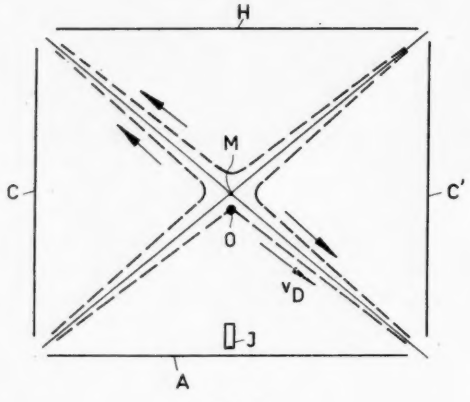

FIG. 3.

When the *rf* field is now applied, a spiral motion is superposed on the cycloidal paths mentioned above. The resulting motion may be approximately described by saying that the ions describe spiral paths, while the ion orbit guiding centres move with a drift velocity v_D.

The special electrostatic field shall influence the movement of the ions in such a way that the non-resonant ions are extracted, thus reducing the space charge, while the guiding centres of the resonant ions keep to a path which will result in an optimal yield of these ions at the collector. In order to satisfy these conditions, we must make certain restrictions on the magnitude of both electric fields. The drift velocity v_D is proportional to the electrostatic field strength E_{st}, and inversely proportional to the magnetic field strength B:

$$v_D \sim \frac{E_{st}}{B} \tag{5}$$

The lower limit of E_{st} is set by the condition that the space charge must not appreciably effect the potential, and the upper limit is determined by the amplitude of the *rf* field, since the rate of increase of the radius of the spiral path of the resonant ions is proportional to the *rf* field strength:

$$v_{rf} \sim \frac{E_0}{B} \tag{6}$$

This rate must be high enough, so that the final radius of the spiral path reaches a value equal to the distance of the equipotential line from the top of the ion collector, in a time given by the drift velocity and the geometrical dimensions of the omegatron. Otherwise the resonant ions will pass the ion collector. Since the amplitude of the *rf* field also determines the resolution, the possible variation of E_{st} is severely limited. The permissible range of both field strengths will be discussed in the next section. It may be mentioned here, however, that equations 5 and 6 are more or less independent of the mass of the ions, so once the omegatron is properly adjusted it will give optimum collection of the resonant ions over the whole mass spectrum.

6. Characteristics

The electrostatic field must be adjusted to the optimum operating conditions by varying the small positive voltage V_R and the large negative voltage $V_{CC'}$, so that maximum resonant ion current is obtained for a given pressure. Some care should be taken when trying to find out the optimum adjustment, since it is a property of this omegatron that an ion current can be measured in the absence of the *rf* field, in which case the omegatron acts as a total-pressure indicator. This condition is reached when the potential of the ion source becomes equal to the potential of the ion collector, caused by a too small negative electrostatic voltage and a resulting space-charge effect. These residual current characteristics are shown as the broken lines in Figs. 4 and 5. The

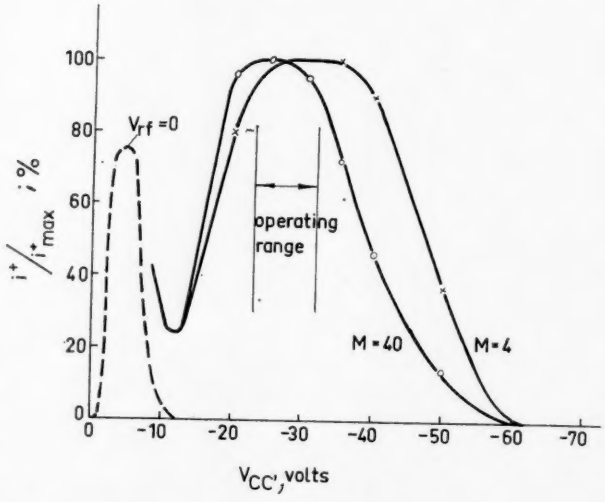

FIG. 4.

full curves show the characteristics of the partial-pressure meter with a *rf* voltage of 1 V r.m.s. for a light ion and a heavy one, in a magnetic field of 5000 G. In the range of values of V_R, where the omegatron can be used as total pressure indicator, also non-resonant ions can reach the ion collector beside the resonant ions in the presence of a *rf* field. Therefore, the full lines of Fig. 5 reach values higher than 100 per cent. The most favourable range of the potential settings is that of the voltage V_R being as small as possible, and $V_{CC'}$ having a large negative value. The precise values vary from tube to tube, because of the above-mentioned

Vol. 10 1960

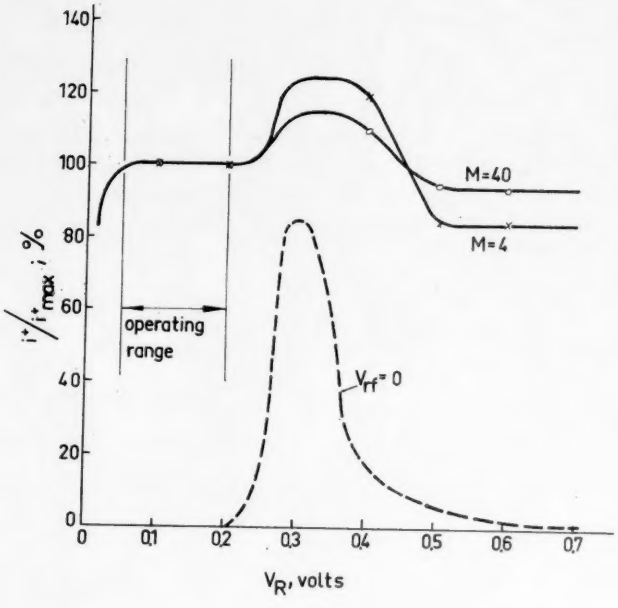

FIG. 5.

surface films on the electrodes, and they may even change with the degree of degassing of the electrodes.

The influence of the voltage of the electron collector, V_T, on the ion current is slight as long as this electrode is clean (see Fig. 6).

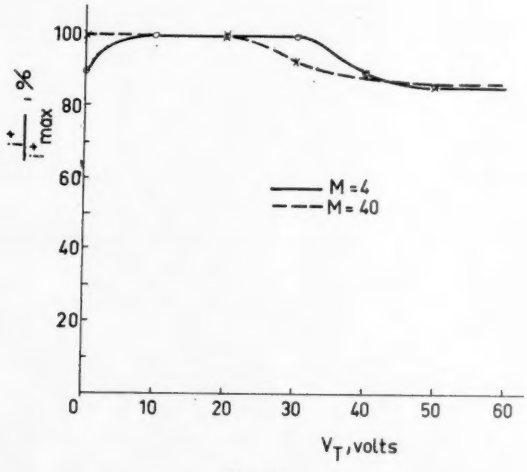

FIG. 6.

According to equation 4, the ion current should be a linear function of the electron current at fixed pressure. The range of values for which this relation holds has been determined experimentally for mixtures of H_2 and N_2 of two different compositions (Fig. 7). In one case the nitrogen pressure was 1.3×10^{-7} Torr, and in the other case it was 7×10^{-6} Torr, while the hydrogen pressure was roughly the same (about 8×10^{-8} Torr) in both mixtures. When the electron current exceeded 1μA, the adjustment of the optimum operating data had to be changed to maintain the maximum ion current. The curvature of the characteristics is caused by space-charge effects produced by the non-resonant ions and the electrons, as has been shown by Edwards.[5] When the electron current is 1μA, an ion must surmount a potential barrier of a few hundredths of a volt in order to reach a distance of 0.5 mm from the electron beam. Moreover, as the electron density increases the resonance frequency inside the electron beam differs more and more from that outside the beam, until finally resonance is no longer possible. The limit of the linear relation between ion current and electron current is at a higher pressure for nitrogen, with its larger mass, than for hydrogen. The theory of the idealized omegatron[1] predicts that the increase of radius of the path of the ion per revolution at resonance depends on the mass of the ion. The diameter of the path of a N_2 ion equals the diameter of the electron beam (0.5 mm) in two revolutions when the magnetic field is 5000 G and the *rf* voltage is 1 V r.m.s., while an H_2 ion requires 28 revolutions to reach the same distance.

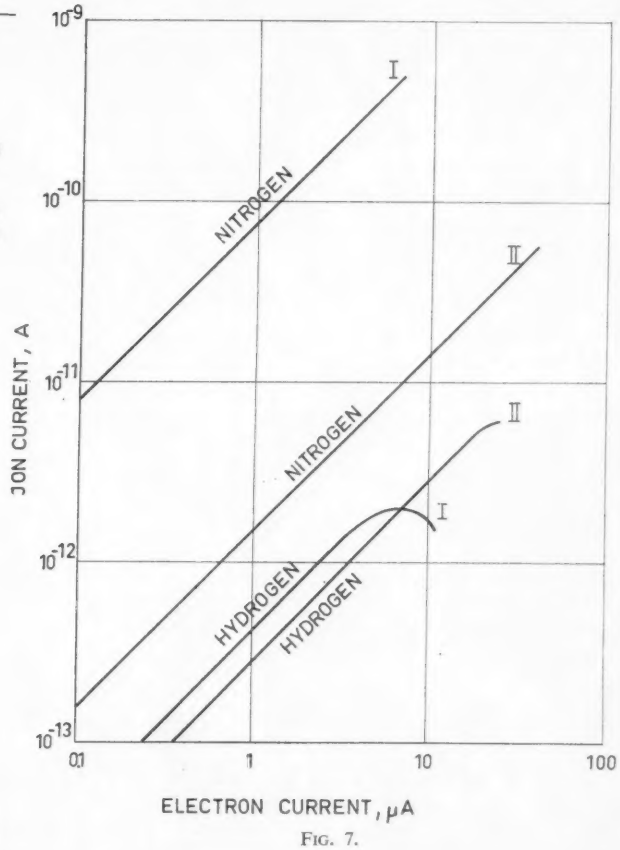

FIG. 7.

TABLE I

Maximum values of the electron current at various pressure ranges

i^-_{max}, μA	p, Torr
30	$\leqslant 10^{-8}$
10	$\leqslant 10^{-7}$
1	$\leqslant 10^{-5}$

Table I gives the maximum values of the electron current for which the ion current is proportional to the electron current, independent of the mass at various pressures.

The relation between ion current and pressure can be calculated from equation (4), if the ionization probability σ, the mean free path λ of the gas and the intensities of the various fragment ions are known. The value of λ for a given gas depends on the pressure, according to the equation :

$$\lambda = \frac{\sqrt{2}\,\lambda_0 p_0}{p} \tag{7}$$

where λ_0 is the mean free path at a pressure p_0. The values of λ_0 are tabulated for a number of gases.[8, 9] The factor of $\sqrt{2}$ is due to the fact that the mean velocity of the ions is higher than that of the gas molecules. The total length of path of the resonant ions is given for the idealized omegatron by[1] :

$$L = \frac{eR_0^2 d_0 B^2}{\sqrt{2}\,V_{rf} M} \tag{8a}$$

$$\text{or} \quad L = \frac{9.6 \times 10^{-5}}{\sqrt{2}} \times \frac{R_0^2 d_0 B^2}{V_{rf} M} \tag{8b}$$

where e = charge of the ion, B = magnetic field strength (G), V_{rf} = r.m.s. *rf* voltage, M = atomic mass numbers, R_0 = distance from ion source to ion collector (cm), or, we can say, R_0 is the final radius of the ion orbit, when the resonant ion reaches the collector and d_0 = distance between the two *rf* electrodes (cm). The number of revolutions needed by the resonant ions to reach the collector is smaller in our omegatron than in an idealized one, because of the drift of the ion orbit guiding centre. The final radius of the ion orbit is therefore reduced in our case and the term R_0 of equation (8) must be replaced by the term $0.75 \times R_0$. The total path length becomes :

$$L = \frac{9.6 \times 10^{-5}}{\sqrt{2}} \times \frac{(0.75\,R_0)^2 d_0 B^2}{V_{rf} M} \tag{8c}$$

TABLE II

Ionization probabilities, measured with the omegatron and compared with the values given in the literature

Gas	Mass number	σ exper.	σ literat.
H_2	2	3.6	3.6
He	4	1.63	1.36
N_2	28	10	10
CO	28	10.7	10
A	40	11.8	12

Since the ion collection is optimal, α may be put equal to 1 in equation (4). As a demonstration that this is justified, Table II gives the values of the ionization probability taken from the literature,[8, 9] together with the values derived from measurements on the omegatron at low pressures, according to the equation :

$$i^+_{\text{exp}} = i^- \times p_{\text{exp}} \times s \times \sigma_{\text{exp}} \tag{9}$$

Combination of equations (4), (7) and (8c) gives the relationship between ion current and pressure, when only one gas is present in the omegatron :

$$i^- = i^- p\, s\, \sigma\, e^{-\frac{4.8 \times 10^{-5} (0.75\,R_0)^2 d_0 B^2}{\lambda_0 p_0 V_{rf} M}} \tag{10}$$

The agreement between the calibration curves determined experimentally and by calculation from equation (10) is shown in Fig. 8 for He. The two curves agree almost exactly for other gases, as is to be expected from the data of Table II.

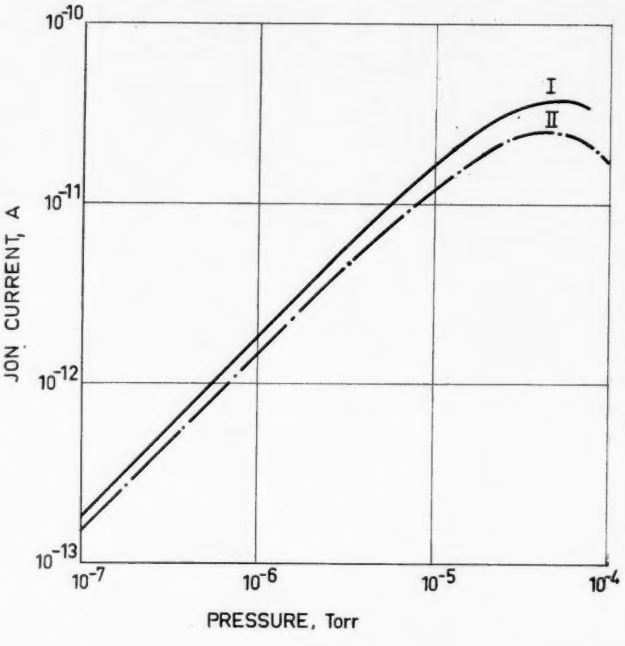

FIG. 8.

The calibration curve is linear for $\lambda \gg L$, has a maximum at $\lambda = L$, and drops rapidly for $\lambda < L$. The highest permissible pressure is determined by the position of the maximum, at which :

$$L = \lambda = \frac{\sqrt{2}\,\lambda_0\, p_0}{p_{\max}} \tag{11a}$$

$$\text{or} \quad p_{\max} = \frac{\lambda_0\, p_0}{4.8 \times 10^{-5}} \times \frac{V_{rf} M}{(0.75\,R_0)^2 d_0 B^2} \tag{11b}$$

If, however, the system in question is a mixture of gases of different masses, the mean free path and thus the value of $p_{\max}$ will be different, and also below the maximum the ion losses will be influenced by collisions with other gases, so that even when the partial pressure of the resonance gas is constant, the ion current will vary with the total pressure and the composition of the gas mixture. A purely theoretical approach to this problem indicates that the mean free path λ of the resonance ion in equation (4) should be replaced by the expression :

$$\lambda^*_1 = \frac{\sqrt{2}\,kT}{\pi} \cdot \frac{1}{\sum_{n=1}^{m} (\varrho_1 + \varrho_n)^2 p_n \sqrt{1 + M_1/M_n}} \tag{12}$$

where p_n = partial pressure of gas n
M_n = mass of molecule of gas n
M_1 = mass of resonance ion
ϱ_1 = radius of resonance ion
ϱ_n = radius of the molecule of gas n
m = number of components of the mixture.

An idea of the magnitude of the effect on the calibration curve may be gained from the calculations assuming a mixture of He and N_2, in which the mass of the resonant gas He is much smaller than that of the non-resonant gas N_2. The ratio of the He^+-current at the ion collector to the ion current produced by the electron beam is plotted in Fig. 9 as a function of the partial pressure of N_2 for various values of the partial pressure of He (full lines). The broken curve shows the behaviour when only helium is present in the omegatron. It may be seen from Fig. 9 that even when the total pressure is 10^{-5} Torr the ion losses in the mixed system only differ by about 5 per cent from the ion losses in a pure gas. The difference is still less with the gases usually met with in clean vacuum systems.

The measuring technique is simplified if the omegatron is only used in the range in which the ion current is proportional to the pressure, according to the simplified equation (9). The relation between current and pressure is then similar to that of an ionization gauge :

$$i^+ = i^- \times C \times p \qquad (13)$$

where C is the sensitivity of the instrument, $C = s \times \sigma = 1.1\sigma$, since the length of the electron path s is constant (1.1 cm). The sensitivities for the gases most frequently found in vacuum systems are given in Table III, and the intensities of the fragment ions expressed with respect to the main peak are given in Table IV. If errors of about 15 per cent can be tolerated, the upper limit of the total pressure for which the linear relation (13) still holds may be put at 1×10^{-5} Torr.

TABLE III

Sensitivities C of the omegatron for various gases

Gas	Mass number	C, Torr^{-1}
H_2	2	4.0
He	4	1.8
A	40	13
H_2O	18	7.2
N_2	28	11.0
CO	28	11.8
CO_2	44	14.0
CH_4	16	7.4
C_2H_2	26	15.5
C_2H_4	28	11.6
C_2H_6	28	14
C_3H_8	29	9

The smallest pressure which can be detected, p_{min}, is determined by the greatest electron current which can still be applied at low pressures, i^-_{max}, and the sensitivity of the amplifier :

$$p_{min} = \frac{i^+_{min}}{s \times \sigma \times i^-_{max}} \qquad (14)$$

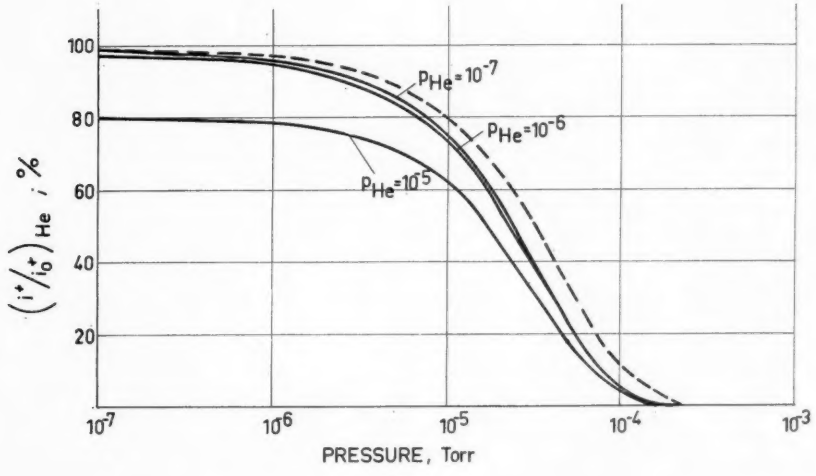

FIG. 9.

If we take i^+_{min} as 10^{-16} A, i^-_{max} as 30μ A, $s = 1.1$ cm and $\sigma = 10$, p_{min} is calculated to about 3×10^{-13} Torr. Partial pressures as low as 1×10^{-12} Torr have been measured in our laboratories. Since fragment ions giving a current of 1 per cent of the main peak frequently have to be detected in gas analysis, the lower limit raises by a factor of 100.

According to equations (4) and (10), the ion current is independent of the *rf* voltage V_{rf} as long as $\lambda \gg L$. If this condition is not fulfilled, the ion current drops. The decrease is greater for light gases than for heavy ones (broken curves in Fig. 10). The decrease actually found with the omegatron described here was greater than was to be expected from equation (10) (full curves of Fig. 10). We have already mentioned the connection between the electrostatic field

TABLE IV

Intensity of the fragment ions (Intensity of the main peak = 100)

2	12	13	14	15	16	17	18	19	20	24	25	26	27	28	29	30	31	32	36	37	38	39	40	41	43	44	Gas
100	—	—	—	—	—	—	—	—	—	—	—	—	—	—	—	—	—	—	—	—	—	—	—	—	—	—	H_2
—	—	—	—	—	—	—	—	—	14.2	—	—	—	—	—	—	—	—	—	0.38	—	0.06	—	100	—	—	—	A
0.6-1.5	—	—	—	—	1.8	21	100	11-17	0.23	—	—	—	—	—	—	—	—	0.13	—	—	—	—	—	—	—	—	H_2O
—	—	—	7.4	0.03	—	—	—	—	—	—	—	—	—	100	0.75	—	—	—	—	—	—	—	—	—	—	—	N_2
—	3.3	0.04	0.55	—	1.3	—	—	—	—	—	—	—	—	100	0.88	0.2	—	0.02	—	—	—	—	—	—	—	—	CO
—	3.5	0.03	0.08	—	7.8	—	—	—	—	—	—	—	—	11.5	0.1	—	—	0.4	—	—	—	—	—	—	—	100	CO_2
	1.8	5.7	12.5	81	100	2.7	—	—	—	—	—	—	—	—	1–5	—	—	—	—	—	—	—	—	—	—	—	CH_4
3.5	1.4	4.0	0.3	0.04	—	—	—	—	—	5.1	19	100	3.2	—	—	—	—	—	—	—	—	—	—	—	—	—	C_2H_2
	0.6	1.0	2.3	0.3	0.4	—	—	—	—	2.0	6.8	47	51.5	100	3.3	—	—	—	—	—	—	—	—	—	—	—	C_2H_4
	0.2	0.55	2.0	3.1	0.15	—	—	—	—	0.5	2.7	18.1	27.6	100	20.5	25.9	0.54	—	—	—	—	—	—	—	—	—	C_2H_6
	0.18	0.36	1.13	3.8	0.12	—	—	—	—	0.13	0.64	8.2	39.1	60.3	100	2.1	—	—	0.64	4.1	5.8	20	—	16	30.8	44.9	C_3H_8

Vol. 10 1960

strength and the *rf* field in section 5, and it may also be mentioned that in the presence of an electrostatic field the resonance frequency becomes a position function in the omegatron. Brubaker and Perkins[3] have shown that there is a critical lower limit for the *rf* voltage, at which the resonance ions just manage to reach the ion collector after passing two potential barriers. If either of these barriers is not passed, the ion returns to the source.

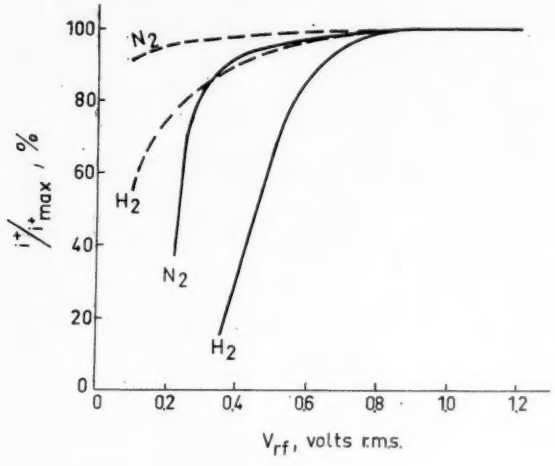

FIG. 10.

Since the ion losses are different for different types of ions when the *rf* voltage is too small, the omegatron must always be used in the saturation range, i.e. the horizontal part of the curve (Fig. 10) for gas analysis ; only then the partial pressures are given correctly.

Sommer *et al.*[1] have given an expression for the resolution of an idealized omegatron :

$$\left(\frac{M}{\Delta M}\right)_{ideal} = \frac{e\,R_0\,B^2}{2\,E_0 M} \tag{15}$$

where B = the magnetic field, E_0 = amplitude of the alternating electric field, M = the mass of the resonance ion, e = the charge of the ion and R_0 = distance from electron beam to ion collector.

Equation (15) is derived on the assumption that the peaks at mass number M and $M \pm \Delta M$ are completely separate from each other. The resolution of the present omegatron is given by the same expression, except that the term R_0 is replaced by the distance from the ion collector to the point on the equipotential lines reached by the guiding centre of the ion orbit during the time of flight of the resonant ion. In general, this omegatron gives a separation of one mass unit at mass number 30 ; while according to equation (15), separation should be possible up to mass number 39 for the idealized omegatron. It is not possible to increase the resolution much by decreasing the *rf* voltage, since the latter must be kept within the saturation range ; however, increasing the magnetic field gives the effect predicted by equation (15). When the resolution changes, the maximum pressure which can be measured also changes, since it can be calculated from equation 8 and 15 that :

$$L = 2\,\frac{M}{\Delta M} \times (0.75\,R_0) \tag{16}$$

whence, according to equation (11), if $\lambda = L$

$$p_{max} = \frac{\lambda_0 p_0}{\sqrt{2}\,(0.75\,R_0)} \times \frac{1}{\frac{M}{\Delta M}} \tag{17}$$

7. Accuracy of measurement and individual tube differences

As long as the electrode surfaces are kept clean, the sensitivity of the tube described here remains constant to within 10 per cent ; and the sensitivity is also constant from tube to tube, as long as the dimensions are kept constant. About 40 tubes have so far been tested for their reproducibility in our laboratories. The sensitivity is not affected by the action of corrosive gases like H_2O, CH_4, C_2H_6 and CO_2 up to pressures of 10^{-5} Torr, even after relatively long periods of time (up to several weeks). The presence of mercury on the electrodes, or of HCl, do have a considerable disturbing effect on the operation of the omegatron, however.

The accuracy of the partial pressure measurements is 10 per cent, except when different gases give a peak at the same mass number. In a gas mixture, however, the error may be considerably greater than this, since all gases which contribute 10 per cent or less to a peak due to another gas are not detected. The greatest ratio of ion currents which can be determined is 10^4. For details of the influence of the adsorption of gases and reactions of gases with the cathode of the omegatron on the partial pressure analysis and the determination of small quantities of gas, see Garbe.[10]

These omegatron tubes are used by Philips for many purposes such as the determination of the residual gases in vacuum apparatus and in electron tubes, and the investigation of getter-gas reactions and the gas evolved by glasses.

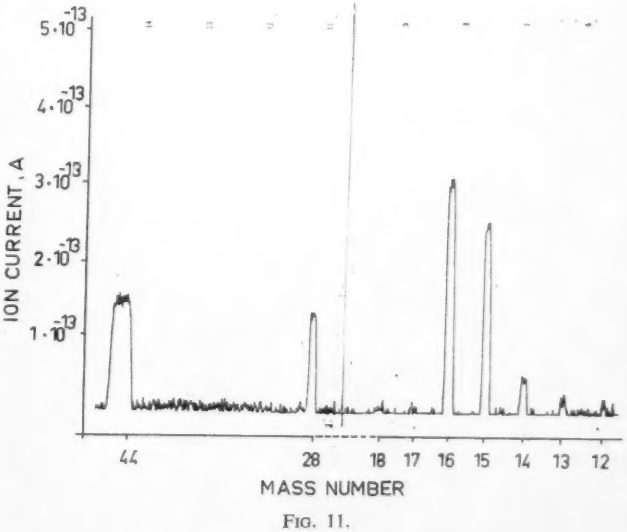

FIG. 11.

As a simple example, the mass spectrum and the partial pressures in a well degassed glass system with a barium getter mirror are shown in Fig. 11.

References

[1] H. Sommer, H. A. Thomas, and J. A. Hipple ; *Phys. Rev.*, **82**, 697 (1951).
[2] D. Alpert and R. S. Buritz ; *J. Appl. Phys.*, **25**, 202 (1954).
[3] W. M. Brubaker and G. D. Perkins ; *Rev. Sci. Instrum.*, **27**, 720 (1956).
[4] C. E. Berry ; *J. Appl. Phys.*, **25**, 28 (1954).
[5] A. G. Edwards ; *Brit. J. Appl. Phys.*, **6**, 44 (1955).
[6] J. Peper ; *Philips Techn. Rundsch.*, **19**, 278 (1957–58).
[7] L. R. McNarry ; *Canad. J. Phys.*, **36**, 1710 (1958).
[8] R. Jaeckel ; *Kleinste Drucke*, Springer Verlag 1950.
[9] S. Dushman ; *Scientific Foundation of Vacuum Technique*, John Wiley and Sons, Inc., New York 1949.
[10] S. Garbe ; Paper No. 32, *1st International Congress on Vacuum Technique, Namur*, 1958, Pergamon Press, London.

Vol.
10
1960

Ion Movements in an Omegatron*

G. SCHUCHHARDT

Institute of Theoretical Physics of the Technische Hochschule, Aachen, Germany

The motion of resonant and nonresonant ions in the omegatron, already described in the preceding paper of A. Klopfer and W. Schmidt, is investigated. It is demonstrated that the auxiliary electrostatic field in this type of omegatron creates conditions which make for optimum collection of the resonant ions and insure consistent reproducibility. Space-charge effects are estimated, and an expression is derived for the resolving power.

Symbols used in the text

x, y, z = coordinates
r = radius, distance in the xy plane
r_0 = radius of the electron beam
t = time (differentiation with respect to t is indicated by a dot, thus $\dot{x} = \frac{dx}{dt}$)
φ = electrostatic potential
B = magnetic flux density
E_0 = amplitude of the *rf* field
i^- = electron current
U = accelerating voltage of the electron beam
e/m = charge-to-mass ratio
M = mass number
$\frac{1}{2\pi}\omega_R$ = resonance frequency in the omegatron
$\frac{1}{2\pi}\omega_{rf}$ = frequency of the *rf* field
σ = ionization probability
p = pressure

Further signs and symbols will be explained in the text.

1. Introduction

The omegatron is a mass spectrometer, developed during the last few years, in which the ratio of e/m of ions can be determined by means of a resonance condition similar to that of the cyclotron.

The ion trajectories in the omegatron were analysed by Berry[1] on the assumption that no electrostatic fields affect the motion of the ions. In the types of omegatrons used for measurements of partial pressures electrostatic fields are, however, always present. In the following, the processes taking place in such an omegatron used in practice will first be treated in a generalized way, and then the obtained result will be applied to the type of omegatron described in the preceding paper of A. Klopfer and W. Schmidt and which will subsequently be referred to as the Philips omegatron.

2. Motion of ions in an omegatron with electrostatic fields

Essentially an omegatron consists of six rectangular electrodes forming the sides of a cube and an ion collector I (see Fig. 1). The electrodes R and R' are electrically connected to one another. A coordinate system (x, y, z) is used with its origin in the geometrical centre of this cube. In order to derive the differential equations for the motion of a charged particle, an uniform alternating electric field

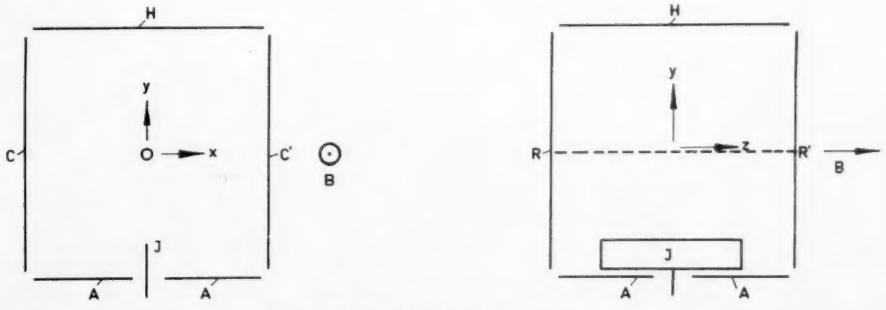

FIG. 1. Schematic view of an omegatron.

*This work was supported by the Research Laboratories of the Allgemeine Deutsche Philips Industrie GmbH, Aachen.

$E_0 \times \sin \omega_{rf} t$ with positive direction along the positive y axis, and an uniform static magnetic field B along the z axis will be assumed. The electrodes may be supplied with any desired electrostatic voltages. As the electrodes R and R' are electrically connected to one another, an electrostatic field results with a plane of symmetry normal to the magnetic field. We will only consider the ion motions in this plane of symmetry. The equation for the motion of a charged particle in an electromagnetic field is then found to be :

$$\ddot{\vec{r}} = \frac{e}{m} (\vec{E} + \dot{\vec{r}} \times \vec{B}) \tag{1}$$

and in our case we have

$$\vec{E} = \vec{E}_0 \sin \omega_{rf} t - \text{grad } \varphi \tag{2}$$

The solution of this system of equations consists of two parts. The first part, which is caused by the *rf* field, describes a spiral with a time-dependent radius[2] :

$$r_s = \frac{E_O}{B(\omega_{rf} - \omega_R)} \cdot \sin\left(\frac{\omega_{rf} - \omega_R}{2} \cdot t\right) \tag{3}$$

The second part describes a cycloidal motion of which in our case only the drift, i.e. the motion of the guiding centre of the ion orbit is significant[3] :

$$\dot{\vec{r}}_D = \frac{1}{B^2} \cdot \vec{B} \times \text{grad } \varphi \tag{4}$$

It may be derived from equation (4), that this drift or macroscopic motion causes a motion of the ion orbit guiding centre along the equipotential lines, regardless to the starting phase.

Thus, the ions in an omegatron, in which an electrostatic field is present, move from the point of origin towards the outside, at a velocity which is nearly independent of the mass of the ions. Simultaneously they are subjected, under the influence of the *rf* field, to spiral paths for which large amplitudes of r_s (equation 3) will result only near resonance, i.e. for small values of $\omega_{rf} - \omega_R$. At resonance, viz. for $\omega_{rf} = \omega_R$, the radius of the spiral increases with time and the ion path will become an Archimedes' spiral[2] :

$$r_k = \frac{E_0 t}{2B} \tag{5}$$

The centres of these spirals drift away with a velocity of $\dot{\vec{r}}_D$ along the equipotential lines.

3. Electrostatic fields in the Philips omegatron

In order to determine the electrostatic field in the Philips omegatron values of the electrostatic potentials were measured point by point in a considerably enlarged model with the aid of an electrolytic tank. From these figures it is possible to derive the values of the first coefficients of equation (6), which shows the development of the electrostatic potential in powers of the coordinates x, y and z :

$$\varphi = \sum_{i=0}^{\infty} \sum_{k=0}^{\infty} \sum_{l=0}^{\infty} a_{ikl} x^i y^k z^l \tag{6}$$

If a voltage of -40 V is applied to the electrodes C and C' and a voltage of $+0.4$ V to the guard rings, while the electrodes A and H are grounded (see Fig. 1 of the preceding paper), the following values are obtained for the first coefficients of equation (6) (dimensions in volts and cm) :

a_{000}	a_{200}	a_{020}	a_{002}	a_{210}	a_{030}	a_{012}
-0.615	-3.5	$+0.4$	$+3.1$	$+0.125$	-0.105	$+0.19$

a_{400}	a_{040}	a_{004}	a_{022}	a_{202}	a_{220}
-2.5	$+1.25$	-0.2	-10.65	$+11.85$	$+3.15$

The coefficients not here listed, up to $i + k + 1 \leqslant 4$, are zero.

Some equipotential lines with their corresponding potential values are represented in Fig. 2. Apart from the region close

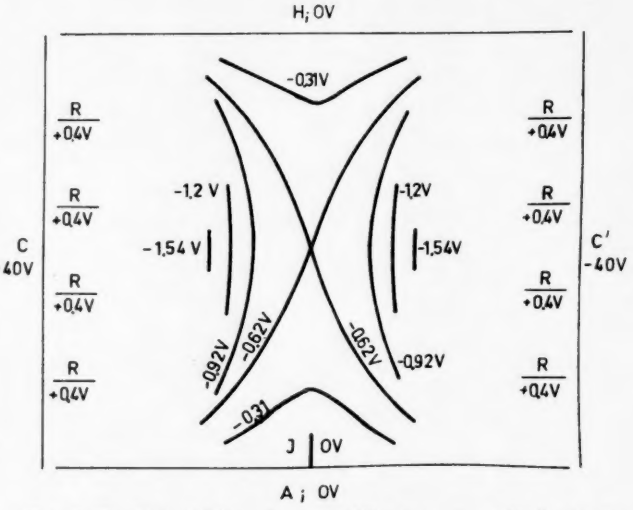

FIG. 2. Equipotential lines in the middle plane perpendicular to the magnetic field for the Philips omegatron, adjusted as partial pressure indicator.

to the electrodes, the expression of equation 6 with components up to the second power ($i + k + 1 \leqslant 2$) satisfies the numerical description of the potential distribution, as shown in Fig. 2. For the same reason the expression for the drift (equation 4) is hardly effected, within the range considered, by an omission of the components with powers higher than two in our treatment of the potential. Whether or not the higher terms cause higher harmonic resonance effects still falls to be considered. Such resonance effects will develop, as the exciting function in equation (1) is a harmonic function. The amplitudes of these harmonic resonances will be considered in further detail in chapter V.

4. Space charge effect of the electrons and of the positive nonresonant ions

In order to estimate the magnitude of the variations of the electrostatical potential in the omegatron, caused by the space charge of the electrons and the nonresonant ions, the following simplifying assumptions will be made : The cylindrically shaped electron beam with a radius r_0 and a length s is assumed to be uniform, i.e. the density of the electron current should be constant inside the beam and zero outside the beam. The kinetic energy of the electrons

Vol. 10 1960

is assumed to be independent of the coordinates. Furthermore, we will only determine the variation $\Delta\varphi$ of the potential at the border of the electron beam with respect to the potential of the ion collector. The variation in potential caused by the space charge of the positive ions and the electrons is then given by :

$$\varphi = \Delta\varphi^+ + \Delta\varphi^- = \frac{1}{4\pi\varepsilon}\left(\frac{\pi i_0^+}{2\dot{r}} \cdot \frac{r_0}{s} - \frac{i^-}{\dot{z}}\right) \ln\frac{er^2}{r_0^2} \quad (8)$$

where ε = dielectric constant, and e = base of the natural logarithms.

The ion current i_0^+ formed by the electron current i^- along the path length s is given by

$$i_0^+ = i^- \cdot s \cdot \sigma \cdot p \quad (9)$$

wherein σ is the ionisation probability and p the pressure. The drift velocity of the ions, according to equation (4), gives the expression

$$\dot{r} = \frac{r_0}{B} 2\sqrt{-a_{200}\, a_{020}} \quad (10)$$

The velocity z of the electrons, which passed a potential difference U, is

$$\dot{z} = \sqrt{2\, U\, e/m} \quad (11)$$

We therefore obtain

$$\varphi = \frac{i^-}{4\pi\varepsilon}\left(\frac{\pi\sigma B}{4\sqrt{-a_{200}\, a_{020}}}\, p - \frac{1}{\sqrt{2\ Ue/m}}\right) \ln\frac{er^2}{r_{02}} \quad (12)$$

If we substitute the numerical values of the operating data of the Philips omegatron, viz.

$B = 5000$ G ; $U = 90$ V ; $2\sqrt{-a_{200}\, a_{020}} = 2.4$ V cm^{-2} ; $r = R_0$; $r_0 = 2.5 \times 10^{-2}$ cm, we obtain at a value $\sigma = 12.5$ Torr^{-1} cm^{-1}

$$\Delta\varphi = (3.5 \times 10^9 \times p - 1.6 \times 10^3) \cdot i^- \text{ (volts)} \quad (13)$$

At pressures below 5×10^{-7} Torr the space charge effect of the electrons predominates the effect of the positive nonresonant ions. At a total pressure of 10^{-5} Torr and an electron current of 1μA we obtain $\Delta\varphi^+ = 35$ mV, $\Delta\varphi^- = -1.6$ mV.

If the normal operating data of the omegatron are used, the space charge of the positive ions and of the electrons will therefore vary the potential on the border of the electron beam at most by 35 mV to a more positive value with respect to the potential which is caused by the voltages applied to the electrodes and which, according to equation (6), amounts to about -600 mV. At an electron current of 10μA and at the maximum admissible measuring pressure of 10^{-5} Torr, however, the variation of the potential caused by the space charge reaches the magnitude of the electrostatic potential, so that the linear relationship between ion current and electron current no longer holds.

5. Operating conditions

The Philips omegatron has two operating conditions, viz. that for the measurement of partial pressures and that for the measurement of total pressures. The more important condition is the measuring of the partial pressures. In this case ions of a certain charge-to-mass ratio e/m satisfy the resonance condition. They take up energy continuously from the *rf* field and thus attain a sufficiently large size of their orbit, finally reaching the ion collector. The nonresonant ions do not take up sufficient energy. Their movement therefore corresponds mainly to the drift which guides the nonresonant ions away from the collector and towards other electrodes, as may be seen from Fig. 3 of the preceding paper. For a treatment of this movement we introduce the collection range (Fig. 3). As long as the macroscopic component of the ion path remains within this range, the

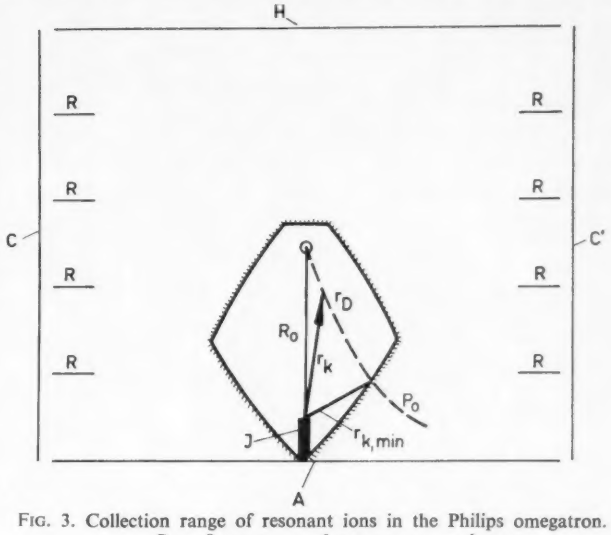

FIG. 3. Collection range of resonant ions in the Philips omegatron. $R_0 = 8$ mm ; $r_k = 6$ mm ; $r_{k,min} = 4$ mm.

resonant ions on their orbits spiral will hit the ion collector ; for in this region the collector is the nearest of all the electrodes. The macroscopic movement in the Philips omegatron is guided by the equipotential line P_0 (Fig. 3). Thus we can ensure that the guiding centre of all resonant ions remains within the collecting range, and that therefore ion collection is at its optimum. The condition for this, however, is that the time t_s required by a spiralling resonant ion to reach the ion collector is less than the time t_D after which the nonresonant ions produced at the border of the electron beam, will leave the collection range. According to equations (4) and (5) this means that

$$t_s = \frac{2B}{E_0} r_k < t_D = \frac{B}{2\sqrt{-a_{200}\, a_{020}}} \ln\frac{r_D}{r_0} \quad (14)$$

For the Philips omegatron, with $V_{rf} = 1$ V r.m.s. and $B = 5000$ G, we obtain the figures

$$\left.\begin{aligned} t_s &= 40\mu s \text{ with } r_k = 0.6 \text{ cm, i.e. the experimental value} \\ t_s &= 55\mu s \text{ with } r_k = R_0 = 0.8 \text{ cm, i.e. the maximum value} \end{aligned}\right\} \quad (15)$$

$$t_D = 65\mu s \text{ with } r_D = 0.7 \text{ cm} \quad (16a)$$

If we calculate the time required for almost all ions to leave the collection range, except for a small fraction of ions whose movement in the centre of the electron beam is delayed, we find a fraction of 1 per cent remaining within the collecting region after a time of

$$t_{1\%} = 150\mu s \quad (16b)$$

and a fraction of 0.01 per cent after a time

$$t_{0.01\%} = 225\mu s \quad (16c)$$

We have now to investigate whether during the drifting period t_D the amplitudes of higher harmonic resonances obtain values so that the corresponding ions can reach the ion collector. Apart from the ions with mass M, which are in their state of fundamental resonance at ω_{rf}, ions with mass $\frac{1}{2}M$, $\frac{1}{3}M \ldots$ would in that case be excited at the same frequency ω_{rf}. As the time of flight t_s of the resonant ions and the drifting period t_D, according to equations (15) and (16), are of approximately the same order of magnitude, the amplitude of the harmonic effects will reach values of $r_{k,\min}$ within the collection range only when the exciting functions of the higher harmonic resonances and that of the fundamental resonance attain equality in value. If the higher terms of the expression (6) may be treated as a perturbation, we thus find for the condition that ions excited by higher resonances should not reach the ion collector (see equations 1 and 2)

$$\text{grad } \varphi_{\text{perturb.}} < B\, r_s \omega_R \tag{17}$$

But this condition is satisfied at low mass numbers, for

$$\text{grad } \varphi_{\text{perturb.}} < 6 \text{ V/cm and}$$

$$B\,\omega_R r_s \simeq \frac{1}{M},\ 2{,}4 \times 10^3 \text{ V/cm}$$

with the values :

$V_{cc'} = -40$ V, $V_R = +0{,}4$ V, $B = 5000$ G, $M \leqslant 100$ mass units.

With the Philips omegatron it is possible to measure total pressures. For this measurement, no *rf* voltage is applied, and the negative voltage $V_{cc'}$ is, for example, reduced so far that a maximum ion current is obtained. In order to enable the ions to reach the collector, the point of origin of the ions must have about the same potential as the ion collector, i.e. a potential $\varphi = 0$, for the path of the ions corresponds to the macroscopic movement as no *rf* field is present. According to equation (4), the drift is practically independent of the mass of the ions, and guides the ions along equipotential lines.

The operating data for total pressure measurement must be adjusted so that the resulting potential, derived from the applied voltages and the space charges, attains the value of $\varphi = 0$. While for instance the values of $V_{cc'} = -40$ V and $V_R = +0.4$ V are required in the operating conditions for partial pressure measurements voltages of $V_{cc'} = -20$ V and $V_R = 0.4$ V must be applied for the measurement of total pressures at pressures of about 10^{-5} Torr. Neglecting the space charge effects, these values yield a potential of -175 mV at the point of origin (Fig. 4). Because of the space charge effects, the potential varies by about $+200$ mV according to equation (12). At low pressures, at which the space charge of the ions becomes small or at which the space charge of the electron beam might even prevail, the ratio of $V_R : V_{cc'}$ must be increased from 1 : 50 up to 1 : 35 or 1 : 30. This accords with the experimental values, according to which the adjustment for measuring total pressures is pressure-dependent.

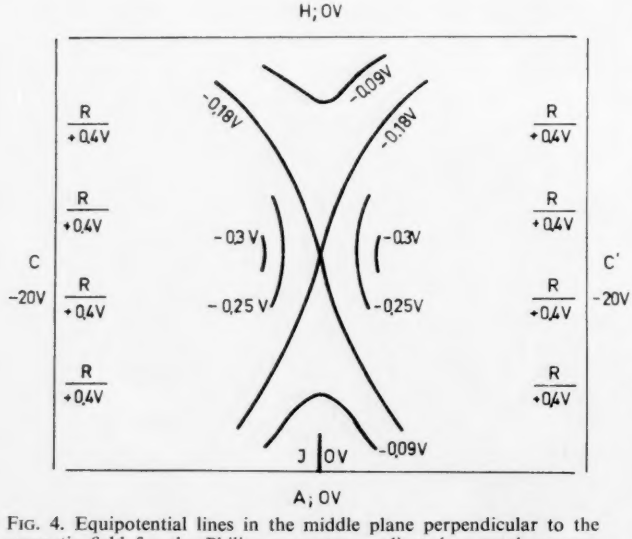

FIG. 4. Equipotential lines in the middle plane perpendicular to the magnetic field for the Philips omegatron, adjusted as total pressure indicator.

6. Resolving power

The resolving power of the omegatron is defined as $A = m/\Delta m$, where $m \pm \Delta m$ are the masses of that non-resonant ions, which just reach the collector.

For the resolving power the expression is derived :

$$A = \frac{m}{\Delta m} = \frac{\omega}{\Delta\omega}$$

and with the aid of equation (3) we obtain

$$A = \frac{e}{m}\,\frac{r_k B^2}{2 E_o} \tag{19}$$

This means that r_k, and thus A are not influenced within certain limits by the dependence of the resonance frequency on the coordinates x, y, z, caused by the electrostatic fields. For the ideal omegatron the following expression[2] is found

$$A_{id} = \frac{e}{m}\,\frac{R_o B^2}{2E_o} \tag{20}$$

A comparison of the resolving power of the Philips omegatron with that of the ideal omegatron amounts to a comparison of the critical distance r_k (Fig. 3) with the distance R_o :

$$\frac{A}{A_{id}} = \frac{r_k}{R_o} \tag{21}$$

The minimum value of this ratio becomes the smaller, the closer the equipotential line passes by the ion collector, for the possible values of r_k are between R_o and $r_{k,\min}$ (Fig. 3) at a given field distribution.

Acknowledgements

For their valuable suggestions and discussions in carrying out the work I wish to express my gratitude to Prof. Dr. J. Meixner and Dr. A. Klopfer.

My thanks are also due to Dr. J. L. Verster and Dr. ter Haar, of the Philips Research Laboratories, Eindhoven, for the measurements of the potential distribution.

References

[1] C. E. Berry ; *J. Appl. Phys.*, **25**, 28 (1954).
[2] H. Sommer, H. A. Thomas, and J. A. Hipple ; *Phys. Rev.*, **82**, 697 (1951).
[3] L. Spitzer, Jr. ; *Physics of Fully Ionized Gases*, Interscience Publishers Inc., New York, 1956.

Vol. 10 1960

A Precision McLeod Gage for Volumetric Gas Measurement

H. H. PODGURSKI and F. N. DAVIS

Edgar C. Bain Laboratory for Fundamental Research, United States Steel Corporation Research Center, Monroeville, Pennsylvania, U.S.A.

The modified McLeod Gage described is designed to measure pressures between 10^{-3} and 10^{-4} Torr with an accuracy of ± 2 per cent. A large-bore side arm isolated from the gage by a cut-off replaces the usual open-end capillary. This feature provides the means for calibrating the variations in capillary depression of mercury at every position along the length of the remaining capillary without contributing to the volume of the gage. A tapered plug used to seal the capillary end eliminates sticking even at 10^{-7} Torr and also extends the range of stable calibration in the ground capillary bore up to the end seal, thus extending the usefulness of the gage to a lower pressure limit. With these innovations, a gage of 200 ml capacity with a capillary of one-half mm bore was found adequate for the accuracy sought. Solution of helium in the pyrex capillary accounts for errors estimated between 1 and 3 per cent.; hence for volumetric calibration neon is preferable to helium.

Introduction

An error of 5 per cent or more can be expected when pressures are measured at 10^{-4} Torr with a conventional McLeod gage having two matched capillaries and a one liter capacity; yet this gage is frequently employed to calibrate ion gages down to pressures approaching 10^{-6} Torr. Such calibrations must be in considerable error. When the atmosphere in the system consists essentially of helium, more than 1 per cent of the gas sample compressed in the gage dissolves in the pyrex capillary during the time interval taken to measure the pressure. This constitutes one of the known sources of error. The variation in capillary depression of mercury noted at different positions along the length of a gage capillary proves of greater concern.

Working below 10^{-6} Torr with a gage equipped with matched precision bore capillaries (ground), the mercury level was observed to rise to a higher rest position in the sealed end capillary than in the matched open-end capillary. Furthermore, the difference in level varied with rest positions taken along the length of the capillary bore. If this source of error is neglected, the measured pressure values will be too low, conceivably by about 20 per cent (at 10^{-4} Torr). When attempts were made to minimize contamination in the mercury, the effect became more pronounced. We believe that a difference in concentration of trace impurities at the surface of the two menisci was produced by the very nature of the gage operation. The mercury-vacuum interface is extended as it enters into the gage bulb and drops several thousandfold as it passes from the bulb into the capillary above it; this large extension and compression of the mercury-gas interface does not occur in the meniscus entering the adjacent capillary. The concentration of soluble or insoluble impurities through adsorption or by mechanical means (turbulence) may well occur to a greater degree at the interface experiencing greater changes in area. Presumably a greater contamination level resulted at the meniscus in the sealed-end capillary above the gage bulb and the wetting of the capillary wall by mercury was enhanced.

With no reference point available in the conventional gage by which to calibrate the wetting behavior in either capillary, no dependable corrections could be made. The new gage design depicted in Fig. 1 solved these problems.

The basic contributions from this investigation are :

(1) Establishment of the need for calibration curves describing the wetting character of mercury at every position in the gage capillary.
(2) Isolation of the large dead space or volume of the reference arm replacing the open-end capillary.
(3) Use of a tapered plug seal on capillaries ; this eliminates sticking and extends the working range of the gage to lower pressures.
(4) Demonstration of helium solubility as the source of error when measuring helium pressures.

Gage design and assembly

A survey of the literature revealed a gage design (adopted by Keevil, Errington, and Newman[1] for use as a microgas burette) in which the capillary depression could be measured and corrected for, i.e., a reference existed for calibrating the wetting character of the capillary tube. The open-end capillary was replaced by a large-bore tube in which the mercury level in any rest position was independent of its wetting character. With this modification Keevil *et al* determined an average depression* of the mercury level in the closed-end capillary relative to the mercury meniscus position in the large-bore tube when the gage was completely

*Established with helium in gage (graphical method).

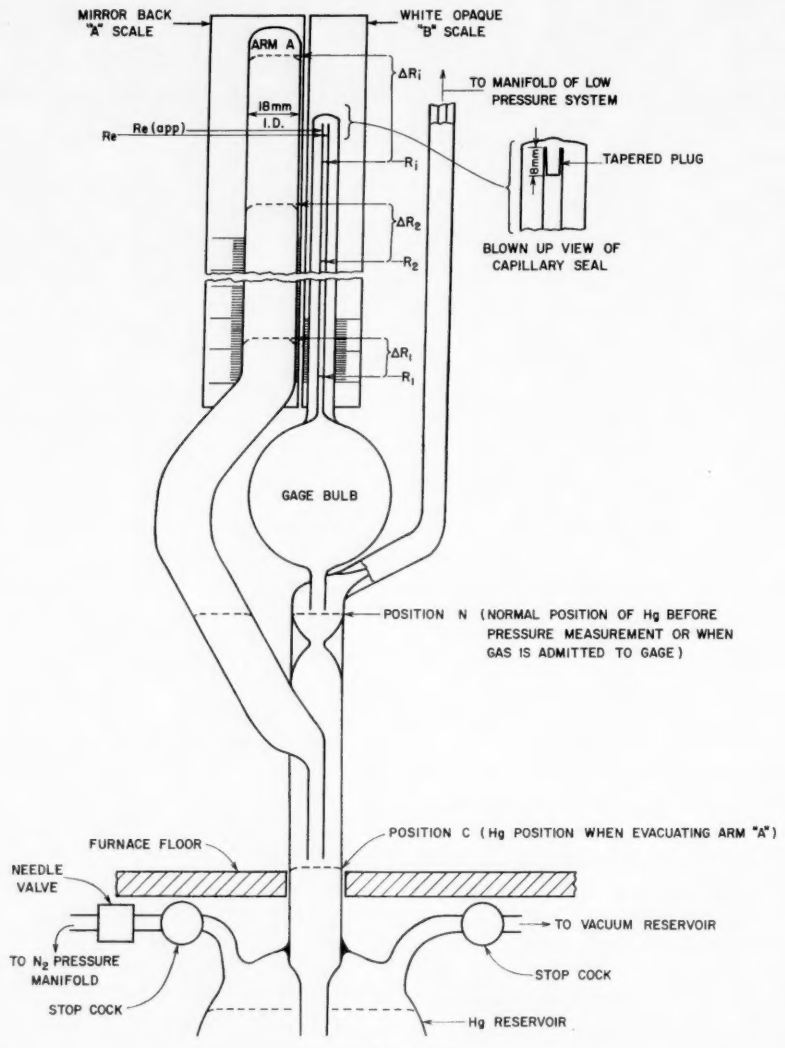

FIG. 1.

evacuated. They then applied this single correction to the pressure measurement of the helium gas sample captured in the burette or gage (one liter capacity). As will be shown later, a single average correction was found to be inadequate in our work. Furthermore, the large-bore side arm also contributes an undesirable dead space. In the design that we finally adopted (Fig. 1), this difficulty was overcome by isolating the large tube with the cut-off arrangement shown between position C and N. It remained to establish a wetting calibration curve for the closed-end capillary, i.e., a capillary depression value for every position along the capillary measured at very low pressures ($<10^{-6}$ Torr), and to demonstrate that the corrections afforded by this curve were valid at measurable pressures.

Another feature added to the new gage is the end seal on the capillary. The significance of this change will be appreciated after the pressure determination procedure has been discussed.

Gage calibration and operation

In normal operation, arm A in the modified gage (Fig. 1) is free of gas ($P < 10^{-6}$ Torr) and the mercury level is raised from position N. From a single value of ΔR_i(cor)* a pressure can be calculated according to conventional methods. As previously stated, the correction, d_i, for a particular R_i (any position in the capillary read on Scale B) has been found to vary along the length of the capillary; hence, the calibration curves of the sort illustrated in Figs. 2A and B were obtained. To insure their usefulness they are frequently checked for time stability. More will be said about this point later. When corrected ΔR_i values are used, the error in pressure determination is reduced to reading errors. If these errors can be assumed to be random in nature, several compression readings in a single pressure determination will increase the accuracy.

To take full advantage of multiple compression readings, the scale position (R_i) is graphed vs. the reciprocal of

*$\Delta R_i(\text{cor}) = \Delta R_i - d_i$.
ΔR_i is the difference between the meniscus levels in arm A and arm B; d_i is the capillary depression correction.

Vol. 10 196

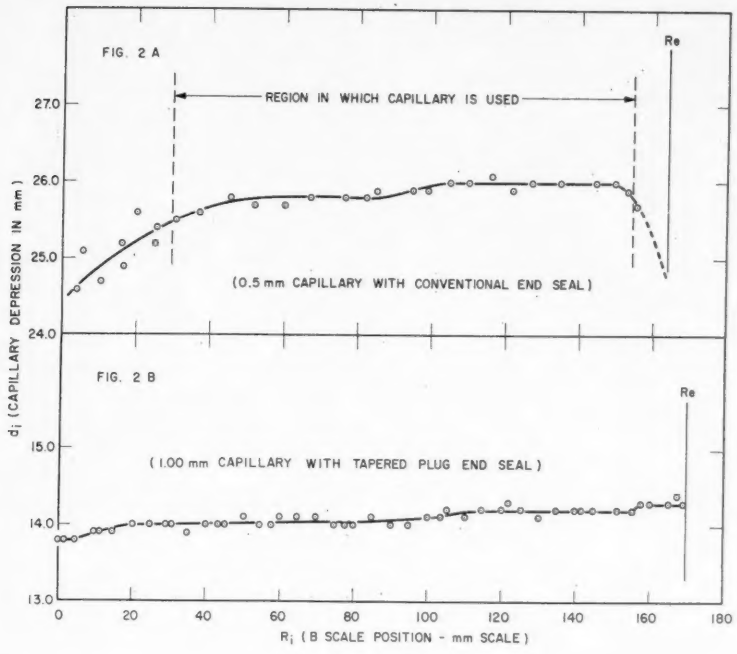

FIG. 2

ΔR_i(cor) as in Fig. 3. The corrections, d_i, now a function of R_i, are read from a calibration curve. The slope, C, of the graph need only be multiplied by the gage factor, F, to yield the absolute pressure*. Although the procedure is time consuming when first employed, many time saving steps may be taken once certain gage characteristics have been evaluated. Much of this information is obtained from the same graphs.

The most regular and most time-stable calibration curves were obtained in precision-bore capillaries with internal surfaces ground according to the method suggested by Rosenberg[2]. Annealing a capillary above 525°C destroys the benefit afforded by previous preparation. So, sealing the capillary end by fusion after grinding destroys the calibration stability some distance from the point of the seal. The effect obviously is quite undesirable as it does not allow reliable high compression values of ΔR_i(cor) to be obtained in the low pressure range of the gage. To effect this end seal, as illustrated in Fig. 1, a drawn tapered pyrex rod is inserted into the end of the capillary and fused only at its end. Thus sealed, an unannealed region for calibration is retained up to the position R_e. The value of this procedure is reflected by the stability and uniformity of the calibration curves in the vicinity of R_e. See Figs. 2*A* and *B*. No time stability was attainable in the calibration curve near R_e, regardless of tube diameter, for the conventional end seal. The volume of the annular space about the plug is not neglected, however, as the extrapolation of the straight line through the ordinate R_e yields R_e(app) rather than R_i†. R_e(app) must be established with certainty inasmuch as it contributes to the gas volume in the capillary above the mercury meniscus. Once established, fewer compression readings are needed to calculate a pressure accurately. This is particularly true when the gage is employed at its upper pressure limit and when a single compression point is taken.

Graphing compression data, as in Fig. 3, although time consuming, does reveal several interesting points which otherwise might remain unnoticed. Straight line curves intersecting the ordinate at the same R_e(app) for all gases establish unambiguously the applicability of the calibration curve for correcting ΔR_i values. Deviations from linearity indicated by the dotted curve in Fig. 3 suggest immediately the need for re-establishing the calibration curve. One exception to this test arises if the mercury is moved up into the capillary too rapidly during compression of a gas sample. Under this condition of gage operation an electric charge‡ builds up in the gage and nonlinearity results. The effect can be eliminated by allowing the mercury to rise slowly to the positions Ri. Experience will establish a reasonable rate to be used. Since the rate of rise is necessarily slow the practice of admitting pure nitrogen slowly into the mercury reservoir via a fine needle valve was adopted.

To check the validity of corrections afforded by calibration curves, volumetric calibrations were conducted with neon

*From the ideal gas law $[R_e(\text{app}) - R_i] \times \Delta R_i(\text{cor}) = C$ where $[R_e(\text{app}) - R_i]$ is proportional to the volume of gas compressed in the capillary at pressure ΔR_i(cor). System pressure $= C \times F$, where C = slope and F (gage factor) $= \pi \times$ (radius of capillary)^2/(gage volume). R_e(app) is the apparent position of the end seal in the capillary on Scale B (established by the point of intercept on the ordinate of the curve in graphs of the type illustrated in Fig. 3).

†R_e and R_e(app) will nearly coincide if the capillary tube is very uniform and the annular space about the plug is kept small.

‡A mercury thermometer suspended near the gage will be attracted to the gage arms and held there when the mercury level is moved rapidly up and down in the gage. An electrical discharge can be observed at certain gas pressures in the gage capillary with similar movement of the mercury level.

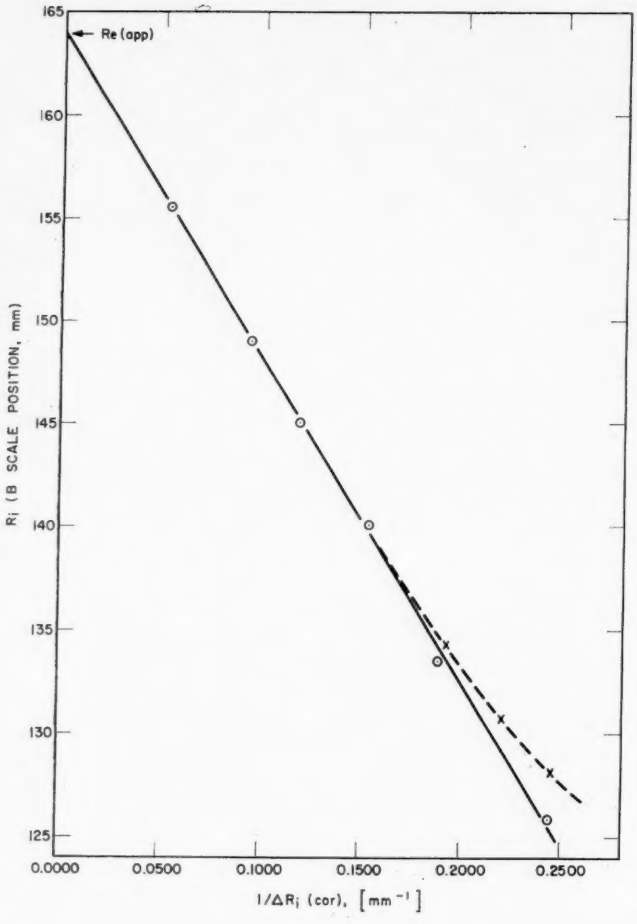

FIG. 3.

and xenon gas at system pressures between 10^{-4} and 10^{-2} Torr corersponding to gas pressures in the gage between 5 and 250 Torr during measurement. The calibration of a glass burette gave values within 0.1 per cent of the volume subsequently determined with mercury. The graphs of the compression data (as in Fig. 3) for the neon and xenon were linear and extrapolated to the same R_e in all instances. On the basis of gas adsorption theory these results leave no doubt that the calibration curves for mercury wetting of the capillary wall obtained at pressures below 10^{-6} Torr were valid with gas in the gage.

Gage conditioning

Several cleaning procedures were investigated to prepare the gage for final calibration : two bear mentioning. The one adopted entailed the use of concentrated nitric acid followed by a thorough rinsing with distilled water. The gage, which (except for the mercury reservoir) is housed in an oven, is baked at 400°C. While baking, with the mercury level set at position *C*, the gage is alternately evacuated and dosed with oxygen ($P_{O_2} \sim 5$ Torr). This operation burns out nonvolatile carbonaceous materials from the system and effects outgassing. Prior to raising the furnace temperature to 400°C, the mercury contained in the gage reservoir is heated while both the gage and reservoir are evacuated, care being taken to condense and return the volatilized mercury to the reservoir. Finally, the mercury level is always adjusted in the gage by pressurizing the reservoir with clean dry nitrogen to avoid unnecessary contamination of the system under normal operation.

The use of a 1 per cent HF solution as a cleansing agent proved disastrous even after extensive rinsing with distilled water. The pyrex glass cleaned in this manner " reacted " with mercury vapor during the bake-out operation as was evidenced by the enhanced and irregular wetting of the capillary wall by the mercury during calibration. The mercury actually was observed to rise higher in a $\frac{1}{2}$ mm capillary bore than in an 18 mm bore side arm and in a very erratic manner.

Helium solution in Pyrex glass

Preliminary calculations* on the possibility of obtaining a significant loss of helium by solution or diffusion into or through pyrex glass when measuring pressures in a McLeod Gage did not reveal cause for concern. Experimental observations did not confirm this conclusion. Very pure helium gas samples (measured in the closed-end capillary), when expanded into the closed evacuated manifold of our adsorption apparatus for dead-space determinations, gave values about 1–$\frac{1}{2}$ per cent lower than when neon and krypton were employed. Agreement existed between the values obtained with the latter two gases. Apparently, helium was disappearing from our system because of solution in the pyrex capillary during the interval between the two compression operations when measuring the two consecutive pressures. The minimum error expected in a single pressure measurement must be greater than 1–$\frac{1}{2}$ per cent, but could not be determined directly. The helium solution rate subsequent to the first pressure reading was measured by noting the loss of pressure with time. The results of the measurements are graphed in Fig. 4. The dashed curve was calculated by using the solubility value and diffusion constant for helium given by Alpert and Buritz[3]. The calculation was made using an equation[4] for the conditions of non-steady state diffusion through a cylindrical surface into an infinite medium. The observed amount of helium dissolved in the pyrex capillary over the first ten minutes, the shortest interval taken for a single pressure determination, is an order of magnitude lower than necessary to account for the estimated 1.5–3 per cent error in dead space determinations. Undoubtedly the initial rate of helium solution in pyrex depends upon the surface roughness and surface strains in the capillary under consideration and is not revealed in long-time experiments where the diffusion rate is established by permeation through a glass membrane. The inner surfaces of our capillaries were ground and not annealed. Recently, McAfee[5] reported that tensile stresses increase the permeability of pyrex glass membranes to helium. The disappearance of helium from the gage could not, under

*Calculations based on solubility and diffusion constant determined by Alpert and Buritz[3].

Vol. 10 196

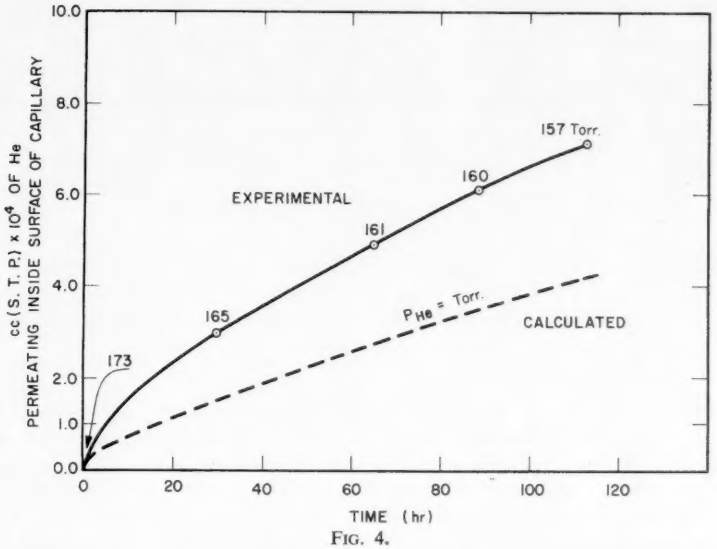

FIG. 4.

any circumstances, be attributed to the presence of gas impurities.

The precision claimed for this modified gage applies only when pressures are measured in a closed system saturated with mercury vapor. A symmetrical* refrigerated *U* trap separating a mercury-saturated atmosphere from one free of mercury can produce a pressure gradient across the trap ; the higher pressure develops in the mercury-free region. The magnitude of this effect is dependent upon the gas in the system. We have had to assume on occasion pressure differentials of 6 ± 2 per cent with xenon and 2 ± 1 per cent with argon in order to account for the distribution of these gases between those parts of a system separated by *U* traps. A value of 1 per cent is calculated employing equation 6, page 178, *Vacuum Technique*, by S. Dushman[6] for argon in a system with a pipe diameter 0.15 cm between the gage and *U* trap.

References

[1] N. G. Keevil, R. F. Errington, and L. T. Newnam, *Rev. Sci. Instrum.*, **12**, 609–611 (1941).
[2] P. Rosenberg ; *Rev. Sci. Instrum.*, **9**, 258–259 (1938).
[3] D. Alpert and R. S. Buritz ; *J. Appl. Phys.*, **25**, 202–209 (1954).
[4] H. S. Carslaw and J. C. Jaeger ; *Conduction of Heat in Solids*, p. 282, Oxford Press (1947).
[5] K. B. McAfee ; *J. Chem. Phys.*, **28**, 218 (1958).
[6] S. Dushman ; *Vacuum Technique*, John Wiley & Sons, Inc., New York.

*Symmetrical *U* traps used to avoid the development of pressure gradients attributable to the thermal transpiration effect.

An Omegatron Spectrometer, its Characteristics and Application*

E. J. ZDANUK, R. BIERIG, L. G. RUBIN and S. P. WOLSKY

Research Division, Raytheon Company, Waltham, Massachusetts, U.S.A.

The development of an omegatron mass spectrometer as a relatively inexpensive and automatic scanning analyzer is described. Operating characteristics of the device in the pressure range 10^{-5} to 10^{-9} Torr are given. Areas of application in which the omegatron is especially suitable are indicated by some preliminary work.

In recent years the demand for relatively simple and inexpensive equipment for gas analysis has led to the development of the omegatron spectrometer. The omegatron is a device of small volume which may be used to determine the composition of a gas in the pressure range from 10^{-5} to 10^{-9} Torr. In this ultra-high vacuum region, the partial pressure of a gas component is often more important than the total gas pressure. The omegatron is suitable for such operation since it has reasonable resolution at high sensitivity and is constructed of materials which can be baked out at elevated temperatures to achieve low residual pressures.

In 1949 Hipple and co-workers[1] first proposed such a device and in 1951[2] described it in detail. In 1954 Alpert and Buritz[3] developed a simplified omegatron for analysis in high vacuum systems. Since then, a number of laboratories[4] have developed omegatrons tailoring them to their specific use and several workers[5] have analyzed theoretically the principle of operation of the device.

This report presents some of the results we have obtained in developing the omegatron as a convenient and reliable analytical tool for high vacuum work.

Principle of operation

The principle of operation of the omegatron is similar to that of the cyclotron. Ions formed by an ionizing electron beam passing through a shielded volume are subject to crossed magnetic and high frequency electric fields. For a given strength of the magnetic field and frequency of the electric field, ions of a selected e/M ratio (e is the electric charge and M the mass of the ion) will spiral until trapped by a suitably placed collector within the shielded volume. The selection of ion may be made by changing either the frequency of the electric field or the strength of the magnetic field. There are in the literature[3, 5, 6] several theoretical analyses of the motion of ions in an omegatron and some of the more useful expressions are given below.

The cyclotron frequency is given by

$$f_c = 1.525\, Bn/M \ (mc) \tag{1}$$

where B is the magnetic field in kilogauss, M is the mass of the ion in atomic mass units, n is the charge of the ion in units of electron charge, and the frequency f_c is in megacycles. In an idealized omegatron, at a particular magnetic field strength and electric field frequency, ions receive energy "kicks" with each revolution and travel in an expanding spiral terminating at the collector. Although all ions within the shielded volume are being affected, those ions having e/M ratios differing from the resonant value tend to lead or lag the coherent motion. After a small number of revolutions, these ions will lose any energy gained from the fields and thus remain near the points of their origin along the electron beam. From the equation of motion of ions near resonance, one finds that ions will not reach the collector if they have a resonant frequency differing from the operating frequency by more than $\Delta\omega^*$, given by

$$\Delta\omega^* = E_0/r_0 B \tag{2}$$

where E_0 is the amplitude of the electric field, r_0 the distance from electron beam to the collector, and $\Delta\omega^*$ is expressed in units of angular frequency. We may use this relationship to determine an expression for resolution. This is given by

$$R = \frac{\omega_c}{2\Delta\omega^*} = \frac{M}{\Delta M} = 96 B^2 r_0/ME \tag{3}$$

where r_0 is in cm, E_0 in V/cm, and others in above mentioned units. An experimental resolution may be obtained from a scan by measuring a Δf at the base of a peak. The time required for the resonant ion to reach the collector, τ, and the number of revolutions made by the ion, N, are given by the following expressions respectively :

$$\tau = \frac{2Br_0}{E_0} \times 10^{-8} \text{ (sec)} \tag{4}$$

$$N = \frac{e}{M}\frac{r_0 B^2}{2\pi E_0} = 2B/\pi \tag{5}$$

The distance travelled by the resonant ion, L, is approximately equal to the average circumference of the spiral times the number of revolutions,

$$L = \pi r_0 N = 2r_0 R \tag{6}$$

For the average sized omegatron having as the shielded

*Of the papers published since this work, the following are of special interest to workers in the field :—
R. Warneche ; Thesis, University of Paris (1959).
D. Charles, R. J. Warneche, Jr. and J. C. Marchois ; *Le Vide*, 23, 274 (1959).
D. Lichtman ; *J. Appl. Phys.*, 31, 1213 (1960).

Vol. 10 1960

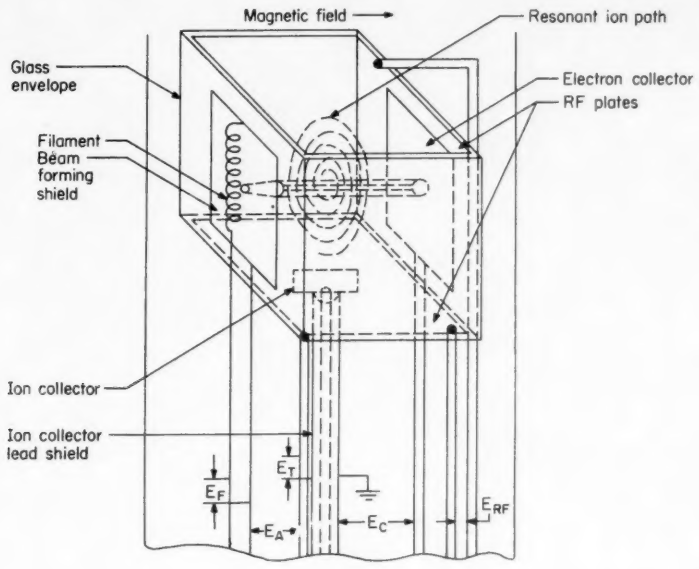

FIG. 1. Diagram of an Omegatron.

volume a cube of about one inch on edge and with magnetic field of several kilogauss, the time of flight is of the order of tenths of a millisecond, the number of revolutions is in the hundreds, and the distance travelled is in the tens of meters.

Apparatus

Fig. 1 shows the essential parts and the geometric arrangement of an omegatron tube. The spiral ion path was confined to a shielded cubic volume. The top and bottom faces of the cube were electrically isolated from the sides of the cube and formed the high freqeuency or *rf* electrode system. For a tube designed to operate with single-ended *rf* excitation only, the bottom plate was connected internally to the tube shielding the ion collector lead. Holes in the center of two opposite faces of the cube permitted an ionizing electron beam to traverse the shielded volume. On the outside opposite one of the holes was a filament with a shield having an aperture which aided in forming the beam and minimized emission to the other structures of the tube. Opposite the other hole was a collector for the electrons which had passed through the cube. Up through the bottom *rf* plate was the ion collector, which protruded into the shielded volume and was oriented in a direction parallel to the electron beam. The lead from this collector, which carried the minute ion currents i^+, passed down through a grounded shielding tube.

For proper operation of the tube, the magnetic field had to be oriented in line with the electron beam. This orientation was very critical as may be estimated from the narrowness of the electron beam path which was determined by apertures several hundredths of an inch in diameter. The electrons were accelerated through the cube by a potential between the filament and cube shield, E_A. The exit electrons were prevented from returning to the cube volume by a positive potential on the electron collector, E_C. Such returns must be minimized to prevent electron beam oscillations which can seriously disturb the field within the shielded cube.[6] A small positive trapping potential, E_T, was applied to the cube sides to control ion drift in the direction of the magnetic field. The *rf* potential, E_{RF}, applied between the *rf* plates and the electron current, i^-, measured by a meter in the collector circuit were two more parameters that determined tube operation.

In the tubes that were used, the cube was 2 cm on edge and the electron-beam-forming holes were about 50 mils in diameter. One of the tubes, Tube *A*[7], had a fine straight wire filament of heavier tungsten wire in the form of a double helix, and the metal sheets were of molybdenum instead of platinum. In the months in which both tubes were in operation, the substitution of molybdenum for platinum in Tube *B* was not detrimental to tube operation and imposed no new limitations on tube use.

The power supply of the omegatron tube was of conventional design. Filament power was supplied by an adjustable, voltage-regulated, sixty-cycle source (6.3 V at 6 amp maximum). Electron acceleration was made possible by the application of up to -150 V (E_A) to the filament with respect to ground. The electron collector potential, E_c, was variable from 0 to ± 45 V above ground, while the trapping voltage, E_T, was variable over the range from 0 to 1.3 V. The wide range adjustability of the supply was a necessary feature for experimental work with different tubes as will become evident when it is shown how the optimum operating characteristics of an omegatron tube will vary, depending on the particular tube and the use being made of it.

Fig. 2 is a block diagram of the omegatron system, showing some of the associated equipment. The permanent magnet, which had three-inch diameter pole faces, yielded a uniform

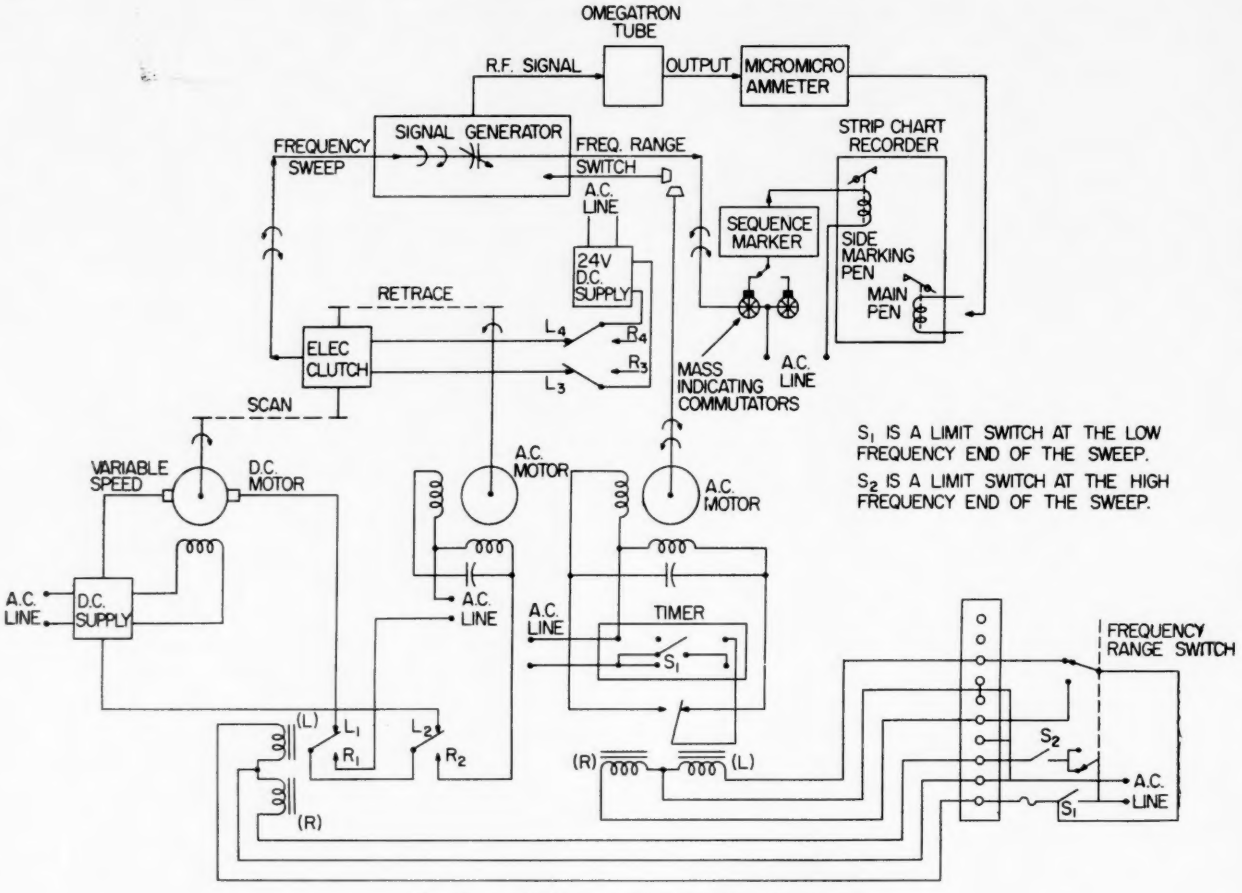

FIG. 2. Block Diagram of the Omegatron System.

field of about 3400 G over an area of about two inches in diameter, inside of a $1\frac{1}{2}$-in. air gap. Similar units are obtainable from the Arnold Engineering Company of Marengo, Illinois.

The function of measuring the low level ion currents flowing in the ion collector circuit was satisfactorily performed by the Keithley Model 410 micro-microammeter which was capable of measuring currents as low as 5×10^{-14} amp. The task of achieving stability at these low levels was made easier by: (1) providing a continuous shield extending from the ion collector itself to the input of the micro-microammeter. A portion of this shield is inside of the tube (Fig. 1); the external shield is carried right up to the glass base; (2) insuring that only high resistance paths (greater than 10^{13} ohms) existed between the ion collector and all other tube elements, including the circuit ground. This necessitated the use of Teflon insulated connectors, as well as a careful cleaning of the tube base to eliminate surface leakage; (3) using "noise free" coaxial cable for the flexible lead between tube and micro-ammeter. This type of cable employs a conductive coating on the outer diameter of the insulation separating the inner and outer conductors to eliminate the build-up of charge as the cable insulation is flexed.

The strip chart recorder was a 10 mV, self-balancing potentiometer type, such as the Leeds and Northrup Speedomax G or the Bristol Dynamaster. A pen lifting mechanism and an auxiliary marking device (either a side marking pen or margin print wheel) were installed on the recorder for reasons to be described below.

From Eq. 1, it is apparent that for a constant value of magnetic field, B, it is the value of the frequency of the applied electric field that will determine the mass of a singly ionized atom picked up by the ion collector. This, the problem of designing an automatic scanning mass spectrometer mainly resolves itself to the design of a sweep for the signal generator. The first model of such a device was based on the use of a Hewlett-Packard Model 650A generator, which will normally supply up to three volts at frequencies from 10 c to 10 mc/sec in six decade steps. The automatic gain control circuit of this instrument provided it with a frequency-independent output amplitude. For a magnetic field of 3400 G, a frequency range of from 60 kc to 6 Mc was required to cover a mass range of from 1 to 100. The frequency determining resistors in the phase shift oscillator section of the 650 A were thus increased sufficiently to lower the normal ranges (0.1–1 Mc; 1–10 Mc) to the desired values.

In order to mechanically sweep the frequency, three motors were employed. The first, a variable speed d.c. motor, was coupled through one shaft of a duplex electromagnetic clutch to the main tuning capacitor. A fixed speed a.c. motor (No. 2) was coupled to the second shaft of the clutch and rotated in a direction such as to drive the tuning capacitor from the high toward the low frequency end. The third motor, a fixed speed, synchronous, reversible unit, engaged the frequency range switch.

With the aid of the necessary circuitry, the scanning sequence was made to follow a prescribed schedule. Starting at the low end of the first frequency range (60 kc), the tuning capacitor was turned slowly up scale by motor No. 1 (speed range 2–30 min per revolution). At the upper limit of the scale (600 kc), the closing of a microswitch contact caused motor No. 2 to quickly return the capacitor to its starting point (4 sec retrace time). Simultaneously, motor No. 3 caused the frequency range switch to advance to the next range (0.6–6 Mc). A timer was used to ensure that this advance was exactly one-sixth of a revolution, corresponding to a 60 degree switch index. The retrace cycle was terminated by the closing of a second microswitch contact, which again started the slow scan—this time for the high range. At the completion of this scan, the retrace cycle was repeated, except for the reversing of motor No. 3 which now returned the frequency range switch to its initial, or low range, position.

By causing the recorder chart to stop and the pen to lift during the retrace time, a continuous spectrum of ion current versus frequency (mass) was obtainable. In addition, a multicontact commutator, rotating synchronously with the frequency drive shaft, was used to mark frequencies along the recorder chart margin. Because the same equipment was normally used on different tubes with different magnets, it was necessary to initially correlate the frequency markers with mass numbers for each tube, after which the spectrum was direct-reading in mass number.

The system described above was designed and fabricated from available components in an effort to save time. A new version of the apparatus is presently being constructed with improvements in both the mechanical and electrical design. It is worth noting that although the Hewlett-Packard generator has only a single-ended output, the addition of a simple two-tube circuit makes possible a balanced output. This is necessary if it is desired to work with omegatron tubes utilizing the "double *rf* plate" structure.[9]

The omegatrons were used in conjunction with two different vacuum systems. One system had a single stage oil diffusion pump with a single liquid nitrogen trap. This system had no provision for high temperature bakeouts, althought bakeouts at temperatures of between 150° and 200°C were carried out using electrical heating tapes. This system was capable of achieving pressures of 5×10^{-8} Torr. A second system used only with Tube *B* had two mercury diffusion pumps in series, two liquid nitrogen traps, one of which was bakeable, and provisions for high temperature bakeout at 450°C. In this system pressures of 1×10^{-9} have been obtained.

Operating characteristics of the omegatron

In an idealized omegatron, the following conditions are assumed to be in existence within the shielded volume :

(a) the magnetic and electric fields are homogeneous
(b) the fields are oriented perpendicular to one another
(c) ions originate in or near the electron beam only
(d) ions are formed with a negligible amount of kinetic energy
(e) no space charge exists to distract the field governing the motion of ions.

For the real tube, some or all of these conditions are only approximated. Other processes in the tube, but outside the shielded volume, can also affect the tube operation ; leakage along surface of glass between leads, changes in contact potential, flow of electron currents not part of the ionizing beam to elements of the tube structure, etc.

A. *Background current.*—One of the limitations on the sensitivity of the omegatron is the presence of a background current which tends to swamp out low level resonant ion currents. This current is made up of ions which are able to reach the collector by means other than the cyclotron type of motion. This current is measureable when no *rf* potential is applied.

Experimentally it has been found that the background current, $i^+(B)$, is affected by each of the operating parameters, E_T, E_A, E_c, i^-, and gas pressure, P. In general, the dependence of $i^+(B)$ on these parameters is not simple.

Fig. 3 shows, for Tube *A*, the dependence of $i^+(B)$, on E_T,

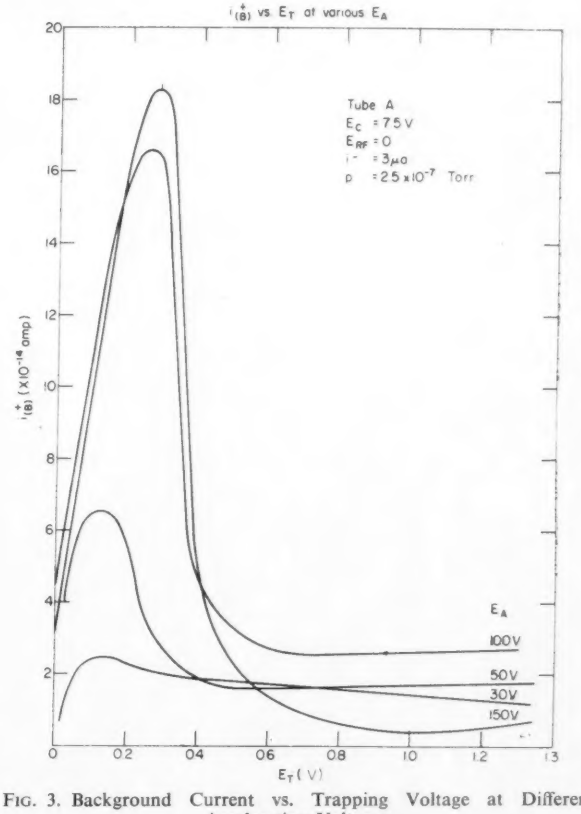

FIG. 3. Background Current vs. Trapping Voltage at Different Accelerating Voltages.

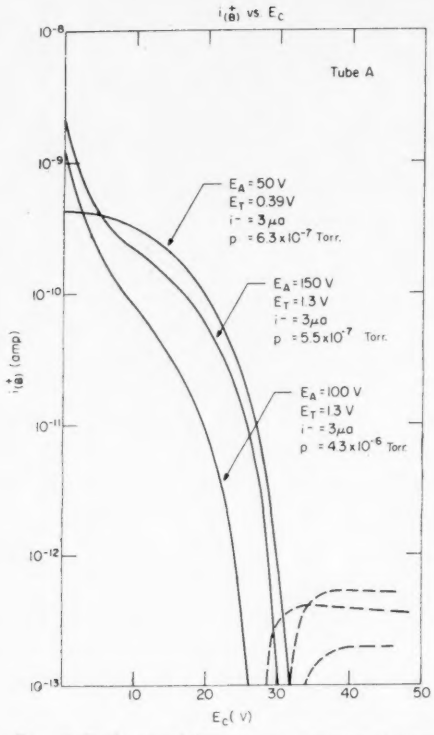

FIG. 4. Background Current vs. Collector Voltage.

for different values of E_A. These curves showed substantial maxima in the region of low E_T. An expected decrease in ion current reflecting a decrease in ionization cross section with increasing electron energy appeared only at the higher trapping voltages. Tube *B* showed a similar behavior. McNary[6], using a more refined omegatron, also found maxima in the curves of $i^+_{(B)}$ vs. E_T.

In Fig. 4, Tube *A* shows a change in $i^+_{(B)}$ of several orders of magnitude for a collector voltage change from 7.5 to 30 For Tube *B*, a similar change in collector voltage changes the background current by only a factor of 2 or 3. Although the tubes differ substantially in this property, operating conditions for both tubes could be found which would bring the background current to equally low values.

B. *Sensitivity and resolution.*—The effect of trapping or bias voltage and *rf* voltage on peak height is shown in Fig. 5. These curves represent the peak heights above background for ions of mass 36, a minor component of the gases in the system, having a partial pressure of about 10^{-8} Torr. It will be noted that these peak height curves for lower E_{RF} voltages are very similar to the $i^+_{(B)}$ vs. E_T curve at E_A = 30 V in Fig. 3.

The change of peak ion current with *rf* voltage and pressure is shown in Fig. 6. The knees in the curves, at about 1.0 V, correspond to points at which large decreases in resolution, $M/\Delta M$, with increasing *rf* voltage takes place. For the conditions as noted on the figure, the theoretical resolution for mass 28 ions at E_{RF} equal to 0.2, 1.0, and 2.0 V, are 200, 40, and 20, respectively. For the same values of E_{RF}, the observed resolutions determined by measuring the base widths of peaks are on the average 40, 15, and 8, respectively. In general, the observed resolution decreased with increasing pressure. For high resolution, operation must be in a region of low *rf* voltages, which requires very stable voltage output to prevent large instrumental variation in peak

Vol. 10 1960

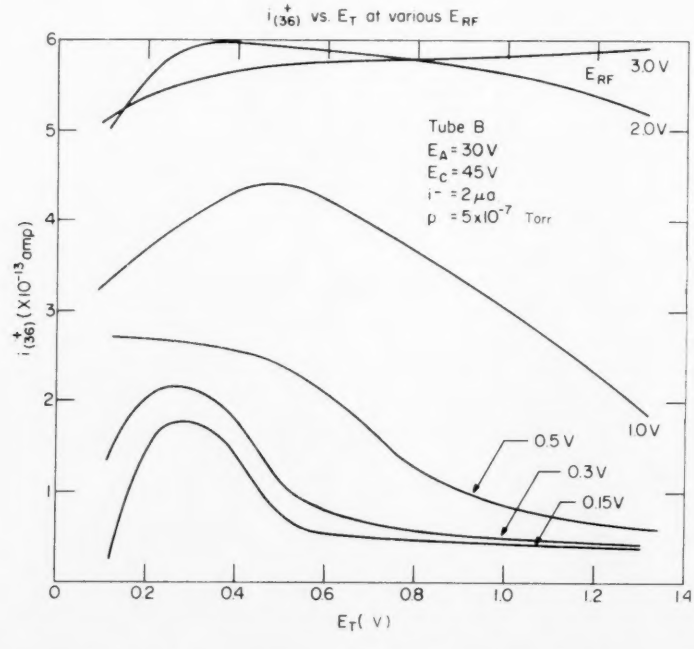

FIG. 5. Mass 36 Peak Ion Current vs. Trapping Voltages at Various Radio Frequency Voltages.

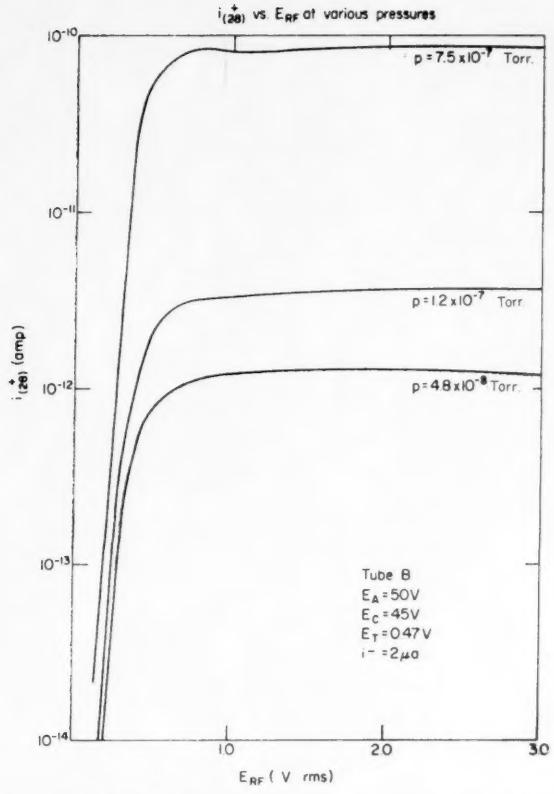

FIG. 6. Mass 28 Peak Ion Current vs. Radio Frequency Voltage at Various Ion Gauge Pressures.

heights. These curves are for peak heights of mass 28 ions, which may correspond to N_2 or CO. Since the mass 28 component represents about 80 per cent of the residual gas, an estimate can be made on the sensitivity. At 0.75 V, the sensitivity is 10^{-9} Torr, where sensivitity is defined as the pressure in Torr yielding an ion current of 10^{-14} a. For *rf* voltage of 0.25 V the sensitivity drops to about 10^{-8} Torr. These values are comparable to those found by other workers[4, 6] although operating conditions were somewhat different. Assuming a linear relationship between partial pressure and peak ion current, an estimated sensitivity of 10^{-9} Torr for krypton at an *rf* of 0.3 V is obtained from experiments in which krypton was added to the system. In some recent experiments with argon a sensitivity of 10^{-11} Torr for this gas was obtained with the above assumption.

C. *Individual tube differences.*—Although the two tubes used in this study displayed differences in the dependence of background current and optimum operating conditions on various parameters, equivalent operating characteristics could be obtained after adjusting the parameters to the particular values associated with each tube. At these equivalent operating conditions there was little difference in the sensivitity of 10^{-9} Torr ($\pm$10 per cent) when operated to yield unit mass difference for ions in the mass 35 region. Over a period of several months during which the tubes were subject to a variety of bakeout treatments and ambient conditions, the reproducibility between ion gauge currents and total omegatron peak ion currents, and of resolution was about 5 per cent for each tube. The primary sources of deviation from such behavior have been traced to poor orientation of the magnetic field or a short term initial instability in tube operation immediately following an exposure to atmospheric pressure or immediately following a bakeout treatment. Operating of the tubes for several hours restores normal tube operation in the latter case.

Applications

An indication of some of the areas in which the omegatron is especially useful is given by a brief description of some initial applications of this device in our laboratory.

The composition of residual gases in vacuum systems is always of interest to workers in high vacuum. At times, such analysis is of major importance, as in the case of efforts to create an inert environment by vacuum.

We have applied the omegatron to determine the composition of residual gases in two types of vacuum systems. Fig. 7 represents a mass spectrum of the residual gases with added krypton in an oil diffusion pump system having liquid nitrogen traps. It will be noted that there are substantial components having masses to 72, which are probably long chained hydrocarbons. This scan also shows the krypton peak of mass 83–85. The much greater resolution of the krypton peak with a loss in sensitivity is shown on the left, which was measured at a reduced *rf* voltage, 0.15 V, and in which the structure in the krypton peak reflects the krypton isotope distribution. Fig. 8 is a scan of a mercury diffusion pump system and we note that there are no detectable components of mass greater than 44. It should be noted that this scan was made with the residual gas pressure almost an order of magnitude greater than the pressure for the oil diffusion pump system.

Another aspect of vacuum systems which is of major importance in the ultra-high vacuum region is the adsorption and desorption properties of various parts of the vacuum system. We have applied the omegatron to determine these properties for an ion gauge. The source and sink behavior of a standard ion gauge, the Bayard-Alpert type, operating at an electron current of 10 mA in the pressure region of 10^{-7} Torr is shown in Fig. 9. The total volume of the system was about 500 ml, and since the mass 28 component constituted more than 80 per cent of the gas in the system, the gas involved in the adsorption and desorption is not negligible for work at high vacuum. The rapid drop in pressure when the hot filament of the gauge is turned off is probably the result of an adsorption action of the cooling tungsten wire, and the rapid rise in pressure when the filament is turned on shows the desorption action of the filament. The slow decrease in pressure, or in ion current of the omegatron, after the maximum reflects the adsorption action of the glass envelope, filament pumping, and the other metal structures of the gauge. A high rate of decrease in pressure was observed when the temperature of the glass envelope was lowered by the use of a fan. As is indicated by the spike in the low nearly constant region after the ion gauge was off, the technique of making a quick pressure reading with the

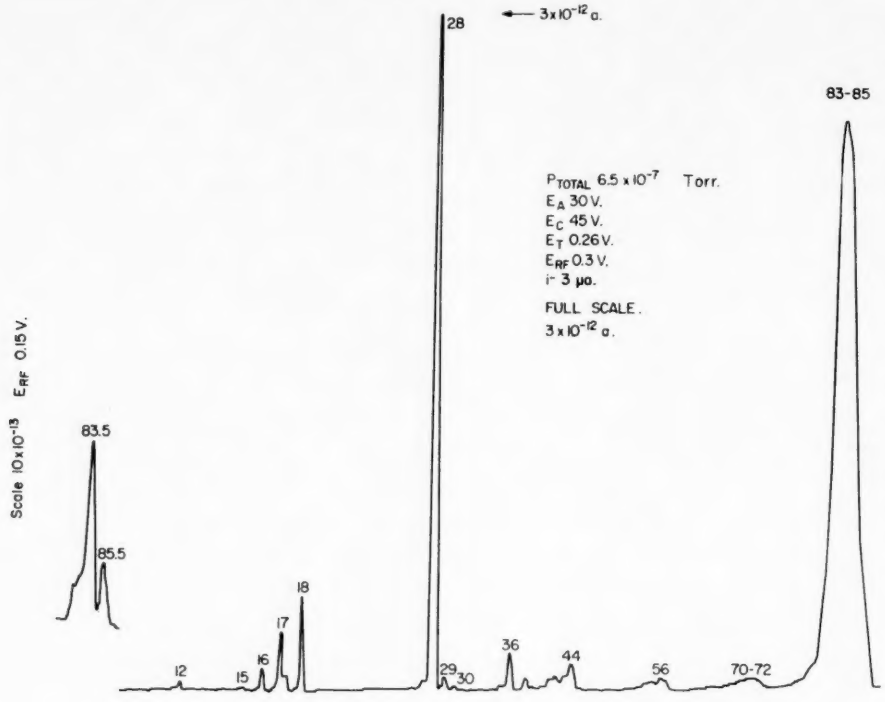

FIG. 7. Mass Scan of Residual Gases with Added Krypton in an Oil Diffusion Pump System.

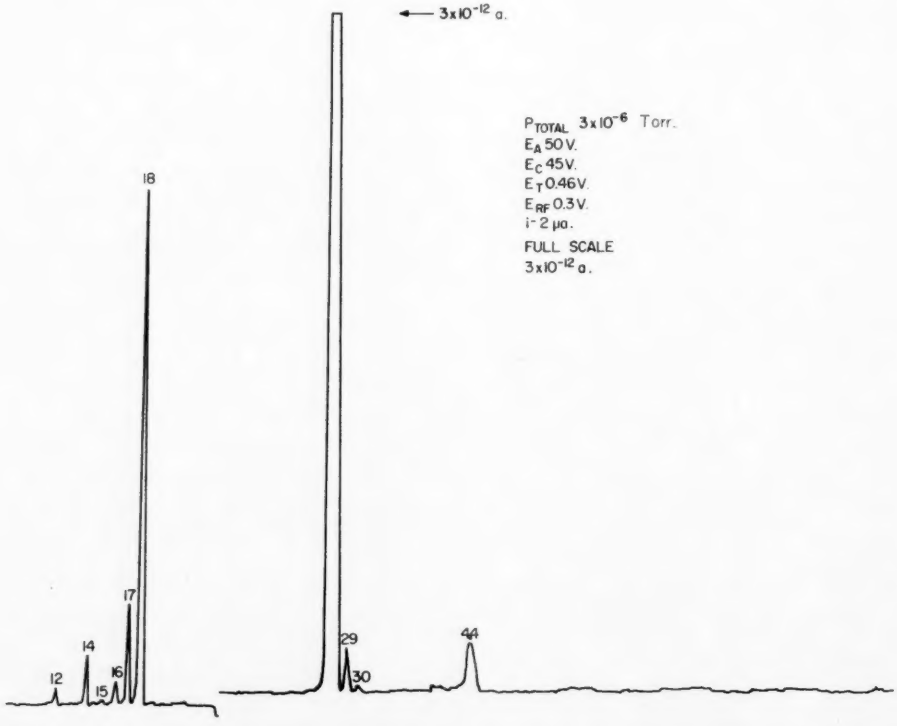

FIG. 8. Mass Scan of Residual Gases in a Mercury Diffusion Pump System.

Vol.
10
1960

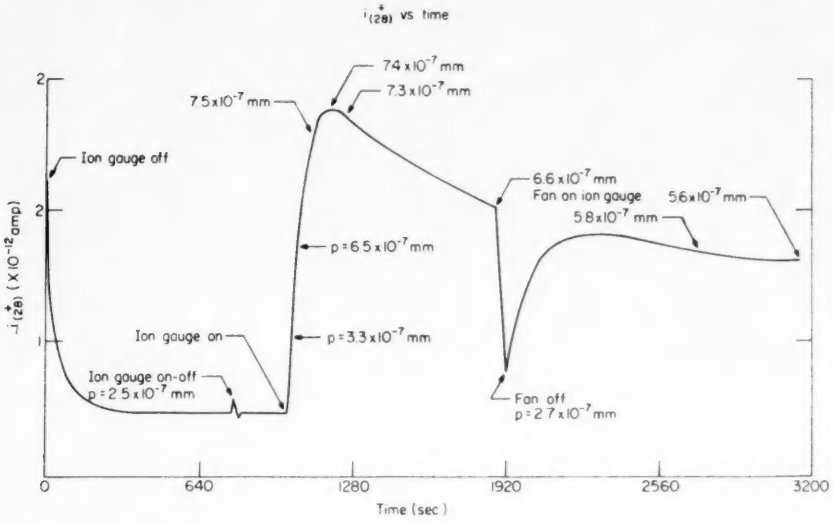

FIG. 9. Adsorption and Desorption Behavior of an Ion Gauge.

gauge does not introduce any substantial change in the pressure of the system.

We have used the omegatron to monitor a gas stream for components which may destroy the inert quality of the gas. In one such system the grease in ground glass joints and stopcocks introduced sufficient hydrocarbons to make the gas unacceptable. This introduction was made with no intervening cold traps. The inclusion of two liquid nitrogen cooled traps and a molybdenum getter bulb in the gas train in a second system gave a gas which showed no hydrocarbon-like components.

Conclusion

Our experience with the omegatron shows it to be a reliable instrument for mass analysis of gases in the pressure region of 10^{-5} to 10^{-9} Torr. The tubes require individual study to determine optimum operating conditions when the tubes are very similar in construction. The associated instrumentation should be chosen with care to exploit the tube capabilities to the highest degree. The data obtained from the omegatron is reproducible and sufficiently accurate to make the device suitable for study of high vacuum systems.

Acknowledgement

The authors wish to acknowledge the assistance of P. Rodriguez and K. Boericke in making omegatron measurements, and T. Driscoll and I. Fish of Raytheon Power Tube Division for handling the fabrication of one of the tubes. We are grateful to Dr. D. Smith of Lincoln Laboratories for the loan of an omegatron during our initial studies.

References

[1] J. A. Hipple, H. Sommer, and H. A. Thomas ; *Phys. Rev.*, **76**, 1877 (1949).
[2] H. Sommer, H. A. Thomas, and J. A. Hipple ; *Phys. Rev.*, **82**, 697 (1951).
[3] D. Alpert and R. S. Buritz ; *J. Appl. Phys.*, **25**, 28 (1954).
[4] R. L. Bell ; *J. Sci. Instrum.*, **33**, 269 (1956).
P. A. Redhead ; *Trans. Roy. Soc. Can.*, **47**, 134 (1953).
R. E. Schlier ; *J. Appl. Phys.*, **29**, 1162 (1958).
D. Charles and R. J. Warnecke, Jr. ; *Le Vide*, **73**, 25 (1958).
[5] C. E. Berry ; *J. Appl. Phys.*, **25**, 28 (1954).
W. M. Brubaker and G. D. Perkins ; *Rev. Sci. Instrum.*, **273**, 720 (1956).
[6] L. R. McNary ; *Canad. J. Phys.*, **36**, 1710 (1958).
[7] Tube A was made by E. Leybold of Germany.
[8] Tube B was made at the Power Tube Division, Raytheon Company, Waltham, Massachusetts.
[9] L. R. McNary, *N.R.C. Report* No. 4259 (ERA–311) (1956).

Book Reviews

TRANSACTIONS OF THE VACUUM METALLURGY CONFERENCE 1959. Edited by Rointan F. Bunshah. xi—212 pp. New York University Press, New York, 1960. $7.50, paper.

DR. BUNSHAH is to be credited with producing a fine edition of the papers presented at the New York University Conference on Vacuum Metallurgy, 1959. It is well organized, carefully edited, and attractively published with many large, clear photographs, tables of data, and graphs. One or two of the papers presented at the Conference do not appear in the proceedings, but are in each case papers that have been presented in substance at meetings of the American Vacuum Society, and other organizations. Having attended this conference, this reviewer regrets that the motion pictures shown there cannot be published and that some of the slides cannot be published in color. The economics and delays of such effort would scarcely be worthwhile, and Dr. Bunshah has edited carefully where motion or color were used by the speaker to bring out a point.

The Proceedings are divided into six sections of several pages each : Vacuum Arc Melting and Casting has seven very advanced papers on handling of the refractory metals and alloys for the Atomic Energy and missile-space applications. This group of papers is clear, concise and authoritative, with data on the design of the equipment as well as on the analysis of results. These papers constitute almost one-third of the publication.

Next are three sections of one or two articles each, Vacuum Investment Casting, Vacuum Induction Melting and Vacuum Degassing. As before, these articles are concerned with more advanced techniques and concentrate on the super alloys, ultra pure iron and forging steels. The articles are all both thorough and concise, with well organized tables of data and graphs.

The fifth section contains five papers on Electron Beam Techniques in Vacuum Metallurgy. The first of these articles is on electron beam melting of titanium and its alloys by Charles Dittmar and Stanley Abkowitz. It contains considerably more detail and data than was available from the same authors at another meeting several months before. The second article on electron beam melting of beryllium is a fourteen page report on a well organized research program of great interest, and remains one of the few articles on the subject that have been published.

The third and fourth papers in this section are on electron beam welding and were of interest at the time of the conference but have since received large amounts of publicity. They do not discuss obsolete equipment, however, simply because no major advances have been made in this technique during the months that have elapsed. The fifth paper, also discussed at a prior meeting, contains the final data and conclusions which were not previously available. A very complete bibliography on electron beam techniques, compiled by Dr. Bunshah, appears at the end of the proceedings.

The final section is composed of individual articles of a wide variety, covering such techniques as vacuum brazing, vacuum melting of Super Duty Steels (Aksoy and Buehl), magnetic properties of vacuum melted alloys, and so forth. These articles are of great importance to certain groups, adhere to the same high standards of the other papers, and do not occupy an unduly large share of the available space.

This publication and the others in the series will be of primary value to the metallurgists and the mechanical engineers that must deal with materials of exceptional properties, and of general interest to those engaged in a wide variety of other activities.

JAMES S. HETHERINGTON
Boston, Mass.

Vol.
10
196

Organisation internationale pour la Science et la Technique du Vide

International Organization for Vacuum Science and Technology

Internationale Organisation für Vakuum-Physik und -Technik

ASSOCIATION SCIENTIFIQUE

30, avenue de la Renaissance, Bruxelles 4, Belgique

Président:
Prof. Dr. E. Thomas

Secrétaire administrative:
Mme A. De Henau

2e année **BULLETIN D'INFORMATION No. 8** **Septembre**

2nd year **NEWS BULLETIN No. 8** **September 1960**

2. Jahrgang **INFORMATIONSBLATT Nr. 8** **September**

ol.
10
960

SOMMAIRE — SUMMARY — INHALT

Editorial — Leitartikel 393

1. 2e Congrès International de la Science et de la Technique du Vide (1961) .. ..
   2nd International Congress on Vacuum Science and Technology (1961) 393
   2. Internationaler Kongress für Vakuum-Physik und -Technik (1961) .. ..

2. Réunions — Meetings — Tagungen 394

3. Comité de normalisation .. ..
   Vacuum Standardization Committee 394
   Normungs-Komitee .. ..

4. Liste des nouveaux membres de l'OISTV .. ..
   List of IOVST new Members 394
   Liste der neuen Mitglieder der IOVPT .. ..

5. Lettre à l'éditeur — Letter to the Editor — Brief an den Herausgeber 395

Nous renouvelons l'appel lancé dans le numéro précédent :
We wish to renew the call appearing in our former number :
Wir erneuern die in unserer vorhergehenden Nummer erlassenen Aufforderung :

*
* *

Deux bulletins d'adhésion sont joints au présent numéro : l'un destiné aux membres fondateurs collectifs (sociétés et associations), l'autre destiné aux membres fondateurs individuels (personnes).

L'OISTV vous saurait gré de l'aider dans son action, en remettant ces bulletins à des sociétés et à des personnes intéressées à la science et à la technique du vide.

*
* *

Vol
10
196

Two application forms are attached to the present number : one is meant for Associate Founder Members (societies and associations), the other is meant for Individual Founder Members (persons).

The IOVST would appreciate your co-operation by transmitting these forms to societies and persons interested in vacuum science and technology.

*
* *

Dem vorliegendem Bericht sind zwei Beitrittsformulare beigelegt : eines ist für Kollektiv-Gründermitglieder (Gesellschaften und Körperschaften) bestimmt und das zweite für individuelle Gründermitglieder (Personen).

Die IOVPT wäre Ihnen verbunden, wenn Sie sie in ihrer Tätigkeit unterstützen würden, indem Sie diese Beitrittsformulare an die an der Vakuum-Physik und -Technik interessierten Gesellschaften und Personen weiterleiten.

2e année | BULLETIN D'INFORMATION No. 8 | Septembre
2nd year | NEWS BULLETIN No. 8 | September 1960
2. Jahrgang | INFORMATIONSBLATT Nr. 8 | September

EDITORIAL — LEITARTIKEL

Maintenant que notre bulletin bénéficie d'une meilleure présentation et d'une diffusion plus large, nous demandons une nouvelle fois à nos membres de nous envoyer des textes, écrits dans une des langues officielles de l'Organisation, sous forme de lettres à l'éditeur, de rapports de recherche, de résumés d'articles soumis aux revues du vide ainsi qu'aux autres revues. Notre bulletin y gagnera beaucoup en intérêt.

Les heureux résultats de la collaboration que nous apportent les sociétés nationales affiliées nous font souhaiter l'adhésion prochaine des autres groupements nationaux du vide. Le groupe national du vide du Royaume-Uni vient d'adhérer à l'OISTV.

Nous continuons à favoriser la création de tels groupements et à étudier la transformation de l'OISTV en une fédération comprenant aussi les spécialistes des pays où n'existent pas de sociétés nationales.

*
* *

Our bulletin being favoured by an improved presentation and a wider distribution, we beg once again our members to send us texts in one of the official languages of the Organization in the form of letters to the editor, abstracts of scientific reports, abstracts of articles submitted to vacuum and other reviews. The interest of our bulletin will so be increased.

The happy results of the collaboration we have obtained from the affiliated national bodies make the future affiliation of the other national vacuum bodies more desirable. The national vacuum group of the United Kingdom has just adhered to the IOVST.

We further recommend the setting up of such bodies and we carry on the study of the evolution of the IOVST towards a federation which would also group the specialists from countries where national bodies do not exist.

*
* *

Da sich nunmehr unser Informationsblatt einer besseren Ausstattung und einer weiteren Verbreitung erfreut, ersuchen wir unsere Mitglieder neuerlich, uns in einer der offiziellen Sprachen der Organisation geschriebenen Texte in Form eines Briefes an den Herausgeber oder einer wissenschaftlichen Berichterstattung, sowie Zusammenfassungen der den anderen Vakuum-oder sonstigen Zeitschriften eingereichten Artikel einzusenden. Unser Informationsblatt würde hiedurch sehr an Interesse gewinnen.

Die durch die Mitarbeit der angeschlossenen nationalen Gesellschaften erreichten günstigen Resultate lassen uns den zukünftigen Anschluss anderer nationaler Vakuum-Gruppen wünschenswert erscheinen. Die nationale Vakuum-Gruppe von Grossbritannien tritt der IOVPT bei.

Wir fahren fort, die Gründung solcher Gruppen zu begünstigen und die Umwandlung der IOVPT in eine Föderation, welche gleicherweise die Spezialisten jener Länder, welche noch keine nationalen Gesellschaften besitzen zusammenfasst, zu studieren.

*
* *

1. 2e Congrès International de la Science et de la Technique du Vide (1961)

2nd International Congress on Vacuum Science and Technology (1961)

2. Internationaler Kongress für Vakuum-Physik und -Technik (1961)

Nous serons bientôt en mesure de donner des informations détaillées en ce qui concerne ce congrès qui a été annoncé dans notre bulletin no. 6.

En attendant, nous vous informons que les langues des communications et discussions seront l'anglais, le français et l'allemand et que l'exposition internationale de matériel de vide se tiendra, ainsi que le congrès et l'assemblée générale statutaire de l'OISTV, au Sheraton-Park Hotel à Washington, D.C.

*
* *

We shall soon be able to give detailed information about the congress which was announced in our bulletin No. 6.

It has been decided that the languages of the papers and discussions will be English, French and German. There will also be an international exhibition of vacuum equipment which together with the congress and the statutory General Assembly of the IOVST will be held at the Sheraton-Park Hotel, Washington, D.C.

*
* *

Wir werden baldigst in der Lage sein, genauere Angaben hinsichtlich des in unserem Informationsblatt Nr. 6 angekündigten Kongress zu machen.

In der Zwischenzeit möchten wir mitteilen, dass die für Berichte und Besprechungen zugelassenen Sprachen englisch, französisch und deutsch sein werden und dass die Internationale Ausstellung der Vakuum-Materialien sowie der Kongress und die statutengemässe Generalversammlung der IOVPT im Sheraton-Park Hotel in Washington, D.C., stattfinden werden.

2. Réunions — Meetings — Tagungen

On constate depuis quelques années que les réunions organisées par les sociétés nationales du vide dans leurs pays respectifs groupent un nombre croissant de conférenciers et d'auditeurs étrangers. Cette tendance contribue au progrès dans le domaine du vide ainsi qu'au développement des relations entre les spécialistes mais elle impose à ceux-ci des déplacements de plus en plus fréquents. Une entente plus étroite entre les sociétés nationales du vide paraît donc désirable.

C'est pourquoi l'OISTV demande aux sociétées nationales de lui faire connaître les dates et si possible les thèmes des réunions nationales qu'elles ont l'intention d'organiser avant la fin de 1961.

L'OISTV centraliserait les renseignements et les communiquerait aux groupements affiliés ainsi qu'à ceux qui ne le sont pas encore. Il serait ainsi éventuellement possible d'éviter des coïncidences de dates.

*
* *

More and more foreign lecturers and participants attended in the last few years, the meetings organized by the national bodies concerned with vacuum science and technology. This tendency certainly contributes to promote progress in the vacuum field and to develop relationship between all specialists but it also imposes on them more and more frequent travels. A closer understanding between the national bodies thus seems desirable.

For this reason the IOVST asks the national bodies to inform the Secretariat of the dates and if possible of the subjects of the national meetings they intend to organize up to December 1961.

The IOVST would centralize this information and send it to the affiliated bodies and to those not yet affiliated. This might prevent unhappy coincidences in the dates.

*
* *

Man kann seit einigen Jahren feststellen, dass die durch die nationalen Vakuum-Gesellschaften in deren entsprechenden Ländern organisierten Zusammenkünfte eine anwachsende Anzahl von ausländischen Vortragenden und Zuhörern umfassen. Diese Tendenz trägt zum Fortschritt auf dem Gebiete des Vakuums wie zur Entwicklung der Relationen zwischen den Spezialisten bei, verlangt jedoch von denselben immer häufiger werdende Reisen. Ein immer engerer Zusammenschluss zwischen den nationalen Vakuum-Gesellschaften erscheint daher wünschenwert.

Aus diesem Grunde ersucht die IOVPT die nationalen Gesellschaften ihr die Daten und wenn möglich die Themen der nationalen Zusammenkünfte, welche dieselben bis zum Ende 1961 die Absicht haben zu veranstalten, freundlichst bekanntzugeben.

Die IOVPT wird die Angaben und Mitteilungen den angeschlossenen Gruppen, wie auch denjenigen welche es noch nicht sind vermitteln und wäre es eventuellerweise auf diese Weise möglich, das Zusammenfallen der Termine zu vermeiden.

3. Comité de Normalisation—Vacuum Standardization Committee—Normungs-Komitee

Le Dr. W. HÄNLEIN, Obmann des Arbeitsausschusses Vakuumtechnik im Deutschen Normenausschuss (DNA), a été désigné comme représentant allemand au sein du Comité de Normalisation de l'OISTV.

*
* *

Dr. W. HÄNLEIN, Obmann des Arbeitsausschusses Vakuumtechnik im Deutschen Normenausschuss (DNA), has been appointed as German representative to the Vacuum Standardization Committee of the IOVST.

*
* *

Dr. W. HÄNLEIN, Obmann des Arbeitsausschusses der Vakuumtechnik im Deutschen Normenausschuss (DNA) wurde als deutscher Vertreter im Schosse des Normungs-Komitees der IOVPT ernannt.

*
* *

4. Liste des nouveaux membres fondateurs de l'OISTV allant du 16 juillet au 25 septembre 1960
List of the new founder members of the IOVST, as from July 16, to September 25, 1960
Liste der neuen Gründer-Mitglieder der IOVPT vom 16. Juli bis 25. September 1960

La liste suivante comprend les noms des nouveaux membres fondateurs classés selon le pays où ils résident :

The following list contains the names of the new founder members who are classified according to their present residing State :

Die nachfolgende Liste umfasst die Namen der neuen Gründer-Mitglieder, eingeteilt nach dem Lande ihres gegenwärtigen Wohnsitzes :

MEMBRES FONDATEURS COLLECTIFS
ASSOCIATE FOUNDER MEMBERS
KOLLEKTIVE GRÜNDER-MITGLEIDER

Royaume-Uni United Kingdom Grossbritannien

Joint British Committee for Vacuum Science and Technology.

MEMBRES FONDATEURS INDIVIDUELS
INDIVIDUAL FOUNDER MEMBERS
INDIVIDUELLE GRÜNDER-MITGLIEDER

Allemagne (Rép. Dém.)—Germany (Dem. Rep)—Deutschland (Demokratische Republik)

Hans JANCKE, Prof. Dr., Berlin.

Belgique—Belgium—Belgien

P. L. CARPENTIER, Directeur, Bruxelles.

Danemark—Denmark—Dänemark

N. O. LASSEN, Prof. Dr., København Ø.

Etats-Unis d'Amérique—U.S.A.—V.S. von Nordamerika
Cal LASKY, New Hyde Park.

Israël
Alexandre ROTH, Ing., Ramat Hen.

Nouvelle Adresse—New Address—Neue Adresse
Hubert BAIRIOT, Ing. Civ., Mol (Belgique).

TABLEAU RÉCAPITULATIF — GENERAL TABLE
ZUSAMMENFASSENDE TABELLE

Pays — Countries — Länder	Membres fondateurs collectifs Associate founder members Kollektive Gründer-Mitglieder	Membres fondateurs individuels Individual founder members Individuelle Gründer-Mitglieder
Org. europ.—Europ. Org.	1	2
Allemagne—Germany—Deutschland :		
Rép. Dém.—Dem. Rep.	1	3
Rép. Féd.—Fed. Rep.—Bundesrep.	6	34
Argentine—Argentinien		2
Australie—Australia—Australien		9
Autriche—Austria—Österreich		1
Belgique—Belgium—Belgien	14	52
Brésil—Brazil—Brasilien		2
Canada		9
Danemark—Denmark—Dänemark		1
Espagne—Spain—Spanien	1	5
Etats-Unis—U.S.A.—V.S. von Amerika	13	291
France—Frankreich	1	12
Hongrie—Hungary—Ungarn		4
Inde—India—Indien		1
Israël		2
Italie—Italy—Italien	2	5
Japon—Japan	3	5
Liechtenstein	1	4
Norvège—Norway—Norwegen		2
Pays-Bas—Netherlands—Niederlande	1	7
Philippines—Philippinen		1
Pologne—Poland—Polen		1
Royaume-Uni—U.K.—Grossbritannien	4	28
Suède—Sweden—Schweden		3
Suisse—Switzerland—Schweiz		11
Tchécoslovaquie—Czecho-Slovakia—Tschechoslowakei		2
Union Sud-Africaine—Un. of S. Africa—Südafrikanische Union		1
Yougoslavie—Yugoslavia—Yugoslavien		3
	48	503

*
* *

Nous saurions gré aux membres changeant d'adresse ou de fonction de bien vouloir nous en aviser le plus rapidement possible. Ils faciliteront ainsi la tâche du Secrétariat.

We would be obliged if the members changing their address or function would kindly advise us of same as quickly as possible. They will in this way facilitate the task of the Secretariat.

*
* *

Wir wären denjenigen Mitgliedern, welche ihre Adresse oder Funktion ändern verbunden, wenn sie uns hiervon so schnell wie möglich verständigen würden ; hierdurch wären die Arbeiten des Sekretariats wesentlich erleichtert.

*
* *

5. Lettre à l'éditeur
Letter to the Editor
Brief an den Herausgeber

GROUPE DE POMPAGE METALLIQUE PERMETTANT D'OBTENIR DES PRESSIONS INFERIEURES À 10^{-7} Torr

par

R. LEYNIERS et J. STEVENS*

Centre des Sciences Nucléaires de l'Ecole Royale Militaire, Bruxelles, Belgique

(reçue le 15 septembre 1960)

Au cours des dernières années, quelques auteurs ont décrit des installations de vide permettant, à l'aide de pompes à diffusion d'huile, de réaliser et maintenir des pressions inférieures à 10^{-9} Torr dans des enceintes métalliques de volume important (par exemple : réf. 1 à 7).

Les moyens proposés à cet effet posent de nombreux problèmes aux laboratoires qui ne disposent pas toujours d'ateliers suffisamment équipés.

Lors de la construction d'une installation de vide équipée d'un omégatron, nous avons tenu compte le plus possible des progrès déja acquis dans la production des ultra-vides, tout en veillant au maximum à la simplicité des moyens mis en oeuvre.

Nous présentons ci-après les résultats obtenus au cours des premiers essais. Sans être comparables à ceux réalisés par d'autres auteurs, ils nous semblent cependant susceptibles d'intéresser de nombreux utilisateurs. Ils confirment entre autres les renseignements publiés par divers fabricants de matériel de vide (réf. 1, 6, 7).

Description de l'appareillage

L'enceinte est constituée d'un tube sans soudure en acier inoxydable du type 18/8 (150 mm de diamètre intérieur) muni de quatre brides de 50 mm de diamètre de passage. Le volume du cylindre est d'environ 7,5 l. L'ensemble a été soudé à l'arc sous argon.

Les différentes pièces constituant l'ensemble ont été choisies dans des nuances d'acier bien adaptée, afin d'éviter des difficultés aux soudures d'étanchéité. La pièce a été prévue de façon à éviter les fuites virtuelles. Les jauges et la verrerie nécessaires sont raccordées par l'intermédiaire de scellements verre-métal du commerce, brasés à l'argent

*Laboratoire de Chimie analytique et minérale de l'Université Libre de Bruxelles, actuellement au Centre des Sciences Nucléaires de l'Ecole Royale Militaire.

sur des brides démontables. Le groupe de pompage, tout à fait classique, est constitué d'une pompe à diffusion d'huile de 500 l/s et d'une pompe mécanique à deux étages de 12 m^3/h. L'huile de la pompe à diffusion est de l'Apiezon C. La partie vide primaire de l'installation, équipée de joints toriques en perbunan, est munie d'une vanne de sécurité d'un type spécial (réf. 8).

Au-dessus de la pompe à diffusion on trouve d'abord un baffle du commerce pouvant être réfrigéré à −40 °C à l'aide d'un groupe frigorifique à usage ménager (réf. 9) puis un second baffle refroidi à l'eau.

Le volume total de l'installation, pompe mécanique non comprise, est d'environ 15 l. Les joints de la partie haut-vide sont des joints toriques en aluminium serrés entre deux brides symétriques du type EF de " Leybold ". C'est le type de rainure qui nous a paru le plus simple à usiner tout en étant à la fois propice à l'emploi de joints métalliques et de joints standards en caoutchouc suivant la nature du travail envisagé.

L'ensemble est équipé de jauges Bayard-Alpert (WL 5966) dans la partie haut-vide et diverses sécurités permettent de laisser fonctionner l'installation avec un minimum de surveillance.

L'installation a été testée à l'aide d'un détecteur de fuites aux halogènes. Remarquons qu'elle comprend neuf joints métalliques dans la partie haut-vide et quatorze joints de caoutchouc dans le vide primaire.

Résultats

1.—Lors d'essais préliminaires les taux globaux de remontée de pression mesurés dans la région de 1–5.10^{-2} Torr ont été inférieurs à 2.10^{-7} Torr l.s.$^{-1}$. dm^{-2}. Cette valeur est difficile à comparer avec les différentes courbes de dégazage des matériaux à la température ambiante qui ont déjà été publiées.

2.—La vitesse de pompage, mesurée au-dessus des deux baffles, est de 200 à 220 l/s à 10^{-5} Torr. On peut observer que le fonctionnement du baffle à −40 °C diminue de 3 pour cent la vitesse apparente de pompage.

3.—Lors de la première mise en marche du groupe nous avons atteint 2.10^{-7} Torr (équivalent N_2) en moins de 24 h de pompage, sans dégazage forcé de la partie haut-vide et sans utiliser le baffle à basse température. Les pièces venant de l'atelier avaient préalablement été dégraissées au benzène et au chloroforme, puis étuvées. Si, en période d'arrêt, on maintient l'installation sous vide, le temps de pompage est naturellement fort diminué mais la pression limite ne s'améliore pas.

4.—Après une nuit de pompage en chauffant l'enceinte à 150 °C environ et en utilisant le baffle à −40 °C, la pression lue après refroidissement atteint 5.10^{-8} Torr, les parties métalliques des jauges n'ayant pas été dégazées. Le chauffage était réalisé en enroulant autour de l'enceinte un ruban chauffant isolé du commerce (1600 W de puissance employée). La même méthode a été utilisée pour le dégazage des parois des jauges.

Remarques

Ayant une pression de travail suffisamment basse, nous nous proposons de tester l'étanchéité de l'enceinte et des joints métalliques à l'aide d'un omégatron. Il est vraisemblable que nous pourrons ainsi améliorer les temps de pompage. Nous essayerons aussi de déterminer l'importance de la qualité du vide primaire (par un piégeage efficace de la pompe mécanique) sur les performances de la pompe à diffusion.

Conclusions

Nos essais sont à rapprocher de ceux de Huber et Trendelenburg (réf. 1) qui ont obtenu une pression de 10^{-9} Torr sans l'intervention d'un piège à l'air liquide. Comme eux, nous avons observé un manque d'efficacité du baffle à basse température. Les résultats ne sont cependant pas directement comparables parce que, dans notre installation :

1.—Les pièges ne sont pas prévus pour un dégazage à chaud.

2.—L'enceinte possède un volume non négligeable.

3.—La partie vide primaire du groupe est réalisée d'une façon tout à fait classique.

4.—Les tests d'étanchéité peuvent être fortement améliorés.

5.—La partie haut-vide comporte plusieurs joints.

6.—L'étuvage de l'installation a été moins poussé.

L'absence de renseignements précis ne permet pas de comparer les vitesses effectives de pompage.

Références

1 W. K. Huber et E. A. Trendelenburg ; *Le Vide*, 15ème année, no. 86, p. 132–139 (1960).

2 H. Ehlers und J. Moll ; *Zeit. f. Angew. Phys.*, **12**, (1960), S.324–328.

3 R. A. Haefer ; *Vakuum-Technik*, **9**, (1960) S.37–43.

4 S. R. Ullman ; *Fourth National Symposium on Vacuum Technology Transactions* (1957), Pergamon Press, p. 95–97.

5 N. Milleron ; *Fifth National Symposium on Vacuum Technology Transactions* (1958), Pergamon Press, p. 140–147.

6 W. Bächler ; *Proceedings of the First International Congress on Vacuum Techniques*, Pergamon Press, p. 182–185.

7 B. D. Power and D. H. Crawley ; *Proceedings of the First International Congress on Vacuum Techniques*, Pergamon Press, p. 211 Discussion.

8 R. Servranckx et R. Leyniers ; *Le Vide*, 14ème année, no. 83, p. 259–299 (1959).

R. Servranckx ; *Bulletin d'information de l'O.I.S.T.V.*, 1ère année, no. 4, p. 11 (1959).

9 R. Servranckx et Ch. Triffois ; *Bulletin d'information de l'O.I.S.T.V.*, 2ème année, no. 5, p. 18–19 (1960).

Vol. 10 1960

Abstracts

General Vacuum Science and Engineering

16. Gases and Solids

16

397. The Sorption of Gaseous Hydrogen Chloride by Dry Lyophilized β-Lactoglobulin.
United States. The sorption of gaseous HCl by dry lyophilized β-lactoglobulin was studied at 27°. HCl is held so firmly on some of the sorption sites that it cannot be removed by pumping to a high vacuum. The results show that the amount remaining sorbed on the protein is some reciprocal function of the temperature. (Author)
W. S. Hnojewyj and L. H. Reyerson, *J. Phys. Chem.*, **64**, 1199–1202, Sept. 1960.

16

398. Electronic Spectra of Adsorbed Molecules : Stable Carbonium Ions on Silica Alumina.
H. P. Leftin, *J. Phys. Chem.*, **64**, 1714–1717, Nov. 1960.

16

399. On the Energetics of Physically Adsorbed Films, With Particular Reference to the Use of Krypton for Surface Area Measurement.
United States. Some simple considerations of the energetics of adsorbed films suggest that fairly complete monolayers of gases such as krypton should be formed before the onset of significant multilayer formation. Such monolayer formation should be experimentally observable by the Brunauer–Emmett–Teller method. It is noted that the experimentally observed variations in the molecular area parameters used to calculate areas may reflect differences in the adsorption energetics for different adsorbate-adsorbent systems. On the basis of these considerations, together with our experimental results for krypton adsorption, it is concluded that recent criticisms of the use of krypton in the BET surface area method are not justified. (Author)
G. L. Gaines, Jr. and P. Cannon, *J. Phys. Chem.*, **64**, 997–1000, Aug. 1960.

16

400. The Extreme Sensitivity of Paramagnetic Sites to Poisoning by Desorbed Gases Evaluated by the Low Temperature Ortho-Parahydrogen Conversion.
Note by D. S. Chapin, C. D. Park and M. L. Corrin, *J. Phys. Chem.*, **64**, 1073–1074, Aug. 1960.

16

401. A Radiotracer Study of an Optical Method for Measuring Adsorption.
Note by L. S. Bartell and J. F. Betts, *J. Phys. Chem.*, **64**, 1075–1076, Aug. 1960.

16

402. Calorimetric Heats of Adsorption for Hydrogen on Nickel, Copper and Some of Their Alloys.
Note by L. S. Shield and W. W. Russell, *J. Phys. Chem.*, **64**, 1592–1594, Oct. 1960.

16

403. Heats of Adsorption and Adsorption Isotherms for Low Boiling Gases Adsorbed on Graphon.
E. L. Pace and A. R. Siebert, *J. Phys. Chem.*, **64**, 961–963, Aug. 1960.

16

404. The Failure of Dispersion Energy Calculations to Reproduce Heats of Adsorption on Graphitic Carbon.
D. Graham, *J. Phys. Chem.*, **64**, 1089–1092, Sept. 1960.

16

405. The Effects of Oxygen Adsorption on the K X-Ray Absorption Edge of Alumina Supported Nickel.
P. H. Lewis, *J. Phys. Chem.*, **64**, 1103–1109, Sept. 1960.

16

406. Sites for Hydrogen Chemisorption of Zinc Oxide.
V. Kesavulu and H. A. Taylor, *J. Phys. Chem.*, **64**, 1124–1131, Sept. 1960.

16

407. Non-Steady-State Fluid Flow and Diffusion in Porous Media Containing Dead-End Pore Volume.
R. C. Goodknight, W. A. Klikoff, Jr. and I. Fatt, *J. Phys. Chem.*, **64**, 1162–1168, Sept. 1960.

16

408. The Frenkel-Halsey-Hill Adsorption Isotherm and Capillary Condensation.
C. Pierce, *J. Phys. Chem.*, **64**, 1184–1187, Sept. 1960.

16

409. Hydrogen Sorption on Graphite at Elevated Temperatures.
United States. The sorption of hydrogen on selected types of nuclear and spectroscopic graphite has been studied. On nuclear graphite, the desorption of hydrogen over the temperature range 1035 to 1375° follows the Elovich equation. The activation energy of desorption over the coverage range (θ), 0.32 to 0.68, can be approximated as $E = 137 - 42(\theta)$ kcal./mole. On the basis of limited results, it is found that the adsorption of hydrogen at 1335° on nuclear graphite can also be expressed by the Elovich equation. Isotherms for sorption of hydrogen on both nuclear and spectroscopic graphites over the temperature range 920 to 1495° are of the Temkin-type. However, at temperatures of 1085° and above, the isotherms consist of two straight-line regions of markedly different slopes. From the isotherms at 1335 and 1495° for the nuclear graphite, the heat of adsorption over the coverage range, 0.50 to 0.80, can be approximated as $Q = 58 - 56(\theta)$ kcal./mole. It is concluded that the adsorption of hydrogen occurs on carbon atoms at the edge of crystallites and that significant intracrystalline sorption does not occur. (Author)
J. P. Redmond and P. L. Walker, Jr., *J. Phys. Chem.*, **64**, 1093–1099, Sept. 1960.

16 : 17

410. Adsorption Studies on Metals. IX. The Nature of the Thermal Regeneration of Oxide-Coated Nickel, Cobalt and Copper.

United States. It is well known that oxidation of nickel, cobalt and copper at 25° proceeds by two steps, a fast followed by a slow process. Upon heating these oxide-coated metals at modest temperatures such as 300° *in vacuo*, oxidation will again proceed multimolecularly by a rapid step at 25° even though no oxygen was evolved during thermal treatment. The regeneration could be due to (a) migration of metal ions to the metal-oxide interface ; (b) dissolution of the oxide film in the bulk metal ; or (c) crystallization of the oxide film to reveal bare metal. In this work, organic vapors were used as a probe for any bare metal surface uncovered during regeneration. The heats of adsorption of *n*-propylamine and acetic acid on the bare, oxide-coated and regenerated metal surfaces support the contention of Dell that recrystallization occurs. That is to say, initial heats of adsorption were much higher on the regenerated surfaces, in accord with the values for the freshly reduced metals, and were much lower on the oxide-coated surfaces. The extents of irreversible adsorption followed the pattern to be expected from the heat measurements. (Author)

A. C. Zettlemoyer, Yung-Fang Yu and J. J. Chessick, *J. Phys. Chem.*, **64**, 1099–1102, Sept. 1960.

16

411. The Chemisorption of Oxygen on Nickel.
United States. The chemisorption of oxygen on nickel-silica catalyst systems has been investigated by the low frequency a.c. permeameter method and volumetric gas adsorption techniques. The nickel particles were in the superparamagnetic range or slightly larger. A method has been developed for distinguishing between true chemisorption of oxygen on nickel as contrasted with surface oxide formation. The method makes use of what appears to be a change of magnetic anisotropy energy in particles of nickel in the 100 Å diameter range. A possible explanation is discussed for the so-called " hydride anomaly " in the chemisorption of hydrogen on nickel at low temperatures. (Author)

R. J. Leak and P .W. Selwood, *J. Phys. Chem.*, **64**, 1114–1120, Sept. 1960.

16 : 17

412. The Heat of Adsorption of Argon and Krypton on Molybdenum Disulfide-Separation of Enthalpies into Rational Components.
United States. The molar integral heats of adsorption of two rare gases on oxide-free MoS_2 are presented as functions of coverage. The data are analyzed in terms of both sorbate-solid and sorbate-sorbate interactions. The values of each separate interaction are calculable from the fundamental physical properties of the components of the system. The calculation of the dispersion forces for the gas-solid pair is most successful using London's form for the dispersion constant. The data cover the ranges $4 \times 10^{-7} < p/p_0 < 2 \times 10^{-3}$ (Ar) and $4 \times 10^{-4} < p/p_0 < 4 \times 10^{-1}$ (Kr). The argon film exhibits a gas-liquid transition and the krypton film shows a maximum self interaction energy equal to one half the heat of liquefaction. (Author)

P. Cannon, *J. Phys. Chem.*, **64**, 1285–1289, Sept. 1960.

17. Thermodynamics

17

413. Heats of Immersion. IV. The Alumina-Water System-Variations with Particle Size and Outgassing Temperature.
United States. Samples of α-, γ- and amorphous-alumina with surface areas from 0.222 to 221 m^2/g. were studied following vacuum outgassing treatments over the temperature range, 100–450°. In addition, weight loss measurements were made as a function of temperature. Usually a substantial increase was noted for the heats of immersion with decreasing specific area and increasing outgassing temperature. These studies are consistent with the normal alumina surface being covered with a maximum of 19 OH'S/100 Å. (Author)

W. H. Wade and N. Hackerman, *J. Phys. Chem.*, **64**, 1196–1199, Sept. 1960.

17

414. Mechanism of the Isothermal Decomposition of Potassium Perchlorate.
Note by K. H. Stern and M. Bufalini, *J. Phys. Chem.*, **64**, 1781–1782, Nov. 1960.

17

415. On the Use of Tantalum Knudsen Cells in High Temperature Thermodynamic Ptudies of Oxides.
Communication to the Editor by H. W. Goldstein, P. N. Walsh and D. White, *J. Phys. Chem.*, **64**, 1087, Aug. 1960.

17 : 52

416. The Dissociation Pressures and the Heats of Formation of the Molybdenum Silicides.
United States. Silicon partial pressures for dissociation of the three molybdenum silicides have been measured by the Knudsen effusion method. The heats of dissociation per gram atom of silicon vapor are calculated to be at 298°K for Mo_3Si 131.9 + 1.2 kcal., for Mo_5Si_3 131.1 + 0.7 kcal., and for $MoSi_2$ 117.2 + 0.6 kcal. The heats of dissociation of the molybdenum silicides when combined with the heat of sublimation of silicon yield the following heats of formation at 298°K : Mo_3Si −23.5 + 4 kcal. ; 1/3 Mo_5Si_3 −22.6 + 5 kcal. ; 1/2 $MoSi_2$ −13.0 + 5 kcal. (Author)

A. W. Search and A. G. Tharp, *J. Phys. Chem.*, **64**, 1539–1542, Oct. 1960.

17 : 16

Adsorption Studies on Metals. IX. The Nature of the Thermal Regeneration of Oxide-Coated Nickel, Cobalt and Copper. See Abstract No. 410.

17 : 16

The Heat of Adsorption of Argon and Krypton on Molybdenum Disulfide-Separation of Enthalieps into Rational Components. See Abstract No. 412.

Vol. 10 1960

Vacuum Apparatus and Auxiliaries

21. Pumps and Pump Fluids

21

417. Experiments on a Simple Getter—Ion Pump.
Japan. For a trial purpose the authors fabricated Penning type cold cathode vacuum-ion pump with a three latticed titanium cells of 15 mm × 45 mm × 20 mm as an anode, and two sheets of titanium plate of 15 mm × 45 mm as cathodes. The operating condition was : anode voltage was 2000 V, strength of the magnetic field was 1200–2000 gauss. The pumping speed was measured as 1 l/sec. Using this tinny pump, the ultra-high vacuum of 10^{-9} mmHg was easily obtained. H. N.

I. Morita, F. Kanematsu and S. Mito, *J. Vac. Soc., Japan*, **3**, 263–268, 1960.

22. Gauges

22

418. An Ultra-High Vacuum Mass Spectrometer.
Japan. To analysis of very small quantity gas, and to investigate the adsorption phenomena in ultra-high vacuum, the authors constructed all metal mass spectrometer which is operated in ultra-high vacuum. Same difficulties which is experienced in constructing all metal ultra-high vacuum equipments, are more serious in this case. A large amount of outgas, difficulties of vacuum tight joints and flanges would be more sensitive to the performance of the mass spectrometer than usual ultra-high vacuum equipment.
The noticeable features of this mass spectrometer are as follows : (1) The analyzing tube is made of stainless steel, and all analyzing parts including tube are set in electric oven, and enable to be baked up to 350°C ; (2) The gaskets of the tube is oxygen free copper ; (3) The trap which contends oxygen free copper foil is equipped ; (4) Vac-ion type ultra-high vacuum pump is equipped ; (5) Sample inlet system is also enable to be evacuated to ultra-high vacuum. The analyzing tube is 60° type single focussing, and radius of ion orbit is 15 cm, and it can identify components with mass range between 1 and 200 a.m.u. The system can be evacuated up to 1–2 = 10^{-8} mmHg, and best operating condition was in 1.4 = 10^{-8} mmHg. The magnet is 1000 gauss electro-magnet, and resolving power was 150. Minimum enquire sample quantity was 10^{-6} cc/N.T.P. By this mass spectrometer, the authors investigated the residual gas in an analyzing tube. Before baking up, the main component of residual gas is H_2O with small quantities of CO, N_2, Ar, CO_2, and hydrocarbons. After baking up and under 1 = 10^{-6} mmHg vacuum CO or N_2 was identified as a main component. Under 1 = 10^{-6} mmHg the gas of M/e = 28 are still main component, but the composition of CO was estimated as 40 per cent, and under 1 × 10^{-8} mmHg the CO occupies 80 per cent. H. N.

K. Kawasaki, T. Sugita, A. Fujinaga, M. Goto and J. Kai, *J. Vacuum Soc., Japan*, **3**, 96–103, 1960.

Vacuum Applications

30. Evaporation and Sputtering

30

419. Evaporation from Liquid Surface under a High and a Medium Vacuum.

Japan. Evaporation of di-2-ethylphthalate under a high and a medium vacuum was investigated. Changing the pressure, the author found that the evaporation mechanism could be thought as it is considered by two different ways. The author proposes these should be called as a " molecular-projective-evaporation " and a " molecular-burst-evaporation ". The former is observed under a high vacuum and follows Knudsen's high vacuum evaporation rate, but the latter is observed under a medium vacuum and its rate is strongly influenced by the vapor pressure of liquid and pressure of inert gas. Under a medium vacuum the evaporation rate is always less than Knudsen rate, and the author proposes the fundamental relation between rate and pressure considering the evaporating molecules slip diffuse through its vapor and inert gas, and presents the following equation : $D = \{MD_f\pi_p/R_oT(x-x')\} \ln(P_{rc}/P_{rv})$ where D : evaporation rate per unit area, D_f : diffusion constant, M : Molecular weight, π_p : total pressure, R_o : ideal gas constant, T : absolute temperature, x : distance from evaporating surface to condensing surface, x' : thickness of molecular-exchange zone, P_{rc} : inert gas pressure at nearer condensing surface, P_{rv} : inert gas pressure at nearer evaporating surface. H. N.

H. Uyeha, T. Kajiura and O. Yoshikawa, *Chem. Eng., Japan*, **24**, 274–280, 1960.

30

420. Thick Vacuum Metallized Coatings are Durable, Corrosion Resistant.

This article describes a new method of vacuum-depositing metal coatings up to thicknesses of a few mils. Various types of coating materials are described together with applications of these materials. A. G.

Philip J. Clough and Howard M. Farrow, *Metal Prog.*, **52**, 12–15, Sept. 1960.

31. Evacuation and Sealing

31

421. The Radiolysis of Deuterated Biphenyls : Mechanism of Hydrogen Formation.

J. G. Burr and J. M. Scarborough, *J. Phys. Chem.*, **64**, 1367–1374, Oct. 1960.

33. General Physics and Electronics

33

422. On the Characteristics of Steam Ejectors and a Method of Calculating Their Performances.

Japan. It is rather difficult to predict the performance of steam ejector, because it is influenced by many factors which cannot be predicated by design, and usually we decide the detailed constructions by our experiences. The author presents the practical method of calculating the performance. H. N.

T. Ueda, *Chem. Eng., Japan*, **24**, 264–273, 1960.

33

423. Photoelectric Devices for Monitoring Thickness of Vacuum Deposition of Multilayer Film.

Japan. A practical and reliable device to measure and control the thickness of multilayer films deposited in vacuum was described. Light source was constructed by 12 V 20 W lamp, condenser lens, hole, project lens, and sector. The light modulated by sector which has frequency of 1000 c.p.s., passes through vacuum deposited thin film, and converted to signed photocell and amplified. Monitoring this signal, the authors say that it is easily possible to measure and control the thickness of the film. H. N.

T. Sawaki, M. Iwata and S. Katsube, *J. Vac. Soc., Japan*, **3**, 304–308, 1960.

36. Drying, Degassing and Concentration

36

424. Fundamental Study of Vacuum Drying.

Japan. Using Shigaraki clay as a testing material, the authors investigated the mechanism of vacuum drying. The pressure was between 4–300 mmHg, and heating device was in two cases : by radiation and conduction. Thickness of the testing material had no influence on the rate. Surface evaporation coefficient Kg is defined as $R = Kg(pm - p) = Kg(\Delta p)$, where R is constant drying rate, Pm is water vapor pressure on the surface of material, P is water vapor pressure in the vessel, and Δp is the difference. Using this Kg, the experimental results were tabulated, the authors concluded as all mechanism was considered as a typical case of drying of the porous material. The influence of air leak varies the rate, and also in this case the equation $Kg = 4.4 \times 10^{-3}\ \pi^{-2/3}$ was fully adoptable, where Kg is surface evaporation coefficient and κ is pressure in mmHg. H. N.

R. Toei, K. Maeda, T. Yamauchi, T. Fuha, K. Wada and H. Yamamoto, *Chem. Eng., Japan*, **24**, 289–297, 1960.

37. Metallurgy, Inorganic Chemistry, Analytical Chemistry

37

425. Which Brazing Alloys for Vacuum Systems ?

The properties of brazing alloys required to produce vacuum-tight joints are discussed with particular emphasis on avoiding high vapor pressure constituents and impurities and the ability to wet and flow. An equilibrium diagram is included to explain brazing problems. A. G.

Walter Hack, *Materials in Design Engineering*, **52**, 116–117, July 1960.

37

426. Electron Beam Welding : Emphasis on Precision and Freedom From Contamination.

Marsbed Hablanian, *Metal Prog.*, **78**, 127–129, July 1960.

37

427. Vacuum Melters Push Expansion—Bank on Growing Markets.

The growth of vacuum melting capacity in the U.S.A., both consumable electrode and induction, is represented in graphical form. The locations of present and planned facilities for vacuum melted metals are listed. The dependence on the defense industry is discussed. A. G.

G. J. McManus, *Iron Age*, **186**, 113–116, Oct. 1960.

37

427a. Welding and Brazing Two Columbium Alloys.

C. F. Burrows, M. M. Schwartz and L. J. Gagola, *Materials in Design Engineering*, **52**, 13–15, Oct. 1960.

38. Distillation, Organic Chemistry and Isotopic Gas Analysis

38

428. Falling-Film Evaporator.
Note by M. S. Tendulkar, *Chem. Eng.*, **67**, 208, Oct. 1960.

38

429. Mass Transfer in Falling-Film Molecular Distillation.
Japan. The performances of molecular distillation still was investigated using sperm oil as of two groups of wax and glyceride. The theoretical analysis of the mechanism of molecular distillation, especially under recycling, is very complicated but the authors introduced several equations. These are (1) The expression of variation of concentration of light component in falling liquid, and (2) the distillating rate of light and heavy components. Comparing these theoretical equations with experimental results, the authors concluded that the mass transfer in falling-film molecular distillation still is expressed fairly well by these equations. H. N.

H. Uyeha, T. Shigemaaa, Y. Tozaki and A. Oyeha, *Chem. Eng., Japan*, **24**, 281–288, 1960.

ol.
10
960

Materials and Techniques used in Vacuum Technology

40. Gases and Vapours

40

430. Pressure Dependence of Some Infrared and Vacuum Ultraviolet Bands Occurring in Active Nitrogen.
Robert A. Young, *J. Chem. Phys.*, **33**, 1112–1230, Oct. 1960.

40

431. Charge Transfer between Atomic Hydrogen and N^+ and O^+.
R. F. Stebbings, Wade L. Fite and David G. Hummer, *J. Chem. Phys.*, **33**, 1226–1116, Oct. 1960.

432. Interchange of Charge between Gaseous Molecules.
Donald Rapp and Irene B. Ortenburger, *J. Chem. Phys.*, **33**, 1230–1233, Oct. 1960.

40

433. Rapid Determination of Gaseous Diffusion Coefficients by Means of Gas Chromatography Apparatus.
Note by J. Calvin Giddings and Spencer L. Seager, *J. Chem. Phys.*, **33**, 1579–1580, Nov. 1960.

40

434. Dielectric Constants of Imperfect Gases. I. Helium, Argon, Nitrogen, and Methane.
D. R. Johnston, G. J. Oudemans and R. H. Cole, *J. Chem. Phys.*, **33**, 1310–1317, Nov. 1960.

40

435. Molecular Friction in Dilute Gases.
J. T. O'Toole and J. S. Dahler, *J. Chem. Phys.*, **33**, 1496–1504, Nov. 1960.

40

436. Dissociation Energies of Diatomic Molecules.
G. R. Somayajulu, *J. Chem. Phys.*, **33**, 1541–1553, Nov. 1960.

40

437. Sparking Potential and Molecular Structure of Unsaturated Hydrocarbon Gases.
R. W. Crowe and J. C. Devins, *J. Chem. Phys.*, **33**, 413–418, Aug. 1960.

40

438. Self-Diffusion of Oxygen in Single Crystal and Polycrystalline Aluminum Oxide.
Y. Oishi and W. D. Kingery, *J. Chem. Phys.*, **33**, 480–486, Aug. 1960.

40

439. Interaction of Condensable Gases with Cold Surfaces.
Deposition from a molecular beam onto a cold target surface only occurs when the beam pressure is many orders of magnitude larger than the vapor pressure of the depositing phase at the substrate temperature. The critical beam pressure for deposition has been interpreted as a critical supersaturation for heterogeneous nucleation of a condensed phase. It is shown that the critical beam pressure is much too large to be accounted for as a critical value for nucleation if the adsorbate temperature and the substrate temperature are alike. The interpretation of critical deposition phenomena as a nucleation event must include the additional assumption that the adsorbate temperature is somewhat higher than the substrate temperature. (Author)
G. W. Sears and J. W. Cahn, *J. Chem. Phys.*, **33**, 494–499, Aug. 1960.

40

440. Heterogeneous Reactions Studied by Mass Spectrometry. I. Reaction of B_2O_3(s) with H_2O(g).
David J. Meschi, William A. Chupka and Joseph Berkowitz, *J. Chem. Phys.*, **33**, 530–533, Aug. 1960.

40

441. Heterogeneous Reactions Studied by Mass Spectrometry. II. Reaction of Li_2O(s) with H_2O(g).
Joseph Berkowitz, David J. Meschi and William A. Chupka, *J. Chem. Phys.*, **33**, 533–540, Aug. 1960.

40

442. Viscosity of Mixtures of Hydrogen and Water Vapor at 295°K.
Note by J. W. Fox and A. C. H. Smith, *J. Chem. Phys.*, **33**, 623–624, Aug. 1960.

40

443. Multiple Ionization in Argon and Krypton by Electron Impact.
R. E. Fox, *J. Chem. Phys.*, **33**, 200–205, July 1960.

40

444. Recombination Kinetics of Atomic Oxygen at Room Temperature.
Note by C. B. Kretschmer and H. L. Petersen, *J. Chem. Phys.*, **33**, 948–949, Sept. 1960.

40

445. Secondary Reactions in a Gas Discharge.
Arene B. Ortenburger, Martin Hertzberg and Richard A. Ogg, Jr., *J. Chem. Phys.*, **33**, 579–583, Aug. 1960.

40

446. Kinetic Absorption Spectra Recorded Through Flash-Heated Grids.
Note by L. S. Nelson and N. A. Kuebler, *J. Chem. Phys.*, **33**, 610–611, Aug. 1960.

40

447. Separation of Gas Mixtures in a Supersonic Jet. II. Behavior of Helium-Argon Mixtures and Evidence of Schock Separation.
S. Alexander Stern, P. C. Waterman and T. F. Sinclair, *J. Chem. Phys.*, **33**, 805–813, Sept. 1960.

40

448. Threshold Law for the Probability of Excitation of Molecules by Photon Impact. A Study of the Photoionization Efficiencies of Br_2, I_2, HI and CH_3I.
J. D. Morrison, H. Hurzeler and Mark G. Inghram, *J. Chem. Phys.*, **33**, 821–824, Sept. 1960.

40

449. Oxygen Diffusion in Periclase Crystals.
Y. Oishi and W. D. Kingery, *J. Chem. Phys.*, **33**, 905–906, Sept. 1960.

41. Metals and Alloys

41

450. Space-Age Beryllium—It's Technology.
The advantages of beryllium as a metal for use in space vehicles and the various fabrication methods currently in use are discussed. The problems encountered in using materials at very low pressures are also considered. A. G.
Robert H. Gassner, *Metal Prog.*, **78**, 88–92, Sept. 1960.

Vol. 10 1960

41

451. Secondary Positive Ion-Emission from Platinum.
R. C. Bradley, A. Arking and D. S. Beers, *J. Chem. Phys.*, **33**, 764–769, Sept. 1960.

41

452. Nucleation and Growth of Mercury Crystals at Low Supersaturation.
In the present paper it is shown that mercury crystals can be nucleated on a cold glass surface at a much lower supersaturation than has been previously reported. The role of ambient temperature in the growth process is described. It is established that the growth habit is intrinsic to the pure mercury and is not characteristic of a growth modification by foreign gases. (Author)
G. W. Sears, *J. Chem. Phys.*, **33**, 563–567, Aug. 1960.

41

453. Low-Temperature Metals : A Roundup.
George H. Zenner, *Chem. Eng.*, **67**, 117–120, Oct. 1960.

41

454. Progress in Aluminum Alloys.
This article summarizes the status of new aluminum alloys and improved techniques for producing and working them. Particular attention is given to vacuum die casting. A. G.
Anon., *Metal Prog.*, **78**, 137–142, Oct. 1960.

41

455. Progress in Copper Alloys.
Anon., *Metal Prog.*, **78**, 143, Oct. 1960.

41

456. Progress in Magnesium Alloys.
Anon., *Metal Prog.*, **78**, 146, Oct. 1960.

41 : 47

457. Vapor Pressures of Platinum Metals. I. Palladium and Platinum.
United States. Langmuir free-evaporation rates for Pd and Pt samples of high purity establish the equilibrium vapor pressures and the heat of sublimation. For Pt : $\log P_{mm}^{solid} = 10.362 - 29.100/T$; $\Delta H^{\circ}_{298} = 135.2 \pm 0.8$ kcal./mole ; estimated b.p. $\approx 4100 \pm 100^{\circ}K$. For Pd : $\log P_{mm}^{solid} = 9.075 - 19{,}425/T$; $\Delta H^{\circ}_{298} = 91.0 \pm 0.8$ kcal./mole ; estimated b.p. $\approx 3200 \pm 100^{\circ}K$. (Author)
L. H. Dreger and J. L. Margrave, *J. Phys. Chem.*, **64**, 1323–1324, Sept. 1960.

41

458. The Niobium-Niobium Carbide System.
E. K. Storms and N. H. Krikorian, *J. Phys. Chem.*, **64**, 1471–1477, Oct. 1960.

41

459. The Preparation, Crystal Structures and Some Properties of Zirconium and Hafnium Dirhenide.
N. H. Krikorian, W. G. Witteman and M. G. Bowman, *J. Phys. Chem.*, **64**, 1517–1519, Oct. 1960.

41

460. Some Solidus Temperatures in Several Metal-Carbon Systems.
United States. Minimum eutectic temperatures were determined for systems involving carbon and some refractory metals. These solidus temperatures for the systems C-, Ta, Os, W, Re, Nb, Ir, Mo, Ru, 50IR-50Rh, Pt, Rh and Pd are 2902, 2732, 2732, 2486, 2328, 2296, 2210, 1942, 1932, 1736, 1694 and 1504°, respectively. For the Nb-C system, the Nb_2C peritectic and the NbC-C eutectic are located at 3080 and 3220°, respectively. For the Ta-C system, the Ta_2C peritectic and the TaC-C eutectic are located at 3500 and 3710°, respectively. The melting points of Mo_2C, WC and NbC are 2410, 2720 and 3480°, respectively. (Author)
M. R. Nadler and C. K. Kempter, *J. Phys. Chem.*, **64**, 1468–1471, Oct. 1960.

41 : 53

461. The Initial Stages of Oxidation of Germanium.
United States. The initial stages of oxidation on a germanium surface freed of combined and adsorbed oxygen by reduction with carbon monoxide at 600° was studied with a vacuum microbalance sensitive to 1/300th of a GeO_2 layer. These experiments were done at an oxygen pressure of 75 mm and at temperatures from 25 to 400°. The oxidation laws were found to change with temperature and the extent of oxidation. The initial oxygen uptake is consistent with the viewpoint that the surfaces prepared by reduction in carbon monoxide behave as if they are atomically clean. The first oxygen layer, as one oxygen per surface germanium atom, forms in less than a minute on the clean surface. At temperatures below 250° a second layer of one oxygen per surface germanium atom forms according to the logarithmic rate law in agreement with the results of Green and Kafalas. Subsequent oxidation beyond the second layer is not logarithmic but obeys a Mott and Cabrera thin film-type equation. At temperatures about 250° the second layer forms in less than one minute. The subsequent oxidation rates beyond the second layer where only GeO_2 is formed, are very slow and even at 400° only 17.5 Å of GeO_2 formed in three hours. Activation energies for the logarithmic law and for the Mott and Cabrera equations were calculated. (Author)
J. R. Ligenza, *J. Phys. Chem.*, **64**, 1017–1022, Aug. 1960.

42. Glass and Ceramics

42

462. Glass-Ceramics.
This article summarizes the manufacturing process involved in producing glass-ceramics and the properties of these materials, which appear suitable for many vacuum applications. A. G.
S. D. Stookey, *Mech. Eng.*, **82**, 65–68, Oct. 1960.

42 : 53

463. The Reactions of Water Vapor with Beryllia and Beryllia-Alumina Compounds.
W. A. Young, *J. Phys. Chem.*, **64**, 1003–1006, Aug. 1960.

45. Soldering, Welding, Brazing

45

464. Progress in Welding Steels : Vapor-Shielded Arc Means Faster Welding.
R. A. Wilson, *Metal Prog.*, **78**, 96–99, Oct. 1960.

47. Outgassing Data, Vapour Pressure Data, and Gettering Data

47 : 41

Vapor Pressures of Platinum Metals. I. Palladium and Platinum.
See Abstract No. 457.

49. Miscellaneous Materials and Techniques

49

465. How Radiation Affects Engineering Materials.
The effects of gamma rays and neutrons on structural metals, inorganic nonmetallics, elastomers, plastics and organic fluids are discussed. Numerous tables summarizing the effects are included. A. G.
Richard E. Bowman, *Materials in Design Engineering*, **78**, 119–134, July 1960.

49

466. Observation of Adsorption on an Atomic Scale. Note by Gert Ehrlich and F. G. Hudda, *J. Chem. Phys.*, **33**, 1253–1254, Oct. 1960.

49

467. Cuprous Halide Films on Alkali Halide Crystals. L. M. Kraemer, *J. Chem. Phys.*, **33**, 991–993, Oct. 1960.

Basic Science and Engineering

53. Metallurgy, Ceramics, Inorganic Chemistry

53 : 41

The Initial Stages of Oxidation of Germanium. See Abstract No. 461.

53 : 42

The Reactions of Water Vapor with Beryllia and Beryllia-Alumina Compounds. See Abstract No. 463.

Vol.
10
1960

VACUUM

Le Traitemente sous Vide des Métaux et de l'Acier en particulier

W. ARMBRUSTER

W. C. Heraeus, Hanau/Main, Allemagne

Au cours des dernières années, l'application dans la métallurgie de procédés sous vide a acquis une importance de plus en plus grande. Il faut citer :

1. Le dégazage sous vide à l'état liquide
2. Le dégazage sous vide et le recuit à l'état solide
3. Le frittage sous vide de poudres métalliques
4. La fusion sous vide.

Pour la fusion sous vide, on utilise le four à induction sous vide, le four de fusion à arc sous vide ou le four à faisceau électronique, dont la construction est visible schématiquement sur les photos suivantes.

La Fig. 1 montre le four à induction à vide. Il offre le plus grand nombre de possibilités dans le domaine métallurgique, lorsqu-une composition d'alliage très précise est nécessaire.

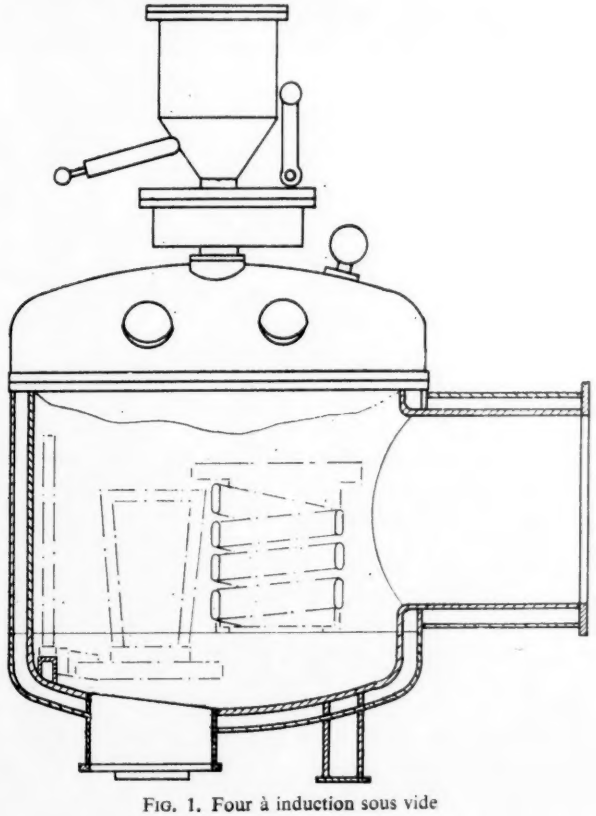

Fig. 1. Four à induction sous vide

La Fig. 2 montre le four à l'arc avec électrode consommable. Dans la partie inférieure, l'on peut observer la coquille refroidie à l'eau, dans laquelle le métal fondu à l'arc forme un lac de fusion peu profond.

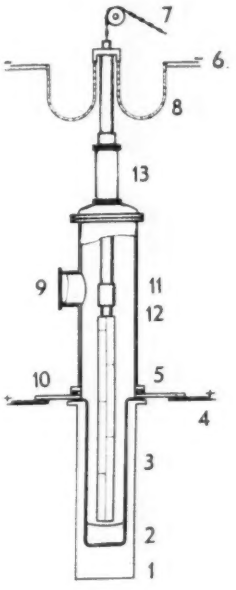

1 Kühlbehälter
2 Tiegel
3 Selbstverzehrende Elektrode
4 Stromzuführung (Anode)
5 Isolationsring
6 Stromzuführung (Kathode)
7 Getriebe für den Elektrodenvorschub
8 Kühlung der Elektrodenstange
9 Flansch zur Vakuumpumpe
10 Ofengehäuse
11 Elektrodeneinspann-Vorrichtung
12 Einspannkopf
13 Druckstufendichtung und Führung der Elektrodenstange

Fig. 2. Four de fusion à l'arc sous vide

La Fig. 3 montre le croquis d'un four de fusion par bombardement électronique. Avec ce modèle, les électrons sont produits dans un canon éléctronique et lancés à l'intérieur du four. Les canons électroniques et l'intérieur du four sont maintenus sous haut vide par des pompes à vide à grand rendement. Grâce à la disposition que je viens de décrire, les difficultés qui sont dues à la formation d'effluves électriques, peuvent être surmontées. Les électrodes consommables sont continuellement fondues par l'énergie des

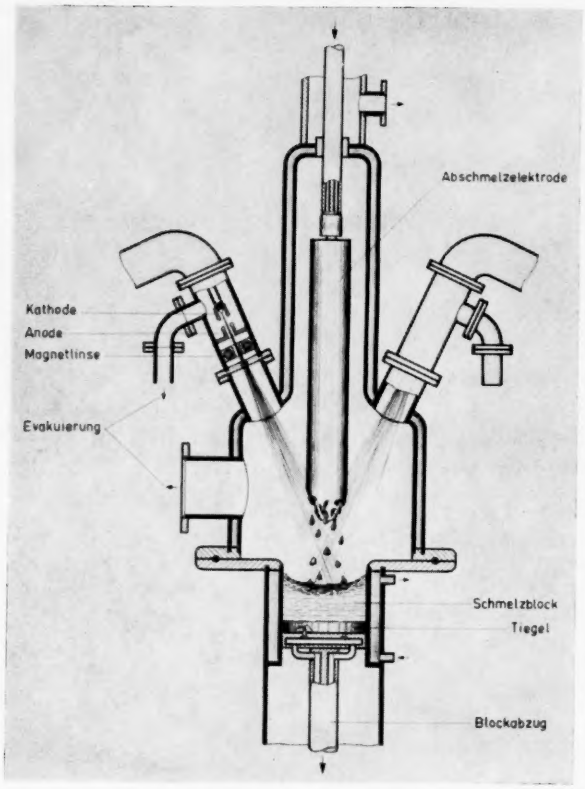

FIG. 3. Four de fusion par bombardement électronique sous vide poussé

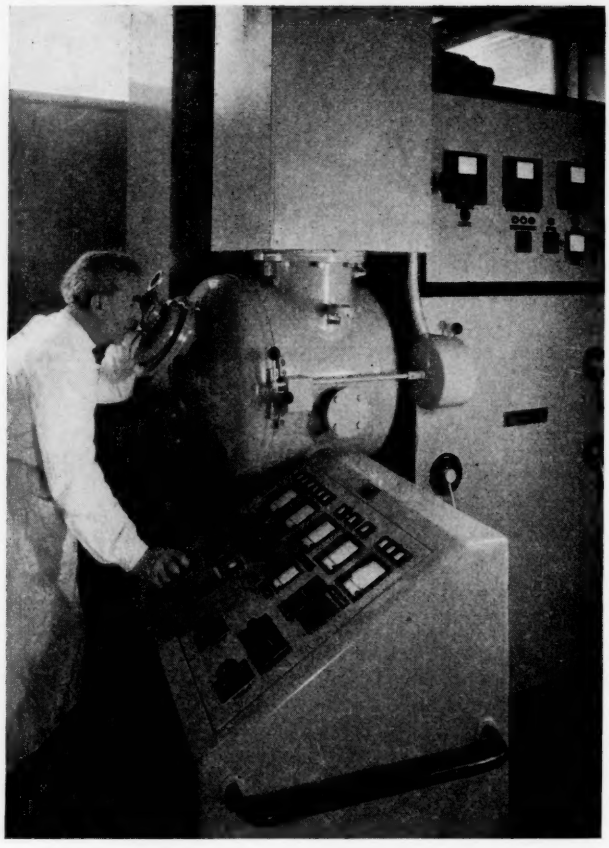

FIG. 4. Four de fusion par bombardement électronique sous vide poussé

électrons, ainsi qu'il est montré sur la photo. Le bloc à fondre se solidifie dans une coquille refroidie à l'eau avec fond abaissable.

Dans la Fig. 4, nous voyons un four de fusion à rayons électroniques utilisé dans un institut de recherches de métaux précieux. Dans ces essais les analyses des gaz sont effectuées avec un appareillage moderne d'extraction à chaud, dont le schéma apparait dans la Fig. 5. A gauche se trouve la partie d'extraction avec creuset en graphite et bobine à haute fréquence, au milieu une pompe à diffusion de mercure et une pompe automatique Toepler. L'amélioration qui a eu lieu par comparaison avec les appareillages d'analyse habituels est visible à droite. La séparation et l'analyse des quantités presque toujours très petites de gaz a lieu dans une colonne chromatographique pour gaz avec chambre à ionisation et dispositif d'enregistrement. La Fig. 6 montre une vue de l'appareillage d'analyse complet.

Il est maintenant question de savoir quelle est la meilleure méthode à suivre dans le traitement d'un métal ou d'un alliage donné. Le tableau de la Fig. 7 montre l'application des différentes méthodes à l'heure actuelle ou dans un futur très proche. Cependant l'examen détaillé des propriétés de tous les métaux en question nous conduirait trop loin. Le coût relatif et le vide le meilleur ont été indiqués. Comme on peut constater, trois procédés sous vide différents peuvent être à présemt utilisés avec les métaux comme le niobium, le vanadium, le tungstène, et le molybdène. Les aciers spéciaux de haute qualité seront seulement fondus, pour des raisons d'économie, dans des fours à induction sous haut vide ou dans des fours à arc sous vide.

Acier

Ce ne sera que le traitement sous vide de l'acier qui sera examiné en détail. Ici deux procédés se présentent :

A. Le dégazage à circulation sous vide d'après le procédé Heraeus-Ruhrstahl.

B. Le procédé du four à arc sous vide avec électrode consommable.

Dans le procédé de dégazage sous vide, on cherche à obtenir une diminution de la teneur en gaz et des inclusions non-métalliques. Dans la production de lourdes pièces forgées, la diminution d'hydrogène, qui empêche la formation de flocons, est de première importance. Dans la production d'acier laminé, il est tout aussi important de diminuer ou d'éliminer complètement les inclusions non-métalliques. Dans le développement du procédé à circulation, on s'était fixé le but de dégazer dans la poche de coulée des quantités d'acier de 80 à 100 t environ, sans trop déranger l'allure normale de l'aciérie. Ceci signifie qu'une installation pareille doit être de la construction la plus robuste et la plus simple possible. Ainsi que A. Lorenz l'avait proposé, les premiers essais furent effectués avec du mercure et, plus tard, avec une installation ayant plusieurs kilogrammes de plomb (Fig. 8).

Vol.
10
196

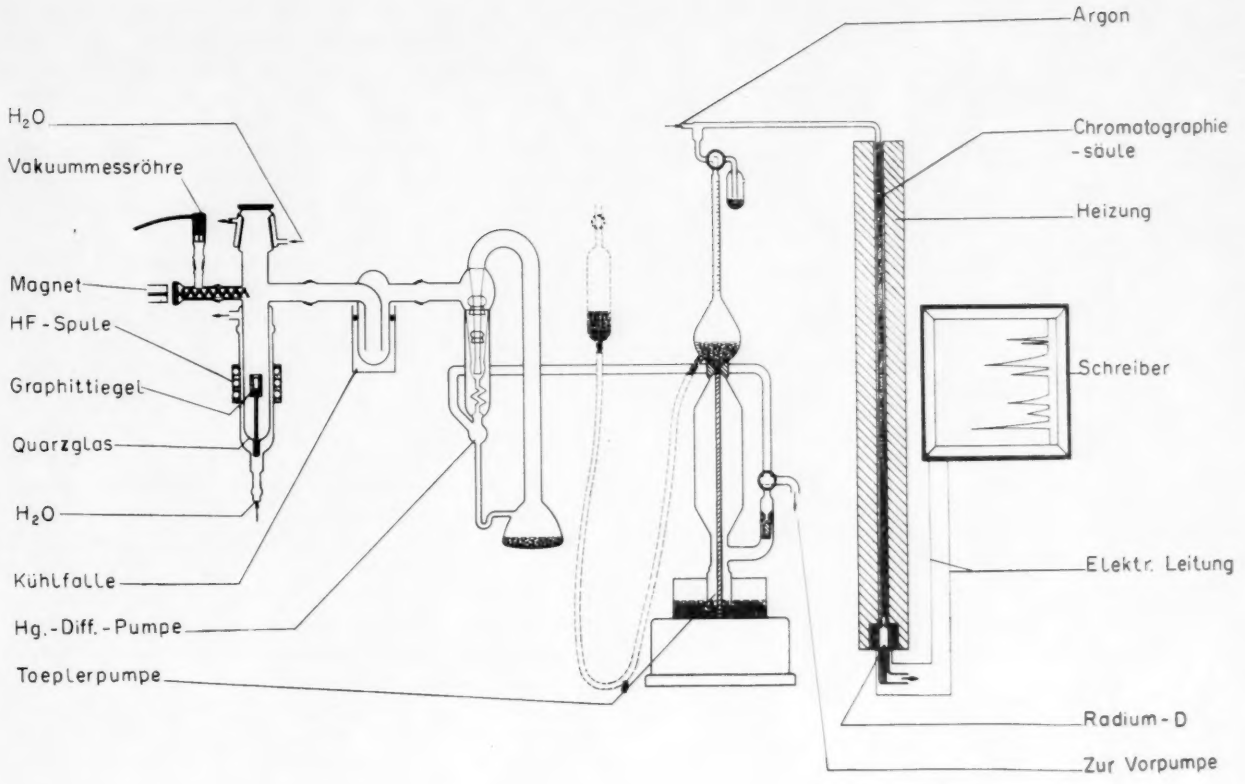

FIG. 5. Principe d'extraction à chaud pour le dosage des gaz dans les métaux

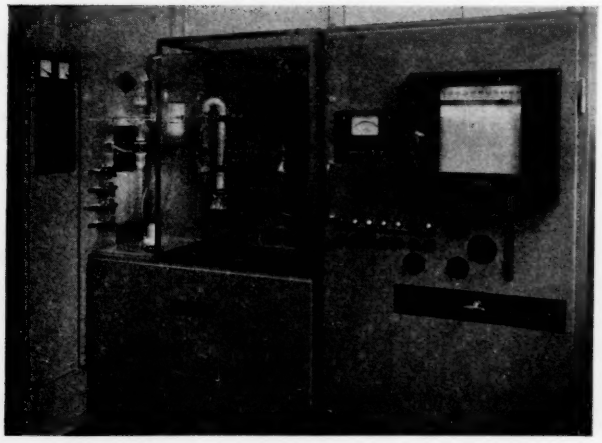

FIG. 6. Installation d'extraction à chaud pour le dosage des gaz dans les métaux

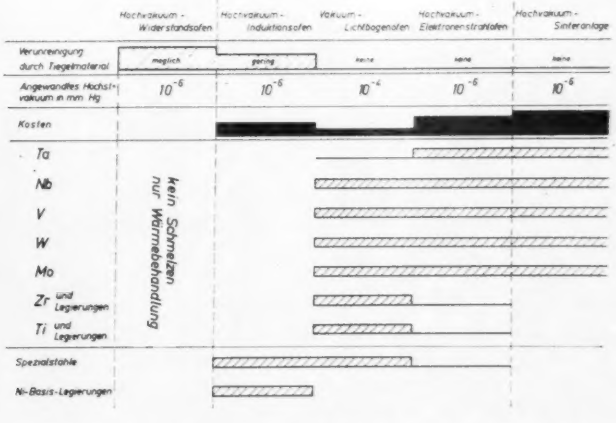

FIG. 7. Différentes méthodes de traitements des métaux

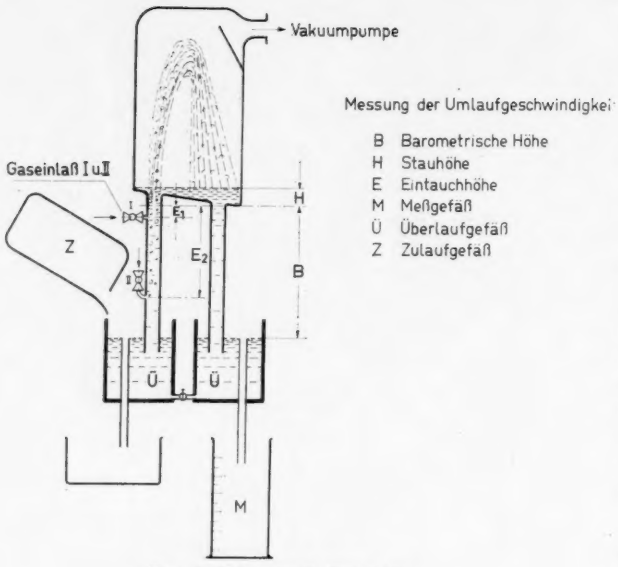

FIG. 8. Dégazage à circulation

Dans ces modèles d'installations, furent étudiés la formation de gouttes, le mécanisme du transport du métal, les effets de l'injection, la vitesse de la circulation en rapport avec la largeur des tuyaux, la profondeur d'immersion et la quantité de gaz.

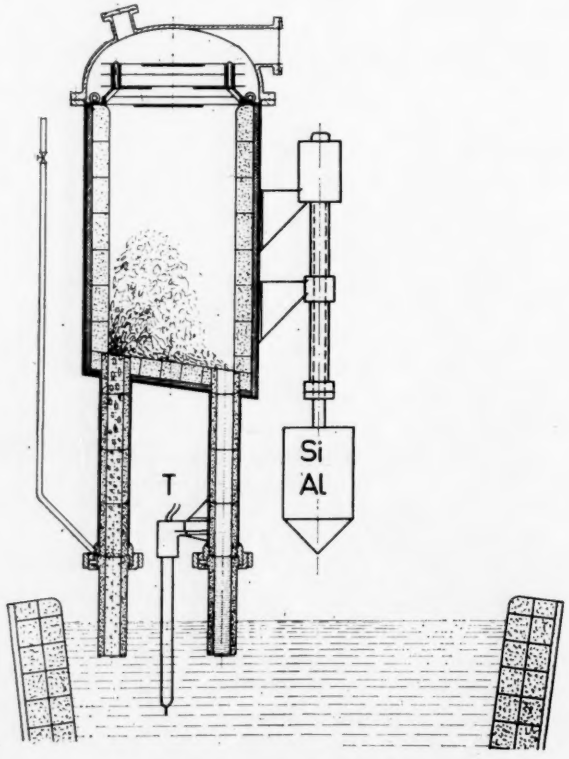

FIG. 9. Dégazage à circulation

Dans la Fig. 9, on peut observer le principe de l'installation de dégazage à circulation pour l'acier. Cette installation consiste en un réservoir étanche au vide, pourvu de deux tubes plongeurs et d'une canalisation de vide qui est raccordée au groupe de pompage par des joints à vide. Les tubes plongeurs descendent dans la charge à dégazer. A l'évacuation du récipient, la charge monte dans les deux tubes jusqu'à la hauteur barométrique qui, pour l'acier, est de 140 cm. Si on amène un gaz à la bride de raccordement de l'un des tubes plongeurs, les bulles de gaz, à la suite de la dilatation du volume, se déplacent vers le haut et transportent ainsi la charge dans le réservoir de dégazage. En même temps, a lieu, dans la charge qui monte, une intense formation de gaz qui favorise le transport. A l'entrée du réservoir de dégazage, l'acier se fractionne en éclaboussures et gouttelettes. Les gouttes, qui retombent en arrière, se rassemblent en formant un lac de fusion en forte ébullition de faible profondeur. La vidange du lac se fait par la conduite de décharge. La turbulence de la coulée de l'acier, la formation de gouttes et le lac de fusion en ébullition laissent prévoir un dégazage favorable qui a lieu aux surfaces limites liquide/gaz.

Ces raisons montrent que les valeurs d'équilibre thermodynamique des teneurs en hydrogène et en oxygène sont atteintes dans une large mesure. Il faut toutefois renoncer ici à des discussions théoriques plus étendues.

Grâce à la turbulence de la coulée, l'acier se mélange vite au contenu de la poche de coulée. A la suite de l'équilibre des concentrations d'acier dégazé et d'acier se trouvant dans la poche, la teneur en gaz de la masse d'acier diminue constamment. Le choix de la largeur des tuyaux, de la grandeur du récipient et de la vitesse de circulation sont choisis de telle façon, qu'en 20 min, on atteint un débit double ou triple du contenu de la poche. La perte en température d'une quantité d'acier de 90 t s'établit aux environs de 30 °C. Si l'on tient compte que l'acier sous vide, par suite d'une viscosité plus faible, permet une température de coulée de 20 °C plus basse, seule une petite surchauffe de l'acier dans le four est indispensable pour récupérer les pertes de chaleur.

L'observation de la vitesse de coulée et du mélange a été effectuée avec de l'or radio-actif. Ces recherches que Pröbstl a mises au point à Ruhrstahl, représentent un bel exemple de l'application dans l'aciérie des méthodes de recherche modernes.

Un échantillon d'or radio-actif est poussé avec une lance sous le tuyau ascendant (Fig. 10). L'or se dissout très rapidement dans l'acier et, transformé en nuage radio-actif, passe à travers le tuyau ascendant dans le récipient de dégazage, et coule à nouveau par le tuyau de vidange dans la poche de coulée. Le tuyau de vidange est muni d'un tube compteur, détecteur de radiations, qui sert à enregistrer la radio-activité. Plus grand est le nombre des impulsions enregistrées par le tube compteur dans une période donnée commençant depuis l'immersion de l'échantillon, plus lente est la coulée, puisqu'alors, la période d'arrêt du nuage radio-actif dans le domaine de fonctionnement du tube compteur est relativement longue. Par une vitesse plus grande de la coulée, le nuage radio-actif coule rapidement devant le tube compteur et ne cause qu'un petit nombre d'impulsions. Afin d'établir s'il se créait éventuellement entre les deux tuyaux plongeurs un court-circuit de la coulée, c.-à-d. si la coulée sortant du tuyau de vidange rejoint tout

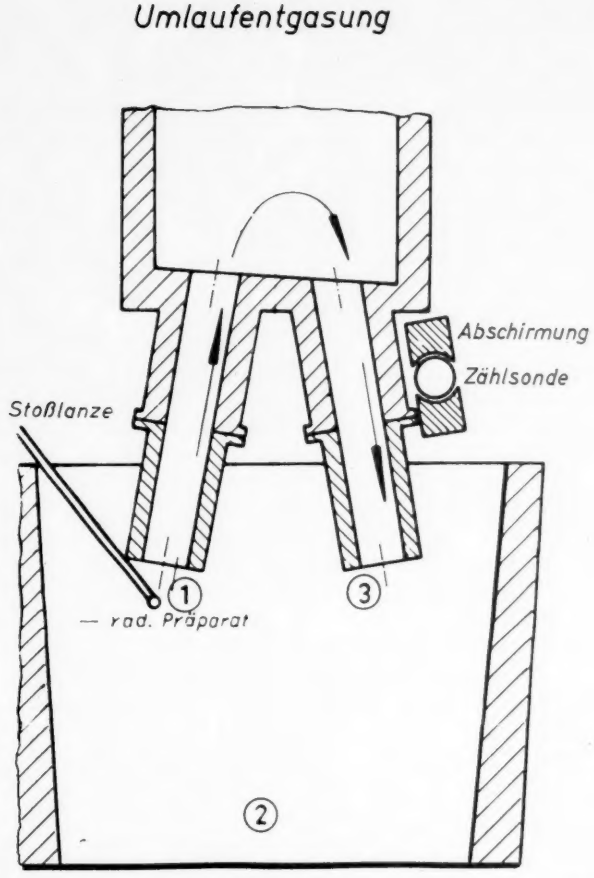

FIG. 10. Mesure de la vitesse de circulation au moyen d'isotopes radioactifs

de suite le tuyau ascendant, les essais suivants ont été effectués : dans un cas, l'échantillon a été porté jusqu'au fond de la poche, dans un autre, immédiatement au-dessous du tuyau de vidange. Aucune différence n'a pu être déduite des courbes enregistrées. Il faut en conclure qu'aucun court-circuit de coulée n'a lieu entre les deux tuyaux plongeurs. D'autres recherches avec isotopes ont servi à déterminer les proportions du mélange dans la poche de coulée.

L'allure de la pression de dégazage, par suite de la diminution constante de la teneur en gaz et du mélange continu, est représentée sous la forme d'une diminution exponentielle. La pression totale dans le récipient de dégazage est continuellement enregistrée, et la composition qualitative des gaz aspirés 'par la pompe à vide est continuellement suivie.

La Fig. 11 donne la variation dans le temps des pressions totale et partielle des gaz les plus importants. La teneur finale en hydrogène établie dans cette analyse de l'acier d'après le procédé de fusion d'étain, s'élevait à 2,9 ppm. Quelques minutes avant la fin du traitement, le silicium et ensuite l'aluminium sont immergés dans la poche de coulée. La circulation favorise une subdivision rapide et uniforme des quantités ajoutées. L'aluminium sert plus à l'amélioration de la texture qu'à la désoxydation qui se fait en grande partie pendant le traitement sous vide et fournit le CO

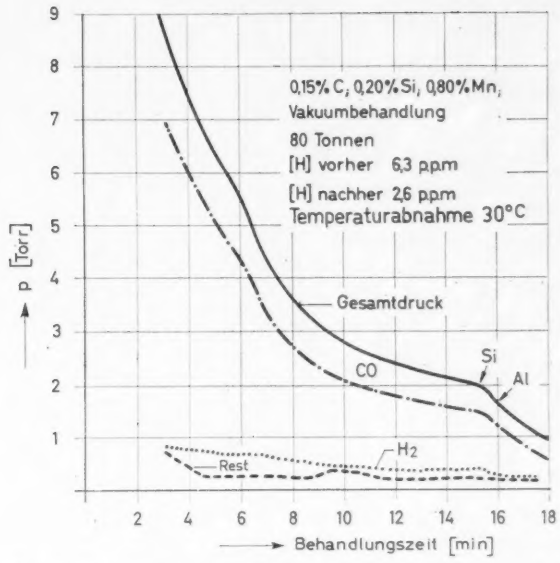

FIG. 11. Dégazage à circulation. Pressions totale et partielle

comme agent gazeux de désoxydation. Le dispositif d'introduction est directement monté sur le récipient de dégazage. Il s'est avéré qu'il suffisait d'immerger les moyens d'alliage et de désoxydation directement dans la poche de coulée, et qu l'on peut se passer d'un sas à vide sur le récipient de dégazage. Au début, le procédé n'a consisté que dans le traitement sous vide de fusions complètement calmes. L'acier avait été préparé de la façon habituelle. Seulement peu à peu, on commença à exploiter plus largement les possibilités métallurgiques de la désoxydation gazeuse en réduisant la désoxydation par le silicium et l'aluminium avant le traitement sous vide.

Plus on renonce aux moyens de désoxydation, particulièrement à ceux ayant une haute affinité pour l'oxygène, comme l'aluminium, plus grande est la possibilité d'obtenir un raffinage précieux par lequel les inclusions non-métalliques sont moindres ou nulles. Dans la production d'aciers faiblement alliés, les éléments d'alliage réactifs peuvent être introduits, aussi simplement que nous l'avons décrit, à la fin du traitement sous vide. Avec le chrome, qui avait déjà été introduit dans le four et était en partie devenu oxyde chromique, on a observé, au cours du traitement sous vide, une petite augmentation de concentration dans l'acier. Cette augmentation du chrome s'explique par le bas potentiel d'oxydation, c.-à-d. que l'oxyde chromique se réduit facilement.

Ces mesures peuvent être considérées comme le commencement d'un procédé chimique nouveau, qui requiert des connaissances physiques et chimiques systématiques. Il est facile de s'imaginer que, après les succès de l'application de l'oxygène dans l'industrie de l'acier, le traitement sous vide par effet de dégazage et de désoxydation peut aussi atteindre un raffinage valable de l'acier.

Si l'on peut adjoindre au traitement sous vide, surtout à la désoxydation gazeuse, les avantages de ségrégation et de solidification que l'on constate dans la coulée continue, un

autre procédé futur peut être entrevu : la coulée continue sous vide.

Bien qu'un tel procédé puisse paraître attrayant, surtout dans la production rationnelle de bandes en acier avec de bonnes qualités de surface, il ne faut pas oublier que les deux procédés, le traitement sous vide à grande échelle industrielle et la coulée continue, sont encore en plein développement.

Toutefois il y a aujourd'hui un procédé dont le développement est déjà très avancé et qui présente les traits caractéristiques du traitement sous vide et de la coulée continue que l'on vient de décrire : la fusion à arc sous vide. Il est intéressant de constater que la fusion à arc sous vide a eu son départ dans la production des métaux tantale et molybdène, qu'elle a plus tard pris une grande importance dans la production du titane et du zirconium, et que son application à l'acier ne s'est affirmée qu'au cours des dernières années.

Une différence fondamentale entre le four à arc sous vide d'une part, et le four à induction et les autres procédés de dégazage d'autre part, réside dans l'emploi d'une coquille en cuivre refroidie à l'eau. Le matériau à fondre se solidifie assez rapidement sur la paroi de la coquille, en préparant ainsi pour la suite une cuvette solide. Le creuset proprement dit est par conséquent constitué du même matériau que celui qui est à fondre. Des réactions nuisibles avec un matériau étranger du creuset ne peuvent pas avoir lieu. C'est pour cette raison que le procédé pour la production de titane et zirconium fut introduit. Jusqu'à présent aucun autre procédé utilisable n'a été trouvé pour ces métaux.

La coquille refroidie à l'eau procure une formation continue du bloc de fusion à la solidification. Des ségrégations, des retassures et des porosités n'apparaissent presque jamais.

Au moyen de quelques exemples, je voudrais vous montrer les améliorations des propriétés des aciers que l'on peut obtenir par la fusion à l'arc sous vide. Bien entendu, ces résultats coïncident jusqu'à un certain degré avec ceux de la fusion par induction sous vide.

(a) *Abaissement de la teneur en gaz*

Comme la quantité de gaz dissous dans une masse métallique fondue est proportionelle à la racine carrée de la pression partielle régnant au-dessus de la masse fondue, un dégazage de celle-ci est favorisée par une basse pression dans la chambre du four. De plus, il y a aussi une dissociation des liaisons gaz-métal les moins stables. Il faut ajouter que des mesures ont montré que, malgré les hautes températures régnant dans un arc électrique, les surfaces liquides à l'électrode de fusion et au bain de fusion ne peuvent être échauffées que légèrement au-dessus du point de fusion. Dans le cas de l'acier, il n'y a pas plus de 100 °C environ. Quand, donc, des oxydes, nitrures et carbo-nitrures très stables ne sont que peu dissociés, ceux-ci se font cependant éliminer d'une manière importante par flottation à la surface du lingot de fusion, de telle manière que la teneur totale en gaz des alliages est abaissée. Il apparaît aussi dans la fusion à l'arc sous vide un certain effet de fusion par zone.

(b) *Augmentation du degré de pureté*

Dans la fusion à pression atmosphérique, les aciers sont normalement désoxydés au moyen d'aluminium, titane, silicium ou manganèse. Les produits de désoxydation, quoique pour la plupart insolubles dans la masse fondue, restent en partie comme inclusions non-métalliques dans les alliages. Comme mentionné auparavant, ces inclusions sont écartées en grande partie par la refonte dans le four à arc sous vide. Les inclusions plus petites sont, en général, dispersées d'une manière homogène dans tout le lingot.

(c) *Effet permettant d'éviter les ségrégations et la porosité d'un lingot*

Dans les lingots coulés de la manière classique, il apparaît au milieu du lingot des ségrégations et des porosités, qui doivent être réduites en réalité par l'habileté de l'aciériste, mais qui ne peuvent jamais être tout à fait évitées dans la plupart des cas. De telles défectuosités provoquent des difficultés lors des transformations ultérieures (forgeage, laminage, usinage) et dégradent les propriétés mécaniques, spécialement dans la direction transversale. Par la formation continue du lingot dans le four à arc sous vide, de tels phénomènes sont éliminés par une technique de fusion correcte, c'est-à-dire par un bain le plus calme possible en profondeur, ce qui peut être obtenu par des paramètres de fusion déterminés. On évite aussi complètement la formation d'une retassure supérieure, en diminuant d'une manière continue le courant de fusion en fin de la fusion. Vanadium Alloys Steel Corp. a fait savoir que, dans les alliages hautement réfractaires, jusqu'à 95 pour cent d'un lingot fondu à l'arc sous vide était sain et pouvait subir des opérations de transformation ultérieures.

(d) *Amélioration des propriétés mécaniques*

Un des avantages les plus importants est la possibilité de transformations essentiellement meilleure des alliages hautement alliés à base de fer et de nickel, qui ne sont normalement que très péniblement transformables à cause des inclusions d'oxydes, de nitrures et de carbonitrures sous forme de dendrites, à cause de la formation de phases intermétalliques cassantes aux limites des grains, à cause des ségrégations et des porosités au milieu du lingot. La refonte en four à arc sous vide aplanit considérablement ces difficultés. Ce moyen donne la possibilité de développer encore d'autres alliages, dont l'utilisation n'aurait pas pu être envisagée à cause de leur manque de capacité de transformations. L'augmentation de rendement par l'amélioration des capacités de transformations est vraiment essentielle. Jusqu'ici il arrivait que des matériaux hautement alliés, fondus à la pression atmosphérique, ne procuraient qu'un gain de 15 pour cent. Rien que cette amélioration était rentable dans beaucoup de cas.

La Fig. 12 montre la durée de vie et la valeur des pertes d'un acier à roulement à billes SAE 100, qui correspond à l'acier allemand 100 Cr. 6.

La différence entre un matériau fondu normalement et un matériau fondu sous vide apparaît particulièrement nette pour des valeurs de pertes comprises entre 3 et 20 pour cent. Pour une perte faible de 5 pour cent, la durée de vie est quintuplée par la mise en oeuvre d'un alliage fondu sous vide.

La température de transition entre la rupture cassante et la rupture tenace des aciers ferritiques inoxydables est

Vol. 10 196

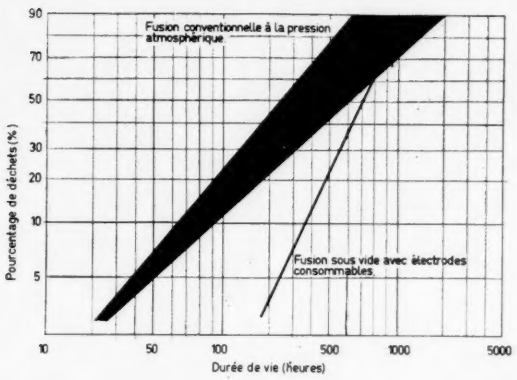
Fusion conventionnelle à la pression atmosphérique
Fusion sous vide avec électrodes consommables
Pourcentage de déchets (%)
Durée de vie (heures)

FIG. 12. Pourcentage de déchets en fonction de la durée de vie pour un acier pour roulements à billes (1,0 %C, 1,5 %Cr) fondu à la pression atmosphérique et fondu sous vide

abaissée substantiellement. La résilience à la température ambiante se relève dans le cas d'un acier, de 1 kgm à 22 kgm, ou encore de 0,3 kgm à 14 kgm.

Comme dernier exemple (Fig. 13) qu'il soit mentionné que la résistance à la fatigue s'élève d'une manière appréciable

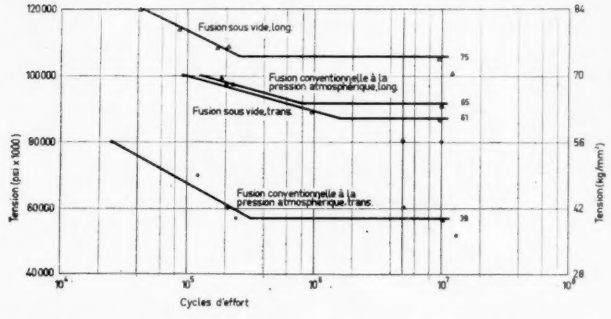
Fusion sous vide, long.
Fusion conventionnelle à la pression atmosphérique, long.
Fusion sous vide, trans.
Fusion conventionnelle à la pression atmosphérique, trans.
Tension (psi x 1000)
Tension (kg/mm²)
Cycles d'effort

FIG. 13. Limite de fatigue d'un acier à haute résistance, fondu à la pression atmosphérique et sous vide (SAE 4340)

et en particulier, la différence de cette caractéristique entre les directions longitudinale et transversale est diminuée sensiblement.

Finalement il faut encore citer un développement intéressant du four à arc dans la direction des blocs d'un poids de 25 t. Ces blocs, qui auront un diamètre d'un mètre, devront être utilisés pour la fabrication de pièces forgées lourdes, comme par exemple d'arbres de rotors et de roues motrices de turbines.

La Maison américaine Midvale-Heppenstall, qui a déjà fabriqué des pièces forgées lourdes avec une installation de dégazage sous vide d'après le procédé du " Giessstrahl ", est le soumissionaire de nouvelles installations à l'arc sous vide.

Les blocs déjà dégazés sous vide dans le " Giessstrahl " doivent être refondus dans le four à l'arc sous vide afin d'obtenir une amélioration ultérieure. Le four est construit de telle façon qu'il permet la réalisation d'un programme d'essais avec des lingots encore plus lourds et plus gros et des diamètres jusqu'à 1,5 m. Une vue de ce four, que la firme Heraeus de Hanau a entrepris de construire, apparait dans la dernière Fig. 14.

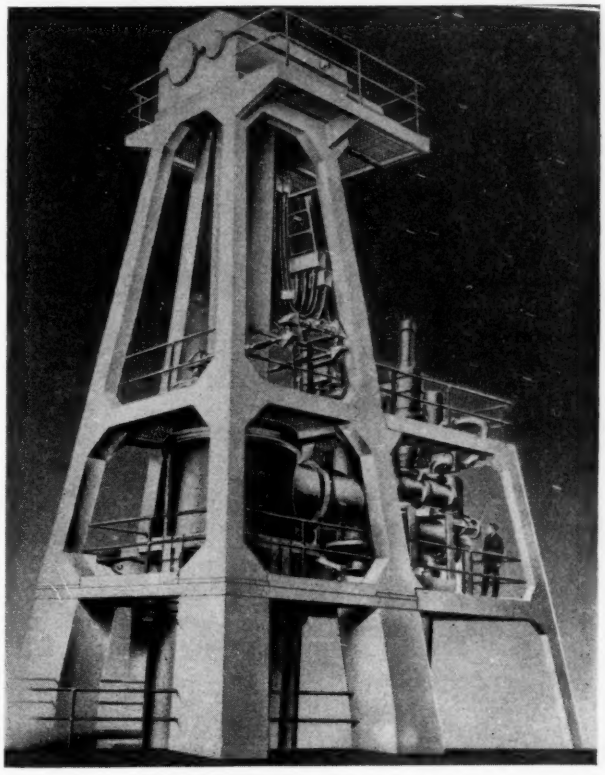

FIG. 14. Four de fusion à l'arc sous vide (25 t)

J'ai voulu montrer dans mon exposé quelle importance le traitement sous vide des métaux a acquis. Je n'ai pas tenu à mettre en lumière des résultats dispersés, mais bien plus à souligner les traits principaux d'une technique nouvelle de la métallurgie sous vide.

Techniques du Vide et Propriétés des Métaux*

L. HABRAKEN

Centre National de Recherches Métallurgiques, Liège, Belgique

Vacuum Techniques and Metal Properties†

L. HABRAKEN

Centre National de Recherches Métallurgiques, Liège, Belgium

Vol.
10
1960

Au cours de leur élaboration, les métaux sont généralement en contact avec des atmosphères gazeuses. Ces atmosphères dont la pression est, le plus souvent, voisine de la pression atmosphérique, sont de compositions très variables.

Le métal liquide ou, au cours de traitements thermiques, le métal solide, tend à se mettre en équilibre avec cette atmosphère. Certains " gaz " se dissolvent dans le métal, d'autres réagissent avec les éléments présents.

Lors de la solidification du métal liquide, la solubilité de ces " gaz " dissous peut décroître avec la température ou les nouvelles phases en présence ; leur affinité pour certains éléments peut se modifier, des composés peuvent même se former à des températures définies. Les qualités du lingot résultant, ses possibilités de mise en forme, les propriétés du produit final seront influencées.

Les techniques du vide, en modifiant la pression, la nature de l'atmosphère au-dessus du bain métallique, ou autour du métal solide, conduisent à un nouvel équilibre, donnant ainsi des possibilités nouvelles dans l'élaboration ou le traitement des métaux et alliages.

Dans le cas de l'élaboration des métaux, il apparaît une métallurgie sous vide où l'on peut distinguer :

— des possibilités pour l'amélioration des alliages existants,

— des moyens pour réaliser de nouveaux alliages.

Il est évident que l'équilibre dont nous parlons ci-dessus est bien différent lorsqu'on passe d'une atmosphère de quelques dizaines de millimètres de Hg, à une atmosphère de quelques microns ou même de quelques centièmes de micron de Hg ; qu'il est tout différent aussi si l'on remplace l'oxygène et l'azote de l'air par un gaz neutre (argon) ou par l'hydrogène, l'oxyde de carbone, etc.

During their preparation, metals are usually in contact with gases. These gases, the pressure of which is usually near that of atmospheric pressure, are of extremely variable composition.

A liquid metal or a solid metal during its heat treatment tends to attain the equilibrium with this atmosphere. Certain gases are dissolved in the metal while others may actually react chemically with the elements present.

During the solidification of a metal, the solubility of these dissolved gases decreases with the temperature or the new phases present. The affinity of the gases for certain elements can change and new compounds can even be formed at well-defined temperatures. The quality of the ingot, its workability as well as the properties of the final product will thus be influenced. Vacuum techniques which modify the pressure and the nature of the atmosphere above the metallic bath or around a solid metal also modifies the equilibrium, thus making it possible to perform new methods of metal and alloy preparation and heat treatment.

There thus exists a vacuum metallurgy where one can distinguish :

(1) Possibilities for the improvement of classical alloys

(2) A means to realize the preparation of new alloys.

It is evident that the equilibrium which we mentioned above is quite different when one passes from a pressure of several tens of millimeters of mercury to a pressure a several microns or even to several hundredths of a micron of mercury.

It is also very different if one replaces atmospheric oxygen and nitrogen by an inert gas such as argon or a mixture of hydrogen and carbon monoxide.

*Ce travail a été réalisé sous les auspices de l'Institut pour l'Encouragement de la Recherche Scientifique dans l'Industrie et l'Agriculture (IRSIA) au Centre National de Recherches Métallurgiques (CNRM).

†This work was conducted under the auspices of the " Institut pour l'Encouragement de la Recherche Scientifique dans l'Industrie et l'Agriculture " IRSIA) at the " Centre National de Recherches Métallurgiques " (CNRM).

Cette qualité ou ce " degré " de vide conditionne les installations, non seulement les types de pompe, mais également les formes d'énergie mise en oeuvre, les quantités de métal que l'on pourra traiter, etc.

Les puissantes pompes à palettes modernes, les " pompes à diffusion " à grand débit permettent de maintenir un vide moyen (quelques mmHg ou dizièmes de mmHg) dans de très grandes enceintes[1] et ainsi de traiter les aciers de masse au moment de la coulée par exemple. Il s'agit en fait alors d'un dégazage sous vide après une fusion classique au four à arc ou au four Siemens-Martin[2].

The quality or the " degree " of the vacuum determines the equipment employed ; not only the types of pumps utilized but also the forms of energy employed, the quantities of material treated, etc. The modern rotary pumps and the high capacity diffusion pumps permit us to realize an average vacuum of several millimeters or tens of millimeters of mercury in a very large volume[1]. These units make it possible to treat large masses of steel during casting, for example. It can thus be employed as a means of degassing after a classical fusion operation in an electric arc or in an open hearth furnace[2].

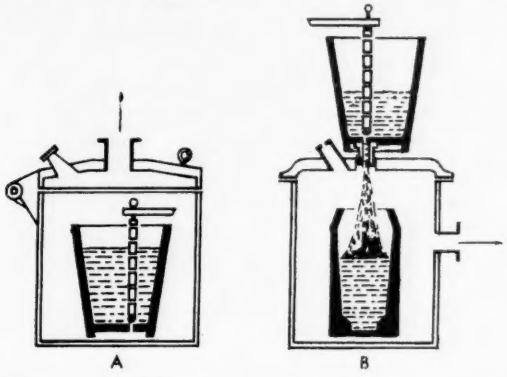

FIG. 1. Techniques de dégazage sous vide[2]

A. dégazage au tiroir
B. dégazage au jet
C. dégazage par tube plongeur
D. dégazage continu par la méthode au siphon (circulation sous vide)

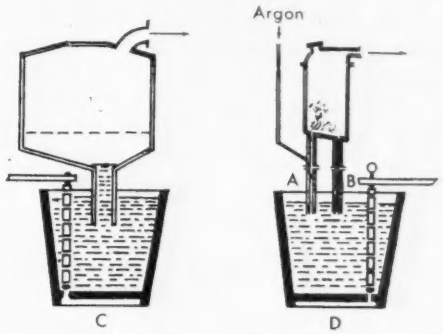

FIG. 1. Four vacuum degassing techniques[2]

A. Ladle degassing
B. Vacuum stream degassing
C. Pipette degassing by lifting
D. Continuous degassing by the siphon method

La Fig. 1 rappelle les méthodes les plus importantes : dégazage en poche, dégazage au jet de coulée, dégazage au siphon. La Fig. 2 montre un exemple de dégazage en

The most important methods are illustrated in Fig. 1 : ladle degassing, stream degassing and siphon degassing. An example of degassing of a ladle sealed directly to the upper part of the mould is shown in Fig. 2. The only

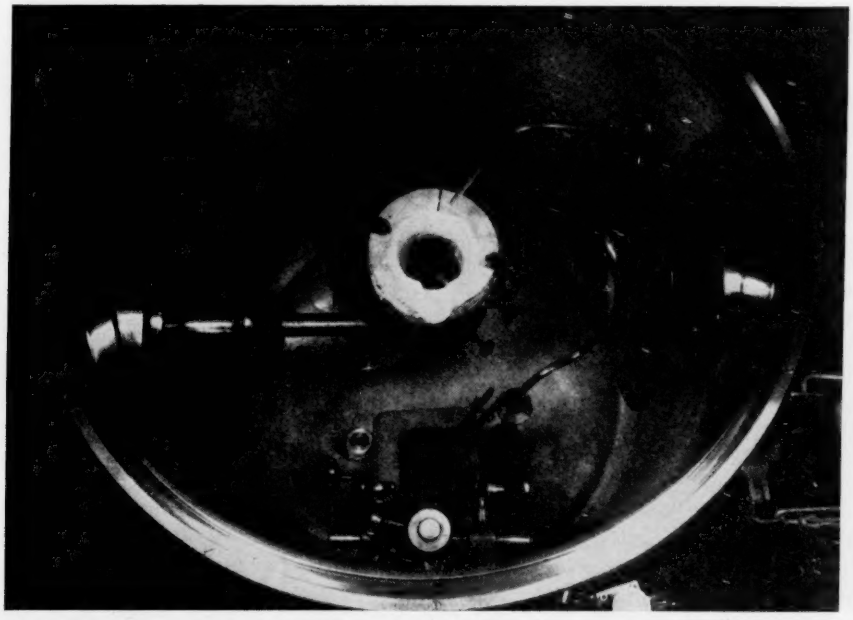

FIG. 2. Méthode de dégazage avec cuve placée directement sur la lingotière[2]

FIG. 2. Degassing method with the ladle sealed directly to the mould[2]

tête de lingotière. La seule énergie nécessaire en dehors de celle utilisée pour le groupe de pompage est l'énergie employée pour porter le métal à une température plus élevée. Ces procédées se répandent de plus en plus et intéressent de grandes quantités de métal.

Dès que l'on veut à la fois fondre et couler sous vide, on doit alors recourir à une installation plus complexe où le vide doit être réalisé dans une enceinte relativement importante puisqu'il faut pouvoir basculer le four pour couler en lingotière. Le vide réalisé à l'aide de pompes à palettes et de pompes à diffusion descend jusqu'à 10^{-4} mmHg. Le chauffage est obtenu par résistance ou, plus couramment, par induction. La fusion se fait généralement dans des creusets frittés *in situ*. De nombreux fours à induction sous vide existent actuellement, permettant la fusion et la coulée de lingots allant de 1 kg à 2½ t et on annonce même jusqu'à 5 t dans les futures installations[3, 4, 5]. Ce mode de fusion s'adresse évidemment à des alliages spéciaux. La Fig. 3 montre un type de four industriel.

energy necessary in addition to that supplied to the pumps is that utilized to increase the temperature of the metallic bath. These examples are becoming increasingly numerous during the last few years for the production of large tonnages of transfromer sheet, rails, construction steels, and forgings.

If one wishes to both melt and cast in vacuum, the installation becomes more complex since the evacuated chamber increases greatly in volume to permit the casting operation. The vacuum realized by a group of rotary and diffusion pumps descends to about 10^{-4} mmHg. Heating is performed by resistance or, more frequently, by induction. Melting is generally done in magnesia or zirconia crucibles rammed and sintered *in situ*. Numerous induction furnaces of this latest model actually exist with capacities from 1 kg to 2½ t, with one of 5 t capacity now under study[3, 4, 5].

The process is especially interesting for special-purpose alloys. An industrial furnace is illustrated in Fig. 3.

FIG. 3. Four à induction sous vide (type Balzers)

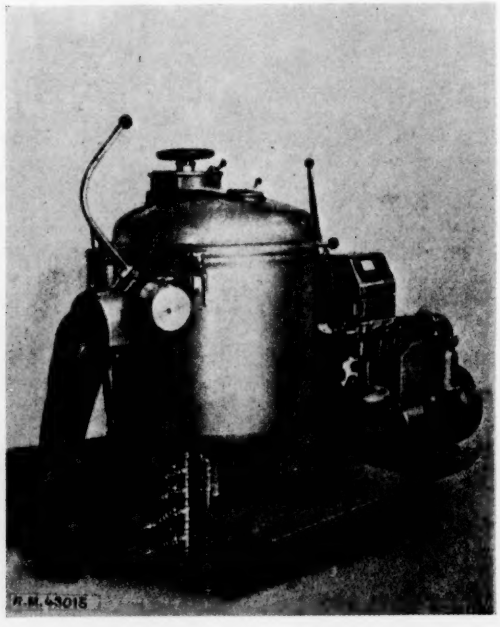

FIG. 3. Vacuum induction furnace (Balzers type)

L'utilisation du vide permet de rechercher une source d'énergie différente des formes d'énergies conventionnelles par exemple, la fusion dans un arc électrique ou sous flux d'électrons. La première forme a donné naissance aux fours à électrodes consommables[6, 7, 8], la deuxième au four à bombardement d'électrons[9, 10, 11].

La Fig. 4 schématise un four à électrodes consommables. L'enceinte est maintenant relativement petite; le vide y est de l'ordre de 10^{-1} à 10^{-2} mmHg. L'énergie nécessaire à la fusion est fournie par l'arc entre l'électrode consommable, formée du produit à fondre et du produit fondu. Il s'agit d'un arc en courant continu de grande intensité—milliers d'ampères—mais sous une tension de quelques dizaines de volts. La fusion se fait dans un " creuset " en cuivre refroidi à l'eau, il n'y a plus de contact, donc de réaction, avec des

The utilization of a vacuum furnace permits one to employ non-conventional sources of energy such as the electric arc and electron flux. The first has resulted in the construction of furnaces utilizing consumable electrodes[6, 7, 8] and the second those employing electron bombardment[9, 10, 11].

Fig. 4 shows schematically a consumable electrode furnace, the vacuum chamber is kept relatively small, the vacuum being of the order of 10^{-1} to 10^{-2} mmHg. The energy necessary for melting is furnished by an arc between the consumable electrode composed of the material to be melted and the material already melted. The arc is produced by direct current of several thousand amperes under a difference of potential of only several tens of volts. One advantage of the method is that melting is performed in a water-cooled copper crucible so there is no contact with and contamination

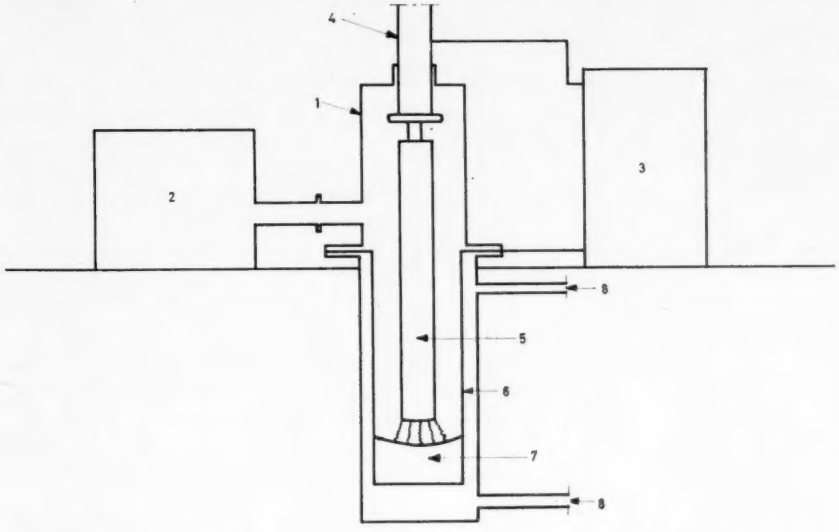

FIG. 4(a). Four de fusion à arc à électrodes consommables

Schéma du four

1—four
2—groupe de pompage
3—source de courant et panneaux de contrôle
4—support d'électrodes
5—électrode consommable
6—creuset refroidi à l'eau
7—lingot
8—entrée et sortie d'eau de refroidissement

FIG. 4(a). Consumable electrode arc melting furnace

Scheme

1—furnace
2—vacuum system
3—power source and control panel
4—electrode holder
5—consumable electrode
6—water cooled crucible
7—ingot
8—water in—out

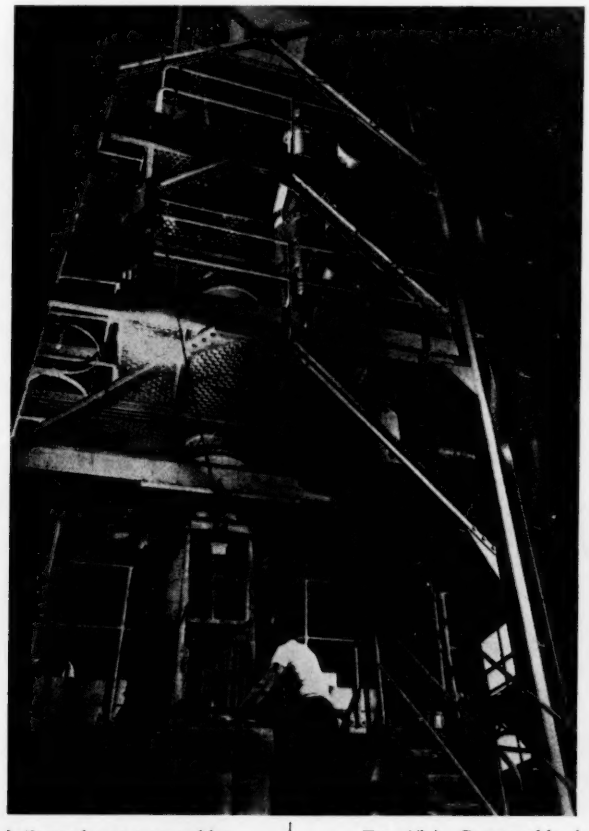

FIG. 4(b). Vue d'un four Heraeus à électrodes consommables

FIG. 4(b.) Consumable electrode furnace—Heraeus type

produits réfractaires. Le temps de fusion est court. Dans les grandes installations, on réalise ainsi une coulée " continue " intéressante, car elle limite l'hétérogénéité qui nait souvent au cours de la solidification des lingots. L'avantage inhérent à la disparition du creuset et le coût moyennement élevé des installations expliquent le développement considérable de ce mode de fusion, qui produit actuellement des lingots de plusieurs tonnes[12].

Lorsqu'un flux d'électrons bombarde une pièce métallique, une anti-cathode d'une ampoule d'un appareil à rayons X par exemple, on constate, si celle-ci n'est pas refroidie, que l'échauffement peut être tel que l'on fond le métal. L'utilisation à une plus grande échelle de ce phénomène est à la base d'une technique de fusion et d'une technique de soudure. L'emploi d'un flux d'électrons est possible grâce à un vide très élevé (10^{-4} à 10^{-5} mmHg).

from refractories. The melting time is also short. In the large units it is possible to realize a " continuous casting " operation and hence reduce or eliminate inhomogeneities usually encountered during solidification of the ingots. The inherent advantages as well as the relatively modest cost of these units explains the considerable development of this means of melting which can actually produce ingots weighing several tons[12].

When an electron beam strikes a metal such as the anti-cathode of an X-ray tube for example, one finds that if the target is not vigourously cooled, it can be eventually melted. The utilization of this phenomenon on a larger scale is the base of a melting technique as well as one of welding. The use of an electron beam is possible due to the high vacuum (10^{-4} to 10^{-5} mmHg).

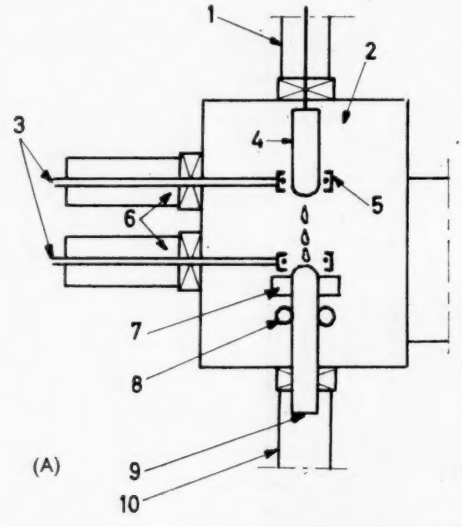

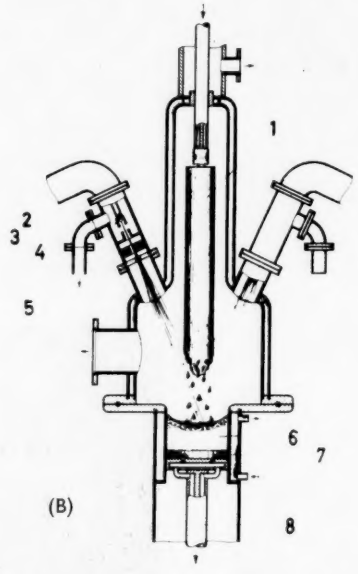

FIG. 5(A et B). Schémas de fours à bombardement d'électrons

A—avec cathodes circulaires
1—chambre de chargement
2—four
3—entrées haute tension en courant continu
4—métal à fondre
5—canon d'électrons
6—chambre de changement des canons d'électrons
7—creuset refroidi à l'eau
8—guides du lingot
9—lingot
10—chambre de refroidissement du lingot

B—avec canons d'électrons
1—métal à fondre
2—cathode
3—anode
4—lentille magnétique
5—vers pompe
6—lingotin
7—creuset
8—dispositif de guidage du lingot

FIG. 5(A and B). Electron bombardment furnace

A. with ring cathode
1—entrance lock
2—melting tank
3—high voltage D.C. power
4—raw ingot
5—electron gun
6—gun locks
7—water cooled crucible
8—ingot puller
9—melted ingot
10—ingot cooling chamber

B. with electron guns
1—raw ingot
2—cathode
3—anode
4—magnetic lens
5—lens to pump groups
6—ingot
7—crucible
8—ingot puller

Pour la fusion, différentes techniques existent : elles sont résumées Fig. 5. La puissame nécessaire est de l'ordre de quelques dizaines de kilowatts. L'émission est réalisée par exemple, sous une tension de 20 à 30 kV. La densité

For melting various techniques exist which are shown in Fig. 5. The energy necessary is of the order of several tens of kilowatts. The emission is realized under a tension of 20 to 30 kV and the current density is about 1 A. The

Vol. 10 196

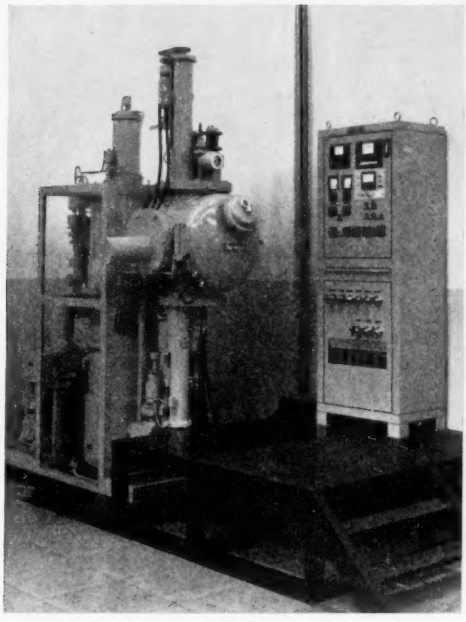

FIG. 5(C). Vue d'un four à bombardement d'électrons type ES Heraeus

FIG. 5(C). Electron bombardment furnace (ES Heraeus type)

du faisceau d'électrons est de l'ordre de l'ampère. Le métal se solidifie dans une enceinte en cuivre refroidie à l'eau. On peut réaliser ici également une méthode semi-continue permettant d'obtenir des lingots d'une centaine de kilogrammes.

A côté de ces procédés les plus importants, en développement constant d'ailleurs, il faut encore mentionner la fusion par zone qui s'adresse à des métaux spéciaux, tels que le germanium[13].

La comparaison des procédés principaux décrits ci-dessus est donnée au tableau I[14, 15]. Le tableau II rappelle les sources de contamination des différents procédés[14, 15]. Enfin, le tableau III donne une idée du développement de certaines de ces techniques aux États-Unis d'Amérique.

TABLEAU I

Comparaison des procédés

	Température °C	Atmosphère (pression)	Temps
Fusion à l'air (four électrique)	1500–1700	1 atm	2 à h
Four à induction sous vide	,,	10^{-1} à 10^{-4} mmHg	1 à 5 h
Four à électrodes consommables	1500–5000	env. 10^{-2} mmHg	$\frac{1}{4}$ à $\frac{1}{2}$ h
Four à bombardement d'électrodes	,,	10^{-5} mmHg	1 h

Les avantages principaux qui découlent de l'utilisation des procédés décrits ci-dessus, dans la préparation des alliages, peuvent se résumer comme suit[2, 14] :

(1) Abaissement de la teneur en gaz
(2) Contrôle plus serré de la composition
(3) Propreté du métal plus grande
(4) Ségrégation ou porosité moindre dans le lingot
(5) Possibilité accrue de travail à chaud ou à froid du métal

molten metal solidifies in a water-cooled copper crucible. It is possible to operate this technique also in a semi-continuous manner for some hundreds of kilograms or to melt only several grams.

In addition to these procedures which are undergoing continuous development, it is also necessary to mention the method of zone melting especially utilized for metals such as germanium[13].

A comparison of the principal procedures described above is given in Table I[14, 15].

The sources of contamination of the different processes are given in Table II.

Table III gives an idea of the development of these techniques in the U.S.A.

TABLE I

Comparison of the different processes

	Temperature (°C)	Atmosphere (pressure)	Time
Air melting	1500–1700	1 atm	2–3 h
Induction vacuum furnace	,,	10^{-1}–10^{-4} mmHg	1–5 h
Consumable electrode furnace	1500–5000	10^{-2} mmHg	$\frac{1}{4}$–$\frac{1}{2}$ h
Electron bombardment furnace	,,	10^{-5} mmHg	1 h

The major aims of the procedures described above not only for mass produced steels, but also for special steels and alloys may be resumed as follows[2, 14] :

(1) Decrease in gas content
(2) Better control of the composition
(3) Increase in metal cleanliness
(4) Decrease in segregation and porosity
(5) Increase the hot and cold workability of the metal

TABLEAU II

Sources de contamination

	Air	Laitier	Réfractaire des creusets
Fusion au four électrique	oui	oui	oui
Fusion au four à induction sous vide	non	non	oui
Fusion au four à électrodes consommables	non	non	non
Fusion au four à bombardement d'électrons	non	non	non

TABLEAU III

	Capacité annuelle en tonnes		Poids des lingots (kg)		Diamètre des lingots	
	1957	1959	1957	1959	1957	1959
Four à induction sous vide	10 000	15 000	1 500	2 500	—	—
Four à électrodes consommables	25 000	50 000	7 000	20 000	65 cm	75 cm

(6) Amélioration des propriétés mécaniques, chimiques et magnétiques

(7) Production de métaux et d'alliages qu'on ne peut obtenir par la fusion classique ou bien, lorsqu'ils sont fondus à l'air, ne peuvent être formés à chaud économiquement.

Suivant les alliages ou les procédés employés, ces avantages peuvent être obtenus individuellement ou collectivement. Il existe une certaine interdépendance entre eux d'ailleurs. Les propriétés optima dans les alliages sont obtenues actuellement par la combinaison de deux des procédés : la fusion au four à induction sous vide suivie d'une refusion au four à électrodes consommables.

La comparaison des procédés de fusion au four à induction sous vide et au four à électrodes consommables, en ce qui concerne les objectifs ci-dessus, est donnée au tableau IV[15].

TABLEAU IV

Procédés de fusion et qualité des lingots par rapport aux modes de fusion classiques

	Four à induction sous vide	Four à électrodes consommables
Propreté	améliorée	améliorée
Teneur en gaz	plus faible	plus faible
Travail à chaud	plus aisé	plus aisé
Propriétés mécaniques (sensibles à la composition)	améliorées	peu d'effet
Propriétés mécaniques (sensibles à la ségrégation)	peu d'effet	améliorée

L'utilisation des techniques du vide a permis l'amélioration de nombreuses nuances d'alliages. Nous voudrions, ci-dessous, indiquer quelques-unes d'entre elles :

TABLE II

Sources of contamination

	Air	Slag	Crucible refr.
Melting in electric furnace	Yes	Yes	Yes
Melting in vacuum induction furnace	No	No	Yes
Melting in consumable electrode furnace	No	No	No
Melting in electron bombardment furnace	No	No	No

TABLE III

	Actual capacity (t)		Ingot weight (kg)		Ingot diameter (cm)	
	1957	1959	1957	1959	1957	1959
Induction furnace	10,000	15,000	1500	2500	—	—
Con. Elect. Fur.	25,000	50,000	7000	20,000	65	75

(6) Increase the mechanical, chemical and magnetic properties

(7) Production of metals and alloys not possible by classical methods or those when melted in air cannot be hot-worked economically.

These improvements in the quality can be obtained individually or collectively. They are interdependent, by the way. The optimum properties of alloys are actually obtained by a combination of two of these processes : melting in a vacuum induction furnace followed by a remelting in a consumable electrode furnace.

A comparison of the procedure by melting in an induction furnace and an electrode furnace in relation to the above-mentioned aims is given in Table IV[15].

TABLE IV

Melting method and ingot quality

	Vacuum induction furnace	Consumable electrode furnace
Cleanliness	better	better
Gas content	lower	lower
Cold workability	easier	easier
Mech. Prop. (influenced by comp.)	better	no effect
Mech. Prop. (influenced by segreg.)	better	no effect

The utilization of vacuum techniques has permitted the preparation of several types of alloys. We would like to indicate several of these below.

— mass produced steels : Cr–Mo, Cr–Mo–V, Ni–Mo–V . . . steels

Vol. 10 1960

— aciers de masse : aciers au Cr–Mo–V, Ni–V–Mo, Cr–V–Mo, . . .
— aciers faiblement alliés : 52100, 6150, 9310, 4340, etc.,*
— aciers à outils : M 2–M 10–M 50, etc.,
— aciers inoxydables : 304, 321, 440 C,
— métaux non ferreux : nickel et ses alliages, . . .
— super-alliages : A 286, Waspalloy, M 252, Incoloy 901.

De plus, les techniques du vide ont permis la réalisation d'alliages nouveaux. On peut mentionner :
— alliages Fe–Al, affenol, thermenol,
— aciers inoxydables au bore (304 + 2 pour cent B–18/8),
— super-alliages (M 308, Udimet, Jettalloy, 1570, Réné 41),
— titane, zirconium et leurs alliages,
— tantale, niobium et leurs alliages.

Le tableau V donne les compositions des principales nuances signalées dans cet article.

Il ne peut être question évidemment d'envisager ce qu'apportent les techniques du vide dans tous ces alliages. Nous allons plutôt, d'une manière générale, analyser les modifications que provoque le vide en reprenant les différents avantages indiqués ci-dessus et en examinant, à cette occasion, des cas précis d'applications.

1. *Teneur en gaz*

La teneur en gaz est réduite considérablement par les techniques envisagées.

(a) La coulée sous faible pression permet déjà de diminuer les teneurs en hydrogène, azote et oxygène. La Fig. 6 donne la diminution de la teneur en hydrogène dans différents

— low-alloyed steels : 52100, 6150, 9310, 4340, etc. . . .*
— tool steels : M 2–M 10–M 50, etc. . . .
— stainless steels : 304, 321, 440 C
— non-ferrous metals and alloys : nickel, copper
— super-alloys : A 286, Waspalloy, M 252, Incoloy 901.

In addition, vacuum techniques have permitted the realization of new alloys. Of these we can list the following :
— Fe–Al alloys : alfenol, thermenol
— Boron-containing stainless steels : (304 + 2 per cent B–18/8)
— Super-alloys (m 308, Udimet, Jettalloy, 1570, Réné 41)
— Titanium, zirconium and their alloys
— Tantalum and columbium.

The compositions of the principal varieties are given in Table V.

There is, in fact, no question to describe the improvements given by vacuum techniques in all these alloys. We will, however, investigate in a general way, the modifications due to vacuum techniques in considering the different aims previously mentioned.

1. *Decrease in gas content*

The gas content is considerably reduced by these techniques.

(A) Casting even under a relatively low vacuum permits one to reduce hydrogen, nitrogen and oxygen contents. Fig. 6 shows the decrease in hydrogen in different steels

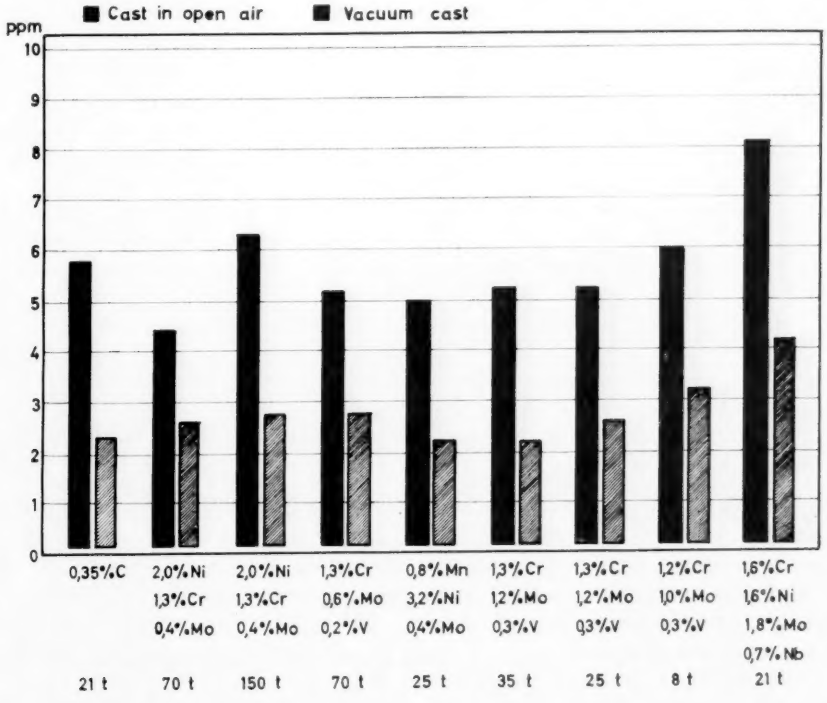

FIG. 6(a). Réduction de la teneur en hydrogène obtenue par la coulée sous vide. Le poids des lingots est mentionné.

*Suivant la classification AISI.

FIG. 6(a). Hydrogen reduction obtained on vacuum spray cast ingots

*According to AISI classification.

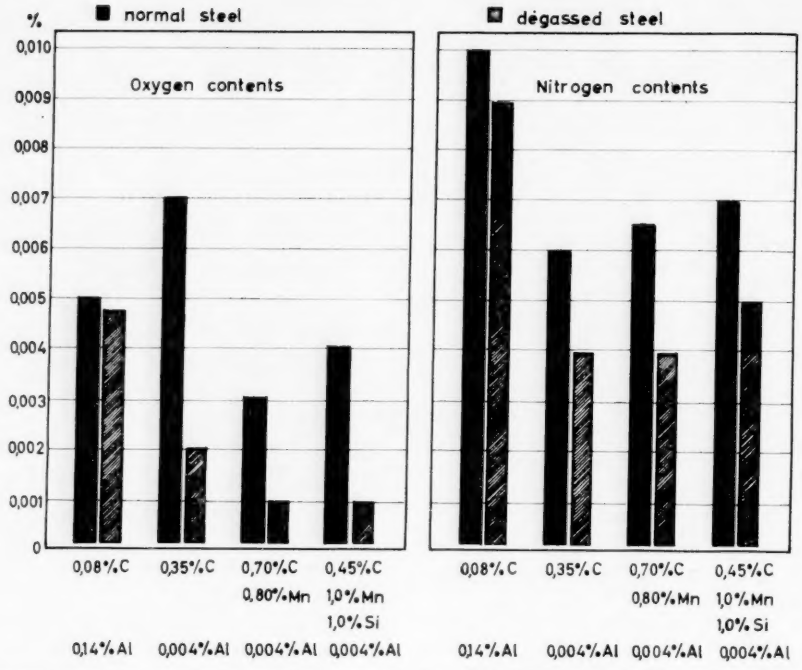

FIG. 6(b). Effet du dégazage sur la teneur en oxygène et azote de lingots d'acier

FIG. 6(b). Effect of degassing on the oxygen and nitrogen contents of steel ingots

aciers coulés sous vide. On peut ainsi éviter dans ces aciers la formation de flocons. L'oxygène et l'azote sont également réduits, mais dans des proportions variables dépendant notamment de la teneur en aluminium.

(b) Les températures élevées et les faibles pressions du four à électrodes consommables sont favorables au dégazage. Toutefois, vu le temps relativement court de la fusion, l'élimination des gaz n'est pas complète, surtout si l'on utilise des électrodes élaborées à l'air.

(c) Dans les fours à induction sous vide, les matériaux utilisés sont souvent plus purs et le temps pour affiner le métal est plus long.

Le tableau VI, dû à C. T. Evans[16] donne une idée générale de la réduction des " gaz ". L'hydrogène est ramené à une teneur très faible. Pour l'oxygène et l'azote, les résultats sont plus nuancés.

Dans un cas précis, un alliage type 305 (18 Cr–11 Ni)–modification de l'alliage 304 (18–8), le tableau VII donne les résultats obtenus après la combinaison des deux méthodes.

2. *Contrôle plus serré de la composition*

Dans les super-alliages, la fusion sous vide permet un contrôle plus précis des éléments tels que Ti, Al, B, Zr et un meilleur rendement de ces éléments. C'est évidemment la fusion par induction sous vide qui est la plus adéquate. Le temps de fusion est plus long ; des analyses intermédiaires et des corrections peuvent être faites au cours de la fusion.

Moore, Darmara, et Huntington[3] estiment que l'aluminium et le titane dans des alliages de nickel peuvent être contrôlés à $\pm$0,12 pour cent, alors que dans les procédés classiques, une précision de $\pm$0,25 pour cent à 0,50 pour cent était jugée satisfaisante.

cast under vacuum. One can, in this way, avoid the formation of flakes. Oxygen and nitrogen are also reduced but the various proportions depend upon the aluminum content.

(B) The elevated temperatures and the low pressures in the consumable electrode furnaces favors dissociation, deoxidation and degassing. Due to the relatively short melting period, however, the extraction of gases is not complete especially if one employs electrodes prepared in air.

(C) In vacuum induction furnaces, the materials utilized are frequently purer and the melting time is longer.

Table VI due to C. T. Evans[16] gives a general idea of this decrease. Hydrogen is reduced to an extremely low value. In the case of oxygen and nitrogen, the results are not so evident.

In one special case, an alloy type 305 (18 Cr–11 Ni) a modification of the alloy 304 (18–8), Table VII shows the results obtained after a combination of the two methods.

2. *Better control of the composition*

This is of special interest in super-alloys. Melting in vacuum permits a more strict control of such elements as Ti, Al, B, Zr as well as a better efficiency of these elements. It is evidently the melting by induction which is the most useful. The melting time is the longest. Intermediate analyses and corrections can be performed during this operation.

Moore, Darmara and Huntington[3] estimate that aluminum and titanium in nickel alloys can be controlled to $\pm$0.12 per cent while in classical procedures a precision of $\pm$0.25 per cent to 0.50 per cent is considered satisfactory.

Vol. 10 1960

TABLEAU V

	C	Ni	Cr	Mo	W	Co	Fe	Ti	Al	Zr	V
A 286	0,05	26,0	15,0	1,25	—	—	Bal.	2,00	0,20	—	0,25
M 308	0,05	33,0	14,0	4,0	6,5	—	Bal.	2,2	0,25	0,20	—
Incoloy 901	0,05	42,0	12,0	6,0	—	—	Bal.	2,5	—	—	—
M 252	0,10	Bal.	19,0	10,0	—	10,0	1,0	2,5	0,8	—	—
Réné 41	0,10	Bal.	19,0	10,0	—	11,0	1,0	3,1	1,6	—	—
Waspalloy	0,07	Bal.	20,0	4,0	—	14,0	1,0	3,2	1,3	—	—
Udimet 500	0,10	Bal.	19,0	4,0	—	19,0	1,0	3,0	3,0	—	—
GMR 235	0,15	Bal.	15,5	5,25	—	—	10,0	2,0	3,0	—	—
Jettalloy 1570	0,15	Bal.	20,0	—	7,0	36,0	1,0	4,4	—	—	—
M 2	0,83	—	4,10	5,00	6,25	—	Bal.	—	—	—	1,90
AM 355	0,13	4,2	15,5	2,75			Bal.				0,100 N_2
52100	1,00	—	1,50				Bal.				
6150	0,50		1%				Bal.	—	—	—	—
9310	0,10	3,25	1,2%	0,12			Bal.				
4340	0,40	1,80	0,80	0,25	—	—	Bal.	—	—	—	—
304	<0,08	8–11	18–20	—	—	—	Bal.	—	—	—	—
321	<0,08	8–11	17–19	—	—	—	Bal.	5 × C	—	—	—
440 C	1	—	16–18	0,75	—	—	Bal.	—	—	—	—

TABLE V

	C	Ni	Cr	Mo	W	Co	Fe	Ti	Al	Zr	V
A 286	0.05	26.0	15.0	1.25	—	—	Bal.	2.00	0.20	—	0.25
M 308	0.05	33.0	14.0	4.0	6.5	—	Bal.	2.2	0.25	0.20	—
Incoloy 901	0.05	42.0	12.0	6.0	—	—	Bal.	2.5	—	—	—
M 252	0.10	Bal.	19.0	10.0	—	10.0	1.0	2.5	0.8	—	—
Réné 41	0.10	Bal.	19.0	10.0	—	11.0	1.0	3.1	1.6	—	—
Waspalloy	0.07	Bal.	20.0	4.0	—	14.0	1.0	3.2	1.3	—	—
Udimet 500	0.10	Bal.	19.0	4.0	—	19.0	1.0	3.0	3.0	—	—
GMR 235	0.15	Bal.	15.5	5.25	—	—	10.0	2.0	3.0	—	—
Jettalloy 1570	0.15	Bal.	20.0	—	7.0	36.0	1.0	4.4	—	—	—
M 2	0.83	—	4.10	5.00	6.25	—	Bal.	—	—	—	1.90
AM 355	0.13	4.2	15.5	2.75			Bal.				0.100 N_2
52100	1.00	—	1.50				Bal.				
6150	0.50		1%				Bal.	—	—	—	—
9310	0.10	3.25	1.2%	0.12			Bal.				
4340	0.40	1.80	0.80	0.25	—	—	Bal.	—	—	—	—
304	<0.08	8–11	18–20	—	—	—	Bal.	—	—	—	—
321	<0.08	8–11	17–19	—	—	—	Bal.	5 × C	—	—	—
440 C	1	—	16–18	0.75	—	—	Bal.	—	—	—	—

TABLEAU VI

Teneurs approximatives en "gaz" dans les aciers et alliages (ppm = 0,0001 pour-cent)

	Aciers faiblement alliés (0,25%C) calmés			Aciers austénitiques ou alliage Fe–Ni–Co pour températures élevées		
Procédés de fusion	H_2	O_2	N_2	H_2	O_2	N_2
Fusion à l'air sous laitier						
Four électrique à arc	1–20	50–125	30–500	5–15	10–200	50–500
Fusion sous vide						
Four à induction	1	5–15	5–50	1–2	5–125	20–200
Four à électrodes consommables	1–2	5–25	10–100	1–2	10–100	20–200

TABLEAU VII

Comparaison des teneurs en "gaz" de l'acier 305 (18 *pour cent Cr–*11 *pour-cent Ni) après différents modes de fusion (ppm = 0,0001 pour-cent)*

Gaz	Fusion à l'air	Fusion simple au four à électrodes consommables		Fusion double au four à électrodes consommables	
	PPM	PPM	% RED	PPM	% RED
Oxygène	101,0	37,7	63	26,2	31
Hydrogène	5,0	1,1	78	1,0	9

Gaz	Four à induction sous vide	Four à induction sous vide et four à électrodes consommables	
	PPM	PPM	% RED
Oxygène	35,4	30,4	14
Hydrogène	2,1	1,1	48

Dans le four à électrodes consommables, c'est la qualité de l'électrode qui conditionne la composition. Ainsi, l'utilisation d'une électrode fondue au four à induction sous vide puis refondue au four à électrodes consommables combine les avantages des deux procédés et assure la production de lingots de grandes dimensions très homogènes.

3. *Plus grande propreté*

Lors de la fusion à l'air, la désoxydation se fait par l'addition d'éléments tels que Si, Mn, Al, Ti. Certains oxydes formés restent dans le métal sous forme d'inclusions. La fusion sous vide permet l'utilisation du carbone et de l'hydrogène pour la désoxydation. La formation d'oxydes gazeux qui sont continuellement éliminés par le pompage permet de réaliser un métal exempt d'inclusions.

Au four à électrodes consommables, la température élevée provoque une désoxydation importante, mais le temps de fusion est relativement court. Les alliages contiennent de très petites inclusions. Au four à induction sous vide, il subsiste de petites inclusions de composés de titane. La

TABLE VI

Approximate "gas" contents in the final product (ppm = 0.0001 per cent)[16]

	Low-alloyed steels (0.25%C) killed			Austenitic steels or Fe–Ni–Co alloys for high temperatures		
Fusion method	H_2	O_2	N_2	H_2	O_2	N_2
Air melting under slag						
Electric arc furnace	1–20	50–125	30–500	5–15	10–200	50–500
Melting in vacuum						
Induction furnace	1	5–15	5–50	1–2	5–125	20–200
Cons. Elect. furnace	1–2	5–25	10–100	1–2	10–100	20–200

TABLE VII

Comparison of "gas" contents. Steel 305 (18 *per cent Cr–*11 *per cent Ni) after different melting methods*[14]

Gas	Melting in air	Single melting in consumable electrodes furnace		Double melting in consumable electrodes furnace	
	PPM	PPM	% RED	PPM	% RED
Oxygen	101.0	37.7	63	26.2	31
Hydrogen	5.0	1.1	78	1.0	9

Gas	Vacuum induction furnace	Vacuum induction furnace and consommable electrodes furnace	
	PPM	PPM	% RED
Oxygen	35.4	30.4	14
Hydrogen	2.1	1.1	48

In the case of the consumable electrode furnaces, the composition is determined by the quality of the electrode. For this reason, the use of electrodes melted in a vacuum induction furnace and then remelted in a consumable electrode furnace combines the advantages of the two methods and assures the production of large homogeneous ingots.

3. *Increase in metal cleanliness*

The deoxidation during melting in air is performed by the addition of such elements as Si, Al and Ti. Certain oxides thus formed are retained in the metal in the form of inclusions. In the induction furnace, the utilization of carbon and hydrogen results in the formation of gaseous oxides which are continually eliminated by pumping.

The elevated temperatures in the consumable electrode furnace provokes a high degree of deoxidation. The alloys contain only extremely small inclusions. In the induction furnace, small inclusions of sulfides or oxides and of nitrides or carbonitrides of titanium are present.

A combination of two procedures permits, here again,

combinaison des deux techniques conduit ici encore à des alliages extrêmement propres, qui peuvent être utilisés dans les cas les plus critiques.

4. *Ségrégation et porosité*

Ces défauts sont caractéristiques des lingots obtenus par les procédés classiques et amenuisent parfois sérieusement les propriétés mécaniques.

Au four à induction, où le mode de coulée est analogue, l'amélioration n'est pas sensible. Par contre, au four à électrodes consommables, la porosité centrale et la ségrégation sont éliminées ou très réduites, ce qui améliore les propriétés en travers et l'homogénéité dans les teneurs.

L'élimination de la ségrégation améliore la ductilité en travers dans les alliages A 286 et N 155. Dans les aciers inoxydables à précipitation structurale (AM 355), l'amélioration de la résistance à la rupture et de la limite élastique, aussi bien que la ductilité, sont obtenues (Fig. 7) par l'élimination d'austénite résiduelle ségrégée dans les billettes[15].

the production of extremely clean alloys suitable for the most important applications.

4. *Decrease in segregation and porosity*

These defects are characteristic of ingots obtained by classical methods and which often decrease considerably the mechanical properties.

In the induction furnace, where the means of casting is similar the increase is not great. On the other hand, in the consumable electrode furnace, central porosity and segregation are either eliminated or greatly reduced. This results in an increase of the transversal properties and the homogeneity of the constituents.

The elimination of segregation increases the transversal ductility in the alloys A 286 and N 155. In the precipitation hardening stainless steels (A M 355), the increase of the yield strength and the elastic limit as well as the ductility are obtained (Fig. 7) by the elimination of residual austenite segregated in the billets[15].

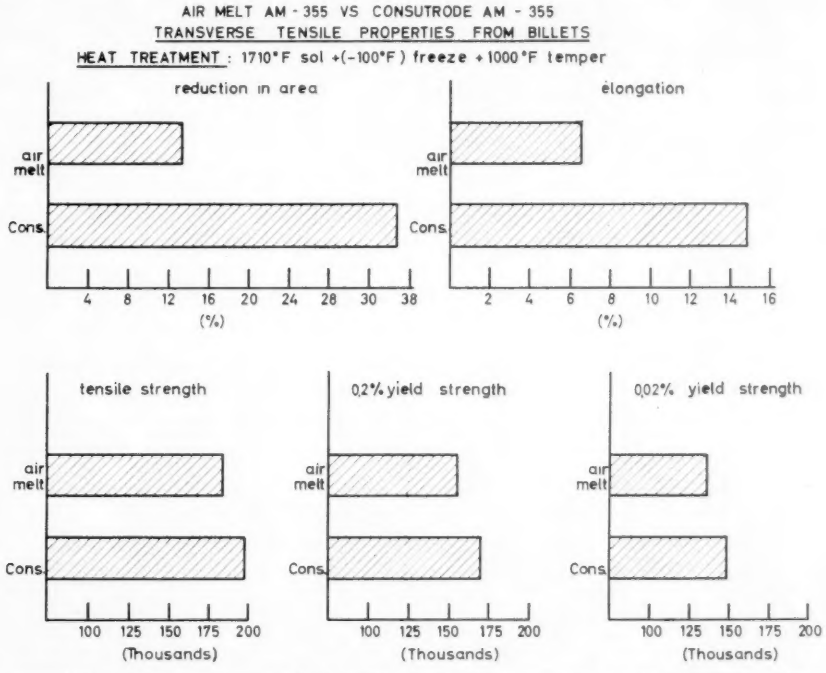
AIR MELT AM - 355 VS CONSUTRODE AM - 355
TRANSVERSE TENSILE PROPERTIES FROM BILLETS
HEAT TREATMENT : 1710°F sol +(-100°F) freeze +1000°F temper
reduction in area
elongation
air melt
Cons.
4 8 12 16 20 24 28 30 38
(%)
2 4 6 8 10 12 14 16
(%)
tensile strength
0,2% yield strength
0,02% yield strength
100 125 150 175 200
(Thousands)

FIG. 7. Comparaison des propriétés de traction en travers des billettes d'alliages AM 355 fondus à l'air et par électrode consommable. Traitement thermique : austénisé 950 °C, refroidi −73 °C, revenu à 550 °C

FIG. 7. Comparison of the transverse tensile properties of billets of the AM 355 alloys, melted in air by a consumable electrode.
Heat treatment : 1710 °F. sol. −100 °F. freeze 1000 °F. temper

5. *Amélioration de la laminabilité*

C'est un des principaux avantages du procédé de fusion sous vide. L'élimination des gaz permet d'obtenir des structures plus pures exemptes d'inclusions, des frontières de grain sans constituants plus fusibles que la masse métallique, etc.

Un très grand nombre d'alliages sont améliorés par les techniques du vide. C'est ce que montre la Fig. 8 pour l'acier A 286.

Cette amélioration permet le développement de nombreux super-alliages de nickel contenant Al, Ti, d'alliages de cobalt, d'aciers inoxydables au bore, d'alliages Fe–Al, etc.

5. *Improvements of rollability*

This is one of the principal advantages of the vacuum melting method. The elimination of the entrapped gas permits one to obtain purer structures free from inclusions and from low-melting grain-boundary constituents.

A very large number of alloys are improved by the use of these vacuum techniques. An example for the steel A 286 is shown in Fig. 8.

This improvement permits the development of numerous super alloys of nickel containing Al and Ti, cobalt-base alloys, stainless steels containing boron and Fe–Al alloys,

FIG. 8. Alliage A 286—amélioration de la forgeabilité par la coulée sous vide. Au-dessus, échantillon élaboré à l'air—en dessous échantillon élaboré sous vide

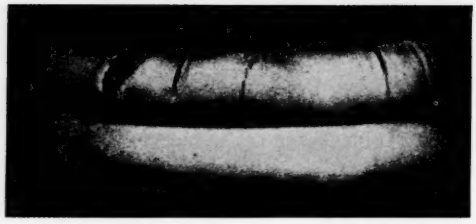

FIG. 8. Comparison of hot workability of A 286 bars on drastic upsetting. Upset test on air melted (top) versus upset on vacuum melted (bottom) material

Ici également, le procédé de double fusion présente un grand intérêt.

Nous allons envisager le cas du cobalt.

Jusqu'en ces derniers temps, on considérait qu'un des avantages importants des alliages à base de cobalt était leur possibilité d'être élaborés à l'air. Toutefois, la plupart de ces alliages ne sont pas forgeables et ne peuvent être utilisés que comme produit moulé.

Afin de contrôler l'influence des éléments résiduels sur la forgeabilité du cobalt commercial, nous avons fondu à l'air et sous vide dans un four à induction, une charge de 6 kg de métal, dans un creuset en magnésie électrofondue.

La coulée à l'air n'a donné lieu à aucune anomalie : fusion en une heure dans un creuset en magnésie ; coulée en lingotière d'acier.

La coulée sous vide a été effectuée dans les conditions suivantes : fusion sous un vide de 10^{-2} mmHg, pression d'hydrogène sur le bain : 360 mmHg pendant 2 h avec circulation continue du gaz. La coulée s'effecture dans un moule en acier lorsque le vide atteint 2.10^{-4} mmHg.

Vu le caractère expérimental des essais, une tranche de $\frac{1}{2}$ cm d'épaisseur des lingotins a été sciée dans la zone centrale et a servi pour les essais de laminage.

Les faces des tranches ont montré que les lingotins étaient sains.

L'analyse des deux produits n'a pas révélé de différences significatives dans les éléments métalliques, par contre, en ce qui concerne les gaz ou les métalloïdes, on note des différences appréciables, comme le montre le tableau VIII.

Nous avons alors fait procéder au laminage des deux tranches après un chauffage prolongé à 1000 °C dans un four à vide partiel (10^{-2} mmHg).

TABLEAU VIII

	Coulée à l'air	Coulée sous vide
	%	%
S	0,0166	0,0100
		0,0098
O_2	0,020	0,006
N_2	0,0012	0,0004
	0,0013	0,0004

Pour la tranche de lingotin coulé à l'air, on a obtenu en trois passes une réduction de 46 pour-cent, mais dès la première passe, 14 pour-cent, un début de fissuration est apparu.

Pour la tranche du lingotin coulé sous vide, on est arrivé à une réduction de 91,5 pour-cent en six passes avec un réchauffage intermédiaire après la 3e passe. On a pu

etc. Here again, the combination of a double melting method presents a great interest.

We will consider here the case of cobalt. Until recently one of the principal advantages of cobalt-base alloys was their ability to be prepared in air. However, the most of these alloys could not be forged and thus had to be used in the cast form.

In order to control the influence of some residual elements in commercial grade cobalt, we have melted in air and in vacuum induction furnaces 6 kg charges in magnesia crucibles. Treatment in air melting time—1 hr casting in steel mould—gave no improvement.

Treatment in vacuum was performed in following manner : melting at 10^{-2} mmHg, hydrogen pressure above metal bath : 360 mmHg for 2 hr—casting in steel mould in a vacuum of 2.10^{-4} mmHg.

In view of the experimental character of the tests, a $\frac{1}{2}$ cm section from the centre of the ingot was selected for rolling studies.

The sawed surfaces of the section showed that the ingot was completely sound.

The analysis of these two products did not reveal any significant difference in metallic element contents. The gas and metalloid contents, on the other hand, were appreciably different as can be seen in Table VIII.

We then performed a rolling operation on the two sections after a prolonged heating at 1000 °C in a vacuum furnace (10^{-2} mmHg).

TABLE VIII

	Elaborated in air	Elaborated in vacuum
	%	%
S	0.0166	0.0100
		0.0098
O_2	0.020	0.006
N_2	0.0012	0.0004
	0.0013	0.0004

With the specimen cast in air we could obtain in three passes a reduction in thickness of 46 per cent. However, after the first pass (reduction 14 per cent) cracks became visible.

In the case of the specimen produced in vacuum we could arrive at a reduction of 91.5 per cent in six passes with intermediate heating after the third pass. We then could

Vol. 10 196

ensuite laminer à froid et obtenir des feuilles de 0,3 mm dont les propriétés mécaniques sont excellentes.

6. *Amélioration des propriétés*

De par son action sur la propreté, la teneur en gaz, l'homogénéité des lingots, la fusion sous vide améliore les propriétés dans de très nombreux alliages et notamment :

(a) La résistance à la fatigue
(b) La résistance au fluage et à la rupture aux températures élevées
(c) Les propriétés mécaniques, limite élastique, charge de rupture, résilience, ainsi que les propriétés chimiques
(d) L'homogénéisation des propriétés en long et en travers
(e) L'amélioration des propriétés magnétiques.

Nous discuterons un cas précis pour chacune de ces propriétés.

(a) *Résistance à la fatigue.* Il est généralement admis que l'amélioration de la résistance à la fatigue est en relation avec l'élimination des inclusions. Moore en 1953[17] mettait déjà ce fait en évidence dans les aciers pour roulements.

Le plus populaire des aciers de ce groupe fondu sous vide est sans conteste l'acier pour roulements du type 52100. Il est élaboré au four à induction sous vide.

Pour réaliser l'acier 52100 sous vide, l'utilisation de métaux relativement purs est de loin préférable aux ferro-alliages. Leur pureté plus grande en différents éléments est plus intéressante, même si les teneurs en gaz sont plus élevées. En effet, les gaz peuvent être éliminés au cours de la fusion.

La fusion se fait généralement à une vitesse de 5 kg/min, sous un vide de quelques mmHg, en présence de carbone. Le dégazage est rapide et peut parfois ramener la pression jusqu'à 14 mmHg.

Le raffinage se fait à une pression inférieure à 10 μHg. Lorsque le dégazage est terminé, on peut faire la mise à nuance et, parfois grâce à l'analyse spectrale, on peut obtenir des produits dont les teneurs sont particulièrement précises.

Les teneurs en gaz dans de telles coulées sont de l'ordre suivant :

O_2 : 4 à 13 ppm
N_2 : 3 à 11 ppm
H_2 : 0,9 à 1,9 ppm

La teneur en hydrogène est du même ordre que celle trouvée dans les aciers fondus dans le four électrique, au moins pour les aciers élaborés au procédé acide. La teneur en azote est nettement plus faible.

L'examen des inclusions résiduelles est difficile. Il exige des observations au banc métallographique à des grossissements élevés. En général, on observe des inclusions du type A si l'on s'en tient aux normes ASTM, c'est-à-dire des inclusions de sulfures.

Toutefois, pour les caractériser, il convient d'améliorer les normes actuelles et notamment de remplacer la catégorie Al par les catégories A$\frac{1}{4}$ et A$\frac{1}{2}$, etc.

Ce problème des inclusions est particulièrement important. Ainsi, l'addition de manganèse avant la coulée, à un métal tenant 0,005 pour-cent S a pour effet d'augmenter le nombre d'inclusions de sulfures, mais non leur dimension. Il y aurait donc lieu dans des aciers de ce genre, de limiter

cold roll this material to sheets of 0.3 mm thickness. Their mechanical properties were excellent.

6. *Improvement of properties*

By its influence on the cleanliness, gas content and homogeneity, vacuum melting improves different properties in the alloys. Among these are the following :

(a) fatigue resistance
(b) creep resistance and rupture at elevated temperatures
(c) mechanical properties—elastic limit, ultimate strength and resilience—as well as chemical properties
(d) homogenization of the properties along and across the ingot
(e) improvement of magnetic properties.

We will discuss an example of each of these properties.

(a) *Fatigue resistance.* It is generally agreed that the increase of the fatigue resistance is due to the elimination of inclusions. Moore in 1953[17] has already shown this in the case of bearing steels.

The most popular of this group of vacuum-treated steels is the type 52100. This steel is usually prepared in a vacuum induction furnace. The use of metals relatively pure is of great advantage even if the gas content is high since the removal of the latter is assured during melting. Fusion is usually performed at a rate of 5 kg/min in the presence of carbon in an initial vacuum of several millimeters of mercury. Degassing is so rapid that the pressure can, at times, increase to 14 mmHg. The refining operation is performed under a pressure of 10 μHg. After the end of the degassing period, the alloying elements are added. The use of spectral analysis permits one to finally arrive at very nearly the composition desired.

The gas contents in the cast products are of the following order :

O_2 : 13 to 14 ppm
N_2 : 3 to 11 ppm
H : 0.9 to 1.9 ppm

Hydrogen content is of the same order as that found in steels prepared by the acid electric process, the nitrogen content is decidedly lower.

Examination of residual inclusions is extremely difficult. This study requires the use of a high magnification. In general, it is possible to observe inclusions of the type A (ASTM specification) that is sulphide inclusions. In order to characterise these inclusions, however, it is necessary to increase the specifications by replacing the Al category by those A $\frac{1}{4}$ and A $\frac{1}{2}$, etc. . . .

The problem of inclusions is particularly important. Thus, the addition of manganese before casting a metal containing 0.005 per cent S serves to increase the number of inclusions but not their size. It is thus necessary in these steels to limit the use of manganese to a degree compatible with the properties desired.

l'emploi du manganèse à des quantités compatibles avec les propriétés de l'acier. On peut même se demander pourquoi on ajoute du silicium et du manganèse puisque la désoxydation se pratique par une technique différente ; en fait, il s'agit souvent de spécifications anciennes et actuellement certaines spécifications pour les aciers coulés sous vide permettent de les omettre. Cette omission simplifie d'ailleurs la réalisation de la fusion sous vide. L'amélioration de la résistance à la fatigue de l'acier 52100 par les techniques de fusion sous vide est représentée aux courbes de la Fig. 9.

One could even ask why silicon and manganese are added since deoxidation is performed by a different means. In fact, it frequently is possible that these are the classical specifications ; in the vacuum melting techniques these can frequently be omitted. Such an omission simplifies the vacuum fusion methods.

This steel is an example of the improvement in the fatigue resistance due to a cleaner metal. (Fig. 9).

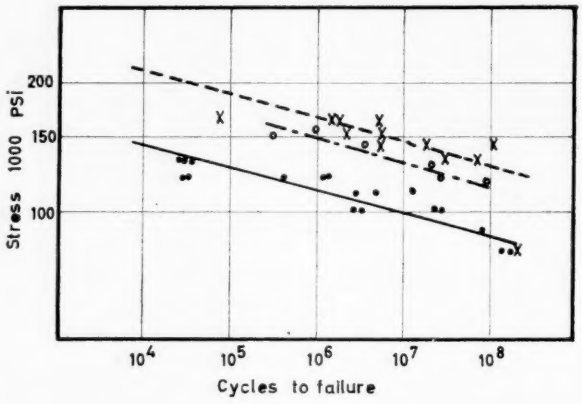

FIG. 9. Comparaison de la résistance à la fatigue de l'acier SAE 52110 fondu par diverses techniques à l'air (—.), au four à induction sous vide (— x), au four à électrodes consommables (— . — o) avec des électrodes fondues à l'air

FIG. 9. Fatigue properties of 52100 steel melted by various techniques (—.) air melted, (— — — x) vacuum induction melted, (— . — o) vacuum arc remelted from air melted electrodes

(b) *Résistance aux températures élevées.* Nous en venons maintenant aux alliages pour températures élevées et nous considérerons des alliages à base de nickel : les " nimonics "[18].

Ces alliages ont une résistance mécanique élevée grâce à la formation de composés intermétalliques d'aluminium et de titane (Ni_3TiAl). Ces deux éléments ayant une forte affinité pour l'oxygène et même pour l'azote, il convient non seulement pour avoir un rendement satisfaisant, mais avant tout pour éviter d'avoir un métal avec trop d'inclusions, de les préparer sous vide. Il convient même que l'addition de ces éléments aluminium et titane se fasse après le retrait de l'oxygène.

Par la fusion et la coulée sous vide (10^{-3} mmHg–1500 °C) on peut augmenter sensiblement les propriétés des " nimonics ", comme le montre le tableau IX.

TABLEAU IX

Comparaison de propriétés de fluage de " nimonics " après fusion à l'air et fusion sous vide

Alliage	Caractéristiques de l'essai de fluage		Fusion à l'air		Fusion sous vide	
	kg/mm²	Tempér.	Temps pour rupture (h)	All. %	Temps pour rupture (h)	All. %
Nimonic 90	14,5	870 °C	51	8	93	33
Nimonic 105	12,8	940 °C	80	10	120	25

On observe une amélioration sensible, principalement de l'allongement à la rupture.

Des essais préliminaires ont révélé que par des modifications de compositions appropriées, les propriétés des

(b) *Resistance to elevated temperatures.* We now reach alloys for high temperatures and we consider nickel-base alloys : the " nimonics "[18]. These alloys owe their high mechanical resistance at elevated temperatures to the formation of intermetallic compounds of aluminum and titanium. Since these elements have a great affinity for oxygen and nitrogen, it is convenient, not only to have a sufficient yield but principally to decrease the number of inclusions, to prepare these alloys in vacuum. It is better to add the aluminum and titanium after the removal of oxygen. In this way, by a simple melting and casting in vacuum (10^{-3} mmHg–1500 °C), the properties are considerably improved as is shown in Table IX.

TABLE IX

Comparison of creep properties of " nimonics " after air and vacuum melting[18]

Alloys	Creep tests		Air melting		Vacuum melting	
	kg/mm²	Temp. (°C)	Rupture time (hr)	Elongation (%)	Rupture time (hr)	Elongation (%)
Nimonic 90	14.5	870	51	8	93	35
Nimonic 105	12.8	940	80	10	120	25

One can detect a decided improvement especially in the elongation at rupture. In all cases, these preliminary tests have revealed, by the appropriate modifications of the composition, that important improvement can be obtained

Vol. 10 1960

" nimonics " pouvaient être améliorées grâce aux techniques du vide. En effet, les diagrammes temps de rupture en fonction de la teneur en élément d'alliage (Fig. 10) pour Ti, Al, Mo, Cr, montrent en général un maximum pour une composition déterminée. Ce maximum est obtenu pour des teneurs plus élevées dans le métal coulé sous vide que dans le métal coulé à l'air. On est conduit ainsi à la réalisation de nouveaux alliages définis actuellement par les vocables: M 14V, M 15V.

Leurs propriétés sont actuellement en cours de détermination. En ce qui concerne la résistance aux températures élevées, la résistance à la fatigue, la résistance à l'oxydation et la corrosion, on note d'une manière générale une amélioration sensible.

(c) *Amélioration des propriétés mécaniques et des propriétés chimiques.* Dans les aciers faiblement alliés, l'emploi de la fusion sous vide peut conduire à des améliorations sensibles des propriétés mécaniques.

Pour l'acier 4340 par exemple, nous avons reporté au tableau X quelques résultats caractéristiques, montrant les améliorations obtenues[19].

FIG. 10. Comparaison de la variation du temps de rupture à une charge déterminée en fonction de la teneur en éléments d'alliages pour des alliages fondus sous vide et à l'air

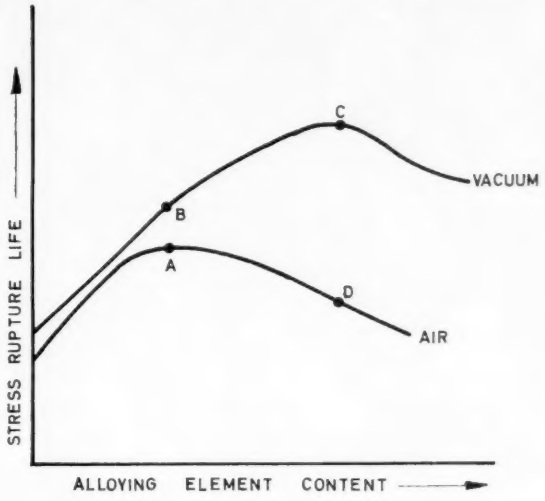

FIG. 10. Variation of stress-rupture life with alloying element content for vacuum melted and air melted alloy

TABLEAU X

Propriétés de l'acier 4340 *après double fusion sous vide* (4 *coulées*)

	Fusion à l'air	1ère fusion sous vide	2me fusion sous vide
Hydrogène	6 ppm	3 ppm	2 ppm
Oxygène	0,045 %	0,0005–0,003	0,0008–0,001
Azote	0,001–0,09	0,002–0,004	0,0006
—essai de fatigue 70 kg/mm² nbre de cycles	10 000	280 000	18 millions
—essai de résilience (Charpy-température de transition)	−3 °C±10 °C	−122 °C±10 °C	inférieure à la température de l'azote liquide
—essai de traction	196 kg/mm²	206 kg/mm²	201,3 kg/mm²
—% striction	fragile	5 à 17%	13 à 17%

by the use of vacuum techniques. In fact, the diagrams rupture time/per cent of alloying element (Fig. 10) for Ti, Al, Mo and Cr show, in most cases, a maximum for a certain composition. This maximum is obtained for higher contents in metal treated in vacuum than those treated in air. For this reason, new alloys possessing such symbols as M 14V, M 15V, etc., are being realized.

Their properties are actually being determined at this time. However, with respect to the resistance to elevated temperatures, fatigue resistance, oxidation and corrosion resistance one can notice, in a general manner, marked improvement.

(c) *Improvement of mechanical and chemical properties.* In the case of low-alloyed steels, vacuum fusion methods result in a decided improvement in these properties.

The improvements obtained in the alloy 4340 are shown in Table X[19].

TABLE X

Properties of steel 4340 *after a double melting in vacuum* (4 *heats*)

	Melting in air	First vacuum melt	Second vacuum melt
Hydrogen	6 ppm	3 ppm	2 ppm
Oxygen	0.045 %	0.0005–0.0003	0.0008–0.001
Nitrogen	0.001–0.09	0.002–0.004	0.0006
Fatigue test 70 kg/mm² nb of cycles	10,000	280,000	18 millions
Resilience tests (Charpy-trans. temp.)	−3 °C±10 °C	−122 °C±10 °C	lower than temp. of liq. N_2
Stress-strain test	196 kg/mm²	206 kg/mm²	201.3 kg/mm²
% at neck	fragile	5–17%	13–17%

Examinons maintenant un alliage préparé par la fusion à électrodes consommables des types AISI 4100, type d'aciers à très grande résistance[20].

La composition : C 0,39, Mn 1,70, Si 1,00, Cr 1,10, Mo 0,25, V 1,15, Co 1,00.

Cet acier, dénommé 4137 Co est préparé au four électrique à arc. Puis, pour obtenir le degré de propreté et le degré d'homogénéité pour certaines applications, notamment celles relatives à l'aviation, aux véhicules spatiaux, le produit est refondu dans un four à arc à électrodes consommables.

Après un traitement thermique adéquat, on obtient une limite élastique de 160 kg/mm^2 et une charge de rupture de 187 kg/mm^2.

L'acier ci-dessus, par rapport à l'acier 4100 dont il dérive contient en plus 1 pour-cent Si et 1 pour-cent Co.

Ces additions et spécialement le silicium tendent à freiner les premiers stades du revenu et diminuer la fragilité qui y apparaît. Le cobalt durcit la ferrite comme le nickel par exemple, sans lui donner toutefois, le même caractère de durcissement à la déformation. Cet effet toutefois ne semble être net que dans un métal relativement pur. De nombreuses études nous ont montré en effet, qu'il était parfois très difficile de se faire une idée satisfaisante de l'effet du cobalt.

Sans entrer dans des détails, mais afin de bien faire ressortir la complexité de l'effet du vide, signalons simplement les résultats de deux mémoires récents.

Decker et Freeman[21] ont étudié le formage à chaud et les propriétés de fluage à 900°C d'un alliage : 55 pour-cent Ni–20 pour-cent Cr–15 pour-cent Co–4 pour-cent Mo–3 pour-cent Ti–3 pour-cent Al
élaborés :
— au four à induction à l'air
— au four à induction sous vide
— au four à arc à électrodes consommables.

Le but était de déterminer le rôle de l'oxygène et de l'azote. Il est d'abord apparu que les traces de bore et de zirconium provenant éventuellement du creuset avaient une influence plus grande que le processus de fusion.

Toutefois, la fusion sous vide présente les avantages suivants :

(1) amélioration de la forgeabilité
(2) uniformisation des propriétés de fluage
(3) amélioration de la résistance au fluage.

Si l'on ajoute volontairement l'oxygène et l'azote après fusion sous vide, on n'a pas d'effet sur le fluage. D'autres considérations encore amènent les auteurs à conclure que l'oxygène et l'azote seraient favorables aux propriétés envisagées et qu'en fait la fusion sous vide éliminerait des éléments inconnus défavorables à la ductilité.

Stutzmann et Cunningham[22] dans une étude analogue sur deux alliages de "cobalt" (Stellite–He 1049) et deux alliages à base de nickel (Udimet 500 et Guy alloy) concluent à l'amélioration des propriétés de fluage par l'emploi des techniques du vide, mais d'une manière générale, si certaines propriétés sont améliorées, d'autres sont détériorées. La ductilité de la Stellite 31 s'accroît par la fusion sous vide, mais la résistance à l'oxydation décroît.

Let us now examine an alloy of the type A ISI 4100—a high strength steel prepared by melting in a consumable electrode furnace. Its composition is as follows : C–0.39 per cent, Mn–0.70 per cent, Si–1.00 per cent, Cr–1.10 per cent, Mo–0.25 per cent, V–1.15 per cent, and Co–1.00 per cent.

This steel is first treated in an electric arc furnace. In order to obtain the degree of homogeneity and properties desired for certain applications such as for the aviation and space vehicles, the initial product is remelted in vacuum.

After a suitable heat treatment, one obtains an elastic limit of 160 kg/mm^2 and an ultimate strength of 187 kg/mm^2. The above steel, by comparison with the steel 4100, from which it is derived, contains in fact 1 per cent Si and 1 per cent Co.

The latter additions specially that of silicon tends to retard the first stage of tempering thus decreasing the fragility. Cobalt hardens the ferrite as does nickel, by the way, without giving the same degree of work-hardening. This effect does not seem clear except in a case of an alloy relatively pure. The results of an extended series of studies have shown that it is difficult to get an exact idea of the influence of cobalt.

Finally, we will briefly describe the result of two different researches.

Decker and Freeman[21] have studied the hot working and creep properties at 900°C of an alloy of the following composition : 55 per cent Ni–20 per cent Cr–15 per cent Co–4 per cent Mo–3 per cent Ti and 3 per cent Al. This alloy was prepared in the following three steps :

(1) melted in air in induction furnace
(2) remelted in vacuum in an induction furnace, and
(3) again melted in vacuum in a consumable electrode furnace.

The purpose was to determine the role played by oxygen and nitrogen (it again became apparent that traces of boron and zirconium had a greater influence than the melting process).

Melting in vacuum presents the following advantages :

(1) increases forgeabiltiy
(2) uniformizes creep properties
(3) increases creep properties.

If one intentionally adds oxygen and nitrogen after melting in vacuum, there is no influence on the creep properties. Still other considerations lead these authors to conclude that oxygen and nitrogen are favorable to the considered properties and that, in fact, vacuum melting would eliminate unknown elements which are unfavorable for the ductility.

Stutzmann and Cunningham[22], in a similar study on cobalt-base alloys (Stellite–He 1049) and nickel-base alloys (500 and Guy alloy) conclude that creep properties were improved by vacuum techniques but, in a general way, the improvement of one property appeared to be detrimental to others. Although the ductility of Stellite 31 is improved by vacuum melting, oxidation resistance was found to

Vol. 10 1960

L'allongement de fluage et la résistance à l'oxydation à température constante pour l'alliage He 1049 est améliorée par la fusion sous vide et la coulée sous argon, mais la résistance à une oxydation intermittente est meilleure après une élaboration à l'air.

D'une manière analogue, d'ailleurs, l'addition de bore et de zirconium à l'alliage Udimet 500 améliore l'allongement au fluage, mais dininue la résistance à l'oxydation.

Chaque alliage et son élaboration doivent donc être étudiés en vue d'une application définie et les techniques du vide, pas plus que des additions spécifiques ou des traitements thermiques spéciaux ne sont des passe-partout.

(d) *Homogénéisation des propriétés en long et en travers.* Child et Harris[7] ont étudié les propriétés d'aciers pour disques de turbines élaborés au four électrique et au four à électrodes consommables. Dans beaucoup d'aciers, ils ont pu obtenir une homogénéisation sensible des propriétés. C'est le cas notamment pour des coulées de disques de turbines forgés en acier martensitique au Cr d'analyse suivante : C 0,08 pour-cent, Mn 0,9 pour-cent, Si 0,2 pour-cent, Cr 10 pour-cent, W 0,85 pour-cent, Co 10 pour-cent, Mo 1,1 pour-cent, Nb 0,4 pour-cent, Ni 0,2 pour-cent, V 0,47 pour-cent.

Cet alliage a été réalisé pour améliorer le comportement au fluage de ces aciers ferritiques.

L'augmentation en éléments d'alliages rendant de plus en plus difficile l'obtention d'une bonne ductilité en travers. Des disques de 65 cm de diamètre ont été forgés à partir de lingot de 50 cm coulé sous vide et de lingot conventionnel de 48 cm. La comparaison des propriétés aux différentes sections est reportée au tableau XI.

On peut constater que le métal fondu sous vide a une ductilité beaucoup plus uniforme notamment à l'axe des pièces.

TABLEAU XI[7]

Position de prélèvement dans la pièce	Fusion à l'air			Fusion sous vide		
	Ch. Rupt. kg/mm²	All. %	Striction %	Ch. Rupt. kg/mm²	All. %	Striction %
en axe long	134,2	18	57	130,7	17,5	56
en axe long	131,3	9	15	129,7	13	43
en axe long	134,8	15	45	131,6	18	50
en axe long	130,1	4,5	6,5	130,6	15,6	52,5
en axe au milieu	129,9	11,1	21	129,7	14,3	43,5
en axe en périphérie	132,6	14,5	40	132,9	16	43
		14,5	50	130,4	18	54
radial en périphérie	129,3	20	60	129,9	17	57
en axe en travers	130,4	16	52	127,8	17	60
en axe en travers	133,1	18	60	131,0	18,5	60
en axe en travers	129,7	18	60	129,6	17	55
en périphérie transv.	130,9	19	59	128,3	18,5	52
anneau de contrôle	130,7	18	55	126,4	15	40,5

decrease. The creep elongation and the oxidation resistance at constant temperature for He 1049 are improved by melting in vacuum and casting in the presence of argon, but the resistance to non-continuous oxidation is better in the case of an alloy prepared in air. In a similar manner, the addition of boron and zirconium to the alloy Udimet 500 improves the creep elongation but decreases the oxidation resistance.

Each alloy and its preparation must thus be studied by keeping in mind its specific application. Vacuum techniques, as well as alloying element additions and special heat treatments, are thus not universally beneficial.

(d) *Homogenization of longitudinal and transversal properties.* Child and Harris[21] have studied the properties of turbine discs prepared in electric and consumable electrode furnaces. In many cases, they have been able to observe a decided homogenization of the properties.

This is especially the case for turbines disc forged from martensitic steel (Cr 10.5 per cent) of the following analysis : C–0.08 per cent, Mn–0.9 per cent, Si–0.2 per cent, Cr–10 per cent, W–0.85 per cent, Co–10 per cent, Mo–1.1 per cent, Nb–0.4 per cent, Ni–0.2 per cent, and V–0.47 per cent.

This alloy has been realized in order to increase the creep properties of the ferritic steels. The increase in the alloying elements makes it more and more difficult to obtain a good transversal ductility. Discs (65 cm diameter) have been forged from 50 cm ingots cast in vacuum and conventional 48 cm diameter ingots.

The comparison of properties in different regions are shown in Table XI. One can notice that the alloy prepared in vacuum has a much more uniform ductility especially along the axis of the disc.

TABLE XI[7]

Comparison of properties of disc forgings in air- and vacuum-arc melted 10.5 per cent Cr martensitic steel

Test-piece position	Air melted			Vacuum melted		
	U.T.S. tonf/in²	El. %	R of A %	U.T.S. tonf/in²	El. %	R of A %
Axial hub	84.4	18.0	57.0	82.2	17.5	56.0
Axial hub	82.6	9.0	15.0	81.6	13.0	43.0
Axial hub	84.8	15.0	45.0	82.8	18.0	50.0
Axial hub	81.8	4.5	6.5	81.8	15.6	52.5
Axial near hub	81.7	11.1	21.0	81.6	14.3	43.5
Axial midway	83.4	14.5	40.0	83.6	16.0	43.0
Axial periphery	81.3	14.5	50.0	82.0	18.0	54.0
Radial periphery	82.0	20.0	60.0	81.7	17.0	57.5
Transverse hub	83.7	16.0	52.0	80.6	17.0	60.0
Transverse hub	81.8	18.0	60.0	80.4	18.5	60.0
Transverse hub	81.6	18.0	60.0	82.4	17.0	55.0
Transverse periphery	82.3	19.0	59.6	81.5	18.5	52.4
Transverse hub	82.2	18.0	55.0	80.7	15.0	40.5

(e) *Amélioration des propriétés magnétiques.* Des travaux récents ont montré que les impuretés avaient un effet important sur les propriétés magnétiques[23, 24].

Ainsi dans les matériaux magnétiques doux, le supermendur (49 pour-cent Fe–49 pour-cent Co–2 pour-cent V) a une rémanence et une perméabilité plus élevées, associées d'ailleurs à une induction de saturation maximum lorsqu'il est coulé sous vide. La Fig. 11 compare la courbe

(e) *Improvement in magnetic properties.* Recent research has shown that impurities have a decided influence on magnetic properties[23, 24].

In soft magnetic materials, the alloy Superminder (49 per cent Fe, 49 per cent Co, 2 per cent V) possesses a higher remanence and permeability associated, by the way, with a maximum saturation induction, when prepared in vacuum. Fig. 11 shows the hysteresis curve of an alloy prepared in air

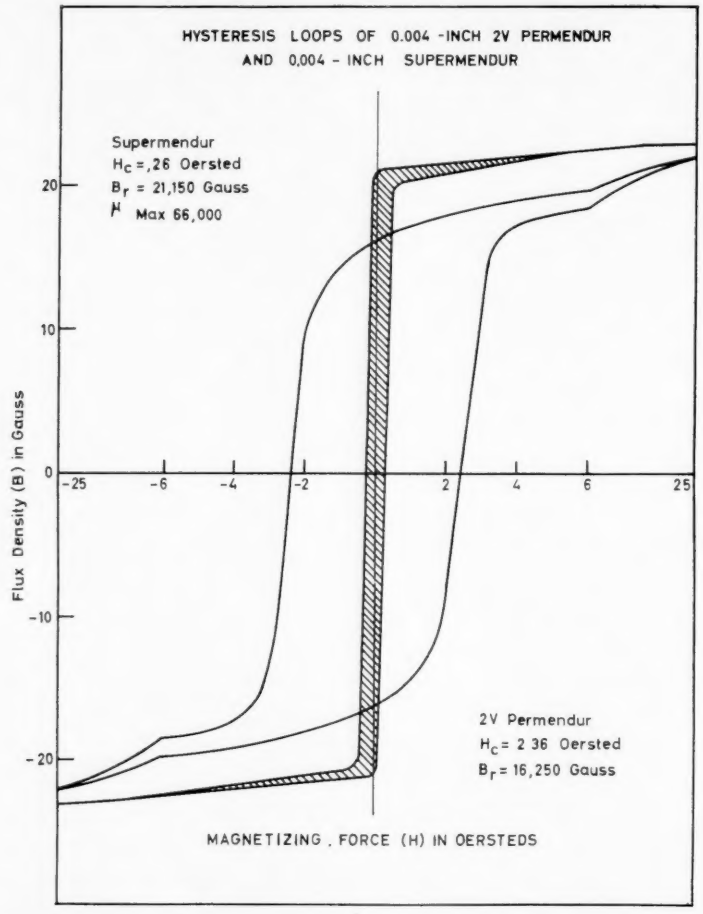

FIG. 11. Caractéristiques magnétiques d'alliages Fe–Co–V coulés sous vide et à l'air

FIG. 11. Magnetic characteristics of Fe–Co–V alloys, air and vacuum melted

d'hystérésis de l'alliage préparé à l'air et préparé sous vide. Cette amélioration est obtenue uniquement grâce à la fusion sous vide au four à induction à l'aide de matériaux sélectionnés de haute pureté.

Nous n'avons guère jusqu'ici insisté sur le nouveau venu, le four à bombardement d'èlectrons. Ses applications les plus intéressantes sont évidemment attendues dans les métaux réfractaires Nb, Mo, Ta, W, Th et leurs alliages ainsi que dans le Be et les aciers spéciaux inoxydables. Le procédé permet d'atteindre des puretés exceptionnelles. Pour les métaux réfractaires, on obtient ainsi des produits laminables et usinables.

Son prix est certes conditionné par un vide plus élevé que dans les autres méthodes, mais par contre, son agrégat haute tension est maintenant relativement bon marché et le rendement en puissance élevé. C'est ainsi que le frittage de tantale par exemple requiert 1000 kWh/kg alors que la

and in vacuum. The improvement is obtained uniquely by melting in a vacuum induction furnace materials of selected high purity.

We have waited until now to discuss what could bring the new type of furnace—the electron bombardment furnace. Its application, the most evident, is the treatment of such highly refractory metals as Nb, Mo, Ta, W, Th and their alloys as well as beryllium, vanadium and special stainless steels.

Extremely high purity can be achieved by this procedure. In the case of refractory metals the finished products are thus rendered rollable and machinable.

Its price is certainly determined by the higher vacuum required when compared to other techniques. On the credit side, one must mention that the power source is not now excessively expensive and that the efficiency is high. As an example, the sintering of tantalum requires 1000 kWh/kg

Vol. 10 196

purification au four à bombardement d'électrons utilise seulement 12 à 15 kWh/kg. Cependant, si cet aspect économique est important, les nouvelles possibilités qu'offre le procédé sont plus importantes encore.

Pour notre part, nous essayons actuellement sur un four de type Heraeus dont le principe a été décrit au début de cette communication d'étudier l'action de ce mode de fusion sur les propriétés des alliages du type Alnico pour aimants permanents.

Ces alliages et notamment l'alliage Alnico V (Al, Co, Ni, Cu, Fe) a un produit BH_{max} 4,5 à 6×10^6 et peut être traité sous champ magnétique. Le métal est dur et fragile et doit être coulé.

Après fusion au four à bombardement d'électrons, on obtient un matériau dont la cristallisation est caractéristique. Elle est presque exclusivement colomnaire, les angles de cristallisation ne dépassant guère 12 à 15°.

Des échantillons de matériaux élaborés au four à bombardement d'électrons et des échantillons de produits classiques ont été traités à 1150°C, dans une ampoule en vycor vidée d'air puis refroidis à une vitesse de 10°C/s, puis ensuite recuits à 600°C pendant 8 h. Ces conditions généralement conduisent au produit BH_{max} le plus élevé.

Les essais au perméamètre ont donné les résultats suivants (tableau XII).

TABLEAU XII

	Alnico classique	Alnico traité sous vide
B_r (gauss)	6500	9850
H_c (oersted)	520	680
BH_{max}	$1{,}4 \times 10^6$	$3{,}65 \times 10^6$

Notons que la dureté varie peu. L'alliage classique a une dureté de 530 kg/mm² (HV 30), tandis qu'après fusion, 490 kg/mm² (HV 30) ; par contre, l'alliage obtenu sous vide est parfaitement usinable par les méthodes classiques et sa forgeabilité est satisfaisante. D'autres essais sont en cours notamment les analyses qui permettent de déterminer le degré de dégazage, l'action de ce mode de fusion sur la teneur en aluminium, etc.

7. *Nouveaux alliages*

Au début de l'exposé, nous avons parlé d'amélioration d'alliages connus, de réalisations d'alliages nouveaux.

Parmi les alliages que les techniques de fusion sous vide permettent de réaliser aisément, il convient de citer les alliages à base de fer-aluminium : les ferral, les alfenols, les alliages plus complexes dérivés : Fe–Al–Mo (Zr), les thermenols.

D'une manière élémentaire, on peut admettre que les propriétés de résistance à l'oxydation, à la corrosion sont en relation avec l'action des éléments Cr–Al et Si sur les couches de passivation dans le fer allié.

Les aciers au chrome sont de très loin les plus couramment utilisés : ils ont donné naissance à la grande classe des aciers inoxydables (stainless) ferritiques, martensitiques et austénitiques. Les conditions d'élaboration classique sont satisfaisantes. L'utilisation des deux autres éléments Si et Al est peu développée ; tout au plus a-t-on élaboré des aciers Si–Cr–Al, des fontes et des fers à haut silicium.

whereas treatment by electron bombardment requires 12 to 15 kWh/kg. However, if the economic point is important, the new possibilities offered by this procedure are even more interesting.

We are actually trying with a furnace developed by Heraeus to study the influence of this method of preparation on the properties of the permanent magnetic alloys of the Alnico type.

The alloys and especially Alnico V (Al, Co, Ni, Cu, Fe) possess a BH_{max} of 4.5 to 6×10^6 and may be treated in a magnetic field. The alloy is hard and brittle and must thus be cast. After melting in an electron bombardment furnace, one obtains a material possessing a characteristic mode of grain growth. This is nearly completely columnar the long axes of crystallization never exceeding 12 to 15°.

Specimens manufactured in the above manner as well as those prepared in the classical manner have been treated at 1150°C in a sealed vycor tube and cooled at a rate of 1°C/s and annealed at 600°C for 8 hr. This treatment generally develops the highest BH_{max} value.

Results of " permeability " tests have given the following results—Table XII.

TABLE XII

	Classical Alnico	Vacuum Alnico
B_r (gauss)	6500	9850
H_c (oersted)	520	680
BH_{max}	1.4×10^6	3.65×10^6

Notice that the hardness does not change appreciably. The classical alloy has a hardness of 530 kg/mm² (HV 30) while after melting 490 kg/mm² (HV 30). The alloy produced in vacuum, however, is easily machinable by classical methods and its forgeability is satisfactory. Other tests are being undertaken such as the analysis permitting the determination of the amount of degassing, the action of the mode of melting on the aluminum content, etc.

7. *New alloys*

At the beginning of this communication, we spoke about the improvement of known alloys and the development of new alloys.

Among those alloys which are easy to prepare by the techniques of vacuum melting we can mention those iron-aluminum-base alloys the ferral, alfenols and more complex alloys Fe–Al–Mo (Zr) the thermenols.

In a general manner, one can admit that corrosion and oxidation resistance are related to the elements : Cr, Al, Si on the passivity layers in the alloyed iron.

Steels containing chromium are by far the most commonly employed ; they have been responsible for the great class of stainless steels : ferritic, martensitic and austenitic. The classical preparation of such alloys is satisfactory. The use of two other elements Si and Al is not highly developed, except for the preparation of Si–Cr–Al steels and high silicon cast-irons.

La fusion classique d'alliages Fe–Al sans être impossible est relativement difficile. En effet, l'aluminium s'oxyde à la surface du bain liquide malgré la protection de laitier et finalement à la coulée les grains sont presque séparés par une peau d'oxyde d'aluminium qui donne une fragilité excessive. L'élaboration sous vide élevé dans un creuset au zirconium permet d'abaisser considérablement la teneur en oxygène et d'obtenir des alliages jusqu'à 17 pour-cent d'aluminium laminables à chaud, mais encore fragiles à froid et présentant malgré tout des microfissures dans le lingot.

L'utilisation de deux méthodes conventionnelles de désoxydation appropriées à la fusion sous vide, la réduction au carbone et à l'hydrogène ont été utilisées pour améliorer cette situation.

La réduction à l'hydrogène est la plus intéressante, mais elle est lente et coûteuse. Elle requiert 4 heures pour amener l'xoygène à 0,0015 pour-cent. Par comparaison, l'addition de carbone en présence de vide élevé réduit en 10 minutes l'oxygène à 0,001 pour-cent. Une teneur de 0,03 pour-cent de carbone est adéquate pour une désoxydation satisfaisante et pour conférer au produit une ductilité satisfaisante. Signalons qu'une teneur de 1 pour-cent C n'affecte pas outre mesure le travail à chaud. mais au-dessus de 0,15 pour-cent, la teneur en carbone affecte le travail à froid.

La résistance à chaud de cet alliage peut être obtenue en y ajoutant les éléments suivants : Ti–Si–Mo et V. On peut obtenir un comportement à chaud supérieur à celui de l'acier inoxydable 302. Le prix peu élevé de l'aluminium compense partiellement la nécessité d'utiliser les techniques du vide. Nous avons, pour notre part, étudié l'action d'une addition de cobalt sur les alliages Fe–Al. On observe une amélioration significative pour de faibles pourcentages en cobalt, sans perte appréciable de propriétés à froid.

La résistance à l'oxydation extraordinaire de cet alliage, sa tenue dans les milieux chimiques où souvent elle est supérieure aux aciers inoxydables, rendent ces alliages intéressants dans de très nombreuses applications : utilisation dans les turbines, les fours de carburation et carbonitruration, éléments de résistance chauffante.

A côté de ce type d'alliages aux propriétés multiples qui cherchent actuellement leur place, les procédés de fusion sous vide les plus développés ont donné naissance à une nouvelle série d'alliages destinés au service des hautes températures tels que Udimet 500, M 308, Super Waspalloy, Jettalloy (voir tableau V).

Il s'agit en fait de ce que l'on appelle couramment des " super-alliages " dans les bases fer, cobalt et surtout nickel.

Ils contiennent 3 à 6 pour-cent Ti et Al et ne peuvent être élaborés d'une manière intéressante par la fusion classique. La fusion par électrodes consommables et par induction a permis une production commerciale de ces alliages qui présentent actuellement les propriétés à chaud les plus élevées. Dans le cas du " Waspalloy ", la résistance au fluage mesurée par le temps de rupture est de 10 fois supérieure dans la coulée à vide par rapport à la coulée à l'air.

Dans le cadre des applications de l'énergie nucléaire, il faut encore citer les aciers inoxydables au bore. L'acier 304 + 2 pour-cent B ne peut être réalisé que par des traitements sous vide. La section efficace aux neutrons thermiques

Although the melting by classical means of Fe–Al alloys is not impossible it is relatively difficult. The aluminum at the surface of the metallic bath, despite the protection offered by the slag, is oxidized. The cast product is thus rendered exceeding brittle due to the presence of this oxide film along grain boundaries. Preparation in vacuum in a zirconia crucible greatly reduces this effect and alloys containing up to 17 per cent Al can be hot-rolled. The ingots are, however, brittle at low temperatures and contain micro cracks.

The employment of two classical deoxidation methods in vacuum-reduction by carbon and by hydrogen can be used to improve this situation. Reduction by hydrogen, although the most interesting, is slow and expensive. It requires 4 hours to decrease the oxygen content to 0.0015 per cent. In contrast, treatment with carbon in a high vacuum decreases the oxygen content to 0.001 per cent in 10 min. A carbon content of 0.03 per cent permits a deoxidation sufficient to obtain the desired ductility.

The high temperature resistance of this alloy can be improved by adding such elenents as Ti, Si, Mo, V. One can thus obtain high-temperature properties superior to those of the stainless steel 302. The lower price of aluminum partially compensates for the necessity to employ vacuum techniques.

We have studied the influence of cobalt additions to the Fe–Al alloys.

One observes a definite improvement for small cobalt additions without a significant loss in low-temperature properties.

The high oxidation resistance of this alloy—frequently higher than that of stainless steels in chemical media—makes it extremely interesting for many applications such as the following : in turbines, in carburizing and nitriding furnaces and electrical resistance heating elements.

In addition to this alloy possessing multiple properties, the employ of the highly developed vacuum processes have resulted in the production of a new series of alloys for high-temperature service : Udimet 500, M 305, Réné 41, Super Waspalloy, Jettalloy (see Table V).

These are, in fact, what one commonly calls " super alloys " rich in iron, nickel and cobalt. These contain 3 to 6 per cent Ti and Al and thus cannot be successfully prepared by classical melting procedures. Melting by induction or by consumable electrodes has permitted the commercial production of these alloys which present the highest elevated temperature properties. In the case of " Waspalloy ", the creep resistance measured by the rupture time is 10 times higher when the alloy is prepared by vacuum techniques.

Among the alloys destined for use in the field of nuclear energy, we must cite also the stainless steels containing boron. The alloy 304 with 2 per cent B can only be successfully prepared in vacuum. Since the effective cross-section of boron for thermal neutrons is large, it is very interesting to prepare alloys as rich as possible in this element.

In all means, these are difficult to prepare by classical

Vol. 10 1960

du bore étant élevée, il est intéressant de disposer d'alliages riches en bore. Toutefois, ceux-ci sont difficiles à élaborer et provoquent finalement la formation d'alliages trop oxydés dont les propriétés mécaniques sont déficientes.

Conclusion

Ce tour d'horizon cherchait à faire ressortir par des exemples précis quelques domaines d'application des techniques du vide en métallurgie.

Nous avons montré comment elles pouvaient apporter aux alliages existants des propriétés nouvelles et permettre l'élaboration d'alliages nouveaux dont certaines propriétés sont sensiblement améliorées.

Comme nous l'avons esquissé, non seulement les alliages spéciaux, mais également les aciers de production sont intéressés par certains aspects de cette technique.

Pour terminer, cependant, nous voudrions rappeler la conclusion de Stutzmann[22] : l'emploi des techniques du vide n'est pas une panacée ; elles doivent être appliquées avec discernement en fonction de la ou des propriétés que l'on désire améliorer dans un métal.

Bibliographie

[1] A. S. D. Barrett et M. E. Harper ; Selection of Pumping System for Vacuum Metallurgical Processes, *J. Inst. Metals*, **87**, 227 (1958–59).

[2] A. Tix ; Production Application of Degassing Steel in Vacuum Especially for Big Forging Ingots, *Stahl und Eisen*, **76**, 61–88 (1956).

G. Garnik et A. Samarin ; Vacuum Metallurgy of Steels—Deoxydation and Desulphurization in Vacuum, *Izv. Akad. Nauk SSSR* (Mai 1957), 77 Brutcher Transl. no. 4054.

L. Levaux et L. Hannon ; La coulée sous vide des gros lingots de forge, *Proc. of the First International Congress on Vacuum Techniques Belgium* 1958, Vol. II, 611. Pergamon Press Ltd.

D. E. Parson et W. A. Morgan ; *Vacuum Degassing of Steels*, Part I, Department of Mines and Technical Survey, Canada, Research no. 47, 1959.

[3] F. Darmara, J. Huntington et E. Machlin ; Vacuum Induction Melting, *J.I.S.I.*, **191**, 266 (1959).

[4] W. Jones ; Vacuum Induction Melting Processes Consideration, *Metal Progr.*, **72**, 133.

[5] J. Byrne ; World's Largest Induction Furnace, *Metal Progr.*, **77**, 83 (1960).

[6] Consumable Electrode Vacuum Remelting of High Temperature Alloys, *High Temperature Materials*, Ed. J. Wiley, 1957, paper no. 25, 378.

[7] R. Pitler, E. Reynolds et W. Dyrkacz ; Vacuum Melting of Steels, *J.I.S.I.*, 414 (1958).

[8] J. L. Ham ; Skull and Permanent Electrode Melting, *Vacuum Metallurgy*, Ed. R. Bunshah, 172 (1958).

[9] T. C. Du Mond, Ultra-Pure Metals Produced in Electron Beam Furnace, *Metal Progr.*, 84 (Déc. 1958).

[10] H. Smith, Ch. D. A. Hunt et Ch. Hauks ; Electron Bombardment Melting, *J. Metals*, 112 (Fév. 1959).

[11] H. R. Smith ; Electron Bombardment Melting Techniques, *Vacuum Metallurgy*, Ed. R. Bunshah, 1958.

[12] W. W. Dyrkacz ; *Thermodynamics in Vacuum Metallurgy*, 1960, Ed. New York Univ. Press.

[13] W. G. Pfann ; *Zone Melting*, Ed. J. Wiley, New York, 1958.

[14] A. M. Aksoy ; Quality Aspects and Properties of Vacuum Melted Super Duty Steels, *A.I.M.E. Metall. Soc. Confer.*, **3**, 267. Quality Requirements of Super Duty Steels.

[15] W. W. Dyrkacz ; Quality Improvements in Stainless Steels and Super Alloys by Vacuum Melting, *A.S.M. Western Metal Congress*, 1959.

[16] C. T. Evans ; Overall Summary of Vacuum Melting, *A.I.M.E. Electric Furnace Steel Conference*, Pitttburgh, Pa. Dec. 1957.

[17] J. H. Moore ; Vacuum Melting Lengthens Fatigue Life Improves Impact Properties, *Iron Age*, **171**, 154–156 (1953).

Promises and Problem Posed by Vacuum Melting, *J. Metals*, **6**, 1368–1369 (1954).

means. In fact, boron reacts with oxygen thus rendering the alloy excessively oxidized and, as a result, of inferior mechanical qualities.

Conclusions

This survey attempts to show by means of several examples the application of vacuum melting techniques in metallurgy.

We have shown how such methods give the metallurgist the possibility to realize important improvements in the various properties of existing alloys as well as the means to prepare new alloys whose properties are greatly increased.

As we have mentioned not only the special alloys, but also those of tonnage production can frequently benefit from the employ of vacuum melting techniques.

In conclusion, however, we would like to state as has Stutzmann[22] that the use of these techniques is not a " panacea " they must be carefully employed by keeping in mind the properties which one desires in the finished alloy.

References

[1] A. S. D. Barrett and M. E. Harper ; Selection of Pumping System for Vacuum Metallurgical Processes, *J. Inst. Metals*, **87**, 227 (1958–59).

[2] A. Tix ; Production Application of Degassing Steel in Vacuum Especially for big Forging Ingots, *Stahl und Eisen*, **76**, 61–88 (1956).

G. Garnik and A. Samarin ; Vacuum Metallurgy of Steels—Deoxydation and Desulphurization in Vacuum, *Izv. Akad. Nauk SSSR*, May 1957, 77, Brutcher Transl. no. 4054.

J. Levaux and L. Hannon ; La coulée sous vide des gros lingots de forge, *Proc. of the First International Congress on Vacuum Techniques, Belgium* 1958, Vol. II, 611. Pergamon Press Ltd.

D. E. Parson and W. A. Morgan ; *Vacuum Degassing of Steels*, Part I, Department of Mines and Technical Survey, Canada. Research no. 47, 1959.

[3] F. Darmara, J. Huntington and E. Machlin ; Vacuum Induction Melting, *J.I.S.I.*, **191**, 266 (1959).

[4] W. Jones ; Vacuum Induction Melting Processes Consideration, *Metal Progr.*, **72**, 133.

[5] J. Byrne ; World's Largest Induction Furnace, *Metal Progr.*, 77, 83 (1960).

[6] Consumable Electrode Vacuum Remelting of High Temperature Alloys, *High Temperature Materials*, Ed. J. Wiley, 1957, paper no. 25, 378.

[7] R. Pitler, E. Reynolds and W. Dyrkacz ; Vacuum Melting of Steels, *J.I.S.I.*, 414 (1958).

[8] J. L. Ham ; Skull and Permanent Electrode Melting, *Vacuum Metallurgy*, Ed. R. Bunshah, 172 (1958).

[9] T. C. Du Mond ; Ultra-Pure Metals Produced in Electron Beam Furnace, *Metal Prog.*, 84 (Dec. 1958).

[10] H. Smith, Ch. D. A. Hunt and Ch. Hauks ; Electron Bombardment Melting, *J. Metals*, 112 (Feb. 1959).

[11] H. R. Smith ; Electron Bombardment Melting Techniques, *Vacuum Metallurgy*, Ed. R. Bunshah (1958).

[12] W. W. Dyrkacz ; *Thermodynamics in Vacuum Metallurgy*, 1960. Ed. New York Univ. Press.

[13] W. G. Pfann ; *Zone Melting*, Ed. J. Wiley, New York, 1958.

[14] A. M. Aksoy ; Quality Aspects and Properties of Vacuum Melted Super Duty Steels, *A.I.M.E. Metall. Soc. Confer.*, **3**, 267. Quality Requirements of Super Duty Steels.

[15] W. W. Dyrkacz ; Quality Improvements in Stainless Steels and Super Alloys by Vacuum Melting, *A.S.M. Western Metal Congress*, 1959.

[16] C. T. Evans ; Overall Summary of Vacuum Melting, *A.I.M.E. Electric Furnace Steel Conference*, Pittsburgh, Pa. (Dec. 1957).

[17] J. H. Moore ; Vacuum Melting Lengthens Fatigue Life Improves Impact Properties, *Iron Age*, **171**, 154–156 (1953).

Promises and Problem Posed by Vacuum Melting, *J. Metals*, 6, 1368–1369 (1954).

[18] J. H. Gittus ; Nickel Based Vacuum Melted Exp.—High Temperature Alloys, *Metal Treatment and Drop Forging*, 76 (Janv. 1960).

[19] B. F. Richardson ; Vacuum Induction Melting of Low Alloy Steels, *A.I.M.E. Metall. Soc. Confer.*, 3, 285. Quality Requirements of Super Duty Steels.

[20] G. K. Bhat ; A New Steel for Rocket Motor Cases, *Metal Progr.*, 75 (Juin 1960).

[21] R. F. Decker, J. Rowe et J. W. Freeman ; Relation of High Temperatures Properties of a Nickel Base Precipitation Hardening Alloys to Contamination by Crucibles, *High Temperature Materials*, Ed. J. Wiley, no. 26, 388 (1957).

[22] M. J. Stutzmann and Cunningham ; Studies and Comparison of the Properties of High Temperatures Alloys Melted and Precision Cast both in Air and in Vacuum, *Wright Air Development Center—Technical Report* 1957, 678 (Dec. 1957). *Trans. A.I.M.E.*

[23] Littmann ; *J. Metals*, 220 (Mars. 1960).

[24] H. Gould and D. Wenny ; *Elect. Engng.* (Mars 1957).

[18] J. H. Gittus ; Nickel Based Vacuum Melted Exp.—High Temperature Alloys, *Metal Treatment and Drop Forging*, 76, (Jan. 1960).

[19] B. F. Richardson ; Vacuum Induction Melting of Low Alloy Steels, *A.I.M.E. Metall. Soc. Confer.*, 3, 285. Quality Requirements of Super Duty Steels.

[20] G. K. Bhat ; A New Steel for Rocket Motor Cases, *Metal Progr.*, 75 (June 1960).

[21] R. F. Decker, J. Rowe, and J. W. Freeman ; Relation of High Temperatures Properties of a Nickel Base Precipitation Hardening Alloys to Contamination by Crucibles, *High Temperature Materials*, Ed. J. Wiley, no. 26, 388 (1957).

[22] M. J. Stutzmann, Cunningham ; Studies and Comparison of the Properties of High Temperatures Alloys Melted and Precision Cast both in Air and in Vacuum, *Wright Air Development Center—Technical Report* 1957, 678 (Dec. 1957). *Trans. A.I.M.E.*

[23] Littmann ; *J. Metals*, 220 (March 1960).

[24] H. Gould and D. Wenny ; *Elect. Engng.* (March 1957).

Vol.
10
1960

Coulée sous Vide de l'Acier

J. LEVAUX et L. HANNON

S.A. Cockerill-Ougrée, Seraing, Belgique

L'Aciérie Martin de Seraing possède une installation LEYBOLD *pour la coulée sous vide de l'acier. On opère la coulée sous vide de deux façons :*

—pour les gros lingots de forge, on dégaze directement à la mise en lingotière,

—pour les petits lingots, on dégaze en transvasant l'acier d'une poche dans une autre, puis on va couler à l'air.

La teneur en hydrogène de l'acier liquide dégazé est de l'ordre de 2 à 3 cm³/100 g. Les fissurations provoquées par les inclusions oxydées disparaissent complètement par la coulée sous vide. L'allongement et la striction sont améliorés et la résilience radiale en travers est nettement favorisée. Cette technique s'applique donc particulièrement aux pièces de forge très sollicitées.

Vacuum Casting of Steel

J. LEVAUX and L. HANNON

S.A. Cockerill-Ougrée, Seraing, Belgium

The open hearth steel plant at Seraing is equipped with a LEYBOLD *installation for vacuum casting of steel. Vacuum casting is carried out in two different ways :*

—for heavy forging ingots : the degassing takes place directly when pouring steel into the ingot mould ;

—for small forging ingots : the degassing is obtained when transferring steel from the tapping ladle to another ladle ; then steel is air-cast.

The hydrogen content of the liquid degassed steel is of the order of 2 to 3 cm³/100 g. The cracks initiated by the oxidized inclusions completely disappear thanks to the vacuum casting technique. Elongation and reduction in area are improved ; as well, the impact values recorded from transverse radial test specimens. This technique is therefore particularly beneficial to heavy stressed forgings.

Appareillage et technologie

Nous disposons de trois cuves de coulée : deux cuves ont un diamètre de 2,900 m et permettent la coulée de lingots de forge jusqu'à 42 t, la troisième cuve a 4 m de diamètre et permet, soit la coulée de lingots jusqu'à 120 t, soit la coulée par transvasement de poche à poche.

Coulée sous vide par transvasement de poche à poche

Ce procédé est utilisé pour la coulée de petits lingots à bloomer (2,5 à 7 t). Le plus souvent, il s'agit de petites poches d'acier électrique, à raison de 20 t par coulée. On dégaze l'acier en transvasant d'une poche dans une autre poche, puis on coule à l'air suivant la pratique normale. Ce procédé permet le contrôle du dégazage par prélèvement

Equipment and technology

Our works are equipped with three vacuum tanks : two are of 2.900 m diameter and permit the casting of forging ingots up to 42 t ; the third tank is of 4 m diameter and permits either casting of ingots up to 120 t or pouring from tapping ladle to transfer ladle.

Vacuum casting by transfer from ladle to ladle

This process is used for casting small ingots intended to be rolled into blooms (2.5 to 7 t). In almost all cases, it is small tapping ladles for electrical steel (20 t per heat). Steel is degassed by transfer from one ladle to another ; then it is poured according to the conventional practice. This

d'une éprouvette lors de la coulée des lingots au bassin ordinaire. L'éprouvette est obtenue par le remplissage d'un moule genre " pencil test ", l'acier étant prélevé au moyen d'une louche directement sous la poche.

Dans le cas du transvasement poche à poche, le dégazage en hydrogène est représenté aux Fig. 1 et 2 ; ces graphiques donnent les résultats de quelques dizaines d'opérations.

Figure 1. La teneur en hydrogène de l'acier liquide au bassin de coulée est représentée en fonction de la teneur en hydrogène de départ au four avant de couler. La corrélation entre ces deux valeurs indique qu'il y a un dégazage de l'ordre de 50 pour cent lorsque l'acier, à la sortie du four, a une teneur en hydrogène de l'ordre de 7 cm^3/100 g, 60 pour cent quand l'acier quitte le four avec une teneur en hydrogène de 10 cm^3/100 g.

process permits to check the degassing through taking a sample when pouring the ingots at the casting pit. The sampling consists in filling with steel a mould of the pencil test type—steel being drawn with a " spoon " directly under the ladle.

In the case of transfer from ladle to ladle, hydrogen removal is represented on Figs. 1 and 2 ; they show the results recorded from some tens of operations.

Figure 1. The hydrogen content of the liquid steel at the casting pit is plotted in relation to the hydrogen content of steel at the furnace outlet before the pouring operation. The relationship of these two values indicates that degassing has been carried out up to about 50 per cent when steel—at the furnace outlet—shows a hydrogen content of the order of 7 cm^3/100 g, about 60 per cent when steel at the furnace outlet shows a hydrogen content of 10 cm^3/100 g.

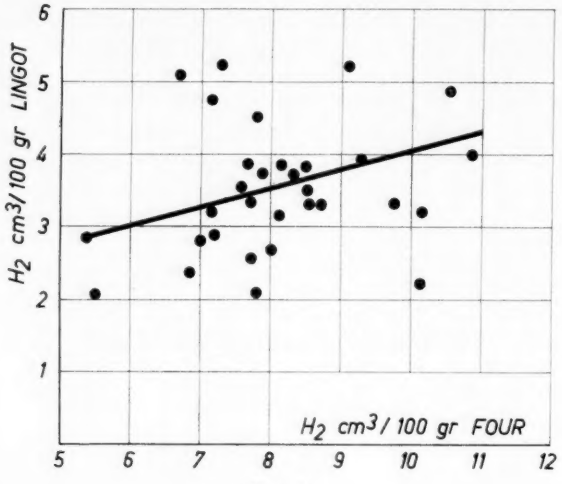

FIG. 1.

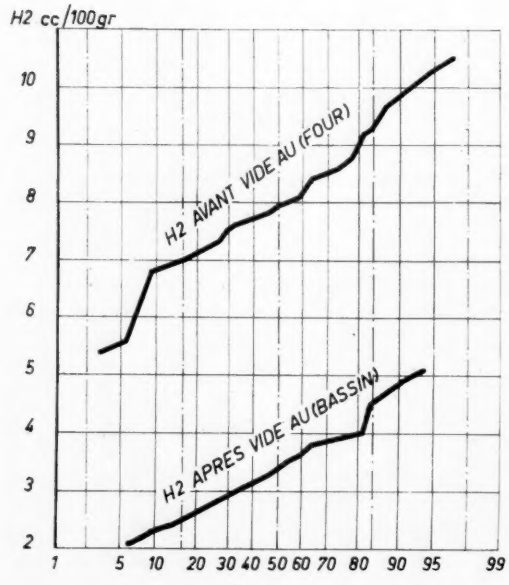

FIG. 2.

Vol. 10 1960

Figure 2. Les mêmes chiffres sont représentés sur un diagramme probabilitaire montrant que plus de 80 pour cent des valeurs de teneur en hydrogène sont inférieurs à 4 $cm^3/100$ g.

Coulée sous vide à la mise en lingotière

Dans ce cas, le dégazage s'effectue dans les meilleures conditions possibles au point de vue du débit d'acier qui ne dépasse pas 3 t/min.

Figure 2. The same values are represented on a " prospective diagram " showing that more than 80 per cent of the values of hydrogen content are below 4 $cm^3/100$ g.

Vacuum casting when pouring into ingot moulds

In this case, degassing is carried out under the most favourable conditions, as the pouring rate does not exceed 3 t/min.

However the possibility of spraying the pouring stream is limited, since it is desirable to avoid spreading the stream outside the hot-top opening.

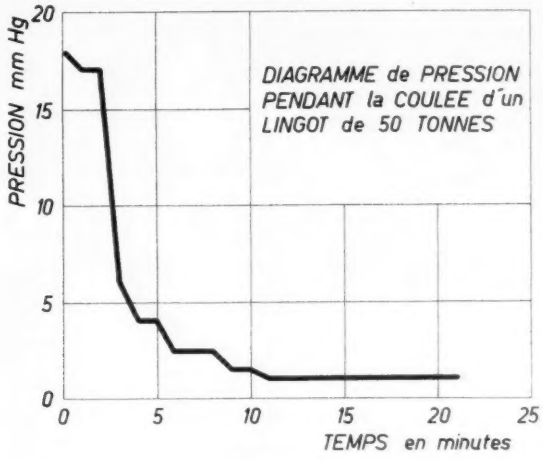

FIG. 3.

Cependant, on est limité dans la possibilité de disperser le jet, puisqu'il convient d'éviter un étalement du jet en dehors de l'ouverture de la masselotte.

Le rendement du dégazage en hydrogène paraît atteindre 65 pour cent, en effet, on quitte la plupart du temps le four Martin à une teneur d'environ 7 $cm^3/100$ g pour atteindre au prélèvement dans la masselotte une teneur d'environ 2 à 2,5 $cm^3/100$ g.

La Fig. 3 montre une courbe de maintien du vide pendant la coulée d'un lingot de 50 t.

L'hydrogène dans les pièces de forge

Nous venons de montrer que le procédé de coulée sous vide éliminait 60 à 65 pour cent de l'hydrogène contenu dans les aciers.

Dans des rapports précédents (Congrès de Namur 1958 et de Londres 1959), nous avons eu l'occasion de noter le raccourcissement de la durée des traitements des pièces de forge par la suppression pure et simple des traitements spéciaux anti-flocons qui permettaient la diffusion partielle de l'hydrogène.

Nous pouvons actuellement, à la suite d'une expérience de plus de deux ans, confirmer l'intérêt de la coulée sous vide : elle assure un seuil de teneur en hydrogène suffisamment bas pour se trouver à l'abri de la création de flocons lors du refroidissement après forgeage.

La valeur moyenne en hydrogène de tous les turbos et rotors exécutés sous vide en nos aciéries a été de :

— à la sortie du four : 6,5 $cm^3/100$ g (s'étalant de 5,5 à 7,5)
— après coulée sous vide : 2,3 $cm^3/100$ g (s'étalant de 1,6 à 2,8).

The extent of hydrogen removal appears to reach 60 per cent ; in fact, in most of the cases, the steel, when leaving the open hearth furnace, has a content of about 7 $cm^3/100$ g and when sampled from the hot-top, about 2 to 2.5 $cm^3/100$ g.

Fig. 3 is a chart of the tank pressure during the casting of a 50-ton ingot.

Hydrogen concentration in forgings

We have already proved that the vacuum casting process removed 60 to 65 per cent of hydrogen from steel.

In previous reports (Namur 1958, and London 1959 meetings) we have had opportunity to mention the shortening of the heat treatment times for forgings thanks to the cancellation of the anti-flaking treatments which permitted partial dispersal of hydrogen.

Basing on over two-year experience, we can now confirm the practical value of this technique ; it ensures a level of hydrogen content sufficiently low to be secure from the flakening occurring when cooling the part after the forging operation.

The average hydrogen value of all the turbine shaft and rotor steels manufactured in our works, has been :

— at the furnace outlet : 6.5 $cm^3/100$ g (ranging from 5.5 to 7.5)
— after vacuum casting : 2.3 $cm^3/100$ g (ranging from 1.6 to 2.8).

Inclusions in the steels

The crack-generating inclusions are a major cause for

Inclusions dans les aciers

Les inclusions fissurantes sont une cause essentielle de raccourcissement de la vie des cylindres de laminoirs.

Si la formation des inclusions fissurantes reste encore à l'heure actuelle un sujet de discussion entre spécialistes, on admet généralement que les fissures internes proviennent d'inclusions oxydées déformées par forgeage et rendues fissurantes sous l'effet de gaz.

Dans un cylindre, possédant à mi-rayon une zone d'inclusions fissurantes, les fissures, qui se développent en surface en cours de service, rejoignent plus rapidement ces fissures internes.

A partir de ce moment, le cylindre est mis hors service.

Les inclusions oxydées, lors de la coulée traditionnelle des lingots de forge, se trouvent souvent sous forme d'alignement en particulier dans la zone dendritique (Fig. 4).

shortening the service life of the rolling-mill rolls. Whilst the formation of crack-generating inclusions is still a much debated question among the specialists, it is generally acknowledged that internal cracks result from oxidized inclusions which have been deformed by the forging operation and which have developed into cracks owing to gas action.

In a roll showing a zone of crack-generating inclusions located under the surface (at about half the radius deep), the cracks which develop on the surface during service operation join more quickly these internal cracks.

From that moment, the roll is to be discarded.

In the case of forging ingots produced according to the conventional casting system, the oxidized inclusions are often found arranged in lines, namely in the dendritic zone (Fig. 4).

They are concentrated in the segregation bands.

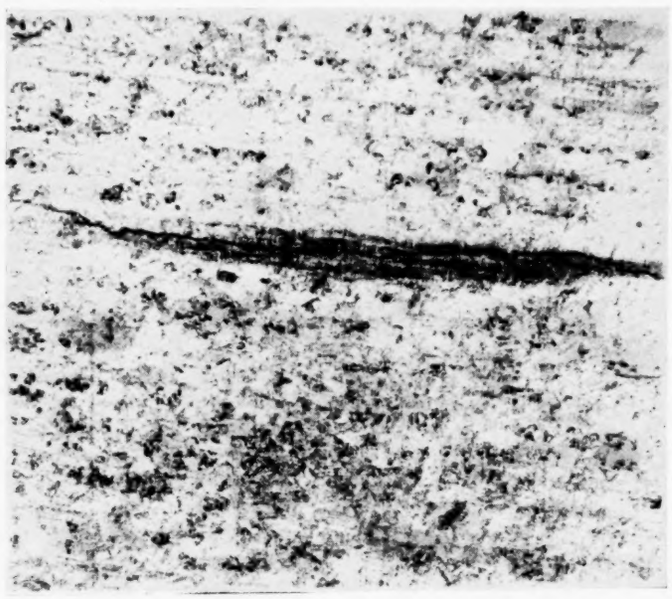

FIG. 4.

Elles se concentrent dans les bandes de ségrégation.

Par l'emploi de la technique du vide, ces inclusions oxydées sont réduites dans des proportions telles qu'elles ne se rencontrent plus que sous forme de nodules isolés, sans alignement et n'ayant plus leur caractère fissurant.

Si nous comparons les sondages ultra-soniques de pièces forgées de même type, nous constatons :

(1) Que toutes les pièces forgées à partir de lingots coulés à l'air sont chargées d'inclusions oxydées souvent fissurantes qui se concentrent en général à mi-rayon, surtout dans la partie haute du lingot.

(2) Que dans les lingots coulés sous vide, une différence nette apparait entre :
   (a) les coulées où le vide a pu être poussé très bas (1 mmHg) ; Aucune inclusion n'apparait aux ultra-sons. Il faudrait utiliser le palpeur de 6 MH pour déceler les inclusions isolées qui, comme nous

Thanks to the vacuum casting process, the amount of oxidized inclusions is minimized to such an extent that the inclusions are only found in the form of separate nuclei without showing any alinement and without retaining their crack-generating characteristic.

When comparing ultrasonic testings conducted on forgings of the same type, we find that :

(1) All the forgings produced from air cast ingots contain a great deal of oxidized inclusions, often of the crack-generating type, which are generally concentrating under the surface (at half the radius deep), mostly in the top part of the ingot.

(2) In the vacuum cast ingots, a marked difference is noted between :
   (a) When casting pressure has been as low as 1 mmHg : no inclusion is detected by ultrasonic inspection. The 6 MH probe should be used to detect the

l'avons dit, sont sans influence sur la vie des pièces forgées.

(b) Les coulées où le vide a été limité à 4 à 5 mmHg. Elles comportent, en général, des traces d'inclusions : celles-ci ne sont pas fissurantes. Elles peuvent cependant, sous des charges exceptionnellement fortes, amorcer des écaillages, comme c'est le cas des cylindres de travail à froid. Une étude systèmatique des teneurs en oxygène total et poids d'inclusions oxydées a permis de tracer les Fig. 5 et 6. On constate (Fig. 5) que pour des teneurs données en oxygène total, la valeur correspondant à la fréquence maximum et la dispersion sont plus faibles pour les coulées sous vide. Pour les poids des inclusions oxydées (Fig. 6), la valeur correspondant à la fréquence maximum est plus faible pour les pièces coulées sous vide mais la dispersion est pratiquement la même pour les deux types de coulée.

isolated inclusions which, as already mentioned, have no effect on the life of the forging.

(b) When casting pressure has been limited to 4 to 5 mmHg : the steel generally shows traces of inclusions and such inclusions are not of the crack-generating type. However, under exceptionally heavy loads, the inclusions are liable to initiate cracks as is the case for working-rolls in cold rolling mills. A systematic study of the total oxygen contents and oxidized inclusion weights has led to plot diagrams 5 and 6. It is found (Fig. 5) that for contents of total oxygen, the value corresponding to maximum frequency and the dispersal are lower for vacuum cast parts. For the weights of oxidized inclusions (Fig. 6), the value corresponding to the maximum frequency is lower for the vacuum cast parts but the dispersal is practically at same level for both types of casting techniques.

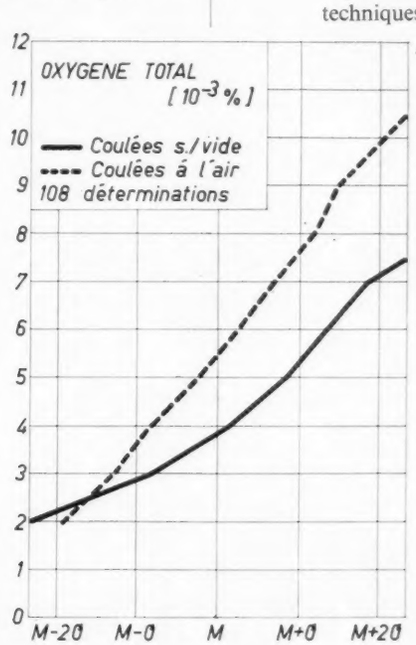

FIG. 5.

Note : La teneur en oxygène total a été déterminée par fusion sous vide. Le poids des inclusions oxydées est obtenu après dissolution et séparation des inclusions oxydées par la méthode de Koch.

Un incident de coulée nous a donné une démonstration péremptoire de l'efficacité de la coulée sous vide.

Il était prévu de couler un gros lingot sous vide. Après la coulée sous vide, dans des conditions normales du demi lingot, un incident nous a mis dans l'obligation de remettre la cuve à la pression atmosphérique. La partie supérieure du lingot fut donc coulée à l'air. Le contrôle ultra-sonique a montré que toute la partie inférieure du lingot était exempte d'inclusions oxydées tandis que la partie supérieure présentait de multiples inclusions.

La Fig. 7 donne une comparaison frappante entre pied et tête du même lingot.

Note : The total oxygen content has been determined through vacuum melting. The weight of oxidized inclusions is determined after dissolution and separation of the oxidized inclusions through the Koch process.

A hitch that occurred during the pouring operation decisively demonstrated the efficiency of vacuum casting process.

We had designed to vacuum-cast a heavy ingot. After we had vacuum-poured half the ingot—under normal conditions—we were obliged to restore the pressure within the vacuum tank to atmospheric conditions. Therefore the top part of the ingot was air-cast.

Ultrasonic testing revealed that the whole bottom part was free from oxidized inclusions whilst the top part showed a great number of inclusions.

Fig. 7 permits us to compare the bottom and top parts of the same ingot.

Vol. 10 1960

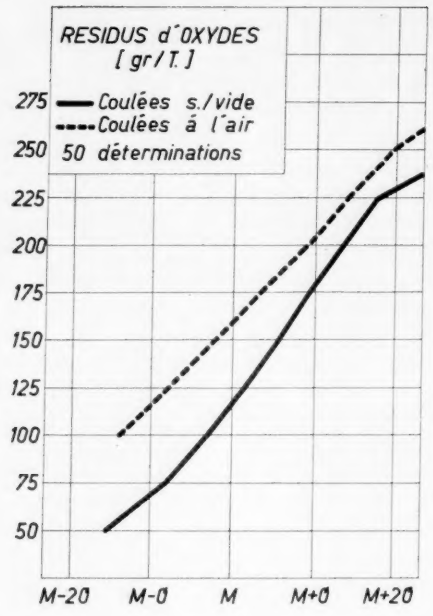

FIG. 6.

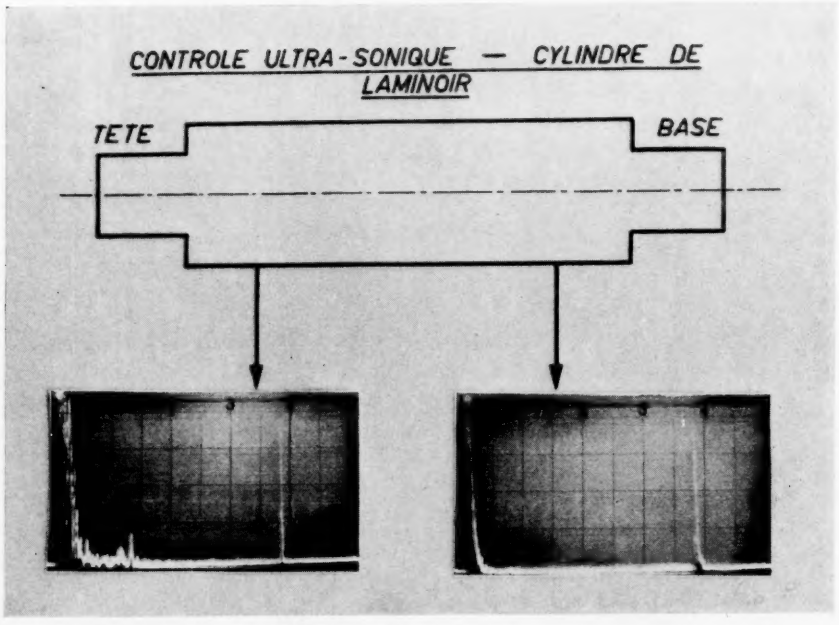

FIG. 7.

Caractéristiques mécaniques des aciers coulés sous vide

Nous avons vu que la quantité et la forme des inclusions oxydées étaient modifiées de façon favorable par la coulée sous vide.

Nous savons que ces inclusions ont une influence néfaste sur certaines caractéristiques mécaniques.

Il est certain également que d'autres inclusions jouent un

Mechanical properties of vacuum-cast steels

We have seen that the amount and shape of oxidized inclusions were favourably changed by vacuum casting.

We know that these inclusions have a detrimental effect on some of the mechanical properties.

It is also acknowledged that other inclusions play a prominent part in the make-up of physical characteristics of steel : here we think of the sulphurous inclusions not

rôle important dans les caractères physiques des aciers : nous pensons ici aux inclusions sulfureuses non éliminées par le vide et non décelées par les ultra-sons.

D'autres techniques, dont nous parlerons plus loin, permettent d'en limiter à la fois l'importance et l'action.

Voyons les caractéristiques sur lesquelles le vide peut avoir une influence.

La coulée sous vide n'améliore pas la période élastique des essais de traction : en effet, la limite élastique et le module d'élasticité ne sont pas influencés par le mode de coulée des lingots.

De la même façon, la charge de rupture n'est pratiquement pas modifiée par la coulée sous vide.

Deux caractéristiques enregistrent une notable amélioration: ce sont l'allongement et la striction des essais en travers.

Des essais de traction dans le sens radial pris dans la zone dendritique des pièces forgées (schéma de prélèvement Fig. 9) ont donné les moyennes reprises à la Fig. 8.

eliminated by vacuum casting process and not detected by ultrasonic inspection.

Other techniques, which will be quoted later, enable us to limit the importance and effect of these inclusions.

We shall now review the properties which can be affected by vacuum casting.

Vacuum casting does not improve the elastic phase of the tension tests ; in fact, yield point and modulus of elasticity are not changed by the process selected for ingot casting.

As well, the breaking load is practically not modified by the vacuum casting technique.

Two characteristics are markedly improved : elongation and reduction in area recorded from transverse test specimens.

The values shown in Fig. 8 have been recorded from radial tension test specimens cut from the dendritic zone of the forgings (sampling location, Fig. 9). They reveal a considerable increase amounting up to 185 per cent for elongation and 234 per cent for reduction in area.

TRACTION ET RESILIENCE RADIALES

TYPE de PIECE	ANALYSE	ALLONGE-MENT VIDE / ALLONGE-MENT AIR en %	STRICTION VIDE / STRICTION AIR en %	RESILIENCE Kgm / cm²	
				LONGITUD.	RADIALE
ROTOR	Ni-Cr-Mo	129	207		
ARBRE	C	168	134		
CYLINDRE	Cr	185	234		
TURBO	Ni-Cr-Mo 67 Kgs Rt			13,9	12

FIG. 8.

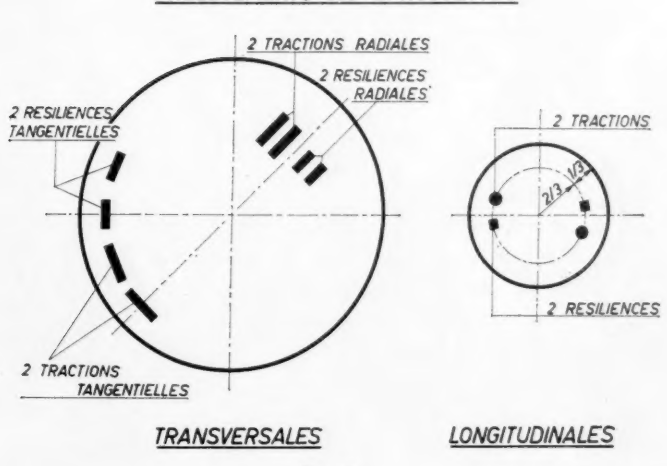

FIG. 9.

Il montre une notable augmentation des allongements et des strictions allant jusque 185 pour cent pour l'allongement et 234 pour cent pour la striction.

L'essai de choc sur éprouvette entaillée du type Mesnager montre également que si la résilience en long est peu modifiée par la technique du vide, il est courant d'obtenir des résiliences en travers atteignant des valeurs très proches de la résilience en long (Fig. 8 et Fig. 9).

Ce point est particulièrement important, car l'expérience confirme qu'un acier ayant une bonne résilience en travers est généralement considéré comme étant à l'abri de ruptures brusques sans déformation.

Propriétés essentielles exigées pour les pièces spéciales telles que rotors, arbres de turbo, coudés, etc.

Procédés d'aciérie

Comme on le sait, la plupart des pièces de forge de la S.A. Cockerill-Ougrée sont coulées soit en acier Martin épuré par le procédé Perrin soit en acier électrique. Le procédé Perrin consiste en un brassage de l'acier dans une poche avec un laitier désulfurant et désoxydant préparé dans un four électrique.

Comme ce procédé est appliqué à la mise en poche, on peut sans aucune difficulté superposer les deux procédés : d'une part, le procédé du laitier Perrin pour assurer une bonne désulfuration et une bonne décantation, en second lieu, la mise en lingotière sous vide pour obtenir un acier dégazé et désoxydé.

L'un ou l'autre procédé permet d'obtenir un acier dont les teneurs en S, O_2 et H_2 sont les plus basses possibles.

Conclusions

On a pu voir que la coulée sous vide, généralement associée au procédé Perrin de désulfuration, permet l'obten-

The impact test conducted on Mesnager notched bars also indicates that while the impact values recorded from longitudinal test specimens are little modified by the vacuum casting technique, it is usual to note from transverse test specimens values approaching those recorded from longitudinal test specimens (Figs. 8 and 9).

This point is particularly important as experience confirms that a steel with good impact values on transverse test specimens is generally considered as being secure from unexpected ruptures without deformation.

These prime properties are required for special parts such as rotors, turbine shafts, crankshafts, etc.

Steelmaking processes

As everyone knows, most of the forgings produced by Cockerill-Ougrée are made of either electric steel or open hearth steel purified by the Perrin process. The Perrin process consists in stirring the steel in a ladle while adding desulphurizing and deoxidizing slag prepared in an electric furnace.

As this operation is carried out when pouring steel in the ladle, it is easy to superpose both processes : on the one hand, the Perrin slag process to ensure an efficient desulphurization and decantation ; on the other hand, the vacuum casting in ingot mould to obtain a degassed and deoxidized steel.

Either process enables the steel to be produced with the lowest practical contents of S, O_2 and H_2.

Conclusions

From the above, it appears that the vacuum casting technique, associated with the Perrin desulphurizing process, allows a steel showing very low content of S as well as O_2 and H_2 to be produced.

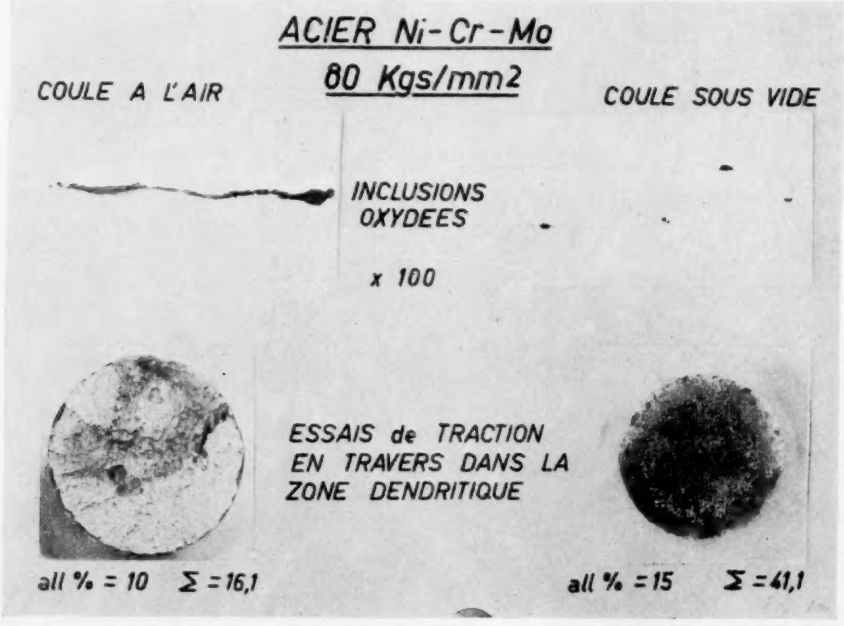
ACIER Ni-Cr-Mo
80 Kgs/mm2
COULE A L'AIR
COULE SOUS VIDE
INCLUSIONS OXYDEES
x 100
ESSAIS de TRACTION EN TRAVERS DANS LA ZONE DENDRITIQUE
all % = 10 Σ = 16,1
all % = 15 Σ = 41,1

FIG. 10.

tion d'un acier à très basse teneur tant en S qu'en O_2 et H_2.

Pratiquement, les fissurations dangereuses provoquées par les inclusions oxydées ont disparu.

Les flocons n'apparaissent plus lors du refroidissement après forgeage.

Les caractéristiques mécaniques d'allongement et de striction sont améliorées sur éprouvette radiale.

La résidence radiale en travers est nettement favorisée.

La Fig. 10 peut résumer complètement l'intérêt du vide dans la coulée des gros lingots de forge : elle se passe de commentaire.

The dangerous cracks caused by oxidized inclusions have been practically eliminated.

Flaking no longer occurs when cooling the part after the forging operation.

Such mechanical properties as elongation and reduction of area are improved on radial test specimens.

The tensile strength from radial tension test specimens is markedly favoured.

Fig. 10 summarizes the features which prove the efficiency of the vacuum casting process for heavy forging ingots : comment is needless.

ol.
10
960

Design Considerations for Vacuum Metallurgical Equipment

M. E. HARPER

Head of Vacuum Metallurgy Research Division, Edwards High Vacuum Limited, Crawley, Sussex

and

W. J. SMITH

Senior Research Assistant

The paper discusses some of the more important considerations to be made in the design of vacuum metallurgical equipments. Comparisons of four types of vacuum pump are made relative to capital cost and efficiency in operation. Design of other components relevant to the operating efficiency of a vacuum system are enumerated and particular reference is made to the design of vacuum induction and resistance heated furnaces.

1. Introduction

The applications of vacuum in the metallurgical field are now very varied and widespread and it is beyond the scope of this paper to carry out a detailed survey. Amongst the most important processes being operated at the present time are melting, degassing, heat treatment, sintering, brazing and welding. Previously published literature[1] has very adequately covered the alternative techniques available for any specified process and it is intended here to review certain applications with a view to pointing out considerations which must be given to a particular design, and to illustrate the variable factors which should be considered in arriving at a particular conclusion.

The problems facing Production Metallurgists in the choice of suitable equipment to carry out a metallurgical process under vacuum, are naturally dictated primarily by the nature of the process itself, the capital and running cost of the equipment, and the type of operating personnel required. A secondary problem is also present in the fact that, for many processes there is an alternative choice in the heating methods employed by the equipment, for example, brazing and sintering can be carried out equally well, using either induction or resistance heating, and the choice in this instance may very well rely upon the importance of capital costs versus the simplicity of maintenance over a long period. Despite the fact that vacuum metallurgy is a relatively new field, developments in high vacuum engineering and equipment in the last decade have resulted in the production of large scale equipment in a field that only a short time ago was confined to research work.

More recent developments in vacuum engineering have led to the possibility of building small scale equipment capable of operating in a pressure range that would be extremely difficult and costly to reproduce on an industrial scale. This fact emphasizes the need for experimental equipment to be designed on principles which can be faithfully reproduced on large scale production plant, thus ensuring that experimental results are not misleading when it comes to production applications.

Results obtained experimentally above a pressure of approximately 10^{-4} Torr* are capable of being reproduced on an industrial scale by equipment which does not require specialized scientific attention, and has an operating cost conducive with supplying a demanding market with a high class product commensurate with the premium that could be charged for better quality. In many instances vacuum processes are able to reduce production cost by the reduction of scrap returns and the use of charge materials which by normal standards could be considered inferior. Obviously the first decision to be made in considering a vacuum process is the value that the particular process can offer on a competitive market, the answer being obtained either by experimentation or by careful study of existing techniques.

It is important to bear in mind that it is not always essential to completely replace existing equipment when installing a vacuum process, and in many cases great economy can be made by integrating the design to make full use of facilities already available.

2. Vacuum pumping equipment

Having decided upon the type of process to be carried out, one of the prime factors affecting both the initial and running cost of the process, is the choice of the vacuum equipment employed, related to the operating pressure demanded. It is most important to realize that the lower the pressure demanded the higher will be the cost both for the initial equipment and its maintenance. This will not only be reflected in the vacuum pumping equipment but in the fabrication cost of the vacuum chamber, the standard of cleanliness that must be maintained and the choice of

* 1 Torr = 1 mmHg.

Vol. 10 1960

materials used for internal construction, which must be compatible with the operating pressure demanded.

It is common practice, in representing graphically the performance characteristics of a vacuum pump, to plot the speed of the pump against the pressure. Fig. 1 illustrates

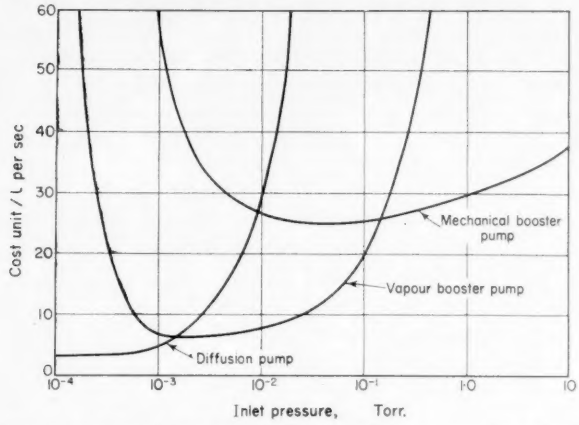

FIG. 1. Cost unit/l./sec. speed plotted against pressure for complete pumping system

the cost of a complete pumping unit in units of speed for three secondary pumps and from this it can be seen that for a given pressure of operation there is an optimum choice to be made. However, such curves can be misleading when considering processes involving large quantities of gas as a cursory perusal of the curves may give the impression that it is relatively inexpensive to operate at low pressures. Therefore, in this case, it is much more pertinent to represent performance characteristics as mass throughputs and Fig. 2 is a replot of Fig. 1 showing the cost per given mass, i.e. pressure × speed, against pressure. From this it will be clearly seen that the cost of handling large quantities of gas

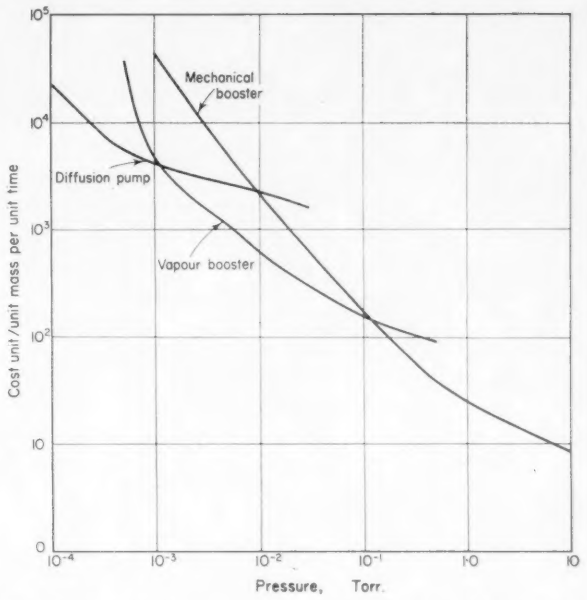

FIG. 2. Cost unit/unit mass/unit time plotted against pressure for complete pumping systems

increases greatly as the pressure decreases. It must be remembered that low pressures can often be achieved quite readily before the main gas load occurs and the pressure of operation during the process must then be decided by the equilibrium state demanded. If a process is required to terminate at a low base pressure following the removal of the majority of the gas, then it is often desirable from a cost and time consideration to design the vacuum system to be capable of handling the major gas load at higher pressures than the base pressure and finally to achieve the ultimate required.

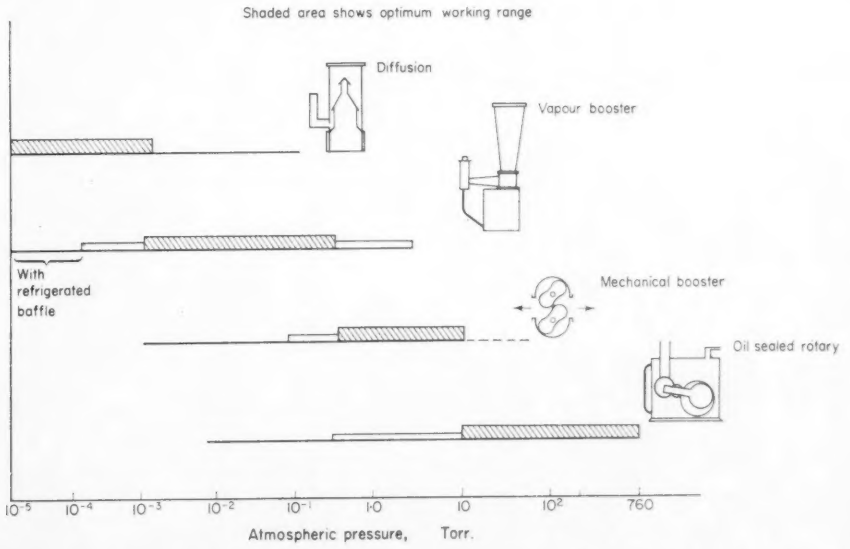

FIG. 3. Operating ranges of the oil sealed rotary, mechanical booster, vapour booster and diffusion pumps. Shaded areas show optimum operating range under gas load

If the pressure range of operation is sufficiently restricted this may be achieved by the use of a single primary or secondary pump (there always being the necessity to employ a primary pump to reduce the furnace pressure from atmosphere to the operating pressure of the secondary pump). If a wider coverage of the pressure spectrum is required then a suitable combination of pumps in either parallel or series will provide the necessary pumping characteristics.

The majority of vacuum metallurgical processes employ either singly or in combination, four main types of vacuum pump ; the rotary mechanical, mechanical booster, vapour booster and vapour diffusion pump. In addition to these pumps, the traditional steam ejection pump in a more advanced design is now being used (primarily in America) with large steel degassing plant. The operating principles of these pumps are well known and although a certain amount of over-lap occurs the four main pumps can be basically considered as complementary, the various application ranges being shown in Fig. 3.

With the exception of steam ejection systems the oil sealed rotary mechanical pump normally forms the basis of every pumping system where it acts as the primary pump to exhaust direct to atmosphere, although on occasions it is replaced by a water-ring pump working in conjunction with mechanical booster pumps (popularly known as rotary or Roots blowers). This latter application is mainly used on processes evolving large quantities of dust though care must be taken with processes of an intermittent nature due to corrosion of dust deposits in the presence of water vapour which may result in the seizure of the mechanical booster pumps.

The mechanical booster is a dry pump whose ultimate pressure is directly related by a given ratio to the pressure prevailing at its exhaust. In conjunction with a primary pump it normally comes into operation at 10 Torr by the action of a pressure switch. The fact that this type of pump employs a relatively high horse power motor makes it highly desirable to include it in the pumping circuit direct from atmospheric pressure. This is achieved in the modern type of pump by employing a limited torque fluid drive. The oil sealed rotary mechanical pump and mechanical booster are started together, the rotary pump pumping through the booster which rotates at a speed limited to the horse power of its driving motor. Thus the controls of the vacuum system are considerably simplified with the added advantage of decreasing the overall evacuation time. If the mechanical booster is to be used for pumping gases lighter than air the decrease in its air pumping speed due to back diffusion is an important point to bear in mind.

Although this type of pump is most advantageously used in the pressure region of 10^{-1} to 10 Torr, it is capable of producing an ultimate far lower than this pressure. Where conditions are such that contamination of the primary pump occurs two or more pumps in series may be required to obtain the desired ultimate, although from the cost point of view these lower pressure applications are better handled by a combination of vapour type pumps.

Vapour pumps working on the principle of the compression of diffused gases and the subsequent condensation of the working vapour consist of two main types ; the normal vapour diffusion pump and the vapour booster diffusion pump, typical speed curves of which are shown in Fig. 4. The vapour diffusion pump has an optimum operating range below 10^{-3} Torr, whereas the vapour booster diffusion pump has a high throughput above 10^{-3} Torr plus a diffusion characteristic below this pressure and is the pump normally used for vacuum melting operations. An added attraction of the vapour booster diffusion pump is its high backing pressure and ability to pump hydrogen at speeds double those with respect to air.

One basic difference of the vapour pump as compared with the mechanical booster is that its performance is not dependent upon its exhaust pressure which is only required to be maintained below the critical backing pressure. It is

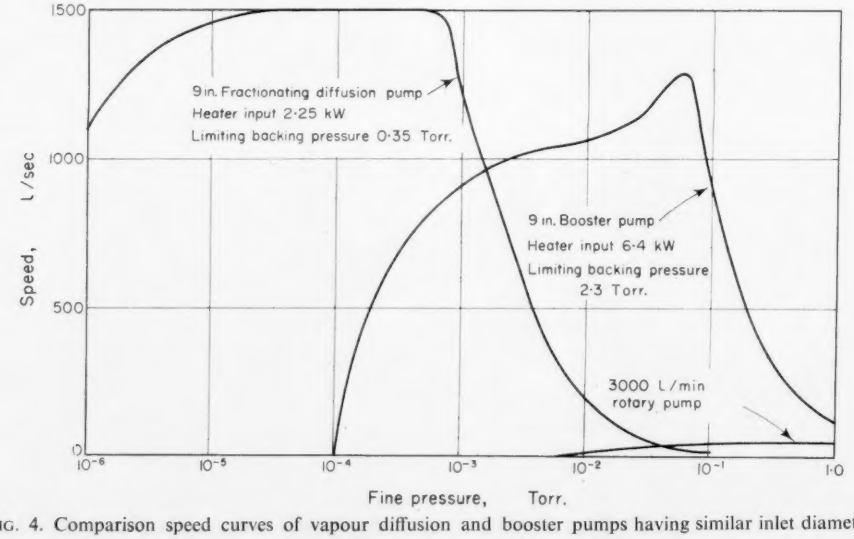

FIG. 4. Comparison speed curves of vapour diffusion and booster pumps having similar inlet diameters

important to realize that with these pumps not only the speed for air carries on below the vapour ultimate of the pump, but also the vapour ultimate of the pump can be reduced further by the use of refrigerated or liquid air traps, although for most industrial purposes these are not required.

A more detailed account of the selection of pumps for vacuum metallurgical processes is given elsewhere[2] and it is sufficient at this stage to point out the main factors governing a choice in specific instances.

3. General vacuum design

Although the vacuum pump is the basic item of the evacuation unit, to ensure optimum performance it is important to give due consideration to the control and layout of the system. In general the vacuum system is isolated from the process chamber by a main control valve which, in conjunction with subsidiary valves, is operated in a sequence which enables the vacuum system to be operated from atmosphere to the working pressure, and also to remain working in isolation whilst the process chamber is open to atmosphere for charging operations, etc. It is extremely important that connections made to the process chamber are dimensioned compatible with the pumping equipment used, and care must be taken that any screening included to suppress heat radiation, etc. does not impair the effective pumping speed in the process area. Similarly, the vacuum measuring devices must be placed to monitor, as nearly as possible, the pressures pertaining in this region.

The choice of the control system is mainly governed by

(i) the complexity of operation,

(ii) the quality of the operator, and

(iii) the maintenance facilities available.

Manual operation is the most economic in capital outlay and if confined to only one or two controls is easily handled by an unskilled operator and avoids the necessity of specialized maintenance. On the other hand, fully automatic controls can be extremely simple to operate, but can cause considerable delay in maintenance if a fault arises. Such systems can also give rise to concern if the pressure sensitive devices used to control the operations respond differently to the various gases which may be evolved, either singly or as mixtures during the process. Whenever the use of manual controls is difficult due to either complexity or inaccessibility, then a remote sequence controlled system provides the most adequate solution. This relies on the operator actuating the control at various stages of the process, but having operated that control the correct sequence of switching is predetermined in the control instrument. Such systems also have the advantage of being quickly operated in an emergency to safeguard the equipment and the process.

The basis of any good design is simplicity and if this can be integrated with robust and practical construction, many of the operator's problems are avoided. In a rapidly expanding field which is bringing to light many new factors, a degree of flexibility initially allowed for, at very little extra cost, enables modifications to be made at a future date to cater for improved techniques without the necessity of replacing major items.

In general, vacuum fabrications are constructed from either mild or stainless steel, the choice being mainly dependent upon cost and operating pressure and whether atmospheric conditions or evolved process gases are of a corrosive nature.

Any mechanical operation that must be carried out within the process chamber requires the control mechanism to be introduced into the chamber through vacuum seals. Such seals are normally made by the use of elastomer " O " rings contained in a variety of shaped grooves which permit adequate compression of the elastomer to secure an efficient seal, and ensure that the effect of atmospheric pressure differential and the weight of components is taken by metal to metal contact and not by the elastomer itself.

Elastomer " O " ring seals are normally effective up to temperatures of 100 °C and if excessive heat is radiated during the process, cooling at the seal is necessary either in the form of a water jacket or water cooling pipes. For certain higher temperature applications metal seals can be employed, but these are not so easily demountable as those of the elastomer type.

Lubrication of dynamic seals is important, there being a sufficient range of low vapour pressure oils and greases available to cater for most applications. In some instances, particularly with sliding seals, it is necessary to double seal and roughly evacuate the interspace to reduce the possibility of direct leakage from atmosphere.

4. Specific applications

The considerations which have been detailed so far apply in general to most vacuum metallurgical equipment and in order to study more specialised design considerations, it is necessary to make a detailed account of specific processes.

At the present time one of the major applications is the vacuum melting or the vacuum treatment of molten metal.

Both the large scale degassing treatment of steel and the vacuum arc melting of metals and alloys present, from a vacuum pumping point of view, the problem of handling relatively constant gas loads over defined pressure ranges. As these two processes are being separately dealt with at this symposium, it is sufficient to state that evacuation for steel degassing is usually carried out by either mechanical booster or steam ejector pumps and for arc melting by vapour booster, mechanical booster or a combination of both.

5. Induction heated vacuum furnaces

A more detailed study is now made of the design of vacuum induction melting equipment which must ensure high quality melting, refining, and consistent alloy making. The basis of the furnace is a lip axis tilted induction melting assembly robustly constructed from materials compatible with the order of vacuum employed which are stainless steel and sindanyo for the support framework and top and bottom boards respectively. The framework is broken with insulation at those points which will prevent induction loops being formed and the sindanyo, baked and impregnated with silicones, to prevent undue degassing. The induction coil

itself, fabricated from special section water-cooled copper tube, has electrical problems associated with its use in vacuum.

In the interests of electrical efficiency it is desirable to employ as high a voltage as possible. Therefore, under the conditions pertaining in a vacuum furnace which are conducive to ionisation, it is necessary to insulate the coil if voltages greater than 200 V are employed. In addition, the power supply must have a frequency which provides adequate stirring for mixing and refining.

In the case of a coil tilting within a stationary chamber, power is conveyed through a co-axial seal which, as well as preventing induced effects, can provide a means of rotation

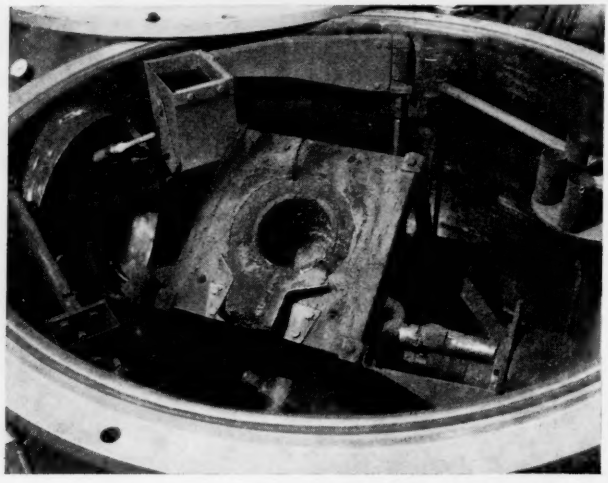

[*By courtesy of G. L. Willan Ltd., Sheffield*]

FIG. 5. Interior view of a 56 to 100 lb capacity vacuum induction melting and casting furnace

for the tilting assembly. The 56 lb (steel) capacity furnace illustrated in Fig. 5 employs this feature together with all the other mechanisms such as bulk charge and multiple alloy feeders, immersion pyrometers and bridge breaker, etc. which are required to provide full manipulation of the melt without disturbing the vacuum.

High frequency power is supplied from a 50 kW 400 V 5000 c/s alternator via water-cooled cables having the necessary flexibility to permit tilting of the induction coil assembly. Evacuation of the furnace is carried out by a vapour booster diffusion pump working in conjunction with a rotary mechanical pump to provide a high gas handling characteristic below 10^{-1} Torr and a diffusion characteristic capable of attaining a pressure below 10^{-3} Torr prior to teeming.

The point previously made that the conditions and mode of operation of the experimental furnace should be reproducible on a production scale is illustrated by Figs. 6 and 7, showing two 5 cwt capacity furnaces operating as twin units from one 200 kW 400 V, 2000 c/s motor alternator supply. All the facilities of the smaller unit are available together with a turntable for multiple ingot casting and a commensurate vacuum pumping characteristic is provided by a large size vapour booster diffusion pump.

The cost of melting in such furnaces is many times that of air melting and although melting cost is important the desirability of vacuum melting a particular alloy is related

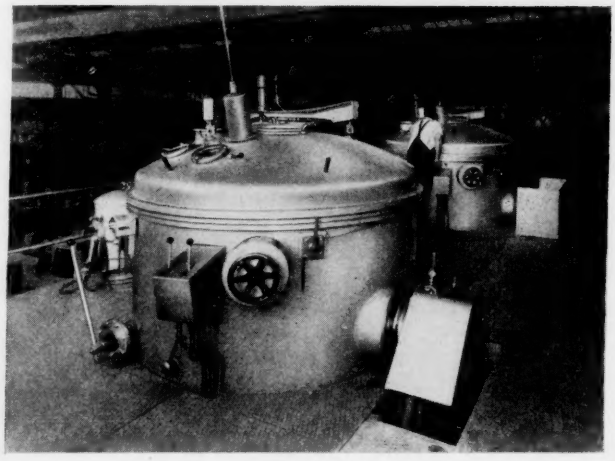

[*By courtesy of Telcon Metals Ltd., Crawley, Sussex*]

FIG. 6. Twin 5 cwt capacity vacuum induction melting and casting furnaces showing operating positions

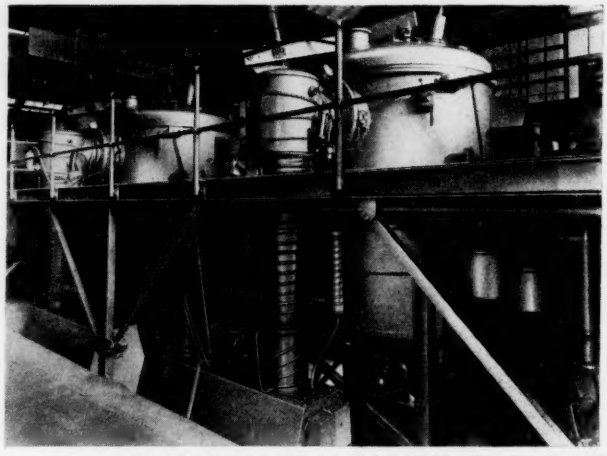

[*By courtesy of Telcon Metals Ltd., Crawley, Sussex*]

FIG. 7. View of vapour booster diffusion pump systems on 5 cwt furnaces illustrated in Fig. 6

to the overall cost involved, bearing in mind the improved quality, reduction in scrap and consistent production.

In certain cases substantial improvements in alloys can be obtained without all the intricacies of the true high vacuum induction melting furnace by using a furnace which refines a liquid charge melted in an existing atmospheric induction furnace. Fig. 8 illustrates such a furnace which has a capacity of 15 cwt and is evacuated by a combination of mechanical booster and rotary mechanical pumps. The furnace is installed on an existing induction power supply of 400 kW at 1100 V which is capable of quickly boosting the charge temperature prior to the evacuation of the furnace

Vol. 10 1960

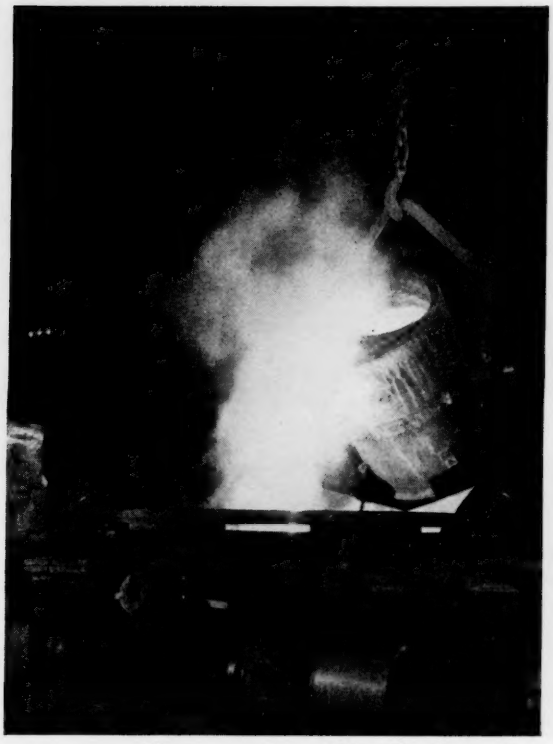

[*By courtesy of Sheepbridge Alloy Castings Ltd., Sutton-in-Ashfield*]

FIG. 8. Liquid charging a 15 cwt capacity induction degassing furnace

and of supplying the power required to hold the temperature constant under vacuum at a coil voltage of 400 V. The degassing procedure takes approximately 15 to 30 min during which time the hydrogen content is reduced by approximately 75 per cent, small quantities of oxygen and carbon are removed, and volatile impurities such as lead are eliminated from the melt. After the treatment the charge is teemed in atmosphere and cast in the conventional manner.

From an economy point of view the operating cost is only about 30 per cent greater than that already entailed in carrying out the initial atmospheric melt with the complete operation being carried out by normal foundry workers. The purpose of the furnace is not to produce super quality metal but to ensure that quality is maintained at a consistent high level even though the starting material may be 100 per cent scrap.

The design differs largely from the previous furnaces illustrated in that it employs a stationary induction melting assembly in a vertical steel chamber pivoted about the lip axis of the melting assembly and hydraulically tilted for the teeming operation, the vacuum connection being made through a rotating vacuum seal on the tilting axis. The use of the static coil enables an extremely robust assembly to be made and laminated magnetic shields prevent induction heating of the adjacent chamber. From the vacuum fabrication point of view, this type of construction enables large quantities of metal to be melted in relatively small diameter chambers compared with those required to accommodate a tilting coil and ingot moulds.

One of the main problems in vacuum induction melting is the refractory lining and as the capacity of the melt increases, the difficulty of ensuring the high strength of this lining becomes increasingly important. The stability offered by the induction degassing furnace design is more conducive to the vacuum treatment of large quantities of the metal than the tilting coil type of furnace. The employment of this principle on a large scale production furnace having all the facilities required for high vacuum melting and casting is shown in Figs. 9 and 10. This furnace consists of two vertical chambers interconnected by a circular manifold and is capable of either melting or accepting a liquid charge

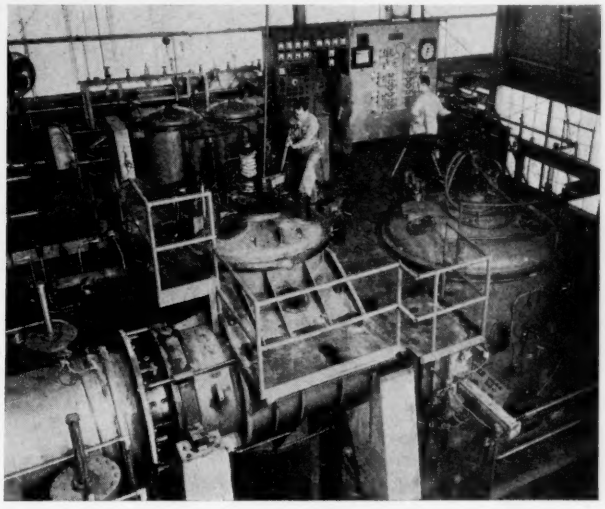

[*By courtesy of A.S.E.A., Sweden*]

FIG. 9. A.S.E.A. 5000 lb capacity twin chamber furnace installed at the Kelsey-Hayes Co., New Hartford, U.S.A., showing furnace in the melting position

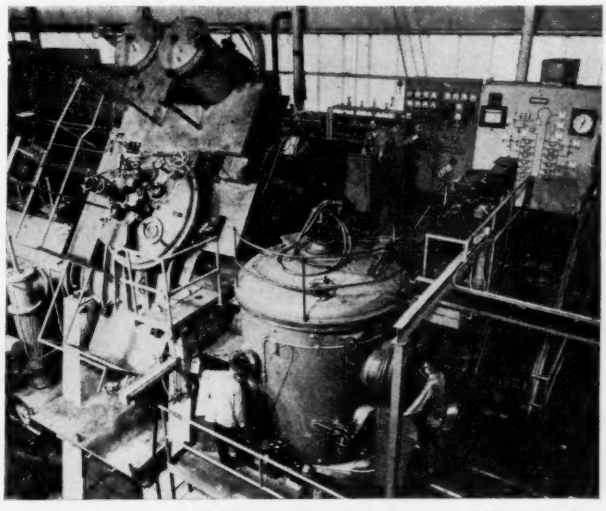

[*By courtesy of A.S.E.A., Sweden*]

FIG. 10. A.S.E.A. 5000 lb capacity furnace illustrated in Fig. 9 showing melting chamber in pouring position

of 5000 lb. Melting is carried out in a static coil mounted in a tilting chamber which is connected by two large diameter rotating vacuum seals to a high capacity vacuum pumping system and a static casting chamber capable of isolation and connected to a separate vacuum pumping system. During the pouring operation the melting chamber is tilted and the molten stream conveyed via a refractory launder to the casting chamber which contains the ingot moulds indexed to the pouring position by the operation of a turntable. Resistance heaters are positioned where required for degassing and pre-heating the ancillary refractory parts such as the launder, tun-dish and hot tops. The ingots are removed from the casting chamber by lowering the casting chamber base which mounts the mould turntable as an integral part.

The many points which must be considered in the design of such a large unit are excellently illustrated by this furnace. The vacuum pumping system combines both vapour booster diffusion pumps and mechanical booster pumps connected to serve in either a parallel or series combination, the whole being backed by conventional oil sealed rotary mechanical pumps.

The mechanical booster pumps handle the high gas loads down to a pressure of approximately 1 Torr at which stage the vapour booster pumps take over. It is in this region that it is highly desirable to overlap the performance of both types of pumps. Where vapour booster pumps having critical backing pressures of 5 to 6 Torr are employed they safeguard the system if severe gas bursts are encountered during the melting operation whereas an overlap on the mechanical boosters to pressures below 1 Torr enables a diminished pumping speed to be employed in controlling a high rate of carbon boil.

The importance of carbon reduction in vacuum is well known and it is essential that such reactions are allowed to continue without suppression if the maximum degree of refining is to be obtained. At this stage the boil which occurs must be carefully controlled by a reduction in pumping speed for if the pressure is reduced to too low a level the bubble size can grow to dimensions which result in an overflow of metal from the melting crucible.

It is important that sufficient and controllable stirring be available to ensure that no reaction becomes pressure limited on large baths of metal where pressures at the base of the melt are high due to the head of metal in the crucible. This essential feature is achieved by superimposing a controllable low frequency supply of 30 to 50 c/s on the normal high frequency. In addition, a means of ionization shielding has been developed by the makers of the furnace illustrated in Figs. 9 and 10 in order that voltages in the region of 800 V may be used and the maximum efficiency obtained from the induction power supply. The shielding itself forms an integral part of the chamber base and may be lowered clear of the furnace when in the vertical position to provide adequate access to the coil for relining and maintenance.

For some specialized work it is necessary to design large scale equipment capable of working at pressures considerably lower than those employed in normal industrial furnaces. Fig. 11 illustrates such a furnace for the melting of 200 kg of uranium. This furnace is evacuated by a combination of vapour booster (with refrigerated baffle) and fractionating diffusion pumps which together provide high pumping speeds down to working pressures of less

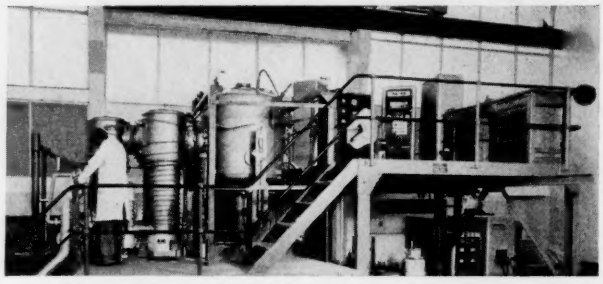

[*By courtesy of the Australian Atomic Energy Commission*]

FIG. 11. A 200 kg uranium vacuum induction and melting bottom pour furnace

than 10^{-5} Torr. Melting is carried out in a static induction coil and pouring is accomplished through the base of the crucible which is sealed during melting by a solid plug formed by the initial molten metal freezing on contact with a water cooled hemispherical copper stopper. The stopper is withdrawn immediately prior to the casting operation and pouring commences after the short time interval taken

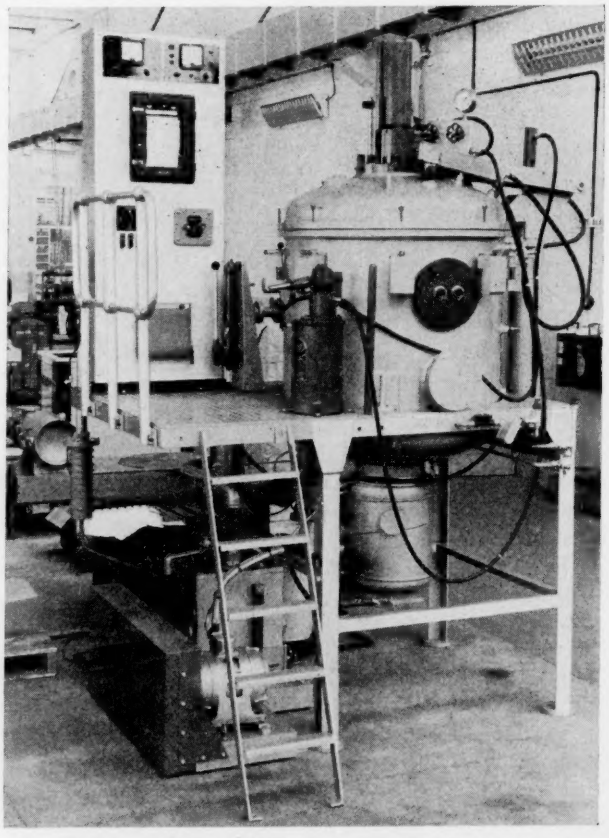

FIG. 12. A 30 ton vacuum hot pressing induction furnace

Vol.
10
1960

for the plug to melt out. With this method the stopper may be replaced immediately after pouring without any of the contact surface treatment normally required with other bottom pouring methods.

Induction heating is by no means confined to melting operations and is widely used for sintering, brazing and high temperature processes. Fig. 12 illustrates a furnace fitted with a static induction coil for heating a graphite susceptor in which metal powder is sintered under pressure. The vacuum chamber acts not only as the vacuum envelope but as a stress frame for a hydraulic ram which enters through the lid of the chamber to exert pressure to the desired value on the powder being compacted.

6. Resistance heated vacuum furnaces

There are, of course, many processes that do not employ induction heating and as an alternative electrical resistance heating, where applicable, is both practical and economical. The simplest type of resistance heated furnace employs a retort fabricated from a suitable heat resistant material to form the vacuum chamber which is heated externally by a conventional type of electric resistance furnace. With this type of furnace there is a temperature limitation imposed by the maximum operating temperature of the retort material and the effect of atmospheric pressure, although this latter limit may be alleviated by constructing the external furnace to hold a rough vacuum to reduce pressure differential.

An example of a hot retort furnace installation for the vacuum annealing of copper wire with an output of 36 tons per week is shown in Figs. 13 and 14. The retorts are vacuum sealed to bases which connect via individual valves to two common vacuum lines. Each retort assembly can accommodate a maximum load to 3500 lb and is raised to the annealing temperature of 500°C by a bell type furnace having a rating of 85 kW over three independently controlled zones.

[*By courtesy of The Electric Resistance Furnace Co., Weybridge*]

FIG. 13. General view of hot retort installation for vacuum annealing copper

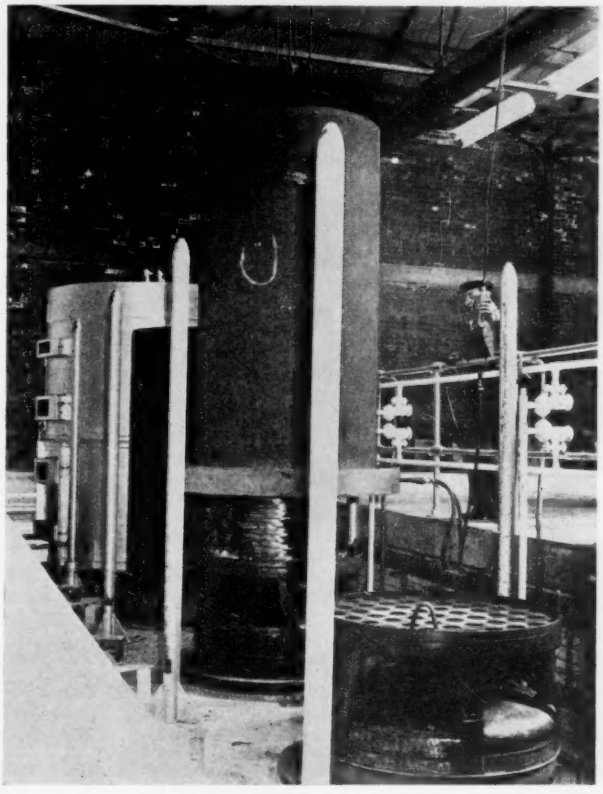

[*By courtesy of The Electric Resistance Furnace Co., Weybridge*]

FIG. 14. View of work base and raised retort of installation illustrated in Fig. 13

The application of vacuum in this case enables coils of copper wire to be bright annealed without discoloration due to drawing lubricants or sticking. There is very little gas evolved and only a single stage oil sealed rotary mechanical pump is used to maintain the pressure below 1 Torr. Two vacuum lines are employed, one to pre-evacuate the retort and the other to maintain the required vacuum during the annealing cycle.

Heat loss from the charge under vacuum is primarily by radiation and, therefore, cooling times are prolonged. An average charge takes six hours to cool from 500°C to 100°C and twelve hours from 500°C to 50°C and although cooling may be accelerated by the admission of an inert gas, it is

often better to employ more retorts per heating furnace than is conventional with controlled atmosphere plant.

Hot retort type furnaces afford an opportunity of utilizing existing furnace equipment. Fig. 15 illustrates a " packaged "

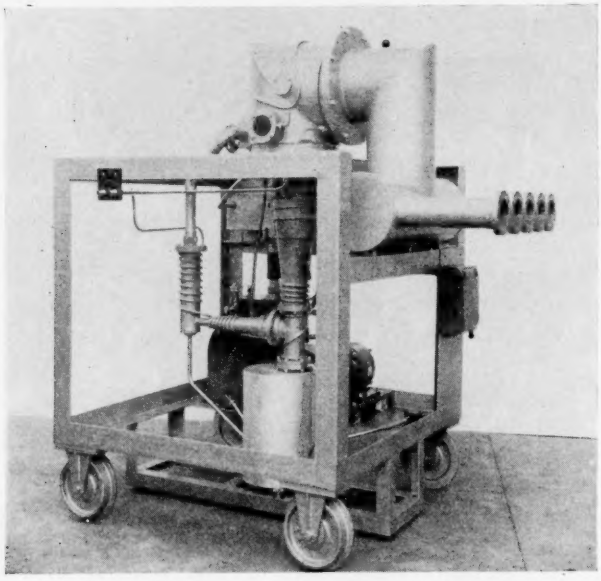

FIG. 15. Mobile vapour booster diffusion pump unit used in conjunction with an atmospheric annealing furnace for the vacuum annealing of tubes

pumping unit for the vacuum annealing of long tubes. The pumping unit terminates in a manifold on to which vacuum tight retort tubes are connected housing the tubes to be annealed. The pumping unit is mobile and the retorts are moved into an existing furnace for heating with subsequent removal when cooling is desired.

With the exception of small laboratory furnaces, the hot retort furnace is limited to an operating temperature of approximately 1100°C and if temperatures in excess of this figure are required, a " cold wall " furnace is used having the heater assembly built within the vacuum chamber.

In this type of furnace the conventional thermal insulation is undesirable from a degassing point of view and for this reason all refractories are kept to a bare minimum. Since under vacuum there is no conduction or convection by an atmosphere, the heat losses are those due mainly to radiation alone and the conventional insulation is replaced by radiation shields.

Obviously the efficiency of these shields is dictated by their surface finish and for optimum conservation of heat they are highly polished on their internal faces. It is not always easy to accurately estimate the power required to reach a given temperature as considerable deterioration of the polished surfaces can occur during the working of the furnace and although this may be rectified by periodic cleaning, it is often more economic to initially power the furnace to ensure that the desired heating characteristics are obtained even after considerable deterioration of the shields has taken place. The more efficient a radiation shield assembly is made the more protracted will be the cooling time and although this can be accelerated by gas circulation, it is often more practical to compromise by reducing the number of radiation shields and increasing the power rating.

There is, of course, no reason why this type of furnace should not be used at temperatures below 1100°C, particularly when quick heating is required, for example brazing, and full use can be made of the low thermal content of the furnace.

The choice of heater materials is most important as it is necessary to obtain a far higher wattage dissipation than that used in a conventional furnace. The most widely used heater materials for temperatures in excess of 1000°C are molybdenum, tungsten or carbon. The electrical characteristics of molybdenum and tungsten are almost identical and both have very high temperature coefficients of resistivity. This means that automatic control systems are best actuated by reference to the secondary current, thus avoiding high current surges when power is switched on to a cold heater. For small furnaces it is often convenient to use single phase heaters but for larger furnaces connection in delta form from a three phase supply is more satisfactory.

There is considerable divergence of opinion as to the correct choice between a metal or carbon heater. Although molybdenum and tungsten heaters have high temperature coefficients, they are capable of a greater degree of flexibility in design and can be used on power supplies having a relatively low ratio of current to voltage compared with that required for a carbon heater. However, the temperature limit of a metal heater is normally set by the supporting refractory insulators, whereas the mechanical strength of carbon at temperature enables self-supporting assemblies to be made. At temperatures in excess of 2000°C, carbon vapour may be an embarrassment and it is difficult to apply any general rules for optimum choice.

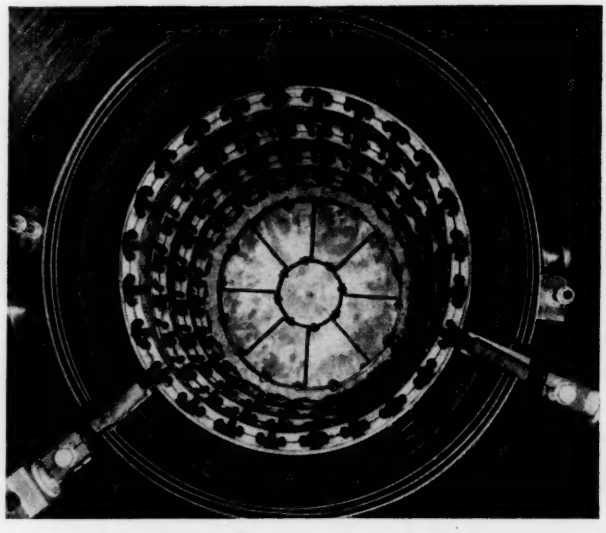

FIG. 16. Internal view of heater assembly and shields of a resistance heated radiant furnace

Vol. 10 196

In choosing a power supply for a resistance heater it is desirable to employ as high a voltage as possible, bearing in mind that it is unwise to exceed 100 V between hot conductors. Fig. 16 illustrates a radiant (i.e. cold wall) furnace designed for operating at temperatures up to 1400°C over a work space 15 in. diameter by 22 in. high. A molybdenum heater is employed being made up of multi-strands of twisted wire to increase the available surface area. The heater is held in position on a molybdenum framework by high grade alumina insulators which consist of two halves and are easily removed if a heater section is required to be replaced. The inner two radiation shields are of molybdenum, followed by a Nimonic 75 shield the remainder being stainless steel. The work support platform is fabricated from molybdenum and its legs pass completely through the bottom radiation shield stack so that the weight of the charge is taken directly to the base of the assembly container which does not reach an elevated temperature.

It is important to note that when using mixtures of materials in these types of furnace great care must be taken to avoid contact of pairs of materials which could form a eutectic alloy. For this reason, the work platform legs are protected by refractory tubes to avoid contact of the molybdenum with the Nimonic and stainless steel shields.

Normally, these types of furnace are designed as very clean systems and used for vacuum brazing, sintering, heat treatment, etc. where gas loads are relatively small. The furnace illustrated is evacuated by a fractionating diffusion pump in combination with an oil sealed rotary mechanical pump and is designed for operation at pressures of better than 10^{-4} Torr. The higher limit of working pressure is dictated not only by the charge but by the effect of bad atmospheres and the efficiency of the heater assembly.

Despite the many attractions of resistance heating, it is advisable to use induction heating techniques in conjunction with a suitable susceptor for certain very high temperature applications or where robustness is an essential feature, even though a higher initial cost is involved.

7. Conclusion

In conclusion, it is relevant to point out that no matter what design the vacuum furnace follows and irrespective of the efficiency of the vacuum pumping system, the charge being processed is often the most efficient vacuum pump available and unless due attention is paid to the correct leak tightness of the entire system, the efforts of good design and all other points are wasted.

Acknowledgements

The authors wish to express their thanks to A.S.E.A. Ltd., Sweden and the Electric Resistance Furnace Co. Ltd., Weybridge, for permission to include technical information relevant to Figs. 9, 10, 13 and 14 respectively, and also to the Directors of Edwards High Vacuum Ltd. for permission to publish this paper.

References

[1] A very useful bibliography of vacuum metallurgy up to 1958 is included in the book " Vacuum Metallurgy ", edited by R. F. Bunshah, published 1958. Reinhold Publishing Corporation, New York. Chapman & Hall Ltd., London.

[2] A. S. D. Barrett and M. E. Harper; *Selection of Pumping Systems for Vacuum Metallurgical Processes ; J. Inst. Metals*, **87**, 227–234 (1959).

Schmelzen im Elektronenstrahlofen

G. OGIERMANN

Degussa, Wolfgang bei Hanau, Deutschland

Melting in the Electron Beam Furnace

G. OGIERMANN

Degussa, Wolfgang bei Hanau, Germany

Die Vakuumetallurgie bedient sich normalerweise zwei verschiedener Schmelzöfen, des Vakuum-Induktions—sowie des Vakuum-Lichtbogenofens. Beide Schmelzverfahren dürften hinreichend bekannt sein und brauchen nicht näher erörtert zu werden. Für weitere Betrachtungen scheint es jedoch nützlich, auf einige grundsätzliche Nachteile beider Schmelzverfahren kurz einzugehen.

Im Induktionsofen bereitet das Tiegelproblem ernsthafte Schwierigkeiten. Auch bei sorgfältigster Auswahl keramischer Stampfmassen, einwandfreier Tiegelzustellung und Durchführung des Schmelzprozesses, ist eine Verunreinigung der Schmelze durch das Tiegelmaterial kaum zu unterbinden. Für die industrielle Schmelzpraxis ist ebenfalls die begrenzte Kapazität solcher Anlagen nachteilig. Die grössten bisher gebauten Öfen dieser Art fassen ca. $2\frac{1}{2}$ t Stahl.

Der Lichtbogenofen mit Abschmelzelektrode ist eine Umschmelzanlage. Als Einsatz sind daher gepresste und gesinterte oder gegossene Elektroden erforderlich. Der Schmelzprozess kann nur durch die in einem relativ engen Bereich regelbare Abschmelzgeschwindigkeit beeinflusst werden. Die Verweilzeit des Schmelzgutes in flüssigem Zustand ist relative kurz, deshalb erreichen die im Lichtbogenofen umgeschmolzenen Werkstoffe nur selten den Reinheitsgrad der im Induktionsofen erschmolzenen.

Es ist daher verständlich, dass verschiedenlich der Versuch unternommen wurde, durch eine Kombination der beiden Verfahren die Nachteile des einen auszuschalten. Als Beispiel sei hier die Anwendung wassergekühlter Kupfertiegel im Induktionsofen genannt. Der Elektronenstrahlofen kommt einer Lösung dieses Problems sehr nahe. Nach einer kurzen Beschreibung der von der Temescal-Stauffer-Co. entwickelten* und von der Degussa gebauten Anlage, soll auf die Vorzüge dieses Schmelzverfahrens noch näher eingegangen werden.

*A. R. Smith, C. d'A. Hunt und C. W. Hanks : The Development of Large Scale Electron Bombardment Melting and its Effect on the Composition of Metals and Alloys. 3. *Plansee Seminar*, Reutte, 1959, S. 336–349.

Vacuum metallurgy normally uses two different types of melting furnaces, viz., the vacuum induction furnace and the vacuum arc furnace. Both melting processes ought to be sufficiently known and therefore need not be discussed in detail. For further considerations, however, it seems to be useful to point out in short some of their principal disadvantages.

In the induction furnace, the crucible provides considerable difficulties. It is hardly possible to prevent contamination of the melt by the crucible material, even when the ceramic tamping material is most carefully selected, the crucible is delivered in perfect condition and the melting process is performed properly. The limited capacity of such units is another disadvantage for industrial melting practice. The biggest furnaces of this type built so far hold about $2\frac{1}{2}$ metric tons of steel.

The arc furnace with consumable electrodes is a remelting unit. Therefore, it requires prefabricated electrodes. The melting process can be influenced solely by the electrode melting rate which can be regulated only within relatively narrow limits. The processed material stays in the molten condition only for a relatively short time. Consequently, the materials remelted in the arc furnace only occasionally reach the degree of purity obtained in the induction furnace.

Therefore, it is understandable that it has been tried in various ways to eliminate the disadvantages of these processes by combining both procedures. As an example, the application of watercooled copper crucibles in the induction furnace shall be mentioned here. The electron bombardment furnace comes very close to the solution of this problem. After a short description of the furnace unit developed by Temescal-Stauffer* and built by Degussa, the advantage of the melting process will be described in more detail.

*A. R. Smith, C. d'A. Hunt and C. W. Hanks : The Development of Large Scale Electron Bombardment Melting and its Effect on the Composition of Metals and Alloys. 3. *Plansee Seminar*, Reutte, 1959, p. 336–349.

Beschreibung der Ofenanlage

Durch Erwärmung treten aus Metallen Elektronen aus, die bei entsprechenden Temperaturen technisch verwertbare Ströme ergeben. Wird diesem Elektronenfluss ein starkes positives Potential gegenübergestellt, so werden die Elektronen in Richtung auf die Anode beschleunigt. Die Anode kann das Schmelzgut sein. Längere Zeit hielt man eine solche Anordnung, die weitgehend einer normalen Diode gleicht, für Schmelzzwecke wenig geeignet. Die Erfahrung zeigte, dass die ursprünglich existierenden Schwierigkeiten durch

(1) Wahl eines leistungsfähigen Pumpsatzes und

(2) Entwicklung eines automatischen Spannungs- und Stromregelsystems sowie eines automatischen Emissionsstrombegrenzers

beseitigt werden können.

Pumpen entsprechender Leistung sind heute verfügbar. Schwieriger ist die Gestaltung des Regelsystems, das die Kompensation der während des Schmelzprozesses zwischen Anode und Kathode auftretenden Widerstandsschwankungen gewährleisten muss. Durch Entwicklung eines solchen elektronischen Regelsystems, das aus einem dem Hochspannungs-Transformator vorgeschalteten Stromkonstanthalter und einem Emissionsstrombegrenzer der Kathodenheizung besteht, wurde ein einwandfreies Schmelzen auch grosser Blöcke möglich. Ein Schema der elektrischen Regelung zeigt Bild 1. Die Regelanlage selbst ist aus Bild 2 ersichtlich.

Teilansichten einer Elektronenschmelzanlage typischer Bauart sind in Bild 3 und 4 dargestellt. Sie besteht aus

(a) dem Ofengehäuse (1) mit Schleuse und Bedienungspult (2) ;

(b) einem Pumpsatz, der sich aus zwei Diffusionspumpen (3), deren Saugleistung je 8000 l/s beträgt, einer Rootspumpe und einer rotierenden Vorpumpe zusammensetzt ;

Description of the furnace unit

When metals are heated to appropriate temperatures, they emit electrons which produce electrical currents of technical interest. If a large positive potential is produced opposite this electron flow, the electrons will be accelerated in the direction of the anode. The melt stock can be used as the anode in such an arrangement. For a long time, this arrangement—resembling largely an ordinary diode—was thought to be rather unsuitable for melting purposes. Experience has shown, however, that the originally existing difficulties can be overcome by

(1) Selecting an efficient pumpset, and

(2) Developing an automatic voltage and current control system as well as an automatic emission current limiter.

Pumps having an adequate efficiency are nowadays available. The design of the control system which must guarantee the compensation of the resistance fluctuations occurring between anode and cathode during the melting process is more difficult. By developing such an electronic control system consisting of a current stabilizer preconnected to the high voltage transformer and an emission current limiter of the cathode heating system, it was possible to melt even large ingots without failures. Fig. 1 shows a scheme of the electrical control. The control unit itself can be seen on Fig. 2.

Partial views of an electron beam melting unit of typical design are shown in Figs. 3 and 4. The unit consists of

(a) the furnace housing (1) with airlock and the operator's desk (2) ;

(b) a pumpset consisting of two diffusion pumps (3) having a pumping speed of 8000 l/s each, a Roots pump, and a rotary pump ;

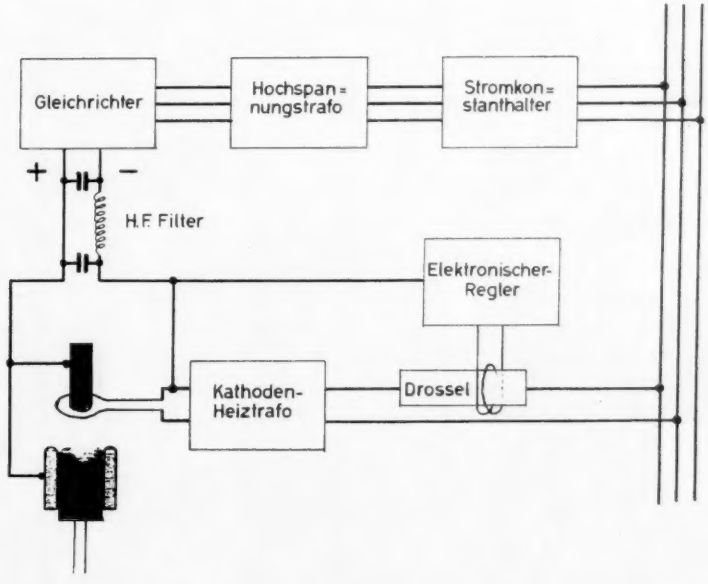

BILD 1. Blockschema der elektrischen Regelung

FIG. 1. Block diagram of the electronic control

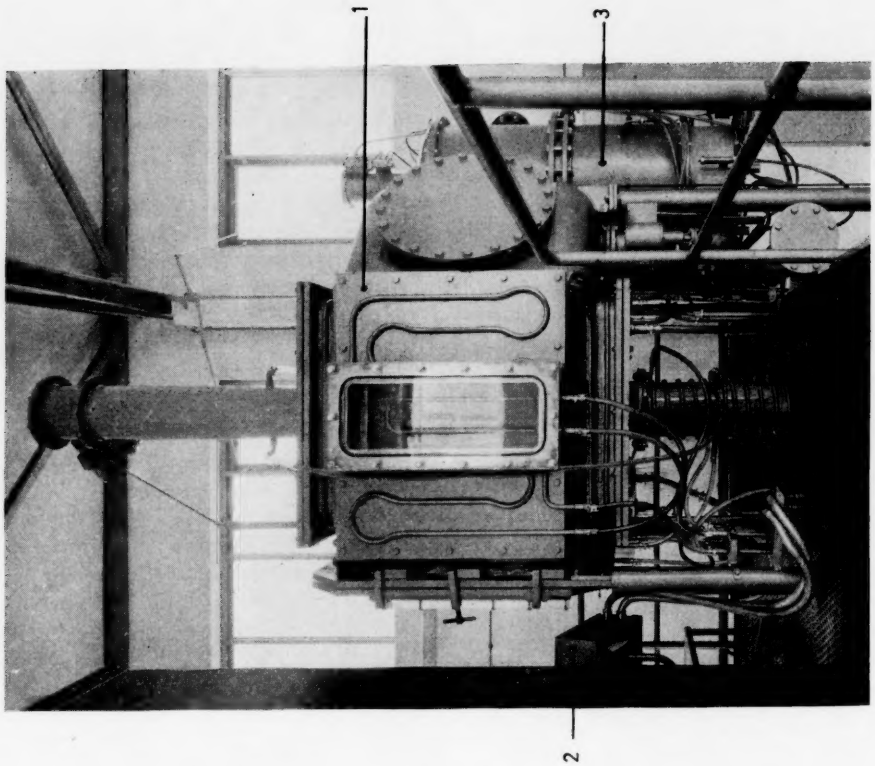

BILD 3.
Seitenansicht des Elektronenstrahlofens

FIG. 3. Lateral view of the electron beam furnace

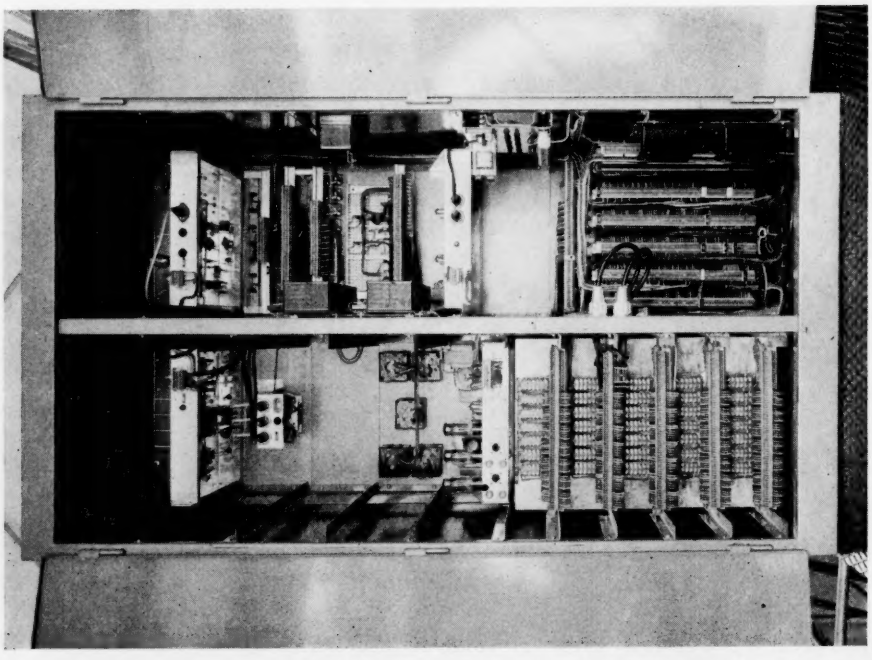

BILD 2.
Regelanlage des Elektronenstrahlofens

FIG. 2. Control unit of the electron beam furnace

Vol.
10
1960

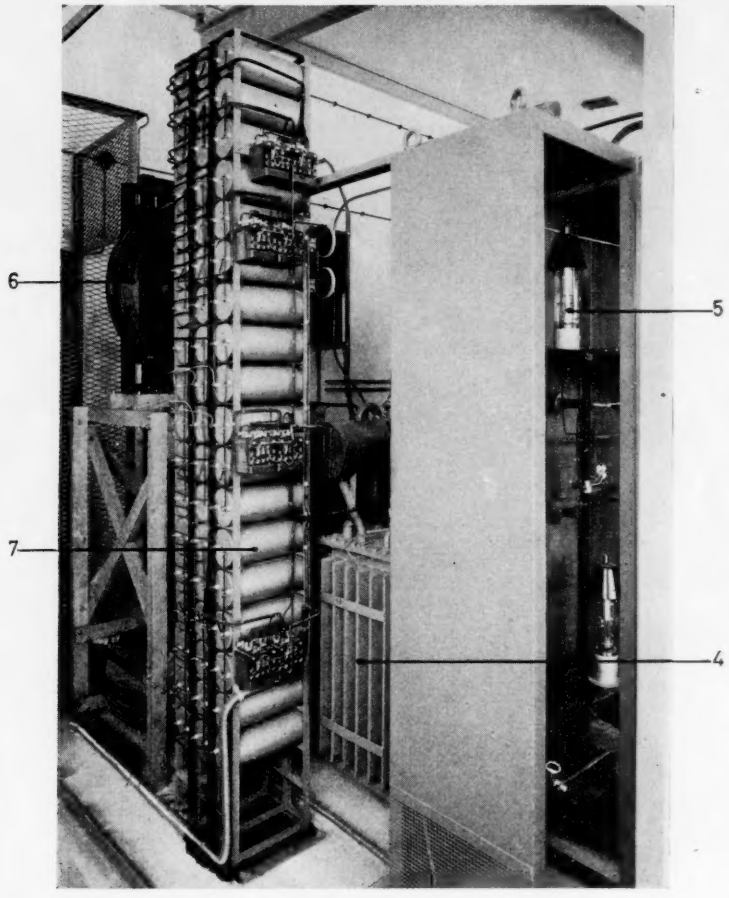

BILD 4. Stromversorgungsanlage

FIG. 4. Current supply unit

(c) der Stromversorgungsanlage mit Hochspannungstrafo (4), Gleichrichter (5), Drosseln (6) und Kondensatoren (7).

Schmelztechnik

Der Schmelzprozess kann mit zwei verschiedenen Kathodenanordnungen durchgeführt werden. Die eine Anordnung wird als Nah- oder Ringkathode, die andere als Fernkathode bezeichnet. Die Ringkathodenanordnung ist in Bild 5, die Prinzipskizzen beider Anordnungen sind in Bild 6 u. 7 gezeigt.

Bei beiden Anordnungen besteht die Kathode aus Wolframdraht (8) 1–2 mm Durchmesser, der auf etwa 2000 °C erhitzt wird. Die dabei emittierten Elektronen werden mit Hilfe einer Fokussierungseinrichtung (9) so gebündelt, dass ein Teil das Schmelzgut, ein Teil den Block trifft. Dadurch, dass das Schmelzgut (10) und der Boden der wassergekühlten Kupferkokille (11) beweglich sind, kann die für die jeweiligen Schmelzbedingungen erwünschte Verteilung des Elektronenstromes beliebig variiert werden. Während die Ringkathode vor allem für die Erschmelzung von geformten Elektroden geeignet ist, kann mit der Fernkathode auch pulverförmiges Material (12) verarbeitet werden, das mittels einer Zugabevorrichtung der Kokille zugeführt wird. Die Erfahrung hat gezeigt, dass mit Hilfe der Ringkathode und einer entsprechend angeordneten Schüttelrinne, Granulat selbst hochschmelzender Metalle einwandfrei einschmelzbar ist.

(c) the current supply unit with high voltage transformer (4), rectifier (5), chokes (6), and capacitors (7).

Melting technique

The melting process can be performed with two different cathode arrangements. The one arrangement is called the near or ring cathode and the other one the distance cathode. The ring cathode arrangement can be seen in Fig. 5, whereas Figs. 6 and 7 show schematic drawings of both arrangements.

The cathode in both arrangements consists of a tungsten filament (8) having a diameter of 1 to 2 mm, which is heated to approx. 2000 °C. The electrons emitted thereby are focused by means of the focusing device (9) in such a way, that part of the electron beam impinges on the melt stock and the other part impinges on the block. Since the melt stock (10) and the bottom of the cold copper mould (11) are movable, the desired distribution of the electron current can be varied to obtain optimum melting conditions. Whereas the ring cathode is suitable mainly for the melting of prefabricated electrodes, the distance cathode can also be used to melt pellets or powder (12) which is fed to the mould by means of a special feeder. Experience has shown that granular material even of refractory metals can be properly melted with the aid of the ring cathode.

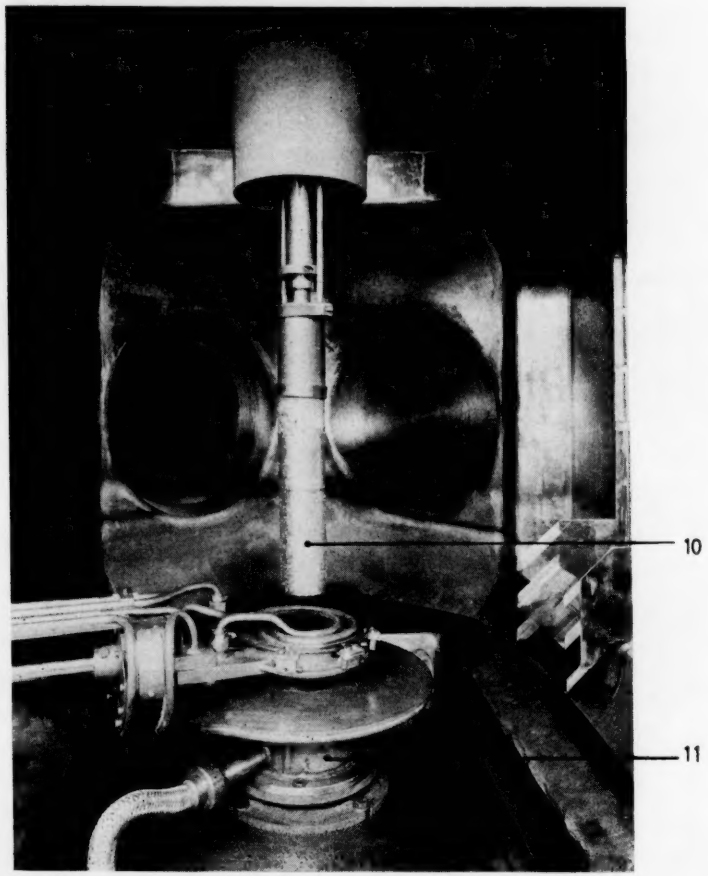

BILD 5.
Ofeninneres mit Ringkathodenanordnung

FIG. 5. Furnace inside with ring cathode arrangement

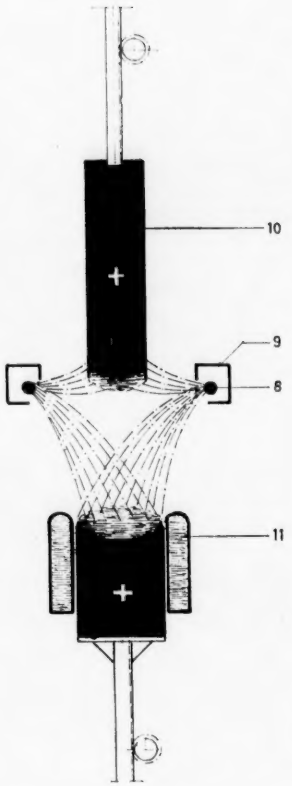

BILD 6.
Prinzipskizze der Ringkathodenanordnung

FIG. 6.
Principle scheme of the ring cathode arrangement

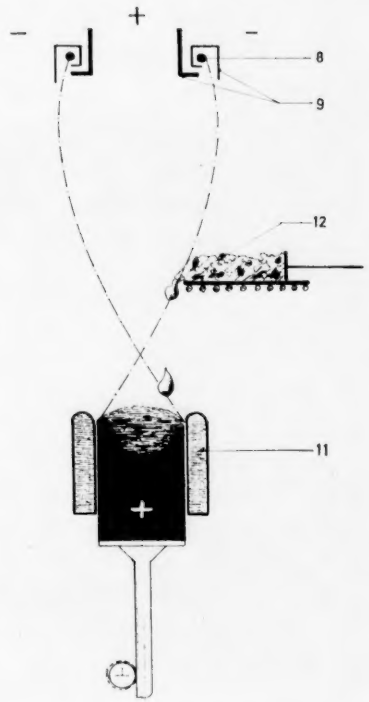

BILD 7.
Prinzipskizze der Fernkathodenanordnung

FIG. 7.
Principle scheme of the distance cathode arrangement

Vol. 10 1960

Die kurz beschriebene Anlage verfügt über eine Leistung von 60 kWh und wird demnächst ohne nennenswerte Änderungen bei gleichbleibender Hochspannung von 12 kV* auf 240 kW erweitert werden. Sie ist somit für eine Produktion z. B. hochschmelzender Metalle im halbtechnischen Massstab geeignet. Eine vorwiegend für Versuchszwecke gedachte Labor-Mehrzweckanlage, die gegenwärtig im Bau begriffen ist, zeigt mit den verschiedenen Zusatzeinrichtungen schematisch Bild 8.

The furnace unit described above has a capacity of 60 kW per hour and will be enlarged in the near future without considerable changes in design to 240 kW at an unchanged high voltage of 12 kV*. Therefore, it is suitable, e.g. for the production of refractory metals on a semi-commercial scale. Fig. 8 schematically shows a laboratory multi-purpose furnace unit with its various auxiliary items which is under construction at present and which is destined chiefly for testing purposes.

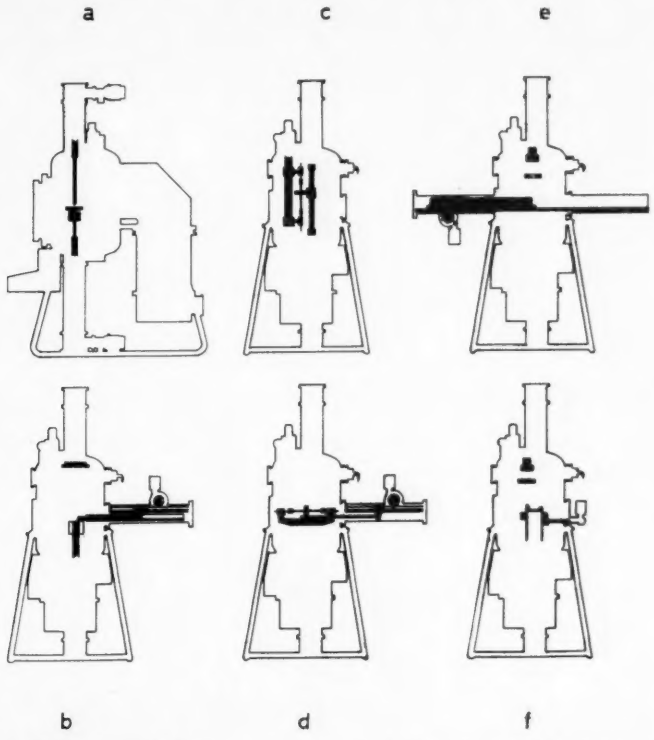

Bild 8. Schema eines Labor-Elektronenstrahlofens mit Zusatzeinrichtung :

(a) Ringkathodenanordnung
(b) Fernkathodenanordnung
(c) Vertikale Zonenschmelzeinrichtung
(d) Horizontale Zonenschmelzeinrichtung
(e) Längsschweisseinrichtung
(f) Rundschweiss—bzw. Knopfeinschmelzeinrichtung

Fig. 8. Scheme of a laboratory type electron beam furnace with auxiliary equipment

(a) Ring cathode arrangement
(b) Distance cathode arrangement
(c) Vertical zone melting arrangement
(d) Horizontal zone melting arrangement
(e) Longitudinal welding arrangement
(f) Circular welding and button melting arrangement

Schmelzpraxis

Im Elektronenstrahlofen sind alle metallischen Werkstoffe schmelzbar. Für Werkstoffe mit relativ hohem Dampfdruck wird man diese Anlage jedoch wegen des hohen Betriebsvakuums noch seltener anwenden, als die bereits üblichen Vakuumschmelzöfen.

Zwischen Kokillendurchmesser, Schmelztemperatur des Schmelzgutes und der erforderlichen Schmelzleistung der Anlage besteht eine ausgeprägte Beziehung, die in Bild 9 graphisch dargestellt ist. Wie daraus zu ersehen ist, kann man mit einer Leistung von 60 kW z.B. Stahlblöcke von etwa 130 mm Durchmesser, Niobblöcke von etwa 65 mm

Melting practice

In the electron bombardment furnace, all metallic materials can be melted. For materials having a relatively high vapour pressure, however, the electron beam furnace will be used less than conventional vacuum melting furnaces due to its high operational vacuum.

A distinct relationship, which is graphically shown in Fig. 9, exists between the mould diameter, the melting temperature of the melt stock, and the necessary melting capacity of the furnace unit. As this graph indicates, a capacity of 60 kW is capable of melting steel ingots of

*Bei 12 kV liegt die Strahlungsenergie unter 0,01 mr/h. Strahlungsschäden sind daher nicht zu befürchten.

*At 12 kV, the radiation energy is less than 0.01 mr/h. Radiation injuries are therefore not experienced.

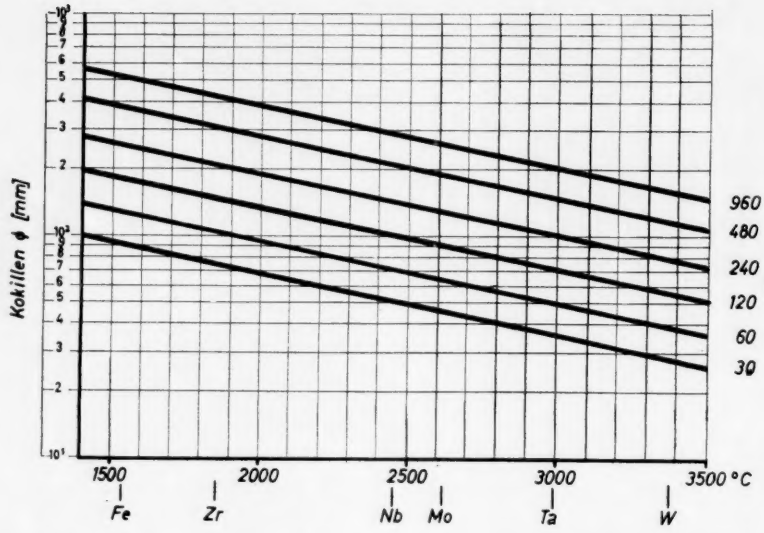

BILD 9. Abhängigkeit der Leistung von Elektronenstrahlöfen mit Ringkathodenanordnung von Schmelztemperatur und Kokillendurchmesser

FIG. 9. Capacity of electron beam furnaces with ring cathode arrangement as a function of melting temperature and mould diameter

Durchmesser bzw. Tantalblöcke von etwa 50 mm Durchmesser erschmelzen.

Die Schmelzgeschwindigkeit hat zwar einen wesentlichen Einfluss auf den Reinheitsgrad des Blockes, beeinflusst aber kaum, wie das im Vakuum-Lichtbogenofen der Fall ist, die Oberflächenbeschaffenheit des Blockes. Typische, mit unterschiedlicher Geschwindigkeit geschmolzene Stahlblöcke sind in Bild 10 angeführt.

about 130 mm diameter, niobium ingots of about 65 mm diameter, or tantalum ingots of approx. 50 mm diameter.

Although the melting rate has a considerable influence on the degree of purity of the ingot, it hardly influences its surface condition as happens in the vacuum arc furnace.

Typical ingots which have been melted at different rates are shown in Fig. 10.

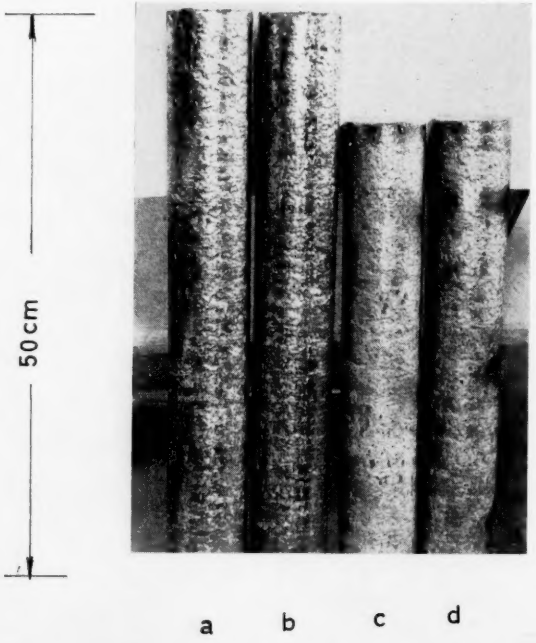

BILD 10. Oberflächenbeschaffenheit von Blöcken 75 mm Durchmesser aus rostfreiem (a und b) und Transformatorenstahl (c und d). Abschmelzgeschwindigkeit der Blöcke:

(a) 230 g/min
(c) 245 g/min
(b) 190 g/min
(d) 170 g/min

FIG. 10. Surface condition of 75 mm dia. ingots of stainless (a and b) and transformer steel (c and d) melting rate of ingots:

(b) 190 g/min
(d) 170 g/min
(a) 230 g/min
(c) 245 g/min

Die Blockbeschaffenheit wird durch die Abzugstechnik des Kokillenbodens mehr beeinflusst, als durch die Schmelzgeschwindigkeit. Trotz einer einwandfreien Bündelung des Elektronenstromes, können an der Blockoberfläche verschiedentlich bis etwa 1 mm tiefe Querrisse entstehen. Der Verlauf der Risse (Bild 11) lässt eine Zugbeanspruchung

The ingot quality is affected more by the lowering technique of the mould bottom than by the melting rate. Despite a proper focusing of the electron beam, transverse cracks up to 1 mm in depth can occur more than once on the ingot surface. The direction of the cracks (Fig. 11) suggests a tensile stress which is to be expected if the ingot head is

Vol. 10 1960

BILD 11 (*links*). Rissbildung in einem elektronenstrahlgeschmolzenen Block

FIG. 11 (*left*). Cracks in an electron beam melted ingot

BILD 12 (*rechts*). Oberflächenbeschaffenheit eines elektronenstrahlgeschmolzenen Niobblockes

FIG. 12 (*right*). Surface of an electron beam melted niobium ingot

BILD 13 (*rechts*). Aussehen von Elektrodenabschmelzköpfen bei geringem Kathodenabstand

BILD 14 (*unten*). Aussehen von Elektrodenabschmelzköpfen bei grossem Kathodenabstand

FIG. 13(*above*). Appearance of electrode melt heads at small cathode distance

FIG. 14 (*left*). Appearance of electrode melt heads at long cathode distance

vermuten, die dann zu erwarten ist, wenn der Blockkopf aus einer Stellung oberhalb des mit einem Radius versehenen Kokillenrades abgezogen wird. Eine einwandfreie Blockoberfläche kann durch Halten der Schmelze unterhalb des Kokillenrandes erreicht werden (Bild 12). Bei einigen besonders rissanfälligen Werkstoffen (18/8–Cr–Ni–Stählen, Uran, Beryllium und Zr–Nb–legierungen) hat sich eine oszillierende Bewegung des Blockes als günstig erwiesen.

Bei Abschmelzelektroden kann der Abschmelzkopf je nach dem während des Schmelzprozesses eingehaltenen Kathodenabstand konvex oder konkav ausgebildet sein (Bild 13 und 14). Bei grösserem Kathodenabstand, wie er bei gedrosselter Abschmelzgeschwindigkeit üblich ist, muss darauf geachtet werden, dass beim Aushöhlen des Abschmelzkopfes das Anschlusstück der Vorschubeinrichtung nicht angeschmolzen wird. Bei der Ringkathode wird allgemein ein vorzeitiger Ausfall des Wolfram-Heizfadens durch Bedampfung vermutet. Beim Schmelzen von Niob, das mit Wolfram eine lückenlose Mischkristallreihe bildet, müsste demnach der Heizfaden eine besonders kurze Lebensdauer aufweisen. Die an einigen hundert kg umgeschmolzenem Niob gesammelten Erfahrungen zeigten jedoch, dass der Heizfaden trotz starker Bedampfung noch einen ausreichenden Elektronenstrom gewährleistete und erst beim Reinigen des Kathodengehäuses durch mechanische Beanspruchung an einer wenig bedampften Anschlussstelle brach (Bild 15).

drawn off from a position above the rounded mould rim.

By keeping the melt below the mould rim, a proper ingot surface can be achieved (Fig. 12). For several of the materials which are particularly sensitive to cracking (stainless steels, uranium, beryllium, and Zr/Nb alloys) an oscillating motion of the ingot has proved to be successful.

The melt head of the consumable electrodes can be shaped either convex or concave depending on the cathode distance maintained during the melting process (Figs. 13 and 14).

With longer cathode distances as are usual at reduced melting rates, care must be taken that the connection between the ingot and the feeding device is not melted if the melt head becomes concave.

With the ring cathode, a premature failure of the tungsten filament is generally suspected to be due to deposits of thin metal layers.

The experience gained by remelting several hundred kilograms of niobium showed, however, that the heating filament yielded a sufficient electron current despite heavy metallization, and broke mostly by mechanical strain at a point of only slight metallization when the cathode assembly was mechanically cleaned (Fig. 15).

Vol.
10
196

BILD 15. Bedampfter Wolfram-Heizfaden

FIG. 15. Metallized tungsten heating filament

Metallurgische Gesichtspunkte des Verfahrens

Aufbau und Arbeitsweise des Elektronenstrahlofens lassen bereits erkennen, dass bei diesem Verfahren die Vorteile der beiden konventionellen Vakuum-Schmelzöfen weitgehend vereinigt sind. Man macht sich die Vorteile der wassergekühlten Kupferkokille zu Nutze und hat darüberhinaus die Möglichkeit, das Schmelzgut bliebig lange in flüssigem Zustand zu halten, was bei der gleichzeitig möglichen hohen Überhitzung und sehr niedrigem Druck überaus günstige Bedingungen für die Erhöhung des Reinheitsgrades darstellt. Die Anordnung der Kathode im Schmelzraum bringt ausserdem mit sich, dass die durch Elektronenbeschuss ionisierten Moleküle, darunter auch die der Verunreinigungen, durch geeignete elektrische Felder angezogen werden. Dadurch wird eine Rückkehr solcher Ionen ins Bad unterbunden und der Reinheitsgrad der Schmelze zusätzlich erhöht.

Natürlich muss bei optimalen Reinigungsbedingungen mit erhöhten Verdampfungsverlusten gerechnet werden. Konkrete Unterlagen fehlen jedoch diesbezüglich noch. Bekannt ist lediglich, dass in Stählen der Mangangehalt um durchschnittlich 90% verringert wird. Überraschenderweise kann der Chromgehalt auch in hochchromhaltigen Stählen in den vorgeschriebenen-Analysengrenzen erhalten bleiben.

Bei reinen Metallen, insbesondere den hochschmelzenden ist der Umschmelzeffekt wesentlich stärker ausgeprägt, als bei Legierungen, bei denen man bei der Wahl der Schmelzbedingungen verständlicherweise auf Verdampfungsverluste einiger Komponenten Rücksicht nehmen muss. Die angelaufenen systematischen Untersuchungen lassen eine deutliche Abnahme von Verunreinigungen erkennen. Die Analyse von Spurenelementen im Bereich von einigen ppm bereitet jedoch erhebliche Schwierigkeiten. Man begnügt sich deshalb sehr oft, zumindest im praktischen Schmelzbetrieb, mit einer Beurteilung des Reinheitsgrades anhand der Härte.

Niob, mit z.B. 0,25% O_2 und 0,05% C im Ausgangszustand weist nach Einschmelzen unter Argon bzw. im Vakuum-Lichtbogenofen eine Härte von 180 HB auf. Das entsprechende Schliffbild zeigt Bild 16. Nach Einschmelzen

Metallurgical aspects of the procedure

Design and operation of the electron beam furnace already indicates that this procedure combines the advantages of the two conventional vacuum melting processes to a large degree. The main advantages of electron beam melting are the possibility to

(a) keep the melt liquid for any length of time ;

(b) superheat the melt to the desired temperature ;

(c) keep a very low pressure above the melt.

The arrangement of the cathode in the melting space, moreover, permits the molecules which are ionized by the electron bombardment—amongst them the molecules of the impurities—to be attracted by appropriate electrical fields. Thereby, such ions are prevented from returning to the liquid melt, effecting an additional purification of the melt.

Of course, increased vaporization losses must be expected at these optimum purification conditions. Substantial results on this matter are not yet available, however. So far it is only known that the manganese content of steel is reduced on the average by 90 per cent. Surprisingly, the chromium content even of high chromium alloy steels can be kept within the specified analysis limits.

With pure metals, and especially with the refractory metals, the remelting effect is much more pronounced than with alloys. With these, of course, vaporization losses of some of their components must be taken into consideration when selecting the melting conditions. The systematic studies performed at present indicate a distinct decrease of the impurities. The analysis of trace elements in the range of several ppm, however, provides considerable difficulties. Therefore, it is very often satisfactory, at least for practical purposes, to control the degree of purity by hardness measurements.

Niobium, for instance, with an initial content of 0.25 per cent O_2 and 0.05 per cent C, has a hardness of 180 BHN after melting under argon or in the vacuum arc furnace. The corresponding microstructure can be seen in Fig. 16.

BILD 16. Gefüge von im Lichtbogenofen unter Argon eingeschmolzenem Niob ; 180 HB chemisch poliert 150 : 1

FIG. 16. Micrograph of argon arc melted niobium, 180 BHN chemically polished 150 : 1

im Elektronenstrahlofen liegt die Härte desselben Ausgangsmaterials bei 90 bis 100 HB. Das ensprechende Schliffbild zeigt Bild 17. Durch nochmaliges Umschmelzen nimmt die Härte auf 35–45 HB ab, wobei die Schliffe fast keine Verunreinigungen mehr zeigen (Bild 18). Grundsätzlich ist das

After electron beam melting, the hardness of the same original material lies at 90 to 100 BHN. Its microstructure is shown in Fig. 17. A second remelting further decreases the hardness to 35–45 BHN, whereby the microstructure shows hardly any impurity at all (Fig. 18). In principle, it is not

BILD 17. Gefüge von elektronenstrahlgeschmolzenem Niob ; Erstschmelze, 96 HB chemisch poliert 150 : 1

FIG. 17. Micrograph of electron beam melted niobium first melt : 96 BHN chemically polished 150 : 1

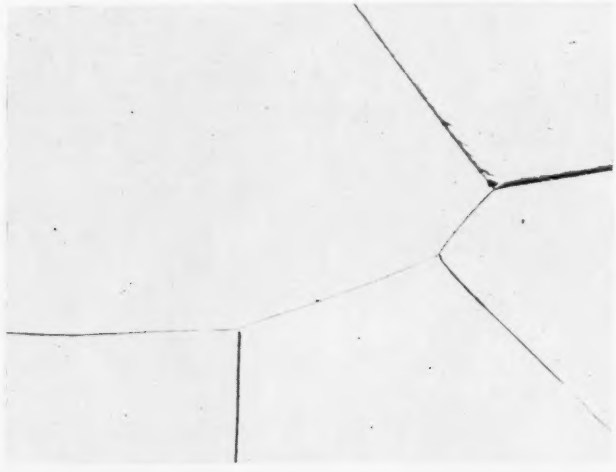

BILD 18. Gefüge von elektronenstrahlgeschmolzenem Niob ; Zweitschmelze, 38 HB chemisch poliert 150 : 1

FIG. 18. Micrograph of electron beam melted niobium second melt ; 38 BHN chemically polished 150 : 1

zweimalige Schmelzen der Blöcke nicht unbedingt erforderlich. Bei entsprechend niedriger Abschmelzgeschwindigkeit kann eine Härte von 45 HB bereits an Niob-Erstschmelzen gemessen werden. Die relative schlechte Oberflächenbeschaffenheit von aus Granulat hergestellten Erstschmelzen macht jedoch eine Umschmelzung oft notwendig.

Sämtliche Niobschliffe wurden unter gleichen Bedingungen in einer aus 50 cm^3 H_2SO_4, 20 cm^3 HNO_3 und 20 cm^3 HF bestehenden Lösung chemisch poliert. Die Lösung hat sich bereits für den Nachweis von orientierungsabhängigen Oxyd-, Nitrid- und Hydrid-Ausscheidungen in Tantal* als brauchbar erwiesen.

*R. Bakish : Some Observations of the Effect of Interaction of Tantalium with Oxygen, Nitrogen and Hydrogen. *J. Electrochem. Soc.*, **105** (1958), S. 574.

necessary in every case to melt the ingots twice. At an appropriately slow melting rate, a hardness of 45 BHN can be measured already on first melts of niobium. The relatively bad surface of first melts produced from granular melt stock, however, makes remelting frequently necessary.

All niobium metallographic specimens have been chemically polished under the same conditions in a bright deep solution of 50 ml sulphuric acid, 20 ml nitric acid, and 20 ml hydrofluoric acid.

This reagent has already proved useful for the detection of orientation-dependent gas-metal precipitations in tantalum*.

*R. Bakish : Some Observations of the Effect of Interaction of Tantalum with Oxygen, Nitrogen and Hydrogen. *J. Electrochem. Soc.*, **105** (1958), p. 574.

Vol. 10 1960

Die an anderen im Elektronenstrahlofen ein-bzw. umgeschmolzenen Metallen gemessenen Härteabnahme ist in Tab. 1 zusammengestellt.

TABELLE I

Metall	Ausgangshärte HB 10/5–60	Härte HB 10/5–60 Erstschmelzen	Zweitschmelzen
Ti	140	75	—
Zr	180	95	—
Mo	160	138	—
Ta*	—	65	45–55
W*	—	260	—
U	202	—	160

*In Pulverform angeliefert, daher Ausgangshärte nicht bekannt.

Wolfram-Erstschmelzen zeigten bei mikroskopischen Betrachtungen einen relativ hohen Reinheitsgrad (Bild 19 und 20). Trotzdem war das Metall sehr spröde. Nach Literaturangaben wurde eine zufriedenstellende Duktilität lediglich an Wolfram-Einkristallen festgestellt, die in einer Elektronenstrahl-Zonenschmelzanlage hergestellt wurden. Ob durch mehrmaliges Elektronenstrahlschmelzen die Duktilität von polykristallinem Wolfram verbessert werden kann, muss noch geprüft werden.

The hardness decrease measured on other metals, which are melted once or twice in the electron bombardment furnace, are summarized in Table I.

TABLE I

Metal	Initial hardness BHN 10/5–60	Hardness BHN 10/5–60 First melt	Second melt
Ti	140	75	—
Zr	180	95	—
Mo	160	138	—
Ta*	—	65	45—55
W*	—	260	—
U	202	—	160

*Supplied as powder, initial hardness therefore unknown.

Tungsten first melts showed a relatively high degree of purity under the microscope (Figs. 19 and 20). Nevertheless, the metal was very brittle. According to literature, a satisfactory ductility has been observed only on electron beam zone melted tungsten single crystals.

It must still be examined whether the ductility of polycrystalline tungsten can be improved by multiple electron beam melting.

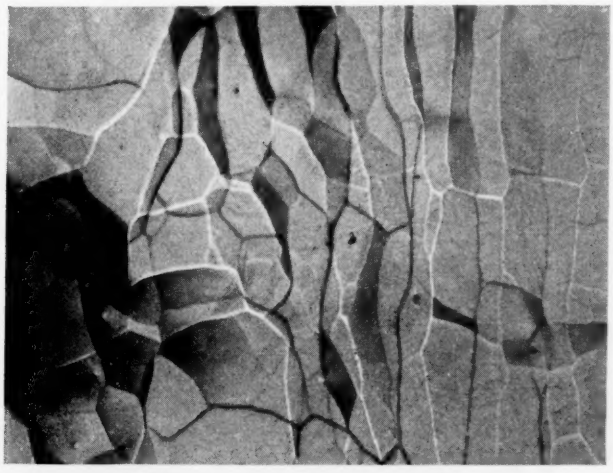

BILD 19. Bruchgefüge von elektronenstrahlgeschmolzenem Wolfram; Erstschmelze, 261 HB 200 : 1

FIG. 19. Fracture of electron beam melted tungsten first melt; 261 BHN 200 : 1

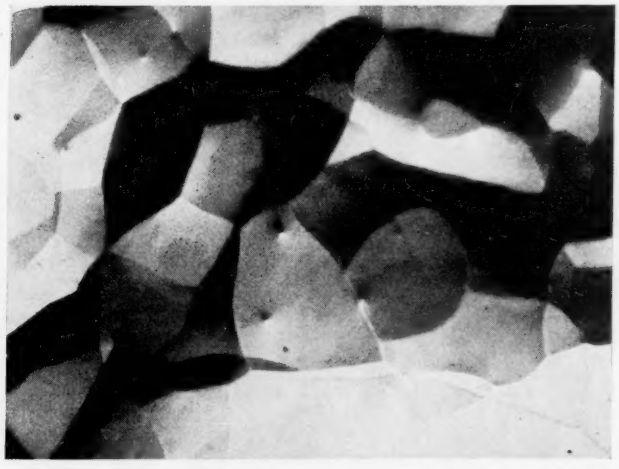

BILD 20. Bruchgefüge von elektronenstrahlgeschmolzenem Wolfram; Erstschmelze, 261 HB 300 : 1

FIG. 20. Fracture of electron beam melted tungsten first melt; 261 BHN 300 : 1

Quelques Cas d'Application pratique du Vide dans la Métallurgie des Métaux non ferreux

B. TOUGARINOFF

Société Générale Métallurgique de Hoboken, Hoboken, Belgique

Some Practical Examples of the Use of Vacuum in Non-ferrous Metallurgy

B. TOUGARINOFF

Société Générale Métallurgique de Hoboken, Hoboken, Belgium

Vol. 10 1960

Au cours de cette journée, nous avons entendu plusieurs exposés émanant des firmes spécialisées dans l'appareillage utilisé dans la métallurgie sous vide et donnant des indications très complètes sur les pompes, les fours, les moyens de chauffage, le contrôle des circuits électriques et ceux de l'eau de refroidissement, etc. Aussi, négligeant un peu la partie " instrumentale ", nous limiterons-nous à vous exposer brièvement quelques cas d'application pratique du vide dans les traitements utilisés à Hoboken en nous plaçant du point de vue " utilisateur " : pourquoi pratique-t-on le vide, qu'est-ce qu'on en attend et qu'est-ce qu'on en obtient ?

1. Dézingage du plomb sous vide

Nous commencerons par cette opération pratiquée à l'échelle de quelques 5000 t/mois.

Le plomb désargenté par le procédé Parkes contient, à la fin de cette opération, un pourcentage de zinc déterminé par la température et la teneur en argent résiduaire du plomb ; à Hoboken on trouve environ 0,5 pour cent Zn dans le plomb désargenté. La récupération au moindre coût de ce zinc est une des exigences de l'économie du procédé Parkes ; pour ce faire, on a tout avantage àfaire distiller le zinc de saturation et à le recueillir sous forme métallique directement réutilisable à la désargentation.

Sans entrer dans les détails, rappelons brièvement que la pression partielle de métaux à l'état fondu est proportionnelle à la concentration molaire du métal dans la phase liquide, corrigée par le coefficient d'activité (loi de Raoult). Dans le cas du Zn dans le Pb, la déviation de la loi de Raoult est positive, c'est-à-dire, la pression partielle du Zn est supérieure à la pression calculée ; on dit que le Zn est expulsé du Pb (le cas inverse est p. ex. celui du Zn dans le Cu ; la déviation de la loi de Raoult est négative, le Zn est retenu par le Cu sous forme de combinaisons intermétalliques).

During this day, we have heard several speakers from firms specialized in the equipment used in vacuum metallurgy who have given us many details regarding the pumps, furnaces, heating apparatus, control equipment for electrical circuits and for cooling water, etc., used in this technique. Therefore, neglecting somewhat the " instrument " side, we shall limit our talk to a brief description of a few practical cases of the use of vacuum in the technology at Hoboken, from the point of view of the user. Why is vacuum used, what advantages can be expected from its use and what results are obtained in practice ?

1. Vacuum de-zincing of lead

We shall begin with this operation carried out at a scale of about 5000 tons per month.

After de-silverizing by the Parkes process, lead contains a quantity of zinc proportional to the temperature and to the residual silver content of the lead ; at Hoboken about 0.5 per cent Zn is found in the de-silverized lead. The recovery at the least possible cost of this zinc is a primordial factor in the economics of the Parkes process. It is therefore advantageous to distil almost all of the zinc of saturation and to recover it in metal form directly reusable for further de-silverizing.

Without going into details, let us briefly recall that the partial pressure of molten metals is proportional to the molar concentration of the metal in the liquid phase, corrected by the activity coefficient (Raoult's law). In the case of Zn in Pb, the deviation of Raoult's law is positive ; it means that the partial pressure of zinc is higher than the calculated pressure and it is said that Zn is expelled from Pb (the opposite case being, e.g. that of Zn in Cu ; the deviation of Raoult's law is negative, Zn is retained in Cu under the form of inter-metallic compounds).

Nous avons fait figurer sur le tableau ci-dessous quelques données de base du procédé ; la tension de vapeur de 1,5 mmHg pour le Zn dans l'alliage 0,5 pour cent Zn dans Pb est une valeur expérimentale. La valeur théorique, —si l'on ne tient pas compte du coefficient d'écart de la loi de Raoult,— est environ 10 fois plus faible.

	Zn pur	Pb pur	0,5 % Zn dans Pb
Température d'ébullition sous 760 mmHg	907 °C	1 740 °C	—
Tension de vapeur à 600 °C	10 mmHg	négligeable	1,5 mmHg

Dans le choix des conditions opératoires, on tient compte :

(1) de la résistance des matériaux des cuves qui sont en acier et chauffées au mazout,

(2) du vide qu'on peut obtenir au moyen de pompes robustes,

(3) d'une vitesse de volatilisation admissible pour un procédé industriel.

La vitesse de distillation est fonction de la surface du métal exposé et de la concentration Zn à l'interface solide/gaz ; il est essentiel d'assurer un renouvellement continu de la surface par brassage énergique.

L'opération se fait à 600 °C et sous un vide de 5.10^{-2} mmHg.

L'appareillage adopté par Hoboken, comme satisfaisant plus particulièrement aux conditions de travail par batch de sa raffinerie de plomb, est celui mis au point par la " St. Joseph Lead Cy " aux U.S.A. Il se compose d'une cloche de dézingage et d'un groupe de pompage schématisé ci-dessous :

La cloche de dézingage en acier extra-doux est introduite dans une cuve à plomb, également en acier extra-doux,

The following table gives a few of the basic points of the process ; the vapour pressure of 1.5 mmHg for Zn in the ZnPb alloy with 0.5 per cent Zn is an experimental value. The theoretical value, if no account is taken of the coefficient of Raoult's law, is approximately 10 times smaller.

	Pure Zn	Pure Pb	0.5 % Zn in Pb
Boiling point under 760 mmHg	907 °C	1740 °C	—
Vapour pressure at 600 °C	10 mmHg	negligible	1.5 mmHg

In practice, due account has to be taken of some practical factors such as :

(1) the resistance of the kettles made of steel and heated by oil,

(2) the vacuum that can be reached with use of strongly built pumps,

(3) the speed of volatilization that can be tolerated in an industrial process.

The speed of volatilization is function of the surface of the exposed metal and of the concentration of Zn at the solid/gas interface ; it is essential to insure a continuous renewal of the surface by thorough stirring. The operation is carried out at 600 °C under a vacuum of 5×10^{-2} mmHg.

The equipment adopted by Hoboken, as best suitable to the conditions of operation of its lead refinery (batch process) is that developed by the St. Joseph Lead Company in the U.S.A. It consists in a de-zincing bell and a pumping assembly represented schematically as follows :

The mild steel de-zincing bell is lowered in a lead kettle,

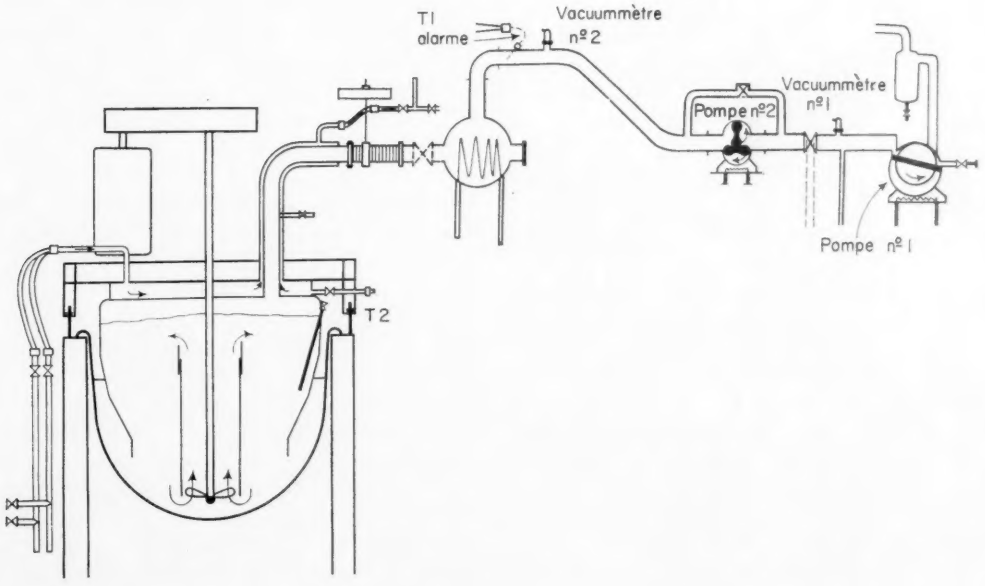

FIG. 1. Dézingage du plomb sous vide

FIG. 1. Vacuum de-zincing of lead

contenant 75 t de plomb désargenté et préalablement porté à 600 °C ; on fait le vide dans la cloche et on met en marche l'agitateur qui chasse le plomb vers le haut dans la cheminée disposée au-dessus de l'hélice et le répartit à la surface du bain. Le zinc distille de cette surface toujours renouvelée et se condense sur le caisson refroidi à l'eau qui forme le plafond de la cloche.

L'avancement de l'opération de dézingage est facilement suivi à l'examen de la cristallisation de lingotins coulés à cet effet.

Après 3 h environ d'opération à 600 °C, la teneur en zinc du plomb est tombée à $\pm$0,010 pour cent ; l'agitateur est arrêté, le vide coupé et la cloche extraite de la cuve à plomb.

Le zinc distillé, qui se présente sous la forme d'une couche irrégulière de quelques centimètres d'épaisseur, est détaché du plafond de la cloche en faisant vibrer violemment cette tôle. Dans ce but un marteau pneumatique est introduit dans le caisson par de petits puits prévus à cet effet. La couche de zinc distillé se brise facilement et est recueillie aux pieds de la cloche ; elle contient 70 à 75 pour cent de zinc, le reste étant du plomb avec un peu de cadmium apporté par le Zn. Théoriquement, le dépôt de Zn ne devrait contenir qu'un très faible pourcentage de Pb (env. 0,1 pour cent) ; pratiquement, il y a un entraînement non négligeable de Pb par primage (env. 0,15 pour cent du Pb mis au dézingage). Le Zn plombifère est réutilisé tel quel à la désargentation avec un rendement de près de 100 pour cent en zinc.

Le groupe de pompage, protégé par un réfrigérant de gaz, est composé d'une pompe Roots d'un débit de 1500 m^3/h à 5.10^{-2} mmHg et d'une pompe préliminaire à piston rotatif d'un débit de 180 m^3/h à la pression atmosphérique ; ces débits et le vide de 10^{-3} mmHg sont largement suffisants pour atteindre le résultat recherché.

2. La fusion sous vide de l'uranium

L'uranium brut ex Ca- ou Mg-thermie ne convient pas à l'utilisation dans les piles ; sa surface est irrégulière ou même malsaine et il contient trop d'impuretés volatiles et non-volatiles. On corrige ces défauts par la refusion sous vide.

L'uranium brut contient normalement 5 à 10 ppm d'H_2 présent sous forme d'inclusions d'hydrure qui est décomposé par fusion sous vide ; la teneur finale en H_2 après refusion descend à environ 1 ppm. En même temps que l'H_2, on élimine les inclusions de Ca ou Mg et d'autres impuretés volatiles.

Au cours de la refusion du métal brut, les impuretés insolubles se séparent par densité et surnagent sur le métal : c'est le cas pour les restes de scories (CaF_2 ou MgF_2), les oxydes d'uranium, le nitrure d'uranium (15 à 30 ppm N_2) et le carbure d'uranium (env. 200 ppm C). Le four de fusion sous vide utilisé à Olen pour la purification et la mise en forme de l'uranium est du type classique : une enceinte étanche contenant le creuset de fusion, disposé au-dessus des lingotières. Le vide est obtenu au moyen d'un train de pompage comprenant une pompe mécanique abaissant la pression jusqu'à environ 0,2 mmHg, puis une pompe " booster " passant de 0,2 à 0,5–1.10^{-2} mmHg.

Le creuset de fusion en graphite est chauffé par induction

also made of mild steel, containing 75 t of de-silverized lead and preheated to 600 °C. Vacuum is applied to the bell and the screw mixer is put in operation, lead being forced up the central sleeve and spread over the surface of the bath. Zinc distils from this ever renewed surface and is condensed on the watercooled jacket forming the roof of the bell.

The progress of the de-zincing operation is easily followed by inspection of the crystalline structure of small test pieces cast for the purpose.

After approximately three hours of operation at 600 °C the Zn content of the lead has been reduced to $\pm$0.01 per cent ; the mixer is stopped, vacuum is broken and the bell is raised from the kettle.

The condensed zinc which has formed an irregular layer about 1 in. thick, is detached from the roof of the bell by vibrating very strongly the steel plate. An air hammer is introduced through the waterjacket in small hollow shafts provided for the purpose. The layer of condensed zinc is easily broken and is collected at the foot of the bell. It contains about 70 to 75 per cent Zn, the remaining being lead with a little cadmium brought about by the Zn. In theory, the condensed Zn should only contain very small amounts of Pb (about 0.1 per cent) ; in practice there is a non-negligible entrainment of Pb through priming (about 0.15 per cent of the lead put through de-zincing). The lead rich zinc is reused as such for further de-silverizing with almost a 100 per cent efficiency.

The pumping assembly, protected by a gas cooler, consists of a Roots pump of 1500 m^3/hr capacity at 5×10^{-2} mmHg and of a pre-pump with rotating piston of 180 m^3/hr capacity at atmospheric pressure. These capacities and a vacuum of about 10^{-3} mmHg are quite ample for reaching the desired results.

2. Vacuum melting of uranium

Uranium as produced through calcium or magnesium-thermy is not suitable for use in atomic piles ; its surface is irregular or even unsound and it contains many volatile and non-volatile impurities. These defects are corrected by remelting under vacuum.

Raw uranium contains usually 5 to 10 ppm H_2 as hydride inclusions which are decomposed by melting under vacuum. The final content in H_2 is reduced to 1 ppm after remelting. At the same time as H_2, inclusions of Ca or Mg and other volatile impurities are removed.

During remelting of the raw metal, the insoluble impurities are separated by density and float on the metal : such is the case for remains of slags (CaF_2 or MgF_2), oxides of uranium, uranium nitride (15 to 30 ppm N_2) and uranium carbide (about 200 ppm C). At Olen, the vacuum furnace for remelting uranium and for casting in wanted shapes is of standard design and consists of an air tight enclosure containing the melting crucible placed above the moulds. Vacuum is obtained by means of a pumping assembly consisting of a mechanical pump lowering the pressure to about 0.2 mmHg, followed by a booster pump going from 0.2 to $0.5–1 \times 10^{-2}$ mmHg.

en moyenne fréquence (2500 cycles). Afin d'atténuer la réaction entre l'uranium et le graphite (carburation de l'U), l'intérieur du creuset est recouvert d'un enduit réfractaire : MgO, ZrO_2, $MgZrO_3$, Al_2O_3, etc. L'enduit est appliqué soit à l'état de suspension aqueuse, soit à l'état de pellicule frittée au moyen d'un chalumeau spécial. On dispose de deux jeux de creusets (avec leurs inducteurs) : les uns pour les charges de $\pm$50 kg U, les autres pour $\pm$200 kg U. La coulée se fait par le fond du creuset, qui reste fixe. Le trou de coulée est obturé soit par une plaquette soulevée d'en bas, soit par un tampon traversant la charge de haut en bas (ce qui nécessite le forage préalable de la billette chargée).

Pour la coulée du métal, on utilise soit une lingotière unique en graphite donnant une billette de 3 in. pesant $\pm$41 kg, soit une batterie de 6 lingotières en acier ou en graphite, donnant des barreaux de petit diamètre, environ 1 in. qui ne subissent plus de laminage ou d'extrusion, mais uniquement un léger usinage avant d'être utilisés dans les piles (après gainage).

Les lingots de l'U brut ont une tête malsaine dans laquelle s'est rassemblée, par liquation, la majeure partie des inclusions : scories, carbures, oxydes, nitrures. Cette tête est enlevée à la scie, avant la refusion. Au besoin, on perce ensuite un trou dans la charge pour livrer passage au tampon obturateur du creuset. Le lingot est ensuite dégraissé, décapé et chargé dans le creuset pourvu de son badigeon en réfractaire.

On pompe sur four froid et on démarre le chauffage ayant atteint le vide de 5.10^{-2} mmHg ; on constate immédiatement un dégazage assez bref dû au départ de l'humidité absorbée par le graphite et par l'écran en réfractaire disposé entre les inducteurs et le creuset. Le vide s'améliore rapidement pendant que la température s'élève. Lorsque la charge fond, elle bouillonne, suite au départ de l'H_2 + métaux volatils (Mg), et on note une nouvelle et brève augmentation de pression.

On porte la température à environ 200 °C au-dessus du point de fusion et la maintient environ 20 min.

Cette façon d'opérer est un compromis entre les exigences suivantes :

— d'une part, chauffage assez long à température élevée nécessaire au bon dégazage et une bonne liquation des impuretés insolubles,

— d'autre part, chauffage assez bref et peu intense limitant l'inévitable carburation de l'uranium par le graphite du creuset.

La protection du creuset par le badigeon n'est, en effet, jamais parfaite et le creuset est plus ou moins endommagé pendant " l'ébullition " de la charge (la teneur finale en carbone monte de 200 ppm dans l'U brut vers 300 à 500 ppm dans l'U refondu sous vide).

La température de coulée dépend de la nature de la lingotière et de son préchauffage ; on vise à éviter la formation de gouttes froides. Le refroidissement se fait sous vide ; on décharge 6 h environ après la fermeture du four.

3. Application du vide au tantale et au niobium

Le tantale et le niobium métal réagissent très facilement

The graphite melting crucible is heated by medium frequency (2500 cycles) induction. In order to lessen the reaction between uranium and graphite (formation of U carbides), the inside of the crucible is protected with a refractory coating : MgO, ZrO_2, $MgZrO_3$, Al_2O_3, etc. This coating is applied either as an aqueous suspension or as a sintered layer using a special blow-pipe. Two sets of crucibles are available (with their respective induction coils), one for 50 kg uranium charges, the other for about 200 kg U. The metal is poured through the bottom of the crucible which remains stationary. The tap-hole is closed with a plate raised from underneath or through a rod reaching from the top (which necessitates the drilling of the ingot to be melted).

The metal is cast either in a single graphite mould giving a 3 in. billet weighing about 41 kg, or in a set of six steel or graphite moulds, giving small diameter bars of about 1 in. dia. which do not request further rolling or extrusion, but only light turning before being used in piles (after cladding).

The raw U ingots have an unsound head into which most of the inclusions have been collected through liquation : slags, carbides, oxides and nitrides. This head is sawed off before remelting. If necessary a hole is then drilled in the ingot allowing the use of a rod to close the crucible. The ingot is further degreased, pickled and placed in the crucible protected with its refractory coating.

Pumping is started before heating which is applied when a vacuum of 5×10^{-2} mmHg is reached ; a first short degassing is then observed due to the removal of the humidity absorbed by the graphite and by the refractory screen placed between the inductors and the crucible. Vacuum rises rapidly during the increase in temperature. When the charge is melted, it boils due to the evolution of H_2 and the volatile metals (Mg) and a new and short increase in pressure is noted.

The temperature is brought to about 200 °C above the melting point and kept for about 20 min.

This procedure is a compromise between the following requirements :

— on the one side, prolonged heating at high temperature to insure good removal of gases and a good liquation of insoluble impurities,

— on the other side, limitation of the carbon pick up of the U through fairly short period of heating at reasonably low temperature.

The coating of the crucible is, indeed, never perfect and the crucible is always more or less corroded during the " boiling " of the charge (the carbon content of the U increases from 200 ppm in the raw metal to 300 to 500 ppm in the vacuum remelted metal).

The casting temperature depends on the type of mould used and of its degree of preheating. The formation of cold drops is avoided as far as possible. Cooling is effected under vacuum, it is only after 6 hr that the charge is removed.

3. Use of vacuum technology in tantalum and niobium metallurgy

Tantalum and niobium metals react very strongly with

avec les gaz hydrogène, oxygène et azote : témoin leur utilisation comme getter dans les lampes radio. Dès 20°C, ces métaux absorbent de l'hydrogène (si l'atmosphère environnante est de l'hydrogène pur). A 350°C, la réaction avec l'oxygène de l'air devient notable ; à 400°C, l'azote commence à se fixer.

Les gaz fixés par le Ta ou le Nb changent la structure et les propriétés physiques de ces métaux ; ils affectent particulièrement la dureté et la malléabilité, caractéristiques recherchées par l'utilisateur. Il s'en suit que toute opération métallurgique exigeant une température élevée doit se dérouler soit en atmosphère inerte soit sous vide élevé.

Argon, hélium et autres gaz rares peuvent être utilisés lorsque l'opération métallurgique ne vise pas un dégazage poussé du métal. Cependant, même dans ce cas on donne actuellement la préférence au vide parce que les gaz inertes sont coûteux et doivent avoir des puretés très élevées, difficilement atteintes (le Ta ou Nb sont avides de la moindre trace résiduelle de gaz réactionnel dans l'atmosphère protectrice).

Le vide utilisé généralement dans les opérations métallurgiques à haute température intéressant Ta et Nb varie de 10^{-3} à 10^{-6} mmHg.

Le groupe classique de pompage comprend en série la pompe à diffusion accolée directement à l'enceinte, la pompe Roots, la pompe à palettes ou à piston rotatif.

Dégazage pendant les opérations métallurgiques

1. *Hydrogène.* L'absorption de l'hydrogène par Ta et Nb est une réaction réversible régie par l'équation d'équilibre :

$$\log_{10} P_{\text{mm}} = -A/T_k + B$$

On désorbe l'hydrogène par pompage en augmentant le terme T_k.

L'élimination d'hydrogène devient industriellement applicable à 600°C. Elle s'intensifie à plus haute température ; en partant de poudre de Ta ou Nb, sous vide à 10^{-4} mmHg et la température à 1100°C, on descend la teneur H_2 à $<$0,005 pour cent.

2. *Oxygène–Carbone.* Dans la plupart des cas, le Ta et le Nb soumis au traitement à haute température sous vide poussé contiennent ces deux impuretés simultanément ; dès 1700°C, l'oxygène réagit avec le carbone libre ou combiné pour former CO qui se dégage.

Cette réaction est particulièrement intéressante, parce qu'elle permet d'éliminer simultanément les deux impuretés : O_2 et C.

La désoxygénation se complète à partir de 2100–2200°C par la volatilisation de l'oxygène résiduaire sous forme d'un sous-oxyde métallique qui forme une phase gazeuse stable. La teneur finale résiduaire à cette température est pour O_2 $<$0,01 pour cent, pour C environ 0,01 pour cent.

3. *Azote.* La température de 2300°C est nécessaire pour décomposer les nitrures de Ta et Nb.

La teneur finale dans Ta après traitement à 2600°C et 10^{-4} mmHg s'élève à 0,008 pour cent ; dans le Nb, à 2300°C et 10^{-4} mmHg, on descend vers 0,01 pour cent ou moins.

Opérations métallurgiques sous vide

1. *Frittage.* Pratiquement, la montée en température se

gases such as hydrogen, oxygen and nitrogen : as proof of this fact is their use as " getter " in radio tubes. From 20°C on, these metals absorb hydrogen (if placed in pure hydrogen atmosphere). At 350°C reaction with oxygen from the air becomes quite marked and at 400°C nitrogen begins to be fixed.

The gases fixed by Ta and Nb bring about a change in the structure and the physical properties of these metals ; they modify mainly the hardness and malleability, characteristics particularly desired by the users. It follows that every metallurgical operation necessitating a high temperature must be carried out under inert atmosphere or high vacuum.

Argon, helium and other rare gases may be used when the metallurgical operation does not aim at a severe degassing of the metal. However, even in these cases, preference is at present given to vacuum because inert gases are costly and must be available in very pure state. This is a difficult goal to reach (Ta or Nb absorb the smallest trace of residual reactive gas in the protective atmosphere with avidity).

The degree of vacuum mostly used in high temperature metallurgical operations concerning Ta and Nb varies between 10^{-3} and 10^{-6} mmHg.

The typical pumping assembly consists of a diffusion pump connected directly to the furnace tank, followed in series by the Roots pump, the vane pump or rotating piston pump.

Degassing during metallurgical operations

1. *Hydrogen.* The absorption of hydrogen in Ta and Nb is a reversible reaction governed by the equilibrium equation :

$$\log_{10} P_{\text{mm}} = -A/T_k + B$$

Hydrogen is desorbed through pumping by increase of the factor T_k.

The removal of H_2 is industrially applicable at 600°C. It becomes more intense at higher temperatures. Starting from Ta or Nb powder, under a vacuum of 10^{-4} mmHg and at a temperature of 1100°C, the hydrogen content decreases to less than 0.005 per cent.

2. *Oxygen–Carbon.* In the majority of applications, Ta and Nb treated under high vacuum at high temperatures, contain simultaneously these two impurities. At 1700°C, oxygen reacts with free or combined carbon to form CO which is liberated. This reaction is of particular advantage because both impurities C and O_2 are eliminated at the same time.

The de-oxidation is completed at about 2100–2200°C through volatilization of residual oxygen under the form of a metallic sub-oxide in a stable gaseous phase. The final residual content at this temperature is for O_2 less than 0.01 per cent and for C about 0.01 per cent.

3. *Nitrogen.* A temperature of 2300°C is needed in order to decompose Ta and Nb nitrides.

The final N_2 content in Ta after treatment at 2600°C and 10^{-5} mmHg reaches 0.008 per cent ; in Nb, at 2300°C and 10^{-4} mmHg N_2 is lowered to 0.01 per cent or less.

fait par paliers successifs correspondant aux trois périodes de dégazage :

(a) désorption de H_2 entre 600 et 900 °C,
(b) réaction du carbone sur l'oxygène entre 1700 et 1900 °C,
(c) volatilisation des sous-oxydes et N_2 : vers 2300 °C pour Nb et vers 2600 °C pour Ta.

Les impuretés métalliques, dont la tension de vapeur est suffisamment élevée, sont également éliminées en partie ; le fer par exemple descend de 0,04 dans le barreau non-fritté à 0,02 pour cent après frittage.

2. *Fusion.* La fusion du tantale et du niobium s'effectue actuellement surtout dans des fours à arc et à électrode consommable et dans des fours par bombardement électronique (B.E.).

Les deux se pratiquent sous vide respectivement vers 10^{-3} et 10^{-5} mmHg. On y porte très rapidement le métal à son point de fusion de sorte que les dégazages ne correspondent plus à des périodes bien définies mais se passent quasi simultanément. D'où la nécessité de disposer de capacités de pompage très grandes, plus particulièrement pour le four à B.E. où un vide de 10^{-4} mmHg est essentiel pour la stabilité de la décharge électronique. Par exemple, pour le four Degussa-Temescal de 60 kW dont nous disposons à Hoboken et dans lequel on refond du Ta à l'allure de plus de 50 kg/h, la capacité de pompage est de 16000 l/s à 10^{-4} mmHg.

La fusion par bombardement électronique sous haut vide conduit à des purifications très poussées non seulement des gaz mais également des impuretés métalliques. Celles-ci s'éliminent soit sous forme métallique soit sous forme d'oxydes suivant les tensions de vapeur.

Ainsi, lors de la fusion par B.E. du niobium, le vanadium, le fer, l'aluminium, le nickel, le chrome, le cobalt, s'évaporent rapidement sous forme métallique jusqu'à des concentrations inférieures à 0,01 pour cent (après double fusion).

Le zirconium, par contre, se volatilise sous forme de ZrO, dix fois plus volatil que NbO et cent fois plus volatil que Nb métal. Le NbO se volatilise également à raison de 10^{-8} moles/cm².s lorsque la concentration initiale en O_2 est de 0,1 pour cent. Sous cette forme, O_2 se volatilise quatre fois plus vite que par combinaison sous forme de CO (alors qu'au frittage effectué à plus basse température la réaction CO est de loin la plus rapide).

Une première fusion par B.E. réduit p. ex. O_2 dans Nb de 0,250 à 0,050 pour cent ; une seconde passe l'amène à 0,015 pour cent.

Le recuit du Ta ou du Nb n'implique pas de dégazage ; il peut se faire en atmosphère gazeuse inerte mais la préférence va au vide (10^{-3} à 10^{-4} mmHg) pour les raisons données au début ; la recristallisation s'opère vers 1300–1400 °C ; accessoirement on constate un très léger dégazage.

4. Application du vide au Si et Ge

La métallurgie des semi-conducteurs est polarisée vers l'obtention des corps extrêmement purs ; on vise à éliminer plus spécialement les " poisons " affectant les propriétés recherchées dans les dispositifs tels que les redresseurs, les diodes et les transistors. Comme impuretés principales citons le bore, le phosphore, l'arsenic, le cuivre, l'aluminium

Metallurgical operations under vacuum

1. *Sintering.* In practice the temperature is increased in successive steps corresponding to three degassing periods :

(a) desorption of H_2 between 600 and 900 °C,
(b) reaction between C and O_2 between 1700 and 1900 °C,
(c) volatilization of N_2 sub-oxides around 2300 °C for Nb and 2600 °C for Ta.

Some metallic impurities of sufficiently high vapour pressure are also partially eliminated : iron for example decreases from 0.04 per cent in the non sintered bar to 0.02 per cent after sintering.

2. *Fusion.* Fusion of Ta and Nb is at present mostly carried out in consumable electrode arc furnaces and in electron beam furnaces (E.B.).

Both operate under vacuum at 10^{-3} mmHg and 10^{-5} mmHg respectively. The metal is brought to its melting point so quickly that well definite degassing periods are not observed but occur simultaneously. It is therefore necessary to supply the furnaces with very large pumping capacities, more particularly for the E.B. furnace where a vacuum of 10^{-4} mmHg is essential to the stability of the electron discharge. For example, the pumping capacity of the Degussa–Temescal 60 kW furnace in use at Hoboken and where Ta is remelted at the rate of more than 50 kg/hr, reaches about 16,000 l/sec at 10^{-4} mmHg.

Melting through electron beam under high vacuum brings about a very high purification not only regarding gases but also of metallic impurities. These are removed either as metals or oxides depending on the vapour pressures.

Thus in niobium, after melting through E.B., metals such as vanadium, iron, aluminium, nickel, chromium and cobalt evaporate rapidly under metal form up to concentrations of less than 0.01 per cent (after double melting).

Zirconium, however, volatilises as ZrO, ten times more volatile than NbO and one hundred times more volatile than Nb metal. NbO volatilizes also at the rate of 10^{-8} moles/cm².s when the initial O_2 concentration is of 0.1 per cent. Under this form, O_2 is eliminated four times as fast as under the form of CO (during lower temperature sintering however the CO reaction is by far the quickest).

A first E.B. melting reduced, e.g. O_2 in Nb from 0.25 to 0.05 per cent ; a second operation brings it down to 0.015 per cent.

Annealing of Ta and Nb does not involve degassing, it can be done under protective inert atmosphere but vacuum of 10^{-3} to 10^{-4} mmHg is preferred for reasons given above. Recrystallization occurs around 1300 to 1400 °C ; a light degassing effect is also observed.

4. Use of vacuum for Si and Ge technology

Semi-conductor metallurgy is mostly concerned with the production of extremely pure substances. One particular object aims at the removal of the " poisons " which affect the desired properties of devices such as rectifiers, diodes and

et nombreux autres qui influencent défavorablement soit la résistivité de l'élément, soit la durée de vie des porteurs minoritaires.

Les performances industrielles dans ce domaine sont caractérisées par le fait que les qualités les plus élevées au point de vue pureté ne sont plus désignées par le nombre 9 (p. ex. cinq 9, ou six 9), ni même par le pourcentage de l'impureté, mais par le nombre d'atomes étrangers au cm^3 de matière ; p. ex., on vend un Ge avec la garantie qu'il contient moins de 10^{12} atomes de " porteurs excédentaires " par cm^3 (en pourcentage ce chiffre correspond à environ 2.10^{-9} pour cent).

La technique du vide a sa place parmi les procédés de purification conduisant à la pureté recherchée pour les semi-conducteurs.

D'une manière générale, le vide peut remplacer avantageusement les atmosphères protectrices à base d'argon, ou d'azote, ou d'hydrogène (ou d'un mélange de ces gaz). L'application du vide élimine la sujétion constante des producteurs quant à la pureté de leurs gaz au point de vue " poisons électroniques " (As, P, etc.) ; en effet, d'une part, tout train d'épuration est faillible et, d'autre part, les limites de tolérance sont extraordinairement faibles (fractions de microgramme d'impureté au m^3 de gaz). L'application du vide présente, cependant, un inconvénient dans le cas du Ge, plus spécialement : les impuretés des nacelles en graphite ou des nacelles en quartz graphitisées sont facilement diffusées dans le germanium, ce qui oblige à effectuer un prétraitement des nacelles par long chauffage sous vide avec charge de Ge sacrifié.

Une application courante du vide consiste dans le dégazage du silicium déposé ex-phase gazeuse et qui contient des occlusions des dérivés gazeux de silicium ; ce dégazage se pratique au-dessous du point de fusion du silicium et sous un vide de 10^{-2} à 10^{-3} mmHg.

Une autre application, trés importante, est l'élimination des impuretés lors de la fusion sous vide de silicium : Ga, In, As, Sb s'évaporent très rapidement, P, Al, Mn plus lentement, tandis que l'élimination de B, Fe, Cu est extrêmement faible.

L'élimination de l'As et, surtout, du P dans le silicium présente une importance pratique considérable ; le P est en effet, l'impureté—poison principale du Si obtenu par les procédés actuels de fabrication par réduction des composés volatils de Si.

L'élimination des traces ultimes de phosphore—de l'ordre de 0,1 à 10 ppm—est très difficile ; la technique habituelle de purification des semi-conducteurs au moyen de raffinage par zones est peu efficace, le coefficient de ségrégation du phosphore étant peu favorable (env. 0,4, alors que pour le Cu p. ex. il est égal à 0,004).

En principe, le bas point d'ébullition du phosphore (282 °C) devrait permettre son élimination lors de la fusion du Si à pression atmosphérique, c.-à-d. à 1450 °C environ ; cette élimination se fait effectivement, mais elle est lente. Toutes conditions égales, on accélère la volatilisation du phosphore d'un facteur 8 en opérant sous vide poussé (10^{-4} mmHg) ; il est actuellement de pratique courante d'opérer sous vide pour la purification du Si aussi bien par

transistors. As principal impurities are found : boron, phosphorus, arsenic, copper, aluminium and many other substances which affect unfavourably either the resistivity of the element or the life-time of minority carriers.

The industrial performances in this field are better characterized by the fact that the highest quality products are not given by the numbers of 9 (e.g. five 9 or six 9), nor even by the percentage of impurity but by the quantity of foreign atoms per cm^3 of product. For example, Ge is sold with the guarantee that it contains less than 10^{12} atoms of " excess carriers " per cm^3 (this corresponds to about 2×10^{-9} per cent).

Vacuum technology has its place amongst other processes of purification in the achievement of the desired purity of the semi-conductors.

In general, vacuum can replace with advantage the protective atmospheres composed of argon, nitrogen and hydrogen (or of a mixture of these gases). The use of vacuum removes one of the main worries of the producers, that of the purity of the gases from the viewpoint of " electronic poisons " such as As, P, etc. Indeed, every gas purification system can fail and on the other hand the tolerated impurities limits are excessively small (a fraction of microgramme impurity per m^3 of gas). However the use of vacuum in the metallurgy of Ge especially, gives rise to some difficulty : the impurities of the graphite or quartz boats coated with graphite are easily diffused in the Ge. It is therefore necessary to pretreat the boats through prolonged heating under vacuum with sacrified Ge charges.

A current application of vacuum consists in the degassing of silicon deposited ex gaseous phase which occludes normally gaseous compounds of silicon. This gas removal is operated at a temperature below the melting point of silicon and under a vacuum of 10^{-2}–10^{-3} mmHg.

Another very important use of vacuum is the removal of impurities during vacuum melting of silicon. Galium, indium, arsenic and antimony are quickly evaporated, phosphorus, Al and Mn more slowly whilst the removal of boron, Fe and Cu is very limited.

Removal of As and especially that of P in silicon are of considerable practical importance ; P is the principal impurity in silicon produced by the present processes through reduction of volatile compounds of Si.

The removal of final traces of P of the order of 0.1 to 10 ppm is very difficult. The usual zone refining technique is unefficient, the segregation coefficient of P being very unfavourable (about 0.4 ; when for Cu for example it reaches 0.004).

In theory, the low boiling point of P (282 °C) should permit the removal of P during melting of Si at atmospheric pressure (at 1450 °C) ; this occurs in fact but at a very slow rate.

All conditions remaining constant, the volatilization of P can be increased by a factor of 8 through operation under high vacuum (10^{-4} mmHg). It is at present usual to operate under vacuum for the purification of Si through floating zone or through molten bath. It has to be noted that the

Vol. 10 1960

" zone flottante " que par travail sur bain fondu. Il est bon de souligner que la volatilisation du Sb, dont le point d'ébullition est de 1645 °C sous pression atmosphérique (alors que celui du phosphore est de 282 °C), est plus facile que celle du phosphore. Il s'agit des déviations à la loi de Raoult, positive (avec fort coefficient) pour le Sb et négative pour P, très fortement retenu par le Si. L'étirage des monocristaux de Si sous vide poussé d'après la technique de Czochralski vous est exposé en détails dans une communication séparée ; aussi nous bornerons-nous à souligner que l'emploi du vide diminue la teneur en oxygène du cristal étiré parce qu'on volatilise l'oxygène sous forme de SiO ; en contre-partie, la distribution de l'O_2 dans le cristal est moins homogène, la périphérie en contenant moins que le centre.

Enfin une application intéressante du vide est la production des monocristaux de silicium, dopés au phosphore, de résistivité constante ; on compense la concentration du phosphore dans la phase liquide—due à la ségrégation—par l'évaporation à la surface du bain fondu. Il faut, bien entendu, régler les conditions expérimentales de très près pour réaliser l'automaticité de l'étirage.

Les cas du plomb, de l'uranium, du tantale, du niobium, du germanium et du silicium ne sont pas les seuls où nous avons recours au vide. Nous citerons encore :

— la distillation du Cd sous vide, permettant d'opérer à plus basse température (matériaux) et assurer une meilleure rectification (le primage étant moins important dans le vide, les particules entraînées chutent plus facilement) ; le Cd distille à 810 °C à la pression atmosphérique, et à 385 °C sous pression de 10^{-3} mmHg ;
— le désarséniage du cuivre qui n'est pas pratique à grande échelle à cause des difficultés technologiques encore insurmontées ;
— la purification de l'étain sous vide, à l'état expérimental ;
— le séchage sous vide de différents sels métalliques, sensibles à l'oxygène (certains sels de Co).

Cette variété des applications du vide est la meilleure preuve de sa valeur dans notre branche de métallurgie.

volatilization of Sb, whose boiling point reaches 1645 °C under atmospheric pressure (compared to 282 °C for P), is more important than that of P. This is due to the deviation of Raoult's law, positive (with high coefficient) for Sb and negative for P, very strongly retained by Si.

The crystal pulling process under vacuum following the Czochralski method is given in detail in a separate paper and we shall only mention the removal of oxygen through the use of vacuum, due to volatilization of oxygen as SiO ; however, distribution of O_2 in the crystal is less homogeneous, the periphery containing less O_2 than the centre.

Lastly, an interesting case of the use of vacuum is the production of single crystals of Si doped with P to a constant resistivity level ; the process involves a compensation between the concentration of P in the liquid phase—due to segregation —and the evaporation at the surface of the molten bath. It is of course of prime importance to control closely the conditions of the process to insure successful pulling of the crystals.

Besides lead, uranium, tantalum, niobium, germanium and silicon we have recourse to vacuum in many other cases ; we shall mention :

— Vacuum distillation of Cd, allowing to operate at lower temperature (materials) and to insure a better rectification (priming being less notable in vacuum, the entrained particles falling back more easily) ; Cd distils at 810 °C at atmospheric pressure and at 385 °C under a vacuum of 10^{-3} mmHg.
— The removal of As from copper which is not adopted on a large scale because of technological problems still unsolved.
— Purification of tin under vacuum, still in the experimental stage.
— Vacuum drying of several metal salts which are sensitive to oxygen (some Co salts).

The variety of the applications of vacuum is the best proof of its value in our field of metallurgy.

Application de la Technique du Vide à la Fabrication des Transistors

H. BUMM et O. KORN

Leybold-Hochvakuum-Anlagen, Cologne, Allemagne

1. Introduction

L'électronique moderne est étroitement liée au développement des éléments miniatures. Nous avons enregistré ces dernières années de continuels progrès dans la réduction de volume et de poids des équipements. Diodes à semi-conducteurs et transistors représentent dans ce domaine les éléments à caractéristique non linéaire, redresseuse et amplificatrice.

Le transistor—qui n'a pas encore dix années d'existence—a déjà atteint une petitesse de dimension au-dessous de laquelle les lampes ne pourront sans doute jamais descendre.

Comme résistance pouvant être pratiquement commandée sans inertie, semblablement au tube, le transistor n'exige en outre, comme pur amplificateur solide, aucune puissance de chauffage. La tension de diffusion ou tension thermale assure le déplacement des porteurs de charge dans le corps cristallin.

Il existe ainsi une certaine analogie entre la température du filament d'une lampe et la température cristalline d'un transistor. L'agencement de champs d'accélération dans l'espace de base par l'introduction d'atomes étrangers dans le réseau cristallin, suivant un programme de partage, a déjà rendu les propriétés de haute fréquence de ces éléments amplificateurs semblables aux tubes électroniques, et cela bien que les transistors n'atteignent pas encore, à hautes fréquences, la puissance de sortie des tubes électroniques.

Les difficultés inhérentes à la mise au point d'un transistor commercial ne sont pas soupçonnées par la plupart des utilisateurs. Il faut ici satisfaire à des conditions de pureté de la matière première comme jamais il n'en a été exigé dans aucune technique.

On exige en outre une structure avec une orientation de réseau exacte à quelques minutes près—ceci afin de sauvegarder les propriétés physiques qui en dépendent.

L'influence des éléments à l'état de traces sur les propriétés physiques des semi-conducteurs est très grande et ressort des considérations suivantes :

Un atome d'arsenic sur 100 millions d'atomes de germanium abaisse la résistivité électrique de celui-ci de 50 Ωcm à 7 Ωcm. Les méthodes d'analyse chimiques et spectrographiques habituelles ne permettent plus de déterminer les contaminations admissibles.

Jusqu'ici, on a employé dans la pratique comme semi-conducteurs des éléments du IV^{e} groupe du système périodique, en particulier le germanium et le silicium.

Des recherches sont en cours avec des éléments des III^{e} et V^{e} groupes—des liaisons A III B V—et on a déjà pu obtenir, même par traitement final de substances organiques, des propriétés semi-conductrices. On ne peut encore entrevoir où ces recherches aboutiront. Mais une chose semble déjà certaine : le germanium et le silicium conserveront leurs domaines d'application.

D'autre part les exigences quant à la pureté, aussi bien lors de la fabrication du matériau de base que lors de son utilisation technique, ne feront que croître avec les connaissances.

Après la mise au point d'appareillages appropriés de purification, à l'aide de méthodes physiques, l'emploi de la technique du vide est venu améliorer considérablement ces procédés. Ainsi, p. ex., la technique de mesa ne peut pas être réalisée sans le vide moléculaire.

2. Production de cristaux et usinage

2.1. *Purification par " fusion en zones " (méthode de Pfan)*

La méthode de purification physique, c'est-à-dire la ségrégation des impuretés lors de la solidification du bain de fusion, a été employée pour la première fois par W. G. Pfan et introduite dans la pratique, sous la dénomination de " fusion en zones ", en 1952, pour purifier du germanium.

Pfan put démontrer théoriquement et pratiquement que la plupart des impuretés s'accumulent dans le bain de fusion de la fin au cours de sa lente solidification, étant donné que sa solubilité est plus grande dans le métal liquide que dans le métal solide.

Si l'on fond maintenant par exemple non un barreau entier de germanium, mais seulement différentes zones et fait ensuite courir celles-ci lentement le long du barreau, du métal de plus en plus purifié se sépare des zones de fusion lors de la resolidification.

Les impuretés sont transportées au cours de ce processus à l'extrémité du barreau par les zones de fusion se déplaçant à sens unique.

Dans l'application pratique de ce procédé de fusion en zones, on opère, pour la purification, avec des barreaux de germanium de 40 à 50 cm de long et avec des zones de fusion de 1 à 2 cm. Pour le germanium, une vitesse de migration de zones de fusion de l'ordre de 2 à 6 cm/h le long du barreau donne des cristaux très purs, ayant une résistivité électrique de 50 Ωcm.

Pour éliminer les gaz encore solubles dans le métal (hydrogène, oxygène et azote), on exécute ce procédé de purification de préférence sous vide moléculaire (Fig. 1).

On place, pour opérer, le métal à purifier dans une nacelle en graphite, qu'on introduit ensuite dans un tube de quartz

Vol. 10 1960

horizontal. On chauffe par induction en différents points à l'aide d'un générateur à haute fréquence.

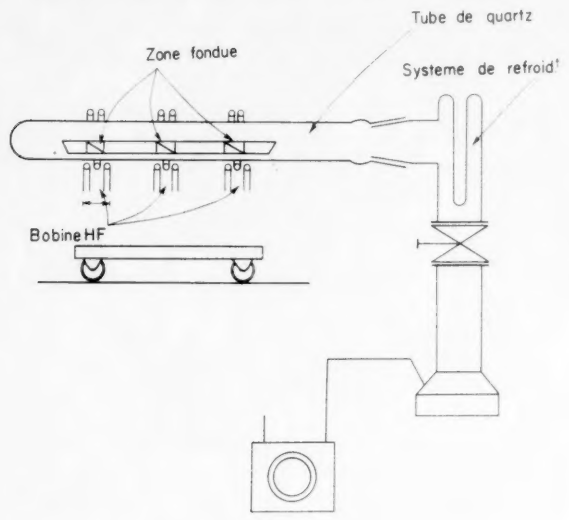

FIG. 1.

Comme la vitesse de migration d'une zone le long du barreau est relativement lente, on applique simultanément plusieurs bobines d'induction à des intervalles très rapprochés.

Le creuset renfermant le métal à purifier reste dans la plupart des cas immobile, tandis que les bobines se déplacent à une vitesse constante le long de la nacelle.

Avec une vitesse d'étirage uniforme et un barreau d'un diamètre constant, on peut maintenir la largeur des zones de fusion, en réglant le générateur, constamment à 1 cm.

De tels appareils épurateurs travaillent alors de façon pratiquement automatique. On peut fondre du germanium dans des creusets en graphite très purs et ne souillant pas le métal en fusion, et sans que ces creusets réagissent avec le germanium ni ne soient détruits par lui lors de la solidification.

Le silicium, par contre, réagit à l'état liquide avec tous les matériaux de creuset connus. Il fait en outre éclater, lors de sa solidification, le tube en quartz, par suite de son grand coefficient de dilatation.

Pour tourner ces difficultés, Keck a, en 1954, disposé le barreau de silicium à purifier en position verticale et a procédé à la fusion en zones sans creuset.

Naturellement, on ne peut opérer ainsi qu'avec une seule zone de fusion, qui doit ensuite courir, pour la purification, plusieurs fois de suite—jusqu'à 10 fois—le long du barreau de silicium.

Pour ce faire, on opère de la façon suivante :

Le barreau de silicium, qui a 40 à 50 cm de long et 10 à 15 mm de diamètre, est fixé à ses extrémités dans des supports mobiles et chauffé par induction en un point.

Par suite de la tension superficielle du silicium (720 dyn/cm), le silicium liquide est maintenu entre les deux tronçons solides du barreau de cristal.

On peut faire fondre localement un tel barreau à l'aide d'un générateur à haute fréquence, de 5 mégacycles et 10 kW, et faire courir la zone de fusion le long de celui-ci. Le barreau à traiter est sous vide afin d'éviter toute oxydation.

On obtient généralement par la fusion en zones une matière première polycristalline très pure à partir de laquelle doivent être produits des monocristaux d'une orientation déterminée, suivant la méthode de Czochralski p. ex., vu que les limites à grains agiraient, tout comme chaque écart de la périodicité idéale du réseau dans les semi-conducteurs électroniques, naturellement comme barrières perturbatrices.

2.2. Etirage de monocristaux à partir d'un creuset

Suivant le procédé de Czochralski, on tire du creuset, dans lequel se trouve la matière de départ purifiée et à l'état liquide—mais à une température tout juste au-dessus du point de fusion—un monocristal à l'aide d'un germe.

Le cristal-germe, d'une certaine orientation cristallographique, p. ex. [111], est fixé à un support, qui tourne à une vitesse uniforme en se déplaçant en même temps vers le haut.

Si l'on règle convenablement entre elles la température du creuset et la vitesse d'étirage, toute la phase liquide se cristallise progressivement sur le germe plongé dans le bain de fusion et forme un nouveau monocristal pouvant atteindre une longueur quelconque et un diamètre d'environ 40 mm.

Bien que la température de fusion ou celle de solidification doivent régner sur la surface interne de prise du monocristal croissant à l'état liquide, la paroi du creuset a, suivant la vitesse d'étirage, une température supérieure de 20 à 50 °C.

Les monocristaux de germanium ou de silicium sont généralement étirés à des vitesses allant de 1 à 5 cm/h.

Des dispositifs spéciaux de contrôle doivent maintenir constantes pendant des heures la température du creuset et la vitesse d'étirage.

On travailla tout d'abord avec des appareils remplis de gaz rares ou d'hydrogène purifiés, en vue de protéger la fusion contre toute oxydation.

Mais on a récemment démontré que, du point de vue technique, des appareils à vide moléculaire offraient de gros avantages et produisaient plus économiquement en service continu.

Il convient en outre de signaler que le nombre de défauts de structure des monocristaux (défauts de dislocations) se réduit fort dans l'étirage sous vide moléculaire.

Naturellement de tels cristaux doivent être refroidis avec d'infinies précautions après l'étirage—à l'aide p. ex. de dispositifs réchauffeurs auxiliaires.

Le réchauffement des bains de fusion peut se faire soit par induction et haute fréquence, soit dans des fours à résistances, en se servant de la fréquence du secteur.

La régulation de la température exige dans les deux cas des dispositifs électriques perfectionnés, vu qu'il est impossible d'introduire des thermo-éléments dans le bain de fusion—à cause des contaminations. Le plus simple est de régler la température du bain de fusion de telle façon que l'épaisseur du monocristal croissant, une fois atteinte, reste constante.

La firme Leybold, de Cologne, a mis au point récemment une installation technique à vide moléculaire, répondant tant aux besoins de la production industrielle qu'à ceux du laboratoire (Fig. 2).

Cette installation tient compte de toutes les conditions devant être remplies pour produire des monocristaux de

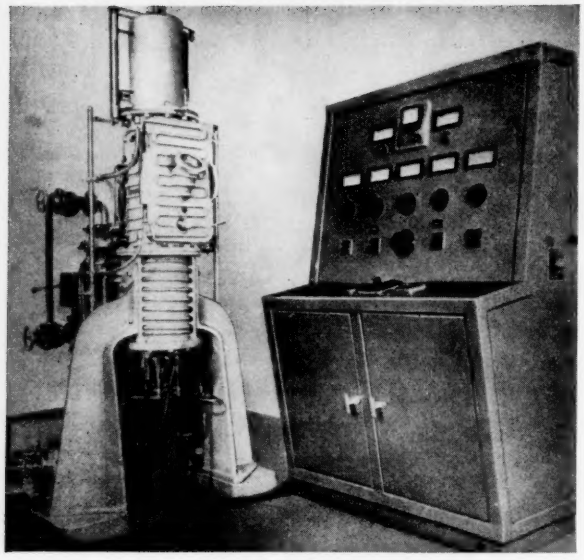

FIG. 2.

germanium ou de silicium de haute qualité. Cette réalisation est le fruit d'une étroite collaboration avec des producteurs et des utilisateurs de semi-conducteurs. Grâce à cette collaboration, on a pu perfectionner cet appareil à un tel point qu'il peut être confié à du personnel sommairement initié, donc inexpérimenté, avec la certitude d'obtenir des produits impeccables.

Le four proprement dit se compose de trois parties reliées entre elles par des brides étanches au vide moléculaire. Les deux parties inférieures sont refroidies par circulation d'eau et sont en acier laminé.

La partie la plus inférieure renferme le four proprement dit, dans lequel se trouve une spirale bifilaire en graphite chauffée par passage direct de courant à la fréquence du réseau. Cette spirale est entourée de plusieurs écrans de protection, pour obtenir une température régulière à l'intérieur du four.

Le creuset lui-même peut tourner, ce qui permet d'obtenir une répartition uniforme de la température et une bonne homogénéité du bain de fusion.

En sus du mouvement rotatif et en même temps que celui-ci, le creuset peut être déplacé vers le haut par un moteur réglable, afin que la surface de fusion reste toujours à la même hauteur dans le four pendant l'étirage, malgré la baisse du niveau de la matière dans le creuset.

On tient ainsi compte de la nécessité de maintenir constant le gradient de température entre le cristal croissant et le bain de fusion pendant toute l'opération.

La partie inférieure fendue du tube en graphite est serrée dans une douille également refroidie à l'eau pour assurer un contact électrique parfait.

Le raccordement de la pompe à diffusion, d'une vitesse d'aspiration de 500 l/s à 10^{-4} mmHg, est réalisé par une tubulure latérale de grand diamètre, renfermant un filtre antipoussières, une bride facilement démontable, un raccord d'angle et une vanne à clapet.

La partie médiane, constituée par une carcasse métallique refroidie par eau, est fermée par une grande porte étanche au vide moléculaire et pourvue en même temps d'une fenêtre d'observation. C'est par cette porte que se fait le chargement du creuset avec du silicium ou du germanium, ainsi que la mise en place du germe, qui peut être aisément fixé et centré dans son dispositif d'entraînement.

On peut suivre à travers la fenêtre vitrée le processus de fusion et l'étirage, qui peuvent être ainsi surveillés sans que l'observateur soit incommodé par la chaleur ou le rayonnement lumineux intense du métal en fusion.

La partie supérieure de l'installation renferme le dispositif mécanique d'étirage proprement dit avec son variateur de vitesse. Tout le mécanisme se trouve en dehors du vide moléculaire.

La broche tournante à laquelle est fixé le support avec le germe pénètre dans le four par une traversée spéciale. La longueur des barreaux de monocristaux étirés peut atteindre jusqu'à 20 cm.

Ce four d'étirage sous vide moléculaire permit d'obtenir des monocristaux de silicium correspondant, en ce qui concerne la résistivité électrique et la durée de vie des porteurs minoritaires, aux valeurs de silicium " hyperpur ".

Le nombre des défauts de structure relevés dans les cristaux étudiés fut très faible. Enfin la croissance des monocristaux se poursuivit jusqu'à la fin sans incident.

La fusion n'exige qu'environ 20 min, en comptant à partir du moment où l'on enclenche le four. La durée du processus d'étirage dépend de la longueur et de l'épaisseur du cristal. Ce processus est achevé dans la plupart des cas au bout de 1½ à 2 h. Le refroidissement demande à peu près autant de temps.

La fusion sous vide moléculaire et l'étirage d'épais monocristaux à l'aide d'un germe, à partir d'un creuset, ne perdront pas de leur intérêt, malgré la production par fusion en zones, employée ces derniers temps pour obtenir des monocristaux de silicium jouissant de meilleures propriétés physiques.

C'est que la production de tels cristaux par le procédé de fusion en zones exige beaucoup plus de temps, du fait qu'on ne peut faire parcourir le barreau de matière que par une zone à la fois et qu'il faut répéter l'opération 5 à 10 fois pour obtenir une pureté suffisante.

Des cristaux, hautement dotés, comme ceux utilisés pour les diodes-tunnel ne peuvent être pratiquement obtenus que par étirage à partir d'un creuset.

Il ne nous reste plus guère que de donner un aperçu du procédé de fabrication des transistors. Il convient pourtant de parler plus en détail du processus où intervient la technique du vide.

Le monocristal étiré dans l'installation que nous venons de décrire est, après qu'on a testé ses propriétés électriques (Fig. 3) (1), d'abord découpé en plaquettes avec des scies circulaires diamantées (2). Ensuite les plaquettes sont rectifiées et rodées à l'épaisseur désirée (3), pour être finalement découpées en pastilles de diverses grosseurs (4) ou, plus exactement, celles-ci sont entaillées au diamant et cassées.

L'épaisseur définitive des pastilles est obtenue par décapage (5). Cette épaisseur dépend de la durée du traitement et elle est contrôlée par des appareils automatiques

Vol. 10 196

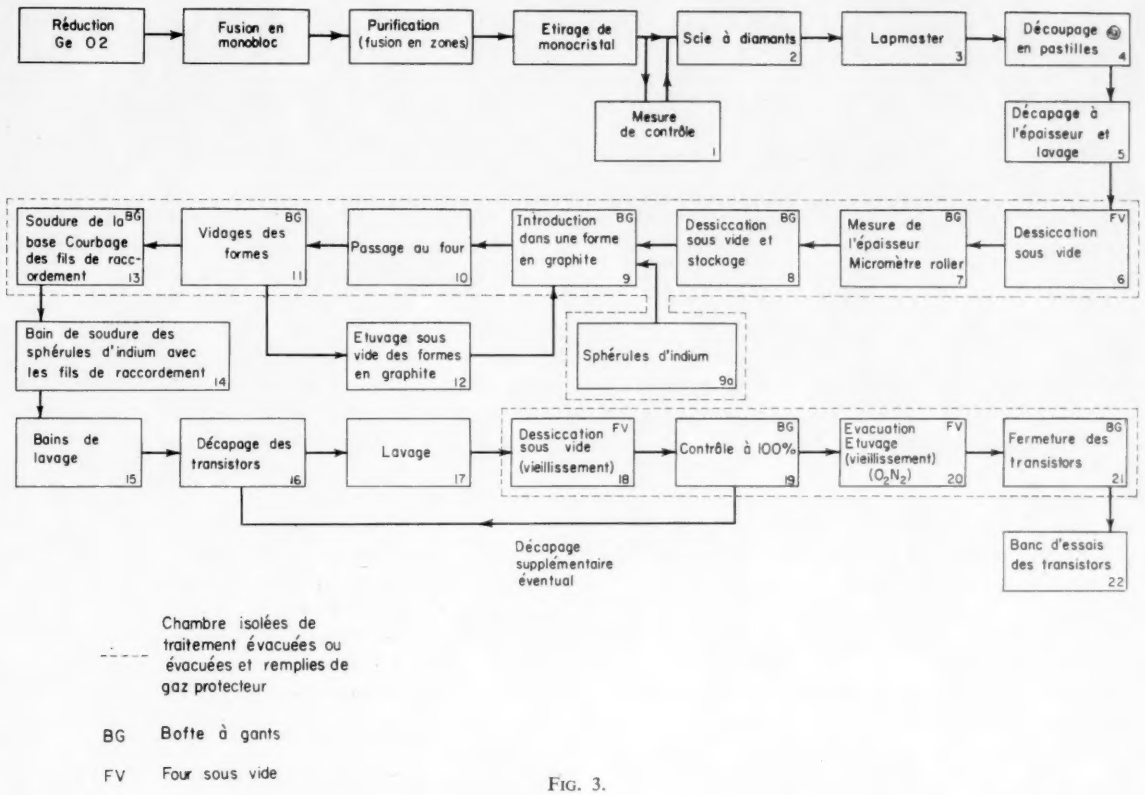
Réduction Ge O2
Fusion en monobloc
Purification (fusion en zones)
Etirage de monocristal
Scie à diamants 2
Lapmaster 3
Découpage en pastilles 4
Mesure de contrôle 1
Décapage à l'épaisseur et lavage 5
Soudure de la base Courbage des fils de raccordement 13
Vidages des formes 11
Passage au four 10
Introduction dans une forme en graphite 9
Dessiccation sous vide et stockage 8
Mesure de l'épaisseur Micromètre rolier 7
Dessiccation sous vide 6
Bain de soudure des sphérules d'indium avec les fils de raccordement 14
Etuvage sous vide des formes en graphite 12
Sphérules d'indium 9a
Bains de lavage 15
Décapage des transistors 16
Lavage 17
Dessiccation sous vide (vieillissement) 18
Contrôle à 100% 19
Evacuation Etuvage (vieillissement) (O_2N_2) 20
Fermeture des transistors 21
Décapage supplémentaire éventual
Banc d'essais des transistors 22
Chambre isolées de traitement évacuées ou évacuées et remplies de gaz protecteur
BG Boîte à gants
FV Four sous vide

FIG. 3.

équipés de micromètres Roller. Enfin, les pastilles sont triées suivant leur épaisseur et classées par groupes (7).

La dessiccation et le stockage se font de préférence dans des récipients exempts de poussières et pouvant être évacués. Ce genre de stockage doit être préféré à celui dans un liquide quelconque.

3. Technologie des transistors

3.1. Technique de l'alliage

Normalement, l'alliage des transistors se fait dans des formes en graphite (voir Fig. 3) (9), et sphérules émettrices et collectrices (dots) qui, dans les transistors Ge-pnp sont en indium ou en alliage d'indium, sont placés dans ces formes avec les pastilles de cristal et une tôle-support de connexion. Les formes passent ensuite dans une batterie de fours (10) dans lesquels les sphérules émettrices et collectrices se soudent par alliage intime avec la matière cristalline, à l'exception d'une fine couche.

Après le vidage des formes (11), les systèmes alliés sont soudés avec des machines de précision sur les supports de transistor (13), tandis que les fils de connexion sont recourbés sur les émetteurs et les collecteurs.

Les systèmes installés sur rampes sont, après avoir subi un décapage et un lavage pour les nettoyer, plongés dans un bain de soudure (14). Là, les pastilles d'indium sont soudées avec les fils de connexion.

Les bains de rinçage et de nettoyage (15) enlèvent les restes de soudure pour le bain décapant électrolytique (16), en vue de dégager les barrières critiques.

Le liquide décapant doit être complètement éliminé dans d'autres bains de lavage (17). Puis le système est soumis à une dessiccation poussée (18).

Un test à 100 pour cent décide (19), après le processus de dessiccation ou de dessiccation-vieillissement, si le transistor doit être fermé ou non.

Des systèmes se trouvant encore en dehors des caractéristiques requises peuvent être ici remis dans le circuit précédent des traitements (décapage, etc.) à travers des écluses.

Après le test à 100 pour cent, on peut répéter le vieillissement ou y procéder seulement maintenant—cela dépend du fabricant—dans des fours pouvant être évacués (20) et remplis ensuite de gaz.

Enfin, dernière phase, le système est fermé (21) en opérant dans une boîte à gants, dans laquelle règne une atmosphère contrôlée. L'étanchéité de l'enveloppe du transistor est contrôlée au banc d'essai (22) qui suit. On doit en outre procéder à des mesures électriques pour classer les transistors en types et en groupes de caractéristiques, c.-à-d. pour déterminer si les caractéristiques électriques existent bien dans les types sélectionnés.

Les mesures sont effectuées statiquement, c.-à-d. à l'aide de courant continu ou de demi-ondes de 50 cycles, et dynamiquement, c.-à-d. sous divers types de fréquence.

Après ce bref aperçu du processus de fabrication employé pour les types de transistors courants, parlons maintenant de quelques phases de ce processus pouvant être améliorées par 'a technique du vide.

Par le décapage des plaquettes de cristal à l'épaisseur désirée, la partie de la structure cristalline détruite par l'usinage mécanique est enlevée et les pastilles ont après le lavage une surface très pure, qui doit être sauvegardée pour l'usinage ultérieur.

La dessiccation sous vide et le stockage dans des récipients exempts de poussières assurent mieux cette sauvegarde que le stockage dans n'importe quel liquide ou gaz protecteur.

Le chargement des formes exige une atmosphère exempte de poussières et le plus possible inerte, étant donné que des impuretés et des oxydes superficiels perturbent les processus suivants, aussi bien sur les pastilles d'alliage que sur les plaquettes de cristal.

Des boîtes à gants pouvant être évacuées et remplies de gaz protecteur—d'azote desséché p. ex.—sont très indiquées pour procéder au chargement des formes.

Les formes ainsi chargées passent sous la même atmosphère à travers une batterie de fours, dans lesquels règne une température différente et bien déterminée.

On atteint dans une zone de soudure un mouillement à la fois le plus rapide et le plus parfait possible de la pastille d'indium sur la surface prescrite par la forme.

Dans une zone d'alliage suivante, les sphérules d'indium liquéfient localement les surfaces des plaquettes.

La température de la zone alliée doit être maintenue la plus constante possible, pour atteindre de faibles tolérances des épaisseurs séparant dans la plaquette de cristal les émetteurs et les collecteurs.

Dans la zone de refroidissement suivante, la matière cristalline dissoute dans l'indium—modifié d'ailleurs suivant " p " dans ses caractéristiques conductrices—croît de nouveau de façon monocristalline sur le cristal de départ, dans la mesure, bien entendu, où la vitesse de refroidissement le permet. Les formes quittent le four normalement à des températures inférieures à 100 °C.

Le processus d'alliage exige une atmosphère inactive ou réductrice, si les phases précédentes n'ont pu empêcher une oxydation des constituants de l'alliage. Il est nécessaire d'employer des fours à gaz protecteur avec des écluses d'azote des deux côtés des zones de chauffage, cela pour empêcher la pénétration de l'oxygène de l'air et de l'humidité dans l'espace où se fait l'alliage.

Il faut avoir du gaz protecteur d'une grande pureté. Pour des raisons d'économie, on emploie la plupart du temps de l'hydrogène absolument pur, sinon du gaz rare.

Quelques ppm d'oxygène et d'eau se font déjà sentir dans le mouillement des pastilles sur les plaquettes de cristal, de sorte que les qualités de gaz protecteur dites " pures " ou " super-purifiées " et obtenues industriellement ne suffisent pas. Il est alors nécessaire de disposer d'installations supplémentaires pour purifier les gaz—si l'on veut naturellement tenir compte des conditions à remplir pour les alliages.

Les dépenses occasionnées par l'achat d'une telle installation ainsi que son entretien—auxquelles vient s'ajouter le coût du gaz lui-même—correspondent sensiblement au prix d'un four d'alliage par passage. C'est pourquoi Leybold s'est décidé à construire un tel four sous vide. Ce four possède 8 zones réglables, et comprenant des zones de chauffage ou des zones de chauffage et de refroidissement. Son agencement permet de modifier, dans une zone allant jusqu'à 800 °C et cela dans de larges limites, les gradients thermiques des zones de soudure et de refroidissement.

Cela vaut également pour la position et la largeur de la zone de température maxima, avec une constance thermique de ± 1 °C.

Les formes entrent dans le four ou en sortent à une cadence réglée par 2 écluses sous vide. Plusieurs groupes de pompage assurent le maintien du vide de la partie chauffée et des écluses. Un vacustat veille de son côté au maintien de la pression de travail du four et signale tout dépassement de la limite supérieure.

Des thermo-éléments installés dans le four permettent de contrôler la température de chaque zone.

Après l'alliage, les transistors ne devraient plus normalement quitter, jusqu'à ce qu'ils soient scellés, une atmosphère exempte de poussières et inactive. Les impuretés ne pouvant pas être enlevées au décapage et au lavage le suivant rendent le transistor inutilisable.

Il est indispensable d'étuver sous vide les formes débarrassées de leur contenu (voir Fig. 3 (12)). Cet étuvage sous vide doit se faire sous des températures d'environ 1000 °C, afin d'éliminer les impuretés provenant des pastilles (Fig. 4). On le fait après que les formes ont servi à plusieurs alliages.

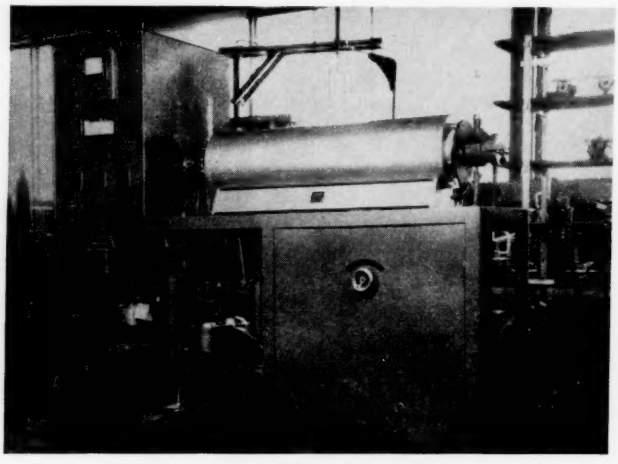

FIG. 4.

Après le décapage il faut sécher les transistors. Il faut éviter de souiller les faces des transistors décapés. Pour la dessiccation, il est surtout indiqué de procéder sous vide et en chauffant. Divers fabricants font suivre cette dessiccation d'un vieillissement. Celui-ci peut être exécuté dans l'installation à vide, en observant de rigoureuses conditions de propreté, et en introduisant le cas échéant, après l'évacuation et l'étuvage—qu'on effectue en continuant à chauffer de l'oxygène seul ou un mélange d'oxygène et d'azote dans des proportions bien définies—une humidité déterminée pour accélérer la réaction.

Le test à 100 pour cent doit être également fait dans une atmosphère et sous une température définies. Des humidités

Vol. 10 196

relatives inférieures à 1 pour cent sont absolument indispensables pour obtenir des transistors d'une bonne durée de vie utile, et de nouvelles connaissances dans ces domaines prescrivent déjà des humidités résiduelles plus réduites. Or, cette exigence peut être pleinement satisfaite en recourant à des appareillages à vide pour l'évacuation préalable et l'introduction de gaz protecteurs desséchés et purifiés lui succédant.

Le degré d'étanchéité de la capsule du transistor nous renseigne directement sur la durée de vie qu'on peut en attendre. La méthode la plus sûre employée actuellement consiste en un contrôle avec un gaz radioactif (on peut détecter des fuites de l'ordre de 10^{-13} mmHg l/s.

Le transistor est mis dans un récipient ne laissant pas sortir de radiations. Ce récipient est évacué et rempli ensuite de crypton 85, à une pression de quelques atm au-dessus de la pression atmosphérique.

Les transistors non étanches absorbent, suivant la grandeur de leur fuite, plus ou moins de gaz et deviennent ainsi diversement radioactifs. Le crypton 85 est alors repompé dans le réservoir.

Un rinçage d'air élimine l'activité superficielle et les transistors sont classés alors, à l'aide du scintillomètre, en bons ou mauvais, ou encore quantitativement suivant leur degré d'étanchéité, c.-à-d. suivant la durée de vie qu'on peut en attendre.

3.2. Technique de " mesa "

La technique de " mesa " représente actuellement le procédé le plus moderne de fabrication de transistors pour des fréquences maxima.

Si l'on considère le développement de la technique des transistors vers les fréquences supérieures, on peut constater pour l'essentiel les progrès suivants :

3.2.1. La réduction de volume des sphérules porta les fréquences de 1–2 mégacycles à 10–15 mégacycles.

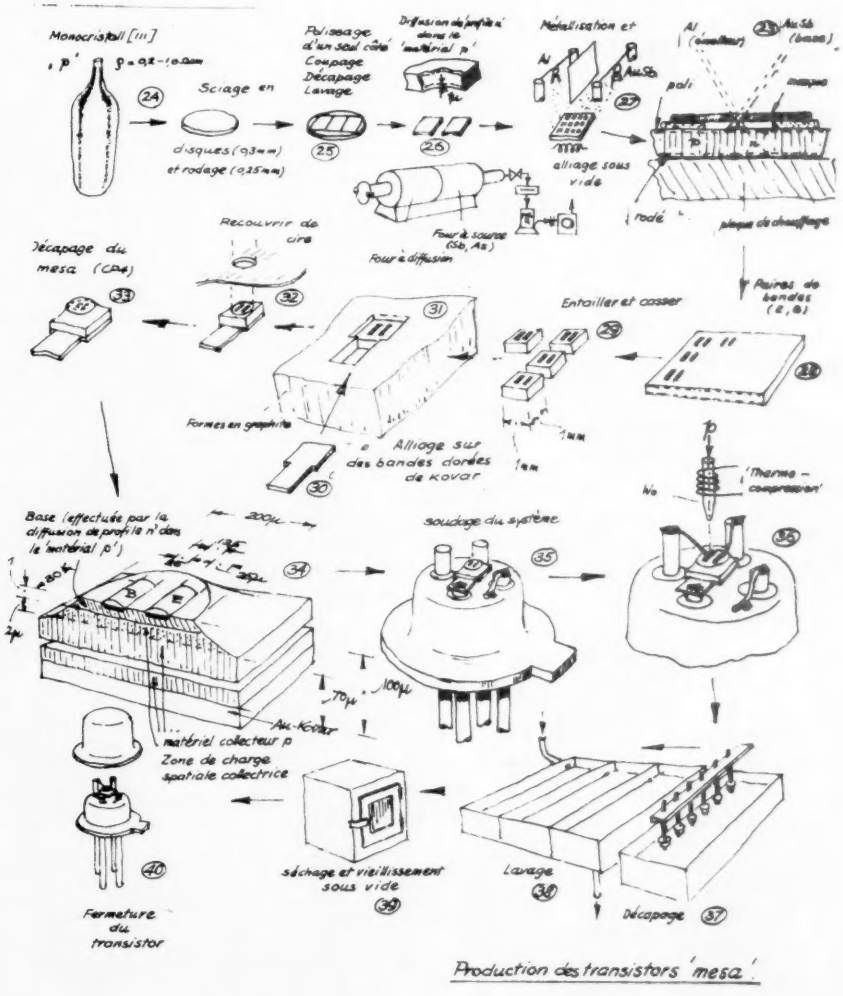

FIG. 5.

3.2.2. La technique du décapage par jet en réduisant encore la surface, permit de porter la fréquence à 30–80 mégacycles.

3.2.3. L'aménagement d'un champ d'accélération dans l'espace de base par Krömer—des drifttransistors et plus tard des transistors alliés par diffusion—repoussèrent encore la zone des fréquences jusqu'à environ 150 mégacycles.

3.2.4. Mais seule la mise en oeuvre de la technique de la vaporisation sous vide, et avec elle la possibilité de reproduire les plus petites surfaces, permit de réaliser des transistors pour des fréquences de 1200 à 2000 mégacycles. (Transistors de " mesa ").

La vaporisation sous vide se fait à l'aide de masques en nickel ou en molybdène, fabriqués par la technique de décapage photographique (Fig. 5 (23)).

Les diverses phases de fabrication de tels transistors sont les suivantes :

Le cristal est scié en plaquettes (24) qui sont ensuite rodées et polies d'un seul côté.

Ensuite, ces plaquettes sont sciées en rectangles de 10 × 15 mm et brièvement nettoyées par décapage (25).

Le matériau de départ a une résistivité de 0,2–1 Ωcm, et l'orientation cristallographique [111] (24).

Dans un four à diffusion sous vide à deux zones de chauffage (26) se trouvent, à l'endroit le plus chaud, les plaquettes de cristal devant être diffusées et, en autre endroit moins chaud, la source (le diffusant, p. ex. antimoine ou arsenic).

La température de la source détermine la pression de vapeur du diffusant et avec elle la concentration du gaz à la surface des plaquettes de cristal.

La température des plaquettes et le temps de diffusion fournissent la profondeur de pénétration du profil à points perturbateurs (atomes étrangers). Sur des transistors " mesa " cette profondeur atteint 1–2 μ.

Vaporisation et alliages des bandes d'émetteur et de base

Un appareillage de vaporisation sous vide possède deux sources (filaments de tungstène) séparées l'une de l'autre par un écran pour de l'aluminium et un mélange d'or-antimoine (27).

La plaquette de cristal est installée, côté poli tourné vers le masque, à quelques dizaines de microns de celui-ci et près d'un dispositif de chauffage (23).

Après qu'on atteint un vide d'environ 5.10^{-5} mmHg, la plaquette de cristal est chauffé à environ 500 °C pour en nettoyer la surface.

Après le refroidissement, on vaporise tout d'abord l'aluminium, puis le mélange d'or-antimoine, chaque fois sous un autre angle par la fente du masque.

Cette vaporisation donne naissance sur la plaquette de cristal, au-dessous de chaque fente à une paire de bandes d'aluminium et d'or-antimoine.

La plaquette de cristal est portée maintenant au-dessus de la température eutectique de la substance vaporisée et du cristal. De cette façon les bandes pénètrent faiblement en s'alliant à la plaquette de cristal. L'épaisseur des bandes vaporisées atteint environ 1/3 de micron.

La bande d'aluminium fournit l'émetteur et celle d'or-antimoine la connexion de base exempte de couches redresseuses.

La plaquette de cristal est maintenant entaillée au diamant (28) puis cassée en pastilles d'environ 1 × 1 mm, renfermant chacune une paire de bandes (29).

Ces pastilles sont fixées par alliage intime sous vide ou gaz protecteur (31), sous une température d'environ 400 à 450 °C, sur des bandes dorées de Kovar (30) jouant le rôle de conducteur de chaleur et de connexion électrique du collecteur.

A l'aide d'un pochoir les deux bandes vaporisées et fixées par alliage intime sont recouvertes de cire (32).

Le mesa est attaqué à l'acide tout autour de la couche de cire (33). De cette façon, la jonction du collecteur est dégagée. On enlève ensuite la couche de cire (34). (Coupe d'un système de mesa avec dimensions moyennes). La bande de Kovar est soudée au support du transistor (35), puis les fils de connexion en or (5–25μ, suivant le type) sont soudés par thermo-compression—micro-alliage par pression—aux fils-supports du transistor (36).

Un léger lavage à l'acide et puis à l'eau désionisée (38) élimine les perturbations superficielles (37) que pourrait apporter l'usinage mécanique ultérieur et nettoie la zone se trouvant entre les deux bandes.

Comme dans la technique des transistors alliés, les systèmes sont maintenant séchés sous vide et vieillis (39) et ensuite mesurés électriquement tous, sans exception, évacués de nouveau, étuvés et remplis de gaz inerte (azote ou hélium).

D'autre fabricants les remplissent d'oxygène ou d'un mélange d'oxygène et d'azote.

La fermeture des transistors " mesa " (40) est la même que celle employée pour les transistors alliés. Le banc d'essai tient compte des paramètres sous de hautes fréquences des transistors " mesa ".

Pour la vaporisation des bandes d'émetteur et de base et pour le processus d'alliage, Leybold a développé une

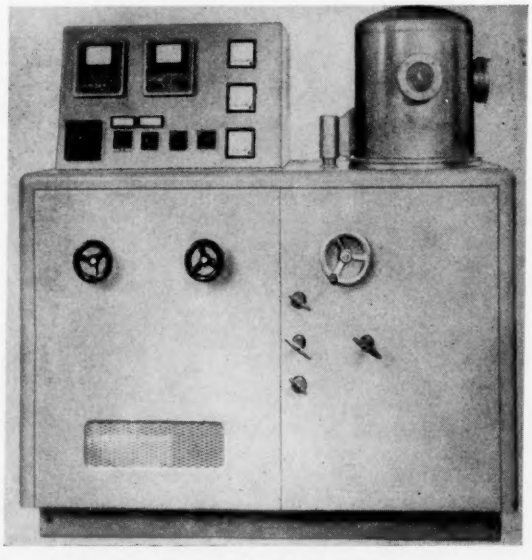

FIG. 6.

Vol. 10 1960

installation spéciale de métallisation sous vide (Fig. 6).

Il va sans dire qu'on aurait pu dire davantage de chacun des processus employés par la technologie des transistors. On aurait même peut-être pu parler des derniers degrés atteints par le développement, tels que ceux de la technique du micromodule et de la technique moléculaire, mais ce n'était pas possible dans ce cadre. Il aurait fallu pour cela renoncer à la vue d'ensemble.

Nous espérons, malgré l'étendue du domaine, avoir réussi à donner un clair aperçu général et à montrer toute l'importance de la technique du vide dans l'état actuel des choses, ainsi que le développement des transistors à l'avenir.

ol.
10
960

Index to Abstracts

Volume 9

General Vacuum Science and Engineering

10. Vacuum Technology

1. High Vacuum Practice.

11. Production of Low Pressures

2. Sur le Pompage des Tubes à Vide.
3. Means for Attaining Vacua without the Use of Pump Fluids.
4. Ionic Vacuum Pumps.
134. Cryopumping.

12. Measurement of Low Pressures

135. The Speed of Evacuation of High Vacuum Plant.
136. Two Methods for the Measurement of Low Vapour Pressures.
137. Density Determinations based on the Explorer and Vanguard Satellites.
138. Partial Pressure of Ammonia in Alveolar Air.

13. Vacuum Applications

5. Hypothermia.
347. Proceedings of the Fourth Conference on Magnetism and Magnetic Materials.
348. Sputtered Resistors Make High Component-Density Possible.

14. Kinetic Theory of Gases

6. Kinetic Theory of the Flow of Gas through a Cylindrical Tube.
7. Note on Diffusive Separation of Gas Mixtures in Flow Fields.
349. The Diffusion of Impurities into Evaporating Silicon.

15. Fluid Dynamics

8. Mean Gas Flow Velocity and Gas Flow Rate in Jets of High Vacuum Pumps.
9. Velocity and Temperature Discontinuities near the Walls of a Body around which Rarified Gases Flow with Transonic Velocities.
10. The Design, Instrumentation and Operation of the Utia Low Density Wind Tunnel.
139. Polyhedral Satellite for more accurate Measurement of Orbit Data of Earth Satellites.
140. Stabilized Pinch and Controlled Fusion Power.
141. Flow through Capillary Tubing with Eccentric Annular Sections.

16. Gases and Solids

11. Adsorption of Oxygen and Carbon Monoxide on Tungsten.
12. Work Function and Sorption Properties of Silicon Crystals.
13. Ion Induced Re-emission of Noble Gases from a Nickel Surface.
14. Using Cathode Resistance to Measure Adsorption of Gases on Metals.
15. Adsorption of Water Vapour on Lead Borosilicate Glass in Vacuum.
16. Dissociative Adsorption of Methane and Ethane on Evaporated Metal Films.
17. Evidence for Permeability Minima in Low Pressure Gas Flow through Porous Media.
18. Theoretical Analysis of Ultra-High Vacuum Condensers.
19. Some Observations Regarding the Present Status of Measurements of the Diffusion Coefficients of Hydrogen in Iron and Mild Steel.
20. Diffusion of Hydrogen in Palladium.
21. Properties of Hydrogen Chemisorbed on Tungsten.
22. Evidence for Permeability Minima in Low-Pressure Gas Flow through Porous Media.
142. The Influence of the Gas Atmosphere on the Pulverisation Process in Vibratory and Rotary Mills.
143. First Adsorbed Layer of He at 4.2°K.
350. Oxide Nucleation and the Substructure of Iron.
351. Enhanced Surface Reactions. III. Adsorption of Gases on Prepared Ruthenium Surfaces.

17. Thermodynamics

18. Theoretical Analysis of Ultra-High Vacuum Condensers.
23. A Simple, Automatic, High-Temperature Thermal Analysis Apparatus.
24. Precision Liquid Nitrogen Trap Level Controller.
25. Heat of Formation of BaC_2.
134. Cryopumping.
144. Simple Continuous He^3 Refrigeration System.
145. Extremely Low Temperatures.
146. Cryostat for Electron Bombardment and Electron Diffraction Work.
147. Use of Neon in Cryogenics.
148. The Selection of Stainless Steels for Use in Liquid Hydrogen Bubble Chambers.
149. Hydrogen Liquefaction.
150. Resistance Thermometer Bridge for Measurement of Temperatures in the Liquid Helium Range.
151. Growth and Properties of " Whiskers ".
152. Ultrahigh-Pressure Research.
153. Atmospheres of other Planets.
154. Air Conservation.
155. On Evaporation from Wind-swept Surfaces.
156. How Does a Raindrop Grow ?
352. Equilibrium Reduction of Tungsten Dioxide by Hydrogen.
353. Sublimation Freeze-Drying without Vacuum.

18. Gaseous Electronics

13. Ion Induced Re-emission of Noble Gases from a Nickel Surface.
26. Mechanism of Cataphoretic Segregation in Inert Gas Glow Discharges.
27. Formation of Plasma Structure in a Developing Discharge.
28. Microwave Investigation of Disintegrating Gaseous Discharge Plasmas.
29. Microwave Method for Measuring the Probability of Elastic Collision of Electrons in a Gas.
30. Impedance and Recovery Time of Glow Discharges in Mixtures of Rare Gases.

Vol.
10
1960

31. Anode Region in a Low Pressure Gas Discharge.
32. The Influence of the Electrode Temperature on the Electrical Breakdown Strength of a Vacuum Gap.
33. Secondary Positive Ion Emission from Metal Surfaces.
34. Collisions of Metastable Atoms.
35. Inelastic Ion–Atom Collisions.
36. Inelastic Atomic Collision Processes.
37. Electron Emission at High Fields Due to Positive Ions.
38. Electron Cooling by Heat Exchange.
39. Thermionic Ions from Hydrogen Palladium.
157. Effect of Humidity on the Spark Breakdown Voltage.
158. Alfven Waves in a Gas Discharge.
159. Some Experiments with an Electrodeless Discharge.
160. Townsend's First Ionization Coefficient in Pure Nitrogen.
161. Production of High Concentrations of Hydrogen Atoms.
162. Vacuum Arcs on Tungsten Cathodes.
163. High Power Vacuum Spark Gap.
164. Investigation of Breakdown in Vacuum.
165. New Developments of Air Cooled Condensers for the Processing Industry.

19. Radiation

40. Electroluminescent Thin Films.
41. Photoconductive Response of Single Crystal Germanium Layers Prepared by the Pyrolytic Decomposition of GeI_2.
42. Infrared Absorptivities and Emissivities of Gases.
43. Relation between Gas Absorptivities and Emissivities.
44. A Mechanical Version of the Smith Chart.
166. Electroluminescence of Zinc Sulfide Phosphors as an Equilibrium Process.
167. Reflexion Coefficient of Optically Inhomogeneous Layers.
168. Optical Transmission of Evaporated IN, SN, and BI Films in the Vacuum Ultraviolet.
169. Optical Constants of Evaporated Se Films by Successive Approximations.
170. Optical Properties of Various Evaporated Rare Earth Oxides and Fluorides.
171. Transmittance and Reflectance of Cesium Iodide in the Far Infrared Region.
172. Infrared Spectra of Monolayers on Metal Mirrors.
173. Luminescent Phases in Willemite Films.
174. Stokes' Equations and their Application to the Refractivity of Thin Films.
175. Obtaining Low Orders of Interference in Measuring Film Thicknesses by Multiple Beam Interferometry.
176. Ultraviolet Transmission Properties of Conducting Coatings on Glass.
177. Pressure Modulation of Infrared Absorption. I. Entire Vibration–Rotation Bands.
178. Antireflexion Coatings for Ge and Si in the Infrared.
179. Index of Refraction of Ge.
180. Spectral Effects in Interferometry.
181. Light Guide Radiation Pyrometry.
182. Design of Multilayer Filters by Successive Approximations.
183. Primary Frequency Standard Using Resonant Caesium.
184. Semiconductor P-N Junction Radiation Counter.
354. Phase Charge on Reflection from Evaporated Chromium Films.

Vacuum Apparatus and Auxiliaries

20. Pumping Systems

185. Measurement of Partial Pressures of HCl and H_2O in the $MgCl_2$–H_2O–HCl System.
186. The Attainment of High Pumping Speeds Using Ionization Pumps.
187. The Pumping Speed of an Ion and Absorption Pump of the Comsa-Musa Type.
188. Application of New Vacuum Pump Combinations.

21. Pumps and Pump Fluids

2. Sur le Pompage des Tubes à Vide.
3. Means for Attaining Vacua without the Use of Pump Fluids.
4. Ionic Vacuum Pumps.
8. Mean Gas Flow Velocity and Gas Flow Rate in Jets of High Vacuum Pumps.
9. Velocity and Temperature Discontinuities near the Walls of a Body around which Rarified Gases Flow with Transonic Velocities.
45. Preventing Steam " Slipping " at Ejector Pumps.
46. Vapour Cut-off for Vacuum Plant.
47. Interior Component of Vapour Pumps.
48. A New Type of Titanium Getter Pump.
189. Annular Jet Pump.
190. Dual Pumping Speeds of Some Ionization Pumps.
191. Étude d'une Pompe à Évaporation et Ionisation. Study of an Evapor-ion Pump.
192. Theory and Design of Getter-Ion Pumps.
193. A New Molecular Pump.
194. Removal of Gases in High Vacuum Systems by Metal Abrasion.
355. On the Pumping Speed of Oil Diffusion Pumps.

22. Gauges

11. Adsorption of Oxygen and Carbon Monoxide on Tungsten.
49. A High-Precision Differential Manometer.
195. Liquid Manometer with Electromagnetic Balance Indicator.
196. Construction of a Mcleod Type Vacuum Gauge having a Linear Scale.
197. Pressure Gauge for Corrosive Gases in the Micron and Submicron Region.
198. Investigations of Radiometer Forces in the Pressure Range 10^{-3} to 3 Torr.
199. Vacuum Gauges in Glass.
200. Thermocouple for Vapor Pressure Measurement in Biological and Soil Systems at High Humidity.

23. Plumbing

50. Vacuum Limitations of Rubber O-Ring Joints.
51. Simple Vacuum Coupling.
52. Demountable Vacuum Seal for Attaching an End-Plate to a Glass Tube.
53. Electrical Lead for Vacuum Systems.
54. A Note on the Use of P.T.F.E. in Vacuum Seals.
55. A Neoprene Vacuum Gasket for Wires.
56. A Metal through Glass Seal.
201. Vacuum Seals at Liquid Nitrogen Temperatures.
202. Coolable Vacuum-tight Window Seals for Optical Use.
203. O-Ring Seals for Pressures of 10 Kilobars.
204. Cleaning Techniques for Rubber O-Rings Used in Vacuum Systems.
205. Valve for Pressures of 10 Kilobars.
206. Glass Problems in Electron Tube Technology.
207. Transmission Specimen Holder for Electron Diffraction.

24. Valves

46. Vapour Cut-Off for Vacuum Plant.
57. The Construction of Small Vacuum Leaks of Constant Value.
58. Valve for the Grease-free Manipulation of Mercury.
59. Kinetic Theory of Nonspherical Molecules. III.

208. O-Ring Vacuum Valve for Use with a Visible Flow Industrial Glass Apparatus.
209. Vacuum Type Gas Flow Calibrator.
210. Small Valves for Instrumentation.
211. Mercury Glass Check Valves.

25. Baffles, Traps, and Refrigeration Equipment

24. Precision Liquid Nitrogen Trap Level Controller.
60. Helium Dewar with Incorporated Magnet Pole Tips.
149. Hydrogen Liquefaction.
212. Liquid-Air Level Controller for Cold Traps.

26. Automatic Protective and Control Equipment

24. Precision Liquid Nitrogen Trap Level Controller.
46. Vapour Cut-Off for Vacuum Plant.
61. Pressures under 1 mmHg.
213. Vacuum Valve Indicator Light.
214. Bellows-Operated Water Switch.
215. Two Emission Stabilizers for Electron-Bombardment Furnaces.

27. Leak Detectors and Leak Detection

1. High Vacuum Practice.
57. The Construction of Small Vacuum Leaks of Constant Value.
216. Thermal Conductivity Leak Detector.
217. Experiments on Flow of Gases through Leaks.
218. Application of Mass Spectrometry to Vacuum Technique.
356. Materials and Processes of Electron Devices.

28. Heating Equipment

219. Electron Bombardment Apparatus for Vacuum Evaporation.
220. Concerning a Large Capacity Uranium Melting Furnace.
221. High Temperature Laboratory Vacuum Furnace.
357. Microfurnace for Thermal Microscopy and Studies at High Temperatures.

29. Miscellaneous

175. Obtaining Low Orders of Interference in Measuring Film Thicknesses by Multiple Beam Interferometry.
176. Ultraviolet Transmission Properties of Conducting Coatings on Glass.
222. Molybdenum Disilicide for High Temperature Sliding.
223. Method for Breaking Open Sealed Electronic Devices in Vacuum.
224. Five Ways to Automatically Control Pressure for Ejector Vacuum Systems.
225. Use of Borosilicate Glass in Ozonizer Tubes.
226. Le Spectromètre à Rayons β du Centre de Physique Nucléaire Liège. β Spectrometer of the Nuclear Physics Center of Liège (Belgium).

Vacuum Applications

30. Evaporation and Sputtering

16. Dissociative Adsorption of Methane and Ethane on Evaporated Metal Films.
40. Electroluminescent Thin Films.
44. A Mechanical Version of the Smith Chart.
62. On P. A. Kurov's Letter on the Structure and Properties of Layers Obtained on Evaporation of InSb in Vacuum.
63. Structure of Thin Films of Sb_2S_3 Obtained by Sublimation at Pressures of Nitrogen below 4 mmHg.
64. Stability of Evaporated Films.
65. Electrodes for Thin Metal Films.
66. Thin Film Magnetization Reversal by Coherent Rotation.
67. Crystal Growth on Cathode Sputtered Copper Films by Pairs of Double Spiral Mechanisms Analogous to Frank-Read Sources.
68. Selective Delineation of Screw Dislocations by Cathodic Sputtering.
69. Production of Cadmium Sulfide Crystals by Coevaporation in a Vacuum.
70. n-Type and p-Type Conduction in Alkali–Anti-monide Photo-emitters.
71. Magnetic Writing with an Electron Beam.
72. Variation in the Temperature Derivative of Resistivity.
167. Reflexion Coefficient of Optically Inhomogeneous Layers.
168. Optical Transmission of Evaporated In, Sn, and Bi Films in the Vacuum Ultraviolet.
169. Optical Constants of Evaporated Se Films by Successive Approximations.
170. The Optical Properties of Various Evaporated Rare Earth Oxides and Fluorides.
171. Transmittance and Reflectance of Cesium Iodide in the Far Infrared Region.
173. Luminescent Phases in Willemite Films.
174. Stokes' Equations and their Application to the Refractivity of Thin Films.
175. Obtaining Low Orders of Interference in Measuring Film Thicknesses by Multiple Beam Interferometry.
178. Antireflexion Coatings for Ge and Si in the Infrared.
182. A Design of Multilayer Filters by Successive Approximations.
219. Electron Bombardment Apparatus for Vacuum Evaporation.
227. Optically Active Fluorite Films.
228. The Production of Thin Films by Thermal Evaporation of Inorganic Materials in High Vacuum.
229. Thin Magnetic Films.
230. Calculation of Absorption Peaks in Thin Metal Films.
231. Errors in the Measurement of Film Thickness by Multiple-Beam Interferometry.
232. Mechanical Properties of Whiskers and Thin Films.
233. Measurement of the Optical Constants of the Thin Dielectric Films by Means of Frustrated Total Reflexion.
234. Use of Fe^{55} for Measuring Titanium Coating Thickness.
235. Two-Layer Anti-Reflexion Coating for Low Refractive Index Glass.
236. Ultraviolet Normal Incidence Grating Vacuum Spectograph.
237. Interfacial Phenomena.
238. Ionization Potential and Absorption Coefficients of Nitrogen Dioxide.
239. Thermal Conductivity and Euckin Correction for Diatomic Gases and Mixtures.
240. Control Vacuum Evaporation by Temperature.
241. Evaporation of Metals by Electron Bombardment.
242. Evaporated Layers Formed from Semi-conducting III–V Combinations.
243. Electrical Breakdown of 1d-S Evaporated Layers.
347. Proceedings of the Fourth Conference on Magnetism and Magnetic Materials.
348. Sputtered Resistors Make High Component-Density Possible.
349. The Diffusion of Impurities into Evaporating Silicon.
358. Tungsten Coils for Vacuum Metallizing.
359. Reflecting Coatings for the Extreme Ultra-violet.
360. Optical and Photoelectric Properties of Thin Metallic Films in the Vacuum Ultraviolet.
361. Improved Metallic Coatings by Vacuum, Vapor Plating.

Vol.
10
196

362. Temperature Stabilization of Highly Reflecting Spherical Satellites.
363. Growth of Molybdenum, Tungsten and Columbium Crystals by Floating Zone Melting in Vacuum.

31. Evacuation and Sealing

364. Titanium Coatings on Molybdenum Wire.

32. Nucleonics

73. Neutron Generation from Straight Pinches.
74. A High Voltage Electron Injector Gun for Synchrotrons.
75. A Nuclear Plate Camera for Angular Distribution Measurements with Gaseous or Solid Targets over a Wide Range of Angles.
76. A Cryostat for Reactor Irradiations in Liquid Nitrogen.
77. Research on Controlled Thermonuclear Reactions at the Atomic Energy Institute of the USSR Academy of Sciences.
78. 150 kV Cockcroft–Walton Type Particle Accelerator.
79. New Proportional Counters for Gases and Vapors.
80. Evacuated Pinhole Camera Maps Beta-Active Deposits.
183. Primary Frequency Standard Using Resonant Caesium.
244. Isotopic Analysis of Lithium by Mass Spectrometry.
245. Surface Ionization Source for Mass Spectrometry.
246. The Resnatron as a 200 Mc/s Power Amplifier.
247. Low Background Gas-Flow Counter.
248. Simple Pulsed Neutron Source Based on Crossed-Field Trapping.
249. He^3 Recirculation and Purification System for a Cyclotron Ion Source.
250. Possibility of Ion Runaway in ZETA.
251. Development of an Occluded-Gas Ion Source.
252. A 22-MeV Electron Linear Accelerator.
253. Gas Scattering in a Strong Focusing Synchrotron.
254. Catalytic Activity and Surface Structure after Ion Bombardment.
255. The Electron Temperature in Sceptre III.
256. New Investigations with Sceptre III.
365. Stratospheric Carbon-14, Carbon Dioxide, and Tritium.
366. Which Approach to Controlled Fusion—The Machine Called DCX.

33. General Physics and Electronics

12. Work Function and Sorption Properties of Silicon Crystals.
14. Using Cathode Resistance to Measure Absorption of Gases on Metals.
32. The Influence of the Electrode Temperature on the Electrical Breakdown Strength of a Vacuum Gap.
33. Secondary Positive Ion Emission from Metal Surfaces.
34. Collisions of Metastable Atoms.
37. Electron Emission at High Fields due to Positive Ions.
38. Electron Cooling by Heat Exchange.
41. Photoconductive Response of Single Crystal Germanium Layers Prepared by the Pyrolytic Decomposition of GeI_2.
60. Helium Dewar with Incorporated Magnet Pole Tips.
66. Thin Film Magnetization Reversal by Coherent Rotation.
72. Variation in the Temperature Derivative of Resistivity.
70. n-Type and p-Type Conduction in Alkali–Antimonide Photoemitters.
71. Magnetic Writing with an Electron Beam.
76. A Cryostat for Reactor Irradiations in Liquid Nitrogen.
81. Electrically Driven Shock Tube.
82. Contact Potential Measurements on Graphite.
83. Beam Noise in Crossed Electric and Magnetic Fields.
84. Vacuum Arcs on Tungsten Cathodes.
85. Production of High Concentrations of Hydrogen Atoms.
86. The Recombination of Oxygen Atoms at Surfaces.
87. Grating Vacuum Monochromator for the Spectral Range 1000–6500 Å.
88. A Broadband Oscilloscope Tube.
89. A Mass Spectrometer Mass Marker.
90. Soft X-Ray Spectroscopy Using an Electron Multiplier.
91. An X-Ray Tube Target Current Stabilizer.
92. Properties of a Thermoelectric Cell.
93. Noise in Oxide Cathode Coatings.
94. Thermometric Study of the Frozen Products from the Nitrogen Microwave Discharge.
95. High Vacuum Studies of Surface Recombination Velocity of Germanium.
96. Application of the Ion Bombardment Cleaning Method to Titanium, Germanium, Silicon, and Nickel as Determined by Low-Energy Electron Diffraction.
97. Preparation and Regeneration of Clean Germanium Surfaces.
98. Measured Thermal Efficiencies of a Diode Configuration of a Thermo Electron Engine.
99. Helium Atoms from a Tungsten Target.
207. Transmission Specimen Holder for Electron Diffraction.
257. Effect of Cathode Inclusions on Electrical Discharges.
258. Electron Microscope Study of Finback Whale Myoglobin Crystals.
259. Microscopy with X-Rays.
260. High-Current Ion Sources.
261. Mass Spectrometer Ion Source for Solid Samples.
262. An Effect of Oxide Layers on the Behaviour of Vacuum Arc Cathode Spots.
263. Emission of Slow Secondary Electrons.
264. Helium Temperatures from Vapour Pressure Measurements.
265. Simple Attachment to the Sucksmith Ring Balance for Use at Low Temperatures.
266. Calorimeter with Automatic Control.
267. Space-charge Grid High-Transconductance Electron Gun.
268. Microscopic Examination of Interior of Highly Curved Surfaces by Means of Replicas.
269. Photoconductivity and the Visual Receptor Process.
270. Improved, Single Flash, Continuum Source for Use below 2000 A.
271. High-Sensitivity Crystal Infrared Detectors.
272. High-Temperature X-ray Diffractometer.
273. Electron Microscope and Electron Diffraction Study of Optically Transparent Electrically Conducting Coating on Glass and Acrylic Plastics.
274. Some Properties of Thin Barium–Strontium–Titanate Single Crystal Layers Evaporated in the Presence of an Electrical Field.
275. Investigations on Ion Absorption and Corrosion using Radioactive Indicators.
276. Investigations of a High Frequency Ion Source.
277. Vacuum Sampling Device.
278. Note on the Observation of Molecules by Field Emission Microscopy.
279. Thermal Contact at Low Temperatures.
280. Automatic Recording Vacuum Microbalance.
281. Electron-permeable Window for Cathode Ray Tubes.
282. Low-temperature Optical Window Seal used at 80°K.
283. Vacuum Plant for Crystal Pulling.
284. Mica as Constructional Material for Use in High Vacuum.
367. Studies of the Effect of Anode Materials on Oxide Cathode Performance.
368. Infrared Vacuum Spectrometer with Prism Grating Double Monochrometer.

34. High Altitude and Space Technology

18. Theoretical Analysis of Ultra-High Vacuum Condensers.
137. Density Determinations Based on the Explorer and Vanguard Satellites.
153. Atmosphere of other Planets.
285. Stratospheric Fallout of Strontium-89 and Barium-140.
286. Concentrations of Radioactive Materials in the Air during 1957.
287. Mass of the Moon from Satellite Observations.
288. Ground Rules for Space Research.
289. Radar Echoes from Venus.

290. Effect of Transverse Atmospheric Drag on Satellite Orbits.
291. Optical Tracking of Artificial Earth Satellites.
292. Cloud Physics.
293. Earth Oblateness in Terms of Satellite Orbital Periods.
294. Frontal Cloud System Pictures obtained by Rocket.
295. " IGY " Conference in Moscow.
296. International Geophysical Year.
297. International Geophysical Year.
298. Modifying Weather on a Large Scale.
362. Temperature Stabilization of Highly Reflecting Spherical Satellites.
365. Stratospheric Carbon-14, Carbon Dioxide, and Tritium.
369. Research in Space.
370. Effect on the Solar Wind on the Lunar Atmosphere.

35. Impregnation and Potting

299. Vacuum Drying.

36. Drying, Degassing and Concentration

100. Low Temperature Evaporation plus Energy Economy.
101. Method of Freeze Drying Sensitive Material.
102. A Machine for Freeze-Drying and Storing Tissues under Aseptic Conditions.
103. Continuous Freeze-Drying of *Serratia marcescens*.
104. Pilot-Plant Production of Ground *Serratia marcescens*.
105. Freezing and Drying.
300. Large Scale Laboratory Freeze-Drying Apparatus.
353. Sublimation Freeze-Drying without Vacuum.

37. Metallurgy, Inorganic Chemistry and Analytical Chemistry

95. High Vacuum Studies of Surface Recombination Velocity of Germanium.
106. Sampling from a Vessel under Vacuum.
107. Factors Determining the Oxygen Content of Liquid Silicon at its Melting Point.
108. Sampling System for High-Vacuum Furnace Atmosphere.
109. The Preparation of Single-Crystal Ingots of Silicon by the Pulling Technique.
110. Vacuum Degassing at Bethlehem.
111. Vacuum Degassing.
112. Preparation of Indium Arsenide.
113. Whisker Growth from Iodide Titanium Wire.
114. Resolution of Electron Probe Microanalyzers.
115. Production of Discaloy by Vacuum Arc Melting.
116. Removal of Gases in High Vacuum Systems by Metal Abrasion.
117. The Achema Meeting 1958. Chemical Plant Exhibition.
118. Report on U.S. Reactor Fuel Technology.
215. Two Emission Stabilizers for Electron-Bombardment Furnaces.
301. General Purpose Vacuum Furnace.
302. Vacuum Arc Furnace for Laboratory Operation.
303. Vacuum Levitation Melting.
304. Vacuum Melting Stainless Steels and Super-alloys.
305. Vacuum-Melting of Metals.
306. Vacuum Furnaces.
307. Vacuum Flow Steel Degassing.
308. Vacuum Furnace for Continuous Strip.
309. Vacuum Furnace Features Quick Changeover.
310. Hydrogen in Heavy Forgings.
311. Welding with an Electron Beam.
312. Pattern for Better Alloys.
313. Spectrographic Analysis of Oxygen in Titanium.
314. Beryllium—Present and Potential Uses.
315. The Effect of Oxygen, Hydrogen and Water Vapour on the Electrical Conductivity of Barium Oxide and Barium-Strontium Dioxide.
316. Préparation du Fluorure de Zirconium Anhydre pur. Preparation of Pure Anhydrous Zirconium Fluoride.
317. Contribution à l'Étude de l'Élimination par Vaporisation du Zinc Contenu dans les Alliages Zirconium–Zinc. Contribution to the Study of the Elimination by Vaporization of Zinc contained in Zirconium–Zinc Alloys.
318. Contribution à l'Étude de la Préparation du Zirconium et de Certains de ses Alliages par Réduction Métallothermique. Contribution to the Study of the Preparation of Zirconium and Certain Alloys by Metallothermic Reduction.
319. Aluminium Nitride Precipitates in α-Iron.
320. Vacuum as a Furnace " Atmosphere ".
321. Vacuum Metallurgy in Europe.
347. Proceedings of the Fourth Conference on Magnetism and Magnetic Materials.
348. Sputtered Resistors Make High Component-Density Possible.
356. Materials and Processes of Electron Devices.
371. Vacuum Casting Steel.
372. Vacuum Melted Metals and Alloys.

38. Distillation, Organic Chemistry and Isotopic Gas Analysis

117. The Achema Meeting 1958. Chemical Plant Exhibition.
119. Low Temperature Distillation of Hydrogen Isotopes.
120. Removal of some Volatile Impurities from Uranium Hexafluoride.
121. A Fraction Collector (with Drop Counter).

39. Miscellaneous Applications

96. Application of the Ion Bombardment Cleaning Method to Titanium, Germanium, Silicon, and Nickel as Determined by Low-Energy Electron Diffraction.
97. Preparation and Regeneration of Clean Germanium Surfaces.
122. Cooling Cannula for use in the Treatment of Cerebral Neoplasms.
123. Effect of Hypothermia on the Adrenocortical Response to Operation.
124. Hyperpyrexia in Encephalitis Treated by Hypothermia.
125. Accidental Hypothermia.
126. Accidental Hypothermia.
127. Hypothermia by Internal Cooling in Man.
128. An Apparatus, Capable of being Heated for High Vacuum Grinding of Solids.

Materials and Techniques used in Vacuum Technology

40. Gases and Vapours

21. Properties of Hydrogen Chemisorbed on Tungsten.
59. Kinetic Theory of Non-spherical Molecules. III.
129. Effect of Pressure on Ion Formation in Propane–Air Flames.
130. Gas or Vapour Filled Discharge Vessel Fitted with a Hollow Cathode and a Starting Electrode Located outside the Main Discharge Path.
217. Experiments on Flow of Gases through Leaks.
322. Pressure Induced Shifts of HCl Absorption Lines in the Infrared.
323. Paramagnetic Line Widths in Gaseosy Atomic Hydrogen.
324. Multiple Ionization of Sodium Vapor by Electron Impact.
325. Alkali Halide Complex Ions and the Hydrated Ion $K(H_2O)^+$.
326. Interaction of Rare Gases with Metal Surfaces I, A, Kr, and Xe on Tungsten.

Vol. 10 1960

327. Production of Atoms by a Glow Discharge in Dry Hydrogen.
328. Adsorption of Oxygen on Silicon.
329. Adsorption of Oxygen on Tungsten.
330. Electrical Properties of Hydrogen Adsorbed on Silicon.
331. Mutual Diffusion of Pairs of Rare Gases at Different Temperatures.
332. Kinetics of Nitrogen Atom Recombination.
349. The Diffusion of Impurities into Evaporating Silicon.
356. Materials and Processes of Electron Devices.
373. Separation of Gas Mixtures in a Supersonic Jet.
374. Thermal Conductivity of Nitrogen–Carbon Dioxide Mixtures.
375. Adsorption of Nitrogen on Tungsten at Very Low Pressures.

41. Metals and Alloys

62. On P. A. Kurov's Letter on the Structure and Properties of Layers Obtained on Evaporation of InSb in Vacuum.
131. Cleanliness of Vacuum-Melted Alloys.
132. Comments on a Theory of Double Block Walls in Thin Films.
148. The Selection of Stainless Steels for Use in Liquid Hydrogen Bubble Chambers.
376. Tungsten Zone Melting by Electron Bombardment.

42. Glass and Ceramics

164. Investigation of Breakdown in Vacuum.
206. Glass Problems in Electron Tube Technology.
333. Quartz Glass, Fused Quartz and Quartzlike Glasses as Constructional Materials in High Vacuum Technique.
334. A Contribution to the Technology of Large Ceramic Bodies.
377. Ceramic Electrical Insulating Materials.
378. Young's Modulus of Various Refactory Materials as a Function of Temperature.
379. Thermal Expansion of Al_2O_3, BeO, MgO,B_1C, SiC, and TiC above 1000°C.
380. Rate of Thermal Dehydration of Muscovite.

43. Plastics and Elastomers

50. Vacuum Limitations of Rubber O-Ring Joints.
54. A Note on the Use of P.T.F.E. in Vacuum Seals.
164. Investigation of Breakdown in Vacuum.
335. Electron Spin Resonance Studies of Irradiated Teflon : Effects of Various Gases.

44. Waxes, Lubricants, Cements, Lacquers, Paints, Oils

381. Health Legislation Concerning Paint Ingredients.
382. Exciting Developments in Better Finishing Facilities.

45. Soldering, Welding and Brazing

336. The Technique of Soldering in Vacuum.
383. Wetting of Original and Metallized High-Alumina Surfaces by Molten Brazing Solders.

46. Glass Blowing, Glass-to-Metal and Ceramic-to-Metal Sealing Techniques

284. Mica as Constructional Material for use in High Vacuum.
337. Precision Ends for Fused Silica Tubes.
338. Contribution to the Question of Electrolysis of Glass in Electronic Valves.
339. Vacuum Tight Seals between Molybdenum and Glass.
384. Fundamentals of Glass-to-Metal Bonding. IV. Wettability of Gold and Platinum by Molten Sodium Disilicate.
385. Tension Stress in Glass Coatings and in Glass–Metal Seals in the Annealing Range.

47. Outgassing Data, Vapour Pressure Data, and Gettering Data

339. Vapor Pressure, Mass and Infrared Spectra of Hexaborane.
356. Materials and Processes of Electron Devices.
386. Carbon as an Indicator of Gas Content of Metallic Tube Elements.
387. Measurements of Gas Evolution or Sorption of Anode Materials under Simulated Life Conditions.

49. Miscellaneous Materials and Techniques

133. Size Reduction in Ball Mills.
340. Vaporization of Beryllium Oxide and its Reaction with Tungsten.
341. Free Evaporation of Alkali Halide Crystals.
342. Structure and Adsorption Characteristics of Clean Surfaces of Germanium and Silicon.
343. Adsorption of Hydrogen on Silicon.
344. Adsorption of Carbon Dioxide on Tungsten.
345. Evaporation of Aluminium Oxide.
364. Titanium Coatings on Molybdenum Wire.
388. Surface Phenomena Associated with Application of Organic Films to Phosphor Screens.
389. A Study of the Molded Nickel Cathode.

Basic Science and Engineering

51. Physics, Astronomy and Geophysics

134. Cryopumping.
139. Polyhedral Satellite for more Accurate Measurement of Orbit Data of Earth Satellites.
151. Growth and Properties of " Whiskers."
152. Ultrahigh-Pressure Research.
166. Electroluminescence of Zinc Sulfide Phosphors as an Equilibrium Process.
167. Reflexion Coefficient of Optically Inhomogeneous Layers.
171. Transmittance and Reflectance of Cesium Iodide in the Far Infrared Region.
173. Luminescent Phases in Willemite Films.
176. Ultraviolet Transmission Properties of Conducting Coatings on Glass.
177. Pressure Modulation of Infrared Adsorption. I. Entire Vibration-rotation bands.
178. Antireflexion Coatings for Ge and Si in the Infrared.
179. Index of Refraction of Ge.
285. Stratospheric Fallout of Strontium-89 and Barium-140.
287. Mass of the Moon from Satellite Observations.
346. Formation of Elements in the Stars.
354. Phase Charge on Reflection from Evaporated Chromium Films.
369. Research in Space.
370. Effect of the Solar Wind on the Lunar Atmosphere.
390. Experimental Determination of the Oscillator Strength of the First Negative Bands of N_2^+.

53. Metallurgy, Ceramics and Inorganic Chemistry

301. General Purpose Vacuum Furnace.
302. Vacuum Arc Furnace for Laboratory Operation.

305. Vacuum-Melting of Metals.
306. Vacuum Furnaces.
307. Vacuum Flow Steel Degassing.
313. Spectrographic Analysis of Oxygen in Titanium.
314. Beryllium—Present and Potential Uses.

56. Electrical Engineering, Electronic Circuits

165. New Developments of Air Cooled Condensers for the Processing Industry.
246. The Resnatron as a 200 Mc/s Power Amplifier.
267. Space-Charge Grid High-Transconductance Electron Gun.
299. Vacuum Drying.
391. Design of Broadband Ceramic Coaxial Output Windows for Microwave Power Tubes.

58. Nucleonics

140. Stabilized Pinch and Controlled Fusion Power.
286. Concentration of Radioactive Materials in the Air during 1957.

59. Miscellaneous

222. Molybdenum Disilicide for High Temperature Sliding.

Vol.
10
1960

Index to Abstracts

Volume 10

General Vacuum Science and Engineering

10. Vacuum Technology

207. Summarized Proceedings of a Symposium on Current Developments in the Production of High Vacua.

11. Production of Low Pressures

1. Molecular Pumping.

12. Measurement of Low Pressures

208. Forced Periodic Changes of Kinetic Energy of Gas Molecules as a Means of Vacuum Measurement.

13. Vacuum Applications

209. Methods of Cleaning Glass by Vapour Degreasing and Ultrasonically Agitated Solvents.

14. Kinetic Theory of Gases

2. Gas-Kinetic Collision Diameters of the Halomethanes.
3. Calcium Atomic Beam Source and Interference Beyond Two Meter Retardation.
210. Torsion Balance Measurements with Molecular Beams.

15. Fluid Dynamics

4. Transitional Correction to the Drag of a Sphere in Free Molecule Flow.
5. Laminar Steady-State Magnetohydrodynamic Flow in an Annular Channel.
6. Magnetohydrodynamic Flow in a Shock Tube.
7. Some Exact Solutions of the Navier-Stokes and the Hydromagnetic Equations.
8. Laminar Flow in the Entrance Region of a Porous Pipe.
9. Integration Theory for One-Dimensional Viscous Flow.
10. Evaporation into a Boundary Layer. II. Dissociation in Evaporation.
11. Vacuum Type Gas Flow Calibrator.

16. Gases and Solids

12. Secondary Positive Ion Emission from Metal Surfaces.
13. Alkane Adsorption on Silica, Alumina and Silica-Alumina Catalysts.
14. Effects of Interparticle Condensation on Heats of Adsorption and Isotherms of Powder Samples.
15. Model Calculation of the Temperature Dependence of Small Molecule Diffusion in High Polymers.
16. Surface Properties of Germanium.
17. The Slow Step in Chemisorption. The Possible Role of the Solid Adsorbent. II.
18. Adsorption of Inert Gases by Modified Carbons.
19. Effects of Interparticle Condensation on Heats of Adsorption and Isotherms of Powder Samples.
20. Model Calculation of the Temperature Dependence of Small Molecule Diffusion in High Polymers.
23. The Sorption of Hydrocarbon Vapors by Silica Gel.
24. The Determination of Surface Areas from Krypton Adsorption Isotherms.
25. The Rates of Adsorption of Water and Carbon Monoxide by Zinc Oxide.
26. Heat of Adsorption of Parahydrogen and Orthodeuterium on Graphon.
27. Effect of Poisoning on the Infrared Spectrum of Carbon Monoxide Adsorbed on Nickel.
28. Infrared Spectra of Hydrocarbons Adsorbed on Silica Supported Metal Oxides.
29. Sorption and Magnetic Susceptibility Studies on Nitric Oxide–Silica Gel Systems at a Number of Temperatures.
30. Adsorption Studies on Metals. VIII. Mono-functional Organic Molecules on Reduced Oxide-Coated Nickel and Copper.
31. Thermal Aging of Silica Gels.
32. The Adsorption of Some Gases on Evaporated Metal Films and on Oxidized Films of Nickel.
33. Acid-Base Interaction in the Adsorption of Olefins on Aluminium Kaolinite.
34. A Precision Adsorption Apparatus for the Study of the Interactions Between Gas Atoms and Surfaces.
35. The Time Lag in Diffusion. IV.
36. The Sorptive Properties of a Zeolite Containing a Preadsorbed Phase.
37. Adsorption and Diffusion of Argon on Tungsten.
38. The Interaction of Krypton with Metals. An Appraisal of Several Interaction Theories.
39. The Influence of a Chemisorbed Layer of Carbon Monoxide on Subsequent Physical Adsorption.
40. The Exchange of Deuterium Gas with the Hydrogen Associated with Solid Catalysts. I. The Model Tantalum–Hydrogen System.
41. The Chemisorption of Oxygen on Silver.
42. Relations Between Different Definitions of Physical Adsorption.
43. An Infrared Study of the Water–Silica Gel System.
44. The Structure of Gas-Adsorbent Carbons.
45. Surface Reactions on Evaporated Palladium Films.
46. The Adsorption of Krypton on Germanium.
47. The Adsorption of Water Vapor on Quartz and Calcite.
48. A Useful Adsorption Isotherm.
49. Adsorption of Fluorinated Methanes by Linde Molecular Sieves.
50. Infrared Studies of Physically Adsorbed Polar Molecules and of the Surface of a Silica Adsorbent Containing Hydroxyl Groups.
51. Adsorption and Catalysts.
52. Theory of Permeation Through Metal Coated Polymer Films.
53. Oxygen Sorption and Electrical Conductivity of Copper Oxide Films.
54. The Time Lag in Diffusion. III.
211. The Chemisorption of Gases on Chromia Surfaces at Low Temperatures.
212. Physical Adsorption on Chemisorbed Films.
213. The Diffusion of Hydrocarbons in Polyisobutylene.
214. Successive Differential Adsorptions of Vapors by Glassy Polymers.
215. The Theory of Diffusion Controlled Adsorption Kinetics with Accompanying Evaporation.

216. Coefficients of Evaporation and Condensation.
217. Diffusion of Hydrogen in Thorium.
218. The Oxidation of Evaporated Barium Films (Getters).
219. Properties of Getters in Electronic Tubes.
220. The Submonolayer Adsorption of Argon and Krypton on Molybdenum Disulfide ; Phenomenological Comparison with Studies on Graphite.
221. New Technique for Measurement of Low Dissolved-Air Content of Water.
222. Evaporation and Diffusion Rate Measurements on Cathodes of Sintered Nickel Containing Alkaline-Earth Oxides.
223. Adsorption on Porous Solids.
224. The Quantum Mechanical Correction for the High Temperature Van der Waals Interaction of Light Gases and Surfaces. A New Method of Determining Surface Area.
225. Reactions of Titanium and Zirconium with Oxygen, Air, Nitrogen and Carbon Dioxide.
397. The Sorption of Gaseous Hydrogen Chloride by Dry Lyophilized β-Lactoglobulin.
398. Electronic Spectra of Adsorbed Molecules : Stable Carbonium Ions on Silica Alumina.
399. On the Energetics of Physically Adsorbed Films, with Particular Reference to the Use of Krypton for Surface Area Measurement.
400. The Extreme Sensitivity of Paramagnetic Sites to Poisoning by Desorbed Gases Evaluated by the Low Temperature Ortho-Parahydrogen Conversion.
401. A Radiotracer Study of an Optical Method for Measuring Adsorption.
402. Calorimetric Heats of Adsorption for Hydrogen on Nickel, Copper and Some of their Alloys.
403. Heats of Adsorption and Adsorption Isotherms for Low Boiling Gases Adsorbed on Graphon.
404. The Failure of Dispersion Energy Calculations to Reproduce Heats of Adsorption on Graphite Carbon.
405. The Effects of Oxygen Adsorption on the K X-Ray Absorption Edge of Alumina Supported Nickel.
406. Sites for Hydrogen Chemisorption of Zinc Oxide.
407. Non-Steady-State Fluid Flow and Diffusion in Porous Media Containing Dead-End Pore Volume.
408. The Frenkel-Halsey-Hill Adsorption Isotherm and Capillary Condensation.
409. Hydrogen Sorption on Graphite at Elevated Temperatures.
410. Adsorption Studies on Metals. IX. The Nature of the Thermal Regeneration of Oxide-Coated Nickel, Cobalt and Copper.
411. The Chemisorption of Oxygen on Nickel.
412. The Heat of Adsorption of Argon and Krypton on Molybdenum Disulfide-Separation of Enthalpies into Rational Components.

17. Thermodynamics

10. Evaporation into a Boundary Layer. II. Dissociation in Evaporation.
55. The Dissociation Pressure of Aluminum Carbide.
56. A Mass Spectrometric Study of the Vaporization of Ferrous Bromide.
57. Oxygen Dissociation Pressures over Uranium Oxides.
58. High-Altitude Atmospheric Density.
59. Satellite Density Measurements.
60. Approximate Formula for the Thermal Conductivity of Gas Mixtures.
61. Dissociation Pressure and Stability of Beryllium Carbide.
62. Kinetic Theory of Moderately Dense Gases.
63. Condensation of an Imperfect Boson Gas.
64. The Vaporization of Molybdenum and Tungsten Oxides.
65. Applicability of the Knudsen Effusion Method to the Study of Decomposition Reactions. The Decomposition of Magnesium Hydroxide.
66. Thermodynamics of Electrically Conducting Fluids.
67. Compressibility and Intermolecular Forces in Gases : Methane.
68. Evaporation into a Boundary Layer.
69. Heat Transfer to a Sphere at the Transition from Free Molecule Flow.
216. Coefficients of Evaporation and Condensation.
226. Viscosity and Thermal Conductivity of Liquid Boron Trifluoride.
227. The Dissociation Pressure of CdSb.
228. Sublimation Pressures of Solid Solutions. I. The Systems Tin (IV), Bromide-Tin (IV), Iodide and Tin (IV), Bromide-Titanium (IV). The System Tin (V), Bromide-Tin (IV), Iodide-Carbon Tetrachloride.
229. Dewar System for Low Temperature Experiments.
410. Adsorption Studies on Metals. IX. The Nature of the Thermal Regeneration of Oxide-Coated Nickel, Cobalt and Copper.
412. The Heat of Adsorption of Argon and Krypton on Molybdenum Disulfide-Separation of Enthalpies into Rational Components.
413. Heats of Immersion. IV. The Alumina-Water System-Variations with Particle Size and Outgassing Temperature.
414. Mechanism of the Isothermal Decomposition of Potassium Perchlorate.
415. On the Use of Tantalum Knudsen Cells in High Temperature Thermodynamic Studies of Oxides.
416. The Dissociation Pressures and the Heats of Formation of the Molybdenum Silicides.

18. Gaseous Electronics

66. Thermodynamics of Electrically Conducting Fluids.
70. Electron Acceleration against an Opposing Field in a Vacuum Electromagnetic Discharge.
71. The Stellarator Concept.
72. Electrical Breakdown between Close Electrodes in Air.
73. On the Research and Development of Electron Emitting Substances for Gas Discharges.
74. Supersonic Motion of Vacuum Spark Plasmas along Magnetic Fields.
75. Response of Electrostatic Probes to Ionized Gas Flow in a Shock Tube.
76. Adsorption of Gases in the Low Pressure Arc.
77. Micro-discharges and Pre-discharge Currents between Metal Electrodes in High Vacuum.
78. Automatic Cloud Chamber for Gas Discharge Studies.
79. Design and Performance of a Hot Cathode Magnetically Collimated Arc Discharge Ion Source.
80. Cold Cathode Electric Discharge at Low Pressures in a Magnetic Field.
81. Anode Region in a Low Pressure Gas Discharge.
222. Evaporation and Diffusion Rate Measurements on Cathodes of Sintered Nickel Containing Alkaline-Earth Oxides.
230. Noise Propagation on Uniformly Accelerated Multivelocity Electron Beams.
231. Propagation Characteristics of Detonation-Generated Plasmas.
232. Charge Localization on the Surfaces of Oxide-Coated Cathodes.
233. Anode Surface Effects in Diodes Containing Oxide-Coated Cathodes.
234. Cathode Work Function, Sparking Potentials and Secondary Ionization Coefficients for Oxide-Coated Cathodes in Hydrogen.
235. Influence of the Cathode Work Function on the Sparking Potential in Hydrogen.
236. Glow Discharge Characteristics of Helium–Neon Mixtures.
237. Deuterium-Filled Thyratrons.
238. Deuterium as a Filling for High-Voltage Thyratrons.
239. The Grid Emitting Properties of Titanium.
240. The Magnetic Stabilization of Low Pressure D.C. Arcs.
241. The Cleaning of Glass in a Glow Discharge.
242. Thermionic and Related Properties of Calcium Oxide.

Vol.
10
1960

243. Cathode Emission Measurements in Low Pressure Discharges.
244. Reversible Poisoning by Sulphur, Oxygen and Other Gases of Oxide-Coated Cathodes at High Temperatures.
245. Microwave Method of Investigating the Afterglow of Pulsed Gaseous Discharges.
246. First Ionization Coefficients in Hydrogen, Neon and Argon.
247. Excitation and Ionization Rates of Mercury in Discharge Plasmas.
248. Production of X-Ray during a Low-Pressure Gas Discharge.
249. Thermionic Properties of Thorium Deposits on Control Grid Materials.
250. Evaporation of Thorium from Carburized Thoriated Tungsten Cathodes.
251. Studies of Cold Cathode Discharges in Magnetic Fields.

19. Radiation

82. Design of High-Resolution Monochromator for the Vacuum Ultra-violet. An Application of Off-Plane Eagle Mounting.
83. Phase Changes on Reflection from Evaporated Chromium Films.
84. The Theory of the High Frequency Brush Discharge.
85. Preparation of Phase Diffraction Gratings by Vacuum Evaporation.
86. Method for Obtaining Uniform Evaporated Layers.
87. On the Measurement of the Temperatures of Unenclosed Objects by Radiation Methods.
252. Summarized Proceedings of a Conference on Electron Microscopy.
253. Absolute Intensity Measurements of the Carbon and Aluminium X-Ray K-Lines with a Proportional Counter.
254. Some Developments and Applications of Micro-focus X-Ray Diffraction Techniques.
255. Summarized Proceedings of a Colloquium on X-Ray Fluorescence Analysis.
256. Summarized Proceedings of a Conference on X-Ray Analysis.
257. Apparent Loss of Efficiency in Multilayer Cathodo-luminescent Films.
258. Reflectance-Increasing Coatings for the Vacuum Ultraviolet and their Applications.
259. Selective Modulation of Radiation by Periodical Variation of Gas Temperature.
260. Effect of Foreign Gases on the Adsorption of Infrared Radiation by Water Vapors in the Region of an Individual Line in Band 2.7μ.
261. Candoluminescence and Surface Recombination Luminescence of Phosphors in the Atmosphere of Activated Gas.
262. Thin Film Optics. V. The Properties of Silicon.
263. Optical Properties of Metal Films in the Region of Anomalous Skin-Effect.
264. Investigation of the Thermal Activation Energy of Photostimulated Flashes in Zns-Cu-Pb Phosphors.
265. Initial Stages of the Rise of Luminescence in Phosphors with Levels of Several Kinds.
266. Study of the Absorption Spectrum of Zinc Sulfide.
267. On the Temperature Dependence of the Intensities of Vibrational Absorption Bands of Gases in the Case of Fermi Resonance.
268. Study of the Temperature Dependence of the Intensity of the Infrared Absorption Bands in Solutions.

Vacuum Apparatus and Auxiliaries

20. Pumping Systems

207. Summarized Proceedings of a Symposium on Current Developments in the Production of High Vacua.
269. Vacuum Pumping Set.
270. Vacuum Pump Selection.

21. Pumps and Pump Fluids

1. Molecular Pumping.
88. Improvements in or Relating to Vapor Operated Vacuum Pumps.
89. Improvements in or Relating to Vapor Vacuum Pumps.
90. Annular Jet Pump.
91. Rough Pumping with Activated Charcoal.
271. Centripetal Air-Pump Operated Electro-magnetically.
272. Studies on the Construction of a Mechanical Booster Pump.
273. Performance of the Booster Pump of Multi-Nozzle Type (1).
274. Selection of Pumping Fluid which can be Safely Used in Oil Rotary Pump and Oil Ejector.
417. Experiments on a Simple Getter-Ion Pump.

22. Gauges

92. Small, Lightweight Ionization Gauge Control Circuit.
93. Principle of a Semiconductor Manometer in the Pressure Range of 1 mm to 10^{-6} mmHg.
275. Bistable Behaviour of the Bayard–Alpert Ionization Gauge.
276. The Sub-Standard Ionization Gauge, its Characteristics and Utility.
277. High Speed Ionization Gauge.
278. An Ultra-High Vacuum Mass Spectrometer.

23. Plumbing

94. Improvements in and Relating to Vacuum Vessels.
95. Inflatable Gasket for the 72 in. Bubble Chamber.
279. Leak-proof Joint for High Vacuum Work.
280. Method for Sealing Stainless Steel to Glass.
281. Platinum to Pyrex Tubular Housekeeper Seals.
282. Plastic-to-Metal Vacuum Seal for Rotating Targets.
283. Metallic Valve Seals.

24. Valves

96. Metal Bakeout Valve for Ultrahigh Vacuum.
97. New Techniques with Attainment of High Vacua.
98. Ultrahigh Vacuum Valve.
99. Large Ultrahigh Vacuum Valve.
284. Magnetically Driven Fast-Acting Valve for Gas Injection into High Vacua.
285. Mercury Float Valve.

25. Baffles, Traps and Refrigeration Equipment

286. Principles of Thermoelectric Devices.

27. Leak Detectors and Leak Detection

100. This Simple Method Finds Vacuum Leaks.
101. A New Mass Spectrometer Leak Detector for General Use.
207. Summarized Proceedings of a Symposium on Current Developments in the Production of High Vacua.
287. One Year Operating Experience with CEC Helium Leak Detector, Type 24-210.
288. Vacuum Testing of Tube Elements for Steam-Raising Units.

28. Heating Equipment

289. Resistance-Heated High Vacuum Furnace for Temperature to 1400°C.
290. Apparatus for the Measurement of Specific Heats of Metals.
291. Linear Voltage Temperature Furnace for Thermal Analysis.

29. Miscellaneous

292. Thermoplastic Recording.

Vacuum Applications

30. Evaporation and Sputtering

10. Evaporation into a Boundary Layer. II. Dissociation in Evaporation.
12. Secondary Positive Ion Emission from Metal Surfaces.
32. The Adsorption of Some Gases on Evaporated Metal Films and on Oxidized Films of Nickel.
38. The Interaction of Krypton with Metals. An Appraisal of Several Interaction Theories.
45. Surface Reactions on Evaporated Palladium Films.
52. Theory of Permeation Through Metal Coated Polymer Films.
68. Evaporation into a Boundary Layer.
85. Preparation of Phase Diffraction Gratings by Vacuum Evaporation.
86. Method for Obtaining Uniform Evaporated Layers.
102. Diffusion of Silver in Silver Sulfide.
103. Heterogeneous Reaction Studies by Infrared Absorption.
104. Physical Techniques in the Study of Silver Catalysts for Ethylene Oxidation.
105. Temperature Stabilization of Highly Reflecting Spherical Satellites.
106. Calculation of the Performance of a High-Vacuum Thermionic Energy Converter.
107. Selective Delineation of Screw Dislocations by Cathodic Sputtering.
108. Improvements in or Relating to the Deposition of Metals and the like Substances on Webs by Evaporation *in vacuo*.
109. A Method of Applying Films by Deposition in Vacua and Electrical Impedances when Made by the Method.
110. Substrate Damage in Film Thickness Measurement by Beam Interferometry.
111. Interferometric Studies of Synthetic Diamonds.
112. Investigation of Thin Films Produced by Evaporating Indium Antimonide in Vacuum.
113. Control of the Thickness of Evaporated Layers During Evaporation.
293. Vacuum Evaporator for Copper.
294. Low Cost Coatings for Metal Products.
295. Studies on the Manufacturing Process of Selenium Photocell.
296. Annealing Silicon Monoxide Films on Aluminium Mirrors.
297. The Effect of Gettering on the Reflectivity of Aluminium Films.
298. Preparation of Metal Film Resistors on Laminated Plastics.
299. Deposition by Thermal Evaporation of Thin Films of Titanium and Zirconium for Tritium Targets.
300. Technique for Preparing Thin Films of α-Iron.
301. Superconducting Computer Elements.
302. Simple Evaporator for Radioactive Metals.
419. Evaporation from Liquid Surface under a High and a Medium Vacuum.
420. Thick Vacuum Metallized Coatings are Durable, Corrosion Resistant.

31. Evacuation and Sealing

249. Thermionic Properties of Thorium Deposits on Control Grid Meterials.
303. Progress in Electric Lamps.
304. Discharge Lamp Production Development.
305. Absorption of Sodium and Argon by Glass.
306. On the High Temperature Reaction of Silica Glass with Copper and Copper Oxide.
307. Analysis of the Residual Gases in Several Types of High Vacuum Evaporators.
308. Sublimatography.
309. Some Properties of a Grade Vacuum Spark Gap.
421. The Radiolysis of Deuterated Biphenyls : Mechanism of Hydrogen Formation.

32. Nucleonics

53. Oxygen Sorption and Electrical Conductivity of Copper Oxide Films.
114. New Electrostatic Accelerator.
115. 22 MeV Electron Linear Accelerator.
116. Duo Plasmatron Ion Source for Use in Accelerators.
117. Zero Gradient Synchrotron at the Argonne National Laboratory.
207. Summarized Proceedings of a Symposium on Current Developments in the Production of High Vacua.
253. Absolute Intensity Measurements of the Carbon and Aluminium X-Ray K-Lines with a Proportional Counter.
299. Deposition by Thermal Evaporation of Thin Films of Titanium and Zirconium for Tritium Targets.
302. Simple Evaporator for Radioactive Metals.
310. Cern Proton Synchrotron.
311. Large Double-Focusing Mass Spectrometer.

33. General Physics and Electronics

12. Secondary Positive Ion Emission from Metal Surfaces.
71. The Stellarator Concept.
118. Recombination of Atoms at Surfaces.
119. Theory and Application of Molecular Beam Techniques for the Design of Collision Free Sampling Systems. Part 1. Molecular Beam Formation by Multiple Aperture Collimating Systems. Part 2. Molecular Beam Formation by Adiabatic Expansion of Gas through Apertures in Thin Diaphragms.
120. Emission of Relatively High-Energy Ions from Low-Voltage Arcs.
121. Improvements in or Relating to Methods of Forming Luminescent Screens Coated with Thin Films of Organic Material.
122. A Comparison of Charges on the Electron, Proton, and Neutron.
123. Field Effects on Chemisorbed Films in Electron Emission Microscopy.
124. Ionization Phenomena in Gases.
125. Tensile Strength of Liquid Argon, Helium, Nitrogen and Oxygen.
126. Precision Thermometer System for Liquid Helium Range.
127. Precooling Device for Liquid Helium Transfer Tube.
128. Strong Focusing Ion Source for Mass Spectrometers.
129. Ion Optics for the V-Type Surface Ionization Filament Used in Mass Spectrometry.
130. A New Method of Comparing the Mass of Bodies in a Vacuum.
131. Interferometric Calibration of Quartz End-Measuring Rods.
207. Summarized Proceedings of a Symposium on Current Developments in the Production of High Vacua.
219. Properties of Getters in Electronic Tubes.
233. Anode Surface Effects in Diodes Containing Oxide-Coated Cathodes.
237. Deuterium-Filled Thyratrons.
238. Deuterium as a Filling for High-Voltage Thyratrons.
242. Thermionic and Related Properties of Calcium Oxide.
248. Production of X-Ray during a Low Pressure Gas Discharge.
252. Summarized Proceedings of a Conference on Electron Microscopy.
253. Absolute Intensity Measurements of the Carbon and Aluminium X-Ray K-Lines with a Proportional Counter.
300. Technique for Preparing Thin Films of α-Iron.
312. Method for Size-Distribution Determination of Non-Volatile Droplets by Electron Microscopy.
313. Summarized Proceedings of a Conference on Electron Microscopy.
314. Reflexion Electron Microscopy Using Diffracted Electrons.
315. Accuracy of Selected-Area Microdiffraction in the Electron Microscope.
316. Selected Area Microdiffraction in the Electron Microscope.

Vol. 10 196

317. The Theory of Ballast Tubes or Barretters.
318. Heat-Reflecting Windows Using Gold and Bismuth Oxide Films.
319. The Ageing of Vacuum Standard Lamps on a.c. and d.c.
320. The X-Ray Scanning Microanalyser.
321. New Method for the Determination of Grain or Crystallite Size from Spotty Diffraction Rings.
322. High-Resolution Shadow-Casting Technique for the Electron Microscope Using the Simultaneous Evaporation of Platinum and Carbon.
323. Analysis of the Lighter Elements by Total Reflexion of Their Characteristic X-Ray Wavelengths.
324. New Method for Increasing the X-Ray Reflection Power of Lithium Fluoride Crystals.
325. Recent Techniques in Ultra-High Vacuum.
326. A Vacuum Microbalance and its Use in Studies of Electron Tube Materials.
422. On the Characteristics of Steam Ejectors and a Method of Calculating their Performances.
423. Photoelectric Devices for Monitoring Thickness of Vacuum Deposition of Multilayer Film.

34. High Altitude and Space Technology

58. High Altitude Atmospheric Density.
59. Comparison of High-Altitude Rocket and Satellite Density Measurements.
105. Temperature Stabilization of Highly Reflecting Spherical Satellites.
132. Change of Cosmic Rays in Space.
133. Air Density in the Upper Atmosphere from Satellite Orbit Observations.
134. Dissipation of Planetary Atmospheres.

35. Impregnation and Potting

135. Low-Melting Inorganic Glasses with High Melt Fluidities below 400°C.
136. Impregnants for Castings.

36. Drying, Degassing and Concentration

137. Processing Techniques used in Degassing during Casting of Rolling and Forging Steels based on the Vacuum Lift Process.
138. Vacuum Degassing of Low Carbon Unkilled Steel during Casting or during Solidification into Block Form. I. Degassing of Unkilled Soft Steel under Vacuum.
139. Vacuum Degassing of Low Carbon Unkilled Steel during Casting or during Solidification into Block Form. II. Casting by Stream Degassing of Unkilled Soft Steel.
140. Methods of Heating for Large Scale Industrial Degassing of Molten Steel.
141. Steel Degassing Based on the Circulating Degassing Process.
142. Measurements and Control during the Vacuum Degassing of Molten Steel.
143. The Removal of Oxygen in the Treatment of Steel Melts in Vacuum.
424. Fundamental Study of Vacuum Drying.

37. Metallurgy, Inorganic Chemistry and Analytical Chemistry

144. Production Mass Spectrometer.
145. Oxidation of Silicon Carbide in the Temperature Range 1200 to 1500°C.
146. The Fractionation of Oxygen Isotopes between Water and Sulfur Dioxide.
147. New Vacuum-Melting Furnace.
148. High-Temperature Pressure-Vacuum Furnace.
149. High Temperature Laboratory Vacuum Furnace.
150. Vacuum Degassing in Ladle—A New Technique in Steelmaking.
151. Mechanical Testing with a 3000°F Radiant Heat Furnace.
152. A New Tool for Case Carbon Evaluation.
153. Degassing and Vacuum Refining Furnace.
226. Viscosity and Thermal Conductivity of Liquid Boron Trifluoride.
252. Summarized Proceedings of a Conference on Electron Microscopy.
289. Resistance-Heated High Vacuum Furnace for Temperature to 1400°C.
318. Heat-Reflecting Windows Using Gold and Bismuth Oxide Films.
320. The X-Ray Scanning Microanalyser.
321. New Method for the Determination of Grain or Crystallite Size from Spotty Diffraction Rings.
322. High-Resolution Shadow-Casting Technique for the Electron Microscope Using the Simultaneous Evaporation of Platinum and Carbon.
323. Analysis of the Lighter Elements by Total Reflexion of their Characteristic X-Ray Wavelengths.
327. Brazing in Vacuum by Induction Heating.
328. Vacuum Treatment of Molten Steel in Germany.
329. Steel Vacuum Degassed in the Ladle.
330. Missiles Boost Vacuum Melting.
331. World's Largest Vacuum Induction Furnace.
332. Levitation—New Tool for Metallurgy.
333. Vacuum Furnace Brazed Parts at Temperatures to 4500°F.
334. New Furnace Permits Recovery of Reactive Metal Scrap.
335. Vacuum Furnace for Creep-Rupture Testing.
336. Air Hardening Grade and Vacuum Degassing Offer New Possibilities.
337. Welding Processes.
338. Vacuum Furnace.
339. 4 MeV Linear Accelerator for Radiographic Examination of Welds.
340. Preparation of High Purity Single Crystal Silicon.
425. Which Brazing Alloys for Vacuum Systems ?
426. Electron Beam Welding : Emphasis on Precision and Freedom from Contamination.
427. Vacuum Melters Push Expansion—Bank on Growing Markets.
427a. Welding and Brazing Two Columbium Alloys.

38. Distillation, Organic Chemistry and Isotopic Gas Analysis

252. Summarized Proceedings of a Conference on Electron Microscopy.
428. Falling-Film Evaporator.
429. Mass Transfer in Falling-Film Molecular Distillation.

39. Miscellaneous Applications

154. Synthesis of Boron Phosphide and Nitride.
209. Methods of Cleaning Glass by Vapour Degreasing and Ultrasonically Agitated Solvents.
224. The Quantum Mechanical Correction for the High Temperature Van der Waals Interaction of Light Gases and Surfaces. A New Method of Determining Surface Area.
341. Measurement of the Thickness of Thick Layers.

Materials and Techniques used in Vacuum Technology

40. Gases and Vapours

155. Non-Equilibrium Properties of Rare Gases.
156. Heating by Electron Bombardment.
157. Effect of Argon and Helium on the Thermal Conductivity of the N_2O_4 $2NO_2$ System.
158. Adsorption Diffusion and Evaporation of Carbon Monoxide on Tungsten.

159. Molecular Ions.
160. Probability of Double Ionization by Electron Impact for Neon, Argon and Xenon.
161. Diffusion Coefficient of Atomic Hydrogen through Multicomponent Mixtures.
162. Effect of Water Vapor on the Dissociation of Hydrogen in an Electrical Discharge.
163. Molecular Dissociation and Reconstitution on Solids.
164. On the Velocity Distribution in a Chemically Reacting Gas.
245. Microwave Method of Investigating the After-glow of Pulsed Gaseous Discharges.
305. Adsorption of Sodium and Argon by Glass.
326. A Vacuum Microbalance and its Use in Studies of Electron Tube Materials.
342. Calorimetric Heat of Adsorption—Nitrogen on Tungsten.
343. Total Collision Cross Sections for the Interaction of Atomic Beams of Alkali Metals with Gases.
344. Studies of Evaporation of Condensates Containing Nitrogen Atoms.
345. On Chemical Reactions in Free Molecule Flow.
346. Negative Ion Formation in NO_2 by Electron Attachment.
347. Pressure Induced Shifts of HCl Lines due to Foreign Gases.
348. Pressure Induced Shifts to HCl Lines due to Foreign Gases.
349. Pressure Shifting of Spectrum Lines : Some Empirical Generalizations.
350. Threshold Ionization of HCl by Electron Impact.
351. Thermal Conductivity of Binary Mixtures of Diatomic and Monatomic Gases.
352. Molecular Diffusion Studies in Gases at High Temperature IV. Results and Interpretations of the CO_2–O_2, CH–O_2, H_2–O_2, CO–O_2, and H_2O–O_2 Systems.
353. Infrared Emission Spectra of Gaseous B_2O_3 and B_2O_2.
354. Infrared Emission Spectrum of Gaseous HBO_2.
355. Excitation of the Auroral Green Line in Nitrogen Afterglows.
356. Vibrational Distribution in Late Nitrogen Afterglows.
357. Formation of Excited NO and N_2 by Wall Catalysis.
358. Use of Constant-Boiling Systems in Calibration of Mass Spectrometers and other Molecular Beam Instruments.
359. Thermal Conductivity of Condensed Films : Methane.
360. Interaction of Hydrogen with Tungsten.
361. Surface Migration of Nitrogen on Tungsten.
362. On the Mechanism of the Lewis-Rayleigh Nitrogen Afterglow.
363. Emission Spectra of N_2, O_2 and NO Molecules Trapped in Solid Matrices.
364. Collision of a Gas Atom with a Cold Surface.
365. Electron Capture by Neutral Molecules.
366. Thermal Conductivity of Helium and Hydrogen at High Temperatures.
367. Interactions between Molecules Adsorbed on a Surface.
368. Measurements of Multicomponent Diffusion Coefficients for the CO_2–He–N_2 System using the Point Source Technique.
369. Chemisorption of CO on Ni using a Radioactive Tracer.
370. Ionization Potential of Fluorine.
371. Transport in Dilute Gases and Chemical Forces.
430. Pressure Dependence or Some Infrared and Vacuum Ultraviolet Bands Occurring in Active Nitrogen.
431. Charge Transfer between Atomic Hydrogens and N^+ and O^+.
432. Interchange of Charge between Gaseous Molecules.
433. Rapid Determination of Gaseous Diffusion Coefficients by Means of Gas Chromatography Apparatus.
434. Dielectric Constants of Imperfect Gases. I. Helium, Argon, Nitrogen and Methane.
435. Molecular Friction in Dilute Gases.
436. Dissociation Energies of Diatomic Molecules.
437. Sparking Potential and Molecular Structure of Unsaturated Hydrocarbon Gases.
438. Self-Diffusion of Oxygen in Single Crystal and Polycrystalline Aluminum Oxide.
439. Interaction of Condensable Gases with Cold Surfaces.
440. Heterogeneous Reactions Studied by Mass Spectrometry. I. Reactions of B_2O_3(s) with H_2O(g).
441. Heterogeneous Reactions Studied by Mass Spectrometry. II. Reactions of Li_2O(s) with H_2O(g).
442. Viscosity of Mixtures of Hydrogen and Water Vapor at 295°K.
443. Multiple Ionization in Argon and Krypton by Electron Impact.
444. Recombination Kinetics of Atomic Oxygen at Room Temperature.
445. Secondary Reactions in a Gas Discharge.
446. Kinetic Adsorption Spectra Recorded through Flash-Heated Grids.
447. Separation of Gas Mixtures in a Supersonic Jet. II. Behaviour of Helium–Argon Mixtures and Evidence of Schock Separation.
448. Threshold Law for the Probability of Excitation of Molecules by Photon Impact. A Study of the Photionization Efficiencies of Br_2, I_2, HI and CH_3I.
449. Oxygen Diffusion in Periclase Crystals.

41. Metals and Alloys

16. Surface Properties of Germanium.
137. Processing Techniques used in Degassing during Casting of Rolling and Forging Steels based on the Vacuum Lift Process.
138. Vacuum Degassing of Low Carbon Unkilled Steel during Casting or during Solidification into Block Form. I. Degassing of Unkilled Soft Steel under Vacuum.
139. Vacuum Degassing of Low Carbon Unkilled Steel during Casting or during Solidification into Block Form. II. Casting by Stream Degassing of Unkilled Soft Steel.
140. Methods of Heating for Large Scale Industrial Degassing of Molten Steel.
141. Steel Degassing Based on the Circulating Degassing Process.
142. Measurements and Control during the Vacuum Degassing of Molten Steel.
143. The Removal of Oxygen in the Treatment of Steel Melts in Vacuum.
165. Measuring the Thermal Emissivity of Strip Materials.
166. Spectral Emittance of Ceramic-Coated and Uncoated Specimens of Inconel and Stainless Steel.
167. The Behavior of a Rhenium in Electron Tube Environments.
305. Adsorption of Sodium and Argon by Glass.
372. The Heat Capacity and Thermodynamic Functions of Uranium from 5 to 350°K.
373. The Volatility of Actinium.
374. Vapor Pressure of Thorium.
375. Thermionic Properties of Uranium.
376. Materials below —100°F.
377. The Measurement of the Heats of Sublimation of Zinc and Cadmium with the Mass Spectrometer.
378. Extended Theory of Sputtering.
379. Sputtering of Silver by Light Ions with Energies from 2 to 12 keV.
450. Space-Age Beryllium—Its Technology.
451. Secondary Positive Ion-Emission from Platinum.
452. Nucleation and Growth of Mercury Crystals at Low Supersaturation.
453. Low-Temperature Metals : A Roundup.
454. Progress in Aluminum Alloys.
455. Progress in Copper Alloys.
456. Progress in Magnesium Alloys.
457. Vapor Pressures of Platinum Metals. I. Palladium and Platinum.
458. The Niobium–Niobium Carbide System.
459. The Preparation, Crystal Structures and Some Properties of Zirconium and Hafnium Dirhenide.
460. Some Solidus Temperatures in Several Metal-Carbon Systems.
461. The Initial Stages of Oxidation of Germanium.

Vol. 10 1960

42. Glass and Ceramics

131. Interferometric Calibration of Quartz End-Measuring Rods.
135. Low-Melting Inorganic Glasses with High Melt Fluidities below 400°C.
168. Precipitation in Microscopic Cracks.
169. Breaking Stress of Glass Determined from Dimensions of Fracture Mirrors.
170. Strength of Synthetic Single Crystal Sapphire and Ruby as a Function of Temperature and Orientation.
171. Internal Stresses in Model Ceramic Systems.
172. The Dielectric Behavior of Solids Embedded in a Homogeneous Medium.
173. Improved Apparatus for Rapid Measurement of Viscosity of Glass at High Temperatures.
174. Strength and Static Fatigue of Abraded Glass under Controlled Ambient Conditions. I. General Concepts and Apparatus.
175. Strength and Static Fatigue of Abraded Glass under Controlled Ambient Conditions. II. Effect of Various Abrasions and the Universal Fatigue Curve.
176. Effect of Fluorides on Infrared Transmittance of Certain Silicate Glasses.
177. Thermal Conductivity. XIV. Conductivity of Multicomponent Systems.
178. Fifth International Glass Congress organised by the International Commission for Glass in Munich.
179. "Araldite". An Artificial Resin for Preparing Working Models in the Ceramics Industry.
209. Methods of Cleaning Glass by Vapour Degreasing and Ultrasonically Agitated Solvents.
305. Adsorption of Sodium and Argon by Glass.
462. Glass-Ceramics.
463. The Reactions of Water Vapor with Beryllia and Beryllia–Alumina Compounds.

43. Plastics and Elastomers

179. "Araldite". An Artificial Resin for Preparing Working Models in the Ceramics Industry.
180. Cleaning Techniques for Rubber O-Rings Used in Vacuum Systems.
181. Irradiation of Polyethylene. IV. Oxidation Effects.
380. Rubber Developments—1957-1959

44. Waxes, Lubricants, Cements, Lacquers, Paints, Oils

182. When to Consider Automatic Spray Equipment.
183. Applying Decorative Effects to Moulded Plastics.
184. The Oscicator, a new Flow Coater.
381. Lacquering Techniques for Vacuum Metallizing on Metals and Thermosetting Plastics.

45. Soldering, Welding and Brazing

185. Copper Welding for Maximum RF Conductivity.
382. New Alloy Points up Advantages of Electron Beam Melting.
383. Which Copper-Base Alloy for a Brazed Part ?
384. Electron-Beam Welding—Machining.
464. Progress in Welding Steels : Vapor-Shielded Arc Means Faster Welding.

46. Glass Blowing, Glass-to-Metal and Ceramic-to-Metal Sealing Techniques

186. Metal–Glass Vacuum Seal for Use at Low Temperatures.
306. On the High Temperature Reaction of Silica Glass with Copper and Copper Oxide.
385. A Method of Improving the Glass-to-Metal Seal Resistance to High Humidity Deterioration in Electron Tubes.
386. Electroformed Ceramic-to-Metal Seal for Vacuum Tubes.
387. A High Temperature Ceramic–Metal Seal Made with Low Vapor Pressure Materials.

47. Outgassing Data, Vapour Pressure Data, and Gettering Data

44. The Structure of Gas-Adsorbent Carbons.
61. Dissociation Pressure and Stability of Beryllium Carbide.
64. The Vaporization of Molybdenum and Tungsten Oxides.
187. Titanium as a Gettering Material.
188. Vapor Pressure of Thorium Tetrafluoride.
189. Vapor Pressures and Molecular Composition of Vapors of the $RbF–ZrF_4$ and $LiF–ZrF_4$ Systems.
190. Vaporization Characteristics of p-Dibromobenzine.
191. Method for Rapid Determination of Vacuum Outgassing Rates.
192. An Investigation of Some Vacuum Properties of Epoxy Resins.
219. Properties of Getters in Electronic Tubes.
374. Vapour Pressure of Thorium.
377. The Measurement of the Heats of Sublimation of Zinc and Cadmium with the Mass Spectrometer.
388. Vapor Pressures of $FeCl_2$, $FeBr_2$ and FeI_2 by Torsion Effusion Method.
389. Molecular Sieves in Atmosphere Control.
457. Vapor Pressures of Platinum Metals. I. Palladium and Platinum.

49. Miscellaneous Materials and Techniques

145. Oxidation of Silicon Carbide in the Temperature Range 1200 to 1500°.
193. Translucent Phosphor Coatings in High-Pressure Mercury-Vapor Lamps.
194. Molybdenum Disulfide of High Surface Area.
195. Electrical Conductivity of Single Crystals of MgO.
390. Low Friction of Metals in Reciprocating Sliding.
391. Kinetics of Strontium Oxide on Tungsten.
392. Mass Spectrometric Investigation of the Sublimation of Molybdenum Dioxide.
393. Check for Vacuum Producers.
394. The New Welding Process.
465. How Radiation Affects Engineering Materials.
466. Observation of Adsorption on an Atomic Scale.
467. Cuprous Halide Films on Alkali Halide Crystals.

Basic Science and Engineering

51. Physics, Astronomy and Geophysics

3. Calcium Atomic Beam Source and Interference Beyond Two Meter Retardation.
82. Design of High-Resolution Monochromator for the Vacuum Ultra-violet. An Application of Off-Plane Eagle Mounting.
83. Phase Changes on Reflection from Evaporated Chromium Films.
84. The Theory of the High Frequency Brush Discharge.
134. Dissipation of Planetary Atmospheres.
269. Effect of Foreign Gases on the Absorption of Infrared Radiation by Water Vapours in the Region of an Individual Line in Band 2.7μ.
261. Candoluminescence and Surface Recombination Luminescence of Phosphors in the Atmosphere of Activated Gas.
262. Thin Film Optics. V. The Properties of Silicon.
263. Optical Properties of Metal Films in the Region of Anomalous Skin-Effect.

395. Study of Electroluminescence of Zns-Cu Single Crystals.
396. The Influence of an Activator on the Stability of F-Centers.

52. Physical Chemistry

35. The Time Lag in Diffusion IV.
45. Surface Reactions on Evaporated Palladium Films.
102. Diffusion of Silver in Silver Sulfide.
103. Heterogeneous Reaction Studies by Infrared Absorption.
104. Physical Techniques in the Study of Silver Catalysts for Ethylene Oxidation.
106. Calculation of the Performance of a High-Vacuum Thermionic Energy Converter.
107. Selective Delineation of Screw Dislocations by Cathodic Sputtering.
180. Irradiation of Polyethylene. IV. Oxidation Effects.
196. Surface Functionality of Amorphous Silica by Infrared Spectroscopy.
197. The Molecular Composition of Sodium Iodide Vapor from Molecular Weight Measurements.
198. Ion-Molecule Reactions of 1, 3-Butadiene, of Acetylene and of Acetylene–Methane Mixtures.
199. Interaction of Oxygen with Titanium Dioxide.
200. Chemical Effects of Low Energy Electrons.
201. Dissociation of C_2H_5T and 1, 2-$C_2H_4BrBr^{82}$ by β-Decay.
218. The Oxidation of Evaporated Barium Films.
227. The Dissociation Pressure of CdSb.
228. Sublimation Pressures of Solid Solutions. I.

53. Metallurgy, Ceramics and Inorganic Chemistry

169. Strength of Synthetic Single Crystal Sapphire and Ruby as a Function of Temperature and Orientation.
170. Internal Stresses in Model Ceramic Systems.
202. Magnetic Ceramics. VI. Evaluation of Some Methods of Nickel Ferrite Formation.
203. Corrosion Research at the National Bureau of Standards.
461. The Initial Stages of Oxidation of Germanium.
463. The Reactions of Water Vapor with Beryllia and Beryllia-Alumina Compounds.

54. Biology, Biochemistry, Pharmaceutics, Toxicology, Organic Chemistry

204. Mass Spectrometer for Respiratory Studies.

56. Electrical Engineering, Electronic Circuits

237. Deuterium-Filled Thyratrons.
238. Deuterium as a Filling for High-Voltage Thyratrons.
298. Preparation of Metal Film Resistors on Laminated Plastics.
301. Superconducting Computer Elements.

59. Miscellaneous

205. Spectral Study of a Visible, Short-Duration Afterglow in Nitrogen.
206. On the Trapping of Free Radicals of Oxygen and Chlorine.

Vol.
10
196

ol.
10
960

END OF VOL.